Scientific and Technical Aerospace Reports

STAR

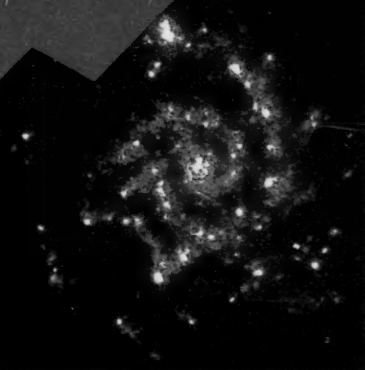

An Abstract Journal

Volume 30, Number 1
January 8,1992
N92-10001 to N92-10971

Scientific and Technical Aerospace Reports

Scientific and Technical Aerospace Reports (STAR) is an abstract journal that provides comprehensive coverage of worldwide aerospace-related reports. It is a major product of the International Aerospace Database managed by the NASA Scientific and Technical Information (STI) Program. The coverage includes reports on aeronautics, space, and supporting disciplines. *STAR* lists current, publicly available reports entered into the NASA STI Database during the 2-week period preceding publication. A typical citation and abstract appear on page viii. They explain how to read the items that are announced in this journal.

NASA sponsors a companion journal, *International Aerospace Abstracts (IAA)* (*NOVA* for internal NASA use) that lists abstracts of the open literature on aerospace subjects available worldwide. *IAA* is available for sale through the AIAA.

Entries found in *STAR* and *IAA* are available through NASA's online service, RECON, as the International Aerospace Database and through DIALOG as the Aerospace Database.

Information on aerospace and related subjects is gathered by the NASA STI Program through national and international agreements and exchanges and is made available to the NASA community as well as to the public in many forms through various outlets. The section on NASA STI Program Products and Services contains additional information.

For further information please contact:
NASA Center for AeroSpace Information (CASI)
P.O. Box 8757
Baltimore, Maryland 21240-0757
(301) 621-0390

US ISSN 0036-8741

***Scientific and Technical Aerospace Reports* (*STAR*)** is an abstract journal that provides comprehensive coverage of worldwide aerospace-related reports. It is a major product of the International Aerospace Database managed by the NASA Scientific and Technical Information (STI) Program. The coverage includes reports on aeronautics, space, and supporting disciplines. *STAR* lists current, publicly available reports entered into the NASA STI Database during the 2-week period preceding publication. A typical citation and abstract appear on page viii. They explain how to read the items that are announced in this journal.

NASA sponsors a companion journal, *International Aerospace Abstracts* (*IAA*), that lists abstracts of the open literature on aerospace subjects available worldwide. *IAA* is available through the American Institute of Aeronautics and Astronautics.

Entries found in *STAR* and *IAA* are available through NASA's online service, RECON, as the International Aerospace Database and through DIALOG as the Aerospace Database.

Information on aerospace and related subjects is gathered by the NASA STI Program through national and international agreements and exchanges and is made available to the NASA community as well as to the public in many forms through various outlets. The section on NASA STI Program Products and Services contains additional information.

US ISSN 0036-8741

Volume 30 Number 1 / JANUARY 8, 1992

TABLE OF CONTENTS

AERONAUTICS For related information see also *Astronautics.*

01 AERONAUTICS (GENERAL) 1

02 AERODYNAMICS 1
Includes aerodynamics of bodies, combinations, wings, rotors, and control surfaces; and internal flow in ducts and turbomachinery. For related information see also *34 Fluid Mechanics and Heat Transfer.*

03 AIR TRANSPORTATION AND SAFETY 4
Includes passenger and cargo air transport operations; and aircraft accidents. For related information see also *16 Space Transportation* and *85 Urban Technology and Transportation.*

04 AIRCRAFT COMMUNICATIONS AND NAVIGATION 4
Includes digital and voice communication with aircraft; air navigation systems (satellite and ground based); and air traffic control. For related information see also *17 Space Communications, Spacecraft Communications, Command and Tracking* and *32 Communications and Radar.*

05 AIRCRAFT DESIGN, TESTING AND PERFORMANCE 4
Includes aircraft simulation technology. For related information see also *18 Spacecraft Design, Testing and Performance* and *39 Structural Mechanics.* For land transportation vehicles see *85 Urban Technology and Transportation.*

06 AIRCRAFT INSTRUMENTATION 5
Includes cockpit and cabin display devices; and flight instruments. For related information see also *19 Spacecraft Instrumentation* and *35 Instrumentation and Photography.*

07 AIRCRAFT PROPULSION AND POWER 5
Includes prime propulsion systems and systems components, e.g., gas turbine engines and compressors; and onboard auxiliary power plants for aircraft. For related information see also *20 Spacecraft Propulsion and Power, 28 Propellants and Fuels,* and *44 Energy Production and Conversion.*

08 AIRCRAFT STABILITY AND CONTROL 6
Includes aircraft handling qualities; piloting; flight controls; and autopilots. For related information see also *05 Aircraft Design, Testing and Performance.*

09 RESEARCH AND SUPPORT FACILITIES (AIR) ..... N.A.
Includes airports, hangars and runways; aircraft repair and overhaul facilities; wind tunnels; shock tubes; and aircraft engine test stands. For related information see also *14 Ground Support Systems and Facilities (Space).*

ASTRONAUTICS For related information see also *Aeronautics.*

12 ASTRONAUTICS (GENERAL) 6
For extraterrestrial exploration see *91 Lunar and Planetary Exploration.*

13 ASTRODYNAMICS 7
Includes powered and free-flight trajectories; and orbital and launching dynamics.

14 GROUND SUPPORT SYSTEMS AND FACILITIES (SPACE) 7
Includes launch complexes, research and production facilities; ground support equipment, e.g., mobile transporters; and simulators. For related information see also *09 Research and Support Facilities (Air).*

15 LAUNCH VEHICLES AND SPACE VEHICLES ..... N.A.
Includes boosters; operating problems of launch/space vehicle systems; and reusable vehicles. For related information see also *20 Spacecraft Propulsion and Power.*

16 SPACE TRANSPORTATION 8
Includes passenger and cargo space transportation, e.g., shuttle operations; and space rescue techniques. For related information see also *03 Air Transportation and Safety* and *18 Spacecraft Design, Testing and Performance.* For space suits see *54 Man/System Technology and Life Support.*

17 SPACE COMMUNICATIONS, SPACECRAFT COMMUNICATIONS, COMMAND AND TRACKING 8
Includes telemetry; space communications networks; astronavigation and guidance; and radio blackout. For related information see also *04 Aircraft Communications and Navigation* and *32 Communications and Radar.*

N.A.—no abstracts were assigned to this category for this issue.

18 SPACECRAFT DESIGN, TESTING AND PERFORMANCE **8**
Includes satellites; space platforms; space stations; spacecraft systems and components such as thermal and environmental controls; and attitude controls. For life support systems see *54 Man/System Technology and Life Support.* For related information see also *05 Aircraft Design, Testing and Performance, 39 Structural Mechanics,* and *16 Space Transportation.*

19 SPACECRAFT INSTRUMENTATION ..... **N.A.**
For related information see also *06 Aircraft Instrumentation* and *35 Instrumentation and Photography.*

20 SPACECRAFT PROPULSION AND POWER **9**
Includes main propulsion systems and components, e.g., rocket engines; and spacecraft auxiliary power sources. For related information see also *07 Aircraft Propulsion and Power, 28 Propellants and Fuels, 44 Energy Production and Conversion,* and *15 Launch Vehicles and Space Vehicles.*

CHEMISTRY AND MATERIALS

23 CHEMISTRY AND MATERIALS (GENERAL) **12**

24 COMPOSITE MATERIALS **13**
Includes physical, chemical, and mechanical properties of laminates and other composite materials. For ceramic materials see *27 Nonmetallic Materials.*

25 INORGANIC AND PHYSICAL CHEMISTRY **14**
Includes chemical analysis, e.g., chromatography; combustion theory; electrochemistry; and photochemistry. For related information see also *77 Thermodynamics and Statistical Physics.*

26 METALLIC MATERIALS **16**
Includes physical, chemical, and mechanical properties of metals, e.g., corrosion; and metallurgy.

27 NONMETALLIC MATERIALS **18**
Includes physical, chemical, and mechanical properties of plastics, elastomers, lubricants, polymers, textiles, adhesives, and ceramic materials. For composite materials see *24 Composite Materials.*

28 PROPELLANTS AND FUELS **21**
Includes rocket propellants, igniters and oxidizers; their storage and handling procedures; and aircraft fuels. For related information see also *07 Aircraft Propulsion and Power, 20 Spacecraft Propulsion and Power,* and *44 Energy Production and Conversion.*

29 MATERIALS PROCESSING **22**
Includes space-based development of products and processes for commercial application. For biological materials see *55 Space Biology.*

ENGINEERING For related information see also *Physics.*

31 ENGINEERING (GENERAL) **23**
Includes vacuum technology; control engineering; display engineering; cryogenics; and fire prevention.

32 COMMUNICATIONS AND RADAR **23**
Includes radar; land and global communications; communications theory; and optical communications. For related information see also *04 Aircraft Communications and Navigation* and *17 Space Communications, Spacecraft Communications, Command and Tracking.* For search and rescue see *03 Air Transportation and Safety,* and *16 Space Transportation.*

33 ELECTRONICS AND ELECTRICAL ENGINEERING **28**
Includes test equipment and maintainability; components, e.g., tunnel diodes and transistors; microminiaturization; and integrated circuitry. For related information see also *60 Computer Operations and Hardware* and *76 Solid-State Physics.*

34 FLUID MECHANICS AND HEAT TRANSFER **31**
Includes boundary layers; hydrodynamics; fluidics; mass transfer and ablation cooling. For related information see also *02 Aerodynamics* and *77 Thermodynamics and Statistical Physics.*

35 INSTRUMENTATION AND PHOTOGRAPHY **34**
Includes remote sensors; measuring instruments and gauges; detectors; cameras and photographic supplies; and holography. For aerial photography see *43 Earth Resources and Remote Sensing.* For related information see also *06 Aircraft Instrumentation* and *19 Spacecraft Instrumentation.*

36 LASERS AND MASERS **36**
Includes parametric amplifiers. For related information see also *76 Solid-State Physics.*

37 MECHANICAL ENGINEERING **37**
Includes auxiliary systems (nonpower); machine elements and processes; and mechanical equipment.

38 QUALITY ASSURANCE AND RELIABILITY **38**
Includes product sampling procedures and techniques; and quality control.

39 STRUCTURAL MECHANICS **39**
Includes structural element design and weight analysis; fatigue; and thermal stress. For applications see *05 Aircraft Design, Testing and Performance* and *18 Spacecraft Design, Testing and Performance.*

GEOSCIENCES For related information see also *Space Sciences.*

42 GEOSCIENCES (GENERAL) ..... **N.A.**

43 EARTH RESOURCES AND REMOTE SENSING **40**
Includes remote sensing of earth resources by aircraft and spacecraft; photogrammetry; and aerial photography. For instrumentation see *35 Instrumentation and Photography.*

44 ENERGY PRODUCTION AND CONVERSION **42**
Includes specific energy conversion systems, e.g., fuel cells; global sources of energy; geophysical conversion; and windpower. For related information see also *07 Aircraft Propulsion and Power, 20 Spacecraft Propulsion and Power,* and *28 Propellants and Fuels.*

45 ENVIRONMENT POLLUTION **43**
Includes atmospheric, noise, thermal, and water pollution.

46 GEOPHYSICS **47**
Includes aeronomy; upper and lower atmosphere studies; ionospheric and magnetospheric physics; and geomagnetism. For space radiation see *93 Space Radiation.*

47 METEOROLOGY AND CLIMATOLOGY **51**
Includes weather forecasting and modification.

48 OCEANOGRAPHY **52**
Includes biological, dynamic, and physical oceanography; and marine resources. For related information see also *43 Earth Resources and Remote Sensing.*

LIFE SCIENCES

51 LIFE SCIENCES (GENERAL) **52**

52 AEROSPACE MEDICINE **53**
Includes physiological factors; biological effects of radiation; and effects of weightlessness on man and animals.

53 BEHAVIORAL SCIENCES **54**
Includes psychological factors; individual and group behavior; crew training and evaluation; and psychiatric research.

54 MAN/SYSTEM TECHNOLOGY AND LIFE SUPPORT **55**
Includes human engineering; biotechnology; and space suits and protective clothing. For related information see also *16 Space Transportation.*

55 SPACE BIOLOGY ..... **N.A.**
Includes exobiology; planetary biology; and extraterrestrial life.

MATHEMATICAL AND COMPUTER SCIENCES

59 MATHEMATICAL AND COMPUTER SCIENCES (GENERAL) **55**

60 COMPUTER OPERATIONS AND HARDWARE **56**
Includes hardware for computer graphics, firmware, and data processing. For components see *33 Electronics and Electrical Engineering.*

61 COMPUTER PROGRAMMING AND SOFTWARE **58**
Includes computer programs, routines, algorithms, and specific applications, e.g., CAD/CAM.

62 COMPUTER SYSTEMS **63**
Includes computer networks and special application computer systems.

63 CYBERNETICS **64**
Includes feedback and control theory, artificial intelligence, robotics and expert systems. For related information see also *54 Man/System Technology and Life Support.*

64 NUMERICAL ANALYSIS **64**
Includes iteration, difference equations, and numerical approximation.

65 STATISTICS AND PROBABILITY **66**
Includes data sampling and smoothing; Monte Carlo method; and stochastic processes.

66 SYSTEMS ANALYSIS ..... **N.A.**
Includes mathematical modeling; network analysis; and operations research.

67 THEORETICAL MATHEMATICS **68**
Includes topology and number theory.

PHYSICS For related information see also *Engineering.*

70 PHYSICS (GENERAL) **68**
For precision time and time interval (PTTI) see *35 Instrumentation and Photography;* for geophysics, astrophysics or solar physics see *46 Geophysics, 90 Astrophysics,* or *92 Solar Physics.*

71 ACOUSTICS **103**
Includes sound generation, transmission, and attenuation. For noise pollution see *45 Environment Pollution.*

72 ATOMIC AND MOLECULAR PHYSICS **105**
Includes atomic structure, electron properties, and molecular spectra.

73 NUCLEAR AND HIGH-ENERGY PHYSICS **113**
Includes elementary and nuclear particles; and reactor theory. For space radiation see *93 Space Radiation.*

74 OPTICS **114**
Includes light phenomena and optical devices. For lasers see *36 Lasers and Masers.*

75 PLASMA PHYSICS **116**
Includes magnetohydrodynamics and plasma fusion. For ionospheric plasmas see *46 Geophysics.* For space plasmas see *90 Astrophysics.*

76 SOLID-STATE PHYSICS **121**
Includes superconductivity. For related information see also *33 Electronics and Electrical Engineering* and *36 Lasers and Masers.*

77 THERMODYNAMICS AND STATISTICAL PHYSICS **129**
Includes quantum mechanics; theoretical physics; and Bose and Fermi statistics. For related information see also *25 Inorganic and Physical Chemistry* and *34 Fluid Mechanics and Heat Transfer.*

SOCIAL SCIENCES

80 SOCIAL SCIENCES (GENERAL) ..... **N.A.**
Includes educational matters.

81 ADMINISTRATION AND MANAGEMENT **130**
Includes management planning and research.

82 DOCUMENTATION AND INFORMATION SCIENCE **130**
Includes information management; information storage and retrieval technology; technical writing; graphic arts; and micrography. For computer documentation see *61 Computer Programming and Software.*

83 ECONOMICS AND COST ANALYSIS ..... **N.A.**
Includes cost effectiveness studies.

84 LAW, POLITICAL SCIENCE AND SPACE POLICY ..... **N.A.**
Includes NASA appropriation hearings; aviation law; space law and policy; international law; international cooperation; and patent policy.

85 URBAN TECHNOLOGY AND TRANSPORTATION **132**
Includes applications of space technology to urban problems; technology transfer; technology assessment; and surface and mass transportation. For related information see *03 Air Transportation and Safety, 16 Space Transportation,* and *44 Energy Production and Conversion.*

SPACE SCIENCES For related information see also *Geosciences.*

88 SPACE SCIENCES (GENERAL) ..... **N.A.**

89 ASTRONOMY **133**
Includes radio, gamma-ray, and infrared astronomy; and astrometry.

90 ASTROPHYSICS **133**
Includes cosmology; celestial mechanics; space plasmas; and interstellar and interplanetary gases and dust. For related information see also *75 Plasma Physics.*

91 LUNAR AND PLANETARY EXPLORATION **136**
Includes planetology; and manned and unmanned flights. For spacecraft design or space stations see *18 Spacecraft Design, Testing and Performance.*

92 SOLAR PHYSICS **178**
Includes solar activity, solar flares, solar radiation and sunspots. For related information see *93 Space Radiation.*

93 SPACE RADIATION **180**
Includes cosmic radiation; and inner and outer earth's radiation belts. For biological effects of radiation see *52 Aerospace Medicine.* For theory see *73 Nuclear and High-Energy Physics.*

GENERAL

Includes aeronautical, astronautical, and space science related histories, biographies, and pertinent reports too broad for categorization; histories or broad overviews of NASA programs.

99 GENERAL ..... **N.A.**

SUBJECT INDEX **I-1**

PERSONAL AUTHOR INDEX **I-63**

CORPORATE SOURCE INDEX **I-73**

CONTRACT NUMBER INDEX **I-83**

REPORT/ACCESSION NUMBER INDEX **I-85**

APPENDIX **A-1**

TYPICAL CITATION AND ABSTRACT

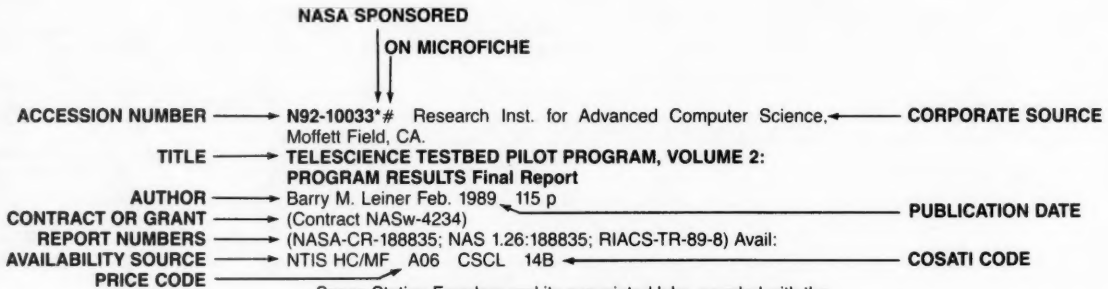

Space Station Freedom and its associated labs, coupled with the availability of new computing and communications technologies, have the potential for significantly enhancing scientific research. A Telescience Testbed Pilot Program (TTPP), aimed at developing the experience base to deal with issues in the design of the future information system of the Space Station era. The testbeds represented four scientific disciplines (astronomy and astrophysics, earth sciences, life sciences, and microgravity sciences) and studied issues in payload design, operation, and data analysis. This volume, of a 3 volume set, which all contain the results of the TTPP, contains the integrated results. Background is provided of the program and highlights of the program results. The various testbed experiments and the programmatic approach is summarized. The results are summarized on a discipline by discipline basis, highlighting the lessons learned for each discipline. Then the results are integrated across each discipline, summarizing the lessons learned overall.

Author

VOLUME 30 NUMBER 1 / JANUARY 8, 1992

Scientific and Technical Aerospace Reports

A Semimonthly Publication of the National Aeronautics and Space Administration

01 AERONAUTICS (GENERAL)

N92-10001* National Aeronautics and Space Administration, Washington, DC.
AERONAUTICAL ENGINEERING: A CONTINUING BIBLIOGRAPHY WITH INDEXES (SUPPLEMENT 267)
Jul. 1991 188 p
(NASA-SP-7037(267); NAS 1.21:7037(267)) Avail: NTIS HC A09; NTIS standing order as PB91-914100, $17.00 domestic, $34.00 foreign CSCL 01B

This bibliography lists 661 reports, articles, and other documents introduced into the NASA scientific and technical information system in June, 1991. Subject coverage includes design, construction and testing of aircraft and aircraft engines; aircraft components, equipment and systems; ground support systems; theoretical and applied aspects of aerodynamics and general fluid dynamics; electrical engineering; aircraft control; remote sensing; computer sciences; nuclear physics; and social sciences. Author

N92-10002*# National Aeronautics and Space Administration. Lewis Research Center, Cleveland, OH.
TECHNICAL EVALUATION REPORT, AGARD FLUID DYNAMICS PANEL SYMPOSIUM ON EFFECTS OF ADVERSE WEATHER ON AERODYNAMICS
J. J. Reinmann Oct. 1991 19 p Meeting held in Toulouse, France, 29 Apr. - 1 May 1991
(NASA-TM-105192; E-6460; NAS 1.15:105192) Avail: NTIS HC/MF A03 CSCL 01B

The purpose of the meeting on Effects of Adverse Weather on Aerodynamics was to provide an update of the stae-of-the-art with respect to the prediction, simulation, and measurement of the effects of icing, anti-icing fluids, and various precipitation on the aerodynamic characteristics of flight vehicles. Sessions were devoted to introductory and survey papers and icing certification issues, to analytical and experimental simulation of ice frost contamination and its effects of aerodynamics, and to the effects of heavy rain and deicing/anti-icing fluids. Author

N92-10003*# National Aeronautics and Space Administration. Ames Research Center, Moffett Field, CA.
PASSIVE RANGE ESTIMATION FOR ROTORCRAFT LOW-ALTITUDE FLIGHT
B. Sridhar, R. Suorsa, and B. Hussien Oct. 1991 37 p
(NASA-TM-103897; A-91242; NAS 1.15:103897) Avail: NTIS HC/MF A03 CSCL 01B

The automation of rotorcraft low-altitude flight presents challenging problems in control, computer vision and image understanding. A critical element in this problem is the ability to detect and locate obstacles, using on-board sensors, and modify the nominal trajectory. This requirement is also necessary for the safe landing of an autonomous lander on Mars. This paper examines some of the issues in the location of objects using a sequence of images from a passive sensor, and describes a Kalman filter approach to estimate the range to obstacles. The Kalman filter is also used to track features in the images leading to a significant reduction of search effort in the feature extraction step of the algorithm. The method can compute range for both straight line and curvilinear motion of the sensor. A laboratory experiment was designed to acquire a sequence of images along with sensor motion parameters under conditions similar to helicopter flight. Range estimation results using this imagery are presented. Author

02 AERODYNAMICS

Includes aerodynamics of bodies, combinations, wings, rotors, and control surfaces; and internal flow in ducts and turbomachinery.

For related information see also *34 Fluid Mechanics and Heat Transfer.*

N92-10004*# Eloret Corp., Sunnyvale, CA.
HYPERSONIC FLOWS AS RELATED TO THE NATIONAL AEROSPACE PLANE Semiannual Research Report, 1 Aug. 1990 - 28 Feb. 1991
Marvin Kussoy, Lionel Levy, and F. Menter 19 Mar. 1991 60 p (Contract NCC2-452)
(NASA-CR-187985; NAS 1.26:187985) Avail: NTIS HC/MF A04 CSCL 01A

Experimental data for a series of 2-D and 3-D shock wave/boundary layer interaction flows at Mach 8.2 are presented. The test bodies, composed of simple geometric shapes fastened to a flat plate test bed, were designed to generate flows with varying degrees of pressure gradient, boundary layer separation, and turning angle. The data include surface pressure and heat transfer distributions as well as limited mean flowfield surveys both in the undisturbed and interaction regimes. The data are presented in a convenient form to be used to validate existing or future computational models of these hypersonic flows. Author

N92-10005*# National Aeronautics and Space Administration. Langley Research Center, Hampton, VA.
MEASUREMENTS OF FORCES, MOMENTS, AND PRESSURES ON A GENERIC STORE SEPARATING FROM A BOX CAVITY AT SUPERSONIC SPEEDS
Robert L. Stallings, Jr. (Lockheed Engineering and Sciences Co., Hampton, VA.), Floyd J. Wilcox, Jr., and Dana K. Forrest Sep. 1991 186 p
(NASA-TP-3110; L-16866; NAS 1.60:3110) Avail: NTIS HC/MF A09 CSCL 01A

An experimental investigation was conducted to measure the forces, moments, and pressure distributions on the generic store separating from a rectangular box cavity contained in a flat plate surface at supersonic speeds. Pressure distributions inside the cavity and oil flow and vapor-screen photographs of the cavity flow field were also obtained. The measurements were obtained for the store separating from a flat plate surface, from two shallow cavities having length to depth ratios (L/h) of 16.778 and 12.073, and from a deep cavity having L/h = 6.730. Measurements for the shallow cavities were obtained both with and without rectangular doors attached to sides of the cavities. The tests were conducted at free stream Mach numbers of 1.69, 2.00 and 2.65 for a free stream Reynolds number per foot of 2 x 10(exp 6). Presented here are a discussion of the results, a complete tabulation of the pressure data, figures of both the pressure and force and moment data, and representative oil flow and vapor screen photographs. Author

N92-10006*# National Aeronautics and Space Administration. Langley Research Center, Hampton, VA.
MASS FLUX SIMILARITY FOR SLOTTED TRANSONIC-WIND-TUNNEL WALLS
Joel L. Everhart and Suresh H. Goradia Washington Aug. 1991 22 p
(NASA-TM-4281; L-16864; NAS 1.15:4281) Avail: NTIS HC/MF A03 CSCL 01A

A discussion of the flow field measurements obtained in the vertical plane at several stations along the centerline of slots in two different longitudinally slotted wind tunnel walls is presented. The longitudinal and transverse components of the data are then transformed using the concept of flow similarity to demonstrate the applicability of the technique to the development of the viscous shear flow along and through a slotted wall of an airfoil tunnel. Results are presented showing the performance of the similarity transformations with variations in tunnel station, Mach number, and airfoil induced curvature of the tunnel free stream. Author

N92-10007 North Carolina State Univ., Raleigh.
A COMPUTATIONAL AND EXPERIMENTAL INVESTIGATION OF A THREE-DIMENSIONAL HYPERSONIC SCRAMJET INLET FLOW FIELD Ph.D. Thesis
Scott Douglas Holland 1991 679 p
Avail: Univ. Microfilms Order No. DA9123361

Since careful design of primary engine parts such as the inlet is necessary to exploit effectively the potential of propulsion-airframe integration, a combined computational and experimental parametric study of the internal aerodynamics of a generic 3-D side wall compression scramjet inlet configuration was performed. The study was designed to show the utility of computational fluid dynamics as a design tool in hypersonic inlet fluid fields, to provide a detailed account of the nature and structure of the internal flow interactions, and to provide a comprehensive surface property and flow field data base to determine the effects of contraction ratio, cowl position, and Reynolds number on the performance of a hypersonic scramjet inlet configuration. The work proceeded in several phases: the initial inviscid assessment of the internal shock structure, the preliminary computational parametric study, the coupling of the optimized configuration with the physical limitations of the facility, the wind tunnel blockage assessment, and the computational and experimental parametric study of the final configuration. A total of 256 channels of pressure data, including static pressure orifices, pilot pressures, and entrance and exit flow rates, along with oil flow and infrared thermography provided a detailed experimental description of the flow. Author

N92-10008*# National Aeronautics and Space Administration. Langley Research Center, Hampton, VA.
REFLECTION TYPE SKIN FRICTION METER Patent Application
Promode R. Bandyopadhyay, inventor (to NASA) (AS&M, Inc., Hampton, VA.) and Leonard M. Weinstein, inventor (to NASA) 8 Aug. 1991 11 p
(NASA-Case-LAR-14520-1-SB; NAS 1.71:LAR-14520-1-SB; US-Patent-Appl-SN-743238) Avail: NTIS HC/MF A03 CSCL 01A

A housing block is provided having an upper surface conforming to the test surface of a model or aircraft. An oil film is supplied upstream of a transparent wedge window located in this upper surface by an oil pump system located external to the housing block. A light source located within the housing block supplies a light beam which passes through this transparent window and is reflected back through the transparent window by the upper surface of the oil film to a photo-sensitive position sensor located within the housing. This position sensor allows the slope history of the oil film caused by and aerodynamic flow to be determined. The skin friction is determined from this slope history. Internally located mirrors augment and sensitize the reflected beam as necessary before reaching the position sensor. In addition, a filter may be provided before this sensor to filter the beam. NASA

N92-10009# National Aerospace Lab., Tokyo (Japan).
NUMERICAL SIMULATION OF HYPERSONIC VISCOUS FLOW FOR THE DESIGN OF H-2 ORBITING PLANE (HOPE-2)
Yukimitsu Yamamoto and Toshio Akimoto Jan. 1991 78 p In JAPANESE; ENGLISH summary
(NAL-TR-1093; ISSN-0389-4010) Avail: NTIS HC/MF A05

An unmanned winged vehicle for space transportation, the H-II Orbiting Plane (HOPE), is being studied. Hypersonic computational fluid dynamics (CFD) analyses were performed on the proposed HOPE 63 model, with the effects of Reynolds number, Mach number, angles of attack, and yaw angles. In order to use CFD for more practical design purposes, analyses of control surfaces and the gas jet are also discussed. The objectives were to: (1) demonstrate the numerical code's validity for aerothermodynamic heating; (2) investigate the applicability of CFD to control problems; and (3) utilize CFD as the main design tool of the HOPE configuration, i.e., utilize it as a numerical wind tunnel. Numerical simulations were conducted using the flux split upwind Navier-Stokes code, and results showed excellent agreement with heat transfer distribution experiments, thereby demonstrating the present code's validity. Author

N92-10010# Oak Ridge National Lab., TN.
RECENT ADVANCES ON A FINITE ELEMENT ALGORITHM FOR COMPUTATIONAL AERODYNAMICS: TRANSONICS-HYPERSONICS
J. D. Freels, A. J. Baker, and G. S. Ianelli (Tennessee Univ., Knoxville.) 1991 7 p Presented at the 4th International Symposium on Computational Fluid Dynamics, Davis, CA, 9-12 Sep. 1991
(Contract DE-AC05-84OR-21400)
(DE91-018176; CONF-9109257-1) Avail: NTIS HC/MF A02

A weak statement forms the theoretical basis for identifying the range of choices/decisions for constructing approximate solutions to the compressible Navier-Stokes equations. The Galerkin form is intrinsically non-dissipative, and a Taylor series analysis identifies the extension needed for shock capturing. Thereafter, the approximation trial space is constructed with compact support using a spatial domain semi-discretization into finite elements. An implicit temporal algorithm produces the terminal algebraic form, which is iteratively solved using a tensor product factorization quasi-Newton procedure. Computational results verify algorithm performance for a range of aerodynamics specifications. DOE

N92-10011*# National Aeronautics and Space Administration. Ames Research Center, Moffett Field, CA.
TRANSONIC AND SUPERSONIC EULER COMPUTATIONS OF VORTEX-DOMINATED FLOW FIELDS ABOUT A GENERIC FIGHTER
Aga M. Goodsell and John E. Melton Nov. 1991 44 p
(NASA-TP-3156; A-90161; NAS 1.60:3156) Avail: NTIS HC/MF A03 CSCL 01A

Flow fields about a generic flighter model were computed using FL057, a 3-D, finite volume Euler code. Computed pressure coefficients, forces, and moments at several Mach numbers (0.6, 0.8, 1.2, 1.4, and 1.6) are compared with wind tunnel data over a wide range of angles of attack in order to determine the applicability of the code for the analysis of fighter configurations. Two configurations were studied, a wing-body and a wing-body-chine. FL057 predicted pressure distributions, forces, and moments well at low angles of attack, at which the flow was fully attached. The FL057 predictions were also accurate for some test conditions once the leading edge vortex became well established. At the subsonic speeds, FL057 predicted vortex breakdown earlier than that seen in the experimental results. Placing the chine on the forebody delayed the onset of bursting and improved the correlation between numerical and experimental data at the subsonic conditions. Author

N92-10012*# National Aeronautics and Space Administration. Lewis Research Center, Cleveland, OH.
THE STRUCTURE AND DEVELOPMENT OF STREAMWISE VORTEX ARRAYS EMBEDDED IN A TURBULENT BOUNDARY LAYER Ph.D. Thesis - Case Western Reserve Univ.
Bruce J. Wendt, Isaac Greber (Case Western Reserve Univ., Cleveland, OH.), and Warren R. Hingst Sep. 1991 319 p
(Grant NAG3-520)
(NASA-TM-105211; E-6523; NAS 1.15:105211) Avail: NTIS HC/MF A14 CSCL 01A

An investigation of the structure and development of streamwise vortices embedded in a turbulent boundary layer was conducted. The vortices were generated by a single spanwise row of rectangular vortex generator blades. A single embedded vortex was examined, as well as arrays of embedded counter rotating vortices produced by equally spaced vortex generators. Measurements of the secondary velocity field in the crossplane provided the basis for characterization of vortex structure. Vortex structure was characterized by four descriptors. The center of each vortex core was located at the spanwise and normal position of peak streamwise vorticity. Vortex concentration was characterized by the magnitude of the peak streamwise vorticity, and the vortex strength by its circulation. Measurements of the secondary velocity field were conducted at two crossplane locations to examine the streamwise development of the vortex arrays. Large initial spacings of the vortex generators produced pairs of strong vortices which tended to move away from the wall region while smaller spacings produced tight arrays of weak vortices close to the wall. A model of vortex interaction and development is constructed using the experimental results. The model is based on the structure of the Oseen Vortex. Vortex trajectories are modelled by including the convective effects of neighbors.
Author

N92-10013# Tulane Univ., New Orleans, LA. Dept. of Mathematics.
A GRID-FREE METHOD FOR HIGH REYNOLDS NUMBER FLOW AROUND AN IMMERSED ELASTIC STRUCTURE Final Report, Jun. 1988 - Dec. 1990
Lisa J. Fauci May 1991 25 p
(Grant AF-AFOSR-0295-89; AF Proj. 7755)
(AD-A239851; AL-TR-1991-0045) Avail: NTIS HC/MF A03 CSCL 20/4

This report is concerned with the computational modeling of problems in biological fluid mechanics. Typically, these problems involve the study of flow about highly flexible, moving boundaries; for instance, distensible vessels, moving heart walls, and valves. The fluid along with the boundary constitutes a coupled mechanical system in the sense that the motion of the boundary is determined by that of the fluid, but at the same time the boundary exerts force on the fluid and alters its motion. Finite difference schemes do not perform well in simulations of high Reynolds number flow because a restrictive number of grid points must be used to resolve boundary layers. In this report we present a grid-free numerical method which may be used to calculate flows around an immersed elastic structure. Numerical results are presented in 2 simple cases: flow past a circular cylinder and flow past a flat plate. The boundary motion is specified and is not time dependent. However, this algorithm can be used to simulate more complicated, time dependent problems in biological fluid mechanics. GRA

N92-10014# Naval Postgraduate School, Monterey, CA.
THE EFFECTS OF FOREBODY STRAKES ON ASYMMETRIC VORTICES ON A VERTICALLY LAUNCHED MISSILE M.S. Thesis
Chih-Chung Yuan Sep. 1990 173 p
(AD-A239948) Avail: NTIS HC/MF A08 CSCL 16/2

Wind tunnel tests were conducted on a vertically launched surface-to-air missile model to investigate the effects of forebody stakes on the side forces and yawing moments induced by nose-generated asymmetric vortices at high angles of attack. The effects of body configuration and a turbulent flowfield on the induced side forces and yawing moments were also examined. Test angles of attack ranged from 0 to 90 at Reynolds number of 150,000 based on the model diameter, and at a March number of 0.11. Three forebody configurations, two body configurations and two flowfield conditions were investigated. The flowfield with a turbulence length scale on the order of the vortex scale was found to have no significant influence on the induced side forces and yawing moments. The change of body configuration had no strong effects on the side forces and yawing moments either. The 4 STRAKES forebody demonstrated dramatic results in the yawing moment alleviation; the ranges of angle of attack in the induced side forces and yawing moments were also decreased by this modification. The 8 STRAKES forebody gave no significant improvement in the induced side force and yawing moment reduction. GRA

N92-10015# Naval Postgraduate School, Monterey, CA.
NUMERICAL INVESTIGATION OF THE EFFECT OF LEADING EDGE GEOMETRY ON DYNAMIC STALL OF AIRFOILS M.S. Thesis
Steven P. Grohsmeyer Sep. 1990 180 p
(AD-A239949) Avail: NTIS HC/MF A09 CSCL 01/3

The dynamic stall of rapidly pitching and oscillating airfoils is investigated by the numerical solution of the full compressible unsteady two-dimensional Navier-Stokes equations using an alternating-direction-implicit scheme. The flow is assumed to be fully turbulent, and the turbulent stresses are modelled by the Baldwin-Lomax eddy viscosity model. Three airfoils (NACA 0012, NACA 0012-33, and NACA 0012-63) are analyzed for the purpose of examining the influence of leading-edge geometry on unsteady flow separation. It is found that a larger leading edge radius, thicker contouring of the forward part of the airfoil, or increasing reduced frequency results in delaying flow separation and formation of the dynamic stall vortex to a higher angle of attack, yielding higher peak Cl. Within the scope of this study, the pressure gradient encountered by the flow at initial separation is found to be independent of reduced frequency and freestream speed. The critical pressure gradient is dependent on leading edge radius and increases for decreasing leading edge radius. GRA

N92-10016# Air Force Academy, CO.
DOWNWASH MEASUREMENTS ON A PITCHING CANARD-WING CONFIGURATION Final Report, 16 Jun. 1990 - 15 Sep. 1991
John E. Burkhalter 15 Sep. 1991 64 p
(AF Proj. 2307)
(AD-A239956; FJSRL-TR-91-0001) Avail: NTIS HC/MF A04 CSCL 01/1

Experimental wind tunnel tests were conducted using a splitter plate model of a two wing configuration oscillating through an unsteady pitch maneuver. Of primary interest were measurements of circulation lag on each wing and the downwash on the aft wing due to the forward wing. It was found that circulation lag associated with oscillating wings is independent of externally induced downwash flow fields but is dependent on the location of the pivot point for the wing or airfoil section, the starting and ending angle, and the angle of attack history. Downwash from a forward wing on an aft lifting surface can make a significant contribution to the lifting properties of the aft wing. The magnitude of these downwash forces are dependent on the forward wing normal force magnitudes and may enhance or degrade the potential of an aft wing to produce lift. The downwash induced in this case, however, is not synchronized with the circulation lag associated with the forward wing but the shift in the downwash curve is more or less synchronized with the circulation lag associated with the aft wing. Consequently a forward wing producing positive lift can produce upwash on an aft wing increasing its potential to produce lift. Enhancement of maneuverability for an aircraft can also be increased by placing the forward canard above the main wing lifting surface. GRA

03 AIR TRANSPORTATION AND SAFETY

Includes passenger and cargo air transport operations; and aircraft accidents.

For related information see also *16 Space Transportation* and *85 Urban Technology and Transportation.*

N92-10017*# National Aeronautics and Space Administration. Langley Research Center, Hampton, VA.
FEASIBILITY OF USING A KNOWLEDGE-BASED SYSTEM CONCEPT FOR IN-FLIGHT PRIMARY FLIGHT DISPLAY RESEARCH
Wendell R. Ricks Sep. 1991 19 p Previously announced as A91-19335
(NASA-TM-4279; L-16917; NAS 1.15:4279) Avail: NTIS HC/MF A03 CSCL 01C

A study was conducted to determine the feasibility of using knowledge-based systems architectures for inflight research of primary flight display information management issues. The feasibility relied on the ability to integrate knowledge-based systems with existing onboard aircraft systems. And, given the hardware and software platforms available, the feasibility also depended on the ability to use interpreted LISP software with the real time operation of the primary flight display. In addition to evaluating these feasibility issues, the study determined whether the software engineering advantages of knowledge-based systems found for this application in the earlier workstation study extended to the inflight research environment. To study these issues, two integrated knowledge-based systems were designed to control the primary flight display according to pre-existing specifications of an ongoing primary flight display information management research effort. These two systems were implemented to assess the feasibility and software engineering issues listed. Flight test results were successful in showing the feasibility of using knowledge-based systems inflight with actual aircraft data. Author

N92-10018# Loughborough Univ. of Technology (England). Dept. of Transport Technology.
A COMPARISON BETWEEN THE CONSEQUENCES OF THE LIBERAL AND NON-LIBERAL UK-EUROPE BILATERALS
Robert Caves and Christopher Higgins May 1991 36 p
(TT-9101; ISBN-0-904947-30-0; ETN-91-99891) Copyright Avail: NTIS HC/MF A03

The history of newly liberized routes between the UK (United Kingdom) and the continent of Europe is examined. Through this examination it is hoped that the value of competition for the consumer will be established and a basis for estimating the impacts of further European Economic Community (EEC) induced liberalization on traffic and route structures will be provided. ESA

N92-10019# Massachusetts Inst. of Tech., Lexington. Lincoln Lab.
THE 1990 AIRPORT SURVEILLANCE RADAR WIND SHEAR PROCESSOR (ASR-WSP) OPERATIONAL TEST AT ORLANDO INTERNATIONAL AIRPORT
T. A. Noyes, S. W. Troxel, M. E. Weber, O. J. Newell, and J. A. Cullen 17 Jul. 1991 68 p
(Contracts F19628-90-C-0002; DTFA-01-L-83-4-10579)
(AD-A239852; ATC-178; DOT/FAA/NR-91/1) Avail: NTIS HC/MF A04 CSCL 17/9

Lincoln Laboratory, under sponsorship from the Federal Aviation Administration (FAA), is conducting a program to evaluate the capability of the newest Airport Surveillance Radars (ASR-9) to detect hazardous weather phenomena--in particular, low-altitude wind shear created by thunderstorm-generated microbursts and gust fronts. The ASR-9 could provide coverage at airports not slated for a dedicated Terminal Doppler Weather Radar (TDWR) and could augment the TDWR at high-priority (high traffic volume, severe weather) facilities by providing a more rapid update of wind shear products, a better viewing angle for some runways, and redundancy in the event of a TDWR failure. An operational evaluation of a testbed ASR Wind Shear Processor (ASR-WSP) was conducted at the Orlando International Airport in Orlando, FL during August and September 1990. The ASR-WSP operational system issued five distinct products to Air Traffic Control: microburst detections, gust front detections, gust front movement predictions, precipitation reflectivity and storm motion. This document describes the operational system, the operational products, and the algorithms employed. An assessment of system performance is provided as one step in evaluating the operational utility of the ASR-WSP. Author (GRA)

04 AIRCRAFT COMMUNICATIONS AND NAVIGATION

Includes digital and voice communication with aircraft; air navigation systems (satellite and ground based); and air traffic control.

For related information see also *17 Space Communications, Spacecraft Communications, Command and Tracking* and *Communications and Radar.*

N92-10020# Federal Aviation Administration, Atlantic City, NJ.
SOLID-STATE RADAR BEACON DECODER (SSRBD) OPERATIONAL TEST AND EVALUATION (OT/E) INTEGRATION TEST PLAN
Thomas D. Bratton Oct. 1991 41 p
(DOT/FAA/CT-TN91/30) Avail: NTIS HC/MF A03

The Solid State Radar Beacon Decoder (SSRBD) operational and integration tests are defined that will be conducted at the FAA operational facilities. These tests will be executed following the contractor site acceptance test. Each SSRBD test configuration will be addressed in conjunction with the associated interfaces which will be required to perform the testing in as near an operational environment as possible. The National Airspace System (NAS) requirements and test objectives can be traced to those designated in the SSRBD Master Test Plan (MTP). In addition to providing requirements traceability, this plan contains a description of the tests which will be executed, associated success criteria, roles and responsibilities of test personnel, and the overall flow of activities required for a successful test program. Author

05 AIRCRAFT DESIGN, TESTING AND PERFORMANCE

Includes aircraft simulation technology.

For related information see also *18 Spacecraft Design, Testing and Performance* and *39 Structural Mechanics.* For land transportation vehicles see *85 Urban Technology and Transportation.*

N92-10021*# National Aeronautics and Space Administration. Langley Research Center, Hampton, VA.
ROTATABLE NON-CIRCULAR FOREBODY FLOW CONTROLLER Patent Application
Cary Moskovitz, inventor (to NASA) (North Carolina State Univ., Raleigh.) 10 Aug. 1990 16 p
(NASA-Case-LAR-14212-1-CU; NAS 1.71:LAR-14212-1-CU; US-Patent-Appl-SN-565090) Avail: NTIS HC/MF A03 CSCL 01C

The invention is a rotatable, non-circular forebody flow controller. The apparatus comprises a small geometric device located at a nose of a forebody of an aircraft or missile. The geometric device has a circular base that fits flush upon the remaining forebody of the aircraft and a non-circular cross-sectional area that extends toward the apex of the aircraft. The device is symmetrical about a reference plane and preferably attaches to a connecting means or axel which in turn attaches to a rotating means such as a motor. The motor rotates the device about and axis of rotation. Preferable, a control means connected to an aircraft flight control computer signals to the rotating means the proper rotational positioning of the geometric device. NASA

N92-10022# Naval Postgraduate School, Monterey, CA.
CH-53E/AV-8B AIRCRAFT SLING LOAD RECOVERY SYSTEM ANALYSIS M.S. Thesis
Rose M. Zammit Sep. 1990 142 p
(AD-A239950) Avail: NTIS HC/MF A07 CSCL 01/2

This report reviews some of the problems encountered in the analysis of the CH-53E/AV-8B Aircraft Recovery System. Equations are developed for use in determining optimum sling lengths and AV-8B attachment point locations that will allow for damage free pickup, transport and set down of an AV-8B aircraft by a CH-53E helicopter. Based on the formulation, a computer program is written that may be used to determine various features of the recovery system, such as, attachment point locations, hook, pendant, sling and AV-8B attachment point loads. The program, with slight modification, may be used to analyze any helicopter/external sling load combination. Furthermore, the effects of rotor downwash on hook, pendant, sling and AV-8B attachment point loads was evaluated both in a hover and in forward flight. Results from an analysis of two different configurations at the range of CH-53E airspeeds and longitudinal center of gravity positions are presented. GRA

N92-10023# Naval Air Development Center, Warminster, PA. Air Vehicle and Crew Systems Technology Dept.
PHYSIOLOGIC TRANSECTION OF THE BRAIN STEM IN HEALTHY HUMANS AND THE NEUROLOGIC BASIS OF UNCONSCIOUSNESS Final Report, Jan. 1988 - Feb. 1990
James E. Whinnery 10 Feb. 1990 20 p
(AD-A240122; NADC-91053-60) Avail: NTIS HC/MF A03 CSCL 01/3

Investigation of the kinetic relationships of the symptom complex associated with abrupt onset ischemic insult of the central nervous system (CNS) in over 700 completely healthy humans has revealed considerable insight into the neurologic substrates underlying conscious function, its loss, and its recovery. Acceleration +G sub z -induced CNS ischemia of a magnitude to alter conscious function (G-LOC) is associated with loss of vision, postural motor control, and memory along with induction of myoclonic convulsions, dreaming, and transient confusion/disorientation. It is evident that regional ischemic differences are established within the CNS and these neurologic alterations suggest that a reversible physiologic transection of the brain stem results from +G sub z -induced ischemia. GRA

06 AIRCRAFT INSTRUMENTATION

Includes cockpit and cabin display devices; and flight instruments.

For related information see also *19 Spacecraft Instrumentation* and *35 Instrumentation and Photography.*

N92-10024*# National Aeronautics and Space Administration. Langley Research Center, Hampton, VA.
A COMPENSATORY ALGORITHM FOR THE SLOW-DOWN EFFECT ON CONSTANT-TIME-SEPARATION APPROACHES
Terence S. Abbott Washington Sep. 1991 19 p
(NASA-TM-4285; L-16922; NAS 1.15:4285) Avail: NTIS HC/MF A03 CSCL 01D

In seeking methods to improve airport capacity, the question arose as to whether an electronic display could provide information which would enable the pilot to be responsible for self-separation under instrument conditions to allow for the practical implementation of reduced separation, multiple glide path approaches. A time based, closed loop algorithm was developed and simulator validated for in-trail (one aircraft behind the other) approach and landing. The algorithm was designed to reduce the effects of approach speed reduction prior to landing for the trailing aircraft as well as the dispersion of the interarrival times. The operational task for the validation was an instrument approach to landing while following a single lead aircraft on the same approach path. The desired landing separation was 60 seconds for these approaches. An open loop algorithm, previously developed, was used as a basis for comparison. The results showed that relative to the open loop algorithm, the closed loop one could theoretically provide for a 6 pct. increase in runway throughput. Also, the use of the closed loop algorithm did not affect the path tracking performance and pilot comments indicated that the guidance from the closed loop algorithm would be acceptable from an operational standpoint. From these results, it is concluded that by using a time based, closed loop spacing algorithm, precise interarrival time intervals may be achievable with operationally acceptable pilot workload. Author

07 AIRCRAFT PROPULSION AND POWER

Includes prime propulsion systems and systems components, e.g., gas turbine engines and compressors; and onboard auxilliary power plants for aircraft.

For related information see also *20 Spacecraft Propulsion and Power, 28 Propellants and Fuels,* and *44 Energy Production and Conversion.*

N92-10025# National Aerospace Lab., Tokyo (Japan).
TEST APPARATUS AND TENSILE PROPERTIES OF LE-7 TURBINE BLADE MATERIALS IN HIGH PRESSURE HYDROGEN CONDITIONS
Makoto Yoshida, Yoshiaki Watanabe, Yoshimasa Tajima, and Kenjiro Kamijo (National Aerospace Lab., Kakuda, Japan) Jan. 1991 21 p In JAPANESE; ENGLISH summary
(NAL-TR-1092; ISSN-0389-4010) Avail: NTIS HC/MF A03

A launch vehicle, the H-II, was developed. This vehicle uses a large liquid oxygen (LOX) liquid hydrogen (LH2) engine, the LE-7. The turbine blades of LE-7 LOX/LH2 turbopumps are subjected to great thermal stress due to the temperature changes during the start sequence which increases from approx. the LOX temperature to greater than the hydrogen rich combustion gas temperature (900 K) within a few seconds, with the turbine blades being exposed to drafts of cold hydrogen gas during the preburner cutoff. At steady state operation, the LOX turbopump is driven by high pressure, hydrogen rich, hot combustion gas, thus the turbine blades must be strong enough to withstand not only thermal stress but also high pressure hydrogen embrittlement. Much research has focussed on industrial application hydrogen embrittlement effects, however, rocket turbopump hydrogen embrittlement must be studied in more detail. This led to the construction of a hydrogen embrittlement test facility to perform fatigue and tensile tests of blade materials in high pressure hydrogen at high temperatures, thereby actually simulating actual turbine driving conditions. Both Inconel 718 and MAR-M247 LC DS were tested using this facility, with the former being used as a disk material for the integrally machined blades of research, prototype, and flight models, whereas the latter is being used for prototype/flight model turbopump turbine blades. Author

N92-10026# Astron Research and Engineering, Sunnyvale, CA.
GAS TURBINE COMBUSTER EXIT TEMPERATURE MEASUREMENT Final Report, 13 Jan. 1987 - 31 May 1989
John D. Sullivan and John E. Kendall Aug. 1991 111 p
(Contract F40600-87-C-0002)
(AD-A239936; AEDC-TR-91-11) Avail: NTIS HC/MF A06 CSCL 21/5

A new gas temperature measurement technique is presented that has the capability to eliminate radiation errors typically observed in high-temperature environments. The technique should allow high measurement accuracy and high spatial resolution and can be implemented in rugged probe designs capable of surviving in a gas turbine combustor exit environment. The theoretical operation of the probe is described, and sources of measurement uncertainty are investigated. Probes fabricated for demonstration purposes are capable of surviving prolonged operation at temperatures up to 3000 F. Tests were run in two facilities, the Astron High-Temperature Furnace and the NASA Lewis Combustor Rig, and results are presented in this report. The test results are

favorable; however, further analysis should be performed and the method of qualifying probe accuracy should be defined. Currently the probe does not operate satisfactorily in a real-time mode, but algorithms developed for posttest data reduction should be suitable for implementation in a microprocessor-based controller allowing real-time operation. GRA

08 AIRCRAFT STABILITY AND CONTROL

Includes aircraft handling qualities; piloting; flight controls; and autopilots.

For related information see also *05 Aircraft Design, Testing and Performance.*

N92-10027*# National Aeronautics and Space Administration. Langley Research Center, Hampton, VA.
ON THE FORMULATION OF A MINIMAL UNCERTAINTY MODEL FOR ROBUST CONTROL WITH STRUCTURED UNCERTAINTY
Christine M. Belcastro, B.-C. Chang, and Robert Fischl (Drexel Univ., Philadelphia, PA.) Sep. 1991 34 p
(NASA-TP-3094; L-16893; NAS 1.60:3094) Avail: NTIS HC/MF A03 CSCL 01C

In the design and analysis of robust control systems for uncertain plants, representing the system transfer matrix in the form of what has come to be termed an M-delta model has become widely accepted and applied in the robust control literature. The M represents a transfer function matrix M(s) of the nominal closed loop system, and the delta represents an uncertainty matrix acting on M(s). The nominal closed loop system M(s) results from closing the feedback control system, K(s), around a nominal plant interconnection structure P(s). The uncertainty can arise from various sources, such as structured uncertainty from parameter variations or multiple unsaturated uncertainties from unmodeled dynamics and other neglected phenomena. In general, delta is a block diagonal matrix, but for real parameter variations delta is a diagonal matrix of real elements. Conceptually, the M-delta structure can always be formed for any linear interconnection of inputs, outputs, transfer functions, parameter variations, and perturbations. However, very little of the currently available literature addresses computational methods for obtaining this structure, and none of this literature addresses a general methodology for obtaining a minimal M-delta model for a wide class of uncertainty, where the term minimal refers to the dimension of the delta matrix. Since having a minimally dimensioned delta matrix would improve the efficiency of structured singular value (or multivariable stability margin) computations, a method of obtaining a minimal M-delta would be useful. Hence, a method of obtaining the interconnection system P(s) is required. A generalized procedure for obtaining a minimal P-delta structure for systems with real parameter variations is presented. Using this model, the minimal M-delta model can then be easily obtained by closing the feedback loop. The procedure involves representing the system in a cascade-form state-space realization, determining the minimal uncertainty matrix, delta, and constructing the state-space representation of P(s). Three examples are presented to illustrate the procedure.

Author

N92-10028# National Aerospace Lab., Tokyo (Japan).
DEVELOPMENT OF DIGITAL/OPTICAL ROTARY POSITION TRANSDUCER
Mitsuyoshi Mayanagi, Minoru Takizawa, and Tadao Uchida May 1991 24 p In JAPANESE; ENGLISH summary
(NAL-TR-1106; ISSN-0389-4010) Avail: NTIS HC/MF A03

Two different types of digital optical rotary position transducers were developed for use in future aircraft Fly-By-Light (FBL) control systems, i.e., one uses a collimated light on a code plate and the other a focussed light. These transducers can be used for sensing the pilot's control stick positions and/or control surface deflection in FBL control systems. The transducer system consists of two different transducers, four fiber cables, and an electronic interface unit having two light sources. This transducer system features the following: (1) resistance against electromagnetic interference and antilightning are obtained by an electrically passive transducer which uses no electronic parts; (2) connection between hardware is simplified by the use of serial digital optical signals obtained through optical pulses, optical fiber delay lines, an optical coupler, and the use of a time domain multiplexing concept; (3) system extendability is attained by using a time sharing processing system in which multiple optical encoders can be handled by a single processing circuit; and (4) optical power energy is reduced by utilizing optical pulses. These transducers cover a displacement of 360 deg. with a digital resolution of 12 bits (0.09 deg.).

Author

09 RESEARCH AND SUPPORT FACILITIES (AIR)

Includes airports, hangars and runways; aircraft repair and overhaul facilities; wind tunnels; shock tubes; and aircraft engine test stands.

For related information see also *14 Ground Support Systems and Facilities (Space).*

N92-10464# Jyvaskyla Univ. (Finland). Dept. of Physics.
THERMAL HELIUM DESORPTION FACILITY IN JYVASKYLA (FINLAND) Abstract Only
E. Kautto, O.-P. Kaehkoenen, S. Maekinen, and M. Manninen *In* Oulu Univ., Proceedings of the 25th Annual Conference of the Finnish Physical Society 1991 1 p (For primary document see N92-10362 01-70)
Avail: NTIS HC/MF A12

12 ASTRONAUTICS (GENERAL)

For extraterrestrial exploration see *91 Lunar and Planetary Exploration.*

N92-10029# Norwegian Space Center, Oslo.
[ACTIVITIES REPORT OF THE NORWEGIAN SPACE CENTER] Annual Report, 1990
1990 17 p
(ETN-91-90052) Avail: NTIS HC/MF A03

The activities of the Norwegian Space Center during 1990 are presented. The management and organization of the Space Center is introduced, key figures from annual accounts are presented, and a report by the board of directors or the 1990 activities, the Tromso satellite station and future space plans is given. The contracts obtained by Norwegian companies active in space are considered. Reflections on the work of the Norwegian Space Center and Norwegian companies in telecommunications, connected to the Columbus Free Flying Laboratory, space transport, Earth observation and Space research are given. The activities of Andoya Rocket range, one of Norway's high technology companies are considered, as are the Earth observation activities of the Tromso (Norway) satellite stations. ESA

N92-10548# Helsinki Univ. of Technology, Espoo (Finland). Astrophysics Lab.
FINNISH SPACE PROJECTS: PLANETARY STUDIES Abstract Only
Kari Lumme *In* Oulu Univ., Proceedings of the 25th Annual Conference of the Finnish Physical Society 1991 1 p (For primary document see N92-10362 01-70)
Avail: NTIS HC/MF A12

13 ASTRODYNAMICS

Includes powered and free-flight trajectories; and orbital and launching dynamics.

N92-10030# Aerospace Corp., El Segundo, CA. Lab. Operations.
A NEURAL NETWORK MODEL OF THE RELATIVISTIC ELECTRON FLUX AT GEOSYNCHRONOUS ORBIT
Harry C. Koons and David J. Gorney 10 Apr. 1991 33 p
(Contract F40701-88-C-0089)
(AD-A239827; TR-0090(5940-06)-5; SSD-TR-91-14) Avail: NTIS HC/MF A03 CSCL 20/7

A neural network has been developed to model the temporal variations of relativistic (greater than 3 MeV) electrons at geosynchronous orbit based on model inputs consisting of ten consecutive days of the daily sum of the planetary magnetic index Sigma Kp. The neural network (in essence, a nonlinear prediction filter) consists of three layers of neurons, containing 10 neurons in the input layer, 6 neurons in a hidden layer, and 1 output neuron. The output is a prediction of the daily-averaged electron flux for the tenth day. The neural network was trained using 62 days of data from 1 July 1984 through 31 August 1984 from the SEE spectrometer on the geosynchronous spacecraft 1982-019. The performance of the model was measured by comparing model outputs with measured fluxes over a 6-year period from 19 April 1982 to 4 June 1988. For the entire data set the RMS logarithmic error of the neural network is 0.76 and the average logarithmic error is 0.58. The neural network is essentially zero-biased, and for accumulation intervals of three days or longer the average logarithmic errors is less than 0.1. The neural network provides results that are significantly more accurate than those from linear prediction filters. The model has been used to simulate conditions that are rarely observed in nature, such as long periods of quiet (Sigma Kp = 0) and ideal impulses. It has also been used to make reasonably accurate day-ahead forecasts of the relativistic electron flux at geosynchronous orbit. GRA

14 GROUND SUPPORT SYSTEMS AND FACILITIES (SPACE)

Includes launch complexes, research and production facilities; ground support equipment, e.g., mobile transporters; and simulators.

For related information see also *09 Research and Support Facilities (Air).*

N92-10031*# Research Inst. for Advanced Computer Science, Moffett Field, CA.
TELESCIENCE TESTBED PILOT PROGRAM, VOLUME 1: EXECUTIVE SUMMARY Final Report
Barry M. Leiner Feb. 1989 45 p
(Contract NASw-4234)
(NASA-CR-188833; NAS 1.26:188833; RIACS-TR-89-7) Avail: NTIS HC/MF A03 CSCL 14B

Space Station Freedom and its associated labs, coupled with the availability of new computing and communications technologies, have the potential for significantly enhancing scientific research. A Telescience Testbed Pilot Program (TTPP), aimed at developing the experience base to deal with issues in the design of the future information system of the Space Station era. The testbeds represented four scientific disciplines (astronomy and astrophysics, earth sciences, life sciences, and microgravity sciences) and studied issues in payload design, operation, and data analysis. This volume, of a 3 volume set, which all contain the results of the TTPP, is the executive summary. Author

N92-10032*# Research Inst. for Advanced Computer Science, Moffett Field, CA.
TELESCIENCE TESTBED PILOT PROGRAM, VOLUME 3: EXPERIMENT SUMMARIES Final Report
Barry M. Leiner Feb. 1989 142 p
(Contract NASw-4234)
(NASA-CR-188834; NAS 1.26:188834; RIACS-TR-89-9) Avail: NTIS HC/MF A07 CSCL 14B

Space Station Freedom and its associated labs, coupled with the availability of new computing and communications technologies, have the potential for significantly enhancing scientific research. A Telescience Testbed Pilot Program (TTPP), aimed at developing the experience base to deal with issues in the design of the future information system of the Space Station era. The testbeds represented four scientific disciplines (astronomy and astrophysics, earth science, life sciences, and microgravity sciences) and studied issues in payload design, operation, and data analysis. This volume, of a 3 volume set, which all contain the results of the TTPP, presents summaries of the experiments. This experiment involves the evaluation of the current Internet for the use of file and image transfer between SIRTF instrument teams. The main issue addressed was current network response times. Author

N92-10033*# Research Inst. for Advanced Computer Science, Moffett Field, CA.
TELESCIENCE TESTBED PILOT PROGRAM, VOLUME 2: PROGRAM RESULTS Final Report
Barry M. Leiner Feb. 1989 115 p
(Contract NASw-4234)
(NASA-CR-188835; NAS 1.26:188835; RIACS-TR-89-8) Avail: NTIS HC/MF A06 CSCL 14B

Space Station Freedom and its associated labs, coupled with the availability of new computing and communications technologies, have the potential for significantly enhancing scientific research. A Telescience Testbed Pilot Program (TTPP), aimed at developing the experience base to deal with issues in the design of the future information system of the Space Station era. The testbeds represented four scientific disciplines (astronomy and astrophysics, earth sciences, life sciences, and microgravity sciences) and studied issues in payload design, operation, and data analysis. This volume, of a 3 volume set, which all contain the results of the TTPP, contains the integrated results. Background is provided of the program and highlights of the program results. The various testbed experiments and the programmatic approach is summarized. The results are summarized on a discipline by discipline basis, highlighting the lessons learned for each discipline. Then the results are integrated across each discipline, summarizing the lessons learned overall. Author

N92-10034*# Research Inst. for Advanced Computer Science, Moffett Field, CA.
A SYSTEM PERFORMANCE THROUGHPUT MODEL APPLICABLE TO ADVANCED MANNED TELESCIENCE SYSTEMS
Richard F. Haines 1 Jan. 1990 23 p Presented at the HCI International '89 Meeting, Boston MA, 18-22 Sep. 1988 Sponsored in part by USRA
(Contract NCC2-387)
(NASA-CR-188860; NAS 1.26:188860; RIACS-TR-90-1) Avail: NTIS HC/MF A03 CSCL 14B

As automated space systems become more complex, autonomous, and opaque to the flight crew, it becomes increasingly difficult to determine whether the total system is performing as it should. Some of the complex and interrelated human performance measurement issues are addressed that are related to total system validation. An evaluative throughput model is presented which can be used to generate a human operator-related benchmark or figure of merit for a given system which involves humans at the input and output ends as well as other automated intelligent agents. The concept of sustained and accurate command/control data information transfer is introduced. The first two input parameters of the model involve nominal and off-nominal predicted events. The first of these calls for a detailed task analysis while the second is for a contingency event assessment. The last two required input parameters involving actual (measured) events, namely human performance and continuous semi-automated system performance. An expression combining these four parameters was

found using digital simulations and identical, representative, random data to yield the smallest variance. Author

15 LAUNCH VEHICLES AND SPACE VEHICLES

Includes boosters; operating problems of launch/space vehicle systems; and reusable vehicles.

For related information see also *20 Spacecraft Propulsion and Power.*

No abstracts in this category.

16 SPACE TRANSPORTATION

Includes passenger and cargo space transportation, e.g., shuttle operations; and space rescue techniques.

For related information see also *03 Air Transportation and Safety* and *18 Spacecraft Design, Testing and Performance.* For space suits see *54 Man/System Technology and Life Support.*

N92-10035*# National Aeronautics and Space Administration. Langley Research Center, Hampton, VA.

SHUTTLE ORBITER WITH TELESCOPING MAIN PROPULSION UNIT AND PAYLOAD Patent Application

Ian O. MacConochie, inventor (to NASA) 7 Aug. 1991 12 p
(NASA-Case-LAR-13586-1; NAS 1.71:LAR-13586-1; US-Patent-Appl-SN-743469) Avail: NTIS HC/MF A03 CSCL 22B

An improved Space Shuttle with variable internal volume is provided. The Space Shuttle Orbiter includes a telescoping main propulsion unit. This main propulsion unit contains the main rocket engines and fuel tanks and telescopes into the Space Shuttle. A variable cavity is located between this unit and the crew compartment. Accordingly, the positioning of the telescoping main propulsion unit determines the volume of the variable cavity. Thus, the volume of the variable length of the entire Space Shuttle may be increased or decreased to achieve desired configurations for optimal storage. In one embodiment of the invention, the payload also telescopes within the variable cavity. NASA

17 SPACE COMM., SPACECRAFT COMM., COMMAND & TRACKING

Includes telemetry; space communications networks; astronavigation and guidance; and radio blackout.

For related information see also *04 Aircraft Communications and Navigation* and *32 Communications and Radar.*

N92-10036*# National Aeronautics and Space Administration. Lyndon B. Johnson Space Center, Houston, TX.

MANAGEMENT OF THE SPACE STATION FREEDOM ONBOARD LOCAL AREA NETWORK

Frank W. Miller and Randy C. Mitchell (Mitre Corp., Houston, TX.) Nov. 1991 18 p
(NASA-TM-104741; S-649; NAS 1.15:104741) Avail: NTIS HC/MF A03 CSCL 09F

An operational approach is proposed to managing the Data Management System Local Area Network (LAN) on Space Station Freedom. An overview of the onboard LAN elements is presented first, followed by a proposal of the operational guidelines by which management of the onboard network may be effected. To implement the guidelines, a recommendation is then presented on a set of network management parameters which should be made available in the onboard Network Operating System Computer Software Configuration Item and Fiber Distributed Data Interface firmware. Finally, some implications for the implementation of the various network management elements are discussed. Author

18 SPACECRAFT DESIGN, TESTING AND PERFORMANCE

Includes satellites; space platforms; space stations; spacecraft systems and components such as thermal and environmental controls; and attitude controls.

For life support systems see *54 Man/System Technology and Life Support.* For related information see also *05 Aircraft Design, Testing and Performance, 39 Structural Mechanics,* and *16 Space Transportation.*

N92-10037*# Dayton Univ., OH. Dept. of Engineering Management and Systems.

THE DETERMINATION OF OPERATIONAL AND SUPPORT REQUIREMENTS AND COSTS DURING THE CONCEPTUAL DESIGN OF SPACE SYSTEMS

Charles Ebeling 8 Oct. 1991 111 p
(Grant NAG1-1327)
(NASA-CR-188817; NAS 1.26:188817) Avail: NTIS HC/MF A06 CSCL 22B

The primary objective is to develop a methodology for predicting operational and support parameters and costs of proposed space systems. The first phase consists of: (1) the identification of data sources; (2) the development of a methodology for determining system reliability and maintainability parameters; (3) the implementation of the methodology through the use of prototypes; and (4) support in the development of an integrated computer model. The phase 1 results are documented and a direction is identified to proceed to accomplish the overall objective. Author

N92-10038*# Research Inst. for Advanced Computer Science, Moffett Field, CA.

MODELING OF THE SPACE STATION FREEDOM DATA MANAGEMENT SYSTEM

Marjory J. Johnson Aug. 1990 31 p Submitted for publication
(Contract NCC2-387)
(NASA-CR-188869; NAS 1.26:188869; RIACS-TR-90-32) Avail: NTIS HC/MF A03 CSCL 22B

The Data Management System (DMS) is the information and communications system onboard Space Station Freedom (SSF). Extensive modeling of the DMS is being conducted throughout NASA to aid in the design and development of this vital system. Activities discussed at NASA Ames Research Center to model the DMS network infrastructure are discussed with focus on the modeling of the Fiber Distributed Data Interface (FDDI) token-ring protocol and experimental testbedding of networking aspects of the DMS. Author

N92-10039# European Space Agency, Paris (France). Directorate for the Observation of the Earth and its Environment.

THE DATA BOOK OF ERS-1: THE EUROPEAN REMOTE SENSING SATELLITE

Norman Longdon, ed. Apr. 1991 41 p Original contains color illustrations
(ESA-BR-75; ISBN-92-9092-079-3; ISSN-0250-1589; ETN-91-90073) Copyright Avail: NTIS HC/MF A03; ESA, EPD, Noordwijk, Netherlands, HC 20 Dutch guilders

A summary of technical elements of the ERS-1 spacecraft and its payload is given. The following are considered: programmatics (overall schedule, assembly, integration, and verification, preparation for the receipt and use of ERS-1 data, launch and early orbit phase, deployment method, special technologies and test equipment); the spacecraft subsystems (structure, power supply, pyrotechnics, attitude and orbital control, thermal control, on board data handling and telemetry); scientific instruments (Active Microwave Instruments (AMI), Radar Altimeter (RA)26, Along Track Scanning Radiometer and Microwave sounder (ATSR-M), the Laser

Retro Reflector (LRR) Precise Range and Range-rate Equipment (PRAFE). ESA

N92-10040# Sandia National Labs., Albuquerque, NM.
AN ASSESSMENT OF THE RADIATION TOLERANCE OF LARGE SATELLITE MEMORIES IN LOW EARTH ORBITS
J. S. Browning, J. W. Griffee, D. B. Holtkamp, and W. C. Priedhorsky (Los Alamos National Lab., NM.) 1991 10 p Presented at the RADECS 91: Radiation Effects on Components and Systems, Montpellier, France, 9-12 Sep. 1991
(Contract DE-AC04-76DP-00789)
(DE91-018353; SAND-89-0167C; CONF-9109232-2) Avail: NTIS HC/MF A02

A procedure is described that assures the reliable operation in space radiation environments of memory systems that are approximately ten times larger and can be built at about one tenth of the cost of recent, comparable satellite projects. The procedure accounts for combined radiation effects, permitting the radiation tolerance of the memory system to be accurately estimated. Using the procedure a 1-gigabit memory with error detection and correction capability has been designed for miniature satellite applications. The memory system is constructed entirely out of commercial grade microelectronics. DOE

N92-10041# Naval Postgraduate School, Monterey, CA.
DESIGN RESTRICTIONS AND LICENSING FOR PETITE AMATEUR NAVY SATELLITE (PANSAT) M.S. Thesis
Robert R. Rowsey Sep. 1990 157 p
(AD-A239951) Avail: NTIS HC/MF A08 CSCL 22/2

The small, inexpensive Petite Amateur Navy SATellite (PANSAT) is the Naval Postgraduate School (NPS) Space Systems Academic Group's first experience with real-time space operations. Propelled by the success of PANSAT, NPS will follow this project with more complex space systems such as ORION. This thesis discusses the general and specific design considerations and constraints encountered during the design of PANSAT, along with providing descriptions of the satellite's various subsystems. The study also addresses the problems and procedures associated with obtaining a license frequency assignment for PANSAT. Three viable licensing options, an amateur, a military and an experimental option are presented. The thesis also includes a detailed description of the national and international frequency regulatory agencies, for better understanding of the licensing procedures. GRA

19 SPACECRAFT INSTRUMENTATION

For related information see also *06 Aircraft Instrumentation* and *35 Instrumentation and Photography.*

N92-10563# Helsinki Univ. of Technology, Espoo (Finland). Astrophysics Lab.
THE MEASURING MODES AND OBSERVATIONS WITH THE X-RAY SPECTROMETER ARRAY SIXA ONBOARD SPECTRUM-X-GAMMA Abstract Only
J. Huovelin, H. Paeivike, O. Vilhu, and V. Kaemaeraeinen (Outokumpu Oy, Tapiola, Finland) *In* Oulu Univ., Proceedings of the 25th Annual Conference of the Finnish Physical Society 1991 1 p (For primary document see N92-10362 01-70)
Avail: NTIS HC/MF A12

N92-10565# Oulu Univ. (Finland). Dept. of Physics.
CAPS-PLASMA SPECTROMETER FOR THE CASSINI SPACECRAFT Abstract Only
P. Tanskanen, K. Mursula, V. Kelha, and H. Huomo (Technical Research Centre of Finland, Espoo.) *In its* Proceedings of the 25th Annual Conference of the Finnish Physical Society 1991 1 p (For primary document see N92-10362 01-70)
Avail: NTIS HC/MF A12

20 SPACECRAFT PROPULSION AND POWER

Includes main propulsion systems and components, e.g., rocket engines; and spacecraft auxilliary power sources.

For related information see also *07 Aircraft Propulsion and Power, 28 Propellants and Fuels, 44 Energy Production and Conversion,* and *15 Launch Vehicles and Space Vehicles.*

N92-10042*# Alabama Univ., Huntsville.
PC PROGRAMS FOR THE PREDICTION OF THE LINEAR STABILITY BEHAVIOR OF LIQUID PROPELLANT PROPULSION SYSTEMS AND APPLICATION TO CURRENT MSFC ROCKET ENGINE TEST PROGRAMS, VOLUME 1 Final Report
George B. Doane, III and W. C. Armstrong Jun. 1990 171 p
(Contract NAS8-36955)
(NASA-CR-184228; NAS 1.26:184228; Rept-5-32176-Vol-1)
Avail: NTIS HC/MF A08 CSCL 21H

Research on propulsion stability (chugging and acoustic modes), and propellant valve control was investigated. As part of the activation of the new liquid propulsion test facilities, it is necessary to analyze total propulsion system stability. To accomplish this, several codes were built to run on desktop 386 machines. These codes enable one to analyze the stability question associated with the propellant feed systems. In addition, further work was adapted to this computing environment and furnished along with other codes. This latter inclusion furnishes those interested in high frequency oscillatory combustion behavior (that does not couple to the feed system) a set of codes for study of proposed liquid rocket engines. Author

N92-10043*# National Academy of Sciences - National Research Council, Washington, DC. Commission on Engineering and Technical Systems.
THE SPACE SHUTTLE ADVANCED SOLID ROCKET MOTOR: QUALITY CONTROL AND TESTING
1991 65 p
(Contract NASw-4003)
(NASA-CR-188800; NAS 1.26:188800) Avail: NTIS HC/MF A04 CSCL 21H

The Congressional committees that authorize the activities of NASA requested that the National Research Council (NRC) review the testing and quality assurance programs for the Advanced Solid Rocket Motor (ASRM) program. The proposed ASRM design incorporates numerous features that are significant departures from the Redesigned Solid Rocket Motor (RSRM). The NRC review concentrated mainly on these features. Primary among these are the steel case material, welding rather than pinning of case factory joints, a bolted field joint designed to close upon firing the rocket, continuous mixing and casting of the solid propellant in place of the current batch processes, use of asbestos-free insulation, and a lightweight nozzle. The committee's assessment of these and other features of the ASRM are presented in terms of their potential impact on flight safety. Author

N92-10044*# National Aeronautics and Space Administration. Lewis Research Center, Cleveland, OH.
MAGNETOPLASMADYNAMIC THRUSTER WORKSHOP
1991 178 p Workshop held in Washington, DC, 16 May 1991; sponsored in part by NASA, Washington
(NASA-CP-10084; E-6518; NAS 1.55:10084) Avail: NTIS HC/MF A09 CSCL 21H

On May 16, 1991, the NASA Headquarters Propulsion, Power, and Energy Division and the NASA Lewis Research Center Low Thrust Propulsion Branch hosted a workshop attended by key experts in magnetoplasmadynamic (MPD) thrusters and associated sciences. The scope was limited to high power MPD thrusters suitable for major NASA space exploration missions, and its purpose was to initiate the process of increasing the expectations and prospects for MPD research, primarily by increasing the level

of cooperation, interaction, and communication between parties within the MPD community. For individual titles, see N92-10045 through N92-10053.

N92-10045*# Sverdrup Technology, Inc., Cleveland, OH.
NEP MISSION SENSITIVITIES
James H. Gilland *In* NASA. Lewis Research Center, Magnetoplasmadynamic Thruster Workshop 1991 12 p (For primary document see N92-10044 01-20)
Avail: NTIS HC/MF A09 CSCL 21H

The Nuclear Electric Power (NEP) Mission requirements and evolution are presented. Application of NEP to the following areas is addressed: a lunar cargo mission, a Mars cargo mission, and a piloted Mars mission. Author

N92-10046*# Jet Propulsion Lab., California Inst. of Tech., Pasadena.
THE MPD THRUSTER PROGRAM AT JPL
John Barnett, Keith Goodfellow, James Polk, and Thomas Pivirotto *In* NASA. Lewis Research Center, Magnetoplasmadynamic Thruster Workshop 1991 12 p (For primary document see N92-10044 01-20)
Avail: NTIS HC/MF A09 CSCL 21H

The main topics covered include: (1) the Space Exploration Initiative (SEI) context; (2) critical issues of MPD Thruster design; and (3) the Magnetoplasmadynamic (MPD) Thruster Program at JPL. Under the section on the SEI context the nuclear electric propulsion system and some electric thruster options are addressed. The critical issues of MPD Thruster development deal with the requirements, status, and approach taken. The following areas are covered with respect to the MPD Thruster Program at JPL: (1) the radiation-cooled MPD thruster; (2) the High-Current Cathode Test Facility; (3) thruster component thermal modeling; and (4) alkali metal propellant studies. Author

N92-10047*# Lawrence Livermore National Lab., CA.
LLNL CONTRIBUTIONS TO MPD THRUSTERS FOR SEI
Edwin Bickford Hooper *In* NASA. Lewis Research Center, Magnetoplasmadynamic Thruster Workshop 1991 16 p (For primary document see N92-10044 01-20)
Avail: NTIS HC/MF A09 CSCL 21H

Some of the topics covered with respect to the Lawrence Livermore National Laboratory's (LLNL's) contributions to Magnetoplasmadynamic (MPD) Thrusters for the Space Exploration Initiative (SEI) include: an IR camera, plasma-induced erosion/redeposition, the Mirror Fusion Test Facility-B (MFTF-B), the Thruster Lifetime Test Facility, the RACE Compact Torus Accelerator Facility, and a RACE program summary. Some of the other topics addressed include: flux contours for HAM simulation, comparison of RACE data of plasma ring formation with the HAM 2-D magnetohydrodynamic code, and the 2-D Ring Acceleration Code (TRAC). Author

N92-10048*# Sverdrup Technology, Inc., Cleveland, OH.
MPD THRUSTER TECHNOLOGY
Roger M. Myers *In* NASA. Lewis Research Center, Magnetoplasmadynamic Thruster Workshop 1991 13 p (For primary document see N92-10044 01-20)
Avail: NTIS HC/MF A09 CSCL 21H

Inhouse magnetoplasmadynamic (MPD) thruster technology is discussed. The study focussed on steady state thrusters at powers of less than 1 MW. Performance measurement and diagnostics technologies were developed for high power thrusters. Also developed was a MPD computer code. The stated goals of the program are to establish: performance and life limitation; influence of applied fields; propellant effects; and scaling laws. The presentation is mostly through graphs and charts. E.R.

N92-10049*# Los Alamos National Lab., NM.
LOS ALAMOS NEP RESEARCH IN ADVANCED PLASMA THRUSTERS
Kurt Schoenberg and Richard Gerwin *In* NASA. Lewis Research Center, Magnetoplasmadynamic Thruster Workshop 1991 20 p (For primary document see N92-10044 01-20)
Avail: NTIS HC/MF A09 CSCL 21H

Research was initiated in advanced plasma thrusters that capitalizes on lab capabilities in plasma science and technology. The goal of the program was to examine the scaling issues of magnetoplasmadynamic (MPD) thruster performance in support of NASA's MPD thruster development program. The objective was to address multi-megawatt, large scale, quasi-steady state MPD thruster performance. Results to date include a new quasi-steady state operating regime which was obtained at space exploration initiative relevant power levels, that enables direct coaxial gun-MPD comparisons of thruster physics and performance. The radiative losses are neglible. Operation with an applied axial magnetic field shows the same operational stability and exhaust plume uniformity benefits seen in MPD thrusters. Observed gun impedance is in close agreement with the magnetic Bernoulli model predictions. Spatial and temporal measurements of magnetic field, electric field, plasma density, electron temperature, and ion/neutral energy distribution are underway. Model applications to advanced mission logistics are also underway. Author

N92-10050*# Massachusetts Inst. of Tech., Cambridge.
MPD WORK AT MIT
Manuel Martinez-Sanchez *In* NASA. Lewis Research Center, Magnetoplasmadynamic Thruster Workshop 1991 17 p (For primary document see N92-10044 01-20)
Avail: NTIS HC/MF A09 CSCL 21H

MPD work at MIT is presented in the form of the view-graphs. The following subject areas are covered: the MIT program, its goals, achievements, and roadblocks; quasi one-dimensional modeling; two-dimensional modeling - transport effects and Hall effect; microscopic instabilities in MPD flows and modified two stream instability; electrothermal stability theory; separation of onset and anode depletion; exit plane spectroscopic measurements; phenomena of onset as performance limiter; explanations of onset; geometry effects on onset; onset at full ionization and its consequences; relationship to anode depletion; summary on self-field MPD; applied field MPD - the logical growth path; the case for AF; the challenges of AF MPD; and recommendations. Author

N92-10051*# Ohio State Univ., Columbus. Dept. of Aeronautical and Astronautical Engineering.
MPD THRUSTER RESEARCH ISSUES, ACTIVITIES, STRATEGIES
In NASA. Lewis Research Center, Magnetoplasmadynamic Thruster Workshop 1991 20 p (For primary document see N92-10044 01-20)
Avail: NTIS HC/MF A09 CSCL 21H

The following activities and plans in the MPD thruster development are summarized: (1) experimental and theoretical research (magnetic nozzles at present and high power levels, MPD thrusters with applied fields extending into the thrust chamber, and improved electrode performance); and (2) tools (MACH2 code for MPD and nozzle flow calculation, laser diagnostics and spectroscopy for non-intrusive measurements of flow conditions, and extension to higher power). National strategies are also outlined. Author

N92-10052*# Princeton Univ., NJ. Electric Propulsion and Plasma Dynamics Lab.
[EPPDYL: RESEARCH FOCUS; PAST ACCOMPLISHMENTS; AND CURRENT RESEARCH]
In NASA. Lewis Research Center, Magnetoplasmadynamic Thruster Workshop 1991 8 p (For primary document see N92-10044 01-20)
Avail: NTIS HC/MF A09 CSCL 21H

Graphs and charts relative to magnetoplasmadynamic thruster power conditioning are given. Graphs show cathode evaporative mass loss, anode power friction, and anode fall. Past accomplishments and current research are outlined. Author

N92-10053*# Stuttgart Univ. (Germany, F.R.). Inst. for Space Systems.
IRS ORGANIGRAM
Ernst Messerschmid *In* NASA. Lewis Research Center, Magnetoplasmadynamic Thruster Workshop 1991 19 p (For primary document see N92-10044 01-20)
Avail: NTIS HC/MF A09 CSCL 21H

Charts and graphs relative to magnetoplasmadynamic (MPD) thruster technology are given. The research activities at the Institute of Space Transportation, University of Stuttgart, are summarized. Information is given on the Institute's Electric Propulsion and Plasma Wind Tunnel; thermal arcjet research; the nozzle-type thruster, DT-IRS; nozzle-type MPD thrusters; a hot anode thruster; the DT6 thruster; the ZT-1 thruster; the cylindrical MPD thruster; and a comparison of continuous and quasi-steady MPD. Author

N92-10054* National Aeronautics and Space Administration. Lewis Research Center, Cleveland, OH.
EXTENDED TEMPERATURE RANGE ROCKET INJECTOR
Patent
Steven J. Schneider, inventor (to NASA) 8 Oct. 1991 5 p Filed 30 Nov. 1989 Supersedes N90-15130 (28 - 7 p 887)
(NASA-Case-LEW-14846-1; US-Patent-5,054,287; US-Patent-Appl-SN-443523; US-Patent-Class-60-240; US-Patent-Class-60-258; US-Patent-Class-60-39.281; Int-Patent-Class-F02R-9/52) Avail: US Patent and Trademark Office CSCL 21H

A rocket injector is provided with multiple sets of manifolds for supplying propellants to injector elements. Sensors transmit the temperatures of the propellants to a suitable controller which is operably connnected to valves between these manifolds and propellant storage tanks. When cryogenic propellant temperatures are sensed, only a portion of the valves are opened to furnish propellants to some of the manifolds. When lower temperatures are sensed, additional valves are opened to furnish propellants to more of the manifolds.
Official Gazette of the U.S. Patent and Trademark Office

N92-10055*# National Aeronautics and Space Administration. Lewis Research Center, Cleveland, OH.
DESCRIPTION OF THE PMAD DC TEST BED ARCHITECTURE AND INTEGRATION SEQUENCE
R. F. Beach, L. Trash, D. Fong, and B. Bolerjack (Rockwell International Corp., Canoga Park, CA.) 1991 10 p Presented at the 26th Intersociety Energy Conversion Engineering Conference, Boston, MA, 4-9 Aug. 1991; sponsored by ANS, SAE, ACS, AIAA, ASME, IEEE, and AIChE
(NASA-TM-105284; E-6614; NAS 1.15:105284) Avail: NTIS HC/MF A02 CSCL 21H

NASA-Lewis is responsible for the development, fabrication, and assembly of the electric power system (EPS) for the Space Station Freedom (SSF). The SSF power system is radically different from previous spacecraft power systems in both the size and complexity of the system. Unlike past spacecraft power system the SSF EPS will grow and be maintained on orbit and must be flexible to meet changing user power needs. The SSF power system is also unique in comparison with terrestrial power systems because it is dominated by power electronic converters which regulate and control the power. Although spacecraft historically have used power converters for regulation they typically involved only a single series regulating element. The SSF EPS involves multiple regulating elements, two or more in series, prior to the load. These unique system features required the construction of a testbed which would allow the development of spacecraft power system technology. A description is provided of the Power Management and Distribution (PMAD) DC Testbed which was assembled to support the design and early evaluation of the SSF EPS. A description of the integration process used in the assembly sequence is also given along with a description of the support facility. Author

N92-10056# National Aerospace Lab., Tokyo (Japan).
EXPERIMENTAL INVESTIGATION OF A 12 cm DIAMETER KAUFMAN XENON ION THRUSTER
Katsuhiro Miyazaki, Yukio Hayakawa, and Shoji Kitamura Mar. 1991 19 p In JAPANESE; ENGLISH summary
(NAL-TR-1099; ISSN-0389-4010) Avail: NTIS HC/MF A03

An experimental study was performed on discharge performance improvement of an 12 cm diameter Kaufman-type xenon ion thruster to study the effects of discharge chamber configurations on discharge performance. Various discharge chamber configurations were constructed by changing the shapes and heights of the pole piece, the positions of the main hollow cathode, the cathode baffle diameters, and the discharge chamber magnets. These parameters were selected because they are relatively easy to change and have a large influence on discharge performance. Thruster operation tests were then conducted using each of these experimental configurations. Results revealed that a straight cylinder type pole piece provided lower ion production costs and higher discharge voltages than an inside brim pole piece, although differences are only slight. Larger diameter cathode baffles gave higher discharge voltages, with the effects of baffle diameter changes on the characteristics of ion production cost with respect to propellant utilization efficiency, being larger in the brim pole piece than in the straight cylinder one. A 30 mm high brim pole piece gave the best discharge performance. Discharge chamber configurations appropriate for operational use ion thrusters were selected based on these results. Author

N92-10057*# National Aeronautics and Space Administration. Lewis Research Center, Cleveland, OH.
MULTI-REACTOR POWER SYSTEM CONFIGURATIONS FOR MULTIMEGAWATT NUCLEAR ELECTRIC PROPULSION
Jeffrey A. George Sep. 1991 9 p
(NASA-TM-105212; E-6607; NAS 1.15:105212) Avail: NTIS HC/MF A02 CSCL 10B

A modular, multi-reactor power system and vehicle configuration for piloted nuclear electric propulsion (NEP) missions to Mars is presented. Such a design could provide enhanced system and mission reliability, allowing a comfortable safety margin for early manned flights, and would allow a range of piloted and cargo missions to be performed with a single power system design. Early use of common power modules for cargo missions would also provide progressive flight experience and validation of standardized systems for use in later piloted applications. System and mission analysis are presented to compare single and multi-reactor configurations for piloted Mars missions. A conceptual design for the Hydra modular multi-reactor NEP vehicle is presented. Author

N92-10058# Oak Ridge National Lab., TN.
MATERIALS IN SPACE NUCLEAR POWER SYSTEMS
R. H. Cooper and J. P. Moore 1991 3 p Presented at the Winter Meeting of the American Nuclear Society (ANS), San Francisco, CA, 10-15 Nov. 1991
(Contract DE-AC05-84OR-21400)
(DE91-017688; CONF-911107-28-Extd-Abst) Avail: NTIS HC/MF A01

Man's presence in space has been limited by the availability of reliable lightweight sources of power. Over the course of the last 30 years, a variety of space nuclear power systems have been designed and, in some cases, built and flown. Although a number of technology issues effect the overall performance of these systems, technical issues associated with the materials of construction have most often been a major limitation in obtaining the desired system performance goals. This paper will review selected materials limitations associated with the three major nuclear power systems being considered at this time: radioisotope power, nuclear power, and nuclear propulsion systems. DOE

N92-10059# Oak Ridge National Lab., TN.
STATUS OF RANKINE-CYCLE TECHNOLOGY FOR SPACE NUCLEAR POWER APPLICATIONS
R. S. Holcomb 1991 4 p Presented at the AIAA/NASA/OAI Conference on Advanced SEI Technologies, Cleveland, OH, 3-4 Sep. 1991 Previously announced in IAA as A91-52474

(Contract DE-AC05-84OR-21400)
(DE91-017859; CONF-9109226-11) Avail: NTIS HC/MF A01

A substantial effort on the development of the liquid metal Rankine cycle space nuclear power system was carried out in programs jointly sponsored by the National Aeronautics and Space Administration (NASA) and the Atomic Energy Commission (AEC) during the period of 1960 to 1972. Component tests were conducted which have established a considerable technology base for the concept. The development effort and technology status of each component are presented. The key technology issues remaining for development of the system are refractory metal parts fabrication, turbine blade endurance, turbine bearings and seals, and generator winding seal. DOE

N92-10060# Sandia National Labs., Albuquerque, NM.
COMPARISON OF SELECTED NUCLEAR THERMAL PROPULSION CONCEPTS
G. F. Polansky 1991 15 p Presented at the AIAA/NASA/OAI Conference on Advanced SEI Technologies, Cleveland, OH, 3-4 Sep. 1991
(Contract DE-AC04-76DP-00789)
(DE91-017982; SAND-91-1905C; CONF-9109226-13) Avail: NTIS HC/MF A03

The rationale for employing nuclear thermal propulsion on a piloted Mars mission is clear. Significant reductions in the required initial mass in low earth orbit are possible, as compared to chemical propulsion systems. However, many different nuclear thermal propulsion systems have been proposed and achieving consensus on the technology path to pursue within this area is difficult. Much of this difficulty results from the various levels of technology that have been assumed in each proposed concept. To address this difficulty, quantitative methods are employed to initiate consistent comparisons between a selected group of the proposed concepts. DOE

N92-10061# Sandia National Labs., Albuquerque, NM.
INSTRUMENTATION AND CONTROL FOR SPACE NUCLEAR PROPULSION
F. V. Thome and D. B. King 1991 6 p Presented at the AIAA/NASA/OAI Conference on Advanced SEI Technologies, Cleveland, OH, 3-4 Sep. 1991
(Contract DE-AC04-76DP-00789)
(DE91-018351; SAND-91-1987C; CONF-9109226-14) Avail: NTIS HC/MF A02

Space nuclear propulsion represents a major change for developers of Instrumentation and Control (I&C) systems. The reactor operates at much higher temperatures and at greater power densities than today's power reactors. Reliability requirements are much greater for high cost manned and unmanned missions. Today's reactor I&C engineers resort to out-of-core flux and temperature measurements because of the severe environments. This practice of indirectly monitoring reactor conditions has caused the industry problems from TMI-2 to Chernobyl. These problems may get worse for higher power densities, for higher temperature, and for fast reactors. I&C serves the purpose of plant integration. It must detect, measure, evaluate, and control the reactor and its cooling system, the power conversion system, and distribution system. The lack of emphasis on this aspect of reactor designs is a contributor to reliability problems and poor reactor on times for U.S. power reactors. The major I&C issues for space nuclear propulsion and some of the solutions are presented. DOE

N92-10062# Colorado Univ., Boulder. Dept. of Mechanical Engineering.
CONTRACTORS MEETING IN PROPULSION
M. A. Birkan and J. M. Tishkoff 2 Aug. 1991 283 p Meeting held in Boulder, CO, 10-14 Jun. 1991
(Grant AF-AFOSR-0541-89; AF Proj. 2308)
(AD-A240057; AFOSR-91-0713TR) Avail: NTIS HC/MF A13 CSCL 21/2

Abstracts are given for research in airbreathing combustion, rocket propulsion, and diagnostics in reacting media supported by the Air Force Office of Scientific Research. Major topics include: Gas turbines, Shear layer, Lasers, Fluorescence, Spectroscopy, Rocket, Engines, and Scramjets. GRA

N92-10063# Rocket Research Corp., Redmond, WA.
SMALL UPPER STAGE BASIC PROGRAM Final Report
T. E. Frei 27 Aug. 1991 140 p
(Contract N00014-90-C-2309)
(AD-A240059; RRC-91-R-1511) Avail: NTIS HC/MF A07 CSCL 22/3

The goal of this effort was to create a generic, low cost propulsion stage design capable of being integrated to several different launch vehicles (LV's) and capable of providing a mission enabling orbit transfer function to a variety of different small satellite missions. In order to accomplish this goal, a launch vehicle survey was conducted to establish the current LV capability and environments with respect to small satellites. In addition, a small satellite survey was conducted to establish the orbital needs of the small satellite community. With this information, the SUS specification was created. Based on this specification, the preliminary design of the SUS was developed. This design is capable of being integrated onto several different LV's and is capable of providing the orbit adjust requirements for approx. 75 pct. of the small satellite missions identified. The SUS design has capabilities of providing small satellites with several orbit transfer maneuvers from a LEO parking orbit (e.g., Hohmann Transfer, circularization, plane change and de-orbit). The SUS, containing a single or multiple small satellites, can be integrated onto a host LV as a primary on the SLV's, as a secondary on the MLV's or as multiples on a dedicated LV. GRA

23 CHEMISTRY AND MATERIALS (GENERAL)

N92-10064*# National Aeronautics and Space Administration. Lewis Research Center, Cleveland, OH.
RELATIVE SLIDING DURABILITY OF TWO CANDIDATE HIGH TEMPERATURE OXIDE FIBER SEAL MATERIALS
Christopher DellaCorte and Bruce M. Steinetz Sep. 1991 18 p
(NASA-TM-105199; E-6502; NAS 1.15:105199) Avail: NTIS HC/MF A03 CSCL 07A

A test program to determine the relative sliding durability of two candidate ceramic fibers for high temperature sliding seal applications is described. Pin on disk tests were used to evaluate potential seal materials. Friction during the tests and fiber wear, indicated by the extent of fibers broken in a test bundle or yarn, was measured at the end of a test. In general, friction and wear increase with test temperature. This may be due to a reduction in fiber strength, a change in the surface chemistry at the fiber/counterface interface due to oxidation, adsorption and/or desorption of surface species and, to a lesser extent, an increase in counterface surface roughness due to oxidation at elevated temperatures. The relative fiber durability correlates with tensile strength indicating that tensile data, which is more readily available than sliding durability data, may be useful in predicting fiber wear behavior under various conditions. A simple model developed using dimensional analysis shows that the fiber durability is related to a dimensionless parameter which represents the ratio of the fiber strength to the fiber stresses imposed by sliding. Author

N92-10065# Colorado State Univ., Fort Collins.
DIOSMACYCLOALKANES AS MODELS FOR THE FORMATION OF HYDROCARBONS FROM SURFACE METHYLENES
J. R. Norton 1991 5 p
(Contract DE-FG02-84ER-13299)
(DE91-017854; DOE/ER-13299/7) Avail: NTIS HC/MF A01

We have developed a method for the preparation of CH3CD(OTf)2 and CD3CD(OTf)2, and have used them for the preparation of Os2(CO)8(mu-CDCH3) and Os2(CO)8(mu-CDCD3). We have examined the mechanism of the extrusion of propene

from a diosmacyclobutane. It is clear that the majority of the product is formed by the expected beta elimination. However, the formation of a significant amount of CH3CD=CHD shows that, contrary to the conventional wisdom, some alpha elimination is occurring. We investigating the mechanism of olefin and acetylene exchange with diosmacyclobutanes. We have also discovered a novel allenyl Claisen rearrangement while exploring the reactions of an 1(3) reagent with triple bonds. Finally, we have learned that a side chain ether oxygen can control the regioselectivity with which the reagent adds to triple bonds. DOE

N92-10066*# National Aeronautics and Space Administration. Langley Research Center, Hampton, VA.
POLY 1, 2, 4-TRIAZOLES VIA AROMATIC NUCLEOPHILIC DISPLACEMENT Patent Application
John W. Connell, inventor (to NASA), Paul M. Hergenrother, inventor (to NASA), and Peter Wolf, inventor (to NASA) (Badische Anilin- und Soda-Fabrik A.G., Mogendorf, Germany, F.R.) 24 Jan. 1991 17 p
(NASA-CASE-LAR-14440-1; NAS 1.71:LAR-14440-1; US-Patent-Appl-SN-650336) Avail: NTIS HC/MF A03 CSCL 07A

The primary object of this invention constitutes new compositions of matter and a new process to prepare poly(1,2,4-triazoles) (PT). It concerns new PT, novel monomers, and the process for preparing the same. Another object of the present invention is to provide new PT that are useful as composite matrix resins for aircraft and dielectric interlayers in electronic devices. Another object of the present invention is the composition of several new di(hyproxyphenyl)-1,2,4-triazole monomers. According to the present invention, the foregoing and additional objects were obtained by synthesizing PT by the nucleophilic displacement reaction of di(hydroxyphenyl)-1,2,4-triazole monomers with activated aromatic dihalides. The inherent viscosities of the PT ranged from 1.37 to 3.4 dL/g and the glass transition temperatures ranged from 192 to 216 C. One polymer exhibited a crystalline melting temperature of 377 C. Thermogravimetric analysis (TGA) showed no weight loss occuring below 300 C in air or nitrogen with a 5 perceet weight loss occuring at approximately 500 C in air and nitrogen. The synthesis of the di(hydroxphenyl)-1,2,4-triazole monomer is represented in an equation. The monomer can be prepared by either of the two routes shown. The chemistry can easily be extended to prepare similar di(hydroxyphenyl)-1,2,4-triazole monomers as shown in a second equation. The aromatic dihydrazides in some cases are commercially available or readily prepared from hydrazine and a di(acid chloride). The substitution of the hydroxy groups in either type of monomer may be meta-meta, para-para, or para-meta. The general reaction sequence of PT from each type of di(hydroxyphenyl)-1,2,4-triazole monomer is shown in equations 3 and 4. NASA

N92-10580# Royal Inst. of Tech., Stockholm (Sweden). Inst. foer Materialfysik.
MATERIALS SCIENCE AND TECHNOLOGY CENTRA IN SWEDEN AND DENMARK: A RESEARCH POLICY FOR THE FUTURE Abstract Only
A. Flodstroem *In* Oulu Univ., Proceedings of the 25th Annual Conference of the Finnish Physical Society 1991 1 p (For primary document see N92-10362 01-70)
Avail: NTIS HC/MF A12

24 COMPOSITE MATERIALS

Includes physical, chemical, and mechanical properties of laminates and other composite materials.

For ceramic materials see *27 Nonmetallic Materials.*

N92-10067*# National Aeronautics and Space Administration. Langley Research Center, Hampton, VA.
PROPERTIES OF THREE GRAPHITE/TOUGHENED RESIN COMPOSITES
Donald L. Smith (Lockheed Engineering and Sciences Co., Hampton, VA.) and Marvin B. Dow Washington Sep. 1991 50 p
(NASA-TP-3102; L-16910; NAS 1.60:3102) Avail: NTIS HC/MF A03 CSCL 11D

Results are presented from an experimental evaluation of IM7/977-2, IM7/F655, and T800/F3900. Data presented include ply-level (unidirectional laminate) strength and moduli, unnotched and notched (open hole) tension and compression properties of quasi-isotropic laminates, and compression-after-impact strengths. These data are compared with properties of other toughened (IM7/8551-7 and IM6/18081) and brittle (T300/5208) graphite-epoxy materials. The IM7/977-2, IM7/F655, and T800/F3900 materials are substantially stronger and more damage tolerant than widely used first generation composite materials such as T300/5208. The T800/F3900 outperforms IM7/977-2 and IM7/F655 materials in tolerance to projectile impacts. Compression-after-impact strengths were found to be dependent on impactor velocity for a given impact energy. The open hole compression properties of all three materials are degraded by the combination of heat and moisture. Author

N92-10068# Construcciones Aeronauticas S.A., Madrid (Spain). Subdireccion de Investigacion y Desarrollo de Tecnologia y Materiales.
CORROSION TESTS OF MESHES IN CARBON FIBER LAMINATES: IMPACT BEAM TESTS [ENSAYO DE CORROSION DE MALLAS EN LAMINADOS DE FIBRA DE CARBONO PROBETAS DE IMPACTO AL RAYO]
1990 9 p In SPANISH
(Informe-I-522/90; ETN-91-90059) Avail: NTIS HC/MF A02

Corrosion resistance test results of copper alloy metal meshes, used in beam impact tests, are summarized. The use of a painting system is advised to avoid corrosion appearance in the metal meshes during an aircraft's service lifetime. ESA

N92-10069*# Boeing Co., Seattle, WA. Defense and Space Group.
ADVANCED THERMOPLASTIC RESINS, PHASE 1 Final Report
C. L. Hendricks, S. G. Hill, A. Falcone, and N. T. Gerken Sep. 1991 155 p
(Contract NAS1-17432)
(NASA-CR-178402; NAS 1.26:178402; D180-32725-1) Avail: NTIS HC/MF A08 CSCL 11D

Eight thermoplastic polyimide resin systems were evaluated as composite matrix materials. Two resins were selected for more extensive mechanical testing and both were versions of LaRC-TPI (Langley Research Center - Thermoplastic Polyimide). One resin was made with LaRC-TPI and contained 2 weight percent of a di(amic acid) dopant as a melt flow aid. The second system was a 1:1 slurry of semicrystalline LaRC-TPI powder in a polyimidesulfone resin diglyme solution. The LaRC-TPI powder melts during processing and increases the melt flow of the resin. Testing included dynamic mechanical analysis, tension and compression testing, and compression-after-impact testing. The test results demonstrated that the LaRC-TPI resins have very good properties compared to other thermoplastics, and that they are promising matrix materials for advanced composite structures. Author

N92-10070* National Aeronautics and Space Administration. Langley Research Center, Hampton, VA.
PROCESS FOR APPLICATION OF POWDER PARTICLES TO FILAMENTARY MATERIALS Patent
Robert M. Baucom, inventor (to NASA), John J. Snoha, inventor (to NASA), and Joseph M. Marchello, inventor (to NASA) 15 Oct. 1991 8 p Filed 16 May 1990 Supersedes N91-28290 (29 - 20, p 3305)
(NASA-Case-LAR-14231-1; US-Patent-5,057,338; US-Patent-Appl-SN-524109; US-Patent-Class-427-185; US-Patent-Class-427-195; US-Patent-Class-427-375; US-Patent-Class-118-DIG.5; US-Patent-Class-156-166;

US-Patent-Class-156-283; Int-Patent-Class-B05D-1/24) Avail: US Patent and Trademark Office CSCL 11D

This invention is a process for the uniform application of polymer powder particles to a filamentary material in a continuous manner to form a uniform composite prepreg material. A tow of the filamentary material is fed under carefully controlled tension into a spreading unit, where it is spread pneumatically into an even band. The spread filamentary tow is then coated with polymer particles from a fluidized bed, after which the coated filamentary tow is fused before take-up on a package for subsequent utilization. This process produces a composite prepreg uniformly without imposing severe stress on the filamentary material, and without requiring long, high temperature residence times for the polymer.

Official Gazette of the U.S. Patent and Trademark Office

N92-10071*# College of William and Mary, Williamsburg, VA.
QUANTITATIVE NONDESTRUCTIVE EVALUATION OF MATERIALS AND STRUCTURES Semiannual Report, 1 Feb. - 1 Jul. 1991
Barry T. Smith 1 Jul. 1991 75 p
(Grant NAG1-1063)
(NASA-CR-188975; NAS 1.26:188975) Avail: NTIS HC/MF A04 CSCL 11D

An experimental investigation was undertaken to quantify damage tolerance and resistance in composite materials impacted using the drop-weight method. Tests were conducted on laminates of several different carbon-fiber composite systems, such as epoxies, modified epoxies, and amorphous and semicrystalline thermoplastics. Impacted composite specimens were examined using destructive and non-destructive techniques to establish the characteristic damage states. Specifically, optical microscopy, ultrasonic, and scanning electron microscopy techniques were used to identify impact induced damage mechanisms. Damage propagation during post impact compression was also studied.

Author

N92-10072# Naval Air Development Center, Warminster, PA. Air Vehicle and Crew Systems Technology Dept.
IN SITU LIQUID-CRYSTAL-POLYMER FIBER REINFORCED ALUMINUM MATRIX COMPOSITE Final Report, 1 Oct. 1989 - 1 Oct. 1990
William E. Frazier and Gilbert J. London 1 May 1991 27 p
(NR Proj. RS3-4-A-50)
(AD-A239860; NADC-91041-60) Avail: NTIS HC/MF A03 CSCL 11/4

POLYMETS are a new class of hybrid materials composed of metals and polymers. The microstructure and mechanical properties of POLYMETS can be customized to meet a wide variety of design requirements. In this research, five to twenty volume percent of a thermotropic, wholly aromatic, liquid crystal polymer was mixed with -240/+325 mesh commercially pure aluminum powder and hot extruded at 300 C. The tensile properties of these POLYMETS were evaluated and the results compared to a pure aluminum control specimen. Optical and electron microscopy were used to examine the microstructures of the extruded rods and fracture surfaces of the tensile specimens. It was observed that polymer fibrils aligned in the extrusion direction. GRA

25 INORGANIC AND PHYSICAL CHEMISTRY

Includes chemical analysis, e.g., chromatography; combustion theory; electrochemistry; and photochemistry.

For related information see also *77 Thermodynamics and Statistical Physics.*.

N92-10073* National Aeronautics and Space Administration. Pasadena Office, CA.
REGENERATIVE Cu/La ZEOLITE SUPPORTED DESULFURIZING SORBENTS Patent
Gerald E. Voecks, inventor (to NASA) and Pramod K. Sharma, inventor (to NASA) (Jet Propulsion Lab., California Inst. of Tech., Pasadena.) 15 Oct. 1991 8 p Filed 12 Apr. 1990 Supersedes N90-26098 (28 - 20, p 2830)
(NASA-Case-NPO-17480-1-CU; US-Patent-5,057,473; US-Patent-Appl-SN-508386; US-Patent-Class-502-73; Int-Patent-Class-B01J-29/10) Avail: US Patent and Trademark Office CSCL 07D

Efficient, regenerable sorbents for removal of H2S from fluid hydrocarbons such as diesel fuel at moderate condition comprise a porous, high surface area aluminosilicate support, suitably a synthetic zeolite, and most preferably a zeolite having a free lattice opening of at least 6 Angstroms containing from 0.1 to 0.5 moles of copper ions, lanthanum ions or their mixtures. The sorbent removes sulfur from the hydrocarbon fuel in high efficiency and can be repetitively regenerated without loss of activity.

Official Gazette of the U.S. Patent and Trademark Office

N92-10074# Los Alamos National Lab., NM.
DETERMINING DESORPTION PRE-EXPONENTIAL FACTORS FROM TEMPERATURE-PROGRAMMED DESORPTION SPECTRA WHEN THE SURFACE IS NONUNIFORM
L. F. Brown and R. M. Chemburkar 15 Mar. 1991 14 p Presented at the American Institute of Chemical Engineers (AIChE) Annual Meeting, Los Angeles, CA, 17-22 Nov. 1991
(Contract W-7405-eng-36)
(DE91-009971; LA-UR-91-1031; CONF-911133-1) Avail: NTIS HC/MF A03

To find desorption pre-exponential factors from temperature-programmed desorption (TPD) spectra, we develop procedures using both the TPD spectra and their derivatives. First, an approximate method is derived using peak temperatures. This method is formally identical with one used for determining pre-exponential factors and desorption activation energies when desorptions are energetically uniform. The method can be used when the pre-exponential factor is constant. We next develop an iterative process that also uses peak temperatures, and again is usable when the pre-exponential factor is constant. This iterative approach should give more exact values of pre-exponential factors than the approximate approach. Using the first derivatives of TPD spectra over the entire range of temperatures leads to a second iterative process. This last procedure allows determination of energy-dependent pre-exponential factors. DOE

N92-10075# San Diego State Univ., CA. Dept. of Chemistry.
DEVELOPMENT AND OPTIMIZATION OF METHODOLOGIES FOR ANALYSIS OF COMPLEX HYDROCARBON MIXTURES
R. J. Laub 1990 30 p
(Contract DE-FG03-87ER-13658)
(DE91-017954; DOE/ER-13658/T1) Avail: NTIS HC/MF A03

Several aspects of liquid-chromatographic (LC) retentions were examined. The results from each were employed in efforts at understanding fundamental contributions to the partitioning process extant in LC. Thus, studies of LC separations with silica and reverse-phase sorbents were carried out. Several phases were then used singly and in admixture with isochratic as well as gradient-elution mobile phases. Selective mobile-phase additives was also evaluated, as were temperature effects. A unified theory of retentions with multicomponent phases, applicable to all forms of chromatography (including ion-exchange), was also developed. The theory made use of an extended form of the Langmuir sorption-isotherm relations. The selection and evaluation of standard stationary phases that exhibit high efficiency with concomitant high selectivity was carried out. The results included the synthesis and characterization of a unique class of mesomorphic polysiloxane stationary phases. Next, studies of blended stationary phases in open-tubular columns was undertaken. This was then followed by a detailed theoretical evaluation of the effects of blended mobile phases. The results from this portion of the work included the formulation and evaluation of a unique equation of state for gases that is valid in many cases from 200 to 900 K. DOE

N92-10076# Pacific Northwest Lab., Richland, WA.
ELECTROMIGRATION OF CARRIER-FREE RADIONUCLIDES

F. Roesch, T. Reimann, G. V. Buglanov, M. Milanov, V. A. Khalkin, and R. Dreyer (Zentralinstitut fuer Kernforschung, Rossendorf bei Dresden, German D.R.) 1990 24 p Original document announced as ZFK-634
(Contract DE-AC06-76RL-01830)
(DE91-017840; PNL-TR-484; ZFK-634) Avail: NTIS HC/MF A03

The purpose of the present paper was to study the hydrolysis and migration of carrier-free (241)Am-Am(III) in aqueous inert electrolytes in the absence of concurrent reactions, such as occur in migration systems when solid phases are added. Therefore, a modified electromigration measurement of carrier-free radionuclides in electrolytic solutions without addition of stabilizing materials was used, which assured the constancy of parameters relating to apparatus and electrolyte during the electromigration experiment. DOE

N92-10077# Oak Ridge National Lab., TN.
DEFINITION AND MEASUREMENT AT HIGH TEMPERATURES OF pH
R. E. Mesmer and H. F. Holmes 1991 33 p Presented at the 2nd International Symposium on Chemistry in High Temperature Water, Provo, UT, 19-22 Aug. 1991
(Contract DE-AC05-84OR-21400)
(DE91-017945; CONF-9108114-3) Avail: NTIS HC/MF A03

The NBS standardized definition of pH in terms of -log a(sub H) with an arbitrary definition of ion activity, has led to much confusion and ambiguity in the measurement of acidity. For many years, physical chemists have recognized and dealt with this problem, but still some continue the use of unnecessarily ambiguous assumptions. Several methods for defining pH are discussed and strong arguments are given for the use of a concentration or molality scale, especially for measurements in concentrated brines. Applications of hydrogen electrode concentration cells will be emphasized, and data available for calibrations for cells at high temperatures are given. Also, problems originating from the association of electrolytes near the critical conditions on the choice of standards for electrochemical measurements are discussed. DOE

N92-10078# Washington State Univ., Pullman. Dept. of Chemistry.
GROUND STATE PROPERTIES OF A He-3 IMPURITY IN LIQUID He-4 MONOLAYERS
C. I. Um, S. K. Yoo, and Thomas F. George Aug. 1991 27 p
(Contract N00014-90-J-1193)
(AD-A239993; WSU/DC/91/TR-60) Avail: NTIS HC/MF A03 CSCL 07/2

We present the results of ground-state energies, radial distribution functions, liquid structure functions and effective interactions for a He-3 impurity in a He-4 background in two dimensions. The hypernetted-chain scheme for the system described by a Jastrow-type wave function is used, taking into account the triplet correlations and elementary diagrams up to fifth order. Solving the Euler Lagrange equations for the two-body distribution functions, which contain triplet correlation and elementary diagrams, improves the results considerably. Furthermore, as a He-3 impurity is inserted into the He-4 background the ground-state energy increases, but the equilibrium density decreases from 0.0350 A(exp -2) to 0.0336 A(exp -2). The radial distribution function is broadened, while its maximum is lowered and shifted to the right (the direction of increasing radial distance) due to its larger zero-point energy, with therefore less localization of the He-4 particle. The results are compared with Monte Carlo results and other studies. GRA

N92-10363# Joensuu Univ. (Finland). Dept. of Physics.
A NEW PHASE RETRIEVAL METHOD FOR CARS SPECTRUM ANALYSIS Abstract Only
E. M. Vartiainen and K.-E. Peiponen *In* Oulu Univ., Proceedings of the 25th Annual Conference on the Finnish Physical Society 1991 1 p (For primary document see N92-10362 01-70)
Avail: NTIS HC/MF A12

N92-10380# Tampere Univ. of Technology (Finland). Dept. of Physics.
FLUIDIZED BED COMBUSTION DIAGNOSTICS BY LASER PHOTOCOUSTIC SPECTROSCOPY Abstract Only
Jari Stenberg and Rolf G. Hernberg *In* Oulu Univ., Proceedings of the 25th Annual Conference of the Finnish Physical Society 1991 1 p Sponsored by LIEKKI (For primary document see N92-10362 01-70)
Avail: NTIS HC/MF A12

N92-10381# Tampere Univ. of Technology (Finland). Dept. of Physics.
SIMULTANEOUS PYROMETRIC MEASUREMENT OF TEMPERATURE AND SIZE OF FUEL PARTICLES IN FLUIDIZED BED COMBUSTIONS Abstract Only
Jari Stenberg, M. Urponen, and Rolf G. Hernberg *In* Oulu Univ., Proceedings of the 25th Annual Conference of the Finnish Physical Society 1991 1 p (For primary document see N92-10362 01-70)
Avail: NTIS HC/MF A12

N92-10454# Helsinki Univ. of Technology, Espoo (Finland). Dept. of Technical Physics.
POLARIZATION SPECTROSCOPY IN OH AND FLAME TEMPERATURE MEASUREMENTS Abstract Only
R. Meier, K. Nyholm, M. Kaivola, and C. G. Aminoff *In* Oulu Univ., Proceedings of the 25th Annual Conference of the Finnish Physical Society 1991 1 p (For primary document see N92-10362 01-70)
Avail: NTIS HC/MF A12

N92-10455# Helsinki Univ. of Technology, Espoo (Finland). Dept. of Technical Physics.
ELECTRONICALLY RESONANT CARS SPECTROSCOPY OF NO2 Abstract Only
L. Oikarinen, K. Nyholm, M. Kaivola, and C. G. Aminoff *In* Oulu Univ., Proceedings of the 25th Annual Conference of the Finnish Physical Society 1991 1 p (For primary document see N92-10362 01-70)
Avail: NTIS HC/MF A12

N92-10484# Helsinki Univ. of Technology, Espoo (Finland). Physics Lab.
CHEMISORPTION OF CO ON Mg-O/Co(0001) Abstract Only
A. Talo, J. Vaari, J. Lahtinen, and P. Hautojarvi *In* Oulu Univ., Proceedings of the 25th Annual Conference of the Finnish Physical Society 1991 1 p (For primary document see N92-10362 01-70)
Avail: NTIS HC/MF A12

N92-10525# Helsinki Univ. of Technology, Espoo (Finland). Dept. of Physics.
AEROSOL DYNAMICS: BINARY NUCLEATION Abstract Only
Markku Kulmala, Ari Laaksonen, Mihalis Lazaridis, Jyrki Makela, Kaarle Hameri, and Timo Vesala *In* Oulu Univ., Proceedings of the 25th Annual Conference of the Finnish Physical Society 1991 1 p (For primary document see N92-10362 01-70)
Avail: NTIS HC/MF A12

N92-10526# Helsinki Univ. of Technology, Espoo (Finland). Dept. of Physics.
AEROSOL DYNAMICS: CONDENSATION AND EVAPORATION Abstract Only
Timo Vesala, Markku Kulmala, Jussi Kalkkinne, Jyrki Maekela, Kaarle Hameri, and Ari Laaksonen *In* Oulu Univ., Proceedings of the 25th Annual Conference of the Finnish Physical Society 1991 1 p (For primary document see N92-10362 01-70)
Avail: NTIS HC/MF A12

N92-10532# Tampere Univ. of Technology (Finland). Dept. of Physics.
ELECTROSTATIC PRECIPITATOR MODELLING Abstract Only
Jukka Hautanen and Markku Kilpelainen *In* Oulu Univ., Proceedings of the 25th Annual Conference of the Finnish Physical

Society 1991 1 p (For primary document see N92-10362 01-70)
Avail: NTIS HC/MF A12

N92-10535# Environics Oy, Mikkeli (Finland).
ION MOBILITY SPECTROMETER TO TRACE GAS ANALYSIS Abstract Only
Tero Katto, Harri Tyrvainen, and Kimmo Pietarinen (Tampere Univ. of Technology, Finland) *In* Oulu Univ., Proceedings of the 25th Annual Conference of the Finnish Physical Society 1991 1 p (For primary document see N92-10362 01-70)
Avail: NTIS HC/MF A12

26 METALLIC MATERIALS

Includes physical, chemical, and mechanical properties of metals, e.g., corrosion; and metallurgy.

N92-10079*# Alabama Univ., Huntsville.
HIGH TEMPERATURE MATERIALS CHARACTERIZATION Final Report
Gary L. Workman 31 Dec. 1990 31 p
(Contract NAS8-36955)
(NASA-CR-184231; NAS 1.26:184231) Avail: NTIS HC/MF A03 CSCL 11F

A lab facility for measuring elastic moduli up to 1700 C was constructed and delivered. It was shown that the ultrasonic method can be used to determine elastic constants of materials from room temperature to their melting points. The ease in coupling high frequency acoustic energy is still a difficult task. Even now, new coupling materials and higher power ultrasonic pulsers are being suggested. The surface was only scratched in terms of showing the full capabilities of either technique used, especially since there is such a large learning curve in developing proper methodologies to take measurements into the high temperature region. The laser acoustic system does not seem to have sufficient precision at this time to replace the normal buffer rod methodology. Author

N92-10080*# Alabama Univ., Huntsville.
EXPERT SYSTEMS FOR SUPERALLOY STUDIES Final Report
Gary L. Workman and William F. Kaukler 31 Dec. 1990 41 p
(Contract NAS8-36955)
(NASA-CR-184236; NAS 1.26:184236) Avail: NTIS HC/MF A03 CSCL 11F

There are many areas in science and engineering which require knowledge of an extremely complex foundation of experimental results in order to design methodologies for developing new materials or products. Superalloys are an area which fit well into this discussion in the sense that they are complex combinations of elements which exhibit certain characteristics. Obviously the use of superalloys in high performance, high temperature systems such as the Space Shuttle Main Engine is of interest to NASA. The superalloy manufacturing process is complex and the implementation of an expert system within the design process requires some thought as to how and where it should be implemented. A major motivation is to develop a methodology to assist metallurgists in the design of superalloy materials using current expert systems technology. Hydrogen embrittlement is disasterous to rocket engines and the heuristics can be very complex. Attacking this problem as one module in the overall design process represents a significant step forward. In order to describe the objectives of the first phase implementation, the expert system was designated Hydrogen Environment Embrittlement Expert System (HEEES). Author

N92-10081# Oak Ridge National Lab., TN.
EVALUATION OF ADVANCED AUSTENITIC ALLOYS RELATIVE TO ALLOY DESIGN CRITERIA FOR STEAM SERVICE
R. W. Swindeman and P. J. Maziasz Jun. 1991 59 p
(Contract DE-AC05-84OR-21400)
(DE91-017800; ORNL-6629/P2) Avail: NTIS HC/MF A04

The results are summarized for a task within a six-year activity to evaluate advanced austenitic alloys for heat recovery systems. Commercial, near-commercial, and development alloys were evaluated relative to criteria for metallurgical stability, fabricability, weldability, mechanical properties, and corrosion in fireside and steamside environments. Alloys that were given special attention in the study were 800HT, NF709, HR3C, and a group of 20/25 percent chromium - 30 percent nickel-iron alloys identified as HT-UPS (high-temperature, ultrafine-precipitation strengthened) alloys. Excellent metallurgical stability and creep strength were observed in the NF709 and HR3C steels that contained niobium and nitrogen. One group of HT-UPS alloys was strengthened by solution treating to temperatures above 1150 C and subsequent cold or warm working. Test data to beyond 35,000 h were collected. The ability to clad some of the alloys for improved fireside corrosion resistance was demonstrated. Weldability of the alloys was a concern. Hot cracking and heat-affected-zone (HAZ) liquation cracking were potential problems in the HR3C stainless steel and HT-UPS alloys, and the use of dissimilar metal filler wire was required. By the reduction of phosphorous content and selection of either a nickel-base filler metal or alloy 556 filler metal, weldments were produced with minimum HAZ cracking. The major issues related to the development of the advanced alloys were identified and methods to resolve the issues suggested. DOE

N92-10082# Sandia National Labs., Albuquerque, NM.
HIGH TEMPERATURE CREEP PROPERTIES OF EUTECTIC AND NEAR EUTECTIC SILVER-COPPER ALLOYS: APPLICATION TO METAL/CERAMIC JOINING
J. J. Stephens, S. N. Burchett, and F. M. Hosking 1991 31 p Presented at the Fall Meeting of the Minerals, Metals, and Materials Society of AIME and Materials Week of the American Society of Metals, Cincinnati, OH, 20-24 Oct. 1991
(Contract DE-AC04-76DP-00789)
(DE91-017987; SAND-91-0006C; CONF-911003-10) Avail: NTIS HC/MF A03

Calculations of residual stresses in eutectic Ag-Cu braze joints are often required to validate designs for a variety of metal/ceramic joining applications. In particular, Finite Element Analysis (FEA) codes have the capability of incorporating either elastic-plastic or minimum creep rate constitutive models for the braze material. Unfortunately, neither high temperature stress-strain or creep data are available in the literature for eutectic Ag-Cu alloy in the microstructural form encountered in braze joints. This paper presents the preliminary results of a study of the high temperature mechanical properties of eutectic 72Ag-28Cu and near-eutectic 67Ag-33Cu alloys at temperatures from 250 C to 750 C. For the case of the 67Ag-33Cu alloy, the stress exponent obtained from creep testing is observed to be a function of temperature. At 750 C, a stress exponent of 1.5 is observed, which suggest that grain boundary sliding controls of deformation while at 350 C, the stress exponent of 4.6 suggests that matrix creep of the Ag-rich phase controls deformation at this temperature. Creep data for both alloys have been fit to a power law equation which incorporates a temperature-dependent stress exponent. Compressive stress-strain tests using an engineering strain rate of 5 percent/min., were made over a temperature range of 27 to 750 C. The linear work hardening slope is found to be fairly constant from room temperature up to 350 C, followed by a steep decrease in value above 450 C. FEA calculations are presented for a eutectic Ag-Cu braze joint between metallized alumina ceramic and Fe-29Ni-17Co alloy using two different types of constitutive relations for the brazement: a high temperature minimum creep rate correlation and an elastic/plastic correlation using the temperature dependent yield stress and work hardening data. DOE

N92-10083# Sandia National Labs., Albuquerque, NM.
WETTABILITY OF LOW TEMPERATURE SOLDER ALLOYS FOR STEP-SOLDERING
F. M. Hosking, P. T. Vianco, and D. R. Frear 1991 20 p
(Contract DE-AC04-76DP-00789)
(DE91-018348; SAND-90-3248C) Avail: NTIS HC/MF A03

The electronics industry relies on step-soldering during device

attachment or subsequent reworking of heavily populated hybrid microcircuits and multilevel networks. Although there are many low to intermediate melting solder alloys that are commercially available, their wettability on typical base metals, such as Cu, Ni, Au, and Sn, are not well characterized. This investigation examines the wetting behavior of several In, Sn, Pb, Bi, and Ag containing solder alloys on Ni-Sn plated aluminum alloy substrates with soldering temperatures ranging from 145 to 200 C. Two rosin mildly activated (RMA) fluxes were included in the study. The wettability experiments were conducted with a Sandia designed wetting balance system. Wetting differences were observed between the two fluxes. The more active flux gave better wetting results and less variability in the meniscus terminations at the lower soldering temperatures. Wetting generally varied from adequate to very good. The Bi-bearing alloys generally gave the lowest wetting values. Work is in progress to determine the effects of aging on intermetallic growth and subsequent mechanical strength. DOE

N92-10084# Sandia National Labs., Albuquerque, NM.
THERMAL- AND IGNITION-TYPE STEAM EXPLOSIONS OF SINGLE DROPS OF MOLTEN ALUMINUM
L. S. Nelson, P. M. Duda, and D. A. Hyndman 1991 6 p Presented at the Winter Meeting of the American Nuclear Society (ANS), San Francisco, CA, 10-15 Nov. 1991
(Contract DE-AC04-76DP-00789)
(DE91-014705; SAND-91-1354C; CONF-911107-8) Avail: NTIS HC/MF A02

The contact of aluminum-based melts with liquid water has been shown to be explosive in many experiments performed by the aluminum industry and in several nuclear reactor experiments and accidents. In order to obtain quantitative information relating to the fuel-coolant interactions that might occur with aluminum-based fuel, a laboratory-scale experimental study is being performed at Sandia National Laboratories. The overall objective of this research program is to provide an understanding of the mechanism of steam explosions with the melt compositions expected in several hypothetical core meltdown accident scenarios in production reactors. In this program it has been demonstrated that rapid exothermic metal-water reactions can accompany the steam explosions under certain conditions resulting in enhanced energy release and in the concomitant generation of hydrogen. DOE

N92-10085# Argonne National Lab., IL.
EXAMINATION OF MECHANICAL BEHAVIOR IN NANOCRYSTALLINE MATERIALS
G. W. Nieman, J. R. Weertman (Northwestern Univ., Evanston, IL.), and R. W. Siegel Aug. 1991 5 p Presented at the Fall Meeting of the Minerals, Metals and Materials Society of AIME and Materials Week of the American Society of Metals, Cincinnati, OH, 20-24 Oct. 1991
(Contracts W-31-109-eng-38; DE-FG02-86ER-45229)
(DE91-018552; ANL/CP-74019; CONF-911003-14) Avail: NTIS HC/MF A01

It is well known that a decrease in grain size generally leads to an increase in yield and flow stress in metals and alloys. Processing methods now permit the preparation of samples with grain sizes in the nanometer range. In this paper we consider mechanisms which may control the mechanical behavior of nanocrystalline metals and compare predicted behavior with the limited experimental results available at present. DOE

N92-10086# Argonne National Lab., IL.
TRANSPORT PROPERTIES AND OXIDATION IN CHROMIUM AND Fe-Cr ALLOYS EXPOSED TO OXYGEN AT HIGH TEMPERATURES
J. H. Park and K. Natesan Mar. 1991 15 p Presented at the 1st International Conference on Heat-Resistant Materials, Lake Geneva, WI, 22-26 Sep. 1991
(Contract W-31-109-eng-38)
(DE91-018571; ANL/CP-71551; CONF-910909-12) Avail: NTIS HC/MF A03

Alloys samples of Fe-25Cr, Fe-25Cr-0.3 and 1Y, and Fe-25Cr-1Ce were subjected to oxidation tests in a microbalance at temperatures between 700 and 1000 C and at oxygen partial pressures in a range of 1 to 10(exp -20) atm for time periods of 19 to 160 h. Integrity of the scales was also evaluated by quenching from the oxidation temperature to room temperature in approx. 20 minutes. During quenching, the 24 h oxidized samples of Fe-25Cr showed total spallation of oxide layers from the alloy substrate. However, the Y and Ce containing alloys did not show scale spallation during thermal quenching. To determine total spallation behavior in Fe-25Cr, the oxidation and quenching tests were repeated twice with the same samples. To learn why the scale in the second and third oxidation/quenching runs did not spall as in the first run, we focused on alloy grain growth behavior during oxidation. Cation mixing properties obtained by electrical conductivity measurements on oxidized specimens were compared with the oxygen diffusivity in the corrosion product formed on the Fe-25Cr alloy. DOE

N92-10087# Naval Air Development Center, Warminster, PA. Air Vehicle and Crew Systems Technology Dept.
MICROSTRUCTURAL STABILITY AND CREEP RESPONSE OF A NEW Al-Fe-W-Si ALLOY Final Report, Sep. 1989 - Dec. 1990
John Benci and William E. Frazier 1 Apr. 1991 30 p
(AD-A239861; NADC-91030-60) Avail: NTIS HC/MF A03
CSCL 11/6

The microstructural stability and creep properties of a new aluminum alloy for potential aerospace applications at service temperatures up to 700 F (371 C) were evaluated. The Al alloy composition is 11.50 percent iron, 3.75 percent tungsten and 2.25 percent silicon by weight. The material was rapidly solidified via planar flow casting, vacuum hot-pressed, and then extruded into bar form. The room temperature yield strength and ultimate tensile strength are 603 MPa and 626 MPa, respectively, with an 11.3 percent elongation and a 33.0 percent reduction of area at fracture. A series of creep experiments were performed on this alloy at 700 F (371 C), and the results were compared to alloys FVS0812 (8009) and FVS1212. A change in creep deformation mechanism was discovered at a stress level of approximately 85 MPa defining the maximum allowable stress for components made from this material. The microstructural stability was evaluated by aging samples at either 700 F (371 C) or 900 F (482 C) and measuring the average grain and dispersoid sizes as a function of aging time with transmission electron microscopy. Upon aging at 371 C, the room temperature hardness did not change even after times greater than 1000 hrs., indicating the microstructure is stable at this temperature. The hardness decreased slightly during 482 C aging over a period of 670 hrs. indicating minor microstructural changes (e.g., dispersoid coarsening) were occurring over long periods of time. GRA

N92-10472# Helsinki Univ. of Technology, Espoo (Finland).
REDISTRIBUTION OF NITROGEN ATOMS AND MAGNETIC ORDERING IN Fe-N MARTENSITE AT LOW TEMPERATURES Abstract Only
K. Ullakko, V. G. Gavriljuk, and V. M. Nadutov (Academy of Sciences of the Ukrainian SSR, Kiev.) *In* Oulu Univ., Proceedings of the 25th Annual Conference of the Finnish Physical Society 1991 1 p (For primary document see N92-10362 01-70)
Avail: NTIS HC/MF A12

N92-10488# Turku Univ. (Finland). Dept. of Physics.
A BAND THEORETICAL STUDY ON THE ELECTRONIC PROPERTIES IN THE PHASE TRANSITION CuAu 1 TO CuAu 2 Abstract Only
K. Kokko *In* Oulu Univ., Proceedings of the 25th Annual Conference of the Finnish Physical Society 1991 1 p (For primary document see N92-10362 01-70)
Avail: NTIS HC/MF A12

N92-10507# Helsinki Univ. of Technology, Espoo (Finland). Low Temperature Lab.
NEUTRON DIFFRACTION EXPERIMENTS ON NUCLEAR MAGNETIC ORDER IN COPPER Abstract Only
A. J. Annila, K. N. Clausen, A. S. Oja, J. T. Tuoriniemi, and H. Weinfurter (Hahn-Meitner-Inst. G.m.b.H., Berlin, Germany, F.R.) *In* Oulu Univ., Proceedings of the 25th Annual Conference of the Finnish Physical Society 1991 1 p (For primary document see N92-10362 01-70)
Avail: NTIS HC/MF A12

N92-10509# Helsinki Univ. of Technology, Espoo (Finland). Low Temperature Lab.
ANTIFERROMAGNETIC ORDERING IN SILVER AT PICOKELVIN TEMPERATURES Abstract Only
P. J. Hakonen, K. K. Nummila, R. Vuorinen, and S. Yin *In* Oulu Univ., Proceedings of the 25th Annual Conference of the Finnish Physical Society 1991 1 p (For primary document see N92-10362 01-70)
Avail: NTIS HC/MF A12

27 NONMETALLIC MATERIALS

Includes physical, chemical, and mechanical properties of plastics, elastomers, lubricants, polymers, textiles, adhesives, and ceramic materials.

For composite materials see *24 Composite Materials.*

N92-10088*# Alabama Univ., Huntsville. Center for Applied Optics.
GLASS SAMPLE CHARACTERIZATION Final Report
Anees Ahmad 16 Aug. 1990 37 p
(Contract NAS8-36955)
(NASA-CR-184230; NAS 1.26:184230) Avail: NTIS HC/MF A03 CSCL 11C

The development of in-house integrated optical performance modelling capability at MSFC is described. This performance model will take into account the effects of structural and thermal distortions, as well as metrology errors in optical surfaces to predict the performance of large an complex optical systems, such as Advanced X-Ray Astrophysics Facility. The necessary hardware and software were identified to implement an integrated optical performance model. A number of design, development, and testing tasks were supported to identify the debonded mirror pad, and rebuilding of the Technology Mirror Assembly. Over 300 samples of Zerodur were prepared in different sizes and shapes for acid etching, coating, and polishing experiments to characterize the subsurface damage and stresses produced by the grinding and polishing operations. Author

N92-10089# Materials Research Labs., Melbourne (Australia).
FIRE RETARDANT PERFORMANCE OF SOME INTERIOR SHIPBOARD PAINT SCHEMES
L. V. Wake 1991 25 p
(MRL-TR-91-31; AR-006-821) Copyright Avail: NTIS HC/MF A03

The fire retardant performance of alternative paints to the alkyd paint system presently protecting the interior areas of Royal Australian Navy (RAN) ships was evaluated. Topcoats studied were: (1) a polyvinylidene chloride (PVDC) latex paint; (2) an acrylic latex paint; (3) an epoxy polyester paint; and (4) the RAN alkyd paint. The paints were examined in a number of primer/topcoat systems by combustion under limiting oxygen index (LOI), radiant heat exposure, direct flame exposure, and reverse panel heating. Some rating variation between procedures was observed although the latex based PVDC topcoat had the highest rating by all test methods. The variability was exemplified by the present RAN fire retardant alkyd paint which successfully passed the reverse panel heating test, had a self-extinguishing LOI of 28.9 pct., yet had a high flame spread by radiant heating and direct flame exposure. A paint scheme comprising an epoxy polyamide primer and a PVDC topcoat exhibited excellent fire retardant and maintenance properties and should be considered by RAN for a trial to determine in-Service shipboard performance. Author

N92-10090* National Aeronautics and Space Administration. Lewis Research Center, Cleveland, OH.
BROMINATED GRAPHITIZED CARBON FIBERS Patent
Ching-Cheh Hung, inventor (to NASA) 22 Oct. 1991 83 p Filed 30 Nov. 1989 Supersedes N90-15262 (28 - 7, p 910) Continuation-in-part of abandoned US-Patent-Appl-SN-219016, filed 14 Jul. 1988
(NASA-Case-LEW-14698-2; US-Patent-5,059,409;
US-Patent-Appl-SN-443289; US-Patent-Appl-SN-219016;
US-Patent-Class-423-448; US-Patent-Class-423-439;
US-Patent-Class-423-460; US-Patent-Class-252-502;
Int-Patent-Class-C01B-31/04) Avail: US Patent and Trademark Office CSCL 11C

Low cost, high break elongation graphitized carbon fibers having low degree of graphitization are inert to bromine at room or higher temperatures, but are brominated at -7 to 20 C, and then debrominated at ambient. Repetition of this bromination-debromination process can bring the bromine content to 18 percent. Electrical conductivity of the brominated fibers is three times of the before-bromination value.

Official Gazette of the U.S. Patent and Trademark Office

N92-10091* National Aeronautics and Space Administration. Lyndon B. Johnson Space Center, Houston, TX.
HELMET OF A LAMINATE CONSTRUCTION OF POLYCARBONATE AND POLYSULFONE POLYMERIC MATERIAL Patent
Joseph J. Kosmo, inventor (to NASA) and Frederic S. Dawn, inventor (to NASA) 15 Oct. 1991 60 p Filed 30 Nov. 1989 Supersedes N90-16925 (28 - 9, p 1195)
(NASA-Case-MSC-21503-1; US-Patent-5,056,156;
US-Patent-Appl-SN-443414; US-Patent-Class-2-2.1A;
US-Patent-Class-2-411; US-Patent-Class-2-424;
US-Patent-Class-428-412; US-Patent-Class-428-419;
US-Patent-Class-428-458; US-Patent-Class-428-215) Avail: US Patent and Trademark Office CSCL 11C

An article of laminate construction is disclosed which is comprised of an underlayer of polycarbonate polymer material to which is applied a chemically resistant outer layer of polysulfone. The layers which are joined by compression-heat molding, are molded to form the shape of a body protective shell such as a space helmet comprising a shell of polycarbonate, polysulfone laminate construction attached at its open end to a sealing ring adapted for connection to a space suit. The front portion of the shell provides a transparent visor for the helmet. An outer visor of polycarbonate polysulfone laminate construction is pivotally mounted to the sealing ring for covering the transparent visor portion of the shell during extravehicular activities. The polycarbonate under layer of the outer visor is coated on its inner surface with a vacuum deposit of gold to provide additional thermal radiation resistance.

Official Gazette of the U.S. Patent and Trademark Office

N92-10092# Brookhaven National Lab., Upton, NY.
THE SEARCH FOR LOW PHOTODESORPTION COATINGS
C. L. Foerster and G. Korn 1990 7 p Presented at the Vacuum Design of Synchrotron Light Sources, Argonne, IL, 13-15 Nov. 1991
(Contract DE-AC02-76CH-00016)
(DE91-017473; BNL-46492; CONF-911178-1) Avail: NTIS HC/MF A02

Low photo desorption (PSD) from surfaces of vacuum chambers increases the beam lifetime and reduces the cost of the pumping system of any storage ring. In compact rings where all radiated power (approx. 10 kW) is incident on a few meters only, low PSD and good thermal conductivity of photon absorbers are of particular importance. An experimental chamber in which one meter long bars can be exposed to white photon beam with 500 eV critical energy has been built and installed on the U10B beamline in the

VUV ring at the NSLS. Several reference bars made of high purity copper and a TiN coating on copper have been measured. Subsequent runs will include gold coating on copper, aluminum (200 C baked), diamond coating on copper and uncoated beryllium bars. In this paper the desorption coefficients will be measured and compared. DOE

N92-10093# Delaware Univ., Newark. Dept. of Chemical Engineering.
THE GENERALIZED VAN DER WAALS THEORY OF PURE FLUIDS AND MIXTURES
S. I. Sandler Aug. 1991 16 p
(Contract DE-FG02-85ER-13436)
(DE91-017549; DOE/ER-13436/6) Avail: NTIS HC/MF A03

A goal of our continuing work in this area is to develop equations of state based on theory and computer simulation for complex chain molecules and polymers. Over the last year we have been concentrating our efforts on small, rigid molecular fluids, models for molecules such as nitrogen, ethane, carbon disulfide, and propane, and trying to understand what are the important features of these fluids which must be accounted for in their thermodynamic description, as well as developing methods for dealing with long chain molecules. Our principal tools for gaining insight into the thermodynamic and structural behavior of molecular fluids has been the generalized van der Waals partition function, a generalization of perturbation theory based on other than hard-core reference fluids, Monte Carlo computer simulation and more recently molecular dynamics simulation based on a new program we have developed. DOE

N92-10094# Tennessee Univ., Knoxville.
INVESTIGATIONS OF THE EFFECTS OF ISOTOPIC SUBSTITUTION AND PRESSURE ON MISCIBILITY IN POLYMER-POLYMER AND POLYMER-SOLVENT SYSTEMS
A. VanHook 1991 23 p
(Contract DE-FG05-88ER-45374)
(DE91-018010; DOE/ER-45374/3) Avail: NTIS HC/MF A03

This report is for the approximately 2.5 years from 9/1/88 to 2/1/91. It documents significant progress in all the areas for which funds were requested. The report is divided into four sections: (1) development of light scattering apparatus and techniques to detect coexistence and spinodal loci for polymer-solvent mixtures over wide pressure and temperature ranges; (2) determination of pressure, solvent and solute isotope, and molecular weight dependences of coexistence and spinodal loci of acetone/polystyrene and methyl cyclopentane/polystyrene solutions (theoretical analysis); (3) development of light scattering apparatus to determine demixing loci in films of polymer-polymer blends (preliminary results); and (4) other efforts (demixing results in small molecule solutions; progress in synthesis and characterization of perdeutero methyl cyclopenthane; mass spectroscopic determination of polymer molecular weight distributions; and theoretical efforts. DOE

N92-10095# Los Alamos National Lab., NM.
OXIDE PROPERTIES OF A GAMMA TITANIUM ALUMINIDE: A SURFACE SCIENCE STUDY
T. N. Taylor and M. T. Paffett 1991 18 p Presented at the International Conference on High Temperature Aluminides and Intermetallics, San Diego, CA, 17-19 Sep. 1991
(Contract W-7405-eng-36)
(DE91-018024; LA-UR-91-2679; CONF-910938-1) Avail: NTIS HC/MF A03

The surface properties of oxides grown on a gamma titanium aluminide (2 at. percent Nb) have been examined using a x-ray photoelectron spectroscopy (XPS) and secondary-ion mass spectroscopy (SIMS). An oxide formed on the sample during air exposure at room temperature was thermally destabilized in ultra-high vacuum. The heating largely decomposed the advanced Ti oxidation states to give a predominate +2 valence configuration at 600 C, while the Al oxide was somewhat enhanced for the same treatment. Growth of a post chemisorption oxide for various temperatures and exposure times at pressures less than or equal to 10(exp -6) Torr oxygen revealed the progressive development of Ti and Al oxide. At a temperature of 600 C the Ti component was greatly enhanced relative to the Al content in the surface region. This separation of Ti from Al was clearly visible in SIMS measurements. The development and thermal stability of these oxides is in agreement with the heats of formation and available valence states for the two majority components in the material. DOE

N92-10096# Sandia National Labs., Albuquerque, NM.
THERMAL MODELING OF AN EPOXY ENCAPSULATION PROCESS
R. G. Baca and J. A. Schutt 1991 21 p Presented at the PATRAN Users Conference, Newport Beach, CA, 1-3 Oct. 1991
(Contract DE-AC04-76DP-00789)
(DE91-017845; SAND-90-3048C; CONF-9110196-2) Avail: NTIS HC/MF A03

The encapsulation of components is a widely used process at Sandia National Laboratories for packaging components to withstand structural loads. Epoxy encapsulants are also used for their outstanding dielectric strength characteristics. The production of high voltage assemblies requires the encapsulation of ceramic and electrical components (such as transformers). Separation of the encapsulant from internal contact surfaces or voids within the encapsulant itself in regions near the mold base have caused high voltage breakdown failures during production testing. In order to understand the failure mechanisms, a methodology was developed to predict both the thermal response and gel front progression of the epoxy during the encapsulation process. A thermal model constructed with PATRAN Plus (1) and solved with the P/THERMAL (2) analysis system was used to predict the thermal response of the encapsulant. This paper discusses the incorporation of an Arrhenius kinetics model into Q/TRAN (2) to model the complex volumetric heat generation of the epoxy during the encapsulation process. As the epoxy begins to cure, it generates heat and shrinks. The total cure time of the encapsulant (transformation from a viscous liquid to solid) is dependent on both the initial temperature and the entire temperature history. Because the rate of cure is temperature dependent, the cure rate accelerates with a temperature increase and, likewise, the cure rate is quenched if the temperature is reduced. The temperature and conversion predictions compared well against experimental data. The thermal simulation results were used to modify the temperature cure process of the encapsulant and improve production yields. DOE

N92-10097# Argonne National Lab., IL.
DEVELOPMENT OF NONDESTRUCTIVE CHARACTERIZATION TECHNOLOGIES FOR PROCESS CONTROL OF CERAMICS
W. A. Ellingson, N. Gopalsami, S. L. Dieckman, and T. Luethi Jul. 1991 23 p Presented at the 5th International Symposium on Nondestructive Characterization of Materials, Karuizawa, Japan, 27-30 May 1991
(Contract W-31-109-eng-38)
(DE91-018540; ANL/CP-72749; CONF-910572-2) Avail: NTIS HC/MF A03

Ceramic matrix composites using either continuous ceramic fibers or ceramic whiskers have been shown to have significantly higher fracture toughness than monolithic ceramics. High fracture toughness is necessary for ceramic applications in many advanced heat engines. Nondestructive characterization methods to measure different properties therefore are important for both types of materials. Mass production methods such as slip casting and injection molding, for composites or monolithics, require high reliability; thus, the development of nondestructive characterization methods for process control can have a high payoff. A method of producing continuous-fiber composites is by chemical vapor infiltration (CVI). In this technology, production and process development requires knowledge of the as-infiltrated density distribution and the orientation of the fibers after infiltration. We have demonstrated on injection molded Si3N4 with 10 to 15 wt. pct. binder that by appropriate use of high-gradient-field nuclear magnetic resonance (NMR) imaging and microfocus 3-D X ray

computed tomography (CT), the distribution of polymeric binders can be mapped to with + or - 0.5 wt. pct. In the case of SiC/SiC CVI continuous-fiber composites made with 0,+, -30 degree cloth layups, we have shown that density variations attributed to process conditions can be detected and that fiber orientations can be determined to better than + or - 2 degs by 3-D X ray microfocus CT data, together with advanced image processing. All data were acquired on NMR and X ray CT machines designed and built at Argonne National Laboratory. DOE

N92-10098# Argonne National Lab., IL.
UPDATE ON THE PROSPECTS FOR CERAMIC ENGINE COMPONENTS
R. P. Larsen and A. D. Vyas 1991 6 p Presented at the 1st International Conference on Heat-Resistant Materials, Lake Geneva, WI, 22-26 Sep. 1991
(Contract W-31-109-eng-38)
(DE91-018574; ANL/CP-73571; CONF-910909-9) Avail: NTIS HC/MF A02

Ceramic components have the potential to improve the performance of automative heat engines. Earlier work by the authors involved predicting the timing and size of the ceramic engine component market using a worldwide Delphi survey. Relevant information from that earlier work is presented, and developments since then are summarized. DOE

N92-10099# Edgerton, Germeshausen and Grier, Inc., Idaho Falls, ID.
INSTRUMENTAL DESIGN FOR MEASUREMENT OF SURFACE CHARGE ON INSULATING MATERIALS Ph.D. Thesis
S. T. Beck May 1991 144 p
(Contract DE-AC07-76ID-01570)
(DE91-018695; EGG-CS-9762) Avail: NTIS HC/MF A07

The study of electric charge buildup on nonconducting samples requires additional research and development in an attempt to gain knowledge of its behavior. One area affected by charge buildup is the charged particle spectroscopies, specifically, secondary ion mass spectroscopy (SIMS). In SIMS, a sample is bombarded with a primary particle beam that results in secondary ions being displaced from the sample's surface. The secondary ions are focused into the mass spectrometer where they are filtered out with respect to their individual atomic masses. When the sample is an insulating material, sample charging eventually occurs due to an imbalance of charged particles leaving the surface. The generated surface charge has severe consequences on the SIMS instrument's ability to perform an analysis. An instrument has been designed and constructed that studies the behavior of charge buildup on insulating materials in an attempt to uncover superior methods that will alleviate its effects in SIMS and other surface analysis techniques. The instrument uses two ion beams: one to apply charge to the sample and the second to determine the voltage located on the surface of the sample. As charge is generated on the sample, a positive cesium ion beam passes parallel to the surface and is deflected by the electrostatic potential on the sample. The cesium beam deflects a specific direction and magnitude, depending on the polarity and magnitude of the sample charge. The displacement of the beam is monitored with the aid of a microchannel plate and photodiode array combination. Experiments performed show that the instrument has a sensitivity of 0.05 volts and an uncertainty drift of 1.5 volts over a 2 hour period. Mylar surface charging data illustrates that the sample voltage is highly dependent on the magnitude and polarity of voltage gradients surrounding the sample. DOE

N92-10100# McDonnell Aircraft Co., Saint Louis, MO.
NONFLAMMABLE HYDRAULIC POWER SYSTEM FOR TACTICAL AIRCRAFT. VOLUME 2: EQUIPMENT AND SYSTEMS TEST AND EVALUATION Final Report, Jun. 1988 - Mar. 1990
J. B. Greene, M. A. Orf, J. J. Sheahan, J. A. Wieldt, and A. O. Harmon Apr. 1991 240 p
(Contract F33615-86-C-2600)
(AD-A239805; WRDC-TR-89-2026-Vol-2) Avail: NTIS HC/MF A11 CSCL 13/7

The objective of the Nonflammable Hydraulic Power System for Tactical Aircraft program was to develop and demonstrate an advanced hydraulic system design operating at a maximum pressure of 8000 psi using an Air Force Developed, nonflammable fluid, chlorotrifluoroethylene (CTFE). It followed four previous programs directed at this technology at Boeing and MCAIR. It was further complemented by three other Air Force sponsored programs which embrace either 8000 psi, CTFE or both. These programs were conducted by Parker Bertea Aerospace (Seal Evaluation), by Vickers Incorporated (High Pressure Pump Development) and by Rockwell International (High Pressure Distribution System Evaluation). GRA

N92-10101# Dayton Univ., OH.
AN EXPERIMENTAL EVALUATION OF THE IMPACT RESISTANCE OF RECOATED F-16A MONOLITHIC POLYCARBONATE FLAT SHEET Interim Report, Oct. 1984 - Mar. 1989
Michael P. Bouchard May 1991 60 p
(Contract F33615-84-C-3404)
(AD-A239984; UDR-TR-89-41; WRDC-TR-90-3078) Avail: NTIS HC/MF A04 CSCL 01/3

F-16A coated monolithic polycarbonate forward canopies experiencing coating degradation are being reworked by the vendor by stripping the degraded coating and applying a new protective coating, thereby restoring the canopy for additional useful service life. The basic objective of the current investigation was to determine whether or not the impact resistance of monolithic polycarbonate flat sheet material for the F-16A forward canopy is degraded by the stripping and recoating process. The effects of laboratory storage and QUV weathering were also evaluated. Coupons (beams) were fabricated and subjected to QUV weathering, laboratory storage, and/or stripping/recoating (which was performed by the vendor). The coupons were then impact tested using either the falling weight beam test technique (ASTM F736-81) or a high rate (40,000 in/min center deflection rate) open loop servohydraulic (MTS) beam test technique. The primary conclusion of the investigation was that the strip and recoat process did not degrade the impact resistance of the polycarbonate relative to the impact resistance of new coated polycarbonate. In other words, the strip and recoat process restored the impact resistance of the reworked polycarbonate to its original newly-fabricated, newly-coated state, regardless of prior conditioning (QUV weathering or laboratory storage). GRA

N92-10102# Pennsylvania State Univ., University Park. Dept. of Materials Science and Engineering.
CHEMICAL SYNTHESIS AND MICROSTRUCTURAL TOUGHENING OF INFRARED WINDOW MATERIALS Final Report, 1 Mar. 1986 - 30 Sep. 1989
Carlo G. Pantano, Gregory Geoffroy, and Gary L. Messing 1991 5 p
(Contract N00014-86-K-0191)
(AD-A239987) Avail: NTIS HC/MF A01 CSCL 20/6

The objectives of this program were: (1) to develop methods for chemical synthesis of high purity ZnS whiskers, fibers and matrix materials; (2) to use these materials for enhancing the fracture toughness of ZnS ceramics through microstructural control and matrix reinforcement; and (3) to model the infrared optical response of the composite. GRA

N92-10103# Southwest Research Inst., San Antonio, TX. Fuels and Lubricants Research Facility.
EVALUATION OF PRESERVATIVE ENGINE OIL CONTAINING VAPOR-PHASE CORROSION INHIBITOR AND A SIMPLIFIED ENGINE PRESERVATION TECHNIQUE Interim Report, Jul. 1985 - Sep. 1990
Edwin A. Frame Dec. 1990 156 p
(Contracts DAAK70-85-C-0007; DAAK70-87-C-0043; DA Proj. 1L7-62786-AH-20)

(AD-A240100; BFLRF-269) Avail: NTIS HC/MF A08 CSCL 21/4

The objectives of this project were: (1) to determine the feasibility of adding a vapor-phase corrosion inhibitor (VCI) component to improve the preservation performance of MIL-L-21260, and (2) to evaluate a less complicated engine preservation procedure. A simultaneous two-phase approach was conducted. Phase 1 involved the formulation and evaluation of experimental VCI oils, while Phase 2 was the evaluation of a simplified engine preservation procedure. VCI oil formulation was conducted by Ronco Laboratory under subcontract. Compatibility of the experimental VCI oils with metal coupons, elastomers, and fuel filters was determined. Effectiveness of the experimental VCI oil was evaluated in a 3-year outdoor engine storage test. The engines were preserved using an experimental, simplified preservation procedure. The simplified engine preservation procedure proved to be acceptable as engines stored for 3 years in a very severe environment were judged to have been adequately preserved. Engine oil meeting specification MIL-L-21260 provided satisfactory protection during the 3-year storage test. The experimental VCI oil also provided satisfactory storage protection during this test; however, there was no observable advantage for the VCI oil. The VCI oil had acceptable compatibility with an elastomeric flex ring, metal coupons (except lead), and fuel filters. GRA

N92-10104# York Univ. (Ontario). Dept. of Chemistry.
SURFACE ELECTROCHEMISTRY OF CHLORO(PHTHALOCYANINATO)RHODIUM(III) SPECIES, AND OXYGEN REDUCTION ELECTROCATALYSIS, FORMATION OF A DIMERIC SPECIES Technical Report, Aug. 1990 - Aug. 1991
Y.-H. Tse, P. Seymour, N. Kobayashi, H. Lam, and C. C. Leznoff 20 Aug. 1991 40 p
(Contract N00014-84-G-0201)
(AD-A240148; TR-42) Avail: NTIS HC/MF A03 CSCL 07/4

The deposition of Chloro (phthalocyaninato) rhodium(III) onto a highly oriented pyrolytic graphite (HOPG) electrode leads to a surface which can be organized by polarizing to potentials negative of the reduction of rhodium(III) to rhodium(II). The organized surface contains dinuclear rhodium phthalocyanine which is fairly stable in its (RhIIPc)2 oxidation state. It is reversibly oxidized to a (RhIIIPc)2 dinuclear species which decomposes slowly to monomeric RhIIIPc detected upon the surface through its electroactivity. Reduction of this mononuclear RhIIIPc back to RhIIPc leads to redimerization. The surface electrochemistry of this dynamic interplay between mononuclear and dinuclear species is explored in depth. The dinuclear (RhIIPc)2 species reacts with oxygen to form oxygen adducts which appear to be involved in both the 2-electron reduction of oxygen to hydrogen peroxide, and the 4-electron reduction to water. However these two processes proved difficult to characterize. GRA

N92-10105*# National Aeronautics and Space Administration. Langley Research Center, Hampton, VA.
A PROCESS FOR PREPARING 1,3-DIAMINO-5-PENTAFLUOROSULFANYLBENZENE AND POLYMERS THEREFROM Patent Application
Anne K. St.Clair, inventor (to NASA), Terry L. St.Clair, inventor (to NASA), and Joseph S. Thrasher, inventor (to NASA) (Alabama Univ., Huntsville.) 5 Sep. 1991 18 p
(NASA-Case-LAR-14773-1-CU; NAS 1.71:LAR-14773-1; US-Patent-Appl-SN-755207) Avail: NTIS HC/MF A03 CSCL 11C

Diamines have shown their utility in the formation of many polymers. Examples of these polymers include polyimides, polyamides, and epoxies. The properties of these polymers are often dependent on the diamine which is used to make the polymer. By the present invention, a process was developed to make a diamine containing pentafluorosulfanylbenzene moiety. This process involves two steps: the preparation of a dinitro precursor and the reduction of the dinitro compound to form the diamine. This diamine was then reacted with various dianhydrides, diacidchlorides, and epoxy resins to yield the corresponding polyimide, polyamide, and epoxy polymers. These polymers were then used to make films, a wire coating enamel, and a semi-permeable membrane. The novelty of this invention resides in the process to make the diamine. Traditionally, dinitro compounds are reduced with hydrazine or a catalyst such as palladium on charcoal. The catalyst which is used in this invention is platinum oxide. When this catalyst is used, it makes it possible to form a polymer-grade diamine. NASA

N92-10492# Odessa State Univ. (USSR). Dept. of Experimental Physics.
THE FIELD DRIFT OF IONS AND ITS INFLUENCE ON THE ELECTRICAL PROPERTIES OF SnO2 Abstract Only
A. V. Ignatov, A. V. Burlak, V. V. Serdyuk, V. Lantto, and S. Leppavuori (Oulu Univ., Finland) *In* Oulu Univ., Proceedings of the 25th Annual Conference of the Finnish Physical Society 1991 1 p (For primary document see N92-10362 01-70)
Avail: NTIS HC/MF A12

N92-10524# Neste Oy, Porvoo (Finland). Corporate Research and Development.
CONDUCTING POLYMERS Abstract Only
Tapani Taka *In* Oulu Univ., Proceedings of the 25th Annual Conference of the Finnish Physical Society 1991 1 p (For primary document see N92-10362 01-70)
Avail: NTIS HC/MF A12

28 PROPELLANTS AND FUELS

Includes rocket propellants, igniters, and oxidizers; their storage and handling procedures; and aircraft fuels.

For related information see also *07 Aircraft Propulsion and Power, 20 Spacecraft Propulsion and Power,* and *44 Energy Production and Conversion.*

N92-10106# Advisory Group for Aerospace Research and Development, Neuilly-Sur-Seine (France). Propulsion and Energetics Panel.
COMBUSTION OF SOLID PROPELLANTS
Jul. 1991 172 p In ENGLISH and FRENCH Lecture series held in Quebec City, Quebec, 4-5 Sep. 1991, in Saint-Medard-en-Jalles, France, 16-17 Sep. 1991, and in Ankara, Turkey, 19-20 Sep. 1991 Original contains color illustrations
(AGARD-LS-180; ISBN-92-835-0630-8) Copyright Avail: NTIS HC/MF A08; Non-NATO Nationals requests available only from AGARD/Scientific Publications Executive

The theoretical and experimental analysis of the complex combustion phenomena is presented. The following subject areas are covered: overview on solid propellant combustion within a rocket motor; solid propellant steady combustion; erosive burning; special effects in solid propellant combustion; combustion instabilities; ignition and unsteady combustion; and combustion and safety of solid propellant rocket motors. For individual titles, see N92-10107 through N92-10110.

N92-10107# Office National d'Etudes et de Recherches Aerospatiales, Paris (France). Energetics Dept.
SOLID PROPELLANT STEADY COMBUSTION: PHYSICAL ASPECTS
Guy Lengelle, Jean-Robert Duterque, Jean-Claude Godon, and Jean-Francois Trubert *In* AGARD, Combustion of Solid Propellants Jul. 1991 25 p Sponsored in part by Societe Nationale des Poudres et Explosifs and Ecole Nationale Superieure des Techniques Avancees (For primary document see N92-10106 01-28)
Copyright Avail: NTIS HC/MF A08; Non-NATO Nationals requests available only from AGARD/Scientific Publications Executive

A review of the understanding of the combustion mechanisms of solid propellants is presented. Such an understanding is an important part of the process carried out to master the behavior of solid propellants and to obtain desired characteristics (with

respect to energetic level, burning rate level, sensitivity to pressure and initial temperature, nature of emitted combustion products, vulnerability to various aggressions, etc.). Author

N92-10108# National Science Foundation, Washington, DC. Chemical and Thermal Systems Div.
EROSIVE BURNING OF SOLID PROPELLANTS
Merrill K. King *In* AGARD, Combustion of Solid Propellants Jul. 1991 26 p (For primary document see N92-10106 01-28) Copyright Avail: NTIS HC/MF A08; Non-NATO Nationals requests available only from AGARD/Scientific Publications Executive

Presented here is a review of the experimental and modeling work concerning erosive burning of solid propellants (augmentation of burning rate by flow of product gases across a burning surface). A brief introduction describes the motor design problems caused by this phenomenon, particularly for low port/throat area ratio motors and nozzleless motors. Various experimental techniques for measuring crossflow sensitivity of solid propellant burning rates are described, with the conclusion that accurate simulation of the flow, including upstream flow development, in actual motors is important since the degree of erosive burning depends not only on local mean crossflow velocity and propellant nature, but also upon this upstream development. In the modeling area, a brief review of simplified models and correlating equations is presented, followed by a description of more complex numerical analysis models. Both composite and double-base propellant models are reviewed. A second generation composite model is shown to give good agreement with data obtained in a series of tests in which composite propellant composition and heterogeneity (particle size distribution) were systematically varied. Finally, the use of numerical models for the development of erosive burning correlations is described, and a brief discussion of scaling is presented. Author

N92-10109# National Science Foundation, Washington, DC. Chemical and Thermal Systems Div.
EFFECTS OF WIRES ON SOLID PROPELLANT BALLISTICS
Merrill K. King *In* AGARD, Combustion of Solid Propellants Jul. 1991 13 p (For primary document see N92-10106 01-28) Copyright Avail: NTIS HC/MF A08; Non-NATO Nationals requests available only from AGARD/Scientific Publications Executive

Metallic wires have been employed in numerous end-burning solid propellant rocket motors over the last thirty years to provide desired burning rate amplifications needed for certain applications. These wires provide such amplification by serving as a thermal short-circuit between the hot final products of the propellant combustion and the unburned solid material, with resultant development of cones penetrating into the propellant adjacent to the wires (creating an increase in burning surface area) which lead the propellant regression. A brief review of models developed by others and of a systematic data base with regard to burning of wired strands is presented. The major emphasis is on modeling. A model of the processes by which wires amplify the burning of strands (at fixed pressure) was developed and applied to analysis of the systematic data base referred to above. This model is capable of treating unsteady-state phenomena and the effects of local (sporadic) gaps between wire and propellant. Accordingly, the strand model was subsequently coupled with a chamber ballistic analysis and a geometrical analysis of cone shaped evolution to permit prediction of pressure-time histories along the wired motors with various distributions along the wire of gaps between the wire and the propellant. Author

N92-10110# Naval Weapons Center, China Lake, CA. Research Dept.
COMBUSTION AND SAFETY OF SOLID PROPELLANT ROCKET MOTORS
T. L. Boggs *In* AGARD, Combustion of Solid Propellants Jul. 1991 14 p (For primary document see N92-10106 01-28) Copyright Avail: NTIS HC/MF A08; Non-NATO Nationals requests available only from AGARD/Scientific Publications Executive

The subject of munition safety is one of continuing importance, with recent emphasis in various insensitive munition requirements, because of the potential damage that can be caused by any device highly loaded with energetic materials. It is a difficult task to prevent inadvertent initiation and to mitigate the effects of reactions once initiation has occurred. This difficulty is compounded by several considerations such as: (1) the initiation can occur via many mechanisms; and (2) solid propellants have evolved to meet increased performance requirements. The need for high burn rates have led to some propellants that are extremely easy to ignite, especially as they age. Similarly, the need for increased range and decreased signature has led to propellants having high specific impulse with little or no metal ingredients. Herein, the ignition and combustion aspects are presented of solid propellant rocket motors. An overview is presented of the subject. The reader is referred to AGARDograph no. 316 for more detailed data. Author

N92-10111# Midwest Research Inst., Golden, CO.
THE ALTERNATIVE FUELS DATA CENTER
Aug. 1991 4 p
(Contract DE-AC02-83CH-10093)
(DE91-015003; SERI/SP-220-4403) Avail: NTIS HC/MF A01

In 1988, the Alternative Motor Fuels Act (AMFA) became Public Law 100-494. The AMFA encourages the production and use of motor vehicles designed to operate on alternative fuels. The alternative fuels specified in the law are methanol, ethanol, and natural gas. The Department of Energy (DOE), along with several other Federal, state, and local agencies, has undertaken numerous activities aimed at fulfilling the AMFA directives. Among these activities is the establishment of the Alternative Fuels Data Center (AFDC), operated and managed by the Solar Energy Research Institute (SERI) in Golden Colorado. The AMFA targets activities for three vehicle types using alternative fuels: (1) light-duty vehicles such as automobiles, mini-vans, and light-duty; (2) heavy-duty vehicles such as tractor trailers and garbage trucks; and (3) urban transit buses. The primary purpose of the AFDC is to gather and analyze information on the fuel consumption, emissions, operation, and durability of these vehicles types. The AFDC staff work with an Oracle Relational Database Management System and statistical software to provide information to users. DOE

29 MATERIALS PROCESSING

Includes space-based development of products and processes for commercial applications.
For biological materials see *55 Space Biology*.

N92-10112*# Alabama Univ., Huntsville. Center for Microgravity and Materials Research.
PROCESS MODELLING FOR SPACE STATION EXPERIMENTS Final Report
J. Iwan D. Alexander, Franz Rosenberger, Arunan Nadarajah, Jalil Ouazzani, and Sakir Amiroudine 17 Oct. 1990 141 p
(Contract NAS8-36955)
(NASA-CR-184227; NAS 1.26:184227) Avail: NTIS HC/MF A07 CSCL 22A

Examined here is the sensitivity of a variety of space experiments to residual accelerations. In all the cases discussed the sensitivity is related to the dynamic response of a fluid. In some cases the sensitivity can be defined by the magnitude of the response of the velocity field. This response may involve motion of the fluid associated with internal density gradients, or the motion of a free liquid surface. For fluids with internal density gradients, the type of acceleration to which the experiment is sensitive will depend on whether buoyancy driven convection must be small in comparison to other types of fluid motion, or fluid motion must be suppressed or eliminated. In the latter case, the experiments are sensitive to steady and low frequency accelerations. For experiments such as the directional solidification of melts with two or more components, determination of the velocity response alone is insufficient to assess the sensitivity. The effect of the velocity on the composition and temperature field must be considered, particularly in the vicinity of the melt-crystal interface. As far as the response to transient disturbances is concerned,

the sensitivity is determined by both the magnitude and frequency of the acceleration and the characteristic momentum and solute diffusion times. The microgravity environment, a numerical analysis of low gravity tolerance of the Bridgman-Stockbarger technique, and modeling crystal growth by physical vapor transport in closed ampoules are discussed. Author

31 ENGINEERING (GENERAL)

Includes vacuum technology; control engineering; display engineering; cryogenics; and fire prevention.

N92-10113# Edgerton, Germeshausen and Grier, Inc., Idaho Falls, ID.
THE EH SAFETY REPRESENTATIVE INFORMATION SYSTEM ON THE SAFETY PERFORMANCE MEASUREMENT SYSTEM IS WHERE YOU WILL FIND... WORD PROCESSING AND HELPS WITH A V-PLUS
P. I. Loo 1991 9 p Presented at the 1991 INTEREX HP Users Conference, San Diego, CA, 5-8 Aug. 1991
(Contract DE-AC07-76ID-01570)
(DE91-018709; EGG-M-91232; CONF-9108133-2) Avail: NTIS HC/MF A02

What are some of the current environmental, safety, and health problems being found at different DOE facilities? What are some of latest software products available for HP-3000 on-line application? How can I meet my customer's ever-changing requirements? These and many other questions will be focused on within this review of the Environment, Safety, and Health (EH) Safety Representative Information System (SRIS) located on the Safety Performance Measurement System (SPMS). SPMS is a collection of automated environmental, safety, and health information modules for references by DOE and DOE contractors. SPMS is operated by the Management Information Systems (MIS) Unit of the System Safety Development Center at EG&G Idaho, Inc. In the following sections an overview of SRIS, an on-line system designed for the HP-3000, will be presented along with an analysis of design methods and software packages used to develop the system. DOE

32 COMMUNICATIONS AND RADAR

Includes radar; land and global communications; communications theory; and optical communications.

For related information see also *04 Aircraft Communications and Navigation* and *17 Space Communications, Spacecraft Communications, Command and Tracking.* For search and rescue see *03 Air Transportation and Safety,* and *16 Space Transportation.*

N92-10114# Loughborough Univ. of Technology (England). Dept. of Electrical and Electronic Engineering.
THE DESIGN OF SPACEBORNE SYNTHETIC APERTURE RADAR M.S. Thesis
P. J. Gow 1988 128 p
(ETN-91-99986) Copyright Avail: NTIS HC/MF A07

The design concepts, the potential applications and the construction of spaceborne SAR (Synthetic Aperture Radar) systems are examined and advantages of SAR over conventional radar, particularly at orbital altitudes are discussed. The Seasat A mission is used as a baseline system to assimilate an overall design procedure. The antenna, sensor, datalink and processor subsystems are examined in detail and potential improvements highlighted. A SAR design is proposed in the light of the Seasat post mission analysis and technological advances, and a range of operational modes of the system and how the design could be maximized for a variety of enduser requirements are explained. Military aspects and applications of spaceborne SAR are included. ESA

N92-10115 Institute for Perception RVO-TNO, Soesterberg (Netherlands). Audiology Group.
DIGITAL SIMULATION OF SPEECH TRANSMISSION CHANNELS Final Report
J. L. vanRaaij and H. J. M. Steeneken 28 Jan. 1991 19 p
(Contract A89/KLu/321)
(IZF-1991-A-7; TD-91-0035; ETN-91-99989) Copyright Avail: Institute for Perception RVO-TNO, P.O. Box 23, 3769 ZG Soesterberg, Kampweg 5, Netherlands

A system was designed to simulate speech transmission channels by a series of successive elementary speech processing units. These modules include: filtering, automatic gain control, peak clipping, soft clipping, center clipping, noise addition, noise filtering, echo addition, delta modulation, pulse code modulation and bit error addition. The system is based on a digital signal processor and is computer controlled. The input and output is analog. With this system a number of representative reference channels will be established. These channels will be specified in terms of intelligibility, and will provide a framework for the evaluation of speech communication systems. ESA

N92-10116*# Jet Propulsion Lab., California Inst. of Tech., Pasadena.
PERSONAL ACCESS SATELLITE SYSTEM (PASS) STUDY. FISCAL YEAR 1989 RESULTS
Miles K. Sue, ed. Sep. 1990 322 p
(NASA-CR-188808; JPL-D-7382; NAS 1.26:188808) Avail: NTIS HC/MF A14 CSCL 17B

The Jet Propulsion Laboratory is exploring the potential and feasibility of a personal access satellite system (PASS) that will offer the user greater freedom and mobility than existing or currently planned communications systems. Studies performed in prior years resulted in a strawman design and the identification of technologies that are critical to the successful implementation of PASS. The study efforts in FY-89 were directed towards alternative design options with the objective of either improving the system performance or alleviating the constraints on the user terminal. The various design options and system issues studied this year and the results of the study are presented. For individual titles, see N92-10117 through N92-10124.

N92-10117*# Jet Propulsion Lab., California Inst. of Tech., Pasadena.
INTRODUCTION TO THE PERSONAL ACCESS SATELLITE SYSTEM STUDY
Miles K. Sue *In its* Personal Access Satellite System (PASS) Study. Fiscal Year 1989 Results Sep. 1990 48 p (For primary document see N92-10116 01-32)
Avail: NTIS HC/MF A14 CSCL 17B

A recent study by the National Telecommunications and Information Administration (NTIA) has concluded that the 21st century will be the age of information in which the telecommunication infrastructure will be vital to the social and economic well being of society. To meet the challenge of the coming age, JPL has been performing studies on a personal access satellite system (PASS) for the 21st century. The PASS study can be traced back to a study in which the technical feasibility and potential applications of a high frequency, low data rate satellite system were identified using small fixed terminals. Herein, the PASS concept is described along with the strawman design. Then the key challenges are identified along with possible solutions. Finally, the plan for the future is summarized from the key results. Author

N92-10118*# Jet Propulsion Lab., California Inst. of Tech., Pasadena.
MULTIPLE ACCESS TRADE STUDY
Masoud Motamedi *In its* Personal Access Satellite System (PASS) Study. Fiscal Year 1989 Results Sep. 1990 30 p (For primary document see N92-10116 01-32)
Avail: NTIS HC/MF A14 CSCL 17B

The Personal Access Satellite System (PASS) strawman design uses a hybrid Time Division Multiple Access (TDMA)/Frequency

Division Multiple Access (FDMA) implementation. TDMA is used for the forward direction (from Suppliers to Users), and FDMA for the return direction (from Users to Suppliers). An alternative architecture is proposed that will require minimal real time coordination and yet provide a fast access method by using random access Code Division Multiple Access (CDMA). The CDMA system issues are addressed such as connecting suppliers and users, both of whom may be located anywhere in the CONUS, when the user terminals are constrained in size and weight; and providing efficient traffic routing under highly variable traffic requirements. It is assumed that bandwidth efficiency is not of paramount importance. CDMA or Spread Spectrum Multiple Access (SSMA) communication is a method in which a group of carriers operate at the same nominal center frequency but are separable from each other by the low cross correlation of the spreading codes used. Interference and multipath rejection capability, ease of selective addressing and message screening, low density power spectra for signal hiding and security, and high resolution ranging are among the benefits of spread spectrum communications.
Author

N92-10119*# Jet Propulsion Lab., California Inst. of Tech., Pasadena.
ANTENNA BEAM COVERAGE CONCEPTS
Polly Estabrook and Masoud Motamedi *In its* Personal Access Satellite System (PASS) Study. Fiscal Year 1989 Results Sep. 1990 51 p (For primary document see N92-10116 01-32)
Avail: NTIS HC/MF A14 CSCL 17B

The strawman Personal Access Satellite System (PASS) design calls for the use of a CONUS beam for transmission between the supplier and the satellite and for fixed beams for transmission between the basic personal terminal and the satellite. The satellite uses a 3 m main reflector for transmission at 20 GHz and a 2 m main reflector for reception at 30 GHz. There are several types of spot beams under consideration for the PASS system besides fixed beams. The beam pattern of a CONUS coverage switched beam is shown along with that of a scanning beam. A switched beam refers to one in which the signal from the satellite is connected alternatively to various feed horns. Scanning beams are taken to mean beams whose footprints are moved between contiguous regions in the beam's coverage area. The advantages and disadvantages of switched and/or scanning beams relative to fixed beams. The consequences of using switched/scanning in lieu of fixed beams in the PASS design and attempts are made to evaluate the listed advantages and disadvantages. Two uses of switched/scanning beams are examined. To illustrate the implications of switched beams use on PASS system design, operation at two beam scan rates is explored. Author

N92-10120*# Jet Propulsion Lab., California Inst. of Tech., Pasadena.
IMPACT OF NON-GEOSTATIONARY ORBITS ON PASS
Polly Estabrook and Masoud Motamedi *In its* Personal Access Satellite System (PASS) Study. Fiscal Year 1989 Results Sep. 1990 39 p (For primary document see N92-10116 01-32)
Avail: NTIS HC/MF A14 CSCL 17B

The use of satellites in non-geostationary orbits (NGO) for PASS (Personal Access Satellite System) is discussed. The following subject areas are covered: (1) orbit parameters (circular and elliptical orbit characteristics); (2) link characteristics (Doppler shift, propagation loss, CONUS coverage antenna, multibeam antenna gain, and impact on link equations); (3) number of satellites required for continuous CONUS coverage (circular and elliptical orbit results); and (4) advantages and disadvantages of NGOs. Author

N92-10121*# Jet Propulsion Lab., California Inst. of Tech., Pasadena.
USER ANTENNAS
Vahraz Jamnejad and Paul Cramer *In its* Personal Access Satellite System (PASS) Study. Fiscal Year 1989 Results Sep. 1990 57 p (For primary document see N92-10116 01-32)
Avail: NTIS HC/MF A14 CSCL 17B

The following subject areas are covered: (1) impact of frequency change of user and spacecraft antenna gain and size; (2) basic personal terminal antennas (impact of 20/30 GHz frequency separation; parametric studies - gain, size, weight; gain and figure of merit (G/T); design data for selected antenna concepts; critical technologies and development goals; and recommendations); and (3) user antenna radiation safety concerns. Author

N92-10122*# Jet Propulsion Lab., California Inst. of Tech., Pasadena.
SPACECRAFT ANTENNAS
Vahraz Jamnejad, Farzin Manshadi, Yahya Rahmat-Samii, and Paul Cramer *In its* Personal Access Satellite System (PASS) Study. Fiscal Year 1989 Results Sep. 1990 52 p (For primary document see N92-10116 01-32)
Avail: NTIS HC/MF A14 CSCL 17B

Some of the various categories of issues that must be considered in the selection and design of spacecraft antennas for a Personal Access Satellite System (PASS) are addressed, and parametric studies for some of the antenna concepts to help the system designer in making the most appropriate antenna choice with regards to weight, size, and complexity, etc. are provided. The question of appropriate polarization for the spacecraft as well as for the User Terminal Antenna required particular attention and was studied in some depth. Circular polarization seems to be the favored outcome of this study. Another problem that has generally been a complicating factor in designing the multiple beam reflector antennas, is the type of feeds (single vs. multiple element and overlapping vs. non-overlapping clusters) needed for generating the beams. This choice is dependent on certain system design factors, such as the required frequency reuse, acceptable interbeam isolation, antenna efficiency, number of beams scanned, and beam-forming network (BFN) complexity. This issue is partially addressed, but is not completely resolved. Indications are that it may be possible to use relatively simple non-overlapping clusters of only a few elements, unless a large frequency reuse and very stringent isolation levels are required. Author

N92-10123*# Jet Propulsion Lab., California Inst. of Tech., Pasadena.
PASS SPACECRAFT ANTENNA TECHNOLOGY ASSESSMENT
R. E. Freeland *In its* Personal Access Satellite System (PASS) Study. Fiscal Year 1989 Results Sep. 1990 18 p (For primary document see N92-10116 01-32)
Avail: NTIS HC/MF A14 CSCL 17B

The purpose was to generate estimates of mechanical performance for the classes of spacecraft antenna under construction for application to the Personal Access Satellite System (PASS). These performance data are needed for the support of trade studies involving antenna system development. The classes of antenna considered included: (1) rigid non-deployable antenna structures; (2) mechanical deployable antenna concepts; (3) inflatable deployable antenna concepts; and (4) mesh deployable antenna concepts. The estimates of mechanical performance are presented in terms of structural weight and cost as a function of the reflector size. Estimates of aperture surface precision are presented for a few discrete antenna sizes. The range of reflector size is 1 to 4 meters for non-deployable structures and 2 to 8 meters for deployable structures. The range of reflector surface precision is lambda/30 to lambda/50 for 20 and 30 GHz, respectively. Author

N92-10124*# Jet Propulsion Lab., California Inst. of Tech., Pasadena.
TECHNOLOGY ASSESSMENT AND EXPERIMENTATION PLAN
Polly Estabrook *In its* Personal Access Satellite System (PASS) Study. Fiscal Year 1989 Results Sep. 1990 18 p (For primary document see N92-10116 01-32)
Avail: NTIS HC/MF A14 CSCL 17B

An assessment is given of the critical and enhancing technologies necessary to build the basic personal terminal (BPT), the supplier, and the Network Management Center (NMC). The experimentation plan for testing the Personal Access Satellite System (PASS) utilizing ACTS is detailed. The experiment plan

gives a list of candidate experiments and describes the proposed experimental set-up. ACTS will be used in the Microwave Switch Matrix (MSM) mode. The Microwave Switch Matrix - Link Evaluation Terminal (MSM-LET) at the NASA Lewis Research Center will serve as the microwave front-end for the PASS supplier and the NMC. Link budgets are given for both the forward and return links between the supplier and the basic personal terminal. The equipment required for the experiments is identified. Author

N92-10125*# National Aeronautics and Space Administration. Pasadena Office, CA.
METHOD AND APPARATUS FOR FREQUENCY SPECTRUM ANALYSIS Patent Application
Steven W. Cole, inventor (to NASA) (Jet Propulsion Lab., California Inst. of Tech., Pasadena.) 25 Feb. 1991 22 p
(Contract NAS7-918)
(NASA-Case-NPO-17759-1-CU; NAS 1.71:NPO-17759-1-CU; US-Patent-Appl-SN-660371) Avail: NTIS HC/MF A03 CSCL 17B

The invention relates to a method and apparatus for frequency spectrum analysis of an unknown signal in real time based upon integration of 1-bit samples of signal voltage amplitude corresponding to sine or cosine phases of a controlled center frequency clock which is changed after each integration interval to sweep the frequency range of interest in steps. Integration of samples during each interval is carried out over a number of cycles of the center frequency clock spanning a number of cycles of an input signal to be analyzed. The invention may be used to detect the frequency of at least two signals simultaneously. By using a reference signal of known frequency and voltage amplitude (added to the two signals for parallel processing in the same way, but in a different channel with a sampling at the known frequency and phases of the reference signal), the absolute voltage amplitude of the other two signals may be determined by squaring the sine and cosine integrals of each channel and summing the squares to obtain relative power measurements in all three channels and, from the known voltage amplitude of the reference signal, obtaining an absolute voltage measurement for the other two signals by multiplying the known voltage of the reference signal with the ratio of the relative power of each of the other two signals to the relative power of the reference signal. NASA

N92-10126*# National Aeronautics and Space Administration. Pasadena Office, CA.
COMPOSITE VIDEO AND GRAPHICS DISPLAY FOR MULTIPLE CAMERA VIEWING SYSTEM IN ROBOTICS AND TELEOPERATION Patent Application
Daniel B. Diner, inventor (to NASA) and Steven C. Venema, inventor (to NASA) (Jet Propulsion Lab., California Inst. of Tech., Pasadena.) 17 Jun. 1991 24 p
(Contract NAS7-918)
(NASA-Case-NPO-17836-1-CU; NAS 1.71:NPO-17836-1-CU; US-Patent-Appl-SN-716150) Avail: NTIS HC/MF A03 CSCL 17B

A system for real-time video image display for robotics or remote-vehicle teleoperation is described that has at least one robot arm or remotely operated vehicle controlled by an operator through hand-controllers, and one or more television cameras and optional lighting element. The system has at least one television monitor for display of a television image from a selected camera and the ability to select one of the cameras for image display. Graphics are generated with icons of cameras and lighting elements for display surrounding the television image to provide the operator information on: the location and orientation of each camera and lighting element; the region of illumination of each lighting element; the viewed region and range of focus of each camera; which camera is currently selected for image display for each monitor; and when the controller coordinate for said robot arms or remotely operated vehicles have been transformed to correspond to coordinates of a selected or nonselected camera. NASA

N92-10127# Ceskoslovenska Akademie Ved, Prague. Inst. of Plasma Physics.
APPROXIMATE ANALYTIC THEORY OF THE MULTIJUNCTION GRILL
O. Hurtak and J. Preinhaelter Mar. 1991 38 p
(IPPCZ-309) Avail: NTIS HC/MF A03

Approximate analytic theory of the general multijunction grill is developed. Omitting the evanescent modes in the subsidiary waveguides both at the junction and at the grill mouth and neglecting multiple wave reflection between the same places, simple formulae are derived for the reflection coefficient, the amplitudes of the incident and reflected waves, and the spectral power density. All these quantities are expressed through the basic grill parameters (the electric length of the structure and phase shift between adjacent waveguides) and two sets of the reflection coefficients describing wave reflections in the subsidiary waveguides at the junction and at the plasma. The approximate expressions for these coefficients are also given. The results are compared with numerical solution of two specific examples and they prove to be useful for the optimization and design of the multijunction grills. For the JET structure, it is shown that, in the case of the dense plasma, many results can be obtained from the simple formulae for two waveguide multijunction grill. Author

N92-10128* National Aeronautics and Space Administration. Lewis Research Center, Cleveland, OH.
REAL-TIME DATA COMPRESSION OF BROADCAST VIDEO SIGNALS Patent
Mary Jo W. Shalkauser, inventor (to NASA), Wayne A. Whyte, Jr., inventor (to NASA), and Scott P. Barnes, inventor (to NASA) 15 Oct. 1991 30 p Filed 9 Nov. 1990 Supersedes N91-15469 (29 - 7, p 996) Continuation-in-part of US-Patent-Appl-SN-540976, filed 20 Jun. 1990
(NASA-Case-LEW-14945-2; US-Patent-5,057,917; US-Patent-Appl-SN-611214; US-Patent-Appl-SN-540976; US-Patent-Class-358-135; US-Patent-Class-358-133; Int-Patent-Class-H04N-7/13) Avail: US Patent and Trademark Office CSCL 17B

A non-adaptive predictor, a nonuniform quantizer, and a multi-level Huffman coder are incorporated into a differential pulse code modulation system for coding and decoding broadcast video signals in real time.
Official Gazette of the U.S. Patent and Trademark Office

N92-10129# Oak Ridge National Lab., TN.
THREE EXPERIMENTS WITH STEREOSCOPIC TELEVISION: WHEN IT WORKS AND WHY
J. V. Draper, S. Handel, C. C. Hood (Human Machine Interfaces, Inc., Knoxville, TN.), and C. T. Kring 1991 7 p Presented at the Institute of Electrical and Electronics Engineers (IEEE) International Conference on Systems, Man, and Cybernetics, Charlottesville, VA, 4 Nov. 1991
(Contract DE-AC05-84OR-21400)
(DE91-016277; CONF-911162-1) Avail: NTIS HC/MF A02

Three experiments evaluated the impact of a stereoscopic television (STV) system on teleoperator performance. In the first, subjects performed Fitts' tapping task by hand using direct binocular, direct monocular, STV, and mono-image television (MTV) viewing. In the second, subjects performed the same task with a teleoperator using STV and MTV. In the third, subjects performed a prototypical task using STV and MTV. The results indicate that STV sometimes conferred a performance advantage, but the amount of the STV impact varied greatly across tasks. The results are discussed from the perspective of information availability during teleoperation and the need for a multi-measure approach to performance assessment. DOE

N92-10130# Oak Ridge National Lab., TN.
PHASE CONTROL IN A TWO-ELEMENT FOLDED WAVEGUIDE ARRAY
G. R. Haste 1991 4 p Presented at the 9th Topical Conference on Radio Frequency Power in Plasmas, Charleston, SC, 12-14

Aug. 1991
(Contract DE-AC05-84OR-21400)
(DE91-018251; CONF-910869-3) Avail: NTIS HC/MF A01

A pair of folded waveguides have been used to determine the mutual coupling and to measure the field distributions for the magnetic field components for single units and for a pair. The phase difference controls the field distribution and the Fourier spectrum. DOE

N92-10131# Sandia National Labs., Albuquerque, NM.
A DIGITAL ASIC IMPLEMENTATION OF A VIDEO FILTER FOR SYNTHETIC APERTURE RADAR
B. L. Remund, J. Chow, and J. Salinas (GigaBit Logic, Newbury Park, CA.) 1991 10 p Presented at the 1991 IEEE GaAs IC Symposium, Monterey, CA, 20 Oct. 1991
(Contract DE-AC04-76DP-00789)
(DE91-018400; SAND-91-0967C; CONF-9110202-1) Avail: NTIS HC/MF A02

Two GaAs Application Specific Integrated Circuits (ASICs) have been designed and implemented for a synthetic aperture radar which eliminate the dc bias in the sampled video data and increase the signal to noise ratio by summing the data across consecutive bursts. The High Pass Filter and Presummer ASICs process data at a maximum sample rate of 170 MHz and 125 MHz respectively. The chips are fully ECL and TTL compatible. The high pass filter is packaged in GigaBit's standard 132-pin ceramic package, while the presummer is packaged in TriQuint's standard 196-pin ceramic package. The presummer has been successfully tested in a prototype synthetic aperture radar at Sandia National Laboratories. The high pass filter has been successfully tested in a high speed test fixture. These ASICs provide flexibility and low power consumption at data rates previously unattainable with comparable hardware. DOE

N92-10132# Sandia National Labs., Albuquerque, NM.
ELECTROMAGNETIC OIL FIELD MAPPING FOR IMPROVED PROCESS MONITORING AND RESERVOIR CHARACTERIZATION
J. R. Waggoner and A. J. Mansure 1991 8 p Presented at the 3rd International Reservoir Characterization Technical Conference, Tulsa, OK, 3-5 Nov. 1991
(Contract DE-AC04-76DP-00789)
(DE91-017452; SAND-91-0980C; CONF-911125-1) Avail: NTIS HC/MF A02

Electromagnetic (EM) techniques are being developed to monitor oil recovery processes and improve overall process performance. Just as seismic surveys generate acoustic waves to detect changes in sonic velocity, and then infer rock properties, EM surveys generate electromagnetic fields to detect changes in electrical resistivity, and then infer fluid properties. The potential impact of the EM survey is very significant, primarily in the areas of locating oil, identifying oil inside and outside the pattern, characterizing flow units, and pseudo-real time process control to optimize process performance and efficiency. Since a map of resistivity is of no direct use to a reservoir engineer, an essential part of the EM technique is understanding the relationship between the process and the formation resistivity at all scales, and integrating this understanding into reservoir simulation. This abstract discusses the process we have developed for integrating EM measurements into reservoir characterization and simulation. DOE

N92-10133# Lawrence Livermore National Lab., CA.
RADAR APPLICATIONS OF GIGAWATT SOURCES AT MILLIMETER WAVE FREQUENCIES
J. A. Bruder and M. L. Belcher (Georgia Inst. for Research, Atlanta.) Jun. 1991 4 p Presented at the 16th International Conference on Infrared and Millimeter Waves, Lausanne (Switzerland), 26-30 Aug. 1991
(Contract W-7405-eng-48)
(DE91-017541; UCRL-CR-107206; CONF-9108146-1) Avail: NTIS HC/MF A01

The high transmit powers provided by free electron laser (FEL) sources in combination with the narrow antenna beamwidths achievable at millimeter wave (MMW) frequencies offer potential for use in a number of radar applications. Potential applications of high power millimeter wave sources include satellite imaging, low angle radar tracking, radar astronomy, and a number of other possible applications such as atmospheric research, space debris detection, and space vehicle tracking. DOE

N92-10134# Los Alamos National Lab., NM.
HARDWARE DESCRIPTION ADSP-21020 40-BIT FLOATING POINT DSP AS DESIGNED IN A REMOTELY CONTROLLED DIGITAL CW DOPPLER RADAR
R. E. Morrison and S. H. Robinson 1991 14 p Presented at the 2nd International Conference on Digital Signal Processing (DSP) Applications and Technology, Berlin (Germany), 28-31 Oct. 1991
(Contract W-7405-eng-36)
(DE91-018004; LA-UR-91-2804; CONF-9110199-1) Avail: NTIS HC/MF A03

A continuous wave Doppler radar system has been designed which is portable, easily deployed, and remotely controlled. The heart of this system is a DSP/control board using Analog Devices ADSP-21020 40-bit floating point digital signal processor (DSP) microprocessor. Two 18-bit audio A/D converters provide digital input to the DSP/controller board for near real time target detection. Program memory for the DSP is dual ported with an Intel 87C51 microcontroller allowing DSP code to be up-loaded or down-loaded from a central controlling computer. The 87C51 provides overall system control for the remote radar and includes a time-of-day/day-of-year real time clock, system identification (ID) switches, and input/output (I/O) expansion by an Intel 82C55 I/O expander. DOE

N92-10135# Los Alamos National Lab., NM.
THE APPLICATION OF THE ADSP-21020 40-BIT FLOATING POINT DSP MICROPROCESSOR IN A DIGITAL DOPPLER RADAR
S. H. Robinson and R. E. Morrison 26 Aug. 1991 7 p Presented at the 2nd International Conference on Digital Signal Processing (DSP) Applications and Technology, Berlin (Germany), 28-31 Oct. 1991
(Contract W-7405-eng-36)
(DE91-018005; LA-UR-91-2803; CONF-9110199-2) Avail: NTIS HC/MF A02

A continuous wave Doppler radar system has been designed which is portable, easily deployable and can be remotely controlled. The system is immune to ground clutter and is used for wind speed detection and direction determination. Nearly real time digital signal processing is performed by an Analog Devices ADSP-21020, a 40-bit floating point Digital Signal Processing (DSP) microprocessor. This paper provides an overview of the design of the system including the radio frequency (RF) to digital interface. The various DSP detection algorithms are discussed and compared to system performance and sensitivity. Finally, DSP performance is compared to the performance of an earlier system using Analog Device's ADSP-2100. DOE

N92-10136# Sandia National Labs., Albuquerque, NM.
A 500 MHz PHASE GENERATOR FOR SYNTHETIC APERTURE RADAR WAVEFORM SYNTHESIZERS
B. L. Remund and C. R. Srivatsa (GigaBit Logic, Newbury Park, CA.) 1991 4 p Presented at the 1991 IEEE GaAs IC Symposium, Monterey, CA, 20 Oct. 1991
(Contract DE-AC04-76DP-00789)
(DE91-018399; SAND-91-0966C; CONF-9110202-2) Avail: NTIS HC/MF A01

A GaAs Phase Generator ASIC has been developed using GigaBit's SC10000 standard cell library which produces the quadratic phase necessary to generate a linear-FM chirp waveform. Fully functional chips have been fabricated using a 3-layer metal, 0.9 (mu)m gate E/D-MESFET process. Measured maximum accumulation rates vary from 450 MHz to 590 MHz. The chip is fully ECL and TTL compatible and is packaged in GigaBit's standard 132-pin ceramic package. The phase generator has been

successfully tested in a prototype synthetic aperture radar at Sandia National Laboratories. Sample rates as high as 800 Msamples/sec have been synthesized using two phase generator/sine ROM combinations in parallel driving a TriQuint TQ6112 DAC. DOE

N92-10137# IIT Research Inst., Chicago, IL.
COMPILATION OF 1990 ANNUAL REPORTS OF THE NAVY ELF COMMUNICATIONS SYSTEM ECOLOGICAL MONITORING PROGRAM. VOLUME 1: TABS A, B Annual Report, Jan. - Dec. 1990
J. E. Zapotosky Aug. 1991 571 p
(Contract N00039-88-C-0065)
(AD-A239868; IITRI-E06628-4-Vol-1) Avail: NTIS HC/MF A24
CSCL 06/6

The Navy initiated studies in 1982 for possible bioelectromagnetic effects from operation of their ELF transmitters in Michigan and Wisconsin. Since then, resident biota have been monitored for effects while transmitters were operated at both intermittent low-power and continuous full-power conditions. This ninth compilation of investigator reports documents the technical progress of biological studies that were performed near the Michigan transmitter through 1989-1990. Near the Wisconsin transmitter, similar studies were completed during 1989. To date, investigators have not found any effects on biota from either an intermittent or a fully energized transmitter. Partial contents include: (1) development, installation and operation of the ambient monitoring system for air temperature, soil temperature, soil moisture, precipitation, global solar radiation, relative humidity, photo synthetically active radiation and soil chemistry; (2) tree productivity and growth of hardwoods and red pine; and (3) litter production including weight and nutrients. GRA

N92-10138# IIT Research Inst., Chicago, IL.
COMPILATION OF 1990 ANNUAL REPORTS OF THE NAVY ELF COMMUNICATIONS SYSTEM ECOLOGICAL MONITORING PROGRAM. VOLUME 2: TABS C THRU F Annual Report, Jan. - Dec. 1990
J. E. Zapotosky Aug. 1991 368 p
(Contract N00039-88-C-0065)
(AD-A239869; IITRI-E06628-4-Vol-2) Avail: NTIS HC/MF A16
CSCL 06/6

This portion of the report includes monitoring of and data for arthropoda and earthworms; pollinating insects; and small mammals and nesting birds. During the 1990 growing season the ELF antenna was operated more frequently than in prior years. This provides 2 years of intermittent ELF exposure for the biological systems to react to the radiation, one year of very limited exposure and greater exposure in 1990. Arthropod and earthworm sampling was conducted at intervals of two weeks from early May to late October. High voltage transmission lines and magnetic fields have been shown to affect honeybee reproduction, survival, orientation, and nest structure. ELF EM fields could have similar effects on native megachild bees. Changes in cell length, number of cells per nest, number of leaver per cell, orientation of nest entrances, and time to collect a round leaf pierce to cap a cell were monitored. We have not detected significant changes that could be attributed to ELF EM fields. Small mammal and nesting bird biological studies in the western Upper Peninsula of Michigan for the year 1990 are reported. GRA

N92-10139# IIT Research Inst., Chicago, IL.
COMPILATION OF 1990 ANNUAL REPORTS OF THE NAVY ELF COMMUNICATIONS SYSTEM ECOLOGICAL MONITORING PROGRAM. VOLUME 3: TABS G THRU I Annual Report, Jan. - Dec. 1990
J. E. Zapotosky Aug. 1991 503 p
(Contract N00039-88-C-0065)
(AD-A239870; IITRI-E06628-4-Vol-3) Avail: NTIS HC/MF A22
CSCL 06/6

This portion of the report includes monitoring of and data for bird species and communities, aquatic ecosystem and a listing of technical reports. Effects of extremely-low-frequency electromagnetic fields on most aspects of a bird species' life history are poorly understood. This investigation was designed to isolate effects of EM fields produced by ELF antenna systems on bird species breeding in or migrating through Wisconsin and Michigan. Specifically, we seek to determine if bird species richness and abundance differ between areas that are close to the antenna and those that are far enough away to be unaffected by the antenna. The goal of the aquatic ecosystems portion of the project is to determine the effects of low-level, long-term, electromagnetic radiation on the biota of streams. This electromagnetic radiation will be derived from the U.S. Navy's extremely low frequency submarine communication system (ELF) located in the upper peninsula of Michigan. The specific ecosystem being studied is the Ford River, a fourth order stream that arises in northern Dickinson and southern Marquette Counties and enters the Michigan portion of Green Bay south of Escanaba, Michigan. Detailed ecological sample and analyses are being conducted simutaneously at two sites. GRA

N92-10140# Marine Corps, Washington, DC.
C4I2 IN SPACE: SOLVING THE SATCOM SHORTFALL
Harold E. Bullock, Arthur J. Leeper, Michael S. McGuire, Hideo Sato, and Donald J. Singer 1 Apr. 1991 52 p
(AD-A239880) Avail: NTIS HC/MF A04 CSCL 22/2

Without a coordinated team-effort, an army can not hope for control on the battlefield. Without effective communication, a commander can not hope for effective command and control of his army. In today's highly-centralized, global command network, standard terrestrial communications alone are insufficient. Satellite communication is indispensable for command and control on today's battlefield, but requirements for SatCom far outstrip available resources. To exacerbate this problem, demand for reliable, long-haul, high-quality communication continues to grow geometrically. Satellites offer many well-known advantages for C4I2 in battlefield operations. These advantages include long range, freedom from obstructions, high quality, and increased interoperability. Satellite transmission allows units to communicate reliably over long distances. GRA

N92-10141# Test Group (6585th), Holloman AFB, NM. Ratscat Div.
THE USE AND MISUSE OF AIRCRAFT AND MISSILE RCS STATISTICS Final Report
Lee R. Bishop 31 Jul. 1991 10 p
(AD-A239892; RATSCAT-TM-91-001) Avail: NTIS HC/MF A02
CSCL 17/9

Both static and dynamic radar cross sections measurements are used for RCS predictions, but the static data are less complete than the dynamic. Integrated dynamics RCS data also have limitations for prediction radar detection performance. When raw static data are properly used, good first-order detection estimates are possible. The research to develop more-usable RCS statistics is reviewed, and windowing techniques for creating probability density functions from static RCS data are discussed. GRA

N92-10142# Michigan Univ., Ann Arbor. Ultrafast Science Lab.
TRANSPORT IN HETEROSTRUCTURES AND DEVICES IN MICROWAVE AND MILLIMETER-WAVE REGIMES Annual Report, 1 Apr. 1990 - 31 Mar. 1991
Gerard A. Mourou, John F. Whitaker, and Theodore B. Norris 19 Jul. 1991 18 p
(Grant AF-AFOSR-0214-90; AF Proj. 3484)
(AD-A239943; Rept-026845-910719) Avail: NTIS HC/MF A03
CSCL 20/12

Transport phenomena has been studied in semiconductors and superconductor materials, and devices, using ultrafast optical and electrical signals. Femtosecond optical absorption spectroscopy has been used to study the carrier dynamics in low-temperature epitaxially grown (LT) Gallium Arsenide. Optical techniques have also been used to observe for the first time the ballistic acceleration of electrons from the bandedge in a GaAs quantum well and the domain formation in superlattices as well as excitonic transport in quantum wells. Using LT GaAs ultrafast electrical signals, less than 1 ps in duration, have been produced

with amplitude up to 1 KV. These pulses have a frequency spectrum extending to 1 THz and have been used to study the physics of semiconductors and semiconductor devices in the high-field and high-frequency regime. Using LT GaAs photoconductive switches, and in conjunction with the electrooptic sampling we built an electro-optic analyzer capable of extracting S-parameters of active devices, up to 100 GHz. These techniques have been applied for the measurement of the fastest photoconductive response times of GaAs and In-GaAs epitaxially grown at 200 C. GRA

N92-10143# Mitre Corp., Bedford, MA.
INTEGRATION OF ELECTRONIC SUPPORT MEASURES (ESM) AND ALPHA-BETA RADAR TRACKER Final Report
Kwang H. Kim Aug. 1991 46 p Previously announced in IAA as A91-36928
(Contract F19628-89-C-0001)
(AD-A240031; MTR-11093; ESD-TR-91-208) Avail: NTIS HC/MF A03 CSCL 17/4

In target environments that include electronic countermeasures (ECM), where availability of radar range measurements is severely reduced, an integration of ESM data into a multi-sensor tracker provides an inexpensive but effective approach to augmenting radar tracking systems. Tracking-filter equations are presented for a multi-heterogenous sensor tracking system consisting of radars and ESM sensors. Measurement time-based track updating is performed, due to non-periodicity of ESM measurement acquisition times, instead of the usual track-based updating times. Track updating, using ESM measurements, is accomplished via an extended Kalman filter (EKF)-based algorithm and radar measurement via an alpha-beta tracking algorithm. The integration of data from different sensor types is a logical response to increasingly hostile airborne threats. The technique described in this paper is a straightforward and cost-effective approach for accomplishing that integration. GRA

N92-10144# Delaware Univ., Newark. Dept. of Mathematics.
OPTIMIZATION METHODS IN CONTROL OF ELECTROMAGNETIC FIELDS Final Report, 1 Sep. 1989 - 31 May 1991
Thomas S. Angell and Ralph E. Kleinman 31 May 1991 11 p
(Grant AF-AFOSR-0269-86; AF Proj. 2304)
(AD-A240044; AFOSR-91-0719TR) Avail: NTIS HC/MF A03 CSCL 20/14

This program is developing constructive methods for certain constrained optimization problems arising in the design and control of electromagnetic fields and in the identification of scattering objects. The problems addressed fall into three categories: (1) the design of antennas with optimal radiation characteristics measured in terms of directivity; (2) the control of the electromagnetic scattering characteristics of an object, in particular the minimization of its radar cross section, by the choice of material properties; and (3) the determination of the shape of scattering objects with various electromagnetic properties from scattered field data. The main thrust of the program is toward the development of constructive methods based on the use of complete families of solutions of the time-harmonic Maxwell equations in the infinite domain exterior to the radiating or scattering body. During the course of the work an increasing amount of attention has been devoted to the use of iterative methods for the solution of various direct and inverse problems. The continued investigation and development of these methods and their application in parameter identification has become a significant part of the program. GRA

N92-10914*# Geological Survey, Flagstaff, AZ.
TRIANGULATION USING SYNTHETIC APERTURE RADAR IMAGES
Sherman S. C. Wu and Annie E. Howington-Kraus *In* NASA, Washington, Reports of Planetary Geology and Geophysics Program, 1990 Jun. 1991 p 489 (For primary document see N92-10728 01-91)
Avail: NTIS HC/MF A25 CSCL 03B

33 ELECTRONICS AND ELECTRICAL ENGINEERING

Includes test equipment and maintainability; components, e.g., tunnel diodes and transistors; microminiaturization; and integrated circuitry.

For related information see also *60 Computer Operations and Hardware* and *76 Solid-State Physics.*

N92-10145# Lintel Technology, Inc., Roslyn, NY.
DIAMOND HEAT SINKS FOR ELECTRONIC CIRCUITS Progress Report
Chou H. Li 1990 4 p
(Contract N00014-90-C-0143)
(AD-A239750) Avail: NTIS HC/MF A01 CSCL 20/13

During the interim stage of this Phase 1 R and D, a useful metallizing procedure for bulk diamond has been developed, with natural diamond chips, granules, and polished wafers from two vendors. Small-scale statistical experiments were designed and executed by systematically varying several material and processing variables including: metallizing and brazing compositions, processing temperature and time, ambient control, and other procedural changes. Under selected combinations of these variables, metallizing of these diamond samples was achieved. Surface wetting appears to be excellent. The metallized surfaces were brazed or soldered to metal for future heat sink uses in high-power electronic circuits. These results clearly demonstrate the proof of the principle that is our main objective in Phase 1. The remainder of the Phase 1 work will be directed to metallizing and brazing polished diamond wafers to metal (copper and/or Kovar) substrates; detailed sample characterization including scanning electron microscopy (SEM), microstructural and microprobing analyses; thermal conductance measurements of mounted diamond wafers; and analyzing all results for the final report. GRA

N92-10146*# National Aeronautics and Space Administration. Pasadena Office, CA.
FORMATION OF SELF-ALIGNED GUARD RINGS FOR MONOLITHIC SCHOTTKY-BARRIER DIODE ARRAYS Patent Application
True-Lon Lin, inventor (to NASA) (Jet Propulsion Lab., California Inst. of Tech., Pasadena.) 16 May 1991 16 p
(Contract NAS7-918)
(NASA-Case-NPO-17734-1-CU; NAS 1.71:NPO-17734-1-CU; US-Patent-Appl-SN-700830) Avail: NTIS HC/MF A03 CSCL 09A

A method for fabricating self-aligned n-type guard rings in a body of p-type silicon for a silicide/Schottky-barrier diode array consists of depositing SiO2 with uniformly distributed phosphorus ions as a masking layer on the surface of the p-doped silicon body before etching the masking layer in the desired pattern of guard rings. N-type guard rings buried in the p-type silicon substrate are then formed by heating the structure to diffuse the phosphorus ions remaining on the surface functions as a mask for the remaining steps of the process which are to deposit metal over the entire surface of the structure and then form a silicide in those areas inside the SiO2 grid pattern by heating the structure. Metal not converted to a silicide is then removed by etching. The silicide and p-type silicon form a Schottky-barrier diode at their junction in areas inside the buried guard rings. Overlap of the silicide and the guard rings is minimized by this self-aligning technique to maximize the fill factor of the array. NASA

N92-10147# Danish Space Research Inst., Lyngby.
THE SHORT-CIRCUITED FLUXGATE SENSITIVITY PARAMETERS
F. Primdahl, P. Ripka, J. R. Petersen, and O. V. Nielsen (Technical Univ. of Denmark, Lyngby.) Feb. 1991 28 p
(ISSN-0109-6605) Avail: NTIS HC/MF A03

The short circuited fluxgate output current impulses depend on the input magnetic field, and on a number of parameters such as the fraction of time spent in saturation during the excitation

cycle, on the synchronous detection time impulse timing, and on core properties like the cross sectional area and the demagnetization factor. Following a theoretical treatment, experimental tests of these parameter dependences are reported, and additional experimental evidence of the noise performance is presented. Author

N92-10148# Sandia National Labs., Albuquerque, NM.
PROCEEDINGS OF THE SECOND SWITCH TUBE ADVANCED TECHNOLOGY MEETING
L. C. Beavis Jul. 1991 200 p Meeting held in Salem, MA, 21 Feb. 1991
(Contract DE-AC04-76DP-00789)
(DE91-017718; SAND-91-1045; CONF-9102131) Avail: NTIS HC/MF A09

The Second Switch Tube Technology Review Meeting was held at EG&G Salem, MA, on February 21, 1991. This document is a compilation of the abstracts, viewgraphs and written materials supplied by the presenters from Allied Signal Kansas City Division, EG&G Salem and Sandia National Laboratories. It has not been reviewed nor edited in any way. Also included is an agenda of the meeting and a list of attendees. Covered topics include, Temperature of Uniformity Survey, Brazing Furnace Atmosphere Purity Studies, Creep of Cu Braze Materials and Area Seal Braze Joints, Characterization of the Screen Printing Process, Purity and Structures, Grain Growth and Thermal Treatment of KOVAR, Laser Weldability Testing of KOVAR, Decarburization -- Is It Required, Gross Impurities in KOVAR, Carbon Doping Desorption Studies Update, and MC3857 Sprytron Carbon Doping Matrix Evaluation. DOE

N92-10149# Stanford Linear Accelerator Center, CA.
AUTOMATIC NETWORK ANALYZER PROCEDURES FOR 5045 KLYSTRON CAVITIES
J. G. Judkins Jul. 1991 7 p
(Contract DE-AC03-76SF-00515)
(DE91-018015; SU-SLAC-TN-91-10) Avail: NTIS HC/MF A02

This note describes the results of using Automatic Network Analyzers in measuring SLAC 5045 klystron cavities. Two different analyzers were compared; the HP8753 and HP8510. Both analyzers have frequency synthesizer accuracy and stability to perform the measurement without the need for a frequency counter. The klystron has six cavities which can be put into three categories; input, gain and output. The input and output cavities require an external Q measurement (Q(sub e)) to determine coupling (beta) and center frequency (f(sub 0)). The gain cavities require a resonant frequency measurement only. DOE

N92-10150# Northwestern Univ., Evanston, IL. Center for Quality Engineering and Failure Prevention.
QUANTITATIVE NON-DESTRUCTIVE EVALUATION OF HIGH-TEMPERATURE SUPERCONDUCTING MATERIALS
J. D. Achenbach 14 Jun. 1991 13 p
(Contract DE-FG02-86ER-13484)
(DE91-018284; DOE/ER-13484/5) Avail: NTIS HC/MF A03

Even though the currently intensive research efforts on high-temperature superconducting materials have not yet converged on a well specified practical material, the indications are that such a material may be quite brittle, anisotropic, and may contain many flaws such as microcracks and voids at grain boundaries. Consequently, practical applications of high temperature superconducting materials will require a very careful strength analysis based on fracture mechanics considerations. Because of the high sensitivity of the strength of such materials to the presence of defects, methods of quantitative non-destructive evaluation may be expected to play an important role in strength determinations. This proposal is concerned with the use of ultrasonic methods to detect and characterize isolated cracks, clusters of microcracks and microcracks distributed throughout the material. Particular attention has been, and will continue to be devoted to relating ultrasonic results to fracture mechanics considerations. DOE

N92-10151# Sandia National Labs., Albuquerque, NM.
A MINIATURE ACOUSTO-OPTIC IMAGE CORRELATOR
P. A. Molley, W. C. Sweatt, and D. S. Strong 1991 7 p Presented at the Society of Photo-Optical Instrumentation Engineers (SPIE) Meeting, San Diego, CA, 21-26 Jul. 1991
(Contract DE-AC04-76DP-00789)
(DE91-018002; SAND-90-3161C; CONF-9107115-44) Avail: NTIS HC/MF A02

An acousto-optic (AO) image correlator architecture will be presented that minimizes the overall system size while maintaining excellent image quality for large input scenes. The correlator can accommodate grayscale input scenes with dimensions of 512 x 244 pixels and grayscale reference templates of size 64 x 64 pixels. The size of the optical system, however is less than ten cubic inches, 1 in. x 1 in. x 9 in. This design incorporates a surface emitting laser diode array that has a center-to-center spacing of the laser elements matched to the row spacing on the CCD. Furthermore, the space-bandwidth and center frequency of the AO cell are chosen to match the length of the input image information in the cell to the width of the CCD. These two design decisions allow close to one-to-one imaging through the entire optical system producing the shortest possible path length. The optics were then designed with a goal of producing nearly diffraction-limited quality. DOE

N92-10152# Sandia National Labs., Albuquerque, NM.
STATUS OF THE REPETITIVE HIGH ENERGY PULSED POWER PROJECT
H. C. Harjes, K. J. Penn, K. W. Reed, C. R. McClenahan, G. E. Laderach, R. W. Wavrik, J. Adcock, M. Butler, G. A. Mann, and L. Martinez et al 1991 6 p Presented at the 8th IEEE Pulsed Power Conference, San Diego, CA, 17-19 Jun. 1991
(Contract DE-AC04-76DP-00789)
(DE91-018359; SAND-91-0178C; CONF-910640-44) Avail: NTIS HC/MF A02

High average power pulse compression systems are being considered for use in several applications. The Repetitive High Energy Pulsed Power (RHEPP) system will consist of a 7 stage magnetic pulse compressor driving a linear induction voltage adder with an e-beam diode load. It is being designed to deliver 350 kW of average power to the diode in 60 ns FWHM, 2.5 MV, 2.9 kJ pulses. Input power for the module is presently supplied by a 600 kW, 120 Hz, alternator (developed by Westinghouse Electric Corporation). Two stages in a bipolar, 2.5 kJ/pulse output mode. These stages are now being modified to operate in a unipolar, 5 kJ/pulse output mode. The design of the system is proceeding and several experiments are being conducted to support the design effort. A discussion of these experiments, the system design, and the status of the project is presented. DOE

N92-10153# Sandia National Labs., Albuquerque, NM.
SINTERED COMPACTS FOR HEAT SINKS AND PROCESS FOR FABRICATING SAME Patent Application
Akio Hara, inventor (to Sumitomo) and Shuji Yatsu, inventor (to Sumitomo) (Sumitomo Electric Industries Ltd., Itami, Japan) Nov. 1990 8 p Transl. into ENGLISH of Japanese Patent Application No. 32,154, 1987
(Contract DE-AC04-76DP-00789)
(DE91-018438; ALS/TR-90-021) Avail: NTIS HC/MF A02

The present invention relates to sintered compacts for heat sinks and to a process for their fabrication. Over the past few years, the semiconductor devices employed in high-field and high-current density applications have been adopted for practical use. Because power consumption density is especially high in the active regions of semiconductor lasers and IMPATT devices, modifications that prevent temperature rises in the devices are necessary. As a result, much attention has been devoted to materials which have a high thermal conductivity and are capable of serving as heat sinks. DOE

N92-10154# General Atomic Co., San Diego, CA.
HIGH TEMPERATURE CERAMIC SUPERCONDUCTORS Final Quarterly Report No. 8, 1 Apr. - 30 Jun. 1991

K. S. Mazdiyasni, K. C. Chen, and S. Paguio Jun. 1991 17 p
(Contract N00014-88-C-0714)
(AD-A239813; GA-C19465) Avail: NTIS HC/MF A03 CSCL 09/1

This is the eighth and final quarterly progress report on High Temperature Ceramic Superconductors. The principal objectives of this program are to demonstrate fabrication of high temperature ceramic superconductors that can operate at or above 90 K with appropriate current density, Jc, in forms useful for application in resonant cavities, magnets, motors, sensors, computers, and other devices; and to fabricate and demonstrate selected components made of these materials, including microwave cavities and magnetic shields. GRA

N92-10155# California Univ., Santa Barbara. Dept. of Electrical and Computer Engineering.
EFFICIENT, HIGH-SPEED, MONOLITHIC OPTOELECTRONIC CIRCUITS USING QUANTUM-CONFINED STRUCTURES
Larry A. Coldren 25 Jul. 1991 54 p
(Contract DAAL03-89-K-0078)
(AD-A239841; ARO-26922.13-EL) Avail: NTIS HC/MF A04 CSCL 20/10

This is the final report for DAAL03-89-K-0078, a program aimed at developing highly efficient quantum-confined structures for use in optoelectronic circuits using molecular beam epitaxy (MBE) technology. The focus has been primarily on the development of the enabling technologies for high efficiency and speed in integrable diode lasers. Improved MBE growth control for in situ grown quantum-wire structures and the creation of UHV in situ processing techniques have been key technological outcomes of this work. In the device area, one high-risk, high-payoff emphasis has been the growth and analysis of quantum-wire diode lasers. A new growth procedure has been developed for more uniform closely-packed wire arrays. Another device emphasis has been the design and fabrication of highly-efficient vertical-cavity surface-emitting lasers. In this latter area, record device performance has been greatly facilitated by many new theoretical contributions. In this report, we shall attempt to summarize our progress in the materials and processing as well as the device areas. GRA

N92-10156# Naval Postgraduate School, Monterey, CA.
ANALYSIS OF LOSS FOR INDUCTIVE STRIPS IN FINLINE M.S. Thesis
Levent Kurtoglu Sep. 1990 68 p
(AD-A239947) Avail: NTIS HC/MF A04 CSCL 09/1

This thesis introduces the effect of the loss to the homogeneous finline strip model. The expressions for the Quality Factors associated with the ohmic losses for inductive strips in homogeneous finline are derived and included in the CAD compatible circuit model in terms of the finite Q inductances. It is shown that the lossy circuit models more accurately predict the experimental response of an X band finline filter. Author (GRA)

N92-10157# Coriolis Corp., Saratoga, CA.
THERMAL MANAGEMENT OF HIGH HEAT FLUX ELECTRONIC COMPONENTS IN SPACE AND AIRCRAFT SYSTEMS, PHASE 1 Final Report, 28 Sep. 1989 - 5 May 1990
Arthur H. Iversen 18 Mar. 1991 51 p
(Contract F33615-89-C-2970)
(AD-A239982; WRDC-TR-90-2122-Phase-1) Avail: NTIS HC/MF A04 CSCL 09/1

The objectives of this Phase 1 program were to analyze, design, construct and demonstrate the application of curved surface cooling to power devices with the goal of demonstrating greater than 200 W/sq cm chip dissipation while maintaining junction temperatures within specification. Major components of the experiment comprised the test fixture for mounting the device under test and the cooling loop equipment and instrumentation. The work conducted in this Phase 1 study was to establish the basic parameters for the design of an entire class of efficient, compact, lightweight and cost competitive power conversion/conditioning systems for space, aircraft and general DOD requirements. This has been accomplished. Chip power dissipation of greater than 400 W/sq cm was demonstrated, and a general packaging and the thermal management design has been devised to meet the above requirements. The power limit reached was dictated by the junction temperature and not power dissipation, i.e., critical heat flux. The key to the packaging design is a basic construction concept that provides low junction to fluid thermal resistance. High heat flux dissipation without low thermal resistance is useless because excessive junction temperatures will results. GRA

N92-10158# Army Lab. Command, Fort Monmouth, NJ. Electronics Technology and Devices Lab.
PERFORMANCE CHARACTERIZATION OF MAGNESIUM/MANGANESE DIOXIDE BATTERIES Research and Development Technical Report, Sep. 1990 - Feb. 1991
Louis Jarvis Jul. 1991 13 p
(AD-A240037; SLCET-TR-91-22) Avail: NTIS HC/MF A03 CSCL 10/3

The effects of storage and temperature on the performance of magnesium/manganese dioxide batteries produced by two different manufacturers was studied. Both batteries performed extremely poorly at -17 C (0 F), losing over 70 percent capacity, compared with performance at 21 C (70 F) and above. After partial usage, and storage, both battery types lost as much as 25 hours of service. Overall, no appreciable difference existed between the batteries of the two manufacturers. GRA

N92-10159# Manlabs, Inc., Cambridge, MA.
CHARACTERIZATION OF ELECTRONIC MATERIALS Final Report, May 1987 - Apr. 1990
Edward P. Warekois Jul. 1991 15 p
(Contract F19628-87-C-0125)
(AD-A240063; RL-TR-91-118) Avail: NTIS HC/MF A03 CSCL 20/3

This report describes development and implementation of experimental techniques to fabricate specimens from new or novel materials developed under several Air Force programs. X-ray orientation, optical polishing and metallurgical processing are discussed. Specimen materials include hydrothermally grown quartz crystals, nonoxide based glasses, indium phosphide crystals, bismuth containing electro-optic materials and several other miscellaneous materials. GRA

N92-10382# Kuopio Univ. (Finland). Dept. of Applied Physics.
DUAL PIN DIODE PREAMPLIFIER FOR LASER DOPPLER VELOCIMETRY Abstract Only
H. Olkkonen *In* Oulu Univ., Proceedings of the 25th Annual Conference of the Finnish Physical Society 1991 1 p (For primary document see N92-10362 01-70)
Avail: NTIS HC/MF A12

N92-10529# Humboldt Univ., Berlin (German D.R.). Dept. of Electronics.
FABRICATION OF GaAs: MESFET's AND TEST STRUCTURES FOR ELECTRICAL MATERIAL CHARACTERIZATION Abstract Only
K. Wilke, G. Heymann, J. Varrio, and M. Pessa (Tampere Univ. of Technology, Finland) *In* Oulu Univ., Proceedings of the 25th Annual Conference of the Finnish Physical Society 1991 1 p (For primary document see N92-10362 01-70)
Avail: NTIS HC/MF A12

34 FLUID MECHANICS AND HEAT TRANSFER

Includes boundary layers; hydrodynamics; fluidics; mass transfer; and ablation cooling.

For related information see also *02 Aerodynamics* and *77 Thermodynamics and Statistical Physics.*

N92-10160*# Alabama Univ., Huntsville. Dept. of Chemical Engineering.
A NON-ISOTROPIC MULTIPLE-SCALE TURBULENCE MODEL Final Report, 15 Mar. 1989 - 15 Sep. 1990
C. P. Chen 15 Aug. 1990 38 p
(Contract NAS8-36955)
(NASA-CR-184217; NAS 1.26:184217) Avail: NTIS HC/MF A03 CSCL 20D

A newly developed non-isotropic multiple scale turbulence model (MS/ASM) is described for complex flow calculations. This model focuses on the direct modeling of Reynolds stresses and utilizes split-spectrum concepts for modeling multiple scale effects in turbulence. Validation studies on free shear flows, rotating flows and recirculating flows show that the current model perform significantly better than the single scale k-epsilon model. The present model is relatively inexpensive in terms of CPU time which makes it suitable for broad engineering flow applications. Author

N92-10161*# National Aeronautics and Space Administration. Langley Research Center, Hampton, VA.
NUMERICAL ANALYSIS AND SIMULATION OF AN ASSURED CREW RETURN VEHICLE FLOW FIELD
K. James Weilmuenster, Robert E. Smith, Jr., and Francis A. Greene Washington Sep. 1991 37 p
(NASA-TP-3101; L-16836; NAS 1.60:3101) Avail: NTIS HC/MF A03 CSCL 20D

A lifting body was proposed as a candidate for the Assured Crew Return Vehicle (ACRV) which will serve as a crew rescue vehicle for the Space Station Freedom. The focus is on body surface definition, both surface and volume grid definition, and the computation of inviscid flow fields about the vehicle at wind tunnel conditions. Very good agreement is shown between the computed aerodynamic characteristics of the vehicle at M(sub infinity) = 10 and those measured in wind tunnel tests at high Reynolds numbers. Author

N92-10162# Office National d'Etudes et de Recherches Aerospatiales, Paris (France). Direction de l'Aerodynamique.
NUMERICAL SIMULATION OF VORTEX BREAKDOWN Final Summary Report [SIMULATION NUMERIQUE DE L'ECALTEMENT TOURBILLONAIRE]
P. Mege and T. H. Le Jun. 1990 68 p In ENGLISH and FRENCH
(Contract DRET-89-34-001)
(ONERA-RSF-6/4368-AY-008A; ETN-91-90027) Avail: NTIS HC/MF A04

Isolated vortex breakdown is calculated. Second order time and fourth order spatial finite different schemas are used. A breakdown test in terms of the Roosby number is given. Breakdown provoked by an adverse pressure gradient is considered. Two other papers are included which cover the numerical simulation of vortex breakdown by solving the Euler equations for an incompressible fluid. For individual titles, see N92-10163 through N92-10164.

N92-10163# Office National d'Etudes et de Recherches Aerospatiales, Paris (France).
NUMERICAL SIMULATION OF VORTEX BREAKDOWN BY SOLVING THE EULER EQUATIONS FOR AN INCOMPRESSIBLE FLUID
T. H. Le, P. Mege, and Y. Morchoisne (Paris VI Univ., France) *In its* Numercical Simulation of Vortex Breakdown Jun. 1990 p 32-46 In FRENCH; ENGLISH summary Sponsored by Direction des Recherches, Etudes et Techniques (For primary document see N92-10162 01-34)
Avail: NTIS HC/MF A04

A method of calculating unsteady, three dimensional flows of inviscid incompressible fluid was used in research on vortex breakdown. This method is based on the solution of the unsteady Euler equations in a velocity-pressure formulation, discretized by centered finite difference schemes, accurate to the second order. The application dealt with relates to a single vortex that has an initial velocity profile resembling delta wing vortices. Comparisons are made with experimental data and with other simulation methods. ESA

N92-10164# Office National d'Etudes et de Recherches Aerospatiales, Paris (France).
NUMERICAL SIMULATION OF VORTEX BREAKDOWN VIA 3-D EULER EQUATIONS
T. H. Le, P. Mege, and Y. Morchoisne (Paris VI Univ., France) *In its* Numerical Simulation of Vortex Breakdown Jun. 1990 p 47-69 Presented at Turbulence 89, Grenoble, France, 18-21 Sep. 1989 (For primary document see N92-10162 01-34)
Avail: NTIS HC/MF A04

The long term goal is the modeling of vortex breakdown that occurs in some aerodynamic configurations at high angle of attack, (i.e., fighters with highly swept delta wings or missiles). A numerical simulation was made based on solving the 3-D Euler equations for an usteady incompressible flow. Preliminary results were obtained using a pressure-velocity formulation with periodic boundary conditions, the Euler equations being discretized by 2nd order finite difference schemes. The continuation to this work by implementing more realistic boundary conditions and 4th order finite difference discretization schemes are presented. ESA

N92-10165 North Carolina State Univ., Raleigh.
NONEQUILIBRIUM RADIATIVE HEATING PREDICTION METHOD FOR AEROASSIST FLOWFIELDS WITH COUPLING TO FLOWFIELD SOLVERS Ph.D. Thesis
Lin Clara Hartung 1991 176 p
Avail: Univ. Microfilms Order No. DA9123406

A method for predicting radiation absorption and emission coefficients in thermochemical nonequilibrium flows is developed. The method is called LORAN (Langley Optimized RAdiative Nonequilibrium code). It applies the smeared band approximation for molecular radiation to produce moderately detailed results and is intended to fill the gap between detailed but costly prediction methods, and very fast but highly approximate methods. The optimization of the method to provide efficient solutions allowing coupling to flow field solvers is discussed. Representative results are obtained and compared to previous nonequilibrium radiation methods, as well as to ground and flight measured data. Reasonable agreement is found in all cases. A multidimensional radiative transport method is also developed for axisymmetric flows. Its predictions for wall radiative flux are 20 to 25 pct. lower than those of the tangent slab transport method, as expected. The method was applied to the peak heating condition of the Aeroassist Flight Experiment (AFE) trajectory, with results comparable to predictions from other methods. The LORAN method was also applied in conjunction with the CFD code, LAURA, to study the sensitivity of the radiative heating prediction to various models used in nonequilibrium CFD. Author

N92-10166# National Aerospace Lab., Tokyo (Japan).
NUMERICAL ANALYSIS OF FULLY DEVELOPED LAMINAR FLOW IN CURVED RECTANGULAR CHANNELS
Hitoshi Yamada, Hiroshi Ishigaki, and Munekazu Mochizuki (National Aerospace Lab., Kakuda, Japan) May 1991 10 p In JAPANESE; ENGLISH summary
(NAL-TR-1111; ISSN-0389-4010) Avail: NTIS HC/MF A02

The Navier-Stokes equations were numerically solved using a finite volume method to simulate steady, fully developed, incompressible, and laminar flow in curved rectangular channels. Accurate solutions were obtained for a Dean number up to 550 by using the power-law scheme, whereas up to 900 using the

up-wind scheme. Numerical results were compared with available experimental and theoretical results, and it was subsequently determined that the friction factor is approximately 6 percent larger when the secondary flow changes from a two vortex to a four vortex pattern (Dean number = 116). In addition, the friction factor's slope was found to be different in the two and four vortex region. The calculated friction factor showed better agreement with the experimental results than did the other investigated theoretical results. Author

N92-10167*# National Aeronautics and Space Administration. Lewis Research Center, Cleveland, OH.
PULSE THERMAL ENERGY TRANSPORT SYSTEM Patent Application
Mark W. Weislogel, inventor (to NASA) 26 Jul. 1991 15 p
(NASA-Case-LEW-15235-1; NAS 1.71:LEW-15235-1; US-Patent-Appl-SN-736145) Avail: NTIS HC/MF A03 CSCL 20D

A pulse-thermal pump having a novel fluid flow wherein heat admitted to a closed system raises the pressure in a closed evaporator chamber, while another interconnected evaporator chamber remains open, is described. This creates a pressure differential, and at a predetermined pressure, the closed evaporator is opened and the opened evaporator is closed. The difference in pressure initiates fluid flow in the system. NASA

N92-10168# Los Alamos National Lab., NM.
RIPPLE: A NEW MODEL FOR INCOMPRESSIBLE FLOWS WITH FREE SURFACES
D. B. Kothe and R. C. Mjolsness 1991 9 p Presented at the AIAA/NASA/OAI Conference on Advanced SEI Technologies, Cleveland, OH, 3-4 Sep. 1991 Previously announced in IAA as A91-52433
(Contract W-7405-eng-36)
(DE91-017830; LA-UR-91-2818; CONF-9109226-10) Avail: NTIS HC/MF A02

A new free surface flow model, RIPPLE, is summarized. RIPPLE obtains finite difference solutions for incompressible flow problems having strong surface tension forces at free surfaces of arbitrarily complex topology. The key innovation is the Continuum Surface Force (CSF) model which represents surface tension as a (strongly) localized volume force. Other features include a high-order momentum advection model, a volume-of-fluid free surface treatment, and an efficient two-step projection solution method. RIPPLE'S unique capabilities are illustrated with two example problems: low-gravity jet-induced tank flow, and the collision and coalescence of two cylindrical rods. DOE

N92-10169# Los Alamos National Lab., NM.
A 3-D ADAPTIVE MESH REFINEMENT ALGORITHM FOR MULTIMATERIAL GAS DYNAMICS
E. G. Puckett (California Univ., Davis.) and J. S. Saltzman 12 Aug. 1991 18 p Presented at the 11th Annual Center for Nonlinear Studies (CNLS) Conference, Los Alamos, NM, 20-24 May 1991
(Contract W-7405-eng-36)
(DE91-018040; LA-UR-91-2745; CONF-9105252-1) Avail: NTIS HC/MF A03

Adaptive Mesh Refinement (AMR) in conjunction with high order upwind finite difference methods has been used effectively on a variety of problems. In this paper we discuss an implementation of an AMR finite difference method that solves the equations of gas dynamics with two material species in three dimensions. An equation for the evolution of volume fractions augments the gas dynamics system. The material interface is preserved and tracked from the volume fractions using a piecewise linear reconstruction technique. DOE

N92-10170*# Mississippi State Univ., Mississippi State. NSF Engineering Research Center for Computational Field Simulation.
TRANSFORMATION OF TWO AND THREE-DIMENSIONAL REGIONS BY ELLIPTIC SYSTEMS Semiannual Status Report, 1 Apr. - 30 Sep. 1991
C. Wayne Mastin 31 Oct. 1991 13 p
(Grant NsG-1577)
(NASA-CR-188982; NAS 1.26:188982) Avail: NTIS HC/MF A03 CSCL 20D

A reliable linear system is presented for grid generation in 2-D and 3-D. The method is robust in the sense that convergence is guaranteed but is not as reliable as other nonlinear elliptic methods in generating nonfolding grids. The construction of nonfolding grids depends on having reasonable approximations of cell aspect ratios and an appropriate distribution of grid points on the boundary of the region. Some guidelines are included on approximating the aspect ratios, but little help is offered on setting up the boundary grid other than to say that in 2-D the boundary correspondence should be close to that generated by a conformal mapping. It is assumed that the functions which control the grid distribution depend only on the computational variables and not on the physical variables. Whether this is actually the case depends on how the grid is constructed. In a dynamic adaptive procedure where the grid is constructed in the process of solving a fluid flow problem, the grid is usually updated at fixed iteration counts using the current value of the control function. Since the control function is not being updated during the iteration of the grid equations, the grid construction is a linear procedure. However, in the case of a static adaptive procedure where a trial solution is computed and used to construct an adaptive grid, the control functions may be recomputed at every step of the grid iteration. Author

N92-10171*# Institute for Computer Applications in Science and Engineering, Hampton, VA.
STABILITY OF THE FLOW AROUND A CYLINDER: THE SPIN-UP PROBLEM Final Report
S. R. Otto (Manchester Univ., England) Sep. 1991 26 p Submitted for publication
(Contract NAS1-18605)
(NASA-CR-187636; NAS 1.26:187636; ICASE-91-74) Avail: NTIS HC/MF A03 CSCL 20D

A concern is the flow around an infinite cylinder, which at a certain instant impulsively starts to spin. The growth of vortices in the resulting boundary layer occurring outside the cylinder is investigated. This layer is essentially a Rayleigh layer which grows with time, so the mechanism involved is similar to that studied in Hall (1983). Vortices with wavenumber comparable to the layer thickness are shown to be described by partial differential equations that govern the system numerically. It is assumed that the Rayleigh layer is thin, so particles are confined to move in a path with radius of curvature the same as the cylinder. The Goertler number is a function of time, so the time scale which produces an order, is considered one Goertler number. The right hand branch calculation is considered by letting the time tend to infinity, also inviscid Goertler modes are considered. Author

N92-10172# Westinghouse Hanford Co., Richland, WA.
AIR PULSED PLATE LIQUID-LIQUID EXTRACTOR SIMULATION
C. A. Barrington May 1991 434 p
(Contract DE-AC06-87RL-10930)
(DE91-018155; WHC-MR-0187) Avail: NTIS HC/MF A19

A simulation of bulk fluid behavior in pneumatically pulsed sieve-plate columns is developed primarily through application of fundamental concepts in thermodynamics and fluid mechanics. The simulation allows estimation of the time variation of many basic parameters such as gas and liquid pressures and positions of liquid interfaces. The simulation includes sufficient detail to allow use as an aid to the design of pneumatic pulse columns. An open system and adiabatic gas dynamics are assumed. A new pulse leg design is proposed and included in the mathematical development of the stimulation. The use of the simulation as an aid in designing a pulse leg for a hypothetical column is demonstrated. This entire work has been developed solely for the purpose of satisfying requirements for the degree of Master of Science in Chemical Engineering for the University of Washington in Seattle, Washington. DOE

N92-10173# Texas Univ., Austin.
NONLINEAR INTERACTIONS OF TEARING MODES IN THE PRESENCE OF SHEAR FLOW
X. L. Chen and P. J. Morrison Aug. 1991 29 p
(Contract DE-FG05-80ET-53088)
(DE91-018420; DOE/ET-53088/511; IFSR-511) Avail: NTIS HC/MF A03

The interaction of two near marginal tearing modes in the presence of shear flow is studied. To find the time asymptotic states, the resistive magnetohydrodynamic (MHD) equations are reduced to four amplitude equations, using center manifold reduction. These amplitude equations are subject to the constraints due to the symmetries of the physical problem. For the case without flow, the model which we adopted has translation and reflection symmetries. Presence of flow breaks the reflection symmetry, while the translation symmetry is preserved, and hence flow allows the coefficients of the amplitude equations to be complex. Bifurcation analysis is employed to find various possible time asymptotic states. In particular, the oscillating magnetic island states discovered numerically by Person and Bondeson are discussed. It is found that the flow introduced parameters (imaginary part of the coefficients) play an important role in driving these oscillating islands. DOE

N92-10174# Pittsburgh Energy Technology Center, PA.
STEADY FLOW OF A FLUID-SOLID MIXTURE IN A CIRCULAR CYLINDER
G. Johnson, K. R. Rajagopal (Pittsburgh Univ., PA.), M. Massoudi, and M. P. Mathur Sep. 1991 61 p Prepared in cooperation with Oak Ridge Associated Universities, Inc., TN
(Contract DE-AC05-76OR-00033)
(DE91-018698; DOE/PETC-TR/91/10) Avail: NTIS HC/MF A04

A mathematical description for a flowing mixture of solid particulates and a fluid similar to a coal-water slurry, is developed within the context of Mixture Theory. Specifically, the equations governing the flow of a two-component mixture of a Newtonian fluid and a granular solid are derived. These relatively general equations are then reduced to a system of coupled ordinary differential equations describing steady flow of the mixture through a pipe. The resulting boundary value problem is solved numerically and results are presented for cases in which drag and lift interactions are important. DOE

N92-10175# Naval Postgraduate School, Monterey, CA. Dept. of Mechanical Engineering.
A GENERAL-PURPOSE FINITE-DIFFERENCE CODE FOR SOLVING STEADY-STATE THREE-DIMENSIONAL FLUID-FLOW AND HEAT TRANSFER PROBLEMS Final Report, Jan. - Dec. 1990
Larry O. Haukenes, Sanjeev B. Sathe, Yogendra Joshi, and Matthew D. Kelleher Jul. 1991 59 p
(AD-A239857; NPS-ME-91-001) Avail: NTIS HC/MF A04 CSCL 12/5

A general purpose FORTRAN code is described for the computations of three dimensional steady heat transfer and fluid flow in rectangular geometries. The code is designed to handle combined conduction convection problems within domains comprising of both solid and fluid regions. This is accomplished through the use of the harmonic mean formulation for evaluating interface diffusivities. A control volume formulation is used to discretize the governing equations for the dependent variables in the primitive form. The velocity-pressure coupling is handled by the SIMPLER algorithm. THe iterative solution scheme employs the tri-diagonal matrix algorithm of Thomas. A sample example of three-dimensional natural convection in a rectangular enclosure is used to validate the code against existing numerical solutions. GRA

N92-10176# Universal Energy Systems, Inc., Dayton, OH.
THERMAL ENERGY STORAGE AND HEAT TRANSFER SUPPORT PROGRAM. VOLUME 1: TASK-1 HEAT TRANSPORT SYSTEM STUDY COPPER-WATER AND STEEL-SODIUM DWAHP Final Report, Jun. 1987 - Sep. 1990
R. Ponnappan 1 Mar. 1991 140 p
(Contract F33615-87-C-2738)
(AD-A239928; UES-799-TR-90-001-Vol-1; WRDC-TR-90-2121-Vol-1) Avail: NTIS HC/MF A07 CSCL 13/1

This report covers the test results of some extended research conducted on both 2 m copper-water double wall artery heat pipe and 2 m stainless steel-sodium heat pipe. The experimental results of the effective thermal conductivity of the wick agree with the predicted results. It is shown that the double wall wick is a boiling-tolerant wick and it can support high radial heat flux. The 2 m sodium-SS 304 heat pipe was successfully tested using a pyrolytic graphite heater after facing several failures with nichrome and cartridge type heaters. Inert gas-filled mode and conventional mode startup tests were conducted. The startup from frozen state was smooth in gas-filled mode whereas similar startup attempt was rough in the conventional mode. Calorimetric measurement of heat losses and tilt test results are also presented. GRA

N92-10177# Universal Energy Systems, Inc., Dayton, OH.
THERMAL ENERGY STORAGE AND HEAT TRANSFER SUPPORT PROGRAM. TASK-5 HEAT PIPE LIFE TEST STUDY. FACILITIES UPGRADING AND MAINTENANCE Final Report, Jun. 1987 - Sep. 1990
R. Ponnappan 1 Mar. 1991 79 p
(Contract F33615-87-C-2738)
(AD-A239929; UES-799-TR-90-005-Vol-3; WRDC-TR-90-2121-Vol-3) Avail: NTIS HC/MF A05 CSCL 20/13

This report describes the recommissioning, upgrading, and maintaining of thirty low and five high temperature heat pipe life test rigs. This is an ongoing research effort, originally put together by NASA LeRC, continued by the Air Force. The 92 cm long 1.27 cm dia. spacecraft-type heat pipes have completed nearly 74,000 hours of life tests. They exhibit varying Delta Ts across the length and symptoms of gas accumulation. Life test status and temperature profile for each pipe are presented. The sodium and potassium pipes have undergone relatively less hours of testing (34,000 hours) only. These five pipes are exhibiting normal status. All the life tests will continue till failure and there will be updates of this report. GRA

N92-10178# Universal Energy Systems, Inc., Dayton, OH.
THERMAL ENERGY STORAGE AND HEAT TRANSFER SUPPORT PROGRAM. VOLUME 2: TASK 4 THERMIONIC ENERGY CONVERSION STUDIES Final Report, 1 Jul. 1987 - 30 Sep. 1990
Mysore L. Ramalingam 1 Mar. 1991 147 p
(Contract F33615-87-C-2738)
(AD-A239968; UES-799-TR-90-004-Vol-2; WRDC-TR-90-2121-Vol-2) Avail: NTIS HC/MF A07 CSCL 10/2

This report provides the technical details on the research activities for Task-4 on the fabrication and utility installation for the three thermionic diode test stations and the diode processing station are discussed along with the instrumentation for actually testing the diodes. Experimental results as well as analytical characterization results have been provided in the form of J-V characteristics and discrepancies between the two have been explained. Emitter temperature calibration results have also been provided. Efforts are currently directed towards developing an automated pulse generating circuit to sweep (voltage) the diminiode and generate in ignited mode J-V characteristic in less than 5 msecs thereby taking advantage of the converter's thermal inertia properties. Performance verification tests were conducted on a planar diminiode with sintered Lanthanum Hexaboride as the emitter material and arc melted Lanthanum Hexaboride as the collection material. It was found that the performance of the diode was well in agreement with similar characteristics generated earlier. GRA

N92-10179# Pennsylvania State Univ., University Park. Dept. of Mechanical Engineering.
COUPLING BETWEEN RADIATION AND GAS DYNAMICS Final Report, 1 Feb. 1990 - 1 Feb. 1991
Charles L. Merkle and Michael M. Micci 31 May 1991 75 p
(Grant AF-AFOSR-0312-89; AF Proj. 2308)
(AD-A240004; AFOSR-91-0715TR) Avail: NTIS HC/MF A04 CSCL 21/3

Detailed experimental and analytic studies of microwave thermal propulsion are presented. Results are obtained for four geometric configurations: bluff-body stabilized resonant cavity plasmas; swirl-stabilized resonant cavity plasmas; free-floating plasmas in resonant cavities; and propagating, bluff-body stabilized plasmas in waveguides. Swirl stabilization proved to be less effective than bluff-body stabilization and was not modeled analytically. The experimental studies included both helium and nitrogen plasmas, while the analytic results are for helium only. In the free-floating plasmas, non-axisymmetric effects in the experimental setup led to arcing to the wall, limiting maximum power levels to about 500 W, although analysis suggests substantially higher upper power levels for this configuration. The bluff-body stabilized, resonant cavity plasmas, however, allowed power absorptions up to the maximum source power of 2.5 kW and 5 atm pressure for helium, although experiments in nitrogen were limited to lower powers. The analytic predictions agree well with the experiments in terms of plasma size, location, and response to parameters such as input power, mass flow rate, electromagnetic wave form, and pressure. The predicted coupling efficiencies and peak temperatures also agree well with measurements. Coupling efficiencies of near 100 percent can be obtained for the resonant cavity configurations, with somewhat lower efficiencies for the propagating plasmas. GRA

N92-10180# Illinois Inst. of Tech., Chicago. Fluid Dynamics Research Center.
MANAGEMENT AND CONTROL OF UNSTEADY AND TURBULENT FLOWS Final Technical Report, Oct. 1986 - Mar. 1990
Hassan M. Nagib, Mukund Acharya, Thomas C. Corke, Patrick H. Reisenthel, and Candace C. Wark Jul. 1991 15 p
(Contract F49620-86-C-0133)
(AD-A240050; AFOSR-91-0726TR) Avail: NTIS HC/MF A03 CSCL 20/4

Conclusions from a wide range of experiments in transitioning, turbulent, separated and unsteady flow fields include the following highlights: The simultaneous generation of controlled phase-coupled plane TS waves and oblique waves was used to investigate the development of three dimensional disturbances and mechanisms of transition in a Blasius boundary layer. From these experiments, the detuning of the fundamental/subharmonic resonance emerges as a primary candidate for the transition process under natural conditions. Three dimensional mappings of the Reynolds stress producing events in turbulent boundary layers over a range of Reynolds numbers and initial conditions have demonstrated that an integral size of these dynamical motions scales better with outer variables as compared with inner variables. While the wall or inner layer is responsible for their initial, the hierarchy of their scales in the log layer expands with Reynolds number according to this outer scaling. Real-time reactive control of a model unsteady separating flow was successfully implemented using a simple scheme for the detention of the separation. GRA

N92-10181# Kentucky Univ., Lexington. Dept. of Mechanical Engineering.
AN ADDITIVE TURBULENT DECOMPOSITION OF THE NAVIER-STOKES EQUATIONS IMPLEMENTED ON HIGHLY PARALLEL COMPUTER SYSTEMS Final Report
J. M. McDonough, E. C. Hylin, Tony F. Chan, Matthew T. Chan, and Y. Yang 5 Aug. 1991 49 p Prepared in cooperation with California Univ., Los Angeles
(Contract AF-AFOSR-0271-90; AF Proj. 2707)
(AD-A240131; AFOSR-91-0733TR) Avail: NTIS HC/MF A03 CSCL 20/4

Progress is reported on a study of a new turbulence simulation technique based on unaveraged, additive decomposition of the Navier Stokes equations. The decomposition formalism provides a natural separation of the governing equations into large- and small-scale parts, with the small scale solved in local subdomains. The method thus exhibits a high degree of automatic parallelism, and in addition is well-suited for application of domain decomposition methods as part of the solution process. Results presented include validation of a 2-D version of the small-scale equations, initial studies associated with bifurcation of solutions to these equations, qualitative comparisons with data, and analysis of the additive turbulent decomposition in two dimensional, generalized coordinates. GRA

35 INSTRUMENTATION AND PHOTOGRAPHY

Includes remote sensors; measuring instruments and gages; detectors; cameras and photographic supplies; and holography.

For aerial photography see *43 Earth Resources and Remote Sensing*. For related information see also *06 Aircraft Instrumentation*, and *19 Spacecraft Instrumentation*.

N92-10182*# National Aeronautics and Space Administration. Langley Research Center, Hampton, VA.
CONSTANT FREQUENCY PULSED PHASE-LOCKED LOOP MEASURING DEVICE Patent Application
William T. Yost, inventor (to NASA), Peter W. Kushnick, inventor (to NASA) (PRC Kentron, Inc., Hampton, VA.), and John H. Cantrell, inventor (to NASA) 26 Aug. 1991 23 p
(NASA-Case-LAR-13823-1; NAS 1.71:LAR-13823-1; US-Patent-Appl-SN-749737) Avail: NTIS HC/MF A03 CSCL 14B

A measuring apparatus is presented that uses a fixed frequency oscillator to measure small changes in the phase velocity ultrasonic sound when a sample is exposed to environmental changes such as changes in pressure, temperature, etc. The invention automatically balances electrical phase shifts against the acoustical phase shifts in order to obtain an accurate measurement of electrical phase shifts. NASA

N92-10183*# National Aeronautics and Space Administration. Lyndon B. Johnson Space Center, Houston, TX.
TWO-COLOR HOLOGRAPHY CONCEPT (T-CHI) Final Report
C. S. Vikram, H. J. Caulfield, G. L. Workman, J. D. Trolinger, C. P. Wood, R. L. Clark, A. D. Kathman, and R. M. Ruggiero (Teledyne Brown Engineering, Huntsville, AL.) Apr. 1990 65 p
(Contract NAS8-38078)
(NASA-CR-184240; NAS 1.26:184240) Avail: NTIS HC/MF A04 CSCL 14E

The Material Processing in the Space Program of NASA-MSFC was active in developing numerous optical techniques for the characterization of fluids in the vicinity of various materials during crystallization and/or solidification. Two-color holographic interferometry demonstrates that temperature and concentration separation in transparent (T-CHI) model systems is possible. The experiments were performed for particular (succinonitrile) systems. Several solutions are possible in Microgravity Sciences and Applications (MSA) experiments on future Shuttle missions. The theory of the T-CHI concept is evaluated. Although particular cases are used for explanations, the concepts developed will be universal. A breadboard system design is also presented for ultimate fabrication and testing of theoretical findings. New developments in holography involving optical fibers and diode lasers are also incorporated. Author

N92-10184*# Massachusetts Inst. of Tech., Cambridge. Center for Space Research.
EXPLOSIVE TRANSIENT CAMERA (ETC) PROGRAM Final Report
George Ricker Oct. 1991 254 p

(Grant NsG-7339)
(NASA-CR-188957; NAS 1.26:188957; MIT-85469) Avail: NTIS HC/MF A12 CSCL 14E

Since the inception of the ETC program, a wide range of new technologies was developed to support this astronomical instrument. The prototype unit was installed at ETC Site 1. The first partially automated observations were made and some major renovations were later added to the ETC hardware. The ETC was outfitted with new thermoelectrically-cooled CCD cameras and a sophisticated vacuum manifold, which, together, made the ETC a much more reliable unit than the prototype. The ETC instrumentation and building were placed under full computer control, allowing the ETC to operate as an automated, autonomous instrument with virtually no human intervention necessary. The first fully-automated operation of the ETC was performed, during which the ETC monitored the error region of the repeating soft gamma-ray burster SGR 1806-21. Author

N92-10185* National Aeronautics and Space Administration. Langley Research Center, Hampton, VA.
DUAL STRAIN GAGE BALANCE SYSTEM FOR MEASURING LIGHT LOADS Patent
Paul W. Roberts, inventor (to NASA) 15 Oct. 1991 9 p Filed 18 Sep. 1990 Supersedes N91-13687 (29 - 5, p 663)
(NASA-Case-LAR-14419-1; US-Patent-5,056,361; US-Patent-Appl-SN-584018; US-Patent-Class-73-147; US-Patent-Class-73-862.04; US-Patent-Class-73-862.65; Int-Patent-Class-G01L-5/16; Int-Patent-Class-G01M-9/00) Avail: US Patent and Trademark Office CSCL 14B

A dual strain gage balance system for measuring normal and axial forces and pitching moment of a metric airfoil model imparted by aerodynamic loads applied to the airfoil model during wind tunnel testing includes a pair of non-metric panels being rigidly connected to and extending towards each other from opposite sides of the wind tunnel, and a pair of strain gage balances, each connected to one of the non-metric panels and to one of the opposite ends of the metric airfoil model for mounting the metric airfoil model between the pair of non-metric panels. Each strain gage balance has a first measuring section for mounting a first strain gage bridge for measuring normal force and pitching moment and a second measuring section for mounting a second strain gage bridge for measuring axial force.
Official Gazette of the U.S. Patent and Trademark Office

N92-10186* National Aeronautics and Space Administration. Goddard Space Flight Center, Greenbelt, MD.
CONTROL SYSTEM FOR RULING BLAZED, ABERRATION CORRECTED DIFFRACTION GRATINGS Patent
Douglas B. Leviton, inventor (to NASA) 22 Oct. 1991 8 p Filed 23 Aug. 1990 Supersedes N91-13692 (29 - 5, p 664)
(NASA-Case-GSC-13240-1; US-Patent-5,058,281; US-Patent-Appl-SN-571344; US-Patent-Class-33-19.2; US-Patent-Class-33-23.02; Int-Patent-Class-B43L-13/24) Avail: US Patent and Trademark Office CSCL 14B

The grooved surface of an aberration-corrected holographic model grating is sensed by utilizing the sensing head of a scanning tunneling microscope. The sensing head is mechanically connected to a blazing type stylus for replicating the groove pattern of the holographic model on a ruled grating blank. A ruling engine causes the sensing head not only to scan the surface of the holographic grating model but also drive a blazing type ruling stylus or an equivalent type device in accordance with an error signal resulting from a departure of a sensing tip from the top of the holographic model groove as a function of tunneling current.
Official Gazette of the U.S. Patent and Trademark Office

N92-10187# Lawrence Livermore National Lab., CA.
SUBPICOSECOND X RAY STREAK CAMERA
M. W. Bowers, R. L. Shepherd, and R. E. Stewart 12 Jul. 1991 4 p Presented at the Society of Photo-Optical Instrumentation Engineers (SPIE) Meeting, San Diego, CA, 21-26 Jul. 1991
(Contract W-7405-eng-48)
(DE91-017664; UCRL-JC-107984; CONF-9107115-38) Avail: NTIS HC/MF A01

We have designed and built an x ray streak camera with subpicosecond time resolution. This camera attains its fast temporal resolution through a very strong extraction field, 100,000 V/cm, at the photocathode. It incorporates a narrow electron emission band photocathode that will also help the time resolution. The total time resolution has been calculated to be near 600 fs. DOE

N92-10188# CSA Engineering, Inc., Palo Alto, CA.
DEVELOPMENT OF A PRESSURE TRANSDUCER CALIBRATION SYSTEM (DYNAMIC PRESSURE RESPONSE CALIBER), PHASE 2 Final Report, Jun. 1989 - May 1991
Joseph R. Maly and David A. Kienholz Aug. 1991 53 p
(Contract F40600-89-C-0004)
(AD-A239859; AEDC-TR-91-13-Phase-2) Avail: NTIS HC/MF A04 CSCL 14/2

Current dynamic pressure calibrators are restricted in ultimate peak pressure, bandwidth, and accuracy; in fact, static calibrations are commonly performed for dynamic transducers. A dynamic transducer calibration system has been developed for the bandwidth of 2 to 2,500 Hz. Controlled pressure can be provided, in sine or random format, for a standard transducer and a test transducer. For the frequency bands of 2 to 150 Hz and 1600 to 2400 Hz, acoustic pressure levels up to 1.0 psi RMS can be attained. The development of this system demonstrated the application to acoustic-mechanical systems of a hybrid technique known as admittance modeling. (This technique combines experimentally derived test data with finite element model results.) The system can be used with a variety of dynamics transducers.
Author (GRA)

N92-10412# Helsinki Univ. of Technology, Espoo (Finland). Research Inst. for High Energy Physics.
THE DELPHI MICROVERTEX DETECTOR, A SILICON TRACKING CHAMBER Abstract Only
R. Brenner, Iiro Hietanen, Jukka Lindgren, R. Orava, C. Ronnqvist, and T. Tuuva *In* Oulu Univ., Proceedings of the 25th Annual Conference of the Finnish Physical Society 1991 1 p (For primary document see N92-10362 01-70)
Avail: NTIS HC/MF A12

N92-10413# European Organization for Nuclear Research, Geneva (Switzerland).
STUDY OF MUON TRIGGERS AND MOMENTUM RECONSTRUCTION IN A STRONG MAGNETIC FIELD FOR A MUON DETECTOR AT LHC Abstract Only
M. DellaNegra, K. Eggert, C. Bacci, S. Bettini, R. Cardarelli, S. Centro, F. Ceradini, G. Ciapetti, D. Cline, and D. Dau (Kiel Univ., Germany, F.R.) et al *In* Oulu Univ., Proceedings of the 25th Annual Conference of the Finnish Physical Society 1991 1 p (For primary document see N92-10362 01-70)
Avail: NTIS HC/MF A12

N92-10414# Helsinki Univ. of Technology, Espoo (Finland). Research Inst. for High Energy Physics.
DEVELOPMENT OF DOUBLE-SIDED SILICON STRIP DETECTORS Abstract Only
Iiro Hietanen, Richard Brenner, Jukka Lindgren, Tuure Tuuva, Kari Leinonen, and Hannu Ronkainen (Technical Research Centre of Finland, Espoo.) *In* Oulu Univ., Proceedings of the 25th Annual Conference of the Finnish Physical Society 1991 1 p (For primary document see N92-10362 01-70)
Avail: NTIS HC/MF A12

N92-10415# Helsinki Univ. of Technology, Espoo (Finland). Research Inst. for High Energy Physics.
RADIATION DAMAGE MEASUREMENTS ON DOUBLE-SIDED Si STRIP DETECTORS Abstract Only
Iiro Hietanen, Mikko Laakso, Tom Schulman, and Tuure Tuuva (European Organization for Nuclear Research, Geneva, Switzerland) *In* Oulu Univ., Proceedings of the 25th Annual Conference of

the Finnish Physical Society 1991 1 p (For primary document see N92-10362 01-70)
Avail: NTIS HC/MF A12

N92-10416# Helsinki Univ. of Technology, Espoo (Finland).
BEAM TEST RESULTS OF ION-IMPLANTED SILICON STRIP DETECTORS ON A 100 mm WAFER Abstract Only
Iiro Hietanen, Jukka Lindgren, R. Orava, Tuure Tuuva, R. Brenner, Mikael Andersson, Kari Leinonen, Hannu Ronkainen, L. Hubbeling, and M. Turala (European Organization for Nuclear Research, Geneva, Switzerland) et al *In* Oulu Univ., Proceedings of the 25th Annual Conference of the Finnish Physical Society 1991 1 p (For primary document see N92-10362 01-70)
Avail: NTIS HC/MF A12

N92-10417# Jyvaskyla Univ. (Finland). Dept. of Physics.
ION-GUIDE QUADRUPOLE MASS SPECTROMETER (IGQMS) Abstract Only
A. Iivonen, K. Morita, R. Saintola, K. Valli, and A. Yoshida (Institute of Physical and Chemical Research, Saitama, Japan) *In* Oulu Univ., Proceedings of the 25th Annual Conference of the Finnish Physical Society 1991 1 p (For primary document see N92-10362 01-70)
Avail: NTIS HC/MF A12

N92-10418# Helsinki Univ. of Technology, Espoo (Finland). Research Inst. for High Energy Physics.
STUDIES ON NEW LOW NOISE SILICON RADIATION DETECTOR Abstract Only
Mikko Laakso, P. Jalas, M. Juntunen, T. Tikkanen, E. Tuominen, K. Grahn, and Kari Leinonen (Technical Research Centre of Finland, Espoo.) *In* Oulu Univ., Proceedings of the 25th Annual Conference of the Finnish Physical Society 1991 1 p (For primary document see N92-10362 01-70)
Avail: NTIS HC/MF A12

N92-10448# Joensuu Univ. (Finland). Dept. of Physics.
PHOTORESIST CROSSED GRATINGS Abstract Only
Pekka Savander, Olli Salminen, and Tuula Keinonen *In* Oulu Univ., Proceedings of the 25th Annual Conference of the Finnish Physical Society 1991 1 p (For primary document see N92-10362 01-70)
Avail: NTIS HC/MF A12

N92-10449# Helsinki Univ. of Technology, Espoo (Finland). Dept. of Technical Physics.
RECONFIGURABLE OPTICAL INTERCONNECTIONS BY ACOUSTO-OPTIC HOLOGRAMS Abstract Only
Eero Tervonen, Ari T. Friberg, and Jari Turunen (Heriot-Watt Univ., Edinburgh, Scotland) *In* Oulu Univ., Proceedings of the 25th Annual Conference of the Finnish Physical Society 1991 1 p (For primary document see N92-10362 01-70)
Avail: NTIS HC/MF A12

N92-10451# Joensuu Univ. (Finland). Dept. of Physics.
HOLOGRAPHIC NONDESTRUCTIVE TESTING IN BONE BIOMECHANICS Abstract Only
Raimo Silvennoinen, Kaarlo Nygren, Juha Paatsama (Helsinki Univ. of Technology, Espoo, Finland), and Markku Kaernae *In* Oulu Univ., Proceedings of the 25th Annual Conference of the Finnish Physical Society 1991 1 p (For primary document see N92-10362 01-70)
Avail: NTIS HC/MF A12

N92-10521# Finnish Centre for Radiation and Nuclear Safety, Helsinki. Surveillance Dept.
CALIBRATION OF SCINTILLATION CELLS FOR RADON-222 MEASUREMENTS Abstract Only
Kyllikki Aakko and Eero Oksanen *In* Oulu Univ., Proceedings of the 25th Annual Conference of the Finnish Physical Society 1991 1 p (For primary document see N92-10362 01-70)
Avail: NTIS HC/MF A12

N92-10528# Oulu Univ. (Finland). Microelectronics Lab.
NOVEL TYPE OF CRYOGENIC LIQUID LEVEL SENSOR WITH HIGH SENSITIVITY Abstract Only
E. Immonen, A. Uusimaki, J. Hagberg, S. Leppavuori, and T. Porjesz (Eoetvoes Lorand Univ., Budapest, Hungary) *In its* Proceedings of the 25th Annual Conference of the Finnish Physical Society 1991 1 p (For primary document see N92-10362 01-70)
Avail: NTIS HC/MF A12

N92-10534# Tampere Univ. of Technology (Finland). Dept. of Physics.
LOW PRESSURE IMPACTOR WITH ELECTRICAL CONCENTRATION DETECTION Abstract Only
J. Keskinen and Kimmo Pietarinen *In* Oulu Univ., Proceedings of the 25th Annual Conference of the Finnish Physical Society 1991 1 p (For primary document see N92-10362 01-70)
Avail: NTIS HC/MF A12

N92-10537# Institute of Occupational Health, Turku (Finland).
A MEASURING ROBOT FOR THERMAL ENVIRONMENT, CONTAMINANT CONCENTRATION AND VENTILATION STUDIES Abstract Only
E. Minni, H. Koskela, J. Pekkarinen, and R. Niemela (Institute of Occupational Health, Helsinki, Finland) *In* Oulu Univ., Proceedings of the 25th Annual Conference of the Finnish Physical Society 1991 1 p (For primary document see N92-10362 01-70)
Avail: NTIS HC/MF A12

36 LASERS AND MASERS

Includes parametric amplifiers.
For related information see also *76 Solid-State Physics.*

N92-10189# Tokyo Univ. (Japan). Inst. of Space and Astronautical Science.
LASER INTERFEROMETER (TENKO-10 AND -100) FOR GRAVITATIONAL WAVE ANTENNA DEVELOPMENT
Nobuki Kawashima Jul. 1991 15 p
(ISAS-640; ISSN-0285-6808) Avail: NTIS HC/MF A03

Development of 10 m 102 bounce laser interferometer gravitational wave antenna (TENKO-10) at ISAS is described. The objective is to establish the engineering background for the laser interferometer gravitational wave antenna in Japan so that a km class antenna can be constructed for the detection of gravitational waves in the future. A particular emphasis was on the achievement of a long term stable operation, 127 hour operation was realized in Feb. to Mar. 1989 and more than 5 hour continuous operation was done without any adjustment. An upgrade of the interferometer to 100 m (TENKO-100) is going to be started in 1991 and will be completed in 1994. Author

N92-10190# Lawrence Livermore National Lab., CA.
CAVITY ISSUES FOR Ni-LIKE Ta X RAY LASERS
D. C. Eder, L. B. DaSilva, R. A. London, B. J. MacGowan, and S. Maxon Jun. 1991 7 p Presented at the Society of Photo-Optical Instrumentation Engineers (SPIE) Meeting, San Diego, CA, 21-26 Jul. 1991
(Contract W-7405-eng-48)
(DE91-017668; UCRL-JC-105900; CONF-9107115-37) Avail: NTIS HC/MF A02

Lasing has been demonstrated at 44.83 Angstrom in Ni-like Ta (Phys. Rev. Lett. 65, 420 (1990)) with a gain of order 3/cm over a length of 3 cm. This wavelength is suitable for holography of biological specimens provided that sufficient energy is available. The duration of the x ray laser pulse (FWHM of order 0.35 ns) allows the possibility of a second pass through the lasing medium to increase the output energy. The dependences of the output energy on the reflectivity of the multilayer mirror, the separation of the mirror from the lasing medium, and the duration of lasing are explored in this paper. The x ray laser plasma is a strong source of x rays (energies up to 2 keV) that can damage the

multilayer mirror. We examine the heating of the multilayer mirror as a function of the separation from the lasing medium. The effect of the mirror shape (radius of curvature and whether the surface is flat, concave, or convex) on the output energy and degree of coherence of the x ray laser is given. DOE

N92-10191# Los Alamos National Lab., NM.
OPTICAL AND ELECTRICAL INVESTIGATIONS INTO CATHODE IGNITION AND DIODE CLOSURE
J. J. Coogan, E. A. Rose, and R. P. Shurter 1991 5 p Presented at the 8th IEEE Pulsed Power Conference, San Diego, CA, 17-19 Jun. 1991
(Contract W-7405-eng-36)
(DE91-017823; LA-UR-91-1955; CONF-910640-43) Avail: NTIS HC/MF A01

The temporal behavior of high-power diodes is closely related to the impedance collapse caused by the movement of the cathode and/or anode plasmas. This impedance collapse can be especially problematic when a constant power electron beam is required. This is the case for the very large area (square meters) diodes used to pump the amplifiers within the Aurora KrF laser system. The electron beam technology development program at Los Alamos utilizes the Electron Beam Test Facility (EGTF) to study diode physics in an attempt to better understand the basic phenomenology of ignition and closure. A combination of optical and electric diagnostics has been fielded on the Electron Beam Test Facility to study ignition and closure in large area electron beam diodes. A four-channel framing camera is used to observe the formation of microplasmas on the surface of the cathode and the subsequent movement of these plasmas toward the anode. Additionally, a perveance model is used to extract information about this plasma from voltage and current profiles. Results from the two diagnostics are compared. Closure velocity measurements are presented showing little dependence on applied magnetic field for both velvet and carbon felt emitters. We also report the first observation of the screening effect in large area cold cathode diodes. DOE

N92-10192# California Univ., Santa Barbara.
ELECTRON ACCELERATION BY LASER FIELDS IN A GAS
J. R. Fontana Aug. 1991 98 p
(Contract DE-AS03-84ER-40136)
(DE91-018269; DOE/ER-40136/T10) Avail: NTIS HC/MF A05

This report discusses electron acceleration by passes through a Gaussian-mode laser beam in an index matching gas; electron beam dynamics in gas media; energy loss and scattered trajectory simulations for electrons in gases; interaction within an optical waveguide; refractive index enhancement techniques; and collaboration with SDI Optronics. DOE

N92-10193# Edgerton, Germeshausen and Grier, Inc., Idaho Falls, ID.
LASER ACOUSTIC TECHNOLOGY DEMONSTRATION AND EQUIPMENT FIELD TRAILS
J. G. Rodriguez and D. M. Tow May 1991 20 p
(Contract DE-AC07-76ID-01570)
(DE91-018759; EGG-MS-9726) Avail: NTIS HC/MF A03

A fieldable, noncontacting, laser acoustic method to characterize chemical weapon (CW) containers has been demonstrated. The laser sensor detects the vibrational response of CW containers to acoustic excitation. Laboratory results demonstrated that the vibrational signatures are unique to the fill material of the munition containers. The field trials, at Tooele Utah Army Depot, demonstrated that this noncontacting inspection technique could identify distinctive vibrational signatures for various chemical and conventional agents in munitions containers in a nonlaboratory environment. DOE

N92-10194# Center for Night Vision and Electro-Optics, Fort Belvoir, VA.
LASER INDUCED OPTICAL DAMAGE IN SOLIDS Final Report
Gary L. Wood and Edward J. Sharp Jul. 1991 36 p
(AD-A240124; AMSEL-NV-TR-0097) Avail: NTIS HC/MF A03 CSCL 09/3

This report examines some of the many mechanisms that lead to catastrophic damage of solids by high intensity optical radiation. Both surface and bulk damage are explored including: the different mechanisms of avalanche breakdown, thermal runaway, acoustic damage, nonlinear effects, the role of plasmas in damage, and the effects of surface preparation on damage thresholds. The relevant radiation and material characteristics are given for each damage mechanism, and the damage thresholds for a variety of materials are reported. Suggestions are offered on ways to raise the threshold for optical damage. GRA

N92-10452# Helsinki Univ. of Technology, Espoo (Finland). Dept. of Technical Physics.
SINGLE-SHOT SPECTRAL MEASUREMENTS OF MULTIMODE PULSED DYE LASERS Abstract Only
T. Kajava, H. Lauranto, and Rainer Salomaa *In* Oulu Univ., Proceedings of the 25th Annual Conference of the Finnish Physical Society 1991 1 p (For primary document see N92-10362 01-70)
Avail: NTIS HC/MF A12

N92-10453# Helsinki Univ. of Technology, Espoo (Finland). Inst. of Metrology Research.
A SIMPLE METHOD TO STABILIZE THE FREQUENCY OF SEMICONDUCTOR LASERS Abstract Only
Hanne Ludvigsen, Christer Holmlund (Technical Research Centre of Finland, Espoo.), and Erkki Ikonen *In* Oulu Univ., Proceedings of the 25th Annual Conference of the Finnish Physical Society 1991 1 p (For primary document see N92-10362 01-70)
Avail: NTIS HC/MF A12

37 MECHANICAL ENGINEERING

Includes auxiliary systems (nonpower); machine elements and processes; and mechanical equipment.

N92-10195*# National Aeronautics and Space Administration. Lewis Research Center, Cleveland, OH.
A METHOD FOR DETERMINING SPIRAL-BEVEL GEAR TOOTH GEOMETRY FOR FINITE ELEMENT ANALYSIS
Robert F. Handschuh and Faydor L. Litvin (Illinois Univ., Chicago.) Aug. 1991 16 p Original contains color illustrations
(DA Proj. 1L1-62211-A-47A)
(NASA-TP-3096; E-5837; NAS 1.60:3096; AVSCOM-TR-91-C-020)
Avail: NTIS HC/MF A03; 1 functional color page CSCL 13I

An analytical method was developed to determine gear tooth surface coordinates of face-milled spiral bevel gears. The method uses the basic gear design parameters in conjunction with the kinematical aspects of spiral bevel gear manufacturing machinery. A computer program, SURFACE, was developed. The computer program calculates the surface coordinates and outputs 3-D model data that can be used for finite element analysis. Development of the modeling method and an example case are presented. This analysis method could also find application for gear inspection and near-net-shape gear forging die design. Author

N92-10196*# National Aeronautics and Space Administration. Langley Research Center, Hampton, VA.
APPARATUS AND METHOD FOR EXPLOSIVE BONDING TO EDGE OF FLYER PLATE Patent Application
Laurence J. Bement, inventor (to NASA) and Anne C. Kushnick, inventor (to NASA) (PRC Kentron, Inc., Hampton, VA.) 2 Oct. 1991 17 p
(NASA-Case-LAR-14096-1; NAS 1.71:LAR-14096-1;
US-Patent-Appl-SN-591644) Avail: NTIS HC/MF A03 CSCL 13H

The invention is an apparatus and a process for the explosive joining of a flyer plate and a base plate. The apparatus consists of a flyer plate positioned over a base plate. The flyer plate has a notch containing a filler material in intimate contact with the flyer

plate. An adhesive means holds a ribbon explosive partially overlapping the notch in the flyer plate. A detonating means initiates the ribbon explosive that drives the flyer plate to accomplish a high velocity, angular collision between the mating surfaces. This collision creates surface melts and effacing bonding, resulting in electron-sharing linkups between the plates. An unbonded tap of the flyer plate is lifted and levered to apply a peeling stress to the limit of the bond. The unbonded tab fractures at a base of the notch leaving a bond to an edge of the attached flyer plate.
NASA

N92-10197* National Aeronautics and Space Administration. Lyndon B. Johnson Space Center, Houston, TX.
MECHANIZED FLUID CONNECTOR AND ASSEMBLY TOOL SYSTEM WITH BALL DETENTS Patent
Ronald C. Zentner, inventor (to NASA) and Steven A. Smith, inventor (to NASA) 22 Oct. 1991 10 p Filed 9 Nov. 1989
Supersedes N90-17138 (28 - 9, p 1230)
(NASA-Case-MSC-21434-1; US-Patent-5,058,929; US-Patent-Appl-SN-433881; US-Patent-Class-285-39; US-Patent-Class-285-353; US-Patent-Class-285-23; US-Patent-Class-285-912; Int-Patent-Class-F16L-15/00) Avail: US Patent and Trademark Office CSCL 13K

A fluid connector system is disclosed which includes a modified plumbing union having a rotatable member for drawing said union into a fluid tight condition. A drive tool is electric motor actuated and includes a reduction gear train providing an output gear engaging an integral peripheral spur gear on the rotatable member. Coaxial alignment means are attached to both the connector assembly and the drive tool. A hand lever actuated latching system includes a plurality of circumferentially spaced latching balls selectively wedged against the alignment means attached to the connector assembly or to secure the drive tool with its output gear in mesh with the integral peripheral spur gear. The drive motor is torque, speed, and direction controllable.
Official Gazette of the U.S. Patent and Trademark Office

N92-10198# Oak Ridge National Lab., TN.
BES WELDING SCIENCE CONTRACTORS SUMMARY REPORT, 1990--1991
S. A. David, comp. 1991 33 p
(Contract DE-AC05-84OR-21400)
(DE91-018510; ORNL/M-1677) Avail: NTIS HC/MF A03

This is a compilation of four short papers on the subject of welding. Researchers from Oak Ridge National Laboratory, Pennsylvania State University, Colorado School of Mines, and the University of Alabama contributed to this coordinated research effort. Weld metal microstructure, crack propagation, mass transfer, surface tension, composite materials, grain boundaries, and the properties of various alloys are topics of discussion. DOE

N92-10199# Naval Ocean Systems Center, San Diego, CA.
ADVANCES AND EXPERIENCE WITH TELEOPERATED SYSTEMS INCORPORATING REMOTE PRESENCE
Professional Paper
D. W. Murphy Aug. 1991 7 p
(AD-A239980) Avail: NTIS HC/MF A02 CSCL 13/9

This paper discusses progress at the Hawaii Laboratory over the past three years in the development of three teleoperated systems: the Advanced Tethered Vehicle (ATV), the TeleOperated Vehicle (TOV), and the TeleOperated/telePresence System (TOPS). We will comment on experience to data with these systems, pointing to the need for additional sensory information by the remote system operator to achieve increased performance. Each of these systems addresses a different mission, but all share common approaches to subsystem design and to various degrees incorporate remote presence. ATV and TOV utilize a fiber optic data link for high band width, small size, ruggedness, and in the case of the TOV, jam resistance and covertness. GRA

38 QUALITY ASSURANCE AND RELIABILITY

Includes product sampling procedures and techniques; and quality control.

N92-10200*# Alabama Univ., Huntsville.
AUTOMATED EDDY CURRENT ANALYSIS OF MATERIALS Final Report
Gary L. Workman 24 Jun. 1990 54 p
(Contract NAS8-36955)
(NASA-CR-184216; NAS 1.26:184216) Avail: NTIS HC/MF A04 CSCL 14D

This research effort focused on the use of eddy current techniques for characterizing flaws in graphite-based filament-wound cylindrical structures. A major emphasis was on incorporating artificial intelligence techniques into the signal analysis portion of the inspection process. Developing an eddy current scanning system using a commercial robot for inspecting graphite structures (and others) has been a goal in the overall concept and is essential for the final implementation for expert system interpretation. Manual scans, as performed in the preliminary work here, do not provide sufficiently reproducible eddy current signatures to be easily built into a real time expert system. The expert systems approach to eddy current signal analysis requires that a suitable knowledge base exist in which correct decisions as to the nature of the flaw can be performed. In eddy current or any other expert systems used to analyze signals in real time in a production environment, it is important to simplify computational procedures as much as possible. For that reason, we have chosen to use the measured resistance and reactance values for the preliminary aspects of this work. A simple computation, such as phase angle of the signal, is certainly within the real time processing capability of the computer system. In the work described here, there is a balance between physical measurements and finite element calculations of those measurements. The goal is to evolve into the most cost effective procedures for maintaining the correctness of the knowledge base. Author

N92-10201# Cincinnati Univ., OH. Dept. of Aerospace Engineering.
APPROXIMATE EVALUATION OF RELIABILITY AND RELATED QUANTITIES VIA PERTURBATION TECHNIQUES Final Technical Report, 1 Sep. 1989 - 30 Sep. 1990
Bruce K. Walker and Ramaswamy Srichander Dec. 1990 107 p
(Grant AF-AFOSR-0486-89; AF Proj. 2304)
(AD-A240049; AFOSR-91-0716TR) Avail: NTIS HC/MF A06 CSCL 12/4

The evaluation of the reliability, stability, and performance of fault tolerant control systems (FTCS) is considered. New sufficient conditions for stochastic stability of FTCS with standard Markovian component failure behavior and Markovian failure detection decision behavior are derived. By specializing these results to the class of linear time-invariant (LTI) FTCS with linear state feedback control laws that are reconfigured by switching the feedback gain matrix according to the identified failure configuration, the stability results are strengthened to necessary and sufficient conditions for stochastic stability of a special type (exponential in mean square) that implies a very strong sense of stability (a.s. in probability). An approximate feedback control design technique for LTI FTCS is then proposed and demonstrated on a simple numerical case. In addition, previous results on semi-Markov analysis of FTCS reliability are used to derive a numerical method for establishing approximately optimal failure detection test thresholds for sequential failure detection tests. This method, though approximate, is shown to yield thresholds that provide a considerable increase in system reliability relative to those provided by a method based on a rigorously derived reliability approximation for one numerical example. GRA

39 STRUCTURAL MECHANICS

Includes structural element design and weight analysis; fatigue; and thermal stress.

For applications see *05 Aircraft Design, Testing and Performance* and *18 Spacecraft Design, Testing and Performance.*

N92-10202*# National Aeronautics and Space Administration. Langley Research Center, Hampton, VA.
MULTI-DEGREE OF FREEDOM, ACTIVE VIBRATION CONTROL METHOD, AND SYSTEM Patent Application
Richard J. Silcox, inventor (to NASA), Chris R. Fuller, inventor (to NASA), and Gary P. Gibbs, inventor (to NASA) (Virginia Polytechnic Inst. and State Univ., Blacksburg.) 4 Mar. 1991 27 p
(NASA-Case-LAR-14508-1-CU; NAS 1.71:LAR-14508-1-CU; US-Patent-Appl-SN-664194) Avail: NTIS HC/MF A03 CSCL 20K

Arrays of actuators are affixed to structural elements to impede the transmission of vibrational energy. A single pair is used to provide control of bending and extensional waves and two pairs are used to control torsional motion. The arrays are applied to a wide variety of structural elements such as a beam structure that is part of a larger framework that may or may not support a rigid or non-rigid skin. Electrical excitation is applied to the actuators that generate forces on the structure. These electrical inputs may be adjusted in their amplitude and phase by a controller in communication with appropriate vibrational wave sensors to impede the flow of vibrational power in all of the above mentioned wave forms beyond the actuator location. Additional sensor elements can be used to monitor the performance and adjust the electrical inputs to maximize the attenuation of vibrational energy. NASA

N92-10203*# National Aeronautics and Space Administration. Langley Research Center, Hampton, VA.
PREDICTION OF MATRIX FATIGUE CRACK INITIATION IN NOTCHED SCS-6/Ti-15-3 METAL MATRIX COMPOSITES
B. M. Hillberry (Purdue Univ., West Lafayette, IN.) and W. S. Johnson Oct. 1991 16 p
(NASA-TM-104141; NAS 1.15:104141) Avail: NTIS HC/MF A03 CSCL 20K

Several lay-ups of SCS-6/Ti-15-3 metal matrix composites were tested in either a center hole or a double edge notched geometry. At different cyclic strss levels, the number of cycles required to develop matrix fatigue cracks at the notches was recorded. A fatigue strat-life curve was developed for the Ti-15-3 matrix material. This modified parameter predicted the number of cycles required for matrix crack initiation at the notches. The predictions were in good agreement with the experimental data. Author

N92-10204# Sandia National Labs., Albuquerque, NM.
A FREQUENCY DOMAIN METHOD FOR THE GENERATION OF PARTIALLY COHERENT NORMAL STATIONARY TIME DOMAIN SIGNALS
D. O. Smallwood and T. L. Paez 1991 10 p Presented at the 62nd Shock and Vibration Symposium, Springfield, VA, 29-31 Oct. 1991
(Contract DE-AC04-76DP-00789)
(DE91-017058; SAND-91-0983C; CONF-9110189-1) Avail: NTIS HC/MF A02

A procedure for generating vectors of time domain signals which are partially coherent in a prescribed manner is described. The procedure starts with the spectral density matrix, (G(sub xx)(f)), that relates pairs of elements of the vector random process (x(t)), -infinity less than t less than infinity. The spectral density matrix is decomposed into the form: (G(sub xx)(f)) = (U(f)) (S(f)) (U(f))' where (U(f)) is a matrix of complex frequency response functions, and (S(f)) is a diagonal matrix of real functions which can vary with frequency. The factors of the spectral density matrix, (U(f)) and (S(f)), are then used to generate a frame of random data in the frequency domain. The data is transformed into the time domain using an inverse FFT to generate a frame of data in the time domain. Successive frames of data are then windowed, overlapped, and added to form a vector of normal stationary sampled time histories, (x(t)), of arbitrary length. DOE

N92-10205*# Illinois Univ., Chicago. Dept. of Civil Engineering, Mechanics, and Metallurgy.
PROBABILITY OF BRITTLE FAILURE Final Report
A. Kim, C. P. Bosnyak (Dow Chemical Co., Freeport, TX.), and A. Chudnovsky Sep. 1991 26 p
(Grant NAG3-1034)
(NASA-CR-187174; NAS 1.26:187174) Avail: NTIS HC/MF A03 CSCL 20K

A methodology was developed for collecting statistically representative data for crack initiation and arrest from small number of test specimens. An epoxy (based on bisphenol A diglycidyl ether and polyglycol extended diglycyl ether and cured with diethylene triamine) is selected as a model material. A compact tension specimen with displacement controlled loading is used to observe multiple crack initiation and arrests. The energy release rate at crack initiation is significantly higher than that at a crack arrest, as has been observed elsewhere. The difference between these energy release rates is found to depend on specimen size (scale effect), and is quantitatively related to the fracture surface morphology. The scale effect, similar to that in statistical strength theory, is usually attributed to the statistics of defects which control the fracture process. Triangular shaped ripples (deltoids) are formed on the fracture surface during the slow subcritical crack growth, prior to the smooth mirror-like surface characteristic of fast cracks. The deltoids are complementary on the two crack faces which excludes any inelastic deformation from consideration. Presence of defects is also suggested by the observed scale effect. However, there are no defects at the deltoid apexes detectable down to the 0.1 micron level. Author

N92-10206# Massachusetts Inst. of Tech., Cambridge. Acoustics and Vibration Lab.
THE MEASUREMENT OF PLATE VIBRATION AND SOUND RADIATION FROM A TURBULENT BOUNDARY LAYER MANIPULATOR
M. Phillips, K. Herbert, and P. Leehey 15 Aug. 1991 50 p
(Contract N00014-89-J-1176)
(AD-A240127; Rept-71435-2) Avail: NTIS HC/MF A03 CSCL 20/11

Two Boundary Layer Manipulators (BLM's) made of thin honeycombed aluminum were placed in a turbulent boundary layer flow. Sound intensity measurements were taken in order to determine the Mach number dependence of sound radiation. We found that sound intensity levels follow a power law consistent with dipole radiation. We made estimates of intensity levels for the BLM's in water using our measurements in air. Our estimates predict low radiation levels when mounted on naval vessels. Vibration levels were increased when undamped BLM's were installed in our wind tunnel facility. However, vibration levels were very low, and consequently sound radiation due to plate vibration was too low to be measured. Damping of the BLM's dramatically reduced vibration levels as well as direct radiation from the BLM's. GRA

N92-10207# Naval Civil Engineering Lab., Port Hueneme, CA.
BOND OF REINFORCEMENT UNDER CONTROLLED CONFINEMENT Final Report, Oct. 1989 - Feb. 1991
L. J. Malvar Jun. 1991 46 p
(AD-A240142; NCEL-TN-1833) Avail: NTIS HC/MF A03 CSCL 13/3

Twelve specimens were tested to determine the local bond stress-slip characteristics of a No. 6 rebar embedded in a 3-inch diameter concrete cylinder. Radial confining stress around the concrete specimen and radial deformation were assumed to be fundamental variables, together with bond stress and slip, needed to properly describe the interface behavior. Configuration independent bond stress-slip, relationships for a short five-lug embedded length were obtained for various degrees of confining pressure. Maximum bond stresses could be increased almost

threefold by increasing the confining stress from 500 to 4500 psi at the bar level. Two types of No. 6 bars with different deformations were investigated. GRA

42 GEOSCIENCES (GENERAL)

No abstracts in this category.

43 EARTH RESOURCES AND REMOTE SENSING

Includes remote sensing of earth resources by aircraft and spacecraft; photogrammetry; and aerial photography.

For instrumentation see *35 Instrumentation and Photography.*

N92-10208*# National Aeronautics and Space Administration. Langley Research Center, Hampton, VA.

MISSION DESCRIPTION AND IN-FLIGHT OPERATIONS OF ERBE INSTRUMENTS ON ERBS AND NOAA 9 SPACECRAFT, NOVEMBER 1984 - JANUARY 1986

William L. Weaver, Kathryn A. Bush, Chris J. Harris, Clayton E. Howerton, and Carol J. Tolson (STX Corp., Hampton, VA.) Washington Aug. 1991 282 p

(NASA-RP-1256; L-16895; NAS 1.61:1256) Avail: NTIS HC/MF A13 CSCL 04A

Instruments of the Earth Radiation Budget Experiment (ERBE) are operating on three different Earth orbiting spacecrafts: the Earth Radiation Budget Satellite (ERBS), NOAA-9, and NOAA-10. An overview is presented of the ERBE mission, in-orbit environments, and instrument design and operational features. An overview of science data processing and validation procedures is also presented. In-flight operations are described for the ERBE instruments aboard the ERBS and NOAA-9. Calibration and other operational procedures are described, and operational and instrument housekeeping data are presented and discussed. Author

N92-10209*# Oregon State Univ., Corvallis. Dept. of Bioresource Engineering.

USING LANDSAT TO PROVIDE POTATO PRODUCTION ESTIMATES TO COLUMBIA BASIN FARMERS AND PROCESSORS

1991 44 p

(Contract NCC2-569)

(NASA-CR-188783; NAS 1.26:188783) Avail: NTIS HC/MF A03 CSCL 02C

The estimation of potato yields in the Columbia basin is described. The fundamental objective is to provide CROPIX with working models of potato production. A two-pronged approach was used to yield estimation: (1) using simulation models, and (2) using purely empirical models. The simulation modeling approach used satellite observations to determine certain key dates in the development of the crop for each field identified as potatoes. In particular, these include planting dates, emergence dates, and harvest dates. These critical dates are fed into simulation models of crop growth and development to derive yield forecasts. Purely empirical models were developed to relate yield to some spectrally derived measure of crop development. Two empirical approaches are presented: one relates tuber yield to estimates of cumulative intercepted solar radiation, the other relates tuber yield to the integral under GVI (Global Vegetation Index) curve. Author

N92-10210 Technische Univ., Munich (Germany, F.R.). Inst. fuer Geographie.

EVALUATION OF HIGH ALTITUDE PHOTOGRAPHY FOR CITY REGIONAL AREAS [AUSWERTUNG VON HOCHBEFLIEGUNGEN FUER STADTREGIONEN]

H.-G. Gierloff-Emden, ed., Ute Krueger, Nicolas Prechtel, Frank W. Strathmann, and F. Wilhelm, ed. 1990 131 p In ENGLISH and GERMAN

(MGA-A-44; ISBN-3-925-308-66-0; ISSN-0932-3147; ETN-91-99832) Copyright Avail: Technische Univ. Munich, Inst. fuer Geographie, Luisenstrasse 37, D-8000 Munich 2, Fed. Republic of Germany

Subjects dealt with are the recording of urban land use by high altitude photography, taking Munich (Fed. Republic of Germany) as an example; the possibility of producing land use information for city regional area planning by high altitude photography, taking south west Munich regional area as an example; image evaluation of high altitude photographs, taking Boston and Foster City (U.S.) as examples; evaluation of high altitude photography for city cartography, taking Seattle (U.S.) as an example. For individual titles, see N92-10211 through N92-10214.

N92-10211 Technische Univ., Munich (Germany, F.R.).

RECORDING OF URBAN LAND USE BY HIGH ALTITUDE PHOTOGRAPHY: THE MUNICH (FED. REPUBLIC OF GERMANY) EXAMPL [ERFASSUNG STAEDTISCHER FLAECHENNUTZUNGEN DURCH HOCHBEFLIEGUNGEN: DAS BEISPIEL MUENCHEN]

Nikolas Prechtel and Frank W. Strathmann *In its* Evaluation of High Altitude Photography for City Regional Areas 1990 p 7-23 In GERMAN (For primary document see N92-10210 01-43)

Copyright Avail: Technische Univ. Munich, Inst. fuer Geographie, Luisenstrasse 37, D-8000 Munich 2, Fed. Republic of Germany

Mapping properties of aerial photographs with scales of 1:120,000 to 1:140,000 are evaluated, using the method of image detail analysis. Five experimental high altitude photographs on Munich regional area are used with different film materials. The method is a comparison of measurement of local frequencies in the image, and of local frequencies in the ground. The possibilities of application of the image material for land use differentiation in representative urban structures are derived. The results show that a small derivation of surface information is possible, particularly when using SO131 color infrared film. ESA

N92-10212 Technische Univ., Munich (Germany, F.R.).

POSSIBILITIES OF PRODUCING LAND USE INFORMATION FOR CITY REGIONAL AREA PLANNING BY HIGH ALTITUDE PHOTOGRAPHS, TAKING SOUTH WEST MUNICH (FED. REPUBLIC OF GERMANY) REGIONAL AREA AS AN EXAMPLE [MOEGLICHKEITEN DER GEWINNUNG VON FLAECHENNUTZUNGSINFORMATION FUER DIE STADT-UMLAND-PLANUNG AUS HOCHBEFLIEGUNGSAUFNAHMEN - BEISPIELE IM SUEDWESTLICHEN STADTUMLAND VON MUENCHEN]

Nikolas Prechtel *In its* Evaluation of High Altitude Photography for City Regional Areas 1990 p 25-54 In GERMAN; ENGLISH summary (For primary document see N92-10210 01-43)

Copyright Avail: Technische Univ. Munich, Inst. fuer Geographie, Luisenstrasse 37, D-8000 Munich 2, Fed. Republic of Germany

Panchromatic high altitude photographs with scales of 1:120,000 are evaluated with regard to their potentials for land use mapping in a regional area size. Typical land use patterns around the city of Munich are selected to compare the image information contents with data derived from existing maps or ground checks. It is found that photographs are a valuable source for thematic mapping, especially in built up areas, where ground element sizes of high resolution satellite data do not give a good representation of the basic structures. ESA

N92-10213 Technische Univ., Munich (Germany, F.R.).
IMAGE EVALUATION OF HIGH ALTITUDE PHOTOGRAPHS. EXAMPLES: BOSTON AND FOSTER CITY (US) [BILDAUSWERTUNGEN VON HOCHBEFLIEGUNGEN - BEISPIELE: BOSTON UND FOSTER CITY]
H.-G. Gierloff-Emden *In its* Evaluation of High Altitude Photography for City Regional Areas 1990 p 55-78 In GERMAN (For primary document see N92-10210 01-43)
Copyright Avail: Technische Univ. Munich, Inst. fuer Geographie, Luisenstrasse 37, D-8000 Munich 2, Fed. Republic of Germany

Three examples of image evaluation of Ultra High Altitude Photography (UHAP) for use in city and city regional area mapping are presented for Boston and Foster City. The sequence of photo scales of UHAP are analyzed with regard to applicability for city and city regional area. Map scale equivalents for topographic maps of the U.S. are given. The possibility of application of the UHAP of the single scales for the detailed area Boston city regional area, Boston city, Foster city problems is verified. The aspects of the application of UHAP to photointerpretation, with regard to city regional area are reported. ESA

N92-10214 Technische Univ., Munich (Germany, F.R.).
EVALUATION OF HIGH ALTITUDE PHOTOGRAPHY FOR CITY CARTOGRAPHY, WITH THE EXAMPLE OF SEATTLE, US [AUSWERTUNG VON HOCHBEFLIEGUNGEN ZUR STADTKARTOGRAPHIE: DAS BEISPIEL SEATTLE/USA]
Ute Krueger *In its* Evaluation of High Altitude Photography for City Regional Areas 1990 p 79-127 In GERMAN (For primary document see N92-10210 01-43)
Copyright Avail: Technische Univ. Munich, Inst. fuer Geographie, Luisenstrasse 37, D-8000 Munich 2, Fed. Republic of Germany

Dimensions and detail discernibility are evaluated in high altitide photographs. High altitude mapping is compared with existing maps, with regard to topographic contents, for the various quarters of Seattle. The utilization potentials of evaluated high altitude photography in city cartography are examined. It is shown that high altitude photographs meet the requirements of the production of topographic maps up to scale 1:25,000, with regard to resolution, accuracy, dimensions, and detail discernibility. High altitude photographs can be used for land use maps, in order to carry out a level II classification of the Multilevel Classification System. ESA

N92-10215# Beleidscommissie Remote Sensing, Delft (Netherlands).
THE REMOTE SENSING LOOSDRECHT LAKES (NETHERLANDS) PROJECT
A. G. Dekker, T. J. Malthus, S. W. M. Peters, and E. Seyhan (Vrije Univ., Amsterdam, Netherlands) Mar. 1991 118 p Original contains color illustrations
(BCRS-90-29; TD-91-2194; ETN-91-90049) Avail: NTIS HC/MF A06

The objectives were to study and detect the temporal and spatial variations in water quality of the Loosdrecht lakes using the general purpose satellite systems Thematic Mapper and SPOT, the airborne remote sensing instrument CAESAR and low altitude aerial color photography. Within this context water quality is defined as: the changes in type and/or concentration of water constituents caused by mean induced eutrophication. First phase research results showed, however, that in order to detect temporal and spatial variations in water quality parameters with sufficient quantitative accuracy, the above remote sensing methods lacked both the required spectral band positioning and accuracy and the required radiometric sensitivity (with the exception of CAESAR). Digital image processing was used as a tool, rather than as a research topic. Simple algorithms which relate water quality parameters to remote sensing data were developed based on understanding the physical processes which lead to the validity of the algorithm. ESA

N92-10216# Beleidscommissie Remote Sensing, Delft (Netherlands).
REMOTE SENSING AND WATERSHED MODELLING: TOWARDS A HYDROLOGICAL INTERFACE MODEL
Mar. 1991 98 p Prepared in cooperation with IWACO B.V., Rotterdam, Netherlands; Winand Staring Centre, Wageningen, Netherlands; and International Inst. for Aerospace Survey and Earth Sciences, Enschede, Netherlands
(BCRS-90-42; TD-91-2195; ETN-91-90051) Avail: NTIS HC/MF A05

The aim is to identify an extension to a combined Geographic Information System (GIS) and image processing system, in such a way that it can be used as an input and output generator for a large variety of hydrologic models, i.e., a hydrological information system. The basic information system selected for this project is ILWIS (Integrated Land and Water Information System), and a high performance personal computer based system. The developments taking place in hydrology with respect to remote sensing and GIS are discussed. The hydrologic processes in a watershed and a categorization of hydrological models are considered and the selection of representative models for each category is presented, including an extensive description of each selected model. The current possibilities and the extensions of ILWIS required to come to a versatile data processing system that can be used in combination with a variety of hydrologic models are given. An overview of users in the field of hydrological applications is presented andexamples of remote sensing and TIS applications in the different hydrological processes are shown. Recommendations for a continuation of this study are given. ESA

N92-10217# Earth Satellite Corp., Rockville, MD.
NEW METHODS OF CHANGE DETECTION USING MULTISPECTRAL DATA Final Report
Charles Sheffield and Gil Richardson 15 May 1991 130 p
(Contract DACA76-86-C-0018)
(AD-A239370; ETL-0586) Avail: NTIS HC/MF A07 CSCL 20/6

This report discusses the final phase of a project to develop multispectral change detection methods with emphasis on human activities. Two new algorithms were developed and tested: a Spectral/Spatial Classifier and a Feature Vector Spectral Classifier. The Spectral/Spatial method appears to be a powerful new tool. The Feature Vector results were inconclusive. GRA

N92-10218# Los Alamos National Lab., NM.
REMOTE DETECTION OF ATMOSPHERICALLY DISPERSED VEGETATIVE CELLS USING FLUORESCENCE LIDAR
J. J. Tiee, W. E. Eichinger, D. E. Hof, D. B. Holtkamp, R. R. Karl, Jr., R. J. Martinez, D. S. Moore, C. R. Quick, and R. J. Joseph 1991 5 p Presented at the Optical Society of America (OSA) Remote Sensing of the Atmosphere, Williamsburg, VA, 18-21 Nov. 1991
(Contract W-7405-eng-36)
(DE91-016077; LA-UR-91-2185; CONF-911165-1) Avail: NTIS HC/MF A01

An UV fluorescence LIDAR system is employed for the long range detection of atmospherically dispersed biological particles (e.g., Bacillus thuringiensis) released from an aerosol generator. DOE

N92-10219# Sparta, Inc., Lexington, MA.
A TECHNIQUE FOR ESTIMATING SURFACE METEOROLOGICAL RANGES OVER OCEANS FROM SATELLITE MEASUREMENTS OF AEROSOL OPTICAL DEPTH Technical Report, 1 Aug. 1989 - 1 Oct. 1990
David R. Longtin, Eric P. Shettle, and John R. Hummel 16 Oct. 1990 66 p
(Contract F19628-88-C-0038)
(AD-A239985; LTR90-010; GL-TR-90-0284; SR-5) Avail: NTIS HC/MF A04 CSCL 04/1

Measurements of aerosol optical depth obtained from NOAA's Advanced Very High Resolution Radiometers (AVHRR) aboard

polar-orbiting satellites have been used to estimate the surface meteorological range over oceans. To do this, a lookup table of optical depth versus meteorological range had been developed which is based on the aerosol extinction profiles in LOWTRAN 7. To better simulate conditions over oceans, the boundary layer height has been lowered to 0.5 km and an extinction profile corresponding to a 150 km meteorological range has been added. The lookup table has been applied to AVHRR aerosol optical depths near selected island locations where, in turn, the inferred meteorological ranges were validated against surface observations. Results show reasonable success in locating regions where meteorological ranges exceed 30 km, but more precise classification may not be possible due to uncertainties in both the measurements and observations. The algorithm tends to produce higher than observed meteorological ranges when the observed values are less than 30 kilometers. Limited comparisons with SAGE II data, suggest that the assumed model aerosol extinction profiles used by the algorithm may contain too much aerosol loading above the boundary layer, which could account for some, but not all, of this discrepancy. Other explanations include the possibility the island sites have lower visibilities than the surrounding open ocean or the AVHRR optical depths are too small. GRA

N92-10514# Joensuu Univ. (Finland). Faculty of Sicences.
SPECTRAL REFLECTANCE OF PINE AND INTENSITY OF MOOSE BROWSING Abstract Only
Raimo Silvennoinen, Kaarlo Nygren (Game and Fisheries Research Inst., Ilomantsi, Finland), Kim vonWeissenberg, and Rauno Hamalainen *In* Oulu Univ., Proceedings of the 25th Annual Conference of the Finnish Physical Society 1991 1 p (For primary document see N92-10362 01-70)
Avail: NTIS HC/MF A12

N92-10844*# Washington Univ., Saint Louis, MO.
THE GEOLOGIC REMOTE SENSING FIELD EXPERIMENT (GRSFE)
Mary A. Dale-Bannister, Raymond E. Arvidson, Edward E. Guinness, Susan H. Slavney, and Thomas C. Stein *In* NASA, Washington, Reports of Planetary Geology and Geophysics Program, 1990 Jun. 1991 p 306-307 (For primary document see N92-10728 01-91)
Avail: NTIS HC/MF A25 CSCL 03B

N92-10847*# Arizona State Univ., Tempe. Dept. of Geology.
REMOTE SENSING OBSERVATIONS OF KELSO DUNES, CALIFORNIA Abstract Only
Ronald Greeley, N. Lancaster, L. Gaddis, and E. C. I. Paisley *In* NASA, Washington, Reports of Planetary Geology and Geophysics Program, 1990 Jun. 1991 p 313 (For primary document see N92-10728 01-91)
Avail: NTIS HC/MF A25 CSCL 03B

44 ENERGY PRODUCTION AND CONVERSION

Includes specific energy conversion systems, e.g., fuel cells; global sources of energy; geophysical conversion; and windpower.

For related information see also *07 Aircraft Propulsion and Power, 20 Spacecraft Propulsion and Power,* and *28 Propellants and Fuels.*

N92-10220*# Cleveland State Univ., OH. Dept. of Engineering Technology.
DEVELOPMENT OF A MODEL OF SPACE STATION SOLAR ARRAY Final Report, 15 Sep. 1989 - 15 Mar. 1990
Paul A. Bosela 15 Mar. 1990 228 p
(Grant NAG3-1008)
(NASA-CR-188911; NAS 1.26:188911) Avail: NTIS HC/MF A11 CSCL 10B

Space structures, such as the space station solar arrays, must be extremely lightweight, flexible structures. Accurate prediction of the natural frequencies and mode shapes is essential for determining the structural adequacy of components, and designing a control system. The tension preload in the blanket of photovoltaic solar collectors, and the free/free boundary conditions of a structure in space, causes serious reservations on the use of standard finite element techniques of solution. In particular, a phenomena known as grounding, or false stiffening, of the stiffness matrix occurs during rigid body rotation. The grounding phenomena is examined in detail. Numerous stiffness matrices developed by others are examined for rigid body rotation capability, and found lacking. Various techniques are used for developing new stiffness matrices from the rigorous solutions of the differential equations, including the solution of the directed force problem. A new directed force stiffness matrix developed by the author provides all the rigid body capabilities for the beam in space. Author

N92-10221*# National Aeronautics and Space Administration. Lewis Research Center, Cleveland, OH.
TRADE STUDIES FOR NUCLEAR SPACE POWER SYSTEMS
John M. Smith, David J. Bents, and Harvey S. Bloomfield 1991 12 p Presented at the Conference on Advanced Space Exploration Initiative Technologies, Cleveland, OH, 4-6 Sep. 1991; cosponsored by AIAA, NASA, and OAI Previously announced in IAA as A91-52413
(NASA-TM-105231; E-6554; NAS 1.15:105231; AIAA-91-3518)
Avail: NTIS HC/MF A03 CSCL 10B

As human visions of space applications expand and as we probe further out into the universe, our needs for power will also expand, and missions will evolve which are enabled by nuclear power. A broad spectrum of missions which are enhanced or enabled by nuclear power sources have been defined. These include Earth orbital platforms, deep space platforms, planetary exploration, and terrestrial resource exploration. The recently proposed Space Exploration Initiative (SEI) to the Moon and Mars has more clearly defined these missions and their power requirements. Presented here are results of recent studies of radioisotope and nuclear reactor energy sources, combined with various energy conversion devices for Earth orbital applications, SEI lunar/Mars rovers, surface power, and planetary exploration. Author

N92-10222*# National Aeronautics and Space Administration. Lewis Research Center, Cleveland, OH.
ALKALI METAL CARBON DIOXIDE ELECTROCHEMICAL SYSTEM FOR ENERGY STORAGE AND/OR CONVERSION OF CARBON DIOXIDE TO OXYGEN Patent Application
Norman H. Hagedorn, inventor (to NASA) 26 Sep. 1991 15 p
(NASA-Case-LEW-14973-1; NAS 1.71:LEW-14973-1;
US-Patent-Appl-SN-766593) Avail: NTIS HC/MF A03 CSCL 10C

An alkali metal, such as lithium, is the anodic reactant, carbon dioxide or a mixture of carbon dioxide and carbon monoxide is the cathodic reactant, and carbonate of the alkali metal is the electrolyte in an electrochemical cell for the storage and delivery of electrical energy. Additionally, alkali metal-carbon dioxide battery systems include a plurality of such electrochemical cells. Gold is a preferred catalyst for reducing the carbon dioxide at the cathode. The fuel cell of the invention produces electrochemical energy through the use of an anodic reactant which is extremely energetic and light, and a cathodic reactant which can be extracted from its environment and therefore exacts no transportation penalty. The invention is therefore especially useful in extraterrestrial environments. NASA

N92-10223# Sandia National Labs., Albuquerque, NM.
A GENERIC GUIDE FOR THE PREPARATION OF A QUALITY ASSURANCE/QUALITY CONTROL MANUAL FOR THE DESIGN, PRODUCTION, AND INSTALLATION OF PHOTOVOLTAIC CONCENTRATOR SYSTEMS
V. S. Murty Jul. 1991 42 p Prepared in cooperation with Texas Southern Univ., Houston
(Contract DE-AC04-76DP-00789)
(DE91-017716; SAND-91-7010) Avail: NTIS HC/MF A03

The United States National Photovoltaic (PV) program considers the production of energy using PV concentrator systems a viable renewable energy technology. To this end it has launched the National Photovoltaic Concentrator Initiative. One of the main objectives of the initiative is to achieve an energy price goal of $0.06/kwh by the year 2000. These cost goals involve calculations that assume the systems are operating with the minimum of maintenance for periods of twenty to thirty years. This rigid reliability requirement necessitates, the implementation of a strict Quality Assurance/Quality Control plan in all phases of design, development, manufacturing, testing, installation and operation. This document is intended as a guide for any company involved in design and manufacture of PV concentrator modules and systems. The contents of this document incorporate the collective input of representatives of the PV industry and the Sandia Photovoltaic Technology Research Division. DOE

N92-10224# Sandia National Labs., Albuquerque, NM.
THE SOLARTRAK SOLAR ARRAY TRACKING CONTROLLER
A. B. Maish Jul. 1991 328 p
(Contract DE-AC04-76DP-00789)
(DE91-017721; SAND-90-1471) Avail: NTIS HC/MF A15

Sandia National Laboratories has developed an advanced self-contained tracking control system for use with one- or two-axis tracking solar arrays. The SolarTrak system computes the sun's position based on the time and stored position data, and then controls two motors to point the tracker at the sun without using sun sensors. When used with a photovoltaic concentrator array, the system initially performs a self-alignment routine using array-generated current to locate the sun. The routine computes six numbers that are used during the normal operation to correct the array pointing for the tracker's installation misalignment. This enables the tracker to point accurately even with installation misalignments of up to several degrees. The SolarTrak system consists of a control board, which contains a Motorola 68HC11 microcontroller, a power supply board, motor-interface boards, and a hand-held user interface board, which contains a liquid-crystal display and an input keypad. This report contains a thorough discussion of the controller software and hardware, including control algorithms, parts lists and estimated costs (about $300 per system). The performance measured on two trackers is reviewed. Tracking accuracy was better than plus minus 0.1 degrees over a full day on one system. A thorough user's manual is included. Companies interested in licensing the technology should contact the Technology Transfer Division of Sandia National Laboratories. DOE

N92-10225# Department of Energy, Washington, DC. Office of the Deputy Assistant Secretary for Oil, Gas, Shale and Special Technologies.
FUEL CELL SYSTEMS PROGRAM PLAN, FISCAL YEAR 1991
1991 38 p
(DE91-017215; DOE/FE-0238P) Avail: NTIS HC/MF A03

The Department of Energy (DOE), Office of Fossil Energy, is sponsoring the development of phosphoric acid fuel cell (PAFC), molten carbonate fuel cell (MCFC), and advanced concepts including solid oxide fuel cell (SOFC) technologies for application in the utility, commercial and industrial sectors. In addition, the DOE Office of Conservation and Renewable Energy is evaluating the use of fuel cells in transportation propulsion systems. Their focus is primarily on the development of polymer electrolyte or proton exchange membrane fuel cells, although they also have a congressionally mandated demonstration program for phosphoric acid fuel cells buses. These research and development (R&D) efforts are also supported by private sector funding. This Plan describes the fuel cell activities of the Office of Fossil Energy. DOE

N92-10226# Spire Corp., Bedford, MA.
HIGH EFFICIENCY GaAs/Ge MONOLITHIC TANDEM CELLS FOR SPACE CONCENTRATOR ARRAYS, PHASE 1 Interim Report, Aug. 1988 - Aug. 1989
Steven J. Wojtczuk May 1991 21 p
(Contract F33615-88-C-2844)
(AD-A239931; WL-TR-91-2047-Phase-1) Avail: NTIS HC/MF A03 CSCL 10/2

The goal of this program is to develop a 30 percent efficient 2-junction solar cell that is monolithic, two terminal, and that will operate in 25-100x solar concentrator elements with operating temperatures of 75 to 100 C. The cell design is a GaAs/Ge compound configuration with the Ge bottom cell utilizing the 0.9 to 1.8 micron portion of the AM0 solar spectrum and contributing 7 percent to the total stack efficiency. During the first Phase of this effort individual component cells were developed that had efficiencies of 22 percent for Gallium Arsenide and 6 percent for Germanium. Monolithically grown 2-junction devices were also fabricated with efficiencies exceeding 20 percent when characterized at the defined operating temperatures and solar concentration. Author (GRA)

N92-10227# Dayton Univ., OH.
HIGH TEMPERATURE SOLAR CELL CONTACTS Final Report, Jan. 1989 - Jan. 1990
Steven Smith May 1991 26 p
(Contract F33615-86-C-2722)
(AD-A239932; UDRI-FR-60136; WL-TR-91-2044) Avail: NTIS HC/MF A03 CSCL 10/2

Gallium arsenide solar cells may be subjected to extreme temperature excursions as high as 600 C during processing steps and while operating in space orbits. To prevent solar cell failure during fabrication and its operating life, the electrical contacts to the active semiconductor material must remain electrically and chemically stable during these high temperature excursions. The objective of this effort is to develop an electrical contact material to the gallium arsenide solar cell which will survive temperatures up to 600 C (873 K) for periods up to 15 minutes. During this contracting period a thermodynamic phase equilibrium computer model was developed which calculates the liquidus and solidus phase boundaries of metal-Ga-As systems of interest to determine their potential high temperature stability. Author (GRA)

N92-10581# Finnish National Fund for Research and Development, Helsinki.
ENERGY SYSTEMS AND THEIR TECHNICAL, ECONOMIC AND ENVIRONMENTAL BOUNDARY CONDITIONS Abstract Only
Jorma Routti *In* Oulu Univ., Proceedings of the 25th Annual Conference of the Finnish Physical Society 1991 1 p (For primary document see N92-10362 01-70)
Avail: NTIS HC/MF A12

N92-10583# Helsinki Univ. of Technology, Espoo (Finland). Dept. of Technical Physics.
FUSION ENERGY: STATUS AND PROSPECTS Abstract Only
Rainer Salomaa *In* Oulu Univ., Proceedings of the 25th Annual Conference of the Finnish Physical Society 1991 1 p (For primary document see N92-10362 01-70)
Avail: NTIS HC/MF A12

N92-10584# Helsinki Univ. of Technology, Espoo (Finland). Dept. of Technical Physics.
SOLAR ENERGY IN MITIGATING GLOBAL ENVIRONMENTAL PROBLEMS Abstract Only
P. D. Lund *In* Oulu Univ., Proceedings of the 25th Annual Conference of the Finnish Physical Society 1991 1 p (For primary document see N92-10362 01-70)
Avail: NTIS HC/MF A12

45 ENVIRONMENT POLLUTION

Includes atmospheric, noise, thermal, and water pollution.

N92-10228# Resources for the Future, Inc., Washington, DC. Energy and Natural Resources Div.
GREENHOUSE WARMING: ABATEMENT AND ADAPTATION
Norman J. Rosenberg, ed., William E. Easterling, III, ed., Pierre R.

Crosson, ed., and Joel Darmstadter, ed. 1991 184 p Workshop held in Washington, DC, 14-15 Jun. 1988; sponsored by Resources for the Future, Inc., NOAA, DOE, Dept. of Agriculture, EPA, and the International Federation of Inst. for Advanced Studies
(ISBN-0-915707-50-0; LC-89-8483) Avail: NTIS HC/MF A09

The papers presented herein grew out of a workshop organized by the Climate Resources Program at Resources for the Future. The workshop was held to study the prospects for future climate change and the far reaching physical and socioeconomic impacts that may follow in the wake of such change. The aim was to provide information on policies and practices that can be effective for government and the private sector in delaying and abating climate change and in coping with such change as may be unavoidable. For individual titles, see N92-10229 through N92-10240.

N92-10229# National Center for Atmospheric Research, Boulder, CO. Interdisciplinary Climate Systems Section.
THE GREENHOUSE EFFECT: ITS CAUSES, POSSIBLE IMPACTS, AND ASSOCIATED UNCERTAINTIES
Stephen H. Schneider and Norman J. Rosenberg (Resources for the Future, Inc., Washington, DC.) *In* Resources for the Future, Inc., Greenhouse Warming: Abatement and Adaptation 1991 p 7-34 (For primary document see N92-10228 01-45)
Avail: NTIS HC/MF A09

The Earth's climate changes. The climatic effects of having polluted the atmosphere with gases such as carbon dioxide (CO2) may already be felt. There is no doubt that the concentration of CO2 in the atmosphere has been rising. CO2 tends to trap heat near the Earth's surface. This is known as the greenhouse effect, and its existence and basic mechanisms are not questioned by atmospheric scientists. What is questioned is the precise amount of warming and the regional pattern of climatic change that can be expected on the Earth from the anthropogenic increase in the atmospheric concentration of CO2 and other greenhouse gases. It is the regional patterns of changes in temperature, precipitation, and soil moisture that will determine what impact the greenhouse effect will have on natural ecosystems, agriculture, and water supplies. These possible effects are discussed in detail. It is concluded, however, that a detailed assessment of the climatic, biological, and societal changes that are evolving and should continue to occur into the next century cannot reliably be made with available scientific capabilities. Nevertheless, enough is known to suggest a range of plausible futures with attendant impacts, both positive and negative, on natural resources and human well being. Author

N92-10230# Resources for the Future, Inc., Washington, DC.
HUMAN DEVELOPMENT AND CARBON DIOXIDE EMISSIONS: THE CURRENT PICTURE AND THE LONG-TERM PROSPECTS
Joel Darmstadter and Jae Edmonds (Pacific Northwest Lab., Washington, DC.) *In its* Greenhouse Warming: Abatement and Adaptation 1991 p 35-51 Sponsored in part by DOE (For primary document see N92-10228 01-45)
Avail: NTIS HC/MF A09

The scale of human activity has grown to the point that gaseous emissions produced by four areas of human endeavor (energy, agriculture, land use, and chemical manufacture) are changing the stock of gases in the atmosphere. That change, in turn, affects the global temperature and climate. Such gases are called greenhouse, or radiatively important, gases (RIGs). The nature and timing of future climate change depend on three things: the rate of emission of RIGs into the atmosphere, the capacity of removal mechanisms, and the interaction between atmospheric composition and the climate. Herein, the first of these is examined: the rate of emission of RIGs and its determinants. The broad diversity of RIGs is briefly reviewed, but particular emphasis is on the relationship between energy use and the release of carbon dioxide from fossil fuels. Author

N92-10231# Ministry of Housing, Physical Planning, and Environment, Leidschendam (Netherlands).
SEA-LEVEL RISE: REGIONAL CONSEQUENCES AND RESPONSES
Gjerrit P. Hekstra *In* Resources for the Future, Inc., Greenhouse Warming: Abatement and Adaptation 1991 p 53-67 (For primary document see N92-10228 01-45)
Avail: NTIS HC/MF A09

Climatic change and its possible impact on sea level, hydrology, agriculture, and other dimensions of human development have concerned physical and social scientists for some time. Public authorities in nations with coastal lowlands have shown heightened worry about the foreseeable long term effects of accelerated sea level rise (SLR). By constrast with the last century, during which SLR amounted to approx. 0.12 to 0.15 m, assessments of prospective change over the next 100 years range from increases of around 0.6 to 4.0 m, though scenarios can be constructed that point to the possibility of a far greater rise. Such a circumstance could result from the disintegration and rapid melting of the West Antarctic ice sheet. But such global averages may mask both substantial variability among different coastal regions and the storm surges and other intensified perturbations which, in given localities, can greatly magnify SLR damage to human settlements, croplands, and ground water quality. A detailed analysis is made of region-specific SLR effects and adaptive and protective measures to counter them are discussed. Author

N92-10232# Resources for the Future, Inc., Washington, DC.
CLIMATE CHANGE: PROBLEMS OF LIMITS AND POLICY RESPONSES
Pierre R. Crosson *In its* Greenhouse Warming: Abatement and Adaptation 1991 p 69-82 (For primary document see N92-10228 01-45)
Avail: NTIS HC/MF A09

Present emission rates of carbon dioxide (CO2) and the other principle greenhouse gases (radiatively important gases (RIG's)) - methane, nitrous oxide, and chlorofluorocarbons - exceed the capacity of the oceanic, terrestrial, and tropospheric sinks to absorb them. Consequently, their concentrations in the troposphere are increasing and will continue to increase so long as emissions exceed sink capacities. It is assumed that an indefinitely persistent gap between emissions and sinks of RIG's implies indefinite global warming and related changes in regional climates. The high monetary and environmental costs that would be imposed by global warming are discussed along with the changes in energy policy that are needed to insure that these high costs will not be past on to future generations. Author

N92-10233# Resources for the Future, Inc., Washington, DC. Center for Risk Management.
ASSESSING AND MANAGING THE RISKS OF CLIMATE CHANGE
Paul R. Portney *In its* Greenhouse Warming: Abatement and Adaptation 1991 p 83-104 (For primary document see N92-10228 01-45)
Avail: NTIS HC/MF A09

Some similarities and differences between the assessment and management of climate problems are presented along with ordinary environmental regulatory problems. The applicability of a familiar rule often invoked in thinking about the management of traditional environmental risks, namely, that an once of prevention is worth a pound of cure, is addressed with respect to the optimal management of climate-related risks. Author

N92-10234# Resources for the Future, Inc., Washington, DC.
CLIMATE AND FORESTS
Roger A. Sedjo and Allen M. Solomon (International Inst. for Applied Systems Analysis, Laxenburg, Austria) *In its* Greenhouse Warming: Abatement and Adaptation 1991 p 105-119 (For primary document see N92-10228 01-45)
Avail: NTIS HC/MF A09

The effects of forests on climate change and the effects of climate change on forests are examined. In particular, the

mechanisms whereby changing CO2 levels and global warming might affect forest growth and composition are examined. The economic cost required to establish plantation forests in temperate and tropical regions are estimated. In addition, the economic uses to which the newly established forest stock might be put are investigated. The possible effects of these higher stocking levels on world industrial wood markets and on investments in traditional industrial forestry activities are addressed, and the broad economic implications are examined. The question of the source of financing is addressed briefly and the possibility/necessity of foreign assistance is examined. Author

N92-10235# Virginia Polytechnic Inst. and State Univ., Blacksburg.
THE BIOLOGICAL CONSEQUENCES OF CLIMATE CHANGES: AN ECOLOGICAL AND ECONOMIC ASSESSMENT
Sandra S. Batie and Herman H. Shugart (Virginia Univ., Charlottesville.) *In* Resources for the Future, Inc., Greenhouse Warming: Abatement and Adaptation 1991 p 121-131 (For primary document see N92-10228 01-45)
Avail: NTIS HC/MF A09

The following subject areas are covered: (1) the level of climate change; (2) impacts of climate change on ecological systems (short-term (decadal), medium term (centenary), and long-term (millennial) effects); and (3) ecological consequences of climate change - evaluating the social costs (the problem of valuing consequences, intergenerational problem, and safe minimum standard strategies and policies). Author

N92-10236# Resources for the Future, Inc., Washington, DC.
WATER RESOURCES AND CLIMATE CHANGE
Kenneth D. Frederick and Peter H. Gleick (California Univ., Berkeley.) *In its* Greenhouse Warming: Abatement and Adaptation 1991 p 133-143 (For primary document see N92-10228 01-45)
Avail: NTIS HC/MF A09

The following subject areas are covered: (1) risks to water supplies associated with climate change; (2) coping with hydrologic change (infrastructure, managing the infrastructure for more water and greater security, demand management for urban and agricultural water use, and technological change); and (3) vulnerability to climate change. Author

N92-10237# International Centre for Integrated Mountain Development, Kathmandu (Nepal). Mountain Farming Systems Div.
POTENTIAL STRATEGIES FOR ADAPTING TO GREENHOUSE WARMING: PERSPECTIVES FROM THE DEVELOPING WORLD
N. S. Jodha *In* Resources for the Future, Inc., Greenhouse Warming: Abatement and Adaptation 1991 p 147-158 (For primary document see N92-10228 01-45)
Avail: NTIS HC/MF A09

The following subject areas are covered: (1) the developing world and its high-risk sector; and (2) abatement and adaptation strategies (prevention of further warming, adaptation options, and impediments to adaptation). Adaptation options in the developing countries are discussed in the framework of the following components: (1) uncertainties with respect to the impact of the greenhouse warming; (2) indifference of public policies and programs to greenhouse warming issues; and (3) potential agroclimatic changes following greenhouse warming. Author

N92-10238# International Federation of Inst. for Advanced Study, Toronto (Ontario).
HUMAN DIMENSIONS OF GLOBAL CHANGE: TOWARD A RESEARCH AGENDA
Ian Burton *In* Resources for the Future, Inc., Greenhouse Warming: Abatement and Adaptation 1991 p 159-174 (For primary document see N92-10228 01-45)
Avail: NTIS HC/MF A09

The Earth's environment is being transformed by human activity. Human activity, in turn, is being affected by these transformations. This interaction is being studied under the aegis of global change in the geosphere-biosphere. The purpose here is to explore the basis for and the substance of a proposed research program focused on the human dimensions of global change. Global warming due to the greenhouse effect, CO2 reduction, environment impacts, land use management, and the removal of greenhouse gases from the atmosphere are among the topics covered. Author

N92-10239# California Univ., San Diego, La Jolla.
THOUGHTS ON ABATEMENT AND ADAPTATION
Roger R. Revelle *In* Resources for the Future, Inc., Greenhouse Warming: Abatement and Adaptation 1991 p 167-174 (For primary document see N92-10228 01-45)
Avail: NTIS HC/MF A09

A number of questions having to do with the themes of abatement and adaptation are discussed. Under the first rubric are questions of future concentrations of radiatively active trace gases, the linkage of these gases with greenhouse warming, and other environmental problems. Also examined in the abatement context are opportunities to reduce fossil fuel use and therefore the emission of greenhouse gases, and the likelihood that natural forest expansion may provide an opportunity to control the rate of carbon dioxide (CO2) accumulation in the atmosphere. Also discussed are the possible effects of greenhouse warming on agriculture in the United States and in the developing world. Finally, some suggestions are given on capturing and retaining interest in greenhouse warming on the part of the decision making public. Author

N92-10240# Resources for the Future, Inc., Washington, DC.
EPILOGUE
Chester L. Cooper *In its* Greenhouse Warming: Abatement and Adaptation 1991 p 175-182 (For primary document see N92-10228 01-45)
Avail: NTIS HC/MF A09

A general discussion of the issues raised during the conference is given. Global warming due to the greenhouse effect, climate change, agricultural, and forestry are discussed. General policy considerations, the improvement of energy efficiency, fuel switching as a way of reducing the rate of CO2 emissions, capturing of CO2 through forest management, water management, and adapting to sea level rises are covered. Author

N92-10241# Midwest Research Inst., Golden, CO.
SOLAR DETOXIFICATION TECHNOLOGY: USING ENERGY FROM THE SUN TO DESTROY HAZARDOUS WASTE
J. V. Anderson and R. J. Clyne Aug. 1991 8 p Presented at the Challenge of the Environment: New Technologies, Restono, VA, 5-6 Sep. 1991
(Contract DE-AC02-83CH-10093)
(DE91-015007; SERI/TP-250-4474; CONF-9109255-1) Avail: NTIS HC/MF A02

Solar energy is being applied to one of the most difficult environmental problems our country faces in the coming decades: the destruction of hazardous waste. DOE Researchers are developing two separate technologies -- solar detoxification of water and solar decontamination of soil -- that could revolutionize the way toxic wastes are removed from the environment. Unlike many remediation techniques in use today, these solar-based processes actually destroy hazardous contaminants; the wastes are not transferred to other media for disposal. Solar detoxification of water uses solar energy to power a reaction that eliminates organic contaminants from polluted surface water and groundwater. The process uses a solar-activated photocatalyst, such as titanium dioxide, to break the bonds holding organic compounds together. Researchers are currently working to increase the efficiency and reduce the costs of the process to make it economically competitive with traditional remediation methods. In a related program researchers are investigating the ability of high solar flux (upwards of 300 times the sun's normal intensity) to decontaminate polluted solids such as soils. The solar decontamination of soil is a two-step process: in the first step contaminants are desorbed from the solid either by solar thermal energy or by conventional means

(such as heating or vacuum extraction); in the second step the desorbed contaminants are destroyed. The contaminants can be destroyed by using either a high-flux photolytic process or a low-flux process that employs a photocatalyst. Solar Energy Research Institute's state-of-the-art high-flux solar furnace is home to a large portion of the soil decontamination research. DOE

N92-10242# Resources for the Future, Inc., Washington, DC.
PROCESSES FOR IDENTIFYING REGIONAL INFLUENCES OF AND RESPONSES TO INCREASING ATMOSPHERIC CO2 AND CLIMATE CHANGE: THE MINK PROJECT
Pierre R. Crosson, L. A. Katz, and J. Wingard Aug. 1991 123 p
(Contract DE-AC06-76RL-01830)
(DE91-018602; DOE/RL-01830T-H7) Avail: NTIS HC/MF A06

The second report of a series contributing to the study Processes for Identifying Regional Influences of and Responses to Increasing Atmospheric CO2 and Climate Change. The MINK Project is composed of two parts. This Report (2A) treats agriculture in MINK in terms of state and region-wide production and resource use for the main crops and animals in the baseline periods of 1984/87 and 2030. The effects of the analog climate on the industry at this level of aggregation are considered in both baseline periods. DOE

N92-10243# Resources for the Future, Inc., Washington, DC.
PROCESSES FOR IDENTIFYING REGIONAL INFLUENCES OF AND RESPONSES TO INCREASING ATMOSPHERIC CO2 AND CLIMATE CHANGE: THE MINK PROJECT
William E. Easterling, III, M. S. McKenney, Norman J. Rosenberg, and K. M. Lemon Aug. 1991 222 p
(Contract DE-AC06-76RL-01830)
(DE91-018603; DOE/RL-01830T-H8) Avail: NTIS HC/MF A10

The second report of a series Processes for Identifying Regional Influences of and Responses to Increasing Atmospheric CO2 and Climate Change. The MINK Project is composed of two parts. This Report (2B) deals with agriculture at the level of farms and Major Land Resource Areas (MLRAs). The Erosion Productivity Impact Calculator (EPIC), a crop growth simulation model developed by scientists at the U.S. Department of Agriculture, is used to study the impacts of the analog climate on yields of main crops in both the 1984/87 and the 2030 baselines. The results of this work with EPIC are the basis for the analysis of the climate change impacts on agriculture at the region-wide level undertaken in this report. Report IIA treats agriculture in MINK in terms of state and region-wide production and resource use for the main crops and animals in the baseline periods of 1984/87 and 2030. The effects of the analog climate on the industry at this level of aggregation are considered in both baseline periods. DOE

N92-10244# Resources for the Future, Inc., Washington, DC.
PROCESSES FOR IDENTIFYING REGIONAL INFLUENCES OF AND RESPONSES TO INCREASING ATMOSPHERIC CO2 AND CLIMATE CHANGE: THE MINK PROJECT
Kenneth D. Frederick Aug. 1991 153 p
(Contract DE-AC06-76RL-01830)
(DE91-018605; DOE/RL-01830T-H10) Avail: NTIS HC/MF A08

This is the fourth of a series of reports of research contributing to the study Processes for Identifying Regional Influences of and Responses to Increasing Atmospheric CO2 and Climate Change -- The MINK Project. This report is directed to an analysis of the possible impacts of climatic change on water resources in the Missouri -- Iowa -- Nebraska -- Kansas (MINK) region. It follows a uniform methodological strategy that is applied to the four resource sectors most likely to be impacted by climate change, i.e., agriculture, forestry, water resources and energy. The methodological strategy is fully explained in Report 1 of this series. DOE

N92-10245# Johns Hopkins Univ., Baltimore, MD. Dept. of Environmental Health Sciences.
THE 14TH INTERNATIONAL CONFERENCE ON COMBINED EFFECT OF ENVIRONMENTAL FACTORS Final Report, 30 Sep. 1990 - 29 Mar. 1991
Lawrence D. Fechter 9 Aug. 1991 4 p Conference held in Baltimore, MD, 30 Sep. - 3 Oct. 1990
(Grant AF-AFOSR-0344-90; AF Proj. 2312)
(AD-A240045; AFOSR-91-0732TR) Avail: NTIS HC/MF A01 CSCL 24/3

Issues discussed during the conference included interactions between gases and particulates, health effects of combined exposure in the psychosocial work environment, health effects from combined exposure to solvents, and mechanisms of oto-and vestibulo-toxicity. The material presented at the scientific sessions included both laboratory based research and epidemiological study. GRA

N92-10246# Harvard Univ., Cambridge, MA. Div. of Applied Sciences.
REGIONAL SCALE DYNAMICAL MODELLING OF BIOGEOCHEMICAL PROCESSES Final Technical Report, 1 Oct. 1989 - 14 Aug. 1990
Allan R. Robinson and Gordon McKay 14 Aug. 1990 31 p
(Contract N00014-88-K-0617)
(AD-A240115) Avail: NTIS HC/MF A03 CSCL 08/3

This project involved the design and development of 3D regional biogeochemical models. The biogeochemical models were designed for attachment to the Harvard Hierachy of models, including the surface boundary layer (SBL) component of the open ocean baroclinic eddy resolving quasigeostrophic (QG) model, or its coastal extensions, and the open boundary primitive equation (PE) model with hybrid vertical coordinates. Selection of these physical models is motivated by the interest to study the time evolution of biogeochemical components with realistic physical fields, as they all have data assimilation schemes associated. The approach taken in this model design was first to construct simplified models with a minimal number of biogeochemical components, and then step-by-step to introduce further components and detailed intercomponent interactions. These simplifications allow focused research on important biological mechanisms in the presence of realistic physical fields. Construction of regional biogeochemical models with data assimilation schemes will provide a unique tool to determine processes and sensitivities operative in the real ocean and to facilitate efficient experimental design and model validation. The simplest biogeochemical model of interest is of the nitrogen cycle. During this contract we constructed two models with two different compartmentalizations of the nitrogen components. GRA

N92-10533# Technical Research Centre of Finland, Espoo.
ABATEMENT STRATEGIES BASED ON CRITICAL LOADS Abstract Only
M. Johansson, I. Savolainen, and M. Tahtinen *In* Oulu Univ., Proceedings of the 25th Annual Conference of the Finnish Physical Society 1991 1 p (For primary document see N92-10362 01-70)
Avail: NTIS HC/MF A12

N92-10547# Geophysical Observatory, Sodankyla (Finland).
OZONE DEPLETION RATES IN THE LATE WINTER/EARLY SPRING ARCTIC AND ANTARCTIC STRATOSPHERE ACCORDING TO RECENT OZONE SOUNDING OBSERVATIONS Abstract Only
Esko Kyro and P. Taalas (Finnish Meteorological Inst., Helsinki.) *In* Oulu Univ., Proceedings of the 25th Annual Conference of the Finnish Physical Society 1991 1 p (For primary document see N92-10362 01-70)
Avail: NTIS HC/MF A12

N92-10586# Imatran Voima Oy, Vantaa (Finland).
FOSSIL FUELS AND THE ENVIRONMENT Abstract Only
H. Niininen *In* Oulu Univ., Proceedings of the 25th Annual

Conference of the Finnish Physical Society 1991 1 p (For primary document see N92-10362 01-70)
Avail: NTIS HC/MF A12

N92-10587# Helsinki Univ. of Technology, Espoo (Finland). Dept. of Meteorology.
THE GREENHOUSE EFFECT Abstract Only
E. Holopainen *In* Oulu Univ., Proceedings of the 25th Annual Conference of the Finnish Physical Society 1991 1 p (For primary document see N92-10362 01-70)
Avail: NTIS HC/MF A12

46 GEOPHYSICS

Includes aeronomy; upper and lower atmosphere studies; ionospheric and magnetospheric physics; and geomagnetism.

For space radiation see *93 Space Radiation.*

N92-10247# Atomic Weapons Research Establishment, Aldermaston (England).
THE DETECTION AND LOCATION OF NEAR-REGIONAL SEISMIC DISTURBANCES BY THE ESKDALEMUIR ARRAY: A STUDY USING NOISE AND SIGNAL CORRELATIONS
R. C. Lilwall Feb. 1991 41 p
(AWE-RE-0-20/90; BR116726; ETN-91-99862) Copyright Avail: NTIS HC/MF A03; HMSO, London, England, HC 5 sterling pounds

Recordings of noise and signals from seismic disturbances at near regional (0 to 500 km) disturbances are used to investigate the noise and signal correlations for the Eskdalemuir array. The observed spatial variation of the signal and noise correlations enable predictions to be made on the beamforming capability of the array in terms of potential signal to noise gain. Predicted gains are 3.8 in the 2 to 4 Hz band falling to 3.0 in the 6 to 8 Hz band when using the full 20 seismometer array. The uniform spacing of the seismometers in the array leads to strong grating lobes in the array response which in turn can lead to ambiguities or aliasing in estimates on the slowness and backbearing of incoming signals. This problem is considerably reduced if only signals with slowness less than 0.2 s/km (apparent velocity in excess of 5 Km/s) are considered. Standard errors on the backbearing estimates for near regional signals are found to be in the range 3 to 4 degrees.
ESA

N92-10248*# National Aeronautics and Space Administration. Lyndon B. Johnson Space Center, Houston, TX.
PROGRAM AND ABSTRACTS FOR CLAY MINERALS SOCIETY 28TH ANNUAL MEETING
1991 232 p Meeting held in Houston, TX, 5-10 Oct. 1991 Prepared in cooperation with Lunar and Planetary Inst., Houston, TX
(Contract NASw-4574)
(NASA-TM-105098; NAS 1.15:105098; LPI-Contrib-773) Avail: NTIS HC/MF A11 CSCL 08G

This volume contains abstracts that were accepted for presentation at the annual meeting. Some of the main topics covered include: (1) fundamental properties of minerals and methods of mineral analysis; (2) surface chemistry; (3) extraterrestrial clay minerals; (4) geothermometers and geochronometers; (5) smectite, vermiculite, illite, and related reactions; (6) soils and clays in environmental research; (7) kaolinite, halloysite, iron oxides, and mineral transformations; and (8) clays in lakes, basins, and reservoirs. For individual titles, see N92-10249 through N92-10256.

N92-10249*# National Aeronautics and Space Administration. Lyndon B. Johnson Space Center, Houston, TX.
COMBINED BACKSCATTER MOESSBAUER SPECTROMETER AND X RAY FLUORESCENCE ANALYZER (BaMS/XRF) FOR PLANETARY SURFACE MATERIALS Abstract Only
D. G. Agresti, T. D. Shelfer, M. M. Pimperl, E. L. Wills (Alabama Univ., Birmingham.), and R. V. Morris *In its* Program and Abstracts for Clay Minerals Society 28th Annual Meeting 1991 p 1 (For primary document see N92-10248 01-46)
Avail: NTIS HC/MF A11 CSCL 08G

A backscatter Moessbauer spectrometer (BaMS) with included x ray fluorescence (XRF) capability for the Mars Environment Survey (MESUR) Mission, which has been proposed by NASA for 1998, is being developed. The instrument will also be suitable for other planetary missions such as those to the Moon, asteroids, and other solid solar-system objects. The BaMS would be unique for MESUR in providing information about iron mineralogy in rocks, clays, and other surface materials, including relative proportions of iron-bearing minerals. It requires no sample preparation and can identify all the normal oxidation states of iron (3+, 2+, 0). Thus, BaMS is diagnostic for weathering and other soil-forming processes. Backscatter design allows the addition of XRF elemental analysis with little or no modification. The BaMS/XRF instrument complements the thermal analyzer with evolved gas analyzer (TA-EGA) and the alpha-proton x-ray spectrometer (APXS) proposed (along with BaMS) for geochemical analysis on MESUR.
Author

N92-10250*# National Aeronautics and Space Administration. Ames Research Center, Moffett Field, CA.
CLAYS ON MARS: REVIEW OF CHEMICAL AND MINERALOGICAL EVIDENCE Abstract Only **c91**
Amos Banin and James L. Gooding (Hebrew Univ. of Jerusalem, Rehovot, Israel) *In* NASA. Johnson Space Center, Program and Abstracts for Clay Minerals Society 28th Annual Meeting 1991 p 10 (For primary document see N92-10248 01-46)
Avail: NTIS HC/MF A11 CSCL 03B

Mafic igneous bedrock is inferred for Mars, based on spectrophotometric evidence for pyroxene (principally in optically dark areas of the globe) and the pyroxenite-peridotite petrology of shergottite nakhlite chassignite (SNC) meteorites. Visible and infrared spectra of reddish-brown surface fines (which dominate Martian bright areas) indicate ferric iron and compare favorably (though not uniquely) with spectra of palagonitic soils. Laboratory studies of SNC's and Viking Lander results support a model for Martian soil based on chemical weathering of mafic rocks to produce layer structured silicates (clay minerals), salts, and iron oxides.
Author

N92-10251*# National Aeronautics and Space Administration. Lyndon B. Johnson Space Center, Houston, TX.
TRANSFORMATION PRODUCTS OF SUBMICRON-SIZED ALUMINUM-SUBSTITUTED MAGNETITE: COLOR AND REDUCTANT SOLUBILITY Abstract Only **c91**
D. C. Golden, D. W. Ming, and H. V. Lauer, Jr. (Lockheed Engineering and Sciences Co., Houston, TX.) *In its* Program and Abstracts for Clay Minerals Society 28th Annual Meeting 1991 p 61 (For primary document see N92-10248 01-46)
Avail: NTIS HC/MF A11 CSCL 03B

Magnetite, when present as fine particles, is soluble in acid ammonium oxalate (pH equals 3). However, the commonly used extractant for free iron oxides (i.e., citrate dithionite-bicarbonate (CDB) is not very effective in dissolving magnetite in soils and geologic materials. Upon oxidation, magnetite transforms to maghemite; at elevated temperatures, maghemite inverts to hematite. This transformation causes a change in color from black to red and may affect the reductant solubility as well. The objectives here were to examine the color and reflectance spectral characteristics of products during the transformation of magnetite to maghemite to hematite and to study the effect of Al-substitution in magnetite on the above process. Reductant solubility of Al-substituted magnetite, maghemite, and hematite was also studied. In summary, the transformation of magnetite to maghemite was accompanied by a change in color from black to red because of the oxidation of Fe2(+) to Fe3(+). The phase change maghemite to hematite had a relatively minor effect on the color and the reflectance spectra.
Author

N92-10252*# National Aeronautics and Space Administration. Lyndon B. Johnson Space Center, Houston, TX.
CLAY MINERALS IN PRIMITIVE METEORITES AND INTERPLANETARY DUST 2. SMECTITES AND MICAS Abstract Only **c90**
L. P. Keller and M. E. Zolensky *In its* Program and Abstracts for Clay Minerals Society 28th Annual Meeting 1991 p 87 (For primary document see N92-10248 01-46)
Avail: NTIS HC/MF A11 CSCL 03B

The classification is briefly summarized of stony meteorites and cosmic dust, and the mineralogy and chemistry is described of serpentine group minerals. The occurrence of smectites and micas in extraterrestrial materials is examined. The characterization of fine grained minerals in meteorites and IDPs relies heavily on electron beam instruments, especially the transmission electron microscope (TEM). Typically, phyllosilicates are identified by a combination of high resolution imaging of basal spacings, electron diffraction, and chemical analysis. Smectites can be difficult to differentiate from micas because the smectites lose their interlayer water and the interlayer partly collapse in the high vacuum of the TEM. Author

N92-10253*# National Aeronautics and Space Administration. Lyndon B. Johnson Space Center, Houston, TX.
MINERALOGY OF CRETACEOUS/TERTIARY BOUNDARY CLAYS IN THE CHICXULUB STRUCTURE IN NORTHERN YUCATAN Abstract Only **c90**
D. W. Ming, Virgil L. Sharpton, and B. C. Schuraytz (Lunar and Planetary Inst., Houston, TX.) *In its* Program and Abstracts for Clay Minerals Society 28th Annual Meeting 1991 p 114 (For primary document see N92-10248 01-46)
Avail: NTIS HC/MF A11 CSCL 03B

The Cretaceous/Tertiary (K/T) boundary clay layer is thought to be derived from ejecta material from meteorite impact, based on the anomalous concentrations of noble metals in the layer. Because of recent findings of a half-meter thick ejecta deposit at the K/T boundary in Haiti, efforts have focused on locating a large impact feature in the Caribbean and the Gulf of Mexico. One of the leading candidates for the site of a large impact is the Chicxulub structure located on the northern Yucatan Peninsula in Mexico. The Chicxulub structure is a subsurface zone of upper Cretaceous igneous rocks, carbonates, and breccias. The structure has been interpreted to be a 200 km diameter; however, there is some question to the size of the structure or to the fact that it even is an impact feature. Little is known about the mineralogy of this structure; the objective of this study was to determine the clay mineralogy of core samples from within the Chicxulub structure. Author

N92-10254*# National Aeronautics and Space Administration. Lyndon B. Johnson Space Center, Houston, TX.
UV, VISIBLE, AND NEAR-IR REFLECTIVITY DATA FOR MAGNETIC SOILS/ROCKS FROM BRAZIL Abstract Only
R. K. Vempati, R. V. Morris, H. V. Lauer, Jr., and J. M. D. Coey (Trinity Coll., Dublin, Ireland) *In its* Program and Abstracts for Clay Minerals Society 28th Annual Meeting 1991 p 161 (For primary document see N92-10248 01-46)
Avail: NTIS HC/MF A11 CSCL 08G

The objective is to obtain UV, visible, and near-IR reflectivity spectra for several magnetic Brazilian soils/rocks and compare them to corresponding data for Mars to see if these materials satisfy both magnetic and spectral constraints for Mars. Selected physical properties of the magnetic Brazilian soils/rocks are presented. In general, the spectral features resulting from ferric crystal-field transitions are much better defined in the spectra of the magnetic Brazilian soils/rocks than in Martian spectral data. Presumably, this results from a relatively higher proportion of crystalline ferric oxides for the former. The apparent masking of the spectral signature of maghemite by hematite or goethite for the Brazilian samples implies the magnetic and spectral constraints for Mars can be decoupled. That is, maghemite may be present in magnetically-significant but optically-insignificant amounts compared to crystalline hematite. Author

N92-10255*# National Aeronautics and Space Administration. Lyndon B. Johnson Space Center, Houston, TX.
SYNTHESIS AND PROPERTIES OF TI-SUBSTITUTED GOETHITES AND HEMATITES Abstract Only **c91**
R. K. Vempati, R. V. Morris, H. V. Lauer, Jr. (Lunar and Planetary Inst., Houston, TX.), and J. DeHart *In its* Program and Abstracts for Clay Minerals Society 28th Annual Meeting 1991 p 162 (For primary document see N92-10248 01-46)
Avail: NTIS HC/MF A11 CSCL 03B

The objective was to synthesize Ti-substituted goethites and hematites and to characterize them using x-ray diffraction, thermogravimetric analysis, coulimetry, optical and Mossbauer spectroscopies, and magnetic data in order to determine the evidence of Ti substitution for Martian spectral data. Evidence is provided that up to 4 mole percent can be incorporated into the goethite structure during the low temperature synthesis. Because the spectral data in the visible and near-IR are not sensitive to the degree of Ti-substitution in goethites and hematites, such data cannot be used to infer the presence or absence of Ti substitution in Martian hematites and goethites. Author

N92-10256*# National Aeronautics and Space Administration. Lyndon B. Johnson Space Center, Houston, TX.
CLAY MINERALS IN PRIMITIVE METEORITES AND INTERPLANETARY DUST 1 Abstract Only **c90**
M. E. Zolensky and L. P. Keller *In its* Program and Abstracts for Clay Minerals Society 28th Annual Meeting 1991 p 184 (For primary document see N92-10248 01-46)
Avail: NTIS HC/MF A11 CSCL 03B

Many meteorites and interplanetary dust particles (IDPs) with primitive compositions contain significant amounts of phyllosilicate minerals, which are generally interpreted as evidence of protoplanetary aqueous alteration at an early period of the solar system. These meteorites are chondrites (near solar composition) of the carbonaceous and ordinary varieties. The former are subdivided (according to bulk composition and petrology) into CI, CM, CV, CO, CR, and ungrouped classes. IDPs are extraterrestrial particulates, collected in stratosphere, which have chemical compositions indicative of a primitive origin; they are typically distinct from the primitive meteorites. Characterization of phyllosilicates in these materials is a high priority because of the important physico-chemical information they hold. The most common phyllosilicates present in chondritic extraterrestrial materials are serpentine-group minerals, smectites, and micas. We discuss these phyllosilicates and describe the interpretation of their occurrence in meteorites and IDPs and what this indicates about history of their parent bodies, which are probably the hydrous asteroids. Author

N92-10257*# National Aeronautics and Space Administration. Goddard Space Flight Center, Greenbelt, MD.
GEOID UNDULATIONS AND GRAVITY ANOMALIES OVER THE ARAL SEA, THE BLACK SEA AND THE CASPIAN SEA FROM A COMBINED GEOS-3/SEASAT/GEOSAT ALTIMETER DATA SET
Andrew Y. Au, Richard D. Brown (ST Systems Corp., Lanham, MD.), and Jean E. Welker Jul. 1991 57 p Original contains color illustrations
(NASA-TM-104543; Rept-91E02481; NAS 1.15:104543) Avail: NTIS HC/MF A04; 2 functional color pages CSCL 08C

Satellite-based altimetric data taken by GOES-3, SEASAT, and GEOSAT over the Aral Sea, the Black Sea, and the Caspian Sea are analyzed and a least squares collocation technique is used to predict the geoid undulations on a 0.25x0.25 deg. grid and to transform these geoid undulations to free air gravity anomalies. Rapp's 180x180 geopotential model is used as the reference surface for the collocation procedure. The result of geoid to gravity transformation is, however, sensitive to the information content of the reference geopotential model used. For example, considerable detailed surface gravity data were incorporated into the reference model over the Black Sea, resulting in a reference model with significant information content at short wavelengths. Thus, estimation of short wavelength gravity anomalies from gridded geoid

heights is generally reliable over regions such as the Black Sea, using the conventional collocation technique with local empirical covariance functions. Over regions such as the Caspian Sea, where detailed surface data are generally not incorporated into the reference model, unconventional techniques are needed to obtain reliable gravity anomalies. Based on the predicted gravity anomalies over these inland seas, speculative tectonic structures are identified and geophysical processes are inferred. Author

N92-10258# Tokyo Univ. (Japan). Inst. of Space and Astronautical Science.
THEORETICAL ESTIMATION OF THE VIBRATIONAL TEMPERATURES OF N2 MOLECULES IN THE IONOSPHERE AND IN THE LABORATORY SIMULATED PLASMA
K. S. Kalpuri and K.-I. Oyama Jun. 1991 16 p
(ISAS-642; ISSN-0285-6808) Avail: NTIS HC/MF A03

The vibrational temperature of excited nitrogen molecules (N2) are estimated theoretically for the case of ionosphere as well as for the lab simulated plasma, considering the various chemical reactions leading to the production and loss of N2 molecules. It was found that even in the case when quenching of the excited molecules by O and CO2 is considered, the vibrational temperature, T sub v, is higher than the neutral temperature, T sub n, below about 105 km but the difference decreases and about 120 km, the value of T sub v is less than T sub n. However, for no quenching case, the vibrational temperature can be as high as 1600 K at 150 km. The vibrational temperature for the lab simulated plasma on the other hand was found to be high (1500 K or more), the absolute value being dependent upon the concentration of O2 in the gas mixture taken and the intensity of UV light used for excitation of nitrogen molecules. Author

N92-10259# Tokyo Univ. (Japan). Inst. of Space and Astronautical Science.
ELECTRON TEMPERATURES IN THE E-REGION OF THE IONOSPHERE
K. S Zalpuri and K.-I. Oyama Jun. 1991 20 p
(ISAS-641; ISSN-0285-6808) Avail: NTIS HC/MF A03

Various heating and cooling mechanisms which are operative in the lower E region are discussed and their relative importance in different altitude range is shown. These heating and cooling rates are then used to derive the electron temperature, T sub e. The calculated values of electron temperatures are found to be higher than neutral temperature through out the altitude range 100 to approx. 150 km, with the difference increasing with increase in altitude. However, compared to observed values of T sub e, the calculated values are still smaller below about 130 km. Above this altitude, the calculated values become larger. Estimation of T sub e for different, suggested values of heating efficiency due to dissociative recombination, show that T sub e profile obtained even by assuming a constant value of 1.3 eV is in fairly good agreement with those derived based on variable values of this parameter. Author

N92-10260# Los Alamos National Lab., NM.
ATMOSPHERIC MEASUREMENTS USING A SCANNING, SOLAR-BLIND RAMAN LIDAR
W. E. Eichinger, D. I. Cooper, D. B. Holtkamp, R. R. Karl, Jr., C. R. Quick, and J. J. Tiee 1991 5 p Presented at the Optical Society of America (OSA) Remote Sensing of the Atmosphere, Williamsburg, VA, 18-21 Nov. 1991
(Contract W-7405-eng-36)
(DE91-016078; LA-UR-91-2184; CONF-911165-2) Avail: NTIS HC/MF A01

The study of the water cycle by Lidar has many applications. Because micro-scale structures can be identified by their water content, the technique offers new opportunities to visualize and study the phenomena. There are applications to many practical problems in agricultural and water management as well as at waste storage sites. Conventional point sensors are limited and are inappropriate for use in complex terrain or varied vegetation and cannot be extrapolated over even modest ranges. To this end, techniques must be developed to measure the variables associated with evapotranspirative processes over large areas and varied surface conditions. A scanning water-Raman Lidar is an ideal tool for this task - it can measure the water vapor concentration rapidly with high spatial resolution without influencing the measurements by the presence of the sensor. DOE

N92-10261# Geological Survey, Denver, CO.
GEOLOGIC MAPPING OF TUNNELS USING PHOTOGRAMMETRY: CAMERA AND TARGET POSITIONING
J. A. Coe and K. S. Dueholm (Technical Univ. of Denmark, Lyngby.) 1991 15 p
(Contract DE-AI08-78ET-44802)
(DE91-018394; USGS-OFR-90-49) Avail: NTIS HC/MF A03

A photogrammetric method has been developed by the U.S. Geological Survey and the U.S. Bureau of Reclamation for the use in geologic mapping of tunnels (drifts). The method requires photographing the tunnel walls and roof with a calibrated small-format camera to obtain stereo pairs of photos which are then oriented in an analytical stereo plotter for measurement of geologic features. The method was tested in G-tunnel at Rainier Mesa on the Nevada Test Site. Calculations necessary to determine camera and target positions and problems encountered during testing were used to develop a set of generic formulas that can be applied to any tunnel. DOE

N92-10262# Range Commanders Council, White Sands Missile Range, NM.
RANGE REFERENCE ATMOSPHERE, NELLIS AIR FORCE BASE, NEVADA
Aug. 1991 161 p
(AD-A239816; RCC-377-91) Avail: NTIS HC/MF A08 CSCL 04/2

A reference atmosphere is a statistical model of the earth's atmosphere, derived from upper-air observations over a specific location. The individual RRA is the authoritative source for upper-atmosphere climatology over the launch and recovery site for which it has been prepared. The RRA's are used to plan, evaluate, and establish environmental launch constraints for aerospace vehicles launched from a particular location. GRA

N92-10263# Massachusetts Inst. of Tech., Cambridge.
IONOSPHERIC AND MAGNETOSPHERIC PROCESSES Final Report, 28 Feb. 1986 - 28 Feb. 1991
Tom Chang 17 May 1991 108 p
(Contract F19628-86-K-0005)
(AD-A239967; PL-TR-91-2117) Avail: NTIS HC/MF A06 CSCL 04/1

Results of a five-year study of a variety of kinetic plasma processes in the ionosphere and magnetosphere are described. Specific topics discussed in detail include: (1) the formation of ion conics due to electromagnetic ion cyclotron and/or lower hybrid turbulence; (2) auroral beam-plasma interactions and VLF turbulence; (3) heating of charged particles in the ionosphere and magnetosphere due to strong plasma turbulence; (4) formation of counterstreaming electron distributions along auroral field lines; and (5) double layer formation along discrete auroral field lines. The following subject areas are discussed: particle acceleration by electromagnetic ion cyclotron turbulence; particle acceleration by intense auroral VLF turbulence; equatorially generated ULF waves as a source for the turbulence associated with ion conics; and a 3-D model of double layer formation on auroral field lines are described. A complete listing of published papers and books during the years 1986-1991 is also included. GRA

N92-10264# Science Applications International Corp., San Diego, CA.
PLASMA CLOUD BEHAVIOR Technical Report, 1 Jul. 1980 - 1 Feb. 1983
Lewis M. Linson 1 Aug. 1991 48 p
(Contract DNA001-80-C-0246H; DNA Proj. 125-AAXH)
(AD-A240000; SAIC-89/1097; DNA-TR-89-55) Avail: NTIS HC/MF A03 CSCL 04/1

Participation in PLACES (Position Location And

Communications Effects Simulations) and Midnight Sky field operations is described. In the former, four barium releases were made during the period 4 to 12 December 1980. The range of velocities experienced was greater than before at this location. The principal challenge was to perform real-time tracking of the ion cloud so as to predict a future aim point for use in targeting beacon and probe rockets. Recommendations for obtaining smoother tracking data involve determining the motion of a field line through the ion cloud rather than an indeterminate point in the cloud, making measurements at set intervals, and coordinating measurements by more than one observer. During Midnight Sky, 2 barium releases were made on 29 March 81 and 2 April 81. The first went westerly at 450 m/s while the second was nearly motionless. A small aircraft was positioned so as to take photographs up the magnetic field line during the second release. It is strongly urged that a complete dry run including all participants, communications links, and necessary operations be carried out before a test event. GRA

N92-10265# Royal Norwegian Council for Scientific and Industrial Research, Kjeller.
INTEGRATED ARRAY AND 3-COMPONENT PROCESSING USING A SEISMIC MICROARRAY Report, 1 Feb. - 30 Apr. 1991
T. Kvaerna and F. Ringdal 31 May 1991 40 p
(Contract F49620-89-C-0038)
(AD-A240139; PL-TR-91-2142; SR-9) Avail: NTIS HC/MF A03
CSCL 08/11

A microarray is modeled on a subgeometry of the NORESS array, and comprises a 3-component center seismometer surrounded by 3 closely spaced vertical-component sensors deployed over a typical aperture of 0.3 km. Analysis of five days of continuous data has shown that such a system combines the benefits of array and 3-component processing in providing reliable automatic detection, phase identification, and location of weak seismic events at local and regional distances. The data processing has comprised: (1) multiple-band filtering, (2) coherent and incoherent beamforming, (3) STA/LTA threshold detection, (4) broadband frequency-wavenumber (f-k) analysis, and (5) automatic phase association and event location. Using vertical components only, broadband f-k array analysis enables correct phase identification (P-type og S-type phase) in 95 percent of the cases, and gives S-wave azimuths with a root-mean-square (RMS) deviation of 13.9 degrees from the estimates of the full NORESS array. It is particularly significant that the small array eliminates the need for introducing particle motion models, which creates ambiguities in 3-component analysis of secondary phases when interfering SH and SV phases occur. GRA

N92-10368# EISCAT Scientific Association, Kiruna (Sweden).
THE STRUCTURE AND DYNAMICS OF THE POLAR MESOSPHERE INVESTIGATED WITH THE EISCAT RADAR SYSTEMS Abstract Only
J. Roettger *In* Oulu Univ., Proceedings of the 25th Annual Conference of the Finnish Physical Society 1991 1 p (For primary document see N92-10362 01-70)
Avail: NTIS HC/MF A12

N92-10551# Oulu Univ. (Finland). Dept. of Geophysics.
LITHOSPHERE PHYSICS: GEOELECTRICS AND SEISMICS Abstract Only
T. Korja *In its* Proceedings of the 25th Annual Conference of the Finnish Physical Society 1991 1 p (For primary document see N92-10362 01-70)
Avail: NTIS HC/MF A12

N92-10552# Academy of Sciences (USSR), Moscow. Inst. of the Physics of the Earth.
ON THE IONOSPHERIC INFLUENCE UPON THE SPECTRAL STRUCTURE ON THE Pc1 GEOMAGNETIC PULSATIONS Abstract Only
F. Z. Feygin, A. K. Nekrasov, Jorma Kangas, K. Mursula, and T. Pikkarainen (Oulu Univ., Finland) *In* Oulu Univ., Proceedings of the 25th Annual Conference of the Finnish Physical Society 1991 1 p (For primary document see N92-10362 01-70)
Avail: NTIS HC/MF A12

N92-10553# Oulu Univ. (Finland). Dept. of Physics.
EISCAT RESEARCH PROGRAM Abstract Only
Jorma Kangas *In its* Proceedings of the 25th Annual Conference of the Finnish Physical Society 1991 1 p (For primary document see N92-10362 01-70)
Avail: NTIS HC/MF A12

N92-10554# Oulu Univ. (Finland). Dept. of Physics.
THE USE OF WHISTLERS FOR MAGNETOSPHERIC DIAGNOSTICS Abstract Only
Jyrki Manninen *In its* Proceedings of the 25th Annual Conference of the Finnish Physical Society 1991 1 p (For primary document see N92-10362 01-70)
Avail: NTIS HC/MF A12

N92-10555# Oulu Univ. (Finland). Dept. of Physics.
EXAMPLES OF VLF EMISSIONS RECORDED IN THE AURORAL ZONE Abstract Only
Jyrki Manninen, Tauno Turunen, and Timo Turunen (Geophysical Observatory, Sodankyla, Finland) *In its* Proceedings of the 25th Annual Conference of the Finnish Physical Society 1991 1 p (For primary document see N92-10362 01-70)
Avail: NTIS HC/MF A12

N92-10556# Oulu Univ. (Finland). Dept. of Physics.
AVERAGE PROPERTIES OF ENERGETIC IONS IN DIFFERENT PARTS OF THE CUSP/CLEFT REGION Abstract Only
K. Mursula, G. Kremser, and B. Wilken (Max-Planck-Inst. fuer Aeronomie, Katlenburg-Lindau, Germany, F.R.) *In its* Proceedings of the 25th Annual Conference of the Finnish Physical Society 1991 1 p (For primary document see N92-10362 01-70)
Avail: NTIS HC/MF A12

N92-10557# Academy of Sciences (USSR), Moscow. Inst. of the Physics of the Earth.
INHOMOGENEITY AND NONLINEARITY EFFECTS ON STOP BANDS OF ALFVENIC ION CYCLOTRON WAVES IN MULTICOMPONENT PLASMA Abstract Only
A. K. Nekrasov, K. Mursula, Jorma Kangas, T. Pikkarainen (Oulu Univ., Finland), and N. F. Maltseva *In* Oulu Univ., Proceedings of the 25th Annual Conference of the Finnish Physical Society 1991 1 p Previously announced in IAA as A91-25582 (For primary document see N92-10362 01-70)
Avail: NTIS HC/MF A12

N92-10558# Oulu Univ. (Finland). Dept. of Physics.
ENERGY-LATITUDE DISPERSION OF ENERGETIC IONS IN THE DAYSIDE OF THE EARTH'S MAGNETOSPHERE: A SUBSTORM-RELATED PHENOMENON Abstract Only
R. Rasinkangas, G. Kremser, B. Wilken, and F. Soraas (Bergen Univ., Norway) *In its* Proceedings of the 25th Annual Conference of the Finnish Physical Society 1991 1 p (For primary document see N92-10362 01-70)
Avail: NTIS HC/MF A12

N92-10559# Geophysical Observatory, Sodankyla (Finland).
EISCAT INCOHERENT SCATTER RADAR OBSERVATIONS AND MODEL STUDIES ON DAY TO NIGHT VARIATIONS IN THE IONOSPHERIC D-REGION DURING THE PCA EVENT OF AUGUST 1989 Abstract Only
E. Turunen *In* Oulu Univ., Proceedings of the 25th Annual Conference of the Finnish Physical Society 1991 1 p (For primary document see N92-10362 01-70)
Avail: NTIS HC/MF A12

N92-10560# Oulu Univ. (Finland). Dept. of Physics.
OBSERVATIONS OF SEMIDIURNAL ATMOSPHERIC TIDES USING THE EISCAT INCOHERENT SCATTER RADAR Abstract Only
A. Huuskonen and T. Nygren *In its* Proceedings of the 25th

Annual Conference of the Finnish Physical Society 1991 1 p (For primary document see N92-10362 01-70)
Avail: NTIS HC/MF A12

N92-10561# Geophysical Observatory, Sodankyla (Finland).
VARIATION OF D-REGION PARAMETERS DURING POLAR CAP ABSORPTION EVENTS IN THE YEAR 1989 Abstract Only
H. Ranta *In* Oulu Univ., Proceedings of the 25th Annual Conference of the Finnish Physical Society 1991 1 p (For primary document see N92-10362 01-70)
Avail: NTIS HC/MF A12

N92-10746*# Jet Propulsion Lab., California Inst. of Tech., Pasadena.
HORIZONTAL STRESS IN PLANETARY LITHOSPHERES FROM VERTICAL PROCESSES
W. B. Banerdt *In* NASA, Washington, Reports of Planetary Geology and Geophysics Program, 1990 Jun. 1991 p 46-48 (For primary document see N92-10728 01-91)
Avail: NTIS HC/MF A25 CSCL 03B

N92-10957*# Lancaster Univ. (England). Environmental Science Div.
FACTORS CONTROLLING THE STRUCTURES OF MAGMA CHAMBERS IN BASALTIC VOLCANOES
L. Wilson and James W. Head (Brown Univ., Providence, RI.) *In* NASA, Washington, Reports of Planetary Geology and Geophysics Program, 1990 Jun. 1991 p 579-580 (For primary document see N92-10728 01-91)
Avail: NTIS HC/MF A25 CSCL 03B

47 METEOROLOGY AND CLIMATOLOGY

Includes weather forecasting and modification.

N92-10266# Lamont-Doherty Geological Observatory, Palisades, NY.
RECENT CHANGES OF WEATHER PATTERNS IN NORTH AMERICA
1991 7 p
(Contract DE-FG02-85ER-60372)
(DE91-017706; DOE/ER-60372/6) Avail: NTIS HC/MF A02

Much effort in the last several years has been spent in the preparation of digitized quality controlled and homogenized data basis suitable for the time series analysis. This work has taken considerably more time than originally expected due to many serious and unexpected problems in the data. It has been necessary to balance the quality requirements with the needs of uniform geographic coverage, the uncertainty due to the data gaps with the uncertainties involved in the applied corrections. In general we prefer to end up with less data of higher quality than with more data of low quality. Today most of the work on the preparation of the necessary data sets is completed. Other research groups within NOAA-NCDC or cooperating with NOAA are currently working on the addition of quality controlled data sets which will become available for the study. Thus the bulk of our effort may be oriented toward the analysis. This will be done by similar statistical procedures as those used in our earlier work. The bulk of the analysis is done using Monte Carlo techniques. DOE

N92-10267*# ST Systems Corp., Hampton, VA.
SOLAR CONSTANT (SOLCON) EXPERIMENT: GROUND SUPPORT EQUIPMENT (GSE) SOFTWARE DEVELOPMENT Final Report
M. Alan Gibson, Susan Thomas, and Robert Wilson Jun. 1991 77 p
(Contract NAS1-18460)
(NASA-CR-187596; NAS 1.26:187596) Avail: NTIS HC/MF A05 CSCL 04B

The Solar Constant (SOLCON) Experiment, the objective of which is to determine the solar constant value and its variability, is scheduled for launch as part of the Space Shuttle/Atmospheric Laboratory for Application and Science (ATLAS) spacelab mission. The Ground Support Equipment (GSE) software was developed to monitor and analyze the SOLCON telemetry data during flight and to test the instrument on the ground. The design and development of the GSE software are discussed. The SOLCON instrument was tested during Davos International Solar Intercomparison, 1989 and the SOLCON data collected during the tests are analyzed to study the behavior of the instrument.
Author

N92-10268# Naval Oceanography Command Center/Joint Typhoon Warning Center, FPO San Francisco, CA.
ANNUAL TROPICAL CYCLONE REPORT, 1990 Report, Jan. - Dec. 1990
Dieter K. Rudolph and Charles P. Guard 1990 288 p
(AD-A239910) Avail: NTIS HC/MF A13 CSCL 04/2

This annual publication summarizes tropical cyclone activity in the Western North Pacific Bay of Bengal, Arabian Sea, Western South Pacific and South Indian Oceans. A best track is provided for each significant tropical cyclone. A brief narrative is given for all tropical cyclones in the Western North Pacific and North Indian Oceans. All reconnaissance and fix data used to construct the best tracks can be provided, upon request, on floppy diskettes. Forecast verification data and statistics for the Joint Typhoon Warning Center (JTWC) are submitted. GRA

N92-10269# Phillips Lab., Hanscom AFB, MA.
A SURVEY OF LASER LIGHTNING ROD TECHNIQUES Scientific Proceedings
Arnold A. Barnes, Jr. and Robert O. Berthel 21 Aug. 1991 7 p Presented at the International Conference on Lightning and Static Electricity, Cocoa Beach, FL, 16-19 Apr. 1991 Previously announced in IAA as N91-32645
(AF Proj. ILIR)
(AD-A239988; PL-TR-91-2201) Avail: NTIS HC/MF A02 CSCL 13/12

The concept of using a laser to create an ionized path in the atmosphere to act as a lightning rod is not new. Over the past four decades since the invention of the laser, there have been many documented investigations into the ionization of atmospheric gases with an eye towards creating a laser lightning rod. Initial experimental attempts using lasers operating in the IR were not successful. Although some ionization was attained, it was found that the laser beam was self-quenching so that distances of only tens of meters were obtained in the atmosphere near sea level. This paper briefly reviews the work which has been done in trying to create a laser lightning rod and discusses some ongoing research which has potential for achieving an operational laser lightning rod for use in the protection of missile launch sites, launch vehicles, and other property. Author (GRA)

N92-10270# Phillips Lab., Hanscom AFB, MA.
PREDICTING CLOUD-TO-GROUND LIGHTNING WITH NEURAL NETWORKS Scientific Proceeding
Arnold A. Barnes, Jr., Donald Frankel, and James S. Draper (KTAADN, Inc., Newton, MA.) 20 Aug. 1991 11 p Presented at the International Conference on Lightning and Static Electricity, Cocoa Beach, FL, 16-19 Apr. 1991
(AF Proj. 6670)
(AD-A239989; PL-TR-91-2199) Avail: NTIS HC/MF A03 CSCL 04/2

Lightning is a hazard to ground operations, launch operations and recovery at Cape Canaveral. The Air Force is responsible for providing the forecasts of lightning for these operations. Neural networks (a sub-discipline of artificial intelligence which deals with the relationships between sets of data) are being applied in an effort to improve the forecasting of cloud to ground lightning. The excellent data sets from Cape Canaveral are used as inputs and lightning strike data are used as the output (predicted) data to train the networks. Wind data from 32 towers were used to predict lightning strikes in 16 blocks over Cape Canaveral for four time periods: 0-15 min., 15-30 min., 30-60 min., and 1-2 hours. The network was trained by backpropagation using the data from one day and was verified on independent data. Comparisons made

with the currently used convergence method gave similar results. The neural network results improved with larger training sets and with the addition of other readily available data. Five minute averaged field mill data did not improve the predictions, indicating that short term variations of the field mill data should be used. GRA

N92-10271# Naval Postgraduate School, Monterey, CA. Dept. of Meteorology.
ONR TROPICAL CYCLONE MOTION RESEARCH INITIATIVE: DATA USERS GUIDE TO OBSERVATIONS Interim Report, Oct. 1990 - Sep. 1991
Patrick A. Harr, Tamar Neta, and Russell L. Elsberry Jul. 1991 126 p
(AD-A240061; NPS-MR-91-002) Avail: NTIS HC/MF A07 CSCL 04/2

The Tropical Cyclone Motion (TCM-90) Data User's Guide addresses the collection, types, preparation, quality control, format and data base structure for all data collected during the field phase of TCM-90. Additionally, this Guide addresses the data collected from the three concurrent tropical cyclone field experiments (Elsberry 1990): (1) ESCAP/WMO Typhoon Committee Special Experiment Concerning Typhoon Recurvature and Unusual Movement (SPECTRUM); (2) USSR TYPHOON-90 expedition; and (3) Taiwan Area Typhoon Experiment (TATEX). The Data Management Plan contained in Elsberry et al. (1990) describes a framework for construction of a comprehensive data set that utilizes all of the data from the concurrent tropical cyclone experiments. This Data User's Guide will aid researchers who wish to utilize this complete data set. GRA

48 OCEANOGRAPHY

Includes biological, dynamic, and physical oceanography; and marine resources.

For related information see also *43 Earth Resources and Remote Sensing.*

N92-10272# Academy of Sciences (USSR), Moscow. Space Research Inst.
RADIOHYDROPHYSICAL AEROSPACE RESEARCH OF OCEAN
V. S. Etkin, M. D. Raev, M. G. Bulatov, Yu. A. Militsky, A. V. Smirnov, V. Yu. Raizer, Yu. A. Trokhimovsky, V. G. Irisov, A. V. Kuzmin, and K. Ts. Litovchenko et al 1991 84 p
(SRI-PR-1749) Avail: NTIS HC/MF A05

A review of theoretical and experimental papers devoted to microwave, infrared, and optic remote sensing of ocean is presented. The active and passive techniques and tools and their application to such physical parameters and phenomena as sea surface temperature, near surface wind, sea wave spectra, waves breaking, internal waves in ocean and atmosphere, surface and internal waves nonlinear interactions, sea currents, hydrological fronts, etc., are considered. Author

N92-10273# Princeton Univ., NJ. Dept. of Geological and Geophysical Sciences.
SIMULATIONS OF THE CARBON CYCLE IN THE OCEANS
J. L. Sarmiento 1991 4 p
(Contract DE-FG02-90ER-61052)
(DE91-018475; DOE/ER-61052/1) Avail: NTIS HC/MF A01

A perturbation approach for simulating carbon dioxide uptake which estimates oceanic uptake of CO2 in excess of 2 GtC/yr over the last decade is being readied for publication. The recent estimate of less than 1 GtC/yr is believed to be due to an undersampling bias. A major effort was put into studies of the effect of iron fertilization on uptake of anthropogenic CO2 by the oceans. We find that while fertilization will reduce the CO2 increase, it will not reverse the trend. Also, iron fertilization may double nitrous oxide flux out of the ocean, partially canceling the CO2 reduction and having an unknown effect on the ozone layer. A paper in preparation describes the three-dimensional seasonal variations in nitrogen concentration in the ocean. The model does a reasonable job of matching observations, although performance could be improved by adjusting the biological parameters and increasing the physical resolution. A dual-currency carbon-nitrogen model is being constructed, with a first version recently completed. DOE

N92-10274# Institute for Naval Oceanography, Bay Saint Louis, MS.
VERMOD CAPABILITIES. VERMOD 1.0 AND FUTURE
Harsh Anand, Michael S. Foster, Ramesh Krishnamagaru, and Ranjit M. Passi Jun. 1991 35 p
(NR Proj. RM3-5-G-97)
(AD-A239801; AD-E040098; INO-TM-4) Avail: NTIS HC/MF A03 CSCL 08/3

The Institute for Naval Oceanography (INO) has established the Experimental Center for Mesoscale Ocean Prediction (ECMOP) to facilitate research and development of ocean models. ECMOP aims to take advantage of existing infrastructures to provide support to Navy and academic researchers in an end-to-end model evaluation effort. In addition, if and when necessary, ECMOP performs internal research and development as an adjunct to this support. ECMOP is composed of three functional subsystems, or modules: the Verification Module (VERMOD), the Visualization Module (VISMOD), and the Data Sub-System (DASS). This technical memorandum describes the current state of VERMOD, in particular, its statistical and physical criteria for model verification, and the software structural characteristics of the module. Finally, we discuss several of the verification concepts anticipated as future enhancements of VERMOD. GRA

N92-10275# Washington Univ., Seattle. Applied Physics Lab.
SEA ICE ELASTIC MODULI: DETERMINATION OF BIOT PARAMETERS USING IN-FIELD VELOCITY MEASUREMENTS
K. L. Williams and R. E. Francois Jun. 1991 34 p
(Contract N00039-91-C-0072)
(AD-A239803; AD-E040115; NOARL-CR-036-91) Avail: NTIS HC/MF A03 CSCL 08/12

The elastic moduli of sea ice are determined from high frequency velocity measurements made on small samples extracted from the ice canopy. The experimental apparatus for determining the velocities is described and was designed to allow quick in-field measurement. The experimental procedure included measurement of the ice sample salinity and temperature and the results given here allow prediction of elastic moduli from knowledge of these more easily obtainable physical parameters. The elastic moduli determined are those appropriate for a specialized Biot model in which the ice is viewed as a closed pore isotropic material. With the Biot model put forth here, seven parameters are needed to predict acoustic velocities, all of which are easily interpreted physically and are given here in terms of their salinity and temperature dependences. PACS numbers: 43.20.Bi, 43.20.Hg, 43.30.Ma, 43.35.Cg. GRA

51 LIFE SCIENCES (GENERAL)

N92-10276# California Univ., Davis.
PAUCITY OF MODERATELY REPETITIVE SEQUENCES
C. W. Schmid 1991 3 p
(Contract DE-FG03-88ER-60693)
(DE91-017953; DOE/ER-60693/T1) Avail: NTIS HC/MF A01

We examined clones of renatured repetitive human DNA to find novel repetitive DNAs. After eliminating known repeats, the remaining clones were subjected to sequence analysis. These clones also corresponded to known repeats, but with greater sequence diversity. This indicates that either these libraries were depleted of short interspersed repeats in construction, or these repeats are much less prevalent in the human genome than is indicated by data from Xenopus or sea urchin DNA studies. We directly investigated the sequence composition of human DNA through traditional renaturation techniques with the goal of

estimating the limits of abundance of repetitive sequence classes in human DNA. Our results sharply limit the maximum possible abundance to 1 to 2 percent of the human genome. Our estimate, minus the known repeats in this fraction, leaves about 1 percent (3 x 10(exp 7) nucleotides) of the human genome for novel repetitive elements. DOE

52 AEROSPACE MEDICINE

Includes physiological factors; biological effects of radiation; and effects of weightlessness on man and animals.

N92-10277 Institute for Perception RVO-TNO, Soesterberg (Netherlands). Thermophysiology Group.
PHYSIOLOGICAL RESPONSES OF THE HUMAN EXTREMITIES TO COLD WATER IMMERSION Final Report
H. A. M. Daanen and M. B. Ducharme (Defence and Civil Inst. of Environmental Medicine, North York, Ontario) 5 Apr. 1991 31 p
(Contract A87/M/124)
(IZF-1991-A-15; TD-91-0044; ETN-91-99992) Copyright Avail: Institute for Perception RVO-TNO, P.O. Box 23, 3769 ZG Soesterberg, Kampweg 45, Netherlands

Five subjects immersed their hands and feet twice during 1 hour sessions in a calorimeter bath, filled with water at 25 C. Before immersion the hand (33.0 + or -2.2 C) was warmer than the foot (30.6 + or -2.1 C) and so was the blood flow: repectively 5.8 + or -5.2 versus 0.7 + or -0.3 ml./min.100 ml/tissue) as determined by strain gauge plethysmography and 10.8 + or -5.1 versus 6.7 + or -5.3 by the doppler method. At the end of the immersion period the blood flow had decreased a factor of 2.9 (doppler) and 4.3 (plethysmography). The local heat transfer, determined by heat flux tranducers, was highest immediately after immersion. The maximum was higher at the ventral sides than at the dorsal sides of the hand (225 plus or minus 93 versus 186 plus or minus 61 W./sq m) and the foot (178 + or -53 versus 160 + or -57 W./sq m). The total heat transferred to the water by hand or foot during the 60 minutes of immersion, determined by calorimetry, was 47 + or -21 and 36 + or -18 kJ respectively and was not statistically different due to considerale interindividual differences. Interindividual differences were also found for heat flux, rectal and local skin temperature and blood flow. These differences will have to be taken into account if a comparison is made with data from subjects with local cold injuries. ESA

N92-10278# Hebrew Univ., Jerusalem (Israel). Laser Center.
FUNDAMENTAL STUDIES IN THE MOLECULAR BASIS OF LASER INDUCED RETINAL DAMAGE Final Report, 1 Nov. 1987 - 31 Oct. 1990
Aaron Lewis 15 Apr. 1991 23 p
(Contract DAMD17-88-Z-8008; DA Proj. 3M1-62787-A-878)
(AD-A239941) Avail: NTIS HC/MF A03 CSCL 06/5

The past three years has seen considerable advancements in our understanding of the fundamental basis of laser interaction with retinal and ocular tissue. In this section we will review our achievements during the past three years of support by the Ocular Hazards Program of the United States Letterman Army Institute of Research. This support has resulted in 15 published papers. These papers have reported for the first time second harmonic generation in rhodopsin. The data provide an understanding of the very efficient second harmonic generation that is occurring in visual pigments. The fundamental understanding that we have obtained begins to elucidate the interactions that could underlie the psychophysical phenomena that have been indicated green sensation with Nd:YAG laser illumination. In addition, these results are leading to a more detailed understanding of the photodynamics of the rhodopsin spectral alterations under both one and two photon illumination. This photodynamics is the basic information that is required in order to design the constraints that must be met in order to develop photodynamic filters. GRA

N92-10279# Letterman Army Inst. of Research, San Francisco, CA.
TWO INFORMATIVE CASES OF Q-SWITCHED LASER EYE INJURY Institute Report, Jul. 1989 - Jul. 1991
H. Zwick, B. E. Stuck, D. Gagliano, V. C. Parmley, and J. Lund Jul. 1991 26 p
(AD-A240001; LAIR-IR-463) Avail: NTIS HC/MF A03 CSCL 06/5

We describe two cases of parafoveal Q-switched laser retinal injuries which illustrate the variability of the processes set in motion by retinal laser injuries. The first case demonstrates that parafoveal lesions may cause an immediate degradation in visual functions which may recover spontaneously to almost normal levels. In the second, multiple parafoveal exposure sites produced central retinal scars at the parafoveal lesion sites and resulted in retinal traction over an extensive region of the retina with local retinal hole formation at the edge of the central scar. A central arucate absolute scotoma appeared shortly after exposure. The central scotoma, as well as visual acuity, stationary and dynamic contrast sensitivity functions were permanently altered. No treatment presently exists to alleviate or minimize the effects of this retinal scarring process. GRA

N92-10280# Northwestern Univ., Evanston, IL.
PROGRAM AND ABSTRACTS OF THE 2ND MEETING OF THE SOCIETY FOR RESEARCH ON BIOLOGICAL RHYTHMS Final Report, 1 May 1990 - 30 Apr. 1991
Fred W. Turek 15 Jul. 1991 121 p Meeting held in Jacksonville, FL, 9-13 May 1990
(Grant AF-AFOSR-0270-90; AF Proj. 2312)
(AD-A240007; AFOSR-91-0725TR) Avail: NTIS HC/MF A06 CSCL 06/4

From May 9-13, 1990 the Society for Research on Biological Rhythms held its second meeting at Amelia Island Plantation, Florida. The Society was formed to promote the advancement of basic and applied research in all aspects of biological rhythms, to disseminate important research results concerning biological rhythms to the general public, to develop and enhance the education and training of students and researchers in the field and to foster interdisciplinary communication. This second meeting was successful in meeting the goals of the Society, particularly in the area of interdisciplinary communication. This second meeting promoted the interaction of workers in the various areas in a variety of different ways. First, there was a mixture of Symposia as well as slide and poster sessions on clinical and basic research topics. The Symposia were organized to insure that the entire frequency range of biological rhythms would be presented. GRA

N92-10281# University of Southern Mississippi, Hattiesburg.
AUDITORY AND VISUAL EVOKED POTENTIALS AS A FUNCTION OF SLEEP DEPRIVATION AND IRREGULAR SLEEP Final Report
John R. Harsh 30 Apr. 1991 172 p
(Contract DAMD17-88-C-8016; DA Proj. 3E1-62777-A-879)
(AD-A240097) Avail: NTIS HC/MF A08 CSCL 06/10

This report describes progress in a program of research concerned with whether event-related brain potentials (ERPs) provide a reliable, valid, and practical way of predicting performance. Two objectives of the program were to develop the capacity to measure, analyze, and interpret ERPs and to demonstrate that ERPs are sensitive to factors influencing performance. Experiments are described that show ERP variation in studies of orienting responses, habituation, and Pavlovian conditioning. Additional experiments show ERP changes in relation to time-of-day and ultradian variation in performance. Several experiments describe the relationship between ERP and performance changes during the wake/sleep transition. These experiments encourage the view that ERPs are closely related to both arousal and cognitive factors influencing performance. GRA

N92-10539# Kuopio Univ. (Finland). Dept. of Applied Physics.
SPECTRAL REPRESENTATION IN VISION Abstract Only
J. Hallikainen, J. Parkkinen, and T. Jaaskelainen *In* Oulu Univ.,

Proceedings of the 25th Annual Conference of the Finnish Physical Society 1991 1 p Sponsored by Academy of Finland (For primary document see N92-10362 01-70)
Avail: NTIS HC/MF A12

N92-10540# Helsinki Univ. of Technology, Espoo (Finland). Low Temperature Lab.
INTEGRATION OF MAGNETOENCEPHALOGRAPHY AND MAGNETIC RESONANCE IMAGING Abstract Only
S. O. Tissari and M. S. Hamalainen *In* Oulu Univ., Proceedings of the 25th Annual Conference of the Finnish Physical Society 1991 1 p (For primary document see N92-10362 01-70)
Avail: NTIS HC/MF A12

N92-10541# Kuopio Univ. (Finland). Dept. of Applied Physics.
CLUSTERING: A POWERFUL AID IN CLASSIFYING QRS WAVEFORMS Abstract Only
L. Patomaki and M. Jarviluoto *In* Oulu Univ., Proceedings of the 25th Annual Conference of the Finnish Physical Society 1991 1 p (For primary document see N92-10362 01-70)
Avail: NTIS HC/MF A12

N92-10542# Kuopio Univ. (Finland). Dept. of Applied Physics.
ALGORITHM FOR DETECTION OF VFIB IN REAL TIME FROM ECG Abstract Only
L. Patomaki and A. Nieminen *In* Oulu Univ., Proceedings of the 25th Annual Conference of the Finnish Physical Society 1991 1 p (For primary document see N92-10362 01-70)
Avail: NTIS HC/MF A12

N92-10543# Kuopio Univ. (Finland). Dept. of Applied Physics.
ANALYSIS OF ESOPHAGEAL pH-RECORDINGS FOR REFLUX DISEASE Abstract Only
L. Patomaki, P. Vainio, E. Lansimies, and K. Jarvinen *In* Oulu Univ., Proceedings of the 25th Annual Conference of the Finnish Physical Society 1991 1 p (For primary document see N92-10362 01-70)
Avail: NTIS HC/MF A12

N92-10545# Oulu Univ. (Finland). Dept. of Physics.
PROTON NMR STUDIES ON HUMAN BLOOD PLASMA: AN APPLICATION TO CANCER RESEARCH Abstract Only
M. Ala-Korpela, Y. Hiltunen, Jukka Jokisaari, S. Eskelinen, and K. Kiviniitty *In its* Proceedings of the 25th Annual Conference of the Finnish Physical Society 1991 1 p (For primary document see N92-10362 01-70)
Avail: NTIS HC/MF A12

53 BEHAVIORAL SCIENCES

Includes psychological factors; individual and group behavior; crew training and evaluation; and psychiatric research.

N92-10282*# Research Inst. for Advanced Computer Science, Moffett Field, CA.
HUMAN PERFORMANCE MEASUREMENT: VALIDATION PROCEDURES APPLICABLE TO ADVANCED MANNED TELESCIENCE SYSTEMS
Richard F. Haines 12 Feb. 1990 35 p Sponsored in part by USRA
(Contract NCC2-387)
(NASA-CR-185447; NAS 1.26:185447; RIACS-TR-90-10) Avail: NTIS HC/MF A03 CSCL 05I

As telescience systems become more and more complex, autonomous, and opaque to their operators it becomes increasingly difficult to determine whether the total system is performing as it should. Some of the complex and interrelated human performance measurement issues are addressed as they relate to total system validation. The assumption is made that human interaction with the automated system will be required well into the Space Station Freedom era. Candidate human performance measurement-validation techniques are discussed for selected ground-to-space-to-ground and space-to-space situations. Most of these measures may be used in conjunction with an information throughput model presented elsewhere (Haines, 1990). Teleoperations, teleanalysis, teleplanning, teledesign, and teledocumentation are considered, as are selected illustrative examples of space related telescience activities. Author

N92-10283# City Univ. of New York, NY.
TEST ANXIETY AND POST PROCESSING INTERFERENCE, 2 Interim Report, Sep. 1982 - Sep. 1986
Sigmund Tobias and Joanne Sacks Jul. 1991 18 p
(Contract MDA903-82-0353)
(AD-A239819; ARI-RN-91-88) Avail: NTIS HC/MF A03 CSCL 05/8

This experiment was performed to determine whether test anxiety interferes in the retrieval of prior learnings from long-term memory and to investigate the degree to which anxiety affected post processing interference. Thirty students were administered Sarason's Text Anxiety Scale and four subtests of Weinstein's Learning and Study Skills Inventory (LASSI). Students were asked to memorize two 18-word lists, each consisting of three different categories, to a criterion of one perfect recall. Students were randomly assigned to one of three conditions: (1) acquisition stress ego involving instruction administered prior to the beginning of the task, (2) ego involving instructions after acquisition, or (3) no ego involving instruction of any kind. It is conceivable that study skills, like test anxiety, affect performance mainly in the presence of effective stress. GRA

N92-10284# Yale Univ., New Haven, CT. Dept. of Psychiatry.
FEAR-POTENTIATED STARTLE AS A MODEL SYSTEM FOR ANALYZING LEARNING AND MEMORY Final Report, 1 Jul. 1987 - 31 Jan. 1991
Michael Davis 31 Jan. 1991 4 p
(Grant AF-AFOSR-0336-87; AF Proj. 2312)
(AD-A239994; AFOSR-91-0749TR) Avail: NTIS HC/MF A01 CSCL 05/8

Research during this funding period has focussed on the role of a particular brain area, the amygdala, in fear conditioning, using increased acoustic startle amplitude in the presence of a stimulus previously paired with shock as a measure of fear in rats. We have found that: (1) electrical stimulation of the amygdala increases startle; (2) mechanical or chemical lesions of the amygdala prevent either footshock or stimuli paired with footshock from elevating startle; (3) there is a direct anatomical connection between the central nucleus of the amygdala and a specific point along the acoustic startle pathway; (4) lesions at several levels of this connection between the amygdala and the startle circuit block conditioned and unconditioned fear; (5) local infusion of specific receptor antagonists into the amygdala prevent the development of fear conditioning; and (6) presentation of a conditioned fear stimulus activates early expression genes (c-fos) in the amygdala. The data strongly implicate the amygdala as a critical brain structure for both the acquisition and expression of conditioned and unconditioned fear. Drugs that reduce anxiety in humans may act by interacting with specific receptors in the amygdala. GRA

N92-10285# California Univ., Irvine. Center for the Neurobiology of Learning and Memory.
SYNAPTIC PLASTICITY AND MEMORY FORMATION Annual Technical Report, 15 May 1990 - 14 May 1991
Gary Lynch 14 Jun. 1991 6 p
(Grant AF-AFOSR-0383-89; AF Proj. 2312)
(AD-A240121; AFOSR-91-0708TR) Avail: NTIS HC/MF A02 CSCL 05/8

The goal of the project is to define the mechanisms responsible for inducing, expressing, and stabilizing long-term synaptic potentiation (LTP), a form of physiological plasticity that is likely to be responsible for the encoding of memory in telencephalic networks. Studies in the past year defined the cellular changes likely to be responsible for expressions. The nootropic (cognitive enhancing) drug aniracetam prolongs the open time of post-synaptic receptors mediating fast synaptic transmission. The

LTP changes the effect of the drug on synaptic responses in hippocampus; manipulations that enhance responses by increasing release do not interact with the drug. By far the most plausible explanation of this result is that LTP modifies receptors. This conclusion is supported by negative results from experiments testing the hypotheses that LTP is due to changes in release, receptor number, or spine resistance. GRA

N92-10286# New York Univ., New York. Dept. of Psychology.
VISUAL MOTION PERCEPTION Final Report, 1 Feb. 1988 - 31 Jan. 1991
George Sperling 15 Aug. 1991 279 p
(Grant AF-AFOSR-0140-88; AF Proj. 2313)
(AD-A240133; AFOSR-91-0757TR) Avail: NTIS HC/MF A13 CSCL 06/4

The articles enclosed with this report describe work related to five aspects of visual information processing: (1) Continuing studies of two separate motion-computation systems in human vision and the derivation of the functional properties of each. (2) The investigation of three dimensional structure derived from two dimensional visual inputs. (3) A potent form of spatial contrast-gain-control was discovered and found to be not only frequency selective but also orientation specific. This form of local gain control may exemplify a universal form of neural normalization. (4) Studies of human pattern recognition of familiar shapes (such as letters) show that its statistical efficiency approaches an incredible 50 percent of the ideal detector's efficiency when the pattern is spatially bandpass filtered in a band whose wavelength is of the same order as the pattern itself. (5) Studies of real and simulated saccadic eye movements in which the same sequence of images that is produced on the retina during saccadic eye movements is artificially produced on a stationary retina. GRA

54 MAN/SYSTEM TECHNOLOGY AND LIFE SUPPORT

Includes human engineering; biotechnology; and space suits and protective clothing.

For related information see also *16 Space Transportation.*

N92-10287*# National Aeronautics and Space Administration. Lyndon B. Johnson Space Center, Houston, TX.
DISPLAY FORMAT, HIGHLIGHT VALIDITY, AND HIGHLIGHT METHOD: THEIR EFFECTS ON SEARCH PERFORMANCE
Kimberly A. Donner, Tim D. McKay, Kevin M. OBrien (Lockheed Engineering and Sciences Co., Houston, TX.), and Marianne Rudisill Oct. 1991 15 p
(NASA-TM-104742; S-654; NAS 1.15:104742) Avail: NTIS HC/MF A03 CSCL 05H

Display format and highlight validity were shown to affect visual display search performance; however, these studies were conducted on small, artificial displays of alphanumeric stimuli. A study manipulating these variables was conducted using realistic, complex Space Shuttle information displays. A 2x2x3 within-subjects analysis of variance found that search times were faster for items in reformatted displays than for current displays. Responses to valid applications of highlight were significantly faster than responses to non or invalidly highlighted applications. The significant format by highlight validity interaction showed that there was little difference in response time to both current and reformatted displays when the highlight validity was applied; however, under the non or invalid highlight conditions, search times were faster with reformatted displays. A separate within-subject analysis of variance of display format, highlight validity, and several highlight methods did not reveal a main effect of highlight method. In addition, observed display search times were compared to search time predicted by Tullis' Display Analysis Program. Benefits of highlighting and reformatting displays to enhance search and the necessity to consider highlight validity and format characteristics in tandem for predicting search performance are discussed.
Author

N92-10288# Army Research Inst. of Environmental Medicine, Natick, MA.
A COMPUTER SIMULATION FOR PREDICTING THE TIME COURSE OF THERMAL AND CARDIOVASCULAR RESPONSES TO VARIOUS COMBINATIONS OF HEAT STRESS, CLOTHING, AND EXERCISE
Kenneth K. Kraning, II Jun. 1991 54 p
(AD-A240023; USARIEM-T13-91) Avail: NTIS HC/MF A04 CSCL 06/10

This report describes a new computer simulation of human temperature regulation for predicting limiting physiological responses to work under heat stress. Possible military applications include adjustment of work: rest cycles during intermittent work in protective clothing or confined spaces and determining optimal recovery periods and environments following exercise and/or exposure to hot environments. Using data bases from 7 independent studies of widely varying workload and environment, the simulation was validated by comparing the standard deviations (sd) of variable means (internal temperature, skin temperature and heart rate) in the data sets with the root mean squared deviations (rmsd) between the variable means and the corresponding simulator outputs. Results suggest that, on the average and within the range of data tested, the present simulation is able to forecast results with the same order of precision as laboratory studies of the same problems. Future applications could include incorporation into on-line expert systems used as tactical decision aids and as a tool to aid the experimental design of studies on the competing stresses of work, heat, dehydration, sleep deprivation and chemical protective drugs. GRA

55 SPACE BIOLOGY

Includes exobiology; planetary biology; and extraterrestrial life.

No abstracts in this category.

59 MATHEMATICAL AND COMPUTER SCIENCES (GENERAL)

N92-10289*# National Aeronautics and Space Administration. Lewis Research Center, Cleveland, OH.
ON THE MOST GENERAL TENSOR B(SUB ij) WHICH IS ZERO FOR i DOES NOT EQUAL j, AND THE MOST GENERAL ISOTROPIC TENSOR I(SUB ij)
Robert G. Deissler Oct. 1991 8 p
(NASA-TM-105236; E-6561; NAS 1.15:105236) Avail: NTIS HC/MF A02 CSCL 12A

It is shown that the most general second order tensor B sub ij which is zero for i not = j is proportional to the Kronecker delta (Delta sub ij). By a slight modification of that argument, the known result was obtained that the most general second order isotropic tensor is also proportional to Delta sub ij. These results are useful for instance in obtaining the stress tensor for a viscous fluid.
Author

60 COMPUTER OPERATIONS AND HARDWARE

Includes hardware for computer graphics, firmware, and data processing.

For components see *33 Electronics and Electrical Engineering.*

N92-10290*# Research Inst. for Advanced Computer Science, Moffett Field, CA.
THE PARADIGM COMPILER: MAPPING A FUNCTIONAL LANGUAGE FOR THE CONNECTION MACHINE
Jack B. Dennis Apr. 1989 16 p
(Contract NCC2-387)
(NASA-CR-188839; NAS 1.26:188839; RIACS-TR-89-15) Avail: NTIS HC/MF A03 CSCL 09B

The Paradigm Compiler implements a new approach to compiling programs written in high level languages for execution on highly parallel computers. The general approach is to identify the principal data structures constructed by the program and to map these structures onto the processing elements of the target machine. The mapping is chosen to maximize performance as determined through compile time global analysis of the source program. The source language is Sisal, a functional language designed for scientific computations, and the target language is Paris, the published low level interface to the Connection Machine. The data structures considered are multidimensional arrays whose dimensions are known at compile time. Computations that build such arrays usually offer opportunities for highly parallel execution; they are data parallel. The Connection Machine is an attractive target for these computations, and the parallel for construct of the Sisal language is a convenient high level notation for data parallel algorithms. The principles and organization of the Paradigm Compiler are discussed. Author

N92-10291*# Research Inst. for Advanced Computer Science, Moffett Field, CA.
AN ALTERNATIVE DESIGN FOR A SPARSE DISTRIBUTED MEMORY
Louis A. Jaeckel Jul. 1989 47 p
(Contracts NCC2-387; NCC2-408)
(NASA-CR-188847; NAS 1.26:188847; RIACS-TR-89-28) Avail: NTIS HC/MF A03 CSCL 09B

A new design for a Sparse Distributed Memory, called the selected-coordinate design, is described. As in the original design, there are a large number of memory locations, each of which may be activated by many different addresses (binary vectors) in a very large address space. Each memory location is defined by specifying ten selected coordinates (bit positions in the address vectors) and a set of corresponding assigned values, consisting of one bit for each selected coordinate. A memory location is activated by an address if, for all ten of the locations's selected coordinates, the corresponding bits in the address vector match the respective assigned value bits, regardless of the other bits in the address vector. Some comparative memory capacity and signal-to-noise ratio estimates for the both the new and original designs are given. A few possible hardware embodiments of the new design are described. Author

N92-10292*# Research Inst. for Advanced Computer Science, Moffett Field, CA.
BIRD: A GENERAL INTERFACE FOR SPARSE DISTRIBUTED MEMORY SIMULATORS
David Rogers Jan. 1990 100 p
(Contract NCC2-387)
(NASA-CR-188858; NAS 1.26:188858; RIACS-TR-90-3) Avail: NTIS HC/MF A05 CSCL 09B

Kanerva's sparse distributed memory (SDM) has now been implemented for at least six different computers, including SUN3 workstations, the Apple Macintosh, and the Connection Machine. A common interface for input of commands would both aid testing of programs on a broad range of computer architectures and assist users in transferring results from research environments to applications. A common interface also allows secondary programs to generate command sequences for a sparse distributed memory, which may then be executed on the appropriate hardware. The BIRD program is an attempt to create such an interface. Simplifying access to different simulators should assist developers in finding appropriate uses for SDM. Author

N92-10293*# Research Inst. for Advanced Computer Science, Moffett Field, CA.
ON THE SUITABILITY OF THE CONNECTION MACHINE FOR DIRECT PARTICLE SIMULATION
Leonard Dagum Jun. 1990 179 p Sponsored in part by USRA
(Contracts NCC2-387; NCA2-313; NAGw-965)
(NASA-CR-188863; NAS 1.26:188863; RIACS-TR-90-26)
Copyright Avail: NTIS HC/MF A09 CSCL 09B

The algorithmic structure was examined of the vectorizable Stanford particle simulation (SPS) method and the structure is reformulated in data parallel form. Some of the SPS algorithms can be directly translated to data parallel, but several of the vectorizable algorithms have no direct data parallel equivalent. This requires the development of new, strictly data parallel algorithms. In particular, a new sorting algorithm is developed to identify collision candidates in the simulation and a master/slave algorithm is developed to minimize communication cost in large table look up. Validation of the method is undertaken through test calculations for thermal relaxation of a gas, shock wave profiles, and shock reflection from a stationary wall. A qualitative measure is provided of the performance of the Connection Machine for direct particle simulation. The massively parallel architecture of the Connection Machine is found quite suitable for this type of calculation. However, there are difficulties in taking full advantage of this architecture because of lack of a broad based tradition of data parallel programming. An important outcome of this work has been new data parallel algorithms specifically of use for direct particle simulation but which also expand the data parallel diction. Author

N92-10294*# Research Inst. for Advanced Computer Science, Moffett Field, CA.
SPARSE DISTRIBUTED MEMORY: PRINCIPLES AND OPERATION
M. J. Flynn, P. Kanerva, and N. Bhadkamkar Dec. 1989 57 p
(Contract NCC2-387; NAGw-419)
(NASA-CR-188901; NAS 1.26:188901; RIACS-TR-89-53; CSL-TR-89-400) Avail: NTIS HC/MF A04 CSCL 09B

Sparse distributed memory is a generalized random access memory (RAM) for long (1000 bit) binary words. Such words can be written into and read from the memory, and they can also be used to address the memory. The main attribute of the memory is sensitivity to similarity, meaning that a word can be read back not only by giving the original write address but also by giving one close to it as measured by the Hamming distance between addresses. Large memories of this kind are expected to have wide use in speech recognition and scene analysis, in signal detection and verification, and in adaptive control of automated equipment, in general, in dealing with real world information in real time. The memory can be realized as a simple, massively parallel computer. Digital technology has reached a point where building large memories is becoming practical. Major design issues were resolved which were faced in building the memories. The design is described of a prototype memory with 256 bit addresses and from 8 to 128 K locations for 256 bit words. A key aspect of the design is extensive use of dynamic RAM and other standard components. Author

N92-10295# Los Alamos National Lab., NM.
THE ROLE OF THE COMPUTER IN SCIENCE FAIR PROJECTS: CURRENT STATUS AND POTENTIAL
M. S. Trainor 1991 14 p Presented at the 33rd International Association for the Development of Computer-Based Instruction of Systems (ADCIS) Conference, St. Louis, MO, 10-14 Nov. 1991

(Contract W-7405-eng-36)
(DE91-008606; LA-UR-91-702; CONF-911130-1) Avail: NTIS HC/MF A03

The need for more students to enter the field of science is acute in the nation, and science fair projects provide a motivational mechanism to entice students into pursuing scientific careers. Computers play a major role in science today. Because computers are a major source of entertainment for our children, one would expect them to play a significant role in many science fair projects. This study investigated current and potential uses of computers in science fair projects and incorporated an informal case study of scientists, teachers, and students involved in science fair projects from a highly scientific community. Interviews, a survey, and observations were conducted. Results indicated that most projects either do not use or inadequately use computers and that a significant potential for more effective use of computers for science fair projects exists. DOE

N92-10296# Los Alamos National Lab., NM.
MAGNETO-OPTICAL DISK AS A CD-ROM DEVELOPMENT TOOL
F. K. Houghton and A. L. Leuttgen 1991 6 p Presented at the 33rd International Association for the Development of Computer-Based Instruction of Systems (ADCIS) Conference, St. Louis, MO, 10-14 Nov. 1991
(Contract W-7405-eng-36)
(DE91-009973; LA-UR-91-1100; CONF-911130-2) Avail: NTIS HC/MF A02

Computer-based training (CBT) programs are becoming more sophisticated. They are no longer electronic papers, but are large multi-media systems which incorporate computer-generated graphics and digital audio as well as text. The numerous computer-generated graphics, large audio files, and complex hypertext structures place a great demand on the computer system's binary storage capacity (disk space). If the use of interactive video is prohibitive because of cost or other restraints, a compact disk read-only memory (CD-ROM) delivery system is a viable delivery system. Because CD-ROM is a read-only system, the development and delivery system must be different. There are several alternatives for the development system, including a very large hard-disk and a magneto-optical disk drive. Recently a CBT package for radiation protection workers (RPT's) that was developed at Los Alamos National Laboratory (LANL) was delivered on CD-ROM. A magneto-optical drive was used for the development system. This paper will discuss some reasons for selecting a CD-ROM delivery system and the use of magneto-optical disk drive as the development system. DOE

N92-10297# Los Alamos National Lab., NM.
MEASUREMENT OF MEMORY ACCESS CONTENTIONS IN MULTIPLE VECTOR PROCESSOR SYSTEMS
I. Y. Bucher and M. L. Simmons 1991 13 p Presented at the Conference on Supercomputing 1991, Albuquerque, NM, 18-22 Nov. 1991
(Contract W-7405-eng-36)
(DE91-013205; LA-UR-91-1665; CONF-911103-6) Avail: NTIS HC/MF A03

The purpose of this paper is to study delays encountered when several vector processors access a common memory. Such delays may be caused by access conflicts at the memory or by contentions within the network connection processors to common memory. Because such delays are potentially the limiting performance bottleneck of common memory architectures, it is important to understand how they depend on design parameters, in particular the number of processors serviced by the common memory, the degree of memory interleaving, and the speed of the memory chips. Such understanding will make it possible to assess the performance of systems with increasing number of processors and new memory technologies. It is essential for any assessment of the future potential of common memory systems. There are three possible approaches to the study of this problem, analytical models, simulations, and measurements on existing machines. All three approaches are necessary because each has advantages and limitations. Analytical models owe their effectiveness to simplifying assumptions that need to be checked by the other two methods. In particular, stochastic methods and queueing theory offer not techniques to deal with regular memory access patterns that are common in scientific and engineering applications. Simulations can generally approximate reality more closely, however, even simulations do not replace real measurements. They are often very slow and contain assumptions that need to be tested. This paper presents a set of measurements of memory access delay performed on several computers of the Cray family under carefully controlled conditions. DOE

N92-10298# Los Alamos National Lab., NM.
A PERFORMANCE COMPARISON OF THREE SUPERCOMPUTERS: FUJITSU VP-2600, NEC SX-3, AND CRAY Y-MP
M. L. Simmons, H. J. Wasserman, O. M. Lubeck, C. Eoyang, R. Mendez, Hiroo Harada, and Misako Ishiguro (Japan Atomic Energy Research Inst., Ibaraki.) 1991 11 p Presented at the Supercomputing 1991, New York, NY, 18-22 Nov. 1991
(Contract W-7405-eng-36)
(DE91-016304; LA-UR-91-2554; CONF-911164-1) Avail: NTIS HC/MF A03

The performance of two second-generation supercomputers, the NEC SX-3 and the Fujitsu VP2600, is analyzed using the Standard Los Alamos Benchmark Set, the Mendez Fluid Dynamics Codes, and some highly vectorizable production-type codes from Los Alamos. For comparison, data are also given for a single processor of the CRAY Y-MP8/264. Factors affecting performance such as memory bandwidth, vector register organization, and the effects of multiple vector pipelines are examined. On a highly vectorizable code that can take advantage of multiple vector pipes, the SX-3 and VP2600 are faster than the single CRAY Y-MP processor by factors of seven to eight. DOE

N92-10299*# Rutgers - The State Univ., New Brunswick, NJ. Lab. for Computer Science Research.
CONTENT ADDRESSABLE MEMORY PROJECT Semiannual Progress Report No. 2, Mar. - Aug. 1991
Josh Hall, Saul Levy, D. Smith, S. Wei, K. Miyake, and M. Murdocca 1 Oct. 1991 29 p
(Grant NAG2-668)
(NASA-CR-188981; NAS 1.26:188981) Avail: NTIS HC/MF A03 CSCL 09B

The progress on the Rutgers CAM (Content Addressable Memory) Project is described. The overall design of the system is completed at the architectural level and described. The machine is composed of two kinds of cells: (1) the CAM cells which include both memory and processor, and support local processing within each cell; and (2) the tree cells, which have smaller instruction set, and provide global processing over the CAM cells. A parameterized design of the basic CAM cell is completed. Progress was made on the final specification of the CPS. The machine architecture was driven by the design of algorithms whose requirements are reflected in the resulted instruction set(s). A few of these algorithms are described. Author

N92-10300# Department of Energy, Washington, DC. Scientific Computing Staff.
PROCEEDINGS OF THE FIRST ENERGY RESEARCH POWER SUPERCOMPUTER USERS SYMPOSIUM
1991 173 p Symposium held in Gaithersburg, MD, 21-22 May 1991
(DE91-018877; CONF-9105202) Avail: NTIS HC/MF A08

The Energy Research Power Supercomputer Users Symposium was arranged to showcase the richness of science that has been pursued and accomplished in this program through the use of supercomputers and now high performance parallel computers over the last year: this report is the collection of the presentations given at the Symposium. Power users were invited by the ER Supercomputer Access Committee to show that the use of these computational tools and the associated data communications network, ESNet, go beyond merely speeding up computations.

Today the work often directly contributes to the advancement of the conceptual developments in their fields and the computational and network resources form the very infrastructure of today's science. The Symposium also provided an opportunity, which is rare in this day of network access to computing resources, for the invited users to compare and discuss their techniques and approaches with those used in other ER disciplines. The significance of new parallel architectures was highlighted by the interesting evening talk given by Dr. Stephen Orszag of Princeton University. DOE

N92-10419# Jyvaskyla Univ. (Finland). Dept. of Physics.
CONTROL SYSTEM OF THE JYVASKYLA (FINLAND) K130 CYCLOTRON Abstract Only
J. Lampinen and V. Hanninen *In* Oulu Univ., Proceedings of the 25th Annual Conference of the Finnish Physical Society 1991 1 p (For primary document see N92-10362 01-70)
Avail: NTIS HC/MF A12

61 COMPUTER PROGRAMMING AND SOFTWARE

Includes computer programs, routines, alogorithms, and specific applications, e.g., CAD/CAM.

N92-10301*# Alabama Univ., Huntsville.
METHODOLOGY FOR AUTOMATING SOFTWARE SYSTEMS Final Report
Warren Moseley 1990 96 p
(Contract NAS8-36955)
(NASA-CR-184233; NAS 1.26:184233) Avail: NTIS HC/MF A05 CSCL 09B

Applying ITS technology to the shuttle diagnostics would not require the rigor of the Petri Net representation, however it is important in providing the animated simulated portion of the interface and the demands placed on the system to support the training aspects to have a homogeneous and consistent underlying knowledge representation. By keeping the diagnostic rule base, the hardware description, the software description, user profiles, desired behavioral knowledge, and the user interface in the same notation, it is possible to reason about the all of the properties of petri nets, on any selected portion of the simulation. This reasoning provides foundation for utilization of intelligent tutoring systems technology. Author

N92-10302*# National Aeronautics and Space Administration. Langley Research Center, Hampton, VA.
EFFICIENT MULTITASKING OF CHOLESKI MATRIX FACTORIZATION ON CRAY SUPERCOMPUTERS
Andrea L. Overman and Eugene L. Poole (Analytical Services and Materials, Inc., Hampton, VA.) Sep. 1991 63 p
(NASA-TM-4259; L-16901; NAS 1.15:4259) Avail: NTIS HC/MF A04 CSCL 09B

A Choleski method is described and used to solve linear systems of equations that arise in large scale structural analysis. The method uses a novel variable-band storage scheme and is structured to exploit fast local memory caches while minimizing data access delays between main memory and vector registers. Several parallel implementations of this method are described for the CRAY-2 and CRAY Y-MP computers demonstrating the use of microtasking and autotasking directives. A portable parallel language, FORCE, is used for comparison with the microtasked and autotasked implementations. Results are presented comparing the matrix factorization times for three representative structural analysis problems from runs made in both dedicated and multi-user modes on both computers. CPU and wall clock timings are given for the parallel implementations and are compared to single processor timings of the same algorithm. Author

N92-10303*# Southwest Research Inst., San Antonio, TX.
CONTINUATION OF RESEARCH INTO LANGUAGE CONCEPTS FOR THE MISSION SUPPORT ENVIRONMENT: SOURCE CODE
Timothy J. Barton and Jeremiah M. Ratner 5 Sep. 1991 480 p
(Grant NAG9-435; SwRI Proj. 05-3531)
(NASA-CR-187816; NAS 1.26:187816) Avail: NTIS HC/MF A21 CSCL 09B

Research into language concepts for the Mission Control Center is presented. A computer code for source codes is presented. The file contains the routines which allow source code files to be created and compiled. The build process assumes that all elements and the COMP exist in the current directory. The build process places as much code generation as possible on the preprocessor as possible. A summary is given of the source files as used and/or manipulated by the build routine. Author

N92-10304*# Illinois Univ., Urbana. Center for Supercomputing Research and Development.
PARALLEL MACHINE ARCHITECTURE AND COMPILER DESIGN FACILITIES Final Report
David J. Kuck, Pen-Chung Yew, David Padua, Ahmed Sameh, and Alex Veidenbaum 20 Dec. 1990 51 p
(Contract NCC2-559)
(NASA-CR-188784; NAS 1.26:188784) Avail: NTIS HC/MF A04 CSCL 09B

The objective is to provide an integrated simulation environment for studying and evaluating various issues in designing parallel systems, including machine architectures, parallelizing compiler techniques, and parallel algorithms. The status of Delta project (which objective is to provide a facility to allow rapid prototyping of parallelized compilers that can target toward different machine architectures) is summarized. Included are the surveys of the program manipulation tools developed, the environmental software supporting Delta, and the compiler research projects in which Delta has played a role. Author

N92-10305# Defense Systems Support Organization, Arlington, VA.
FUNCTIONAL DESCRIPTION FOR THE MAPPING AND GRAPHIC INFORMATION CAPABILITY (MAGIC)
David W. Hall 14 Jun. 1991 103 p
(AD-A239436; DISA/DSSO-FD-4-91) Avail: NTIS HC/MF A06 CSCL 12/7

This Functional Description (FD) for the Mapping and Graphic Information Capability (MAGIC) is written to provide: (1) A bridging document that clearly delineates and documents both the structure and functionality of the current Graphic Information Presentation System (GIPSY) while providing complete and yet, concise information linking those functions to the architecture and components of MAGIC; (2) Documentation of all requirements (system, functional, user, performance, etc.) that MAGIC will satisfy such that, this FD shall serve as a basis for mutual understanding between the Government and the contractor; (3) A basis for discussion of planned system processing, assumptions, constraints, and expected impacts upon users; (4) Preliminary, top-level design information related to MAGIC; and (5) A basis for the development of system integration tests and formal qualification testing (FQT). GRA

N92-10306*# Research Inst. for Advanced Computer Science, Moffett Field, CA.
THE ROLE OF GRAPHICS SUPER-WORKSTATIONS IN A SUPERCOMPUTING ENVIRONMENT
E. Levin Sep. 1989 14 p
(Contract NCC2-387)
(NASA-CR-188852; NAS 1.26:188852; RIACS-TR-89-37) Avail: NTIS HC/MF A03 CSCL 09B

A new class of very powerful workstations has recently become available which integrate near supercomputer computational performance with very powerful and high quality graphics capability. These graphics super-workstations are expected to play an increasingly important role in providing an enhanced environment for supercomputer users. Their potential uses include: off-loading

the supercomputer (by serving as stand-alone processors, by post-processing of the output of supercomputer calculations, and by distributed or shared processing), scientific visualization (understanding of results, communication of results), and by real time interaction with the supercomputer (to steer an iterative computation, to abort a bad run, or to explore and develop new algorithms). Author

N92-10307*# Research Inst. for Advanced Computer Science, Moffett Field, CA.
MODELING REALITY
Peter J. Denning 27 Nov. 1990 13 p Submitted for publication
(Contract NCC2-387)
(NASA-CR-188881; NAS 1.26:188881; RIACS-TR-90-49) Avail: NTIS HC/MF A03 CSCL 09B

Although powerful computers have allowed complex physical and manmade hardware systems to be modeled successfully, we have encountered persistent problems with the reliability of computer models for systems involving human learning, human action, and human organizations. This is not a misfortune; unlike physical and manmade systems, human systems do not operate under a fixed set of laws. The rules governing the actions allowable in the system can be changed without warning at any moment, and can evolve over time. That the governing laws are inherently unpredictable raises serious questions about the reliability of models when applied to human situations. In these domains, computers are better used, not for prediction and planning, but for aiding humans. Examples are systems that help humans speculate about possible futures, offer advice about possible actions in a domain, systems that gather information from the networks, and systems that track and support work flows in organizations. Author

N92-10308*# Research Inst. for Advanced Computer Science, Moffett Field, CA.
QUEUEING IN NETWORKS OF COMPUTERS
Peter J. Denning 17 May 1991 15 p Submitted for publication
(Contract NCC2-387)
(NASA-CR-188892; NAS 1.26:188892; RIACS-TR-91-14) Avail: NTIS HC/MF A03 CSCL 09B

The designers of networks of computers must assess the capacity of the network to complete work within reasonable times. The utilization law, Little's law, forced-flow law, and response time formula are simple tools that can be used to calculate throughput and response times of networks. Bottleneck analysis can be used to calculate simple lower bounds on response time in terms of individual server parameters and the load on network as a whole. These simple results are important tools for all users of scientific networks - back of the envelope calculations can quickly reveal the effects of distant servers on local throughput and response time. Author

N92-10309*# Research Inst. for Advanced Computer Science, Moffett Field, CA.
GLOBALLY CONVERGENT TECHNIQUES IN NONLINEAR NEWTON-KRYLOV
Peter N. Brown (Lawrence Livermore National Lab., CA.) and Youcef Saad Nov. 1989 40 p
(Contracts NCC2-387; W-7405-eng-48)
(NASA-CR-188894; NAS 1.26:188894; RIACS-TR-89-57) Avail: NTIS HC/MF A03 CSCL 09B

Some convergence theory is presented for nonlinear Krylov subspace methods. The basic idea of these methods is to use variants of Newton's iteration in conjunction with a Krylov subspace method for solving the Jacobian linear systems. These methods are variants of inexact Newton methods where the approximate Newton direction is taken from a subspace of small dimensions. The main focus is to analyze these methods when they are combined with global strategies such as linesearch techniques and model trust region algorithms. Most of the convergence results are formulated for projection onto general subspaces rather than just Krylov subspaces. Author

N92-10310*# Research Inst. for Advanced Computer Science, Moffett Field, CA.
A RESTRICTED SIGNATURE NORMAL FORM FOR HERMITIAN MATRICES, QUASI-SPECTRAL DECOMPOSITIONS, AND APPLICATIONS
Roland W. Freund and Thomas Huckle (Wuerzburg Univ., Germany, F.R.) Dec. 1989 23 p
(Contract NCC2-387)
(NASA-CR-188895; NAS 1.26:188895; RIACS-TR-89-55) Avail: NTIS HC/MF A03 CSCL 09B

In recent years, a number of results on the relationships between the inertias of Hermitian matrices and the inertias of their principal submatrices appeared in the literature. We study restricted congruence transformation of Hermitian matrices M which, at the same time, induce a congruence transformation of a given principal submatrix A of M. Such transformations lead to concept of the restricted signature normal form of M. In particular, by means of this normal form, we obtain short proofs of most of the known inertia theorems and also derive some new results of this type. For some applications, a special class of almost unitary restricted congruence transformations turns out to be useful. We show that, with such transformations, M can be reduced to a quasi-diagonal form which, in particular, displays the eigenvalues of A. Finally, applications of this quasi-spectral decomposition to generalize inverses and Hermitian matrix pencils are discussed. Author

N92-10311*# Research Inst. for Advanced Computer Science, Moffett Field, CA.
AN IMPLEMENTATION OF THE LOOK-AHEAD LANCZOS ALGORITHM FOR NON-HERMITIAN MATRICES, PART 1
Roland W. Freund, Martin H. Gutknecht, and Noel M. Nachtigal (Massachusetts Inst. of Tech., Cambridge.) Nov. 1990 34 p
(Contract NCC2-387)
(NASA-CR-188909; NAS 1.26:188909; RIACS-TR-90-45) Avail: NTIS HC/MF A03 CSCL 09B

The nonsymmetric Lanczos method can be used to compute eigenvalues of large sparse non-Hermitian matrices or to solve large sparse non-Hermitian linear systems. However, the original Lanczos algorithm is susceptible to possible breakdowns and potential instabilities. We present an implementation of a look-ahead version of the Lanczos algorithm which overcomes these problems by skipping over those steps in which a breakdown or near-breakdown would occur in the standard process. The proposed algorithm can handle look-ahead steps of any length and is not restricted to steps of length 2, as earlier implementations are. Also, our implementation has the feature that it requires roughly the same number of inner products as the standard Lanczos process without look-ahead. Author

N92-10312*# Research Inst. for Advanced Computer Science, Moffett Field, CA.
AN IMPLEMENTATION OF THE LOOK-AHEAD LANCZOS ALGORITHM FOR NON-HERMITIAN MATRICES, PART 2
Roland W. Freund and Noel M. Nachtigal (Massachusetts Inst. of Tech., Cambridge.) Nov. 1990 67 p
(Contract NCC2-387)
(NASA-CR-188910; NAS 1.26:188910; RIACS-TR-90-46) Avail: NTIS HC/MF A04 CSCL 09B

It is shown how the look-ahead Lanczos process (combined with a quasi-minimal residual QMR) approach) can be used to develop a robust black box solver for large sparse non-Hermitian linear systems. Details of an implementation of the resulting QMR algorithm are presented. It is demonstrated that the QMR method is closely related to the biconjugate gradient (BCG) algorithm; however, unlike BCG, the QMR algorithm has smooth convergence curves and good numerical properties. We report numerical experiments with our implementation of the look-ahead Lanczos algorithm, both for eigenvalue problem and linear systems. Also, program listings of FORTRAN implementations of the look-ahead algorithm and the QMR method are included. Author

N92-10313*# Research Inst. for Advanced Computer Science, Moffett Field, CA.
INTEGRITY AND SECURITY IN AN Ada RUNTIME ENVIRONMENT
Rodney L. Bown Jun. 1991 9 p
(Contract NCC9-16; RICIS Proj. SE-26)
(NASA-CR-188826; NAS 1.26:188826) Avail: NTIS HC/MF A02 CSCL 09B

A review is provided of the Formal Methods group discussions. It was stated that integrity is not a pure mathematical dual of security. The input data is part of the integrity domain. The group provided a roadmap for research. One item of the roadmap and the final position statement are closely related to the space shuttle and space station. The group's position is to use a safe subset of Ada. Examples of safe sets include the Army Secure Operating System and the Penelope Ada verification tool. It is recommended that a conservative attitude is required when writing Ada code for life and property critical systems. Author

N92-10314*# Research Inst. for Advanced Computer Science, Moffett Field, CA.
ART/Ada DESIGN PROJECT, PHASE 1. TASK 3 REPORT: TEST PLAN Status Report, Mar. - Oct. 1988
Bradley P. Allen (Inference Corp., Los Angeles, CA.) 24 Oct. 1988 11 p
(Contract NCC9-16; RICIS Proj. SE-19)
(NASA-CR-188945; NAS 1.26:188945) Avail: NTIS HC/MF A03 CSCL 09B

The plan is described for the integrated testing and benchmark of Phase Ada based ESBT Design Research Project. The integration testing is divided into two phases: (1) the modules that do not rely on the Ada code generated by the Ada Generator are tested before the Ada Generator is implemented; and (2) all modules are integrated and tested with the Ada code generated by the Ada Generator. Its performance and size as well as its functionality is verified in this phase. The target platform is a DEC Ada compiler on VAX mini-computers and VAX stations running the VMS operating system. Author

N92-10315# Sandia National Labs., Albuquerque, NM.
PARALLEL QR FACTORIZATION ON A HYPERCUBE USING THE TORUS WRAP MAPPING
B. Hendrickson 1 Apr. 1991 19 p Presented at the Conference on Supercomputing 1991, Albuquerque, NM, 18-22 Nov. 1991
(Contract DE-AC04-76DP-00789)
(DE91-011502; SAND-91-8-0874C; CONF-911103-5) Avail: NTIS HC/MF A03

We present an algorithm for the QR factorization of a dense matrix without column pivoting on a hypercube multiprocessor. The algorithm combines the optimal numerical efficiency of Householder reflections with the excellent communication properties of the torus wrap mapping. Analytical results indicate that the communication cost for this algorithm is less than that for other common approaches. Numerical results on an nCUBE 2 confirm the efficiency of our technique. DOE

N92-10316# Los Alamos National Lab., NM.
PERFORMANCE OF CONJUGATE GRADIENT-LIKE ALGORITHMS IN TRANSIENT TWO-PHASE SUBCHANNEL ANALYSIS
J. A. Turner and M. J. Doster (North Carolina State Univ., Raleigh.) 1991 19 p Presented at the Winter Meeting of the American Nuclear Society (ANS), San Francisco, CA, 10-15 Nov. 1991
(Contract W-7405-eng-36)
(DE91-013373; LA-UR-91-1802; CONF-911107-3) Avail: NTIS HC/MF A03

A transient, drift-flux subchannel analysis code (SWIRL) has been created for the development and evaluation of algorithms for the solution of weakly 3-D fluid flow problems. Spatial discretization on a staggered grid, semi-implicit temporal discretization, and algebraic reduction of the conservation equations of mass, energy, and momentum result in nonsymmetric block-tridiagonal linear systems of equations that must be solved for the pressure distribution at each time step of a transient. The solution of these systems of equations is the most time-consuming portion of the code, and direct, stationary iterative, and preconditioned conjugate gradient (CG)-like methods have been investigated both for a simple approach to steady state and for a severe transient. The best direct algorithm appears to be an efficient implementation of block elimination, and iterative methods are compared to this algorithm for accuracy, robustness, and efficiency. Results presented here indicate that preconditioned CG-like methods such as Sonneveld's conjugate gradients squared are superior to an efficient direct method. DOE

N92-10317# Lawrence Livermore National Lab., CA.
RETIRE FORTRAN? A DEBATE REKINDLED
D. Cann 24 Jul. 1991 11 p Presented at the Conference on Supercomputing 1991, Albuquerque, NM, 18-22 Nov. 1991 Revised
(Contract W-7405-eng-48)
(DE91-016565; UCRL-JC-107018-Rev-1; CONF-911103-3-Rev-1)
Avail: NTIS HC/MF A03

In the May 1984 issue of Physics Today, Jim McGraw debated David Kuck and Michael Wolfe on the question of retiring FORTRAN. They addressed such questions as: (1) is FORTRAN the best tool for decomposing problems for parallel execution?; (2) is FORTRAN the programming language we should carry into the 21st century?; and (3) Are there any alternatives? While McGraw argued forcefully in favor of retiring FORTRAN, concerns about performance crippled his position. He could not rebut the claim that only FORTRAN could provide the performance required for scientific computing. We use the current performance of CRAY SISAL, a functional language for large-scale scientific computing to counter that claim. If McGraw had had our data in 1984, he could have countered what some say is the only defense in favor of keeping FORTRAN. The results show that we can move beyond the constraints of imperative programming. We can raise the level of abstraction and retain performance. DOE

N92-10318# Los Alamos National Lab., NM.
INTEGRA MANUAL: ROUTINES FOR ELECTRONIC SPREADSHEET INTEGRATION (UNDER FRAMEWORK 3)
M. G. Fonseca Aug. 1991 100 p In ENGLISH and SPANISH
(Contract W-7405-eng-36)
(DE91-017518; LA-12182-M) Avail: NTIS HC/MF A05

INTEGRA is a collection of routines for general use that facilities the integrated execution of spreadsheets. INTEGRA has been programmed with FRED language from the commercial software package FRAMEWORK 3. The routines can be used in systems of very different technical areas, in spite of the fact that initially they served to create models for energy planning. INTEGRA is also an easy-to-learn methodology that speeds up application development. This report is written in English and in Spanish. The Spanish version is the more complete report containing the actual programming and examples of applications and utilization. DOE

N92-10319# Argonne National Lab., IL. Mathematics and Computer Science Div.
A PORTABLE RUN-TIME SYSTEM FOR PCN
I. Foster, S. Tuecke, and S. Taylor (California Inst. of Tech., Pasadena.) Jul. 1991 43 p
(Contract W-31-109-eng-38)
(DE91-017700; ANL/MCS-TM-137) Avail: NTIS HC/MF A03

This report describes a run time system to support Program Composition Notation (PCN), a high level concurrent programming notation. The run time system is described in terms of an abstract machine. We specify an abstract architecture that represents the state of a PCN computation and executes abstract machine instructions that encode tests on or modifications to the computation state. Programs to be executed on the abstract machine are encoded as sequences of abstract machine instructions. The abstract machine may be implemented by an emulator written in a low level language. Alternatively, sequences

of abstract machine instructions may be further compiled to machine code. The run time system is designed to run on uniprocessors, multiprocessors, and multicomputers. DOE

N92-10320# Westinghouse Hanford Co., Richland, WA.
PATRAN AND P/THERMAL APPLICATIONS FOR THERMAL MODELING
R. Valdiviez and B. A. Crea Jul. 1991 9 p Presented at the PATRAN Users Conference, Newport Beach, CA, 1-3 Oct. 1991
(Contract DE-AC06-87RL-10930)
(DE91-017767; WHC-SA-1076; CONF-9110196-1) Avail: NTIS HC/MF A02

The standard that has been established over the last decade or so in performing numerical modeling for analysis purposes is to make creation of the computational grid and results presentation less time and effort consuming than the analysis function itself. Software packages known as pre- and post-processors have been developed and made available in various forms and sizes for the engineering analyst's use. These packages reduce the effort and time required of the analyst to perform pre- and post-operations on a given model. PATRAN is one such pre- and post-processing software package. PATRAN provides a large array of capabilities to enable geometric representation and creation of the analysis model. This software package also incorporates interfacing routines which enable a model created in PATRAN to be translated into the input format of many other analysis codes. This paper discusses the use of PATRAN as a pre- and post-processor and the software package P/THERMAL as the analysis code for the steady state and transient thermal analysis of a vacuum vessel. The design objective of the vessel is to duplicate the conditions of outer space and provide containment for a test nuclear reactor designed for space application. This objective creates a challenging thermal analysis effort. The use of P/THERMAL in meeting this challenge is also discussed. P/THERMAL's ability to facilitate and perform thermal analysis is recognized in this analysis task. DOE

N92-10321# Sandia National Labs., Albuquerque, NM.
MERLIN 2: A COMPUTER PROGRAM TO TRANSFER SOLUTION DATA BETWWEN FINITE ELEMENT MESHES
D. K. Gartling Jul. 1991 40 p
(Contract DE-AC04-76DP-00789)
(DE91-018130; SAND-89-2989) Avail: NTIS HC/MF A03

The MERLIN 2 program is designed to transfer data between finite element meshes of arbitrary geometry. The program is structured to accurately interpolate previously computed solutions onto a given mesh and format the resulting data for immediate use in another analysis program. Data from either two-dimensional or three-dimensional meshes may be considered. The theoretical basis and computational algorithms used in the program are described and complete user instructions are presented. Several example problems are included to demonstrate program usage. DOE

N92-10322# Stanford Univ., CA. Dept. of Operations Research.
SOLVING PROBLEMS UNDER UNCERTAINTY
Jun. 1991 53 p
(Contract DE-FG03-87ER-25028)
(DE91-017940; DOE/ER-25028/T2) Avail: NTIS HC/MF A04

This final technical report covers mainly the progress made solving large scale linear programs and the recent successes in optimizing large-scale planning problems under uncertainty (stochastic programs). The general goal of the research was the development of effective methods for solving stochastic linear programs. Stochastic programming models are designed to deal with the uncertainty in the values of the parameters of complex scheduling, planning and control problems. Because solutions obtained from such models properly hedge against future uncertainties they are much to be preferred to solutions produced by deterministic models. The stochastic linear program, if it could be solved efficiently, is consequently a problem of greatest practical importance, especially in the fields of energy planning, industry and finance. Our recent work has made it possible to efficiently solve certain important classes of stochastic linear programs. Our approach combines large scale system decomposition techniques and advanced sampling methods with the use of parallel processors. The use of adaptive importance sampling in tests conducted so far has so significantly reduced required sample sizes that it is now possible to solve some previously intractable problems on a personal computer. We have successfully solved several very large scale energy planning and finance models; these problems are discussed in the technical appendix. DOE

N92-10323# Stanford Linear Accelerator Center, CA.
OBJECT ORIENTED PROGRAMMING
P. F. Kunz Aug. 1991 19 p Presented at the 1991 CERN School of Computing, Ystad, Sweden, 23 Aug. - 2 Sep. 1991
(Contract DE-AC03-76SF-00515)
(DE91-018151; SU-SLAC-PUB-5629; CONF-9108155-1) Avail: NTIS HC/MF A03

This paper is an introduction to object oriented programming. The object oriented approach is very powerful and not inherently difficult, but most programmers find a relatively high threshold in learning it. Thus, this paper will attempt to convey the concepts with examples rather than explain the formal theory. DOE

N92-10324# Sandia National Labs., Albuquerque, NM.
NORMALIZATION OF CORRELATIONS
B. A. Kast and F. M. Dickey 1991 9 p Presented at the Society of Photo-Optical Instrumentation Engineers (SPIE) Meeting, San Diego, CA, 21-26 Jul. 1991
(Contract DE-AC04-76DP-00789)
(DE91-018398; SAND-90-3204C; CONF-9107115-45) Avail: NTIS HC/MF A02

Correlation is often used as an approach to automated pattern recognition. Generally, correlation provides a measure of the similarity between a reference template and regions of an input image. This measure is also highly dependent on intensity variations in the input image, thereby hindering the performance of simple peak detection decision algorithms. Normalization can be used to achieve intensity invariance of correlation results. This paper will address some aspects of normalization for a few filter types. For matched filters, the Cauchy-Schwarz inequality provides an effective method by taking into account the energy of the input image within the spatial region of support of the template. For many other types of filters being considered for pattern recognition applications, the regions of support are not always limited to the area occupied by the template pattern. This excessive support can produce undesirable effects in the correlation results whether normalized or not. Benefits of normalized correlation such as intensity invariance and resistance to high energy clutter will be discussed along with some problems associated with regions of support. Matched filters, phase-only filters, and binary phase-only filters will be investigated. Computer simulations of several cases will be used to to demonstrate results. DOE

N92-10325# Lawrence Livermore National Lab., CA.
A BRIEF INTRODUCTION TO CONDOR
J. J. Ambrosiano, S. Brandon, D. E. Nielsen, Jr., and S. Ray 1 Aug. 1991 4 p
(Contract W-7405-eng-48)
(DE91-018652; UCRL-ID-108037) Avail: NTIS HC/MF A01

The CONDOR computer code evolved at the Lawrence Livermore National Laboratory (LLNL) from MASK in the early 80's. CONDOR is a two-dimensional particle-in-cell plasma simulation program. Orbits of charged particles are followed in self-consistent electromagnetic fields using the Lorentz force law. The full set of Maxwell's equations (with particle source terms) are solved to generate time dependent electric and magnetic fields. CONDOR is capable of simulations in three geometries, Cartesian XY, cylindrical RZ and R(Theta). Internal structures (metal, resistive, and insulating) which conform to the uniformly spaced-rectangular mesh cells can be specified. Interactions between the simulation particles and any internal structures can also be included in the calculation. DOE

N92-10326# Lawrence Livermore National Lab., CA.
TAURUS: AN INTERACTIVE POST-PROCESSOR FOR THE ANALYSIS CODES NIKE3D, DYNA3D, AND TOPAZ3D
T. Spelce May 1991 81 p
(Contract W-7405-eng-48)
(DE91-019012; UCRL-MA-105401) Avail: NTIS HC/MF A05

This report provides an update to the user's manual for the TAURUS finite element analysis post processor. TAURUS is designed for use with the family of nonlinear finite element codes DYNA3D, NIKE3D, and TOPAZ3D developed in the Methods Development Group at Lawrence Livermore National Laboratory and the structural analysis code GEMINI. TAURUS provides the ability to display deformed geometries and contours or fringes of a large number of quantities on meshes consisting of beam, plate, shell, and solid type elements. Time history plotting is also available for a wide variety of primitive and derived quantities. TAURUS is operational on a variety of platforms from workstations to supercomputers. DOE

N92-10327# Syracuse Univ., NY. Dept. of Electrical and Computer Engineering.
ON ADAPTIVE MULTIBAND DETECTION OF TARGETS IN NONSTATIONARY NONHOMOGENEOUS INTERFERENCE Final Report, Jan. - Dec. 1989
H. Wang and L. Cai Jun. 1991 133 p
(Contract F30602-88-D-0027)
(AD-A239983; RL-TR-91-119) Avail: NTIS HC/MF A07 CSCL 17/9

Addressed in this report is the problem of detecting a known signal in strong, severely non-stationary/nonhomogeneous interference of unknown statistics. Two approaches are proposed. The first one is the multiband signaling and detection scheme which makes possible a trade-off between data quantity and signal quality. Two multiband algorithms, the MultiBand Sample Matrix Inversion (MB-SMI) and Generalized Likelihood Ratio (MB-GLR) algorithms, are thus developed and shown to be able to significantly outperform the corresponding single-band algorithms, providing a potential solution to the problem which exists when the data available for learning are severely limited by the environment. To obtain the desirable CFAR feature in colored Gaussian interference at a lower computational cost, we modify the MB-SMI and obtain the MultiBand Modified-SMI (MB-MSMI) algorithm. The performance comparisons of the MB-MSMI and MB-GLR show that in Gaussian interference, the detection performance difference between the two algorithms is practically negligible and therefore, the use of the MB-GLR is unnecessary as it requires more implementation complexity. In non-Gaussian interference, however, the MB-GLR is preferable due to its much lower performance sensitivity than the MB-MSMI. To further improve the system performance, also proposed in this report is an approach which explores interference covariance structure to reduce the uncertainty in estimating unknown statistics. GRA

N92-10328# Unisys Corp., Reston, VA. Tactical Systems Div.
SOFTWARE TECHNOLOGY FOR ADAPTABLE, RELIABLE SYSTEMS (STARS): DOMAIN SPECIFIC ENVIRONMENT REPOSITORY COMPOSITE PARADIGM REPORT
30 May 1991 38 p
(Contract F19628-88-D-0031)
(AD-A240107; STARS-SC-03068/001/00; GR-7670-1195(NP))
Avail: NTIS HC/MF A03 CSCL 25/5

This document defines a risk-driven Composite Paradigm as an interim step toward the definition of a reuse-based paradigm for the development of trusted Navy Command and Control systems. This report represents an adaptation and melding of previous Defense Advanced Research Projects Agency (DARPA), the Software Engineering Institute (SEI), Software Technology for Adaptable, Reliable Systems (STARS), and industry process modeling work, as appropriate, in the areas of risk-based activities; high performance, trusted system developments; software reuse; library support for reuse; and trusted system reuse issues. It directly addresses the STARS goals for a technology for building adaptable, highly reliable and cost effective software systems. In particular, it provides an initial framework for the development of trusted systems, a high risk domain growing in importance as the need for more complex systems and more systems interoperability increases. This report presents a tutorial description of the Composite Paradigm for a reuse-driven system development. GRA

N92-10329# Unisys Corp., Reston, VA. Tactical Systems Div.
SOFTWARE TECHNOLOGY FOR ADAPTABLE, RELIABLE SYSTEMS (STARS): UUS40 RISK-REDUCTION REASONING-BASED DEVELOPMENT PARADIGM TAILORED TO NAVY C2 SYSTEMS
30 Jul. 1991 99 p
(Contract F19628-88-D-0031)
(AD-A240108; STARS-SC-03070/001/00; GR-7670-1219(NP))
Avail: NTIS HC/MF A05 CSCL 25/5

This report defines a STARS trusted, reuse-oriented Navy Command and Control (C2) Process Model (NCCPM) for system development. The NCCPM describes the entire system development lifecycle from early concept through contract award, design, development, and operations and maintenance with an emphasis on software development. The NCCPM description combines the STARS Composite Process Model (SCPM) and preliminary Navy C2 domain analysis work contained in the appendix in the Spiral 0 descriptions of Subsection 3.2. This work integrates and adapts previous DARPA, STARS, SEI, and industry process modeling work, as appropriate. The work incorporates the process model concepts and issues of risk-based activities; high performance, trusted system development; software reuse; library support for reusable assets; and domain considerations within the Navy C2 application domain. These results directly address the STARS goals for a technology for building adaptable, highly reliable and cost effective software systems. Specifically, they provide a framework for the development of reuse-driven, trusted systems within the Navy C2 application domain. GRA

N92-10330# Unisys Corp., Reston, VA. Tactical Systems Div.
SOFTWARE TECHNOLOGY FOR ADAPTABLE, RELIABLE SYSTEMS (STARS): US40-STARS REUSE CONCEPT OF OPERATIONS. VOLUME 1: VERSION 0.5-DRAFT
27 Aug. 1991 61 p Prepared in cooperation with The Boeing Co., Seattle, WA and IBM Federal Sector Div., Gaithersburg, MD
(Contract F19628-88-D-0031)
(AD-A240109; STARS-SC-03725/001/00; GR-7670-1259(NP))
Avail: NTIS HC/MF A04 CSCL 12/5

The purpose of this document is to articulate STARS concepts and expectations for reuse with respect to system and software development by: (1) elaborating on the STARS reuse vision; (2) stating STARS goals for reuse; (3) defining a framework for definition of reuse processes; (4) identifying low level reuse processes that STARS may provide as process building blocks (precise, composable process definitions) in the context of the reuse process framework and specific life cycles; (5) establishing a common terminology for reuse; (6) addressing the impact and opportunities for use of distributed, heterogeneous asset libraries as a reuse-enabling technology; and (7) providing a context for understanding STARS reuse plans and products. GRA

N92-10331*# National Aeronautics and Space Administration. Lyndon B. Johnson Space Center, Houston, TX.
RECONFIGURABLE FUZZY CELL Patent Application
George A. Salazar, inventor (to NASA) 18 Sep. 1991 70 p
(NASA-Case-MSC-21613-1; NAS 1.71:MSC-21613-1;
US-Patent-Appl-SN-761566) Avail: NTIS HC/MF A04 CSCL 09B

This invention relates to a reconfigurable fuzzy cell comprising a digital control programmable gain operation amplifier, an analog-to-digital converter, an electrically erasable PROM, and 8-bit counter and comparator, and supporting logic configured to achieve in real-time fuzzy systems high throughput, grade-of-membership or membership-value conversion of multi-input sensor data. The invention provides a flexible multiplexing-capable configuration, implemented entirely in hardware, for effectuating S-, Z-, and

PI-membership functions or combinations thereof, based upon fuzzy logic level-set theory. A membership value table storing 'knowledge data' for each of S-, Z-, and PI-functions is contained within a nonvolatile memory for storing bits of membership and parametric information in a plurality of address spaces. Based upon parametric and control signals, analog sensor data is digitized and converted into grade-of-membership data. In situ learn and recognition modes of operation are also provided. NASA

N92-10374# Tampere Univ. of Technology (Finland). Microelectronics Lab.
GATE MATRIX OPTIMIZATION USING SIMULATED ANNEALING Abstract Only
Harri Raittinen, Jarkko Niittylahti, and Kimmo Kaski *In* Oulu Univ., Proceedings of the 25th Annual Conference of the Finnish Physical Society 1991 1 p (For primary document see N92-10362 01-70)
Avail: NTIS HC/MF A12

N92-10375# Kuopio Univ. (Finland). Dept. of Applied Physics.
RUNNING DISCRETE COSINE TRANSFORM ALGORITHM Abstract Only
H. Olkkonen *In* Oulu Univ., Proceedings of the 25th Annual Conference of the Finnish Physical Society 1991 1 p (For primary document see N92-10362 01-70)
Avail: NTIS HC/MF A12

N92-10544# Helsinki Univ. of Technology, Espoo (Finland). Dept. of Physics.
USE OF IN-111 IN QUANTITATIVE SPECT Abstract Only
S. Savolainen, A. Kiuru, and J. Kankare *In* Oulu Univ., Proceedings of the 25th Annual Conference of the Finnish Physical Society 1991 1 p (For primary document see N92-10362 01-70)
Avail: NTIS HC/MF A12

62 COMPUTER SYSTEMS

Includes computer networks and special application computer systems.

N92-10332*# Alabama Univ., Huntsville.
COOPERATING SYSTEMS: LAYERED MAS Final Report
Daniel Rochowiak May 1990 55 p
(Contract NAS8-36955)
(NASA-CR-184232; NAS 1.26:184232; JRC-RR-90-21) Avail: NTIS HC/MF A04 CSCL 09B

Distributed intelligent systems can be distinguished by the models that they use. The model developed focuses on layered multiagent system conceived of as a bureaucracy in which a distributed data base serves as a central means of communication. The various generic bureaus of such a system is described and a basic vocabulary for such systems is presented. In presenting the bureaus and vocabularies, special attention is given to the sorts of reasonings that are appropriate. A bureaucratic model has a hierarchy of master system and work group that organizes E agents and B agents. The master system provides the administrative services and support facilities for the work groups. Author

N92-10333*# Research Inst. for Advanced Computer Science, Moffett Field, CA.
TOTALLY PARALLEL MULTILEVEL ALGORITHMS FOR SPARSE ELLIPTIC SYSTEMS
Paul O. Frederickson Mar. 1989 7 p
(Contract NCC2-387)
(NASA-CR-188837; NAS 1.26:188837; RIACS-TR-89-10) Avail: NTIS HC/MF A02 CSCL 09B

The fastest known algorithms for the solution of a large elliptic boundary value problem on a massively parallel hypercube all require O(log(n)) floating point operations and O(log(n)) distance-1 communications, if massively parallel is defined to mean a number of processors proportional to the size n of the problem. The Totally Parallel Multilevel Algorithm (TPMA) that has, as special cases, four of these fast algorithms is described. These four algorithms are Parallel Superconvergent Multigrid (PSMG), Robust Multigrid, the Fast Fourier Transformation (FFT) based Spectral Algorithm, and Parallel Cyclic Reduction. The algorithm TPMA, when described recursively, has four steps: (1) project to a collection of interlaced, coarser problems at the next lower level; (2) apply TPMA, recursively, to each of these lower level problems, solving directly at the lowest level; (3) interpolate these approximate solutions to the finer grid, and to verage them to form an approximate solution on this grid; and (4) refine this approximate solution with a defect-correction step, using a local approximate inverse. Choice of the projection operator (P), the interpolation operator (Q), and the smoother (S) determines the class of problems on which TPMA is most effective. There are special cases in which the first three steps produce an exact solution, and the smoother is not needed (e.g., constant coefficient operators). Author

N92-10334# Sandia National Labs., Albuquerque, NM.
MASSIVELY PARALLEL COMPUTING AT SANDIA AND ITS APPLICATION TO NATIONAL DEFENSE
S. S. Dosanjh 1991 10 p Presented at the Nuclear Explosives Code Developers Conference, Monterey, CA, 14 Nov. 1991
(Contract DE-AC04-76DP-00789)
(DE91-008178; SAND-91-0278C; CONF-911129-1) Avail: NTIS HC/MF A02

Two years ago, researchers at Sandia National Laboratories showed that a massively parallel computer with 1024 processors could solve scientific problems more than 1000 times faster than a single processor. Since then, interest in massively parallel processing has increased dramatically. This review paper discusses some of the applications of this emerging technology to important problems at Sandia. Particular attention is given here to the impact of massively parallel systems on applications related to national defense. New concepts in heterogenous programming and load balancing for MIMD computers are drastically increasing synthetic aperture radar (SAR) and Strategic Defense Initiative (SDI) modeling capabilities. Also, researchers are showing that the current generation of massively parallel MIMD and SIMD computers are highly competitive with a CRAY on hydrodynamic and structural mechanics codes that are optimized for vector processors. DOE

N92-10335# Sandia National Labs., Albuquerque, NM.
MASSIVELY PARALLEL COMPUTING AND THE MID-COURSE TRACKING PROBLEM
J. L. Tomkins and J. P. VanDyke 1991 18 p Presented at the Conference on Supercomputing 1991, Albuquerque, NM, 18-22 Nov. 1991
(Contract DE-AC04-76DP-00789)
(DE91-010864; SAND-91-0765C; CONF-911103-1) Avail: NTIS HC/MF A03

The Strategic Defense Initiative (SDI) mid-course tracking problem is a very computationally intensive problem that must be solved in real time. It is generally believed that a real-time solution is only possible through massively parallel computing. This paper discusses the implementation of the TRC code, a mid-course tracking code, on a 1024 processor nCUBE/ten computer. A brief discussion of the modeling approach used in the TRC is provided together with a discussion of how the TRC was restructured to make it run efficiently in parallel. The performance of the parallel version of the TRC over a wide range of problem sizes is discussed and results obtained on a Cray X-MP single processor are compared to the nCUBE/ten results. These results demonstrate the applicability of massively parallel MIMD computing to the SDI mid-course tracking problem. Also, the successful implementation of the TRC code and the performance of the nCUBE/ten versus a Cray X-MP processor (approximate run time speed up of six) demonstrate the potential of massively parallel MIMD computing for performing large, complex simulations. DOE

N92-10336# Lawrence Livermore National Lab., CA.
GANG SCHEDULING A PARALLEL MACHINE
B. C. Gorda and E. D. Brooks, III Mar. 1991 9 p Presented at the Conference on Supercomputing 1991, Albuquerque, NM, 18-22 Nov. 1991

(Contract W-7405-eng-48)
(DE91-011539; UCRL-JC-107020; CONF-911103-4) Avail: NTIS HC/MF A02

Program development on parallel machines can be a nightmare of scheduling headaches. We have developed a portable time sharing mechanism to handle the problem of scheduling gangs of processors. User program and their gangs of processors are put to sleep and awakened by the gang scheduler to provide a time sharing environment. Time quantums are adjusted according to priority queues and a system of fair share accounting. The initial platform for this software is the 128 processor BBN TC2000 in use in the Massively Parallel Computing Initiative at the Lawrence Livermore National Laboratory. DOE

N92-10337# Harvard Univ., Boston, MA. Dept. of Genetics.
COMPUTER ASSISTED MULTIPLEX SEQUENCING
G. M. Church Aug. 1991 5 p
(Contract DE-FG02-87ER-60565)
(DE91-017851; DOE/ER-60565/5) Avail: NTIS HC/MF A01

The objectives of this project are automation and optimization of multiplex sequencing. Dideoxy reactions were combined in a label duplex system. A chemical reaction set has been developed in which all four reactions are free of precipitations and hazardous waste. Direct transfer electrophoresis was adapted, yielding runs readable beyond 850 bases with an error rate less than 0.6 percent overall. Per gel, 24 reaction sets are used, with each reaction set capable of yielding 28 or more separate sequence ladders on reprobing. A new chemiluminescent substrate CSPD yields three times faster exposures. The REPLICA automated film reading software was extended from its multiplex-specific origins to new handle conventional sequencing and duplex sequencing. A sequence assembly system for ordered and shotgun data called GTAC was benchmark tested - the run time of is near-linear with increasing project size (N(sup 1.15)). A sample data set of 2 million bases of raw DNA sequence with an initial 2 percent error rate was assembled in 9 hours on a desktop computer. Hybridization acceleration conditions were explored. DOE

N92-10338# Argonne National Lab., IL.
FIBER NETWORKING AT ARGONNE: A DISTRIBUTED, MULTIAPPLICATION, MULTIVENDOR COMPUTING ENVIRONMENT
T. C. Kuhfuss, P. T. Phillips, and W. W. Morgan 1991 14 p Presented at the SPIE Meeting, Boston, MA, 3-6 Sep. 1991
(Contract W-31-109-eng-38)
(DE91-018560; ANL/CP-74007; CONF-9109230-5) Avail: NTIS HC/MF A03

In order to support existing and future applications, Argonne is installing a Laboratory-wide fiber optic cable plant. It has been designed to support an integrated data/video service consisting of a Laboratory-wide FDDI network and video teleconferencing system and has the capacity for future gigabit per second networks. This paper describes Argonne applications expected to push existing network capacity, our current network configuration, networking research activities, and future networking plans. DOE

N92-10339# Argonne National Lab., IL.
PARALLEL PROGRAMMING WITH PCN
I. Foster and S. Tuecke Sep. 1991 66 p
(Contract W-31-109-eng-38)
(DE91-019005; ANL-91/32) Avail: NTIS HC/MF A04

Program composition Notation (PCN) is a system for developing and executing parallel programs. It comprises a high-level programming language, a set of tools for developing and debugging programs in this language, and interfaces to Fortran and C that allow the reuse of existing code in multilingual parallel programs. Programs developed using PCN are portable across many different workstations, networks, and parallel computers. This document provides all the information required to develop parallel programs with the PCN programming system. It includes both tutorial and reference material. It also presents the basic concepts that underlie PCN, particularly where these are likely to be unfamiliar to the reader, and provides pointers to other documentation on the PCN language, programming techniques, and tools. PCN is in the public domain. DOE

N92-10376# Jyvaskyla Univ. (Finland). Dept. of Physics.
A MODEL FOR A DATA ACQUISITION SOLUTION FOR A MEDIUM SIZE ACCELERATOR LABORATORY Abstract Only
A. Lampinen, K. Loberg, M. Lahtinen, and J. Rauma *In* Oulu Univ., Proceedings of the 25th Annual Conference of the Finnish Physical Society 1991 1 p (For primary document see N92-10362 01-70)
Avail: NTIS HC/MF A12

63 CYBERNETICS

Includes feedback and control theory, artificial intelligence, robotics and expert systems.

For related information see also *54 Man/System Technology and Life Support.*

N92-10340*# Alabama Univ., Huntsville.
DESIGN CONTROLS FOR LARGE ORDER SYSTEMS Final Technical Report, 10 Jan. 1990 - 9 Jan. 1991
George B. Doane, III 9 Jan. 1991 118 p
(Contract NAS8-36955)
(NASA-CR-184237; NAS 1.26:184237; UAH-5-32323) Avail: NTIS HC/MF A06 CSCL 01C

The output of this task will be a program plan which will delineate how MSFC will support and implement its portion of the Inter-Center Computational Controls Program Plan. Another output will be the results of looking at various multibody/multidegree of freedom computer programs in various environments. Author

N92-10447# Kuopio Univ. (Finland). Dept. of Applied Physics.
RECOGNIZING OF SPECTRAL MIXTURES, THEIR COMPONENTS AND SPECTRAL PATTERNS Abstract Only
K. Mantere, J. Parkkinen, and T. Jaaskelainen *In* Oulu Univ., Proceedings of the 25th Annual Conference of the Finnish Physical Society 1991 1 p (For primary document see N92-10362 01-70)
Avail: NTIS HC/MF A12

64 NUMERICAL ANALYSIS

Includes iteration, difference equations, and numerical approximation.

N92-10341# Universiteit Twente, Enschede (Netherlands). Faculty of Applied Mathematics.
THE CONNECTIVITY OF THE BASIS GRAPH OF A BRANCHING GREEDOID
H. J. Broersma and Xueliang Li (Xinjiang Univ., Urumchi, China) Feb. 1991 11 p
(MEMO-937; ISSN-0169-2690; ETN-91-99735) Avail: NTIS HC/MF A03

A result of Korte and Lovasz implies that the basis graph of every two connected greedoid is connected. It is proven that the basis graph of every three connected branching greedoid is (gamma one) connected, where gamma is the minimum in degree (disregarding the root) of the underlying rooted digraph. Examples showing that this result is the best possible are presented. ESA

N92-10342# Universiteit Twente, Enschede (Netherlands). Faculty of Applied Mathematics.
SOME RESULTS ON CONSTRAINED CONTROLLABILITY IN DISCRETE-TIME CONVEX PROCESSES
Vu Ngoc Phat and Trinh Cong Dieu (Pedagogical Inst., Ho Chi Minh City, Vietnam) Jan. 1991 14 p
(MEMO-926; ISSN-0169-2690; ETN-91-99727) Avail: NTIS HC/MF A03

Controllability properties of nonlinear discrete time systems described by discrete time inclusion whose right hand sides are

convex processes are studied. These systems include linear systems with constrained controls and states. Necessary and sufficient conditions for constrained null controllability and reachability are established. The main tool used is an extension of Krein-Rutman's theorem and use of separation theorem in Banach spaces. ESA

N92-10343*# Research Inst. for Advanced Computer Science, Moffett Field, CA.
OVERVIEW OF KRYLOV SUBSPACE METHODS WITH APPLICATIONS TO CONTROL PROBLEMS
Youcef Saad May 1989 13 p
(Contract NCC2-387)
(NASA-CR-188842; NAS 1.26:188842; RIACS-TR-89-23) Avail: NTIS HC/MF A03 CSCL 12A

An overview of projection methods based on Krylov subspaces are given with emphasis on their application to solving matrix equations that arise in control problems. The main idea of Krylov subspace methods is to generate a basis of the Krylov subspace Span and seek an approximate solution the the original problem from this subspace. Thus, the original matrix problem of size N is approximated by one of dimension m typically much smaller than N. Krylov subspace methods have been very successful in solving linear systems and eigenvalue problems and are now just becoming popular for solving nonlinear equations. It is shown how they can be used to solve partial pole placement problems, Sylvester's equation, and Lyapunov's equation. Author

N92-10344*# Research Inst. for Advanced Computer Science, Moffett Field, CA.
OPTIMAL MOVING GRIDS FOR TIME-DEPENDENT PARTIAL DIFFERENTIAL EQUATIONS
A. J. Wathen (Bristol Univ., England) Sep. 1989 30 p
(Contract NCC2-387)
(NASA-CR-188850; NAS 1.26:188850; RIACS-TR-89-42) Avail: NTIS HC/MF A03 CSCL 12A

Various adaptive moving grid techniques for the numerical solution of time-dependent partial differential equations were proposed. The precise criterion for grid motion varies, but most techniques will attempt to give grids on which the solution of the partial differential equation can be well represented. Moving grids are investigated on which the solutions of the linear heat conduction and viscous Burgers' equation in one space dimension are optimally approximated. Precisely, the results of numerical calculations of optimal moving grids for piecewise linear finite element approximation of partial differential equation solutions in the least squares norm. Author

N92-10345*# National Aeronautics and Space Administration. Lewis Research Center, Cleveland, OH.
MULTIGRID CALCULATION OF THREE-DIMENSIONAL VISCOUS CASCADE FLOWS
A. Arnone (Florence Univ., Italy), M.-S. Liou, and L. A. Povinelli Oct. 1991 25 p Previously announced in IAA as A91-53754
(NASA Order C-99066-G)
(NASA-TM-105257; ICOMP-91-18; E-6587; NAS 1.15:105257)
Avail: NTIS HC/MF A03 CSCL 12A

A 3-D code for viscous cascade flow prediction was developed. The space discretization uses a cell-centered scheme with eigenvalue scaling to weigh the artificial dissipation terms. Computational efficiency of a four stage Runge-Kutta scheme is enhanced by using variable coefficients, implicit residual smoothing, and a full multigrid method. The Baldwin-Lomax eddy viscosity model is used for turbulence closure. A zonal, nonperiodic grid is used to minimize mesh distortion in and downstream of the throat region. Applications are presented for an annular vane with and without end wall contouring, and for a large scale linear cascade. The calculation is validated by comparing with experiments and by studying grid dependency. Author

N92-10346# Reynolds Electrical and Engineering Co., Inc., Las Vegas, NV. Defense Waste Management Dept.
FOURIER COMPONENT ANALYSIS OF THREE EULER-LAGRANGIAN METHODS APPLIED TO THE ONE-DIMENSIONAL ADVECTION-DISPERSION MODEL
F. T. Lindstrom Jul. 1991 41 p
(Contract DE-AC08-89NV-10630)
(DE91-017733; DOE/NV-10630/21) Avail: NTIS HC/MF A03

Numerical approximations of the parabolic- and hyperbolic-class transport and fate of chemicals in porous media models are extremely useful and valuable tools in both research and practical environmental remediation situations. The ever increasingly popular Euler-Lagrangian methods for solving the complex transport and fate problems, in one- through three-space dimensions, have the attractive feature of being able to have no constraints placed on the maximum allowable Peclet number. The unfortunate trade-off is possibly (1) a large amount of numerical diffusion, or dissipation, when using simple linear, bilinear, or trilinear interpolation schemes, or (2) stable, but nuisance, wiggles (sometimes referred to as oscillations) in the neighborhoods of steep fronts when using higher degree polynomials. The word fronts is used in the generic sense so as to include both leading and lagging edges in a concentration profile. This work derives and then studies the resulting Fourier (von Neumann) spectrum of the three most often occurring Lagrange interpolation approximations for advection: the classical 2-point, a polynomial degree one method; the 3-point, a polynomial degree two method; and the 5-point, a polynomial degree four method. DOE

N92-10347*# Brown Univ., Providence, RI. Div. of Engineering.
PARAMETER IDENTIFICATION FOR NONLINEAR AERODYNAMIC SYSTEMS Semiannual Progress Report No. 4, 24 Apr. - 22 Oct. 1991
Allan E. Pearson 1991 9 p
(Grant NAG1-1065)
(NASA-CR-188985; NAS 1.26:188985) Avail: NTIS HC/MF A02 CSCL 12A

Work continues on frequency analysis for transfer function identification, both with respect to the continued development of the underlying algorithms and in the identification study of two physical systems. Some new results of a theoretical nature were recently obtained that lend further insight into the frequency domain interpretation of the research. Progress in each of those areas is summarized. Although not related to the system identification problem, some new results were obtained on the feedback stabilization of linear time lag systems. Author

N92-10348*# Institute for Computer Applications in Science and Engineering, Hampton, VA.
THE IMPROVED ROBUSTNESS OF MULTIGRID ELLIPTIC SOLVERS BASED ON MULTIPLE SEMICOARSENED GRIDS Final Report
Naomi H. Naik (Vassar Coll., Poughkeepsie, NY.) and John VanRosendale Sep. 1991 19 p Submitted for publication
(Contract NAS1-18605)
(NASA-CR-187633; NAS 1.26:187633; ICASE-91-70) Avail: NTIS HC/MF A03 CSCL 12A

Multigrid convergence rates degenerate on problems with stretched grids or anisotropic operators, unless one uses line or plane relaxation. For 3-D problems, only plane relaxation suffices, in general. While line and plane relaxation algorithms are efficient on sequential machines, they are quite awkward and inefficient on parallel machines. A new multigrid algorithm is presented based on the use of multiple coarse grids, that eliminates the need for line or plane relaxation in anisotropic problems. This algorithm was developed and the standard multigrid theory was extended to establish rapid convergence for this class of algorithms. The new algorithm uses only point relaxation, allowing easy and efficient parallel implementation, yet achieves robustness and convergence rates comparable to line and plane relaxation multigrid algorithms. The algorithm described is a variant of Mulder's multigrid algorithm for hyperbolic problems. The latter uses multiple coarse grids to achieve robustness, but is unsuitable for elliptic problems, since

its V-cycle convergence rate goes to one as the number of levels increases. The new algorithm combines the contributions from the multiple coarse grid via a local switch, based on the strength of the discrete operator in each coordinate direction. Author

N92-10349*# Institute for Computer Applications in Science and Engineering, Hampton, VA.
MULTI-DIMENSIONAL ENO SCHEMES FOR GENERAL GEOMETRIES Final Report
Ami Harten and Sukumar R. Chakravarthy (Rockwell International Science Center, Thousand Oaks, CA.) Sep. 1991 71 p Submitted for publication
(Contracts NAS1-18605; NSF DMS-88-11863; N00014-86-K-0691) (NASA-CR-187637; NAS 1.26:187637; ICASE-91-76) Avail: NTIS HC/MF A04 CSCL 12A

A class of ENO schemes is presented for the numerical solution of multidimensional hyperbolic systems of conservation laws in structured and unstructured grids. This is a class of shock-capturing schemes which are designed to compute cell-averages to high order accuracy. The ENO scheme is composed of a piecewise-polynomial reconstruction of the solution form its given cell-averages, approximate evolution of the resulting initial value problem, and averaging of this approximate solution over each cell. The reconstruction algorithm is based on an adaptive selection of stencil for each cell so as to avoid spurious oscillations near discontinuities while achieving high order of accuracy away from them. Author

N92-10350# Florida State Univ., Tallahassee. Dept. of Statistics.
IDENTIFICATION OF NONLINEAR TIMES SERIES FROM FIRST ORDER CUMULATIVE CHARACTERISTICS
Ian W. McKeague and Mei-Jie Zhang Aug. 1991 25 p
(Contracts DAAL03-86-G-0204; DAAL03-90-G-0103)
(AD-A239822; FSU-Statistics-TR-M-853; ARO-27868.10-MA)
Avail: NTIS HC/MF A03 CSCL 12/3

We consider the problem of identifying the class of time series model to which a series belongs based on observation of part of the series. Techniques of nonparametric estimation have been applied to this problem by various authors using kernel estimates of the one-step lagged conditional mean and variance functions. We study cumulative versions of Tukey regressogram estimators of such functions. These are more stable than estimates of the mean and variance functions themselves and can be used to construct confidence bands. Goodness of fit tests for specific parametric models are also developed. GRA

N92-10351# Air Force Inst. of Tech., Wright-Patterson AFB, OH.
A MATHEMATICAL MODEL FOR A PAIRED COMPARISON EXPERIMENT ON A CONTINUUM OF RESPONSE Ph.D. Thesis
Kaye A. deRuiz Dec. 1990 120 p
(AD-A239858; AFIT/CI/CIA-90-041D) Avail: NTIS HC/MF A06 CSCL 12/3

This research uses a Bradley-Terry paired comparison model, extending the possible outcomes from a simple binary response to any point along a continuum. An integrated mean squared error approach is used as a basis for parameter estimation based on an underlying logistic model and for estimating a function that maps a response from the real line onto the interval (0,1). Evaluation of the parameter estimates is performed using an underlying logistic sampling distribution with a logistic mapping function. The asymptotic behavior of the estimates involves the use of linear combinations of order statistics, also called L-statistics. Using this approach it is shown that the parameter estimates are consistent but slightly biased. A simulation study with randomly generated values from a standard logistic distribution were used for response values in a paired comparison experiment. Samples for 3, 4, and 5 treatments with 5, 10, 25, and at times 50, replications for each pairing were considered. The values for the parameter estimates for these samples are presented along with the graphs of the estimated inverse mapping function. Density smoothing techniques using a kernel estimator were employed to further explore the shape of the derivative of the inverse mapping function. This continuous model was then reformulated into a Likert scale with five possible responses from any comparison. An ad hoc method and weighed least squares were used to determine the discriminating values for the Likert scale. GRA

N92-10352# Missouri Univ., Columbia. Dept. of Mathematics.
APPLICATIONS OF MULTIPARAMETER BIFURCATIONS OF PERIOD FUNCTIONS Final Report, 1 Nov. 1988 - 30 Jun. 1991
Carmen Chicone 24 Jul. 1991 17 p
(Grant AF-AFOSR-0078-89; AF Proj. 2304)
(AD-A240046; AFOSR-91-0722TR) Avail: NTIS HC/MF A03 CSCL 12/2

The objective of the research project was a mathematical analysis of multiparameter bifurcation problems which arise in the study of ordinary differential equations, especially, the bifurcation of critical points of period functions and the bifurcation of continuous families of periodic trajectories. GRA

N92-10353# Naval Postgraduate School, Monterey, CA. Dept. of Operations Research.
A POLYNOMIAL-TIME ALGORITHM FOR COMPUTING THE YOLK IN FIXED DIMENSION
Craig A. Tovey Aug. 1991 35 p
(AD-A240060; NPSOR-91-024) Avail: NTIS HC/MF A03 CSCL 12/4

The yolk developed in (16,22), is a key solution concept in the Euclidean spatial model as the region of policies where a dynamic voting game will tend to reside. However, determining the yolk is NP-hard for arbitrary dimension. This paper derives an algorithm to compute the yolk in polynomial time for any fixed dimension. GRA

N92-10369# Helsinki Univ. of Technology, Espoo (Finland). Dept. of Physics.
EARLY 19TH-CENTURY LEAST SQUARES CALCULATIONS IN FINLAND REPEATED WITH MODERN TECHNIQUES Abstract Only
T. Sundius *In* Oulu Univ., Proceedings of the 25th Annual Conference of the Finnish Physical Society 1991 1 p (For primary document see N92-10362 01-70)
Avail: NTIS HC/MF A12

N92-10371# Jyvaskyla Univ. (Finland). Dept. of Physics.
DYNAMICS OF DISCRETE QUANTUM NONLINEAR SCHROEDINGER EQUATIONS Abstract Only
R. Lohikoski, E. Viitala, and J. Timonen *In* Oulu Univ., Proceedings of the 25th Annual Conference of the Finnish Physical Society 1991 1 p Sponsored by Academy of Finland (For primary document see N92-10362 01-70)
Avail: NTIS HC/MF A12

N92-10379# Tampere Univ. of Technology (Finland). Plasma Technology Lab.
ABEL INVERSION WITH THE FAST FOURIER TRANSFORM Abstract Only
S. M. Jaffe (Stanford Univ., CA.), J. Larjo, and Rolf G. Hernberg *In* Oulu Univ., Proceedings of the 25th Annual Conference of the Finnish Physical Society 1991 1 p (For primary document see N92-10362 01-70)
Avail: NTIS HC/MF A12

65 STATISTICS AND PROBABILITY

Includes data sampling and smoothing; Monte Carlo method; and stochastic processes.

N92-10354# Los Alamos National Lab., NM.
A NEW METHOD TO ASSESS THE STATISTICAL CONVERGENCE OF MONTE CARLO SOLUTIONS
R. A. Forster 1991 7 p Presented at the Winter Meeting of the American Nuclear Society (ANS), San Francisco, CA, 10-15 Nov. 1991

(Contract W-7405-eng-36)
(DE91-016013; LA-UR-91-2391; CONF-911107-19) Avail: NTIS HC/MF A02

Accurate Monte Carlo confidence intervals (CIs), which are formed with an estimated mean and an estimated standard deviation, can only be created when the number of particle histories N becomes large enough so that the central limit theorem can be applied. The Monte Carlo user has a limited number of marginal methods to assess the fulfillment of this condition, such as statistical error reduction proportional to 1/square root of N with error magnitude guidelines and third and fourth moment estimators. A new method is presented here to assess the statistical convergence of Monte Carlo solutions by analyzing the shape of the empirical probability density function (PDF) of history scores. Related work in this area includes the derivation of analytic score distributions for a two-state Monte Carlo problem. Score distribution histograms have been generated to determine when a small number of histories accounts for a large fraction of the result. This summary describes initial studies of empirical Monte Carlo history score PDFs created from score histograms of particle transport simulations. DOE

N92-10355# Oak Ridge National Lab., TN.
ARE LIMIT CYCLE CALCULATIONS A STOCHASTIC PROCESS?
J. March-Leuba 1991 4 p Presented at the Winter Meeting of the American Nuclear Society (ANS), San Francisco, CA, 10-15 Nov. 1991
(Contract DE-AC05-84OR-21400)
(DE91-017681; CONF-911107-27-Extd-Abst) Avail: NTIS HC/MF A01

Stochasticity is typically associated with processes that produce uncertain results which, in many cases, are due to process nonlinearities and/or extreme sensitivity to initial conditions. By its name, a stochastic process should have a probabilistic or random nature; however, it is well known that many if not all, of the processes that behave stochasticly are indeed deterministic. This is the case with computer calculations to predict the stability of boiling water reactors (BWRs). This paper attempts to introduce the reader to some of the stochastic uncertainties involved in this topic, and in particular the errors introduced by the approximations used to integrate numerically the solutions in the time domain. The knowledge of this type of errors is relevant not only in BWR stability calculations but also in time domain calculations involving nonlinear or stochastic processes. DOE

N92-10356# Los Alamos Nuclear Corp., NM.
CHARACTERIZATION OF NONLINEAR INPUT-OUTPUT SYSTEMS USING TIME SERIES ANALYSIS
N. F. Hunter and J. Theiler 1991 11 p Presented at the 1st Experimental Chaos Conference, Arlington, VA, 1-3 Oct. 1991
(Contract W-7405-eng-36)
(DE91-018003; LA-UR-91-2816; CONF-9110200-1) Avail: NTIS HC/MF A03

Data obtained from time series analysis has been used for a number of years for the characterization and response prediction of linear systems. This paper describes a time series technique for the analysis of nonlinear systems through the use of embeddings using delay coordinates or appropriate transformations of delay coordinates (local singular value decomposition or local canonical variate analysis). Local linear approaches are used to characterize the state evolution. Application of the technique is illustrated for a single degree of freedom oscillator with nonlinear stiffness, a mechanical chaos beam, and a climatic data time series. In each application analysis from measured data is emphasized. State rank, Lyapunov exponents, and expected iterated prediction errors are quantified. The technique illustrated should be useful in the analysis of many forms of experimental data, especially where the state rank is not excessively large. DOE

N92-10357# Los Alamos National Lab., NM.
USING SURROGATE DATA TO DETECT NONLINEARITY IN TIME SERIES
J. Theiler, B. Galdrikian, A. Longtin, S. Eubank, and J. D. Farmer 31 Jul. 1991 17 p Presented at the North Atlantic Treaty Organization (NATO) Advanced Research Workshop on Nonlinear Modelling and Forecasting, Santa Fe, NM, 17-21 Sep. 1990
(Contract W-7405-eng-36)
(DE91-018017; LA-UR-91-2615; CONF-900986-1) Avail: NTIS HC/MF A03

We address the issue of reliably discriminating between chaos and noise from a time series. In particular, we are interested in avoiding claims of chaos when simpler models (such as linearly correlated noise) can explain the data. We take a statistical approach, and use a form of bootstrapping to detect nonlinearity by showing that a given linear model is unlikely to have produced the data. Our method requires the careful statement of a null hypothesis which characterizes a candidate linear process, the generation of an ensemble of surrogate data sets which are similar to the original time series but consistent with the null hypothesis, and the computation of a discriminating statistic for the original and for each of the surrogate data sets. The idea is to test the original time series against the null hypothesis by checking whether the discriminating statistic computed for the original time series differs significantly from the statistics computed for each of the surrogate sets. We present algorithms for generating surrogate data under various null hypotheses, and we show the results of numerical experiments on artificial data using correlation dimension, Lyapunov exponent, and forecasting error as discriminating statistics. Finally, we consider a number of experimental time series -- including sunspots, electroencephalogram (EEG) signals, and fluid convection -- and evaluate the statistical significance of the evidence for nonlinear structure in each case. DOE

N92-10358# Los Alamos National Lab., NM.
MEAN ESTIMATION IN HIGHLY SKEWED SAMPLES
S. P. Pederson Sep. 1991 8 p
(Contract W-7405-eng-36)
(DE91-018513; LA-12114-MS) Avail: NTIS HC/MF A02

The problem of inference for the mean of a highly asymmetric distribution is considered. Even with large sample sizes, usual asymptotics based on normal theory give poor answers, as the right-hand tail of the distribution is often under-sampled. This paper attempts to improve performance in two ways. First, modifications of the standard confidence interval procedure are examined. Second, diagnostics are proposed to indicate whether or not inferential procedures are likely to be valid. The problems are illustrated with data simulated from an absolute value Cauchy distribution. DOE

N92-10359# Oak Ridge National Lab., TN.
THE CHANGING FACE OF PROBABILITY
Bruce E. Tonn and L. James. ValverdeA, Jr. (Electric Power Research Inst., Palo Alto, CA.) Sep. 1991 13 p Presented at the Symposium on Expert System Applications for the Electric Power Industry, Boston, MA 9-11 Sep. 1991
(Contract DE-AC05-84OR-21400)
(DE91-018857; CONF-9109121-4) Avail: NTIS HC/MF A03

During the course of the past several centuries, the concept of probability has evolved in both interesting and varied ways. In this paper we consider various facets of the conceptual evolution of probability. We begin with a brief historical overview of the earliest conceptions of probability. We then consider the rise of probability in the twentieth century, and some of the central views that have emerged. The paper concludes with a discussion of some of the current trends in modern probability theory. DOE

N92-10360# Naval Postgraduate School, Monterey, CA.
DETECTION OF ABRUPT CHANGES IN STATISTICAL MODELS Ph.D. Thesis
David Aviv Jun. 1991 250 p
(AD-A240116) Avail: NTIS HC/MF A11 CSCL 12/3

This dissertation investigates different types of disorder problems by using sequential procedures for on-line implementation. The problem is considered within the framework of detecting abrupt changes in an observed random process when

the disorder can occur at unknown times. The focus of this work is on quickest detection methods for cumsum procedures implemented for different parametric and nonparametric nonlinearities and their performance evaluation. Both the non-Bayesian (Maximum-Likelihood) and the Bayesian frameworks are presented but the focus is mainly on non-Bayesian methods for which detailed analysis is provided. The use of Brownian motion approximations is also included and provides an additional viewpoint of analyzing the performance for both the non-Bayesian and Bayesian methods. GRA

66 SYSTEMS ANALYSIS

Includes mathematical modeling; network analysis; and operations research.

No abstracts in this category.

67 THEORETICAL MATHEMATICS

Includes topology and number theory.

N92-10361# National Academy of Sciences - National Research Council, Washington, DC. Board on Mathematical Sciences.
ACTIVITIES OF THE BOARD ON MATHEMATICAL SCIENCES Annual Report
1991 12 p
(Contract DE-FG05-89ER-25080)
(DE91-017931; DOE/ER-25080/2) Avail: NTIS HC/MF A03

This is a progress report on the activities of the Board on Mathematical Sciences (BMS) of the Commission on Physical Sciences, Mathematics, and Applications, National Research Council (NRC), for the second year of the referenced grant for Board core support, and a request to the Department of Energy for the third year of funding in the amount of $32,390 under that grant for the period August 1, 1991 to July 31, 1992. As this request is for the third year of funding for activities covered by a three-year proposal and award, this report is limited to an update of progress over the second funding year. Some of the projects discussed are: Number theory; the import of mathematics; some of the spatial statistics and image processing; and BMS strategic plan. DOE

70 PHYSICS (GENERAL)

For precision time and time interval (PTTI) see *35 Instrumentation and Photography;* for geophysics, astrophysics or solar physics see *46 Geophysics, 90 Astrophysics,* or *92 Solar Physics.*

N92-10362# Oulu Univ. (Finland). Dept. of Physics.
PROCEEDINGS OF THE 25TH ANNUAL CONFERENCE OF THE FINNISH PHYSICAL SOCIETY Abstracts Only
Jukka Jokisaari, ed. and Maarit Levasalmi, ed. 1991 257 p
Conference held in Oulu, Finland, 21-23 Mar. 1991
(Rept-119(1991); ISBN-951-42-3087-6; ISSN-0356-1852;
ETN-91-99838) Avail: NTIS HC/MF A12

A book of abstracts of the proceedings is presented. The following subjects were addressed: general physics; elementary particles and fields; nuclear physics; atomic and molecular physics; classical areas of phenomenology; fluids, plasmas and electrical discharges; structure, thermal and mechanical properties of condensed matter; electronic structure electrical, magnetic, and optical properties of condensed matter; cross disciplinary physics and related areas of science and technology; geophysics, astronomy, and astrophysics. Invited lectures and some papers on energy and evironment are abstracted. For individual titles, see N92-10363 through N92-10587.

N92-10363# Joensuu Univ. (Finland). Dept. of Physics.
A NEW PHASE RETRIEVAL METHOD FOR CARS SPECTRUM ANALYSIS Abstract Only **c25**
E. M. Vartiainen and K.-E. Peiponen *In* Oulu Univ., Proceedings of the 25th Annual Conference on the Finnish Physical Society 1991 1 p (For primary document see N92-10362 01-70)
Avail: NTIS HC/MF A12

Coherent Anti-Stokes Raman Scattering (CARS) has proven to be a powerful tool in spectroscopic and diagnostic applications. CARS signal intensity is proportional to the squared modulus of the effective third order susceptibility, chi(3), which in turn can be resonantly enhanced by the rotational and vibrational relaxation processes in the sample. Therefore, the amount of information obtained from a CARS measurement depends mainly on how accurate the theoretical lineshape model is for the chi(3) used, and how well the measured values can be fitted to the theoretical model. A noniterative phase retrieval method for CARS spectrum analysis is developed. By this method the phase (or the real and imaginary parts) of chi(3) can be uniquely determined only when the modulus of chi(3) is known. This result is obtained by approximating the squared modulus by the Maximum Entropy Method (MEM) and using some a priori information of the function chi(3). When the real and imagery parts are known some important physical properties of the system, hidden in the original spectrum, are revealed. Since this method is independent of any theoretical lineshape model, one is also able to check whether a certain model is reasonable or not for the measured spectrum. ESA

N92-10364# Oulu Univ. (Finland). Dept. of Theoretical Physics.
ANOMALOUS e(+)e(-) PAIRS IN HEAVY ION COLLISIONS AND SOLAR NEUTRINOS: TWO PUZZLES WITH COMMON SOLUTION? Abstract Only **c92**
P. Mahonen and M. Pitkanen (Helsinki Univ. of Technology, Espoo, Finland) *In its* Proceedings of the 25th Annual Conference of the Finnish Physical Society 1991 1 p (For primary document see N92-10362 01-70)
Avail: NTIS HC/MF A12

The production of anomalous electron-positron pairs in heavy ion collisions and solar neutrino puzzle are two seemingly unrelated problems of the standard model of electroweak interactions. The generalization of PCAC ideas is shown to lead to a prediction for the lifetime and production cross section of leptopion in agreement with data. The model is also consistent with constraints coming from Babbha scattering and supernova physics. ESA

N92-10365# Stockholm Univ. (Sweden). Inst. of Physics.
QUANTUM WORLD IN 2+1 DIMENSIONS Abstract Only **c77**
H. Hansson *In* Oulu Univ., Proceedings of the 25th Annual Conference of the Finnish Physical Society 1991 1 p (For primary document see N92-10362 01-70)
Avail: NTIS HC/MF A12

Some of the physics and mathematics related to Chern-Simons gauge theory are reviewed. The main emphasis is on various aspects of anyon physics, but the relevance for relativistic spinning particles and the topological theory of links and knots is also discussed. ESA

N92-10366# Cornell Univ., Ithaca, NY. Dept. of Applied and Engineering Physics.
SYNCHROTRON RADIATION: NEW RESEARCH OPPORTUNITIES FOR THE NEXT DECADE Abstract Only **c73**
Boris W. Batterman *In* Oulu Univ., Proceedings of the 25th Annual Conference of the Finnish Physical Society 1991 1 p (For primary document see N92-10362 01-70)
Avail: NTIS HC/MF A12

The availability of intense synchrotron radiation beams has affected the general field of X ray crystallography and scattering in a manner similar to lasers in the field of optics. In addition to enormous increases of available flux on a specimen there are

additional properties, heretofore unavailable from conventional sources. Some of these are: time structure, polarization and tuneability, each of which has had a special impact on a conventional technique in structure determination. These features, as utilized in recent experiments, as well as future prospects for new synchrotron sources and the next generation of experimentation are discussed. ESA

N92-10367# European Organization for Nuclear Research, Geneva (Switzerland). Theory Div.
THE QUARK-HADRON PHASE TRANSITION Abstract Only **c75**
Helmut Satz (Bielefeld Univ., Germany, F.R.) *In* Oulu Univ., Proceedings of the 25th Annual Conference of the Finnish Physical Society 1991 1 p (For primary document see N92-10362 01-70)
Avail: NTIS HC/MF A12

From Quantum Chromodynamics (QCD) it is expected that at sufficiently high density, strongly interacting matter should become a plasma of deconfined quarks and gluons. The physical basis of this transition is discussed and quantitative predictions for the critical behavior using the lattice evaluation of statistical QCD are obtained. Following a brief excursion to the cosmological quark-hadron transition shortly after the big bang, experimental attempts to produce a quark-gluon plasma by means of high energy heavy ion collisions, are surveyed and assessed. The conditions which can be achieved in such collisions are examined and possible ways to obtain information about the primordial state of the matter thus produced are considered. ESA

N92-10368# EISCAT Scientific Association, Kiruna (Sweden).
THE STRUCTURE AND DYNAMICS OF THE POLAR MESOSPHERE INVESTIGATED WITH THE EISCAT RADAR SYSTEMS Abstract Only **c46**
J. Roettger *In* Oulu Univ., Proceedings of the 25th Annual Conference of the Finnish Physical Society 1991 1 p (For primary document see N92-10362 01-70)
Avail: NTIS HC/MF A12

The principle of incoherent backscatter of radar waves from the ionized part of the mesosphere, namely the D region of the ionosphere, is discussed. The coherent backscatter process, resulting from ionization irregularities due to clear air turbulence and related processes in the mesosphere, are considered. The measurable ionospheric/atmospheric parameters, namely electron density, temperature, wind vector velocity, turbulence intensity etc., are outlined. Examples of data collected from incoherent and coherent backscatter using the EISCAT UHF and VHF radars are presented and explained. ESA

N92-10369# Helsinki Univ. of Technology, Espoo (Finland). Dept. of Physics.
EARLY 19TH-CENTURY LEAST SQUARES CALCULATIONS IN FINLAND REPEATED WITH MODERN TECHNIQUES Abstract Only **c64**
T. Sundius *In* Oulu Univ., Proceedings of the 25th Annual Conference of the Finnish Physical Society 1991 1 p (For primary document see N92-10362 01-70)
Avail: NTIS HC/MF A12

The least squares method was introduced in Finland by the professor in physics G. G. Hallstrom (1775 to 1844), and was first used in a dissertation by his student H. J. Walbeck. The aim of his investigation was to find the temperature, at which the density of water is a maximum. Hallstrom refined both the measurement and calculation techniques in two subsequent papers, which can be considered to be of pioneering importance. The calculations in these papers were critically examined, using modern computational methods and facilities. ESA

N92-10370# Turku Univ. (Finland). Dept. of Physics.
DROMIONS: THE MOVIE Abstract Only **c77**
Jarmo Hietarinta and J. Ruokolainen (Centre for Scientific Computing, Espoo, Finland) *In* Oulu Univ., Proceedings of the 25th Annual Conference on the Finnish Physical Society 1991 1 p (For primary document see N92-10362 01-70)
Avail: NTIS HC/MF A12

The most interesting recent development in the soliton theory is concerned with new kind of solutions, the dromions. They are solutions to 2 + 1 dimensional nonlinear evolution equations (e.g., the Davey-Stewartson equation) that decay exponentially in all directions of the (x,y) plane. The basic concept behind the dromions is the existence of ghost solitons which are not physical themselves, but whose interaction creates a physical local effect. Hietarinta and Hirota constructed dromion solutions by the bilinear method, which yields more general solutions than those obtained by any other method. This was subsequently generalized into other equations, and are illustrated here by a video animation. ESA

N92-10371# Jyvaskyla Univ. (Finland). Dept. of Physics.
DYNAMICS OF DISCRETE QUANTUM NONLINEAR SCHROEDINGER EQUATIONS Abstract Only **c64**
R. Lohikoski, E. Viitala, and J. Timonen *In* Oulu Univ., Proceedings of the 25th Annual Conference of the Finnish Physical Society 1991 1 p Sponsored by Academy of Finland (For primary document see N92-10362 01-70)
Avail: NTIS HC/MF A12

The discrete quantum nonlinear Schroedinger equations in the form which can be derived in the adiabatic approximation from the Scott-Davydov equations are studied. These equations describe the dynamics at zero temperature of a vibrational quantum coupled to sound waves in the alpha helix protein. ESA

N92-10372# Oulu Univ. (Finland). Dept. of Theoretical Physics.
DYNAMIC LATTICE COMPUTING IN GENERAL RELATIVITY Abstract Only **c77**
P. Mahonen and V. Punkka (Texas Univ., Austin.) *In its* Proceedings of the 25th Annual Conference of the Finnish Physical Society 1991 1 p (For primary document see N92-10362 01-70)
Avail: NTIS HC/MF A12

A comprehensive method to numerically calculate time evolution of gravitational field in general relativity is introduced. Vierbain (tetraed) formalism, dynamic lattice and massively parallellized computation are suggested as they are expected to speed up the calculations considerably and enable problems previously considered too hard to be solved, such as the time evolution of a system consisting of two or more black holes or the structure of wormholes. The basic implementation is presented and initial results are reported. ESA

N92-10373# Tampere Univ. of Technology (Finland). Dept. of Physics.
DRIVEN GROWTH IN THE RESTRICTED SOLID ON SOLID MODEL Abstract Only **c76**
Tapio Ala-Nissila, J. M. Kim, and J. M. Kosterlitz (Brown Univ., Providence, RI.) *In* Oulu Univ., Proceedings of the 25th Annual Conference of the Finnish Physical Society 1991 1 p (For primary document see N92-10362 01-70)
Avail: NTIS HC/MF A12

Results of numerical simulations of growth in a restricted solid on solid model are described. The exponent beta is calculated by comparing the surface width with a spatially averaged height correlation function. The latter is shown to yield more reliable results, even for relatively small systems. The exponent chi is obtained from saturation of the interface fluctuations in the late time regime. The results lead to a new conjecture of dimension dependent exponents as beta (d) = 1/(d+1), chi (d) = 2/(d+2). How crossover effects may affect the values of these exponents is shown and the relation of the model to the continuum growth equations is discussed. ESA

N92-10374# Tampere Univ. of Technology (Finland). Microelectronics Lab.
GATE MATRIX OPTIMIZATION USING SIMULATED ANNEALING Abstract Only **c61**
Harri Raittinen, Jarkko Niittylahti, and Kimmo Kaski *In* Oulu

Univ., Proceedings of the 25th Annual Conference of the Finnish Physical Society 1991 1 p (For primary document see N92-10362 01-70)
Avail: NTIS HC/MF A12

A computational method for simulated annealing optimization is described. This is used on programmable boolean logic gates for application specific vector mapping. These logic gates form a feed forward neural network, which is capable of learning the general mapping rule on the basis of a few correct mapping examples introduced to the network. The network consists of programmable logic gates and a connection matrix, which defines the connections between these gates. ESA

N92-10375# Kuopio Univ. (Finland). Dept. of Applied Physics.
RUNNING DISCRETE COSINE TRANSFORM ALGORITHM Abstract Only **c61**
H. Olkkonen *In* Oulu Univ., Proceedings of the 25th Annual Conference of the Finnish Physical Society 1991 1 p (For primary document see N92-10362 01-70)
Avail: NTIS HC/MF A12

The Discrete Cosine Transform (DCT) has become the industry standard in digital signal processing (digital filtering, data compression, image coding, high definition television, etc.). Performance of the DCT is close to the statistically optimal Karhunen-Loeve transform, which decomposes the signal into correlated signal vectors and minimizes the mean square error between a truncated representation and the actual signal. The DCT is a fast transform and commonly its computation goes through the fast Fourier transform algorithm. For real time computation, the Running DCT (RDCT) is introduced and defined. With the aid of the Z transform, a recursive algorithm for computation of the RDCT coefficients is deduced. ESA

N92-10376# Jyvaskyla Univ. (Finland). Dept. of Physics.
A MODEL FOR A DATA ACQUISITION SOLUTION FOR A MEDIUM SIZE ACCELERATOR LABORATORY Abstract Only **c62**
A. Lampinen, K. Loberg, M. Lahtinen, and J. Rauma *In* Oulu Univ., Proceedings of the 25th Annual Conference of the Finnish Physical Society 1991 1 p (For primary document see N92-10362 01-70)
Avail: NTIS HC/MF A12

A plan for a data acquisition system for a new cyclotron laboratory is presented. The design is based on a six stage pipeline architecture resulting in a high level of parallelism and, consequently, a very low effective dead time. A new optical local area network topology is proposed for media connecting separate front end systems to control units. The majority of the system software will be programmed on a high level real time operating system. ESA

N92-10377# Oulu Univ. (Finland). Dept. of Physics.
SYNCHROTRON RADIATION RESEARCH AND FINNISH BEAMLINE AT MAX-LAB Abstract Only **c73**
Seppo Aksela *In its* Proceedings of the 25th Annual Conference on the Finnish Physical Society 1991 1 p (For primary document see N92-10362 01-70)
Avail: NTIS HC/MF A12

Basis characteristics of the synchrotron radiation, its generation and some of its applications are discussed. In order to provide better possibilities, especially for the Finnish photoemission research below 100 eV photon energy range, official cooperation with MAX laboratory, at the University of Lund, was initiated. The agreement involves financing and construction of the Finnish beamline with a high resolution monochromator at MAX lab. The beamlines and available experimental set ups for solid state as well as atomic and molecular physics measurements are described. Some examples of synchrotron radiation studies of atomic gases and metal vapors are presented. ESA

N92-10378# Tampere Univ. of Technology (Finland). Dept. of Physics.
DOPPLER SHIFT VELOCIMETRY IN DISPERSE FLOWS Abstract Only **c74**
V. Hayrinen and Rolf G. Hernberg *In* Oulu Univ., Proceedings of the 25th Annual Conference of the Finnish Physical Society 1991 1 p Sponsored by Academy of Finland (For primary document see N92-10362 01-70)
Avail: NTIS HC/MF A12

The objective was to develop a device for measuring the particle flow fields in plasma spray jets and similar environments. Particular emphasis was set on measuring capability in heavily loaded flows and rough industrial conditions. A technique based on the direct measurement of the Doppler shift between laser light illuminating the measurement volume and light backscattered from it is described. The instrument developed makes use of fiberguides to communicate the light signals, and a planar mirror scanning Fabry-Perot and a PMT were used. ESA

N92-10379# Tampere Univ. of Technology (Finland). Plasma Technology Lab.
ABEL INVERSION WITH THE FAST FOURIER TRANSFORM Abstract Only **c64**
S. M. Jaffe (Stanford Univ., CA.), J. Larjo, and Rolf G. Hernberg *In* Oulu Univ., Proceedings of the 25th Annual Conference of the Finnish Physical Society 1991 1 p (For primary document see N92-10362 01-70)
Avail: NTIS HC/MF A12

A method in which the FFT (Fast Fourier Transform) allows side on data to be determined, is presented. The FFT is further used to process the data by optimal filtering of the noise, determining the location of the center, measuring the asymmetry, and symmetrizing. The resulting Fourier coefficients are used directly in a Bessel series representation of the volumetric emission. The integration can be performed analytically, because the cosine and J sub 0 Bessel functions are Abel transform pairs. The method was tested on artificial distributions and is now being employed as a standard research tool in the laboratory. In conclusion, this method allows more information from the side on distributions to be extracted and forms a more exact basis for the Abel inversion of noisy data than polynomial fitting methods. ESA

N92-10380# Tampere Univ. of Technology (Finland). Dept. of Physics.
FLUIDIZED BED COMBUSTION DIAGNOSTICS BY LASER PHOTOCOUSTIC SPECTROSCOPY Abstract Only **c25**
Jari Stenberg and Rolf G. Hernberg *In* Oulu Univ., Proceedings of the 25th Annual Conference of the Finnish Physical Society 1991 1 p Sponsored by LIEKKI (For primary document see N92-10362 01-70)
Avail: NTIS HC/MF A12

A method under development for in situ gas analysis based on laser photoacoustic spectroscopy is described. To demonstrate the laser photoacoustic effect, a laboratory test was performed using the 3s to 3p transition of sodium at 285.29 nm. At present a high temperature photoacoustic probe design is being tested. Future developments incorporate tests in a laboratory combustion facility, and field tests in industrial fluidized bed combustors. ESA

N92-10381# Tampere Univ. of Technology (Finland). Dept. of Physics.
SIMULTANEOUS PYROMETRIC MEASUREMENT OF TEMPERATURE AND SIZE OF FUEL PARTICLES IN FLUIDIZED BED COMBUSTIONS Abstract Only **c25**
Jari Stenberg, M. Urponen, and Rolf G. Hernberg *In* Oulu Univ., Proceedings of the 25th Annual Conference of the Finnish Physical Society 1991 1 p (For primary document see N92-10362 01-70)
Avail: NTIS HC/MF A12

In studying the reactivities of solid fuels used in fluidized bed combustors it is of great interest to know the temperature and size of a burning fuel particle in the char burning stage. A new

device was developed which makes possible the measurement of pyrometric signals from the bed and the fuel particles by means of a fiberguide optical probe. The instrument was used successfully in full scale industrial environments for particle temperature measurement. Further development resulted in a method which allows for the extraction of particle size data from the pyrometric signals collected by the probe resulting in simultaneous measurement of temperature and size of individual fuel particles. ESA

N92-10382# Kuopio Univ. (Finland). Dept. of Applied Physics.
DUAL PIN DIODE PREAMPLIFIER FOR LASER DOPPLER VELOCIMETRY Abstract Only **c33**
H. Olkkonen *In* Oulu Univ., Proceedings of the 25th Annual Conference of the Finnish Physical Society 1991 1 p (For primary document see N92-10362 01-70)
Avail: NTIS HC/MF A12

Laser Doppler Velocimetry (LDV) is widely used for nondestructive assessment of velocity distributions of flowing materials and vibrating surfaces. Most LDV methods are based on the detection of the photons due to the interference between the laser emitted light wavelength and the Doppler shifted wavelength. In practice, disturbances are due to the surrounding light and the laser cavity interference, which are difficult to eliminate. An LDV preamplifier, which is based on the detection of the interference photons by two parallel PIN diodes placed in opposite directions, is described. The dual diode preamplifier minimizes the disturbances due to common mode laser light and transient noise due to the laser mode variation. Also the 50 Hz+ harmonics pickup due to the surrounding light effectively vanishes. ESA

N92-10383# Jyvaskyla Univ. (Finland). Dept. of Physics.
THERMAL EMISSION OF GAMMAS AND LEPTON PAIRS FROM QUARK-GLUON PLASMAS Abstract Only **c72**
P. V. Ruuskanen *In* Oulu Univ., Proceedings of the 25th Annual Conference of the Finnish Physical Society 1991 1 p (For primary document see N92-10362 01-70)
Avail: NTIS HC/MF A12

Thermal production rates of lepton pairs and photons are calculated for central nucleus-nucleus collisions at several energies. The cross sections of basic processes in quark gluon plasma are calculated in lowest order quantum chromodynamics perturbation theory. For dileptons the contribution from hadron gas is included assuming that the hadron gas consists only of pions. Hydrodynamics is used to describe the thermal evolution. Results are compared with dominant background sources. ESA

N92-10384# Jyvaskyla Univ. (Finland). Dept. of Physics.
THERMAL PHOTON PRODUCTION FROM HIGH-TEMPERATURE NUCLEAR MATTER Abstract Only **c72**
D. Seibert, J. Kapusta, and P. Lichard (Comenius Univ., Bratislava, Czechoslovakia) *In* Oulu Univ., Proceedings of the 25th Annual Conference of the Finnish Physical Society 1991 1 p (For primary document see N92-10362 01-70)
Avail: NTIS HC/MF A12

Thermal production of photons from hot hadronic matter and from quark-gluon plasma is calculated. Both the overall production rate and and the shape of the energy distribution are found to be very similar for both production mechanisms at fixed temperature. As a result, photon production rates can be used as a thermometer to measure the temperature of hot nuclear matter, with results that depend only weakly on the state of the matter. ESA

N92-10385# Cape Town Univ., Rondebosch (South Africa). Dept. of Physics.
EXACT STRANGENESS CONSERVATION AND PARTICLE PRODUCTION Abstract Only **c72**
J. Cleymans, K. Redlich, and E. Suhonen (Oulu Univ., Finland) *In* Oulu Univ., Proceedings of the 25th Annual Conference of the Finnish Physical Society 1991 1 p Submitted for publication (For primary document see N92-10362 01-70)
(BI-TP-90/35) Avail: NTIS HC/MF A12

The production of strange particles is studied in terms of a statistical formalism requiring strangeness to be exactly conserved while baryon number is treated grand canonically using a chemical potential. The gas is considered to be in thermal and chemical equilibrium and to have zero overall strangeness. All particles and resonances having masses up to approximately 2 GeV and strangeness up to plus or minus 3 are included. General formulas for different particle multiplicities in terms of infinite series of modified Bessel functions are derived. In contrast to the integral representation of particle numbers in the canonical ensemble, results can be easily handled numerically since the series converge very rapidly. As an illustration, the above formalism is applied to the description of particle production in proton-proton, proton-nucleus and nucleus-nucleus collisions. In particular the K/pi ratio shows a strong dependence on the interaction volume on the system while, in contrast, the antiLambda/Lambda ratio is almost independent of the volume. These results are in qualitative agreement with experimental data. ESA

N92-10386# Cape Town Univ., Rondebosch (South Africa). Dept. of Physics.
HADRONIC EQUATION OF STATE AND THE ONSET OF KAON CONDENSATION Abstract Only **c72**
J. Cleymans, J. Staalnacke, and E. Suhonen (Oulu Univ., Finland) *In* Oulu Univ., Proceedings of the 25th Annual Conference of the Finnish Physical Society 1991 1 p (For primary document see N92-10362 01-70)
Avail: NTIS HC/MF A12

An equation of state which takes the finite size of baryons and optionally of mesons consistently into account and incorporates the contributions of both non strange and strange hadrons with strangeness conservation is presented. The difference of the original and new equations of state are large in a dense hadronic matter. To demonstrate them, the onset of Bose-Einstein condensation of kaons is considered. The phase diagrams of the deconfinement phase transition of hadronic matter are calculated using the MIT bag model for the quark gluon plasma. ESA

N92-10387# European Organization for Nuclear Research, Geneva (Switzerland). UA1 Collaboration.
INTERMITTENCY STUDIES IN PROTON-ANTIPROTON COLLISIONS AT SQUARE ROOT OF S = 630 GeV Abstract Only **c72**
C. Albajar, M. G. Albrow, O. C. Allkofer, B. Andrieu, K. Ankoviak, R. Apsimon, B. Aubert, C. Bacci, S. Bartha (Kiel Univ., Germany, F.R.), and G. Bauer, 8RZ958
et al *In* Oulu Univ., Proceedings of the 25th Annual Conference of the Finnish Physical Society 1991 1 p Submitted for publication (For primary document see N92-10362 01-70)
(CERN-PPE/90-153) Avail: NTIS HC/MF A12

A significant intermittency signal is observed in 630 GeV proton-antiproton collisions measured in the UA1 central detector. It occurs with similar magnitude in different variables: pseudorapidity, rapidity and azimuthal angle. The signal increases with decreasing charged particle multiplicity in the event. Its strength in a sample of low p sub t tracks and its multiplicity dependence are not reproduced by commonly used Monte Carlo models of high energy interactions. ESA

N92-10388# European Organization for Nuclear Research, Geneva (Switzerland). UA1 Collaboration.
BEAUTY PRODUCTION AT THE CERN PROTON-ANTIPROTON COLLIDER Abstract Only **c72**
C. Albajar, R. Kinnunen, J. Tuominiemi, V. Karimaki, M. Pimia, and E. Pietarinen (Helsinki Univ. of Technology, Espoo, Finland) *In* Oulu Univ., Proceedings of the 25th Annual Conference of the Finnish Physical Society 1991 1 p Submitted for publication (For primary document see N92-10362 01-70)
(CERN-PPE/90-155) Avail: NTIS HC/MF A12

Measurements of b-quark and B-hadron production in proton-antiproton collisions at square root of s = 0.063 TeV are reported. Muon data samples are used to extract beauty production cross sections over a wide range of transverse momentum in the

central rapidity range, the absolute value of y is less than 1.5.
ESA

N92-10389# European Organization for Nuclear Research, Geneva (Switzerland). UA1 Collaboration.
A SEARCH FOR RARE B MESON DECAYS AT THE CERN PROTON-ANTIPROTON COLLIDER Abstract Only c72
C. Albajar, R. Kinnunen, J. Tuominiemi, V. Karimaki, M. Pimia, and E. Pietarinen (Helsinki Univ. of Technology, Espoo, Finland) *In* Oulu Univ., Proceedings of the 25th Annual Conference of the Finnish Physical Society 1991 1 p Submitted for publication (For primary document see N92-10362 01-70)
(CERN-PPE/91) Avail: NTIS HC/MF A12

A search for the decays B zero to mu(+)mu(-), B to mu(+)mu(-)X and B zero sub d to mu(+)Mu(-)K zero, which are expected to be rare if mediated by flavor changing neutral currents, is reported. Using data collected during the 1984 to 1989 CERN proton-antiproton collider runs, the UA1 search was carried out using muon(+)muon(-) events with 3.9 GeV/c squared less than M sub mumu less than 5.5 GeV/c squared. Ninty percent confidence level upper limits were found on the branching ratios for B zero to mu(+)mu(-) of 0.0000083, for B to mu(+)mu(-)X of 0.00005 and for B zero sub d to mu(+)mu(-)K zero of 0.000023. Implications of upper limits on the t-quark mass are discussed.
ESA

N92-10390# European Organization for Nuclear Research, Geneva (Switzerland). UA1 Collaboration.
J/PSI AND PSI' PRODUCTION AT THE CERN PROTON-ANTIPROTON COLLIDER Abstract Only c72
C. Albajar, R. Kinnunen, J. Tuominiemi, V. Karimaki, M. Pimia, and E. Pietarinen (Helsinki Univ. of Technology, Espoo, Finland) *In* Oulu Univ., Proceedings of the 25th Annual Conference of the Finnish Physical Society 1991 1 p Submitted for publication (For primary document see N92-10362 01-70)
(CERN-PPE/90-154) Avail: NTIS HC/MF A12

The production cross section times branching ratio is given for J/psi to mu+mu- in proton-antiproton interactions at square root of s = 630 GeV in the kinematic range y less than 2.0 and p sub t greater than 5 GeV, BR (J/psi to mu+mu-)sigma (proton antiproton to J/psi) 6.18 plus or minus 0.24 plus or minus 0.81 nb. The data sample collected in 1988 and 1989 for an integrated luminosity of 4.7 pb to the minus 1st power represents a fivefold improvement over the statistics in an earlier study of the J/psi production process, and the p sub t distribution which is measured extends to 28 GeV/c. Using event topology it is shown that the rate for the direct production of J/psi, probably via radiative decays of chi states, is larger than that for production via B-hadrons. Production of psi' is also studied using the decay modes psi' to mu+mu- and psi' to J/psi pi+pi-.
ESA

N92-10391# European Organization for Nuclear Research, Geneva (Switzerland). UA1 Collaboration.
LIMITS ON T-QUARK DECAY INTO CHARGED HIGGS FROM A DIRECT SEARCH AT THE CERN PROTON-ANTIPROTON COLLIDER Abstract Only c72
C. Albajar, R. Kinnunen, J. Tuominiemi, V. Karimaki, M. Pimia, and E. Pietarinen (Helsinki Univ. of Technology, Espoo, Finland) *In* Oulu Univ., Proceedings of the 25th Annual Conference of the Finnish Physical Society 1991 1 p Submitted for publication (For primary document see N92-10362 01-70)
(CERN-PPE/90-180) Avail: NTIS HC/MF A12

A search for t-quark decay into charged Higgs, t to H+(b), with the charged Higgs decaying via the H+ to tau+(nu sub tau) mode, was performed in proton-antiproton collisions at square root of s = 0.63 TeV with the UA1 experiment. No evidence for this decay has been observed. Mass limits at 95 and 90 pcts. CL for the t-quark and the charged Higgs are presented. The results were also interpreted in terms of the tan beta parameter of a two doublet Higgs sector.
ESA

N92-10392# European Organization for Nuclear Research, Geneva (Switzerland).
MEASUREMENTS OF THE RATIO R = SIGMA(SUB W)Br(W TO MU(NU))/SIGMA(SUB Z)Br(Z TO MU(MU)) AND GAMMA(SUP tot)(SUB W) AT THE CERN PROTON-ANTIPROTON COLLIDER Abstract Only c72
C. Albajar, R. Kinnunen, J. Tuominiemi, V. Karimaki, M. Pimia, and E. Pietarinen (Helsinki Univ. of Technology, Espoo, Finland) et al *In* Oulu Univ., Proceedings of the 25th Annual Conference of the Finnish Physical Society 1991 1 p Submitted for publication (For primary document see N92-10362 01-70)
(CERN-PPE/90-141) Avail: NTIS HC/MF A12

An analysis of W and Z boson production at UA1, using 4.66 pb(exp -1) of data from the 1988 and 1989 CERN proton-antiproton collider runs at square root of s = 0.63 TeV, yields R (sigma sub W)Br(W to mu(nu))/(sigma sub Z)Br(Z to mu(mu)) = 10.4 (upper limit 1.8)(lower limit -1.5)(stat) + or - 0.8 (syst). R = 9.5 (upper limit 1.1)(lower limit -1.0) (stat+syst) is found when combining all available UA1 data, in both the electron and muon channel, taken in the period 1983 to 1989. In the framework of the standard model, the value of R is used to infer the total width of the W boson, Gamma(sup tot)(sub W) = 2.18 (upper limit 0.26)(lower limit -0.24)(exp) + or - 0.04 (theory) GeV/c squared.
ESA

N92-10393# Helsinki Univ. of Technology, Espoo (Finland). Dept. of High Energy Physics.
LOCAL CHARGE COMPENSATION IN Z(SUP 0) HADRONIC DECAYS Abstract Only c72
P. Eerola, J. Pennanen, and R. Orava *In* Oulu Univ., Proceedings of the 25th Annual Conference of the Finnish Physical Society 1991 1 p (For primary document see N92-10362 01-70)
Avail: NTIS HC/MF A12

The charged particle distribution in rapidity space in Z zero hadronic decays was studied by using rapidity zone analysis. The events were collected with the DELPHI experiment at 91 GeV central of mass energy at LEP (Large Electron Positron) collider. The length of a rapidity zone is defined as the length in which the cumulative hadronic charge is compensated. If there are correlations between oppositely charged hadrons, the average length of the zones should be shorter than in the situation in which all the charged hadrons are randomly distributed in the rapidity space. The rapidity zone analysis is a model independent way to study quark fragmentation. When the results are compared with low energy experiments, they support the local charge compensation hypothesis which states that the average length of the rapidity zones and the number of charged particles in a zone should become independent of square root of s at high energies.
ESA

N92-10394# Helsinki Univ. of Technology, Espoo (Finland). Research Inst. for High Energy Physics.
RECENT PHYSICS RESULTS FROM DELPHI Abstract Only c72
Reino Keranen *In* Oulu Univ., Proceedings of the 25th Annual Conference of the Finnish Physical Society 1991 1 p (For primary document see N92-10362 01-70)
Avail: NTIS HC/MF A12

The Large Electron Positron (LEP) collider at CERN, operating at the Z zero mass pole, was tested at precisely the electroweak sector in a model independent fashion, and more knowledge was gained of the quantum chromodynamic parameters at jet energies significantly higher than in previous electron-positron studies. The couplings of the Z zero boson have constituted a unique frame for searches for new particles and phenomena. The result obtained with the DELPHI detector at LEP are reviewed.
ESA

N92-10395# Turku Univ. (Finland). Dept. of Physics.
SEARCHES FOR HEAVY NEUTRINOS FROM DECAYS OF THE Z Abstract Only c72
Kenneth Osterberg (Helsinki Univ. of Technology, Espoo, Finland) *In* Oulu Univ., Proceedings of the 25th Annual Conference of the Finnish Physical Society 1991 1 p (For primary document

see N92-10362 01-70)
Avail: NTIS HC/MF A12

Evidence was sought for a heavy unstable neutrino, either a Dirac or Majorana particle, pairproduced in the decays of the Z zero. Results of a direct search, using about 50,000 hadronic Z zeros collected with the DELPHI detector are presented. The heavy neutrino events are characterized by two isolated particles and at least two jets. No evidence was found. The invisible width of the Z zeros was used to exclude new long lived neutrinos and the total width to exclude new low mass neutrinos. A new Dirac neutrino is excluded at a 95 pct. confidence level up to 41.0 GeV for all mixing angles and limits dependent on the mixing angle up to 45.7 GeV are obtained. A new Majorana neutrino is excluded at a 95 pct. confidence level up to 32.4 GeV for all mixing angles and limits dependent on the mixing angle and the decay channel up to 44.8 GeV are obtained. ESA

N92-10396# Bern Univ. (Switzerland). Inst. fuer Theoretische Physik.
PION-NUCLEON SIGMA-TERM AND THE STRANGE QUARK CONTENT OF THE PROTON Abstract Only **c72**
J. Gasser, H. Leutwyler, and M. E. Sainio (Helsinki Univ. of Technology, Espoo, Finland) *In* Oulu Univ., Proceedings of the 25th Annual Conference of the Finnish Physical Society 1991 1 p Sponsored in part by Schweizerischer Nationalfonds (For primary document see N92-10362 01-70)
Avail: NTIS HC/MF A12

Exploiting unitarity and analyticity, a set of integral equations which determine the behavior of the S and P wave phase shifts near threshold in terms of two subtraction constants is derived. These constants also fix the value of the Sigma term when information on pion scattering is used in addition to fix the curvature of the D+ amplitude as well as the t-dependence of the scalar form factor sigma(t). The result of the analysis including the low energy pion-nucleon data is sigma approx. = 60 MeV and sigma = sigma(0) approx. = 45 MeV. The corresponding value for the strange quark constant of the proton is given. ESA

N92-10397# Helsinki Univ. of Technology, Espoo (Finland). Research Inst. for Theoretical Physics.
GLUON OVERLAP FACTORS EXTRACTED FROM MONTE CARLO LATTICE CALCULATIONS Abstract Only **c72**
A. M. Green, O. Morimatsu, and J. Paton (Oxford Univ., England) *In* Oulu Univ., Proceedings of the 25th Annual Conference of the Finnish Physical Society 1991 1 p (For primary document see N92-10362 01-70)
Avail: NTIS HC/MF A12

Strategies are proposed for the extraction of the appropriate gluon field overlap factors from Monte Carlo lattice calculations involving static (quark antiquark)(quark antiquark) configurations. One aspect is demonstrated by means of an existing lattice calculation that restricts the quarks and antiquarks to a rectangular geometry. The results are in qualitative agreement with weak coupling at short distances, but more definite conclusions could not be made at this stage, since the appropriate Monte Carlo calculations are as yet not sufficiently precise. ESA

N92-10398# Helsinki Univ. of Technology, Espoo (Finland). Research Inst. for Theoretical Physics.
HEAVY NEUTRINOS IN e(+)e(-) COLLISIONS Abstract Only **c72**
J. Maalampi, K. Mursula (Oulu Univ., Finland), and R. Vuopionpera *In* Oulu Univ., Proceedings of the 25th Annual Conference of the Finnish Physical Society 1991 1 p (For primary document see N92-10362 01-70)
Avail: NTIS HC/MF A12

Detailed production and decay properties of a heavy neutrino, N, are investigated in view of the coming high energy electron-positron machines as e.g., LEP200. Concentrating on two heavy neutrino production processes, the N(N bar) pairproduction and the N(nu bar) channel, both the Dirac and Majorana neutrino cases are studied and left and right handed heavy neutrino couplings are compared. The correlated production of two same signed leptons of the same flavor is discussed. Such a pair appears in approximately half of the decays of the NN system if N is a Majorana particle. Studying these correlations will offer a promising method to experimentally distinguish between heavy Dirac and Majorana neutrinos. ESA

N92-10399# Helsinki Univ. of Technology, Espoo (Finland). Dept. of Theoretical Physics.
SUPERNOVA NEUTRINOS Abstract Only **c90**
Juha T. Peltoniemi *In* Oulu Univ., Proceedings of the 25th Annual Conference of the Finnish Physical Society 1991 1 p (For primary document see N92-10362 01-70)
Avail: NTIS HC/MF A12

The supernova 1987A showed that it is possible to detect neutrinos from gravitational collapse. If the statistics were better the neutrinos from a supernova would give a lot of information about the properties of neutrinos and the collapse of a star. The detectors are now ready to observe the explosion of a supernova in the Galaxy. This is likely to occur during this generation. ESA

N92-10400# Helsinki Univ. of Technology, Espoo (Finland). Accelerator Lab.
LIFETIME OF THE 1.959 MeV STATE IN Cl-36 Abstract Only **c72**
A. Kuronen, J. Keinonen, P. Tikkanen, and A. Kangasmaki *In* Oulu Univ., Proceedings of the 25th Annual Conference of the Finnish Physical Society 1991 1 p (For primary document see N92-10362 01-70)
Avail: NTIS HC/MF A12

A standard lifetime value is needed in Cl-36 for the analysis of GRID data. The lifetime values reported in the literature are not sufficiently accurate and reliable for this purpose. The lifetime of the 1.959 MeV state in Cl-36 was measured to be 68 + or - 5 fs using the Doppler shift attenuation method through the S-36(p,n) Cl-37 reaction at E sub p = 4.2 MeV. An S-36 target implanted into Ta was used in the measurements. The lifetime was deduced by comparing the measured and simulated gamma ray line shapes. In the simulations experimental stopping power was used. Polycrystalline structure of the backing material was taken into account. ESA

N92-10401# Turku Univ. (Finland). Dept. of Physics.
SHAPE COEXISTENCE IN TRANSITIONAL (132,133,134)Ba Abstract Only **c72**
T. Loennroth, P. Ahonen, M. Carpenter, C. Fahlander, J. Gascon, R. Julin, S. Juutinen (Jyvaskyla Univ., Finland), K.-M. Kaellman, A. Lampinen, and P. Manngaard, 9J9928 et al *In* Oulu Univ., Proceedings of the 25th Annual Conference of the Finnish Physical Society 1991 1 p (For primary document see N92-10362 01-70)
Avail: NTIS HC/MF A12

Nuclei in the transitional region Z greater than or = 50 and N less than or = 82 are of interest because they show a large variety of coexisting structures. They exhibit clear shell model structure close to Sn-132, and band structures are found in e.g., the Sb isotopes, whereas in the Te and Xe isotopes vibrational like bands and two quasiparticle excitations co-exist. The excited structure was studied of the transitional Z = 50+6 nuclides Ba-(132,133,134), thus having N = 76 to 78 is presented. ESA

N92-10402# Jyvaskyla Univ. (Finland). Dept. of Physics.
OBSERVATIONS ON VERY NEUTRON-RICH NUCLEI BELOW Z = 50 Abstract Only **c72**
J. Aysto, K. Eskola, P. P. Jauho, A. Jokinen, M. Leino, S. Malm, J. Parmonen, H. Penttila, and H. Salminen *In* Oulu Univ., Proceedings of the 25th Annual Conference of the Finnish Physical Society 1991 1 p Sponsored by Academy of Finland Prepared in cooperation with Warsaw Univ., Katholieke Univ., and Lyon Univ. (For primary document see N92-10362 01-70)
Avail: NTIS HC/MF A12

New neutron rich exotic nuclei were produced for the first time via symmetric fission of U-238 induced by light charged particles. Data obtained for the isotopic A and isobaric Z distributions on

over 50 nuclides allowed unique experimental information on the (N/Z) degree of freedom and consequently on the time scale and dynamics of the symmetric fission to be obtained. A new region of rather strongly deformed nuclei with a breaking of the axial symmetry along the most n-rich Ru isotopes was identified. Candidates for the shape isomers are also suggested by data on the quasiparticle structures and isomeric states populated in fission. The spectroscopic investigations resulted in new information on the strength and splitting of the allowed beta decay and, especially, on its connection with nuclear deformation. During the course of the spectroscopic studies new or improved beta half lives were obtained for over 20 n-rich isotopes in the mass region A = 109 to 120. The shortest lived isomeric states discovered are the 1.5 ms Ag-114m and the 19 ms Pd-117m. ESA

N92-10403# Jyvaskyla Univ. (Finland). Dept. of Physics.
HIGH-SPIN STATES IN Cd-109 Abstract Only **c72**
S. Juutinen, P. Ahonen, J. Hattula, R. Julin, J. Kumpulainen, A. Lampinen, D. Mueller, A. Pakkanen, M. Piiparinen, and S. Toermaenen et al *In* Oulu Univ., Proceedings of the 25th Annual Conference of the Finnish Physical Society 1991 1 p (For primary document see N92-10362 01-70)
Avail: NTIS HC/MF A12

Excited states in Cd-109 were studied by means of gamma spectroscopic methods. A target made of enriched Zr-96 was bombarded with the O-18 ions (E sub lab = 73 MeV) and emitted gamma rays were detected in the NORDBALL detector system at the Tandem accelerator facility of the Niels Bohr Institute (Finland). ESA

N92-10404# Jyvaskyla Univ. (Finland). Dept. of Physics.
SHAPES OF Cd-110 AT HIGH SPINS Abstract Only **c72**
S. Juutinen, R. Julin, P. Ahonen, C. Fahlander, J. Hattula, J. Kumpulainen, A. Lampinen, T. Loennroth, D. Mueller, and J. Nyberg (Niels Bohr Inst., Copenhagen, Denmark) et al *In* Oulu Univ., Proceedings of the 25th Annual Conference of the Finnish Physical Society 1991 1 p (For primary document see N92-10362 01-70)
Avail: NTIS HC/MF A12

A high spin study of Cd-110 via the (O-18, 4n) reaction carried out by the employment of the NORDBALL array at the Tandem accelerator facility (Niels Bohr Institute, Denmark) is addressed. Observed well developed collective bands are discussed. The bands must involve both high j proton and high j neutron configurations. The behavior of the yrast band is described. ESA

N92-10405# Jyvaskyla Univ. (Finland). Dept. of Physics.
EVIDENCE FOR BAND TERMINATION IN Xe-118 Abstract Only **c72**
S. Tormanen, S. Juutinen, B Cederwall, I. Ragnarsson, A. Johnson, R. Julin, S. Mitarai, J. Mukai, P. Ahonen, and B. Fant (Helsinki Univ. of Technology, Espoo, Finland) et al *In* Oulu Univ., Proceedings of the 25th Annual Conference of the Finnish Physical Society 1991 1 p (For primary document see N92-10362 01-70)
Avail: NTIS HC/MF A12

High spin states in the Xe-118 nucleus were studied via the Mo-92(S-32,alpha2p)Xe-118 reaction. A 145 MeV S-32 beam was provided by the Tandem and Booster facility at the Niels Bohr Institute, Denmark. The target was an enriched, 1.2 mg/sq cm thick selfsupporting Mo-92 foil. The NORDBALL of 15 Compton suppressed Ge detectors and a Si detector inner ball were employed to collect gamma-gamma events in coincidence with evaporated charged particles. ESA

N92-10406# Jyvaskyla Univ. (Finland). Dept. of Physics.
PROTON-NEUTRON SYMMETRY IN BOSON MODELS OF NUCLEAR STRUCTURE Abstract Only **c72**
P. O. Lipas *In* Oulu Univ., Proceedings of the 25th Annual Conference of the Finnish Physical Society 1991 1 p (For primary document see N92-10362 01-70)
Avail: NTIS HC/MF A12

Collective behavior of nucleons in nuclei has been long established both experimentally and theoretically. The Bohr-Mottelson collective Model (BMM) provides a mechanical picture of it in terms of vibrations and rotations of the nuclear body. An alternative description, due to Iachello and Arima, emerges from the algebra of bosons built from correlated pairs of like nuclei. This model is known as the Interacting Boson Approximation (IBA). Its results are largely equivalent with those of the BMM. Most features of low energy nuclear spectra indicate that in the collective motion the proton and neutron components behave together as one fluid. However, nuclear magnetism does distinguish between proton and neutron collectivity so that two fluids participate in the motion. The most spectacular manifestation of this is provided by magnetic dipole excitation in inelastic electron and photon scattering. The excited states, of spin-parity 1+, are viewed mechanically as resulting from a counterflow of the proton and neutron fluids. In the IBA such states are interpreted as states breaking the symmetry between proton and neutron bosons. ESA

N92-10407# Oulu Univ. (Finland). Dept. of Physics.
CONTRIBUTION OF THE DELTA RESONANCE TO THE GAMOW-TELLER DECAY OF HEAVY NUCLEI Abstract Only **c72**
J. Suhonen *In its* Proceedings of the 25th Annual Conference of the Finnish Physical Society 1991 1 p (For primary document see N92-10362 01-70)
Avail: NTIS HC/MF A12

The contribution of the delta isobars to the nuclear beta decay strength function has previously been studied within simple approximation schemes. The effect of the Delta is studied using the charge changing form of the Quasi particle Random Phase Approximation (QRPA) and applied to the Beta decay of neutron deficient tin isotopes Sn-(102 to 110). The principle aim is to address the question of the observed quenching of the low energy positron decay rate of several neutron deficient nuclei. The results of the calculation indicate that the Delta degree of freedom does not affect the low energy distribution of the Beta+/EC strength to such a measure that it would give an important contribution the the quenching. Thus, in the light of the calculation, the question about the role of the Delta can be removed from the discussion. ESA

N92-10408# Jyvaskyla Univ. (Finland). Dept. of Physics.
DOUBLE BETA DECAY IN THE PARTICLE-NUMBER PROJECTED QRPA FORMALISM Abstract Only **c72**
J. Suhonen *In* Oulu Univ., Proceedings of the 25th Annual Conference of the Finnish Physical Society 1991 1 p (For primary document see N92-10362 01-70)
Avail: NTIS HC/MF A12

The O+ to O+ two neutrino double beta and the neutrinoless double beta decay were studied in the framework of the particle number Projected BCS theory (PBCS) and constructing the particle number projected RPA (Random Phase Approximation) equations in the quasi-proton-quasi-neutron mode on top of the PBCS solution of the even-event parent and daughter nucleus. ESA

N92-10409# Jyvaskyla Univ. (Finland). Dept. of Physics.
NEUTRINOLESS BETA DECAY IN THE FRAMEWORK OF A RELATIVISTIC QUARK MODEL Abstract Only **c72**
J. Suhonen *In* Oulu Univ., Proceedings of the 25th Annual Conference of the Finnish Physical Society 1991 1 p (For primary document see N92-10362 01-70)
Avail: NTIS HC/MF A12

The 0+ to 0+ neutrinoless double beta decay of the nuclei Ge-76, Se-82, Kr-86, Cd-114, Te-(128,130) and Xe-(134,136) is calculated starting from the Relativistic Harmonic oscillator Model (RHM) and using the proton-neutron Quasi-particle Random Phase Approximation Approach (QRPA) to evaluate the nuclear structure matrix elements involved in the neutrinoless double beta decay amplitude. The quark current is evaluated using wave functions obtained from the Dirac equation with a harmonic confinement potential. ESA

N92-10410# Jyvaskyla Univ. (Finland). Dept. of Physics.
GAMMA-DECAY BRANCHING OF 1(+)-STATES IN Gd-156 AND Dy-164 Abstract Only **c72**
E. Hammaren, K. W. Schmid, P. Heikkinen, I. Koivistoinen, and A. Faessler (Tuebingen Univ., Germany, F.R.) *In* Oulu Univ., Proceedings of the 25th Annual Conference of the Finnish Physical Society 1991 1 p (For primary document see N92-10362 01-70)
Avail: NTIS HC/MF A12

Branching Ratio (BR) states were investigated using nuclear resonance fluorescence experiments. The findings are in agreement with the general wisdom that there is no one to one correspondance between an observable such as BR and an intrinsic quantum number such as K. Nevertheless, it would be important to improve the experimental sensitivity for verifying some of the small and large BR values predicted by the microscopic calculation. ESA

N92-10411# Helsinki Univ. of Technology, Espoo (Finland). Dept. of Physics.
INDEPENDENT AND CUMULATIVE YIELDS OF NEUTRON-RICH NUCLEI IN SYMMETRIC FISSION INDUCED BY p AND d ON U-238 Abstract Only **c72**
M. Leino, P. P. Jauho, J. Aysto, P. Decrock, P. Dendooven, K. Eskola, M. Huyse, A. Jokinen, J. M. Parmonen, and H. Penttila (Jyvaskyla Univ., Finland) et al *In* Oulu Univ., Proceedings of the 25th Annual Conference of the Finnish Physical Society 1991 1 p Sponsored by Academy of Finland (For primary document see N92-10362 01-70)
Avail: NTIS HC/MF A12

Independent and cumulative yields in nearly symmetric fission were measured for the first time by bombarding U-238 with 20 MeV protons and with 18, 25 and 41 MeV deuterons. Charge dispersion was determined in the A = 110, A = 112, and A = 114 mass chains and, from asymmetric fission, in the A = 80 mass chain. ESA

N92-10412# Helsinki Univ. of Technology, Espoo (Finland). Research Inst. for High Energy Physics.
THE DELPHI MICROVERTEX DETECTOR, A SILICON TRACKING CHAMBER Abstract Only **c35**
R. Brenner, Iiro Hietanen, Jukka Lindgren, R. Orava, C. Ronnqvist, and T. Tuuva *In* Oulu Univ., Proceedings of the 25th Annual Conference of the Finnish Physical Society 1991 1 p (For primary document see N92-10362 01-70)
Avail: NTIS HC/MF A12

A silicon strip vertex detector was installed into the DELPHI detector in the Spring 1990. The DELPHI detector is one of the four mammoth experiments run at the 27 km LEP (Large Electron Positron) collider at CERN on the Swiss-Franco border. The aim of the microvertex detector is to improve the recognition of primary and secondary vertices in the DELPHI experiment. During the year 1990, 120,000 Z zeros were observed with the microvertex detector and an impact parameter better than 75 microns was achieved. The performance of the microvertex detector during the first year in the DELPHI experiment is presented. The detector upgrade for next period of running was ended in the beginning of this year and is also presented. ESA

N92-10413# European Organization for Nuclear Research, Geneva (Switzerland).
STUDY OF MUON TRIGGERS AND MOMENTUM RECONSTRUCTION IN A STRONG MAGNETIC FIELD FOR A MUON DETECTOR AT LHC Abstract Only **c35**
M. DellaNegra, K. Eggert, C. Bacci, S. Bettini, R. Cardarelli, S. Centro, F. Ceradini, G. Ciapetti, D. Cline, and D. Dau (Kiel Univ., Germany, F.R.) et al *In* Oulu Univ., Proceedings of the 25th Annual Conference of the Finnish Physical Society 1991 1 p (For primary document see N92-10362 01-70)
Avail: NTIS HC/MF A12

The construction of a small fraction of a muon detector in a strong magnetic field, for possible use in an LHC (Large Hadron Collider) experiment, and its testing in a beam containing hadrons and muons are proposed. Properties of muons from hadron decays and of hadron punch-through, i.e., angle, momentum and timing distributions of the outgoing particles, are measured for various absorber thicknesses, including the effect of strong magnetization of the absorber. The efficiency of different muon triggers and the rejection against hadron punch-through and decay muons are investigated, including the effect of catastrophic energy losses of high momentum muons. The performance of resistive plate chambers as fast tracking trigger hodoscopes will be studied. ESA

N92-10414# Helsinki Univ. of Technology, Espoo (Finland). Research Inst. for High Energy Physics.
DEVELOPMENT OF DOUBLE-SIDED SILICON STRIP DETECTORS Abstract Only **c35**
Iiro Hietanen, Richard Brenner, Jukka Lindgren, Tuure Tuuva, Kari Leinonen, and Hannu Ronkainen (Technical Research Centre of Finland, Espoo.) *In* Oulu Univ., Proceedings of the 25th Annual Conference of the Finnish Physical Society 1991 1 p (For primary document see N92-10362 01-70)
Avail: NTIS HC/MF A12

Silicons trip detectors with 2-D readout were designed, processed and tested. IC processing steps were utilized to manufacture AC coupled silicons strip electrodes on both sides of 4 inch high resistivity silicon wafers. Double metal processing on the detector n side enabled the design of additional cross electrodes in order to perform readout of the perpendicular strips on one detector edge. Detectors equipped with LSI readout electronics were tested with tracks from an Sr-90 source and with a laser spot focused on the detector surface. In the beta measurements the most probable signal pulse height on the p side was found to be excellent; 37 times the sigma noise of any individual channel. Due to a temporary processing problem the separation of the n side silicon strips was incomplete in the first prototype batch. The charge from the Sr-90 electrons was spread to approx. 10 neighboring strips and was not properly recorded by the n side electrodes. In the laser measurments the larger signal charge was clearly seen on both detector sides. A new processing run was recently completed without problems and detectors from this batch are currently being tested. ESA

N92-10415# Helsinki Univ. of Technology, Espoo (Finland). Research Inst. for High Energy Physics.
RADIATION DAMAGE MEASUREMENTS ON DOUBLE-SIDED Si STRIP DETECTORS Abstract Only **c35**
Iiro Hietanen, Mikko Laakso, Tom Schulman, and Tuure Tuuva (European Organization for Nuclear Research, Geneva, Switzerland) *In* Oulu Univ., Proceedings of the 25th Annual Conference of the Finnish Physical Society 1991 1 p (For primary document see N92-10362 01-70)
Avail: NTIS HC/MF A12

Results from radiation tests on new double sided microstrip detectors are presented. The radiation effects on the detectors were studied using a Co-60 gamma source. The test results suggest a modification in the detector layout design, which would lead to increased radiation resistance. Detectors with the modified design were manufactured and are currently under tests. ESA

N92-10416# Helsinki Univ. of Technology, Espoo (Finland).
BEAM TEST RESULTS OF ION-IMPLANTED SILICON STRIP DETECTORS ON A 100 mm WAFER Abstract Only **c35**
Iiro Hietanen, Jukka Lindgren, R. Orava, Tuure Tuuva, R. Brenner, Mikael Andersson, Kari Leinonen, Hannu Ronkainen, L. Hubbeling, and M. Turala (European Organization for Nuclear Research, Geneva, Switzerland) et al *In* Oulu Univ., Proceedings of the 25th Annual Conference of the Finnish Physical Society 1991 1 p (For primary document see N92-10362 01-70)
Avail: NTIS HC/MF A12

The use of planar silicons trip detectors in both position sensitive and energy dispersive applications has rapidly increased. Detector systems of large angular coverage unavoidably consist of a large number of individual detector plates traditionally processed on 3 inch silicon wafers. The effective wafer processing area is almost doubled by the use of 100 mm wafers, enabling detector designs

with less inactive material and fewer electrical connections. Two detectors, processed on a 100 mm wafer, were tested in a pion beam. The one detector was directly coupled with a 25 micron readout pitch and the other capacitively coupled with a 50 microns readout pitch. The detectors were equipped with LSI readout chips. The spatial resolution was measured to be 3.9 micron for the DC and 4.9 micron for the AC detector. The corresponding signal to noise values were 20 and 31. ESA

N92-10417# Jyvaskyla Univ. (Finland). Dept. of Physics.
ION-GUIDE QUADRUPOLE MASS SPECTROMETER (IGQMS) Abstract Only **c35**
A. Iivonen, K. Morita, R. Saintola, K. Valli, and A. Yoshida (Institute of Physical and Chemical Research, Saitama, Japan) *In* Oulu Univ., Proceedings of the 25th Annual Conference of the Finnish Physical Society 1991 1 p (For primary document see N92-10362 01-70)
Avail: NTIS HC/MF A12

The IGQMS is intended to separate ions that are created in helium by any means. In test experiments the transmission yield of 215Po(+) through the entire IGQMS varied from 5 to 25 pct. of that through the nozzle, depending on the choice of mass resolution (typically a few hundred). A typical separation is one milliseond. The kinetic energy of the separated ions is 10 to 100 eV. ESA

N92-10418# Helsinki Univ. of Technology, Espoo (Finland). Research Inst. for High Energy Physics.
STUDIES ON NEW LOW NOISE SILICON RADIATION DETECTOR Abstract Only **c35**
Mikko Laakso, P. Jalas, M. Juntunen, T. Tikkanen, E. Tuominen, K. Grahn, and Kari Leinonen (Technical Research Centre of Finland, Espoo.) *In* Oulu Univ., Proceedings of the 25th Annual Conference of the Finnish Physical Society 1991 1 p (For primary document see N92-10362 01-70)
Avail: NTIS HC/MF A12

In connection with a research project for developing room temperature energy dispersive detectors for X ray spectroscopy the possibility of integrating a signal amplifying transistor directly on the detector is studied. The idea is to integrate a normal FET (Field Effect Transistor) structure on high resistivity n-type semiconductor wafer with p-type layer on the other side of the bulk. This kind of structure acts as a detector when it is completely depleted from the p-side. The amplification of the transistor is based on the shape of the electric potential in the detector. First detectors based on this method were manufactured using MOS transistor technology. Results on transistor characteristics, detector depletion behavior and readout electronics are presented. The shape of the electric potential and charge carrier (concentration distribution of a detector utilizing JFET (Junction FET) technology was studied by simulation using the knowledge of the possible processing steps as parameters. The simulations suggested that detectors based on a FJET structure can be manufactured. ESA

N92-10419# Jyvaskyla Univ. (Finland). Dept. of Physics.
CONTROL SYSTEM OF THE JYVASKYLA (FINLAND) K130 CYCLOTRON Abstract Only **c60**
J. Lampinen and V. Hanninen *In* Oulu Univ., Proceedings of the 25th Annual Conference of the Finnish Physical Society 1991 1 p (For primary document see N92-10362 01-70)
Avail: NTIS HC/MF A12

The control system consists of nine process modules, each containing a processor card and up to 16 input/output cards. The operator interface includes two monitors with touch sensitive screens. The monitors are driven by two operator module processors. One manager module processor is used for computationally intensive tasks and interfacing intelligent devices. Two design modules (program development workstations) are used for application design. ESA

N92-10420# Jyvaskyla Univ. (Finland). Dept. of Physics.
THE JYVASKYLA (FINLAND) K130 CYCLOTRON PROJECT Abstract Only **c73**
Esko Liukkonen *In* Oulu Univ., Proceedings of the 25th Annual Conference of the Finnish Physical Society 1991 1 p (For primary document see N92-10362 01-70)
Avail: NTIS HC/MF A12

Tests and delivery dates of the components and cyclotron building and installation are given. A vacuum level of 0.00002 Pa was obtained after 200 hours pumping of the vacuum chamber. After venting with nitrogen the vacuum level of 0.0001 Pa was achieved. The specified level of 0.00001 Pa could not be achieved. It is possible that first experiments can be run just before the end of the year 1992. ESA

N92-10421# Jyvaskyla Univ. (Finland). Dept. of Physics.
MAGNETIC FIELD SETTINGS FOR THE K130 CYCLOTRON Abstract Only **c73**
M. Rinta-Nikkola *In* Oulu Univ., Proceedings of the 25th Annual Conference of the Finnish Physical Society 1991 1 p (For primary document see N92-10362 01-70)
Avail: NTIS HC/MF A12

Precalculation of trim coil currents for the whole operation range of the K130 cyclotron were carried out by using measured magnetic fields and the program FIELDER. FIELDER uses an iterated least squares process to adjust the trim coil currents and the RF frequency. The least square fitting is subjected to the constraints which serve to produce energy stability as well as energy focusing in the extracted beam. Results were mainly satisfactory. ESA

N92-10422# Jyvaskyla Univ. (Finland). Dept. of Physics.
STATUS OF THE JYFL-ECR ION SOURCE Abstract Only **c73**
J. Arje, V. Nieminen, J. Choinski, and T. A. Antaya (Michigan State Univ., East Lansing.) *In* Oulu Univ., Proceedings of the 25th Annual Conference of the Finnish Physical Society 1991 1 p (For primary document see N92-10362 01-70)
Avail: NTIS HC/MF A12

In the University of Jyvaskyla (Finland), construction of a new accelerator laboratory was started in June 1989. The cyclotron type heavy ion accelerator will be equipped with an external ECR (Electron Cyclotron Resonance) ion source. In addition to the use as an injector for the accelerator, the source will also be used in research of atomic and condensed matter physics. Some features and present status of the JYFL-ECR ion source are described. ESA

N92-10423# Technische Univ., Dresden (German D.R.). Inst. of Low Temperature Physics.
ULTRA-COLD POLARIZED HYDROGEN SOURCE Abstract Only **c73**
M. Mertig, V. G. Luppov, and Y. K. Pilipenko (Joint Inst. for Nuclear Research, Dubna, USSR) *In* Oulu Univ., Proceedings of the 25th Annual Conference of the Finnish Physical Society 1991 1 p (For primary document see N92-10362 01-70)
Avail: NTIS HC/MF A12

Results of stabilization experiments, where a flux of up 5 x 10(exp 15) polarized hydrogen atoms per second into the storage cell was achieved are presented. Recombination losses in the critical transition from 4 to 0.5 K were reduced to less than 50 by using a new thermal accommodator. A method for creating a cold, electron polarized hydrogen beam without microwave extraction is discussed. This method is based merely on separation of hydrogen atoms due to their electron spins in the fringe gradient of a high magnetic field. The separation is achieved by cooling the atoms down to less than 1 K at the location where the field is approximately half of its maximum (center) value. Consequently, spin down state atoms are attracted into the high field where they are forced to recombine. The spin up atoms are accelerated towards the low field region, where they leave the cell and form a polarized beam. ESA

N92-10424# Jyvaskyla Univ. (Finland). Dept. of Physics.
PLAN FOR THE JYFL GAS-FILLED RECOIL SEPARATOR Abstract Only **c73**
M. Leino, J. Aysto, K. Eskola (Helsinki Univ. of Technology, Espoo, Finland), P. Heikkinen, R. Julin, J. Kumpulainen, and T. Enqvist

In Oulu Univ., Proceedings of the 25th Annual Conference of the Finnish Physical Society 1991 1 p Sponsored by Academy of Finland (For primary document see N92-10362 01-70)
Avail: NTIS HC/MF A12

A heavy ion cyclotron laboratory is under construction in Jyvaskyla (Finland). A gas filled recoil separator was chosen for the study of heavy ion reaction products. The aim is to diversify the use of the separator considerably. The layout of the magnetic elements will differ slightly from the conventional one and the separator will be rotatable. The dipole will have a 1.4 m radius and the maximum design B(sub rho) value is 2 Tm. Besides the gas filled mode, the separator is designed for operation in vacuum when high transmission can be sacrificed in order to improve the resolving power. ESA

N92-10425# Oulu Univ. (Finland). Dept. of Physics.
STRUCTURE AND OPTICAL POLARIZABILITIES OF SMALL SILICON CLUSTERS Abstract Only **c76**
Tapio T. Rantala, Mark I. Stockman, Daniel A. Jelski, and Thomas F. George (State Univ. of New York, Buffalo.) *In its* Proceedings of the 25th Annual Conference of the Finnish Physical Society 1991 1 p (For primary document see N92-10362 01-70)
Avail: NTIS HC/MF A12

Possible structures of an Si10 cluster were examined using a tight binding model. Obtained stable geometries agree well with those from ab initio methods and classical potential methods. However, a new lowest energy geometry was found. It appears to be Jahn-Teller distorted, and therefore, it was not found with the other methods quoted above. The new structure also explains experimental photoelectron and chemical reactivity data. Electronic contributions of the linear and nonlinear optical properties of the Si10 cluster above and high symmetry clusters Si7 and Si13 were examined. The (hyper)polarizabilities alpha, beta and gamma were evaluated using one electron density matrix techniques in the form of sum over one electron states. The absorption cross section spectra were calculated in order to stimulate experimental work. Nonlinear polarizabilities were found to depend primarily on the symmetry of the cluster and proved to be high for low symmetry clusters. Possible experiments on the nonlinear properties are discussed. ESA

N92-10426# Oulu Univ. (Finland). Dept. of Physics.
DECAY CHANNELS OF RESONANTLY EXCITED 2p(-1)ns, md STATES OF Ar AND 3d(-1)np STATES OF Kr Abstract Only **c72**
Seppo Aksela, H. Aksela, Y. Furusawa, and A. Yagishita (National Lab. for High Energy Physics, Tsukuba, Japan) *In its* Proceedings of the 25th Annual Conference of the Finnish Physical Society 1991 1 p (For primary document see N92-10362 01-70)
Avail: NTIS HC/MF A12

The electron spectra of Ar and Kr were measured covering wider kinetic energy region and using several photon energies from the first resonance to the threshold. Resonance excitation obeying the dipole transition selection rules populates the states 2p(-1)ns, md of Ar and 3d(-1)np of Kr. The excited states decay predominantly via two electron transitions where the excited electron stays as a spectator during the decay. Shake up/down of the spectator electron plays a predominent role, especially in the case of the dacay of the 2p(-1)3d state of Ar. Final states of the de-excitation processes are the same as the satellite states involved in the valence-electron photoionization. Comparison between different intensity distributions arising from different pathways provides a useful method for the interpretation of the very complicated level structures of the two holes one electron states. ESA

N92-10427# Oulu Univ. (Finland). Dept. of Physics.
Li 1s PHOTOIONIZATION AND PHOTOEXCITATION WITH SATELLITES Abstract Only **c72**
Seppo Aksela, H. Aksela, Maarit Levasalmi, Y. Furusawa, and A. Yagishita (National Lab. for High Energy Physics, Tsukuba, Japan) *In its* Proceedings of the 25th Annual Conference of the Finnish Physical Society 1991 1 p (For primary document see N92-10362 01-70)
Avail: NTIS HC/MF A12

Lithium is an ideal test case for studying different processes giving rise to satellite structure in photoelectron spectra. Measurements were carried out using monochromatized synchrotron radiation. The spectra were measured with a commercial spherical mirror type electron analyzer. The photoelectron spectrum of lithium was studied by using synchrotron radiation in the photon energy range 60 to 150 eV. When the photon energy is above the 1s ionization limit (64.4 eV) direct 1s ionization is the dominant process. ESA

N92-10428# Oulu Univ. (Finland). Dept. of Physics.
ELECTRON CORRELATION IN THE 4d HOLE STATE OF Cs AND Ba Abstract Only **c76**
A. Mantykentta, H. Aksela, Seppo Aksela, J. Tulkki, and T. Aaberg (Helsinki Univ. of Technology, Espoo, Finland) *In its* Proceedings of the 25th Annual Conference of the Finnish Physical Society 1991 1 p (For primary document see N92-10362 01-70)
Avail: NTIS HC/MF A12

Correlation effects in the 4d hole states of Cs (Z 55) and Ba (Z 56) are studied in relation to various shake-up processes. Experimental photoelectron spectra and outer-shell Auger electron spectra are compared with theoretical results calculated by using the relativistic multiconfiguration Dirac-Fock method (MCDF). The measurements were carried out using monochromatized synchrotron radiation. The electron spectra were measured below, at, and above the 4d threshold energies. ESA

N92-10429# Helsinki Univ. of Technology, Espoo (Finland). Physics Lab.
KRYPTON 4p,4s AND 3d PARTIAL PHOTOIONIZATION CROSS SECTIONS BELOW 260 eV PHOTON ENERGY Abstract Only **c72**
J. Tulkki, Seppo Aksela, H. Aksela, Y. Furusawa, A. Yagishita, and E. Shigemasa (National Lab. for High Energy Physics, Tsukuba, Japan) *In* Oulu Univ., Proceedings of the 25th Annual Conference of the Finnish Physical Society 1991 1 p (For primary document see N92-10362 01-70)
Avail: NTIS HC/MF A12

Theoretical and experimental data on krypton 4p, 4s and 3d partial photoionization cross sections for photon energies ranging from the Kr 4p threshold up to 260 eV are presented. Experimental results are presented for the 95 to 260 eV photon energy range. Theoretical partial cross sections were obtained by the multichannel Dirac-Fock method. Calculations include 18 leading singly excited ionization channels and the relaxation is fully taken into account. Comparison with earlier experimental and theoretical data shows that relaxation contributes at the level of 20 to 30 percent to the 4s and 3d subshell sections, while it is found to be less important for 4p ionization. The remaining discrepancy between theory and experiment is attributed to strong initial state correlation effects in the case of 4p and to coupling between singly and doubly excited ionization channels for 4s. ESA

N92-10430# Helsinki Univ. of Technology, Espoo (Finland). Physics Lab.
RELAXATION AND FINAL-STATE CORRELATION EFFECTS IN THE 3p AND 3s PHOTOIONIZATION OF Ar, K(+), AND Ca(++) Abstract Only **c72**
J. Tulkki *In* Oulu Univ., Proceedings of the 25th Annual Conference of the Finnish Physical Society 1991 1 p (For primary document see N92-10362 01-70)
Avail: NTIS HC/MF A12

The 3p and 3s partial cross sections were calculated for Ar, K(+) and Ca(++) using the multichannel Dirac-Fock method. Relaxation is included by using separately optimized initial and final bound states and by including all the resulting overlap integrals and partial amplitudes in the transition matrix. The results are compared with calculations excluding body effects and with available experimental data. Results indicate that the relative

correlation effect does not decrease dramatically for the singly and doubly charged ions in the Ar isoelectronic sequence. ESA

N92-10431# Oulu Univ. (Finland). Dept. of Physics.
THE ROTATIONAL STRUCTURE OF THE NU(SUB 6) VIBRATION BAND OF CH3I Abstract Only **c72**
S. Alanko and R. Paso *In its* Proceedings of the 25th Annual Conference of the Finnish Physical Society 1991 1 p (For primary document see N92-10362 01-70)
Avail: NTIS HC/MF A12

High resolution Fourier transform infrared spectrum associated with the fundamental nu(sub 6)vibration of CH3I from 766 to 1050/cm is reported. The spectrum was measured by means of the Bruker IFS-120HR spectrometer. The fundamental nu(sub 6) band is a perpendicular band where only the I resonance must be considered. The assignment was straightforward and more than 400 lines with maximum J approximately equal to 79 and K(sub max) equal to 18 were found. The analysis and the resulting molecular constants are presented. The nature of hyperfine structure in the infrared spectra and a method of utilizing the shifted lines in conventional analysis are discussed. ESA

N92-10432# Oulu Univ. (Finland). Dept. of Physics.
THE NU(SUB 4) AND NU(SUB 7) BANDS OF CD3CN WITH CORIOLIS COUPLING AND OTHER RESONANCE PERTURBATIONS Abstract Only **c72**
M. Koivusaari and R. Anttila *In its* Proceedings of the 25th Annual Conference of the Finnish Physical Society 1991 1 p (For primary document see N92-10362 01-70)
Avail: NTIS HC/MF A12

A series of studies on the high resolution infrared spectrum of CD3CN is reported. The parallel fundamental nu(sub 4) (831.44/cm) and the perpendicular fundamental nu(sub 7) (847.10/cm) and the resonance perturbations appearing in these bands were studied. The measurements were performed with the aid of Bruker IFS 120 HR FT spectrometer using a Globar source and an MCT detector. The absorption path length was 9.6 cm and the sample pressure 0.6 Torr. The linewidth is about 0.003/cm. The calibration was done with CO2 nu(sub 2) band lines. ESA

N92-10433# Oulu Univ. (Finland). Dept. of Physics.
THE NU(SUB 8) AND 2NU(SUB 8) BANDS OF CD3CN Abstract Only **c72**
M. Koivusaari, V.-M. Horneman, and R. Anttila *In its* Proceedings of the 25th Annual Conference of the Finnish Physical Society 1991 1 p (For primary document see N92-10362 01-70)
Avail: NTIS HC/MF A12

The measurement and analysis of the lowest fundamental vibration nu(sub 8) band of CD3CN at high resolution and the study of the overtone 2nu(sub 8) are reported. The measurements were carried out with the Fourier transform spectrometer Bruker IFS 120HR. ESA

N92-10434# Oulu Univ. (Finland). Dept. of Physics.
THE INFRARED ROTATION-VIBRATION SPECTRUM OF C2H2 IN THE NU(SUB 2) + NU(SUB 5) BAND REGION; l-RESONANCES IN THE BANDS NU(SUB 2) + NU(SUB 5), NU(SUB 2) + 2(NU(SUB 5)) BACK ARROW NU(SUB 5) AND NU(SUB 1) BACK ARROW NU(SUB 5) Abstract Only **c72**
A.-M. Tolonen and S. Alanko *In its* Proceedings of the 25th Annual Conference of the Finnish Physical Society 1991 1 p (For primary document see N92-10362 01-70)
Avail: NTIS HC/MF A12

The infrared rotation-vibration spectra of the various species of acetylene (C2H2) are investigated in order to make a comparison with the bending fundamental nu(sub 5) and the hot bands accompanying it and to determine vibrational and rotational constants for the v(sub 1)=1 vibrational level. In the analysis of the vibrational levels, the rotational l-doublings and l-resonances were taken into account. The molecular constants characterizing the energy levels and the parameters describing the l-resonances were derived. ESA

N92-10435# Oulu Univ. (Finland). NMR-Lab.
THE Kr-83 NMR IN PROBING ELECTRIC FIELD GRADIENTS IN THERMOTROPIC LIQUID CRYSTALS Abstract Only **c76**
L. P. Ingman and Jukka Jokisaari *In its* Proceedings of the 25th Annual Conference of the Finnish Physical Society 1991 1 p (For primary document see N92-10362 01-70)
Avail: NTIS HC/MF A12

Studies of Kr-83 NMR (Nuclear Magnetic Resonance) spectra were continued in a mixture of the thermotropic liquid crystals ZLI1132 (55 wt percent) and EBBA (45 wt percent). The Electric Field Gradients (EFG)s generated by the ZLI1132 and EBBA possess opposite signs. Previously, behavior indicated that the total EFG experienced by krypton is a sum of at least two contributions. In this particular mixture the resultant gradient is proposed to vanish. The maximum has disappeared and the quadrupole coupling increases monotonically when temperature decreases: one of the contributions was removed. ESA

N92-10436# Oulu Univ. (Finland). Dept. of Physics.
NMR DETERMINATION OF THE Ne-21 QUADRUPOLE COUPLING FOR NEON GAS DISSOLVED IN LIQUID CRYSTALS Abstract Only **c76**
Jukka Jokisaari, O. Pulkkinen, P. Diehl, and O. Muenster (Basel Univ., Switzerland) *In its* Proceedings of the 25th Annual Conference of the Finnish Physical Society 1991 1 p (For primary document see N92-10362 01-70)
Avail: NTIS HC/MF A12

The Ne-21 QC (Quadrupole Coupling) was studied over the temperature range 305 to 352 K in the liquid crystal Merck ZLI 1167. The results indicate that the total EFG (Electric Field Gradient) experienced by the isotope must be a sum of at least two contributions. The comparison of the EFG's derived in similar environments by Xe-131, Kr-83, and Ne-21 NMR (Nuclear Magnetic Resonance) will most probably make it possible to separate the various contributions, one of them being the external EFG created by the liquid crystal. ESA

N92-10437# Oulu Univ. (Finland). Dept. of Physics.
NMR-RELAXATION TIME MEASUREMENTS OF NOBLE GAS ISOTOPE Xe-129 DISSOLVED IN ISOTROPIC AND ANISOTROPIC LIQUIDS Abstract Only **c76**
Kari Oikarinen and Jukka Jokisaari *In its* Proceedings of the 25th Annual Conference of the Finnish Physical Society 1991 1 p (For primary document see N92-10362 01-70)
Avail: NTIS HC/MF A12

The spin lattice relaxation time of the noble gas isotope Xe-129 dissolved in isotropic and anisotropic liquids was measured by using inversion recovery method over quite large temperature ranges: in the isotropic solvents from 298 to 323 K, and in the liquid crystal solvents from 300 to 360 K. Used solvents were benzene (C6H6), deuterated benzene (C6D6), cyclohexane (C6H12), deuterated cyclohexane (C6D12), liquid crystal, 7AB and binary mixture of liquid crystals EBBA (73.5 percent) and ZLI1132 (26.5 percent). In the isotropic solvents it was found that the relaxation time is inversely proportional to temperature. Liquid crystals and liquid crystal mixtures have several phase transition temperatures. Previously, the Xe-129 shieldings were measured to be changing strongly at these transition points. Here, the spin lattice relaxation times are changing too, but only slightly. ESA

N92-10438# Turku Univ. (Finland). Dept. of Applied Physics.
A NEW LINE-NARROWING METHOD LOMEP Abstract Only **c77**
Jyrki K. Kauppinen, Matti R. Hollberg, and Douglas J. Moffatt (National Research Council of Canada, Ottawa, Ontario) *In* Oulu Univ., Proceedings of the 25th Annual Conference of the Finnish Physical Society 1991 1 p (For primary document see N92-10362 01-70)
Avail: NTIS HC/MF A12

The characteristics and utility of the LOMEP (Lineshape Optimized Maximum Entropy Linear Prediction) method are detailed and its application to experimental data are discussed. In particular, such characteristics as the effect of the S/N (Signal to Noise)

ratio on the output S/N, the maximum achievable line narrowing factor, and the accuracy of the output line position are addressed. A quantity (q), the quality factor, which indicates the reliability of the linear prediction and hence the usefulness of the LOMEP method itself, is defined. ESA

N92-10439# Helsinki Univ. of Technology, Espoo (Finland). Dept. of Physics.
INTERACTION-INDUCED LIGHT SCATTERING AS A SOURCE OF INFORMATION ON PROPERTIES AND INTERACTIONS OF SPHERICAL TOP MOLECULES Abstract Only **c74**
N. Meinander, G. C. Tabisz, and S. M. El-Sheikh (Cairo Univ., Egypt) *In* Oulu Univ., Proceedings of the 25th Annual Conference of the Finnish Physical Society 1991 1 p (For primary document see N92-10362 01-70)
Avail: NTIS HC/MF A12

The two body collision induced light scattering spectra of pure SF6 and CF4 and of their mixtures with inert gases were measured at 295 K. Spectra of CH4 were measured at several temperatures. The spectrum consists of an intense, broadened depolarized Rayleigh component termed the translational spectrum, which arises from the participation of the relative kinetic energy of the colliding molecules in the scattering process through the Dipole Induced Dipole (DID) and electron overlap interactions. This component has distinct contributions coming from free-free transitions occurring in unbound interacting molecules and from transitions in bound dimers. A third component of the spectrum results from high order multiple polarizabilities and is termed the induced rotational spectrum. The data were compared with computed spectral profiles. These comparisons allowed: testing of a scaling law for the pair polarizability anisotropy responsible for the translational spectra; determination of refined values for the magnitude of the dipole-quadrupole and dipole-octopole molecular polarizabities; and assessment of available intermolecular potentials. ESA

N92-10440# Tampere Univ. of Technology (Finland). Dept. of Physics.
SUPERSONIC MOLECULAR BEAM APPARATUS TO STUDY SURFACE REACTIONS Abstract Only **c72**
M. Valden, Q. Wang, and I. Vattulainen *In* Oulu Univ., Proceedings of the 25th Annual Conference of the Finnish Physical Society 1991 1 p (For primary document see N92-10362 01-70)
Avail: NTIS HC/MF A12

A supersonic molecular beam system which provides a well defined method of dosing, both in terms of surface collision rate and the energy distribution of the incident molecules, is presented. Recent experiments that principally make use of molecular beam technique have revealed that the energy at which an incident molecule collides with a surface can be the key factor in determining its reactivity with or on the surface. This provides new mechanisms for chemistry at surfaces. Reactions that are normally observed only at high reactant pressures, and which are the ones most often of practical importance, can now be carried out in low pressure, ultrahigh vacuum environments. ESA

N92-10441# Jyvaskyla Univ. (Finland). Dept. of Physics.
EQUIVALENCE IN THE SHELL STRUCTURE OF THE TIGHT BINDING AND FREE ELECTRON CLUSTERS Abstract Only **c72**
J. Mansikka-aho, E. Hammaren, and M. Manninen *In* Oulu Univ., Proceedings of the 25th Annual Conference of the Finnish Physical Society 1991 1 p (For primary document see N92-10362 01-70)
Avail: NTIS HC/MF A12

Alkali metal clusters show an electronic shell structure which resembles free electrons in a spherical potential well. On the other hand the tight binding (Huckel) model has been found to describe qualitatively correctly the geometries and electronic structure of the smallest clusters. This puzzle is solved by showing that the discretized free electron Hamiltonian equals the Huckel Hamiltonian. A consequence of this is that the lowest energy levels of the Huckel model approach those of the free electron model when the cluster size increases, as previously calculated. For spherical clusters the Huckel model then gives the same shell structure as the free electron model. ESA

N92-10442# Helsinki Univ. of Technology, Espoo (Finland). Dept. of Technical Physics.
ISOTOPE SELECTIVE RESONANCE IONIZATION MEASUREMENTS OF LITHIUM Abstract Only **c72**
T. Kajava, H. Lauranto, P. Duex (Heidelberg Univ., Germany, F. R.), and Rainer Solomaa *In* Oulu Univ., Proceedings of the 25th Annual Conference of the Finnish Physical Society 1991 1 p (For primary document see N92-10362 01-70)
Avail: NTIS HC/MF A12

As a very sensitive and spectrally selective method, Resonance Ionization Spectroscopy (RIS) is widely applied to trace element analysis. To test the performance of RIS apparatus in accurate analysis of isotope/isomer ratios, a series of RIS measurements of lithium, which has two stable isotopes Li-6 and Li-7 with natural abundancies of 7.5 and 92.5 percent respectively, was made. The observed fine structure splitting and the isotope shifts of the levels involved are in perfect agreement with the tabulated values. ESA

N92-10443# Helsinki Univ. of Technology, Espoo (Finland). Accelerator Lab.
TORSIONAL POTENTIAL FOR THE C(sp2)-C(sp2) BOND Abstract Only **c72**
B. Mannfors, L.-O. Pietila, and K. Palmo (Michigan Univ., Ann Arbor.) *In* Oulu Univ., Proceedings of the 25th Annual Conference of the Finnish Physical Society 1991 1 p (For primary document see N92-10362 01-70)
Avail: NTIS HC/MF A12

A torsional potential model is tested on simple model molecules, such as butadiene, styrene, stilbene, and some of their methyl substituted derivatives. The torsional potential for the central C-C bond in butadiene is discussed in more detail since it offers a good test case for the steric term. The second stable conformer is well characterized by several ab initio calculations with reasonably large basis sets with electron correlation taken into account. All these calculations suggest a gauche form, and that the gauche-trans energy difference is about 3 kcal/mol. ESA

N92-10444# Oulu Univ. (Finland). Dept. of Physics.
ANALYSIS OF THE INTERACTING LEVELS V(SUB 9) = 1 AND V(SUB 10) = 2 OF PROPYNE Abstract Only **c72**
K. Pekkala, G. Graner, G. Wlodarczak, and J. Demaison (Lille-1 Univ., Villeneuve-d'Asoq, France) *In its* Proceedings of the 25th Annual Confernece of the Finnish Physical Society 1991 1 p (For primary document see N92-10362 01-70)
Avail: NTIS HC/MF A12

A global simultaneous study of the interacting levels v(sub 9)=1 and v(sub 10)=2 of propyne was performed. In the analysis three kinds of data were used. The infrared spectrum of propyne between 580/cm and 690/cm was recorded and analyzed. The spectrum includes the fundamental band nu(sub 9). A Fermi resonance was detected, mainly on the K Delta K=-2 subband. The spectrum was measured at a resolution of 0.003/cm with the aid of a Fourier spectrometer. The rotational energy levels both of v(sub 10)=2, l(sub 10)=0 and v(sub 10)=2, l(sub 10) equal to minus/plus 2, computed from the nu(sub 10) band and the hot bands 2nu(sub 10) to nu(sub 10). These measurements were performed with the Bruker Fourier instrument at a resolution of 0.002/cm. The third data set includes the pure rotational transitions at v(sub 9)=1 and v(sub 10)=2 measured with microwave and millimeter wave spectroscopy. In the analysis, altogether 1488 infrared transitions from the nu(sub 9) band, 1147 energies from the v(sub 10)=2, and 217 submillimeter transitions in the v(sub 9)=1 and v(sub 10)=2 vibrational states were used. The new set of molecular parameters for the states v(sub 9)=1; v(sub 10)=2, l(sub 10)=0 and l(sub 10) equal to minus/plus 2 as well as the l(2,2) and Fermi elements were obtained. ESA

N92-10445# Helsinki Univ. of Technology, Espoo (Finland). Dept. of Energy Engineering.
ABSORPTION MEASUREMENTS WITH AN INTEGRATING SPHERE AND AN FT-IR SPECTROMETER Abstract Only **c74**
K. T. Ojala and M. J. Lampinen *In* Oulu Univ., Proceedings of the 25th Annual Conference of the Finnish Physical Society 1991 1 p (For primary document see N92-10362 01-70)
Avail: NTIS HC/MF A12

Methods to measure reflection and transmission spectra of scattering materials were developed. These methods are based on the use of integrating spheres and FT-IR (Fourier Transform-Infrared) spectrometer. Because of the geometrical and optical properties of the system itself, specific correction formulas for results are required. Such new formulas are derived. Integrated spheres and FT-IR spectrometer are used in order to measure the optical properties of paper samples and several different materials used in infrared dryers. These spectral data are than used in new computer models developed for different types of dryers used for drying of paper in paper machines. By using these models, the efficiencies of these dryers are calculated. ESA

N92-10446# Oulu Univ. (Finland). Dept. of Physics.
STUDY OF DIFFERENT SX-700 DESIGNS FOR THE UNDULATOR BEAMLINE (BL51) AT MAX-LAB Abstract Only **c74**
Seppo Aksela, A. Kivimaki, R. Nyholm, and S. Svensson (Uppsala Univ., Sweden) *In its* Proceedings of the 25th Annual Conference of the Finnish Physical Society 1991 1 p (For primary document see N92-10362 01-70)
Avail: NTIS HC/MF A12

The undulator Beam Line BL51 is under construction at MAX-LAB. It is planned to cover the photon energy range 60 to 600 eV. In order to compare the performance of the different SX-700 designs analytical considerations and accurate ray tracing calculations were carried out. The focusing with an elliptical mirror is ideal but the image is curved resulting in the use of curved slits. This disadvantage can be eliminated by using two plane elliptic mirrors to decouple focusing in vertical and horizontal planes. In both cases the practical resolution is limited by slope errors of elliptical mirrors. Spherical mirrors can be fabricated by essentially higher tolerances than elliptical or plane elliptical mirrors. On the other hand spherical mirror suffer from coma aberration, which degrades resolution. However, this effect can be reduced and the source size limited resolution achieved by the extension of the exit arm. ESA

N92-10447# Kuopio Univ. (Finland). Dept. of Applied Physics.
RECOGNIZING OF SPECTRAL MIXTURES, THEIR COMPONENTS AND SPECTRAL PATTERNS Abstract Only **c63**
K. Mantere, J. Parkkinen, and T. Jaaskelainen *In* Oulu Univ., Proceedings of the 25th Annual Conference of the Finnish Physical Society 1991 1 p (For primary document see N92-10362 01-70)
Avail: NTIS HC/MF A12

The problem to find the composition of the unknown color mixture and to recognize a noisy spectrum is considered. Data consists of 39 reflectance spectra of Munsell color chips with maximum chroma, and mixtures were generated from these measured spectras. Four different methods including neural networks and an eigenvector based method were applied. A neural network model was simulated to recognize a spectrum from the original set of spectras. The spectras coded to two dimensional patterns in a matrix whose size was 21 by 41, and hence the interconnection matrix was of size 861 by 861. The system can store all the desired patterns to the asymptotically stable equilibrium points and all pure spectras which were stored to the net were recognized correctly. The noise simulations were achieved by adding 5 percent random noise to each wavelength. Ten simulations were generated with each spectra in a total of 390 experiments and the recognizing rate of the system was 98.5 percent. ESA

N92-10448# Joensuu Univ. (Finland). Dept. of Physics.
PHOTORESIST CROSSED GRATINGS Abstract Only **c35**
Pekka Savander, Olli Salminen, and Tuula Keinonen *In* Oulu Univ., Proceedings of the 25th Annual Conference of the Finnish Physical Society 1991 1 p (For primary document see N92-10362 01-70)
Avail: NTIS HC/MF A12

Crossed gratings were made by using the mixture of two commercial Shipley positive photoresists having different viscosities. By mixing the photoresists with proper ratio emulsion thickness 1.3 microns was achieved by using spincoating method. Gratings were exposed by using an Ar laser of 488 nm wavelength. The recording was carried out in two ways: with pre-exposure and without pre-exposure. The gratings without pre-exposure contain semimaxima between peaks and do not present perfect recording of information. The use of pre-exposure eliminates these semimaxima and the profile of the grating is more sinusoidal. ESA

N92-10449# Helsinki Univ. of Technology, Espoo (Finland). Dept. of Technical Physics.
RECONFIGURABLE OPTICAL INTERCONNECTIONS BY ACOUSTO-OPTIC HOLOGRAMS Abstract Only **c35**
Eero Tervonen, Ari T. Friberg, and Jari Turunen (Heriot-Watt Univ., Edinburgh, Scotland) *In* Oulu Univ., Proceedings of the 25th Annual Conference of the Finnish Physical Society 1991 1 p (For primary document see N92-10362 01-70)
Avail: NTIS HC/MF A12

An experimental set up for the demonstration of the reconfigurable optical interconnections by acousto-optics is presented. With the set up, the generation of both binary and weighted programmable interconnection patterns is demonstrated. An acoustic carrier signal forms a propagating Bragg grating. The carrier is angle modulated with a periodic waveform (electronic equivalent of a computer optimized multilevel phase hologram) to create a dynamic Raman-Nath regime acousto-optic hologram. The desired optical spot pattern is formed with high efficiency in the output Fourier plane. From the memory the control unit selects a hologram structure that is copied into the ring buffer. Presently binary and cellular four level phase holograms are used. The reconfiguration time is essentially the deflector access time. ESA

N92-10450# Kuopio Univ. (Finland). Dept. of Applied Physics.
OPTICAL CORRELATORS IN TEXTURE ANALYSIS Abstract Only **c74**
V. Honkonen, T. Jaaskelainen, and J. Parkkinen *In* Oulu Univ., Proceedings of the 25th Annual Conference of the Finnish Physical Society 1991 1 p (For primary document see N92-10362 01-70)
Avail: NTIS HC/MF A12

Many type of filters for optical correlators are introduced. The performance test of a novel filter was frequently restricted to use of very simple and very few test patterns (alphabet, figure of aeroplane, etc.). The discrimination powers of the complex matched filter, phase only filter and binary phase only filter in texture recognition, were studied. Twelve natural textures of Brodatz were used as test images. These pictures were first digitized into 256 by 256 images. The experiments were then made by computer simulation with 128 by 128 images (upper left corner from 256 by 256 images). The ratios of the energy in the correlation peak, and the energy in the output plane of all the auto and crosscorrelation images, were determined. All of the above mentioned filters were easily able to recognize the texture corresponding to the filter, but there are remarkable differences in the energy within the correlation peaks, and in the shape of the correlation peak. This depends on the applied filter type and on the structure of the texture. Experiments with noise free, noisy and distorted cases, are underway. ESA

N92-10451# Joensuu Univ. (Finland). Dept. of Physics.
HOLOGRAPHIC NONDESTRUCTIVE TESTING IN BONE BIOMECHANICS Abstract Only **c35**

Raimo Silvennoinen, Kaarlo Nygren, Juha Paatsama (Helsinki Univ. of Technology, Espoo, Finland), and Markku Kaernae *In* Oulu Univ., Proceedings of the 25th Annual Conference of the Finnish Physical Society 1991 1 p (For primary document see N92-10362 01-70)
Avail: NTIS HC/MF A12

Holographic interferometry is widely used in nondestructive testing of objects. During the work of the bone biomechanics the antler stress in nasal bone region of five Finnish male moose skulls showing four different nasal bone types were tested with the forces representing dynamic and static stresses. ESA

N92-10452# Helsinki Univ. of Technology, Espoo (Finland). Dept. of Technical Physics.
SINGLE-SHOT SPECTRAL MEASUREMENTS OF MULTIMODE PULSED DYE LASERS Abstract Only c36
T. Kajava, H. Lauranto, and Rainer Salomaa *In* Oulu Univ., Proceedings of the 25th Annual Conference of the Finnish Physical Society 1991 1 p (For primary document see N92-10362 01-70)
Avail: NTIS HC/MF A12

A pulsed multimode laser is an immensely complicated system and therefore reliable theoretical estimates of its statistical fluctuations are difficult to obtain. A solution is to measure directly the spectral properties of the laser pulses. For this purpose a high resolution interferometric spectrum analyzer capable of recording successive single-shot spectra was built. The optical design of the instrument is based on a Burleigh RC-140 Fabry-Perot interferometer, whose mirrors are slightly tilted with respect to each other to form a configuration called Fizeau interferometer. In the case of collimated illumination the interference pattern consists of parallel, equally spaced fringes, which are detected with a linear photodiode array. The measured output spectra of Lambda Physik FI2002E dye lasers show a clearly resolved longitudinal mode structure with strong shot to shot fluctuations in mode intensities. To get a smooth, nearly Lorentzian line profile without noticeable mode structure one needs an average of about 100 shots. Less averaging should cause noise in signal, especially in the case of nonlinear optical processes. ESA

N92-10453# Helsinki Univ. of Technology, Espoo (Finland). Inst. of Metrology Research.
A SIMPLE METHOD TO STABILIZE THE FREQUENCY OF SEMICONDUCTOR LASERS Abstract Only c36
Hanne Ludvigsen, Christer Holmlund (Technical Research Centre of Finland, Espoo.), and Erkki Ikonen *In* Oulu Univ., Proceedings of the 25th Annual Conference of the Finnish Physical Society 1991 1 p (For primary document see N92-10362 01-70)
Avail: NTIS HC/MF A12

A method to stabilize the frequency of a semiconducotr laser is described. Results based on stabilization to an absorption line of iodine vapor are presented and compared with those of the purely electrical stabilization method. Beside the simplicity the advantages of this method include high reproducibility, unmodulated laser output and freedom to stabilize the laser frequency to any desired value. The laser will be particularly suited for interferometric applications in optical metrology. ESA

N92-10454# Helsinki Univ. of Technology, Espoo (Finland). Dept. of Technical Physics.
POLARIZATION SPECTROSCOPY IN OH AND FLAME TEMPERATURE MEASUREMENTS Abstract Only c25
R. Meier, K. Nyholm, M. Kaivola, and C. G. Aminoff *In* Oulu Univ., Proceedings of the 25th Annual Conference of the Finnish Physical Society 1991 1 p (For primary document see N92-10362 01-70)
Avail: NTIS HC/MF A12

Work directed towards alternative nonlinear laser methods providing sufficient detection sensitivity for the analysis of trace molecules in flames is addressed. The use of polarization spectroscopy for the analysis of OH radicals and temperature determination in atmospheric pressure flames is reported. ESA

N92-10455# Helsinki Univ. of Technology, Espoo (Finland). Dept. of Technical Physics.
ELECTRONICALLY RESONANT CARS SPECTROSCOPY OF NO2 Abstract Only c25
L. Oikarinen, K. Nyholm, M. Kaivola, and C. G. Aminoff *In* Oulu Univ., Proceedings of the 25th Annual Conference of the Finnish Physical Society 1991 1 p (For primary document see N92-10362 01-70)
Avail: NTIS HC/MF A12

The applicability of resonance CARS (Coherent Anti-Stokes Raman Scattering) for the detection and spectroscopy of NO2 is studied. A frequency doubled injection seeded single mode Nd:YAG laser and a tunable dye laser are used. Preliminary studies are performed in a cell, where the pressure dependence of the signal is measured. With this high resolution method, sharp distinct lines are detected in the NO2 spectrum with efficient background discrimination. Resonance CARS spectra are strongly dependent on the precise tuning of the pump beam frequency. The dependence of the NO2 spectrum on the Nd:YAG laser frequency was investigated by temperature tuning of the Nd:YAG injection laser. The use of broadband dye laser pulses for resonance CARS in NO2 was demonstrated by applying an optical multichannel analyzer for signal detection. This shows that applications in turbulent flows may become possible. ESA

N92-10456# Kuopio Univ. (Finland). Dept. of Applied Physics.
COUPLED WAVE ANALYSIS IN INVERSE GRATING DIFFRACTION PROBLEMS Abstract Only c74
M. Kuittinen and T. Jaaskelainen *In* Oulu Univ., Proceedings of the 25th Annual Conference of the Finnish Physical Society 1991 1 p (For primary document see N92-10362 01-70)
Avail: NTIS HC/MF A12

Diffraction of a thin grating, which refraction index is modulated, can be solved for example by using the Multiwave Coupled Wave Theory (MWCWT), if the Fourier coefficients of modulation are known. The inverse problem, which are the Fourier coefficients to produce a desired diffraction pattern, is considered. By neglecting second derivates (boundary effect) MWCWT equations can be easily solved in matrix form. This form is also suitable for solving unknown coefficients of refraction index modulation by some optimization method. The applied numerical method is described and examples from the synthesis procedure are given. One to one connections are considered and it is shown that it is possible to plan thin gratings which diffract a given power distribution to different diffraction orders. The grating parameters, like thickness, grating period and incident angle are included in the MWCWT, and these parameters can be chosen quite flexible after optimization. Because only few Fourier coefficients are needed, individual sinusoidal gratings could be arranged as a stack structure in the final product. ESA

N92-10457# Helsinki Univ. of Technology, Espoo (Finland). Dept. of Technical Physics.
PARAMETRIC OPTIMIZATION OF SYNTHETIC GRATINGS USING VECTOR DIFFRACTION THEORY Abstract Only c74
Eero Noponen, Antti Vasara, and Jari Turunen (Heriot-Watt Univ., Edinburgh, Scotland) *In* Oulu Univ., Proceedings of the 25th Annual Conference of the Finnish Physical Society 1991 1 p (For primary document see N92-10362 01-70)
Avail: NTIS HC/MF A12

Vector diffraction theory was used to reoptimize the grating parameters to take into account the resonance effect. The optimization procedure is based on a gradient algorithm in which the transition points are first searched keeping the period length and the relief depth constant until no futher improvement is possible. Then, the solution is optimized further by changing the period and the depth of the relief using a local search. This two step procedure is repeated until a satisfactory result is obtained or the optimization stagnates in a local minimum. So far, gratings have been designed producing up to 15 equally intense beams with 90 to 99 percent diffraction efficiencies even if the reflection losses at the dielectric boundaries are included. ESA

N92-10458# Helsinki Univ. of Technology, Espoo (Finland). Dept. of Technical Physics.
WAVEGUIDE DAMMANN GRATINGS AND KINOFORMS Abstract Only **c74**
Jyrki Saarinen, Juhani Huttunen, Antti Vasara, Jari Turunen, and Arto Salin (Technical Research Centre of Finland, Espoo.) *In* Oulu Univ., Proceedings of the 25th Annual Conference of the Finnish Physical Society 1991 1 p (For primary document see N92-10362 01-70)
Avail: NTIS HC/MF A12

The application of an integrated optic equivalent of a synthetic Fourier domain phase grating, for splitting the incoming field into N diffraction orders of equal power, is proposed. The grating modulates the phase of the wavefront periodically and thus generates a set of diffracted plane wave components, which can be focused with a Fresnel lens to channel waveguides or to optical fibers. The same kind of coding schemes of the phase gratings that are now standard in free space computer generated holography, such as the Dammann's method and the kinoform technique, were used. The performance of waveguide gratings was analyzed numerically using the effective index method and paraxial beam propagation calculations. ESA

N92-10459# Tampere Univ. of Technology (Finland). Plasma Technology Lab.
VELOCIMETRY IN GAS FLOWS USING PULSED LASER INDUCED PHOTOTHERMAL EFFECTS Abstract Only **c75**
J. P. Vattulainen and Rolf G. Hernberg *In* Oulu Univ., Proceedings of the 25th Annual Conference of the Finnish Physical Society 1991 1 p Sponsored by Academy of Finland (For primary document see N92-10362 01-70)
Avail: NTIS HC/MF A12

The status of theoretical studies and laboratory experiments to apply the laser induced photothermal measurement techniques to diagnose high rate thermal plasma diamond coating deposition performed using an industrial scale induction plasma torch is presented. At the first stage the aim is to measure the plasma flow velocity in the 1000 to 3000 K temperature region near the substrate using the so called time of flight method. The possibility of determining the local concentration of the excited species using the photothermal signals will then be studied. ESA

N92-10460# Tampere Univ. of Technology (Finland). Plasma Technology Lab.
KINETIC GAS AND ELECTRON TEMPERATURES IN RF INDUCTION PLASMA Abstract Only **c75**
S. M. Jaffe (Stanford Univ., CA.), Rolf G. Hernberg, J. Larjo, and J. P. Vattulainen *In* Oulu Univ., Proceedings of the 25th Annual Conference of the Finnish Physical Society 1991 1 p Sponsored by Academy of Finland (For primary document see N92-10362 01-70)
Avail: NTIS HC/MF A12

Measurements to produce an experimental characterization of an RF induction plasma in terms of gas temperature and electron temperature under well defined conditions were carried out. The purpose of this is to serve as an experimental reference for the verification of numerical models and to study the extent of non equilibrium in the plasma. The temperature distributions and a discussion of the results are presented. ESA

N92-10461# Helsinki Univ. of Technology, Espoo (Finland). Dept. of Technical Physics.
NUMERICAL CALCULATIONS OF WAVE PROPAGATION IN TOKAMAK PLASMAS Abstract Only **c75**
S. Sipila, S. Karttunen (Technical Research Centre of Finland, Espoo.), T. Pattikangas, and Rainer Salomaa *In* Oulu Univ., Proceedings of the 25th Annual Conference of the Finnish Physical Society 1991 1 p (For primary document see N92-10362 01-70)
Avail: NTIS HC/MF A12

A geometric optics ray tracing code for numerical calculations of wave propagation in a toroidal plasma with a circular cross section was developed. The SCARGO code uses the general cold plasma dispersion relation, which makes it applicable to ray tracing over a wide frequency spectrum. Single rays and beams consisting of several rays can be traced with user defined starting point, direction, frequency and plasma parameters. The SCARGO ray tracing code was utilized in a study of plasma current drive based on stimulated Raman scattering. ESA

N92-10462# Tampere Univ. of Technology (Finland). Dept. of Electrical Engineering.
MOLECULAR DYNAMICS STUDIES OF LIQUID-SOLID INTERFACES Abstract Only **c72**
J. A. Nieminen, M. Karttunen, and Kimmo Kaski *In* Oulu Univ., Proceedings of the 25th Annual Conference of the Finnish Physical Society 1991 1 p (For primary document see N92-10362 01-70)
Avail: NTIS HC/MF A12

Molecular Dynamics (MD) method is applied to a variety of problems in materials science. This method offers a very versatile tool to study problems in liquids in which, as the detailed atomic structure becomes essential at nanometer scale, the continuum theories such as hydrodynamics fail. The spreading of a very viscose liquid drop on a solid substrate was investigated. This gives new insight to the dynamics of wetting and it gives information of the essential time scales, e.g., in lubrication. The behavior of a liquid film between two solid surfaces was studied. It has been observed experimentally that structural ordering and quantization of the properties of the film take place as the distance between the solids is few lattice constants. The simulations agree qualitatively with the experiments. ESA

N92-10463# Tampere Univ. of Technology (Finland). Dept. of Physics.
DETERMINATION OF THE (1X2) STRUCTURE OF A Pt FILM ON Pd(110) Abstract Only **c76**
P. Kaukasoina, M. Lindroos, H. C. Kang, O. L. Warren, P. J. Schmitz, and P. A. Thiel (Iowa State Univ. of Science and Technology, Ames.) *In* Oulu Univ., Proceedings of the 25th Annual Conference of the Finnish Physical Society 1991 1 p (For primary document see N92-10362 01-70)
Avail: NTIS HC/MF A12

The surface structure of a Pt film on Pd(110) was determined using Low Energy Electron Diffraction (LEED) and was compared with the (1x2) reconstruction of clean Pt. Theoretical LEED I(E) spectra were calculated for several possible overlayer structures. The origin of the (1x2) structure can be either pairing or buckling of atoms in some layer or some layer with a missing row structure. The optimum structure could contain any mixture of these layers with the normal (1x1) atomic layers. Tested model systems were systematic combinations of these layer elements down to three layers counting from the topmost layer. After this Pd bulk was assumed to have formed of the normal (1x1) atomic layers. The distances between atomic layers were systematically varied. Chemical composition of each overlayer was considered as a variable, i.e., atomic layer was either of palladium of platinum. Theoretical spectra were compared against measured ones using Pendry's r-factor. ESA

N92-10464# Jyvaskyla Univ. (Finland). Dept. of Physics.
THERMAL HELIUM DESORPTION FACILITY IN JYVASKYLA (FINLAND) Abstract Only **c09**
E. Kautto, O.-P. Kaehkoenen, S. Maekinen, and M. Manninen *In* Oulu Univ., Proceedings of the 25th Annual Conference of the Finnish Physical Society 1991 1 p (For primary document see N92-10362 01-70)
Avail: NTIS HC/MF A12

The building of a thermal helium desorption facility was reported. The fully UHV compatible vacuum chamber (volume 35 l) is pumped by a turbo-molecular pump. According to the preliminary tests, a pressure level of 10(exp -6) Pa was attained after 24 hours pumping. After being baked for 24 hours in 150 C the pressure decreased to the low 10(exp -8) Pa range. This can be regarded as a good result, considering the pumping system is based on a turbopump unit. The ion gun can ionize inert gases with energy range of 0.1

to 3.0 keV. This is enough for helium implantation and for sputtering the target. The gun can also be used to produce crystal defects with heavy noble gas ions. The mass spectrometer is provided with channeltron multiplier. The lowest detectable partial pressure is of the order of 3 x 10(exp -11) Pa. The facility is operational and test measurements using tungsten and molybdenum samples are being carried out. ESA

N92-10465# Helsinki Univ. of Technology, Espoo (Finland). Physics Lab.
MOLECULAR DYNAMICS USING THE TIGHT-BINDING APPROXIMATION: APPLICATION TO LIQUID SILICON Abstract Only **c72**
R. Virkkunen, K. Laasonen, and R. M. Nieminen *In* Oulu Univ., Proceedings of the 25th Annual Conference of the Finnish Physical Society 1991 1 p (For primary document see N92-10362 01-70)
Avail: NTIS HC/MF A12

The Tight Binding (TB) approximation is used in a Molecular Dynamical (MD) study of liquid silicon. In the TB scheme the quantum mechanics of the electrons is approximately calculated from the parametrized Hamiltonian. The parameters are adjusted to reproduce experimental data of the different structures of silicon. This simplified approach to the electronic effects is computationally much less demanding than ab initio molecular dynamics. Still the TB model succeeds in predicting properties that are similar to ab initio results and to the experimental observations. A molecular dynamical simulation of 64 silicon atoms in a cubic cell with periodic boundary conditions is performed. The average temperature is 1820 K which is well above the experimental melting point. A transferable set of TB parameters was used. Structural and dynamical properties of liquid Si are calculated and the results are compared to those of ab initio simulations and classical molecular dynamics. ESA

N92-10466# Oulu Univ. (Finland). Dept. of Physics.
COMPUTER SIMULATIONS ON THE ORIENTATION OF MOLECULAR HYDROGEN IN LIQUID CRYSTALS Abstract Only **c76**
Juhani Lounila and Tapio T. Rantala *In its* Proceedings of the 25th Annual Conference of the Finnish Physical Society 1991 1 p (For primary document see N92-10362 01-70)
Avail: NTIS HC/MF A12

The suggestion that negative orientational order parameters (S values) of molecular hydrogen dissolved in various nematic liquid crystals might be due to the attractive Van der Waals force between the atoms in H2 and the liquid crystal surroundings was studied. The model for a nematic solvent was a rigid lattice consisting of parallel, axially symmetric molecules of infinite length. These molecules were taken to be chains of benzene rings, whose interactions with the hydrogen atoms of H2 were described by the Lennard-Jones 6-12 potential function. Two different (two dimensional) crystal structures were used: a simple square lattice and an imperfect hexagonal lattice having vacancies at the centers of the hexagons. The thermal motion of the H2 molecule (at 300 K) was simulated by two independent techniques, Monte Carlo and molecular dynamics methods. In the latter case the thermal contact with the heat bath was effected by simulated random inelastic collisions of H2 with its environment. The van der Waals forces acting on the atoms of the hydrogen molecule are not capable of explaining the negative S values. The presence of other interactions, such as the electrostatic forces between the molecular quadrupole moments, seems to be essential. ESA

N92-10467# Helsinki Univ. of Technology, Espoo (Finland). Physics Lab.
OBSERVATION OF A MONOVACANCY IN THE METASTABLE STATE OF THE EL2 DEFECT IN GaAs BY POSITRON ANNIHILATION Abstract Only **c76**
K. Saarinen, R. Krause, P. Hautojarvi, and C. Corbel (Institut National des Sciences et Techniques Nucleaires, Saclay, France) *In* Oulu Univ., Proceedings of the 25th Annual Conference of the Finnish Physical Society 1991 1 p Previously announced in IAA as A91-19549 (For primary document see N92-10362 01-70)
Avail: NTIS HC/MF A12

A monovacancy defect is observed by positron lifetime and Doppler broadening experiments in semi insulating GaAs after photoquenching the EL2 defects. The monovacancy exhibits the same thermal and optical recoveries as the metastable state of EL2 and its concentration is proportional to that of the EL2 defect. It is concluded that the metastable state of the EL2 defect involves the monovacancy. The results indicate that the monovacancy or its immediate surrounding is negatively charged. ESA

N92-10468# Jyvaskyla Univ. (Finland). Dept. of Physics.
THE SHAPE EFFECT OF MAGNETIC DAMAGES IN IRRADIATED Nd2Fe14B-PERMANENT MAGNETS Abstract Only
O.-P. Kaehkoenen, S. Maekinen, M. Talvitie (Outokumpu Oy, Tapiola, Finland), and M. Manninen *In* Oulu Univ., Proceedings of the 25th Annual Conference of the Finnish Physical Society 1991 1 p (For primary document see N92-10362 01-70)
Avail: NTIS HC/MF A12

The detailed picture of the temperature dependence of the flux loss in Nd2Fe14B magnets was measured. The flux loss is shown to be connected to the demagnetizing field created by the magnet itself: the magnetic damages caused by irradiations are strongly dependent on the shape of the irradiated magnet. A theoretical model based on the domain nucleation due to the local heating at the collision cascade explains the observed temperature dependence of the flux loss. ESA

N92-10469# Centre for Scientific Computing, Espoo (Finland).
ADSORBATE INDUCED SURFACE RECONSTRUCTION Abstract Only
K. Kankaala, Tapio Ala-Nissila, and S.-C. Ying (Brown Univ., Providence, RI.) *In* Oulu Univ., Proceedings of the 25th Annual Conference of the Finnish Physical Society 1991 1 p (For primary document see N92-10362 01-70)
Avail: NTIS HC/MF A12

An absorbate induced surface reconstruction on W(100) surface is discussed. This surface is known to exhibit a spontaneous reversible reconstruction of the surface layer as a function of temperature. The calculations show that there exists an additional order-order transition in the system as the amount of adsorbate is increased. Mean field calculations and Monte Carlo results for the phase diagram are presented. This order-order transition is of first order at low temperatures and of second order at higher temperatures. The transition and its order are explained in terms of an XY model with four fold and eight fold anisotropy fields. ESA

N92-10470# Tampere Univ. of Technology (Finland). Dept. of Physics.
DIFFUSION ANOMALY AT A SURFACE RECONSTRUCTION Abstract Only **c76**
Tapio Ala-Nissila, W. K. Han, and S.-C. Ying (Brown Univ., Providence, RI.) *In* Oulu Univ., Proceedings of the 25th Annual Conference of the Finnish Physical Society 1991 1 p (For primary document see N92-10362 01-70)
Avail: NTIS HC/MF A12

The dynamical structure function associated with the reconstruction of the W(100) surface is calculated using a combination of analytic methods and Monte Carlo computer simulations. The dynamical behavior of the surface is dominated by a central peak, which diverges at the transition temperature. It is shown how such a diverging central peak generally leads to the vanishing of the diffusion coefficient D of an adatom on the surface, using a recently developed microscopic theory of diffusion. For the W(100) surface, the behavior of D as a function of temperature is calculated and the finite size dependence of D is studied. ESA

N92-10471# Helsinki Univ. of Technology, Espoo (Finland). Lab. of Engineering Materials.
INTERNAL FRICTION ASSOCIATED WITH INTERACTION BETWEEN CARBON ATOMS AND DISLOCATIONS AT LOW TEMPERATURE Abstract Only **c76**
Y. Liu, K. Ullakko, and J. Pietikainen *In* Oulu Univ., Proceedings of the 25th Annual Conference of the Finnish Physical Society 1991 1 p (For primary document see N92-10362 01-70)
Avail: NTIS HC/MF A12

A model to describe the internal friction behavior due to carbon atoms diffusing to and interacting with dislocations at low temperature is proposed. In this case the relaxation strength is temperature and heating rate dependent which is in line with the experimental results. ESA

N92-10472# Helsinki Univ. of Technology, Espoo (Finland).
REDISTRIBUTION OF NITROGEN ATOMS AND MAGNETIC ORDERING IN Fe-N MARTENSITE AT LOW TEMPERATURES Abstract Only **c26**
K. Ullakko, V. G. Gavriljuk, and V. M. Nadutov (Academy of Sciences of the Ukrainian SSR, Kiev.) *In* Oulu Univ., Proceedings of the 25th Annual Conference of the Finnish Physical Society 1991 1 p (For primary document see N92-10362 01-70)
Avail: NTIS HC/MF A12

Alloyed Fe-C martensites are characterized by abnormal tetragonality which changes during low temperature aging. The change of tetragonality and the redistribution of nitrogen atoms during aging of a freshly formed Fe-N martensite in the temperature range between 5 and 300 K are studied. The tetragonality of Fe-2.4 wt percent N during aging, measured with X-ray diffraction, is shown. ESA

N92-10473# Helsinki Univ. of Technology, Espoo (Finland). Physics Lab.
HELIUM IN SILICON: A FIRST PRINCIPLE MOLECULAR DYNAMICS STUDY Abstract Only **c72**
M. Alatalo, K. Laasonen, and R. M. Nieminen *In* Oulu Univ., Proceedings of the 25th Annual Conference of the Finnish Physical Society 1991 1 p (For primary document see N92-10362 01-70)
Avail: NTIS HC/MF A12

Ab initio molecular dynamics calculations to study diffusion of He atoms in a silicon crystal are performed. The unified approach of Molecular Dynamics and Density Functional theory (MD-DF) was used. In this approach the interatomic potential is obtained directly from the electronic ground state, corresponding to the instantaneous ionic configuration. As in ordinary molecular dynamics the ionic coordinates are treated classically. In the MD-DF the single particle electronic orbitals are expanded in planewaves. The coefficients of the plane wave expansion are treated classically by using the effective Lagrangian method. The silicon crystal is described by a supercell containing 64 atoms. The cutoff energy of 8 Ry is used for the plane wave expansion. The migration barriers and relaxation energies for tetrahedral and hexagonal interstitial sites are studied. The diffusion paths in finite temperatures and clusterization of two He atoms are studied. ESA

N92-10474# Helsinki Univ. of Technology, Espoo (Finland). Low Temperature Lab.
TWO-PHONON ABSORPTION BY THE REAL SQUASHING COLLECTIVE MODE IN SUPERFLUID He-3 Abstract Only **c72**
H. Alles, J. M. Kyynarainen, A. J. Manninen, J. P. Pekola, and K. Torizuka *In* Oulu Univ., Proceedings of the 25th Annual Conference of the Finnish Physical Society 1991 1 p (For primary document see N92-10362 01-70)
Avail: NTIS HC/MF A12

Ultrasound is a powerful probe of collective modes of superfluid He-3 which are temporal oscillations of its order parameter. The nonlinear interaction of zero sound with certain collective modes allows a two-phonon absorption: in a pulsed sound transmission experiment the real squashing collective mode in He-3-B is excited with two coincident pulses of frequencies f(sub s) and f(sub p) at the temperature T(+), h(f(sub s) + f(sub p)) = (square root of (8/5))Delta(T(+)), where Delta(T(+)) is the energy gap of superfluid He-3. Two T(+) peaks are seen: the main peak is accompanied by a smaller one on the low temperature side. The heights of the attenuation peaks at the frequency f(sub s) scale almost linearly with the energy of the pump wave at frequency f(sub p). ESA

N92-10475# Landau Inst. for Theoretical Physics, Moscow (USSR).
MUTUAL FRICTION IN SUPERFLUID He-3: EFFECTS OF BOUND STATES IN THE VORTEX CORE Abstract Only **c72**
N. B. Kopnin and M. M. Salomaa (Helsinki Univ. of Technology, Espoo, Finland) *In* Oulu Univ., Proceedings of the 25th Annual Conference of the Finnish Physical Society 1991 1 p Sponsored by Soviet Academy of Sciences, and Academy of Finland (For primary document see N92-10362 01-70)
Avail: NTIS HC/MF A12

The motion of singlar quantized vortex lines in superfluid He-3 is considered for the A and B phases. Mutual friction is calculated within a microscopic quantum mechanical Green's function formalism, valid for dynamical processes. This enables all the different physical phenomena in a unified approach to be included. Axisymmetric vortices for temperatures considerably lower than Tc are considered. ESA

N92-10476# Helsinki Univ. of Technology, Espoo (Finland). Low Temperature Lab.
VORTEX NUCLEATION IN ROTATING SUPERFLUID He-3-B Abstract Only **c72**
U. Parts, Y. M. Bunkov, Y. Kondo, N. B. Kopnin, J. S. Korhonen, M. Krusius, and D. A. Sergatskov *In* Oulu Univ., Proceedings of the 25th Annual Conference of the Finnish Physical Society 1991 1 p (For primary document see N92-10362 01-70)
Avail: NTIS HC/MF A12

The nucleation of quantized vortices with a singular core has proven to be a frustrated process in both the A and B phases of superfluid He-3. In He-3-A coreless continuous vortices are prevailing, although they are assumed to correspond to a higher energy state. The thermally activated process and the critical velocity for the surface energy barrier are identified for vortex nucleation in vortex free superflow of He-3-B. ESA

N92-10477# Oulu Univ. (Finland). Dept. of Theoretical Physics.
EFFECTIVE MASS AND EXCITATION SPECTRUM OF He-3 IMPURITIES IN SUPERFLUID He-4 Abstract Only **c72**
M. Saarela *In its* Proceedings of the 25th Annual Conference of the Finnish Physical Society 1991 1 p (For primary document see N92-10362 01-70)
Avail: NTIS HC/MF A12

A microscopic calculation based on the Jasrow-Feenberg wavefunction is presented for both the effective mass and the excitation spectrum of the impurity in two and three dimensional homogeneous superfluid He-4 as well as on thin films. The calculation optimizes two and three particle correlation functions and includes elementary diagrams up to five body diagrams. The chemical potentials of He-4 and He-3 as a function of density as well as the effective mass of the He-3 impurity are found to be in good agreement with experiments. A monotonic increase of the excitation spectrum with no evidence of the roton like minimum is found for the single He-3 impurity. ESA

N92-10478# Helsinki Univ. of Technology, Espoo (Finland). Low Temperature Lab.
SUPERFLUID INTERFACES IN LIQUID He-3: SUPERCONDUCTING COSMIC DOMAIN WALLS IN THE LABORATORY Abstract Only **c72**
M. M. Salomaa *In* Oulu Univ., Proceedings of the 25th Annual Conference of the Finnish Physical Society 1991 1 p Sponsored by Academy of Finland (For primary document see N92-10362 01-70)
Avail: NTIS HC/MF A12

The interface between superfluid He-3-A and He-3-B, as the most novel surface known to exist in condensed matter physics,

was studied. The most important (and most surprising) finding is the discovery of completely new classes of A-A interphasons displaying a fractional quantum jump in the phase psi of the superfluid condensate: for these novel interphasons, the phase difference delta(psi) between the left and the right A-phase vacua, is only pi/2 (or -pi/2 congruence 3pi/2), not pi. These half soliton vacuum interfaces provide the most elementary possible processes of phase slippage in superfluid He-3-A. Symmetry analysis and numerical calculations have revealed that the number of superfluid A-B interfaces is doubled in the presence of an external magnetic field. In particular, the rotating A-B interface is intriguing, since it is theoretically predicted to contain a plenitude of different hedgehogs: Dirac monopoles with fractional charge. ESA

N92-10479# Helsinki Univ. of Technology, Espoo (Finland). Low Temperature Lab.
SUPERFLUID VORTEX NUCLEATION IN He-3 FLOW Abstract Only **c72**
P. I. Soininen, N. B. Kopnin (Landau Inst. for Theoretical Physics, Moscow, USSR), and M. M. Salomaa *In* Oulu Univ., Proceedings of the 25th Annual Conference of the Finnish Physical Society 1991 1 p (For primary document see N92-10362 01-70)
Avail: NTIS HC/MF A12

Computer simulations for superfluid vortex formation in He-3 flow through narrow channels are described. Phase slippage is found to occur through vortex formation and motion. The dynamics of the order parameter field is described by the Time Dependent Ginzburg-Landau (TDGL) equation, with a chemical potential term to guarantee gauge invariance. The chemical potential is calculated assuming that the normal component executes Knudsen flow. This constitutes the simplest physical model for the multicomponent order parameter dynamics in superfluid He-3. The numerical results confirm Anderson's proposal. In particular, vortex creation is found in the flow channel; phase slip lines are predicted in narrow channels. ESA

N92-10480# Turku Univ. (Finland). Wihuri Physical Lab.
STRONG MAGNETIC COMPRESSION OF SPIN-POLARIZED HYDROGEN Abstract Only **c72**
E. Tjukanov, P. Arvela, M. Karhunen, S. Jaakkola, A. Katunin, A. Safonov, S. Vasilyev, G. Shlyapnikov, and I. I. Lukashevich (Kurchatov, I. V. Inst. of Atomic Energy, Moscow, USSR) *In* Oulu Univ., Proceedings of the 25th Annual Conference of the Finnish Physical Society 1991 1 p (For primary document see N92-10362 01-70)
Avail: NTIS HC/MF A12

Experiments where bulk densities higher than n = 10 exp 19/cu cm and surface densities over n = 10 exp 13/sq cm were obtained for spin polarized atomic hydrogen gas are reported. Compression ratios n/n sub 0 greater than 1000 were obtained, but conditions for Bose-Einstein condensation were not attained in these experiments. ESA

N92-10481# Tampere Univ. of Technology (Finland).
MODELING THE DYNAMICS OF MOLECULAR FILMS BY MONTE CARLO SIMULATION Abstract Only **c72**
J. Heinio, Kimmo Kaski, and D. B. Abraham (Oxford Univ., England) *In* Oulu Univ., Proceedings of the 25th Annual Conference of the Finnish Physical Society 1991 1 p (For primary document see N92-10362 01-70)
Avail: NTIS HC/MF A12

The spreading characteristics of a fluid on an attractive solid substrate are studied using standard vertical but also horizontal solid on solid models. In the case of the horizontal solid on solid model, the wetting dynamics is investigated both with the Langevin theory and Monte Carlo simulations. In the partially wet case, relaxation to stable wetting angle is observed, whereas in the completely wet system a precursor film is found to behave linearly in time and the layers next to the precursor as (t log t) to the 1/2 power in agreement with the theory. The layers above the precursor fluid of molecular thickness seem to show diffusive fluid profiles as found previously in the continuum theory. The case of long range surface potential of the integrated Lennart-Jones type, which decays as z(- 3) from the substrate surface, is studied. Apart from finding similar results as in the case of short range chemical potantial, clear indications of dynamic layering are seen. For the first few layers from the surface the time dependence is found to be linear. ESA

N92-10482# Tampere Univ. of Technology (Finland). Dept. of Electrical Engineering.
NUMERICAL SIMULATION STUDIES OF FLUID SPREADING Abstract Only **c72**
A. Lukkarinen, J. Heinio, and Kimmo Kaski *In* Oulu Univ., Proceedings of the 25th Annual Conference of the Finnish Physical Society 1991 1 p (For primary document see N92-10362 01-70)
Avail: NTIS HC/MF A12

The problem of fluid spreading is investigated, solving numerically the dicrete time Langevin equation of motion for a fluid wedge. This wedge is assumed semi-infinite and nonvolatible, and on investigating the dynamical exponents for the fluid profiles, the precusor film and the foot of a sessile drop are demonstrated. When the conditions are favorable for complete wetting, the precursor film is found to proceed with constant velocity, i.e., the time dependency is linear. On the other hand the foot seems to behave diffusively, i.e., the time dependency is t(alpha) where alpha is about 1/2. In the partial wetting case, the wedge stabilizes to nonzero contact angles that are dependent on the chemical potential and surface tension. ESA

N92-10483# Jyvaskyla Univ. (Finland). Dept. of Physics.
SURFACE RECONSTRUCTION AND MANY-ATOM MODELS Abstract Only **c76**
H. Hakkinen, J. Merikoski, and M. Manninen *In* Oulu Univ., Proceedings of the 25th Annual Conference of the Finnish Physical Society 1991 1 p Sponsored by Emil Aaltonen Foundation and Academy of Finland (For primary document see N92-10362 01-70)
Avail: NTIS HC/MF A12

The (110)(1 by 2) missing row reconstruction of seven fcc metals Ni, Pd, Pt, Cu, Ag, Au and Al was studied with the effective medium theory. A clear trend in tendency to reconstruct was observed when going from the 3d metals Ni and Cu to 5d metals Pt and Au. The results are discussed together with some previous calculations using other many atom models for total energy calculation in metals. The tendency to undergo reconstruction is found to be related to the anisotropy of surface energies on (111) and (100). By investigating the effective two body and three body interactions on the surface, it is shown that the missing row reconstruction is related to the effective repulsion between adjacent nearest neighbor rows on the unreconstructed (110) surface. Restriction of the atomic interactions to the nearest neighbors only makes all the recent many atom models favor the missing row structure. ESA

N92-10484# Helsinki Univ. of Technology, Espoo (Finland). Physics Lab.
CHEMISORPTION OF CO ON Mg-O/Co(0001) Abstract Only **c25**
A. Talo, J. Vaari, J. Lahtinen, and P. Hautojarvi *In* Oulu Univ., Proceedings of the 25th Annual Conference of the Finnish Physical Society 1991 1 p (For primary document see N92-10362 01-70)
Avail: NTIS HC/MF A12

Metal oxides deposited on Group VIII metals were used as model catalysts to study metal support interactions observed in heterogeneous catalysis. The growth of Mg-O overlayers on Co(0001) and chemisorption properties of CO on Mg-O/Co(0001) was studied. The CO adsorption capacity of the Mg-O/Co(0001) system was studied by measuring TDS yields as a function of time. From the resulting curve, the MgO is concluded to block the adsorption sites of CO on cobalt. Although CO is found to adsorb moleculary on Co(0001) and only negligible, adsorption is observed on pure MgO; measurements show the dissociation of CO occurs on Mg-O/Co even at room temperature. This is explained by a

model where MgO(x) that is located in the perimeter of Mg-O island dissociates CO. As a result MgO(x) is oxidized to MgO.
ESA

N92-10485# Tampere Univ. of Technology (Finland). Micro-Electronics Lab.
THE STABILITY ANALYSIS OF A DOUBLE BARRIER RESONANT TUNNELING DEVICE Abstract Only **c76**
H. P. Joosten, H. J. M. F. Noteborn, Kimmo Kaski, and D. Lenstra (Technische Univ., Eindhoven, Netherlands) *In* Oulu Univ., Proceedings of the 25th Annual Conference of the Finnish Physical Society 1991 1 p (For primary document see N92-10362 01-70)
Avail: NTIS HC/MF A12

The stability of a Self-consistent Potential Distribution (SPD) of a Double Barrier Resonant Tunneling Device (DBRTD) was analyzed. Based on a static model of a DBRTD, a model for the dynamics was developed. This model, implemented in a circuit consisting of a battery and a resistor, leads to two stability criteria. The static model of the DBRTD is based on the capacitor like behavior in the intrinsic layer structure, combined with quantum mechanically coherent transport of electrons. The self-consistency demand causes, in a certain bias voltage regime, three SPD's. By introducing dynamics, the stability of these SPD's can be investigated. The dynamics consist of two items: the current charge conservation in the system (Kirchhoff's current law), and the coherent current through the barriers in a non-self-consistent case. The resulting time dependency of the whole system shows that until the point of contact of the load line to the I-V bias curve the resonant current carrying SPD are stable. ESA

N92-10486# Thomson-CSF, Orsay (France).
HIGHLIGHTS OF MATERIAL RESEARCH FOR OPTOELECTRONICS IN THE EIGHTIES, TRENDS AND CHALLENGES FOR THE NINETIES Abstract Only **c74**
M. Razeghi *In* Oulu Univ., Proceedings of the 25th Annual Conference of the Finnish Physical Society 1991 1 p (For primary document see N92-10362 01-70)
Avail: NTIS HC/MF A12

The highlights of semiconductor multilayers technology for high performance photonic and electronic devices and trends and challenges for the 1990's are reviewed. Materials targeted to satisfy society's future needs in electronics and optoelectronics are semiconductors, superconductors, organic materials, and conducting polymers. ESA

N92-10487# Helsinki Univ. of Technology, Espoo (Finland). Physics Lab.
INTERATOMIC INTERACTIONS IN THE LOCAL DENSITY APPROXIMATION Abstract Only **c72**
A. P. Seitsonen, M. J. Puska, and R. M. Nieminen *In* Oulu Univ., Proceedings of the 25th Annual Conference of the Finnish Physical Society 1991 1 p (For primary document see N92-10362 01-70)
Avail: NTIS HC/MF A12

Electron structure calculations in the Local Density Approximation (LDA) of the density functional theory were performed. The systems studied range from bulk metals and rare gas solids to diatomic molecules. The methods used include the Linear Muffin Tin Orbital (LMTO) method within the Atomic Spheres Approximation (ASA) for solids with different lattice structures, the Effective Medium Theory (EMT) which approximates fcc solids, and the commercial program DMOL for small molecules. The aims of the work are to study the effects of different, mainly numerical, approximations used in different programs, and errors due to LDA which are made in all methods, and to construct interatomic potentials to be used in simulations of many atom systems. The calculations gave information about the tendency of LMDA to overbind molecules and solids. The main conclusion is that the electron self-interaction in LDA makes the electron structures of atoms too deformable and therefore the bonds between atoms become too strong. ESA

N92-10488# Turku Univ. (Finland). Dept. of Physics.
A BAND THEORETICAL STUDY ON THE ELECTRONIC PROPERTIES IN THE PHASE TRANSITION CuAu 1 TO CuAu 2 Abstract Only **c26**
K. Kokko *In* Oulu Univ., Proceedings of the 25th Annual Conference of the Finnish Physical Society 1991 1 p (For primary document see N92-10362 01-70)
Avail: NTIS HC/MF A12

A study to find the factors which dominate in the change of the specific heat in the phase transition between CuAu I to CuAu II was undertaken. It was shown that the formation of the antiphase boundaries in CuAu II is the dominating factor in the change of specific heat as the transition takes place. It was also found that the charge transfer does not occur only perpendicular to the b axis but also parallel to it. In addition to this, the calculations show that the charge transfer oscillates inside the antiphase doman. ESA

N92-10489# Tampere Univ. of Technology (Finland). Dept. of Physics.
BERYLLIUM DOPING OF InP GROWN BY GAS-SOURCE MOLECULAR BEAM EPITAXY Abstract Only **c76**
T. Hakkarainen, K. Rakennus, K. Tappura, M. Hovinen, M. Pessa, and H. Asonen *In* Oulu Univ., Proceedings of the 25th Annual Conference of the Finnish Physical Society 1991 1 p (For primary document see N92-10362 01-70)
Avail: NTIS HC/MF A12

Beryllium (Be) doped InP was grown on semi-insulating InP(100) substrates by GSMBE (Gas Source Molecular Beam Epitaxy) to examine its doping characteristics. The Be source temperature in the range 630 to 950 C was studied. The electrical properties of the films were evaluated by standard Hall measurements. The slope of the vapor pressure curve of Be agrees well with the temperature dependence of the hole concentration over the doping range from 10 exp 16 to 10 exp 19/cu cm. This suggests that, over the concentration range studied, the Be doping level is proportional to the Be arrival rate. By comparing the Be doping characteristics of GaAs and InP, it is concluded that about 60 percent of the incorporated Be is electrically activated, assuming 100 percent electrical activity of Be in GaAs. ESA

N92-10490# Tampere Univ. of Technology (Finland). Dept. of Physics.
INTERFACE EFFECTS ON ELECTRICAL PROPERTIES OF HIGH PURITY InP GROWN BY GAS-SOURCE MOLECULAR BEAM EPITAXY Abstract Only **c76**
K. Rakennus, K. Tappura, T. Hakkarainen, M. Pessa, H. Asonen, and R. Laiho (Turku Univ., Finland) *In* Oulu Univ., Proceedings of the 25th Annual Conference of the Finnish Physical Society 1991 1 p (For primary document see N92-10362 01-70)
Avail: NTIS HC/MF A12

The effect of the substrate epilayer interface of InP on Hall mobilities and carrier concentrations at 300 and 77 K is studied. It is shown that photoluminescence and Hall results are contradictory due to the highly conductive interface of InP, which falsifies the Hall results. ESA

N92-10491# Tampere Univ. of Technology (Finland). Dept. of Physics.
THE INFLUENCE OF GROWTH CONDITIONS ON THE COMPOSITION OF GaInAsP GROWN BY GAS-SOURCE MOLECULAR BEAM EPITAXY Abstract Only **c76**
K. Tappura, T. Hakkarainen, K. Rakennus, M. Hovinen, and H. Asonen *In* Oulu Univ., Proceedings of the 25th Annual Conference of the Finnish Physical Society 1991 1 p (For primary document see N92-10362 01-70)
Avail: NTIS HC/MF A12

The effect of growth temperature and growth rate on the composition of GaInAsP grown by gas source molecular beam epitaxy on Inp substrates was studied. The composition of GaInAsP was found to be independent of substrate temperature below a transition temperature, approximately 530 C, at which appeared an abrupt change in the group V composition of GaInAsP for the

wavelengths greater than 1.05 and less than or equal to 1.3 microns. The magnitude of the abrupt change in the composition, as well as group V composition as a whole, is observed to be a function of growth rate, or V/III ratio. Some of the observations related to the influence of growth rate on the alloy composition were explained qualitatively. However, the mechanics causing the abrupt change are not yet understood. ESA

N92-10492# Odessa State Univ. (USSR). Dept. of Experimental Physics.
THE FIELD DRIFT OF IONS AND ITS INFLUENCE ON THE ELECTRICAL PROPERTIES OF SnO2 Abstract Only **c27**
A. V. Ignatov, A. V. Burlak, V. V. Serdyuk, V. Lantto, and S. Leppavuori (Oulu Univ., Finland) *In* Oulu Univ., Proceedings of the 25th Annual Conference of the Finnish Physical Society 1991 1 p (For primary document see N92-10362 01-70)
Avail: NTIS HC/MF A12

The effect of high electric fields at elevated temperatures on some electrical properties of ceramic SnO2 thick film samples was studied by measuring both the I-V characteristics and the potential distribution along the field direction for samples annealed in the presence of high electric fields at temperatures between 300 and 400 C. It was found that annealing of the samples in electric fields of 100 to 3000 V/cm changed both the room temperature I-V characteristics and the potential distribution of the samples dramatically. A very high asymmetry, for instance, was found between the potential distribution of the forward and reverse bias (under annealing) directions. This means that some field drift of ions (or defects) appeared in SnO2 at elevated temperatures between 300 and 400 C in the presence of high electric fields. ESA

N92-10493# Tampere Univ. of Technology (Finland). Dept. of Physics.
ELECTRICAL CHARACTERIZATION OF Li AND N DOPED ZnSe Abstract Only **c76**
E. Kuusisto, J. Lilja, K. Imai, and M. Pessa *In* Oulu Univ., Proceedings of the 25th Annual Conference of the Finnish Physical Society 1991 1 p (For primary document see N92-10362 01-70)
Avail: NTIS HC/MF A12

The conduction type of Li doped ZnSe films were analyzed by a novel I-V measurement employing Schottky contacts. The impurity type and net concentration (N sub D-N sub A) was measured by an extended C-V measurement. The contacts were made by evaporating two Au spots of different area. The results of the characterization of N doped samples are discussed. ESA

N92-10494# National Research Council of Canada, Ottawa (Ontario). Div. of Physics and Inst. for Microstructural Sciences.
MAGNETO-OPTICAL TRANSITIONS IN A COULOMB COUPLED PAIR OF QUANTUM DOTS Abstract Only **c74**
Tapash Chakraborty, V. Halonen, and P. Pietilainen (Oulu Univ., Finland) *In* Oulu Univ., Proceedings of the 25th Annual Conference of the Finnish Physical Society 1991 1 p (For primary document see N92-10362 01-70)
Avail: NTIS HC/MF A12

Optical transitions for a pair of Coulomb coupled quantum dots in a magnetic field are investigated. It is shown that for a parabolic confinement potential, the electric dipole transition energies reveal interesting anticrossing behavior which is due to the many electron interaction. The results for the ground state single particle density in these systems also reflect the correlated behavior of the electrons. ESA

N92-10495# National Research Council of Canada, Ottawa (Ontario).
RECOMBINATION RADIATION IN THE FRACTIONAL QUANTUM HALL EFFECT REGIME Abstract Only **c74**
Tapash Chakraborty and P. Pietilainen (Oulu Univ., Finland) *In* Oulu Univ., Proceedings of the 25th Annual Conference of the Finnish Physical Society 1991 1 p (For primary document see N92-10362 01-70)
Avail: NTIS HC/MF A12

The observed magneto-optical transitions in the fractional quantum Hall effect regime were studied theoretically. In particular, its dependence on the various spin configurations of the initial state was studied. It was found that the intensities of the recombination radiation at 2/3 filling factor are grouped according to the spin polarization of the initial state. It is expected that, depending upon the magnetic field strength, the luminescence line would exhibit splitting or a blue shift, reflecting the various spin polarizations of the ground state. These features are absent for filling factor where no incompressible state is expected. ESA

N92-10496# Helsinki Univ. of Technology, Espoo (Finland). Physics Lab.
TUNNELING IN OSCILLATING DOUBLE BARRIER HETEROSTRUCTURES Abstract Only **c76**
M. F. Bjorksten, R. M. Nieminen, and K. Laasonen *In* Oulu Univ., Proceedings of the 25th Annual Conference of the Finnish Physical Society 1991 1 p (For primary document see N92-10362 01-70)
Avail: NTIS HC/MF A12

One particle wave packet tunneling in sinusoidal oscillating Doubler Barrier Heterostructures (DBH) is discussed on the basis of numerical simulation results performed by using a fast Fourier transform based split operator algorithm. The oscillations of the DBH can be interpreted as a phonon spectrum of the structure and the interaction of the oscillations and the incoming wave packet as absorption/emission of modulation quanta. The absorption/emissions can be seen as sidelobes in the momentum space representation of the wave packet. The sizes of these sidelobes and the effects of these on the resonance tunneling are analyzed. The numerical results are compared to a simple analytical expression obtained for spatially homogeneous Hamiltonian giving the probabilities of inelastic interactions between the oscillating potential and the wave packet. The split operator algorithm is found to be effective and of general utility in analyzing the effects of time dependent potentials on wave packet tunneling. ESA

N92-10497# Helsinki Univ. of Technology, Espoo (Finland). Physics Lab.
SCANNING TUNNELING MICROSCOPE MEASUREMENTS IN AIR:LANGMUIR-BLODGETT FILMS ON HOPG AND GROWTH OF EVAPORATED GOLD ON HOPG Abstract Only **c76**
H. Niemi and K. Fallstroem *In* Oulu Univ., Proceedings of the 25th Annual Conference of the Finnish Physical Society 1991 1 p (For primary document see N92-10362 01-70)
Avail: NTIS HC/MF A12

Atomic resolution images of highly oriented pyrolytic graphite (HOPG) were used for calibrating a Scanning Tunneling Microscope (STM) operating in air. As HOPG is atomically flat on large area it is also very suitable as a substrate for Langmuir-Blodgett (LB) films, biological matter, evaporation of metals, etc. and is widely used in scanning tunneling measurements. The LB films of bacteriohodopsin (BR) in soya phosphatidycholine matrix on HOPG substrate were studied. The BR is a protein pigment of the purple membrane of halobilic bacteria. Atomic resolution images reveal the surface structure of the LB film. Distances between atoms or molecules can be determined. Large area scans of the gold surface evaporated on HOPG substrate were made with layers of gold of different thickness. Some of the images show that the gold is evaporated unevenly on the surface and islands of gold could be found on the HOPG surface. ESA

N92-10498# Technical Univ. of Budapest (Hungary). Dept. of Electron Devices.
WORK FUNCTION CHANGES OF HIGH-T(SUB c) SUPERCONDUCTORS AROUND THE T(SUB c) Abstract Only **c76**
J. Mizsei, A. Uusimaki, and V. Lantto (Oulu Univ., Finland) *In* Oulu Univ., Proceedings of the 25th Annual Conference of the

Finnish Physical Society 1991 1 p (For primary document see N92-10362 01-70)
Avail: NTIS HC/MF A12

In order to measure the work function Phi of high temperature superconducting materials, an electrical alternative, the so called Kelvin probe method, was used instead of a second alternative of using photoelectric measurements. Polycrystalline bulk materials, namely hot pressed YBa2Cu3O(x) and cold pressed B(1.84)Pb(0.34)Sr(1.94)Ca(2.00)Cu(3.08)O(y) in the form of cylindrical disc, were used as samples and a graphite sheet was used as the reference electrode. The resistivity of the sample was measured using the four probe method and the temperature was measured by a thermocouple as well as the pn junction of a transistor. All the measurements were done simultaneously with the recording of the differences in the contact potentials by the Kelvin probe during the cooling and warming processes. In the case of YBa2Cu3O(x), the work function of the sample increased by more than 10 MeV during the warming from 77 K to the normal state of about 92 K. This is in agreement with the hole nature of the charge. ESA

N92-10499# Oulu Univ. (Finland). Dept. of Theoretical Physics.
PREDICTIONS OF THE ELECTRON-HOLE LIQUID MODEL FOR HIGH T(SUB c) SUPERCONDUCTORS Abstract Only **c76**
A. Kallio, X. Xiong, and V. Apaja *In* Oulu Univ., Proceedings of the 25th Annual Conference of the Finnish Physical Society 1991 1 p (For primary document see N92-10362 01-70)
Avail: NTIS HC/MF A12

Electron Hole Liquid (EHL) in semiconductors can be described as a mixture of electrons and holes forming an interpenetrating mixture of two strongly correlated fermi liquids. By replacing the holes with hole bosons, a model for high Tc superconductors is obtained. The model predicts a nonvanishing normal state fraction at $T = 0$ due to the electrons which seem to be needed to understand the surface resistivity at $T = 0$, which is found to be orders of magnitude larger than for BCS superconductors. Within the EHL model the scenario is this: the holes and hence bosons are situated at oxygen sites O(1) in the CuO2 planes and the electrons can cross the planes at Cu sites. This comes out of the O(1) nuclear magnetic resonance experiments where the Knight shift continues to change for T greater than Tc. This is a proof for the existence of bosons above Tc. ESA

N92-10500# Landau Inst. for Theoretical Physics, Moscow (USSR).
VORTEX LATTICE: VORTEX LIQUID STATES IN ANISOTROPIC HIGH-T(SUB c) SUPERCONDUCTORS Abstract Only **c76**
B. I. Ivlev, N. B. Kopnin, and M. M. Salomaa (Helsinki Univ. of Technology, Espoo, Finland) *In* Oulu Univ. Proceedings of the 25th Annual Conference of the Finnish Physical Society 1991 1 p Sponsored by Soviet Academy of Sciences and Academy of Finland (For primary document see N92-10362 01-70)
Avail: NTIS HC/MF A12

Vortex lattice structures in highly anisotropic superconductors are investigated for a situation where the vortices are slightly inclined with respect to the easy plane of the crystal. The equilibrium configuration is found to be a vortex lattice with a rhombic unit cell highly compressed along the direction perpendicular to the easy plane. The elastic modulus for a shear deformation along this direction is exponentially small, which should result in melting of the vortex lattice already at quite low temperatures. The implications of the theoretical results are discussed for experiments on the angular dependence of the torque for anisotropic high Tc superconductors in an applied magnetic field. The torque is found to display quite a narrow peak for small tilting angles. ESA

N92-10501# Helsinki Univ. of Technology, Espoo (Finland). Low Temperature Lab.
DYNAMICS OF VORTICES IN HIGH-TEMPERATURE SUPERCONDUCTORS Abstract Only **c76**
N. B. Kopnin (Landau Inst. for Theoretical Physics, Moscow, USSR) *In* Oulu Univ., Proceedings of the 25th Annual Conference of the Finnish Physical Society 1991 1 p (For primary document see N92-10362 01-70)
Avail: NTIS HC/MF A12

The effects of the intrinsic pinning on the flux flow and flux creep for magnetic fields parallel or inclined with respect to the layers are considered. A simple theoretical model based on the Lawrence-Doniach theory for layered compounds, which can be used for calculating both energy barrier for thermally activated flux creep, and the flux flow conductivity of layered and anisotropic conductors, is discussed. ESA

N92-10502# Turku Univ. (Finland). Wihuri Physical Lab.
PHOTOINDUCED SUPERCONDUCTIVITY IN FILMS OF YBaCuO Abstract Only **c76**
E. Lahderanta, V. I. Kudinov, A. I. Kirilyuk, N. M. Kreines (Academy of Sciences, USSR, Moscow), and R. Laiho *In* Oulu Univ., Proceedings of the 25th Annual Conference of the Finnish Physical Society 1991 1 p (For primary document see N92-10362 01-70)
Avail: NTIS HC/MF A12

Photoinduced superconductivity in YBa2Cu3O7-delta films with delta near the semiconductor metal transition was studied. Resisitivity and magnetic properties of the film were followed during an illumination of the sample with argon/krypton laser. The observation of superconductivity (resistivity decrease and Meissner effect) due to the illumination was obvious. The growing of the superconducting properties due to illumination was temperature dependent and stabilized on a saturation level after long illumination. The relaxation of these properties (after switching off the illumination) was large at room temperature and decreased when decreasing the temperature. At 4.2 K there was practically no relaxation and the photoinduced superconductivity was permanent. The mechanism of photoinduced superconductivity is discussed on the basis of photoinduced free carriers which become trapped at the oxygen site in the material. ESA

N92-10503# Turku Univ. (Finland). Dept. of Applied Physics.
VALENCE ELECTRON STATES OF THE Bi-Sr-Ca-Cu-O HIGH-T(SUB c) COMPOUND Abstract Only **c76**
J. A. Leiro, F. Werfel, and G. Drager (Martin Luther-Univ., Halle-Wittenberg, German D.R.) *In* Oulu Univ., Proceedings of the 25th Annual Conference of the Finnish Physical Society 1991 1 p (For primary document see N92-10362 01-70)
Avail: NTIS HC/MF A12

Polarized soft x-ray emission measurements of the high Tc superconducting Bi-Sr-Ca-Cu-O compound are presented. The OK sub alpha spectrum shows a strong anisotropy and three main features can be identified. When the c axis of the crystal is nearly perpendicular to the polarization vector, alpha, the OK sub alpha shows a shoulder at about 1.2 eV from the Fermi level. It is assumed that this shoulder can be assigned to local singlets in the CuO2 plane. In the case of c axis almost parallel to the polarization vector alpha, the spectrum has a feature at about 5.8 eV from the Fermi level. A possible explanation for this feature can be local triplets. The most striking property of the CuL(alpha) spectrum is the energy shift between the main peaks in the case of the two different polarization directions. This is in accordance with the suggestion that the largely Pi bonded Cu3d(xy) states should have a smaller binding energy than that of the corresponding Cu3d(xz,yz) states. ESA

N92-10504# Helsinki Univ. of Technology, Espoo (Finland). Dept. of Technical Physics.
STUDIES ON SUPERCONDUCTING Bi2Sr2Ca(n-1) Cu(n)O(4+2n) COMPOUNDS WITH Fe-57 AND Eu-151 MOESSBAUER SPECTROSCOPY Abstract Only **c76**
J. Linden, J. Hietaniemi, T. Karlemo, M. Karppinen, T. Katila, M. Lippmaa, L. Niinisto, I. Tittonen, and K. Ullakko *In* Oulu Univ., Proceedings of the 25th Annual Conference of the Finnish Physical Society 1991 1 p (For primary document see N92-10362 01-70)
Avail: NTIS HC/MF A12

In order to study the dependence of superconductivity on the

sample preparation, Bi2Sr2Ca(n-1)Cu(n)O(4+2n) samples were prepared using various sintering temperatures and nominal starting compositions. After sintering the samples were characterized with x-ray diffraction and magnetic AC susceptibility measurements. In all cases the corresponding Fe-57 doped samples were also made for Mossbauer measurements. The Mossbauer measurements show usually three quadrupole components arising from the different phases in the samples. The site assignment of Fe-57 is discussed. Samples corresponding to the nominal n + 2 were studied by means of Eu-151 Mossbauer spectroscopy, by replacing 20 to 100 percent of the calcium atoms with europium. The crystallites of these samples were oriented in a strong magnetic field to enable Mossbauer and x-ray studies as a function of different angles between the c axis and the photon beam. ESA

N92-10505# Oulu Univ. (Finland). Microelectronics and Material Physics Labs.
EPITAXIAL HIGH T(SUB c) SUPERCONDUCTING THIN FILMS AND SUPERLATTICES DEPOSITED BY LASER ALBATION Abstract Only **c76**
J. Levoska, T. Murtoniemi, and S. Leppavuori *In its* Proceedings of the 25th Annual Conference of the Finnish Physical Society 1991 1 p (For primary document see N92-10362 01-70)
Avail: NTIS HC/MF A12

High Tc superconducting YBa2Cu3O7-delta thin films and YBa2Cu3O7-delta containing superlattices were deposited by laser ablation on SrTiO3 (001) and MgO (001) single crystal substrates by an in situ process using sintered superconducting pellets as targets. The films were characterized by optical microscopy, SEM/EDS X-ray diffraction, and electrical measurements. From the measurements of current voltage characteristics of laser patterned films in a zero applied magnetic field, the critical current as a function of temperature was obtained, and the Kosterlitz-Thouless transitions observed. The transport critical currents were in the range above 2,000,000 A/sq cm at 77 K. Epitaxial YBa2Cu3O7-delta/PrBa2CuO7-delta and YBa2Cu3O7-delta/Nd(2-x)Ce(x)Cu3O(4-d) layered structures and superlattices with various periods were also deposited and their electrical and structural properties were characterized. ESA

N92-10506# Oulu Univ. (Finland). Microelectronics and Material Physics Labs.
HIGH T(SUB c) SUPERCONDUCTING Li-DOPED Bi-Sr-Ca-Cu-O THIN FILMS DEPOSITED BY LASER ABLATION Abstract Only **c76**
J. Levoska, T. Murtoniemi, and S. Leppavuori *In its* Proceedings of the 25th Annual Conference of the Finnish Physical Society 1991 1 p (For primary document see N92-10362 01-70)
Avail: NTIS HC/MF A12

High Tc superconducting Bi-Sr-Ca-Cu-O thin films doped with Li were deposited by laser ablation. The purpose of Li doping was to increase the T(sub c 0) of the 2212 phase. For a sintered bulk material, enhancement of the T(sub c 0) from 80 to 87 K was obtained by annealing at 740 C. The films and target materials were characterized by optical microscopy, SEM/EDS, X-ray diffraction, and electrical measurements. ESA

N92-10507# Helsinki Univ. of Technology, Espoo (Finland). Low Temperature Lab.
NEUTRON DIFFRACTION EXPERIMENTS ON NUCLEAR MAGNETIC ORDER IN COPPER Abstract Only **c26**
A. J. Annila, K. N. Clausen, A. S. Oja, J. T. Tuoriniemi, and H. Weinfurter (Hahn-Meitner-Inst. G.m.b.H., Berlin, Germany, F.R.) *In* Oulu Univ., Proceedings of the 25th Annual Conference of the Finnish Physical Society 1991 1 p (For primary document see N92-10362 01-70)
Avail: NTIS HC/MF A12

Spontaneous antiferromagnetic ordering in the nuclear spin system of copper was studied by neutron diffraction experiments. Below the critical temperature 60 nK and the critical field 0.25 mT, the system displays two different neutron Bragg reflections, (1 0 0) and (0 2/3 2/3), depending on the strength and direction of the magnetic field. The (1 0 0) peak characterizes the conventional type-I-antiferromagnet but the recently found (0 2/3 2/3) reflection has not been observed in any other fcc magnet. In conclusion, the nuclear spin system of copper revealed a variety of different antiferromagnetic structures. The richness, in this regime of extremely low temperatures, is interesting also from the theoretical point of view. As the interactions between the spins can be determined from first principles, copper nuclei provided an exceptional model system for calculations. ESA

N92-10508# Jyvaskyla Univ. (Finland). Dept. of Physics.
FERROMAGNETISM IN SMALL CLUSTERS Abstract Only
J. Merikoski, J. Timonen, M. Manninen, and P. Jena (Virginia Commonwealth Univ., Richmond.) *In* Oulu Univ., Proceedings of the 25th Annual Conference of the Finnish Physical Society 1991 1 p (For primary document see N92-10362 01-70)
Avail: NTIS HC/MF A12

Magnetization of small ferromagnetism clusters at finite temperatures was studied by using the nearest neighbor Ising model and Monte Carlo techniques. The clusters are formed such that complete layers of successive neighbors are added to an atom in a lattice site of the fcc structure. The results explain qualitatively recent experimental observations. The average magnetization per spin in zero external field is shown as a function of temperature. Below or slightly above the Curie temperature of the smallest cluster, magnetization increases with the cluster size. Adding a new layer of atoms has the effect of pushing the inner layers towards higher magnetization because their average coordination number is increased. Above the Curie temperature, the decay with temperature of the magnetization is slowest for the smallest cluster as a result of increasing fluctuations with decreasing cluster size and of the absolute value of magnetization. It is shown that there is, for each cluster size, a kind of scaling behavior of magnetization. Even clusters of small size satisfy the scaling reasonably well, and it may also be possible to extend the known scaling arguments. ESA

N92-10509# Helsinki Univ. of Technology, Espoo (Finland). Low Temperature Lab.
ANTIFERROMAGNETIC ORDERING IN SILVER AT PICOKELVIN TEMPERATURES Abstract Only **c26**
P. J. Hakonen, K. K. Nummila, R. Vuorinen, and S. Yin *In* Oulu Univ., Proceedings of the 25th Annual Conference of the Finnish Physical Society 1991 1 p (For primary document see N92-10362 01-70)
Avail: NTIS HC/MF A12

The dynamic susceptibility of polycrystalline foils was measured down to about 0.5 nK (S greater than 0.4RIn2) using SQUID-NMR techniques. Saturation and a decrease of the static susceptibility were observed at the lowest temperatures as well as clear changes in the NMR line shapes which are associated with spontaneous, first order antiferromagnetic ordering of silver nuclei. In addition to the construction of the phase diagram, an attempt to resolve different ordered structures predicted for silver was made. The NMR measurements reveal variations in the line shapes depending on the details of the final demagnetization procedure. The line shapes display two distinct, coexistent maxima, which either reflect the presence of two simultaneous phases or, more probably, a single phase with two antiferromagnetic resonance modes. Resolving between these two possibilities could not be done because of the polycrystalline structure of the sample. The latter interpretation is preferred, but if the theoretical ideas are considered, data could also be viewed as evidence for the existence of two different ordered structures. ESA

N92-10510# Kurchatov (I. V.) Inst. of Atomic Energy, Moscow (USSR).
NMR AND ESR EXPERIMENTS ON SOLID MOLECULAR HYDROGEN CONTAINING ATOMIC HYDROGEN Abstract Only **c72**
V. A. Shevtsov, E. E. Ylinen, A. Frolov, I. I. Lukashevich, and Matti Punkkinen *In* Oulu Univ., Proceedings of the 25th Annual Conference of the Finnish Physical Society 1991 1 p Prepared

in cooperation with Turku Univ., Finland (For primary document see N92-10362 01-70)
Avail: NTIS HC/MF A12

A probehead which allows nearly simultaneous Nuclear Magnetic Resonance (NMR) and Electron Spin Resonance (ESR) experiments at liquid helium temperatures was constructed. The ESR setup utilizes a normal X-band microwave bridge near the top of the cryostat. The cavity arm consists of a special low temperature cable and a loop gap resonator around the sample space. The 100 kHz signal from the microwave detector diode is amplified and phase detected in a lock in amplifier. The spectra are collected by a computer, which also controls the slow sweep on the magnetic field. The NMR coil is wound around the shield of the loop gap resonator and it is tuned to about 14.5 MHz by a nearby series capacitance. Other NMR operations are provided by a Bruker spectrometer MSL300. Before the preparation of the sample, hydrogen gas is purified by letting it flow through a palladium foil. A microwave dissociator, positioned at the top of the cryostat, breaks hydrogen molecules. From the dissociator the gas is led to the surface of a quartz crystal (cooled by liquid helium) at the bottom of the cryostat. Preliminary results were obtained on the spin conversion of orthomolecules by NMR and on the recombination of atoms by ESR. ESA

N92-10511# Turku Univ. (Finland). Wihuri Physical Lab.
NMR PULSE RESPONSES OF PAIRS OF TRIADS OF 1/2 SPINS IN SOLIDS Abstract Only **c76**
Antti Vuorimaki and Matti Punkkinen *In* Oulu Univ., Proceedings of the 25th Annual Conference of the Finnish Physical Society 1991 1 p (For primary document see N92-10362 01-70)
Avail: NTIS HC/MF A12

To study many interesting phenomena it is desirable to use single crystals where all the triads are equivalently oriented. However, in the known crystals containing parallel CH3 and CF3 units these groups are arranged in approximate pairs. A pair of such groups or the system of six dipolar coupled 1/2 spins has 34 eigenfunctions. Therefore, its Nuclear Magnetic Resonance (NMR) properties were analyzed either without solving the eigenvalue problem or by using the simplified model of two dipolar coupled quasiparticles of spin 3/2. The first method is applicable to numerical evaluation and such closed form calculations which are independent of the basis. The quasiparticle model can lead to erroneous results even for a pair of rather distant groups. The aim is to find analytical expressions relating the observed Fourier spectra of the NMR signals after various pulse sequences to the 64 energy level populations, the pulse angles, and intervals. Some such problems were not solved even for the isolated triads until recently. The first results for the system of pairs of triads are in good agreement with experimental spectra. ESA

N92-10512# Helsinki Univ. of Technology, Espoo (Finland). Dept. of Technical Physics.
GAMMA ECHO EXPERIMENTS Abstract Only **c72**
P. Helisto, I. Tittonen, M. Lippmaa, and T. Katila *In* Oulu Univ., Proceedings of the 25th Annual Conference of the Finnish Physical Society 1991 1 p (For primary document see N92-10362 01-70)
Avail: NTIS HC/MF A12

When observed through a thick resonant sample the exponential decay of a Mossbauer gamma state appears to be considerably accelerated. It is shown that by applying a phase change to the emitted gamma radiation field this accelerated decay signal can be generated. The amplitude of this novel echo signal can be much higher than the corresponding source intensity. Sample saturation by an intense source is not required. Experimental results with Fe-57 Mossbauer resonance are in good accordance with the theory. ESA

N92-10513# Joensuu Univ. (Finland). Dept. of Physics.
AN IMPROVED TECHNIQUE FOR ELECTROLYTIC COLOURATION OF ALKALI HALIDE CRYSTALS Abstract Only **c76**
P. Raerinne and P. Ketolainen *In* Oulu Univ., Proceedings of the 25th Annual Conference of the Finnish Physical Society 1991 1 p (For primary document see N92-10362 01-70)
Avail: NTIS HC/MF A12

In the electrolytic coloration method, color centers are produced in alkali halide by electron injection into anion vacancies at high temperatures. This procedure is normally carried out using a flat anode and one pointed cathode. Usage of this electrode configuration causes an inhomogeneous color center distribution in the colored crystal. In addition, it is quite difficult to achieve a suitably low F center concentration. These disadvantages can be removed by dividing the total charge to be injected into crystal between several cathode points. A coloration apparatus was modified with a ninepoint cathode element. The current going through the crystal was controlled electronically so that equal amounts of charge were injected through each cathode point. Experiments show that this method is a significant improvement. By using a nine point cathode, the color center distribution was observed to be more homogeneous and the concentration suitably low. This method will be applied to produce color center laser crystals. ESA

N92-10514# Joensuu Univ. (Finland). Faculty of Sicences.
SPECTRAL REFLECTANCE OF PINE AND INTENSITY OF MOOSE BROWSING Abstract Only **c43**
Raimo Silvennoinen, Kaarlo Nygren (Game and Fisheries Research Inst., Ilomantsi, Finland), Kim vonWeissenberg, and Rauno Hamalainen *In* Oulu Univ., Proceedings of the 25th Annual Conference of the Finnish Physical Society 1991 1 p (For primary document see N92-10362 01-70)
Avail: NTIS HC/MF A12

The dehydration and water infiltration of intercellular spaces of leaves of vegetation are shown to increase and decrease the spectral reflectance values of the leaves. Due to the moisture contents of the needles of pine the extreme types are assumed to reflect light differently. Other histochemical properties and metabolic changes may also be measurable with the light reflected from mesophyll, chloroplasts, and other cell organelles. The lack of elements and effects of fertilization are observed to change the reflectance properties of the plants; pest and pollution damages are also noted to change the spectral reflectance of pine. The chemical characteristics of Scotch pine needles preferred or rejected by moose have been studied and it was found that significant differences in dry matter percentage and the ether soluble fraction between totally browsed and hardly touched pine cones. In this study, the spectra of light reflected from the same cones that showed differences in moose browsing preference were measured. The differences of light spectra measured can be used in the interpretation work of aerial multispectral pictures. ESA

N92-10515# Brookhaven National Lab., Upton, NY. Physics Dept.
POSITRON ANNIHILATION INDUCED AUGER-ELECTRON SPECTROSCOPY: A STUDY OF A Ge(100) SURFACE Abstract Only **c76**
E. Soininen (Helsinki Univ. of Technology, Espoo, Finland), A. Schwab, and K. G. Lynn *In* Oulu Univ., Proceedings of the 25th Annual Conference of the Finnish Physical Society 1991 1 p (For primary document see N92-10362 01-70)
Avail: NTIS HC/MF A12

Positron annihilation induced Auger Electron Spectroscopy (PAES) was used to study the effects of oxygen, residual gases, and temperature on a Ge(100) surface. Three low energy Auger peaks were detected at 50 eV, 90 eV, and 100 to 150 eV. An estimated 4 (+/- 1) of the surface trapped positrons annihilate with Ge 3p level electrons. This is an indication of the good efficiency of the method. The PAES proved more sensitive than the conventional electron impact Auger spectroscopy to the carbon contamination of the surface. In exposing the clean surface to oxygen, PAES revealed two phases in oxygen sticking: a sudden uptake with low exposures (less than 0.3 L) and a subsequent passivation of the surface. Further exposure (10 L to 1 ML) seems to lead to a logarithmically increasing coverage of oxygen. ESA

N92-10516# Turku Univ. (Finland). Dept. of Applied Physics.
THE NORMAL INCIDENCE GRATING INVERSE PHOTOEMISSION SPECTROMETER IN THE ENERGY RANGE 8-28 eV Abstract Only **c76**
T. Ollonqvist, L. Saisa, and J. Vayrynen *In* Oulu Univ., Proceedings of the 25th Annual Conference of the Finnish Physical Society 1991 1 p (For primary document see N92-10362 01-70)
Avail: NTIS HC/MF A12

An Ultraviolet Inverse Photoemission Spectrometer (IPES) is used to study unoccupied electronic states of solids and the surfaces. Geometrical aberration theory and a ray tracing program (SHADOW) were used in the design of the spectrometer. The effect of the angle of the grating and the position and orientation of the MCP detector on the photon energy range and the resolution of the spectrometer was calculated. The optical parameters of the spectrometer and other aspects concerning the design and construction of the spectrometer are discussed. ESA

N92-10517# Oulu Univ. (Finland). Dept. of Physics.
SUPER COSTER KRONIG AND RESONANCE SUPER COSTER KRONIG SPECTRA OF SOLID Ge AROUND 3p-IONIZATION THRESHOLD Abstract Only **c76**
A. Kivimaki, H. Aksela, Seppo Aksela, and O.-P. Sairanen *In its* Proceedings of the 25th Annual Conference of the Finnish Physical Society 1991 1 p (For primary document see N92-10362 01-70)
Avail: NTIS HC/MF A12

Electron spectra following excitations and ionization of 3p electrons of solid Ge were measured using synchrotron radiation. On both sides of the ionization limits, some extra resonance like structure can be found. Unlike the normal super Coster Kronig lines, the two new peaks clearly follow the photon energy with the energy difference between them being the same spin orbit splitting. Most probably they are caused by the resonance Coster Kronig decay in which core holes are created by the excitation of the 3p electrons to empty surface and conduction band states. Thus, the intensity distribution of these peaks reflects the amount of unoccupied states available for excitation. ESA

N92-10518# Oulu Univ. (Finland). Dept. of Physics.
SYNCHROTRON RADIATION STUDY OF RECOMBINATION PROCESSES IN SOLID STATE Tb AND Dy AFTER 4d TO 4f GIANT RESONANCE EXCITATION Abstract Only **c76**
O.-P. Sairanen and Seppo Aksela *In its* Proceedings of the 25th Annual Conference of the Finnish Physical Society 1991 1 p (For primary document see N92-10362 01-70)
Avail: NTIS HC/MF A12

The eletron spectra of solid state Tb and Dy after 4d to 4f excitations with synchrotron radiation were studied. The measurements were performed at the synchrotron radiation laboratory using a 4.7 m toroidal grating monochromator. The spectra were recorded with a high vacuum solid state spectrometer including a commercial double pass cylindrical mirror analyzer. The spectra were measured with photon energies below, at, and above the giant resonance energies. Below the main resonance, autoionization from 5s and 5p orbitals was found to be the dominant decay channel (especially 5(p)(1/2) component is strong), whereas the excitation corresponding to the main giant resonance decays by autoionization from 4f. Worth noticing are the almost complete absence of resonance Auger and Auger effect found in the case of solid state La, Gd, and Eu (4,5) and the changes in intensity ratios of different 4f components. ESA

N92-10519# Oulu Univ. (Finland). Dept. of Physics.
THE N(4,5)N(6,7)N(6,7) AND N(4,5)O(2,3)N(6,7) RESONANCE AUGER EFFECTS IN THE ELECTRON SPECTRA OF SOLID STATE Gd AND Eu Abstract Only **c76**
O.-P. Sairanen and Seppo Aksela *In its* Proceedings of the 25th Annual Conference of the Finnish Physical Society 1991 1 p (For primary document see N92-10362 01-70)
Avail: NTIS HC/MF A12

In order to study the N sub(4,5)N sub(6,7)N sub(6,7) and N sub(4,5)O sub(2,3)N sub(6,7) resonance Auger processes, the electron spectra of solid state Gd and Eu were measured using photon energies covering the range of 4d to 4f resonance excitations. The measurements were carried out in the synchrotron radiation laboratory using the 4.7 m toroidal grating monochromator with 1200 l/mm laminar grating. The spectra were recorded with a commercial double pass cylindrical mirror analyzer applying a constant 12 eV pass energy. As expected, autoionization from 5s and 5p orbitals was found to be the dominating decay channel. However, there can also be seen structure caused by the NNN and NON resonance Auger processes. The observed energy shifts relative to the normal Auger energies in gadolinium are 5.5 eV for NNN processes and 2 eV for NON processes. In europium, the energy shifts are found to be smaller: only about 1 eV for both processes. ESA

N92-10520# Turku Univ. (Finland). Materials Research.
SURFACE CHARACTERIZATION OF COATED POWDERS WITH XPS: Al2O3-SiO2 COATED TiO2 PIGMENTS Abstract Only **c76**
Leena-Sisko Johansson and Tuomo Losoi (Kemira Oy Vuorikemia, Pori, Finland) *In* Oulu Univ., Proceedings of the 25th Annual Conference of the Finnish Physical Society 1991 1 p (For primary document see N92-10362 01-70)
Avail: NTIS HC/MF A12

A study aimed at finding experimental strategies to characterize surface structures of coated powders with X-ray Photoelectron Spectroscopy (XPS) was reported. As an example, industrial TiO2 pigments, coated with hydrous alumina and silica were studied using different XPS methods. Isoeletric points and x-ray fluorescence analyses were also measured for comparison. The applicability of an XPS analysis method introduced by Tougaard et al was studied. In the method, the depth an element is calculated, analyzing elastic and inelastic photoelectron emissions from a low resolution XPS spectra. Used together with conventional analysis, two independent analyses may be calculated from line low resolution XPS spectrum. For fast and simple analysis, peak to background ratio D for the element can be measured. Good correlation was found between the results from conventional XPS layer calculations and the Tougaard equation. The methods are independent of each other. Together they seemed to give more reliable information on the nonideal powder surfaces studied than either of the methods alone. ESA

N92-10521# Finnish Centre for Radiation and Nuclear Safety, Helsinki. Surveillance Dept.
CALIBRATION OF SCINTILLATION CELLS FOR RADON-222 MEASUREMENTS Abstract Only **c35**
Kyllikki Aakko and Eero Oksanen *In* Oulu Univ., Proceedings of the 25th Annual Conference of the Finnish Physical Society 1991 1 p (For primary document see N92-10362 01-70)
Avail: NTIS HC/MF A12

The calibration, of a radon-222 measurement system is described. The detector of the system is based on ZnS(Ag) coated scintillation cell. Evacuated cells are used for grab sample measurements of radon-222 in air. Three types of radioactive sources were used to evaluate the calibration coefficient. Standard activities were generated from commercially available solid and liquid radium-226 sources, and from a self-made radon-222 source whose activity was crosschecked by gamma spectrometric measurements. Radium-226 sources are traceable to US National Institute of Standards and Technology reference standards. Sources of error on calibration are discussed. Best accuracy was obtained by gamma spectrometrically crosschecked radon source. Considerable difficulties were encountered with the traditional method of emanating a known activity of radon-222 from a standard liquid radium-226 source. Three separate solid radium-226 sources gave results with rather large deviations. The final error weighted coefficients agree well with international intercalibration results. ESA

N92-10522# Turku Univ. (Finland). Dept. of Physics.
THE CRYSTAL STRUCTURE AND MOISTURE SENSITIVITY OF (+)-4-(1-(2,3 DIMETHYLPHENYL) ETHYL) 1H-IMIDAZOLE HYDROCHLORIDE Abstract Only **c76**
E. Laine, R. Rajala, R. Sillanpaa, and J. Pirttimaki *In* Oulu Univ., Proceedings of the 25th Annual Conference of the Finnish Physical Society 1991 1 p (For primary document see N92-10362 01-70)
Avail: NTIS HC/MF A12

The preliminar crystal structure determination of dexmedetomidine hydrochloride was carried out. The diffraction data was collected on Rigaku AFC5S diffractometer with graphite monogromated Mo(K sub alpha) radiation at 23 C. The molecular structure and packing in the unit cell was solved by using direct methods. The structure was refined by using full matrix least squares refinement to an R value of 6.8 with 870 observed reflections. ESA

N92-10523# Tampere Univ. of Technology (Finland). Dept. of Physics.
COMPOUND SEMICONDUCTOR TECHNOLOGY: MATERIALS AND DEVICES Abstract Only **c76**
M. Pessa, H. Asonen, T. Hakkarainen, M. Hovinen, J. Keskinen, M. Korteoja, J. Lammasniemi, J. Nappi, K. Rakennus, and A. Salokatve et al *In* Oulu Univ., Proceedings of the 25th Annual Conference of the Finnish Physical Society 1991 1 p (For primary document see N92-10362 01-70)
Avail: NTIS HC/MF A12

One of the main objectives of the national microelectronics research and development project during 1987 to 1990 was to create the basic technology for the use of III-V compound semiconductors in Finland. The work was focused on developing thin film materials and devices for optoelectronics and optical telecommunication. Two pilot lines, one of them for growing films of desired layer structures, the other for processing devices on top of these films, were constructed in laboratory within the framework of the national project. Facilities for the quality control and system capacity verification were also developed to some extent. Present state of the art materials, grown by Molecular Beam Epitaxy (MBE) and gas source MBE, as well as the properties of the novel laser diodes, photoreflectors, and solar cells processed in laboratory are presented. Industrial spinoffs resulting, in part, from these studies and prospects for the future are discussed. ESA

N92-10524# Neste Oy, Porvoo (Finland). Corporate Research and Development.
CONDUCTING POLYMERS Abstract Only **c27**
Tapani Taka *In* Oulu Univ., Proceedings of the 25th Annual Conference of the Finnish Physical Society 1991 1 p (For primary document see N92-10362 01-70)
Avail: NTIS HC/MF A12

Polyalkylthiophenes (PAT's) which are melt processable and easily mixed with other polymers to form a conducting material with the desired properties were studied. The conductivity of PAT's was shown to decrease with time, but for practical purposes this appears to be manageable. ESA

N92-10525# Helsinki Univ. of Technology, Espoo (Finland). Dept. of Physics.
AEROSOL DYNAMICS: BINARY NUCLEATION Abstract Only **c25**
Markku Kulmala, Ari Laaksonen, Mihalis Lazaridis, Jyrki Makela, Kaarle Hameri, and Timo Vesala *In* Oulu Univ., Proceedings of the 25th Annual Conference of the Finnish Physical Society 1991 1 p (For primary document see N92-10362 01-70)
Avail: NTIS HC/MF A12

Homogeneous, heterogeneous, and ion induced binary nucleation are used theoretically and numerically. The classical hydrates interaction model and the classical condensation model are compared in wide temperature and gas phase chemical activity ranges. An extended version of the hydrate interaction model is developed. Sulphuric acid-water, nitric acid-water, and hydrogen iodide-water systems are considered. Numerical results are applied to stratospheric conditions, flow reactor studies, etc. ESA

N92-10526# Helsinki Univ. of Technology, Espoo (Finland). Dept. of Physics.
AEROSOL DYNAMICS: CONDENSATION AND EVAPORATION Abstract Only **c25**
Timo Vesala, Markku Kulmala, Jussi Kalkkinne, Jyrki Maekela, Kaarle Hameri, and Ari Laaksonen *In* Oulu Univ., Proceedings of the 25th Annual Conference of the Finnish Physical Society 1991 1 p (For primary document see N92-10362 01-70)
Avail: NTIS HC/MF A12

A presentation on condensation and evaporation as an aerosol physical problem considering behavior of liquid and solid particles was given. The model for condensation and evaporation was applied in various practical situations. It was used for estimating the dynamics of acidic and radioactive particles, describing particle formation and behavior in a X-ray irradiated flow reactor, and also for estimating the atmospheric dispersion of accidental releases of liquefied toxic or flammable gases. ESA

N92-10527# Technische Univ., Chemnitz (Germany, F.R.). Dept. of Physics.
SEMICONDUCTING ORGANIC THIN FILMS AS MONITORING DEVICES FOR NO2 AIR POLLUTION Abstract Only **c76**
A. Heilmann and V. Lantto (Oulu Univ., Finland) *In* Oulu Univ., Proceedings of the 25th Annual Conference of the Finnish Physical Society 1991 1 p. (For primary document see N92-10362 01-70)
Avail: NTIS HC/MF A12

The chemisorption of NO2 on lead phthalocyanine (PbPc) thin films changes the electrical conductivity of this semiconducting organic material and so the detection of NO2 concentration in the ppb range is possible. Some mesurements concerning the NO2 concentration in city air (Oulu, Finland) were carried out using this kind of device (PbPc thin film on metal slit electrodes). In the first part of the study, the sensor devices were heated in a test chamber up to 170 C and air from outside the laboratory was pumped into the test chamber using a conventional pump. In the second part of the study, a PbPc sensor with internal heating and measuring amplifier was installed directly at the city air pollution monitoring station where a commercial equipment based on chemiluminescnece was also used for continuous monitoring of the NO2 concentration in the city air. Good correlation between the sensor response and the chemiluminescence values was obtained under these circumstances. The measurements show that NO2 sensors based on PbPc thin films are suited to monitor NO2 as an air pollutant in city air. ESA

N92-10528# Oulu Univ. (Finland). Microelectronics Lab.
NOVEL TYPE OF CRYOGENIC LIQUID LEVEL SENSOR WITH HIGH SENSITIVITY Abstract Only **c35**
E. Immonen, A. Uusimaki, J. Hagberg, S. Leppavuori, and T. Porjesz (Eoetvoes Lorand Univ., Budapest, Hungary) *In its* Proceedings of the 25th Annual Conference of the Finnish Physical Society 1991 1 p (For primary document see N92-10362 01-70)
Avail: NTIS HC/MF A12

The results of experiments carried out during the investigation of the thermoelectric force of different high Tc superconductors led to the development of a cryogenic liquid level indicator. These sensors can be easily realized using high temperature superconductors based on different high Tc compounds, such as compounds of the Y-Ba-Cu-O 123, iron doped 123, 124, and 5611 and Bi-(Pb)-Ca-Sr-Cu-O systems in both bulk ceramic and thick film form. The measuring equipment designed in the study is suitable for examination of different high Tc materials to be used as cryogenic liquid level indicators. An example demonstrates the method of selection of the proper high Tc material, the sensitivity of the material, and the simplicity of the application. ESA

N92-10529# Humboldt Univ., Berlin (German D.R.). Dept. of Electronics.
FABRICATION OF GaAs: MESFET's AND TEST STRUCTURES FOR ELECTRICAL MATERIAL CHARACTERIZATION Abstract Only c33
K. Wilke, G. Heymann, J. Varrio, and M. Pessa (Tampere Univ. of Technology, Finland) *In* Oulu Univ., Proceedings of the 25th Annual Conference of the Finnish Physical Society 1991 1 p (For primary document see N92-10362 01-70)
Avail: NTIS HC/MF A12

Gallium arsenide layers were grown on both GaAs and Si substrates by Molecular Beam Epitaxy (MBE) and then MESFETS's were fabricated on top of these samples. The pattern used consists of special test fields and high frequency MESFET's. The included test field is quite useful because it consists of structures for the determination of material parameters (Hall and TLM structures), large Schottky diodes for C-V or DLTS measurements, and also various MESFET structures including a dual gate MESFET, a short channel MESFET, and a FATFET. These test structures are used to characterize heteroepitaxial GaAs on Si MBE layers which are then compared with homoepitaxial GaAs on GaAs epilayers. ESA

N92-10530# Tampere Univ. of Technology (Finland). Dept. of Physics.
In(0.5)3Ga(0.47)As/InP SAM AVALANCHE PHOTODIODES GROWN BY GAS SOURCE MBE Abstract Only c76
G. Zhang, T. Hakkarainen, K. Tappura, K. Rakennus, H. Asonen, and M. Pessa *In* Oulu Univ., Proceedings of the 25th Annual Conference of the Finnish Physical Society 1991 1 p (For primary document see N92-10362 01-70)
Avail: NTIS HC/MF A12

The In(0.53)Ga(0.4)As/InP back illuminated Separate Absorption and Multiplication (SAM) Avalanche Photodiodes (ADP's) by the Gas Source Molecular Beam Epitaxy (GSMBE) technique. The APD's exhibit low dark current (less than 1 nA at 20 V reverse bias) and high avalanche gain (M 60), comparable to the results recently obtained by Chemical Beam Epitaxy (CBE). ESA

N92-10531# Tampere Univ. of Technology (Finland). Dept. of Physics.
InP SOLAR CELLS GROWN BY GAS-SOURCE MOLECULAR BEAM EPITAXY Abstract Only c76
J. P. Zibin, K. Rakennus, K. Tappura, G. Zhang, J. Lammasniemi, and H. Asonen *In* Oulu Univ., Proceedings of the 25th Annual Conference of the Finnish Physical Society 1991 1 p (For primary document see N92-10362 01-70)
Avail: NTIS HC/MF A12

Indium phosphide (InP) solar cells were grown on InP substrates by the Gas Source Molecular Beam Epitaxy (GSMBE) technique. The cells were of the n+/p/p+ shallow homojunction type and included an InGaAs contact layer. The aim was to assess the capability of GSMBE in InP solar cell growth, and in particular to investigate the design of the emitter layer and the nature of the surface grown by GSMBE. The properties of the emitter layer are known to be important in the performance of n+/p/p+ shallow homojunction InP solar cells. Cells with emitter thicknesses ranging from 3000 to 200 angstrom were grown. The effect of a plasma deposited SiN(x) Antireflection Coating (ARC) was examined. Anomalously high improvements in spectral response were found after the deposition of such a coating. This was especially apparent in the cells with the 200 angstrom emitters, for which the AMO (space illumination) active area short circuit current density increased from 10 mA/sq cm before ARC to 32 mA/sq cm after ARC deposition. ESA

N92-10532# Tampere Univ. of Technology (Finland). Dept. of Physics.
ELECTROSTATIC PRECIPITATOR MODELLING Abstract Only c25
Jukka Hautanen and Markku Kilpelainen *In* Oulu Univ., Proceedings of the 25th Annual Conference of the Finnish Physical Society 1991 1 p (For primary document see N92-10362 01-70)
Avail: NTIS HC/MF A12

The effect of the process changes to the function of an electrostatic precipitator at a coal fired power plant was investigated. The effect of a sulfur removal process was of specific interest. Sulfur removal can change the properties of the flue gas and the fly ash so that the precipitator does not work properly. Two computer models were compared calculating the particle emission as a function of different input parameters. Some studied input parameters were: gas flow and temperature, particle concentration and size distribution, collection voltage, particle charging, and precipitator collection area. The calculations were compared with experimental results from 250 MW power plant. Sizing of the precipitator was studied. ESA

N92-10533# Technical Research Centre of Finland, Espoo.
ABATEMENT STRATEGIES BASED ON CRITICAL LOADS Abstract Only c45
M. Johansson, I. Savolainen, and M. Tahtinen *In* Oulu Univ., Proceedings of the 25th Annual Conference of the Finnish Physical Society 1991 1 p (For primary document see N92-10362 01-70)
Avail: NTIS HC/MF A12

An optimization model was used to find out where sulfur emission reduction measures could be made and how much a desired strategy would cost. Various scenarios for reducing sulfur emissions in Europe are presented under different critical load definitions. In general, it is difficult to achieve the most stringent critical loads, if considerable reductions are not made also outside Finland. The model system (HAKOMA) used in these comparisons was developed in cooperation with IIASA and several research institutes in Finland, e.g., the Finnish Meteorological Institute, Finnish Forest Research Institute and National Board of Waters and Environment. Input data was collected, for example, in measurement programs of the Finnish Research Project on Acidification (HAPRO). This comprehensive model was developed both for the assessment of importance of different factors related to acidification and for the assessment of various emission abatement policies. ESA

N92-10534# Tampere Univ. of Technology (Finland). Dept. of Physics.
LOW PRESSURE IMPACTOR WITH ELECTRICAL CONCENTRATION DETECTION Abstract Only c35
J. Keskinen and Kimmo Pietarinen *In* Oulu Univ., Proceedings of the 25th Annual Conference of the Finnish Physical Society 1991 1 p (For primary document see N92-10362 01-70)
Avail: NTIS HC/MF A12

To achieve automatic operation, the Quartz Crystal Microbalance (QCM) technique was applied to the measurement of collected mass. The sensisivity of QCM is good for large particles but rather poor for submicrometer particles. Inertial impactors are widely used devices for the measurement of aerosol particle size distribution and concentration, partly because of their large size range. The concepts of electrical detection with aerodynamic sizing is extended to subtenth micrometer particles. For size classification, a modified commercial low pressure impactor is used. The lowest cutoff size of the device is 15 nm. A multichannel electrometer was constructed using low cost monolithic eletrometer op amps. The main problem of using these circuits is the input bias current and its sensitivity to temperature variations. This problem was solved using automatic zeroing. As a result, input current an order of magnitude smaller than the bias current can be measured. The instrument combines aerodynamics size classification of particles with good sensitivity for submicrometer particles and automatic operation. Preliminary results of a study are presented. ESA

N92-10535# Environics Oy, Mikkeli (Finland).
ION MOBILITY SPECTROMETER TO TRACE GAS ANALYSIS Abstract Only c25
Tero Katto, Harri Tyrvainen, and Kimmo Pietarinen (Tampere Univ. of Technology, Finland) *In* Oulu Univ., Proceedings of the 25th

Annual Conference of the Finnish Physical Society 1991 1 p (For primary document see N92-10362 01-70)
Avail: NTIS HC/MF A12

A laboratory instrument based on the ion mobility spectrometer technique was constructed to investigate the possibility of utilizing the method in detection of toxic solvents and chemicals, especially in the field of occupational safety. In the construction, the needs of basic research of ions were taken into construction. The instrument is of the time of flight type with a cylindrical drift tube and personal computer control. The function parameters of the instrument can be adjusted over a wide range. These include the shutter timing, the field strength, and ion polarity. The system was tested with vapors of common solvents and some toxic chemicals. ESA

N92-10536# Tampere Univ. of Technology (Finland). Dept. of Physics.
A SIMPLE RADON WELL Abstract Only c72
Katariina Lahti and Gunnar Graeffe *In* Oulu Univ, Proceedings of the 25th Annual Conference of the Finnish Physical Society 1991 1 p (For primary document see N92-10362 01-70)
Avail: NTIS HC/MF A12

The development of a simple radon well, as effective but less expensive and technically easier to put into practice than is usual, was addressed. The wall was accomplished by a drill well technique. A long plastic tube, partly perforated, is put into the ground. To the top end of the tube an exhaust fan is connected to suck the air from the soil to make an underpressure. By this method radon is prevented from entering dwellings. Measurements were carried out in a one family house in four-day periods by a continuously monitoring radon detector. The radon concentration was usually 3000 to 4000 Bq/cu m without the use of the well. When the fan was turned on it reduced the radon concentration below 200 Bq/cu m. ESA

N92-10537# Institute of Occupational Health, Turku (Finland).
A MEASURING ROBOT FOR THERMAL ENVIRONMENT, CONTAMINANT CONCENTRATION AND VENTILATION STUDIES Abstract Only c35
E. Minni, H. Koskela, J. Pekkarinen, and R. Niemela (Institute of Occupational Health, Helsinki, Finland) *In* Oulu Univ., Proceedings of the 25th Annual Conference of the Finnish Physical Society 1991 1 p (For primary document see N92-10362 01-70)
Avail: NTIS HC/MF A12

A description of the accuracy of the measuring system and demonstrative results of the use of the laboratory were given. On the basis of the measurements the system seems to meet the requirements that were set when planning the system. Spatial distribution of air velocity and turbulence intensity can be measured even at low room air velocity. The concentration field of contaminants or tracer gases and the temperature distribution in test space can be measured. ESA

N92-10538# Turku Univ. (Finland). Wihuri Physical Lab.
SCANNING TUNNELING MICROSCOPY OF POLYSIALIC ACID Abstract Only c72
L. Haikkila, J. P. S. Aalto, L. J. Pelliniemi, R. Laiho, and J. Finne *In* Oulu Univ., Proceedings of the 25th Annual Conference of the Finnish Physical Society 1991 1 p (For primary document see N92-10362 01-70)
Avail: NTIS HC/MF A12

Polysialic Acid (PSA) fragments consisting of 13 and 17 residues were transferred to aqueous solution and applied as droplets on freshly cleft pyrolytic graphite for Scanning Tunneling Microscopy (STM) investigations. Structures of carbohydrates are generally difficult to investigate in detail. In experiments the conductivity and stability of PSA on a graphite substrate was found to be sufficient for stable operation of STM. The results reveal hillocks and their tendency to form prolonged arrangements on the substrate. The dimensions of subunits of these structures correspond to those of single particles (length about 3 mm) occasionally observed on the otherwise atomically flat surface of graphite. These results give further evidence for usefulness of STM in investigations of structures formed by macromolecules. ESA

N92-10539# Kuopio Univ. (Finland). Dept. of Applied Physics.
SPECTRAL REPRESENTATION IN VISION Abstract Only c52
J. Hallikainen, J. Parkkinen, and T. Jaaskelainen *In* Oulu Univ., Proceedings of the 25th Annual Conference of the Finnish Physical Society 1991 1 p Sponsored by Academy of Finland (For primary document see N92-10362 01-70)
Avail: NTIS HC/MF A12

A simplified color vision model is described and analyzed. The Principal Component Analysis (PCA) is used to find out the spectral information content of the model. Instead of traditional calorimetry, the human color vision and physical color measurments are compared more directly. This can be done by comparing the spectral information content of the Munsell color chips, natural color samples, physiological data measured from the macaque monkey and a simplified model of human color visions. The results show clearly that there exists connections between the color subspace representations derived from the PCA and human color vision models. The subspace representation of colors was shown to be an effective tool to compress information, without significant loss of the spectral information and the subspace model could also be a working hypothesis for higher level color recognition by the brain. ESA

N92-10540# Helsinki Univ. of Technology, Espoo (Finland). Low Temperature Lab.
INTEGRATION OF MAGNETOENCEPHALOGRAPHY AND MAGNETIC RESONANCE IMAGING Abstract Only c52
S. O. Tissari and M. S. Hamalainen *In* Oulu Univ., Proceedings of the 25th Annual Conference of the Finnish Physical Society 1991 1 p (For primary document see N92-10362 01-70)
Avail: NTIS HC/MF A12

Magnetic Resonance Imaging (MRI) data provided by the Siemens 1-Tesla MRI system at the Helsinki University Central Hospital was utilized. The coordinate systems of MRI and MEG (Magnetoencephalography) were aligned by attaching small oil filled capsules on the head's landmarks before MR imaging. Three orthogonal MRI data sets, each consisting of 20 T sub 2 and proton density weighted images, were collected at 7 to 8 mm spacing to cover the whole brain. For accurate three dimensional reconstructions, another set comprising 128 parallel slices at 1.3 to 1.5 mm spacing was obtained with a special pulse sequence enhancing the brain with respect to the surrounding tissue. The software is based on the X Window system on a UNIX workstation and, therefore, several concurrent processes can be smoothly integrated. Image viewing software allowing the inspection of the three orthogonal image sets in parallel was written. The three orthogonal slices can also be displayed in a three dimensional view to get a better perception of the relative orientation and position of the slices. The locations of the sources can be directly superimposed on the MR images. ESA

N92-10541# Kuopio Univ. (Finland). Dept. of Applied Physics.
CLUSTERING: A POWERFUL AID IN CLASSIFYING QRS WAVEFORMS Abstract Only c52
L. Patomaki and M. Jarviluoto *In* Oulu Univ., Proceedings of the 25th Annual Conference of the Finnish Physical Society 1991 1 p (For primary document see N92-10362 01-70)
Avail: NTIS HC/MF A12

A method for classifying quasi random shaker (QRS) waveforms in electrocardiography (ECG) using two different methods in parallel was developed. The A classification was based on the width, height, area and RR intervals of QRS waveforms. The B classification was, on the other hand, based on the clustering of the waveforms by their morphology. The B classification depends on the A classification and the B is the final one (output). Using clustering in QRS classification in this way shows two clear advantages: seldom occurring waveforms, most probably noise, are filtered out and the classification is improved through stabilizing

the classification when the A classification lies on some borderline between N and V groups. ESA

N92-10542# Kuopio Univ. (Finland). Dept. of Applied Physics.
ALGORITHM FOR DETECTION OF VFIB IN REAL TIME FROM ECG Abstract Only **c52**
L. Patomaki and A. Nieminen *In* Oulu Univ., Proceedings of the 25th Annual Conference of the Finnish Physical Society 1991 1 p (For primary document see N92-10362 01-70)
Avail: NTIS HC/MF A12

A simple and fast algorithm for the detection of the Ventricular Fibrillation (VF) in ECG in real time was developed and tested. Depending on the first derivative of the signal, the data points are classified either to belong to a horizontal or to a vertical part of the signal. The distance of the point from the baseline is taken into account so that only those points which situate close enough to the baseline are accepted into the class of horizontal point. The second derivative is used to detect sharp peaks in the signal expected to be R waves, to avoid false positive detection of VF. ESA

N92-10543# Kuopio Univ. (Finland). Dept. of Applied Physics.
ANALYSIS OF ESOPHAGEAL pH-RECORDINGS FOR REFLUX DISEASE Abstract Only **c52**
L. Patomaki, P. Vainio, E. Lansimies, and K. Jarvinen *In* Oulu Univ., Proceedings of the 25th Annual Conference of the Finnish Physical Society 1991 1 p (For primary document see N92-10362 01-70)
Avail: NTIS HC/MF A12

The five year use of a battery operated, portable and light weighted data logger and an IBM personal computer compatible software to measure and analyze pH signal for 24 hours, at every 3 seconds, was addressed. A study to find out the best way to use the results, to find the best clinically valuable threshold values in the decision making of the patients care, medication or operation, was undertaken. Preliminary results show the following data. The reflux time being more than 10 percent of the whole measurement period was with 22 percent of the patients. In none was the reflux index more than 40 percent of the measurement time. Sixty-one of the patients showed reflux time index less than 6 percent of the time. The refluxes appear mainly during the upright position and only 30 percent of patients had percentages between 1 to 36 while lying down. ESA

N92-10544# Helsinki Univ. of Technology, Espoo (Finland). Dept. of Physics.
USE OF IN-111 IN QUANTITATIVE SPECT Abstract Only **c61**
S. Savolainen, A. Kiuru, and J. Kankare *In* Oulu Univ., Proceedings of the 25th Annual Conference of the Finnish Physical Society 1991 1 p (For primary document see N92-10362 01-70)
Avail: NTIS HC/MF A12

Data on properties of In-111 were collected in order to develop an optimal reconstruction procedure for SPECT (Single Photon Computed Tomography) imaging. Included is data such as the linear attenuation coefficient of photopeaks with different imaging geometry and with different collimator energy window combinations. In an open geometry (a normal clinical situation) with medium energy collimator (energy windows 245 and 171 keV, plus or minus 20), the linear attenuation coefficient for In-111 in water was found to be 0.119 plus or minus 0.005. The Compton scatter correction seems to be more complex for a dual photopeak isotope than for one with a simple and rather low photopeak. The scatter correction needs to be taken into account in SPECT, particularly, for quantitation of images with a very low signal to noise ratio. ESA

N92-10545# Oulu Univ. (Finland). Dept. of Physics.
PROTON NMR STUDIES ON HUMAN BLOOD PLASMA: AN APPLICATION TO CANCER RESEARCH Abstract Only **c52**
M. Ala-Korpela, Y. Hiltunen, Jukka Jokisaari, S. Eskelinen, and K. Kiviniitty *In its* Proceedings of the 25th Annual Conference of the Finnish Physical Society 1991 1 p (For primary document see N92-10362 01-70)
Avail: NTIS HC/MF A12

The use of proton NMR (Nuclear Magnetic Resonance) spectroscopy of human blood plasma for cancer research is shown to be complicated even when combined with the division of the spectral region into the components corresponding the various lipoproteins VLDL, LDL, and HDL, and with the efficient model for the analysis. However, the presented technique, which is a combination of the very informative and fast proton NMR experiments and the efficient, accurate, and adaptable lineshape fitting analysis method, can be used as a rapid research tool for figuring out the relative concentrations of the lipoproteins in blood plasma and explaining the reasons behind the changes in the spectra. ESA

N92-10546# Helsinki Univ. of Technology, Espoo (Finland).
VARIABLE OPTICAL POLARIZATION IN Her X-1 Abstract Only **c74**
P. J. Hakala and J. Egonsson *In* Oulu Univ., Proceedings of the 25th Annual Conference of the Finnish Physical Society 1991 1 p Prepared in cooperation with Lund Observatory, Sweden (For primary document see N92-10362 01-70)
Avail: NTIS HC/MF A12

The results of the optical photopolarimetry of Her X-1, a low mass X-ray binary system consisting of an early A dwarf and a neutron star were reported. The system has an orbital period of 1.7 days and lies almost edge on. The A star fills its Roche lobe and the mass stream from it forms an accretion disk around the mass accreting neutron star. In the case of Her X-1 there is some evidence for the tilted accretion disk i.e., the disk is precessing around the neutron star with about 30 days period. It is assumed that the tilt of an accretion disk could cause phase dependent polarimetric variations due to Thomson scattering from the optically thin disk. The results from observations carried out on the Nordic Optical Telescope (NOT) show that an accretion disk confined to the orbital plane is not capable of processing the observed polarimetric variations. ESA

N92-10547# Geophysical Observatory, Sodankyla (Finland).
OZONE DEPLETION RATES IN THE LATE WINTER/EARLY SPRING ARCTIC AND ANTARCTIC STRATOSPHERE ACCORDING TO RECENT OZONE SOUNDING OBSERVATIONS Abstract Only **c45**
Esko Kyro and P. Taalas (Finnish Meteorological Inst., Helsinki.) *In* Oulu Univ., Proceedings of the 25th Annual Conference of the Finnish Physical Society 1991 1 p (For primary document see N92-10362 01-70)
Avail: NTIS HC/MF A12

The temporal behavior of the polar ozone layer was analyzed based on the ozone sounding data obtained from Sodankyla, Marambio, Alert, and Heiss Island. The scanding profiles obtained from Sadonkyla and Marambio show large variability as regards both the vertical distribution and temporal variation. This is probably due to the large scale mixing which affects the ozone layer during the times when these stations are situated outside the vortex edge. Very pronounced layering or stratification in Marambio profiles indicates that some mixing of ozone poor air from the ozone hole and ozone rich air outside the vortex is taking place across the vortex wall, as well. Similar ozone layering has been observed also at another Antarctic station McMurdo. The profiles obtained from Alert and Heiss Island show much less variability and layering because the flow at these high latitudes are strictly confined inside the vortex boundaries. A strong decreasing temporal trend in ozone was found in Marambio at most altitudes between 15 km and 25 km averaging to (-1.2 plus or minus 0.3 percent)/day (one sigma) over the period mid August to Mid October/1990. ESA

N92-10548# Helsinki Univ. of Technology, Espoo (Finland). Astrophysics Lab.
FINNISH SPACE PROJECTS: PLANETARY STUDIES Abstract Only **c12**
Kari Lumme *In* Oulu Univ., Proceedings of the 25th Annual Conference of the Finnish Physical Society 1991 1 p (For primary document see N92-10362 01-70)
Avail: NTIS HC/MF A12

Since the active Finnish participation in the Soviet Phobos project several research groups in Finland are planning to continue scientific collaboration with the Soviet, ESA and NASA planetary missions. This participation takes place both at the theoretical analysis level and at the level where various instruments will be delivered to the missions. The theoretical planetary group at the University of Helsinki Observatory, for instance, is developing several new techniques which can be applied to the mission data. An example of this is the flyby of the NASA Galileo spacecraft of an asteroid Gaspra next October for which new shape determination methods can be used. Planetary science is a highly multidisciplinic new area. In addition to traditional planetary astronomy, several physical sciences are merging. For this reason graduate students from various fields should consider this as an option for their research. Unfortunately we are still missing in Finland a good coordination of space sciences and it might be worth considering if a national center for these would be a solution. ESA

N92-10549# Helsinki Univ. of Technology, Espoo (Finland). Astrophysics Lab.
FINNISH SPACE PROJECTS: SPACE ASTRONOMY Abstract Only **c89**
O. Vilhu *In* Oulu Univ., Proceedings of the 25th Annual Conference of the Finnish Physical Society 1991 1 p (For primary document see N92-10362 01-70)
Avail: NTIS HC/MF A12

Finland is an associate member of the ESA and will become a full member starting the year 1995. The following projects and their science, and how to benefit from the Horizon 2000 program, of which a major part is basic astronomy covering the whole range of electromagnetic spectrum to study various astronomical structures from stars to cosmology, are reviewed: ERNE solar flare particle detector (ESA); SPECTRUM-X-GAMMA High Energy X-ray Observatory (USSR, NASA, ESA, several European countries); ISOPHOT Infrared Space Observatory Photometer (ESA); RADIOASTRON Radio Interferometer (USSR, NASA, ESA, several other countries). ESA

N92-10550# Helsinki Univ. of Technology, Espoo (Finland). Lab. of Engineering Materials.
THE 1990 SOLAR ECLIPSE AS SEEN BY A TORSION PENDULUM Abstract Only **c92**
K. Ullakko, Yong Liu, and Zeliang Xie *In* Oulu Univ., Proceedings of the 25th Annual Conference of the Finnish Physical Society 1991 1 p (For primary document see N92-10362 01-70)
Avail: NTIS HC/MF A12

In July 1990 there was a total solar eclipse in Helsinki, Finland. The results of Saxl and Allen, made at Harvard University (U.S.) during the total solar eclipse in March 1970, were tested using equipment which was quite similar to that used in Harvard. Because the possible effects were expected to be extremely small, special attention was paid to avoid vibrations of the surroundings. Also the temperature of the equipment was controlled in order to eliminate changes of temperature due to thermal expansion of the bars of the pendulum and the suspension wire. Ten times better resolution than Saxl and Allen was achieved. Four measurements, each lasting nine hours, were performed during the night preceding the eclipse, during the eclipse and the night after the eclipse and two weeks after the eclipse. In the limits of errors no effects were observed. The origin of the effects reported by Saxl and Allen must have been in the experimental system. ESA

N92-10551# Oulu Univ. (Finland). Dept. of Geophysics.
LITHOSPHERE PHYSICS: GEOELECTRICS AND SEISMICS Abstract Only **c46**
T. Korja *In its* Proceedings of the 25th Annual Conference of the Finnish Physical Society 1991 1 p (For primary document see N92-10362 01-70)
Avail: NTIS HC/MF A12

Deep seismic (reflection and refraction) and geoelectromagnetic (magnetotelluric) soundings are among the main methods of lithosphere investigations. The seismic and geoelectromagnetic methods are presented. The work includes magnetometer array studies, magnetotelluric and quarry blast seismic soundings along several profiles, and a marine seismic BABEL survey. Deep seismic soundings and geoelectromagnetic investigations have shown that the Earth's crust has a very complicated structure in the Fennoscandian Shield: the crust is exceptionally thick beneath the shield, 2000 Ma old collisional structures are detected, a number of elongated conductors, which probably represent old fossile plate boundaries, are identified. The geological processes, which took place in the course of thousands of millions of years, developed the crust and left traces for us to identify and to use for prediction of the Earth's future. ESA

N92-10552# Academy of Sciences (USSR), Moscow. Inst. of the Physics of the Earth.
ON THE IONOSPHERIC INFLUENCE UPON THE SPECTRAL STRUCTURE ON THE Pc1 GEOMAGNETIC PULSATIONS Abstract Only **c46**
F. Z. Feygin, A. K. Nekrasov, Jorma Kangas, K. Mursula, and T. Pikkarainen (Oulu Univ., Finland) *In* Oulu Univ., Proceedings of the 25th Annual Conference of the Finnish Physical Society 1991 1 p (For primary document see N92-10362 01-70)
Avail: NTIS HC/MF A12

Pc1 micropulsations are oscillations of the geomagnetic field in the frequency range between 0.2 and 5 Hz. They are a fairly common phenomenon at high latitudes, especially in the low solar activity years, and can be associated with the ion cyclotron waves generated and propagating in the magnetospheric plasma. Using data from the Finnish pulsation magnetometer network, a few examples of multiple band Pc1 events were analyzed. They show a coherent structure of individual pulsations over the whole pulsation chain, which is difficult to understand in any other mechanism, e.g., the effect of heavy ions in the magnetosphere. Multiple band structured Pc1 events may therefore give important information about the properties of the ionospheric Alfven resonator. ESA

N92-10553# Oulu Univ. (Finland). Dept. of Physics.
EISCAT RESEARCH PROGRAM Abstract Only **c46**
Jorma Kangas *In its* Proceedings of the 25th Annual Conference of the Finnish Physical Society 1991 1 p (For primary document see N92-10362 01-70)
Avail: NTIS HC/MF A12

The scientific interests of the Finnish scientists have been in technical development of the radar system, geophysics and plasmaphysics. They have made important contributions to the design of experiments and data analysis. Original contributions have also been made in the studies of ionospheric E and D regions and non-thermal F region plasma. Although major results are still expected by the present EISCAT system, two important extensions of EISCAT activities will be made in near future. The heating facility in Tromso will become an integral part of the EISCAT. By this system, artificial ionospheric modification experiments can be conducted to study fundamental plasma processes. On the other hand, EISCAT is planning to install a polar cap incoherent scatter radar on Spitzbergen for the studies of the physics of the upper atmosphere in polar cap and cusp regions. Such a radar system would be an important ground support for several future satellite programs. ESA

N92-10554# Oulu Univ. (Finland). Dept. of Physics.
THE USE OF WHISTLERS FOR MAGNETOSPHERIC DIAGNOSTICS Abstract Only **c46**
Jyrki Manninen *In its* Proceedings of the 25th Annual Conference of the Finnish Physical Society 1991 1 p (For primary document see N92-10362 01-70)
Avail: NTIS HC/MF A12

The plasmapause, first discovered by whistler technique, is a permanent feature of the magnetosphere that results from a large scale convection of the magnetospheric plasma driven by the solar wind. Another application of the whistler technique is the measurement of plasma drift velocity. If a whistler duct drifts radially

inward (outward), the nose frequency increases (decreases) with time. Electric fields as small as 0.00001 v/m in the equatorial plane can be measured by this technique. The whistler analysis also gives the electron density of the equator plane. Middle latitude observations have shown that isolated bursts of precipitating electrons can often found in association with whistlers and triggered emissions. ESA

N92-10555# Oulu Univ. (Finland). Dept. of Physics.
EXAMPLES OF VLF EMISSIONS RECORDED IN THE AURORAL ZONE Abstract Only **c46**
Jyrki Manninen, Tauno Turunen, and Timo Turunen (Geophysical Observatory, Sodankyla, Finland) *In its* Proceedings of the 25th Annual Conference of the Finnish Physical Society 1991 1 p (For primary document see N92-10362 01-70)
Avail: NTIS HC/MF A12

During 1989 to 1990 about 100 hours of VLF emission measurements were made in the auroral zone. The data was collected for auroral research in general. Some measurements were coordinated with equipments on board the Active satellite. The recordings were made at Sodankyla (L = 5.1) and at Inari (L = 5.6) in northern Finland. Some examples of the recorded phenomena are presented. ESA

N92-10556# Oulu Univ. (Finland). Dept. of Physics.
AVERAGE PROPERTIES OF ENERGETIC IONS IN DIFFERENT PARTS OF THE CUSP/CLEFT REGION Abstract Only **c46**
K. Mursula, G. Kremser, and B. Wilken (Max-Planck-Inst. fuer Aeronomie, Katlenburg-Lindau, Germany, F.R.) *In its* Proceedings of the 25th Annual Conference of the Finnish Physical Society 1991 1 p (For primary document see N92-10362 01-70)
Avail: NTIS HC/MF A12

The energy distributions of energetic ions in the mid altitude cusp/cleft region of the Earth's magnetosphere were studied using measurements by the Magnetospheric Ion Composition Spectrometer (MICS) on the Swedish Viking satellite. The results show that the energetic ion populations in the cusp, cusp proper and cleft resemble each other very much, whereas the ion intensity in the mantle is very low and some of the energy distributions there have different properties from those of the other regions. O+ ions seem to be a substantial component in the cleft, cusp and cusp proper. The energy distributions of the H+ and particularly the He++ ions resemble a kappa distribution, while all other ion distributions are well fitted by a power law function. ESA

N92-10557# Academy of Sciences (USSR), Moscow. Inst. of the Physics of the Earth.
INHOMOGENEITY AND NONLINEARITY EFFECTS ON STOP BANDS OF ALFVENIC ION CYCLOTRON WAVES IN MULTICOMPONENT PLASMA Abstract Only **c46**
A. K. Nekrasov, K. Mursula, Jorma Kangas, T. Pikkarainen (Oulu Univ., Finland), and N. F. Maltseva *In* Oulu Univ., Proceedings of the 25th Annual Conference of the Finnish Physical Society 1991 1 p Previously announced in IAA as A91-25582 (For primary document see N92-10362 01-70)
Avail: NTIS HC/MF A12

The existence of stop bands for left handed Alfvenic ion cyclotron waves propagating in the direction of magnetic field in a multicomponent plasma is studied. Three effects are discussed: finite ion temperature, inhomogeneous magnetic field and nonlinear wave amplitude. All of them affect the existence of stop bands and set critical bounds on the relevant physical parameters, particularly on the density of heavy ions. Using the model of a linearly varying, longitudinally inhomogenous magnetic field, the critical lower bound on heavy ion density is calculated as a function of longitudinal inhomogeneity, and the difference between the truly inhomogeneous and essentially homogeneous situations is discussed. Typical values for the wave vector in the resonance region are derived. The upper bound on the wave amplitude for the linear theory to be applicable is found and the condition for stop band formation in the nonlinear case is derived. The obtained results are applied to the magnetospheric environment and shown to lead to relevant modifications. ESA

N92-10558# Oulu Univ. (Finland). Dept. of Physics.
ENERGY-LATITUDE DISPERSION OF ENERGETIC IONS IN THE DAYSIDE OF THE EARTH'S MAGNETOSPHERE: A SUBSTORM-RELATED PHENOMENON Abstract Only **c46**
R. Rasinkangas, G. Kremser, B. Wilken, and F. Soraas (Bergen Univ., Norway) *In its* Proceedings of the 25th Annual Conference of the Finnish Physical Society 1991 1 p (For primary document see N92-10362 01-70)
Avail: NTIS HC/MF A12

A working model for the explanation of a new type of energy latitude dispersion of high energy ions (10 to 326 keV/e) observed by the Viking satellite in the magnetosphere of the Earth is presented. The dispersion events are characterized by a decrease of the ion energy with increasing latitude. They occur on the dayside at 0800 to 1500 MLT and invariant latitudes of 69 to 77 degrees. The source region of the ions is located in the midnight sector of the magnetosphere, as has been shown by backtracing the observed ions in model magnetic and electric fields. In order to explain the transport of these ions towards the dayside and the formation of the energy latitude dispersion, a series of magnetospheric processes is needed. These include magnetospheric substorms, the drift of charged particles in realistic (although steady state) magnetospheric magnetic and electric fields, drift shell splitting, and pitch angle diffusion. The working model provides an explanation of all major characteristics of the dispersion events, if some ion energy dependence on the radial distance already exists in the source region. ESA

N92-10559# Geophysical Observatory, Sodankyla (Finland).
EISCAT INCOHERENT SCATTER RADAR OBSERVATIONS AND MODEL STUDIES ON DAY TO NIGHT VARIATIONS IN THE IONOSPHERIC D-REGION DURING THE PCA EVENT OF AUGUST 1989 Abstract Only **c46**
E. Turunen *In* Oulu Univ., Proceedings of the 25th Annual Conference of the Finnish Physical Society 1991 1 p (For primary document see N92-10362 01-70)
Avail: NTIS HC/MF A12

An intense Polar Cap Absorption (PCA) solar proton event causing enhanced ionization in ionospheric D region occurred on 12 Aug. 1989. The event was partially observed during three successive nights by the incoherent scatter radar at Ramfjordmoen near Tromso. The quantitative interpretation of EISCAT data as physical parameters is discussed. Ion production rate calculation from GOES-7 satellite measurements of proton flux and one dimensional steady state ion chemistry model of the D region are used together with the raw radar data to deduce the time variations of the electron concentration, negative ion of electron density ratio, neutral temperature and mean ion mass. The solar radiation control of these time variations is shown to be understood. The deduced temperature variations are compared with simultaneous temperature measurements at Andoya based on lidar technique. ESA

N92-10560# Oulu Univ. (Finland). Dept. of Physics.
OBSERVATIONS OF SEMIDIURNAL ATMOSPHERIC TIDES USING THE EISCAT INCOHERENT SCATTER RADAR Abstract Only **c46**
A. Huuskonen and T. Nygren *In its* Proceedings of the 25th Annual Conference of the Finnish Physical Society 1991 1 p (For primary document see N92-10362 01-70)
Avail: NTIS HC/MF A12

The motion of ionospheric plasma at E region heights is controlled by electric fields and neutral winds. Because the electric field direction is always perpendicular to the geomagnetic field, plasma flow along the magnetic field is only caused by air drag due to meridional neutral winds. Therefore, measurements of plasma velocity along the magnetic field line by the EISCAT facility provide an estimate of neutral wind in the magnetic meridional plane. In March, April and August 1988 such observations were made during afternoon and pre midnight periods and the results were used to fit the amplitude and phase of the semidiurnal component of neutral velocity. An attempt was made to relate the

observations to the various modes of the atmospheric semidiurnal tide. ESA

N92-10561# Geophysical Observatory, Sodankyla (Finland).
VARIATION OF D-REGION PARAMETERS DURING POLAR CAP ABSORPTION EVENTS IN THE YEAR 1989 Abstract Only **c46**

H. Ranta *In* Oulu Univ., Proceedings of the 25th Annual Conference of the Finnish Physical Society 1991 1 p (For primary document see N92-10362 01-70)
Avail: NTIS HC/MF A12

Four intense Solar Cap Absortion (PCA) events were observed in Autumn 1989 during the increasing phase of the sunspotcycle 22. The recurrence periods for these PCA events were 47, 20 and 41 days. For one event studied in detail spatial nonuniformity was observed in the latitude profiles of the electron density in the D region. During the course of the PCA, two clear maxima in the electron density were found. The first maximum was seen at latitude about 69 N (North) and the second at 64 N. After sudden storm commencement during a PCA, the electron density was decreased south of L value 6. The day to night ratio of the absorption was found to be a function of the solar zenith angle. ESA

N92-10562# Turku Univ. (Finland). Space Research Lab.
PERFORMANCE TESTS OF ERNE HED SENSOR Abstract Only **c92**

E. Valtonen, J. Peltonen, T. Eronen, J. J. Torsti, M. Lumme, M. Mahonen, A. Nieminen, and J. B. Viano (Grenoble-1 Univ., France) *In* Oulu Univ., Proceedings of the 25th Annual Conference of the Finnish Physical Society 1991 1 p (For primary document see N92-10362 01-70)
Avail: NTIS HC/MF A12

The Energetic and Relativistic Nuclear and Electron (ERNE) experiment will investigate the Sun from onboard the Solar and Heliospheric Observatory (SOHO) by measuring the composition and energy spectra of energetic ions from hydrogen up to nickel and by detecting electrons. A preliminary test run has been carried out to estimate the light yield in CsI(Tl) and BGO scintillators by different ions. The prototype of HED, a sensor designed to combine a good mass resolution with a large geometric factor to overcome the problem of low intensity of rare elements, was tested in an accelerator run by using a calcium beam at 35 MeV/n. The beam energy was sufficient for producing light elements penetrating through all the silicon detectors and reaching the CsI(Tl) scintillator. First results were obtained of the identification capabilities of relatively high energy ions. Results of the analysis are presented. ESA

N92-10563# Helsinki Univ. of Technology, Espoo (Finland). Astrophysics Lab.
THE MEASURING MODES AND OBSERVATIONS WITH THE X-RAY SPECTROMETER ARRAY SIXA ONBOARD SPECTRUM-X-GAMMA Abstract Only **c19**

J. Huovelin, H. Paeivike, O. Vilhu, and V. Kaemaeraeinen (Outokumpu Oy, Tapiola, Finland) *In* Oulu Univ., Proceedings of the 25th Annual Conference of the Finnish Physical Society 1991 1 p (For primary document see N92-10362 01-70)
Avail: NTIS HC/MF A12

The Spectrum-X-Gamma satellite is scheduled for launch in 1993, and one of the main instruments on the satellite will be the Silicon X-ray Array (SIXA). A Finnish consortium is constructing this in collaboration with Denmark and USSR. A project at the University of Helsinki is responsible for the definitions of the measurement modes available in SIXA, and planning of its scientific usage. The instrument is a 1024 channel spectrometer with 19 elements in the energy range from 0.5 to 30 keV. It is programmed to work in several modes to adjust for various observing programs and targets. The properties are described, the use of these modes are discussed, and the scientific perspectives of SIXA are reviewed. ESA

N92-10564# Turku Univ. (Finland).
PROPERTIES OF SHOCKED RELATIVISTIC JETS Abstract Only **c93**

Markku Lainela and Esko Valtaoja (Helsinki Univ. of Technology, Espoo, Finland) *In* Oulu Univ., Proceedings of the 25th Annual Conference of the Finnish Physical Society 1991 1 p (For primary document see N92-10362 01-70)
Avail: NTIS HC/MF A12

Variable extragalactic radio sources, associated with the nuclei of galaxies and quasars, are interpreted in terms of a supersonic relativistic jet. It is proposed that radio emission originates both from the quasi steady jet itself and from behind strong shock waves which propagate in the jet. A skeleton model for radio outbursts in active galactic nuclei is described using 3C 273 as example. The construction of a computer code that utilizes this model to study the properties of the radiation from shocked, parsec scale extragalactic jets is presented. Runs of this code with example shock patterns show that the characteristics of the total and polarized flux evolution of variable compact radio sources may be understood in terms of one shock, or a sequence of closely spaced shocks; propagating along a diverging flow. The agreement with observations seems much better for BL Lac type objects than for quasars. ESA

N92-10565# Oulu Univ. (Finland). Dept. of Physics.
CAPS-PLASMA SPECTROMETER FOR THE CASSINI SPACECRAFT Abstract Only **c19**

P. Tanskanen, K. Mursula, V. Kelha, and H. Huomo (Technical Research Centre of Finland, Espoo.) *In its* Proceedings of the 25th Annual Conference of the Finnish Physical Society 1991 1 p (For primary document see N92-10362 01-70)
Avail: NTIS HC/MF A12

The Space Physics group at the Department of Physics, University of Oulu together with the Instrument Laboratory of the Technical Research Center of Finland will take part in the science definition, design and fabrication of the Ion Beam Spectrometer (IBS) to be included as one of the three spectrometers to be built in the CAPS plasma spectrometer instrument. CAPS will also include an ion mass spectrometer and an electron spectrometer. All instruments will be designed and built, using the state of the art technique based on a long term heritage of participating co-investigator institutes. A description the Cassini project, of the IBS instrument as well as of the goals of the mission, is given. ESA

N92-10566# Helsinki Univ. of Technology, Espoo (Finland). Astrophysics Lab.
THEORETICAL STUDIES OF OPTICAL PHENOMENA AND RELATED INVERSE PROBLEMS OF SOLAR SYSTEM BODIES Abstract Only **c89**

Mikko K. J. Kaasalainen, Sauli Jamsa, Kari Lumme, Karri O. Muinonen, and Jouni I. Peltoniemi *In* Oulu Univ., Proceedings of the 25th Annual Conference of the Finnish Physical Society 1991 1 p (For primary document see N92-10362 01-70)
Avail: NTIS HC/MF A12

Various optical processes that take place on the surfaces of solar system bodies are under study. Using theoretical models for such processes, inverse methods based on photopolarimetric observations for obtaining information about these objects are being developed. Most asteroids appear as point like sources, so only variations in their total brightnesses as they rotate can be observed. Such variations contain information about an object's shape and surface light scattering properties. New inversion schemes, called photomorphographic methods, for obtaining as much of this information as possible, were developed. A method, called statistical photoclinometry, for recovering topographic information from planetary images at pixel resolution was developed. Rather than producing the exact topography, the method yields statistical parameters of the surface. The thermal emission from atmosphereless bodies does not behave as if they were smooth spheres. The ways in which porosity and surface roughness at different length scales affect heat transport in the body and

absorption and emission of electromagnetic radiation on the surface, are under investigation. ESA

N92-10567# Oulu Univ. (Finland). Dept. of Physics.
EARTH, URANUS, AND NEPTUNE: A COMPARISON OF THEIR MAGNETOSPHERES Abstract Only **c91**
G. Kremser *In its* Proceedings of the 25th Annual Conference of the Finnish Physical Society 1991 1 p (For primary document see N92-10362 01-70)
Avail: NTIS HC/MF A12

The magnetosphere of Uranus and Neptune have been detected recently by the Voyager 2 space probe. This spacecraft crossed the magnetospheres of Uranus and Neptune in January 1986 and August 1989 respectively. One of the surprising results of these observations was the very large tilt angle between the rotation axes of these planets and the symmetry axes of their magnetic fields. The title angle amounts to 60 degrees for Uranus and to 50 degrees for Neptune. Another important result is that contrary to the magnetosphere of the Earth, the charged particles in the magnetospheres play no role in the interaction with the solar wind. They are therefore designated as empty magnetospheres. These and other observations as well as their implications on the formation of the magnetospheres of these planets are reported and are compared to characteristics of the magnetosphere of the Earth. The variability of the interaction of the solar wind with the planetary environments is pointed out. ESA

N92-10568# Turku Univ. (Finland).
THE STABILITY OF THE PLANETARY TRIANGULAR LAGRANGE POINTS Abstract Only **c91**
Seppo Mikkola (York Univ., Toronto, Ontario) and K. A. Innanen *In* Oulu Univ., Proceedings of the 25th Annual Conference of the Finnish Physical Society 1991 1 p (For primary document see N92-10362 01-70)
Avail: NTIS HC/MF A12

From the starting point of the observed existence of Jupiter's two Trojan asteroid families, the question of whether or not stability of motions at their analogous triangular Lagrange points can exist for the other planets is asked. Numerical body integrations of the solar system show significant indications of such stability for the planets from Venus to Neptune. For the terrestrial planets, during a 2 million year integration, stability clearly exist. Near the Lagrangian L4, L5 points the test particles oscillate in tadpole regions. Beyond this the orbits of the particles remain stable but are horseshoe like. In the outer solar system (from Jupiter to Neptune) calculations indicate (at least) 20 million year stability for tadpole like orbits of the Trojans' of various planets. In 20 June 1990 D. H. Levy and H. E. Homlt discovered the asteroid 1990 MB. After orbit calculation E. Bowell suggested that this object may be a Mars' Trojan. This result is now confirmed. A one million year numerical integration of the orbit, based on the orbital elements calculated from observations, indicated stable motion in the neighborhood of Mars' L5 point. ESA

N92-10569# Oulu Univ. (Finland). Dept. of Astronomy.
VENUS BEHIND THE CLOUDS Abstract Only **c91**
J. Raitala, T. Tormanen, and K. Kauhanen *In its* Proceedings of the 25th Annual Conference of the Finnish Physical Society 1991 1 p (For primary document see N92-10362 01-70)
Avail: NTIS HC/MF A12

Magellan radar orbiter began its imaging task last Autumn. Its Synthetic Aperture Radar allows the surface of Venus be studied from the registered echoes. The 120 m per pixel resolution is 20 to 1000 times better than that of previous Venera 15/16 and Pioneer Venus orbiters, repectively. This year most of the Cytherean surface will be imaged by Magellan. Recent radar images reveal that surface of Venus displays evidences of strong endogenic activity. Volcanism has been important on lowlands which are resurfaced by extrusives in 0.1 to 1 times 10 to the 9th power years. Volcanic domes are abundant and there are also calderas formed by magma reservoir roof collapses. Fault systems are regular over wide areas with major grabens being 100 m to 10 km wide and 200 to 300 km long. Lavas and gas particle flows have been extremely low viscous causing stream like structures. On leeward sides of some volcanic pits there are wind deposits. Most of the impact craters are fresh looking with their interiors filled by radar dark lavas. Some small impact craters are unsymmetric due to the effects of dense atmosphere during fall and impact explosion. ESA

N92-10570# Finnish Meteorological Inst., Helsinki. Dept. of Geophysics.
THE EFFECT OF LATITUDINALLY VARYING SOLAR WIND FLUX ON THE LYMAN ALPHA SKY BACKGROUND Abstract Only **c92**
T. Summanen, E. Kyrola, R. Lallement, and J.-L. Bertaux (Centre National de la Recherche Scientifique, Verrieres-Le Buisson, France) *In* Oulu Univ., Proceedings of the 25th Annual Conference of the Finnish Physical Society 1991 1 p (For primary document see N92-10362 01-70)
Avail: NTIS HC/MF A12

A model for the ionization rate, which accepts any latitudinal structure for the solar wind flux was used. It is possible to study different kinds of models for the latitudinal density structure, if the latitudinal dependence of the solar wind velocity is known (e.g., from interplanetary scintillation observations). Simulated measurements were compared with the Lyman alpha intensity data from Prognoz 5 and 6 satellites. The latest results are presented. The SOHO spacecraft, to be launched in 1995 to the first Lagrange point between the Sun and the Earth, will provide new data from the SWAN (a study of Solar Wind ANisotropies) experiment measuring Lymann alpha intensity. ESA

N92-10571# Oulu Univ. (Finland). Dept. of Astronomy.
STRUCTURE AND EVOLUTION OF TURBULENT PREPLANETARY DISC Abstract Only **c90**
M. Verronen, H. Vanhala, and K. A. Hameen-Anttila *In its* Proceedings of the 25th Annual Conference of the Finnish Physical Society 1991 1 p (For primary document see N92-10362 01-70)
Avail: NTIS HC/MF A12

A model of a small mass (0.03 M sub O) turbulent disc which consists of gas (H 73.2 percent, He 25.0 and H2O 1.4 percent) and dust (Fe 0.4 percent) is presented. Evolution of temperature and disc thickness are discussed and effects of grain growth and varied initial size of patricles are considered. The treatment is based on the theory of collisional systems which is applied to encounters of turbulent eddies as well as impacts of macroscopic particles and gas molecules. Radiational processes are included in the formalism. The theory allows derivation of the critical size of turbulent eddies below which the turbulence decays in an interval required for two adjacent eddies to interchange positions. ESA

N92-10572# Oulu Univ. (Finland). Dept. of Astronomy.
RING SATELLITE INTERACTION IN PLANETARY RINGS Abstract Only **c91**
J. Hanninen, H. Salo, and J. Lukkari *In its* Proceedings of the 25th Annual Conference of the Finnish Physical Society 1991 1 p (For primary document see N92-10362 01-70)
Avail: NTIS HC/MF A12

The ringlet structure observed by the Pioneer and Voyager probes during their Saturn flybys is addressed. Particular interest lies in studying the angular momentum exchange between the satellite and the ring. Besides exerting the torque, the satellite perturbs streamlines of the ring particles. If the perturbation is strong enough, the normal viscous angular momentum transport in the rings typically leading to ringlet spreading can reverse its direction. Theoretical calculations show that this mechanism could be responsible for the sharp edges of the planetary rings. These results are verified in the terms of numerical simulations. ESA

N92-10573# Oulu Univ. (Finland). Dept. of Astronomy.
NUMERICAL SIMULATIONS OF DENSE COLLISIONAL SYSTEMS Abstract Only **c91**
H. Salo *In its* Proceedings of the 25th Annual Conference of

the Finnish Physical Society 1991 1 p (For primary document see N92-10362 01-70)
Avail: NTIS HC/MF A12

The numerical simulation of the dynamical evolution of dense planetary rings, such as Saturn's rings, which is mainly governed by the mutual impacts between macroscopic icy particles, is addressed. The wealth of radial structure in planetary rings, a puzzling feature not always explained in terms of external perturbations, is addressed. Another interesting problem discussed is the influence of self gravity in the dynamics of dense rings. ESA

N92-10574# Turku Univ. (Finland). Lab. of Electronics and Information Technology.
ELECTRONICS OF THE COSMIC RAY AIR SHOWER ARRAY AT TURKU (FINLAND) Abstract Only **c93**
H. Arvela, A.-M. Elo (Oulu Univ., Finland), J. J. Torsti, and E. Valtonen *In* Oulu Univ., Proceedings of the 25th Annual Conference of the Finnish Physical Society 1991 1 p (For primary document see N92-10362 01-70)
Avail: NTIS HC/MF A12

An experimental arrangement to detect extensive air showers with multiple hadrons was constructed at the University of Turku. The apparatus consists of an air shower array (400 sq m), hadron spectrometer and three planes of streamer tubes. The parameters to be determined are the following the size, core location and arrival direction of showers and the distribution of hadrons in showers. The data collecting system is based on Computer Automated Measurement and Control (CAMAC) and GPIB. The shower size and core location are determined by recording the charge of the density detector scintillation pulses. The arrival direction of the shower is calculated by using the data from the fast timing detectors. The hadron composition of the showers can be measured with a hadron spectrometer. The trigger system is composed of the coincidence of core detectors and the central fast timing detector. The data collecting system will be cleared automatically within 1 microsecond in the case of uninteresting event. ESA

N92-10575# Oulu Univ. (Finland). Dept. of Physics.
TEST RESULTS OF DENSITY DETECTORS OF THE COSMIC RAY AIR SHOWER ARRAY IN TURKU (FINLAND) Abstract Only **c93**
A.-M. Elo, H. Arvela (Turku Univ., Finland), J. Peltonen, J. J. Torsti, and E. Valtonen *In its* Proceedings of the 25th Annual Conference of the Finnish Physical Society 1991 1 p (For primary document see N92-10362 01-70)
Avail: NTIS HC/MF A12

The air shower array in Turku is designed to detect multiple hadrons in the cores of small air showers. Test results of the density detector performance and their calibration procedure are presented. The pulse charge distributions of individual photomultiplier tubes as well as the density detectors as a whole are measured in order to check their performance. The shape of the pulse charge spectrum to cosmic ray muons is known and therefore the measured spectra can also be used to calibrate the detectors when the light production of charged particles in the scintillation medium is known. ESA

N92-10576# Turku Univ. (Finland).
SELF-REGULATION MECHANISMS IN GALACTIC DISCS Abstract Only **c90**
Alessandro B. Romeo *In* Oulu Univ., Proceedings of the 25th Annual Conference of the Finnish Physical Society 1991 1 p (For primary document see N92-10362 01-70)
Avail: NTIS HC/MF A12

A global collective heating mechanism leading to a self regulation process of the kind suggested by the spiral structure theory, when both the linear effects of wave-wave interactions and the quasilinear effects of wave-particle interactions at the relevant resonances are taken into account, is proposed. The cold interstellar gas is expected to play a crucial role in ensuring self regulation together with the internal excitation and feedback mechanisms invoked for the maintenance of global spiral modes. As a result, the planar and vertical components of the stellar velocity dispersion are expected to have a different age dependence. Some observational evidences in support of this qualitative prediction are discussed. ESA

N92-10577# Turku Univ. (Finland).
EXPLANATION FOR OPTICAL FREQUENCY DEPENDENT POLARIZATION IN BLAZARS Abstract Only **c93**
L. Valtaoja *In* Oulu Univ., Proceedings of the 25th Annual Conference of the Finnish Physical Society 1991 1 p (For primary document see N92-10362 01-70)
Avail: NTIS HC/MF A12

Shocked jet models have had success in explaining the detailed variations associated with radio outbursts. It is suggested that the early stages of the same shock could cause the observed variable frequency dependence in the optical polarization. The model agrees with the available observations. ESA

N92-10578# Turku Univ. (Finland).
DOUBLE RADIO SOURCES AS STANDARD RODS OF TESTING COSMOLOGICAL MODELS Abstract Only **c90**
M. Valtonen, K. Nilsson, J. Kotilainen, and T. Jaakkola *In* Oulu Univ., Proceedings of the 25th Annual Conference of the Finnish Physical Society 1991 1 p (For primary document see N92-10362 01-70)
Avail: NTIS HC/MF A12

A new large sample of 425 double radio sources is studied. A strong inverse correlation between the absolute brightness and the linear size of a double radio source is shown to exist. Since there is a tendency of observing preferentially bright and thus small doubles at large redshifts and faint (and thus large) doubles at small redshifts, the expected minimum of the angular size is lost in the selection process. The standard rod with absolute luminosity is calculated: it turns out that the calibrated standard rod behaves as expected in standard cosmologies, especially if the mean density parameter of the Universe Omega is less than or equal to 1. The absolute luminosity of the largest double radio sources decays exponentially with the size in Omega less than or equal to 1 Friedman models. This is an agreement with the simple model of Jackson for the decay of brightness in double radio source components. However, it is not possible to exclude totally the Omega equal to 1 models or the static Euclidean Universe on the basis of the double radio source data. ESA

N92-10579# Oulu Univ. (Finland). Dept. of Astronomy.
N-BODY SIMULATIONS OF INTERACTING GALAXIES Abstract Only **c90**
H. Salo *In its* Proceedings of the 25th Annual Conference of the Finnish Physical Society 1991 1 p (For primary document see N92-10362 01-70)
Avail: NTIS HC/MF A12

In order to systematically survey the influence of gravitational encounters, a fast N body code was developed, capable of following the simultaneous evolution of two or more realistically modeled systems, including both stellar and gaseous components. The simulation method is based on the use of overlapping, comoving logarithmic spherical polar grids for the calculation of gravitational potential, with the help of a fast Fourier transformation. Orbital integrations are, however, performed in a cartesian center of mass coordinate system. So far the code has been applied to tidally triggered formation of stellar bars, and their influence on gas flows. The three dimensional version allows for an arbitrary orbital geometry and relative orientation of the systems, and combined with orbit fitting procedures can thus be used for modeling of individual interacting pairs. As an example, numerical models for the M51 system are presented, and compared to observed morphology and velocity fields. ESA

N92-10580# Royal Inst. of Tech., Stockholm (Sweden). Inst. foer Materialfysik.
MATERIALS SCIENCE AND TECHNOLOGY CENTRA IN SWEDEN AND DENMARK: A RESEARCH POLICY FOR THE FUTURE Abstract Only **c23**
A. Flodstroem *In* Oulu Univ., Proceedings of the 25th Annual Conference of the Finnish Physical Society 1991 1 p (For primary document see N92-10362 01-70)
Avail: NTIS HC/MF A12

Materials science and technology policy in general are discussed and the materials center concepts is focused on. Its advantages and disadvantages in promoting interdisciplinary research are discussed and the actual research performed within the Swedish and Danish materials center is reviewed. ESA

N92-10581# Finnish National Fund for Research and Development, Helsinki.
ENERGY SYSTEMS AND THEIR TECHNICAL, ECONOMIC AND ENVIRONMENTAL BOUNDARY CONDITIONS Abstract Only **c44**
Jorma Routti *In* Oulu Univ., Proceedings of the 25th Annual Conference of the Finnish Physical Society 1991 1 p (For primary document see N92-10362 01-70)
Avail: NTIS HC/MF A12

Energy systems consisting of energy supply, transportation conversion and consumption form a cornerstone of industrial societies. Their evolution is dictated by technical, economic and environmental possibilities and constraints, as well as by political and societal aspects. Fossil fuels still cover 80 percent of world energy supplies. Future energy systems are based in both nuclear energy and renewable solar based supplies. Shorter term questions in Finland concentrate on the options of building additional and replacing old electricity whose market share has increased rapidly. Increasing energy efficiencies provide partial solutions, but also new capacity of the order of 1 to 2 GWe based on nuclear, coal, natural gas and/or domestic fuels is needed. Recent studies of thse equations are discussed. ESA

N92-10582# Technical Research Centre of Finland, Espoo. Electrical Engineering Lab.
THE POSSIBILITIES TO CONTROL AND TO REGULATE THE ENERGY CONSUMPTION Abstract Only **c75**
A. Lepisto *In* Oulu Univ, Proceedings of the 25th Annual Conference of the Finnish Physical Society 1991 1 p (For primary document see N92-10362 01-70)
Avail: NTIS HC/MF A12

The prognostication of energy consumption and adaptation of energy to consumption are discussed. In Finland, the possibilities for more efficient energy economy are quite limited, and thus to achieve the progress of other countries, measures must be scaled toughly. ESA

N92-10583# Helsinki Univ. of Technology, Espoo (Finland). Dept. of Technical Physics.
FUSION ENERGY: STATUS AND PROSPECTS Abstract Only **c44**
Rainer Salomaa *In* Oulu Univ., Proceedings of the 25th Annual Conference of the Finnish Physical Society 1991 1 p (For primary document see N92-10362 01-70)
Avail: NTIS HC/MF A12

A review of the present state of the international fusion research is given. In the largest tokamak devices (JET, TFTR, JT-60) fusion relevant temperatures are routinely obtained and the scientific feasibility of plasma confinement has been demonstrated. Plans concerning the next step are described. A critical view is presented on questions as to what extent the generic advantages of fusion (availability, sufficiency, safety, environmental acceptability, etc.) can be exploited in a practical power reactor where the formidable technological problems call for compromises. ESA

N92-10584# Helsinki Univ. of Technology, Espoo (Finland). Dept. of Technical Physics.
SOLAR ENERGY IN MITIGATING GLOBAL ENVIRONMENTAL PROBLEMS Abstract Only **c44**
P. D. Lund *In* Oulu Univ., Proceedings of the 25th Annual Conference of the Finnish Physical Society 1991 1 p (For primary document see N92-10362 01-70)
Avail: NTIS HC/MF A12

The potential of solar energy is discussed. Solar energy is an inherently clean energy source and may thus have an important contribution in mitigating global environmental problems. For global climate change questions with a strong coupling with the growing energy demands of the less developed countries situated around the Sun belt region, solar energy offers also an interesting future possibility. ESA

N92-10585# Imatran Voima Oy, Helsinki (Finland).
NUCLEAR ENERGY: ITS STRENGTHS, WEAKNESSES AND ROLE IN FINLAND Abstract Only **c73**
A. Ruuskanen *In* Oulu Univ., Proceedings of the 25th Annual Conference of the Finnish Physical Society 1991 1 p (For primary document see N92-10362 01-70)
Avail: NTIS HC/MF A12

Nuclear energy has, in principle, various strengths as an energy form. In spite of the drawbacks of nuclear power, the benefits exceed its cost. That is why power companies in Finland have decided to apply for the construction, of the fifth nuclear power plant during Spring 1991. Electricity consumption is increasing, and new power producing capacity will be needed. Nuclear power is seen as the best alternative for producing baseload power in Finnish conditions. ESA

N92-10586# Imatran Voima Oy, Vantaa (Finland).
FOSSIL FUELS AND THE ENVIRONMENT Abstract Only **c45**
H. Niininen *In* Oulu Univ., Proceedings of the 25th Annual Conference of the Finnish Physical Society 1991 1 p (For primary document see N92-10362 01-70)
Avail: NTIS HC/MF A12

In 1989, fossil fuels accounted for slightly over 50 percent of Finland's primary energy use; globally, the corresponding figure was over 80 percent. Both percentages are rising. Finland's emissions in their own acid load account for 20 to 25 percent. The development of the purification and combustion technologies for reducing acid emissions has been rapid. International negociations on restricting the greenhouse gas emissions have been started. So far it is not practically possible to separate carbon dioxide from flue gases. Thus the solution has to be found in energy conservation and replacement of fuels by energy sources which are either free from or produce less CO2. The initial setup in Finland for international CO2 restrictions is poor, because most of the thinkable means for reducing emissions are already in exceptionally wide use in the country. ESA

N92-10587# Helsinki Univ. of Technology, Espoo (Finland). Dept. of Meteorology.
THE GREENHOUSE EFFECT Abstract Only **c45**
E. Holopainen *In* Oulu Univ., Proceedings of the 25th Annual Conference of the Finnish Physical Society 1991 1 p (For primary document see N92-10362 01-70)
Avail: NTIS HC/MF A12

The atmospheric concentration of carbon dioxide has increased by about 25 since preindustrial times. During recent decades this increase has been primarily due to burning of fossil fuels. Concentrations of some other greenhouse gases such as the CFC's, methane and nitrous oxide are also increasing. Numerical climate models, based on laws of physics, predict that increase of atmopsheric greehouse gases will eventually warm the climate. Associated with the warming there will be other changes, such as the rise of the gobal mean sea level. Confidence on the predictions of regional climate changes is still low. Some of the regional features in the model results deserve attention, however. In high latitudes the wintertime increase of temperature and precipitation is expected to be much larger than on the average over the

globe. There may be reduction in summertime precipitation and soil moisture e.g., in Southern Europe and central North America. According to recent model results, the Gulf Stream may weaken when the climate warms. If this happens, the wintertime warming in Scandinavia could be smaller than the average warming in the high northern latitudes. ESA

N92-10588# Max-Planck-Inst. fuer Physik und Astrophysik, Garching (Germany, F.R.).
[ACTIVITIES REPORT OF THE WERNER HEISENBERG INSTITUTE FOR PHYSICS, MUNICH (FEDERAL REPUBLIC OF GERMANY)] Annual Report, 1990
[WERNER-HEISENBERG-INSTITUT FUER PHYSIK MUENCHEN, JAHRESBERICHT 1990]
Dec. 1990 152 p In GERMAN
(ISSN-0173-6256; ETN-91-99833) Copyright Avail: NTIS HC/MF A08

The research activities are covered from October 1989 to 1990. Elementary particles and their interactions were the subject of theoretical and experimental studies. Experiments and studies carried out in the two experimental divisions and in the theoretical division are reported. The organization of the technical division is presented. The cooperation with industrial companies, scientific publications, conferences, in particular the workshop on two dimensional quantum field theories, are reported. For individual titles, see N92-10589 through N92-10592.

N92-10589# Max-Planck-Inst. fuer Physik und Astrophysik, Garching (Germany, F.R.).
THE THEORETICAL DIVISION (OF THE WERNER HEISENBERG INSTITUTE FOR PHYSICS) [THEORETISCHE ABTEILUNG]
H.-P. Duerr, L. Stodolsky, J. Wess, and W. Zimmermann *In its* Activities Report on the Werner Heisenberg Institute for Physics, Munich (Fed. Republic of Germany) Dec. 1990 p 1-13 In GERMAN (For primary document see N92-10588 01-70)
Copyright Avail: NTIS HC/MF A08

Progress achieved from Oct. 1989 to Sep. 1990 within the theoretical division was reported in the fields of perturbation theory renormalizing, statistical mechanics methods in quantized field theory, standard model quantized field theory problems, elementary particle physics, gravitation, cosmology, nonrelativistic multiple particle physics, and history of physics. Editorial publications are given. ESA

N92-10590# Max-Planck-Inst. fuer Physik und Astrophysik, Garching (Germany, F.R.).
THE A EXPERIMENTAL DIVISION (OF THE WERNER HEISENBERG INSTITUTE FOR PHYSICS) [EXPERIMENTELLE ABTEILUNG]
G. Buschhorn and N. Schmitz *In its* Activities Report of the Werner Heisenberg Institute for Physics, Munich (Fed. Republic of Germany) Dec. 1990 p 14-51 In GERMAN (For primary document see N92-10588 01-70)
Copyright Avail: NTIS HC/MF A08

Progress achieved within the A experimental division from Oct. 1989 to Sep. 1990 is reported, on the following themes: the interaction of neutrinos and antineutrinos with protons in the bubble chamber, the interaction of neutrinos and antineutrinos with neon neuclei in the bubble chamber, the deep inelastic lepton nucleon scattering in muon stream, the shocks of relativistic ions on atom nuclei, the tevatron accelerator of the Fermi laboratory, the PETRA electron positron storage ring with CELLO detector, the H1 detector for the HERA electron proton storage ring, the development of a low energy particle detector, electronics for experiments, data processing, and evaluating system. ESA

N92-10591# Max-Planck-Inst. fuer Physik und Astrophysik, Garching (Germany, F.R.).
THE B EXPERIMENTAL DIVISION (OF THE WERNER HEISENBERG INSTITUTE OF PHYSICS) [EXPERIMENTELLE ABTEILUNG B]
U. Stierlin *In its* Activities Report of the Werner Heisenberg Institute for Physics, Munich (Fed. Republic of Germany) Dec. 1990 p 52-76 In GERMAN (For primary document see N92-10588 01-70)
Copyright Avail: NTIS HC/MF A08

Progress achieved within the B experimental division from Oct. 1989 to Sep. 1990 is reported on the following themes: the ALEPH experiment, the ALEPH minivertex detector, the High Energy Gamma Ray Astronomy (HEGRA) experiment, semiconductor detectors and microelectronics, calorimeter improvement and particle identification, drift velocity in electrical and magnetic fields, and the production and dissociation of particles with the charm quantum number. ESA

N92-10592# Max-Planck-Inst. fuer Physik und Astrophysik, Garching (Germany, F.R.).
THE TECHNICAL DIVISION (OF THE WERNER HEISENBERG INSTITUTE OF PHYSICS) [TECHNISCHE ABTEILUNG]
H. Schmuecker *In its* Activities Report on the Werner Heisenberg Institute for Physics, Munich (Fed. Republic of Germany) Dec. 1990 p 77-81 In GERMAN (For primary document see N92-10588 01-70)
Copyright Avail: NTIS HC/MF A08

The organization of the technical division, whose task is to design and build devices and appliances for physical experiments, is presented. From Oct. 1989 to Sep. 1990, the tasks covered the H detector for HERA, the ALEPH minivertex detector, the Time Projection Chamber (TPC), and the High Energy Gamma Ray Astronomy (HEGRA) detectors. The tasks carried out in coooperation with industrial companies are reported. ESA

N92-10593*# Ohio State Univ., Columbus. ElectroScience Lab.
CONSTITUTIVE PARAMETER EXTRACTION FOR HEATED MATERIALS Annual Report
J. Munk and A. Dominek Feb. 1991 43 p
(Grant NAG3-1108)
(NASA-CR-186208; NAS 1.26:186208; Rept-723224-2) Avail: NTIS HC/MF A03 CSCL 20C

The focus is the determination of the electrical constitutive paramaters of materials with general complex epsilon and mu values at elevated temperatures. Measurement fixtures and techniques are evaluated for frequencies between 8 and 12 GHz using a rectangular waveguide with the sample completely filling the fixture. Three different measurement techniques are evaluated to obtain the necessary measured quantities for parameter extraction. The most desirable technique used two reflection measurements from material samples of different thickness backed with a short. Temperatures up to 600 F were investigated.
Author

N92-10594# National Academy of Sciences - National Research Council, Washington, DC. Board on Physics and Astronomy.
PLASMA SCIENCE COMMITTEE (PLSC)
17 Dec. 1990 4 p
(Contract DE-FG05-88ER-53279)
(DE91-018011; DOE/ER-53279/1) Avail: NTIS HC/MF A01

The Plasma Science Committee (PLSC) is a standing committee under the auspices of the Board on Physics and Astronomy, Commission on Physical Sciences, Mathematics, and Applications of the National Academy of Sciences - National Research Council. Plasma sciences represent a broad and diverse field. The PLSC has accepted the responsibility of monitoring the continuing development and assessing the general health of the field as whole. Although select advisory bodies have been created to address specific issues that affect plasma science, such as the Fusion Policy Advisory Committee (FPAC), the PLSC provides a focus for the plasma science community that is unique and essential. The membership of the PLSC is drawn from research laboratories in universities, industry, and government. Areas of expertise on the committee include accelerators and beams, space physics, astrophysics, computational physics and applied mathematics, fusion plasmas, fundamental experiments and theory, radiation sources, low temperature plasmas, and plasma-surface

interactions. The PLSC is well prepared to respond to requests for studies on specific issues. DOE

N92-10595# Texas Univ., Austin. Inst. for Fusion Studies.
VLASOV-MAXWELL SYSTEM: 2-D EQUILIBRIA, REVERSED FIELD PINCHES
S. M. Mahajan, W. Q. Li, and A. Sen (International Centre for Theoretical Physics, Trieste, Italy) Aug. 1991 30 p
(Contract DE-FG05-80ET-53088)
(DE91-018421; DOE/ET-53088/512; IFSR-512) Avail: NTIS HC/MF A03

Exact solutions to the Vlasov-Maxwell system in the two dimensional circular cylindrical model are presented. The magnetic surfaces are shifted circles for the m = 1 case, where the shift is determined by a parameter (epsilon); (epsilon) = 0 gives concentric circles and represents 1-D solutions. For m greater than or equal to 2 cases, the solutions are singular at the origin and the magnetic surfaces contain islands and separatrices. An improved one dimensional model with currents in both the axial and azimuthal directions is also presented. It is shown that this simple finite pressure model can yield field reversed equilibria in the presence of appropriate boundary constraints. DOE

N92-10596# New York Univ., New York. Courant Inst. of Mathematical Sciences.
ANALYTICAL AND COMPUTATIONAL MATHEMATICAL PHYSICS Progress Report, 1 Jan. - 31 Dec. 1991
1991 16 p
(Contract DE-FG02-88ER-25053)
(DE91-018965; DOE/ER-25053/6) Avail: NTIS HC/MF A03

This report briefly discusses research on computational methods for gas dynamics and solidification, and mesh generating techniques. DOE

N92-10597# Army Lab. Command, Fort Monmouth, NJ. Electronics Technology and Devices Lab.
AN OVERVIEW OF MODERN PERMANENT MAGNET DESIGN Technical Report, 1970 - 1990
Herbert A. Leupold and Ernest Potenziani, II Aug. 1990 69 p
(DA Proj. 1L1-61102-AH-47)
(AD-A240144; SLCET-TR-90-6) Avail: NTIS HC/MF A04
CSCL 20/3

The high-energy product magnet materials have made possible many (compact, light weight) high-field magnetic flux sources that were not practicable before their advent. Near-revolutionary device consequences are unfolding as a result. This report discusses the approaches to the design of such devices and gives various examples that apply to electron-beam devices, nuclear magnetic resonance, electric motors, and others. GRA

71 ACOUSTICS

Includes sound generation, transmission and attenuation. For noise pollution see *45 Environmental Pollution.*

N92-10598*# National Aeronautics and Space Administration. Langley Research Center, Hampton, VA.
AEROACOUSTICS OF FLIGHT VEHICLES: THEORY AND PRACTICE. VOLUME 1: NOISE SOURCES
Harvey H. Hubbard, ed. Washington Aug. 1991 601 p
Sponsored in cooperation with Wright Research and Development Center and Army Aviation Systems Command
(Contract F33615-84-C-3202)
(NASA-RP-1258-Vol-1; L-16926-Vol-1; NAS 1.61:1258-Vol-1; WRDC-TR-90-3052-Vol-1) Avail: NTIS HC/MF A99 CSCL 20A

Methodology recommended to evaluate aeroacoustic related problems is provided, and approaches to their solutions are suggested without extensive tables, nomographs, and derivations. Orientation is toward flight vehicles and emphasis is on underlying physical concepts. Theoretical, experimental, and applied aspects are covered, including the main formulations and comparisons of theory and experiment. The topics covered include: propeller and propfan noise, rotor noise, turbomachinery noise, jet noise classical theory and experiments, noise from turbulent shear flows, jet noise generated by large-scale coherent motion, airframe noise, propulsive lift noise, combustion and core noise, and sonic booms. For individual titles, see N92-10599 through N92-10608.

N92-10599*# Hamilton Standard, Windsor Locks, CT.
PROPELLER AND PROPFAN NOISE
B. Magliozzi, D. B. Hanson, and R. K. Amiet (AMI, Wooster, OH.) *In* NASA. Langley Research Center, Aeroacoustics of Flight Vehicles: Theory and Practice. Volume 1: Noise Sources Aug. 1991 p 1-64 (For primary document see N92-10598 01-71)
Avail: NTIS HC/MF A99 CSCL 20A

The characteristics of propellers, their noise-generating mechanisms, propeller noise theories and calculation procedures, and sound propagation effects are described. Comparisons of predictions and measurements, and means for controlling propeller noise are described. Author

N92-10600*# National Aeronautics and Space Administration. Ames Research Center, Moffett Field, CA.
ROTOR NOISE
F. H. Schmitz *In* NASA. Langley Research Center, Aeroacoustics of Flight Vehicles: Theory and Practice. Volume 1: Noise Sources Aug. 1991 p 65-149 (For primary document see N92-10598 01-71)
Avail: NTIS HC/MF A99 CSCL 20A

The physical characteristics and sources of rotorcraft noise as they exist today are presented. Emphasis is on helicopter-like vehicles, that is, on rotorcraft in nonaxial flight. The mechanisms of rotor noise are reviewed in a simple physical manner for the most dominant sources of rotorcraft noise. With simple models, the characteristic time- and frequency-domain features of these noise sources are presented for idealized cases. Full-scale data on several rotorcraft are then reviewed to allow for the easy identification of the type and extent of the radiating noise. Methods and limitations of using scaled models to test for several noise sources are subsequently presented. Theoretical prediction methods are then discussed and compared with experimental data taken under very controlled conditions. Finally, some promising noise reduction technology is reviewed. Author

N92-10601*# National Aeronautics and Space Administration. Lewis Research Center, Cleveland, OH.
TURBOMACHINERY NOISE
John F. Groeneweg, Thomas G. Sofrin, Edward J. Rice, and Phillip R. Gliebe (General Electric Co., Cincinnati, OH.) *In* NASA. Langley Research Center, Aeroacoustics of Flight Vehicles: Theory and Practice. Volume 1: Noise Sources Aug. 1991 p 151-209 (For primary document see N92-10598 01-71)
Avail: NTIS HC/MF A99 CSCL 20A

Summarized here are key advances in experimental techniques and theoretical applications which point the way to a broad understanding and control of turbomachinery noise. On the experimental side, the development of effective inflow control techniques makes it possible to conduct, in ground based facilities, definitive experiments in internally controlled blade row interactions. Results can now be valid indicators of flight behavior and can provide a firm base for comparison with analytical results. Inflow control coupled with detailed diagnostic tools such as blade pressure measurements can be used to uncover the more subtle mechanisms such as rotor strut interaction, which can set tone levels for some engine configurations. Initial mappings of rotor wake-vortex flow fields have provided a data base for a first generation semiempirical flow disturbance model. Laser velocimetry offers a nonintrusive method for validating and improving the model. Digital data systems and signal processing algorithms are bringing mode measurement closer to a working tool that can be frequently applied to a real machine such as a turbofan engine. On the analytical side, models of most of the links in the chain from turbomachine blade source to far field observation point have been formulated. Three dimensional lifting surface theory for blade rows,

including source noncompactness and cascade effects, blade row transmission models incorporating mode and frequency scattering, and modal radiation calculations, including hybrid numerical-analytical approaches, are tools which await further application. Author

N92-10602*# Southampton Univ. (England).
JET NOISE CLASSICAL THEORY AND EXPERIMENTS
G. M. Lilley *In* NASA. Langley Research Center, Aeroacoustics of Flight Vehicles: Theory and Practice. Volume 1: Noise Sources Aug. 1991 p 211-289 (For primary document see N92-10598 01-71)
Avail: NTIS HC/MF A99 CSCL 20A

Lighthill's theory of aerodynamic noise is presented as the foundation on which to build all other theories of aerodynamic noise. The application of the Lighthill acoustic analogy to the estimation of the characteristics of the noise radiated from the jets is central. Attention is given to the assumptions on which the Lighthill acoustic analogy is based and it is shown why the theory gives results different from experiment when flow-acoustic interaction occurs. The details of flow-acoustic interaction are invariably unavailable to provide the necessary fine adjustments to the Lighthill source function to render it such that the noise radiation as calculated is exact. The alternative approaches to the understanding of aerodynamic noise theory are discussed. The emphasis is placed on the flow-acoustic interaction and such theories as are required to complement the results obtained by application of Lighthill's acoustic analogy. The authors discuss some of the dominant features of the mean flow and the turbulent structure of a jet as a guide to modeling the T sub ij four-order covariance, which is central to applications involving Lighthill's acoustic analogy. The results obtained from the acoustic analogy model are compared with experimental data obtained by application of the polar correlation technique to both a model-scale jet and a full-scale jet engine. The relatively close agreement is evidence that the flow field data are pertinent to the description of the acoustic analogy model. A brief description is given of attempts to reduce jet noise without incurring an undue penalty in the loss of nozzle efficiency. Finally, the importance of good, reliable, and accurate experimental data in all studies of aerodynamic noise is stressed. Author

N92-10603*# National Aeronautics and Space Administration. Lewis Research Center, Cleveland, OH.
NOISE FROM TURBULENT SHEAR FLOWS
M. E. Goldstein *In* NASA. Langley Research Center, Aeroacoustics of Flight Vehicles: Theory and Practice. Volume 1: Noise Sources Aug. 1991 p 291-310 (For primary document see N92-10598 01-71)
Avail: NTIS HC/MF A99 CSCL 20A

The generation of sound in turbulent shear flows with high Reynolds numbers is discussed. Solid surface effects, representation of incident turbulence, sound generation and the role of instability waves, sound generation by turbulence interacting with itself (the jet noise problem), compressible Rayleigh equations, sound generation from streamwise variations in mean flow, complex turbulent flows, and supersonic flows are among the topics discussed. Author

N92-10604*# Florida State Univ., Tallahassee.
JET NOISE GENERATED BY LARGE-SCALE COHERENT MOTION
Christopher K. W. Tam *In* NASA. Langley Research Center, Aeroacoustics of Flight Vehicles: Theory and Practice. Volume 1: Noise Sources Aug. 1991 p 311-390 (For primary document see N92-10598 01-71)
Avail: NTIS HC/MF A99 CSCL 20A

The noise generated by large scale turbulence structures and instability waves of jets is discussed. Emphasis is placed on supersonic jets with moderate to high Reynolds numbers. This is because it is in these jets that unambiguous experimental and theoretical evidence is found indicating that large turbulence structures and instability waves are directly responsible for generating the dominant part of the noise. For subsonic jets similar large turbulence structures and instability waves do play a crucial role in the dynamics, spread, and mixing of the jet fluid. However, at subsonic convection speeds, they do not appear to be efficient noise generators. Many investigators believe that the dominant noise source of subsonic jets is, in fact, the small scale turbulence. As yet, this belief has not yet received universal acceptance. The issues involved are complicated and are not easy to resolve. Author

N92-10605*# Cambridge Univ. (England).
AIRFRAME NOISE
David G. Crighton *In* NASA. Langley Research Center, Aeroacoustics of Flight Vehicles: Theory and Practice. Volume 1: Noise Sources Aug. 1991 p 391-447 (For primary document see N92-10598 01-71)
Avail: NTIS HC/MF A99 CSCL 20A

Current understanding of airframe noise was reviewed as represented by experiment at model and full scale, by theoretical modeling, and by empirical correlation models. The principal component sources are associated with the trailing edges of wing and tail, deflected trailing edge flaps, flap side edges, leading edge flaps or slats, undercarriage gear elements, gear wheel wells, fuselage and wing boundary layers, and panel vibration, together with many minor protrusions like radio antennas and air conditioning intakes which may contribute significantly to perceived noise. There are also possibilities for interactions between the various mechanisms. With current engine technology, the principal airframe noise mechanisms dominate only at low frequencies, typically less than 1 kHz and often much lower, but further reduction of turbomachinery noise in particular may make airframe noise the principal element of approach noise at frequencies in the sensitive range. Author

N92-10606*# Norden, Norwalk, CT.
PROPULSIVE LIFT NOISE
Martin R. Fink *In* NASA. Langley Research Center, Aeroacoustics of Flight Vehicles: Theory and Practice. Volume 1: Noise Sources Aug. 1991 p 449-481 (For primary document see N92-10598 01-71)
Avail: NTIS HC/MF A99 CSCL 20A

Propulsive life noise is the increase in noise that occurs when airframe surfaces are placed in the propulsive system's exhaust to increase their lift force. Increased local flow velocities and turbulence levels, due to the propulsive system exhaust gases passing along the airframe lifting surfaces, cause an increase in maximum lift coefficient. The airplane's flight speed required for takeoff and landing can then be significantly reduced, allowing operation from shorter runways than those of conventional commercial airports. Unfortunately, interaction of high velocity turbulent exhaust flow with the airframe's solid surfaces generates additional noise radiation. Aeroacoustic processes that cause propulsive lift noise also are present in airframe noise and propulsive system installation noise. Research studies of propulsive lift noise led to development of improved methods of predicting noise radiation from surfaces in turbulent flows. Noise reduction and prediction methods of aircraft noise are discussed. Author

N92-10607*# National Aeronautics and Space Administration. Lewis Research Center, Cleveland, OH.
COMBUSTION AND CORE NOISE
J. Robert Mahan (Virginia Polytechnic Inst. and State Univ., Blacksburg.) and Allen Karchmer *In* NASA. Langley Research Center, Aeroacoustics of Flight Vehicles: Theory and Practice. Volume 1: Noise Sources Aug. 1991 p 483-517 (For primary document see N92-10598 01-71)
Avail: NTIS HC/MF A99 CSCL 20A

Two types of aircraft power plant are considered: the gas turbine and the reciprocating engine. The engine types considered are: the reciprocating engine, the turbojet engine, the turboprop engine, and the turbofan engine. Combustion noise in gas turbine engines is discussed, and reciprocating-engine combustion noise is also briefly described. The following subject areas are covered:

configuration variables, operational variables, characteristics of combustion and core noise, sources of combustion noise, combustion noise theory and comparison with experiment, available prediction methods, diagnostic techniques, measurement techniques, data interpretation, and example applications. Author

N92-10608*# Eagle Engineering, Inc., Hampton, VA.
SONIC BOOM
Domenic J. Maglieri and Kenneth J. Plotkin (Wyle Labs., Inc., Arlington, VA.) *In* NASA. Langley Research Center, Aeroacoustics of Flight Vehicles: Theory and Practice. Volume 1: Noise Sources Aug. 1991 p 519-561 (For primary document see N92-10598 01-71)
Avail: NTIS HC/MF A99 CSCL 20A

A status of the knowledge of sonic booms is provided, with emphasis on their generation, propagation and prediction. For completeness, however, material related to the potential for sonic boom alleviation and the response to sonic booms is also included. The material is presented in the following sections: (1) nature of sonic booms; (2) review and status of theory; (3) measurements and predictions; (4) sonic boom minimization; and (5) responses to sonic booms. Author

N92-10609*# National Aeronautics and Space Administration. Pasadena Office, CA.
ACOUSTIC DEVICE AND METHOD FOR MEASURING GAS DENSITIES Patent Application
Parthasarathy Shakkottai, inventor (to NASA), Eug Y. Kwack, inventor (to NASA), and Lloyd Back, inventor (to NASA) (Jet Propulsion Lab., California Inst. of Tech., Pasadena.) 19 Feb. 1991 35 p
(Contract NAS7-918)
(NASA-Case-NPO-18155-1-CU; NAS 1.71:NPO-18155-1-CU; US-Patent-Appl-SN-658477) Avail: NTIS HC/MF A03 CSCL 20A

Density measurements can be made in a gas contained in a flow through enclosure by measuring the sound pressure level at a receiver or microphone located near a dipole sound source which is driven at constant velocity amplitude at low frequencies. Analytical results, which are provided in terms of geometrical parameters, wave numbers, and sound source type for systems of this invention, agree well with published data. The relatively simple designs feature a transmitter transducer at the closed end of a small tube and a receiver transducer on the circumference of the small tube located a small distance away from the transmitter. The transmitter should be a dipole operated at low frequency with the kL value preferable less that about 0.3. NASA

N92-10610# Acoustical Society of America, New York, NY.
US TAG FOR ISO/TC43, ACOUSTICS, IEC/TC29 ELECTROACOUSTICS, ISO/TC108/SC4 HUMAN EXPOSURE TO MECHANICAL VIBRATION AND SHOCK: MINUTES OF THE ACCREDITED STANDARDS COMMITTEE ON BIOACOUSTICS, S3
2 May 1991 79 p Meeting held in Baltimore, MD, 2 May 1991
(AD-A239918) Avail: NTIS HC/MF A05 CSCL 06/5

This symposia included the following topics: coupler calibration of earphones, human exposure to mechanical vibration and shock, method for calibration of bone conduction vibrator, hearing aids, criteria for background noise for audiometer testing, hearing conservation criteria, measurement of speech levels, measurement of acoustic impedance and admittance of the ear. GRA

N92-10611# Army Aeromedical Research Lab., Fort Rucker, AL.
THE HAZARD OF EXPOSURE TO IMPULSE NOISE AS A FUNCTION OF FREQUENCY, VOLUME 1 Final Report
James H. Patterson, Jr., Melvin Carrier, Jr., Kevin Bordwell, Ilia M. Gautier, and Roger P. Hamernik Jun. 1991 76 p
(DA Proj. 3E1-62777-A-878)
(AD-A239992; USAARL-91-18-Vol-1) Avail: NTIS HC/MF A05 CSCL 20/1

The energy spectrum of a noise is known to be an important variable in determining the effects of a traumatic exposure. However, existing criteria for exposure to impulse noise do not consider the frequency spectrum of an impulse as a variable in the evaluation of the hazards to the auditory system. This report presents the results of a study that was designed to determine the relative potential that impulsive energy concentrated at different frequencies has in causing auditory system trauma. One hundred and eighteen (118) chinchilla, divided into 20 groups with 5 to 7 animals per group, were used in these experiments. Pre- and post-exposure hearing thresholds were measured at 10 test frequencies between 0.125 and 8 kHz on each animal using avoidance conditioning procedures. Quantitative histology (cochleograms) was used to determine the extent and pattern of the sensory cell damage. The noise exposure stimuli consisted of six different computer-generated narrow band tone bursts having center frequencies located at 0.260, 0.775, 1.350, 2.450, and 3.550 kHz. Each narrow band exposure stimulus was presented at two to four different intensities. An analysis of the audiometric and histological data allowed frequency weighing functions to be derived. GRA

N92-10612# Duke Univ., Durham, NC. Dept. of Psychology.
ON CATEGORIZING SOUNDS Final Report, 1 Sep. 1987 - 30 Jun. 1991
Gregory R. Lockhead 7 Aug. 1991 46 p
(Grant AF-AFOSR-0353-87; AF Proj. 2313)
(AD-A240006; AFOSR-91-0731TR) Avail: NTIS HC/MF A03 CSCL 05/8

Context is important when people judge sounds, or attributes of sounds, or other stimuli. It is shown how judgments depend on what sounds recently occurred (sequence effects), on how those sounds differ from one another (range effects), on the distribution of those differences (set effects), on what subjects are told about the situation (task effects), and on what subjects are told about their performance (feedback effects). Each of these factors determines the overall mean and variability of response times and response choices, which are the standard measures, when people judge attribute amounts. Trial-by-trial analysis of the data show these factors also determine performance on individual trials. Moreover, these momentary data cannot be predicted from the overall data. The opposite is not true; the averaged data can be predicted from the momentary details. These results are consistent with a model having two simple assumptions: successive sounds (not just their attributes) assimilate toward one another in memory, and judgments are based on comparisons of these remembered events. It is suggested that relations between attributes, rather than the magnitudes of the attributes themselves, are the basis for judgment. GRA

72 ATOMIC AND MOLECULAR PHYSICS

Includes atomic structure, electron properties, and molecular spectra.

N92-10613*# Alabama Univ., Huntsville. Center for Space Plasma and Aeronomic Research.
DIFFERENTIAL COLLISION CROSS-SECTIONS FOR ATOMIC OXYGEN: ANALYSIS OF SPACE FLIGHT INSTRUMENTS FOR SOLAR TERRESTRIAL PHYSICS Final Technical Progress Report, 7 Nov. 1989 - 6 Nov. 1990
Douglas G. Torr 19 Feb. 1991 88 p
(Contract NAS8-36955)
(NASA-CR-184235; NAS 1.26:184235; OAL91-2) Avail: NTIS HC/MF A05 CSCL 20H

A summary of the status of the Cross-section Facility at MSFC is presented. A facility was designed, fabricated, assembled, tested, and operated for measurement of differential scattering cross sections important to understand the induced environment for a vehicle (e.g., Space Station) in low earth orbit. A user's manual for the facility is also presented. The performance of the facility was evaluated and found to be satisfactory in all the essential areas. Differential scattering cross sections were measured and

results for the scattering measurements are included. Input to the development of the Ultraviolet Imager Optical System is also discussed. Design, fabrication, and evaluation of UV filters using a four-layer aluminum base are reported. Author

N92-10614# Rutherford Appleton Lab., Chilton (England).
SCALE DEPENDENCE OF LAMBDA SUB (MS BAR) FROM DEEP INELASTIC SCATTERING
A. D. Martin, W. J. Stirling (Durham Univ., England), and R. G. Roberts May 1991 15 p
(RAL-91-044; DTP/91/24; ETN-91-99885) Avail: NTIS HC/MF A03

Precision measurements of lambda sub (MS bar) from deep inelastic scattering traditionally use a fixed renormalization scale mu Q. This is in contrast to measurements in positron electron annihilation, where scale dependence is an important source of uncertainty on the value of lambda sub (MS bar). The previous determination of lambda sub (MS bar) is extended to allow for different scale choices. It is found that the previous value of alpha sub s (M sub Z = between (0.109 + 0.004) and (0.109 - 0.005) becomes alpha sub s (M sub Z = between (0.109 + 0.007) and (0.109 - 0.008) when a reasonable variation of scale is included. The implications of this result for recent attempts to obtain information on the scale of supersymmetry from coupling constant unification are discussed. ESA

N92-10615* Max-Planck-Inst. fuer Physik und Astrophysik, Garching (Germany, F.R.). Inst. fuer Extraterrestrische Physik.
PARSEC-SCALE PENETRATION OF UV INTO MOLECULAR CLOUDS: CII 158 MICRON MAPPING OF W3, NGC 1977, AND NGC 2023
J. E. Howe, D. T. Jaffe, R. Genzel, and G. J. Stacey (California Univ., Berkeley.) Dec. 1990 28 p Submitted for publication
Sponsored in part by NATO
(Grant NAG2-419)
(NASA-CR-188969; NAS 1.26:188969; MPE-Preprint-199; ETN-91-90020) Copyright Avail: Fachinformationszentrum Karlsruhe, 7514 Eggenstein-Leopoldshafen 2, Fed. Republic of Germany CSCL 20H

The spatial distribution of the 158 microns CII fine structure line in the galactic sources W3, NGC 1977, and NGC 2023 is mapped. The emission arises from warm (100 to 300 K), dense photodissociation regions at the surface of molecular gas. In all three sources, the emission extends over parsec scales or greater. For W3 and NGC 1977, where the UV source/molecular cloud geometry presents an edge on view of the variation of CII intensity into the molecular gas, two dimensional models of the CII emission which include the effects of gas clumping and scattering by dust on the transport of UV photons are constructed. The observed CII distribution and intensity is well modeled by a clumpy or filamentary distribution to the molecular gas, with a clump/interclump gas density ratio of 100 or more, which allows deep penetration of carbon ionizing UV photons into the clouds. The penetration of UV into clumped molecular clouds may also explain the extended far IR continuum emission from these sources. The total luminosity of CII emission from a clumpy molecular cloud with adjacent or embedded octave band stars can be as much as an order of magnitude higher than the CII luminosity of a uniform cloud. In addition, the extended penetration of UV into molecular clouds will affect the abundances of atomic and molecular species and increase the fractional ionization of interclump gas and UV illuminated clump surfaces. ESA

N92-10616# Cornell Univ., Ithaca, NY.
EXPERIMENTAL STUDY OF INTERACTIONS OF HIGHLY CHARGED IONS WITH ATOMS AT keV ENERGIES
V. O. Kostroun 2 Jul. 1991 8 p
(Contract DE-FG02-86ER-13519)
(DE91-016962; DOE/ER-13519/5) Avail: NTIS HC/MF A02

This Progress Report describes the experimental work carried out, and the work in progress, at the Cornell EBIS Laboratory during the period 2/16/1990 to 6/30/1991. During this period, the absolute values of the total, one and two electron transfer cross sections for highly charged argon ions (8 less than or = q less than or = 16) colliding with helium and molecular hydrogen at 2.3 qkeV laboratory energy were measured. Although the cross sections exhibit a monotonic increase with charge or in this case with decreasing occupation number of the L shell, the detailed variations are not accounted for by current theories. These measurements are currently being extended down to 0.1 qkeV incident ion energies. In order to gain a better understanding of two and more electron capture processes, electron-recoil ion and projectile-recoil ion coincidence experiments are under way. The spectra of electrons emitted in Ar(q+)+Ar(12 less than or = q less than or = 15) collisions at 2.3 qkeV in the energy range 40 to 320 eV were recorded using a 127 degs cylindrical analyzer. These are the first electron spectra ever obtained using an EBIS as a source of low energy, highly charged ions. The fact that we were able to obtain such spectra can be attributed to the remarkably stability and reliability of our superconducting solenoid, cryogenic electron beam ions source CEBIS. Work is in progress to extend the spectral range of electrons down to a few eV and to interpret all of the observed spectral features. DOE

N92-10617# Kansas State Univ., Manhattan. Dept. of Physics.
ATOMIC PHYSICS OF STRONGLY CORRELATED SYSTEMS
C. D. Lin 1991 3 p Presented at the DOE/DES Atomic Physics Contractor's Meeting, Albuquerque, NM, 15-16 Nov. 1991
(Contract DE-FG02-86ER-13596)
(DE91-012259; DOE/ER-13596/18; CONF-911147-1-Extd-Abst) Avail: NTIS HC/MF A01

This abstract describes the programs just completed in the last year and projects currently underway in our study of strongly correlated atomic systems. The radiative and Auger decays of high doubly-excited states of multiply charged ions have been examined to extract simple systematics and propensity rules. The rotational and vibrational characters of doubly excited states of atoms were examined to understand the molecular characters of these states and their limitations. Double capture to doubly excited states in the collisions between multiply charged ions with helium atoms have been calculated and the angular distributions of the ejected electrons are being investigated. The Classical Trajectory Monte Carlo (CTMC) method has been applied to calculate the coherence parameters of excited states formed in collisions of atomic hydrogen with electrons, positrons, protons and antiprotons to examine the range of validity of the classical theory for such parameters. DOE

N92-10618# Oak Ridge National Lab., TN.
INFLUENCE OF THE ANGULAR CORRELATION OF FISSION NEUTRONS ON NOISE SIGNATURES
F. C. Difilippo 1991 5 p Presented at the Winter Meeting of the American Nuclear Society (ANS), San Francisco, CA, 10-15 Nov. 1991
(Contract DE-AC05-84OR-21400)
(DE91-014577; CONF-911107-6) Avail: NTIS HC/MF A01

Noise signatures, the measurement of the correlation between the fluctuating parts of the signals coming from neutron detectors, are commonly used to measure nuclear parameters (reactivities, mean lives) and to monitor nuclear systems. Several techniques are used, such as the correlation of analog signals in time or frequency domains or the statistical analysis of detection events. Independently of the experimental method, the useful component of the stochastic descriptors is related to the detection of neutrons that have ancestors born in the same fission event. Despite an early work, opened to the inclusion of the n-n angular correlations of neutrons coming from the same fission, practically all the theoretical applications ignore this additional complication by making the implicit or explicit hypothesis that fission neutrons are born uncorrelated. However, there are direct measurements that show angular and energy correlation for the two-fission-neutron distribution. The first attempt to include this experimental evidence into the theory of neutron noise was the calculation of the ratio of spectral densities related to the Cf-252 method of measuring reactivities under the simplest condition: two neutron detectors monitoring a Cf-252 plated fission chamber. The objective of this

communication is to show how noise signatures of more complex systems are sensitive to the joint distribution of two neutrons coming from the same fission with velocities v vector and v vector prime. To avoid mathematical complications, we are going to assume (1) that the system is monitored by two different detectors, Labels 2 and 3, distributed according to the fundamental kinetic mode, and (2) that the subcritical system contains only one fissile specie. The driver of the neutron flux is a Cf-252 fission source. DOE

N92-10619# Lawrence Livermore National Lab., CA.
LIMITATIONS OF THE CONDENSED HISTORY METHOD FOR LOW ENERGY ELECTRONS
C. T. Ballinger, J. A. Rathkopf, and W. R. Martin (Michigan Univ., Ann Arbor.) Jul. 1991 6 p Presented at the Winter Meeting of the American Nuclear Society (ANS), San Francisco, CA, 10-15 Nov. 1991
(Contract W-7405-eng-48)
(DE91-015764; UCRL-JC-107753; CONF-911107-15) Avail: NTIS HC/MF A02

A systematic evaluation of the conventional, condensed history electron transport methodology is performed through comparisons with more accurate single-scatter Monte Carlo calculations. These comparisons highlight the inaccuracies associated with the condensed history method and indicate its range of validity. The condensed history method is used in codes such as MCNP4, SANDYL, ETRAN, ITS, and EGS and requires a number of restrictive assumptions about the scattering characteristics to make tractable the analytical solution to the infinite-medium transport equation. DOE

N92-10620# Oak Ridge National Lab., TN.
OPTIMAL DIFFUSION SYNTHETIC ACCELERATION OF DISCRETE ORDINATES TRANSPORT CALCULATIONS
Y. Y. Azmy 1991 6 p Presented at the Winter Meeting of the American Nuclear Society (ANS), San Francisco, CA, 10-15 Nov. 1991
(Contract DE-AC05-84OR-21400)
(DE91-015924; CONF-911107-16) Avail: NTIS HC/MF A02

The Diffusion Synthetic Acceleration (DSA) method has been very successful in improving the iterative convergence of neutron transport computations. Early tests, and analysis showed the susceptibility of DSA to instability, which led to Alcouffe's Consistency Principle conjecturing that consistent discretization of the transport and diffusion operators is essential for the unconditional stability of the accelerated iterations. This conjecture was shown to be true via a Fourier mode analysis for a variety of numerical methods for solving the transport equation in slab geometry. The question however is whether improved convergence can be achieved by alternative choices of the DSA nuclear parameters, and if yes, how to calculate these alternative parameters for practical problems. In this summary, we consider only the first part of this question, and relegate the second part to a future report when further studies are concluded. DOE

N92-10621# Oak Ridge National Lab., TN.
A NOVEL TECHNIQUE FOR THE MEASUREMENT OF PHOTOENHANCED ELECTRON ATTACHMENT: IMPLICATIONS FOR AN OPTICALLY-CONTROLLED DIFFUSE DISCHARGE OPENING SWITCH
L. A. Pinnaduwage and L. G. Christophorou (Tennessee Univ., Knoxville.) 1991 16 p Presented at the 8th IEEE Pulsed Power Conference, San Diego, CA, 17-19 Jun. 1991
(Contract DE-AC05-84OR-21400)
(DE91-016226; CONF-910640-5) Avail: NTIS HC/MF A03

Enhanced electron attachment to transient electron attaching species, such as electronically-excited molecules produced via laser irradiation, could be employed to switch conduction/insulation properties of a gaseous medium and has potential applications in diffuse-discharge opening switches. We discuss a new technique that is capable of measurement of enhanced electron attachment to very short-lived (lifetime less than 10(exp -8) s) electron attaching species. We also report measurements carried out using this technique on superexcited states (electronically-excited states lying above the first ionization threshold) of triethylamine and nitric oxide; these exhibit several orders of magnitude enhancement in electron attachment compared to the corresponding ground electronic states. Implications of such measurements for an optically-controlled diffuse discharge opening switch are indicated. DOE

N92-10622# California Univ., Davis. Dept. of Applied Science.
BEAT WAVE CURRENT DRIVE EXPERIMENT ON DDT
D. Q. Hwang Mar. 1991 12 p
(Contract DE-FG03-89ER-53289)
(DE91-017407; DOE/ER-53289/T1) Avail: NTIS HC/MF A03

Several improvements have been made to the beat wave experiment this year. We are now able to vary the magnetic field over a much larger range, the plasma density is more uniform, and the electron temperature is significantly higher than last year (making it easier to couple energy from the electrostatic wave into the electron distribution). We have found evidence that at higher magnetic fields, omega(sub ce)/omega(sub pe) greater than 1, that numerous electrostatic modes are excited. This may be due to the fact that for a bounded plasma, omega less than omega(sub pe) is allowed (for small wave numbers). Although we are still not sure why the k(vector) matching criteria (k(sub 0)(vector) = k(sub 1)(vector) + k(sub e)(vector)) is not more restrictive. A 35 GHz microwave scattering diagnostic has been designed, built, and tested in order to make a less perturbing measure of the electrostatic wave. DOE

N92-10623# Virginia Univ., Charlottesville. Dept. of Physics.
EXPERIMENTS ON THE NUCLEAR INTERACTIONS OF PIONS AND ELECTRONS
R. C. Minehart and K. O. H. Ziock Aug. 1991 25 p
(Contract DE-FG05-88ER-40390)
(DE91-017929; DOE/ER-40390/4) Avail: NTIS HC/MF A03

During the past year we analyzed the data on the composition of the beam used in our experiment to study the pi + d yields 2p reaction at incident pion energies from 4 to 20 MeV. Analysis of the LAMPF Exp. on pion absorption in He-4 is proceeding. This experiment, which was originally intended to produce measurements in both He-3 and He-4, was run successfully in the summer of 2990 following an accident at LAMPF that severely damaged the liquid helium cryostat. A replacement target for He-4 only was used along with the LAS spectrometer and an extensive scintillator time-of-flight system capable of detecting neutrons as well as charged particles. We continue to build the apparatus to search for fractionally charged particles attached to steel spheres magnetically suspended in an electric field. We are also fully involved in some major collaborations: the search for the decay mu(+) yields e(+) + gamma(MEGA), and the study of anti-proton absorption in heavy nuclei. We are taking part in an equipment to measure pion beta decay to an accuracy of less than 1 percent, using a large acceptance CsI detector to measure the pi(0) following decay of stopped pi(+) mesons. In conjunction with the construction of the CEBAF accelerator, we are working on the CEBAF Large Acceptance Spectrometer (CLAS) program. We are contributing mainly to the design and construction of the CLAS forward calorimeter. This prototype detector is continuing to be used for further studies of the calorimeter design and the associated electronics. DOE

N92-10624# Oak Ridge National Lab., TN.
NONPERTURBATIVE ELECTROMAGNETIC MUON-PAIR PRODUCTION WITH CAPTURE IN PERIPHERAL RELATIVISTIC HEAVY-ION COLLISIONS
J. C. Wells, V. E. Oberacker, and A. S. Umar (Vanderbilt Univ., Nashville, TN.) 1991 13 p Presented at the Conference on Computational Quantum Physics, Nashville, TN, 22-25 May 1991
(Contract DE-AC05-84OR-21400)
(DE91-018247; CONF-9105238-5) Avail: NTIS HC/MF A03

We discuss preliminary calculations of impact-parameter-dependent probabilities and cross sections for muon-pair production with capture of the negative muon into the

K-shell of the target caused by the time-dependent electromagnetic fields generated in peripheral relativistic heavy-ion collisions. Our approach is nonperturbative in that we calculate probabilities by solving the time-dependent Dirac equation on a three-dimensional Cartesian lattice using the basis-spline collocation method. Use of the axial gauge for the electromagnetic potentials produces an interaction easier to implement on the lattice than the Lorentz gauge. DOE

N92-10625# Oak Ridge National Lab., TN.
VALENCE AND PHONON EXCITATIONS IN HIGH-RESOLUTION ELECTRON MICROSCOPY
Z. L. Wang (Tennessee Univ., Knoxville.) and J. Bentley 1991 5 p Presented at the Biennial Conference of the Electron Microscopy and Analysis Group of the Institute of Physics (EMAG '91): Advances in the Instrumentation and Techniques for Electron and Other Microscopies and Trade Exhibition, Bristol, England
(Contract DE-AC05-84OR-21400)
(DE91-017684; CONF-910972-1) Avail: NTIS HC/MF A01

Based on inelastic scattering wave mechanics, a general theory has been proposed to include the effects of valence excitations in image simulations for high-resolution electron microscopy (HREM) of relatively thick crystals. For very thin foils (less than 5 nm at 400 kV), the general theory reduces to a simple theory in which the image can be considered as an incoherent sum of images from incident electrons of different energies weighted by the intensity distribution in the electron energy-loss spectrum from the same are. The effect of phonon scattering can be included in HREM image calculations by introducing an absorption function. DOE

N92-10626# Pittsburgh Univ., PA. Dept. of Chemistry.
QUANTUM STATE RESOLVED DESORPTION OF CO FROM SOLID SURFACE
1991 14 p
(Contract DE-FG02-88ER-13933)
(DE91-017712; DOE/ER-13933/2) Avail: NTIS HC/MF A03

In this project we have concentrated on three activities. First, we studied the kinetics of recombinative desorption of hydrogen and deuterium atoms on a Si(100) surface. Second, we studied the kinetics of isotope mixing between CO molecules on a potassium promoted Ni(111) surface. Third, we have designed and implemented a laser multiphoton ionization time-of-flight (MPI-TOF) mass spectrometer for measuring the velocity, vibrational and rotational distribution of molecules leaving a surface in our ultrahigh vacuum chamber. DOE

N92-10627# Columbia Univ., New York, NY.
ENERGY PARTITIONING IN ELEMENTARY GAS PHASE REACTIONS
R. Bersohn 1991 11 p
(Contract DE-FG02-86ER-13492)
(DE91-017783; DOE/ER-13492/13) Avail: NTIS HC/MF A03

During the last 2(1/2) years we: Measured the LIF excitation spectrum of H atoms dissociated by 193 nm light from cyclopentadiene and indene as well as the rate of dissociation of indene. A general relation is that the translational temperature of the H atoms and the vibrational temperature of the molecules before dissociation are equal. We measured the H atom channel in the photodissociation of ethylene at 193 nm. The LIF excitation spectrum was measured as well as the quantum yield. Isotope effects were observed and explained by RRKM theory in CH2CD2 and trans-CHDCHD. We studied the photodissociation of hydrogen molecules with two photon excited states of the rare gas atoms, 5p(01/2) of Kr and 6p(01/2) of Xe. A new much stronger source of Lyman alpha light at 121.6 nm enabled the study of processes in which a hydride is photodissociated at 121.6 nm and within the same pulse a second photon excites H atom fluorescence. For the first time the dynamics of photodissociation of methane, water, acetylene and HCl were measured at 121.6 nm. Large isotope effects were seen. In CH3D, CH2D and CD3H the H atoms were twice as likely to dissociate as the D atoms. DOE

N92-10628# George Washington Univ., Washington, DC. Center for Nuclear Studies.
INVESTIGATIONS OF THE STRUCTURE AND ELECTROMAGNETIC INTERACTIONS OF FEW-BODY SYSTEMS
D. R. Lehman Jul. 1991 38 p
(Contract DE-FG05-86ER-40270)
(DE91-017927; DOE/ER-40270/28) Avail: NTIS HC/MF A03

In order to make it easy for the reader to see the specific research carried out and the progress made, the following report of progress is done by topic. Each item has a format layout of Topic, Investigators, Objective, Significance, and Description of Progress, followed at the end by the relevant references. As is clear from the topics listed, the emphasis of the GWU theory group has been on the structure and electromagnetic interactions of few-body nuclei. Both low- and intermediate-energy electromagnetic disintegration of these nuclei is considered. When the excitation energy of the target nucleus is low, the aim has been to carry out the continuum part of the theoretical work exactly, this is, by means of exact three- and four-body dynamics. When structure questions are the issue, exact calculations are always carried through, limited only by the underlying two-body or three-body interactions used as input. Implicit in our work is the question of how far one can go within the traditional nuclear physics framework, i.e., nucleons and mesons in a nonrelativistic setting. Our central goal is to carry through state-of-the-art few-body calculations that will serve as an unambiguous means of determining at what point standard nuclear physics requires quark degrees of freedom in order to understand the phenomena in question. So far, in the problems considered, there has been no evidence of the necessity to go beyond the traditional approach, though we always keep in mind that possibility. As our work is involved with questions in the intermediate-energy realm, moving from a nonrelativistic framework to a relativistic one is always a consideration. Currently, for the problems that have been pursued in this domain of energy, the issues concern far more the mechanisms of the reactions and structural questions than the need to move to relativistic dynamics. DOE

N92-10629# Missouri Univ., Rolla. Div. of Applied Plasma Physics.
EXPERIMENTAL INVESTIGATIONS OF ELECTRON CAPTURE FROM ATOMIC HYDROGEN AND DEUTERIUM BY ALPHA PARTICLES
1991 11 p
(Contract DE-FG02-84ER-53188)
(DE91-018280; DOE/ER-53188/8) Avail: NTIS HC/MF A03

We have undertaken a program at the University of Missouri-Rolla to experimentally determine cross sections for ion-atom collisions of interest in fusion reactor development. During the last grant period, we finished measurements of total sections for the alpha single-capture reaction (1) He(sup ++) + He(1s(sup 2)) (yields) He(sup +)(n) + He(sup +)(1s), and we propose to study (2) He(sup ++) + H(1s) (yields) He(sup +)(n) + H(sup +) this year. Accurate knowledge of these cross sections is fundamental for modeling of neutral-hydrogen beam penetration in fusion plasmas as well as for spectroscopic diagnostics of alpha densities and velocity distributions, especially for the case of capture into the n equals 4 state of the projectile He(sup +). Our measurements are made using a unique collision spectrometer discussed below. Reaction (1) was studied for alpha energies between 45 and 135 keV, using the technique of ion-energy spectroscopy. This technique has two major advantages over optical measurements. First, cascading corrections are avoided because the fast collision partner is detected, rather than a secondary photon. Second, no knowledge of detector efficiencies is required, because a ratio of the scattered to incident beam counting rates is measured. Two sources of possible systematic error in the determination of final cross sections are thereby eliminated. Moreover, we have studied the angular dependence of cross sections for (1), and can thus be certain that the measured total cross sections are not low due to incomplete angular

acceptance of the apparatus, a problem known to exist in some previous total cross section measurements of this type. DOE

N92-10630# Rochester Univ., NY. Coll. of Arts and Science.
THEORETICAL AND EXPERIMENTAL STUDIES OF ELEMENTARY PARTICLES
A. Bodek, T. Ferbel, A. C. Melissinos, S. L. Olsen, P. Slattery, P. Tipton, A. Das, C. R. Hagen, S. G. Rajeev, and S. Okubo 1991 412 p
(Contract DE-AC02-76ER-13065)
(DE91-018285; DOE/ER-13065/672) Avail: NTIS HC/MF A18

This report discusses fixed target experimentation at Fermilab; the D-zero collider experiment at Fermilab; deep inelastic lepton nucleon scattering; non-accelerator experiments and non-linear quantum electrodynamics (QED); the AMY experiment at TRISTAN and other activities at KEK; the collider detector at Fermilab; laser switched linac; preparations for experiments at the SSC; search for massive stable particles; and the Advanced Study Institute on techniques and concepts of high energy physics. DOE

N92-10631# Lawrence Livermore National Lab., CA.
THE RESPONSE HISTORY MONTE CARLO METHOD FOR ELECTRON TRANSPORT Ph.D. Thesis
C. T. Ballinger 1 Aug. 1991 199 p
(Contract W-7405-eng-48)
(DE91-018295; UCRL-ID-108040) Avail: NTIS HC/MF A09

The Response History Monte Carlo (RHMC) method is dependent upon along Monte Carlo calculations to generate the probability distributions in the local calculations. An analog Monte Carlo code was written and is described, along with sampling techniques. Comparisons with experimental data and existing codes were performed to benchmark the analog code. The condensed history methodology used in most electron transport codes is outlined. In an effort to determine why condensed history methods fail, this paper shows results obtained by replacing the multi-scatter distributions currently used in condensed history by those calculated via analog Monte Carlo. The RHMC method is described by outlining the local and global calculation procedures. This paper also contains some RHMC code results that are compared to condensed history codes, experimental measurements, and analog Monte Carlo code results. DOE

N92-10632# Texas Univ., Austin. Center for Particle Theory.
RESEARCH PROGRAM IN PARTICLE PHYSICS
E. C. G. Sudarshan, D. A. Dicus, and J. L. Ritchie Jul. 1991 33 p
(Contract DE-FG05-85ER-40200)
(DE91-018525; DOE/ER-40200/261) Avail: NTIS HC/MF A03

This report discusses research on: Quantum gravity and mathematical physics; high energy phenomenology; quantum mechanics and quantum field theory; a new rare K(sub L) decay search; and SSC activities. DOE

N92-10633# Virginia Univ., Charlottesville. Inst. of Nuclear and Particle Physics.
INCLUSIVE QUASIELASTIC AND DEEP INELASTIC ELECTRON SCATTERING AT HIGH ENERGIES
D. B. Day 1990 17 p Presented at the European Workshop on Hadronic Physics With Electrons Beyond 10 GeV, Dourdan, France, 8-12 Oct. 1990
(Contract DE-FG05-86ER-40261)
(DE91-018755; CONF-9010183-5) Avail: NTIS HC/MF A03

With high electron energies a kinematic regime can be reached where it will be possible to separate quasielastic and deep inelastic scattering. We present a short description of these processes which dominate the inclusive spectrum. Using the highest momentum transfer data available to guide our estimates, we give the kinematic requirements and the cross sections expected. These results indicate that inclusive scattering at high q has a yet unfilled potential. DOE

N92-10634# Brown Univ., Providence, RI. Dept. of Physics.
NUCLEAR EXCITATIONS AND REACTION MECHANISMS
S. Fellieros and F. S. Levin 1 Aug. 1991 9 p
(Contract DE-FG02-87ER-40334)
(DE91-018968; DOE/ER-40334/7) Avail: NTIS HC/MF A02

The main theme of this report is the study and interpretation of the sequence of events that occur during the collisions of nuclear particles. Some of the processes discussed in parts A and B involve short range interactions; others involve interactions of long range. In most of part A one of the particles in the initial or in the final state (or in both) is a photon, which serves as a probe of the second particle, which may be a nucleus, a proton, a pion or any other hadron. The complexity of the processes taking place during the collisions makes it necessary to simplify some aspects of the physical problem. This leads to the introduction of models which are used to describe a limited number of features in as much detail as possible. The main interest is in understanding the hadronic excitations which result from the absorption of a photon and the determination of the fundamental structure constants of the target particle. In part B, all the particles are hadrons. The purpose here is to develop and apply optimal quantal methods appropriate for describing the interacting systems. Of particular interest are three-particle collision systems in which the final state consists of three free particles. Part B also considers the process of nuclear fusion as catalyzed by bound muons. DOE

N92-10383# Jyvaskyla Univ. (Finland). Dept. of Physics.
THERMAL EMISSION OF GAMMAS AND LEPTON PAIRS FROM QUARK-GLUON PLASMAS Abstract Only
P. V. Ruuskanen *In* Oulu Univ., Proceedings of the 25th Annual Conference of the Finnish Physical Society 1991 1 p (For primary document see N92-10362 01-70)
Avail: NTIS HC/MF A12

N92-10384# Jyvaskyla Univ. (Finland). Dept. of Physics.
THERMAL PHOTON PRODUCTION FROM HIGH-TEMPERATURE NUCLEAR MATTER Abstract Only
D. Seibert, J. Kapusta, and P. Lichard (Comenius Univ., Bratislava, Czechoslovakia) *In* Oulu Univ., Proceedings of the 25th Annual Conference of the Finnish Physical Society 1991 1 p (For primary document see N92-10362 01-70)
Avail: NTIS HC/MF A12

N92-10385# Cape Town Univ., Rondebosch (South Africa). Dept. of Physics.
EXACT STRANGENESS CONSERVATION AND PARTICLE PRODUCTION Abstract Only
J. Cleymans, K. Redlich, and E. Suhonen (Oulu Univ., Finland) *In* Oulu Univ., Proceedings of the 25th Annual Conference of the Finnish Physical Society 1991 1 p Submitted for publication (For primary document see N92-10362 01-70)
(BI-TP-90/35) Avail: NTIS HC/MF A12

N92-10386# Cape Town Univ., Rondebosch (South Africa). Dept. of Physics.
HADRONIC EQUATION OF STATE AND THE ONSET OF KAON CONDENSATION Abstract Only
J. Cleymans, J. Staalnacke, and E. Suhonen (Oulu Univ., Finland) *In* Oulu Univ., Proceedings of the 25th Annual Conference of the Finnish Physical Society 1991 1 p (For primary document see N92-10362 01-70)
Avail: NTIS HC/MF A12

N92-10387# European Organization for Nuclear Research, Geneva (Switzerland). UA1 Collaboration.
INTERMITTENCY STUDIES IN PROTON-ANTIPROTON COLLISIONS AT SQUARE ROOT OF S = 630 GeV Abstract Only
C. Albajar, M. G. Albrow, O. C. Allkofer, B. Andrieu, K. Ankoviak, R. Apsimon, B. Aubert, C. Bacci, S. Bartha (Kiel Univ., Germany, F.R.), and G. Bauer, 8RZ958
et al *In* Oulu Univ., Proceedings of the 25th Annual Conference of the Finnish Physical Society 1991 1 p Submitted for publication (For primary document see N92-10362 01-70)
(CERN-PPE/90-153) Avail: NTIS HC/MF A12

N92-10388# European Organization for Nuclear Research, Geneva (Switzerland). UA1 Collaboration.
BEAUTY PRODUCTION AT THE CERN PROTON-ANTIPROTON COLLIDER Abstract Only
C. Albajar, R. Kinnunen, J. Tuominiemi, V. Karimaki, M. Pimia, and E. Pietarinen (Helsinki Univ. of Technology, Espoo, Finland) *In* Oulu Univ., Proceedings of the 25th Annual Conference of the Finnish Physical Society 1991 1 p Submitted for publication (For primary document see N92-10362 01-70)
(CERN-PPE/90-155) Avail: NTIS HC/MF A12

N92-10389# European Organization for Nuclear Research, Geneva (Switzerland). UA1 Collaboration.
A SEARCH FOR RARE B MESON DECAYS AT THE CERN PROTON-ANTIPROTON COLLIDER Abstract Only
C. Albajar, R. Kinnunen, J. Tuominiemi, V. Karimaki, M. Pimia, and E. Pietarinen (Helsinki Univ. of Technology, Espoo, Finland) *In* Oulu Univ., Proceedings of the 25th Annual Conference of the Finnish Physical Society 1991 1 p Submitted for publication (For primary document see N92-10362 01-70)
(CERN-PPE/91) Avail: NTIS HC/MF A12

N92-10390# European Organization for Nuclear Research, Geneva (Switzerland). UA1 Collaboration.
J/PSI AND PSI' PRODUCTION AT THE CERN PROTON-ANTIPROTON COLLIDER Abstract Only
C. Albajar, R. Kinnunen, J. Tuominiemi, V. Karimaki, M. Pimia, and E. Pietarinen (Helsinki Univ. of Technology, Espoo, Finland) *In* Oulu Univ., Proceedings of the 25th Annual Conference of the Finnish Physical Society 1991 1 p Submitted for publication (For primary document see N92-10362 01-70)
(CERN-PPE/90-154) Avail: NTIS HC/MF A12

N92-10391# European Organization for Nuclear Research, Geneva (Switzerland). UA1 Collaboration.
LIMITS ON T-QUARK DECAY INTO CHARGED HIGGS FROM A DIRECT SEARCH AT THE CERN PROTON-ANTIPROTON COLLIDER Abstract Only
C. Albajar, R. Kinnunen, J. Tuominiemi, V. Karimaki, M. Pimia, and E. Pietarinen (Helsinki Univ. of Technology, Espoo, Finland) *In* Oulu Univ., Proceedings of the 25th Annual Conference of the Finnish Physical Society 1991 1 p Submitted for publication (For primary document see N92-10362 01-70)
(CERN-PPE/90-180) Avail: NTIS HC/MF A12

N92-10392# European Organization for Nuclear Research, Geneva (Switzerland).
MEASUREMENTS OF THE RATIO R = SIGMA(SUB W)Br(W TO MU(NU))/SIGMA(SUB Z)Br(Z TO MU(MU)) AND GAMMA(SUP tot)(SUB W) AT THE CERN PROTON-ANTIPROTON COLLIDER Abstract Only
C. Albajar, R. Kinnunen, J. Tuominiemi, V. Karimaki, M. Pimia, and E. Pietarinen (Helsinki Univ. of Technology, Espoo, Finland) et al *In* Oulu Univ., Proceedings of the 25th Annual Conference of the Finnish Physical Society 1991 1 p Submitted for publication (For primary document see N92-10362 01-70)
(CERN-PPE/90-141) Avail: NTIS HC/MF A12

N92-10393# Helsinki Univ. of Technology, Espoo (Finland). Dept. of High Energy Physics.
LOCAL CHARGE COMPENSATION IN Z(SUP 0) HADRONIC DECAYS Abstract Only
P. Eerola, J. Pennanen, and R. Orava *In* Oulu Univ., Proceedings of the 25th Annual Conference of the Finnish Physical Society 1991 1 p (For primary document see N92-10362 01-70)
Avail: NTIS HC/MF A12

N92-10394# Helsinki Univ. of Technology, Espoo (Finland). Research Inst. for High Energy Physics.
RECENT PHYSICS RESULTS FROM DELPHI Abstract Only
Reino Keranen *In* Oulu Univ., Proceedings of the 25th Annual Conference of the Finnish Physical Society 1991 1 p (For primary document see N92-10362 01-70)
Avail: NTIS HC/MF A12

N92-10395# Turku Univ. (Finland). Dept. of Physics.
SEARCHES FOR HEAVY NEUTRINOS FROM DECAYS OF THE Z Abstract Only
Kenneth Osterberg (Helsinki Univ. of Technology, Espoo, Finland) *In* Oulu Univ., Proceedings of the 25th Annual Conference of the Finnish Physical Society 1991 1 p (For primary document see N92-10362 01-70)
Avail: NTIS HC/MF A12

N92-10396# Bern Univ. (Switzerland). Inst. fuer Theoretische Physik.
PION-NUCLEON SIGMA-TERM AND THE STRANGE QUARK CONTENT OF THE PROTON Abstract Only
J. Gasser, H. Leutwyler, and M. E. Sainio (Helsinki Univ. of Technology, Espoo, Finland) *In* Oulu Univ., Proceedings of the 25th Annual Conference of the Finnish Physical Society 1991 1 p Sponsored in part by Schweizerischer Nationalfonds (For primary document see N92-10362 01-70)
Avail: NTIS HC/MF A12

N92-10397# Helsinki Univ. of Technology, Espoo (Finland). Research Inst. for Theoretical Physics.
GLUON OVERLAP FACTORS EXTRACTED FROM MONTE CARLO LATTICE CALCULATIONS Abstract Only
A. M. Green, O. Morimatsu, and J. Paton (Oxford Univ., England) *In* Oulu Univ., Proceedings of the 25th Annual Conference of the Finnish Physical Society 1991 1 p (For primary document see N92-10362 01-70)
Avail: NTIS HC/MF A12

N92-10398# Helsinki Univ. of Technology, Espoo (Finland). Research Inst. for Theoretical Physics.
HEAVY NEUTRINOS IN e(+)e(-) COLLISIONS Abstract Only
J. Maalampi, K. Mursula (Oulu Univ., Finland), and R. Vuopionpera *In* Oulu Univ., Proceedings of the 25th Annual Conference of the Finnish Physical Society 1991 1 p (For primary document see N92-10362 01-70)
Avail: NTIS HC/MF A12

N92-10400# Helsinki Univ. of Technology, Espoo (Finland). Accelerator Lab.
LIFETIME OF THE 1.959 MeV STATE IN Cl-36 Abstract Only
A. Kuronen, J. Keinonen, P. Tikkanen, and A. Kangasmaki *In* Oulu Univ., Proceedings of the 25th Annual Conference of the Finnish Physical Society 1991 1 p (For primary document see N92-10362 01-70)
Avail: NTIS HC/MF A12

N92-10401# Turku Univ. (Finland). Dept. of Physics.
SHAPE COEXISTENCE IN TRANSITIONAL (132,133,134)Ba Abstract Only
T. Loennroth, P. Ahonen, M. Carpenter, C. Fahlander, J. Gascon, R. Julin, S. Juutinen (Jyvaskyla Univ., Finland), K.-M. Kaellman, A. Lampinen, and P. Manngaard, 9J9928 et al *In* Oulu Univ., Proceedings of the 25th Annual Conference of the Finnish Physical Society 1991 1 p (For primary document see N92-10362 01-70)
Avail: NTIS HC/MF A12

N92-10402# Jyvaskyla Univ. (Finland). Dept. of Physics.
OBSERVATIONS ON VERY NEUTRON-RICH NUCLEI BELOW Z = 50 Abstract Only
J. Aysto, K. Eskola, P. P. Jauho, A. Jokinen, M. Leino, S. Malm, J. Parmonen, H. Penttila, and H. Salminen *In* Oulu Univ., Proceedings of the 25th Annual Conference of the Finnish Physical Society 1991 1 p Sponsored by Academy of Finland Prepared in cooperation with Warsaw Univ., Katholieke Univ., and Lyon Univ. (For primary document see N92-10362 01-70)
Avail: NTIS HC/MF A12

N92-10403# Jyvaskyla Univ. (Finland). Dept. of Physics.
HIGH-SPIN STATES IN Cd-109 Abstract Only
S. Juutinen, P. Ahonen, J. Hattula, R. Julin, J. Kumpulainen, A. Lampinen, D. Mueller, A. Pakkanen, M. Piiparinen, and S.

Toermaenen et al *In* Oulu Univ., Proceedings of the 25th Annual Conference of the Finnish Physical Society 1991 1 p (For primary document see N92-10362 01-70)
Avail: NTIS HC/MF A12

N92-10404# Jyvaskyla Univ. (Finland). Dept. of Physics.
SHAPES OF Cd-110 AT HIGH SPINS Abstract Only
S. Juutinen, R. Julin, P. Ahonen, C. Fahlander, J. Hattula, J. Kumpulainen, A. Lampinen, T. Loennroth, D. Mueller, and J. Nyberg (Niels Bohr Inst., Copenhagen, Denmark) et al *In* Oulu Univ., Proceedings of the 25th Annual Conference of the Finnish Physical Society 1991 1 p (For primary document see N92-10362 01-70)
Avail: NTIS HC/MF A12

N92-10405# Jyvaskyla Univ. (Finland). Dept. of Physics.
EVIDENCE FOR BAND TERMINATION IN Xe-118 Abstract Only
S. Tormanen, S. Juutinen, B Cederwall, I. Ragnarsson, A. Johnson, R. Julin, S. Mitarai, J. Mukai, P. Ahonen, and B. Fant (Helsinki Univ. of Technology, Espoo, Finland) et al *In* Oulu Univ., Proceedings of the 25th Annual Conference of the Finnish Physical Society 1991 1 p (For primary document see N92-10362 01-70)
Avail: NTIS HC/MF A12

N92-10406# Jyvaskyla Univ. (Finland). Dept. of Physics.
PROTON-NEUTRON SYMMETRY IN BOSON MODELS OF NUCLEAR STRUCTURE Abstract Only
P. O. Lipas *In* Oulu Univ., Proceedings of the 25th Annual Conference of the Finnish Physical Society 1991 1 p (For primary document see N92-10362 01-70)
Avail: NTIS HC/MF A12

N92-10407# Oulu Univ. (Finland). Dept. of Physics.
CONTRIBUTION OF THE DELTA RESONANCE TO THE GAMOW-TELLER DECAY OF HEAVY NUCLEI Abstract Only
J. Suhonen *In its* Proceedings of the 25th Annual Conference of the Finnish Physical Society 1991 1 p (For primary document see N92-10362 01-70)
Avail: NTIS HC/MF A12

N92-10408# Jyvaskyla Univ. (Finland). Dept. of Physics.
DOUBLE BETA DECAY IN THE PARTICLE-NUMBER PROJECTED QRPA FORMALISM Abstract Only
J. Suhonen *In* Oulu Univ., Proceedings of the 25th Annual Conference of the Finnish Physical Society 1991 1 p (For primary document see N92-10362 01-70)
Avail: NTIS HC/MF A12

N92-10409# Jyvaskyla Univ. (Finland). Dept. of Physics.
NEUTRINOLESS BETA DECAY IN THE FRAMEWORK OF A RELATIVISTIC QUARK MODEL Abstract Only
J. Suhonen *In* Oulu Univ., Proceedings of the 25th Annual Conference of the Finnish Physical Society 1991 1 p (For primary document see N92-10362 01-70)
Avail: NTIS HC/MF A12

N92-10410# Jyvaskyla Univ. (Finland). Dept. of Physics.
GAMMA-DECAY BRANCHING OF 1(+)-STATES IN Gd-156 AND Dy-164 Abstract Only
E. Hammaren, K. W. Schmid, P. Heikkinen, I. Koivistoinen, and A. Faessler (Tuebingen Univ., Germany, F.R.) *In* Oulu Univ., Proceedings of the 25th Annual Conference of the Finnish Physical Society 1991 1 p (For primary document see N92-10362 01-70)
Avail: NTIS HC/MF A12

N92-10411# Helsinki Univ. of Technology, Espoo (Finland). Dept. of Physics.
INDEPENDENT AND CUMULATIVE YIELDS OF NEUTRON-RICH NUCLEI IN SYMMETRIC FISSION INDUCED BY p AND d ON U-238 Abstract Only
M. Leino, P. P. Jauho, J. Aysto, P. Decrock, P. Dendooven, K. Eskola, M. Huyse, A. Jokinen, J. M. Parmonen, and H. Penttila (Jyvaskyla Univ., Finland) et al *In* Oulu Univ., Proceedings of the 25th Annual Conference of the Finnish Physical Society 1991 1 p Sponsored by Academy of Finland (For primary document see N92-10362 01-70)
Avail: NTIS HC/MF A12

N92-10426# Oulu Univ. (Finland). Dept. of Physics.
DECAY CHANNELS OF RESONANTLY EXCITED 2p(-1)ns, md STATES OF Ar AND 3d(-1)np STATES OF Kr Abstract Only
Seppo Aksela, H. Aksela, Y. Furusawa, and A. Yagishita (National Lab. for High Energy Physics, Tsukuba, Japan) *In its* Proceedings of the 25th Annual Conference of the Finnish Physical Society 1991 1 p (For primary document see N92-10362 01-70)
Avail: NTIS HC/MF A12

N92-10427# Oulu Univ. (Finland). Dept. of Physics.
Li 1s PHOTOIONIZATION AND PHOTOEXCITATION WITH SATELLITES Abstract Only
Seppo Aksela, H. Aksela, Maarit Levasalmi, Y. Furusawa, and A. Yagishita (National Lab. for High Energy Physics, Tsukuba, Japan) *In its* Proceedings of the 25th Annual Conference of the Finnish Physical Society 1991 1 p (For primary document see N92-10362 01-70)
Avail: NTIS HC/MF A12

N92-10429# Helsinki Univ. of Technology, Espoo (Finland). Physics Lab.
KRYPTON 4p,4s AND 3d PARTIAL PHOTOIONIZATION CROSS SECTIONS BELOW 260 eV PHOTON ENERGY Abstract Only
J. Tulkki, Seppo Aksela, H. Aksela, Y. Furusawa, A. Yagishita, and E. Shigemasa (National Lab. for High Energy Physics, Tsukuba, Japan) *In* Oulu Univ., Proceedings of the 25th Annual Conference of the Finnish Physical Society 1991 1 p (For primary document see N92-10362 01-70)
Avail: NTIS HC/MF A12

N92-10430# Helsinki Univ. of Technology, Espoo (Finland). Physics Lab.
RELAXATION AND FINAL-STATE CORRELATION EFFECTS IN THE 3p AND 3s PHOTOIONIZATION OF Ar, K(+), AND Ca(++) Abstract Only
J. Tulkki *In* Oulu Univ., Proceedings of the 25th Annual Conference of the Finnish Physical Society 1991 1 p (For primary document see N92-10362 01-70)
Avail: NTIS HC/MF A12

N92-10431# Oulu Univ. (Finland). Dept. of Physics.
THE ROTATIONAL STRUCTURE OF THE NU(SUB 6) VIBRATION BAND OF CH3I Abstract Only
S. Alanko and R. Paso *In its* Proceedings of the 25th Annual Conference of the Finnish Physical Society 1991 1 p (For primary document see N92-10362 01-70)
Avail: NTIS HC/MF A12

N92-10432# Oulu Univ. (Finland). Dept. of Physics.
THE NU(SUB 4) AND NU(SUB 7) BANDS OF CD3CN WITH CORIOLIS COUPLING AND OTHER RESONANCE PERTURBATIONS Abstract Only
M. Koivusaari and R. Anttila *In its* Proceedings of the 25th Annual Conference of the Finnish Physical Society 1991 1 p (For primary document see N92-10362 01-70)
Avail: NTIS HC/MF A12

N92-10433# Oulu Univ. (Finland). Dept. of Physics.
THE NU(SUB 8) AND 2NU(SUB 8) BANDS OF CD3CN Abstract Only
M. Koivusaari, V.-M. Horneman, and R. Anttila *In its* Proceedings of the 25th Annual Conference of the Finnish Physical Society 1991 1 p (For primary document see N92-10362 01-70)
Avail: NTIS HC/MF A12

N92-10434# Oulu Univ. (Finland). Dept. of Physics.
THE INFRARED ROTATION-VIBRATION SPECTRUM OF C2H2 IN THE NU(SUB 2) + NU(SUB 5) BAND REGION; I-RESONANCES IN THE BANDS NU(SUB 2) + NU(SUB 5), NU(SUB 2) + 2(NU(SUB 5)) BACK ARROW NU(SUB 5) AND NU(SUB 1) BACK ARROW NU(SUB 5) Abstract Only
A.-M. Tolonen and S. Alanko *In its* Proceedings of the 25th Annual Conference of the Finnish Physical Society 1991 1 p (For primary document see N92-10362 01-70)
Avail: NTIS HC/MF A12

N92-10440# Tampere Univ. of Technology (Finland). Dept. of Physics.
SUPERSONIC MOLECULAR BEAM APPARATUS TO STUDY SURFACE REACTIONS Abstract Only
M. Valden, Q. Wang, and I. Vattulainen *In* Oulu Univ., Proceedings of the 25th Annual Conference of the Finnish Physical Society 1991 1 p (For primary document see N92-10362 01-70)
Avail: NTIS HC/MF A12

N92-10441# Jyvaskyla Univ. (Finland). Dept. of Physics.
EQUIVALENCE IN THE SHELL STRUCTURE OF THE TIGHT BINDING AND FREE ELECTRON CLUSTERS Abstract Only
J. Mansikka-aho, E. Hammaren, and M. Manninen *In* Oulu Univ., Proceedings of the 25th Annual Conference of the Finnish Physical Society 1991 1 p (For primary document see N92-10362 01-70)
Avail: NTIS HC/MF A12

N92-10442# Helsinki Univ. of Technology, Espoo (Finland). Dept. of Technical Physics.
ISOTOPE SELECTIVE RESONANCE IONIZATION MEASUREMENTS OF LITHIUM Abstract Only
T. Kajava, H. Lauranto, P. Duex (Heidelberg Univ., Germany, F.R.), and Rainer Solomaa *In* Oulu Univ., Proceedings of the 25th Annual Conference of the Finnish Physical Society 1991 1 p (For primary document see N92-10362 01-70)
Avail: NTIS HC/MF A12

N92-10443# Helsinki Univ. of Technology, Espoo (Finland). Accelerator Lab.
TORSIONAL POTENTIAL FOR THE C(sp2)-C(sp2) BOND Abstract Only
B. Mannfors, L.-O. Pietila, and K. Palmo (Michigan Univ., Ann Arbor.) *In* Oulu Univ., Proceedings of the 25th Annual Conference of the Finnish Physical Society 1991 1 p (For primary document see N92-10362 01-70)
Avail: NTIS HC/MF A12

N92-10444# Oulu Univ. (Finland). Dept. of Physics.
ANALYSIS OF THE INTERACTING LEVELS V(SUB 9) = 1 AND V(SUB 10) = 2 OF PROPYNE Abstract Only
K. Pekkala, G. Graner, G. Wlodarczak, and J. Demaison (Lille-1 Univ., Villeneuve-d'Asoq, France) *In its* Proceedings of the 25th Annual Confernece of the Finnish Physical Society 1991 1 p (For primary document see N92-10362 01-70)
Avail: NTIS HC/MF A12

N92-10462# Tampere Univ. of Technology (Finland). Dept. of Electrical Engineering.
MOLECULAR DYNAMICS STUDIES OF LIQUID-SOLID INTERFACES Abstract Only
J. A. Nieminen, M. Karttunen, and Kimmo Kaski *In* Oulu Univ., Proceedings of the 25th Annual Conference of the Finnish Physical Society 1991 1 p (For primary document see N92-10362 01-70)
Avail: NTIS HC/MF A12

N92-10465# Helsinki Univ. of Technology, Espoo (Finland). Physics Lab.
MOLECULAR DYNAMICS USING THE TIGHT-BINDING APPROXIMATION: APPLICATION TO LIQUID SILICON Abstract Only
R. Virkkunen, K. Laasonen, and R. M. Nieminen *In* Oulu Univ., Proceedings of the 25th Annual Conference of the Finnish Physical Society 1991 1 p (For primary document see N92-10362 01-70)
Avail: NTIS HC/MF A12

N92-10473# Helsinki Univ. of Technology, Espoo (Finland). Physics Lab.
HELIUM IN SILICON: A FIRST PRINCIPLE MOLECULAR DYNAMICS STUDY Abstract Only
M. Alatalo, K. Laasonen, and R. M. Nieminen *In* Oulu Univ., Proceedings of the 25th Annual Conference of the Finnish Physical Society 1991 1 p (For primary document see N92-10362 01-70)
Avail: NTIS HC/MF A12

N92-10474# Helsinki Univ. of Technology, Espoo (Finland). Low Temperature Lab.
TWO-PHONON ABSORPTION BY THE REAL SQUASHING COLLECTIVE MODE IN SUPERFLUID He-3 Abstract Only
H. Alles, J. M. Kyynarainen, A. J. Manninen, J. P. Pekola, and K. Torizuka *In* Oulu Univ., Proceedings of the 25th Annual Conference of the Finnish Physical Society 1991 1 p (For primary document see N92-10362 01-70)
Avail: NTIS HC/MF A12

N92-10475# Landau Inst. for Theoretical Physics, Moscow (USSR).
MUTUAL FRICTION IN SUPERFLUID He-3: EFFECTS OF BOUND STATES IN THE VORTEX CORE Abstract Only
N. B. Kopnin and M. M. Salomaa (Helsinki Univ. of Technology, Espoo, Finland) *In* Oulu Univ., Proceedings of the 25th Annual Conference of the Finnish Physical Society 1991 1 p Sponsored by Soviet Academy of Sciences, and Academy of Finland (For primary document see N92-10362 01-70)
Avail: NTIS HC/MF A12

N92-10476# Helsinki Univ. of Technology, Espoo (Finland). Low Temperature Lab.
VORTEX NUCLEATION IN ROTATING SUPERFLUID He-3-B Abstract Only
U. Parts, Y. M. Bunkov, Y. Kondo, N. B. Kopnin, J. S. Korhonen, M. Krusius, and D. A. Sergatskov *In* Oulu Univ., Proceedings of the 25th Annual Conference of the Finnish Physical Society 1991 1 p (For primary document see N92-10362 01-70)
Avail: NTIS HC/MF A12

N92-10477# Oulu Univ. (Finland). Dept. of Theoretical Physics.
EFFECTIVE MASS AND EXCITATION SPECTRUM OF He-3 IMPURITIES IN SUPERFLUID He-4 Abstract Only
M. Saarela *In its* Proceedings of the 25th Annual Conference of the Finnish Physical Society 1991 1 p (For primary document see N92-10362 01-70)
Avail: NTIS HC/MF A12

N92-10478# Helsinki Univ. of Technology, Espoo (Finland). Low Temperature Lab.
SUPERFLUID INTERFACES IN LIQUID He-3: SUPERCONDUCTING COSMIC DOMAIN WALLS IN THE LABORATORY Abstract Only
M. M. Salomaa *In* Oulu Univ., Proceedings of the 25th Annual Conference of the Finnish Physical Society 1991 1 p Sponsored by Academy of Finland (For primary document see N92-10362 01-70)
Avail: NTIS HC/MF A12

N92-10479# Helsinki Univ. of Technology, Espoo (Finland). Low Temperature Lab.
SUPERFLUID VORTEX NUCLEATION IN He-3 FLOW Abstract Only
P. I. Soininen, N. B. Kopnin (Landau Inst. for Theoretical Physics, Moscow, USSR), and M. M. Salomaa *In* Oulu Univ., Proceedings of the 25th Annual Conference of the Finnish Physical Society 1991 1 p (For primary document see N92-10362 01-70)
Avail: NTIS HC/MF A12

N92-10480# Turku Univ. (Finland). Wihuri Physical Lab.
STRONG MAGNETIC COMPRESSION OF SPIN-POLARIZED HYDROGEN Abstract Only
E. Tjukanov, P. Arvela, M. Karhunen, S. Jaakkola, A. Katunin, A. Safonov, S. Vasilyev, G. Shlyapnikov, and I. I. Lukashevich (Kurchatov, I. V. Inst. of Atomic Energy, Moscow, USSR) *In* Oulu Univ., Proceedings of the 25th Annual Conference of the Finnish Physical Society 1991 1 p (For primary document see N92-10362 01-70)
Avail: NTIS HC/MF A12

N92-10481# Tampere Univ. of Technology (Finland).
MODELING THE DYNAMICS OF MOLECULAR FILMS BY MONTE CARLO SIMULATION Abstract Only
J. Heinio, Kimmo Kaski, and D. B. Abraham (Oxford Univ., England) *In* Oulu Univ., Proceedings of the 25th Annual Conference of the Finnish Physical Society 1991 1 p (For primary document see N92-10362 01-70)
Avail: NTIS HC/MF A12

N92-10482# Tampere Univ. of Technology (Finland). Dept. of Electrical Engineering.
NUMERICAL SIMULATION STUDIES OF FLUID SPREADING Abstract Only
A. Lukkarinen, J. Heinio, and Kimmo Kaski *In* Oulu Univ., Proceedings of the 25th Annual Conference of the Finnish Physical Society 1991 1 p (For primary document see N92-10362 01-70)
Avail: NTIS HC/MF A12

N92-10487# Helsinki Univ. of Technology, Espoo (Finland). Physics Lab.
INTERATOMIC INTERACTIONS IN THE LOCAL DENSITY APPROXIMATION Abstract Only
A. P. Seitsonen, M. J. Puska, and R. M. Nieminen *In* Oulu Univ., Proceedings of the 25th Annual Conference of the Finnish Physical Society 1991 1 p (For primary document see N92-10362 01-70)
Avail: NTIS HC/MF A12

N92-10510# Kurchatov (I. V.) Inst. of Atomic Energy, Moscow (USSR).
NMR AND ESR EXPERIMENTS ON SOLID MOLECULAR HYDROGEN CONTAINING ATOMIC HYDROGEN Abstract Only
V. A. Shevtsov, E. E. Ylinen, A. Frolov, I. I. Lukashevich, and Matti Punkkinen *In* Oulu Univ., Proceedings of the 25th Annual Conference of the Finnish Physical Society 1991 1 p Prepared in cooperation with Turku Univ., Finland (For primary document see N92-10362 01-70)
Avail: NTIS HC/MF A12

N92-10512# Helsinki Univ. of Technology, Espoo (Finland). Dept. of Technical Physics.
GAMMA ECHO EXPERIMENTS Abstract Only
P. Helisto, I. Tittonen, M. Lippmaa, and T. Katila *In* Oulu Univ., Proceedings of the 25th Annual Conference of the Finnish Physical Society 1991 1 p (For primary document see N92-10362 01-70)
Avail: NTIS HC/MF A12

N92-10536# Tampere Univ. of Technology (Finland). Dept. of Physics.
A SIMPLE RADON WELL Abstract Only
Katariina Lahti and Gunnar Graeffe *In* Oulu Univ, Proceedings of the 25th Annual Conference of the Finnish Physical Society 1991 1 p (For primary document see N92-10362 01-70)
Avail: NTIS HC/MF A12

N92-10538# Turku Univ. (Finland). Wihuri Physical Lab.
SCANNING TUNNELING MICROSCOPY OF POLYSIALIC ACID Abstract Only
L. Haikkila, J. P. S. Aalto, L. J. Pelliniemi, R. Laiho, and J. Finne *In* Oulu Univ., Proceedings of the 25th Annual Conference of the Finnish Physical Society 1991 1 p (For primary document see N92-10362 01-70)
Avail: NTIS HC/MF A12

73 NUCLEAR AND HIGH-ENERGY PHYSICS

Includes elementary and nuclear particles; and reactor theory.

For space radiation see *93 Space Radiation.*

N92-10635# Argonne National Lab., IL.
ADVANCED PHOTON SOURCE: RADIOLOGICAL DESIGN CONSIDERATIONS
H. J. Moe Jul. 1991 107 p Revised
(Contract W-31-109-eng-38)
(DE91-018014; APS-LS-141-Rev) Avail: NTIS HC/MF A06

The Argonne National Laboratory's Advanced Photon Source (APS) will include a 200 MeV electron linac, a positron converter target, a 450 MeV positron linac, a positron accumulator ring, a 7 GeV booster synchrotron, a 7 GeV positron storage ring and a number of experimental photon beam lines utilizing synchrotron radiation. A number of radiological design considerations for such a facility need to be addressed. In addition to shielding considerations for each of the various components and the experimental beam lines, other issues involve production of radioactive and noxious gases, induced activity in the accelerator structures and other materials, potential radiation doses during abnormal occurrences, radiation fields produced by gas bremsstrahlung, and the off-site doses to the public. The methodology used to estimate the contributions from each of the above-mentioned issues is detailed. Estimates of the magnitude of the contribution of each component are presented, and doses, as well as released quantities, are compared to the relevant DOE and EPA requirements. DOE

N92-10636# Sandia National Labs., Albuquerque, NM.
LONG PULSE ELECTRON BEAMS
J. R. Smith, I. R. Shokair, and K. W. Struve (Mission Research Corp., Albuquerque, NM.) 1991 3 p Presented at the 1991 Institute of Electrical and Electronics Engineers (IEEE) Particle Accelerator Conference (PAC), San Francisco, CA, 6-9 May 1991
(Contract DE-AC04-76DP-00789)
(DE91-018357; SAND-90-3139C; CONF-910505-405) Avail: NTIS HC/MF A01

Pulsed power accelerators used for intense relativistic electron beam applications have generally had pulse lengths of 10 to 100 ns. There are research areas where a pulse length of several 100's of nanoseconds is required or might be advantages (e.g., long distance propagation, microwave generation, free electron lasers). In the last 4 years several long pulse accelerators have come on line. In this report the emphasis is on measurement of the parameters of a long-pulse beam. The Troll accelerator produces the beam, and a conditioning cell is used to adjust beam parameters. This system has typically been operated with the following output parameters: 2.5 MV, 1 to 2 kA, 0.5 to 1 microns. DOE

N92-10637# Duke Univ., Durham, NC. Dept. of Physics.
NUCLEAR PHYSICS AT EXTREME ENERGY DENSITY
B. Mueller 15 May 1991 55 p
(Contract DE-FG05-90ER-40592)
(DE91-018012; DOE/ER-40592/1) Avail: NTIS HC/MF A04

This report discusses research performed under the Nuclear Theory Group at Duke University. The following topics are covered: relativistic parton cascade; quark-gluon plasma; and physics in strong electromagnetic fields. DOE

N92-10366# Cornell Univ., Ithaca, NY. Dept. of Applied and Engineering Physics.
SYNCHROTRON RADIATION: NEW RESEARCH OPPORTUNITIES FOR THE NEXT DECADE Abstract Only

Boris W. Batterman *In* Oulu Univ., Proceedings of the 25th Annual Conference of the Finnish Physical Society 1991 1 p (For primary document see N92-10362 01-70)
Avail: NTIS HC/MF A12

N92-10377# Oulu Univ. (Finland). Dept. of Physics.
SYNCHROTRON RADIATION RESEARCH AND FINNISH BEAMLINE AT MAX-LAB Abstract Only
Seppo Aksela *In its* Proceedings of the 25th Annual Conference on the Finnish Physical Society 1991 1 p (For primary document see N92-10362 01-70)
Avail: NTIS HC/MF A12

N92-10420# Jyvaskyla Univ. (Finland). Dept. of Physics.
THE JYVASKYLA (FINLAND) K130 CYCLOTRON PROJECT Abstract Only
Esko Liukkonen *In* Oulu Univ., Proceedings of the 25th Annual Conference of the Finnish Physical Society 1991 1 p (For primary document see N92-10362 01-70)
Avail: NTIS HC/MF A12

N92-10421# Jyvaskyla Univ. (Finland). Dept. of Physics.
MAGNETIC FIELD SETTINGS FOR THE K130 CYCLOTRON Abstract Only
M. Rinta-Nikkola *In* Oulu Univ., Proceedings of the 25th Annual Conference of the Finnish Physical Society 1991 1 p (For primary document see N92-10362 01-70)
Avail: NTIS HC/MF A12

N92-10422# Jyvaskyla Univ. (Finland). Dept. of Physics.
STATUS OF THE JYFL-ECR ION SOURCE Abstract Only
J. Arje, V. Nieminen, J. Choinski, and T. A. Antaya (Michigan State Univ., East Lansing.) *In* Oulu Univ., Proceedings of the 25th Annual Conference of the Finnish Physical Society 1991 1 p (For primary document see N92-10362 01-70)
Avail: NTIS HC/MF A12

N92-10423# Technische Univ., Dresden (German D.R.). Inst. of Low Temperature Physics.
ULTRA-COLD POLARIZED HYDROGEN SOURCE Abstract Only
M. Mertig, V. G. Luppov, and Y. K. Pilipenko (Joint Inst. for Nuclear Research, Dubna, USSR) *In* Oulu Univ., Proceedings of the 25th Annual Conference of the Finnish Physical Society 1991 1 p (For primary document see N92-10362 01-70)
Avail: NTIS HC/MF A12

N92-10424# Jyvaskyla Univ. (Finland). Dept. of Physics.
PLAN FOR THE JYFL GAS-FILLED RECOIL SEPARATOR Abstract Only
M. Leino, J. Aysto, K. Eskola (Helsinki Univ. of Technology, Espoo, Finland), P. Heikkinen, R. Julin, J. Kumpulainen, and T. Enqvist *In* Oulu Univ., Proceedings of the 25th Annual Conference of the Finnish Physical Society 1991 1 p Sponsored by Academy of Finland (For primary document see N92-10362 01-70)
Avail: NTIS HC/MF A12

N92-10585# Imatran Voima Oy, Helsinki (Finland).
NUCLEAR ENERGY: ITS STRENGTHS, WEAKNESSES AND ROLE IN FINLAND Abstract Only
A. Ruuskanen *In* Oulu Univ., Proceedings of the 25th Annual Conference of the Finnish Physical Society 1991 1 p (For primary document see N92-10362 01-70)
Avail: NTIS HC/MF A12

74 OPTICS

Includes light phenomena; and optical devices.
For lasers see *36 Lasers and Masers.*

N92-10638*# Alabama Univ., Huntsville. Center for Applied Optics.
POLARIZATION ABERRATIONS. 1: ROTATIONALLY SYMMETRIC OPTICAL SYSTEMS Final Report
James P. McGuire, Jr. and Russell A. Chipman 16 Aug. 1990 32 p
(Contract NAS8-36955)
(NASA-CR-184218; NAS 1.26:184218) Avail: NTIS HC/MF A03 CSCL 20F

The analysis of the polarization characteristics displayed by optical systems can be divided into two categories: geometrical and physical. Geometrical analysis calculates the change in polarization of a wavefront between pupils in an optical instrument. Physical analysis propagates the polarized fields wherever the geometrical analysis is not valid, i.e., near the edges of stops, near images, in anisotropic media, etc. Polarization aberration theory provides a starting point for geometrical design and facilitates subsequent optimization. The polarization aberrations described arise from differences in the transmitted (or reflected) amplitudes and phases at interfaces. The polarization aberration matrix (PAM) is calculated for isotropic rotationally symmetric systems through fourth order and includes the interface phase, amplitude, linear diattenuation, and linear retardance aberrations. The exponential form of Jones matrices used are discussed. The PAM in Jones matrix is introduced. The exact calculation of polarization aberrations through polarization ray tracing is described. Author

N92-10639*# Alabama Univ., Huntsville. Center for Applied Optics.
CONTAMINATION STUDY Final Report
R. Barry Johnson and Kenneth A. Herren Sep. 1990 81 p
(Contract NAS8-36955)
(NASA-CR-184225; NAS 1.26:184225; UAH-5-32180) Avail: NTIS HC/MF A05 CSCL 20F

The time dependence of the angular reflectance from molecularly contaminated optical surfaces in the Vacuum Ultraviolet (VUV) is measured. The light scattering measurements are accomplished in situ on optical surfaces in real time during deposition of molecular contaminants. The measurements are taken using non-coherent VUV sources with the predominant wavelengths being the Krypton resonance lines at 1236 and 1600 A. Detection of the scattered light is accomplished using a set of three solar blind VUV photomultipliers. An in-plane VUV BRDF (Bidirectional Reflectance Distribution Functions) experiment is described and details of the ongoing program to characterize optical materials exposed to the space environment is reported. Author

N92-10640# Argonne National Lab., IL.
OPTICAL SIGNAL MULTIPLEXER AND DEMULTIPLEXER
Hideo Tsubata, Nobuaki Oharu, and Kiyoshi Sashida 18 Dec. 1990 5 p Transl. into ENGLISH of Japanese Patent No. 60-60605, (8 Apr. 1985)
(Contract W-31-109-eng-38)
(DE91-017836; ANL-Trans-90-19) Avail: NTIS HC/MF A01

An optical signal multiplexer and demultiplexer are described. A single optical receptor or emission diode is positioned facing the lens surface of a condenser lens at the focal point of said lens. Multiple collimator lens, which make parallel rays incident to the condenser lens or entrap parallel rays from the condenser lens, is positioned facing the respective condenser lens, noted above, on the side of said condenser lens opposite the above-noted light receptor or emission diode. At the focus spot of each collimator lens, another light emission or receptor diode, which faces the corresponding collimator lens, is positioned individually relative to its respective positions. DOE

N92-10641# Argonne National Lab., IL.
FIBER-TILE OPTICAL STUDIES AT ARGONNE

D. G. Underwood, D. J. Morgan, and J. Proudfoot 23 Jul. 1991 31 p
(Contract W-31-109-eng-38)
(DE91-018591; ANL-HEP-TR-91-69; SDC-91-00052) Avail: NTIS HC/MF A03

In support of a fiber-tile calorimeter for SDC, we have done studies on a number of topics. The most basic problems were light output and uniformity of response. Using a small electron beam, we have studied fiber placement, tile preparation, wrapping and masking, fiber splicing, fiber routing, phototube response, and some degradation factors. We found two configurations which produced more light output than the others and reasonably uniform response. We have chosen one of these to go into production for the EM test module on the basis of fiber routing for ease of assembly of the calorimeter. We have also applied some of the tools we developed to CDF end plug tile uniformity, shower max testing and development for a couple of detectors, and development of better techniques for radiation damage studies. DOE

N92-10642# North Carolina State Univ., Raleigh.
MULTI-GIGABIT FIBER OPTIC WIDE AREA NETWORK DEVELOPMENT Final Report, Mar. 1989 - Aug. 1990
J. B. ONeal, Jr., Michael R. Slawson, and J. K. Townsend Jul. 1991 178 p
(Contract F30602-88-D-0025)
(AD-A239850; RL-TR-91-132) Avail: NTIS HC/MF A09 CSCL 25/5

The development of the physical layer for a high speed (greater than 10 Gigabits/sec) fiber optic wide area network, implementable by the Air Force in a five to ten year timeframe is addressed. First, to gain a generally acceptable degree of survivability while maintaining efficiency, it is concluded that a counter-rotating ring physical topology is most appropriate. To obtain high link capacity, links will consist of multiple channels, each operating at data rates manageable using switching. Then, for efficient information transfer in a multi-service environment, each channel will operate with Asynchronous Transfer Mode (ATM), a fast packet switching technique. Many common logical network topologies are then overlayed onto this physical multichannel ATM ring foundation. Based on comparisons relative to several important criteria, a logical multi-ring architecture, with wavelength division multiplexing, is concluded to be the most promising alternative. An investigation of the media level implementation of this network, using the example of an eight channel link where each channel operates at 2.49 Gbps, shows that symmetrical, single-mode grating-based wavelength division demultiplexers and traveling wave optical amplifiers can be used to create bidirectional multichannel link spans exceeding 2000 km without electronic regeneration. GRA

N92-10643# Washington State Univ., Pullman. Dept. of Chemistry.
SURFACE EFFECT ON OPTICAL BISTABILITY IN COUPLED EXCITON-PHONON SYSTEMS INSIDE A CAVITY
D. L. Lin, X. Li, Z. D. Liu, and Thomas F. George Aug. 1991 14 p
(Contract N00014-90-J-1193)
(AD-A240026; WSU/DC/91/TR-58) Avail: NTIS HC/MF A03 CSCL 20/6

When laser beam are directed on an exciton-phonon coupling system inside an optical cavity, the cavity field intensity is investigated as a function of the driving field intensity for various distances between the sample and a metallic surface representing one of the mirrors of the cavity. Optical bistability is found to be induced by the surface when the cavity field is on resonance with the excitonic transition frequency. It is also found that at the threshold, the direction of switch of the optical bistability can be controlled by adjusting the distance from the surface. The investigation of optical properties of molecular systems near a solid surface has been of interest from both the fundamental and practical points of view. Exciton phonon coupling systems such as organic semiconductors have been considered very recently instead of single molecular systems located near ideal metal surfaces. Surface-induced optical bistability has been discovered and its nature and origin investigated. GRA

N92-10644# Naval Postgraduate School, Monterey, CA. Dept. of Electrical and Computer Engineering.
RECOVERING SIGNALS FROM OPTICAL FIBER INTERFEROMETRIC SENSORS Ph.D. Thesis
Charles B. Cameron Jun. 1991 400 p
(AD-A240062; NPS-EC-91-005) Avail: NTIS HC/MF A17 CSCL 14/2

This dissertation examines three methods of recovering signals cheaply from one class of highly sensitive Optical Fiber Interferometric Sensors (OFIS). This class of sensors consists of a laser light source; a 2x2 optical fiber coupler to split the beam in two; a differential transducer which converts a signal of interest into optical phase shift in the laser light transmitted through the two optical fibers in the interferometer; and a 3x3 optical fiber coupler which recombines the two beams, producing interference which can be detected electronically. The three outputs can be operated on symmetrically or asymmetrically to recover the signal of interest. The use of the 3x3 coupler permits Passive Homodyne Demodulation of the phase-modulated signals provided by the interferometer without feedback control or modulation of the laser itself and without requiring the use of electronics within the interferometer. One of the three methods discussed in this dissertation performs symmetric demodulation with analog electronics. Another uses analog-to-digital conversion of the signals and performs asymmetric demodulation in digital hardware. The third method discussed uses asymmetric fringe-rate demodulation. The three methods are characterized by their harmonic distortion, minimum detectable signal, bandwidth, dynamic range, noise, complexity, and approximate cost. GRA

N92-10378# Tampere Univ. of Technology (Finland). Dept. of Physics.
DOPPLER SHIFT VELOCIMETRY IN DISPERSE FLOWS Abstract Only
V. Hayrinen and Rolf G. Hernberg *In* Oulu Univ., Proceedings of the 25th Annual Conference of the Finnish Physical Society 1991 1 p Sponsored by Academy of Finland (For primary document see N92-10362 01-70)
Avail: NTIS HC/MF A12

N92-10439# Helsinki Univ. of Technology, Espoo (Finland). Dept. of Physics.
INTERACTION-INDUCED LIGHT SCATTERING AS A SOURCE OF INFORMATION ON PROPERTIES AND INTERACTIONS OF SPHERICAL TOP MOLECULES Abstract Only
N. Meinander, G. C. Tabisz, and S. M. El-Sheikh (Cairo Univ., Egypt) *In* Oulu Univ., Proceedings of the 25th Annual Conference of the Finnish Physical Society 1991 1 p (For primary document see N92-10362 01-70)
Avail: NTIS HC/MF A12

N92-10445# Helsinki Univ. of Technology, Espoo (Finland). Dept. of Energy Engineering.
ABSORPTION MEASUREMENTS WITH AN INTEGRATING SPHERE AND AN FT-IR SPECTROMETER Abstract Only
K. T. Ojala and M. J. Lampinen *In* Oulu Univ., Proceedings of the 25th Annual Conference of the Finnish Physical Society 1991 1 p (For primary document see N92-10362 01-70)
Avail: NTIS HC/MF A12

N92-10446# Oulu Univ. (Finland). Dept. of Physics.
STUDY OF DIFFERENT SX-700 DESIGNS FOR THE UNDULATOR BEAMLINE (BL51) AT MAX-LAB Abstract Only
Seppo Aksela, A. Kivimaki, R. Nyholm, and S. Svensson (Uppsala Univ., Sweden) *In its* Proceedings of the 25th Annual Conference of the Finnish Physical Society 1991 1 p (For primary document see N92-10362 01-70)
Avail: NTIS HC/MF A12

N92-10450# Kuopio Univ. (Finland). Dept. of Applied Physics.
OPTICAL CORRELATORS IN TEXTURE ANALYSIS Abstract Only
V. Honkonen, T. Jaaskelainen, and J. Parkkinen *In* Oulu Univ., Proceedings of the 25th Annual Conference of the Finnish Physical Society 1991 1 p (For primary document see N92-10362 01-70)
Avail: NTIS HC/MF A12

N92-10456# Kuopio Univ. (Finland). Dept. of Applied Physics.
COUPLED WAVE ANALYSIS IN INVERSE GRATING DIFFRACTION PROBLEMS Abstract Only
M. Kuittinen and T. Jaaskelainen *In* Oulu Univ., Proceedings of the 25th Annual Conference of the Finnish Physical Society 1991 1 p (For primary document see N92-10362 01-70)
Avail: NTIS HC/MF A12

N92-10457# Helsinki Univ. of Technology, Espoo (Finland). Dept. of Technical Physics.
PARAMETRIC OPTIMIZATION OF SYNTHETIC GRATINGS USING VECTOR DIFFRACTION THEORY Abstract Only
Eero Noponen, Antti Vasara, and Jari Turunen (Heriot-Watt Univ., Edinburgh, Scotland) *In* Oulu Univ., Proceedings of the 25th Annual Conference of the Finnish Physical Society 1991 1 p (For primary document see N92-10362 01-70)
Avail: NTIS HC/MF A12

N92-10458# Helsinki Univ. of Technology, Espoo (Finland). Dept. of Technical Physics.
WAVEGUIDE DAMMANN GRATINGS AND KINOFORMS Abstract Only
Jyrki Saarinen, Juhani Huttunen, Antti Vasara, Jari Turunen, and Arto Salin (Technical Research Centre of Finland, Espoo.) *In* Oulu Univ., Proceedings of the 25th Annual Conference of the Finnish Physical Society 1991 1 p (For primary document see N92-10362 01-70)
Avail: NTIS HC/MF A12

N92-10486# Thomson-CSF, Orsay (France).
HIGHLIGHTS OF MATERIAL RESEARCH FOR OPTOELECTRONICS IN THE EIGHTIES, TRENDS AND CHALLENGES FOR THE NINETIES Abstract Only
M. Razeghi *In* Oulu Univ., Proceedings of the 25th Annual Conference of the Finnish Physical Society 1991 1 p (For primary document see N92-10362 01-70)
Avail: NTIS HC/MF A12

N92-10494# National Research Council of Canada, Ottawa (Ontario). Div. of Physics and Inst. for Microstructural Sciences.
MAGNETO-OPTICAL TRANSITIONS IN A COULOMB COUPLED PAIR OF QUANTUM DOTS Abstract Only
Tapash Chakraborty, V. Halonen, and P. Pietilainen (Oulu Univ., Finland) *In* Oulu Univ., Proceedings of the 25th Annual Conference of the Finnish Physical Society 1991 1 p (For primary document see N92-10362 01-70)
Avail: NTIS HC/MF A12

N92-10495# National Research Council of Canada, Ottawa (Ontario).
RECOMBINATION RADIATION IN THE FRACTIONAL QUANTUM HALL EFFECT REGIME Abstract Only
Tapash Chakraborty and P. Pietilainen (Oulu Univ., Finland) *In* Oulu Univ., Proceedings of the 25th Annual Conference of the Finnish Physical Society 1991 1 p (For primary document see N92-10362 01-70)
Avail: NTIS HC/MF A12

N92-10546# Helsinki Univ. of Technology, Espoo (Finland).
VARIABLE OPTICAL POLARIZATION IN Her X-1 Abstract Only
P. J. Hakala and J. Egonsson *In* Oulu Univ., Proceedings of the 25th Annual Conference of the Finnish Physical Society 1991 1 p Prepared in cooperation with Lund Observatory, Sweden (For primary document see N92-10362 01-70)
Avail: NTIS HC/MF A12

75 PLASMA PHYSICS

Includes magnetohydrodynamics and plasma fusion.
For ionospheric plasmas see *46 Geophysics*. For space plasmas see *90 Astrophysics*.

N92-10645# National Inst. for Fusion Science, Nagoya (Japan).
SINGLE PARTICLE AND FLUID PICTURE FOR THE PONDEROMOTIVE DRIFT IN NONUNIFORM PLASMAS
B. Bhattacharyya, T. Watanabe, and Kyoji Nishikawa (Hiroshima Univ., Japan) Apr. 1990 14 p
(NIFS-25; ISSN-0915-633X) Avail: NTIS HC/MF A03

General expressions for the ponderomotive force as a second-order average force acting on a single charged particle are derived in the form of potential force. The result is valid for arbitrary spatial structure of the ambient static magnetic field. Sum of the resulting drift flux and the second-order magnetic flux due to the induced magnetic moments of the particles is found to agree with the second-order averaged flux calculated by the fluid model. Author

N92-10646# National Inst. for Fusion Science, Nagoya (Japan).
SIMULATION STUDY OF SCALINGS IN SCRAPE-OFF LAYER PLASMA BY TWO-DIMENSIONAL TRANSPORT CODE
Sanae-I. Itoh, Noriaki Ueda (Mitsubishi Atomic Power Industries, Inc., Tokyo, Japan), and Kimitaka Itoh Mar. 1990 35 p Sponsored in part by Ministry of Education
(NIFS-24; ISSN-0915-633X) Avail: NTIS HC/MF A03

Numerical analysis on Scrape-Off Layer (SOL) plasma and divertor plasma in tokamaks is made by using 2-D time-dependent transport code (UEDA code). Plasma transport in SOL and the divertor region is calculated for given particle and heat sources from the main plasma. Scaling study of the density, the temperature, and their fall-off lengths is done for JFT-2M tokamak. The results show inter-relations between the divertor plasma parameters and the core plasma confinement. The operational conditions of the core to guarantee the divertor performance are discussed.
Author

N92-10647# National Inst. for Fusion Science, Nagoya (Japan).
OBSERVATION OF PLASMA TOROIDAL ROTATIONS DRIVEN BY THE ELECTRIC FIELD DUE TO A LOSS OF IONS
K. Ida, K. Kawahata, K. Toi, T. Watari, O. Kaneko, Y. Ogawa, H. Sanuki, K. Adati, R. Akiyama, and A. Ando et al Mar. 1990 16 p
(NIFS-23; ISSN-0915-633X) Avail: NTIS HC/MF A03

Plasma toroidal rotations not driven by the momentum input but by the electric field due to a loss of ions were observed for the plasmas heated with perpendicular neutral beam injection. They are found to be increased in the counter direction to the plasma current as plasma ions are heated with ion cyclotron resonance frequency waves. The electric field derived from rotations are quantitatively consistent with those inferred from the ambipolarity of particle fluxes. Author

N92-10648# National Inst. for Fusion Science, Nagoya (Japan).
THE MEANDERING ORBIT EFFECT ON STABILIZATION OF THE TILTING INSTABILITY IN A FIELD-REVERSED CONFIGURATION
Ritoku Horiuchi (Science Project Corp., Hiroshima, Japan) and Tetsuya Sato Mar. 1990 35 p Sponsored by Ministry of Education, Science and Culture
(NIFS-22; ISSN-0915-633X) Avail: NTIS HC/MF A03

Ion kinetic effect in the tilt disruption of a field reversed configuration is studied by means of a 3-D particle simulation. It is found that the tilt disruption is completely suppressed when s(vector) approx. = 1, where s(vector) measures the number of ion gyroradii over the radial distance between the magnetic separatrix line and the field-null line. Prolate magnetic well is formed

around the field-null line, in which ions do not execute gyration but meander along the field-null line. For the case of s(vector) approx. = 1, a large number of ions exist in the magnetic well and move on stable orbits around the major axis with the average rotation velocity nearly equal to half of the thermal velocity. As s(vector) becomes larger than 1, the number of ions in the magnetic well decreases and the stabilization effect is reduced. It is also found that an anisotropy is created in the ion thermal pressure profile owing to the anisotropy of the meandering orbits and that the electric field fluctuation always remain at a low level, thus the electric field plays no essential role in the tilt stabilization.
Author

N92-10649# National Inst. for Fusion Science, Nagoya (Japan).
FAST WAVE HEATING AT INTERMEDIATE ION CYCLOTRON HARMONICS ON THE JIPP T-II U TOKAMAK
Y. Takase (Massachusetts Inst. of Tech., Cambridge.), T. Watari, R. Kumazawa, T. Seki, K. Adati, R. Ando, T. Aoki, Y. Hamada, S. Hirokura, and K. Ida et al Feb. 1990 25 p Sponsored by Ministry of Education
(Contract DE-AC02-78ET-51013)
(NIFS-21; ISSN-0915-633X) Avail: NTIS HC/MF A03

Fast wave absorption and heating at a relatively high ion cyclotron harmonic were studied on the JIPP T-II U tokamak. In spite of the low absorption efficiency predicted by a simple theory for present experimental parameters, appreciable electron and ion heating was observed. Heating is most effective at relatively low densities. Ion trail was observed on the majority deuterium energy spectrum but not on the minority hydrogen spectrum, which suggests the possibility of direct absorption of mode-converted ion Bernstein wave power by deuterium ions. Because of the density rise caused by radio frequency injection, clear evidence of fast wave driven current was not observed. Author

N92-10650# Ceskoslovenska Akademie Ved, Prague. Inst. of Plasma Physics.
ON PONDEROMOTIVE FORCE EFFECTS ON COUPLING OF THE LH AND IBW GRILLS FOR THE FTU TOKAMAK
V. Petrzilka Oct. 1990 15 p
(IPPCZ-305) Avail: NTIS HC/MF A03

A nonlinear coupling theory has been used for estimates of the reflection coefficient for the 8 GHz lower hybrid (LH) and 433 MHz ion Bernstein wave (IBW) grills in the FTU tokamak. For the IBW grill, the plasma density decrease due to strong ponderomotive effects. At the full design power of this grill, the reflection coefficient could be unacceptably high. Author

N92-10651# Ceskoslovenska Akademie Ved, Prague. Inst. of Plasma Physics.
EXPERIMENTAL STUDIES OF TOKAMAK PLASMA IN IPP PRAGUE
F. Zacek, J. Badalec, K. Jakubka, L. Kryska, J. Stoeckel, and M. Valovic Feb. 1991 36 p
(IPPCZ-310) Avail: NTIS HC/MF A03

A short survey of experimental activity on small Prague tokamak CASTOR (Czechoslovak Academy of Sciences TORus) during a few last years is given. This activity consists at present of study of anomalous transport and plasma-wall interaction in tokamak under conditions of combined OH/LHCD regimes. Moreover, some new diagnostics were developed and certain improvements in CASTOR performances were achieved. Author

N92-10652# Ceskoslovenska Akademie Ved, Prague. Inst. of Plasma Physics.
NUMERICAL SIMULATION OF ION BEAM GENERATED IN THE DIODE WITH ANODE PLASMA COLUMN
P. Vrba, P. Sunka, and N. I. Gaponenko (Academy of Sciences of the Ukrainian SSR, Kharkov.) Feb. 1991 24 p
(IPPCZ-306) Avail: NTIS HC/MF A03

The ion beam generation in the high current diode with anode plasma slab was studied. The ions are extracted from the anode plasma by the strong electric field of deep potential well (virtual cathode), arising after the propagation of relativistic electrons through the anode plasma slab. The movement of this potential well with the front part of the ion beam leads to collective ion acceleration approximately up to the 10 MeV energy range.
Author

N92-10653# Ceskoslovenska Akademie Ved, Prague. Inst. of Plasma Physics.
ON ACCELERATION OF CHARGED PARTICLES IN INTENSITY MINIMA OF LASER FIELDS
V. Petrzilka Feb. 1991 17 p
(IPPCZ-307) Avail: NTIS HC/MF A03

Using Klima-Bogoliubov-Zubarev method, the acceleration of charged particles (electrons) in moving intensity minima of interference laser fields is studied. The electromagnetic field intensity threshold for an eventual slipping through of the particle through the potential barrier is found both analytically and numerically. Millimeter and submillimeter electromagnetic waves should be irradiated due to forced electron oscillations in potential wells. Author

N92-10654# National Inst. for Fusion Science, Nagoya (Japan).
HIGH RESOLUTION SPECTROSCOPY OF H(+) ENERGY LOSS IN THIN CARBON FILM
Noriaki Matsunami and Kenshin Kitoh (Nagoya Univ., Japan) May 1991 21 p
(NIFS-88; ISSN-0915-633X) Avail: NTIS HC/MF A03

The energy loss of approximately 100 keV H(+) transmitted through thin carbon film of approximately 7 nm was measured with the resolution of approximately 20 eV. We observed new energy loss peaks around 210 and 400 eV in addition to the normal energy loss peak around 1 keV. We find that the experimental artifacts, ionization of C K-(290 eV) and impurity inner-shells, extreme non-uniformity of films, events associated with elastic scattering are not responsible for these peaks. The origin of these energy loss peaks is discussed. Author

N92-10655# National Inst. for Fusion Science, Nagoya (Japan).
GEOMETRICAL EFFECTS OF THE MAGNETIC FIELD ON THE NEOCLASSICAL FLOW, CURRENT, AND ROTATION IN GENERAL TOROIDAL SYSTEMS
N. Nakajima and M. Okamoto May 1991 34 p Sponsored by Ministry of Education, Science and Culture
(NIFS-86; ISSN-0915-633X) Avail: NTIS HC/MF A03

In order to clarify geometrical effects of the magnetic field on neoclassical theory, the neoclassical parallel particle flow, heat flux, current, and plasma rotation of a multispecies plasma in general toroidal systems are examined in several collisionality regimes. The quantitative and qualitative differences between axisymmetric (tokamak) and non-axisymmetric toroidal systems (stellarators, heliotron/torsatron) appear mainly through a geometrical factor which prescribes the parallel flow due to the gradients of the density, temperature, and electrostatic potential. In axisymmetric toroidal systems the geometrical factor reduces to the same expression in all collisionality regimes due to axisymmetry. By contrast, in non-axisymmetric toroidal systems, it changes drastically depending on the magnetic field structure and the collisionality regime. Thus, the poloidal flow has the radial electric field dependence. When the geometrical factor is very small, the ion parallel flow almost vanishes and the ion rotation consists of the diamagnetic and E(vector) x B(vector) flows (perpendicular flows). Author

N92-10656# National Inst. for Fusion Science, Nagoya (Japan).
DEPENDENCE OF Au(-) PRODUCTION UPON THE TARGET WORK FUNCTION IN A PLASMA-SPUTTER-TYPE NEGATIVE ION SOURCE
Yushirou Okabe, Mamiko Sasao, Hitoshi Yamaoka, Motoi Wada (Doshisha Univ., Kyoto, Japan), and Junji Fujita May 1991 31 p Sponsored in part by Ministry of Education, Science and Culture
(NIFS-85; ISSN-0915-633X) Avail: NTIS HC/MF A03

A method to measure the work function of the target surface in a plasma-sputter-type negative ion source was developed. The

present method can be used to determine the work function by measuring the photoelectric current induced by two lasers (He-Ne, Ar(+) laser). The dependence of Au(-) production upon the work function of the target surface in the ion source was studied using this method. The time variation of the target work function and Au(-) production rate were measured during the cesium coverage decrease due to the plasma ion sputtering. The observed minimum work function of a cesiated gold surface in an AR plasma was 1.3 eV where the negative ion production rate (Au(-) current/target current) took the maximum value. The negative ion production rate showed the same dependence on the incident ion energy as that of the sputtering rate when the work function was constant.
Author

N92-10657# National Inst. for Fusion Science, Nagoya (Japan).
DENSITY PEAKING IN THE JFT-2M TOKAMAK PLASMA WITH COUNTER NEUTRAL BEAM INJECTION
K. Ida, Sanae-I. Itoh, Kimitaka Itoh, S. Hidekuma, Y. Miura, H. Kawashima, M. Mori, T. Matsuda, N. Suzuki, and H. Tamai (Japan Atomic Energy Research Inst., Ibaraki.) et al May 1991 22 p
(NIFS-83; ISSN-0915-633X) Avail: NTIS HC/MF A03

A significant particle pinch and reduction of the effective thermal diffusivity are observed after switching the neutral beam direction from co- to counter- injection in the JFT-2M tokamak. A time delay in the occurrence of density peaking to that of plasma rotation is found. This shows that the particle pinch is related to the profile of the electric field as determined by the plasma rotation profile. The measured particle flux shows qualitative agreement with the theoretically-predicted inward pinch.
Author

N92-10658# Lawrence Livermore National Lab., CA.
NONLINEAR RF PROCESSES IN PLASMA
E. Morse 18 Dec. 1990 3 p Prepared in cooperation with California Univ., Berkeley
(Contract W-7405-eng-48)
(DE91-017441; UCRL-CR-107855) Avail: NTIS HC/MF A01

This report is a final progress report for a research contract with Lawrence Livermore Laboratory entitled Nonlinear RF Processes in Plasma. The purpose of this research contract was to establish some understanding of nonlinear radiofrequency (RF) effects in magnetized and unmagnetized plasma environments driven by strong electromagnetic fields. This research was particularly directed at the development of a nonlinear ray tracing method. This method can be applied to vector wave propagation problems such as electromagnetic wave propagation in plasma. A key issue in this development was the treatment of the nonlinear term in the plasma wave equation by an equivalent nonlinear dielectric tensor epsilon sub 2 E vector, omega, x vector which could then fit into our basic formalism. Calculating a nonlinear dielectric tensor of this form for the relevant driven plasma systems was included as another theoretical task. This was effected by using a computer simulation method known as f-moving, whereby the distribution function f of a plasma system with RF fields present was simulated using an equilibrium distribution function f(sub 0) and directly integrating the Vlasov equation along characteristics in order to obtain the perturbed distribution function f. This approach results in a relatively inexpensive but accurate method for obtaining the plasma response including parametric instabilities caused by strong RF drive. From these simulations, the equivalent epsilon sub 2 could be calculated and used in the nonlinear ray tracing. A third task in this contract was the integration of these techniques (the f-moving and nonlinear ray tracing) to generate a complete ray tracing package for the simulation of lower hybrid wave propagation in compact toroids. The results of these investigations are described below, separated into the three tasks.
DOE

N92-10659# Department of Energy, Washington, DC. Office of the Deputy Assistant Secretary for Oil, Gas, Shale, and Special Technologies.
MHD PROGRAM PLAN, FY 1991
Oct. 1990 39 p
(DE91-017916; DOE/FE-0239P) Avail: NTIS HC/MF A03

The current magnetohydrodynamic MHD program being implemented is a result of a consensus established in public meetings held by the Department of Energy in 1984. The public meetings were followed by the formulation of a June 1984 Coal-Fired MHD Preliminary Transition and Program Plan. This plan focused on demonstrating the proof-of-concept (POC) of coal-fired MHD electric power plants by the early 1990s. MHD test data indicate that while there are no fundamental technical barriers impeding the development of MHD power plants, technical risk remains. To reduce the technical risk three key subsystems (topping cycle, bottoming cycle, and seed regeneration) are being assembled and tested separately. The program does not require fabrication of a complete superconducting magnet, but rather the development and testing of superconductor cables. The topping cycle system test objectives can be achieved using a conventional iron core magnet system already in place at a DOE facility. Systems engineering-derived requirements and analytical modeling to support scale-up and component design guide the program. In response to environmental, economic, engineering, and utility acceptance requirements, design choices and operating modes are tested and refined to provide technical specifications for meeting commercial criteria. These engineering activities are supported by comprehensive and continuing systems analyses to establish realistic technical requirements and cost data. Essential elements of the current program are to: develop technical and environmental data for the integrated MHD topping cycle and bottoming cycle systems through POC testing (1000 and 4000 hours, respectively); design, construct, and operate a POC seed regeneration system capable of processing spent seed materials from the MHD bottoming cycle; prepare conceptual designs for a site specific MHD retrofit plant; and continue supporting research necessary for system testing.
DOE

N92-10660# Michigan Univ., Ann Arbor. Dept. of Nuclear Engineering.
THE MAGNETICALLY INSULATED INERTIAL CONFINEMENT FUSION: A NOVEL APPROACH
T. Kammash Jun. 1991 8 p
(Contract DE-FG02-87ER-13723)
(DE91-018273; DOE/ER-13723/3) Avail: NTIS HC/MF A02

This report summarizes the results of a three-year investigation of the Magnetically Inertial Confinement Fusion (MICF) concept. Although the details of the investigation will not be presented here and will be left to the publications generated by the study, the main results and potential applications will be highlighted. The most important conclusion of the study is that MICF does present a very promising approach to fusion power, and that no serious physics issues appear to stand in the way of its eventual utilization as a fusion reactor.
DOE

N92-10661# General Atomic Co., San Diego, CA.
OVERVIEW OF THE 1990'S D3-D RESEARCH PROGRAM
T. C. Simonen Jun. 1991 8 p Presented at the Annual Meeting and Symposium of the Fusion Power Associates, Princeton, NJ, 25-26 Jun. 1991
(Contract DE-AC03-89ER-51114)
(DE91-018185; GA-A-20569; CONF-9106182-2) Avail: NTIS HC/MF A02

The D3-D tokamak plays a key role in the U.S. Magnetic Fusion Energy Development Strategy. With its focus on understanding and demonstrating the underlying physics and the technologies of heating and current drive, divertor particle and impurity control, high beta plasma production, and confinement, D3-D is uniquely suited to address the critical technology issues of next generation machines. The Burning Plasma Experiment (BPX), Engineering Test Reactor (ITER) and the Steady-State Tokamak (STE) are patterned after D3-D, and their designs will be immeasurably enhanced by timely results from the D3-D program. The D3-D program goal is to carry out an integrated demonstration of non-inductive current drive in a well-confined high-beta divertor plasma. Our reference scenario is to drive 2 MA of current, at 5 percent beta for 10 seconds. This capability will enable D3-D to carry out an integrated physical and technology program in the mid to late 1990's. As such D3-D is both an

advanced tokamak and a divertor test bed; a 1990's fusion facility. The Doublet 3 device was modified to D3-D which began operation in 1986. The addition of substantial RF heating and current drive capability and new divertor hardware are now underway to transform D3-D to a non-inductively current driven divertor tokamak. This modernization will upgrade D3-D into a 1990's tokamak facility capable of impacting the next century's world fusion program. Following initial current drive experiments with 2 MW each of electron cyclotron heating and fast wave current drive in late 1991, D3-D will be ready to begin high power non-inductive current drive. With upgrades to the RF power and divertor systems, D3-D will be an advanced tokamak, capable of operating with non-inductive current drive for long pulses and addressing crucial divertor power and particle control issues. DOE

N92-10662# General Atomic Co., San Diego, CA.
VH-MODE: A NEW VERY HIGH CONFINEMENT REGIME IN THE BORONIZED DIII-D TOKAMAK
T. C. Simonen Jun. 1991 5 p Presented at the International Conference on Systems Analysis in Water Quality Management, Berlin, Fed. Republic of Germany, 3-7 Jun. 1991
(Contract DE-AC03-89ER-51114)
(DE91-018186; GA-A-20552; CONF-910609-21) Avail: NTIS HC/MF A01

A very high confinement mode, well beyond usual H-mode performance, has recently been obtained in DIII-D following boronization. Although these results are preliminary, they have been duplicated on three days of operation. These results could have highly favorable impact on next generation tokamak performance if the VH-mode can be extended to higher parameters and longer discharge durations. The utility of this discovery awaits future work exploring VH-mode scaling with plasma parameters, developing a physics understanding, and extending it to steady state with non-inductive RF current drive profile control. DOE

N92-10663# Texas Univ., Austin. Inst. for Fusion Studies.
ION TEMPERATURE GRADIENT DRIVEN TRANSPORT IN A DENSITY MODIFICATION EXPERIMENT ON THE TFTR TOKAMAK
W. Horton, D. Lindberg, J. Y. Kim, J. Q. Dong, G. W. Hammett, S. D. Scott, M. C. Zarnstorff (Princeton Univ., NJ.), and S. Hamaguchi Jul. 1991 46 p
(Contracts DE-FG05-80ET-53088; DE-AC02-76CH-03073)
(DE91-018215; DOE/ET-53088/501; IFSR-501) Avail: NTIS HC/MF A03

Tokamak Fusion Test Reactor (TFTR) profiles from a supershot density-modification experiment are analyzed for their local and ballooning stability to toroidal (eta)(sub i)-modes in order to understand the initially puzzling results showing no increase in X(sub i) when a pellet is used to produce an abrupt and large increase in the (eta)(sub i) parameter. The local stability analysis assumes that k(parallel) equals 1/qR and ignores the effects of shear, but makes no assumption on the magnitude of k(parallel)v(sub ti)/(omega). The ballooning stability analysis determines a self-consistent linear spectrum of k(parallel)'s including the effect of shear and toroidicity, but it expands in k(parallel)v(sub ti)/(omega) less than or equal to 1, which is a marginal assumption for this experiment. Nevertheless, the two approaches agree well and show that the mixing length estimate of the transport rate does not change appreciably during the density-modification and has a value close to or less than the observed X(sub i), in contrast to most previous theories which predicted X(sub i)'s which were over an order-of-magnitude too large. However, we are still unable to explain the observed increase X(sub i)(r) with minor radius by adding the effects of the finite beta drift - magnetohydrodynmaic mode coupling, the slab-like mode, or the trapped electron response. The experimental tracking 0.2 less than X(sub e)/X(sub i) less than 0.7 suggest that both grad T(sub i) and trapped-electron driving mechanisms are operating. DOE

N92-10664# General Atomic Co., San Diego, CA.
THE DIII-D TOKAMAK AND ENERGY CONFINEMENT AT LOW q
R. Snider Aug. 1991 19 p
(Contract DE-AC03-89ER-51114)
(DE91-018317; GA-A-20556) Avail: NTIS HC/MF A03

A summary of DIII-D capabilities and recent improvements is given. The ability to produce highly shaped plasmas in DIII-D has been exploited to produce (beta)(sub T) values of 11 percent. Stability calculations indicate that the current and pressure profile details effect the maximum (beta)(sub T) that can be achieved. The linear increase of H-mode confinement with plasma current ceases for I(sub p)/B(sub T) larger than approx. 1 (MA/T). The most likely cause for the degradation is increased transport due to sawteeth. It has been determined, experimentally, that the saturation of confinement is not the result of a ceiling imposed by saturated Ohmic confinement, by the plasma reaching a (beta) limit, by enhanced plasma radiation, or by ELMs. DOE

N92-10665# General Atomic Co., San Diego, CA.
THEORY OF ION BERNSTEIN WAVE COUPLING AT LOW EDGE DENSITIES
S. C. Chiu, M. J. Mayberry, R. I. Pinsker, C. C. Petty, and M. Porkolab Aug. 1991 4 p Presented at the 9th Topical Conference on Radio Frequency Power in Plasmas, Charleston, SC, 12-14 Aug. 1991
(Contract DE-AC03-89ER-51114)
(DE91-018321; GA-A-20608; CONF-910869-4) Avail: NTIS HC/MF A01

D3-D Ion Bernstein Wave Coupling results are characterized by: (1) insensitivity of loading to the magnitude of the static magnetic field, and (2) large values of resistive loading (about 3 to 10 Omega). These are in sharp contrast to previous predictions. The experimental observations strongly suggest that the plasma in front of the Faraday shield is the coupling to cold plasma waves. A lower-hybrid resonance layer may exist at the edge, so a cold plasma coupling code has been developed which takes into account the lower-hybrid resonance rigorously. Using this code, and postulating that the density in front of the Faraday shield is always lower than the lower-hybrid resonance density, reasonable agreement between theory and experimental results is obtained. An estimate of the ponderomotive force produced by the wave field suggests that a low density region in front of the Faraday shield can be reasonably expected from the effect of this nonlinear force. DOE

N92-10666# Sandia National Labs., Albuquerque, NM.
THE INFLUENCE OF PLASMA MOTION ON DISRUPTION GENERATED RUNAWAY ELECTRONS
A. J. Russo 1991 28 p Presented at the IAEA Technical Committee Meeting on the Avoidance and Control of Tokamak Disruptions, Abindgon, England, 10-12 Sep. 1991
(Contract DE-AC04-76DP-00789)
(DE91-018356; SAND-91-1937C; CONF-9109252-1) Avail: NTIS HC/MF A03

One of the possible consequences of disruptions is the generation of runaway electrons which can impact plasma facing components and cause damage due to high local energy deposition. This problem becomes more serious as the machine size and plasma current increases. Since large size and high currents are characteristics of proposed future machines, control of runaway generation is an important design consideration. A lumped circuit model for disruption runaway electron generation indicates that control circuitry can strongly influence runaway behavior. A comparison of disruption data from several shots on JET and D3-D with model results, demonstrate the effects of plasma motion on runaway number density and energy. DOE

N92-10667# Texas Univ., Austin. Inst. for Fusion Studies.
GEOMETRIC PHASE, ROTATIONAL TRANSFORMS AND ADIABATIC INVARIANTS IN TOROIDAL MAGNETIC FIELDS
A. Bhattacharjee, G. M. Schreiber (Columbia Univ., New York, NY.), and J. B. Taylor Jul. 1991 8 p

(Contract DE-FG05-80ET-53088)
(DE91-018419; DOE/ET-53088/509; IFSR-509) Avail: NTIS HC/MF A02

The rotational transform associated with the magnetic surfaces of a toroidal magnetic field with a non-planar axis is an example of the angle anholonomy recently much discussed in quantum and classical dynamics (the Berry phase and Hannay angle). The same anholonomic angle appears in the phase of a charged particle spiraling around its guiding center in a strong magnetic field. This accounts for a contribution to the longitudinal invariant, associated with the guiding-center motion, which is different for guiding-center orbits that circulate in opposite directions and is absent for orbits that are reflected between mirrors. DOE

N92-10668# Texas Univ., Austin. Inst. for Fusion Studies.
STABILIZATION OF THE m = 1 TEARING MODE BY RESONANCE DETUNING
A. Thyagaraja (United Kingdom Atomic Energy Authority, Culham, England), R. D. Hazeltine, and A. Y. Aydemir Aug. 1991 16 p
(Contract DE-FG05-80ET-53088)
(DE91-018423; DOE/ET-53088/516; IFSR-516) Avail: NTIS HC/MF A03

The possibility of stabilizing the m = 1 tearing mode by rapidly oscillating the resonance point r(sub s)(t) about its mean position is examined. The calculations are carried out for both externally controlled, coherent oscillations of r(sub s)(t), as well as those resulting from turbulent plasma motions. Complete stabilization is possible in the coherent case, while turbulent fluctuations may yield substantial reduction in the growth rate. The technique seems to apply to any linear mode that depends upon local properties around a resonant surface. DOE

N92-10669# Lawrence Livermore National Lab., CA.
PLASMA PHYSICS RESEARCH INSTITUTE, LAWRENCE LIVERMORE NATIONAL LABORATORY, UNIVERSITY OF CALIFORNIA, DAVIS ANNUAL REPORT FOR FISCAL YEAR 1989
J. Killeen and R. P. Drake 26 Jul. 1991 20 p
(Contract W-7405-eng-48)
(DE91-018490; UCRL-ID-108096) Avail: NTIS HC/MF A03

This report discusses: The Davis Diverted Tokamak; Particle Simulation of Transport in Fusion Devices; Astrophysical Plasmas; Statistical Dynamics of Multi-Field Models for Plasma; Large Scale Density Modifications Induced in the Ionosphere; Studies of the Ion Acoustic Decay Instability; and Computer Simulation of Ionospheric Radio Frequency Heating. DOE

N92-10670# Lawrence Livermore National Lab., CA.
ELECTROMAGNETIC PLASMA SIMULATION IN REALISTIC GEOMETRIES
S. Brandon, J. J. Ambrosiano, and D. Nielsen 1 Aug. 1991 6 p
(Contract W-7405-eng-48)
(DE91-018651; UCRL-ID-108042) Avail: NTIS HC/MF A02

Particle-in-Cell (PIC) calculations have become an indispensable tool to model the nonlinear collective behavior of charged particle species in electromagnetic fields. Traditional finite difference codes, such as CONDOR (2-D) and ARGUS (3-D), are used extensively to design experiments and develop new concepts. A wide variety of physical processes can be modeled simply and efficiently by these codes. However, experiments have become more complex. Geometrical shapes and length scales are becoming increasingly more difficult to model. Spatial resolution requirements for the electromagnetic calculation force large grids and small time steps. Many hours of CRAY YMP time may be required to complete 2-D calculation -- many more for 3-D calculations. In principle, the number of mesh points and particles need only to be increased until all relevant physical processes are resolved. In practice, the size of a calculation is limited by the computer budget. As a result, experimental design is being limited by the ability to calculate, not by the experimenters ingenuity or understanding of the physical processes involved. Several approaches to meet these computational demands are being pursued. Traditional PIC codes continue to be the major design tools. These codes are being actively maintained, optimized, and extended to handle large and more complex problems. Two new formulations are being explored to relax the geometrical constraints of the finite difference codes. A modified finite volume test code, TALUS, uses a data structure compatible with that of standard finite difference meshes. This allows a basic conformal boundary/variable grid capability to be retrofitted to CONDOR. We are also pursuing an unstructured grid finite element code, MadMax. The unstructured mesh approach provides maximum flexibility in the geometrical model while also allowing local mesh refinement. Both innovative approaches to electromagnetic PIC calculations are generalizable to 3-D. DOE

N92-10671# General Atomic Co., San Diego, CA.
THE 110 GHz ECH HEATING SYSTEM FOR DIII-D
R. Callis, W. Cary, C. Moeller, R. Freeman, R. Prater, D. Remsen, and L. Sevier Aug. 1991 5 p Presented at the 9th Topical Conference on Radio Frequency Power in Plasmas, Charleston, SC, 12-14 Aug. 1991
(Contract DE-AC03-89ER-51114)
(DE91-018732; GA-A-20627; CONF-910869-6) Avail: NTIS HC/MF A01

Electron cyclotron heating (ECH) has been demonstrated to be effective at heating tokamak plasmas in DIII-D and other tokamaks. Extension of these results to high frequency and higher power in DIII-D is planned using 110 GHz outside launch X-mode at the second harmonic. A 2 MW system constructed from four modules, each using a Varian 0.5 MW 110 GHz gyrotron, is scheduled to be completed by May 1992; construction of a complete 0.5 MW module is complete and is in checkout. The results of the engineering test will be reported. A unique feature of this design is the use of strongly guided HE(sub 11) modes to transmit the power over the long distances required. The choice of a strongly guided HE(sub 11) mode for transmitting the ECH power was influenced by the compact waveguide, the non-critical alignment which allows waveguide flex, the ability to use mode selective directional couplers, and finally, continuous curvature bends can be used since there are no trapped modes. The waveguide is evacuated to handle the required power density. Implementation of this design required the development of mode converters to convert from the TE(sub 15,2) mode generated by the gyrotron to the desired HE(sub 11). Results of the high power tests of the mode converters and transmission components will be presented. DOE

N92-10672# Edgerton, Germeshausen and Grier, Inc., Idaho Falls, ID.
SELF-CONSISTENT MODELING OF PLASMA SPRAYING PROCESSES
C. H. Chang and J. D. Ramshaw 1991 7 p Presented at the 10th International Symposium on Plasma Chemistry, Jerusalem, Israel, 4-9 Aug. 1991
(Contract DE-AC07-76ID-01570)
(DE91-018820; EGG-M-91257; CONF-910867-1) Avail: NTIS HC/MF A02

A new numerical model is described for simulating thermal plasmas containing entrained particles, with emphasis on plasma spraying applications. The plasma is represented as a continuum multicomponent chemically reacting ideal gas, while the particles are tracked as discrete Lagrangian entities coupled to the plasma. Computational results are presented from a transient simulation of the melting of alumina particles injected into an axisymmetric pure argon plasma jet. DOE

N92-10673# Oak Ridge National Lab., TN.
FAST-WAVE ICRF MINORITY-REGIME HEATING EXPERIMENTS ON THE TORE SUPRA TOKAMAK
T. D. Shepard, G. R. Haste, F. W. Baity, G. Agarici, B. Beaumont, A. Becoulet, H. Kuus, B. Saoutic, and G. Martin 1991 4 p Presented at the 9th Topical Conference on Radio Frequency Power in Plasmas, Charleston, SC, 12-14 Aug. 1991
(Contract DE-AC05-84OR-21400)
(DE91-018866; CONF-910869-8) Avail: NTIS HC/MF A01

Up to 4 MW of RF power at 57 MHz has been coupled to Ohmic target plasmas during the first Inertial Confinement Reactor Fusion (ICRF) heating experiments on Tore Supra. A total of 12 MW of RF power will ultimately be available from six tetrode amplifiers and will be coupled to the plasmas using three Oak Ridge National Laboratory (ORNL)-CEA designed resonant double-loop antennas. During these first experiments, two antennas were used, with one or two energized at a time. The antenna loading with plasma was observed to be well over an order of magnitude greater than that without plasma. In addition, one kilo-electron-volt of electron heating, significant minority nonthermal ions, and significant increases in diamagnetic stored energy were observed. A comparison of in-phase and out-of-phase antenna operation showed the same increase in stored energy, less radiated power, and a larger drop in loop voltage for out-of-phase operation. Confinement scaling agrees with the ITER scaling law. DOE

N92-10674# Phillips Lab., Kirkland AFB, NM.
AN ANALYSIS OF THE FREQUENCY CHARACTERISTICS OF CORONA DISCHARGE AT LOW PRESSURE Report, Jan. 1990 - Apr. 1991
T. G. Lewis, George G. Karady, and Murray D. Sirkis Jul. 1991 82 p
(AF Proj. 9993)
(AD-A239940; PL-TR-91-1043) Avail: NTIS HC/MF A05 CSCL 20/9

Corona discharge is becoming more of a concern now that the space program is looking at higher power and voltage requirements for future missions. Improved detection methods for studying corona discharge will increase the knowledge base of how this phenomenon occurs, what effects it has on power systems, and how it is affected by outside influences. A better understanding of corona discharge will enable designers to improve on the space applications of insulation and dielectrics, and develop proper detection techniques. A test system was designed and constructed to measure the frequency spectrum of corona discharge current in low pressure. Various test samples in different arrangements were energized by ac voltage until corona discharge occurred. This same test was repeated at different pressures. The results indicate that the frequency spectrum of the discharge current changes with a change in pressure. At low pressures, the discharge frequency spectrum is concentrated in a narrow band with a peak at 17 kHz. As the pressure is increased, the spectral width increases to include components across a much broader band. Other tests were performed to correlate the frequency spectrum data to the shape of the discharge pulse and the physical appearance of the glow discharge. Author (GRA)

N92-10675# Naval Ocean Systems Center, San Diego, CA.
COLD FUSION VERIFICATION Final Report, period ending 1989
M. H. North, G. F. Mastny, and E. J. Wesley Mar. 1991 63 p
(NR Proj. RR0-00-N-0)
(AD-A239957; NOSC/TR-1412; OCNR-10P) Avail: NTIS HC/MF A04 CSCL 20/5

The objective of this work to verify and reproduce experimental observations of Cold Nuclear Fusion (CNF), as originally reported in 1989. The method was to start with the original report and add such additional information as became available to build a set of operational electrolytic CNF cells. Verification was to be achieved by first observing cells for neutron production, and for those cells that demonstrated a nuclear effect, careful calorimetric measurements were planned. The authors concluded, after laboratory experience, reading published work, talking with others in the field, and attending conferences, that CNF probably is chimera and will go the way of N-rays and polywater. The neutron detector used for these tests was a completely packaged unit built into a metal suitcase that afforded electrostatic shielding for the detectors and self-contained electronics. It was battery-powered, although it was on charge for most of the long tests. The sensor element consists of He detectors arranged in three independent layers in a solid moderating block. The count from each of the three layers as well as the sum of all the detectors were brought out and recorded separately. The neutron measurements were made with both the neutron detector and the sample tested in a cave made of thick moderating material that surrounded the two units on the sides and bottom. GRA

N92-10367# European Organization for Nuclear Research, Geneva (Switzerland). Theory Div.
THE QUARK-HADRON PHASE TRANSITION Abstract Only
Helmut Satz (Bielefeld Univ., Germany, F.R.) *In* Oulu Univ., Proceedings of the 25th Annual Conference of the Finnish Physical Society 1991 1 p (For primary document see N92-10362 01-70)
Avail: NTIS HC/MF A12

N92-10459# Tampere Univ. of Technology (Finland). Plasma Technology Lab.
VELOCIMETRY IN GAS FLOWS USING PULSED LASER INDUCED PHOTOTHERMAL EFFECTS Abstract Only
J. P. Vattulainen and Rolf G. Hernberg *In* Oulu Univ., Proceedings of the 25th Annual Conference of the Finnish Physical Society 1991 1 p Sponsored by Academy of Finland (For primary document see N92-10362 01-70)
Avail: NTIS HC/MF A12

N92-10460# Tampere Univ. of Technology (Finland). Plasma Technology Lab.
KINETIC GAS AND ELECTRON TEMPERATURES IN RF INDUCTION PLASMA Abstract Only
S. M. Jaffe (Stanford Univ., CA.), Rolf G. Hernberg, J. Larjo, and J. P. Vattulainen *In* Oulu Univ., Proceedings of the 25th Annual Conference of the Finnish Physical Society 1991 1 p Sponsored by Academy of Finland (For primary document see N92-10362 01-70)
Avail: NTIS HC/MF A12

N92-10461# Helsinki Univ. of Technology, Espoo (Finland). Dept. of Technical Physics.
NUMERICAL CALCULATIONS OF WAVE PROPAGATION IN TOKAMAK PLASMAS Abstract Only
S. Sipila, S. Karttunen (Technical Research Centre of Finland, Espoo.), T. Pattikangas, and Rainer Salomaa *In* Oulu Univ., Proceedings of the 25th Annual Conference of the Finnish Physical Society 1991 1 p (For primary document see N92-10362 01-70)
Avail: NTIS HC/MF A12

N92-10582# Technical Research Centre of Finland, Espoo. Electrical Engineering Lab.
THE POSSIBILITIES TO CONTROL AND TO REGULATE THE ENERGY CONSUMPTION Abstract Only
A. Lepisto *In* Oulu Univ, Proceedings of the 25th Annual Conference of the Finnish Physical Society 1991 1 p (For primary document see N92-10362 01-70)
Avail: NTIS HC/MF A12

76 SOLID-STATE PHYSICS

Includes superconductivity.

For related information, see also *33 Electronics and Electrical Engineering* and *36 Lasers and Masers.*

N92-10676*# Alabama Univ., Huntsville. Center for Microgravity and Materials Research.
MODELLING CRYSTAL GROWTH: CONVECTION IN AN ASYMMETRICALLY HEATED AMPOULE Final Report
J. Iwan D. Alexander, Franz Rosenberger, J. P. Pulicani, S. Krukowski, and Jalil Ouazzani 13 Sep. 1990 73 p
(Contract NAS8-36955; NAG8-790)
(NASA-CR-184214; NAS 1.26:184214) Avail: NTIS HC/MF A04 CSCL 20L

The objective was to develop and implement a numerical method capable of solving the nonlinear partial differential equations governing heat, mass, and momentum transfer in a 3-D

cylindrical geometry in order to examine the character of convection in an asymmetrically heated cylindrical ampoule. The details of the numerical method, including verification tests involving comparison with results obtained from other methods, are presented. The results of the study of 3-D convection in an asymmetrically heated cylinder are described. Author

N92-10677*# National Aeronautics and Space Administration. Langley Research Center, Hampton, VA.
POSITRON LIFETIME MEASUREMENTS IN CHIRAL NEMATIC LIQUID CRYSTALS
Jag J. Singh, Abe Eftekhari (Hampton Inst., VA.), and Devendra S. Parmar Oct. 1991 14 p
(NASA-TP-3122; L-16948; NAS 1.60:3122) Avail: NTIS HC/MF A03 CSCL 20L

Positron lifetimes in the isotropic phases of chiral nematic liquid crystal formulations and their mixtures up to the racemic level were measured. The lifetime spectra for all liquid crystal systems were analyzed into three components. Although the individual spectra in the left- and right-handed components are identical, their racemic mixtures exhibit much larger orthopositronium lifetimes; these larger lifetimes indicate the presence of larger microvoids. This result is consistent with the reportedly higher thermodynamic stability and color play range in the racemic mixtures of chiral nematic liquid crystals. Author

N92-10678# Oak Ridge National Lab., TN.
FORMATION OF SMALL METALLIC PRECIPITATES OF NIOBIUM IN (ALPHA)-Al2O3 IMPLANTED WITH Nb IONS
L. Romana, P. Thevenard, S. Ramos, B. Canut, L. Gea, and M. Brunel (Centre National de la Recherche Scientifique, Grenoble, France) 1991 15 p Presented at the 7th International Conference on Surface Modification of Metals By Ion Beams (SMMIB-7), Washington, DC, 15-19 Jul. 1991
(Contract DE-AC05-84OR-21400)
(DE91-015928; CONF-910707-1) Avail: NTIS HC/MF A03

Niobium implantations have been performed in (alpha)-Al2O3 single crystals to study the chemical interactions between the implanted species and the oxide and to study the microstructural evolution of the implanted layer. The investigation focused on both as-implanted specimens and specimens that underwent post-implantation anneals in a reducing atmosphere. Ion implantations were performed at 300 K with 150 keV particle energies and fluences ranging from 10(exp 16) to 2 x 19(exp 17) ions-cm(exp -2). Rutherford backscattering spectroscopy (RBS) and X-ray photoemission spectroscopy (XPS) allowed the characterization of the implanted profiles and determination of the chemical state of the implanted ions. X-ray diffraction at glancing incidence and RBS analysis in a channeling geometry were performed to follow the microstructural evolution of the implanted layer. The oxidation state of niobium and the microstructure of the implanted layer were dependent on the atomic concentration of niobium in (alpha)-Al2O3. An amorphous phase was observed after a threshold fluence of 5 x 10(exp 16) ions-cm(exp -2). The amorphous phase contained small metallic precipitates of niobium with a mean diameter of 1 nm. The physical properties of such niobium clusters embedded in an amorphous oxide layer were studied in detail. Electrical conductivity measurements showed that a hopping process between the metallic precipitates was the likely mechanism operating for this system. DOE

N92-10679# Ceskoslovenska Akademie Ved, Prague. Inst. of Plasma Physics.
NON-UNICITY OF GIBBS STATES OF CZECH MODELS IN A HALF-SPACE
Pavel Kotalik Mar. 1991 29 p
(IPPCZ-311) Avail: NTIS HC/MF A03

A classical lattice model is studied, with the property that, while yielding a unique state in the bulk, there exist at least two equilibrium states once considered in a half-space. The properties of those two states are discussed. In particular, the cluster expansion method is used to evaluate their difference deep in the bulk away from the boundary of the half-space. Author

N92-10680*# National Aeronautics and Space Administration. Goddard Space Flight Center, Greenbelt, MD.
TUNNELING CALCULATIONS FOR GaAs-Al(x)Ga(1-x) AS GRADED BAND-GAP SAWTOOTH SUPERLATTICES Thesis
Kathrine A. Forrest and Paul H. E. Meijer (Catholic Univ. of America, Washington, DC.) Apr. 1991 176 p
(NASA-TM-100726; Rept-89B00121; NAS 1.15:100726) Avail: NTIS HC/MF A09 CSCL 20L

Quantum mechanical tunneling calculations for sawtooth (linearly graded band-gap) and step-barrier AlGaAs superlattices were performed by means of a transfer matrix method, within the effective mass approximation. The transmission coefficient and tunneling current versus applied voltage were computed for several representative structures. Particular consideration was given to effective mass variations. The tunneling properties of step and sawtooth superlattices show some qualitative similarities. Both structures exhibit resonant tunneling, however, because they deform differently under applied fields, the J-V curves differ.
Author

N92-10681* National Aeronautics and Space Administration. Pasadena Office, CA.
PASSIVATION OF HIGH TEMPERATURE SUPERCONDUCTORS Patent
Richard P. Vasquez, inventor (to NASA) (Jet Propulsion Lab., California Inst. of Tech., Pasadena.) 22 Oct. 1991 10 p Filed 28 Jun. 1990 Supersedes N90-26684 (28 - 20, p 2932)
(NASA-Case-NPO-17949-1-CU; US-Patent-5,059,581;
US-Patent-Appl-SN-545016; US-Patent-Class-505-1;
US-Patent-Class-505-728; US-Patent-Class-427-62;
US-Patent-Class-427-343; US-Patent-Class-156-637;
Int-Patent-Class-B05D-5/12; Int-Patent-Class-C23F-1/00) Avail: US Patent and Trademark Office CSCL 20L

The surface of high temperature superconductors such as YBa2Cu3O(7-x) are passivated by reacting the native Y, Ba and Cu metal ions with an anion such as sulfate or oxalate to form a surface film that is impervious to water and has a solubility in water of no more than 10(exp -3) M. The passivating treatment is preferably conducted by immersing the surface in dilute aqueous acid solution since more soluble species dissolve into the solution. The treatment does not degrade the superconducting properties of the bulk material.
Official Gazette of the U.S. Patent and Trademark Office

N92-10682# Argonne National Lab., IL.
HIGH-TEMPERATURE IMPLANTATION OF Au INTO Ni
M. R. James, N. Q. Lam, L. E. Rehn, P. M. Baldo, L. Funk, and J. F. Stubbins (Illinois Univ., Urbana.) Jul. 1991 17 p Presented at the 7th International Conference on Surface Modification of Metals By Ion Beams (SMMIB-7), Washington, DC, 15-19 Jul. 1991
(Contract W-31-109-eng-38)
(DE91-017304; ANL/CP-73745; CONF-910707-5) Avail: NTIS HC/MF A03

The role of irradiation temperature on implant distributions was investigated in the Au-Ni system. Au ions were implanted at 300 keV into polycrystalline Ni samples at temperatures between 25 and 700 C to a dose of 10(exp 16)/sq cm. The spatial Au distributions were analyzed with RBS, using both 1.7 and 3.0 MeV He-4, and SIMS. The results showed that the Au profiles were practically insensitive to target temperature below approx. 200 C. At higher temperatures, systematic decreases in the surface and peak concentrations and longer penetration tails were observed. The evolution of the implant distribution in time and space during implantation was also calculated theoretically by means of a comprehensive kinetic model. In general, the effects observed experimentally can be reproduced theoretically, and interpreted in terms of substantial sputtering at low temperatures, and dominant radiation-induced segregation at higher temperatures. In addition, a systematic fitting of model calculations to experimental measurements allowed the determination of various parameters.
DOE

N92-10683# Brookhaven National Lab., Upton, NY.
POLARIZATION DEPENDENT X RAY SPECTROSCOPY OF HIGH T(SUB c) SUPERCONDUCTORS
S. M. Heald and J. M. Tranquada 1991 9 p Presented at the Society of Photo-Optical Instrumentation Engineers (SPIE) Meeting, San Diego, CA, 21-26 Jul. 1991
(Contracts DE-AC02-76CH-00016; DE-AS05-80ER-10742; DE-AC03-82ER-13000)
(DE91-017475; BNL-45591; CONF-9107115-35) Avail: NTIS HC/MF A02

For anisotropic structures such as those found for the high Tc superconductors, the utility of x ray absorption measurements can be enhanced by taking advantage of the inherent polarization of synchrotron radiation. Polarization dependent measurements have been made on all four classes of high Tc materials (La, Y, Bi, and Tl based Cu oxides) after orienting them magnetically. All show similar polarization dependence for their near edge structure which is characteristic of planar Cu compounds. The paper concentrates on results for YBa2Cu3O(7-x) materials. The two types of Cu sites in this material have different polarization dependence, and measurements with the x ray polarization parallel and perpendicular to the c-axis can be used to distinguish their contributions to the near edge structure. We can clearly resolve the 4p(pi) contributions from the two sites. The extended fine structure also shows distinct polarization dependence which allows the separation of contributions from in-plane and out-of-plane bonds. Measurements on oxygen deficient materials show contributions from Cu(1+) which is determined to be on the Cu(1) (linear chain) sites from the polarization dependence, and to vary linearly with the O concentration. DOE

N92-10684# Los Alamos National Lab., NM.
PHOTOEMISSION IN YbCu2Si2: PROBLEMS WITH THE KONDO IMPURITY MODEL
J. M. Lawrence (California Univ., Irvine.), A. J. Arko, J. J. Joyce, P. C. Canfield, Z. Fisk, and J. D. Thompson 1991 20 p Presented at the International Conference on Magnetism, Edinburgh, Scotland, 1-7 Sep. 1991
(Contract W-7405-eng-36)
(DE91-018018; LA-UR-91-2613; CONF-910903-11) Avail: NTIS HC/MF A03

We report valence band photoemission results for YbCu2Si2. The 4f(sup 13)(J=7/2) final state peak, centered 60 meV below the Fermi level epsilon(sub F), lacks the temperature dependence and is broader than predicted for a Kondo resonance. Together with the recent photoemission results for cerium compounds, these results raise serious doubts about the Kondo impurity explanation of heavy fermion photoemission. DOE

N92-10685# Los Alamos National Lab., NM.
MECHANICAL AFTER-EFFECT STUDIES OF OXYGEN RELAXATION IN YBa2Cu3O(7-DELTA)
J. R. Cost and J. T. Stanley (Arizona State Univ., Tempe.) 1991 8 p Presented at the European Conference on Internal Friction and Ultrasonic Attenuation in Solids, Cracow (Poland), 4-7 Sep. 1991
(Contract W-7405-eng-36)
(DE91-018043; LA-UR-91-2736; CONF-9109213-1) Avail: NTIS HC/MF A02

YBa2Cu3O(7-delta) has an anelastic relaxation involving motion of an oxygen atom or defect. This relaxation has been studied with good agreement by more than seven investigating teams over the temperature range from 200 to 550 C using internal friction techniques. We have extended measurements of this relaxation to a new regime of temperature and relaxation time using the mechanical after-effect method. Our results cover an additional three orders of magnitude in relaxation time over the temperature range from 50 to 110 C. The Arrhenius plot, when combined with internal friction results, now covers eleven orders of magnitude in relaxation time. The fit gives an activation energy, Q=1.12 (+ or -0.015) and pre-exponential, tau sub 0 = 1.9 x 10(exp -13) s. The isothermal mechanical relaxation curves we measured always spanned longer times than predicted for a simple exponential relaxation. This indicates that the process is controlled by a relatively wide spectrum of relaxation times. We have calculated best approximations of this spectrum by deconvoluting the mechanical after-effect curves. The resulting distribution is symmetrical in logarithm of the relaxation time with a width at half-height which is a factor of 20 in relaxation time. The significance of these findings is discussed in terms of our understanding of oxygen mobility in YBa2Cu3O(7-delta). DOE

N92-10686# Los Alamos National Lab., NM.
LANGEVIN DYNAMICS SIMULATIONS OF LARGE FRUSTRATED JOSEPHSON JUNCTION ARRAYS
N. Gronbech-Jensen, A. R. Bishop, and P. S. Lomdahl 1991 4 p Presented at the Phenomenology and Applications of High Temperature Superconductivity, Los Alamos, NM, 22-24 Aug. 1991
(Contract W-7405-eng-36)
(DE91-018046; LA-UR-91-2756; CONF-9108140-1) Avail: NTIS HC/MF A01

Long-time Langevin dynamics simulations of large (N x N, N = 128) 2-D arrays of Josephson junctions in a uniformly frustrating external magnetic field are reported. The results demonstrate: Relaxation from an initially random flux configuration as a universal fit to a glassy stretched-exponential type of relaxation for the intermediate temperatures T (0.3 Tc approx. less than T approx. less than 0.7 Tc), and an activated dynamic behavior for T approx. Tc A glassy (multi-time, multi-length scale) voltage response to an applied current. Intrinsic dynamical symmetry breaking induced by boundaries as nucleation sites for flux lattice defects gives rise to transverse and noisy voltage response. DOE

N92-10687# Oak Ridge National Lab., TN.
DYNAMIC SCREENING AND WAKE EFFECTS ON ELECTRONIC EXCITATION IN ION-SOLID AND ION-SURFACE COLLISIONS
J. Burgdoerfer (Tennessee Univ., Knoxville.) 1991 27 p Presented at the 14th International Conference on Atomic Collisions in Solids, Salford, England, 29 Jul. - 2 Aug. 1991
(Contract DE-AC05-84OR-21400)
(DE91-018224; CONF-9107155-3) Avail: NTIS HC/MF A03

The collective electronic response in a solid effectively alters ionic and atomic potentials giving rise to dynamic screening and to a wake of density fluctuations trailing ions as they propagate through the solid. The presence of dynamic screening modifies electronic excitation processes of projectiles in ion-solid collisions as compared to binary ion-atom collisions. We review recent theoretical and experimental studies directed at the search for and identification of signatures of dynamic screening and wake effects. Examples include the formation of excited projectile bound states under channeling conditions, radiative electron capture, the search for wake riding electrons in antiproton-solid collisions, and the neutralization of highly charged ions near surfaces. DOE

N92-10688# Brookhaven National Lab., Upton, NY.
STRONG CORRELATION THEORIES OF HIGH TEMPERATURE SUPERCONDUCTORS
V. J. Emery 1991 33 p Presented at the 39th Scottish Universities Summer School, St. Andrews, Scotland, 16-19 Jun. 1991
(Contract DE-AC02-76CH-00016)
(DE91-017479; BNL-46454; CONF-9106265-1) Avail: NTIS HC/MF A03

The theory of high-temperature superconductors is at an interesting state. There are by now a wide range of reliable experimental results that severely restrict the possible explanations of what is going on. It is clear that the normal state properties are quite unusual and that they must be explained by any satisfactory theory of these fascinating new materials. It is known that superconductivity is a consequence of pairing but there is an ongoing debate about that mechanism, and whether established theory of Bardeen, Cooper and Schrieffer is applicable in its original form. The difficulty in obtaining a widely accepted theory is compounded by the fact that the charge-carriers may not be

regarded as nearly-free electrons or holes: as will be clear from the ensuing discussion, there are strong correlation effects which are likely to be an integral part of any successful theory. The objective of the present lectures is to give some of the background material that is necessary for an appreciation of the current theoretical debate. Various models of high-temperature superconductors will be introduced and the reasons for believing that strong correlations are important will be described. The start point typically involves high energy physics which, in the solid-state context, means physics on a scale of a few eV. But in the final analysis, we are interested in explaining low energy properties such as magnetism and superconductivity, which occur on a scale of 10(exp -3) to 10(exp -1) eV. Therefore it is desirable to find an effective Hamiltonian from which high-energy processes have been eliminated in order to obtain a (hopefully simpler) description of the low-energy physics. A critical discussion of attempts along these lines will also be given. DOE

N92-10689# Michigan Univ., Ann Arbor.
A STATISTICAL MECHANICS STUDY OF SOLID-SOLID INTERFACES
1991 9 p
(Contract DE-FG02-88ER-45367)
(DE91-017852; DOE/ER-45367/3) Avail: NTIS HC/MF A02

The goal of the research project was to employ concepts from statistical mechanics to simplify and extend the classical approaches to the atomistic simulation of interfaces. The reason for resorting to statistical mechanics method was to determine the thermodynamic properties of interfaces in a sufficiently accurate and computationally efficient manner in order to predict the systematic trends (with temperature, interface crystallography, etc.) in the interfacial properties of real materials. The original approach adopted was based on statistical-mechanical density-functional methods. In these methods, the free energy of the system is written as a functional of the atomic density, that is expanded in terms of order parameters that vary smoothly across the interface. After devoting several months to this procedure, we came to the conclusion that it would not provide a sufficiently accurate and tractable approach to meeting the goals of the project. The failure of this approach forced us to examine alternatives that still allowed for the calculation of interfacial thermodynamic properties but that were more accurate and sufficiently computationally tractable that would allow us to truly investigate the systematics of interfacial properties and structure. The approach that was adopted was to write down an approximate free energy functional (in terms of interatomic potentials and atomic coordinates) that could be minimized with respect to atomic positions to obtain finite temperature equilibrium structure and thermodynamics. DOE

N92-10690# Ames Lab., IA.
ELECTRONIC AND MAGNETIC PROPERTIES OF STRONGLY CORRELATED SYSTEMS Ph.D. Thesis
Tsan-Chuen Leung Aug. 1991 135 p
(Contract W-7405-eng-82)
(DE91-018205; IS-T-1545) Avail: NTIS HC/MF A07

Self consistent, spin-polarized calculations are performed for Sc2CuO4, La2CuO4 with constrained d(exp 9) configuration, and La2NiO4. For Sc2CuO4, both ferromagnetic and antiferromagnetic ground states are investigated and found to be unstable. Magnetic form factors are calculated and are discussed in view of experiments in La2CuO4. In the calculation for La2CuO4, the d(exp 9) configuration is maintained by constraining the d(sub x(exp 2)-y(exp 2)) orbital to have exactly one hole. The Cu projected 3d density of states is compared with XPS data which slow the binding energy of the Cu states is lower than the results from standard band structure calculations. The Cu d states are treated as core states and no hybridization is considered. This results in the d density of states being too narrow compared with experiment and the difference indicates the degree of hybridization with the oxygen 2p states. For La2NiO4, only the antiferromagnetic ground state is investigated and found to be stable but with the local moment on Ni being too small compared with experiment. The magnetic form factor for the antiferromagnetic state is examined and discussed in view of experiments. All these results indicate the local spin density functional approximation does not give correct solutions for these materials. To go beyond the LSDA, we study the extended Hubbard model. A mean field calculation of the two dimensional one and three band Hubbard models based on a Mori-projection operator formalism, which is called the projection operator mean field approximation, is presented. The results are compared with those of the Hartree-Fork approximation, the Hubbard I approximation, and Quantum Monte Carlo simulation. DOE

N92-10691# Oak Ridge National Lab., TN.
ANOMALOUS NEUTRON SCATTERING FROM THE FLUX-LINE LATTICE IN K(0.6)Ba(0.4)BiO3
D. M. Paul, E. M. Forgan, H. A. Mook, R. Cubitt, and S. L. Lee (Birmingham Univ., England) 1991 2 p Presented at the International Conference on Materials and Mechanisms of Superconductivity, Kanazawa, Japan, 22-26 Jul. 1991
(Contract DE-AC05-84OR-21400)
(DE91-018233; CONF-910736-18) Avail: NTIS HC/MF A01

Neutron scattering has been used to observe diffraction from the flux-line lattice in K(0.6)Ba(0.4)BiO3 as a function of temperature (0 to 40 K) and magnetic field (0 to 2 T). An anomalous temperature and magnetic field dependence of the intensities of the Bragg reflections has been observed. DOE

N92-10692# Argonne National Lab., IL.
ANISOTROPIC TWIN BOUNDARY PINNING IN YBa2Cu3O(x)
G. W. Crabtree, W. K. Kwok, U. Welp, J. Downey, S. Fleshler, K. G. Vandevoort, and J. Z. Liu (California Univ., Davis.) 1991 7 p Presented at the International Conference on Materials and Mechanisms of Superconductivity, Kanazawa, Japan, 22-26 Jul. 1991
(Contract W-31-109-eng-38)
(DE91-018536; ANL/CP-74040; CONF-910736-19) Avail: NTIS HC/MF A02

The reduction in flux motion resistivity due to pinning at twin boundaries in single crystal YBa2Cu3O(x) is demonstrated. Pinning takes place only for magnetic fields aligned within a critical angle of the twin boundary plane. The critical angle varies with field direction and with field strength for H (parallel) c. The onset temperature of twin boundary pinning is established by its strong anisotropy, and shown to correspond with a feature in the temperature dependent resistivity for H (parallel) c. DOE

N92-10693# Argonne National Lab., IL.
INITIAL MAGNETIZATION AND MAGNETIC RELAXATION IN A SINGLE CRYSTAL OF Bi2Sr2CaCu2O(x)
Ming Xu, A. Umezawa, and G. W. Crabtree 1991 3 p Presented at the International Conference on Materials and Mechanisms of Superconductivity, Kanazawa, Japan, 22-26 Jul. 1991
(Contracts W-31-109-eng-38; W-7405-eng-82)
(DE91-018537; ANL/CP-74039; CONF-910736-20) Avail: NTIS HC/MF A01

The initial magnetization and the magnetic relaxation in a single crystal of Bi2Sr3CaCu2O(x) over a wide range of temperatures and fields have been measured. The results show that the initial magnetization varies with the measuring time at a given temperature and the relaxation is logarithmic in our measuring windows. DOE

N92-10694# Argonne National Lab., IL.
HETEROEPITAXIAL GROWTH OF TiO2, VO2, AND TiO2/VO2 MULTILAYERS BY MOCVD
H. L. M. Chang, Y. Gao, J. Guo, C. M. Foster, H. You, T. J. Zhang, and D. J. Lam Mar. 1991 9 p Presented at the 8th Meeting of European Chemical Vapor Deposition (EURO CVD), Glasgow, Scotland, 8-13 Sep. 1991
(Contract W-31-109-eng-38)
(DE91-018543; ANL/CP-72131; CONF-9109156-2) Avail: NTIS HC/MF A02

Titanium and vanadium dioxide systems were selected to study the MOCVD process for the growth of oxide epitaxial films. Single crystal TiO2 and VO2 films in single and multilayered configurations

have been successfully grown on sapphire (alpha-Al2O3) single crystal substrates. Seven distinct epitaxial orientation relationship between the films and the substrates were observed. Discussion on these epitaxial relationships based on the consideration of atomic arrangements of the materials is presented. From our experimental results, we concluded that single layer films (both TiO2 and VO2) were grown by the nucleations of 3-D clusters. Quantum mechanical calculations of the electronic structures, charge distributions, and energetics of the free substrate surfaces were performed and some results are presented. DOE

N92-10695# Ames Lab., IA.
DIAMOND THIN FILMS GROWN BY MICROWAVE PLASMA ASSISTED CHEMICAL VAPOR DEPOSITION Ph.D. Thesis
M. Leksono Sep. 1991 133 p
(Contract W-7405-eng-82)
(DE91-018553; IS-T-1558) Avail: NTIS HC/MF A07

Undoped and boron doped diamond thin films have been successfully grown by microwave plasma chemical vapor deposition from CH4, H2, and B2H6. The films were characterized using x ray diffraction techniques, Raman and infrared spectroscopies, scanning electron microscopy, secondary ion mass spectrometry, and various electrical measurements. The deposition rates of the diamond films were found to increase with the CH4 concentration, substrate temperature, and/or pressure, and at 1.0 pct. methane, 900 C, and 35 Torr, the value was measured to be 0.87 micron/hour. The deposition rate for boron doped diamond films, decreases as the diborane concentration increases. The morphologies of the undoped diamond films are strongly related to the deposition parameters. As the temperature increases from 840 to 925 C, the film morphology changes from cubo-octahedron to cubic structures, while as the CH4 concentration increases from 0.5 to 1.0 pct., the morphology changes from triangular (111) faces with a weak preferred orientation to square (100) faces. At 2.0 pct. CH4 or higher the films become microcrystalline with cauliflower structures. Scanning electron microscopy analyses also demonstrate that selective deposition of undoped diamond films has been successfully achieved using a lift-off process with a resolution of at least 2 micron. The x ray diffraction and Raman spectra demonstrate that high quality diamond films have been achieved. The concentration of the nondiamond phases in the films grown at 1.0 pct. CH4 can be estimated from the Raman spectra to be at less than 0.2 pct. and increases with the CH4 concentration. The Raman spectra of the boron doped diamond films also indicate that the presence of boron tends to suppress the nondiamond phases in the films. Infrared spectra of the undoped diamond films show very weak CH stretch peaks which suggest that the hydrogen concentration is very low. DOE

N92-10696# Argonne National Lab., IL.
GRAIN BOUNDARIES IN NANOPHASE MATERIALS
R. W. Siegel and G. J. Thomas (Sandia National Labs., Albuquerque, NM.) Aug. 1991 18 p Presented at the Workshop on Structure and Properties of Interfaces, Wickenburg, AZ, 206 Jan. 1991
(Contracts W-31-109-eng-38; DE-AC04-76DP-00789)
(DE91-018587; ANL/CP-74018; CONF-910197-2) Avail: NTIS HC/MF A03

Among the atoms in nanophase materials (with grain sizes less than 100 nm) a significant fraction are associated with grain boundaries. Properties of these new materials are thus affected not only by their reduced grain size scale, but also by the nature of their grain boundary structures. High resolution electron microscopy observations combined with image simulations, as well as complementary results from Raman spectroscopy and small angle neutron scattering experiments, indicate that nanophase boundaries are similar in structure to those normally encountered in conventional coarse grained polycrystals. They are commonly observed to be relatively flat and faceted with well ordered localized structures. The available information on grain boundary structures in nanophase materials is briefly reviewed and future opportunities for measuring grain boundary properties are considered. DOE

N92-10697# Argonne National Lab., IL.
ELECTRICAL TRANSPORT ACROSS GRAIN BOUNDARIES IN BICRYSTALS OF YBa2Cu3O7(DELTA)
D. C. Larbalestier, S. E. Babcock, X. Y. Cai, M. B. Field, N. F. Heinig, L. K. Williams, N. Zhang (Wisconsin Univ., Madison.), Y. Gao, and K. L. Merkle 1991 7 p Presented at the International Conference on Materials and Mechanisms of Superconductivity, Kanazawa Japan, 22-26 Jul. 1991
(Contract W-31-109-eng-38)
(DE91-018588; ANL/CP-74017; CONF-910736-22) Avail: NTIS HC/MF A02

The superconducting properties of about 20 bulk scale flux grown bicrystals of YBa2Cu3O(7-delta) have been measured in order to deduce the nature of the coupling across their grain boundaries. Bicrystals with types of misorientation relationship were studies: (1) theta (001) C-type, and (2) 90 deg. (010) plus an additional rotation about the a sub I parallel to c sub II axis (P-type). A general trend for a transition from flux pinning (FP) to Josephson Junction (JJ) to resistive (R) behavior was observed as the misorientation angle increased. However, FP character was observed well into the high angle regime, in particular, for P-type bicrystals, and JJ behavior was observed at as low as 10 deg. (001). The J sub ct values of two bicrystals were increased by a second oxygen anneal. In one case (28 deg. (001) boundary), extended oxygenation produced a change from JJ to mixed JJ/FP behavior, markedly raising the transport critical current density (J sub ct) at all fields. HRTEM has been performed on two of the same bicrystals which were electromagnetically characterized. A thin second phase layer unobservable by conventional TEM was observed in a resistive boundary, whereas no such phase was detected at a JJ boundary. We conclude that the character of the boundary cannot be predicted either from its misorientation angle or the magnitude of its J sub c. DOE

N92-10698# Argonne National Lab., IL.
HETEROEPITAXY OF MOCVD GROWN TiO2, VO2 FILMS AND TiO2/VO2 MULTILAYERS ON SAPPHIRE (1120)
H. L. M. Chang, Y. Gao, T. J. Zhang, and D. J. Lam Aug. 1991 12 p Presented at the International Workshop on Science and Technology of Thin Films for the 21st Century, Evanston, IL, 28 Jul. - 2 Aug. 1991
(Contract W-31-109-eng-38)
(DE91-018589; ANL/CP-73356; CONF-9107171-1) Avail: NTIS HC/MF A03

Single crystal TiO2 and VO2 films in single- and multilayered configurations have been successfully grown on sapphire (1120) by the MOCVD technique. The epitaxial orientation relationships were determined by the X ray diffraction and transmission electron microscopy techniques. High resolution electron microscopy studies were performed to examine the microstructures of the films at atomic level. DOE

N92-10699# Argonne National Lab., IL.
REVERSIBLE MAGNETIZATION OF Bi2Sr2CaCu2O8 SINGLE CRYSTALS
H. W. Weber, W. Kritscha, F. M. Sauerzopf, G. W. Crabtree, P. Z. Jiang, and Y. C. Chang Jul. 1991 6 p Presented at the Cryogenic Engineering Conference and International Cryogenic Materials Conference, Huntsville, AL, 11-14 Jun. 1991
(Contract W-31-109-eng-38)
(DE91-018600; ANL/CP-74044; CONF-910635-13) Avail: NTIS HC/MF A02

Magnetization measurements on a large BiSCCO-2212 single crystal have been carried out for fields parallel and perpendicular to the crystallographic c-axis, respectively, in a SQUID magnetometer. The results show that for all temperatures and magnetic fields above 20 K and about 2 T, complete reversibility of the magnetization prevails. Hence, standard procedures to determine intrinsic superconductive parameters, such as the thermodynamic critical field and the penetration depth, could be employed. Near (Tc), large fluctuation effects lead to a breakdown of the usual concepts based on a mean field theory, in particular with regard to a definition of the upper critical field H(c2). DOE

N92-10700# Argonne National Lab., IL.
NEUTRON IRRADIATION EFFECTS ON YBCO SINGLE CRYSTALS
F. M. Sauerzopf, H. P. Wiesinger, H. W. Weber, and G. W. Crabtree Jul. 1991 7 p Presented at the Cryogenic Engineering Conference and International Cryogenic Materials Conference, Huntsville, AL, 11-14 Jun. 1991
(Contract W-31-109-eng-38)
(DE91-018615; ANL/CP-74043; CONF-910635-14) Avail: NTIS HC/MF A02

Fast neutron irradiation of YBCO single crystals has proved to result in significant increases of magnetization hysteresis and consequently an enhancement of critical current densities. In addition, shifts of the irreversibility line have been observed. Both of these observations are discussed in terms of an interaction of three different flux pinning mechanisms. The results near (Tc) prove directly the existence of strong intrinsic pinning, when H is applied parallel to the Cu-O layers. DOE

N92-10701# Argonne National Lab., IL.
CHEMICAL THERMODYNAMIC EQUILIBRIA AND CONDUCTIVITY OF NONSTOICHIOMETRIC YB2Cu3O7-(DELTA): A REVIEW
R. J. Thorn 1991 51 p Presented at the NATO Advanced Study Institute on Surfaces and Interfaces, Neos Marmaras, Greece, 18-30 Aug. 1991
(Contract W-31-109-eng-38)
(DE91-018638; ANL/CP-73957; CONF-910855-1) Avail: NTIS HC/MF A04

To synthesize a comprehensive understanding of the nonstoichiometric phase, YBa2Cu3O2(7-delta), the following topics are discussed: (1) The chemical equilibria involved in nonstoichiometric YBa2Cu3O(7-delta) derived principally from photoelectron spectroscopic observations. (2) Nonstoichiometry: Experimental values of the variation of the partial pressure of oxygen with temperature and composition are rationalized quantitatively in terms of nearest neighbor lattice statistics. Energies of interaction between oxygens in the basal plane are obtained. (3) The structures of the variation of conductivity with temperature and composition are interpreted quantitatively in terms of a model with a narrow conduction band and a small gap, thermally activated valence band. (4) Optical conductivity derived from reflectance; structures of (sigma T, omega). The quantitative studies of these topics lead to the conclusion that small polarons exist in YBa2Cu3O(7-delta) and are the source of the conductivity. This conclusion implies that the superconducting state is bipolaronic. DOE

N92-10702# Argonne National Lab., IL.
ACTIVATION ENERGIES IN A Bi2Si2CaCu2O(x) SINGLE CRYSTAL
M. Reissner, W. Steiner (Technische Univ., Vienna, Austria), W. Kritscha, F. M. Sauerzopf, H. W. Weber, and G. W. Crabtree Jul. 1991 3 p Presented at the International Conference on Materials and Mechanisms of Superconductivity, Kanazawa, Japan, 22-26 Jul. 1991
(Contract W-31-109-eng-38)
(DE91-018640; ANL/CP-73930; CONF-910736-23) Avail: NTIS HC/MF A01

The analysis of the time dependent magnetization measured in a field of 1T for a B12212 single crystal leads to a distribution of activation energies with distinctly larger half width for B(parallel)(a,b) than for B(parallel)c. Within a model of thermally activated flux creep, different values for the relaxation time are obtained depending on the field direction. DOE

N92-10703# Utah Univ., Salt Lake City.
OMVPE GROWTH OF InAsSbBi AND RELATED ALLOYS USING NEW ORGANOMETALLIC GROUP V SOURCES Final Report
G. B. Stringfellow 1 Aug. 1991 10 p
(Contract N00014-91-J-1447)
(AD-A239939) Avail: NTIS HC/MF A02 CSCL 11/6

The major goal of the project is the organometallic vapor phase epitaxial (OMVPE) growth of a new III/V alloy, InAsSbBi, with a band gap less than 0.1 eV at 77 K, expected to be useful for infrared detectors with response extending to 12 microns. The alloy is metastable, but under the correct growth conditions we expect to be able to grow it by OMVPE. This apparently requires low growth temperatures of 250 to 350 C. Thus, new organometallic As and Sb precursors are being developed which pyrolyze at lower temperature than AsH3 and TMSb, the normal group V sources. In addition, Bi precursors must be synthesized. GRA

N92-10704# Bell Telephone Labs., Inc., Reading, PA.
GALLIUM ARSENIDE PILOT LINE FOR HIGH PERFORMANCE COMPONENTS Semiannual Report, Sep. 1990 - Apr. 1991
Robert C. Vehse and E. F. Lapham 8 Aug. 1991 73 p
(Contract F29601-87-C-0202)
(AD-A239955) Avail: NTIS HC/MF A04 CSCL 12/6

The Gallium Arsenide Pilot Line for High Performance Components (Pilot Line III) is to develop a facility for the fabrication of GaAs logic and memory chips. Physical and electrical analysis conclusively demonstrated that the EFET problem was caused by residual AlGaAs remaining in the EFET tubs. For our Self Aligned Refractory Gate Integrated Circuit (SARGIC) process to perform as designed, the FET gates must be placed directly on Gallium Arsenide. Residual AlGaAs increases the FET thresholds and thereby substantially changes device characteristics. We solved the problem by developing a new etch process using a PP etchant (H3PO4 and H2O2). AlGaAs is now completely removed from EFET tubs and EFET threshold control has been restored. With wafer starts suspended and other program work minimized to conserve resources, there was little primary circuit testing. A new result is that the 32-Bit Multiplier is functional at 60 MHz. GRA

N92-10705# Washington State Univ., Pullman. Dept. of Chemistry.
POLARIZABILITIES OF TRANS AND CIS POLYACETYLENE AND INTERACTIONS AMONG CHAINS IN CRYSTALLINE POLYACETYLENE
Z. Huang, D. A. Jelski, R. Wang, D. Xie, and C. Zaho Aug. 1991 21 p
(Contract N00014-90-J-1193)
(AD-A240025; WSU/DC/91/TR-59) Avail: NTIS HC/MF A03 CSCL 07/3

In this paper, we use the semi-empirical Hartree-Fock method, introduced within the finite electric field perturbation approach, to calculate the molecular and pi-system polarizabilities of trans and cis polyene H-(-CH=CH-)n-H (n=3,4,5,...,18). The result is that for a given n, the order of both molecular and pi-system polarizabilities of polyene is trans greater than cis. This result is consistent with the order of experimental values of trans and cis hexatriene. When the n increases from 3 to 18, the contribution of pi-system polarizability to the molecular polarizability increases from 45 to 70 percent. Using these results, we have extrapolated the polarizabilities of both trans and cis polyacetylene. The order is trans greater than cis. These results and crystal parameters lead to an estimate of the dispersion energies among polyacetylene chains. The result is also E(sub disp)(trans) greater than E(sub disp)(cis). GRA

N92-10706# Yale Univ., New Haven, CT. Dept. of Applied Physics.
PREPARATION AND CHARACTERIZATION OF HIGH TEMPERATURE SUPERCONDUCTOR FILM SURFACES Annual Report No. 1, 1 Jun. 1990 - 31 May 1991
Daniel E. Prober 31 Mar. 1991 4 p
(Grant AF-AFOSR-0306-90; AF Proj. 2305)
(AD-A240118; AFOSR-91-0744TR) Avail: NTIS HC/MF A01 CSCL 20/12

Research was conducted on deposition and characterization of high temperature superconductor films. A number of configurations for sputter deposition of films were tested, including three-source co-sputtering with the guns facing, and with the guns off-axis, from the growing film, and single composite-target

sputtering. The best film properties were obtained with off-axis, single target sputtering onto a heated substrate. Films were deposited onto heated magnesium oxide substrates using simultaneous sputtering (co-sputtering) from three metal targets: yttrium, copper, and a barium copper alloy. After a significant number of depositions were carried out to optimize film composition and to maximize transition temperature, we began deposition onto substrates of strontium titanate. These substrates allowed higher transition temperatures and films with lower resistivities. GRA

N92-10373# Tampere Univ. of Technology (Finland). Dept. of Physics.
DRIVEN GROWTH IN THE RESTRICTED SOLID ON SOLID MODEL Abstract Only
Tapio Ala-Nissila, J. M. Kim, and J. M. Kosterlitz (Brown Univ., Providence, RI.) *In* Oulu Univ., Proceedings of the 25th Annual Conference of the Finnish Physical Society 1991 1 p (For primary document see N92-10362 01-70)
Avail: NTIS HC/MF A12

N92-10425# Oulu Univ. (Finland). Dept. of Physics.
STRUCTURE AND OPTICAL POLARIZABILITIES OF SMALL SILICON CLUSTERS Abstract Only
Tapio T. Rantala, Mark I. Stockman, Daniel A. Jelski, and Thomas F. George (State Univ. of New York, Buffalo.) *In its* Proceedings of the 25th Annual Conference of the Finnish Physical Society 1991 1 p (For primary document see N92-10362 01-70)
Avail: NTIS HC/MF A12

N92-10428# Oulu Univ. (Finland). Dept. of Physics.
ELECTRON CORRELATION IN THE 4d HOLE STATE OF Cs AND Ba Abstract Only
A. Mantykentta, H. Aksela, Seppo Aksela, J. Tulkki, and T. Aaberg (Helsinki Univ. of Technology, Espoo, Finland) *In its* Proceedings of the 25th Annual Conference of the Finnish Physical Society 1991 1 p (For primary document see N92-10362 01-70)
Avail: NTIS HC/MF A12

N92-10435# Oulu Univ. (Finland). NMR-Lab.
THE Kr-83 NMR IN PROBING ELECTRIC FIELD GRADIENTS IN THERMOTROPIC LIQUID CRYSTALS Abstract Only
L. P. Ingman and Jukka Jokisaari *In its* Proceedings of the 25th Annual Conference of the Finnish Physical Society 1991 1 p (For primary document see N92-10362 01-70)
Avail: NTIS HC/MF A12

N92-10436# Oulu Univ. (Finland). Dept. of Physics.
NMR DETERMINATION OF THE Ne-21 QUADRUPOLE COUPLING FOR NEON GAS DISSOLVED IN LIQUID CRYSTALS Abstract Only
Jukka Jokisaari, O. Pulkkinen, P. Diehl, and O. Muenster (Basel Univ., Switzerland) *In its* Proceedings of the 25th Annual Conference of the Finnish Physical Society 1991 1 p (For primary document see N92-10362 01-70)
Avail: NTIS HC/MF A12

N92-10437# Oulu Univ. (Finland). Dept. of Physics.
NMR-RELAXATION TIME MEASUREMENTS OF NOBLE GAS ISOTOPE Xe-129 DISSOLVED IN ISOTROPIC AND ANISOTROPIC LIQUIDS Abstract Only
Kari Oikarinen and Jukka Jokisaari *In its* Proceedings of the 25th Annual Conference of the Finnish Physical Society 1991 1 p (For primary document see N92-10362 01-70)
Avail: NTIS HC/MF A12

N92-10463# Tampere Univ. of Technology (Finland). Dept. of Physics.
DETERMINATION OF THE (1X2) STRUCTURE OF A Pt FILM ON Pd(110) Abstract Only
P. Kaukasoina, M. Lindroos, H. C. Kang, O. L. Warren, P. J. Schmitz, and P. A. Thiel (Iowa State Univ. of Science and Technology, Ames.) *In* Oulu Univ., Proceedings of the 25th Annual Conference of the Finnish Physical Society 1991 1 p (For primary document see N92-10362 01-70)
Avail: NTIS HC/MF A12

N92-10466# Oulu Univ. (Finland). Dept. of Physics.
COMPUTER SIMULATIONS ON THE ORIENTATION OF MOLECULAR HYDROGEN IN LIQUID CRYSTALS Abstract Only
Juhani Lounila and Tapio T. Rantala *In its* Proceedings of the 25th Annual Conference of the Finnish Physical Society 1991 1 p (For primary document see N92-10362 01-70)
Avail: NTIS HC/MF A12

N92-10467# Helsinki Univ. of Technology, Espoo (Finland). Physics Lab.
OBSERVATION OF A MONOVACANCY IN THE METASTABLE STATE OF THE EL2 DEFECT IN GaAs BY POSITRON ANNIHILATION Abstract Only
K. Saarinen, R. Krause, P. Hautojarvi, and C. Corbel (Institut National des Sciences et Techniques Nucleaires, Saclay, France) *In* Oulu Univ., Proceedings of the 25th Annual Conference of the Finnish Physical Society 1991 1 p Previously announced in IAA as A91-19549 (For primary document see N92-10362 01-70)
Avail: NTIS HC/MF A12

N92-10470# Tampere Univ. of Technology (Finland). Dept. of Physics.
DIFFUSION ANOMALY AT A SURFACE RECONSTRUCTION Abstract Only
Tapio Ala-Nissila, W. K. Han, and S.-C. Ying (Brown Univ., Providence, RI.) *In* Oulu Univ., Proceedings of the 25th Annual Conference of the Finnish Physical Society 1991 1 p (For primary document see N92-10362 01-70)
Avail: NTIS HC/MF A12

N92-10471# Helsinki Univ. of Technology, Espoo (Finland). Lab. of Engineering Materials.
INTERNAL FRICTION ASSOCIATED WITH INTERACTION BETWEEN CARBON ATOMS AND DISLOCATIONS AT LOW TEMPERATURE Abstract Only
Y. Liu, K. Ullakko, and J. Pietikainen *In* Oulu Univ., Proceedings of the 25th Annual Conference of the Finnish Physical Society 1991 1 p (For primary document see N92-10362 01-70)
Avail: NTIS HC/MF A12

N92-10483# Jyvaskyla Univ. (Finland). Dept. of Physics.
SURFACE RECONSTRUCTION AND MANY-ATOM MODELS Abstract Only
H. Hakkinen, J. Merikoski, and M. Manninen *In* Oulu Univ., Proceedings of the 25th Annual Conference of the Finnish Physical Society 1991 1 p Sponsored by Emil Aaltonen Foundation and Academy of Finland (For primary document see N92-10362 01-70)
Avail: NTIS HC/MF A12

N92-10485# Tampere Univ. of Technology (Finland). Micro-Electronics Lab.
THE STABILITY ANALYSIS OF A DOUBLE BARRIER RESONANT TUNNELING DEVICE Abstract Only
H. P. Joosten, H. J. M. F. Noteborn, Kimmo Kaski, and D. Lenstra (Technische Univ., Eindhoven, Netherlands) *In* Oulu Univ., Proceedings of the 25th Annual Conference of the Finnish Physical Society 1991 1 p (For primary document see N92-10362 01-70)
Avail: NTIS HC/MF A12

N92-10489# Tampere Univ. of Technology (Finland). Dept. of Physics.
BERYLLIUM DOPING OF InP GROWN BY GAS-SOURCE MOLECULAR BEAM EPITAXY Abstract Only
T. Hakkarainen, K. Rakennus, K. Tappura, M. Hovinen, M. Pessa, and H. Asonen *In* Oulu Univ., Proceedings of the 25th Annual Conference of the Finnish Physical Society 1991 1 p (For

primary document see N92-10362 01-70)
Avail: NTIS HC/MF A12

N92-10490# Tampere Univ. of Technology (Finland). Dept. of Physics.
INTERFACE EFFECTS ON ELECTRICAL PROPERTIES OF HIGH PURITY InP GROWN BY GAS-SOURCE MOLECULAR BEAM EPITAXY Abstract Only
K. Rakennus, K. Tappura, T. Hakkarainen, M. Pessa, H. Asonen, and R. Laiho (Turku Univ., Finland) *In* Oulu Univ., Proceedings of the 25th Annual Conference of the Finnish Physical Society 1991 1 p (For primary document see N92-10362 01-70)
Avail: NTIS HC/MF A12

N92-10491# Tampere Univ. of Technology (Finland). Dept. of Physics.
THE INFLUENCE OF GROWTH CONDITIONS ON THE COMPOSITION OF GaInAsP GROWN BY GAS-SOURCE MOLECULAR BEAM EPITAXY Abstract Only
K. Tappura, T. Hakkarainen, K. Rakennus, M. Hovinen, and H. Asonen *In* Oulu Univ., Proceedings of the 25th Annual Conference of the Finnish Physical Society 1991 1 p (For primary document see N92-10362 01-70)
Avail: NTIS HC/MF A12

N92-10493# Tampere Univ. of Technology (Finland). Dept. of Physics.
ELECTRICAL CHARACTERIZATION OF Li AND N DOPED ZnSe Abstract Only
E. Kuusisto, J. Lilja, K. Imai, and M. Pessa *In* Oulu Univ., Proceedings of the 25th Annual Conference of the Finnish Physical Society 1991 1 p (For primary document see N92-10362 01-70)
Avail: NTIS HC/MF A12

N92-10496# Helsinki Univ. of Technology, Espoo (Finland). Physics Lab.
TUNNELING IN OSCILLATING DOUBLE BARRIER HETEROSTRUCTURES Abstract Only
M. F. Bjorksten, R. M. Nieminen, and K. Laasonen *In* Oulu Univ., Proceedings of the 25th Annual Conference of the Finnish Physical Society 1991 1 p (For primary document see N92-10362 01-70)
Avail: NTIS HC/MF A12

N92-10497# Helsinki Univ. of Technology, Espoo (Finland). Physics Lab.
SCANNING TUNNELING MICROSCOPE MEASUREMENTS IN AIR:LANGMUIR-BLODGETT FILMS ON HOPG AND GROWTH OF EVAPORATED GOLD ON HOPG Abstract Only
H. Niemi and K. Fallstroem *In* Oulu Univ., Proceedings of the 25th Annual Conference of the Finnish Physical Society 1991 1 p (For primary document see N92-10362 01-70)
Avail: NTIS HC/MF A12

N92-10498# Technical Univ. of Budapest (Hungary). Dept. of Electron Devices.
WORK FUNCTION CHANGES OF HIGH-T(SUB c) SUPERCONDUCTORS AROUND THE T(SUB c) Abstract Only
J. Mizsei, A. Uusimaki, and V. Lantto (Oulu Univ., Finland) *In* Oulu Univ., Proceedings of the 25th Annual Conference of the Finnish Physical Society 1991 1 p (For primary document see N92-10362 01-70)
Avail: NTIS HC/MF A12

N92-10499# Oulu Univ. (Finland). Dept. of Theoretical Physics.
PREDICTIONS OF THE ELECTRON-HOLE LIQUID MODEL FOR HIGH T(SUB c) SUPERCONDUCTORS Abstract Only
A. Kallio, X. Xiong, and V. Apaja *In* Oulu Univ., Proceedings of the 25th Annual Conference of the Finnish Physical Society 1991 1 p (For primary document see N92-10362 01-70)
Avail: NTIS HC/MF A12

N92-10500# Landau Inst. for Theoretical Physics, Moscow (USSR).
VORTEX LATTICE: VORTEX LIQUID STATES IN ANISOTROPIC HIGH-T(SUB c) SUPERCONDUCTORS Abstract Only
B. I. Ivlev, N. B. Kopnin, and M. M. Salomaa (Helsinki Univ. of Technology, Espoo, Finland) *In* Oulu Univ. Proceedings of the 25th Annual Conference of the Finnish Physical Society 1991 1 p Sponsored by Soviet Academy of Sciences and Academy of Finland (For primary document see N92-10362 01-70)
Avail: NTIS HC/MF A12

N92-10501# Helsinki Univ. of Technology, Espoo (Finland). Low Temperature Lab.
DYNAMICS OF VORTICES IN HIGH-TEMPERATURE SUPERCONDUCTORS Abstract Only
N. B. Kopnin (Landau Inst. for Theoretical Physics, Moscow, USSR) *In* Oulu Univ., Proceedings of the 25th Annual Conference of the Finnish Physical Society 1991 1 p (For primary document see N92-10362 01-70)
Avail: NTIS HC/MF A12

N92-10502# Turku Univ. (Finland). Wihuri Physical Lab.
PHOTOINDUCED SUPERCONDUCTIVITY IN FILMS OF YBaCuO Abstract Only
E. Lahderanta, V. I. Kudinov, A. I. Kirilyuk, N. M. Kreines (Academy of Sciences, USSR, Moscow), and R. Laiho *In* Oulu Univ., Proceedings of the 25th Annual Conference of the Finnish Physical Society 1991 1 p (For primary document see N92-10362 01-70)
Avail: NTIS HC/MF A12

N92-10503# Turku Univ. (Finland). Dept. of Applied Physics.
VALENCE ELECTRON STATES OF THE Bi-Sr-Ca-Cu-O HIGH-T(SUB c) COMPOUND Abstract Only
J. A. Leiro, F. Werfel, and G. Drager (Martin Luther-Univ., Halle-Wittenberg, German D.R.) *In* Oulu Univ., Proceedings of the 25th Annual Conference of the Finnish Physical Society 1991 1 p (For primary document see N92-10362 01-70)
Avail: NTIS HC/MF A12

N92-10504# Helsinki Univ. of Technology, Espoo (Finland). Dept. of Technical Physics.
STUDIES ON SUPERCONDUCTING Bi2Sr2Ca(n-1) Cu(n)O(4+2n) COMPOUNDS WITH Fe-57 AND Eu-151 MOESSBAUER SPECTROSCOPY Abstract Only
J. Linden, J. Hietaniemi, T. Karlemo, M. Karppinen, T. Katila, M. Lippmaa, L. Niinisto, I. Tittonen, and K. Ullakko *In* Oulu Univ., Proceedings of the 25th Annual Conference of the Finnish Physical Society 1991 1 p (For primary document see N92-10362 01-70)
Avail: NTIS HC/MF A12

N92-10505# Oulu Univ. (Finland). Microelectronics and Material Physics Labs.
EPITAXIAL HIGH T(SUB c) SUPERCONDUCTING THIN FILMS AND SUPERLATTICES DEPOSITED BY LASER ALBATION Abstract Only
J. Levoska, T. Murtoniemi, and S. Leppavuori *In its* Proceedings of the 25th Annual Conference of the Finnish Physical Society 1991 1 p (For primary document see N92-10362 01-70)
Avail: NTIS HC/MF A12

N92-10506# Oulu Univ. (Finland). Microelectronics and Material Physics Labs.
HIGH T(SUB c) SUPERCONDUCTING Li-DOPED Bi-Sr-Ca-Cu-O THIN FILMS DEPOSITED BY LASER ABLATION Abstract Only
J. Levoska, T. Murtoniemi, and S. Leppavuori *In its* Proceedings of the 25th Annual Conference of the Finnish Physical Society 1991 1 p (For primary document see N92-10362 01-70)
Avail: NTIS HC/MF A12

N92-10511# Turku Univ. (Finland). Wihuri Physical Lab.
NMR PULSE RESPONSES OF PAIRS OF TRIADS OF 1/2 SPINS IN SOLIDS Abstract Only
Antti Vuorimaki and Matti Punkkinen *In* Oulu Univ., Proceedings of the 25th Annual Conference of the Finnish Physical Society 1991 1 p (For primary document see N92-10362 01-70)
Avail: NTIS HC/MF A12

N92-10513# Joensuu Univ. (Finland). Dept. of Physics.
AN IMPROVED TECHNIQUE FOR ELECTROLYTIC COLOURATION OF ALKALI HALIDE CRYSTALS Abstract Only
P. Raerinne and P. Ketolainen *In* Oulu Univ., Proceedings of the 25th Annual Conference of the Finnish Physical Society 1991 1 p (For primary document see N92-10362 01-70)
Avail: NTIS HC/MF A12

N92-10515# Brookhaven National Lab., Upton, NY. Physics Dept.
POSITRON ANNIHILATION INDUCED AUGER-ELECTRON SPECTROSCOPY: A STUDY OF A Ge(100) SURFACE Abstract Only
E. Soininen (Helsinki Univ. of Technology, Espoo, Finland), A. Schwab, and K. G. Lynn *In* Oulu Univ., Proceedings of the 25th Annual Conference of the Finnish Physical Society 1991 1 p (For primary document see N92-10362 01-70)
Avail: NTIS HC/MF A12

N92-10516# Turku Univ. (Finland). Dept. of Applied Physics.
THE NORMAL INCIDENCE GRATING INVERSE PHOTOEMISSION SPECTROMETER IN THE ENERGY RANGE 8-28 eV Abstract Only
T. Ollonqvist, L. Saisa, and J. Vayrynen *In* Oulu Univ., Proceedings of the 25th Annual Conference of the Finnish Physical Society 1991 1 p (For primary document see N92-10362 01-70)
Avail: NTIS HC/MF A12

N92-10517# Oulu Univ. (Finland). Dept. of Physics.
SUPER COSTER KRONIG AND RESONANCE SUPER COSTER KRONIG SPECTRA OF SOLID Ge AROUND 3p-IONIZATION THRESHOLD Abstract Only
A. Kivimaki, H. Aksela, Seppo Aksela, and O.-P. Sairanen *In its* Proceedings of the 25th Annual Conference of the Finnish Physical Society 1991 1 p (For primary document see N92-10362 01-70)
Avail: NTIS HC/MF A12

N92-10518# Oulu Univ. (Finland). Dept. of Physics.
SYNCHROTRON RADIATION STUDY OF RECOMBINATION PROCESSES IN SOLID STATE Tb AND Dy AFTER 4d TO 4f GIANT RESONANCE EXCITATION Abstract Only
O.-P. Sairanen and Seppo Aksela *In its* Proceedings of the 25th Annual Conference of the Finnish Physical Society 1991 1 p (For primary document see N92-10362 01-70)
Avail: NTIS HC/MF A12

N92-10519# Oulu Univ. (Finland). Dept. of Physics.
THE N(4,5)N(6,7)N(6,7) AND N(4,5)O(2,3)N(6,7) RESONANCE AUGER EFFECTS IN THE ELECTRON SPECTRA OF SOLID STATE Gd AND Eu Abstract Only
O.-P. Sairanen and Seppo Aksela *In its* Proceedings of the 25th Annual Conference of the Finnish Physical Society 1991 1 p (For primary document see N92-10362 01-70)
Avail: NTIS HC/MF A12

N92-10520# Turku Univ. (Finland). Materials Research.
SURFACE CHARACTERIZATION OF COATED POWDERS WITH XPS: Al2O3-SiO2 COATED TiO2 PIGMENTS Abstract Only
Leena-Sisko Johansson and Tuomo Losoi (Kemira Oy Vuorikemia, Pori, Finland) *In* Oulu Univ., Proceedings of the 25th Annual Conference of the Finnish Physical Society 1991 1 p (For primary document see N92-10362 01-70)
Avail: NTIS HC/MF A12

N92-10522# Turku Univ. (Finland). Dept. of Physics.
THE CRYSTAL STRUCTURE AND MOISTURE SENSITIVITY OF (+)-4-(1-(2,3 DIMETHYLPHENYL) ETHYL) 1H-IMIDAZOLE HYDROCHLORIDE Abstract Only
E. Laine, R. Rajala, R. Sillanpaa, and J. Pirttimaki *In* Oulu Univ., Proceedings of the 25th Annual Conference of the Finnish Physical Society 1991 1 p (For primary document see N92-10362 01-70)
Avail: NTIS HC/MF A12

N92-10523# Tampere Univ. of Technology (Finland). Dept. of Physics.
COMPOUND SEMICONDUCTOR TECHNOLOGY: MATERIALS AND DEVICES Abstract Only
M. Pessa, H. Asonen, T. Hakkarainen, M. Hovinen, J. Keskinen, M. Korteoja, J. Lammasniemi, J. Nappi, K. Rakennus, and A. Salokatve et al *In* Oulu Univ., Proceedings of the 25th Annual Conference of the Finnish Physical Society 1991 1 p (For primary document see N92-10362 01-70)
Avail: NTIS HC/MF A12

N92-10527# Technische Univ., Chemnitz (Germany, F.R.). Dept. of Physics.
SEMICONDUCTING ORGANIC THIN FILMS AS MONITORING DEVICES FOR NO2 AIR POLLUTION Abstract Only
A. Heilmann and V. Lantto (Oulu Univ., Finland) *In* Oulu Univ., Proceedings of the 25th Annual Conference of the Finnish Physical Society 1991 1 p (For primary document see N92-10362 01-70)
Avail: NTIS HC/MF A12

N92-10530# Tampere Univ. of Technology (Finland). Dept. of Physics.
In(0.5)3Ga(0.47)As/InP SAM AVALANCHE PHOTODIODES GROWN BY GAS SOURCE MBE Abstract Only
G. Zhang, T. Hakkarainen, K. Tappura, K. Rakennus, H. Asonen, and M. Pessa *In* Oulu Univ., Proceedings of the 25th Annual Conference of the Finnish Physical Society 1991 1 p (For primary document see N92-10362 01-70)
Avail: NTIS HC/MF A12

N92-10531# Tampere Univ. of Technology (Finland). Dept. of Physics.
InP SOLAR CELLS GROWN BY GAS-SOURCE MOLECULAR BEAM EPITAXY Abstract Only
J. P. Zibin, K. Rakennus, K. Tappura, G. Zhang, J. Lammasniemi, and H. Asonen *In* Oulu Univ., Proceedings of the 25th Annual Conference of the Finnish Physical Society 1991 1 p (For primary document see N92-10362 01-70)
Avail: NTIS HC/MF A12

77 THERMODYNAMICS AND STATISTICAL PHYSICS

Includes quantum mechanics; theoretical physics; and Bose and Fermi statistics.

For related information see also *25 Inorganic and Physical Chemistry* and *34 Fluid Mechanics and Heat Transfer.*

N92-10707# Argonne National Lab., IL.
PHYSICS DIVISION ANNUAL REVIEW, APRIL 1, 1990 - MARCH 31, 1991
Jun. 1991 344 p
(Contract W-31-109-eng-38)
(DE91-018704; ANL-91/12) Avail: NTIS HC/MF A15

The following subject areas are covered: Research at ATLAS ion accelerator; operation and development of ATLAS; medium-energy nuclear physics and weak interactions; theoretical nuclear physics; high-resolution laser-RF spectroscopy with beams of atoms and molecules; fast ion-beam/laser studies of atomic and molecular structure; interactions of fast atomic and molecular ions with solid and gaseous targets; theoretical atomic physics;

atomic physics at ATLAS and the ECR source; atomic physics at synchrotron light sources; and accelerator facilities for atomic physics. DOE

N92-10365# Stockholm Univ. (Sweden). Inst. of Physics.
QUANTUM WORLD IN 2+1 DIMENSIONS Abstract Only
H. Hansson *In* Oulu Univ., Proceedings of the 25th Annual Conference of the Finnish Physical Society 1991 1 p (For primary document see N92-10362 01-70)
Avail: NTIS HC/MF A12

N92-10370# Turku Univ. (Finland). Dept. of Physics.
DROMIONS: THE MOVIE Abstract Only
Jarmo Hietarinta and J. Ruokolainen (Centre for Scientific Computing, Espoo, Finland) *In* Oulu Univ., Proceedings of the 25th Annual Conference on the Finnish Physical Society 1991 1 p (For primary document see N92-10362 01-70)
Avail: NTIS HC/MF A12

N92-10372# Oulu Univ. (Finland). Dept. of Theoretical Physics.
DYNAMIC LATTICE COMPUTING IN GENERAL RELATIVITY Abstract Only
P. Mahonen and V. Punkka (Texas Univ., Austin.) *In its* Proceedings of the 25th Annual Conference of the Finnish Physical Society 1991 1 p (For primary document see N92-10362 01-70)
Avail: NTIS HC/MF A12

N92-10438# Turku Univ. (Finland). Dept. of Applied Physics.
A NEW LINE-NARROWING METHOD LOMEP Abstract Only
Jyrki K. Kauppinen, Matti R. Hollberg, and Douglas J. Moffatt (National Research Council of Canada, Ottawa, Ontario) *In* Oulu Univ., Proceedings of the 25th Annual Conference of the Finnish Physical Society 1991 1 p (For primary document see N92-10362 01-70)
Avail: NTIS HC/MF A12

80 SOCIAL SCIENCES (GENERAL)

Includes educational matters.

No abstracts in this category.

81 ADMINISTRATION AND MANAGEMENT

Includes management planning and research.

N92-10708# General Accounting Office, Washington, DC.
NASA PROCUREMENT: MANAGEMENT OVERSIGHT OF CONTRACT COST AND TIME CHANGES COULD BE ENHANCED
Sep. 1991 16 p
(GAO/NSIAD-91-259; B-245559) Avail: NTIS HC/MF A03

At the request of the Subcommittee on Investigation and Oversight of the House Committee on Science, Space, and Technology, the General Accounting Office (GAO) reviewed NASA's contract administration and management practices. Particular attention was paid to contract cost increases and time extensions. GAO sampled contracts at the Goddard, Kennedy, Marshall, and Johnson Centers. Based on a sample of 317 contracts, it was estimated that 32 percent of all contracts increased in cost at an annual rate of 1.4 percent, and 41 percent of all contracts had time extensions. GAO suggested that NASA enhance its Financial And Contractual Status (FACS) computer system to track these cost and time increases, and thereby improve NASA's contract oversight capabilities. NASA agreed and will implement the program changes as soon as is practical. J.P.S.

N92-10709# General Accounting Office, Washington, DC.
NASA MAINTENANCE: STRONGER COMMITMENT NEEDED TO CURB FACILITY DETERIORATION
Dec. 1990 43 p
(GAO/NSIAD-91-34; B-240547) Avail: NTIS HC/MF A03

NASA has a $15 billion network of facilities to house and support its research, development, and flight activities. At the request of the subcommittee, GAO evaluated the condition of NASA facilities and, because the facilities had deteriorated, the reasons for such conditions. GAO also reviewed the accuracy of NASA's accounting and budgeting for its maintenance activities. Many of NASA's facilities have not been adequately maintained and are in degraded condition. Consequently, many need significant repair. In addition, several serious incidents have been caused by the facilities' deterioration, including fire and a steam line explosion. Deferred or insufficient maintenance increases the likelihood of more such events in the future, as well as increased maintenance costs. Although some mission critical facilities like the launch pads and the orbiter processing facility used for the space shuttle are generally well maintained, the eight centers GAO visited all have deteriorating facilities, such as leaking roofs, peeling paint, and leaking steam lines. NASA has recently taken steps to focus on the facilities maintenance problems. Author

N92-10710# General Accounting Office, Washington, DC.
MANAGEMENT ISSUES AT THE NATIONAL AERONAUTICS AND SPACE ADMINISTRATION
Frank C. Conahan 1 Aug. 1991 19 p
(GAO/T-NSIAD-91-48) Avail: NTIS HC/MF A03

Testimony before the Subcommittee on investigations and Oversight Committee on Science, Space, and Technology of the House of Representatives is presented. Management issues at the National Aeronautics and Space Administration (NASA), primarily major assignments performed at NASA in the past four years, are discussed. The discussion is within the framework of experience gained from performing general management reviews of executive branch agencies. The most common issues emerging from the general management reviews concern basic management activities, such as developing strategic planning systems to prepare the agency for further challenges; dealing with leadership problems that result from a high rate of turnover and lack of accountability; addressing long-standing problems involving information resources management, financial management, and internal controls; and focusing on how managers and workers are recruited and trained. The work at NASA is discussed with specific regard to strategic planning, organizational management, human resources management, program and project management, financial management, and information management. Author

82 DOCUMENTATION AND INFORMATION SCIENCE

Includes information management; information storage and retrieval technology; technical writing; graphic arts; and micrography.

For computer documentation see *61 Computer Programming and Software.*

N92-10711*# Research Inst. for Advanced Computer Science, Moffett Field, CA.
WORLDNET
Peter J. Denning 5 Jul. 1989 15 p Submitted for publication
(Contract NCC2-387)
(NASA-CR-188845; NAS 1.26:188845; RIACS-TR-89-26) Avail: NTIS HC/MF A03 CSCL 05B

The expanding use of powerful workstations coupled to ubiquitous networks is transforming scientific and engineering research and the the ways organizations around the world do business. By the year 2000, few enterprises will be able to succeed without mastery of this technology, which will be embodied in an information infrastructure based on a worldwide network. A recurring theme in all the discussions of what might be possible

within the emerging Worldnet is people and machines working together in new ways across distance and time. A review is presented of the basic concepts on which the architecture of Worldnet must be built: coordination of action, authentication, privacy, and naming. Worldnet must provide additional functions to support the ongoing processes of suppliers and consumers: help services, aids for designing and producing subsystems, spinning off new machines, and resistance to attack. This discussion begins to reveal the constituent elements of a theory for Worldnet, a theory focused on what people will do with computers rather than on what computers do. Author

N92-10712*# Research Inst. for Advanced Computer Science, Moffett Field, CA.
RESEARCH INTO THE DEVELOPMENT OF A KNOWLEDGE ACQUISITION TAXONOMY Final Report
Pamela K. Fink and L. Tandy Herren (Southwest Research Inst., San Antonio, TX.) Jul. 1991 522 p
(Contract NCC9-16; RICIS Proj. ET-26; SwRI Proj. 05-3744)
(NASA-CR-188948; NAS 1.26:188948) Avail: NTIS HC/MF A22 CSCL 05B

The focus of the research was on the development of a problem solving taxonomy that can support and direct the knowledge engineering process during the development of an intelligent tutoring system. The results of the research are necessarily general. Being only a small initial attempt at a fundamental problem in artificial intelligence and cognitive psychology, the process has had to be bootstrapped and the results can only provide pointers to further, more formal research designs. Author

N92-10713# Department of Energy, Oak Ridge, TN. Office of Scientific and Technical Information.
INFOTECH '91: DOE TECHNICAL INFOMATION (TI) MEETING
1991 153 p Meeting held in Oak Ridge, TN, 22-23 May 1991
(DE91-018074; CONF-9105153) Avail: NTIS HC/MF A08

The INFOTECH '91 DOE Technical Information Meeting which was sponsored by the DOE Office of Scientific and Technical Information in Oak Ridge, Tennessee, emphasizes the impact of technology on information management and production. The two-day meeting features presentations by professional information science, technology, and management personnel from both DOE and DOE contractor organizations who share the plans and/or results of their experiences, methods, technology, and approaches to information management dissemination. The conference papers have been catalogued separately. DOE

N92-10714# Army Research Inst. for the Behavioral and Social Sciences, Alexandria, VA.
MANPRINT REFERENCE RETRIEVAL SYSTEM (USER'S GUIDE) Final Report, Oct. 1988 - Aug. 1990
David R. Hunter Apr. 1991 33 p
(AD-A239915; ARI-RP-91-10) Avail: NTIS HC/MF A03 CSCL 12/7

This report describes the installation and use of the MANPRINT Reference Retrieval System (MANRRS). MANRRS is a menu driven system used for the identification of references related to one or more of the domains subsumed by MANPRINT. MANRRS includes both a database with indexed entries on MANPRINT domain and record type (i.e., regulation, standard, technical report, etc.) and the retrieval software program written in dBase III command language. A valid copy of dBase III Plus is required to use MANRRS. GRA

N92-10715# RAND Corp., Santa Monica, CA.
IID: AN INTELLIGENT INFORMATION DICTIONARY FOR MANAGING SEMANTIC METADATA
Stephanie Cammarata, Darrell Shane, and Prasad Ram 1991 68 p
(Contract MDA903-90-C-0004)
(AD-A240022; RAND/R-3856-DARPA) Avail: NTIS HC/MF A04 CSCL 12/7

RAND has been investigating the use of semantic data models in object-oriented and knowledge-based simulation under these sponsorships and within RAND's Information Processing Systems Program as part of the Intelligent Databases Project. The research described in this report is one aspect of intelligent databases addressing the derivation of simulation-specific databases from external databases. This report serves two purposes. First, it discusses the data flow gap between (1) external databases acquired from public agencies, and (2) datasets derived from these databases to be used as input to specific simulation models. This gap refers to the lack of interoperability between external databases and simulation databases and to the transformations that are necessary to derive compatible datasets. The second goal of this report is to present the computer software system developed to bridge this data flow gap. The report should be of interest to database administrators, simulation developers, and researchers in database management and information processing technology. GRA

N92-10716# Massachusetts Inst. of Tech., Cambridge. Lab. for Computer Science.
TYPE ABSTRACTION RULES FOR REFERENCES: A COMPARISON OF FOUR WHICH HAVE ACHIEVED NOTORIETY
James W. OToole, Jr. Aug. 1991 12 p
(Contract N00014-83-K-0125)
(AD-A240076; MIT/LCS/TM-390) Avail: NTIS HC/MF A03 CSCL 12/5

I present four type abstraction rules which have been introduced by various authors to permit polymorphic type safety in the presence of mutable data. Each of the type abstraction rules is discussed in the context of the language in which is was introduced, and the various abstraction rules are compared. GRA

N92-10930*# Washington Univ., Saint Louis, MO. Center for Space Sciences.
IMAGE RETRIEVAL AND PROCESSING SYSTEM VERSION 2.0 DEVELOPMENT WORK
Susan H. Slavney and Edward A. Guinness *In* NASA, Washington, Reports of Planetary Geology and Geophysics Program, 1990 Jun. 1991 p 517-519 (For primary document see N92-10728 01-91)
Avail: NTIS HC/MF A25 CSCL 03B

83 ECONOMICS AND COST ANALYSIS

Includes cost effectiveness studies.

No abstracts in this category.

84 LAW, POLITICAL SCIENCE AND SPACE POLICY

Includes NASA appropriation hearings; aviation law; space law and policy; international law; international cooperation; and patent policy.

No abstracts in this category.

85 URBAN TECHNOLOGY AND TRANSPORTATION

Includes applications of space technology to urban problems; technology transfer; technology assessment; and surface and mass transportation.

For related information see also *03 Air Transportation and Safety, 16 Space Transportation,* and *44 Energy Production and Conversion.*

N92-10717* National Aeronautics and Space Administration, Washington, DC.
INDEX TO 1987 NASA TECH BRIEFS, VOLUME 11, NUMBERS 1-10
May 1988 114 p
(NASA-TM-105024; NAS 1.15:105024) Avail: NASA Center for AeroSpace Information, P.O. Box 8757, BWI Airport, MD 21240 HC $10.00 CSCL 05A

Short announcements of new technology derived from the research and development activities of NASA are presented. These briefs emphasize information considered likely to be transferrable across industrial, regional, or disciplinary lines and are issued to encourage commercial application. This index for 1987 Tech Briefs contains abstracts and four indexes: subject, personal author, originating center, and Tech Brief Number. The following areas are covered: electronic components and circuits, electronic systems, physical sciences, life sciences, materials, mechanics, machinery, fabrication technology, and mathematics and information sciences. Author

N92-10718* National Aeronautics and Space Administration, Washington, DC.
INDEX TO 1988 NASA TECH BRIEFS, VOLUME 12, NUMBERS 1-11
Jun. 1989 123 p
(NASA-TM-105077; NAS 1.15:105077) Avail: NASA Center for AeroSpace Information, P.O. Box 8757, BWI Airport, MD 21240 HC $10.00 CSCL 05A

Short announcements of new technology derived from the research and development activities of NASA are presented. These briefs emphasize information considered likely to be transferrable across industrial, regional, or disciplinary lines and are issued to encourage commercial application. This index for 1988 Tech Briefs contains abstracts and four indexes: subject, personal author, originating center, and Tech Brief Number. The following areas are covered: electronic components and circuits, electronic systems, physical sciences, materials, life sciences, mechanics, machinery, fabrication technology, and mathematics and information sciences. Author

N92-10719* National Aeronautics and Space Administration, Washington, DC.
INDEX TO 1989 NASA TECH BRIEFS, VOLUME 13, NUMBERS 1-12
May 1990 135 p
(NASA-TM-105109; NAS 1.15:105109) Avail: NASA Center for AeroSpace Information, P.O. Box 8757, BWI Airport, MD 21240 HC $10.00 CSCL 05A

Short announcements of new technology derived from the research and development activities of NASA are presented. These briefs emphasize information considered likely to be transferrable across industrial, regional, or disciplinary lines and are issued to encourage commercial application. This index for 1989 Tech Briefs contains abstracts and four indexes: subject, personal author, originating center, and Tech Brief Number. The following areas are covered: electronic components and circuits, electronic systems, physical sciences, materials, life sciences, mechanics, machinery, fabrication technology, and mathematics and information sciences. Author

N92-10720* National Aeronautics and Space Administration, Washington, DC.
INDEX TO 1990 NASA TECH BRIEFS, VOLUME 14, NUMBERS 1-12
May 1991 146 p
(NASA-TM-105110; NAS 1.15:105110) Avail: NASA Center for AeroSpace Information, P.O. Box 8757, BWI Airport, MD HC $10.00 CSCL 05A

Short announcements of new technology derived from the research and development activities of NASA are presented. These briefs emphasize information considered likely to be transferrable across industrial, regional, or disciplinary lines and are issued to encourage commercial application. This index for 1990 Tech Briefs contains abstracts and four indexes: subject, personal author, originating center, and Tech Brief Number. The following areas are covered: electronic components and circuits, electronic systems, physical sciences, materials, life sciences, mechanics, machinery, fabrication technology, and mathematics and information sciences. Author

N92-10721* National Aeronautics and Space Administration, Washington, DC.
CUMULATIVE INDEX TO NASA TECH BRIEFS, 1976-1980, VOLUMES 1-5
Jun. 1988 471 p
(NASA-TM-89327; NAS 1.15:89327) Avail: NASA Center for AeroSpace Information, P.O. Box 8757, BWI Airport, MD 21240 HC $25.00. A companion index is available HC $25.00. Set available as HC $40.00 CSCL 05A

Short announcements of new technology derived from the research and development activities of NASA are presented. These briefs emphasize information considered likely to be transferrable across industrial, regional, or disciplinary lines are are issued to encourage commercial application. This cumulative index for 1976-1980 Tech Briefs contains abstracts and four indexes: subject, personal author, originating center, and Tech Brief Number. The following areas are covered: electronic components and circuits, electronic systems, physical sciences, materials, life sciences, mechanics, machinery, fabrication technology, and mathematics and information sciences. Author

N92-10722* National Aeronautics and Space Administration, Washington, DC.
CUMULATIVE INDEX TO NASA TECH BRIEFS, 1981-1985, VOLUMES 6-10
Aug. 1988 408 p
(NASA-TM-89326; NAS 1.15:89326) Avail: NASA Center for AeroSpace Information, P.O. Box 8757, BWI Airport, MD 21240 HC $25.00. A companion index is available HC $25.00. Set available as HC $40.00 CSCL 05A

Short announcements of new technology derived from the research and development activities of NASA are presented. These briefs emphasize information considered likely to be transferrable across industrial, regional, or disciplinary lines and are issued to encourage commercial application. This cumulative index for 1981-1985 Tech Briefs contains abstracts and four indexes: subject, personal author, originating center, and Tech Brief Number. The following areas are covered: electronic components and circuits, electronic systems, physical sciences, materials, life sciences, mechanics, machinery, fabrication technology, and mathematics and information sciences. Author

88 SPACE SCIENCES (GENERAL)

No abstracts in this category.

89 ASTRONOMY

Includes radio, gamma-ray, and infrared astronomy, and astrometry.

N92-10723 Max-Planck-Inst. fuer Physik und Astrophysik, Garching (Germany, F.R.).
AN ATLAS OF OPTICAL COUNTERPARTS OF LOW MASS X RAY BINARIES. PART 1: THE NORTHERN SAMPLE
M. Gottwald, H. Steinle, U. Graser (Max-Planck-Inst. fuer Astronomie, Heidelberg, Germany, F.R.), and W. Pietsch Nov. 1990 47 p Previously announced in IAA as A91-48246 Submitted for publication
(MPE-Preprint-195-Pt-1; ISSN-0178-0719; ETN-91-90016)
Copyright Avail: Fachinformationszentrum Karlsruhe, 7514 Eggenstein-Leopoldshafen 2, Fed. Republic of Germany

The first part of an atlas of optical counterparts of low mass X ray binaries is presented. It comprises those sources that can be observed from a site at moderate northern latitudes. The declination threshold is delta greater than -22 degrees so that the sample of low mass X ray binaries is referred to as the northern sample. In total this part of the atlas includes 18 identified and 10 unidentified objects. The latter define the list of bright X ray sources being possible low mass binary candidates but lacking any obvious optical counterpart. The information presented in this atlas is compiled from various papers from the past two decades. Where appropriate, the most recent X ray source positions and error radii are quoted. Some of them have not been published before or were not reported in the context of optical identification. The maps of the atlas were obtained with a charge coupled device camera at the focus of the 1.23 m, the 2.2 m and the 3.5 m telescope at the German-Spanish astronomical Center/Calar alto, as uniformly as possible, for the complete northern sample. ESA

N92-10724*# Alabama Univ., Huntsville. Dept. of Physics and Astronomy.
IPC TWO-COLOR ANALYSIS OF X RAY GALAXY CLUSTERS Final Technical Report, 1 Aug. 1989 - 31 Jan. 1990
Raymond E. White, III 31 Jan. 1990 9 p
(Grant NAG5-1188)
(NASA-CR-188980; NAS 1.26:188980) Avail: NTIS HC/MF A02 CSCL 03A

The mass distributions were determined of several clusters of galaxies by using X ray surface brightness data from the Einstein Observatory Imaging Proportional Counter (IPC). Determining cluster mass distributions is important for constraining the nature of the dark matter which dominates the mass of galaxies, galaxy clusters, and the Universe. Galaxy clusters are permeated with hot gas in hydrostatic equilibrium with the gravitational potentials of the clusters. Cluster mass distributions can be determined from x ray observations of cluster gas by using the equation of hydrostatic equilibrium and knowledge of the density and temperature structure of the gas. The x ray surface brightness at some distance from the cluster is the result of the volume x ray emissivity being integrated along the line of sight in the cluster.
Author

N92-10549# Helsinki Univ. of Technology, Espoo (Finland). Astrophysics Lab.
FINNISH SPACE PROJECTS: SPACE ASTRONOMY Abstract Only
O. Vilhu *In* Oulu Univ., Proceedings of the 25th Annual Conference of the Finnish Physical Society 1991 1 p (For primary document see N92-10362 01-70)
Avail: NTIS HC/MF A12

N92-10566# Helsinki Univ. of Technology, Espoo (Finland). Astrophysics Lab.
THEORETICAL STUDIES OF OPTICAL PHENOMENA AND RELATED INVERSE PROBLEMS OF SOLAR SYSTEM BODIES Abstract Only
Mikko K. J. Kaasalainen, Sauli Jamsa, Kari Lumme, Karri O. Muinonen, and Jouni I. Peltoniemi *In* Oulu Univ., Proceedings of the 25th Annual Conference of the Finnish Physical Society 1991 1 p (For primary document see N92-10362 01-70)
Avail: NTIS HC/MF A12

90 ASTROPHYSICS

Includes cosmology; celestial mechanics; space plasmas; and interstellar and interplanetary gases and dust.
For related information see also *75 Plasma Physics.*

N92-10725# Lawrence Livermore National Lab., CA.
INFORMATION FLOW IN QUANTUM MECHANICS: THE QUANTUM MAXWELL DEMON
G. F. Chapline Aug. 1990 7 p Presented at the Meeting on the Foundation of Quantum Mechanics, Santa Fe, NM, 27-31 May 1991
(Contract W-7405-eng-48)
(DE91-017659; UCRL-JC-107942; CONF-9105251-1) Avail: NTIS HC/MF A02

Quantum information can be lost only when a quantum system is placed in contact with a heat bath, and then only in proportion to the entropy generated. Applied to the universe as a whole this suggests that the universe is in an algorithmically simple nearly pure quantum state. This could be verified by squeezing the vacuum state, and it is quite plausible that this is exactly what is happening inside black holes. DOE

N92-10726# Los Alamos National Lab., NM.
DARK MATTER AND THE EFFECTIVE VALUE OF NEWTON'S CONSTANT AT LARGE DISTANCES
T. Goldman, F. Cooper, M. M. Nieto, and J. Perez-Mercader (Consejo Superior de Investigaciones Cientificas, Madrid, Spain) 1991 4 p Presented at the Particles and Fields '91, Vancouver (Canada), 18-22 Aug. 1991
(Contract W-7405-eng-36)
(DE91-018152; LA-UR-91-2792; CONF-910881-2) Avail: NTIS HC/MF A01

We investigate the implications of the renormalization group applied to one-loop renormalized quantum gravity for the effective value of the Newton's constant on large distance scales. We find a potentially significant contribution to solving the so-called dark matter problem. DOE

N92-10727# Stanford Linear Accelerator Center, CA.
QUANTUM COSMOLOGY ON THE WORLDSHEET
A. R. Cooper, L. Susskind, and L. Thorlacius Aug. 1991 13 p Presented at the Strings and Symmetries Conference, Stony Brook, NY, 20-25 May 1991
(Contract DE-AC03-76SF-00515)
(DE91-018415; SU-SLAC-PUB-5639; CONF-9105113-2) Avail: NTIS HC/MF A03

Two-dimensional quantum gravity coupled to conformally invariant matter central c greater than 25 provides a toy model for quantum gravity in four dimensions. Two-dimensional quantum cosmology can thus be studied in terms of string theory in background fields. The large scale cosmological constant depends on non-linear dynamics in the string theory target space and does not appear to be suppressed by wormhole effects. DOE

N92-10252*# National Aeronautics and Space Administration. Lyndon B. Johnson Space Center, Houston, TX.
CLAY MINERALS IN PRIMITIVE METEORITES AND INTERPLANETARY DUST 2. SMECTITES AND MICAS Abstract Only
L. P. Keller and M. E. Zolensky *In its* Program and Abstracts for Clay Minerals Society 28th Annual Meeting 1991 p 87 (For primary document see N92-10248 01-46)
Avail: NTIS HC/MF A11 CSCL 03B

N92-10253*# National Aeronautics and Space Administration. Lyndon B. Johnson Space Center, Houston, TX.
MINERALOGY OF CRETACEOUS/TERTIARY BOUNDARY CLAYS IN THE CHICXULUB STRUCTURE IN NORTHERN YUCATAN Abstract Only
D. W. Ming, Virgil L. Sharpton, and B. C. Schuraytz (Lunar and Planetary Inst., Houston, TX.) *In its* Program and Abstracts for Clay Minerals Society 28th Annual Meeting 1991 p 114 (For primary document see N92-10248 01-46)
Avail: NTIS HC/MF A11 CSCL 03B

N92-10256*# National Aeronautics and Space Administration. Lyndon B. Johnson Space Center, Houston, TX.
CLAY MINERALS IN PRIMITIVE METEORITES AND INTERPLANETARY DUST 1 Abstract Only
M. E. Zolensky and L. P. Keller *In its* Program and Abstracts for Clay Minerals Society 28th Annual Meeting 1991 p 184 (For primary document see N92-10248 01-46)
Avail: NTIS HC/MF A11 CSCL 03B

N92-10399# Helsinki Univ. of Technology, Espoo (Finland). Dept. of Theoretical Physics.
SUPERNOVA NEUTRINOS Abstract Only
Juha T. Peltoniemi *In* Oulu Univ., Proceedings of the 25th Annual Conference of the Finnish Physical Society 1991 1 p (For primary document see N92-10362 01-70)
Avail: NTIS HC/MF A12

N92-10571# Oulu Univ. (Finland). Dept. of Astronomy.
STRUCTURE AND EVOLUTION OF TURBULENT PREPLANETARY DISC Abstract Only
M. Verronen, H. Vanhala, and K. A. Hameen-Anttila *In its* Proceedings of the 25th Annual Conference of the Finnish Physical Society 1991 1 p (For primary document see N92-10362 01-70)
Avail: NTIS HC/MF A12

N92-10576# Turku Univ. (Finland).
SELF-REGULATION MECHANISMS IN GALACTIC DISCS Abstract Only
Alessandro B. Romeo *In* Oulu Univ., Proceedings of the 25th Annual Conference of the Finnish Physical Society 1991 1 p (For primary document see N92-10362 01-70)
Avail: NTIS HC/MF A12

N92-10578# Turku Univ. (Finland).
DOUBLE RADIO SOURCES AS STANDARD RODS OF TESTING COSMOLOGICAL MODELS Abstract Only
M. Valtonen, K. Nilsson, J. Kotilainen, and T. Jaakkola *In* Oulu Univ., Proceedings of the 25th Annual Conference of the Finnish Physical Society 1991 1 p (For primary document see N92-10362 01-70)
Avail: NTIS HC/MF A12

N92-10579# Oulu Univ. (Finland). Dept. of Astronomy.
N-BODY SIMULATIONS OF INTERACTING GALAXIES Abstract Only
H. Salo *In its* Proceedings of the 25th Annual Conference of the Finnish Physical Society 1991 1 p (For primary document see N92-10362 01-70)
Avail: NTIS HC/MF A12

N92-10738*# Lafayette Coll., Easton, PA. Dept. of Physics.
THE MAGNESIUM SULFATE-WATER SYSTEM AT PRESSURES TO 4 KILOBARS
D. L. Hogenboom, Jeffrey S. Kargel, J. P. Ganasan, and J. S. Lewis (Arizona Univ., Tucson.) *In* NASA, Washington, Reports of Planetary Geology and Geophysics Program, 1990 Jun. 1991 p 27-28 (For primary document see N92-10728 01-91)
Avail: NTIS HC/MF A25 CSCL 03B

N92-10824*# Massachusetts Inst. of Tech., Cambridge. Dept. of Earth, Atmospheric and Planetary Sciences.
PRE-TERRESTRIAL OXIDATION PRODUCTS IN CARBONACEOUS METEORITES IDENTIFIED BY MOSSBAUER SPECTROSCOPY
Roger G. Burns and Duncan S. Fisher *In* NASA, Washington, Reports of Planetary Geology and Geophysics Program, 1990 Jun. 1991 p 256-258 (For primary document see N92-10728 01-91)
(Grant NAGw-2037)
Avail: NTIS HC/MF A25 CSCL 03B

N92-10825*# Massachusetts Inst. of Tech., Cambridge. Dept. of Earth, Atmospheric and Planetary Sciences.
DOES LAFAYETTE = NAKHLA? NOT NECESSARILY SO, BASED ON 4.2K MOSSBAUER SPECTRA OF ALL OF THE SNC METEORITES
Roger G. Burns *In* NASA, Washington, Reports of Planetary Geology and Geophysics Program, 1990 Jun. 1991 p 259-261 (For primary document see N92-10728 01-91)
(Grant NAGw-2037)
Avail: NTIS HC/MF A25 CSCL 03B

N92-10826*# Johns Hopkins Univ., Baltimore, MD. Dept. of Earth and Planetary Sciences.
INFRARED (2.08-14 MICRON) SPECTRA OF POWERED STONY METEORITES
J. W. Salisbury, D. M. DAria, and E. Jarosewich (National Museum of Natural History, Washington, DC.) *In* NASA, Washington, Reports of Planetary Geology and Geophysics Program, 1990 Jun. 1991 p 262-264 (For primary document see N92-10728 01-91)
Avail: NTIS HC/MF A25 CSCL 03B

N92-10827*# Brown Univ., Providence, RI. Dept. of Geological Sciences.
DARKENING IN GAS-RICH ORDINARY CHONDRITES: SPECTRAL MODELLING AND IMPLICATIONS FOR THE REGOLITHS OF ORDINARY CHONDRITE PARENT BODIES
Daniel T. Britt and Carle M. Pieters *In* NASA, Washington, Reports of Planetary Geology and Geophysics Program, 1990 Jun. 1991 p 265-266 (For primary document see N92-10728 01-91)
Avail: NTIS HC/MF A25 CSCL 03B

N92-10828*# Brown Univ., Providence, RI. Dept. of Geological Sciences.
THE BIDIRECTIONAL REFLECTANCE SPECTRA OF FIVE GAS-RICH ORDINARY CHONDRITES
Daniel T. Britt and Carle M. Pieters *In* NASA, Washington, Reports of Planetary Geology and Geophysics Program, 1990 Jun. 1991 p 267-268 (For primary document see N92-10728 01-91)
(Grants NAGw-28; NAGw-748)
Avail: NTIS HC/MF A25 CSCL 03B

N92-10829*# Academy of Sciences (USSR), Moscow.
REFLECTANCE SPECTRA OF SOME FRACTIONS OF MIGEI AND MURCHISON SM CHONDRITES IN THE RANGE OF 0.3-2.6 MICRONS
L. V. Moroz and Carle M. Pieters (Brown Univ., Providence, RI.) *In* NASA, Washington, Reports of Planetary Geology and Geophysics Program, 1990 Jun. 1991 p 269-270 (For primary document see N92-10728 01-91)
Avail: NTIS HC/MF A25 CSCL 03B

N92-10830*# Arizona Univ., Tucson. Lunar and Planetary Lab.
AN INFRARED REFLECTANCE STUDY OF LOW ALBEDO SURFACE CONSTITUENTS
Larry A. Lebofsky *In* NASA, Washington, Reports of Planetary Geology and Geophysics Program, 1990 Jun. 1991 p 271-273 (For primary document see N92-10728 01-91)
Avail: NTIS HC/MF A25 CSCL 03B

N92-10831*# Brown Univ., Providence, RI. Dept. of Geological Sciences.
EFFECTS OF GRAIN SIZE AND SHAPE IN MODELING REFLECTANCE SPECTRA OF MINERAL MIXTURES
T. Hiroi and Carle M. Pieters *In* NASA, Washington, Reports of Planetary Geology and Geophysics Program, 1990 Jun. 1991 p 274-275 (For primary document see N92-10728 01-91)
(Grant NAGw-748)
Avail: NTIS HC/MF A25 CSCL 03B

N92-10832*# Jet Propulsion Lab., California Inst. of Tech., Pasadena.
LIGHT SCATTERING BY LUNAR-LIKE PARTICLE SIZE DISTRIBUTIONS
Jay D. Goguen *In* NASA, Washington, Reports of Planetary Geology and Geophysics Program, 1990 Jun. 1991 p 276-278 (For primary document see N92-10728 01-91)
(Grant NASA-PGP-151-01-70-56-00)
Avail: NTIS HC/MF A25 CSCL 03B

N92-10833*# Brown Univ., Providence, RI.
CHARACTER OF THE OPPOSITION EFFECT AND NEGATIVE POLARIZATION
Carle M. Pieters, Yu. G. Shkuratov, and D. G. Stankevich (Kharkov State Univ., USSR) *In* NASA, Washington, Reports of Planetary Geology and Geophysics Program, 1990 Jun. 1991 p 279 (For primary document see N92-10728 01-91)
Avail: NTIS HC/MF A25 CSCL 03B

N92-10834*# Cornell Univ., Ithaca, NY. Center for Radiophysics and Space Research.
LABORATORY PHOTOMETRIC MEASUREMENT OF PARTICULATE SOILS OUT TO VERY LARGE PHASE ANGLES
Paul Helfenstein, Ulrich A. Bonne, Susan Stolovy, and Joseph Veverka *In* NASA, Washington, Reports of Planetary Geology and Geophysics Program, 1990 Jun. 1991 p 280-282 (For primary document see N92-10728 01-91)
Avail: NTIS HC/MF A25 CSCL 03B

N92-10835*# Cornell Univ., Ithaca, NY.
THE PHOTOMETRIC ROUGHNESS OF MIMAS
A. Verbiscer and Joseph Veverka *In* NASA, Washington, Reports of Planetary Geology and Geophysics Program, 1990 Jun. 1991 p 283-284 (For primary document see N92-10728 01-91)
(Grants NGT-50482; NsG-7156)
Avail: NTIS HC/MF A25 CSCL 03B

N92-10868*# Arizona Univ., Tucson. Lunar and Planetary Lab.
JETTING AND THE ORIGIN OF TEKTITES
A. M. Vickery *In* NASA, Washington, Reports of Planetary Geology and Geophysics Program, 1990 Jun. 1991 p 361 (For primary document see N92-10728 01-91)
Avail: NTIS HC/MF A25 CSCL 03B

N92-10881*# Rensselaer Polytechnic Inst., Troy, NY. Dept. of Geology.
METEORITE SPECTROSCOPY AND CHARACTERIZATION OF ASTEROID SURFACE MATERIALS
Michael J. Gaffey *In* NASA, Washington, Reports of Planetary Geology and Geophysics Program, 1990 Jun. 1991 p 391-393 (For primary document see N92-10728 01-91)
(Grant NAGw-642)
Avail: NTIS HC/MF A25 CSCL 03B

N92-10882*# Hawaii Univ., Honolulu. Dept. of Geology and Geophysics.
WILL GALILEO RESOLVE THE S-ASTEROID CONTROVERSY?
Jeffrey F. Bell *In* NASA, Washington, Reports of Planetary Geology and Geophysics Program, 1990 Jun. 1991 p 394-396 (For primary document see N92-10728 01-91)
Avail: NTIS HC/MF A25 CSCL 03B

N92-10884*# Planetary Science Inst., Tucson, AZ.
UNDERSTANDING ASTEROID COLLISIONAL HISTORY THROUGH EXPERIMENTAL AND NUMERICAL STUDIES
Donald R. Davis, Eileen V. Ryan, and S. J. Weidenschilling *In* NASA, Washington, Reports of Planetary Geology and Geophysics Program, 1990 Jun. 1991 p 399-402 (For primary document see N92-10728 01-91)
Avail: NTIS HC/MF A25 CSCL 03B

N92-10885*# Jet Propulsion Lab., California Inst. of Tech., Pasadena.
ASTEROID FAMILIES
James G. Williams *In* NASA, Washington, Reports of Planetary Geology and Geophysics Program, 1990 Jun. 1991 p 403-404 (For primary document see N92-10728 01-91)
Avail: NTIS HC/MF A25 CSCL 03B

N92-10886*# Florida Univ., Gainesville. Dept. of Astronomy.
ORIGIN AND EVOLUTION OF THE ZODIACAL DUST CLOUD
S. F. Dermott, D. Durda, B. Gustafson, S. Jayaraman, Y.-L. Xu, P. D. Nicholson (Cornell Univ., Ithaca, NY.), and R. S. Gomes *In* NASA, Washington, Reports of Planetary Geology and Geophysics Program, 1990 Jun. 1991 p 405-406 (For primary document see N92-10728 01-91)
Avail: NTIS HC/MF A25 CSCL 03B

N92-10887*# Jet Propulsion Lab., California Inst. of Tech., Pasadena.
PHOTOMETRY OF THE COMET 2060 CHIRON
Bonnie J. Buratti, Robert L. Marcialis, and R. Scott Dunbar *In* NASA, Washington, Reports of Planetary Geology and Geophysics Program, 1990 Jun. 1991 p 407-408 (For primary document see N92-10728 01-91)
Avail: NTIS HC/MF A25 CSCL 03B

N92-10888*# National Aeronautics and Space Administration. Lyndon B. Johnson Space Center, Houston, TX.
WATER/ROCK INTERACTIONS IN EXPERIMENTALLY SIMULATED DIRTY SNOWBALL AND DIRTY ICEBALL COMETARY NUCLEI
James L. Gooding and Judith H. Allton (Lockheed Engineering and Sciences Co., Houston, TX.) *In* NASA, Washington, Reports of Planetary Geology and Geophysics Program, 1990 Jun. 1991 p 412-414 (For primary document see N92-10728 01-91)
Avail: NTIS HC/MF A25 CSCL 03B

N92-10889*# Jet Propulsion Lab., California Inst. of Tech., Pasadena.
THERMAL MODELING OF COMET KOPFF: IMPLICATIONS FOR THE CRAF MISSION
Paul Weissman and Celia Clause *In* NASA, Washington, Reports of Planetary Geology and Geophysics Program, 1990 Jun. 1991 p 415 (For primary document see N92-10728 01-91)
Avail: NTIS HC/MF A25 CSCL 03B

N92-10890*# Heidelberg Univ. (Germany, F.R.).
FORMATION OF THE PROTOSOLAR NEBULA Abstract Only
Werner M. Tscharnuter and Alan P. Boss (Carnegie Institution of Washington, DC.) *In* NASA, Washington, Reports of Planetary Geology and Geophysics Program, 1990 Jun. 1991 p 419 (For primary document see N92-10728 01-91)
Avail: NTIS HC/MF A25 CSCL 03B

N92-10891*# California Univ., Los Angeles. Dept. of Earth and Space Sciences.
FRAGMENTATION IN STELLAR COLLAPSE
E. M. Myhill and W. M. Kaula *In* NASA, Washington, Reports of Planetary Geology and Geophysics Program, 1990 Jun. 1991 p 420-421 (For primary document see N92-10728 01-91)
(Grant NAGw-2085)
Avail: NTIS HC/MF A25 CSCL 03B

N92-10892*# Planetary Science Inst., Tucson, AZ.
AERODYNAMIC AND GASDYNAMIC EFFECTS IN COSMOGONY
S. J. Weidenschilling *In* NASA, Washington, Reports of Planetary Geology and Geophysics Program, 1990 Jun. 1991 p 424-425 (For primary document see N92-10728 01-91)
(Contract NASw-4618)
Avail: NTIS HC/MF A25 CSCL 03B

N92-10893*# National Aeronautics and Space Administration. Ames Research Center, Moffett Field, CA.
PARTICLE-GAS DYNAMICS IN THE PROTOPLANETARY NEBULA
Jeffrey N. Cuzzi, Joelle M. Champney, and Anthony R. Dobrovolskis (California Univ., Santa Cruz.) *In* NASA, Washington, Reports of Planetary Geology and Geophysics Program, 1990 Jun. 1991 p 427-429 (For primary document see N92-10728 01-91)
Avail: NTIS HC/MF A25 CSCL 03B

N92-10894*# Jet Propulsion Lab., California Inst. of Tech., Pasadena.
BENDING WAVES AND ORBITAL INCLINATIONS
William R. Ward (San Juan Capistrano Research Inst., CA.) *In* NASA, Washington, Reports of Planetary Geology and Geophysics Program, 1990 Jun. 1991 p 430-432 (For primary document see N92-10728 01-91)
Avail: NTIS HC/MF A25 CSCL 03B

N92-10895*# Planetary Science Inst., Tucson, AZ.
ACCRETION AND EVOLUTION OF SOLAR SYSTEM BODIES
S. J. Weidenschilling and Donald R. Davis *In* NASA, Washington, Reports of Planetary Geology and Geophysics Program, 1990 Jun. 1991 p 433-435 (For primary document see N92-10728 01-91)
(Contract NASw-4495)
Avail: NTIS HC/MF A25 CSCL 03B

N92-10896*# State Univ. of New York, Stony Brook.
LONG-TERM EVOLUTION OF A PLANETESIMAL SWARM IN THE VICINITY OF A PROTOPLANET
David M. Kary and Jack J. Lissauer *In* NASA, Washington, Reports of Planetary Geology and Geophysics Program, 1990 Jun. 1991 p 436-437 (For primary document see N92-10728 01-91)
(Grant NAGw-1107)
Avail: NTIS HC/MF A25 CSCL 03B

N92-10898*# State Univ. of New York, Stony Brook.
COLLISION PROBABILITIES IN THE PRESENCE OF NEBULAR GAS DRAG
David M. Kary and Jack J. Lissauer *In* NASA, Washington, Reports of Planetary Geology and Geophysics Program, 1990 Jun. 1991 p 441-442 (For primary document see N92-10728 01-91)
(Grant NAGw-1107)
Avail: NTIS HC/MF A25 CSCL 03B

N92-10901*# State Univ. of New York, Stony Brook.
A GEOMETRICAL MODEL FOR SHEPHERDING Abstract Only
Jack J. Lissauer *In* NASA, Washington, Reports of Planetary Geology and Geophysics Program, 1990 Jun. 1991 p 446 (For primary document see N92-10728 01-91)
(Grant NAGw-1107)
Avail: NTIS HC/MF A25 CSCL 03B

N92-10902*# California Univ., Santa Cruz. Dept. of Physics.
DYNAMICS OF LOW VELOCITY COLLISIONS OF ICE PARTICLE, COATED WITH FROST
F. Bridges, D. Lin, L. Boone, and D. Darknell *In* NASA, Washington, Reports of Planetary Geology and Geophysics Program, 1990 Jun. 1991 p 447-448 (For primary document see N92-10728 01-91)
(Grant NAGw-590)
Avail: NTIS HC/MF A25 CSCL 03B

N92-10932*# California Inst. of Tech., Pasadena.
IMPACT AND COLLISIONAL PROCESSES IN THE SOLAR SYSTEM
Thomas J. Ahrens, C. Gazis, R. Pepin, R. Becker, R. Cronin, J. Tyburczy, T. Tingle (California Univ., Davis.), T. Duffy, and L. Rowan *In* NASA, Washington, Reports of Planetary Geology and Geophysics Program, 1990 Jun. 1991 p 525-528 (For primary document see N92-10728 01-91)
(Grant NAGw-1941)
Avail: NTIS HC/MF A25 CSCL 03B

N92-10939*# Arizona Univ., Tucson. Dept. of Planetary Sciences.
GENERATION AND BEHAVIOR OF SOLAR SYSTEM MAGNETIC FIELDS
Eugene H. Levy *In* NASA, Washington, Reports of Planetary Geology and Geophysics Program, 1990 Jun. 1991 p 542-544 (For primary document see N92-10728 01-91)
(Grant NAGw-2176)
Avail: NTIS HC/MF A25 CSCL 03B

N92-10941*# California Univ., San Diego, La Jolla. Space Inst.
ASTEROID SURFACE PROCESSES: EXPERIMENTAL STUDIES OF THE SOLAR WIND ON REFLECTANCE AND OPTICAL PROPERTIES OF ASTEROIDS
Lucy-Ann McFadden *In* NASA, Washington, Reports of Planetary Geology and Geophysics Program, 1990 Jun. 1991 p 547-548 (For primary document see N92-10728 01-91)
(Grant NAGw-2215)
Avail: NTIS HC/MF A25 CSCL 03B

N92-10958*# Cornell Univ., Ithaca, NY. Lab. for Planetary Studies.
STUDIES OF VOLATILES AND ORGANIC MATERIALS IN EARLY TERRESTRIAL AND PRESENT-DAY OUTER SOLAR SYSTEM ENVIRONMENTS
Carl Sagan, W. Reid Thompson, Christopher F. Chyba, and B. N. Khare *In* NASA, Washington, Reports of Planetary Geology and Geophysics Program, 1990 Jun. 1991 p 581-583 (For primary document see N92-10728 01-91)
Avail: NTIS HC/MF A25 CSCL 03B

91 LUNAR AND PLANETARY EXPLORATION

Includes planetology; and manned and unmanned flights.

For spacecraft design or space stations see *18 Spacecraft Design, Testing and Performance.*

N92-10728*# National Aeronautics and Space Administration, Washington, DC.
REPORTS OF PLANETARY GEOLOGY AND GEOPHYSICS PROGRAM, 1990
Jun. 1991 595 p
(NASA-TM-4300; NAS 1.15:4300) Avail: NTIS HC/MF A25 CSCL 03B

Abstracts of reports from NASA's Planetary Geology and Geophysics Program are presented. Research is documented in summary form of the work conducted. Each report reflects significant accomplishments within the area of the author's funded grant or contract. For individual titles, see N92-10729 through N92-10959.

N92-10729*# California Univ., Berkeley. Dept. of Geology and Geophysics.
PROCESSES OF DEEP TERRESTRIAL MANTLES AND CORES Abstract Only
Raymond Jeanloz *In* NASA, Washington, Reports of Planetary Geology and Geophysics Program, 1990 Jun. 1991 p 3-4 (For primary document see N92-10728 01-91)
Avail: NTIS HC/MF A25 CSCL 03B

Ultrahigh pressure experiments are currently focused on

revealing processes occurring deep inside planets. This is in addition to the traditional emphasis on the constitution of planetary interiors, such as the identification of the high pressure perovskite phase of (Mg,Fe)SiO3 as the predominant mineral inside the Earth, and probably Venus. For example, experiments show that the mechanism of geochemical differentiation, separation of partial melts, differs fundamentally in the lower mantles of Earth and Venus than at near surface conditions. In addition to structural transformations, changes in chemical bonding caused by pressure can also be significant for planetary interiors. Measurements of AC and DC electrical conductivity can be obtained at ultrahigh pressures and temperatures, to greater than 80 GPa and 3000 K simultaneously, using the laser heated diamond cell. Anhydrous lower mantle assemblages (perovskite + or - oxide phases) exhibit an electrical conductivity that depends strongly on Fe content. Contrary to traditional assumptions, temperature affects the conductivity of lower mantle assemblages relatively little. The Earth's deep focus seismicity can be explained by the recycling of water into the mantle. Author

N92-10730*# Cornell Univ., Ithaca, NY. Dept. of Geological Sciences.
IMPLICATIONS OF CONVECTION IN THE MOON AND THE TERRESTRIAL PLANETS Abstract Only
Donald L. Turcotte *In* NASA, Washington, Reports of Planetary Geology and Geophysics Program, 1990 Jun. 1991 p 5-6 (For primary document see N92-10728 01-91)
Avail: NTIS HC/MF A25 CSCL 03B

A comprehensive review is made of the thermal chemical evolution of the moon and the terrestrial planets. New results are presented which were obtained for Venus by the Magellan Mission the efforts were concentrated on this planet. Alternative models were examined for the thermal structure of the lithosphere of Venus. The statistical distribution was studied of the locations of the coronae on Venus. Models were examined for the patterns of faulting around the coronae on Venus. A series was considered of viscous models for the development and relaxation of elevation anomalies on Venus. And rates were studied of solidification of volcanic flows on Venus. Both radiative and convective heat transfer were considered. Author

N92-10731*# Massachusetts Inst. of Tech., Cambridge. Dept. of Earth, Atmospheric, and Planetary Sciences.
DYNAMIC MODELS FOR RIDGE BELT FORMATION ON VENUS Abstract Only
Mark Simons, Sean C. Solomon, and Bradford H. Hager *In* NASA, Washington, Reports of Planetary Geology and Geophysics Program, 1990 Jun. 1991 p 7-9 (For primary document see N92-10728 01-91)
Avail: NTIS HC/MF A25 CSCL 03B

The hypothesis is tested that the lithospheric shortening expressed by the ridge belts is the result of convective downwelling beneath the lowland planitia. Dynamical models are developed for the interaction of mantle convection with the crust and the models are compared to the characteristics of the ridge belts in Lavinia Planitia. The models support the hypothesis that convective stresses can produce the broad topographic depression of lowlands on Venus and can lead to the formation of ridge belts on either side of the topographic low. Author

N92-10732*# Massachusetts Inst. of Tech., Cambridge. Dept. of Earth, Atmospheric, and Planetary Sciences.
AN ASSESSMENT OF THE CRUSTAL REMELTING HYPOTHESIS FOR VOLCANISM IN THE FREYJA MONTES DEFORMATION ZONE Abstract Only
Noriyuki Namiki and Sean C. Solomon *In* NASA, Washington, Reports of Planetary Geology and Geophysics Program, 1990 Jun. 1991 p 10-12 (For primary document see N92-10728 01-91)
Avail: NTIS HC/MF A25 CSCL 03B

The linear mountain belts of Ishtar Terra on Venus are notable for their topographic relief and slope and for the intensity of surface deformation. The mountains surround the highland plain Lakshmi Planum, the site of two major paterae and numerous other volcanic features and deposits, and evidence is widespread for volcanism within the mountains and in terrain immediately outward of the mountain belt units. While two hypotheses for magmatism can be distinguished on the basis of the chemistry of the melts, chemical data are presently lacking for the Ishtar region. The competing hypotheses for magmatism in Western Ishtar Terra can also be tested with thermal models, given a kinematic or dynamic model for the evolution of the region. The crustal remelting hypothesis is assessed, using the kinematic scenario of Head for the evolution of Freyja Montes. In that scenario, Freyja Montes formed by a sequence of large scale underthrusts of the lithosphere of the North Polar Plains beneath Ishtar Terra, with successive blocks of underthrust crust sutured in imbricate fashion onto the thickened crust of Lakshmi Planum and the mantle portion of underthrusting lithosphere episodically detached. The numerical experiments thus show that volcanic activity associated with the formation of the Frejya Montes deformation zone can be explained by crustal melting, due either to direct contact of crustal material with the hot asthenosphere or to heat generation in a thickened crustal layer. Author

N92-10733*# Southern Methodist Univ., Dallas, TX. Dept. of Geological Sciences.
MARTIAN SEISMICITY
Roger J. Phillips and Robert E. Grimm *In* NASA, Washington, Reports of Planetary Geology and Geophysics Program, 1990 Jun. 1991 p 13-14 (For primary document see N92-10728 01-91)
Avail: NTIS HC/MF A25 CSCL 03B

The design and ultimate success of network seismology experiments on Mars depends on the present level of Martian seismicity. Volcanic and tectonic landforms observed from imaging experiments show that Mars must have been a seismically active planet in the past and there is no reason to discount the notion that Mars is seismically active today but at a lower level of activity. Models are explored for present day Mars seismicity. Depending on the sensitivity and geometry of a seismic network and the attenuation and scattering properties of the interior, it appears that a reasonable number of Martian seismic events would be detected over the period of a decade. The thermoelastic cooling mechanism as estimated is surely a lower bound, and a more refined estimate would take into account specifically the regional cooling of Tharsis and lead to a higher frequency of seismic events. Author

N92-10734*# Jet Propulsion Lab., California Inst. of Tech., Pasadena.
THERMAL MODELS FOR ICY SATELLITES Abstract Only
Robert H. Brown *In* NASA, Washington, Reports of Planetary Geology and Geophysics Program, 1990 Jun. 1991 p 15-16 (For primary document see N92-10728 01-91)
Avail: NTIS HC/MF A25 CSCL 03B

The solid state greenhouse models were constrained for water ice surfaces using thermal eclipse data. As a result, it was determined that at depths of 3 cm or more Europa can have about a 30 K temperature enhancement over the diurnal mean surface temperature of about 97 K at the equator. It was also determined that the unusual shape of Europa's thermal flux curves during eclipses can be explained by the solid state greenhouse effect. The solid state greenhouse models were applied to the problem of the origin and energy sources of Triton's geyser-like plumes. Two classes of models are examined which may explain the driving energy for Triton's plumes. Triton's internal heatflow is recognized as a major contributor to its global energy balance. Internal heat flow from radioactive decay in Triton's interior along with absorbed thermal energy from Neptune total 5 to 20 pct. of the insolation absorbed by Triton, thus comprising a significant fraction of Triton's surface energy balance. Author

N92-10735*# Lawrence Livermore National Lab., CA.
FLOW AND FRACTURE OF ICE AND ICE MIXTURES
W. B. Durham and S. H. Kirby (Geological Survey, Menlo Park, CA.) *In* NASA, Washington, Reports of Planetary Geology and

Geophysics Program, 1990 Jun. 1991 p 17-19 (For primary document see N92-10728 01-91)
Avail: NTIS HC/MF A25 CSCL 03B

Frozen volatiles make up an important volume fraction of the low density moons of the outer solar system. Understanding the tectonic history of the surfaces of these moons, as well as the evolution of their interiors, requires knowledge of the mechanical strength of these icy materials under the appropriate planetary conditions (temperature, hydrostatic pressure, strain rate). Ongoing lab research is being conducted to measure mechanical properties of several different ices under conditions that faithfully reproduce condition both at the moons' surfaces (generally low temperature, to about 100 K, and low pressures) and in the deep interiors (warmer temperatures, pressures to thousands of atmospheres). Recent progress is reported in two different phases of the work: rheology of ices in the NH3-H2O system at temperatures and strain rates lower than ever before explored, with application to the ammonia-rich moons of Saturn and Uranus; and the water ice I yields II phase transformation, which not only applies directly to process deep in the interiors of Ganymede and Callisto, but holds implications for deep terrestrial earthquakes as well. Author

N92-10736*# Jet Propulsion Lab., California Inst. of Tech., Pasadena.
THE ROLE OF NONUNIFORM INTERNAL HEATING IN TRITON'S ENERGY BUDGET
R. L. Kirk (Geological Survey, Flagstaff, AZ.) and R. H. Brown *In* NASA, Washington, Reports of Planetary Geology and Geophysics Program, 1990 Jun. 1991 p 22-24 (For primary document see N92-10728 01-91)
Avail: NTIS HC/MF A25 CSCL 03B

Triton's large heliocentric distance and high albedo, combined with its unusually large silicate mass fraction, make internal heating more important in its energy budget than in that of any other icy satellite. Brown et al. have recently estimated that the average radiogenic heat flux (which is probably between 3.3 and 6.6 mW/sq m depending on core size and composition) may equal 5 to 20 pct. of the average absorbed insolation. On a global scale, this additional energy input appreciably increases the thermal emissivity required to be consistent with the observed surface temperature. Brown et al. also speculated that spatial variations of the internal flux may change the local sublimation deposition balance enough to lead to observable modifications of the distribution of volatiles on Triton's surface. An attempt is made to estimate the magnitude of internal heat flux variations due to the insulating effect of the polar caps, to mantle convection, and to cryovolcanism; the importance is evaluated of these variations in modifying the volatile distribution. Author

N92-10737*# Arizona Univ., Tucson. Lunar and Planetary Lab.
PHYSICAL PROPERTIES OF CRYOVOLCANIC BRINES: APPLICATIONS TO THE EVOLUTION OF GANYMEDE
Jeffrey S. Kargel *In* NASA, Washington, Reports of Planetary Geology and Geophysics Program, 1990 Jun. 1991 p 25-26 (For primary document see N92-10728 01-91)
Avail: NTIS HC/MF A25 CSCL 03B

Carbonaceous chondrites contain abundant veins of water soluble salts, including carbonates and hydrated sulfates of Mg, Ca, Na, Ni, and Fe. These constitute over 1/4 of the mass of the meteorite Orgueil. Magnesium sulfate is the most abundant salt, constituting nearly half the mass of all salt components combined (anhydrous), and 73 pct. of the highly water soluble salts. The assumption that icy satellites and asteroids contain rock compositionally similar to carbonaceous chondrites suggests that salts may be important in the cryoigneous evolution of icy satellites and asteroids. Ordinary chondrites, an alternative rock component of icy satellites, lack abundant salts, although their anhydrous silicate assemblages are unstable with respect to water and would react to produce salts upon initial melting of ice. Some basic physiochemical properties are reviewed of likely cryovolcanic brines and how the existence of soluble salts in Ganymede might affect its structure and evolution is considered. Observations indicate late stage (post heavy bombardment and post tectonic) volcanism on Ganymede. The highly fluid character of Ganymedian volcanism is consistent with extrusions of either water or salt water brines. Author

N92-10738*# Lafayette Coll., Easton, PA. Dept. of Physics.
THE MAGNESIUM SULFATE-WATER SYSTEM AT PRESSURES TO 4 KILOBARS c90
D. L. Hogenboom, Jeffrey S. Kargel, J. P. Ganasan, and J. S. Lewis (Arizona Univ., Tucson.) *In* NASA, Washington, Reports of Planetary Geology and Geophysics Program, 1990 Jun. 1991 p 27-28 (For primary document see N92-10728 01-91)
Avail: NTIS HC/MF A25 CSCL 03B

Hydrated magnesium sulfate constitutes up to 1/6 of the mass of carbonaceous chondrites, and probably is important in many icy asteroids and satellites. It occurs naturally in meteorites mostly as epsomite. MgSO4, considered anhydrously, comprises nearly 3/4 of the highly soluble fraction of C1 chondrites. Thus, MgSO4 is probably an important solute in cryovolcanic brines erupted on certain icy objects in the outer solar system. While the physiochemical properties of the water-magnesium sulfate system are well known at low pressures, planetological applications of these data are hindered by a dearth of useful published data at elevated pressures. Accordingly, solid-liquid phase equilibria was recently explored in this chemical system at pressures extending to about 4 kilobars. The water magnesium sulfate system in the region of the eutectic exhibits qualitatively constant behavior between pressures of 1 atm and 2 kbar. The eutectic melting curve closely follows that for water ice, with a freezing point depression of about 4 K at 1 atm decreasing to around 3.3 K at 2 kbars. The eutectic shifts from 17 pct. MgSO4 at 1 atm to about 15.3 pct at 2 kbars. Above 2 kbars, the eutectic melting curve again tends to follow ice. Author

N92-10739*# Lawrence Livermore National Lab., CA.
PROPERTIES OF PLANETARY FLUIDS AT HIGH PRESSURES AND TEMPERATURES
W. J. Nellis, N. C. Holmes, and A. C. Mitchell *In* NASA, Washington, Reports of Planetary Geology and Geophysics Program, 1990 Jun. 1991 p 29-31 (For primary document see N92-10728 01-91)
(Contract NASA Order W-16180; W-7405-eng-48)
Avail: NTIS HC/MF A25 CSCL 03B

Observational data obtained by the Voyager space probes to the giant planets Jupiter, Saturn, Uranus, and Neptune have provided valuable information, which is used to refine the picture of the nature of the interiors of these planets. Major results from the Voyager missions include observations of substantial magnetic fields and improved models of internal density distributions. The goal is to obtain equations of state and electrical conductivity data for planetary gases (H2 and He) and the ices (H2O, CH4, and NH3, and their mixtures), which are considered to be the major constituents of the giant planets. These data are needed to test theoretical data bases used to construct models of the chemical composition of planetary interiors, models which are consistent with observables such as mass, diameter, gravitational moments, rotation rate, and magnetic field. The 100 GPa (1 Mbar) pressures and several 1000 K temperatures in the giant planets can be achieved in the lab by the shock compression of liquid specimens. Results are briefly examined. Author

N92-10740*# Arizona State Univ., Tempe. Dept. of Geology.
FLUID DYNAMICS OF MULTIPHASE FLOW IN VOLCANIC ENVIRONMENTS ON THE EARTH, IO, AND OTHER PLANETS Abstract Only
Susan Werner Kieffer *In* NASA, Washington, Reports of Planetary Geology and Geophysics Program, 1990 Jun. 1991 p 32 (For primary document see N92-10728 01-91)
Avail: NTIS HC/MF A25 CSCL 03B

Data was compiled on H2O, CO2, S, and SO2 and it was analyzed by various techniques to prepare phase diagrams relevant to conditions on the Earth, Io, Mars, and other planets. The use of Cray models for volcanic eruptions was examined. Attempts are being made to develop equations of state of the compounds

listed above to be compatible with the Cray code so that they can be called as subroutines for the volcanic models. This is a major project, as the current code uses only the equation of state for a perfect gas, and requires that the atmosphere be the same composition as the volcanic gas. The analysis of the thermodynamic data is time consuming, and was complicated by changes from a VAX/VMS system to Macintosh's, Crays using CTSS, Crays using Unicos, and Sun workstations. Author

N92-10741*# Cornell Univ., Ithaca, NY.
TECTONIC EVOLUTION OF LAVINIA PLANITIA, VENUS
Steven W. Squyres, Sharon L. Frank, George E. McGill, and Sean C. Solomon (Massachusetts Inst. of Tech., Cambridge.) *In* NASA, Washington, Reports of Planetary Geology and Geophysics Program, 1990 Jun. 1991 p 35-37 (For primary document see N92-10728 01-91)
Avail: NTIS HC/MF A25 CSCL 03B

High resolution radar images from the Magellan spacecraft have revealed the first details of the morphology of the Lavinia Planitia region of Venus. Lavinia is a broad lowland over 2000 km across, centered at about 45 deg S latitude, 345 deg E longitude. Herein, the tectonic evolution of Lavinia is discussed, and its possible relationship to processes operating in the planet's interior. The discussion is restricted to the region from 37.3 to 52.6 deg S latitude and from about 340 to 0 deg E longitude. One of the most interesting characteristics of Lavinia is that the entire region possesses a regional tectonic framework of striking regularity. Lavinia is also transected by a complex pattern of belts of intense tectonic deformation known as ridge belts. Despite the gross topographic similarity of all of the ridge belts in Lavinia, they exhibit two rather distinct styles of near surface deformation. One is composed of sets of broad, arch-like ridges rising above the surrounding plains. In the other type, obvious fold-like ridges are rare to absent in the radar images. Both type show evidence for small amounts of shear distributed across the belts. Author

N92-10742*# Cornell Univ., Ithaca, NY.
MORPHOLOGY AND EVOLUTION OF CORONAE AND OVOIDS ON VENUS
Steven W. Squyres, Duane L. Bindschadler, Daniel M. Janes, Gerald Schubert, Virgil L. Sharpton, and Ellen R. Stofan (Jet Propulsion Lab., California Inst. of Tech., Pasadena.) *In* NASA, Washington, Reports of Planetary Geology and Geophysics Program, 1990 Jun. 1991 p 37-38 (For primary document see N92-10728 01-91)
Avail: NTIS HC/MF A25 CSCL 03B

Coronae and ovoids on Venus were first identified in Venera 15/16 data. They are distinctive and apparently unique to the planet, and may be important indicators of processes operating in the Venusian mantle. Magellan images have provided the first high resolution views of coronae and ovoid morphology. Herein, the general geologic character is described of coronae and ovoids, and some inferences are drawn about their geologic evolution. Coronae are circular to elongate features surrounded by an annulus of deformational features, with a relatively raised or indistinct topographic signature and, commonly, a peripheral trough or moat. Ovoids are circular to elongate features other than coronae with either positive or negative topographic signatures, associated with tectonic deformation and volcanism. The relationship of these two geologic features to each other and to Venusian geology is briefly discussed. Author

N92-10743*# Southern Methodist Univ., Dallas, TX. Dept. of Geological Sciences.
HOT-SPOT TECTONICS OF EISTLA REGIO, VENUS: RESULTS FROM MAGELLAN IMAGES AND PIONEER VENUS GRAVITY
Robert E. Grimm and Roger J. Phillips *In* NASA, Washington, Reports of Planetary Geology and Geophysics Program, 1990 Jun. 1991 p 39-40 (For primary document see N92-10728 01-91)
Avail: NTIS HC/MF A25 CSCL 03B

Eistla Regio (ER) is a broad, low, discontinuous topographic rise striking roughly EW at low northern latitudes of Venus. Some 2000 x 7000 km in dimensions, it is the third largest rise in planform on Venus after Aphrodite Terra and Beta Phoebe Regiones. These rises are the key physiographic elements in a hot spot model of global tectonics including transient plume behavior. Since ER is the first such rise viewed by Magellan and the latitude is very favorable for Pioneer Venus gravity studies, some of the predictions of a time dependent hot spot model are tested. Western ER is defined as the rise including Gula and Sif Mons and central ER as that including Sappho Patera. Superior conjunction prevented Magellan from returning data on eastern ER (Pavlova) during the first mapping cycle. It is concluded that the western and central portions of ER, while part of the same broad topographic rise and tectonic framework, have distinctly different surface ages and gravity signatures. The western rise, including Gula and Sif Mons, is the expression of deep seated uplift with volcanism limited to the individual large shields. The eastern portion has been widely resurfaced more recently by thermal anomalies in the mantle. Author

N92-10744*# Massachusetts Inst. of Tech., Cambridge. Dept. of Earth, Atmospheric, and Planetary Sciences.
GRAVITATIONAL SPREADING OF DANU, FREYJA AND MAXWELL MONTES, VENUS
Suzanne E. Smrekar and Sean C. Solomon *In* NASA, Washington, Reports of Planetary Geology and Geophysics Program, 1990 Jun. 1991 p 41-43 (For primary document see N92-10728 01-91)
Avail: NTIS HC/MF A25 CSCL 03B

The potential energy of elevated terrain tends to drive the collapse of the topography. This process of gravitational spreading is likely to be more important on Venus than on Earth because the higher surface temperature weakens the crust. The highest topography on Venus is Ishtar Terra. The high plateau of Lakshmi Planum has an average elevation of 3 km above mean planetary radius, and is surrounded by mountain belts. Freyja, Danu, and Maxwell Montes rise, on average, an additional 3, 0.5, and 5 km above the plateau, respectively. Recent high resolution Magellan radar images of this area, east of approx. 330 deg E, reveal widespread evidence for gravity spreading. Some observational evidence is described for gravity spreading and the implications are discussed in terms of simple mechanical models. Several simple models predict that gravity spreading should be an important process on Venus. One difficulty in using remote observations to infer interior properties is that the observed features may not have formed in response to stresses which are still active. Several causes of surface topography are briefly examined. Author

N92-10745*# Southern Methodist Univ., Dallas, TX. Dept. of Geological Sciences.
INTERPRETATION OF THE NORTHERN BOUNDARY OF ISHTAR TERRA FROM MAGELLAN IMAGES AND ALTIMETRY
S. Mueller, Robert E. Grimm, and Roger J. Phillips *In* NASA, Washington, Reports of Planetary Geology and Geophysics Program, 1990 Jun. 1991 p 44-45 (For primary document see N92-10728 01-91)
Avail: NTIS HC/MF A25 CSCL 03B

Part of the controversy on the origin of western Ishtar Terra (IT) concerns the nature of Uorsar Rupes (UR), the northern boundary of IT. In the hypothesis of lithospheric convergence and underthrusting, UR is held to be the main boundary thrust fault at the toe of an accretionary wedge. A topographic rise parallel to the scarp was interpreted as a flexural bulge similar to those of terrestrial subduction zones, and quantitative models of this feature seemed broadly consistent with the expected lithospheric structure of Venus. In the alternative mantle upwelling hypothesis for western IT, the outer margins of the highland are thought to be collapsing, and UR has been interpreted as a normal fault. Herein, Magellan images and altimetry are interpreted for this region and the hypothesis that a flexural signature can be distinguished is reassessed. The Magellan images of IT show evidence of crustal shortening adjacent to UR, but extension and burial dominate northwards. Altimetric profiles display the same long wavelength trends visible in Venera data, but no clear evidence of the lithospheric flexure. A model of regional extension and burial is herein favored, but regional compression cannot be ruled out. Author

N92-10746*# Jet Propulsion Lab., California Inst. of Tech., Pasadena.
HORIZONTAL STRESS IN PLANETARY LITHOSPHERES FROM VERTICAL PROCESSES **c46**
W. B. Banerdt *In* NASA, Washington, Reports of Planetary Geology and Geophysics Program, 1990 Jun. 1991 p 46-48 (For primary document see N92-10728 01-91)
Avail: NTIS HC/MF A25 CSCL 03B

Understanding the stress states in a lithosphere is of fundamental importance for planetary geophysics. It is closely linked to the processes which form and modify tectonic features on the surface and reflects the behavior of the planet's interior, providing a constraint for the difficult problem of determining interior structure and processes. The tectonics on many extraterrestrial bodies (Moon, Mars, and most of the outer planet satellites) appears to be mostly vertical, and the horizontal stresses induced by vertical motions and loads are expected to dominate the deformation of their lithospheres. Herein, only changes are examined in the state of stress induced by processes such as sedimentary and volcanic deposition, erosional denudation, and changes in the thermal gradient that induce uplift or subsidence. This analysis is important both for evaluating stresses for specific regions in which the vertical stress history can be estimated, as well as for applying the proper loading conditions to global stress models. All references to lithosphere herein should be understood to refer to the elastic lithosphere, that layer which deforms elastically or brittlely when subjected to geologically scaled stresses. Author

N92-10747*# Jet Propulsion Lab., California Inst. of Tech., Pasadena.
MODELLED AND MEASURED STRAIN IN MASCON BASINS ON THE MOON
M. P. Golombek and B. J. Franklin *In* NASA, Washington, Reports of Planetary Geology and Geophysics Program, 1990 Jun. 1991 p 51-53 (For primary document see N92-10728 01-91)
Avail: NTIS HC/MF A25 CSCL 03B

The close association of wrinkle ridges and grabens with mascon basins on the Moon has suggested that the responsible compression and extension resulted from basin subsidence and peripheral flexing of the lithosphere. The distribution of grabens and wrinkle ridges associated with mascon basins has been further used along with elastic plate bending models to constrain the thickness of the lithosphere at the time of their formation. Kinematic models for basin subsidence have also been developed and compared with strains inferred from grabens and wrinkle ridges. Note that kinematic models may be preferable to dynamic models because the strain associated with tectonic features can be compared directly with model predictions and because fewer assumptions are required for their calculations, such as perfect elasticity and specific values of the elastic moduli. Also, if the results from kinematic models compare favorably with the strain estimated across the tectonic features on the Moon, then a global strain field may not be necessary. Herein, the strain inferred for wrinkle ridges and grabens was compared to that calculated from a simple kinematic subsidence model for mascon basins on the Moon. Author

N92-10748*# Jet Propulsion Lab., California Inst. of Tech., Pasadena.
STRAIN ACCOMMODATION BENEATH STRUCTURES ON MARS
M. P. Golombek, Kenneth L. Tanaka (Geological Survey, Flagstaff, AZ.), and W. B. Banerdt *In* NASA, Washington, Reports of Planetary Geology and Geophysics Program, 1990 Jun. 1991 p 54-56 (For primary document see N92-10728 01-91)
Avail: NTIS HC/MF A25 CSCL 03B

A recent review of tectonic features on Mars shows that most of their subsurface structures can be confidently extended only a few kilometers deep (exceptions are rifts, in which bounding normal faults penetrate the entire brittle lithosphere, with ductile flow at deeper levels). Nevertheless, a variety of estimates of elastic lithosphere thickness and application of accepted failure criteria under likely conditions on Mars suggest a brittle lithosphere that is many tens of kilometers thick. This raises the question of how the strain (extension or shortening) accommodated by grabens and wrinkle ridges within the upper few kilometers is being accommodated at deeper levels in the lithosphere. Herein, the nonrift tectonic features present on Mars are briefly reviewed, along with their likely subsurface structures, and some inferences and implications are presented for behavior of the deeper lithosphere. Author

N92-10749*# Arizona State Univ., Tempe. Dept. of Geology.
THE FORMATION OF ANTIPODAL-IMPACT TERRAINS ON MARS
D. A. Williams and Ronald Greeley *In* NASA, Washington, Reports of Planetary Geology and Geophysics Program, 1990 Jun. 1991 p 59-60 (For primary document see N92-10728 01-91)
Avail: NTIS HC/MF A25 CSCL 03B

The regions antipodal to Mars' three largest impact basins, Hellas, Isidis, and Argyre, were assessed for evidence of impact induced seismically disrupted terrains. Photogeology and preliminary computer modeling using the Simplified Arbitrary Lagrangian-Eulerian computer program suggest such terrain could have been formed by the Hellas and Isidis impacts. Previously, the only assessment of potential surface disruptions on Mars antipodal to large impacts was by Peterson (1978). Herein, the results give credence to Peterson's assertions. For Hellas, the computer model clearly suggests that antipodal pressures were probably strong enough to have fractured the crust and disrupted the surface, and may account for aspects of volcanism at Alba Patera. It is suggested that the Hellas impact produced sufficient focused energy at its antipode to produce deep fracture in the Martian crust centered below the current caldera for Alba Petera. With the generation and evolution of magma in the Tharsis area, the fracture system provided a ready conduit for early stage eruptions of Martians lavas derived from deep in the crust and/or upper mantle, perhaps of komatiitic composition. Author

N92-10750*# Arizona State Univ., Tempe. Dept. of Geology.
GLOBAL RELATIONSHIPS BETWEEN VOLCANIC VENTS AND FRACTURES RADIAL TO LARGE IMPACT BASINS ON MARS
Byron D. Schneid and Ronald Greeley *In* NASA, Washington, Reports of Planetary Geology and Geophysics Program, 1990 Jun. 1991 p 61-62 (For primary document see N92-10728 01-91)
Avail: NTIS HC/MF A25 CSCL 03B

The relation of volcanic vents on Mars to impact basins has been previously studied. It has been asserted that the concentric fractures around impact basins extend into the crust and might localize some features, including volcanoes. Herein, the possibility is assessed of radial fractures inferred to be associated with impact basins as an additional control on the location of volcanoes on Mars. Geologic mapping at 1:2 million scale enabled 250 central vents and fissure vents to be identified. Pattern of vent distribution superimposed on a globe show that most are located on three distinct circles. In addition, there are two more possible great circles which may be superimposed onto the Martian globe. These five Martian circles are briefly examined for their geological relationship to volcanoes. Author

N92-10751*# Geological Survey, Flagstaff, AZ.
TECTONIC SETTING OF MARTIAN VOLCANOES AND DEEP-SEATED INTRUSIVES
David H. Scott and James M. Dohm *In* NASA, Washington, Reports of Planetary Geology and Geophysics Program, 1990 Jun. 1991 p 63-64 (For primary document see N92-10728 01-91)
Avail: NTIS HC/MF A25 CSCL 03B

More than 50 volcanoes have been mapped on Mars, and recent geologic studies indicate structural evidence of deep seated intrusive bodies. Most volcanoes in the Tharsis region are volcanotectonic features; they have been associated with large scale tectonic and volcanic processes. They occur along complex systems of faults and grabens having a dominant northwest to southwest trend closely coincident with a great circle, which extends along 90 deg of arc from Tempe Patera to probable volcanic mountains near lat. 40 deg S, long. 150 deg. Deep seated

intrusive bodies are also concentrated in the Tharsis region and are recognized mostly where faults have been deflected around their cores. The Elysium Mons-Amphitrites Patera volcanic alignment is subparallel to that of Tharsis but is longer, extending through about 120 deg of arc; it transects the dichotomy boundary and is radial to the Hellas basin. Volcanoes in the Tharsis region have the widest age range of all volcanoes on Mars, as determined by the size-frequency distribution of their craters having diameters of 2, 5, and 16 km. Author

N92-10752*# Arizona State Univ., Tempe. Dept. of Geology.
TIMING AND FORMATION OF WRINKLE RIDGES IN THE TYRRHENA PATERA REGION OF MARS
Tracy K. Porter, David A. Crown, and Ronald Greeley *In* NASA, Washington, Reports of Planetary Geology and Geophysics Program, 1990 Jun. 1991 p 65-66 (For primary document see N92-10728 01-91)
Avail: NTIS HC/MF A25 CSCL 03B

Wrinkle ridges are distinctive linear to curvilinear arches topped by crenulated ridges and have been identified on the Moon, Mercury, and Mars. The presence of wrinkle ridges on other planetary surfaces has been used as a criterion for identifying volcanic plains. Recently, due to the presence of lava flow lobes and leveed channels, Greeley and Crown identified an area within Hesperia Planum as a flank flow unit associated with Tyrrhena Patera. Hesperia Planum surrounds Tyrrhena Patera and embays the eroded shield of the volcano to the north and south. The Tyrrhena Patera flank flow unit extends approx. 1000 km from the summit caldera to the southwest. More than 55 wrinkle ridges have been identified on this flank flow unit. The relationships between the lava flows and wrinkle ridges within the flank flow unit allow relative ages to be determined. Wrinkle ridges are classified as post flow if flow lobes appear to arch over the rises undeformed, with no evidence of flow ponding on the upstream side of the ridge, or of flows breaching the rises. Wrinkle ridges within Hesperia Planum and Tyrrhena Patera flank flow unit that trend NW-SE appear younger than the flank flow unit. Author

N92-10753*# Jet Propulsion Lab., California Inst. of Tech., Pasadena.
COMPRESSIVE STRAIN IN LUNAE PLANUM-SHORTENING ACROSS WRINKLE RIDGES
J. B. Plescia *In* NASA, Washington, Reports of Planetary Geology and Geophysics Program, 1990 Jun. 1991 p 67-69 (For primary document see N92-10728 01-91)
Avail: NTIS HC/MF A25 CSCL 03B

Wrinkle ridges have long been considered to be structural or structurally controlled features. Most, but not all, recent studies have converged on a model in which wrinkle ridges are structural features formed under compressive stress; the deformation being accommodated by faulting and folding. Given that wrinkle ridges are compressive tectonic features, an analysis of the associated shortening and strain provides important quantitative information about local and regional deformation. Lunae Planum is dominated by north-south trending ridges extending from Kasei Valles in the north to Valles Marineris in the south. To quantify the morphometric character, a photoclinometric study was undertaken for ridges on Lunae Planum using the Davis and Soderblom. More than 25 ridges were examined between long. 57 and 80 deg, lat. 5 to 25 deg N. For each ridge, several profiles were obtained along its length. Ridge width, total relief, and elevation offset were measured for each ridge. Analyses are given. Author

N92-10754*# Geological Survey, Flagstaff, AZ.
LATE NOACHIAN DEVELOPMENT OF THE COPRATES RISE, MARS
Kenneth L. Tanaka and Richard A. Schultz (Nevada Univ., Reno.) *In* NASA, Washington, Reports of Planetary Geology and Geophysics Program, 1990 Jun. 1991 p 70-72 (For primary document see N92-10728 01-91)
Avail: NTIS HC/MF A25 CSCL 03B

The Coprates rise forms a 900 km long, north to northeast trending ridge south of Coprates Chasma between long. 56 and 60 degs. Radar and stereo photogrammetric data indicate that the rise is 2 to 4 km above a neighboring trough to the east. The break in slope between the rise and this trough is well defined topographically and in Viking images. In turn, the trough is bordered to the to the east at long. 52 deg by a much gentler rise. West of the Coprates rise, the terrain dips about 0.2 deg to roughly long. 75 deg. The rise and flanking highs were previously interpreted to be tilted fault blocks formed by either Tharsis tectonism or an ancient impact. Results are now reported of a preliminary geologic study that documents Late Noachian growth of the Coprates rise as a asymmetric fold. More comprehensive work will lead to a mechanical analysis of the kinematic development of the rise. It is concluded that the Coprate rise formed during the Late Noachian by 2 to 4 km of asymmetric uplift (steeper on its east flank). The timing is inconsistent with an origin by an early impact, but it coincides in time with early Tharsis centered radial faulting at Syria Planum. Author

N92-10755*# Jet Propulsion Lab., California Inst. of Tech., Pasadena.
INTERACTIONS OF TECTONIC, IGNEOUS, AND HYDRAULIC PROCESSES IN THE NORTH THARSIS REGION OF MARS
P. A. Davis, Kenneth L. Tanaka (Geological Survey, Flagstaff, AZ.), M. P. Golombek, and J. B. Plescia *In* NASA, Washington, Reports of Planetary Geology and Geophysics Program, 1990 Jun. 1991 p 73-74 (For primary document see N92-10728 01-91)
Avail: NTIS HC/MF A25 CSCL 03B

Recent work on the north Tharsis of Mars has revealed a complex geologic history involving volcanism, tectonism, flooding, and mass wasting. Our detailed photogeologic analysis of this region found many previously unreported volcanic vents, volcaniclastic flows, irregular cracks, and minor pit chains; additional evidence that volcanic tectonic processes dominated this region throughout Martian geologic time; and the local involvement of these processes with surface and near surface water. Also, photoclinometric profiles were obtained within the region of troughs, simple grabens, and pit chains, as well as average spacings of pits along pit chains. These data were used together with techniques to estimate depths of crustal mechanical discontinuities that may have controlled the development of these features. In turn, such discontinuities may be controlled by stratigraphy, presence of water or ice, or chemical cementation. Author

N92-10756*# Geological Survey, Flagstaff, AZ.
VALLES MARINERIS TECTONISM: QUESTIONS AND SUGGESTIONS
Baerbel K. Lucchitta, Mary G. Chapman, and Nancy K. Isbell *In* NASA, Washington, Reports of Planetary Geology and Geophysics Program, 1990 Jun. 1991 p 75-76 (For primary document see N92-10728 01-91)
Avail: NTIS HC/MF A25 CSCL 03B

Much has been learned about the Valles Marineris, and stratigraphic relations inside the troughs have been reasonably well established. However, many questions remain, especially questions pertaining to tectonism and origin. The following issues are briefly considered: the age of the troughs; the evidence for tectonic origin; the relation of Valles Marineris to the Tharsis rise; and the additional factors which may have influenced the origin of the Valles Marineris. Author

N92-10757*# Jet Propulsion Lab., California Inst. of Tech., Pasadena.
EXTENSION AND STRAIN IN NORTHERN THARSIS
J. B. Plescia *In* NASA, Washington, Reports of Planetary Geology and Geophysics Program, 1990 Jun. 1991 p 77-79 (For primary document see N92-10728 01-91)
Avail: NTIS HC/MF A25 CSCL 03B

The northern areas of Tharsis, south of Alba Patera, are remarkable in that they are dominated by extensive, generally north trending graben. Some graben are small isolated features whereas others are complex overlapping features in which individual fault pairs are impossible to separate. This pattern indicates an east-west extensional stress regime, consistent with stress models

for Tharsis. To estimate the regional east-west extension and strain, graben along a profile at 35 N latitude, between longitudes 135 and 93 degs were studied. This profile was chosen because the graben have a northerly trend, the structures are relatively simple, the profile is anchored to ancient Noachian age crust, and high resolution images are available. The western end of the profile begins at Acheron Fossae and ends in the east at the southwestern part of Tempe Fossae. Plains units cut by the graben include Hesperian and Amazonian age members of the Alba Patera and Ceraunius Fossae Formations. Author

N92-10758*# Geological Survey, Flagstaff, AZ.
VALLES MARINERIS, MARS: ARE PIT CHAINS FORMED BY EROSION AND TROUGHS BY TECTONISM?
Baerbel K. Lucchitta, R. A. Balser, and L. M. Bertolini *In* NASA, Washington, Reports of Planetary Geology and Geophysics Program, 1990 Jun. 1991 p 80-81 (For primary document see N92-10728 01-91)
Avail: NTIS HC/MF A25 CSCL 03B

The origin of the Valles Marineris remains controversial. Erosional, tectonic, and hybrid processes have been proposed. To clarify these contradictions, the widths and depths of pit chains and troughs were compared and it was found that the features do not form a continuum. Rather, results are consistent with the hypothesis that pit chains formed by surficial collapse and troughs by deeper seated and coherent failure. All pit chains and linear depressions in the Valles Marineris region were classified by inspection into six morphologic categories: pit chains (linear arrays of small pits); floored chains (arrays of pit chains having flat or hummocky floors); scalloped troughs (wider linear depressions with scalloped wall segments); narrow troughs (depressions of intermediate width with straight wall segments); wide troughs (broad, linear depressions); and chaotic troughs (more irregular depressions displaying some channel morphologies). Topographic profiles were drawn across the classified depressions and the erosional width was determined between plateau margins along with the depth from the surrounding plateau level to the deepest part. Author

N92-10759*# Jet Propulsion Lab., California Inst. of Tech., Pasadena.
MARTIAN SEISMICITY THROUGH TIME FROM SURFACE FAULTING
M. P. Golombek, Kenneth L. Tanaka (Geological Survey, Flagstaff, AZ.), W. B. Banerdt, and D. Tralli *In* NASA, Washington, Reports of Planetary Geology and Geophysics Program, 1990 Jun. 1991 p 82-84 (For primary document see N92-10728 01-91)
Avail: NTIS HC/MF A25 CSCL 03B

An objective of future Mars missions involves emplacing a seismic network on Mars to determine the internal structure of the planet. An argument based on the relative geologic histories of the terrestrial planets suggests that Mars should be seismically more active than the Moon, but less active than the Earth. The seismicity is estimated which is expected on Mars through time from slip on faults visible on the planets surface. These estimates of martian seismicity must be considered a lower limit as only structures produced by shear faulting visible at the surface today are included (i.e., no provision is made for buried structures or non-shear structures); in addition, the estimate does not include seismic events that do not produce surface displacement (e.g., activity associated with hidden faults, deep lithospheric processes or volcanism) or events produced by tidal triggering or meteorite impacts. Calibration of these estimates suggests that Mars may be many times more seismically active than the Moon. Author

N92-10760*# National Aeronautics and Space Administration. Goddard Space Flight Center, Greenbelt, MD.
A 40TH DEG AND ORDER GRAVITATIONAL FIELD MODEL FOR MARS
M. T. Zuber, D. E. Smith, F. J. Lerch, R. S. Nerem, G. B. Patel, and S. K. Fricke (RMS Technologies, Inc., Landover, MD.) *In* NASA, Washington, Reports of Planetary Geology and Geophysics Program, 1990 Jun. 1991 p 85-86 (For primary document see N92-10728 01-91)
Avail: NTIS HC/MF A25 CSCL 03B

Understanding the origin and evolution of major photographic features on Mars, such as the hemispheric dichotomy and Tharsis rise, will require improved resolution of that planet's gravitational and topographic fields. The highest resolution gravity model for Mars published to date was derived from Doppler tracking data from the Mariner 9 and Viking 1 and 2 spacecraft, and is of 18th degree and order. That field has a maximum spatial resolution of approx. 600 km, which is comparable to that of the best topographic model. The resolution of previous gravity models was limited not by data density, but rather by the computational resources available at the time. Because this restriction is no longer a limitation, the Viking and Mariner data sets were reanalyzed and a gravitational field was derived complete to the 40th degree and order with a corresponding maximum spatial resolution of 300 km where the data permit. Author

N92-10761*# Geological Survey, Flagstaff, AZ.
SO2-RICH EQUATORIAL BASINS AND EPEIROGENY OF IO
Alfred S. McEwen *In* NASA, Washington, Reports of Planetary Geology and Geophysics Program, 1990 Jun. 1991 p 87-89 (For primary document see N92-10728 01-91)
Avail: NTIS HC/MF A25 CSCL 03B

Comparison of Io's large scale topography with an SO2 abundance map shows that SO2 is concentrated in equatorial topographic basins. In these basins, about 30 pct. of the surface is covered by SO2 at all elevations above the mean triaxial figure, and SO2 coverage increases with decreasing elevation to as much as 56 pct. at elevations below -1.5 km. The correlation is not good from long 240 to 360 degs where bright areas are covered by red, Pele type plume fallout, and in the polar regions where the topography is poorly known. The histogram of SO2 abundance binned by elevation appears bimodal, with a secondary concentration of SO2 at high elevations, but it is not certain that this is significant. Additional observations suggest that the basins have relatively little higher frequency topographic relief. The distribution of active plumes and hotspots show no obvious correlation with the topography. However, the Pele type plume all erupted from regions higher than the mean figure, and five of the eight Prometheus type plumes are more energetic and are associated with high temperature hotspots, whereas Prometheus type plumes are long lived and require large volatile reservoirs. Author

N92-10762*# Massachusetts Univ., Amherst.
STRUCTURAL GEOLOGY AND GEOLOGICAL HISTORY OF THE PERRINE AND NUN SULCI QUADRANGLES (Jg-2 AND Jg-5), GANYMEDE
George E. McGill and Steven W. Squyres (Cornell Univ., Ithaca, NY.) *In* NASA, Washington, Reports of Planetary Geology and Geophysics Program, 1990 Jun. 1991 p 90-92 (For primary document see N92-10728 01-91)
Avail: NTIS HC/MF A25 CSCL 03B

Grooves are the dominant structural features on Ganymede. While single grooves are found in many areas, it is somewhat more common to find them grouped together in groove sets (groupings of grooves with common structural trends). It is generally believed that the grooves are extensional features. Their underlying geologic nature cannot be determined from Voyager images, however. It appears likely that they are grabens, but the images are insufficient to rule out the possibility that they are modified extension fractures or some kind of ductile necking features. The oldest materials within the Nun Sulci and Perrine quadrangles occur within the cratered dark materials unit, as is generally the case for all of Ganymede. This is the most widespread of the dark units mapped in these two quadrangles. Crater densities within cratered dark materials are consistent with an age on the order of several billion years, and thus cratered dark terrain probably represents crust that has survived from the end of the primordial intense bombardment phase of solar system history. The brief

geologic history is greatly oversimplified as a result of the poor resolution and unfavorable viewing geometry of the images covering the area. Author

N92-10763*# Arizona State Univ., Tempe. Dept. of Geology.
TECTONIC DEFORMATION ON ICY SATELLITES: A MODEL OF COMPENSATING HORSTS
Robert Pappalardo and Ronald Greeley *In* NASA, Washington, Reports of Planetary Geology and Geophysics Program, 1990 Jun. 1991 p 93-94 (For primary document see N92-10728 01-91)
Avail: NTIS HC/MF A25 CSCL 03B

Voyager images demonstrate that the icy satellites have been shaped by a variety of magmatic and tectonic processes, of which ridge and trough terrain is a manifestation. This terrain is observed on Ganymede, Enceladus, Miranda, and Ariel, and many models have been proposed to explain its origin. A likely model is horst and graben style normal faulting, in which horizontal extension results in a series of downdropped grabens and relatively uplifted horsts. The apparent negative elevation of ridges and troughs relative to surrounding terrain has been used to argue such an extensional-tectonic origin for ridge and trough terrain on Ganymede and Enceladus. A ridge or ridge set which stands above a presumed original base level, thus, might be suspect of having a magmatic or compressional origin. It has been shown that rotation of domino-style normal faulting, which involves rotation of fault blocks about a fulcrum, can allow ridges to stand slightly above the original base level, and this relative uplift may be amplified by isostatic uplift. Compensation might also be accomplished through uplift of adjacent horsts. These theories are defended with dynamical equations. Author

N92-10764*# Arizona Univ., Tucson. Lunar and Planetary Lab.
MIMAS: TECTONIC STRUCTURE AND GEOLOGIC HISTORY
Steven K. Croft *In* NASA, Washington, Reports of Planetary Geology and Geophysics Program, 1990 Jun. 1991 p 95-97 (For primary document see N92-10728 01-91)
Avail: NTIS HC/MF A25 CSCL 03B

Mimas, the innermost of the major saturnian satellites, occupies an important place in comparative studies of icy satellites. It is the smallest icy satellite known to have a mostly spherical shape. Smaller icy objects like Hyperion and Puck are generally irregular in shape, while larger ones like Miranda and Enceladus are spherical. Thus Mimas is near the diameter where the combination of increasing surface gravity and internal heating begin to have a significant effect on global structure. The nature and extent of endogenic surface features provide important constraints on the interior structure and history of this transitional body. The major landforms on Mimas are impact craters. Mimas has one of the most heavily cratered surfaces in the solar system. The most prominent single feature on Mimas is Herschel, an unrelaxed complex crater 130 km in diameter. The only other recognized landforms on Mimas are tectonic grooves and lineaments. Groove locations were mapped by Schenk, but without analysis of groove structures or superposition relationships. Mimas' tectonic structures are remapped here in more detail than previously has been done, as part of a general study of tectonic features on icy satellites.
Author

N92-10765*# Arizona Univ., Tucson. Lunar and Planetary Lab.
TETHYS GEOLOGY AND TECTONICS REVISITED
Steven K. Croft *In* NASA, Washington, Reports of Planetary Geology and Geophysics Program, 1990 Jun. 1991 p 98-100 (For primary document see N92-10728 01-91)
Avail: NTIS HC/MF A25 CSCL 03B

Tethys, a medium sized icy satellite of Saturn, was imaged by both Voyager 1 and 2 spacecraft at sufficiently high resolution to allow some geologic analysis. One fairly complete and several brief descriptions of Tethys' geology have been given. Partial results are given herein of a new analysis of Tethys' geology done as part of a comparative tectonic and cryovolcanic study of the saturnian satellites. A new geologic sketch map of Tethys' north polar area is given. This map is based on a sequence of images transformed to a polar stereographic projection at the same scale. The images present the same area under different illuminations, each of which brings out different features. A new global map is in progress. Author

N92-10766*# Arizona Univ., Tucson. Lunar and Planetary Lab.
IAPETUS: TECTONIC STRUCTURE AND GEOLOGIC HISTORY
Steven K. Croft *In* NASA, Washington, Reports of Planetary Geology and Geophysics Program, 1990 Jun. 1991 p 101-103 (For primary document see N92-10728 01-91)
Avail: NTIS HC/MF A25 CSCL 03B

Many papers have been written about the surface of Iapetus, but most of these have discussed either the nature of the strongly contrasting light and dark materials or the cratering record. Little has been said about other geologic features on Iapetus, such as tectonic structures, which would provide constraints on Iapetus' thermal history. Most references have suggested that there is no conclusive evidence for any tectonic activity, even when thermal history studies indicate that there should be. However, a new study of Iapetus' surface involving the use of stereo pairs, an extensive tectonic network has been recognized. A few new observations concerning the craters and dark material were also made. Thus the geology and geologic history of Iapetus can be more fully outlined than before. The tectonic network is shown along with prominent craters and part of the dark material in the geologic/tectonic sketch map. The topology of crater rims and scarps are quite apparent and recognizable in the different image pairs. The heights and slopes of various features given are based on comparison with the depths of craters 50 to 100 km in diameter, which are assumed to have the same depths as craters of similar diameter on Rhea and Titania. Author

N92-10767*# Arizona State Univ., Tempe. Dept. of Geology.
THE STRENGTH OF MIRANDA'S LITHOSPHERE
Robert Pappalardo and Ronald Greeley *In* NASA, Washington, Reports of Planetary Geology and Geophysics Program, 1990 Jun. 1991 p 104-106 (For primary document see N92-10728 01-91)
Avail: NTIS HC/MF A25 CSCL 03B

In attempting to understand the endogenic processes which have shaped the surface of an icy satellite, it is desirable to quantify the failure strength of the satellite's lithosphere. In a crust that is fractured on a large scale, frictional sliding along pre-existing fractures occurs in response to lower differential stresses than required to initiate fracture of pristine rock, thus governing failure of a brittle lithosphere. Failure is predicted along favorably oriented fracture planes; if fractures of all orientations are assumed to be present in the crust (as is expected of a heavily cratered lithosphere), frictional failure relations are directly applicable. The Coulomb criterion predicts that the shear stress (sigma sub t) and normal stress (sigma sub n) components on a fracture plane at failure are related as sigma sub t = mu-sigma sub n + S sub o, where S sub o is the cohesion and mu is the coefficient of friction. At moderate to high pressures, the frictional sliding strength of most materials is found to be sigma sub t = 0.85 sigma sub n.
Author

N92-10768*# Arizona Univ., Tucson. Dept. of Geosciences.
EVOLUTION OF THE MARTIAN HYDROSPHERE
V. Baker *In* NASA, Washington, Reports of Planetary Geology and Geophysics Program, 1990 Jun. 1991 p 111-113 (For primary document see N92-10728 01-91)
(Grant NAGw-285)
Avail: NTIS HC/MF A25 CSCL 03B

The concept of the hydrological cycle is one of the greatest achievements in the understanding of nature. Leonardo da Vinci seems to have held two concurrent views of the cycle: an external process in which evaporation from ponded areas leads to precipitation and runoff from the land; and an internal process in which subsurface pressures from within the Earth force water upward. Endogenetic hypotheses for valley genesis on Mars maintain the necessary prolonged ground water flows by hydrothermal circulation associated with impact cratering or with volcanism. Ocean formation on Mars was episodic, mostly

evidenced by the latest episodes. Coincident cataclysmic flood discharges to the northern plains, probably triggered by Tharsis volcanism, would lead to immense consequences. Potential volumes of ponded water are summarized. The outflow channels have a complex history of flooding events over a prolonged period of planetary history. It is hypothesized that episodic outbursts of concurrent discharge was triggered by planetary scale volcanism. The consequences of such episodes are summarized. Author

N92-10769*# Virginia Univ., Charlottesville. Dept. of Environmental Sciences.
A MARTIAN GLOBAL GROUNDWATER MODEL
Alan D. Howard *In* NASA, Washington, Reports of Planetary Geology and Geophysics Program, 1990 Jun. 1991 p 114-116 (For primary document see N92-10728 01-91)
Avail: NTIS HC/MF A25 CSCL 03B

A global groundwater flow model was constructed for Mars to study hydrologic response under a variety of scenarios, improving and extending earlier simple cross sectional models. The model is capable of treating both steady state and transient flow as well as permeability that is anisotropic in the horizontal dimensions. A single near surface confining layer may be included (representing in these simulations a coherent permafrost layer). Furthermore, in unconfined flow, locations of complete saturation and seepage are determined. The flow model assumes that groundwater gradients are sufficiently low that DuPuit conditions are satisfied and the flow component perpendicular to the ground surface is negligible. The flow equations were solved using a finite difference method employing 10 deg spacing of latitude and longitude.
Author

N92-10770*# Virginia Univ., Charlottesville. Dept. of Environmental Sciences.
ROLE OF GROUNDWATER IN FORMATION OF MARTIAN CHANNELS
Alan D. Howard *In* NASA, Washington, Reports of Planetary Geology and Geophysics Program, 1990 Jun. 1991 p 117-119 (For primary document see N92-10728 01-91)
Avail: NTIS HC/MF A25 CSCL 03B

A global 3-D model of groundwater flow has been used to study possible behavior of groundwater on Mars and its role in creating fluvial features. Conclusions drawn from an earlier 2-D groundwater model are supplemented and expanded. Topical headings are discussed as follows: timescales of groundwater flow; wet areas on Mars and location of outflow channels; implications for valley networks; the enigma of Hellas; absence of fluvial or periglacial features on Syrtis Major; development of chaotic terrain and associated outflow channels; and structurally controlled valley networks.
Author

N92-10771*# Virginia Univ., Charlottesville. Dept. of Environmental Sciences.
ROLE OF ARTESIAN GROUNDWATER IN FORMING MARTIAN PERMAFROST FEATURES
Alan D. Howard *In* NASA, Washington, Reports of Planetary Geology and Geophysics Program, 1990 Jun. 1991 p 120-122 (For primary document see N92-10728 01-91)
Avail: NTIS HC/MF A25 CSCL 03B

Various landforms possibly related to formation (growth), movement, or decay of ground ice have been identified on Mars, including fretted terrain (ft) and associated lobate debris aprons (lda), the chaotic terrain, concentric crater fills (ccf), polygonal ground, softened terrain, small domes that are possibly pingos, and curvilinear (fingerprint) features (cuf). Glaciers may also have been present. Some of these may involve ice derived from artesian groundwater. Topical areas of discussion are: Mars groundwater and the location of permafrost features; the ft, lda, ccf, and cuf; role of artesian groundwater in formation of fretted terrain, lobate debris blankets, and concentric crater fills; sources of glacial ice; and pingos and other pseudovolcanic structures.
Author

N92-10772*# Arizona Univ., Tucson. Lunar and Planetary Lab.
GLACIAL AND MARINE CHRONOLOGY OF MARS
Robert G. Strom, Jeffrey S. Kargel, Natasha Johnson, and Christine Knight *In* NASA, Washington, Reports of Planetary Geology and Geophysics Program, 1990 Jun. 1991 p 123-124 (For primary document see N92-10728 01-91)
Avail: NTIS HC/MF A25 CSCL 03B

A hydrological model involving episodic oceans and ice sheets on Mars has been presented by Baker, et al. One of the main uncertainties concerning this model is the age and correlation of these events. Even more uncertain are their absolute ages. However, based on stratigraphic and cratering evidence, the most recent occurrence of these events was relatively late in Martian history. The cratering record on Mars can be divided into three general periods: (1) the period of late heavy bombardment; (2) a transition period at the end of late heavy bombardment; and (3) the post heavy bombardment era. The crater size/frequency distribution represented by the period of late heavy bombardment is characterized by a complex curve with a differential-2 slope (cumulative-1) at diameters less than about 50 km diameter, while the post heavy bombardment size distribution has a differential-3 slope (cumulative-2) over the same diameter range. An R plot is presented of the size/freqency distribution of ejecta blanket craters on the Argyre esker plains and similar craters in Hellas. The relative chronology is summarized of oceans, ice sheets, and other major events in Martian history.
Author

N92-10773*# Arizona Univ., Tucson. Dept. of Planetary Sciences.
CHRONOLOGY OF GLACIATION IN THE HELLAS REGION OF MARS
N. Johnson, Jeffrey S. Kargel, Roger G. Strom, and Christine Knight *In* NASA, Washington, Reports of Planetary Geology and Geophysics Program, 1990 Jun. 1991 p 125-126 (For primary document see N92-10728 01-91)
Avail: NTIS HC/MF A25 CSCL 03B

The Hellas Impact Basin is one of the oldest features on Mars, as indicated by the high density of large impact craters in parts of the basin. The highly degraded condition of Hellas seems consistent with great antiquity. However, many of the most strikingly modified landscapes in the basin, believed to be glaciogenic, also appear to be geologically youthful. Stratigraphic relations suggest two episodes of glaciation. Chronologic constraints are imposed on glaciation based on the impact cratering record, the focus of which is the southwestern portion of Hellas. Major terrain units are mapped. The lineated terrain and ridged plains form the summit and flanks of a large shield volcano, Amphitrites Patera, which was superimposed over the southwestern rim of Hellas toward the end of heavy bombardment. The ridged plains and lineated terrain are crossed by numerous wrinkle ridges. The lineated terrain is distinguished by a pervasive system of deep erosional troughs and sharp ridges thought to have been glacially sculpted by the Hellas Lobe. It is concluded that glaciation in Hellas occurred during the Middle Amazonian, roughly coeval with glaciation in Argyre.
Author

N92-10774*# Arizona Univ., Tucson. Lunar and Planetary Lab.
GLACIAL GEOLOGY OF THE HELLAS REGION ON MARS
Jeffrey S. Kargel, Robert G. Strom, and Natasha Johnson *In* NASA, Washington, Reports of Planetary Geology and Geophysics Program, 1990 Jun. 1991 p 127-128 (For primary document see N92-10728 01-91)
Avail: NTIS HC/MF A25 CSCL 03B

A glacial geologic interpretation was recently presented for Argyre, which is herein extended to Hellas. This glacial event is believed to constitute an important link in a global cryohydric epoch of Middle Amazonian age. At glacial maximum, ice apparently extended far beyond the regions of Argyre and Hellas, and formed what is termed as the Austral Ice Sheet, an agglomeration of several ice domes and lobes including the Hellas Lobe. It is concluded that Hellas was apparently heavily glaciated. Also glaciation was young by Martian standards (Middle Amazonian), and ancient by terrestrial standards. Glaciation appears to have occurred during the same period that other areas on Mars were experiencing glaciation and periglacial activity. Glaciation seems

to have occurred as a geological brief epoch of intense geomorphic activity in an era characterized by long periods of relative inactivity. Author

N92-10775*# Arizona Univ., Tucson. Lunar and Planetary Lab.
TERRESTRIAL GLACIAL ESKERS: ANALOGS FOR MARTIAN SINUOUS RIDGES
Jeffrey S. Kargel and Roger G. Strom *In* NASA, Washington, Reports of Planetary Geology and Geophysics Program, 1990 Jun. 1991 p 129-130 (For primary document see N92-10728 01-91)
Avail: NTIS HC/MF A25 CSCL 03B

A glacial model was introduced last year for the Argyre region, a concept which is now extended, and which was recently integrated with a Global Hydrologic Model incorporating many other aspects of Martian geology. Despite wide agreement that the Martian ridges strongly resemble glacial eskers, this hypothesis has been presented with great equivocation due to a perceived lack of other glacial landforms. Quite to the contrary, it is shown that the Martian ridges actually do occur in logical ordered sequences with many other types of characteristically glacial appearing landforms. Herein, the esker hypothesis is further supported in isolation from considerations of regional landform assemblages. It is concluded that Martian sinuous ridges are similar in every respect to terrestrial eskers: scale, morphology, planimetric pattern, and associations with other probable glaciogenic landforms. It is found that the esker hypothesis is well supported. Eskers are glaciofluvial structures, and owe their existence to large scale melting of stagnant temporate glaciers. Thus, eskers are indicators of an ameliorating climatic regime after a protracted episode of cold, humid conditions. Author

N92-10776*# Geological Survey, Flagstaff, AZ.
PALEOLAKES AND LACUSTRINE BASINS ON MARS
David H. Scott, James W. Rice, Jr., and James M. Dohm *In* NASA, Washington, Reports of Planetary Geology and Geophysics Program, 1990 Jun. 1991 p 131-132 (For primary document see N92-10728 01-91)
Avail: NTIS HC/MF A25 CSCL 03B

The problems of how warm and wet Mars once was and when climate transitions may have occurred are not well understood. Mars may have had an early environment similar to Earth's that was conducive to the emergence of life. In addition, increasing geologic evidence indicates that water, upon which terrestrial life depends, has been present on Mars throughout its history. This evidence does not detract from the possibility that life may have originated on early Mars, but rather suggests that life could have developed over longer periods of time in longer lasting, more clement local environments than previously envisioned. It is suggested herein that such environments may have been provided by paleolakes, located mostly in the northern lowlands and probably ice covered. Such lakes probably would have had diverse origins. Glacial lakes may have occupied ice eroded hollows or formed in valleys obstructed by moraines or ice barriers. Unlike Earth, the Martian record of the origin and evolution of possible life may have not been erased by extensive deformation of the surface. Thus the basins that may have contained the paleolakes are potential sites for future biological, geological, and climatological study. Author

N92-10777*# Arizona Univ., Tucson. Lunar and Planetary Lab.
STRATIGRAPHY OF THE LAYERED TERRAIN IN VALLES MARINERIS, MARS
G. Komatsu and Roger G. Strom *In* NASA, Washington, Reports of Planetary Geology and Geophysics Program, 1990 Jun. 1991 p 133-134 (For primary document see N92-10728 01-91)
Avail: NTIS HC/MF A25 CSCL 03B

The layered terrain in Valles Marineris provides information about its origin and the geologic history of this canyon system. Whether the terrain is sedimentary material deposited in a dry or lacustrine environment, or volcanic material related to the tectonics of the canyon is still controversial. However, recent studies of Gangis Layered Terrain suggests a cyclic sequence of deposition and erosion under episodic lacustrine conditions. The stratigraphic studies are extended to four other occurrences of layered terrains in Valles Marineris in an attempt to correlate and distinguish between depositional environments. The Juvantae Chasma, Hebes Chasma, Ophir and Candor Chasmata, Melas Chasma, and Gangis Layered Terrain were examined. Although there are broad similarities among the layered terrains, no two deposits are exactly alike. This suggests that there was no synchronized regional depositional processes to form all the layered deposits. However, the similar erosional style of the lower massive weakly bedded unit in Hebes, Gangis, and Ophir-Candor suggests it may have been deposited under similar circumstances. Author

N92-10778*# Geological Survey, Flagstaff, AZ.
HYDROLOGIC ACTIVITY DURING LATE NOACHIAN AND EARLY HESPERIAN DOWNWARPING OF BOREALIS BASIN, MARS
Kenneth L. Tanaka *In* NASA, Washington, Reports of Planetary Geology and Geophysics Program, 1990 Jun. 1991 p 135-137 (For primary document see N92-10728 01-91)
Avail: NTIS HC/MF A25 CSCL 03B

Pronounced global volcanism as well as fracturing and erosion along the highland/lowland boundary (HLB) during the Late Noachian (LN) and Early Hesperian (EH) led McGill and Dimitriou to conclude that the Borealis basin formed tectonically during this period. This scenario provides a basis for interpretation of the initiation and mode of formation of erosional and collapse features along the HLB. The interpretation, in turn, is integral to hypotheses regarding the development of ancient lakes (or an ocean) and their impact on the climate history of Mars. Hydrologic features of Mars are discussed along with their implications for paleolakes and climate history. Author

N92-10779*# Geological Survey, Flagstaff, AZ.
CHANNELING EPISODES OF KASEI VALLES, MARS, AND THE NATURE OF RIDGED PLAINS MATERIAL
Mary G. Chapman and Kenneth L. Tanaka *In* NASA, Washington, Reports of Planetary Geology and Geophysics Program, 1990 Jun. 1991 p 138-139 (For primary document see N92-10728 01-91)
Avail: NTIS HC/MF A25 CSCL 03B

The geologic mapping compiled at 1:500,000 scale of the northern Kasei Valles area of Mars (MTMs 25062 and 25067) indicates (1) at least three periods of Kasei Valles channeling, (2) the development of Sacra Fossae (linear depressions on Tempe Terra and Lunae Planum) in relation to Kasei channeling episodes, and (3) the nature of ridged plains material dissected by Kasei Valles on northern Lunae Planum. (The three channeling periods consists of two flood events and a later, sapping related event). These findings suggest hydrologic conditions and processes that formed Kasei Valles and associated features and terrains. It is concluded that an early period of flooding, whose source is perhaps buried beneath lava flows of Tharsis Montes, may have eroded streamlined features in northern Lunae Planum. Also, later floods originating from Echus Chasma formed after the initial flooding and the mesas adjacent to the plateau. The Sacra Fossae formed after the initial flooding and during the second flooding by sapping, outbreak, scarp retreat, and collapse along joints and fractures in ridged plains materials. Author

N92-10780*# University of Northeast Louisiana, Monroe. Dept. of Geosciences.
FLOOD ROUTING OF THE MAJA OUTFLOW ACROSS XANTHE TERRA
R. A. DeHon *In* NASA, Washington, Reports of Planetary Geology and Geophysics Program, 1990 Jun. 1991 p 140-142 (For primary document see N92-10728 01-91)
Avail: NTIS HC/MF A25 CSCL 03B

The object is to trace a single flood crest through the Maja outflow system and to evaluate the effects of topography on ponding and multiple channel routing. Maja Valles provides a good model because it has a single source and a well defined channel system. The 1500 km long Maja Valles originates in Juventae

Chasma. The outflow system stretches 1100 km northward along the Lunae Planum/Xanthe Terra boundary, then eastward across the Xanthe Terra highlands. It descends to Chryse Planitia where it extends northeastward toward the middle of the basin. It is concluded that flood routing through multiple channels and retardation in local impoundments are responsible for breakup of the initial flood crest and the formation of multiple flood crests. Recombined flow near the mouths of these canyons results in an extended flow regime and multiple flood surges. As a result of ponding along the flood course, depositional sites are localized and renewed erosion downstream (from ponded sites) results in sediment source areas not greatly removed from depositional sites. Author

N92-10781*# National Air and Space Museum, Washington, DC. Center for Earth and Planetary Studies.
ANCIENT FLUVIAL PROCESSES IN THE EQUATORIAL HIGHLANDS OF MARS
Robert A. Craddock and Ted A. Maxwell *In* NASA, Washington, Reports of Planetary Geology and Geophysics Program, 1990 Jun. 1991 p 143-145 (For primary document see N92-10728 01-91)
(Grant NAGw-129)
Avail: NTIS HC/MF A25 CSCL 03B

Martian highland craters typically lack ejecta deposits, have no noticeable rim, and are flat floored. In addition, crater size frequency distribution curves show that highland craters have depleted populations less than 20 km in diameter. A variety of processes have been suggested to explain these observations including deposition of aeolian or volcanic materials up to the crater rim crests, thermal creep, terrain softening, and mass wasting. However, none of these processes adequately explains both the crater morphology and population distribution. In order to explain both the Martian highland crater morphology and population distribution, a fluvial process is proposed which is capable of removing the loose crater rim material. The resulting effect is to decrease the crater diameter, thereby causing the population curves to bendover. The eroded material is redistributed, burying or partially burying smaller diameter craters before complete erosion. This material may also be deposited into local topographic lows, creating the depositional basins observed. A fluvial process explains both sets of observations: crater morphology and crater population distribution curves. Author

N92-10782*# Geological Survey, Flagstaff, AZ.
GEOLOGIC HISTORY AND CHANNELING EPISODES OF THE CHRYSE PLANITIA REGION OF MARS
Susan L. Rotto and Kenneth L. Tanaka *In* NASA, Washington, Reports of Planetary Geology and Geophysics Program, 1990 Jun. 1991 p 146-148 (For primary document see N92-10728 01-91)
Avail: NTIS HC/MF A25 CSCL 03B

The study of the Chryse Planitia region of Mars is based on geologic mapping on a 1:5,000,000 scale shaded relief map. The map area includes Chryse and southern Acidalia Planitiae; the circum Chryse channels and chaotic terrains; Xanthe, southern Tempe, and western Arabia Terrae; Lunae Planum; and northeastern Valles Marineris. The aim of the study is twofold: (1) to obtain relative ages of the outflow channels by performing and compiling detailed stratigraphic analyses; and (2) to correlate channeling episodes with causative mechanisms (such as volcanism and tectonism) and resulting effects (such as climate change). The geologic history given based on this mapping, includes the documentation of a previously unproposed channeling episode in the region as well as the presently favored hypotheses concerning the nature and origin of the channeling events. It is concluded that the history of the Chryse region suggests that two major periods of tectonic activity resulted in two episodes of channeling in the highlands surrounding Chryse Planitia. Author

N92-10783*# Brown Univ., Providence, RI.
GRADATIONAL EVOLUTION OF YOUNG, SIMPLE IMPACT CRATERS ON THE EARTH
J. A. Grant and P. H. Schultz *In* NASA, Washington, Reports of Planetary Geology and Geophysics Program, 1990 Jun. 1991 p 152-153 (For primary document see N92-10728 01-91)
Avail: NTIS HC/MF A25 CSCL 03B

From these three craters, a first order gradational evolutionary sequence can be proposed. As crater rims are reduced by backwasting and downwasting through fluvial and mass wasting processes, craters are enlarged by approx. 10 pct. Enlargement of drainages inside the crater eventually forms rim breaches, thereby capturing headward portions of exterior drainages. At the same time, the relative importance of gradational processes may reverse on the ejecta: aeolian activity may supersede fluvial incisement and fan formation at late stages of modification. Despite actual high drainage densities on the crater exterior during early stages of gradation, the subtle scale of these systems results in low density estimates from air photos and satellite images. Because signatures developed on surfaces around all three craters appear to be mostly gradient dependent, they may not be unique to simple crater morphologies. Similar signatures may develop on portions of complex craters as well; however, important differences may also occur. Author

N92-10784*# Brown Univ., Providence, RI.
STYLES OF CRATER GRADATION IN SOUTHERN ISMENIUS LACUS, MARS
J. A. Grant and P. H. Schultz *In* NASA, Washington, Reports of Planetary Geology and Geophysics Program, 1990 Jun. 1991 p 154-155 (For primary document see N92-10728 01-91)
Avail: NTIS HC/MF A25 CSCL 03B

Preserved morphology around selected impact craters together with results from study of long term gradational evolution are used to assess processes responsible for crater modification in southern Ismenius Lacus. Results are compared with the gradational styles of selected terrestrial craters. Although most craters in the region display complex primary morphologies, some first order comparisons with the gradational styles around simple terrestrial craters may be valid. Nearly complete high resolution coverage provides a basis for studying morphologic features at scales comparable to those observed in LANDSAT TM images of terrestrial craters. It is concluded that the relative importance of gradational processes differs around the terrestrial and Martian craters considered here: Martian rimless morphologies are produced by mass wasting, eolian deposition/erosion, and limited fluvial incisement resulting in downwasting and significant backwasting of crater walls. Author

N92-10785*# Brown Univ., Providence, RI.
THE GRADATIONAL HISTORY OF SOUTHERN ISMENIUS LACUS
J. A. Grant and P. H. Schultz *In* NASA, Washington, Reports of Planetary Geology and Geophysics Program, 1990 Jun. 1991 p 156-157 (For primary document see N92-10728 01-91)
Avail: NTIS HC/MF A25 CSCL 03B

Two epochs of accelerated gradation affected the geomorphic evolution of southern Ismenius Lacus. These periods of enhanced gradational activity were likely related to periods of more clement climate induced by release of either recycled exogenic or juvenile endogenic atmospheric volatiles. Variations in the intensity and duration of gradation during the second epoch are indicated by the variability in the timing of cessation and degree of air fall deposit removal across the study area. Overall intensity of gradation decreased through successive epochs based on: (1) the decreasing diameter at which cumulative statistics from the respective surfaces cease to follow the expected production function; and (2) the decrease in size/increase in density of preserved valley networks incised into surfaces of differing age. A comparable decrease in valley density with time has been noted in the Isidis region. Author

N92-10786*# Geological Survey, Menlo Park, CA.
SOIL CRUSTS ON MARS
H. J. Moore *In* NASA, Washington, Reports of Planetary Geology

and Geophysics Program, 1990 Jun. 1991 p 158-159 (For primary document see N92-10728 01-91)
Avail: NTIS HC/MF A25 CSCL 03B

Three distinct soillike materials sampled by the Viking landers (VL) on Mars are (in order of increasing strength): (1) drift; (2) crusty to cloddy; and (3) blocky. Relative strengths of these materials are manifested by footpad penetrations during landing (VL 1), depths of deep holes, motor currents during sampling, sampler backhoe penetrations, comminutor motor currents, impact pits, trench tailings, and successful acquisitions of the coarse fraction (only blocky material). Cementation by S Cl compounds probably contributes to the relative strengths. This is shown where the weight pct. of SO3 + Cl of each material is plotted against their relative strengths. A similar result is obtained using SO3 alone, but not with Cl which is deficient in VL 2 samples. Author

N92-10787*# Geological Survey, Menlo Park, CA.
SURFACE-MATERIAL MAPS OF VIKING LANDING SITES ON MARS
H. J. Moore and J. M. Keller (Stanford Univ., CA.) *In* NASA, Washington, Reports of Planetary Geology and Geophysics Program, 1990 Jun. 1991 p 160-162 (For primary document see N92-10728 01-91)
Avail: NTIS HC/MF A25 CSCL 03B

Researchers mapped the surface materials at the Viking landing sites on Mars to gain a better understanding of the materials and rock populations at the sites and to provide information for future exploration. The maps extent to about 9 m in front of each lander and are about 15 m wide - an area comparable to the area of a pixel in high resolution Viking Orbiter images. The maps are divided into the near and far fields. Data for the near fields are from 1/10 scale maps, umpublished maps, and lander images. Data for the far fields are from 1/20 scale contour maps, contoured lander camera mosaics, and lander images. Rocks are located on these maps using stereometric measurements and the contour maps. Frequency size distribution of rocks and the responses of soil-like materials to erosion by engine exhausts during landings are discussed. Author

N92-10788*# Arizona State Univ., Tempe. Dept. of Geology.
MAGMA GENERATION ON MARS: ESTIMATED VOLUMES THROUGH TIME
Ronald Greeley and B. Schneid *In* NASA, Washington, Reports of Planetary Geology and Geophysics Program, 1990 Jun. 1991 p 163-164 (For primary document see N92-10728 01-91)
Avail: NTIS HC/MF A25 CSCL 03B

Images of volcanoes and lava flows, chemical analysis by the Viking landers, and studies of meteorites show that volcanism has played an important role in the evolution of Mars. Photogeologic mapping suggests that half of Mars' surface is covered with volcanic materials. Here, researchers present results from new mappings, including estimates of volcanic deposit thicknesses based on partly buried and buried impact craters using the technique of DeHon. The researchers infer the volumes of possible associated plutonic rocks and derive the volumes of magmas on Mars generated in its post-crustal formation history. Also considered is the amount of juvenile water that might have exsolved from the magma through time. Author

N92-10789*# Jet Propulsion Lab., California Inst. of Tech., Pasadena.
CRYSTALLIZATION DURING EMPLACEMENT OF LAVA FLOWS
J. Crisp *In* NASA, Washington, Reports of Planetary Geology and Geophysics Program, 1990 Jun. 1991 p 165-166 (For primary document see N92-10728 01-91)
Avail: NTIS HC/MF A25 CSCL 03B

Thermal models of lava flows provide a way of estimating emplacement durations and eruption rates of planetary lava flows, which can help constrain magma ascent, rheology and composition. Most of the models that have been developed consider only the effects of cooling by radiation. However, heating due to crystallization can be a large component of the overall heat budget of a flow. Little is known about the amount of crystallization and latent heating during flow advance. Crystal size distribution (CSD) measurements were made to quantify and study the effects of crystallization in the 1984 Mauna Loa flow. For flows on Mars, we must assume that the amount of crystallization is similar to that in terrestrial flows and place minimum and maximum bounds on the latent heat effect. Unfortunately, as examples given here show, there can be anywhere from 0 to 60 percent crystallization during flow advance. To improve constraints for Martian flows, we need to search for correlations in terrestrial flows between flow morphology and the amount of crystallization during emplacement. Author

N92-10790*# Arizona State Univ., Tempe. Dept. of Geology.
PHYSICAL PROPERTIES OF LAVA FLOWS ON THE SOUTHWEST FLANK OF TYRRHENA PATERA, MARS
David A. Crown, Tracy K. Porter, and Ronald Greeley *In* NASA, Washington, Reports of Planetary Geology and Geophysics Program, 1990 Jun. 1991 p 167-169 (For primary document see N92-10728 01-91)
Avail: NTIS HC/MF A25 CSCL 03B

Tyrrhena Patera (TP) (22 degrees S, 253.5 degrees W), a large, low-relief volcano located in the ancient southern highlands of Mars, is one of four highland paterae thought to be structurally associated with the Hellas basin. The highland paterae are Hesperian in age and among the oldest central vent volcanoes on Mars. The morphology and distribution of units in the eroded shield of TP are consistent with the emplacement of pyroclastic flows. A large flank unit extending from TP to the SW contains well-defined lava flow lobes and leveed channels. This flank unit is the first definitive evidence of effusive volcanic activity associated with the highland paterae and may include the best preserved lava flows observed in the Southern Hemisphere of Mars. Flank flow unit averages, channelized flow, flow thickness, and yield strength estimates are discussed. Analysis suggests the temporal evolution of Martian magmas. Author

N92-10791*# Geological Survey, Menlo Park, CA.
RHEOLOGICAL ANALYSES OF LAVA FLOWS ON MARS
H. J. Moore and P. A. Davis (Geological Survey, Flagstaff, AZ.) *In* NASA, Washington, Reports of Planetary Geology and Geophysics Program, 1990 Jun. 1991 p 170-171 (For primary document see N92-10728 01-91)
Avail: NTIS HC/MF A25 CSCL 03B

Researchers obtained 183 profiles of lava flows on Mars using photoclinometry. These photoclinometric profiles were leveled by adjusting them until the levee crests or bases had the same elevations (depending on the situation). Here, researchers report some of the results of their analysis of 27 flows on the flanks of Alba Patera (3 flows), near the summit of Ascraeus Mons (6 flows), the flanks of Arsia Mons (3 flows), and the flanks of Olympus Mons (15 flows). Results suggest that the flows examined to date are not felsic or ultramafic; rather, they probably range from basalts to basaltic andesites. Thus, the suggestion that flows on Olympus Mons and elsewhere may be more silicic than Hawaiian basalts is supported by the researchers' results. These suggestions are testable with suitable measurements of silica contents of the flows. Author

N92-10792*# Arizona State Univ., Tempe. Dept. of Geology.
FACTORS CONTROLLING LAVA DOME MORPHOLOGY
Jonathan Fink, Nathan Bridges, and Ross Griffiths (Australian National Univ., Canberra.) *In* NASA, Washington, Reports of Planetary Geology and Geophysics Program, 1990 Jun. 1991 p 172-173 (For primary document see N92-10728 01-91)
Avail: NTIS HC/MF A25 CSCL 03B

Research suggests that variations in lava dome morphology on different planets will depend much more critically on local gravity and the style of eruption than on the magma composition, ambient temperature, or the relative roles of convective and radiative cooling. Eruption style in turn reflects differences in tectonic conditions and the ability of magma to exsolve volatiles. Observed crude correlations between silica content and calculated yield

strengths for terrestrial lava flows and domes probably are do to differences in extrusion rate and volatile solubility, rather than intrinsic rheological properties. Thus, even after taking the known effect of gravity into account, observed differences in gross dome morphology on different planets cannot by themselves be directly related to composition. Additional information such as the distribution of surface textures and structures, or spectroscopic data will be needed to conclusively establish dome compositions. Author

N92-10793*# Hawaii Univ., Honolulu. Dept. of Geology and Geophysics.
NEW STUDIES OF MARTIAN VOLCANOES
P. J. Mouginis-Mark, M. S. Robinson, and S. H. Zisk *In* NASA, Washington, Reports of Planetary Geology and Geophysics Program, 1990 Jun. 1991 p 174-176 (For primary document see N92-10728 01-91)
(Grant NAGw-437)
Avail: NTIS HC/MF A25 CSCL 03B

To investigate the morphology, topography, and evolution of volcanic constructs on Mars, researchers have been studying the volcanoes Olympus Mons, Tyrrhena Patera, and Apollinaris Patera. These studies relied upon the analysis of digital Viking orbiter images to measure the depth and slopes of the summit area of Olympus Mons, upon new Earth-based radar measurements for the analysis of the slopes of Tyrrhena Patera, and upon the color characteristics of the flanks of Apollinaris Patera for information regarding surface properties. Author

N92-10794*# Brown Univ., Providence, RI.
THE PROBABLE CONTINUUM BETWEEN EMPLACEMENT OF PLUTONS AND MARE VOLCANISM IN LUNAR CRUSTAL EVOLUTION
Carle M. Pieters *In* NASA, Washington, Reports of Planetary Geology and Geophysics Program, 1990 Jun. 1991 p 177-178 (For primary document see N92-10728 01-91)
Avail: NTIS HC/MF A25 CSCL 03B

A scenario for the formation of the Moon is advanced and is argued to be consistent with both known data and the leading hypothesis regarding the formation of the Moon. It is concluded that, although the volume of mare basalts is estimated to be only 0.1 percent of the lunar total, this value should not be taken to represent the amount of partial melt produced within the lunar interior, nor should the mare basalts be viewed as representing the only products of internal heating. The actual amount of magnetic activity is certain to be substantially larger, but cannot be estimated without a global assessment of lunar highland heterogeneity and the character, scale, and abundance of lunar plutons. Author

N92-10795*# National Aeronautics and Space Administration. Lyndon B. Johnson Space Center, Houston, TX.
LUNAR WESTERN LIMB PYROCLASTIC DEPOSITS
Cassandra R. Coombs and B. Ray Hawke (Hawaii Univ., Honolulu.) *In* NASA, Washington, Reports of Planetary Geology and Geophysics Program, 1990 Jun. 1991 p 179-180 (For primary document see N92-10728 01-91)
Avail: NTIS HC/MF A25 CSCL 03B

It has become increasingly evident that the lunar pyroclastic volcanism played an important role in the formation and resurfacing of many areas of the Moon. On-going analysis of lunar Orbiter and Apollo photographs continues to locate and identify pyroclastic deposits and suggests that they just may be more ubiquitous than once thought. Located near mare/highland boundaries, many of these deposits formed contemporaneously with effusive mare volcanism. The mantling deposits formed as products of fire-fountaining. Probable source vents for these deposits include irregular depressions at the head of associated sinuous rilles and/or along irregular fractures in the floors of ancient craters. Here, researchers provide a brief synopsis of the nature of the dark mantling deposits and briefly discuss several newly identified deposits on the western limb. Author

N92-10796*# National Aeronautics and Space Administration. Lyndon B. Johnson Space Center, Houston, TX.
LUNAR AND HAWAIIAN LAVA TUBES: ANALOGS AND USES BASED ON TERRESTRIAL FIELD DATA
Cassandra R. Coombs and B. Ray Hawke (Hawaii Univ., Honolulu.) *In* NASA, Washington, Reports of Planetary Geology and Geophysics Program, 1990 Jun. 1991 p 181-182 (For primary document see N92-10728 01-91)
Avail: NTIS HC/MF A25 CSCL 03B

Presented here is an analysis of the data collected for a large number of Hawaiian lava tubes on the islands of Oahu, Molokai, and Hawaii. The results are extrapolated to lunar conditions. It is argued that lava tubes that formed on the Earth and the Moon are relatively stable over time, as illustrated by the ridigity of the Hawaiian prehistoric lava tubes as well as the historic tubes located in the bombing range near Mauna Loa. These natural structures should be considered for use in planning for the expansion and advanced stages of the future manned lunar base. Author

N92-10797*# National Aeronautics and Space Administration. Lyndon B. Johnson Space Center, Houston, TX.
ON USING A PYROCLASTIC DEPOSIT AS A MANNED LUNAR BASE SITE
Cassandra R. Coombs, David S. McKay, B. Ray Hawke, and Grant Heiken (Los Alamos National Lab., NM.) *In* NASA, Washington, Reports of Planetary Geology and Geophysics Program, 1990 Jun. 1991 p 183 (For primary document see N92-10728 01-91)
Avail: NTIS HC/MF A25 CSCL 03B

Hawke et al. (1990) suggest that ilmenite found in Apollo 17-type pyroclastic glass may provide feedstock for the hydrogen reduction of ilmenite process for producing lunar oxygen. They also suggest that the ilmenite may help retain solar wind hydrogen and helium which can be extracted for use at a lunar outpost or even transported back to Earth for fusion fuel in the case of helium-3. Therefore, they suggest that ilmenite-rich material may be the best candidate. Here, researchers propose a somewhat different approach. They propose that the pyroclastic glass can be reduced directly to produce oxygen and one or more metals. Sulfur would be another important byproduct of the processing. This process would eliminate the need for having specific minerals such as ilmenite or for doing any mineral concentration. The bulk pyroclastic would provide the feedstock. Some recent experiments at the Johnson Space Center suggest that an iron-rich composition would be the most suitable for this direct feedstock reduction and that the titanium content may not be important. Also, the lunar pyroclastic deposits would be extremely useful in constructing and supporting a lunar base. Author

N92-10798*# Geological Survey, Menlo Park, CA.
WATER ON MARS: CLUE TO ACCRETIONAL HISTORY
M. H. Carr *In* NASA, Washington, Reports of Planetary Geology and Geophysics Program, 1990 Jun. 1991 p 187-190 (For primary document see N92-10728 01-91)
Avail: NTIS HC/MF A25 CSCL 03B

Geological evidence for large amounts of water at the Martian surface appears to be in conflict with geochemical evidence from SNC meteorites that suggests that the Mars mantle is dry and should have lost almost all of its initially large inventory of water during accretion. Here, several possibilities are suggested as to how the apparently conflicting data from two sources may be reconciled. The considerations examined indicate that several plausible explanations for the apparent conflict between geochemical evidence of little water on Mars and geologic evidence of abundant water. One possible conclusion is that Mars has a primitive volatile-rich crust that has been partly overplated with young, dry, mantle-derived volcanoes of which we have samples in the SNC meteorites. Author

N92-10799*# Arizona Univ., Tucson. Planetary Image Research Lab.
VARIABLE FEATURES IN THE VALLES MARINERIS REGION OF MARS
Paul E. Geissler and Robert B. Singer *In* NASA, Washington,

Reports of Planetary Geology and Geophysics Program, 1990 Jun. 1991 p 191-193 (For primary document see N92-10728 01-91)
Avail: NTIS HC/MF A25 CSCL 03B

Transient phenomena on Mars have long been recognized in Mariner and Viking images as well as in decades of Earth based telescopic observations. These events are of interest because of the information they present on currently active meteorological and geological processes. Changes in surface albedo patterns and atmospheric conditions can also affect the analysis and interpretation of data based on spectral or morphological properties of geologic units on the surface. The mechanism responsible for albedo pattern change is currently under investigation. Generation and subsequent transportation and deposition of dark sands has been interpreted in the Valles. However, the removal of a bright dust layer is more consistent with the rapid time period of the change (about two months) and with preliminary multispectral mapping results which suggest that the dark streak south of Eos and Coprates Chasmata is spectrally distinguishable from the dark saltating materials found elsewhere in the canyon system. If a layer of bright dust was removed to affect the albedo change, questions concerning how such micron-sized particles are mobilized by the winds during a normally quiescent season (Southern Hemisphere Autumn) should be addressed. Author

N92-10800*# Arizona State Univ., Tempe. Dept. of Geology
THE POTENTIAL SCALE OF AEOLIAN STRUCTURES ON VENUS
J. R. Marshall and Ronald Greeley *In* NASA, Washington, Reports of Planetary Geology and Geophysics Program, 1990 Jun. 1991 p 194 (For primary document see N92-10728 01-91)
Avail: NTIS HC/MF A25 CSCL 03B

Simulations of the Venusian aeolian environment with the Venus Wind Tunnel have shown that microdunes are formed during the entrainment of sand-sized material. These structures are several tens of centimeters long (2-3 cm high) and combine the morphological and behavioral characteristics of both full-scale terrestrial dunes and current ripples formed in subaqueous environments. Their similarity to both reflects the fact that the Venusian atmosphere has a density intermediate between air and water. Although the development of microdunes in the wind tunnel experiments was limited by tunnel dimensions, it is possible to make some predictions about their potential size on Venus, and the potential size of related aeolian structures. Microdunes are fluid-filled structures (as are dunes and current ripples) and as such have no theoretical upper limit to their size from a fluid dynamics viewpoint. Limitations to size observed in subaqueous structures are set by, for example, water depth; limitations to the size of dunes are set by, for example, sand supply. It is therefore reasonable to suppose that the microdunes on Venus could evolve into much larger features than those observed in experiments. In addition, the researchers note that current ripples (which are closely related to microdunes) are often found in association with giant ripples that have dimensions similar to aeolian dunes. Thus, it may be reasonable to assume that analogous large scale structures occur on Venus. Both (terrestrial) aeolian and subaqueous environments generate structures in excess of one hundred meters in wavelength. Such dimensions may therefore be applicable to Venusian bedforms. Analysis of Magellan data may resolve the issue. Author

N92-10801*# National Aeronautics and Space Administration. Ames Research Center, Moffett Field, CA.
RELATIONSHIPS BETWEEN TOPOGRAPHIC ROUGHNESS AND AEOLIAN PROCESSES
Ronald Greeley, N. Lancaster, L. Gaddis, K. R. Rasmussen, B. R. White, R. S. Saunders, S. Wall, Anthony R. Dobrovolskis, and J. D. Iversen (Iowa State Univ. of Science and Technology, Ames.) *In* NASA, Washington, Reports of Planetary Geology and Geophysics Program, 1990 Jun. 1991 p 195-197 (For primary document see N92-10728 01-91)
Avail: NTIS HC/MF A25 CSCL 03B

The interaction between winds and desert surfaces has important implications for sediment transport on Earth, Mars, and Venus, and for understanding the relationships between radar backscatter and aerodynamic roughness as part of the NASA Shuttle Imaging radar (SIR-C) Mission. Here, researchers report results from measurements of boundary layer wind profiles and surface roughness at sites in Death Valley and discuss their implications. The sites included a flat to undulating gravel and sand reg, alluvial fans, and a playa. Estimates of average particle size composition of Death Valley sites and arithmetic mean values of aerodynamic roughness are given in tabular form. Author

N92-10802*# Jet Propulsion Lab., California Inst. of Tech., Pasadena.
USE OF RADAR TO ASSESS AEOLIAN PROCESSES Abstract Only
Ronald Greeley, N. Lancaster, L. Gaddis, D. Blumberg, A. Debrovolskis, R. S. Saunders, S. Wall, J. D. Iversen, B. White, and K. R. Rasmussen (Aarhus Univ., Denmark) *In* NASA, Washington, Reports of Planetary Geology and Geophysics Program, 1990 Jun. 1991 p 198 (For primary document see N92-10728 01-91)
Avail: NTIS HC/MF A25 CSCL 03B

The interaction between wind and desert surfaces has important implications for sediment transport on Earth, Mars, and Venus, and for understanding the relationship between radar backscatter and aerodynamic roughness. Here, researchers report results from measurements of atmospheric boundary layer profiles, assessment of radar backscatter at P, L, and C wavelengths, and surface roughness in Death Valley, the Mojave Desert, and Lunar Lake, NV, and discuss the implications for aeolian process. The sites include playas, gravel and sand regs, alluvial fans, and lava flows. Boundary layer wind profiles were measured using anemometers at heights of 0.75, 1.25, 2.07, 3.44, 5.72, and 9.5 m; temperature sensors at heights of 1.3 and 9.6 m; and wind vanes at 9.7 and 1.5 m. Microtopographic measurements were made using a template and a laser-photo device to obtain RMS height. This study demonstrates that radar backscatter coefficients obtained from airborne and perhaps orbiting instruments could permit the derivation of aerodynamic roughness values for large areas. Such values, when combined with wind frequency data, could enable assessment of aeolian processes on a regional scale. Author

N92-10803*# National Aeronautics and Space Administration. Ames Research Center, Moffett Field, CA.
FREE CONVECTION IN THE MARTIAN ATMOSPHERE
G. D. Clow (Geological Survey, Menlo Park, CA.) and R. M. Haberle *In* NASA, Washington, Reports of Planetary Geology and Geophysics Program, 1990 Jun. 1991 p 199-200 (For primary document see N92-10728 01-91)
Avail: NTIS HC/MF A25 CSCL 03B

Researchers investigated the free convective regime for the Martian atmospheric boundary layer (ABL). Researchers generalized Schumann's model describing horizontal fluctuations and mean vertical gradients occurring during free convection to include convection driven by water vapor gradients and to include the effects of circulation above both aerodynamically smooth and rough surfaces. Applying the model to Mars, researchers found that nearly all the resistance to sensible and latent heat transfer in the ABL occurs within the thin interfacial sublayer at the surface. Free convection is found to readily occur at low pressures and high temperatures when surface ice is present. At 7 mb, the ABL should freely convect whenever the mean windspeed at the top of the surface layer drops below about 2.5 m s(-1) and surface temperatures exceed 250 K. Mean horizontal fluctuations within the surface layer are found to be as high as 3 m (-1) for windspeed, 0.5 K for temperature, and 10 (-4) kg m (-3) for water vapor density. Airflow over surfaces similar to the Antarctic Polar Plateau was found to be aerodynamically smooth on Mars during free convection for all pressures between 6 and 1000 mb, while surfaces with z sub o approx. equals 1 cm are aerodynamically rough over this pressure range. Author

N92-10804*# National Aeronautics and Space Administration. Ames Research Center, Moffett Field, CA.

CHARACTERISTICS OF THE MARTIAN ATMOSPHERE SURFACE LAYER

G. D. Clow (Geological Survey, Menlo Park, CA.) and R. M. Haberle *In* NASA, Washington, Reports of Planetary Geology and Geophysics Program, 1990 Jun. 1991 p 201-202 (For primary document see N92-10728 01-91)

Avail: NTIS HC/MF A25 CSCL 03B

Researchers extend elements of various terrestrial boundary layer models to Mars in order to estimate sensible heat, latent heat, and momentum fluxes within the Martian atmospheric surface layer. To estimate the molecular viscosity and thermal conductivity of a CO2-H2O gas mixture under Martian conditions, parameterizations were developed. Parameterizations for specific heat and and binary diffusivity were also determined. The Prandtl and Schmidt numbers derived from these thermophysical properties were found to range from 0.78 - 1.0 and 0.47 - 0.70, respectively, for Mars. Brutsaert's model for sensible and latent heat transport within the interfacial sublayer for both aerodynamically smooth and rough airflow was experimentally tested under similar conditions, validating its application to Martian conditions. For the surface sublayer, the researchers modified the definition of the Monin-Obukhov length to properly account for the buoyancy forces arising from water vapor gradients in the Martian atmospheric boundary layer. This length scale was then utilized with similarity theory turbulent flux profiles with the same form as those used by Businger et al. and others. It was found that under most Martian conditions, the interfacial and surface sublayers offer roughly comparable resistance to sensible heat and water vapor transport and are thus both important in determining the associated fluxes.

Author

N92-10805*# Hawaii Univ., Honolulu. Planetary Geosciences Div.

HEAT FLOW VS. ATMOSPHERIC GREENHOUSE ON EARLY MARS

F. P. Fanale and S. E. Postawko *In* NASA, Washington, Reports of Planetary Geology and Geophysics Program, 1990 Jun. 1991 p 203-205 (For primary document see N92-10728 01-91)

Avail: NTIS HC/MF A25 CSCL 03B

Researchers derived a quantitative relationship between the effectiveness of an atmospheric greenhouse and internal heat flow in producing the morphological differences between earlier and later Martian terrains. The derivation is based on relationships previously derived by other researchers. The reasoning may be stated as follows: the CO2 mean residence time in the Martian atmosphere is almost certainly much shorter than the total time span over which early climate differences are thought to have been sustained. Therefore, recycling of previously degassed CO2 quickly becomes more important than the ongoing supply of juvenile CO2. If so, then the atmospheric CO2 pressure, and thereby the surface temperature, may be approximated mathematically as a function of the total degassed CO2 in the atmosphere plus buried material and the ratio of the atmospheric and regolith mean residence times. The latter ratio can also be expressed as a function of heat flow. Hence, it follows that the surface temperature may be expressed as a function of heat flow and the total amount of available CO2. However, the depth to the water table can simultaneously be expressed as a function of heat flow and the surface temperature (the boundary condition). Therefore, for any given values of total available CO2 and regolith conductivity, there exist coupled independent equations which relate heat flow, surface temperature, and the depth to the water table. This means we can now derive simultaneous values of surface temperature and the depth of the water table for any value of the heat flow. The derived relationship is used to evaluate the relative importance of the atmospheric greenhouse effect and the internal regolith thermal gradient in producing morphological changes for any value of the heat flow, and to assess the absolute importance of each of the values of the heat flow which are thought to be reasonable on independent geophysical grounds.

Author

N92-10806*# Massachusetts Inst. of Tech., Cambridge. Dept. of Earth, Atmospheric and Planetary Sciences.

DEGRADATION OF Fe-Mg SILICATES IN HOT CO2 ATMOSPHERES: APPLICATIONS TO VENUS

DArcy W. Straub and Roger G. Burns *In* NASA, Washington, Reports of Planetary Geology and Geophysics Program, 1990 Jun. 1991 p 207-209 (For primary document see N92-10728 01-91)

(Grant NAGw-2037)

Avail: NTIS HC/MF A25 CSCL 03B

Experiments demonstrated that oxidation of ferromagnesian silicates and magnetite occurs when these minerals are heated at 800 C in 1 atmosphere of CO2, under which conditions hematite is thermodynamically stable. The 30 ppm oxygen impurity in CO2 presumably facilitates the oxidation of some of the ferrous iron initially present in the crystal structures of the minerals. Mossbauer spectral measurements reveal, however, that only CO2 degraded olivine and pigeonite is hematite formed as a magnetically ordered phase at ambient temperatures. In orthopyroxene, some of the ferric iron produced by oxidation is present as nanophase hematite which, because it remains superparamagnetic until 4.2 K, must exist as particles less than or equal to 4 nm in diameter. In the calcic pyroxenes much of the oxidized ferrous iron may still remain as structural Fe3(+) in the host silicates. Some ferric iron may also be present as unit cell sized Fe2O3 inclusions in the pyroxenes, or be segregated along cleavage planes, or be coating mineral grains. In these states of aggregation, the Fe2O3 is unidentifiable by x ray diffraction and in low temperature Mossbauer spectra. Applications of this research to the surface of Venus are discussed.

Author

N92-10807*# Arizona Univ., Tucson. Lunar and Planetary Lab.

THEORETICAL STUDIES OF VOLATILE PROCESSES IN THE OUTER SOLAR SYSTEM

Jonathan I. Lunine *In* NASA, Washington, Reports of Planetary Geology and Geophysics Program, 1990 Jun. 1991 p 210-212 (For primary document see N92-10728 01-91)

Avail: NTIS HC/MF A25 CSCL 03B

Four studies of volatile processes in the outer solar system are discussed. Researchers suggest that the convective and conductive regions of Triton's atmosphere join at the tropopause near 10 km. A model of volatile transport on Triton's surface was constructed that predicts that Triton's surface north of 15 degrees north latitude is experiencing deposition of nitrogen frosts, as are the bright portions of the south polar cap near the equator. Also discussed are numerical models of the evolution of Titan's surface and atmosphere. Results of a study of the rheology of ammonia-water liquids were applied to the icy satellites of the outer solar system. Finally, the researchers examined the frictional heating, sublimation, and re-condensation of grains free-falling into the solar nebula from a surrounding interstellar cloud. The sublimation model includes the effect of various volatile species and accounts for the poor radiating properties of small grains using Mie theory.

Author

N92-10808*# Jet Propulsion Lab., California Inst. of Tech., Pasadena.

CRUSTAL HETEROGENEITY OF THE MOON VIEWED FROM THE GALILEO SSI CAMERA: LUNAR SAMPLE CALIBRATIONS AND COMPOSITIONAL IMPLICATIONS

Carle M. Pieters, M. Belton, T. Becker, M. H. Carr, C. Chapmann, F. P. Fanale, Erich M. Fischer, L. Gaddis, Ronald Greeley, and R. Greenberg (Arizona Univ., Tucson.) et al *In* NASA, Washington, Reports of Planetary Geology and Geophysics Program, 1990 Jun. 1991 p 218-219 (For primary document see N92-10728 01-91)

Avail: NTIS HC/MF A25 CSCL 03B

Summaries are given of the spectral calibration, compositional parameters, nearside color, and limb and farside color of the Moon. The farside of the Moon, a large area of lunar crust, is dominated by heavily cratered terrain and basin deposits that represent the products of the first half billion years of crustal evolution. Continuing analysis of the returned lunar samples suggest a magma ocean

and/or serial magmatism model for evolution of the primordial lunar crust. However, testing either hypothesis requires compositional information about the crustal stratigraphy and lateral heterogeneity. Resolution of this important planetary science issue is dependent on additional data. New Galileo multispectral images indicate previously unknown local and regional compositional diversity of the farside crust. Future analysis will focus on individual features and a more detailed assessment of crustal stratigraphy and heterogeneity. Author

N92-10809*# Hawaii Univ., Honolulu.
REMOTE SENSING AND GEOLOGIC STUDIES OF THE ORIENTALE BASIN REGION
B. Ray Hawke, P. G. Lucey, G. J. Taylor, Jeffrey F. Bell, C. A. Peterson, D. Blewett, K. Horton, and P. D. Spudis (Lunar and Planetary Inst., Houston, TX.) *In* NASA, Washington, Reports of Planetary Geology and Geophysics Program, 1990 Jun. 1991 p 220-222 (For primary document see N92-10728 01-91)
Avail: NTIS HC/MF A25 CSCL 03B

Both visual and near-infrared spectral observations are combined with multispectral imaging to study the Orientale interior and exterior, the Cruger region, Grimaldi Region, the Schiller-Schickard Region, and the Humorum Region of the Moon. It was concluded that anorthosites occur in the Inner Rook Mountains of Orientale, the inner ring of Grimaldi, and the main ring of Humorum. Imaging spectroscopy shows that the entire eastern Inner Rook Mountains are composed of anorthosites. Orientale ejecta are strikingly like the surface materials in the region where Apollo 16 landed. This similarity indicates similar mineralogy, i.e., noritic anorthosite. Thus, Orientile ejecta is more mafic than the Inner Rook Mountains. This situation is also true for the Nectaris, Humorum, and Gramaldi basins. Isolated areas of the Orientale region show the presence of gabbroic rocks, but, in general, Orientale ejecta are noritic anorthosites, which contain much more low-Ca pyroxene than high-Ca pyroxene. Ancient (pre-Orientale) mare volcanism apparently occurred in several areas of the western limb. Author

N92-10810*# National Aeronautics and Space Administration. Lyndon B. Johnson Space Center, Houston, TX.
REMOTE SENSING AND GEOLOGIC STUDIES OF THE TERRAIN NORTHWEST OF HUMORUM BASIN
B. Ray Hawke, C. A. Peterson, P. G. Lucey, G. J. Taylor, Jeffrey F. Bell, D. Blewett, B. Campbell, Cassandra R. Coombs, and P. D. Spudis (Lunar and Planetary Inst., Houston, TX.) *In* NASA, Washington, Reports of Planetary Geology and Geophysics Program, 1990 Jun. 1991 p 223-225 (For primary document see N92-10728 01-91)
Avail: NTIS HC/MF A25 CSCL 03B

A portion of the highlands terrain northwest of the Humorum basin, a large multiringed impact structure on the southwestern portion of the lunar nearside, exhibits anomalous characteristics in several remote sensing data sets. A variety of remote sensing studies of the terrain northwest of Humorum basin were performed in order to determine the composition and origin of the anomalous unit as well as the composition of the highland material exposed by the Humorum impact event. It was found that at least a portion of the mare-bounding ring of Humorum is composed of pure anorthosite. Other details of the study are reported. Author

N92-10811*# Brown Univ., Providence, RI. Dept. of Geological Sciences.
ANALYSES OF THE LUNAR SURFACE WITH ADVANCED REMOTE SENSORS: EXPECTATIONS FOR THE 1990'S
Abstract Only
Carle M. Pieters *In* NASA, Washington, Reports of Planetary Geology and Geophysics Program, 1990 Jun. 1991 p 226 (For primary document see N92-10728 01-91)
Avail: NTIS HC/MF A25 CSCL 03B

Today's advanced sensor capabilities provide unprecedented opportunities for exploration that mesh well with the science requirements for a sophisticated integration of several types of remotely acquired information. Science priorities for the 1990's include an evaluation of the global composition and structure of the primordial lunar crust in order to model its origin and evolution, using the Moon as a natural laboratory to study the impact process and time-cumulative events at 1 AU, and, ultimately, constraining the origin of the Moon and its relation to Earth. Author

N92-10812*# San Juan Capistrano Research Inst., CA.
INFRARED REFLECTANCE SPECTRA (4-12 MICRON) OF LUNAR SAMPLES
Douglas B. Nash *In* NASA, Washington, Reports of Planetary Geology and Geophysics Program, 1990 Jun. 1991 p 227-228 (For primary document see N92-10728 01-91)
Avail: NTIS HC/MF A25 CSCL 03B

Presented here are infrared reflectance spectra of a typical set of Apollo samples to illustrate spectral character in the mid-infrared (4 to 12 microns) of lunar materials and how the spectra varies among three main forms: soil, breccia, and igneous rocks. Reflectance data, to a close approximation, are the inverse of emission spectra; thus, for a given material the spectral reflectance (R) at any given wavelength is related to emission (E) by 1 - R equals E. Therefore, one can use reflectance spectra of lunar samples to predict how emission spectra of material on the lunar surface will appear to spectrometers on orbiting spacecraft or earthbound telescopes. Spectra were measured in the lab in dry air using a Fourier Transform Infrared spectrometer. Shown here is only the key portion (4 to 12 microns) of each spectrum relating to the principal spectral emission region for sunlit lunar materials and to where the most diagnostic spectral features occur. Author

N92-10813*# Colorado Univ., Boulder. Lab. for Atmospheric and Space Physics.
REMOTE SENSING OF THE MARTIAN SURFACE
Bruce M. Jakosky, Bradley G. Henderson, Cora E. Randall, M. Joan Alexander, and Thomas M. McCollom *In* NASA, Washington, Reports of Planetary Geology and Geophysics Program, 1990 Jun. 1991 p 229-230 (For primary document see N92-10728 01-91)
Avail: NTIS HC/MF A25 CSCL 03B

Researchers investigated the physical properties of the Martian surface as inferred from a combination of orbiting and earth-based remote sensing observations and in-situ observations. This approach provides the most detailed and self-consistent view of the global and regional nature of the surface. Results focus on the areas of modeling the diurnal variation of the surface temperature of Mars, incorporating the effects of atmospheric radiation, with implications for the interpretation of surface thermal inertia; modeling the thermal emission from particulate surfaces, with application to observations of the surfaces of the Earth, Moon, and Mars; modeling the reflectance spectrum of Mars in an effort to understand the role of particle size in the difference between the bright and dark regions; and determining the slope properties of different terrestrial surfaces and comparing them with planetary slopes derived from radar observations. Author

N92-10814*# Jet Propulsion Lab., California Inst. of Tech., Pasadena.
MINERALOGY OF THE MARTIAN SURFACE FROM MARINER 6/7 INFRARED SPECTROMETER DATA
T. Z. Martin *In* NASA, Washington, Reports of Planetary Geology and Geophysics Program, 1990 Jun. 1991 p 231-233 (For primary document see N92-10728 01-91)
Avail: NTIS HC/MF A25 CSCL 03B

The Mariner 6/7 Infrared Spectrometer (IRS) experiment data from the 1969 Mars flyby encounters represent a valuable source of information about the IR reflection/emission spectrum of Mars in the 1.9 and 14.4 micron region. During 1990, the wavelength calibration of the IRS data was completely redone, using information from inflight spectra of Mars taken through a polystyrene film and from the locations of Martian CO2 bands. The response functions of the two instruments were then rederived using laboratory black body spectra. Also, a particular approach was taken to study the IRS data in which the effects of uncertain wavelength and intensity

calibration can be minimized. This involves doing ratios of spectra. These are of particular value when applied to study contrasts between various albedo domains on the Mars surface and between spectra with differing emission angle. The latter provide a means of assessing the contribution of the atmosphere and airborne dust to the spectra. Given here are graphs showing two near infrared radiance spectra for very different albedo regions and a ratio of two spectra obtained at very different total solar pathlength (airmass). Author

N92-10815*# Brown Univ., Providence, RI. Dept. of Geology Sciences.

COMPOSITION OF SYRTIS MAJOR VOLCANIC PLATEAU

John F. Mustard, S. Erard, Jean-Pierre Bibring, Yves Langevin (Paris II Univ., Orsay, France), James W. Head, and Carle M. Pieters *In* NASA, Washington, Reports of Planetary Geology and Geophysics Program, 1990 Jun. 1991 p 234-235 (For primary document see N92-10728 01-91)

Avail: NTIS HC/MF A25 CSCL 03B

Syrtis Major, a low-relief volcanic shield centered near 295 degrees 10 degrees N, is an old, well-preserved and exposed volcanic region on Mars which formed at the end of the heavy bombardment period. The composition of these volcanic materials has importance for understanding the thermal and chemical history of Mars. Imaging spectrometer data of the Syrtis Major volcanic plateau are used in this analysis to identify major compositional components. First and second order even channel reflectance spectra between 0.77 and 2.55 microns from four broad classes of materials on Syrtis Major are given. For the volcanic materials, there are three primary classes characterized by albedo, slope, and shape of the 10 micron band. To emphasize the latter, straight line continua were removed from each spectral segment and replotted in another figure. Each spectrum shows a band minima near 0.96 microns and 2.15 microns indicative of pyroxene mineral absorptions. Comparison of these band minima with studies of pyroxene reflectance spectra suggests that the pyroxenes in the volcanics of Syrtis Major are high calcium pyroxene with a Ca/(Mg+Fe+Ca) ratio of 0.2 to 0.3. The most likely pyroxene is an augite. Author

N92-10816*# Brown Univ., Providence, RI. Dept. of Geological Sciences.

THE PERPLEXING CONTINUUM SLOPE OF MARS: EFFECTS OF THIN FERRIC COATINGS AND VIEWING GEOMETRY

Erich M. Fischer, Carle M. Pieters, and Stephen F. Pratt *In* NASA, Washington, Reports of Planetary Geology and Geophysics Program, 1990 Jun. 1991 p 236-237 (For primary document see N92-10728 01-91)

(Grant NAGw-748)

Avail: NTIS HC/MF A25 CSCL 03B

The experiment discussed here was designed to constrain interpretations of variations in continuum slope variations which define several spectral annuli on the flanks of Olympus Mons, observed in the Imaging Spectrometer (IMS) data. The IMS Olympus Mons data reveal that the rings, seen as alternating brighter and darker reflectance in Viking data, correspond to annuli of alternating shallower and steeper continuum slope. At least three factors contributing to continuum slope are identified: ferric coating thickness, viewing geometry, and surface texture. Because the Olympus Mons spectral annuli were observed at nearly constant backscatter geometries in the ISM data, with only slight viewing variations due to the volcanoe's flank slopes, the difference of continuum slope between annuli probably cannot be explained by viewing geometry alone. This suggests that the variation of some fundamental surface characteristics, such as ferric dust/rind thickness or surface texture, is the cause of the Olympus Mons special annuli observed in the ISM imaging spectrometer data. Author

N92-10817*# Arizona Univ., Tucson. Planetary Image Research Lab.

OXIDATION OF BASALTIC TEPHRAS: INFLUENCE ON REFLECTANCE IN THE 1 MICRON REGION

William H. Farrand and Robert B. Singer *In* NASA, Washington, Reports of Planetary Geology and Geophysics Program, 1990 Jun. 1991 p 238-239 (For primary document see N92-10728 01-91)

Avail: NTIS HC/MF A25 CSCL 03B

As part of a ongoing study into the products of hydrovolcanism, tuffs were examined from the Cerro Colorado and Pavant Butte tuff cones. The former resides in the northeastern corner of the Pinacate Volcanic Field in Sonara, Mexico and the latter is in the Black Rock Desert of southern Utah. Numerous samples were collected and many of these had their Vis/IR reflectance measured. It seems likely that in the palagonite tuffs there is a combination of nanocrystalline ferric oxide phases contributing to the UV absorption edge, but not to the 1 micron band, plus more crystalline ferric oxides which do contribute to that band as well as ferrous iron within unaltered sideromelane which is skewing the band center to longer wavelengths. This work has implications for the study of Mars. The present work indicates that when ferrous and ferric iron phases are both present, their combined spectral contribution is a single band in the vicinity of 1 micron. The center, depth, and width of that feature has potential to be used to gauge the relative proportions of ferrous and ferric iron phases. Author

N92-10818*# National Aeronautics and Space Administration. Ames Research Center, Moffett Field, CA.

SPECTROSCOPIC ANALYSES OF Fe AND WATER IN CLAYS: A MARTIAN SURFACE WEATHERING STUDY

J. L. Bishop, Carle M. Pieters, J. O. Edwards, L. M. Coyne (San Jose State Univ., CA.), and S. Chang *In* NASA, Washington, Reports of Planetary Geology and Geophysics Program, 1990 Jun. 1991 p 240-241 (For primary document see N92-10728 01-91)

(Grant NAGw-748)

Avail: NTIS HC/MF A25 CSCL 03B

Martian surface morphology suggests the presence of liquid H2O on Mars in the past. Reflectance spectra of the Martian surface include features which correspond to the crystal field transitions of iron, as well as features supporting the presence of ice and minerals containing structural OH and surface water. Researchers initiated further spectroscopic studies of surface iron and water and structural OH in clays in order to determine what remotely obtained spectra can indicate about the presence of clays on Mars based on a clearer understanding of the factors influencing the spectral features. Current technology allows researchers to better correlate the low frequency fundamental stretching and bending vibrations of O-H bonds with the diagnostic near infrared overtone and combination bands used in mineral characterization and identification. Author

N92-10819*# Jet Propulsion Lab., California Inst. of Tech., Pasadena.

WATER DETECTION AT THE MOON, MARS AND COMETS WITH A COMBINED NEUTRON GAMMA RAY INSTRUMENT

Albert E. Metzger and Eldon L. Haines (Sunrise Research, Inc., Eugene, OR.) *In* NASA, Washington, Reports of Planetary Geology and Geophysics Program, 1990 Jun. 1991 p 242-243 (For primary document see N92-10728 01-91)

Avail: NTIS HC/MF A25 CSCL 03B

Measuring the fluxes of thermal and epithermal neutrons at a planetary object in conjunction with gamma-ray spectroscopic observations will provide information about the chemical composition of the surface which is less model dependent than the gamma ray measurements by themselves. Researchers devised a passive neutron detector for this purpose. An experimental model was designed and built. Three variables provided the basis for a set of experiments: thickness of the Sm and B layers, the presence or absence of the ACS, and the position of the source relative to the PND's cylindrical axis. Experimental results are given. Author

N92-10820*# Geological Survey, Denver, CO.

SPECTRAL EVIDENCE FOR CARBONATES ON MARS: HYDROUS CARBONATES

W. M. Calvin and T. V. V. King *In* NASA, Washington, Reports

of Planetary Geology and Geophysics Program, 1990 Jun. 1991 p 244-245 (For primary document see N92-10728 01-91)
Avail: NTIS HC/MF A25 CSCL 03B

Although many of the spectral features of the Martian samples studied are not unique mineralogical indicators, much of the current spectral data is consistent with (possibly abundant) hydrous carbonates on the surface of Mars. The absorption features in the measured samples were quite weak compared with those of anhydrous carbonates. The weak features imply that significantly more hydrous carbonates can be incorporated onto the surface before becoming spectrally evident; however, exact limits have yet to be determined. The stability of these materials in the Martian environment is not known, but their formation and occurrence in low temperature terrestrial environments makes them appealing candidates for weathering products on Mars. Author

N92-10821*# Washington Univ., Seattle. Geophysics Program.
OPTICAL PROPERTIES OF CO2 ICE AND CO2 SNOW FROM ULTRAVIOLET TO INFRARED: APPLICATION TO FROST DEPOSITS AND CLOUDS ON MARS
Gary B. Hansen, Stephen G. Warren, and Conway B. Leovy *In* NASA, Washington, Reports of Planetary Geology and Geophysics Program, 1990 Jun. 1991 p 246-248 (For primary document see N92-10728 01-91)
(Grant NAGw-1734)
Avail: NTIS HC/MF A25 CSCL 03B

Researchers found that it is possible to grow large clear samples of CO2 ice at Mars-like temperatures of 150-170K if a temperature controlled refrigerator is connected to an isolated two-phase pure CO2 system. They designed a chamber for transmission measurements whose optical path between the 13mm diameter window is adjustable from 1.6mm to 107mm. This will allow measurements of linear absorption down to less than 0.01 cm (exp -1). A preliminary transmission spectrum of a thick sample of CO2 ice in the near infrared was obtained. Once revised optical constants have been determined as a function of wavelength and temperature, they can be applied to spectral reflectance/emissivity models for CO2 snow surfaces, both pure and contaminated with dust and water ice, using previously established approaches. It will be useful, also, to develop an infrared scattering-emission cloud radiance model (especially as viewed from near the limb) in order to develop a strategy for the identification of CO2 cloud layers by the atmospheric infrared radiometer instrument on the Mars Observer. Author

N92-10822*# Brown Univ., Providence, RI. Dept. of Geological Sciences.
DISK-RESOLVED SPECTRAL REFLECTANCE PROPERTIES OF PHOBOS FROM 0.3-3.2 MICRON: PRELIMINARY INTEGRATED RESULTS FROM PHOBOS 2
Scott L. Murchie, Stephane Erard, Yves Langevin, Daniel T. Britt, Jean-Pierre Bibring (Paris II Univ., Orsay, France), John F. Mustard, James W. Head, and Carle M. Pieters *In* NASA, Washington, Reports of Planetary Geology and Geophysics Program, 1990 Jun. 1991 p 249-250 (For primary document see N92-10728 01-91)
Avail: NTIS HC/MF A25 CSCL 03B

The Phobos 2 mission provided multispectral observations of Phobos over a large wavelength range and with relatively high spectral resolution. Here, researchers integrate results from three multispectral detectors by determining the ultraviolet-visible near infrared spectral properties of color and brightness features recognized in VSK TV images. Researchers present evidence that there are two fundamental spectral units within the region of overlapping coverage by the detectors. They describe the units' spectral and reflectance properties and discuss the implications of these results for the composition of Phobos. Author

N92-10823*# Massachusetts Inst. of Tech., Cambridge.
REFLECTANCE SPECTRA OF Fe(2+)-Mg(2+) DISORDERED PYROXENES: IMPLICATIONS TO REMOTE-SENSED SPECTRA OF PLANETARY SURFACES
Roger G. Burns, James R. Besancon, and Stephen F. Pratt (Brown Univ., Providence, RI.) *In* NASA, Washington, Reports of Planetary Geology and Geophysics Program, 1990 Jun. 1991 p 253-255 (For primary document see N92-10728 01-91)
(Grants NAGw-2037; NAGw-748)
Avail: NTIS HC/MF A25 CSCL 03B

The reflectance spectra of Fe(2+)-Mg(2+) disordered orthopyroxenes are relevant to surfaces of terrestrial planets onto which basaltic magma has been extruded. If cooling rates of basalt lava flows were fast, equilibrium iron intersite partitioning may not have been achieved so that abnormal enrichments of Fe(2+) ions in M1 sites would occur. The two intense pyroxene Fe(2+) site CF bands in the 1 micron and 2 micron regions would continue to dominate the the reflectance spectra so that the pyroxene composition and structure type would be readily identified in telescopic spectral profiles. However, abnormal intensification of the Fe(2+)/M1 site CF band at 1.20 microns could lead to the false identification of olivine in remote sensed spectra because in pyroxene-olivine mixtures the inflection around 1.20 microns is the only spectral feature for detecting the presence of olivine. The identification of iron-bearing plagioclase feldspars, too, would be obscured by the pyroxene Fe(2+)/M1 site CF band at 1.20 microns. Such interference would be a major problem if in situ reflectance spectra could be measured on the surface of Venus where ambient temperatures are as high as 475 C. Disordering of Fe(2+) and Mg(2+) ions comparable to that in the orthopyroxenes used in this spectral chemical study might be expected in low Ca pyroxenes occurring on the Venusian surface. Researchers conclude that Fe(2+)/M1 site spectral features need to be carefully assessed in remote-sensed spectra before deductions are made about the presence of olivine on planetary surfaces. Author

N92-10824*# Massachusetts Inst. of Tech., Cambridge. Dept. of Earth, Atmospheric and Planetary Sciences.
PRE-TERRESTRIAL OXIDATION PRODUCTS IN CARBONACEOUS METEORITES IDENTIFIED BY MOSSBAUER SPECTROSCOPY **c90**
Roger G. Burns and Duncan S. Fisher *In* NASA, Washington, Reports of Planetary Geology and Geophysics Program, 1990 Jun. 1991 p 256-258 (For primary document see N92-10728 01-91)
(Grant NAGw-2037)
Avail: NTIS HC/MF A25 CSCL 03B

The occurrence of ferric bearing assemblages, comprising phyllosilicates, oxide hydroxides and magnetite, in carbonaceous chondrites (CC) indicates that these meteorites underwent pre-terrestrial, sub-aqueous oxidation reactions. Reported here are results of a Mossbauer spectral study of a suite of CC demonstrating that a variety of ferrous and ferric bearing phases may be distinguished in different classes of this meteorite type. Author

N92-10825*# Massachusetts Inst. of Tech., Cambridge. Dept. of Earth, Atmospheric and Planetary Sciences.
DOES LAFAYETTE = NAKHLA? NOT NECESSARILY SO, BASED ON 4.2K MOSSBAUER SPECTRA OF ALL OF THE SNC METEORITES **c90**
Roger G. Burns *In* NASA, Washington, Reports of Planetary Geology and Geophysics Program, 1990 Jun. 1991 p 259-261 (For primary document see N92-10728 01-91)
(Grant NAGw-2037)
Avail: NTIS HC/MF A25 CSCL 03B

In previous Mossbauer spectral studies of many of the Shergotite Nakhlite Chassignite (SNC) meteorites, attention was drawn to the close similarities of spectrum profiles between Lafayette and Nakhla, which were once suggested to be identical meteorites. These observations led to the acquisition of Governador Valadares and another specimen of Nakhla, as well as Zagami and Shergotty, for Mossbauer spectral measurements at 4.2K. Results reported here demonstrate that there are subtle differences between the three nakhlites (Nakhla, Lafayette, and Governador Valadares), as there are for three of the shergottites (Shergotty, Zagami, EETA 79001/lithologies A and B) and olivine-dominated

Chassigny and ALHA 77005, indicating that all eight of the SNC meteorites discovered to data fell independently to Earth. Author

N92-10826*# Johns Hopkins Univ., Baltimore, MD. Dept. of Earth and Planetary Sciences.
INFRARED (2.08-14 MICRON) SPECTRA OF POWERED STONY METEORITES **c90**
J. W. Salisbury, D. M. DAria, and E. Jarosewich (National Museum of Natural History, Washington, DC.) *In* NASA, Washington, Reports of Planetary Geology and Geophysics Program, 1990 Jun. 1991 p 262-264 (For primary document see N92-10728 01-91)
Avail: NTIS HC/MF A25 CSCL 03B

Infrared biconical reflectance spectra of 60 powdered meteorite samples, representing 50 different stony meteorites, were measured as analogues of asteroidal regolith. Representative samples were measured in directional hemispherical reflectance to assure that Kirchhoff's Law can be used to predict relative emissivity from the reflectance spectra. These spectral data confirm that the O-H fundamental absorption band near 2.9 microns is an extremely sensitive indicator of incipient alteration, which often has taken place in powdered meteorite samples exposed only to water vapor in the air. Such non-carbonaceous samples typically contain less than 1 percent water by weight. Likewise, the C-H fundamental absorption bands near 3.4 and 3.5 microns are equally sensitive indicators of contamination with volatile hydrocarbons, which can also be absorbed from the air. The heavy, macromolecular hydrocarbons native to chondrites do not display such heavy bands, making detection of these bands in remote sensing of asteroids unlikely. Despite the spectral artifacts introduced by alteration and hydrocarbon contamination, powdered stony meteorites display a wide variety of real spectral features that can be used for their identification, including residual reststrahlen bands, absorption bands, and the Christiansen feature. Researchers found that the wavelengths of the peaks or troughs of each of these spectral features can be used independently to infer meteorite composition, but the best results are obtained when the entire spectral curve is used, or at least the portion of it encompassed by the 8 to 14 micron atmospheric window, in a digital search library. Author

N92-10827*# Brown Univ., Providence, RI. Dept. of Geological Sciences.
DARKENING IN GAS-RICH ORDINARY CHONDRITES: SPECTRAL MODELLING AND IMPLICATIONS FOR THE REGOLITHS OF ORDINARY CHONDRITE PARENT BODIES **c90**
Daniel T. Britt and Carle M. Pieters *In* NASA, Washington, Reports of Planetary Geology and Geophysics Program, 1990 Jun. 1991 p 265-266 (For primary document see N92-10728 01-91)
Avail: NTIS HC/MF A25 CSCL 03B

The dark fine grained matrix of gas-rich ordinary chondrites replicates many of the physical, morphological, and spectral characteristics of the highly shocked and optically altered black chondrites. Spectral mixture modeling shows that the darkening and spectral attenuation seen in the dark matrix can be simulated with realistic mass fractions of light host material and black chondritic material. All these factors point to the conclusion that the dark matrix of gas-rich ordinary chondrites is dark due to the same processes that darkens black chondrites, shock distributed small particle size FeNi metal and troilite. Because the darkening is not seen in any of the non-gas-rich light portions and is only seen in the gas rich grains of the meteorite, the shock darkening would have to occur as part of the matrix's exposure to regolith processes. Since all gas-rich grains are darkened, it follows that darkening is not only common, but pervasive in asteroidal regoliths. These results imply that the upper, optically active layer of an ordinary chondrite parent body should have the spectral characteristics of a black chondrite, which are a dark, relatively featureless spectrum with modest red slope in the infrared. These are the characteristics of special type C asteroids. Author

N92-10828*# Brown Univ., Providence, RI. Dept. of Geological Sciences.
THE BIDIRECTIONAL REFLECTANCE SPECTRA OF FIVE GAS-RICH ORDINARY CHONDRITES **c90**
Daniel T. Britt and Carle M. Pieters *In* NASA, Washington, Reports of Planetary Geology and Geophysics Program, 1990 Jun. 1991 p 267-268 (For primary document see N92-10728 01-91)
(Grants NAGw-28; NAGw-748)
Avail: NTIS HC/MF A25 CSCL 03B

In general, the spectra of the dark areas of gas-rich ordinary chondrites show reductions in both reflectance and band depth relative to the spectra of the light areas and the spectra of normal ordinary chondrites. The dark areas of these samples show spectral alteration despite having substantial fractions of light material intimately mixed with the dark, gas-rich grains. If the spectra of the dark gas-rich grains represent the spectral characteristics of a regolith soil on an ordinary chondrite body, then that surface would display a dark and strongly subdued spectrum. Author

N92-10829*# Academy of Sciences (USSR), Moscow.
REFLECTANCE SPECTRA OF SOME FRACTIONS OF MIGEI AND MURCHISON SM CHONDRITES IN THE RANGE OF 0.3-2.6 MICRONS **c90**
L. V. Moroz and Carle M. Pieters (Brown Univ., Providence, RI.) *In* NASA, Washington, Reports of Planetary Geology and Geophysics Program, 1990 Jun. 1991 p 269-270 (For primary document see N92-10728 01-91)
Avail: NTIS HC/MF A25 CSCL 03B

The reddening observed in CM chondrites is not understood. Johnson and Fanale observed that, as CM chondrites are more finely powdered, their spectra become more reddened. In the process of meteorite crushing, the chondrules are broken up. Those authors suggested that in this case the silicate components of the chondrules (mainly olivine), which have higher IR reflectivities, were able to contribute more to the overall spectrum. Gaffey and McCord proposed two possible physical mechanisms which could produce such an effect. But it is also possible that the presence of the organic polymers in the matrix material results in the reddening of the CM spectra. To test these two hypotheses, the matrix material and the material enriched in olivines were separated from Migei and Murchison CM chondrites using a binocular microscope. The spectra of these fractions were compared with the spectra of the bulk samples of Migei and Murchison. The spectra of the most 'clean' Migei matrix fractions indicate that the reddish slopes of CM spectral curves in the near infrared are due to the enhanced olivine feature, rather than to organic matter. The authors propose that the red slope of the spectra of some C-type asteroids may indirectly suggest the presence of olivine in the surface material. At the same time, the red sloped spectra of more distant D-type asteroids seem to be due to the presence of organic materials. If so, then the chemical or physical form of this organic matter must be quite different from the organic materials which would be on the surfaces of the parent bodies of CM chondrites (most likely C-type asteroids). It is also possible that the content of organic components in the CM matrix is too low to change the slope of the spectra. Author

N92-10830*# Arizona Univ., Tucson. Lunar and Planetary Lab.
AN INFRARED REFLECTANCE STUDY OF LOW ALBEDO SURFACE CONSTITUENTS **c90**
Larry A. Lebofsky *In* NASA, Washington, Reports of Planetary Geology and Geophysics Program, 1990 Jun. 1991 p 271-273 (For primary document see N92-10728 01-91)
Avail: NTIS HC/MF A25 CSCL 03B

Observational testing of the idea that the distribution of water is the key to understanding the volatile content of the asteroid belt relies on the exploration of the 3 micron absorption feature in hydrated silicates - the only diagnostic spectral band evident in the dark, volatile rich CI and CM meteorites. The existence of the band has demonstrated the presence of hydrated silicates on asteroids. An example of this feature is shown in the spectrum of the CI meteorite Orgueil. The feature is characterized by a sharp

reflectance drop at 2.7 microns, due to structural OH, and by an absorption due to H2O that decreases slowly out to about 3.5 microns. In their present observational program, researchers are expanding their observational program to include other low-albedo classes of asteroids - asteroids that range primarily from the middle and outer asteroid belt (greater than 2.5 AU) to the Trojan region at 5.2 AU. Preliminary results indicate that the outer belt and Trojan asteroids do not show feature diagnostic of hydrated silicates. Researchers conclude that these asteroids have not undergone the alteration processes that we see in C-class asteroids. Author

N92-10831*# Brown Univ., Providence, RI. Dept. of Geological Sciences.

EFFECTS OF GRAIN SIZE AND SHAPE IN MODELING REFLECTANCE SPECTRA OF MINERAL MIXTURES **c90**

T. Hiroi and Carle M. Pieters *In* NASA, Washington, Reports of Planetary Geology and Geophysics Program, 1990 Jun. 1991 p 274-275 (For primary document see N92-10728 01-91)
(Grant NAGw-748)
Avail: NTIS HC/MF A25 CSCL 03B

The effects of grain size and shape on the reflectance spectra of mineral mixtures are investigated to improve a reflectance model called the isograin model, whose prototype was proposed by M. Kinoshita in 1985. The sample powder was assumed to consist of an infinite number of layers, each of which has the same thickness with the grain size d. Author

N92-10832*# Jet Propulsion Lab., California Inst. of Tech., Pasadena.

LIGHT SCATTERING BY LUNAR-LIKE PARTICLE SIZE DISTRIBUTIONS **c90**

Jay D. Goguen *In* NASA, Washington, Reports of Planetary Geology and Geophysics Program, 1990 Jun. 1991 p 276-278 (For primary document see N92-10728 01-91)
(Grant NASA-PGP-151-01-70-56-00)
Avail: NTIS HC/MF A25 CSCL 03B

A fundamental input to models of light scattering from planetary regoliths is the mean phase function of the regolith particles. Using the known size distribution for typical lunar soils, the mean phase function and mean linear polarization for a regolith volume element of spherical particles of any composition were calculated from Mie theory. The two contour plots given here summarize the changes in the mean phase function and linear polarization with changes in the real part of the complex index of refraction, n - ik, for k equals 0.01, the visible wavelength 0.55 micrometers, and the particle size distribution of the typical mature lunar soil 72141. A second figure is a similar index-phase surface, except with k equals 0.1. The index-phase surfaces from this survey are a first order description of scattering by lunar-like regoliths of spherical particles of arbitrary composition. They form the basis of functions that span a large range of parameter-space. Author

N92-10833*# Brown Univ., Providence, RI.

CHARACTER OF THE OPPOSITION EFFECT AND NEGATIVE POLARIZATION **c90**

Carle M. Pieters, Yu. G. Shkuratov, and D. G. Stankevich (Kharkov State Univ., USSR) *In* NASA, Washington, Reports of Planetary Geology and Geophysics Program, 1990 Jun. 1991 p 279 (For primary document see N92-10728 01-91)
Avail: NTIS HC/MF A25 CSCL 03B

Photometric and polarimetric properties at small phase angles were measured for silicates with controlled surface properties in order to distinguish properties that are associated with surface reflection from those that are associated with multiple scattering from internal grain boundaries. These data provide insight into the causes and conditions of photometric properties observed at small phase angles for dark bodies of the solar system. Obsidian was chosen to represent a silicate dielectric with no internal scattering boundaries. Because obsidian is free of internal scatterers, light reflected from both the rough and smooth obsidian samples is almost entirely single and multiple Fresnel reflections form surface facets with no body component. Surface structure alone cannot produce an opposition effect. Comparison of the obsidian and basalt results indicates that for an opposition effect to occur, surface texture must be both rough and contain internal scattering interfaces. Although the negative polarization observed for the obsidian samples indicates single and multiple reflections are part of negative polarization, the longer inversion angle of the multigrain inversion samples implies that internal reflections must also contribute a significant negative polarization component. Author

N92-10834*# Cornell Univ., Ithaca, NY. Center for Radiophysics and Space Research.

LABORATORY PHOTOMETRIC MEASUREMENT OF PARTICULATE SOILS OUT TO VERY LARGE PHASE ANGLES **c90**

Paul Helfenstein, Ulrich A. Bonne, Susan Stolovy, and Joseph Veverka *In* NASA, Washington, Reports of Planetary Geology and Geophysics Program, 1990 Jun. 1991 p 280-282 (For primary document see N92-10728 01-91)
Avail: NTIS HC/MF A25 CSCL 03B

In the present study, the objectives were to develop the laboratory methods and tools to conduct photometric observations of dark particulate samples over a large range of phase angles and to demonstrate whether forward scattering behavior can be seen in a surface constructed of low albedo material. The researchers also examined the adequacy of various model formulations of P (alpha) to describe the effective scattering properties of their sample. Author

N92-10835*# Cornell Univ., Ithaca, NY.

THE PHOTOMETRIC ROUGHNESS OF MIMAS **c90**

A. Verbiscer and Joseph Veverka *In* NASA, Washington, Reports of Planetary Geology and Geophysics Program, 1990 Jun. 1991 p 283-284 (For primary document see N92-10728 01-91)
(Grants NGT-50482; NsG-7156)
Avail: NTIS HC/MF A25 CSCL 03B

Voyager imaging observations of Mimas lie between 6 degrees and 132 degrees in phase angle and provide sufficient data with which to model such surface characteristics as large-scale roughness and directional scattering properties. Multiple scattering dominates the photometric behavior of the bright icy surface of Mimas, which has been shown to be moderately backscattering. Researchers analyzed disk-integrated and disk-resolved Voyager clear filter photometric using a modified version of Hapke's (1986) equation which accommodates anisotropic multiple scattering. Author

N92-10836*# Cornell Univ., Ithaca, NY. Center for Radiophysics and Space Research.

ANOMALOUS SCATTERING OF LIGHT ON TRITON

Paul Helfenstein, Pascal Lee, Derek McCarthy, and Joseph Veverka *In* NASA, Washington, Reports of Planetary Geology and Geophysics Program, 1990 Jun. 1991 p 285-287 (For primary document see N92-10728 01-91)
(Grants NAGw-2084; NsG-7156)
Avail: NTIS HC/MF A25 CSCL 03B

Researchers report here the discovery of an isolated region of anomalously forward scattering materials on the surface of Triton. The researchers' best-fit Hapke parameters indicate that regolith particles in the anomalous scattering region are not only less backward scattering, but also slightly lower in single scattering albedo than average materials on Triton's surface. While it might be possible to account for such differences in terms of differences in particle size and transparency, it is also possible that the anomalous region is compositionally distinct from other terrains. It is noteworthy that, for the anomalous region, there exists a distinctively strong spatial correlation between the photometric ratios at different phase angles, and that, relative to other terrains, the anomalous region reddens at a different rate with increasing phase angle. Author

N92-10837*# Jet Propulsion Lab., California Inst. of Tech., Pasadena.
DISK RESOLVED STUDIES OF THE OPTICAL PROPERTIES AND PHYSICAL NATURE OF THE SURFACES OF THE OUTER PLANET SATELLITES
Bonnie J. Buratti, J. A. Mosher, and T. V. Johnson *In* NASA, Washington, Reports of Planetary Geology and Geophysics Program, 1990 Jun. 1991 p 288-290 (For primary document see N92-10728 01-91)
Avail: NTIS HC/MF A25 CSCL 03B

The spatially resolved albedo, color, compaction state, roughness, and constituent particle sizes of the surfaces of the satellites of Saturn, Uranus, and Jupiter provide important constraints in understanding the geologic evolution and relevant exogenic processes operating in these satellite systems. Some details of observations are given. Author

N92-10838*# Virginia Univ., Charlottesville. School of Engineering and Applied Science.
CHARGED-PARTICLE INDUCED ALTERATIONS OF SURFACES IN THE OUTER SOLAR SYSTEM
R. E. Johnson *In* NASA, Washington, Reports of Planetary Geology and Geophysics Program, 1990 Jun. 1991 p 292-293 (For primary document see N92-10728 01-91)
Avail: NTIS HC/MF A25 CSCL 03B

Researchers calculated the plasma bombardment profiles of the surfaces of the icy Saturnian satellites in order to interpret reflection spectra and the effect of charged particles on the surfaces (mantles) of Pluto and of comets in the Oort cloud. Pluto's exposure to cosmic rays results in a slow alteration of the reflectance if the methane condensed on its surface. The UV absorbed in the atmosphere can produce precipitates. The researchers showed that, depending on the rates of the competing regolith processes and rates for replenishment of the methane, the surface can appear bright, red, or dark. Using laboratory data, they showed that the amount of darkening occurring in one orbit is small. Therefore, transport, burial, and re-exposure of organic sediments must control the reflectance, and the average reflectance is established by the radiation altered species accumulated over many orbits with the observed spatial, and possible temporal, differences in albedo due to transport. The cosmic rays, although producing changes in reflectance slowly, do so inevitably. Therefore, the fact that the surface is not dark everywhere implies that it is active and the exposure rates vs. depth into the surface of Pluto can be used to constrain turnover rates. Comets in the Oort cloud experience similar rates. Author

N92-10839*# Geological Survey, Denver, CO.
NEW SPECTRAL OBSERVATIONS OF CALLISTO AND LEADING/TRAILING HEMISPHERE DISTINCTIONS
W. M. Calvin, R. N. Clark, and T. V. V. King *In* NASA, Washington, Reports of Planetary Geology and Geophysics Program, 1990 Jun. 1991 p 294-295 (For primary document see N92-10728 01-91)
Avail: NTIS HC/MF A25 CSCL 03B

In December 1989 and January 1990, new observations of the leading and trailing edges of Callisto were made from the NASA Infrared Telescope Facility on Mauna Kea in Hawaii. Using the Cool Grating Array Spectrometer, spectral coverage was obtained from 1.89 to 2.46 microns and from 2.8 to 4.2 microns for both the leading and trailing hemispheres. In addition, spectral coverage of the leading hemisphere was obtained from 1.30 to 2.55 microns and from 4.2 to 4.8 microns. Interpretations of the data are given. Author

N92-10840*# Jet Propulsion Lab., California Inst. of Tech., Pasadena.
MOJAVE REMOTE SENSING FIELD EXPERIMENT
Raymond E. Arvidson, S. B. Petroy, J. J. Plaut, Michael K. Shepard, D. Evans, T. Farr, Ronald Greeley, L. Gaddis, and N. Lancaster (Arizona State Univ., Tempe.) *In* NASA, Washington, Reports of Planetary Geology and Geophysics Program, 1990 Jun. 1991 p 296-297 (For primary document see N92-10728 01-91)
Avail: NTIS HC/MF A25 CSCL 03B

The Mojave Remote Sensing Field Experiment (MFE), conducted in June 1988, involved acquisition of Thermal Infrared Multispectral Scanner (TIMS); C, L, and P-band polarimetric radar (AIRSAR) data; and simultaneous field observations at the Pisgah and Cima volcanic fields, and Lavic and Silver Lake Playas, Mojave Desert, California. A LANDSAT Thematic Mapper (TM) scene is also included in the MFE archive. TM-based reflectance and TIMS-based emissivity surface spectra were extracted for selected surfaces. Radiative transfer procedures were used to model the atmosphere and surface simultaneously, with the constraint that the spectra must be consistent with field-based spectral observations. AIRSAR data were calibrated to backscatter cross sections using corner reflectors deployed at target sites. Analyses of MFE data focus on extraction of reflectance, emissivity, and cross section for lava flows of various ages and degradation states. Results have relevance for the evolution of volcanic plains on Venus and Mars. Author

N92-10841*# National Aeronautics and Space Administration. Goddard Space Flight Center, Greenbelt, MD.
SURFACE SCATTERING PROPERTIES ESTIMATED FROM MODELING AIRBORNE MULTIPLE EMISSION ANGLE REFLECTANCE DATA
Edward A. Guinness, Raymond E. Arvidson (Washington Univ., Saint Louis, MO.), J. R. Irons, and D. J. Harding *In* NASA, Washington, Reports of Planetary Geology and Geophysics Program, 1990 Jun. 1991 p 298-300 (For primary document see N92-10728 01-91)
Avail: NTIS HC/MF A25 CSCL 03B

Here, researchers apply the Hapke function to airborne bidirectional reflectance data collected over three terrestrial surfaces. The objectives of the study were to test the range of natural surfaces that the Hapke model fits and to evaluate model parameters in terms of known surface properties. The data used are multispectral and multiple emission angle data collected during the Geologic Remote Sensing Field Experiment (GRSFE) over a mud-cracked playa, an artificially roughened playa, and a basalt cobble strewn playa at Lunar Lake Playa in Nevada. Airborne remote sensing data and associated field measurements were acquired at the same time. The airborne data were acquired by the Advanced Solid State Array Spectroradiometer (ASAS) instrument, a 29-spectral band imaging system. ASAS reflectance data for a cobble-strewn surface and an artificially rough playa surface on Lunar Lake Playa can be explained with the Hanke model. The cobble and rough playa sites are distinguishable by a single scattering albedo, which is controlled by material composition; by the roughness parameter, which appears to be controlled by the surface texture and particle size; and the symmetry factor of the single particle phase function, which is controlled by particle size and shape. A smooth playa surface consisting of compacted, fine-grained particles has reflectance variations that are also distinct from either the cobble site or rough playa site. The smooth playa appears to behave more like a Lambertian surface that cannot be modeled with the Hapke function. Author

N92-10842*# Jet Propulsion Lab., California Inst. of Tech., Pasadena.
MAPPING COMPOSITIONAL AND PARTICLE SIZE VARIATIONS ACROSS SILVER LAKE PLAYA: RELEVANCE TO ANALYSES OF MARS TIR DATA
S. B. Petroy, Raymond E. Arvidson (Washington Univ., Saint Louis, MO.), and A. B. Kahle *In* NASA, Washington, Reports of Planetary Geology and Geophysics Program, 1990 Jun. 1991 p 301-303 (For primary document see N92-10728 01-91)
Avail: NTIS HC/MF A25 CSCL 03B

The high spectral and spatial resolution thermal infrared (TIR) data to be acquired from the upcoming Mars Observer-Thermal Emission Spectra (TES) mission will map the composition and texture of the Martian sediments. To prepare for these data, portions of two remote sensing experiments were conducted to test procedures for extracting surface property information from

TIR data. Reported here is the continuing analysis of Thermal Infrared Multispectral Scanner (TIMS) data, field emission spectra, laboratory Fourier Transform Infrared (FTIR) reflectance spectra, and field observations with respect to the physical characteristics (composition, emissivity, etc.) of Silver Lake playa in southern California. Author

N92-10843*# National Aeronautics and Space Administration. Goddard Space Flight Center, Greenbelt, MD.
APPLICATION OF HAPKE PHOTOMETRIC MODEL TO THREE GEOLOGIC SURFACES USING PARABOLA BIDIRECTIONAL REFLECTION DATA
Michael K. Shepard, Raymond E. Arvidson (Washington Univ., Saint Louis, MO.), and Donald W. Deering *In* NASA, Washington, Reports of Planetary Geology and Geophysics Program, 1990 Jun. 1991 p 304-305 (For primary document see N92-10728 01-91)
Avail: NTIS HC/MF A25 CSCL 03B

The Geologic Remote Sensing Field Experiment (GRSFE) was conducted in July and September of 1989 to collect data with both ground and airborne instrumentation. A major objective of GRSFE was to collect data which could be used to test radiative transfer models for the extraction of composition and textural surface properties from remotely acquired data. Reported here are the initial results from an application of the Hapke photometric model, using data from the Portable Apparatus for Remote Acquisition of Bidirectional Observations of Land and Atmosphere (PARABOLA), a ground based radiometer with three spectral channels. PARABOLA data was collected in the Lunar Crater Volcanic Field in Nevada, specifically from the region of Lunar Lake, a playa. The Hapke model was found to be inadequate for three relatively common geologic surfaces (a clay-rich, hard packed surface with decimeter sized mudcracks; a cobble site, similar to a playa site, but strewn with basaltic cobbles and pebbles; and a surface mantled basalt lava flow). The model is not at fault; rather, the complexity of most geologic surfaces is not accounted for in the initial assumptions. Author

N92-10844*# Washington Univ., Saint Louis, MO.
THE GEOLOGIC REMOTE SENSING FIELD EXPERIMENT (GRSFE) **c43**
Mary A. Dale-Bannister, Raymond E. Arvidson, Edward E. Guinness, Susan H. Slavney, and Thomas C. Stein *In* NASA, Washington, Reports of Planetary Geology and Geophysics Program, 1990 Jun. 1991 p 306-307 (For primary document see N92-10728 01-91)
Avail: NTIS HC/MF A25 CSCL 03B

Field measurements for the Geologic Remote Sensing Field Experiment (GRSFE) were concentrated in the Lunar Lake area of Nevada. The GRSFE data are meant to be used in a variety of investigations, including tests of multispectral radiative transfer models for scattering and emission from planetary surfaces in support of the Earth Observing System (EOS), Mars Observer, and Magellan Missions. Studies will also be pursued to establish the neotectonic and paleoclimatic history of the arid southwestern United States. The data will also be used to support Mars Rover Sample Return (MRSR) simulation studies. Author

N92-10845*# Cornell Univ., Ithaca, NY. Dept. of Astronomy.
HIGH RESOLUTION LUNAR RADAR STUDIES: PRELIMINARY RESULTS
Nicholas J. S. Stacy and Donald B. Campbell *In* NASA, Washington, Reports of Planetary Geology and Geophysics Program, 1990 Jun. 1991 p 308-309 (For primary document see N92-10728 01-91)
Avail: NTIS HC/MF A25 CSCL 03B

High resolution radar data for the lunar surface were acquired over 14 sites in June and November 1990 using the new 10 MHz data taking system at the Arecibo Observatory. The raw data collected for each site covers an area approximately 100 by 400 km and will be processed using delay-Doppler techniques into images of backscatter cross section with three fo four independent looks. All observations transmitted a circularly polarized signal and both senses of circular polarization were received containing the polarized and depolarized component of the backscatter signal. The relative power in these two polarizations provides useful information on properties of the surface, in particular surface roughness. The effort to date focused on the initial data analysis with new software written to perform a full synthetic aperture focusing on the raw radar data. This analysis will involve the use of complementary high resolution optical and topographic data sets to aid interpretation of surface scattering mechanisms. Author

N92-10846*# Michigan Univ., Ann Arbor. Dept. of Electrical Engineering and Computer Science.
MODELS OF THE DIFFUSE RADAR BACKSCATTER FROM MARS
A. W. England and R. T. Austin *In* NASA, Washington, Reports of Planetary Geology and Geophysics Program, 1990 Jun. 1991 p 310-312 (For primary document see N92-10728 01-91)
(Contract NCC9-19; NAGw-2199)
Avail: NTIS HC/MF A25 CSCL 03B

The topographies of several debris flow units near the Mount St. Helens Volcano were measured at lateral scales of millimeters to meters in September 1990. The objective was to measure the surface roughness of the debris flows at scales smaller than, on the order of, and larger that the radar wavelength of common remote sensing radars. A laser profiling system and surveying instruments were used to obtain elevation data for square areas that varied in size from 10 to 32 cm. The elevation data were converted to estimates of the power spectrum of surface roughness. The conversions were based upon standard periodogram techniques, and upon a modified spectral estimation technique that was developed. Author

N92-10847*# Arizona State Univ., Tempe. Dept. of Geology.
REMOTE SENSING OBSERVATIONS OF KELSO DUNES, CALIFORNIA Abstract Only **c43**
Ronald Greeley, N. Lancaster, L. Gaddis, and E. C. I. Paisley *In* NASA, Washington, Reports of Planetary Geology and Geophysics Program, 1990 Jun. 1991 p 313 (For primary document see N92-10728 01-91)
Avail: NTIS HC/MF A25 CSCL 03B

The extensive field studies necessary to understand the development of desert sand seas are hampered by their large size and inaccessibility. Remote sensing data used in conjunction with detailed field studies and textural and mineralogical analyses of surface sediments at specific ground-control points can provide a wealth of information on dune types and activity, regional aeolian dynamics, sediment sources and thickness, and depositional history for sand seas. The information available from LANDSAT TM (VNIR), AIRSAR (microwave), and AVIRIS (high spectral resolution VNIR) is compared using Kelso Dunes as a test case. Author

N92-10848*# Geological Survey, Menlo Park, CA.
PRELIMINARY COMPARISON OF 3.5-cm AND 12.6-cm WAVELENGTH CONTINUOUS WAVE OBSERVATIONS OF MARS
H. J. Moore, T. C. OBrien, R. F. Jurgens, M. A. Slade, and T. W. Thompson (Jet Propulsion Lab., California Inst. of Tech., Pasadena.) *In* NASA, Washington, Reports of Planetary Geology and Geophysics Program, 1990 Jun. 1991 p 315-316 (For primary document see N92-10728 01-91)
Avail: NTIS HC/MF A25 CSCL 03B

Radar observations of Mars at Goldstone in 1990 were conducted by transmitting pure sinusoidal signals at 3.5-cm wavelengths and receiving the Doppler-spread echoes from Mars at Earth. Radar transmissions were circularly polarized and the echoes recorded in two senses: depolarized and polarized. Latitudes of the subradar points are between 3.5 deg and 11.1 deg S; longitude coverage is discontinuous. The observed depolarized and polarized echo total cross-sections and their ratios for two wavelengths were compared and discussed. Author

N92-10849*# Stanford Univ., CA. Center for Radar Astronomy.
SURFACE PROPERTIES OF GALILEAN SATELLITES FROM BISTATIC RADAR EXPERIMENTS
R. A. Simpson and G. L. Tyler *In* NASA, Washington, Reports of Planetary Geology and Geophysics Program, 1990 Jun. 1991 p 317-319 (For primary document see N92-10728 01-91)
Avail: NTIS HC/MF A25 CSCL 03B

The icy moons of Jupiter were the first to show unusual radar backscatter behavior in Earth-based experiments. Studies of Europa, Ganymede, and Callisto revealed strong echoes and a reversed sense of circular polarization. No explanations were entirely satisfactory because of the difficult constraints imposed by the existing data. The (scalar) bidirectional coherence model predicts an opposition effect, or enhancement in the backscatter direction, resulting from coherent addition of backscatter from identical (but oppositely directed) ray paths. The mode decoupling model yields a similar, vector result in which the observed polarization properties of the backscattered wave can also be obtained. The possibilities were considered for conducting such experiments using the Galileo spacecraft. Both conventional oblique-forward bistatic experiments (to determine basic electrical and physical properties of the surface material on centimeter-meter scales) and near-backscatter experiments (to sample the enhanced backscatter lobe) were considered. Author

N92-10850*# Stanford Univ., CA. Center for Radar Astronomy.
RADAR BACKSCATTERING BY THE ICY GALILEAN SATELLITES AND THE RADAR GLORY EFFECT
Eric M. Gurrola and Von R. Eshleman *In* NASA, Washington, Reports of Planetary Geology and Geophysics Program, 1990 Jun. 1991 p 320-322 (For primary document see N92-10728 01-91)
(Grants NGL-05-020-014; NGT-70056; NSF AST-87-21880)
Avail: NTIS HC/MF A25 CSCL 03B

Radar echoes from the icy Galilean satellites are unique in character and they may be explained by a phenomenon that was called the radar glory effect. The radar glory backscattering from buried craters was analyzed as a possible model for this effect. These craters have a smaller refractive index below the crater than above. The possibility exists that the rays will be totally internally reflected at the crater walls. The rays which contribute to the backscattering will come from a circular annulus, when viewed before the refraction occurs at the ice-vacuum surface, in a plane orthogonal to the rays reflected from the crater. Author

N92-10851*# Pittsburgh Univ., PA. Dept. of Geology and Planetary Science.
REGOLITHS OF ICY SATELLITES: THE COHERENT BACKSCATTER MODEL Abstract Only
B. Hapke and D. Blewett *In* NASA, Washington, Reports of Planetary Geology and Geophysics Program, 1990 Jun. 1991 p 323 (For primary document see N92-10728 01-91)
Avail: NTIS HC/MF A25 CSCL 03B

The coherent backscatter model of radar scattering from icy satellites argues that most of the received power comes from radio waves that have been multiply scattered from numerous refractive index discontinuities randomly located under the surfaces of the regoliths. In a laboratory analog experiment the circular and linear polarizations were measured in light scattered from a suspension of polystyrene spheres in water illuminated by laser. Results confirm that coherent backscatter from particle media reproduces the large intensity and unusual polarizations observed in the radar data. The model implies that the regoliths of icy satellites consist of matrices of small reflective index containing imbedded scatterers separated by distances of the order of a wavelength. Author

N92-10852*# Geological Survey, Flagstaff, AZ.
IMPACT CRATERS ON VENUS
G. G. Schaber *In* NASA, Washington, Reports of Planetary Geology and Geophysics Program, 1990 Jun. 1991 p 329-331 (For primary document see N92-10728 01-91)
Avail: NTIS HC/MF A25 CSCL 03B

Compared with volcanism and tectonism, impact cratering on Venus has played an overall minor role in sculpting the present-day landscape. The study of Venus impact craters is vital to help place the chronology of the geologic features on the surface in the context of the planet's geological evolution. The degradation of impact craters also provides information on surface and interior processes, particularly alteration by tectonism and volcanism. Through orbit 1422, Magellan mapped about 450 impact craters, with diameters ranging from 2 to 275 km, within an area of about 226 million sq km, or 49 percent of the planet's surface. These craters and their associated deposits show surprisingly little evidence of degradation at the 75 m/pixel resolution of the Magellan SAR. Remarkably few craters in the Magellan images appear to be in the process of being buried by volcanic deposits or destroyed by tectonic activity. Author

N92-10853*# Geological Survey, Flagstaff, AZ.
QUANTITATIVE ANALYSIS OF TERRAIN UNITS MAPPED IN THE NORTHERN QUARTER OF VENUS FROM VENERA 15/16 DATA
G. G. Schaber *In* NASA, Washington, Reports of Planetary Geology and Geophysics Program, 1990 Jun. 1991 p 332-333 (For primary document see N92-10728 01-91)
Avail: NTIS HC/MF A25 CSCL 03B

The contacts between 34 geological/geomorphic terrain units in the northern quarter of Venus mapped from Venera 15/16 data were digitized and converted to a Sinusoidal Equal-Area projection. The result was then registered with a merged Pioneer Venus/Venera 15/16 altimetric database, root mean square (rms) slope values, and radar reflectivity values derived from Pioneer Venus. The resulting information includes comparisons among individual terrain units and terrain groups to which they are assigned in regard to percentage of map area covered, elevation, rms slopes, distribution of suspected craters greater than 10 km in diameter. Author

N92-10854*# Southern Methodist Univ., Dallas, TX. Dept. of Geological Sciences.
VENUS IMPACT CRATERS: IMPLICATIONS FOR ATMOSPHERIC AND RESURFACING PROCESSES FROM MAGELLAN OBSERVATIONS
Roger J. Phillips *In* NASA, Washington, Reports of Planetary Geology and Geophysics Program, 1990 Jun. 1991 p 334-335 (For primary document see N92-10728 01-91)
Avail: NTIS HC/MF A25 CSCL 03B

Observations of impact craters on Venus by Magellan yield important insights into: (1) atmospheric effects on the formation of impact craters and their attendant ejecta deposits and (2) the resurfacing history of the planet. Most craters smaller than 15 km are classified as irregular; they possess irregularly shaped rims, and multiple hummocky floors. The irregular nature of these craters is interpreted to be the consequence of breakup and dispersion of incoming meteoroids by the dense atmosphere. Two major ejecta facies of venusian impact craters are hummocky ejecta and outer ejecta. A number of craters documented in the Magellan images possess often non-radial, flow-like ejecta indicative of a low viscosity materials. Approximately half of the impact craters observed with the Magellan radar are partially or wholly surrounded by areas with low radar backscatter cross sections. Author

N92-10855*# Southern Methodist Univ., Dallas, TX. Dept. of Geological Sciences.
BREAKUP OF METEOROIDS IN THE VENUSIAN ATMOSPHERE AND ITS EFFECTS ON CRATER FORMATION
R. R. Herrick and Roger J. Phillips *In* NASA, Washington, Reports of Planetary Geology and Geophysics Program, 1990 Jun. 1991 p 336-337 (For primary document see N92-10728 01-91)
Avail: NTIS HC/MF A25 CSCL 03B

Early results of the Magellan mission to Venus show that almost all of the observed impact craters appear to be unaffected by erosion, burial, and tectonic deformation. Therefore it is reasonable to assume that the observed paucity of small craters in the

cumulative size-frequency distribution (SFD) relative to the simple power laws observed on airless planets is most likely due to atmospheric effects on the incoming meteoroids. A model was developed earlier for travel and breakup of a meteoroid in an atmosphere, but this model was never used to estimate a SFD. An attempt is made to match the cumulative SFD and the number and size distribution of multiple-floored craters and crater fields using this model. Author

N92-10856*# Brown Univ., Providence, RI. Dept. of Geological Sciences.
ATMOSPHERIC EFFECTS ON OBLIQUE IMPACTS
P. H. Schultz *In* NASA, Washington, Reports of Planetary Geology and Geophysics Program, 1990 Jun. 1991 p 338-339 (For primary document see N92-10728 01-91)
Avail: NTIS HC/MF A25 CSCL 03B

Laboratory experiments and theoretical calculations often use vertical impact angles (90 deg) in order to avoid the complicating effect of asymmetry. Nevertheless, oblique impacts represent the most likely starting condition for planetary cratering. Changing both impact angles and atmospheric pressure not only allows testing previous results for vertical impacts but also reveals phenomena whose signatures would otherwise be masked in the planetary cratering record. The laboratory studies were performed for investigating impact cratering processes. Impact angles can be increased from 0 to 90 deg in 15 deg increments while maintaining a flat target surface. Different atmospheres (nitrogen, argon, and helium) characterized the effects of both gas density and Mach number. Targets varied according to purpose. Because of the complexities in atmosphere-impactor-ejecta interactions, no single combination allows direct simulation of a planetary-scale (10-100 km) event. Nevertheless, fundamental processes and observed phenomena allow formulating first-order models at such broad scales. Author

N92-10857*# Brown Univ., Providence, RI. Dept. of Geological Sciences.
STYLES OF EJECTA EMPLACEMENT UNDER ATMOSPHERIC CONDITIONS
P. H. Schultz *In* NASA, Washington, Reports of Planetary Geology and Geophysics Program, 1990 Jun. 1991 p 340-341 (For primary document see N92-10728 01-91)
Avail: NTIS HC/MF A25 CSCL 03B

Laboratory experiments provide essential first-order constraints on processes affecting ballistic ejecta and styles of ejecta emplacement under different atmospheric environments at planetary scales. The NASA-Ames Vertical Gun allows impacting different fine-grained particulate targets under varying atmospheric pressure and density, thereby helping to isolate controlling variables. Further analysis now permits characterizing distinct modes of emplacement that reflect the degree of ejecta entrainment within a turbidity flow created by ejecta curtain movement through the atmosphere. Author

N92-10858*# Brown Univ., Providence, RI. Dept. of Geological Sciences.
IMPACT DECAPITATION FROM LABORATORY TO BASIN SCALES
P. H. Schultz and D. E. Gault (Murphys Center of Planetology, CA.) *In* NASA, Washington, Reports of Planetary Geology and Geophysics Program, 1990 Jun. 1991 p 342-343 (For primary document see N92-10728 01-91)
Avail: NTIS HC/MF A25 CSCL 03B

Although vertical hypervelocity impacts result in the annihilation (melting/vaporization) of the projectile, oblique impacts (less than 15 deg) fundamentally change the partitioning of energy with fragments as large as 10 percent of the original projectile surviving. Laboratory experiments reveal that both ductile and brittle projectiles produce very similar results where limiting disruption depends on stresses proportional to the vertical velocity component. Failure of the projectile at laboratory impact velocities (6 km/s) is largely controlled by stresses established before the projectile has penetrated a significant distance into the target. The planetary surface record exhibits numerous examples of oblique impacts with evidence fir projectile failure and downrange sibling collisions. Author

N92-10859*# Boeing Co., Seattle, WA.
LABORATORY SIMULATION OF CRATERING ON SMALL BODIES
Robert M. Schmidt *In* NASA, Washington, Reports of Planetary Geology and Geophysics Program, 1990 Jun. 1991 p 344-346 (For primary document see N92-10728 01-91)
Avail: NTIS HC/MF A25 CSCL 03B

A new technique using external pressure was developed to simulate the lithostatic pressure due to self-gravity of small bodies. A 13-in. diameter cylindrical test chamber with L/D of 1 was fabricated to accommodate firing explosive charges with gas overpressures of up to 6000 psi. The chamber was hydrotested to 9000 psi. The method allows much larger scale factors that can be obtained with existing centrifuges and has the correct spherical geometry of self gravity. A simulant for jointed rock to be used in this fixture was developed using weakly cemented basalt. Various strength/pressure scaling theories can now be examined and tested. Author

N92-10860*# Planetary Science Inst., Tucson, AZ.
POSSIBLE MISINTERPRETATION OF LUNAR CRATERING RECORD IN VOYAGER TEAM ANALYSES OF OUTER PLANET SATELLITES
William K. Hartmann *In* NASA, Washington, Reports of Planetary Geology and Geophysics Program, 1990 Jun. 1991 p 347-349 (For primary document see N92-10728 01-91)
Avail: NTIS HC/MF A25 CSCL 03B

While interpreting outer planetary satellites, the Voyager imaging team repeatedly referred to a lunar frontside highland calibration curve. It was assumed that it is unmodified and not in steady state equilibrium, but rather records all impacts that have occurred. It was also assumed that it records the size distribution of an early population of impactors, called Population I, evidence for which was found on various satellites. New evidence is reported that the Voyager team interpretation of this population is wrong, a conclusion that seriously affects the cratering histories reported for outer planet satellites. Author

N92-10861*# Planetary Science Inst., Tucson, AZ.
HYDROCODE PREDICTIONS OF COLLISIONAL OUTCOMES: EFFECTS OF TARGET SIZE
Eileen V. Ryan, Erik Asphaug, and H. J. Melosh (Arizona Univ., Tucson.) *In* NASA, Washington, Reports of Planetary Geology and Geophysics Program, 1990 Jun. 1991 p 350-351 (For primary document see N92-10728 01-91)
Avail: NTIS HC/MF A25 CSCL 03B

Traditionally, laboratory impact experiments, designed to simulate asteroid collisions, attempted to establish a predictive capability for collisional outcomes given a particular set of initial conditions. Unfortunately, laboratory experiments are restricted to using targets considerably smaller than the modelled objects. It is therefore necessary to develop some methodology for extrapolating the extensive experimental results to the size regime of interest. Results are reported obtained through the use of two dimensional hydrocode based on 2-D SALE and modified to include strength effects and the fragmentation equations. The hydrocode was tested by comparing its predictions for post-impact fragment size distributions to those observed in laboratory impact experiments. Author

N92-10862*# Washington Univ., Seattle.
ENERGY COUPLING IN CATASTROPHIC COLLISIONS
K. A. Holsapple and K. Y. Choe *In* NASA, Washington, Reports of Planetary Geology and Geophysics Program, 1990 Jun. 1991 p 352-353 (For primary document see N92-10728 01-91)
Avail: NTIS HC/MF A25 CSCL 03B

The prediction of events leading to the catastrophic collisions and disruption of solar system bodies is fraught with the same difficulties as are other theories of impact events; since one simply

cannot perform experiments in the regime of interest. In the catastrophic collisions of asteroids that regime involves bodies of a few tons to hundred of kilometers in diameter, and velocities of several kilometers pre second. For hundred kilometer bodies, gravitational stresses dominate material fracture strengths, but those gravitational stresses are essentially absent for laboratory experiments. Only numerical simulations using hydrocodes can in principle analyze the true problems, but they have their own major uncertainties about the correctness of the physical models and properties. The question of the measure of the impactor and its energy coupling is investigated using numerical code calculations. The material model was that of a generic silicate rock, including high pressure melt and vapor phases, and includes material nonlinearity and dissipation via a Mie-Gruniesen model. A series of calculations with various size ratios and impact velocities are reported. Author

N92-10863*# Planetary Science Inst., Tucson, AZ.
CONTINUUM MODELING OF CATASTROPHIC COLLISIONS
Eileen V. Ryan, Erik Aspaug, and H. J. Melosh (Arizona Univ., Tucson.) *In* NASA, Washington, Reports of Planetary Geology and Geophysics Program, 1990 Jun. 1991 p 354 (For primary document see N92-10728 01-91)
Avail: NTIS HC/MF A25 CSCL 03B

A two dimensional hydrocode based on 2-D SALE was modified to include strength effects and fragmentation equations for fracture resulting from tensile stress in one dimension. Output from this code includes a complete fragmentation summary for each cell of the modeled object: fragment size (mass) distribution, vector velocities of particles, peak values of pressure and tensile stress, and peak strain rates associated with fragmentation. Contour plots showing pressure and temperature at given times within the object are also produced. By invoking axial symmetry, three dimensional events can be modeled such as zero impact parameter collisions between asteroids. The code was tested against the one dimensional model and the analytical solution for a linearly increasing tensile stress under constant strain rate. Author

N92-10864*# Arizona Univ., Tucson. Lunar and Planetary Lab.
CORE FORMATION BY GIANT IMPACTS
W. B. Tonks and H. J. Melosh *In* NASA, Washington, Reports of Planetary Geology and Geophysics Program, 1990 Jun. 1991 p 355-356 (For primary document see N92-10728 01-91)
Avail: NTIS HC/MF A25 CSCL 03B

Ideas about the accretion and early evolution of the Earth and the other terrestrial planets have recently undergone a number of revolutionary changes. It has become clear that giant impacts were far from rare events. In the later stages of accretion any given planetary embryo is liable to be struck several times by other bodies of up to half its own diameter. Such an impact may have the ability to trigger core formation. Traditional accretion models have had great difficulty explaining the formation of the core. If one admits the importance of infrequent large events that may melt an entire hemisphere, the core formation difficulty vanishes. Millimeter-size iron blebs in the melted region will rain out due to their density difference with the silicate melt. Core formation may not require the melting of the entire hemisphere of the planet. The conditions are explored under which impact induced core formation may occur. Author

N92-10865*# Arizona Univ., Tucson. Lunar and Planetary Lab.
LARGE IMPACTS AND CLIMATIC CATASTROPHES ON THE EARLY EARTH
H. J. Melosh *In* NASA, Washington, Reports of Planetary Geology and Geophysics Program, 1990 Jun. 1991 p 357-358 (For primary document see N92-10728 01-91)
Avail: NTIS HC/MF A25 CSCL 03B

Radiometric data of cratered lunar surfaces suggest that the cratering rate on the ancient Moon was substantially larger than the present rate before about 3.2 Gyr. Since the cratering rate was higher than present on the Moon, it seems likely that is was similarly higher on the Earth. Recently the occurrence of beds of spherules up to 2m thick was reported in 3.2 to 3.5 Gyr old Archean rocks. These spherule beds closely resemble the 3 mm thick spherule beds associated with the K/T boundary (including elevated iridium abundances), widely believed to have been deposited in association of a 10 km diameter comet or asteroid. Author

N92-10866*# Arizona Univ., Tucson. Lunar and Planetary Lab.
IMPACTS AND THE EARLY ENVIRONMENT AND EVOLUTION OF THE TERRESTRIAL PLANETS Abstract Only
H. J. Melosh and A. M. Vickery *In* NASA, Washington, Reports of Planetary Geology and Geophysics Program, 1990 Jun. 1991 p 359 (For primary document see N92-10728 01-91)
Avail: NTIS HC/MF A25 CSCL 03B

It is now admitted that very large impacts may have played an important role in the accretion of the terrestrial planets. The size-frequency distribution of these impacts fits the formal definition of a catastrophic process: the mass and momentum added by a rare large impact is larger than that added by all the more frequent small impacts combined. The effects of such large impacts on the thermal states of growing planets is discussed. At a later stage of planetary evolution, the smaller impacts during late heavy bombardment may have played an important role in stripping the original gaseous atmospheres of the planets and in segregating condensible substances from volatile ones. Author

N92-10867*# Arizona Univ., Tucson. Lunar and Planetary Lab.
VAPOR PLUMES: A NEGLECTED ASPECT OF IMPACT CRATERING Abstract Only
H. J. Melosh *In* NASA, Washington, Reports of Planetary Geology and Geophysics Program, 1990 Jun. 1991 p 360 (For primary document see N92-10728 01-91)
Avail: NTIS HC/MF A25 CSCL 03B

When a meteorite or comet strikes the surface of the planet or satellite at typical interplanetary velocities of 10-40 km/sec, the projectile and a quantity of the target body vaporize and expand out of the growing crater at high speed. The crater continues to grow after the vapor plume has formed and the series of ejecta deposits is laid down ballistically while the crater collapses into its final morphology. Although the vapor plume leaves little evidence of its existence in the crater structure of surface deposits, it may play a major role in a number of impact-related processes. The vapor plume expanding away from the site of an impact carries 25-50 percent of the total impact energy. Although the plume's total mass is only a few times the mass of the projectile, its high specific energy content means that it is the fastest and most highly shocked material in the cratering event. The mean velocity of expansion can easily exceed the escape velocity of the target plane, so that the net effect of a sufficiently high-speed impact is to erode material from the planet. Author

N92-10868*# Arizona Univ., Tucson. Lunar and Planetary Lab. **c90**
JETTING AND THE ORIGIN OF TEKTITES
A. M. Vickery *In* NASA, Washington, Reports of Planetary Geology and Geophysics Program, 1990 Jun. 1991 p 361 (For primary document see N92-10728 01-91)
Avail: NTIS HC/MF A25 CSCL 03B

The scientific consensus is that tektites were produced by impacts on the Earth, but the exact mechanism by impacts might form tektites is still unclear. The most widely cited mechanism is jetting, which results from the extremely high pressures generated at the intersection of two bodies whose surfaces converge obliquely at high speed. Theory of jetting for thin plates is extended to the case of the impact of the sphere onto a half-space. The calculations are done for the impact of a silicate sphere onto a silicate target for impact speeds of 15, 20, and 25 km/sec, spanning the range of reasonable impact speeds for asteroids. The angle of impact is varied from 0 to 75 deg. The mass jetted, the jet velocity, projectile fraction in the jet, azimuthal distribution of the jet, and the phase of the jetted material are calculated as functions of time. The total mass jetted and the overall mass-averages of jet velocity, etc. are also calculated. Author

N92-10869*# Arizona Univ., Tucson. Lunar and Planetary Lab.
MELT DROPLET FORMATION IN ENERGETIC IMPACTS
A. M. Vickery and H. J. Melosh *In* NASA, Washington, Reports of Planetary Geology and Geophysics Program, 1990 Jun. 1991 p 362-363 (For primary document see N92-10728 01-91)
Avail: NTIS HC/MF A25 CSCL 03B

Impacts between rocky bodies at velocities exceeding about 15 km/sec are capable of melting or vaporizing both the impacting object and a portion of the target. Geological materials initially shocked to high pressure approach the liquid-vapor phase boundary from the liquid side as they decompress, breaking up into an expanding spray of liquid droplets. A simple theory is presented for estimating the sizes of these droplets as a function of impactor size and velocity. It is shown that these sizes are consistent with observations of microtektites and spherules found in the Cretaceous-Tertiary boundary layer, the Acraman impact structure, Archean beds in South Africa and lunar regolith. The model may also apply to the formation of chondrules. Author

N92-10870*# Arizona Univ., Tucson. Lunar and Planetary Lab.
PRODUCTION OF IMPACT MELT IN CRATERS ON VENUS, EARTH, AND THE MOON
A. M. Vickery and H. J. Melosh *In* NASA, Washington, Reports of Planetary Geology and Geophysics Program, 1990 Jun. 1991 p 364-365 (For primary document see N92-10728 01-91)
Avail: NTIS HC/MF A25 CSCL 03B

Impact craters imaged by Magellan clearly show large amounts of flow-like ejecta whose morphology suggests that the flows comprise low-viscosity material. It was suggested that this material may be either turbidity flows or very fine-grained ejecta, flows of ejecta plus magma, or impact melts. The last of these hypotheses is considered. If these flows are composed of impact melts, there is much more melt relative to the crater volume than is observed on the moon. The ANEOS equation of state program was used for dunite to estimate the shock pressures required for melting, with initial conditions appropriate for Venus, Earth, and the moon. A simple model was then developed, based on the Z-model for excavation flow and on crater scaling relations that allow to estimate the ratio of melt ejecta to total ejecta as a function of crater size on the three bodies. Author

N92-10871*# Arizona Univ., Tucson. Lunar and Planetary Lab.
IMPACTS AND ATMOSPHERIC EROSION ON THE EARLY EARTH
A. M. Vickery *In* NASA, Washington, Reports of Planetary Geology and Geophysics Program, 1990 Jun. 1991 p 366-367 (For primary document see N92-10728 01-91)
Avail: NTIS HC/MF A25 CSCL 03B

It was suggested that heating and/or vaporization of accreting carbonaceous-chondrite-type planetestimals could result in the release of their volatile components. Modeling of this process strongly suggests that substantial atmospheres/hydrospheres could develop this way. During most of the accretionary process, impact velocities generally differed from the escape velocity of the growing proto-planet because most of the collisions were between bodies in nearly matching orbits. Toward the end of accretion, however, collisions were rarer but more energetic, involving large planetestimals and higher impact velocities. Such impacts result in a net loss of atmosphere from a planet, and the cumulative effect impacts during the period of heavy bombardment might have dramatically depleted the original atmospheres. Models developed to study atmospheric erosion by impacts on Mars and the interaction of the vapor plume produced by KT impactor on Earth are applied to the case of the evolution of Earth's atmosphere. Author

N92-10872*# Brown Univ., Providence, RI.
CHARACTERISTICS OF EJECTA AND ALLUVIAL DEPOSITS AT METEOR CRATER, ARIZONA AND ODESSA CRATERS, TEXAS: RESULTS FROM GROUND PENETRATING RADAR
J. A. Grant and P. H. Schultz *In* NASA, Washington, Reports of Planetary Geology and Geophysics Program, 1990 Jun. 1991 p 368-369 (For primary document see N92-10728 01-91)
Avail: NTIS HC/MF A25 CSCL 03B

Previous ground penetrating radar (GRP) studies around 50,000 year old Meteor Crater revealed the potential for rapid, inexpensive, and non-destructive sub-surface investigations for deep reflectors (generally greater than 10 m). New GRP results are summarized focusing the shallow sub-surfaces (1-2 m) around Meteor Crater and the main crater at Odessa. The following subject areas are covered: (1) the thickness, distribution, and nature of the contact between surrounding alluvial deposits and distal ejecta; and (2) stratigraphic relationships between both the ejecta and alluvium derived from both pre and post crater drainages. These results support previous conclusions indicating limited vertical lowering (less than 1 m) of the distal ejecta at Meteor Crater and allow initial assessment of the gradational state if the Odessa craters. Author

N92-10873*# Hawaii Univ., Honolulu. Planetary Geosciences Div.
DEPTH/DIAMETER RELATIONSHIPS OF FRESH CRATERS WITHIN HESPERIA PLANUM, MARS
P. J. Mouginis-Mark and J. N. Hayashi *In* NASA, Washington, Reports of Planetary Geology and Geophysics Program, 1990 Jun. 1991 p 370-372 (For primary document see N92-10728 01-91)
(Grant NAGw-437)
Avail: NTIS HC/MF A25 CSCL 03B

Meteorite impact craters represent important geological features for revealing the near-surface layers of a planetary surface. In the case of Mars, this characteristic was proposed as a useful method to study spatial variations of such attributes as the distribution of sub-surface volatiles, and heat flow. Using the Planetary Image Cartography System (PICS) software, a quantitative analysis was completed of the geometry of fresh impact craters in the Hesperia Planum region of Mars, where an uniform target material and optimum viewing geometry make possible an analysis of target effects over a large geographic region. Because of the morphologic similarity to the lunar maria, it is likely that Hesperia Planum comprises a series of flood lavas that partially infilled topographic depressions within the Martian highlands. Measurements of partially buried crater rims suggest that the lava flows within Hesperia Planum are between 200-400 m thick. Author

N92-10874*# Arizona Univ., Tucson. Lunar and Planetary Lab.
THE SCALING OF SECONDARY CRATERS
Steven K. Croft *In* NASA, Washington, Reports of Planetary Geology and Geophysics Program, 1990 Jun. 1991 p 373-374 (For primary document see N92-10728 01-91)
Avail: NTIS HC/MF A25 CSCL 03B

Secondary craters are common features around fresh planetary-scale primary impact craters throughout most of the Solar System. They derive from the ejection phase of crater formation, thus secondary scaling relations provide constraints on parameters affecting ejection processes. Secondary crater fields typically begin at the edge of the continuous ejecta blankets (CEB) and extend out several crater radii. Secondaries tend to have rounded rims and bilateral symmetry about an axis through the primary crater's center. Prominent secondary chains can extend inward across the CEB close to the rim. A simple method for comparing secondary crater fields was employed: averaging the diameters and ranges from the center of the primary crater of the five largest craters in a secondary crater field. While not as much information is obtained about individual crater fields by this method as in more complete secondary field mapping, it facilitates rapid comparison of many secondary fields. Also, by quantifying a few specific aspects of the secondary crater field, this method can be used to construct scaling relations for secondary craters. Author

N92-10875*# Los Alamos National Lab., NM.
CHEMICAL FRACTIONATION OF SIDEROPHILE ELEMENTS IN IMPACTITES FROM AUSTRALIAN METEORITE CRATERS
A. Attrep, Jr., C. J. Orth, L. R. Quintana, C. S. Shoemaker, E. M. Shoemaker, and S. R. Taylor (Australian National Univ.,

Canberra.) *In* NASA, Washington, Reports of Planetary Geology and Geophysics Program, 1990 Jun. 1991 p 375-376 (For primary document see N92-10728 01-91)
Avail: NTIS HC/MF A25 CSCL 03B

The abundance pattern of siderophile elements in terrestrial and lunar impact melt rocks was used extensively to infer the nature of the impacting projectiles. An implicit assumption made is that the siderophile abundance ratios of the projectiles are approximately preserved during mixing of the projectile constituents with the impact melts. As this mixture occurs during flow of strongly shocked materials at high temperatures, however there are grounds for suspecting that the underlying assumption is not always valid. In particular, fractionation of the melted and partly vaporized material of the projectile might be expected because of differences in volatility, solubility in silicate melts, and other characteristics of the constituent elements. Impactites from craters with associated meteorites offer special opportunities to test the assumptions on which projectile identifications are based and to study chemical fractionation that occurred during the impact process. Author

N92-10876*# Brown Univ., Providence, RI. Dept. of Geological Sciences.
IGNEOUS INTRUSION MODELS FOR FLOOR FRACTURING IN LUNAR CRATERS
R. W. Wichman and P. H. Schultz *In* NASA, Washington, Reports of Planetary Geology and Geophysics Program, 1990 Jun. 1991 p 377-378 (For primary document see N92-10728 01-91)
Avail: NTIS HC/MF A25 CSCL 03B

Lunar floor-fractured craters are primarily located near the maria and frequently contain ponded mare units and dark mantling deposits. Fracturing is confined to the crater interior, often producing a moat-like feature near the floor edge, and crater depth is commonly reduced by uplift of the crater floor. Although viscous relaxation of crater topography can produce such uplift, the close association of modification with surface volcanism supports a model linking floor fracture to crater-centered igneous intrusions. The consequences of two intrusion models for the lunar interior are quantitatively explored. The first model is based on terrestrial laccoliths and describes a shallow intrusion beneath the crater. The second model is based on cone sheet complexes where surface deformation results from a deeper magma chamber. Both models, their fit to observed crater modifications and possible implications for local volcanism are described. Author

N92-10877*# Arizona Univ., Tucson. Lunar and Planetary Lab.
MAGNETIC EFFECTS OF LARGE-SCALE IMPACTS ON AIRLESS PLANETARY BODIES
L. L. Hood and Z. Huang *In* NASA, Washington, Reports of Planetary Geology and Geophysics Program, 1990 Jun. 1991 p 379-381 (For primary document see N92-10728 01-91)
(Grant NAGw-1881)
Avail: NTIS HC/MF A25 CSCL 03B

The analysis of lunar orbital and sample data combined with laboratory measurements of impact-produced plasmas suggest that large-scale impacts on planetary surfaces may have had significant magnetic effects. These effects may potentially explain part of all lunar crustal magnetization and, by extension, may be responsible for producing paleomagnetism on other airless silicate bodies in the solar system. Theoretical studies are presented of the magnetic field and remanent magnetization effects of basin-scale impacts on the Moon. The specific case of a Moon exposed to the solar wind plasma flow and its embedded magnetic field is investigated. It is shown that maximum compressed field amplitudes occur antipodal to the impact point in agreement with the observed tendency for orbital magnetic anomalies to be concentrated antipodal to young large lunar basins. Generalization of these results to include magnetic effects of impacts on other airless or nearly airless bodies in the solar system is presented. Author

N92-10878*# Brown Univ., Providence, RI. Dept. of Geological Sciences.
THE SPATIAL DISTRIBUTION AND TIME EVOLUTION OF IMPACT-GENERATED MAGNETIC FIELDS
D. A. Crawford and P. H. Schultz *In* NASA, Washington, Reports of Planetary Geology and Geophysics Program, 1990 Jun. 1991 p 382-383 (For primary document see N92-10728 01-91)
Avail: NTIS HC/MF A25 CSCL 03B

The production of magnetic fields was revealed by laboratory hypervelocity impacts in easily vaporized targets. As quantified by pressure measurements, high frame-rate photography, and electrostatic probes, these impacts tend to produce large quantities of slightly ionized vapor, which is referred to as impact-generated plasma. Nonaligned electron density and temperature gradients within this plasma may lead to production of the observed magnetic fields. Past experiments were limited to measuring a single component of the impact-generated magnetic fields at only a few locations about the developing impact crater and consequently gave little information about the field production mechanism. To understand this mechanism, the techniques were extended to map the three components of the magnetic field both in space and time. By conducting many otherwise identical experiments with arrayed magnetic detectors, a preliminary 3-D picture was produced of impact-generated magnetic fields as they develop through time. Author

N92-10879*# Jet Propulsion Lab., California Inst. of Tech., Pasadena.
GRAVITY SURVEY OF THE MT. TOONDINA IMPACT STRUCTURE, SOUTH AUSTRALIA
J. B. Plescia, E. M. Shoemaker, and C. S. Shoemaker (Geological Survey, Flagstaff, AZ.) *In* NASA, Washington, Reports of Planetary Geology and Geophysics Program, 1990 Jun. 1991 p 384-386 (For primary document see N92-10728 01-91)
Avail: NTIS HC/MF A25 CSCL 03B

The Mt. Toondina impact structure is located in northern South Australia, about 45 km south of the town of Oodnadatta. Only the central uplift is exposed. The outcrops at Mt. Toondina reveal a remarkable structural anomaly surrounded by a broad expanse of nearly flat-lying beds of the Bulldog Shale of Early Cretaceous age. A gravity survey was undertaken in 1989 to determine the diameter of the impact structure, define the form of the central uplift, and understand the local crustal structure. Data were collected along two orthogonal lines across the structure. In addition to the profiles, a significant number of measurements were made on and around the central uplift. The 1989 gravity data combined with 1963 gravity data and the seismic reflection data provide an excellent data base to interpret the subsurface structure of the Mt. Toondina feature. Author

N92-10880*# Geological Survey, Flagstaff, AZ.
ASTEROID FLUX AND IMPACT CRATERING RATE ON VENUS
E. M. Shoemaker, R. F. Wolfe, and C. S. Shoemaker *In* NASA, Washington, Reports of Planetary Geology and Geophysics Program, 1990 Jun. 1991 p 389-390 (For primary document see N92-10728 01-91)
Avail: NTIS HC/MF A25 CSCL 03B

By the end of 1990, 65 Venus-crossing asteroids were recognized; these represent 59 percent of the known Earth-crossing asteroids. Further studies, chiefly numerical integrations of orbit evolution, may reveal one or two more Venus crossers among the set of discovered asteroids. A Venus crosser was defined as an asteroid whose orbit can intersect the orbit of Venus as a result of secular (long range) perturbations. Venus crossers revolving on orbits that currently overlap the orbit of Venus are called Venapol asteroids, and those on orbit that don't overlap are called Venamor asteroids; 42 Venapols and 23 Venamors were recognized. Collision probabilities with Venus for 60 of the known Venus crossers were determined. Author

N92-10881*# Rensselaer Polytechnic Inst., Troy, NY. Dept. of Geology.
METEORITE SPECTROSCOPY AND CHARACTERIZATION OF ASTEROID SURFACE MATERIALS **c90**
Michael J. Gaffey *In* NASA, Washington, Reports of Planetary Geology and Geophysics Program, 1990 Jun. 1991 p 391-393

(For primary document see N92-10728 01-91)
(Grant NAGw-642)
Avail: NTIS HC/MF A25 CSCL 03B

The analysis of visible and near-infrared reflectance spectra is the primary means to determine surface mineralogy and petrology of individual asteroids. These individual studies provide the data to investigate the broader relationships between the asteroids and meteorites and between asteroids at different heliocentric distances. The main purpose is to improve the understanding of the origin, evolution, and inter-relationships of the asteroids; of their relationships to the meteorites; and of the processes active and the conditions present in the early inner solar system. Empirical information from the study of asteroids and the meteorites is essential to the adequate development and testing of the theoretical models for the accretion of the terrestrial planets, and for their early post-accretionary evolution. The recent results are outined in the following sections: (1) asteroid igneous processes, and (2) spinel-bearing asteroids and the nebular compositional gradient. Author

N92-10882*# Hawaii Univ., Honolulu. Dept. of Geology and Geophysics.
WILL GALILEO RESOLVE THE S-ASTEROID CONTROVERSY? c90
Jeffrey F. Bell *In* NASA, Washington, Reports of Planetary Geology and Geophysics Program, 1990 Jun. 1991 p 394-396 (For primary document see N92-10728 01-91)
Avail: NTIS HC/MF A25 CSCL 03B

The longest running argument in asteroid science concerns mineral composition and meteoritic association of the asteroids assigned to taxonomic type S. The approaching flyby of the S-type asteroid Gaspra by the Galileo spacecraft will drag an even larger section of the space science community into this argument. The basics of this problem are presented and discussed. The various proposed S asteroid compositions are presented and summarized in roughly the order in which they appeared. Author

N92-10883*# Naval Observatory, Flaggstaff, AZ.
MAPPING THE STABILITY FIELD OF JUPITER TROJANS
H. F. Levison, E. M. Shoemaker, and R. F. Wolfe (Geological Survey, Flagstaff, AZ.) *In* NASA, Washington, Reports of Planetary Geology and Geophysics Program, 1990 Jun. 1991 p 397-398 (For primary document see N92-10728 01-91)
Avail: NTIS HC/MF A25 CSCL 03B

Jupiter Trojans are a remnant of outer solar system planetesimals captured into stable or quasistable libration about the 1:1 resonance with the mean motion of Jupiter. The observed swarms of Trojans may provide insight into the original mass of condensed solids in the zone from which the Jovian planets accumulated, provided that the mechanisms of capture can be understood. As the first step toward this understanding, the stability field of Trojans were mapped in the coordinate proper eccentricity, e(sub p), and libration amplitude, D. To accomplish this mapping, the orbits of 100 particles with e(sub p) in the range of 0 to 0.8 and D in the range 0 to 140 deg were numerically integrated. Orbits of the Sun, the four Jovian planets, and the massless particles were integrated as a full N-body system, in a barycentric frame using fourth order symplectic scheme. Author

N92-10884*# Planetary Science Inst., Tucson, AZ.
UNDERSTANDING ASTEROID COLLISIONAL HISTORY THROUGH EXPERIMENTAL AND NUMERICAL STUDIES c90
Donald R. Davis, Eileen V. Ryan, and S. J. Weidenschilling *In* NASA, Washington, Reports of Planetary Geology and Geophysics Program, 1990 Jun. 1991 p 399-402 (For primary document see N92-10728 01-91)
Avail: NTIS HC/MF A25 CSCL 03B

Asteroids can lose angular momentum due to so called splash effect, the analog to the drain effect for cratering impacts. Numerical code with the splash effect incorporated was applied to study the simultaneous evolution of asteroid sized and spins. Results are presented on the spin changes of asteroids due to various physical effects that are incorporated in the described model. The goal was to understand the interplay between the evolution of sizes and spins over a wide and plausible range of model parameters. A single starting population was used both for size distribution and the spin distribution of asteroids and the changes in the spins were calculated over solar system history for different model parameters. It is shown that there is a strong coupling between the size and spin evolution, that the observed relative spindown of asteroids approximately 100 km diameter is likely to be the result of the angular momentum splash effect. Author

N92-10885*# Jet Propulsion Lab., California Inst. of Tech., Pasadena.
ASTEROID FAMILIES c90
James G. Williams *In* NASA, Washington, Reports of Planetary Geology and Geophysics Program, 1990 Jun. 1991 p 403-404 (For primary document see N92-10728 01-91)
Avail: NTIS HC/MF A25 CSCL 03B

More than 100 asteroid families are presented in Williams. Several examples of cratering events are known including family numbers 150, 162, 169, and 189. These are recognizable as many small fragments adjacent to and to one side (in three dimensions) of a much larger cratered body. Family numbers 138 and 140 are adjacent in proper element space. In population they are an intermediate step between the long recognizable families and the more frequent less populated families. Family number 164 is the fifth most populous family in the belt. All members are faint and nothing is known of the physical properties. Author

N92-10886*# Florida Univ., Gainesville. Dept. of Astronomy.
ORIGIN AND EVOLUTION OF THE ZODIACAL DUST CLOUD c90
S. F. Dermott, D. Durda, B. Gustafson, S. Jayaraman, Y.-L. Xu, P. D. Nicholson (Cornell Univ., Ithaca, NY.), and R. S. Gomes *In* NASA, Washington, Reports of Planetary Geology and Geophysics Program, 1990 Jun. 1991 p 405-406 (For primary document see N92-10728 01-91)
Avail: NTIS HC/MF A25 CSCL 03B

The astrophysical importance of the zodiacal cloud became more apparent. The most useful source of information on the structure of the zodiacal cloud is the Infrared Astronomical Satellite (IRAS) observations. A substantial fraction of the extensive IRAS data set was analyzed. Also, a numerical model was developed (SIMUL) that allows to calculate the distribution of night-sky brightness that would be produced by any particular distribution of dust particle orbits. This model includes the effects of orbital perturbations by both the planets and solar radiation, it reproduces the exact viewing geometry of the IRAS telescope, and allows for the eccentricity of the Earth's orbit. SIMUL now is used to model not just the solar system dust bands discovered by IRAS but the whole zodiacal cloud. Author

N92-10887*# Jet Propulsion Lab., California Inst. of Tech., Pasadena.
PHOTOMETRY OF THE COMET 2060 CHIRON c90
Bonnie J. Buratti, Robert L. Marcialis, and R. Scott Dunbar *In* NASA, Washington, Reports of Planetary Geology and Geophysics Program, 1990 Jun. 1991 p 407-408 (For primary document see N92-10728 01-91)
Avail: NTIS HC/MF A25 CSCL 03B

The comet 2060 Chiron has proven to be an interesting and enigmatic object. Situated between the orbits of Saturn and Uranus, it was originally classified as the most distant asteroid. It began to show cometary behavior in 1987 by increasing a full magnitude in brightness and developing a coma; there is evidence also for similar earlier outbursts. A thorough study of Chiron is important for two reasons: (1) it is a transition object defining the relationship between comets, asteroids, and meteorites; and (2) a full description of its changes in brightness - particularly on time scale of hours - will provide an empirical foundation for understanding the physical mechanisms (including outgassing, sublimation of volatiles, and even significant mass ejections) driving the evolution of comets. Short term outbursts were observed in early 1989, and a rapid decrease in brightness of Chiron's coma was observed

in 1990 in the V and R filters. Also, a rotational lightcurve was detected of the nucleus with an amplitude only 1/4 that observed in its quiescent state: this fact indicates the increased importance of the optically thin coma to the observed brightness. Author

N92-10888*# National Aeronautics and Space Administration. Lyndon B. Johnson Space Center, Houston, TX.
WATER/ROCK INTERACTIONS IN EXPERIMENTALLY SIMULATED DIRTY SNOWBALL AND DIRTY ICEBALL COMETARY NUCLEI **c90**
James L. Gooding and Judith H. Allton (Lockheed Engineering and Sciences Co., Houston, TX.) *In* NASA, Washington, Reports of Planetary Geology and Geophysics Program, 1990 Jun. 1991 p 412-414 (For primary document see N92-10728 01-91)
Avail: NTIS HC/MF A25 CSCL 03B

In the dirty snowball model for cometary nuclei, comet-nucleus materials are regarded as mixtures of volatile ices and relatively non-volatile minerals or chemical compounds. Carbonaceous chondrite meteorites are regarded as useful analogs for the rocky component. To help elucidate the possible physical geochemistry of cometary nuclei, preliminary results are reported of calorimetric experiments with two-component systems involving carbonaceous chondrites and water ice. Based on collective knowledge of the physics of water ice, three general types of interactions can be expected between water and minerals at sub-freezing temperatures: (1) heterogeneous nucleation of ice by insoluble minerals; (2) adsorption of water vapor by hygroscopic phases; and (3) freezing- and melting-point depression of liquid water sustained by soluble minerals. The relative and absolute magnitude of all three effects are expected to vary with mineral composition. Author

N92-10889*# Jet Propulsion Lab., California Inst. of Tech., Pasadena.
THERMAL MODELING OF COMET KOPFF: IMPLICATIONS FOR THE CRAF MISSION **c90**
Paul Weissman and Celia Clause *In* NASA, Washington, Reports of Planetary Geology and Geophysics Program, 1990 Jun. 1991 p 415 (For primary document see N92-10728 01-91)
Avail: NTIS HC/MF A25 CSCL 03B

A thermal model of periodic comet Kopff was developed to aid in planning for the Comet Rendezvous Asteroid Flyby mission. The model is based on the comet nucleus model, which estimates the surface temperature distribution and sublimation rates on a rotating icy sphere in heliocentric orbit. The model results are compared with the observed gas production rates from Kopff in 1983. It is found that approximately 15 percent of the sunlit nucleus surface is active, a relatively high fraction for a typical short-period comet. This suggests that the actual nucleus radius may be larger than the model value. The slope of the observed gas production curve with heliocentric distance is steeper than that predicted by the thermal model. This may indicate the existence of a more complex process than direct sublimation of surface ices, such as gas diffusion through a nonvolatile insulating crust. Author

N92-10890*# Heidelberg Univ. (Germany, F.R.).
FORMATION OF THE PROTOSOLAR NEBULA Abstract Only **c90**
Werner M. Tscharnuter and Alan P. Boss (Carnegie Institution of Washington, DC.) *In* NASA, Washington, Reports of Planetary Geology and Geophysics Program, 1990 Jun. 1991 p 419 (For primary document see N92-10728 01-91)
Avail: NTIS HC/MF A25 CSCL 03B

Theoretical models are discussed of the collapse of a dense molecular cloud core to form the protosolar nebula that produce the sun and the planet. The theoretical models use the equations of hydrodynamics, gravitation, and radiative transfer to follow the time evolution of a cloud collapsing under its own self-gravity. Both semi-analytical and fully numerical solutions (in two and three spatial dimensions) were calculated by several workers, One challenge is to find a set of initial conditions that will lead to the formation of a suitable protosolar nebula. Detailed results are shown for 2-D models, both with and without turbulent viscosity for redistributing angular momentum, and for 3-D models investigating the strength of gravitational torques associated with nonaxisymmetry produced during the collapse phase. Author

N92-10891*# California Univ., Los Angeles. Dept. of Earth and Space Sciences.
FRAGMENTATION IN STELLAR COLLAPSE **c90**
E. M. Myhill and W. M. Kaula *In* NASA, Washington, Reports of Planetary Geology and Geophysics Program, 1990 Jun. 1991 p 420-421 (For primary document see N92-10728 01-91)
(Grant NAGw-2085)
Avail: NTIS HC/MF A25 CSCL 03B

A three dimensional Cartesian code was developed to model molecular cloud collapse and protostellar formation. The basic Eulerian scheme employs spatially second-order accurate, finite difference methods to advance the fluid variables in time. The hydrodynamic equations governing the collapse include the effects of self-gravity, rotation, and radiative transfer. Supplementary equations include Poisson's equation which relates the gravitational potential to the density distribution and a mean intensity equation derived with the Eddington approximation for radiative transfer. The gas pressures and internal energies are determined from equations of state derived for a molecular cloud composed of hydrogen, helium, and heavier elements. Author

N92-10892*# Planetary Science Inst., Tucson, AZ.
AERODYNAMIC AND GASDYNAMIC EFFECTS IN COSMOGONY **c90**
S. J. Weidenschilling *In* NASA, Washington, Reports of Planetary Geology and Geophysics Program, 1990 Jun. 1991 p 424-425 (For primary document see N92-10728 01-91)
(Contract NASw-4618)
Avail: NTIS HC/MF A25 CSCL 03B

An improved numerical code was constructed to model coagulation and settling of particles in disk nebula containing generic turbulence with arbitrary velocities in the gas. The turbulence is assumed to have a Kolmogorov eddy spectrum. Relative velocities of particles, which lead to collisions and possible coagulation, are computed as due all significant causes in their appropriate regimes: thermal motion, shear and inertial effects in turbulent eddies, and systematic motions due to settling and non-keplerian rotation of the gas. Significant improvements to this program were produced. One significant problem was the disparity of timescales for turbulent mixing and coagulation. To accurately compute the former, the timestep must be shorter than the smallest spatial scale (layer thickness) divided by the turbulent velocity. However, the size distribution often varies due to coagulation on much longer timescales. To minimize the computational overhead associated with collisions between particles of all sizes, a dual timestep was introduced. Collisional changes in the size distribution are computed once in every N substeps, where the substep is controlled by the turbulent diffusion velocity, and N is determined by the rate of collisions. This algorithm allowed simulations to be extended to longer times and later stages. Author

N92-10893*# National Aeronautics and Space Administration. Ames Research Center, Moffett Field, CA.
PARTICLE-GAS DYNAMICS IN THE PROTOPLANETARY NEBULA **c90**
Jeffrey N. Cuzzi, Joelle M. Champney, and Anthony R. Dobrovolskis (California Univ., Santa Cruz.) *In* NASA, Washington, Reports of Planetary Geology and Geophysics Program, 1990 Jun. 1991 p 427-429 (For primary document see N92-10728 01-91)
Avail: NTIS HC/MF A25 CSCL 03B

In the past year we made significant progress in improving our fundamental understanding of the physics of particle-gas dynamics in the protoplanetary nebula. Having brought our code to a state of fairly robust functionality, we devoted significant effort to optimizing it for running long cases. We optimized the code for vectorization to the extent that it now runs eight times faster than before. The following subject areas are covered: physical improvements to the model; numerical results; Reynolds averaging

of fluid equations; and modeling of turbulence and viscosity.
Author

N92-10894*# Jet Propulsion Lab., California Inst. of Tech., Pasadena.
BENDING WAVES AND ORBITAL INCLINATIONS c90
William R. Ward (San Juan Capistrano Research Inst., CA.) *In* NASA, Washington, Reports of Planetary Geology and Geophysics Program, 1990 Jun. 1991 p 430-432 (For primary document see N92-10728 01-91)
Avail: NTIS HC/MF A25 CSCL 03B

Disk tides may play an important role in the formation of a planetary system. Modification of protoplanet semi-major axes and eccentricities through density waves was suggested and calculations of linear and non-linear protoplanet-nebula interactions were carried out by a number of researchers. The possible significance of radial drift to the accretion process was discussed, while the evolution of orbital eccentricities was studied for a perturber orbiting external to a ring and for a perturber embedded in the ring. The possible importance of bending waves to the early evolution of protoplanet inclinations is described. Author

N92-10895*# Planetary Science Inst., Tucson, AZ.
ACCRETION AND EVOLUTION OF SOLAR SYSTEM BODIES c90
S. J. Weidenschilling and Donald R. Davis *In* NASA, Washington, Reports of Planetary Geology and Geophysics Program, 1990 Jun. 1991 p 433-435 (For primary document see N92-10728 01-91)
(Contract NASw-4495)
Avail: NTIS HC/MF A25 CSCL 03B

We use a combination of analytical and numerical methods to study dynamical processes involved in the formation of planets and smaller bodies in the solar system. Our goal was to identify and understand critical processes and to link them in a numerical model of planetesimal accretion. We study effects of these processes by applying them in the context of the standard model of solar system formation, which involves accretion of the terrestrial planets and cores of the giant planet from small planetesimals. The principal focus of our research effort is the numerical simulation of accretion of a swarm of planetesimals into bodies of planetary size. Our computer code uses a Monte Carlo method to determine collisional interactions within the swarm. These interactions are not determined simply by a relative velocity, but rather by explicit distributions of keplerian orbital elements. The planetesimal swarm is divided into a number of zones in semimajor axis, which are allowed to interact. The present version of our code has the capability of following detailed distributions of size, eccentricity, and inclination in each zone. Author

N92-10896*# State Univ. of New York, Stony Brook.
LONG-TERM EVOLUTION OF A PLANETESIMAL SWARM IN THE VICINITY OF A PROTOPLANET c90
David M. Kary and Jack J. Lissauer *In* NASA, Washington, Reports of Planetary Geology and Geophysics Program, 1990 Jun. 1991 p 436-437 (For primary document see N92-10728 01-91)
(Grant NAGw-1107)
Avail: NTIS HC/MF A25 CSCL 03B

Many models of planet formation involve scenarios in which one or a few large protoplanets interact with a swarm of much smaller planetesimals. In such scenarios, three-body perturbations by the protoplanet as well as mutual collisions and gravitational interactions between the swarm bodies are important in determining the velocity distribution of the swarm. We are developing a model to examine the effects of these processes on the evolution of a planetesimal swarm. The model consists of a combination of numerical integrations of the gravitational influence of one (or a few) massive protoplanets on swarm bodies together with a statistical treatment of the interactions between the planetesimals. Integrating the planetesimal orbits allows us to take into account effects that are difficult to model analytically or statistically, such as three-body collision cross-sections and resonant perturbations by the protoplanet, while using a statistical treatment for the particle-particle interactions allows us to use a large enough sample to obtain meaningful results. Author

N92-10897*# Arizona Univ., Tucson. Lunar and Planetary Lab.
A REEXAMINATION OF EARLY NUMERICAL SIMULATIONS OF PLANETARY ACCRETION
R. A. Kolvoord and R. Greenberg *In* NASA, Washington, Reports of Planetary Geology and Geophysics Program, 1990 Jun. 1991 p 438-440 (For primary document see N92-10728 01-91)
Avail: NTIS HC/MF A25 CSCL 03B

The intermediate stage of protoplanetary accretion, where sub-km sized bodies accrete in 500-1000 km diameter bodies, is critical in determining the character of subsequent evolution. Greenberg et al. discovered that, at least through the formation of 500 km planetary embryos, the small particle dominate the population and control the velocity distribution, keeping velocities much smaller and setting up the possibility of runaway accretion, where the largest body is able to accumulate quickly a much greater mass and separate itself from the continuum of the size distribution. However, some controversy remains as to the exact methods used by Greenberg et al. I reviewed that planet formation model in detail to address these criticisms and better explain the algorithm used in the study. In particular, the algorithms for mutual velocity stirring among planetesimals and mass shifting between adjacent diameter bins are rederived in detail. I also examined the likelihood of artificial acceleration of the runaway growth phase of the intermediate stage of planetesimal formation. Author

N92-10898*# State Univ. of New York, Stony Brook.
COLLISION PROBABILITIES IN THE PRESENCE OF NEBULAR GAS DRAG c90
David M. Kary and Jack J. Lissauer *In* NASA, Washington, Reports of Planetary Geology and Geophysics Program, 1990 Jun. 1991 p 441-442 (For primary document see N92-10728 01-91)
(Grant NAGw-1107)
Avail: NTIS HC/MF A25 CSCL 03B

We are developing a model to determine what fraction of the planetesimals would have hit a protoplanet on their sunward journey as opposed to having a close approach and passing into an inferior orbit. The model involves direct numerical integration of restricted-three-body orbits using a predictor-corrector integrator. A simple gas drag law with a v(exp 2) dependence was also included in the equations of motion. Runs of 100 to 500 particles were already performed, while some future runs may require several times this number in order to get good impact statistics. All planetesimals start in superior orbits with semi-major axes 5 to 10 R(sub H) from the protoplanets, where R(sub H) is the protoplanet's Hill Sphere radius. The orbit is followed until the planetesimal passed into an inferior orbit at least 10 R(sub H) from the protoplanet. This process typically requires 10(exp 4) to 10(exp 5) orbits. Author

N92-10899*# State Univ. of New York, Stony Brook.
GROWTH OF PLANETS FROM PLANETESIMALS Abstract Only
Jack J. Lissauer and Glen R. Stewart (Colorado Univ., Boulder.) *In* NASA, Washington, Reports of Planetary Geology and Geophysics Program, 1990 Jun. 1991 p 443 (For primary document see N92-10728 01-91)
(Grants NAGw-1107; NAGw-769)
Avail: NTIS HC/MF A25 CSCL 03B

The formation of terrestrial planets and the cores of Jovian planets is reviewed in the framework of the planetesimal hypothesis, wherein planets are assumed to grow via the pairwise accumulation of small solid bodies. The rate of (proto)planetary growth is determined by the size and mass of the protoplanet, the surface density of planetesimals, and the distribution of planetesimal velocities relative to the protoplanet. Planetesimal velocities are modified by mutual gravitational interactions and collisions, which convert energy present in the ordered relative motions of orbiting particles (Keplerian shear) into random motions and tend to reduce

the velocities of the largest bodies in the swarm relative to those of smaller bodies, as well as by gas drag, which damps eccentricities and inclinations. Author

N92-10900*# Carnegie Institution of Washington, DC.
TIDAL DISRUPTION OF INVISCID PROTOPLANETS
Alan P. Boss, A. G. W. Cameron, and W. Benz (Harvard-Smithsonian Center for Astrophysics, Cambridge, MA.) *In* NASA, Washington, Reports of Planetary Geology and Geophysics Program, 1990 Jun. 1991 p 444-445 (For primary document see N92-10728 01-91)
Avail: NTIS HC/MF A25 CSCL 03B

Roche showed that equilibrium is impossible for a small fluid body synchronously orbiting a primary within a critical radius now termed the Roche limit. Tidal disruption of orbitally unbound bodies is a potentially important process for planetary formation through collisional accumulation, because the area of the Roche limit is considerably larger then the physical cross section of a protoplanet. Several previous studies were made of dynamical tidal disruption and different models of disruption were proposed. Because of the limitation of these analytical models, we have used a smoothed particle hydrodynamics (SPH) code to model the tidal disruption process. The code is basically the same as the one used to model giant impacts; we simply choose impact parameters large enough to avoid collisions. The primary and secondary both have iron cores and silicate mantles, and are initially isothermal at a molten temperature. The conclusions based on the analytical and numerical models are summarized. Author

N92-10901*# State Univ. of New York, Stony Brook.
A GEOMETRICAL MODEL FOR SHEPHERDING Abstract Only **c90**
Jack J. Lissauer *In* NASA, Washington, Reports of Planetary Geology and Geophysics Program, 1990 Jun. 1991 p 446 (For primary document see N92-10728 01-91)
(Grant NAGw-1107)
Avail: NTIS HC/MF A25 CSCL 03B

Shepherding is the process by which a satellite secularly exchanges angular momentum with a nearby particle or gaseous disk. The sense of the torque is such that the separation between the orbits of the particles and the shepherd increases secularly with time. I devised a new technique to analyze the physical nature of shepherding through study of evolution of the vector eccentricity of the particles. This method appears to analyze the physical nature of shepherding in sparse particle disks. Thus, it may be very useful in calculating the torque on Neptune's rings and on protoplanets in the solar nebula. Moreover, the techniques are useful in estimating how long numerical simulations of resonant processes must be run in order to reach a quasi-steady state. Author

N92-10902*# California Univ., Santa Cruz. Dept. of Physics.
DYNAMICS OF LOW VELOCITY COLLISIONS OF ICE PARTICLE, COATED WITH FROST **c90**
F. Bridges, D. Lin, L. Boone, and D. Darknell *In* NASA, Washington, Reports of Planetary Geology and Geophysics Program, 1990 Jun. 1991 p 447-448 (For primary document see N92-10728 01-91)
(Grant NAGw-590)
Avail: NTIS HC/MF A25 CSCL 03B

We continued our investigations of low velocity collisions of ice particles for velocities in range 10(exp -3) - 2 cm/s. The work focused on two effects: (1) the sticking forces for ice particles coated with CO2 frost, and (2) the completion of a 2-D pendulum system for glancing collisions. A new computer software was also developed to control and monitor the position of the 2-D pendulum. Author

N92-10903*# National Aeronautics and Space Administration. Ames Research Center, Moffett Field, CA.
PLANETARY RING STUDIES
Jeffrey N. Cuzzi, Anthony R. Dobrovolskis, Luke Dones, Richard H. Durisen, Linda Horn, and Mark R. Showalter (Stanford Univ., CA.) *In* NASA, Washington, Reports of Planetary Geology and Geophysics Program, 1990 Jun. 1991 p 449-451 (For primary document see N92-10728 01-91)
Avail: NTIS HC/MF A25 CSCL 03B

The following topics are covered: (1) characterization of the fine scale structure in Saturn's A and B rings; (2) ballistic transport modeling and evolution of fine ring structure; (3) faint features in the rings of Saturn; (4) the Encke moonlet; (5) dynamics in ringmoon systems; (6) a nonclassical radiative transfer model; and (7) particle properties from stellar occultation data. K.S.

N92-10904*# Cornell Univ., Ithaca, NY.
PHYSICAL PROCESSES IN PLANETARY RINGS
Joseph A. Burns *In* NASA, Washington, Reports of Planetary Geology and Geophysics Program, 1990 Jun. 1991 p 452-453 (For primary document see N92-10728 01-91)
(Grant NAGw-310)
Avail: NTIS HC/MF A25 CSCL 03B

A summary of research performed in 1990 is presented. The subject areas covered include perturbed narrow rings and the dynamics of circumplanetary dust. Progress made in the area of perturbed narrow rings includes: (1) the possible discovery of an undocumented moonlet in the environs of Saturn's F ring; and (2) the investigation of the consequences of a close satellite perturbing a narrow ring using numerical simulation. Progress made in the area of circumplanetary dust includes: (1) studies of the motion of circumplanetary dust under the action of radiation pressure and various electromagnetic processes; and (2) the initiation of a systematic explanation of the curious consequences of some of the perturbations that act on small particles. Author

N92-10905*# National Air and Space Museum, Washington, DC. Center for Earth and Planetary Studies.
PRELIMINARY GEOLOGIC MAPPING OF ARSIA MONS, MARS
James R. Zimbelman *In* NASA, Washington, Reports of Planetary Geology and Geophysics Program, 1990 Jun. 1991 p 457-458 (For primary document see N92-10728 01-91)
(Grant NAGw-1390)
Avail: NTIS HC/MF A25 CSCL 03B

Geologic mapping of the Tharsis Montes at a scale of 1:500,000 was recently initiated as part of the Mars Geologic Mapping Program of NASA. Detailed mapping of the three large shield volcanoes and their surroundings will help to clarify the sequence of events which led to the formation of these features, as well as provide a basis for comparing the complex histories of the three related yet distinctive volcanic centers. Preliminary mapping of Arsia Mons at a scale of 1:2 M was carried out in preparation for detailed mapping. A map is presented along with a discussion of its contents. Author

N92-10906*# National Air and Space Museum, Washington, DC. Center for Earth and Planetary Studies.
PRELIMINARY GEOLOGIC MAPPING OF CENTRAL CHRYSE PLANITIA, MARS
Robert A. Craddock, L. S. Crumpler, and Jayne C. Aubele (Brown Univ., Providence, RI.) *In* NASA, Washington, Reports of Planetary Geology and Geophysics Program, 1990 Jun. 1991 p 459-461 (For primary document see N92-10728 01-91)
(Grants NAGw-2187; NAGw-2171)
Avail: NTIS HC/MF A25 CSCL 03B

Because of the success of the Viking lander mission, central Chryse Planitia represents one of two areas on the Martian surface where planetary geologic mapping is added by ground-truth observations. The broadscale geology of Chryse Planitia and the geology of the Viking 1 landing site have been previously examined by other investigators. A 1:500,000 scale mapping of central Chryse Planitia and the Viking landing site was undertaken to synthesize these results and to address the following: (1) the depositional and erosional history of the Chryse Planitia basin; (2) the degree to which the Viking 1 surface materials are representative of the Chryse Planitia regions and of plains in general; (3) the extent of channel materials versus ridged plains materials; and (4) the primary

objectives of future missions to the surface of Mars. The preliminary results of the investigation are presented. Author

N92-10907*# National Air and Space Museum, Washington, DC. Center for Earth and Planetary Studies.
GEOLOGIC MAPPING OF NORTHERN LUNAE PLANUN, MARS
Robert A. Craddock and Ted A. Maxwell *In* NASA, Washington, Reports of Planetary Geology and Geophysics Program, 1990 Jun. 1991 p 462-464 Presented at the Annual Geological Society of America Conference, Dallas, TX, 29 Oct. - 1 Nov. 1990 and 22nd Lunar and Planetary Science Conference, Houston, TX, 18-22 Mar. 1991 (For primary document see N92-10728 01-91)
(Grant NAGw-1780)
Avail: NTIS HC/MF A25 CSCL 03B

Lunae Planum is an elevated region east of the Tharsis rise, and ridged plains containing numerous Sacra Dorsa wrinkle ridges, cross-cutting Sacra Fossae grabens, and lobate scarps compose this Martian Plateau. Geologic mapping of the northern Lunae Planum region was undertaken to better understand to emplacement history of the ridge plains, the structural history of deformation, and the periods of fluvial processes that have modified the region. These investigations are important for several reasons: (1) the history of plains emplacement yields information valuable for understanding the evolution of Tharsis volcanism; (2) interpretation of structural deformation has implications on the lithology of the Martian crust; and (3) determining the history and fate of Martian volatiles is dependent upon knowing the periods of outflow activity. A discussion of the findings is presented. Author

N92-10908*# DePauw Univ., Greencastle, IN. Dept. of Geology and Geography.
MARS GEOLOGIC MAPPING: DAO, HARMAKHIS, AND REULL VALLES REGION
Katherine H. Price *In* NASA, Washington, Reports of Planetary Geology and Geophysics Program, 1990 Jun. 1991 p 465-467 (For primary document see N92-10728 01-91)
(Grant NAGw-2336)
Avail: NTIS HC/MF A25 CSCL 03B

The east rim of Hellas basin is a complex geologic region affected by volcanic, tectonic, channeling, and resurfacing processes. A regional geologic map of the area between 27.5-42.4 degrees S and 260-275 degrees W was compiled in order to establish general stratigraphic relationships between and among the geologic units exposed in the region. The southern one-third of the regional map, the area convered by three MGM 1:500,000 quadrangles -40272, -40267, and -40262, is to be mapped in more detail in this project. Outflow channel deposits were subdivided into three facies and interpreted. A geologic sketch map of the Hadriaca Patera region on the east rim of the Hellas basin is presented. Author

N92-10909*# Arizona State Univ., Tempe. Dept. of Geology.
EVOLUTION OF THE EAST RIM OF THE HELLAS BASIN, MARS
David A. Crown, Katherine H. Price (DePauw Univ., Greencastle, IN.), and Ronald Greeley *In* NASA, Washington, Reports of Planetary Geology and Geophysics Program, 1990 Jun. 1991 p 468-470 (For primary document see N92-10728 01-91)
Avail: NTIS HC/MF A25 CSCL 03B

The Hellas basin is a dominant feature in the ancient, southern cratered highlands of Mars. The east rim of Hellas is a complex geologic region affected by volcanism, tectonism, and channeling. A detailed study of the area between 27.5-42.4 degrees S and 260-275 degrees W was initiated to analyze the processes forming surface materials and to decipher the evolution of this geologically important highland area. Major units include Hadriaca and Tyrrhena Paterae in the north and Hesperian and Amazonian channeled plains and outflow channels in the south. A brief discussion of the findings is presented. Author

N92-10910*# Lunar and Planetary Inst., Houston, TX.
GEOLOGIC MAPPING OF MTM QUADS 40292 AND 40297: IN THE UTOPIAN LOWLANDS NORTH OF THE NILOSYRTIS MENSAE, MARS
Steven H. Williams and James R. Zimbelman (National Air and Space Museum, Washington, DC.) *In* NASA, Washington, Reports of Planetary Geology and Geophysics Program, 1990 Jun. 1991 p 471-473 (For primary document see N92-10728 01-91)
Avail: NTIS HC/MF A25 CSCL 03B

Geologic mapping at 1:500,000 scale of the Mars transverse Mercator (MTM) quads 40292 and 40297 is being conducted under the auspices of the Mars Geologic Mapping Program. The study area is located in the southwestern portion of Utopia Planitia immediately north of the Nilosyrtis Mensae, between latitudes 37.5 and 42.5 degrees and longitudes 290 and 300 degrees. The goals of the mapping are to identify the major geologic features in the study area and to determine the sequence and scope of the geologic events that have modified the lowland side of the global dichotomy boundary in this region in order to at least partially constrain models of dichotomy boundary origin and evolution. The progress made towards achieving these goals is reported. Author

N92-10911*# Massachusetts Univ., Amherst. Dept. of Geology and Geography.
STRATIGRAPHY OF THE PERRINE AND NUN SULCI QUADRANGLES (Jg-2 AND Jg-5), GANYMEDE
George E. McGill and Steven W. Squyres (Cornell Univ., Ithaca, NY.) *In* NASA, Washington, Reports of Planetary Geology and Geophysics Program, 1990 Jun. 1991 p 474-476 (For primary document see N92-10728 01-91)
Avail: NTIS HC/MF A25 CSCL 03B

Dark and light terrain materials in the Perrine and Nun Sulci quadrangles are divided into nine map units, four dark, and five light. These are placed in time-stratigraphic sequence primarily by means of embayment and cross-cutting relationships. Dark terrain is generally more heavily cratered and thus older that light terrain but, at least in these quadrangles, crater densities are not reliable indicators of relative ages among the four dark material units. The four mapped material units within dark terrain are: cratered dark materials (dc), grooved dark materials (dg), transitional dark materials (di), and dark materials, undivided (d). The five mapped units within light terrain are: intermediate light materials (li), grooved light materials (lg), irregularly grooved light materials (lgl), smooth light materials (ls), and light materials, undivided. Author

N92-10912*# Geological Survey, Flagstaff, AZ.
MARS GEOLOGIC MAPPING PROGRAM: REVIEW AND HIGHLIGHTS
David H. Scott *In* NASA, Washington, Reports of Planetary Geology and Geophysics Program, 1990 Jun. 1991 p 479-480 (For primary document see N92-10728 01-91)
Avail: NTIS HC/MF A25 CSCL 03B

The Mars Geologic Mapping (MGM) Program was introduced by NASA in 1987 as a new initiative in the Planetary Geology and Geophysics (PGG) Program. The overall purpose of the program is to support research on topical science problems that address specific questions. Among the objectives of the project are: (1) to produce highly detailed geologic maps that will greatly increase the knowledge of the materials and processes that have contributed to the evolutionary history of Mars; (2) to define areas of special interest for possible future investigation by planned missions (Mars Observer, Mars Sample Return); and (3) to maintain the interest of the planetary community in the development of new concepts and the re-evaluation of Martian geology as new data in usable form become available. Some interesting highlights of the geologic mapping indicate that multiple flood episodes occurred at different times during the Hesperian Period in both Kasei and Maja Valles. Studies of small channels in the Memnonia, Mangala, and Tharsis regions show that fluvial events appear to have occurred during the Amazonian Period at equatorial latitudes. Flood waters occurred during the Amazonian Period at equatorial latitudes. Flood waters from Mangala Valles may have seeped into surficial materials with

the subsequent development of numerous sapping channels and debris flows; this suggests that the ancient highland terrain consists of relatively unconsolidated materials. Multiple layers were observed for the first time in the ridged plains lava flows covering large areas of Lunae Planum; some wrinkle ridges in this area are associated with grabens and collapse volcanic units at Hadriaca and Tyrrhena Paterae indicates that the units may have been emplaced by gravity-driven pyroclastic flows. Unlike the north polar layered deposits, those in the south polar region show no angular unconformities or evidence of faulting and folding. Water ice in the south polar layered deposits may be protected from solar heating and sublimation by a weathering rind or lag deposit on the surface. Author

N92-10913*# Geological Survey, Flagstaff, AZ.
VENUS MAPPING
R. M. Batson, H. F. Morgan, and Robert Sucharski *In* NASA, Washington, Reports of Planetary Geology and Geophysics Program, 1990 Jun. 1991 p 483-488 (For primary document see N92-10728 01-91)
Avail: NTIS HC/MF A25 CSCL 03B

Semicontrolled image mosaics of Venus, based on Magellan data, are being compiled at 1:50,000,000, 1:10,000,000, 1:5,000,000, and 1:1,000,000 scales to support the Magellan Radar Investigator (RADIG) team. The mosaics are semicontrolled in the sense that data gaps were not filled and significant cosmetic inconsistencies exist. Contours are based on preliminary radar altimetry data that is subjected to revision and improvement. Final maps to support geologic mapping and other scientific investigations, to be compiled as the dataset becomes complete, will be sponsored by the Planetary Geology and Geophysics Program and/or the Venus Data Analysis Program. All maps, both semicontrolled and final, will be published as I-maps by the United States Geological Survey. All of the mapping is based on existing knowledge of the spacecraft orbit; photogrammetric triangulation, a traditional basis for geodetic control on planets where framing cameras were used, is not feasible with the radar images of Venus, although an eventual shift of coordinate system to a revised spin-axis location is anticipated. This is expected to be small enough that it will affect only large-scale maps. Author

N92-10914*# Geological Survey, Flagstaff, AZ.
TRIANGULATION USING SYNTHETIC APERTURE RADAR IMAGES **c32**
Sherman S. C. Wu and Annie E. Howington-Kraus *In* NASA, Washington, Reports of Planetary Geology and Geophysics Program, 1990 Jun. 1991 p 489 (For primary document see N92-10728 01-91)
Avail: NTIS HC/MF A25 CSCL 03B

For the extraction of topographic information about Venus from stereoradar images obtained from the Magellan Mission, a Synthetic Aperture Radar (SAR) compilation system was developed on analytical stereoplotters. The system software was extensively tested by using stereoradar images from various spacecraft and airborne radar systems, including Seasat, SIR-B, ERIM XCL, and STAR-1. Stereomodeling from radar images was proven feasible, and development is on a correct approach. During testing, the software was enhanced and modified to obtain more flexibility and better precision. Triangulation software for establishing control points by using SAR images was also developed through a joint effort with the Defense Mapping Agency. The SAR triangulation system comprises four main programs, TRIDATA, MODDATA, TRISAR, and SHEAR. The first two programs are used to sort and update the data; the third program, the main one, performs iterative statistical adjustment; and the fourth program analyzes the results. Also, input are flight data and data from the Global Positioning System and Inertial System (navigation information). The SAR triangulation system was tested with six strips of STAR-1 radar images on a VAX-750 computer. Each strip contains images of 10 minutes flight time (equivalent to a ground distance of 73.5 km); the images cover a ground width of 22.5 km. All images were collected from the same side. With an input of 44 primary control points, 441 ground control points were produced. The adjustment process converged after eight iterations. With a 6-m/pixel resolution of the radar images, the triangulation adjustment has an average standard elevation error of 81 m. Development of Magellan radargrammetry will be continued to convert both SAR compilation and triangulation systems into digital form. Author

N92-10915*# Geological Survey, Flagstaff, AZ.
NAMING THE NEWLY FOUND LANDFORMS ON VENUS
R. M. Batson and J. F. Russell *In* NASA, Washington, Reports of Planetary Geology and Geophysics Program, 1990 Jun. 1991 p 490-491 (For primary document see N92-10728 01-91)
Avail: NTIS HC/MF A25 CSCL 03B

The mapping of Venus is unique in the history of cartigraphy; never has so much territory been discovered and mapped in so short a period of time. Therefore, in the interest of international scientific communication, there is a unique urgency to the development of a system of names for surface features on Venus. The process began with the naming of features seen on radar images taken from Earth and continued through mapping expeditions of the U.S. and U.S.S.R. However, the Magellan Mission resolves features twenty-five times smaller than those mapped previously, and its radar data will cover an area nearly equivalent to that of the continents and the sea-floors of the Earth combined. The International Astronomical Union (IAU) was charged with the formal endorsement of names of features on the planets. Proposed names are collected, approved, and applied through the IAU Working Group for Planetary System Nomenclature (WGPSN) and its task groups, prior to IAU approval by the IAU General Assembly. Names approved by the WGPSN and its task groups, prior to final approval may be used on published maps and articles, provided that their provisional nature is stipulated. The IAU has established themes for the names to be used on each of the planets; names of historical and mythological women are used on Venus. Names of political entities and those identified with active religions are not acceptable, and a person must have been deceased for three years or more to be considered. Any interested person may propose a name for consideration by the IAU.
Author

N92-10916*# RAND Corp., Santa Monica, CA.
THE CONTROL NETWORK OF MERCURY: APRIL 1991
Merton E. Davies and Patricia G. Rogers *In* NASA, Washington, Reports of Planetary Geology and Geophysics Program, 1990 Jun. 1991 p 492-493 (For primary document see N92-10728 01-91)
Avail: NTIS HC/MF A25 CSCL 03B

Features identified on Mariner 10 high resolution images of Mercury, acquired during three flybys between 1974 and 1975, form the basis of Mercury's planetwide control network. Although images from all three flybys are used in the net, the large amount of contiguous coverage from the second flyby, a southern bright-side pass, make these images the strongest contributors to the control net. Mercury is in synchronous rotation with a period of 58.6462 days and its spin axis is approximately normal to the equatorial plane. The 20 degree meridian is defined by the crater Hun Kal, located just south of the equator. The control network computations involve the photogrammetric determination of control point coordinates and an analytical triangulation solution. The current control network computations for Mercury are performed in the J2000 coordinate system according to the International Astronomical Union (IAU) convention. In recent years, updates to the control network have included improved trajectory solutions and modification of the standard radii (2439) at several points based on Earth-based radar altimetry data. The current status of the control network calculations is presented. Improvements were made to existing control points and new control points were added to the net to strengthen the overall network and improve the standard error of measurement. Author

N92-10917*# RAND Corp., Santa Monica, CA.
A UNIFIED LUNAR CONTROL NETWORK: APRIL 1991
Merton E. Davies *In* NASA, Washington, Reports of Planetary

Geology and Geophysics Program, 1990 Jun. 1991 p 494-496 (For primary document see N92-10728 01-91)
Avail: NTIS HC/MF A25 CSCL 03B

This program was designed to combine and transform various control networks of the Moon into a common center-of-mass coordinate system. The first phase, dealing with the near side, was completed and published. This report contains coordinates of 1166 points on the near side of the Moon. Author

N92-10918*# RAND Corp., Santa Monica, CA.
THE CONTROL NETWORK OF MARS: APRIL 1991
Merton E. Davies and Patricia G. Rogers *In* NASA, Washington, Reports of Planetary Geology and Geophysics Program, 1990 Jun. 1991 p 497-498 (For primary document see N92-10728 01-91)
Avail: NTIS HC/MF A25 CSCL 03B

The modern geodetic control network of Mars was first established based on Mariner 9 images with 1-2 km/pixel resolutions and covered almost the entire Martian surface. The introduction of higher resolution (10-200 meter/pixel) Viking Orbiter images greatly improved the accuracy and density of points in the control network. Analysis of the Viking Lander radio tracking data led to more accurate measurements of Mars' rotation period, spin axis direction, and the lander coordinates relative to the inertial reference frame. The prime meridian on Mars was defined by the Geodesy/Cartography Group of the Mariner 9 Television Team as the crater Airy-0, located about 5 degrees south of the equator. The Viking 1 Lander site was identified on a high resolution Viking frame. The control point measurements form the basis of a least squares solution determined by analytical triangulation after the pixel measurements are corrected for geometric distortions and converted to millimeter coordinates in the camera focal plane. Photogrammetric strips encircling Mars at the equator and at 60 degree north south were used to strengthen the overall net and improve the accuracy of the coordinates of points. In addition, photogrammetric strips along 0, 90, 180, and 270 degrees longitude to the Viking 1 Lander site have all significantly strengthened the control network. Most recently, photogrammetric strips were added to the net along 30 degrees north latitude between 0 and 180 degrees, and along 30 degrees between 180 and 360 degrees. The Viking 1 Lander site and Airy-0 are linked through photogrammetric strips occurring along the 0 degree meridian from Airy-0 to 65 degrees north, from that point through the Viking 1 Lander site to the equator, and along the equator to 180 degrees longitude. The Viking 1 lander site is thus a well calibrated area with coordinates of points accurate to approximately 200 meters relative to the J2000 inertial coordinate system. This will be a useful calibration region for upcoming missions. The current status of the control network calculations is presented. Author

N92-10919*# Geological Survey, Flagstaff, AZ.
PUBLICATION OF TOPOGRAPHIC ATLAS AND CONTROL NETWORK OF MARS
Sherman S. C. Wu, Jennifer S. Billideau, and Beth A. Spare *In* NASA, Washington, Reports of Planetary Geology and Geophysics Program, 1990 Jun. 1991 p 499-502 (For primary document see N92-10728 01-91)
Avail: NTIS HC/MF A25 CSCL 03B

To aid planetary studies and the planning of future Mars missions, the Topographic Atlas and Control Network for Mars will be submitted by the end of fiscal year 1992 for publication as a NASA Special Publication. It will consist of reduced versions of 108 1:2 million-scale photomosaics that show contour lines from topographic maps at the same scale, as well as precisely located control points. The control points are from the planetwide network, which is not only instrumental in the compilation of maps at various scales, but is also widely used in other research such as studies of Mars' gravity and atmosphere. An example, a combination of MC 8-NW and -SW, of the photomosaics to be included in the atlas is presented. Contour lines in the figure are at 1-km intervals. The final adjusted ground coordinates and elevations of the 77 control points shown are given in table form. The last column in the table lists the topographic datum (zero elevation) that can be used to compute the solid radius of the control point from the center of mass of Mars. The atlas will also include information such as the adjusted C-matrices of each image, descriptions of the methods used, and their accuracy, and guidelines for users. Author

N92-10920*# Geological Survey, Flagstaff, AZ.
COLOR-CODED GLOBAL TOPOGRAPHIC MAP OF MARS
Sherman S. C. Wu, Annie E. Howington-Kraus, and Karyn K. Ablin *In* NASA, Washington, Reports of Planetary Geology and Geophysics Program, 1990 Jun. 1991 p 503-505 (For primary document see N92-10728 01-91)
Avail: NTIS HC/MF A25 CSCL 03B

A Digital Terrain Model (DTM) was derived with both Mercator and Sinusoidal Equal-area projections from the global topographic map of Mars at a scale of 1:15 million and a contour interval of 1 km. Elevations on the map are referred to the Mars topographic datum that is defined by the gravity field at a 6.1-millibar pressure surface with respect to the center of mass of Mars. The DTM has a resolution at the equator of 1/59.226 degrees (exactly 1 km) per pixel. By using the DTM, color-coded global maps of Mars' topography were generated in both the Mercator projection and the Sinusoidal Equal-Area projection. On both maps, colors indicate 1 km increments of height. From the equal-are dataset, the positive and negative elevation distributions are calculated to be 67 and 33 percent, respectively. Author

N92-10921*# Geological Survey, Flagstaff, AZ.
MARS ELEVATION DISTRIBUTION
Sherman S. C. Wu, Annie E. Howington-Kraus, and Karyn K. Ablin *In* NASA, Washington, Reports of Planetary Geology and Geophysics Program, 1990 Jun. 1991 p 506-507 (For primary document see N92-10728 01-91)
Avail: NTIS HC/MF A25 CSCL 03B

A Digital Terrain Model (DTM) of Mars was derived with both Mercator and Sinusoidal Equal-Area projections from the global topographic map of Mars (scale 1:15 million, contour interval 1 km). Elevations on the map are referred to Mars' topographic datum that is defined by the gravity field at a 6.1-millibar pressure surface with respect to the center of mass of Mars. The DTM has a resolution at the equator of 1/59.226 degrees (exactly 1 km) per pixel. By using the DTM, the volumetric distribution of Mars topography above and below the datum has previously been calculated. Three types of elevation distributions of Mars' topography were calculated from the same DTM: (1) the frequency distribution of elevations at the pixel resolution; (2) average elevations in increments of 6 degrees in both longitude and latitude; and (3) average elevations in 36 separate blocks, each covering 30 degrees of latitude and 60 degrees of longitude. Author

N92-10922*# Geological Survey, Flagstaff, AZ.
COMPLETION OF COMPILATION OF THE 1:2,000,000-SCALE TOPOGRAPHIC MAP SERIES OF MARS
Sherman S. C. Wu, Raymond Jordan, Patricia A. Garcia, and Karyn K. Ablin *In* NASA, Washington, Reports of Planetary Geology and Geophysics Program, 1990 Jun. 1991 p 508 (For primary document see N92-10728 01-91)
Avail: NTIS HC/MF A25 CSCL 03B

Using special photogrammetric techniques, Mars' topography is being systematically mapped at a scale of 1:2,000,000 from high-altitude Viking Orbiter images. Of the 140 maps in the series, 120 have previously been compiled on the AS-11AM analytical stereoplotters. In fiscal year 1991, the remaining 20 maps will be compiled (most of these are between +/- 30 degrees latitude and the poles). Elevations on the maps are related to the Mars topographic datum. The Mars planetwide control net is used for the control of compilation. The maps have a contour interval of 1 km and a vertical precision of +/- 1 km; thus, they are more detailed than previous maps. Author

N92-10923*# Geological Survey, Flagstaff, AZ.
MARS HIGH-RESOLUTION MAPPING
R. M. Batson and P. K. Thomas *In* NASA, Washington, Reports

of Planetary Geology and Geophysics Program, 1990 Jun. 1991 p 509 (For primary document see N92-10728 01-91)
Avail: NTIS HC/MF A25 CSCL 03B

A series of photomosaics of high-resolution Viking Orbiter images of Mars is being prepared and published to support the Mars 1:500,000 scale geologic mapping program. More than 100 of these photomosaics were made manually, but for the last several years they have all been made digitally. The digital mosaics are published on the Mars Transverse Mercator (MTM) system, and they are also available to the appropriate principal investigators as digital files in the mosaicked digital image model (MDIM) format. The mosaics contain Viking Orbiter images with the highest available resolution: in some areas as high as 10 m/pixel. This resolution, where it exists, will support a 1:100,000 map scale. The full resolution of a mosaic is preserved in a digital file, but conventional lithographic publication of such large-scale inset maps will be done only if required by the geologic map author. When high-resolution images do not full the neatlines of an MTM quadrangle, the medium-resolution (1/256 degrees/pixel, or 231 m/pixel) MDIM is used. The mosaics are tied by image-matching to the planetwide MDIM, in which random errors as large as 5 km (10 mm at 1:500,000 scale) are common; a few much larger, worst-case errors also occur. Because of the distribution of the errors, many large discrepancies appear along the cutlines between frames with very different resolutions. Furthermore, each block of quadrangles is compiled on its own local control system, and adjacent blocks, compiled later, are unlikely to match. Selection of areas to be mapped is based on geologic mapping proposals reviewed and recommended by the Mars 1:500,000 scale geologic mapping review panel. There is no intention to map the entire planet at this scale. Author

N92-10924*# Geological Survey, Flagstaff, AZ.
A NEW EDITION OF THE MARS 1:5,000,000 MAP SERIES
R. M. Batson, Alfred S. McEwen, and Sherman S. C. Wu *In* NASA, Washington, Reports of Planetary Geology and Geophysics Program, 1990 Jun. 1991 p 510 (For primary document see N92-10728 01-91)
Avail: NTIS HC/MF A25 CSCL 03B

A new edition of the Mars 1:5,000,000 scale map series is in preparation. Two sheets will be made for each quadrangle. Sheet one will show shaded relief, contours, and nomenclature. Sheet 2 will be a full-color photomosaic prepared on the Mars digital image model (MDIM) base co-registered with the Mars low-resolution color database. The latter will have an abbreviated graticule (latitude/longitude ticks only) and no other line overprint. The four major databases used to assemble this series are now virtually complete. These are: (1) Viking-revised shaded relief maps at 1:5,000,000 scale; (2) contour maps at 1:2,000,000 scale; (3) the Mars digital image model; and (4) a color image mosaic of Mars. Together, these databases form the most complete planetwide cartographic definition of Mars that can be compiled with existing data. The new edition will supersede the published Mars 1:5,000,000 scale maps, including the original shaded relief and topographic maps made primarily with Mariner 9 data and the Viking-revised shaded relief and controlled photomosaic series. Publication of the new series will begin in late 1991 or early 1992, and it should be completed in two years. Author

N92-10925*# Geological Survey, Flagstaff, AZ.
PLANETARY ATLASES
R. M. Batson, J. L. Inge, and H. F. Morgan *In* NASA, Washington, Reports of Planetary Geology and Geophysics Program, 1990 Jun. 1991 p 511 (For primary document see N92-10728 01-91)
Avail: NTIS HC/MF A25 CSCL 03B

Two kinds of planetary map atlases are in production. Atlases of the first kind contain reduced-scale versions of maps in hard-bound books with dimensions of 11 x 14 inches. These new atlases are intended to: (1) provide concise but comprehensive references to the geography of the planets needed by planetary scientists and others; and (2) allow inexpensive access to the planetary map dataset without requiring acquisition and examination of tens or hundreds of full-size map sheets. Two such atlases have been published and a third is in press. Work was begun of an Atlas of the Satellite of the Outer Planets. The second kind of atlas is a popular or semi-technical version designed for commercial publication and distribution. The first edition, The Atlas of the Solar System, is nearly ready for publication. New funding and contracting constraints now make it unlikely that the atlas can be published in the format originally planned. Currently, the possibility of publishing the maps through the U.S. Geological Survey as a series of folios in the I-map series is being explored. The maps are global views of each solid-surface body of the Solar System. Each map shows airbrushed relief, albedo, and, where available, topography. A set of simplified geologic maps is also included. All of the maps are on equal-area projections. Scales are 1:40,000,000 for the Earth and Venus; 1:2,000,000 for the Saturnian satellites Mimas and Enceladus and the Uranian satellite Miranda; 1:100,000 for the Martian satellites, Phobos and Deimos; and 1:10,000,000 for all other bodies. Author

N92-10926*# Geological Survey, Flagstaff, AZ.
CD-ROM PUBLICATION OF THE MARS DIGITAL CARTOGRAPHIC DATA BASE
R. M. Batson, E. M. Eliason, L. A. Soderblom, Kathleen Edwards, and Sherman S. C. Wu *In* NASA, Washington, Reports of Planetary Geology and Geophysics Program, 1990 Jun. 1991 p 512-513 (For primary document see N92-10728 01-91)
Avail: NTIS HC/MF A25 CSCL 03B

The recently completed Mars mosaicked digital image model (MDIM) and the soon-to-be-completed Mars digital terrain model (DTM) are being transcribed to optical disks to simplify distribution to planetary investigators. These models, completed in FY 1991, provide a cartographic base to which all existing Mars data can be registered. The digital image map of Mars is a cartographic extension of a set of compact disk read-only memory (CD-ROM) volumes containing individual Viking Orbiter images now being released. The data in these volumes are pristine in the sense that they were processed only to the extent required to view them as images. They contain the artifacts and the radiometric, geometric, and photometric characteristics of the raw data transmitted by the spacecraft. This new set of volumes, on the other hand, contains cartographic compilations made by processing the raw images to reduce radiometric and geometric distortions and to form geodetically controlled MDIM's. It also contains digitized versions of an airbrushed map of Mars as well as a listing of all feature names approved by the International Astronomical Union. In addition, special geodetic and photogrammetric processing has been performed to derive rasters of topographic data, or DTM's. The latter have a format similar to that of MDIM, except that elevation values are used in the array instead of image brightness values. The set consists of seven volumes: (1) Vastitas Borealis Region of Mars; (2) Xanthe Terra of Mars; (3) Amazonis Planitia Region of Mars; (4) Elysium Planitia Region of Mars; (5) Arabia Terra of Mars; (6) Planum Australe Region of Mars; and (7) a digital topographic map of Mars. Author

N92-10927*# Geological Survey, Flagstaff, AZ.
DIGITAL CARTOGRAPHY OF IO
Alfred S. McEwen, B. Duck, and Kathleen Edwards *In* NASA, Washington, Reports of Planetary Geology and Geophysics Program, 1990 Jun. 1991 p 514 (For primary document see N92-10728 01-91)
Avail: NTIS HC/MF A25 CSCL 03B

A high resolution controlled mosaic of the hemisphere of Io centered on longitude 310 degrees is produced. Digital cartographic techniques were employed. Approximately 80 Voyager 1 clear and blue filter frames were utilized. This mosaic was merged with low-resolution color images. This dataset is compared to the geologic map of this region. Passage of the Voyager spacecraft through the Io plasma torus during acquisition of the highest resolution images exposed the vidicon detectors to ionized radiation, resulting in dark-current buildup on the vidicon. Because the vidicon is scanned from top to bottom, more charge accumulated toward the bottom of the frames, and the additive error increases from top to bottom as a ramp function. This ramp

function was removed by using a model. Photometric normalizations were applied using the Minnaert function. An attempt to use Hapke's photometric function revealed that this function does not adequately describe Io's limb darkening at emission angles greater than 80 degrees. In contrast, the Minnaert function accurately describes the limb darkening up to emission angles of about 89 degrees. The improved set of discrete camera angles derived from this effort will be used in conjunction with the space telemetry pointing history file (the IPPS file), corrected on 4 or 12 second intervals to derive a revised time history for the pointing of the Infrared Interferometric Spectrometer (IRIS). For IRIS observations acquired between camera shutterings, the IPPS file can be corrected by linear interpolation, provided that the spacecraft motions were continuous. Image areas corresponding to the fields of view of IRIS spectra acquired between camera shutterings will be extracted from the mosaic to place the IRIS observations and hotspot models into geologic context. Author

N92-10928*# Geological Survey, Flagstaff, AZ.
DIGITAL SOLAR SYSTEM GEOLOGY
R. M. Batson, R. C. Kozak, and Nancy K. Isbell *In* NASA, Washington, Reports of Planetary Geology and Geophysics Program, 1990 Jun. 1991 p 515 (For primary document see N92-10728 01-91)
Avail: NTIS HC/MF A25 CSCL 03B

All available synoptic maps of the solid-surface bodies of the Solar System were digitized for presentation in the planned Atlas of the Solar System by Greeley and Batson. Since the last report (Batson et al., 1990), preliminary Uranian satellite maps were replaced with improved versions, Galilean satellite geology was simplified and digitized, structure was added to many maps, and the maps were converted to a standard format, with corresponding standing colors for the mapped units. Following these changes, the maps were re-reviewed by their authors and are now undergoing final editing before preparation for publication. In some cases (for Mercury, Venus, and Mars), more detailed maps were digitized and then simplified for the Atlas. Other detailed maps are planned to be digitized in the coming year for the Moon and the Galilean satellites. For most of the remaining bodies such as the Uranian satellites, the current digitized versions contain virtually all the detail that can be mapped given the available data; those versions will be unchanged for the Atlas. These digital geologic maps are archived at the digital scale of 1/16 degree/ pixel, in sinusoidal format. The availability of geology of the Solar System in a digital database will facilitate comparisons and integration with other data: digitized lunar geologic maps have already been used in a comparison with Galileo SSI observations of the Moon. Author

N92-10929*# Geological Survey, Flagstaff, AZ.
A NEW CATALOG OF PLANETARY MAPS Abstract Only
R. M. Batson and J. L. Inge *In* NASA, Washington, Reports of Planetary Geology and Geophysics Program, 1990 Jun. 1991 p 516 (For primary document see N92-10728 01-91)
Avail: NTIS HC/MF A25 CSCL 03B

A single, concise reference to all existing planetary maps, including lunar ones, is being prepared that will allow map users to identify and locate maps of their areas of interest. This will be the first such comprehensive listing of planetary maps. Although the USGS shows index maps on the collar of each map sheet, periodically publishes index maps of Mars, and provides informal listings of the USGS map database, no tabulation exists that identifies all planetary maps, including those published by DMA and other organizations. The catalog will consist of a booklet containing small-scale image maps with superimposed quadrangle boundaries and map data tabulations. Author

N92-10930*# Washington Univ., Saint Louis, MO. Center for Space Sciences.
IMAGE RETRIEVAL AND PROCESSING SYSTEM VERSION 2.0 DEVELOPMENT WORK **c82**
Susan H. Slavney and Edward A. Guinness *In* NASA, Washington, Reports of Planetary Geology and Geophysics Program, 1990 Jun. 1991 p 517-519 (For primary document see N92-10728 01-91)
Avail: NTIS HC/MF A25 CSCL 03B

The Image Retrieval and Processing System (IRPS) is a software package developed at Washington University and used by the NASA Regional Planetary Image Facilities (RPIF's). The IRPS combines data base management and image processing components to allow the user to examine catalogs of image data, locate the data of interest, and perform radiometric and geometric calibration of the data in preparation for analysis. Version 1.0 of IRPS was completed in Aug. 1989 and was installed at several IRPS's. Other RPIF's use remote logins via NASA Science Internet to access IRPS at Washington University. Work was begun on designing and population a catalog of Magellan image products that will be part of IRPS Version 2.0, planned for release by the end of calendar year 1991. With this catalog, a user will be able to search by orbit and by location for Magellan Basic Image Data Records (BIDR's), Mosaicked Image Data Records (MIDR's), and Altimetry-Radiometry Composite Data Records (ARCDR's). The catalog will include the Magellan CD-ROM volume, director, and file name for each data product. The image processing component of IRPS is based on the Planetary Image Cartography Software (PICS) developed by the U.S. Geological Survey, Flagstaff, Arizona. To augment PICS capabilities, a set of image processing programs were developed that are compatible with PICS-format images. This software includes general-purpose functions that PICS does not have, analysis and utility programs for specific data sets, and programs from other sources that were modified to work with PICS images. Some of the software will be integrated into the Version 2.0 release of IRPS. A table is presented that lists the programs with a brief functional description of each. Author

N92-10931*# Washington Univ., Seattle.
COMPOSITIONAL VARIABILITY OF THE MARTIAN SURFACE
John B. Adams and Milton O. Smith *In* NASA, Washington, Reports of Planetary Geology and Geophysics Program, 1990 Jun. 1991 p 523-524 (For primary document see N92-10728 01-91)
Avail: NTIS HC/MF A25 CSCL 03B

Spectral reflectance data from Viking Landers and Orbiters and from telescopic observations were analyzed with the objective of isolating compositional information about the Martian surface and assessing compositional variability. Two approaches were used to calibrate the data to reflectance to permit direct comparisons with laboratory reference spectra of well characterized materials. In Viking Lander multispectral images (six spectral bands) most of the spectral variation is caused by changes in lighting geometry within individual scenes, from scene to scene, and over time. Lighting variations are both wavelength independent and wavelength dependent. By calibrating lander image radiance values to reflectance using spectral mixture analysis, the possible range of compositions was assessed with reference to a collection of laboratory samples, also resampled to the lander spectral bands. All spectra from the lander images studied plot (in six-space) within a planar triangle having at the apexes the respective spectra of tan basaltic palagonite, gray basalt, and shale. Within this plane all lander spectra fit as mixtures of these three endmembers. Reference spectra that plot outside of the triangle are unable to account for the spectral variation observed in the images. Author

N92-10932*# California Inst. of Tech., Pasadena.
IMPACT AND COLLISIONAL PROCESSES IN THE SOLAR SYSTEM **c90**
Thomas J. Ahrens, C. Gazis, R. Pepin, R. Becker, R. Cronin, J. Tyburczy, T. Tingle (California Univ., Davis.), T. Duffy, and L. Rowan *In* NASA, Washington, Reports of Planetary Geology and Geophysics Program, 1990 Jun. 1991 p 525-528 (For primary document see N92-10728 01-91)
(Grant NAGw-1941)
Avail: NTIS HC/MF A25 CSCL 03B

As impact cratered terrains have been successively recognized on certain planets and planetary satellites, it has become clear

that impact processes are important to the understanding of the accretion and evolution of all solid planets. The noble gases in the normalized atmospheric inventories of the planets and the normalized gas content of meteorites are grossly similar, but demonstrate differences from each other which are not understood. In order to study shock devolatilization of the candidate carrier phases which are principally thought to be carbonaceous or hydrocarbons in planetesimals, experiments were conducted on noble gase implantation in various carbons: carbon black, activated charcoal, graphite, and carbon glass. These were candidate starting materials for impact devolatilization experiments. Initial experiments were conducted on vitreous amorphous carbon samples which were synthesized under vapor saturated conditions using argon as the pressurizing medium. An amino acid and surface analysis by laser ionization analyses were performed on three samples of shocked Murchison meteorite. A first study was completed in which a series of shock loading experiments on a porous limestone and on a non-porous gabbro in one and three dimensions were performed. Also a series of recovery experiments were conducted in which shocked molten basalt a 1700 C is encapsulated in molybdenum containers and shock recovered from up to 6 GPa pressures. Author

N92-10933*# California Inst. of Tech., Pasadena. Seismological Lab.
IMPACT CRATERING CALCULATIONS
Thomas J. Ahrens, J. D. OKeefe, C. Smither, and T. Takata *In* NASA, Washington, Reports of Planetary Geology and Geophysics Program, 1990 Jun. 1991 p 529-531 (For primary document see N92-10728 01-91)
(Grant NAGw-1953)
Avail: NTIS HC/MF A25 CSCL 03B

In the course of carrying out finite difference calculations, it was discovered that for large craters, a previously unrecognized type of crater (diameter) growth occurred which was called lip wave propagation. This type of growth is illustrated for an impact of a 1000 km (2a) silicate bolide at 12 km/sec (U) onto a silicate half-space at earth gravity (1 g). The von Misses crustal strength is 2.4 kbar. The motion at the crater lip associated with this wave type phenomena is up, outward, and then down, similar to the particle motion of a surface wave. It is shown that the crater diameter has grown d/a of approximately 25 to d/a of approximately 4 via lip propagation from Ut/a = 5.56 to 17.0 during the time when rebound occurs. A new code is being used to study partitioning of energy and momentum and cratering efficiency with self- gravity for finite-sized objects rather than the previously discussed planetary half-space problems. These are important and fundamental subjects which can be addressed with smoothed particle hydrodynamic (SPH) codes. The SPH method was used to model various problems in astrophysics and planetary physics. The initial work demonstrates that the energy budget for normal and oblique impacts are distinctly different than earlier calculations for silicate projectile impact on a silicate half space. Motivated by the first striking radar images of Venus obtained by Magellan, the effect of the atmosphere on impact cratering was studied. In order the further quantify the processes of meteor break-up and trajectory scattering upon break-up, the reentry physics of meteors striking Venus' atmosphere versus that of the Earth were studied. Author

N92-10934*# Colorado Univ., Boulder. Lab. for Atmospheric and Space Physics.
MODELS OF PLANETARY RINGS
L. W. Esposito, T. G. Brophy, Glen R. Stewart, and P. A. Yanamandra-Fisher (Jet Propulsion Lab., California Inst. of Tech., Pasadena.) *In* NASA, Washington, Reports of Planetary Geology and Geophysics Program, 1990 Jun. 1991 p 532-533 (For primary document see N92-10728 01-91)
Avail: NTIS HC/MF A25 CSCL 03B

The Voyager occultations provide several uniform and high quality data sets for Saturn, Uranus, and Neptune. These data are intercompared, and theoretical models for the particle sizes and the particle transport are developed. The major topics covered include: ring size distribution, torques and resonances, and satellite wakes. Author

N92-10935*# Wellesley Coll., MA. Dept. of Astronomy.
DYNAMICS AND STRUCTURE OF PLANETARY RINGS
R. G. French *In* NASA, Washington, Reports of Planetary Geology and Geophysics Program, 1990 Jun. 1991 p 534-536 (For primary document see N92-10728 01-91)
Avail: NTIS HC/MF A25 CSCL 03B

Recent research efforts were directed towards sharpening the understanding of kinematical and dynamical properties of the Uranian rings, with the combination of Earth-based and Voyager observations, and in obtaining and interpreting new observations of the Saturn system from the remarkable stellar occultation of 3 Jul. 1989. Some of the highlights studied include: (1) a detailed comparison of structure and dynamics of the Uranus rings from joint analysis of high quality Earth-based data and the complete set of Voyager occultation measurements; (2) a comprehensive search for weak normal modes excited in the Uranian rings, analogous to the m = 2 and m = 0 normal modes previously identified for the delta and gamma rings; (3) an ongoing search for faint rings and ring arcs of Uranus, using both Voyager images of the rings and Earth-based and spacecraft stellar occultation data; (4) a comparison of upper stratospheric temperatures of Uranus inferred from Voyager ultraviolet occultations with results of ground-based occultation observations; and (5) observations of the 3 Jul. 1989 Saturn occultation of 28 Sgr. Author

N92-10936*# California Univ., Santa Barbara. Dept. of Physics.
ACCRETION RATES OF PROTOPLANETS Abstract Only
Yuval Greenzweig and Jack J. Lissauer *In* NASA, Washington, Reports of Planetary Geology and Geophysics Program, 1990 Jun. 1991 p 537 Prepared in cooperation with State Univ. of New York, Stony Brook (For primary document see N92-10728 01-91)
(Grant NAGw-2061)
Avail: NTIS HC/MF A25 CSCL 03B

The rate at which planetesimals in a uniform surface density disk collide with, and are (assumed to be) accreted by, a massive protoplanet is calculated. The collision cross-section of a protoplanet is enhanced relative to its geometric cross-section due to its gravitational focusing of planetesimal trajectories. The gravitation enhancement (eccentricities and inclinations) decrease. For large random velocity planetesimals, encounters are sufficiently rapid (less than or approximately = 5 percent of and orbital period) that F(sub g) is well approximated by the two-body particle in a box formula, which neglects the gravitational effect of the Sun. As planetesimal velocities decrease, F(sub g) increases to approximately twice the two-body value, and then rises less rapidly than the two-body value, eventually dropping below it and asymptotically approaching a constant for sufficiently small random velocities. A scaling argument is presented that generalizes the results to protoplanets of arbitrary mass, radius, and orbital semimajor axis. Gravitational scatterings by a protoplanet prevent random velocities of the planetesimals within its accretion zone from becoming to small. When gravitational stirring is included, the maximum plausible value of the gravitation enhancement factor for rock protoplanets 1 Au from the Sun is F(sub g) of approximately 1000. If one protoplanet dominates gravitational scatterings in a given region of a protoplanetary disk, then it was found that the planetesimal inclinations are excited much less rapidly than eccentricities, in contrast to the two-body approximation, in which energy is roughly equipartitioned between eccentric and inclined random motions. The resulting skewed velocity dispersion allows for a more rapid rate of protoplanet growth. Author

N92-10937*# California Univ., Santa Barbara. Dept. of Physics.
ACCRETION RATES OF PROTOPLANETS 2: GAUSSIAN DISTRIBUTION OF PLANESTESIMAL VELOCITIES Abstract Only
Yuval Greenzweig and Jack J. Lissauer *In* NASA, Washington, Reports of Planetary Geology and Geophysics Program, 1990 Jun.

1991 p 538 Prepared in cooperation with State Univ. of New York, Stony Brook (For primary document see N92-10728 01-91)
(Grants NAGw-2061; NAGw-1107)
Avail: NTIS HC/MF A25 CSCL 03B

The growth rate of a protoplanet embedded in a uniform surface density disk of planetesimals having a triaxial Gaussian velocity distribution was calculated. The longitudes of the aspses and nodes of the planetesimals are uniformly distributed, and the protoplanet is on a circular orbit. The accretion rate in the two body approximation is enhanced by a factor of approximately 3, compared to the case where all planetesimals have eccentricity and inclination equal to the root mean square (RMS) values of those variables in the Gaussian distribution disk. Numerical three body integrations show comparable enhancements, except when the RMS initial planetesimal eccentricities are extremely small. This enhancement in accretion rate should be incorporated by all models, analytical or numerical, which assume a single random velocity for all planetesimals, in lieu of a Gaussian distribution.
Author

N92-10938*# Oregon State Univ., Corvallis. Coll. of Oceanography.
MUD VOLCANOES ON MARS?
Paul D. Komar *In* NASA, Washington, Reports of Planetary Geology and Geophysics Program, 1990 Jun. 1991 p 539-541 (For primary document see N92-10728 01-91)
Avail: NTIS HC/MF A25 CSCL 03B

The term mud volcano is applied to a variety of landforms having in common a formation by extrusion of mud from beneath the ground. Although mud is the principal solid material that issues from a mud volcano, there are many examples where clasts up to boulder size are found, sometimes thrown high into the air during an eruption. Other characteristics of mud volcanoes (on Earth) are discussed. The possible presence of mud volcanoes, which are common and widespread on Earth, on Mars is considered.
Author

N92-10939*# Arizona Univ., Tucson. Dept. of Planetary Sciences.
GENERATION AND BEHAVIOR OF SOLAR SYSTEM MAGNETIC FIELDS **c90**
Eugene H. Levy *In* NASA, Washington, Reports of Planetary Geology and Geophysics Program, 1990 Jun. 1991 p 542-544 (For primary document see N92-10728 01-91)
(Grant NAGw-2176)
Avail: NTIS HC/MF A25 CSCL 03B

A range of problems aimed primarily at elucidating the character and consequences of magnetic-field generation in the solar system and at testing ideas against known properties of natural magnetic fields are covered. Among the specific subjects currently under investigation are the magnetohydrodynamic (MHD) character of the protosolar nebula, including the generation and behavior of magnetic fields, the electrical conductivity of dusty nebular gas, transient magnetodynamic and electrodynamic nebular phenomena, and the generation and dynamical behavior of planetary magnetic fields. During the past year, the focus of this research was on disk magnetic field generation and transient MHD heating events possibly associated with the protoplanetary nebula.
Author

N92-10940*# Arizona State Univ., Tempe. Dept. of Geology.
PLANETARY GEOMORPHOLOGY RESEARCH: FY 1990-1991
M. C. Malin *In* NASA, Washington, Reports of Planetary Geology and Geophysics Program, 1990 Jun. 1991 p 545-546 (For primary document see N92-10728 01-91)
(Grant NAGw-1)
Avail: NTIS HC/MF A25 CSCL 03B

Progress in the following research areas is discussed: (1) volatile ice sublimation in a simulated Martian polar environment; (2) a global synthesis of Venusian tectonics; (3) a summary of nearly a decade of field studies of eolian processes in cold volcanic deserts; and (4) a model for interpretation of Martian sediment distribution using Viking observations. Some conclusions from the research are presented.
Author

N92-10941*# California Univ., San Diego, La Jolla. Space Inst.
ASTEROID SURFACE PROCESSES: EXPERIMENTAL STUDIES OF THE SOLAR WIND ON REFLECTANCE AND OPTICAL PROPERTIES OF ASTEROIDS **c90**
Lucy-Ann McFadden *In* NASA, Washington, Reports of Planetary Geology and Geophysics Program, 1990 Jun. 1991 p 547-548 (For primary document see N92-10728 01-91)
(Grant NAGw-2215)
Avail: NTIS HC/MF A25 CSCL 03B

The effect of the solar wind on the optical properties of meteorites was studied to determine whether the solar wind can alter the properties of ordinary chondrite parent bodies resulting in the spectral properties of S-type asteroids. The existing database of optical properties of asteroids was analyzed to determine the effect of solar wind in altering asteroid surface properties.
Author

N92-10942*# Johns Hopkins Univ., Baltimore, MD. Dept. of Earth and Planetary Sciences.
ARE THE EQUATORIAL HIGHLANDS ON VENUS FORMED BY MANTLE PLUME DIAPIRS?
Peter Olson *In* NASA, Washington, Reports of Planetary Geology and Geophysics Program, 1990 Jun. 1991 p 549-551 (For primary document see N92-10728 01-91)
Avail: NTIS HC/MF A25 CSCL 03B

Several origins have been proposed for the Equatorial Highlands on Venus, including spreading centers and plume-related uplift. Recently, the spreading center hypothesis has been shown to be incompatible with the measured geoid and topography variations over the highlands. It is also difficult to reconcile the range of geoid anomalies over the highlands with a steady-state plum model. There is a large variation in admittance values (geoid/topography ratios) among highland regions. This variation suggests that different uplifted regions represent distinct stages in a time dependent process. It has been proposed that the Beta Regio, Thetis Regio, Ovda Regio, and Artemis Plateau Equatorial Highland Regions are formed by large mantel diapirs. According to this model, topography and geoid height decrease with increasing age of the highland, as the diapir spreads out beneath the lithosphere. In order to determine if the diapir model is compatible with the sequence of tectonic and volcanic events recorded in the surface geology of the highlands, a series of finite difference calculations were made of the ascent and partial melting of a spherical thermal diapir in an incompressible, infinite Prandtl number, isoviscous fluid.
Author

N92-10943*# California Univ., Los Angeles. Dept. of Earth and Space Science.
THERMAL AND ALBEDO MAPPING OF THE NORTH AND SOUTH POLAR REGIONS OF MARS
D. A. Paige and K. D. Keegan *In* NASA, Washington, Reports of Planetary Geology and Geophysics Program, 1990 Jun. 1991 p 552-553 (For primary document see N92-10728 01-91)
Avail: NTIS HC/MF A25 CSCL 03B

The first maps of the thermal properties of the north and south polar region of Mars are presented. The maps complete the mapping of the entire planet. The maps for the north polar region were derived from Viking Infrared Thermal Mapper (IRTM) observations obtained from 10 Jun. to 30 Sep. 1978. This period corresponds to the early summer season in the north, when the north residual water ice cap was exposed, and the polar surface temperatures were near their maximum. The maps in the south were derived from observations obtained between 24 Aug. to 23 Sep. 1977. This period corresponds to the late summer season in the south, when the seasonal polar cap had retreated to close to its residual configuration, and the second global dust storm of 1977 had largely subsided. The major results concerning the following topics are summarized: (1) surface water ice; (2) polar dune material; and (3) dust deposits.
Author

N92-10944*# Brown Univ., Providence, RI. Dept. of Geological Sciences.
THE WIDTH OF FAULT ZONES IN A BRITTLE-VISCOUS LITHOSPHERE: STRIKE-SLIP FAULTS
E. M. Parmentier *In* NASA, Washington, Reports of Planetary Geology and Geophysics Program, 1990 Jun. 1991 p 554-555 (For primary document see N92-10728 01-91)
Avail: NTIS HC/MF A25 CSCL 03B

A fault zone in an ideal brittle material overlying a very weak substrate could, in principle, consist of a single slip surface. Real fault zones have a finite width consisting of a number of nearly parallel slip surfaces on which deformation is distributed. The hypothesis that the finite width of fault zones reflects stresses due to quasistatic flow in the ductile substrate of a brittle surface layer is explored. Because of the simplicity of theory and observations, strike-slip faults are examined first, but the analysis can be extended to normal and thrust faulting. Author

N92-10945*# California Univ., Santa Barbara. Dept. of Physics.
THE RING ARCS OF NEPTUNE
S. J. Peale *In* NASA, Washington, Reports of Planetary Geology and Geophysics Program, 1990 Jun. 1991 p 556-557 (For primary document see N92-10728 01-91)
(Grant NAGw-2061)
Avail: NTIS HC/MF A25 CSCL 03B

After the corotation resonance with an exterior satellite proved inapplicable to the Neptune ring arc confinement, a search for other mechanisms settled on the possible influence of Neptune's magnetic field. The areas of greater optical depth around the ring are much dustier than the low optical depth regions. These particles reside in a plasma; therefore, they must carry some charge. The components of Neptune's magnetic field on the equator at the radius of the ring arcs as a function of Neptunian longitude are shown. The components are those of an offset tilted dipole model. Although the dipole model is probably not a good approximation so close to the planet, the magnitude of the field that is given is probably close to the actual value. The possible importance of the magnetic field on the smallest particles in the ring is indicated by the ratio of the magnetic field on the smallest particles in the ring is indicated by the ratio of the magnetic force to the central gravitation attraction with the field strength of B = 0.01 gauss at the ring distance. A preferred position in the orbit for magnetically perturbed particles seems to require a commensurability between the rotation of the planet and the motion of the particle in the orbit. The period of rotation is assumed to be that of the radio bursts at 16.11 hours. However, without a model for the radio emission, one cannot be absolutely sure. Jupiter's decametric radiation depends on Io's orbital position as well as the rotation, so a synodic periodicity might be appropriate. But the latter radiation is highly directed, whereas Neptune's was seen all along the spacecraft trajectory on the 16.11 hour schedule, i.e., with no shifts in phase relative to a fixed longitude on the planet. The ring orbital period is 10.536 hours which is not commensurate with the rotation period. If the 16.11 hours is interpreted as a synodic period between the rotation and a satellite motion, the closest rotation periods to 16 hours are 15.9 hours if the satellite is 1989N4 and 18.2 hours if the satellite is Triton. The former is near a 3:2 resonance with the ring particle motion. The problem deserves some more thought before a possible herding of small particles by the magnetic field is abandoned. Author

N92-10946*# California Univ., Santa Barbara. Dept. of Physics.
THE TITAN-HYPERION ORBITAL RESONANCE Abstract Only
S. J. Peale *In* NASA, Washington, Reports of Planetary Geology and Geophysics Program, 1990 Jun. 1991 p 558 (For primary document see N92-10728 01-91)
(Grant NAGw-2061)
Avail: NTIS HC/MF A25 CSCL 03B

Considerable effort was spent investigating the applicability of a Hamiltonian averaged over high frequency terms, where long period and secular terms up to second order in eccentricity were kept. The Hamiltonian that is given from the planar, elliptic, restricted three body problem applied to Titan-Hyperion, when the Kepler terms are also expanded to second order in small quantities and several conical transformations are carried out, is presented and discussed. Author

N92-10947*# California Univ., Santa Barbara. Dept. of Physics.
ROTATIONAL PROPERTIES OF PLANETARY SATELLITES Abstract Only
S. J. Peale *In* NASA, Washington, Reports of Planetary Geology and Geophysics Program, 1990 Jun. 1991 p 559 (For primary document see N92-10728 01-91)
(Grant NAGw-2061)
Avail: NTIS HC/MF A25 CSCL 03B

Properties of satellite rotation that are observable in principle, include the rotation period, the orientation of the spin axis relative to the orbit plane, precession of the spin axis due to gravitational torques, nonprincipal axis rotation or wobble, and deviations from uniform principle axis rotation or libration. Considerable order is observed in current satellite rotation states, and it is of interest to ascertain how this order came about and why some satellites do not conform to the dominant norm. There is a strong coupling between the spin and orbital motions that is primarily responsible for maintaining the ordered rotation states in most cases, but this coupling is equally responsible for destroying any chance of orderly rotation for Saturn's satellite Hyperion. Understanding the processes which constrain current rotation states as well as those of an evolutionary nature which could have brought the individual satellites to their observed rotation and orbit states allows us to sometimes infer interior properties of some satellite or even of its primary planet, although, attempts to deduce primordial rotation states are usually frustrated. The observed rotational properties of the planetary satellites are summarized, and the understanding of the processes maintaining and those leading to the observed states are outlined. Some of the inferences that can be drawn about intrinsic properties of the bodies themselves are indicated. Author

N92-10948*# National Aeronautics and Space Administration. Ames Research Center, Moffett Field, CA.
OPTICAL PROPERTIES OF GRAINS IN MOLECULAR CLOUDS AND ACCRETION DISKS Abstract Only
J. B. Pollack, D. Hollenbach, D. Simonelli, S. Beckwith, T. L. Roush, and W. Fong (Synernet Corp., Fremont, CA.) *In* NASA, Washington, Reports of Planetary Geology and Geophysics Program, 1990 Jun. 1991 p 560 (For primary document see N92-10728 01-91)
Avail: NTIS HC/MF A25 CSCL 03B

A baseline model of the composition and abundances of grains and gases in molecular cloud cores and accretion disks around young stars is defined by employing: a wide range of astronomical data and theory; the composition of primitive bodies in the solar system; and solar elemental abundances. It is proposed that in the coldest portions of these objects the major grain species include amorphous olivine, amorphous orthopyroxene, volatile and refractory organics, water ice, troilite, and metallic iron. Using a combination of laboratory measurements of optical constants and asymptotic theory, values of the real and imaginary indices of refraction of these grain species over a wavelength range that runs from the vacuum UV to the radio domain are derived. Auxiliary information for these grain species, such as their vaporization temperatures bulk densities, and their fractional abundances by mass. The above information on grain properties in molecular cloud cores and accretion disks is used to estimate the Rosseland mean opacity of the grains in both environments and the IR and microwave opacity of grains in accretion disks. Author

N92-10949*# Arizona Univ., Tucson. Lunar and Planetary Lab.
STUDIES IN PLANETARY RINGS Abstract Only
Carolyn C. Porco *In* NASA, Washington, Reports of Planetary Geology and Geophysics Program, 1990 Jun. 1991 p 561-562 (For primary document see N92-10728 01-91)
(Grant NAGw-960)
Avail: NTIS HC/MF A25 CSCL 03B

Progress made in research devoted to examining Voyager

imaging data for the purpose of understanding the kinematics and dynamics of the Neptune ring arcs is reported. It was found that a radial distortion of amplitude 30 km is traveling through the arcs with a perturbation by the nearby satellite 1989N4. Two new and smaller arcs within the outer Neptunian ring were also discovered. The longitudinal spacing of all arcs is roughly that expected for corotational arc shepherding by 1989N4 provided that not all corotation sites in the arc region are filled. The semimajor axis of the arcs' orbit inferred from their observed mean motion and the latest Neptune gravitational parameters is, within uncertainties, identical to the location of the 42:43 corotation-inclination resonance of 1989N4: an observation which supports the notion of corotational arc-shepherding. This hypothesis also explains that the 15 km radial width of the arcs are due to a spread in forced orbital eccentricities. Clumps within the arcs were observed at a greater frequency than previously reported. These features may be the manifestation of big bodies within the arcs providing a source of ring dust, or they may be a kinematical effect associated with the crossing of eccentric orbits at quadrature. The inclusion of ground based observations of the arcs taken up to five years ago will lengthen the baseline over which arc dynamics may be studied and should lead to a refinement in the position of the Neptune spin and invariable plane poles. Author

N92-10950*# National Aeronautics and Space Administration. Ames Research Center, Moffett Field, CA.

DERIVATION OF MID-INFRARED (5-25 MICRONS) OPTICAL CONSTRAINTS OF SOME SILICATES AND PALAGONITE

T. L. Roush, J. B. Pollack, and J. B. Orenberg (San Francisco State Univ., CA.) *In* NASA, Washington, Reports of Planetary Geology and Geophysics Program, 1990 Jun. 1991 p 563-564 (For primary document see N92-10728 01-91)

Avail: NTIS HC/MF A25 CSCL 03B

This study was initially conceived in order to aid in the interpretation of Martian surface and atmospheric aerosol mineralogy. As a result, the minerals included are biased toward samples which represent hydrated and hydroxylated silicates. Due to their physical particle size, clays and other materials, such as palagonite, cannot be prepared using typical preparation techniques. Yet in some cases, such as for Mars, these are the materials of perhaps the greatest interest. In order to obtain a suitable sample of these less cohesive materials for the laboratory measurements, a KBr pellet die was used and a pellet of the pure sample was prepared. For all clays and the palagonite, a pellet with highly reflective surfaces at visible wavelengths was produced. The reflectivities of all samples were determined, and to derive the optical constants of a materials as a function of wavelength, dispersion analysis was used which describes the real and imaginary indices of refraction as the contributions due to a sum of classical oscillators and relates them via Frensel's equations for non-normal incidence, the the measured near-normal reflectivity. The final values that were determined represent averages of several model fits to each data set using the same number of oscillators by varying the high frequency dielectric constant. Author

N92-10951*# National Aeronautics and Space Administration. Ames Research Center, Moffett Field, CA.

THERMAL INFRARED OBSERVATIONS OF MARS (7.5-12.8 MICRONS) DURING THE 1990 OPPOSITION

T. L. Roush, F. Witteborn, P. G. Lucy, A. Graps (Hawaii Univ., Honolulu.), and J. B. Pollack *In* NASA, Washington, Reports of Planetary Geology and Geophysics Program, 1990 Jun. 1991 p 565-566 (For primary document see N92-10728 01-91)

Avail: NTIS HC/MF A25 CSCL 03B

Thirteen spectra of Mars, in the 7.5 to 12.8 micron wavelength were obtained on 7 Dec. 1990 from the Infrared Telescope Facility (IRTF). For these observations, a grating with an ultimate resolving power of 120 to 250 was used and wavelengths were calibrated for each grating setting by comparison with the absorption spectrum of polystyrene measured prior to each set of observations. By sampling the Nyquist limit at the shortest wavelengths, an effective resolving power of about 120 over the entire wavelength range was achieved. A total of four grating settings were required to cover the entire wavelength region. A typical observing sequence consisted of: (1) positioning the grating in one of the intervals; (2) calibrating the wavelength of positions; and (3) obtaining spectra for a number of spots on Mars. Several observations of the nearby stellar standard star, alpha Tauri, were also acquired throughout the night. Each Mars spectrum represents an average of 4 to 6 measurements of the individual Mars spots. As a result of this observing sequence, the viewing geometry for a given location or spot on Mars does not change, but the actual location of the spot on Mars's surface varies somewhat between the different grating settings. Other aspects of the study are presented. Author

N92-10952*# California Inst. of Tech., Pasadena. Div. of Geological and Planetary Sciences.

PLANETARY ORIGIN, EVOLUTION, AND STRUCTURE

David J. Stevenson *In* NASA, Washington, Reports of Planetary Geology and Geophysics Program, 1990 Jun. 1991 p 567-569 (For primary document see N92-10728 01-91)

(Grant NAGw-185)

Avail: NTIS HC/MF A25 CSCL 03B

Three areas of recent and ongoing research are presented. The first area is giant planet heatflows. Conventional wisdom attributes the heatflow of the giant planets to the gradual loss of primordial heat, except in the case of Saturn where helium separation is evidently occurring. There are two problems with this picture: (1) the observed helium abundance of Saturn's atmosphere is so low that Jupiter must also be differentiating helium since its internal entropy cannot be much higher than Saturn; and (2) the heatflow of Neptune (not to mention Uranus) is too high to be consistent with adiabatic cooling from an initial hot state. A self-consistent solution to these two problems is presented. The second area covered is that of the despinning protogiant planets. Modeling of the possible despinning of these protoplanets by hydromagnetic torques was performed and the model results are discussed. The third area covered is how Titan hides its ocean. Until recently, the favored picture of Titan's surface was a roughly kilometer-thick ethane/methane ocean, presumably global in extent with at most a few outcroppings of dry land. The depth of the ocean is well constrained by observed atmospheric properties, and the constraints on subaerial topography are obtained indirectly from tidal considerations. A different picture of Titan's surface was pursued which was motivated by the perspective that methane on Titan should more properly be considered as a magmatic fluid. In this picture, methane is stored subsurface in magma chambers fed from deep-seated sources of methane, most probably due to the high pressure breakdown of methane clathrate. Other aspects of this model of Titan are presented. Author

N92-10953*# Arizona Univ., Tucson. Lunar and Planetary Lab.

TIDAL EVOLUTION OF PLANETARY SATELLITES

William C. Tittemore *In* NASA, Washington, Reports of Planetary Geology and Geophysics Program, 1990 Jun. 1991 p 570-571 (For primary document see N92-10728 01-91)

(Grant NAGw-1720)

Avail: NTIS HC/MF A25 CSCL 03B

Early in the history of the Solar System, Europa and Ganymede may have evolved through a 3:1 mean-motion commensurability, which would have been encountered prior to the establishment of the current Laplace resonance involving Io, Europa, and Ganymede. If Europa and Ganymede passed through the 3:1 mean-motion commensurability, the orbital eccentricities of both satellites may have increased to large values during a phase of chaotic behavior, after which the satellites would have escaped from the resonance. In spite of the relatively large J sub 2 of Jupiter, Europa, and Ganymede are sufficiently massive and distant from the planet that resonances at the 3:1 mean-motion commensurability interact strongly, leading to chaotic behavior via the same kinds of dynamical mechanisms present at resonances among the Uranian satellites. As a result of the large eccentricity increases possible during the evolution of Europa and Ganymede through the 3:1 mean-motion commensurability, tidal heating may have melted water ice in the mantles of both satellites, and stresses on the

lithosphere of both satellites due to tidal deformation may have been sufficient to cause extensive fracturing, making resurfacing possible. This may account for the post-heavy bombardment geological activity on both Europa and Ganymede. In addition, the effects of resonance passage on Ganymede may provide an explanation of the Ganymede-Callisto dichotomy by providing Ganymede with an intense source of internal heat and lithospheric stress not present in Callisto. Further possibilities of this evolution are presented. Author

N92-10954*# National Air and Space Museum, Washington, DC. Center for Earth and Planetary Studies.

WRINKLE RIDGE-UPLAND SCARP TRANSITIONS: IMPLICATIONS FOR THE MECHANICAL PROPERTIES OF THE DEFORMED MATERIALS

Thomas R. Watters, Michael J. Tuttle, and Debra Simpson (West Chester Univ., PA.) *In* NASA, Washington, Reports of Planetary Geology and Geophysics Program, 1990 Jun. 1991 p 572-574 Presented at the 22nd Lunar and Planetary Science Conference, Houston, TX, 18-22 Mar. 1991 (For primary document see N92-10728 01-91)

(Grants NAGw-940; NAGw-1172)

Avail: NTIS HC/MF A25 CSCL 03B

Wrinkle ridge-upland scarp transitions are structures that occur at the contact between smooth plains material and highlands or uplands materials on the Moon and Mars. In the smooth plains material the structures have a morphology typical of wrinkle ridges, interpreted to be the result of a combination of folding and thrust faulting. Where the structures extend into the uplands, a distinct change in the morphology occurs. The generally asymmetric cross sectional geometry characteristics of wrinkle ridges becomes that of a one-sided, often lobate scarp. The scarp is indistinguishable from other highland/upland scarps, interpreted to be the result of reverse or thrust faulting. Although these structures are rare, they provide important insight into the mechanical properties of deformed materials. These insights are discussed. Author

N92-10955*# National Air and Space Museum, Washington, DC. Center for Earth and Planetary Studies.

WRINKLE RIDGES IN THE FLOOR MATERIAL OF KASEI VALLES, MARS: NATURE AND ORIGIN

Thomas R. Watters and Robert A. Craddock *In* NASA, Washington, Reports of Planetary Geology and Geophysics Program, 1990 Jun. 1991 p 575-577 Presented at the 22nd Lunar and Planetary Science Conference, Houston, TX, 18-22 Mar. 1991 (For primary document see N92-10728 01-91)

(Grants NAGw-940; NAGw-1172; NAGw-1780)

Avail: NTIS HC/MF A25 CSCL 03B

Wrinkle ridges on Mars occur almost exclusively in smooth plains material referred to as ridged plains. One of the largest contiguous units of ridged plains occurs on Lunae Planum on the eastern flank of the Tharsis rise. The eastern, western, and northern margins of the ridged plains of Lunae Planum suffered extensive erosion in early Amazonian channel-forming events. The most dramatic example of erosion in early Amazonian plains is in Kasei Valles. The nature an origin of the wrinkle ridges in the floor material of Kasei Valles are discussed. Author

N92-10956*# Colorado Univ., Boulder. Lab. for Atmospheric and Space Physics.

PROPERTIES OF DUST AND CLOUDS IN THE MARS ATMOSPHERE: ANALYSIS OF VIKING IRTM EMISSION PHASE FUNCTION SEQUENCES

R. T. Clancy and S. W. Lee *In* NASA, Washington, Reports of Planetary Geology and Geophysics Program, 1990 Jun. 1991 p 578 (For primary document see N92-10728 01-91)

(Grant NAGw-1378)

Avail: NTIS HC/MF A25 CSCL 03B

An analysis of emission-phase-function (EPF) observations from the Viking Orbiter Infrared Thermal Mapper (IRTM) yields a wide variety of results regarding dust and cloud scattering in the Mars atmosphere and atmospheric-corrected albedos for the surface of Mars. A multiple scattering radiative transfer model incorporating a bidirectional phase function for the surface and atmospheric scattering by dust and clouds is used to derive surface albedos and dust and ice optical properties and optical depths for these various conditions on Mars. Author

N92-10957*# Lancaster Univ. (England). Environmental Science Div.

FACTORS CONTROLLING THE STRUCTURES OF MAGMA CHAMBERS IN BASALTIC VOLCANOES **c46**

L. Wilson and James W. Head (Brown Univ., Providence, RI.) *In* NASA, Washington, Reports of Planetary Geology and Geophysics Program, 1990 Jun. 1991 p 579-580 (For primary document see N92-10728 01-91)

Avail: NTIS HC/MF A25 CSCL 03B

The depths, vertical extents, and lateral extents of magma chambers and their formation are discussed. The depth to the center of a magma chamber is most probably determined by the density structure of the lithosphere; this process is explained. It is commonly assumed that magma chambers grow until the stress on the roof, floor, and side-wall boundaries exceed the strength of the wall rocks. Attempts to grow further lead to dike propagation events which reduce the stresses below the critical values of rock failure. The tensile or compressive failure of the walls is discussed with respect to magma migration. The later growth of magma chambers is accomplished by lateral dike injection into the country rocks. The factors controlling the patterns of growth and cooling of such dikes are briefly mentioned. Author

N92-10958*# Cornell Univ., Ithaca, NY. Lab. for Planetary Studies.

STUDIES OF VOLATILES AND ORGANIC MATERIALS IN EARLY TERRESTRIAL AND PRESENT-DAY OUTER SOLAR SYSTEM ENVIRONMENTS **c90**

Carl Sagan, W. Reid Thompson, Christopher F. Chyba, and B. N. Khare *In* NASA, Washington, Reports of Planetary Geology and Geophysics Program, 1990 Jun. 1991 p 581-583 (For primary document see N92-10728 01-91)

Avail: NTIS HC/MF A25 CSCL 03B

A review and partial summary of projects within several areas of research generally involving the origin, distribution, chemistry, and spectral/dielectric properties of volatiles and organic materials in the outer solar system and early terrestrial environments are presented. The major topics covered include: (1) impact delivery of volatiles and organic compounds to the early terrestrial planets; (2) optical constants measurements; (3) spectral classification, chemical processes, and distribution of materials; and (4) radar properties of ice, hydrocarbons, and organic heteropolymers. Author

N92-10959*# Kansas State Univ., Manhattan. Dept. of Geology.

PRELIMINARY 1:500,000-SCALE GEOLOGIC MAPPING OF CLARITAS FOSSAE, MARS

James R. Underwood, Jr. *In* NASA, Washington, Reports of Planetary Geology and Geophysics Program, 1990 Jun. 1991 p 584-585 (For primary document see N92-10728 01-91)

Avail: NTIS HC/MF A25 CSCL 03B

The Claritas Fossae system is a complex, linear fracture zone that extends from its northern intersection with Noctis Labyrinthus 1800 km south-southeast to its southern intersection with Thaumasia Fossae. The width of the fracture zone varies from 150 km in the north to 550 km in the south; topographic relief, based on radar data from Earth, is 1.0 to 1.5 km. Claritas Fossae and its coincident ridge or rise have been interpreted to be a horst with more than 8 km of vertical uplift, the greatest such uplift on Mars. Viking orbital images of sufficiently high resolution exist to provide the basis only for two 1:500,000 scale photomosaic base maps of Claritas Fossae. They extend en in echelon east and west, i.e., the southeast corner of the northern and western quadrangle (MTM-30102) is coincident with the northwest corner of the eastern and southern quadrangle (MTM-25107). Preliminary geologic maps of the two quadrangles were prepared. Materials in the quadrangles are Noachian and Hesperian age, and the

quadrangles are characterized by the widespread occurrence of fractured and cratered plateau material, the oldest material in the map areas. Other information about the quadrangles is presented. Author

N92-10960*# Stanford Univ., CA. Center for Radar Astronomy.
INVESTIGATION OF THE SMALL-SCALE STRUCTURE AND DYNAMICS OF URANUS' ATMOSPHERE Final Technical Report, 15 Sep. 1987 - 31 Mar. 1991
Von R. Eshleman and David P. Hinson 1991 54 p
(Grant NAGw-1180)
(NASA-CR-188819; NAS 1.26:188819) Avail: NTIS HC/MF A04 CSCL 03B

This document constitutes the final technical report of the Uranus Analysis Program. Papers and/or abstracts resulting from this research are presented. The following topics are covered: (1) past and future of radio occultation studies of planetary atmospheres; (2) equatorial waves in the stratosphere of Uranus; (3) the atmosphere of Uranus- results of radio occultation measurements with Voyager 2; (4) Uranus' atmospheric dynamics and circulation; (5) small-scale structure and dynamics in the atmosphere of Uranus; (6) evidence for inertia-gravity waves in the stratosphere of Uranus derived from Voyager 2 radio occultation data; and (7) planetary waves in the equatorial stratosphere of Uranus. Author

N92-10961*# Lunar and Planetary Inst., Houston, TX. Lunar and Planetary Sample Team.
WORKSHOP ON MARE VOLCANISM AND BASALT PETROGENESIS: ASTOUNDING FUNDAMENTAL CONCEPTS (AFC) DEVELOPED OVER THE LAST FIFTEEN YEARS
Lawrence A. Taylor, ed. and John Longi, ed. (Lamont-Doherty Geological Observatory, Palisades, NY.) 1991 75 p Workshop held in Dallas, TX, 27-28 Oct. 1990
(Contract NASw-4574)
(NASA-CR-188810; NAS 1.26:188810; LPI-TR-91-03) Avail: NTIS HC/MF A04 CSCL 03B

Papers presented at the workshop on mare volcanism and basalt petrogenesis are compiled. The discussion of recent ideas and concepts within the context of this workshop permitted to catch up on the developments over the last 15 years. The following subject areas were covered: (1) geological setting; (2) magma evolution and source regions; (3) magma source and ascent processes; and (4) history of volcanism. For individual titles, see N92-10962 through N92-10965.

N92-10962*# National Aeronautics and Space Administration. Lyndon B. Johnson Space Center, Houston, TX.
THE VIOLENT SIDE OF MARE VOLCANISM Abstract Only
Cassandra R. Coombs, David S. McKay, and B. Ray Hawke (Hawaii Univ., Honolulu.) *In* Lunar and Planetary Inst., Workshop on Mare Volcanism and Basalt Petrogenesis: Astounding Fundamental Concepts (AFC) Developed Over the Last Fifteen Years 1991 p 9-10 (For primary document see N92-10961 01-91)
Avail: NTIS HC/MF A04 CSCL 03B

In the past 15 years it has become increasingly evident that lunar pyroclastic volcanism played an important role in the formation and resurfacing of portions of the Moon. Located on mare/highland boundaries, many of these deposits formed in association with mare volcanism. Based on recently acquired geologic and remote sensing data, two generally distinct types of pyroclastic mantling deposits have been identified: regional and localized. Both the regional dark mantling deposits (RDMD) and localized dark mantling deposits (LDMD) are widely distributed across the lunar nearside. The larger RDMD are typically located in lunar highland areas adjacent to many of the major lunar maria, while the smaller LDMD are found on the floors of pre-Imbrian and Inbrian craters. Both deposits are basaltic in composition and are presumed to have originated at great depth (approx. 300 km). The composition, geometry, and vent morphology of the pyroclastic deposits have been used to infer the eruption mechanisms and emplacement styles for both types of deposits. Author

N92-10963*# National Aeronautics and Space Administration. Lyndon B. Johnson Space Center, Houston, TX.
FORMATION OF APOLLO 14 ALUMINOUS MARE BASALTS BY REPLENISHMENT FRACTIONAL CRYSTALLIZATION AND ASSIMILATION OF PRECURSOR CRUST Abstract Only
Tammy L. Dickinson and Dennis O. Nelson (Oregon Dept. of Environmental Quality, Portland.) *In* Lunar and Planetary Inst., Workshop on Mare Volcanism and Basalt Petrogenesis: Astounding Fundamental Concepts (AFC) Developed Over the Last Fifteen Years 1991 p 11-12 (For primary document see N92-10961 01-91)
Avail: NTIS HC/MF A04 CSCL 03B

Apollo 14 aluminous mare basalts (AMB) have been the subject of considerable controversy. These basalts were divided into 5 distinct groups on the basis of RE and HFS element abundances. The groups are similar in major element compositions but display an 8 fold variation in REE abundances. Open-system processes were explored which are common on Earth: combined replenishment fractional crystallization (RFC); and assimilation fractional crystallization (AFC), where the assimilant is a partial melt of precursor crust. RFC often produces decoupled major and trace element variations, while AFC can produce significant variation in incompatible trace element ratios. A model was envisioned by which magmas of Group 5 composition were emplaced in shallow chambers. The Apollo 14 AMB was modeled by RFC using a parental magma of Group 5 composition with the fractionating assemblage consisting of 60 pct. Px, 30 pct. Plag, and 3 pct. Il. Author

N92-10964*# National Aeronautics and Space Administration. Lyndon B. Johnson Space Center, Houston, TX.
EXPLORATION OF RELATIONSHIPS BETWEEN LOW-TI AND HIGH-TI PRISTINE LUNAR GLASSES USING AN ARMALCOLITE ASSIMILATION MODEL Abstract Only
John H. Jones and John W. Delano (State Univ. of New York, Albany.) *In* Lunar and Planetary Inst., Workshop on Mare Volcanism and Basalt Petrogenesis: Astounding Fundamental Concepts (AFC) Developed Over the Last Fifteen Years 1991 p 21-22 (For primary document see N92-10961 01-91)
Avail: NTIS HC/MF A04 CSCL 03B

The pristine glasses of Delano are the most primitive lunar basaltic magma compositions discovered to date. They are grouped into two (and possibly three) arrays: a low-alumina array and a high alumina array. These glasses are very olivine normative and are multiply saturated at pressures of approximately 20 kbar, implying a depth of origin of 400 to 500 km in the Moon. Thus, these glasses appear to be the best candidates for primitive partial melts of the upper lunar mantle. One of the most perplexing characteristics of the pristine glasses is a positive correlation between Ni and SiO2 within each array. This is contrary to the terrestrial experience, where Ni is observed to positively correlate with MgO and negatively correlate with SiO2. These systematics are believed to be due to the depletion of Ni by olivine fractionation. The difference between the lunar and terrestrial Ni vs. SiO2 trends may be partially ascribed to the Ti-rich component. In the case of the pristine glasses, SiO2 increases not because of olivine fractionation, but because they contain less of the high-Ti component. An attempt was made to model this variation in Ni and SiO2 with a simple assimilation-fractional crystallization (AFC) model. Silica and Ni both decreased dramatically as the AFC process proceeded. Only 15 to 20 percent AFC was necessary to produce the observed variation, and the SiO2 vs. Ni variation was modeled quite well. The D(Ni) for olivine/liquid in this model was taken to be 10 and the olivine was assumed to be Fe sub 80. However, the results of this model for Ti and Mg were less than satisfactory. It seemed difficult to achieve the high TiO2 contents of some glasses (16 to 17 wt. percent) by this method. Continual addition of ilmenite by AFC could indeed raise the titania concentrations to the necessary levels, but only by enriching the magma in FeO and greatly depleting the magma in MgO. An attempt was made to circumvent this problem by using armalcolite, (Fe, Mg)Ti2O5, in the AFC model, and the results are presented. Author

N92-10965*# National Aeronautics and Space Administration. Lyndon B. Johnson Space Center, Houston, TX.
THE HISTORY OF LUNAR VOLCANISM Abstract Only
Laurence E. Nyquist and C.-Y. Shih (Lockheed Engineering and Sciences Co., Houston, TX.) *In* Lunar and Planetary Inst., Workshop on Mare Volcanism and Basalt Petrogenesis: Astounding Fundamental Concepts (AFC) Developed Over the Last Fifteen Years 1991 p 39-42 (For primary document see N92-10961 01-91)
Avail: NTIS HC/MF A04 CSCL 03B

The timing and extent of volcanism must have reflected the internal thermal evolution of the moon and a knowledge of the history of lunar volcanism is important for understanding the global evolution of the moon. Recent studies show that lunar volcanism began prior to formation of at least some of the major lunar basins, although the exact provenance of the earliest volcanism remains somewhat obscure. It was shown that the ferroan anorthosites are the best candidates to be remnants of the postulated lunar magma ocean. The Mg-suite rocks are the second major category of highland rocks, and highly evolved. granites and quartz-monzodiorites comprise a third suite of lunar highland rocks. Basalts form the Apollo 12, 15, and 17 landing sites demonstrated that the lunar mantle is greatly depleted in LREE beneath the widely separated landing sites, an observation supportive of a global process of differentiation. Also, KREEP volcanism apparently predated basin formation in the Serenitatis region, but appears to have been contemporaneous with basin formation in the Imbrium region. Recent studies showed that the earliest lunar basaltic volcanism was of mare-like composition. Author

N92-10250*# National Aeronautics and Space Administration. Ames Research Center, Moffett Field, CA.
CLAYS ON MARS: REVIEW OF CHEMICAL AND MINERALOGICAL EVIDENCE Abstract Only
Amos Banin and James L. Gooding (Hebrew Univ. of Jerusalem, Rehovot, Israel) *In* NASA. Johnson Space Center, Program and Abstracts for Clay Minerals Society 28th Annual Meeting 1991 p 10 (For primary document see N92-10248 01-46)
Avail: NTIS HC/MF A11 CSCL 03B

N92-10251*# National Aeronautics and Space Administration. Lyndon B. Johnson Space Center, Houston, TX.
TRANSFORMATION PRODUCTS OF SUBMICRON-SIZED ALUMINUM-SUBSTITUTED MAGNETITE: COLOR AND REDUCTANT SOLUBILITY Abstract Only
D. C. Golden, D. W. Ming, and H. V. Lauer, Jr. (Lockheed Engineering and Sciences Co., Houston, TX.) *In its* Program and Abstracts for Clay Minerals Society 28th Annual Meeting 1991 p 61 (For primary document see N92-10248 01-46)
Avail: NTIS HC/MF A11 CSCL 03B

N92-10255*# National Aeronautics and Space Administration. Lyndon B. Johnson Space Center, Houston, TX.
SYNTHESIS AND PROPERTIES OF Ti-SUBSTITUTED GOETHITES AND HEMATITES Abstract Only
R. K. Vempati, R. V. Morris, H. V. Lauer, Jr. (Lunar and Planetary Inst., Houston, TX.), and J. DeHart *In its* Program and Abstracts for Clay Minerals Society 28th Annual Meeting 1991 p 162 (For primary document see N92-10248 01-46)
Avail: NTIS HC/MF A11 CSCL 03B

N92-10567# Oulu Univ. (Finland). Dept. of Physics.
EARTH, URANUS, AND NEPTUNE: A COMPARISON OF THEIR MAGNETOSPHERES Abstract Only
G. Kremser *In its* Proceedings of the 25th Annual Conference of the Finnish Physical Society 1991 1 p (For primary document see N92-10362 01-70)
Avail: NTIS HC/MF A12

N92-10568# Turku Univ. (Finland).
THE STABILITY OF THE PLANETARY TRIANGULAR LAGRANGE POINTS Abstract Only
Seppo Mikkola (York Univ., Toronto, Ontario) and K. A. Innanen *In* Oulu Univ., Proceedings of the 25th Annual Conference of the Finnish Physical Society 1991 1 p (For primary document see N92-10362 01-70)
Avail: NTIS HC/MF A12

N92-10569# Oulu Univ. (Finland). Dept. of Astronomy.
VENUS BEHIND THE CLOUDS Abstract Only
J. Raitala, T. Tormanen, and K. Kauhanen *In its* Proceedings of the 25th Annual Conference of the Finnish Physical Society 1991 1 p (For primary document see N92-10362 01-70)
Avail: NTIS HC/MF A12

N92-10572# Oulu Univ. (Finland). Dept. of Astronomy.
RING SATELLITE INTERACTION IN PLANETARY RINGS Abstract Only
J. Hanninen, H. Salo, and J. Lukkari *In its* Proceedings of the 25th Annual Conference of the Finnish Physical Society 1991 1 p (For primary document see N92-10362 01-70)
Avail: NTIS HC/MF A12

N92-10573# Oulu Univ. (Finland). Dept. of Astronomy.
NUMERICAL SIMULATIONS OF DENSE COLLISIONAL SYSTEMS Abstract Only
H. Salo *In its* Proceedings of the 25th Annual Conference of the Finnish Physical Society 1991 1 p (For primary document see N92-10362 01-70)
Avail: NTIS HC/MF A12

92 SOLAR PHYSICS

Includes solar activity, solar flares, solar radiation and sunspots.

For related information see *93 Space Radiation.*

N92-10966 Physics and Electronics Lab. TNO, The Hague (Netherlands).
METEO AND IRRADIATION DATA DURING BEST TWO, MOURMELON (NETHERLANDS) Final Report
Y. H. L. Janssen Apr. 1991 45 p
(Contract A90/KL/621)
(FEL-90-A368; TD-99-0403; ETN-91-99998) Copyright Avail: Physics and Electronics Lab. TNO, P.O. Box 96864, 2509 JG The Hague, Netherlands

During their two best measuring periods the infrared research group collected several meteo and irradiation data for support and validation of their transmission, visual and infrared contrast experiments. Meteo data consist of ambient temperature, relative humidity and windspeed. Visual hemispherical radiation on a horizontal surface is measured together with visual radiation on five sides of a cube (top and four vertical sides) and visual irradiation on three boards with elevation angles of 90, 60 and 30 degrees. For support of experiments in the infrared wavelength range, apparent temperatures of a vertical black and white board were measured. ESA

N92-10967# Washington Univ., Seattle. Dept. of Physics.
LONG-TERM NEUTRINO FLUX INTEGRATIONS
W. C. Haxton Nov. 1990 10 p Presented at the International Conference on Trends in Astroparticle Physics, Los Angeles, CA, 28-30 Nov. 1991
(Contract DE-FG06-88ER-40427)
(DE91-013903; DOE/ER-40427/10-N91; CONF-911153-1) Avail: NTIS HC/MF A02

The standard solar model predicts that the sun's luminosity has increased by 40 pct. over the past 5 Gyrs of main-sequence burning, reflecting the evolving chemistry of the solar core. This increase is accompanied by an exponential growth in the B-8 neutrino flux, with a doubling time of 0.85 Gyr. I describe an unusual nuclear system that, in principle, could yield a quantitative terrestrial record of these past changes, and discuss some of the practical obstacles to reading this record. I also argue that there exists a twin of the Cl-37 solar neutrino experiment that could be mounted with modest effort. The experiment, in which neutrinos

incident on an iodine-bearing liquid produce the noble gas Xe-127, should enjoy a number of advantages over Cl-37: a substantially larger counting rate, a potentially greater relative sensitivity to Be-7 neutrinos, lower cosmic ray backgrounds, and a cleaner signal for the Xe-127 decay. I discuss the physics that could be learned from such a detector, emphasizing in particular the virtues of a passive, high counting rate experiment that could be operated cheaply over the long times that might pass before the next galactic supernova. DOE

N92-10968# Washington Univ., Seattle. Dept. of Physics.
SOLAR AND SUPERNOVA NEUTRINO INTERACTIONS
W. C. Haxton Nov. 1990 14 p Presented at the University of California Los Angeles (UCLA) Supernova Watch Workshop, Los Angeles, CA, 28-30 Nov. 1991
(Contract DE-FG06-88ER-40427)
(DE91-013905; DOE/ER-40427/09-N91; CONF-911152-1) Avail: NTIS HC/MF A03

Two topics are addressed, the interactions of neutrinos during a type II supernova and the effect of current eddies on solar neutrino oscillations. The supernova discussion focuses on the nucleosynthesis that accompanies inelastic neutral current interactions of neutrinos in the mantle of a collapsing star, and on the effect of neutrino down scattering and preheating on the explosion mechanism. The second half of the talk deals with the influence of solar turbulence (or density fluctuations) on the neutrino effective mass and the possibility that a time-varying neutrino flux could result. The effects of harmonic density or three-current perturbations on the oscillation probability are explored analytically and numerically. DOE

N92-10969# Los Alamos National Lab., NM.
COMPOSITION AND ENERGETICS OF SOLAR FLARE PARTICLE EVENTS MEASURED BY SATELLITES, 1989 - 1991
G. R. Gisler, R. D. Belian, T. E. Cayton, and G. D. Reeves 1991 5 p Presented at the International Cosmic Ray Conference, Dublin (Ireland), 11-23 Aug. 1991
(Contract W-7405-eng-36)
(DE91-018028; LA-UR-91-2637; CONF-9108141-1) Avail: NTIS HC/MF A01

The Synchronous Orbit Particle Analyzer (SOPA), on board the satellite 1989-046 and others, has detected ions from carbon through nickel at energies from 2 to 50 MeV in the great solar energetic particle events of the current solar cycle. Energetic protons from the same events have been detected by the Charged Particle Analyzer (CPA) on board the satellite 1984-129 and others. We present here a collection of data from these various instruments that includes events of 1989, 1990, and 1991. We demonstrate the association of the events detected by the satellites with solar flares, and examine local solar wind features that in some instances alter the flux. We determine the ionic composition of the events, and compare these compositions among the various events and with those events, and compare these compositions among the various events and with those found in events of previous solar cycles. We obtain time-histories of the energetic particle fluxes, resolved both by ion species and by energy range. These detailed histories are of use, in conjunction with other data, in determining the parameters of the acceleration region. DOE

N92-10970# Los Alamos National Lab., NM.
THE EXTENSION OF SOLAR MAGNETIC FIELDS INTO INTERPLANETARY SPACE
D. J. McComas and J. L. Phillips 1991 13 p Presented at the Solar Connection With Transient Interplanetary Processes (SOLTIP), Castle Liblice, Czechoslovakia, 30 Sep. - 5 Oct. 1991
(Contract W-7405-eng-36)
(DE91-018052; LA-UR-91-2781; CONF-9109254-1) Avail: NTIS HC/MF A03

The flow of coronal plasma into interplanetary space results in outward transport of the solar magnetic field. The prevailing open interplanetary magnetic field is rooted in the corona and wraps up into a spiral due to the rotation of the Sun. This simple configuration, however, is disrupted by magnetically distinct coronal mass ejections (CME's) which erupt from the solar corona into interplanetary space. Observations of CME's at 1 AU reveal electron signatures indicating a closed magnetic topology, postulated to be: (1) magnetic bottles tied to the corona at both ends; (2) plasmoids that are completely disconnected from the Sun; or (3) flux ropes which have topologies intermediate between (1) and (2). With either the magnetic-bottle or flux rope hypothesis, the inward and outward flux at 1 AU should increase indefinitely as CME's continue to erupt. Using a new technique to calculate the 2-D flux through 1 AU from single spacecraft measurements, we show that while there is a solar cycle variation to the magnetic flux, it clearly does not grow without bound. This suggests that either CME's are closed plasmoids which add to no new flux to the interplanetary medium, or that the opening of new flux by CME's is balanced via reconnection elsewhere in the corona. We suggest that the latter process may be dominant and describe observation from the Solar Maximum Mission coronagraph which are consistent with reconnection above helmet streamers in the corona. Such disconnections would serve to return closed field arches to the Sun and release open, U-shaped structures into the solar wind. Coronal disconnections appear in some cases to be triggered by pressure pulses caused by CME eruption elsewhere, suggesting a dynamic flux-balance process. We describe a class of solar wind structures, called heat flux dropouts, in which the solar wind electron heat flux, driven by magnetic connection to the hot corona, is absent or greatly reduced. DOE

N92-10364# Oulu Univ. (Finland). Dept. of Theoretical Physics.
ANOMALOUS e(+)e(-) PAIRS IN HEAVY ION COLLISIONS AND SOLAR NEUTRINOS: TWO PUZZLES WITH COMMON SOLUTION? Abstract Only
P. Mahonen and M. Pitkanen (Helsinki Univ. of Technology, Espoo, Finland) *In its* Proceedings of the 25th Annual Conference of the Finnish Physical Society 1991 1 p (For primary document see N92-10362 01-70)
Avail: NTIS HC/MF A12

N92-10550# Helsinki Univ. of Technology, Espoo (Finland). Lab. of Engineering Materials.
THE 1990 SOLAR ECLIPSE AS SEEN BY A TORSION PENDULUM Abstract Only
K. Ullakko, Yong Liu, and Zeliang Xie *In* Oulu Univ., Proceedings of the 25th Annual Conference of the Finnish Physical Society 1991 1 p (For primary document see N92-10362 01-70)
Avail: NTIS HC/MF A12

N92-10562# Turku Univ. (Finland). Space Research Lab.
PERFORMANCE TESTS OF ERNE HED SENSOR Abstract Only
E. Valtonen, J. Peltonen, T. Eronen, J. J. Torsti, M. Lumme, M. Mahonen, A. Nieminen, and J.B. Viano (Grenoble-1 Univ. France) *In* Oulu Univ., Proceedings of the 25th Annual Conference of the Finnish Physical Society 1991 1 p (For primary document see N92-10362 01-70)
Avail: NTIS HC/MF A12

N92-10570# Finnish Meteorological Inst., Helsinki. Dept. of Geophysics.
THE EFFECT OF LATITUDINALLY VARYING SOLAR WIND FLUX ON THE LYMAN ALPHA SKY BACKGROUND Abstract Only
T. Summanen, E. Kyrola, R. Lallement, and J. L. Bertaux (Centre National de la Recherche Scientifique, Verrieres-Le Buisson, France) *In* Oulu Univ., Proceedings of the 25th Annual Conference of the Finnish Physical Society 1991 1 p (For primary document se N92-10362 01-70)
Avail: NTIS HC/MF A12

93 SPACE RADIATION

Includes cosmic radiation; and inner and outer earth's radiation belts.

For biological effects of radiation see *52 Aerospace Medicine*. For theory see *73 Nuclear and High-Energy Physics*.

N92-10971*# Iowa Univ., Iowa City. Dept. of Physics and Astronomy.
NEW OBSERVATIONS OF THE LOW FREQUENCY INTERPLANETARY RADIO EMISSIONS
W. S. Kurth and D. A. Gurnett Aug. 1991 6 p Submitted for publication
(Contract JPL-957723)
(NASA-CR-188917; NAS 1.26:188917; U-of-Iowa-91-19) Avail: NTIS HC/MF A02 CSCL 03B

Recent Voyager 1 observations reveal reoccurrences of the low frequency interplanetary radio emissions. Three of the new events are weak transient events which rise in frequency from the range of 2-2.5 kHz to about 3 kHz with drift rates of approximately 1.5 kHz/year. The first of the transient events begins in mid-1989 and the more recent pair of events both were first detected in late 1991. In addition, there is an apparent onset of a 2-kHz component of the emission beginning near day 70 of 1991. The new transient emissions are barely detectable on Voyager 1 and are below the threshold of detectability on Voyager 2, which is less sensitive than Voyager 1. The new activity provides new opportunities to test various theories of the triggering, generation, and propagation of the outer heliospheric radio emissions and may signal a response of the source of the radio emissions to the increased solar activity associated with the recent peak in the solar cycle. Author

N92-10564# Turku Univ. (Finland).
PROPERTIES OF SHOCKED RELATIVISTIC JETS Abstract Only
Markku Lainela and Esko Valtaoja (Helsinki Univ. of Technology, Espoo, Finland) *In* Oulu Univ., Proceedings of the 25th Annual Conference of the Finnish Physical Society 1991 1 p (For primary document see N92-10362 01-70)
Avail: NTIS HC/MF A12

N92-10574# Turku Univ. (Finland). Lab. of Electronics and Information Technology.
ELECTRONICS OF THE COSMIC RAY AIR SHOWER ARRAY AT TURKU (FINLAND) Abstract Only
H. Arvela, A.-M. Elo (Oulu Univ., Finland), J. J. Torsti, and E. Valtonen *In* Oulu Univ., Proceedings of the 25th Annual Conference of the Finnish Physical Society 1991 1 p (For primary document see N92-10362 01-70)
Avail: NTIS HC/MF A12

N92-10575# Oulu Univ. (Finland). Dept. of Physics.
TEST RESULTS OF DENSITY DETECTORS OF THE COSMIC RAY AIR SHOWER ARRAY IN TURKU (FINLAND) Abstract Only
A.-M. Elo, H. Arvela (Turku Univ., Finland), J. Peltonen, J. J. Torsti, and E. Valtonen *In its* Proceedings of the 25th Annual Conference of the Finnish Physical Society 1991 1 p (For primary document see N92-10362 01-70)
Avail: NTIS HC/MF A12

N92-10577# Turku Univ. (Finland).
EXPLANATION FOR OPTICAL FREQUENCY DEPENDENT POLARIZATION IN BLAZARS Abstract Only
L. Valtaoja *In* Oulu Univ., Proceedings of the 25th Annual Conference of the Finnish Physical Society 1991 1 p (For primary document see N92-10362 01-70)
Avail: NTIS HC/MF A12

99 GENERAL

No abstracts in this category.

Typical Subject Index Listing

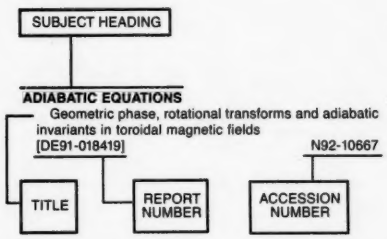

The subject heading is a key to the subject content of the document. Titles, report numbers, and accession numbers of pertinent documents are provided under each subject heading. When the title is insufficiently descriptive of the document content, a title extension has been added, separated from the title by three hyphens. The report number helps to indicate the type of document cited (e.g., NASA report, NASA translation, NASA contractor report). The accession number is the number by which the document abstracts are arranged in this journal and by which the document is sold or requested. The titles, with title extensions if present, are arranged under each subject heading in ascending accession number order. The subject headings have been selected from the latest revision of the *NASA Thesaurus*.

A

ABEL FUNCTION
Abel inversion with the fast Fourier transform N92-10379

ABERRATION
Control system for ruling blazed, aberration corrected diffraction gratings [NASA-CASE-GSC-13240-1] N92-10186
The normal incidence grating inverse photoemission spectrometer in the energy range 8-28 eV N92-10516
Polarization aberrations. 1: Rotationally symmetric optical systems [NASA-CR-184218] N92-10638

ABLATION
Epitaxial high T(sub c) superconducting thin films and superlattices deposited by laser albation N92-10505
High T(sub c) superconducting Li-doped Bi-Sr-Ca-Cu-O thin films deposited by laser ablation N92-10506

ABSORBERS (MATERIALS)
The search for low photodesorption coatings [DE91-017473] N92-10092

ABSORPTION
Fast wave heating at intermediate ion cyclotron harmonics on the JIPP T-II U tokamak [NIFS-21] N92-10649

ABSORPTION SPECTRA
Li 1s photoionization and photoexcitation with satellites N92-10427
The nu(sub 4) and nu(sub 7) bands of CD3CN with coriolis coupling and other resonance perturbations N92-10432
The nu(sub 8) and 2nu(sub 8) bands of CD3CN N92-10433
The infrared rotation-vibration spectrum of C2H2 in the nu(sub 2) + nu(sub 5) band region; l-resonances in the bands nu(sub 2) + nu(sub 5), nu(sub 2) + 2(nu(sub 5)) back arrow nu(sub 5) and nu(sub 1) back arrow nu(sub 5) N92-10434
Absorption measurements with an integrating sphere and an FT-IR spectrometer N92-10445
A simple method to stabilize the frequency of semiconductor lasers N92-10453
Two-phonon absorption by the real squashing collective mode in superfluid He-3 N92-10474
Infrared (2.08-14 micron) spectra of powered stony meteorites N92-10826

ABSTRACTS
Program and Abstracts for Clay Minerals Society 28th Annual Meeting [NASA-TM-105098] N92-10248
Program and abstracts of the 2nd Meeting of the Society for Research on Biological Rhythms [AD-A240007] N92-10280

ABUNDANCE
SO2-rich equatorial basins and epeirogeny of Io N92-10761
Chemical fractionation of siderophile elements in impactites from Australian meteorite craters N92-10875
Formation of Apollo 14 aluminous mare basalts by replenishment fractional crystallization and assimilation of precursor crust N92-10963

ACCELERATED LIFE TESTS
Thermal energy storage and heat transfer support program. Task-5 heat pipe life test study. Facilities upgrading and maintenance [AD-A239929] N92-10177

ACCELERATION (PHYSICS)
Electron acceleration by laser fields in a gas [DE91-018269] N92-10192

ACCESS CONTROL
Multiple access trade study N92-10118
Measurement of memory access contentions in multiple vector processor systems [DE91-013205] N92-10297

ACCRETION DISKS
Bending waves and orbital inclinations N92-10894
Accretion and evolution of solar system bodies N92-10895
Accretion rates of protoplanets N92-10936
Accretion rates of protoplanets 2: Gaussian distribution of planestesimal velocities N92-10937
Generation and behavior of solar system magnetic fields N92-10939
Optical properties of grains in molecular clouds and accretion disks N92-10948

ACETYLENE
The infrared rotation-vibration spectrum of C2H2 in the nu(sub 2) + nu(sub 5) band region; l-resonances in the bands nu(sub 2) + nu(sub 5), nu(sub 2) + 2(nu(sub 5)) back arrow nu(sub 5) and nu(sub 1) back arrow nu(sub 5) N92-10434
Analysis of the interacting levels V(sub 9) = 1 and V(sub 10) = 2 of propyne N92-10444

ACHONDRITES
Does Lafayette = Nakhla? Not necessarily so, based on 4.2K Mossbauer spectra of all of the SNC meteorites N92-10825

ACID RAIN
Abatement strategies based on critical loads N92-10533
Fossil fuels and the environment N92-10586

ACIDITY
Definition and measurement at high temperatures of pH [DE91-017945] N92-10077

ACIDS
Scanning tunneling microscopy of polysialic acid N92-10538

ACOUSTIC MEASUREMENT
Constant frequency pulsed phase-locked loop measuring device [NASA-CASE-LAR-13823-1] N92-10182
Laser acoustic technology demonstration and equipment field trails [DE91-018759] N92-10193
Acoustic device and method for measuring gas densities [NASA-CASE-NPO-18155-1-CU] N92-10609
US TAG for ISO/TC43, acoustics, IEC/TC29 electroacoustics, ISO/TC108/SC4 human exposure to mechanical vibration and shock: Minutes of the Accredited Standards Committee on Bioacoustics, S3 [AD-A239918] N92-10610

ACOUSTICAL HOLOGRAPHY
Reconfigurable optical interconnections by acousto-optic holograms N92-10449

ACOUSTICS
Jet noise classical theory and experiments N92-10602
US TAG for ISO/TC43, acoustics, IEC/TC29 electroacoustics, ISO/TC108/SC4 human exposure to mechanical vibration and shock: Minutes of the Accredited Standards Committee on Bioacoustics, S3 [AD-A239918] N92-10610

ACOUSTO-OPTICS
A miniature acousto-optic image correlator [DE91-018002] N92-10151
Reconfigurable optical interconnections by acousto-optic holograms N92-10449

ACTIVATION ENERGY
Mechanical after-effect studies of oxygen relaxation in YBa2Cu3O(7-delta) [DE91-018043] N92-10685
Activation energies in a Bi2Si2CaCu2O(x) single crystal [DE91-018640] N92-10702

ACTIVE CONTROL
Multi-degree of freedom, active vibration control method, and system [NASA-CASE-LAR-14508-1-CU] N92-10202

ACTIVE GALACTIC NUCLEI
Properties of shocked relativistic jets N92-10564

ACTS
Technology assessment and experimentation plan N92-10124

ACTUATORS
Multi-degree of freedom, active vibration control method, and system [NASA-CASE-LAR-14508-1-CU] N92-10202

ADA (PROGRAMMING LANGUAGE)
Integrity and security in an Ada runtime environment [NASA-CR-188826] N92-10313
ART/Ada design project, phase 1. Task 3 report: Test plan [NASA-CR-188945] N92-10314

ADAPTATION
On adaptive multiband detection of targets in nonstationary nonhomogeneous interference [AD-A239983] N92-10327

ADDRESSING
Content addressable memory project [NASA-CR-188981] N92-10299

ADIABATIC EQUATIONS
Geometric phase, rotational transforms and adiabatic invariants in toroidal magnetic fields [DE91-018419] N92-10667

ADJUSTING
Optical properties of CO2 ice and CO2 snow from ultraviolet to infrared: Application to frost deposits and clouds on Mars N92-10821

ADMIXTURES
Development and optimization of methodologies for analysis of complex hydrocarbon mixtures [DE91-017954] N92-10075

ADSORPTION
Development and optimization of methodologies for analysis of complex hydrocarbon mixtures [DE91-017954] N92-10075
Adsorbate induced surface reconstruction N92-10469

ADVECTION
RIPPLE: A new model for incompressible flows with free surfaces [DE91-017830] N92-10168
Fourier component analysis of three Euler-Lagrangian methods applied to the one-dimensional advection-dispersion model [DE91-017733] N92-10346

AERIAL PHOTOGRAPHY
Evaluation of high altitude photography for city regional areas
[MGA-A-44] N92-10210
Recording of urban land use by high altitude photography: The Munich (Fed. Republic of Germany) exampl N92-10211
Possibilities of producing land use information for city regional area planning by high altitude photographs, taking south west Munich (Fed. Republic of Germany) regional area as an example N92-10212
Evaluation of high altitude photography for city cartography, with the example of Seattle, US N92-10214
Plasma cloud behavior
[AD-A240000] N92-10264

AERIAL RECONNAISSANCE
Surface scattering properties estimated from modeling airborne multiple emission angle reflectance data N92-10841

AEROACOUSTICS
Aeroacoustics of flight vehicles: Theory and practice. Volume 1: Noise sources
[NASA-RP-1258-VOL-1] N92-10598

AEROASSIST
Nonequilibrium radiative heating prediction method for aeroassist flowfields with coupling to flowfield solvers N92-10165

AERODYNAMIC BALANCE
Dual strain gage balance system for measuring light loads
[NASA-CASE-LAR-14419-1] N92-10185

AERODYNAMIC CHARACTERISTICS
Technical evaluation report, AGARD Fluid Dynamics Panel Symposium on Effects of Adverse Weather on Aerodynamics
[NASA-TM-105192] N92-10002

AERODYNAMIC HEATING
Numerical simulation of hypersonic viscous flow for the design of H-2 orbiting plane (HOPE-2)
[NAL-TR-1093] N92-10009

AERODYNAMIC LOADS
CH-53E/AV-8B aircraft sling load recovery system analysis
[AD-A239950] N92-10022

AERODYNAMIC NOISE
Aeroacoustics of flight vehicles: Theory and practice. Volume 1: Noise sources
[NASA-RP-1258-VOL-1] N92-10598
Rotor noise N92-10600
Jet noise classical theory and experiments N92-10602
Airframe noise N92-10605

AERODYNAMIC STABILITY
CH-53E/AV-8B aircraft sling load recovery system analysis
[AD-A239950] N92-10022

AERODYNAMIC STALLING
Numerical investigation of the effect of leading edge geometry on dynamic stall of airfoils
[AD-A239949] N92-10015

AERODYNAMICS
Aeronautical engineering: A continuing bibliography with indexes (supplement 267)
[NASA-SP-7037(267)] N92-10001
Recent advances on a finite element algorithm for computational aerodynamics: Transonics-hypersonics
[DE91-018176] N92-10010
Parameter identification for nonlinear aerodynamic systems
[NASA-CR-188985] N92-10347

AERONAUTICAL ENGINEERING
Aeronautical engineering: A continuing bibliography with indexes (supplement 267)
[NASA-SP-7037(267)] N92-10001

AEROSOLS
Remote detection of atmospherically dispersed vegetative cells using fluorescence lidar
[DE91-016077] N92-10218
A technique for estimating surface meteorological ranges over oceans from satelliite measurements of aerosol optical depth
[AD-A239985] N92-10219
Aerosol dynamics: Binary nucleation N92-10525
Aerosol dynamics: Condensation and evaporation N92-10526
Derivation of mid-infrared (5-25 microns) optical constraints of some silicates and palagonite N92-10950

AEROSPACE ENGINEERING
The determination of operational and support requirements and costs during the conceptual design of space systems
[NASA-CR-188817] N92-10037
Microstructural stability and creep response of a new Al-Fe-W-Si alloy
[AD-A239861] N92-10087
Index to 1987 NASA Tech Briefs, volume 11, numbers 1-10
[NASA-TM-105024] N92-10717
Index to 1988 NASA Tech Briefs, volume 12, numbers 1-11
[NASA-TM-105077] N92-10718
Index to 1989 NASA Tech Briefs, volume 13, numbers 1-12
[NASA-TM-105109] N92-10719
Index to 1990 NASA Tech Briefs, volume 14, numbers 1-12
[NASA-TM-105110] N92-10720
Cumulative index to NASA Tech Briefs, 1976-1980, volumes 1-5
[NASA-TM-89327] N92-10721
Cumulative index to NASA Tech Briefs, 1981-1985, volumes 6-10
[NASA-TM-89326] N92-10722

AEROSPACE ENVIRONMENTS
Differential collision cross-sections for atomic oxygen: Analysis of space flight instruments for solar terrestrial physics
[NASA-CR-184235] N92-10613

AEROSPACE PLANES
Hypersonic flows as related to the National Aerospace plane
[NASA-CR-187985] N92-10004

AEROSPACE SYSTEMS
The determination of operational and support requirements and costs during the conceptual design of space systems
[NASA-CR-188817] N92-10037

AEROTHERMODYNAMICS
Numerical simulation of hypersonic viscous flow for the design of H-2 orbiting plane (HOPE-2)
[NAL-TR-1093] N92-10009

AGING (METALLURGY)
Redistribution of nitrogen atoms and magnetic ordering in Fe-N martensite at low temperatures N92-10472

AGRICULTURE
Processes for identifying regional influences of and responses to increasing atmospheric CO2 and climate change: The MINK project
[DE91-018605] N92-10244

AGROCLIMATOLOGY
Potential strategies for adapting to greenhouse warming: Perspectives from the developing world N92-10237

AIR FLOW
Free convection in the Martian atmosphere N92-10803

AIR POLLUTION
Assessing and managing the risks of climate change N92-10233
Climate and forests N92-10234
Processes for identifying regional influences of and responses to increasing atmospheric CO2 and climate change: The MINK project
[DE91-018603] N92-10243
Processes for identifying regional influences of and responses to increasing atmospheric CO2 and climate change: The MINK project
[DE91-018605] N92-10244
Semiconducting organic thin films as monitoring devices for NO2 air pollution N92-10527
Abatement strategies based on critical loads N92-10533

AIR TRAFFIC CONTROL
The 1990 Airport Surveillance Radar Wind Shear Processor (ASR-WSP) operational test at Orlando International Airport
[AD-A239852] N92-10019
Solid-State Radar Beacon Decoder (SSRBD) Operational Test and Evaluation (OT/E) integration test plan
[DOT/FAA/CT-TN91/30] N92-10020

AIR WATER INTERACTIONS
Radiohydrophysical aerospace research of ocean
[SRI-PR-1749] N92-10272
Simulations of the carbon cycle in the oceans
[DE91-018475] N92-10273

AIRCRAFT APPROACH SPACING
A compensatory algorithm for the slow-down effect on constant-time-separation approaches
[NASA-TM-4265] N92-10024

AIRCRAFT CONTROL
Rotatable non-circular forebody flow controller
[NASA-CASE-LAR-14212-1-CU] N92-10021
Development of digital/optical rotary position transducer
[NAL-TR-1106] N92-10028

AIRCRAFT ENGINES
Aeronautical engineering: A continuing bibliography with indexes (supplement 267)
[NASA-SP-7037(267)] N92-10001

AIRCRAFT EQUIPMENT
Aeronautical engineering: A continuing bibliography with indexes (supplement 267)
[NASA-SP-7037(267)] N92-10001

AIRCRAFT GUIDANCE
Passive range estimation for rotorcraft low-altitude flight
[NASA-TM-103897] N92-10003

AIRCRAFT INSTRUMENTS
The use and misuse of aircraft and missile RCS statistics
[AD-A239892] N92-10141

AIRCRAFT NOISE
Aeroacoustics of flight vehicles: Theory and practice. Volume 1: Noise sources
[NASA-RP-1258-VOL-1] N92-10598
Rotor noise N92-10600
Airframe noise N92-10605

AIRCRAFT POWER SUPPLIES
Nonflammable hydraulic power system for tactical aircraft. Volume 2: Equipment and systems test and evaluation
[AD-A239805] N92-10100

AIRFOIL OSCILLATIONS
Numerical investigation of the effect of leading edge geometry on dynamic stall of airfoils
[AD-A239949] N92-10015
Downwash measurements on a pitching canard-wing configuration
[AD-A239956] N92-10016

AIRFOIL PROFILES
Downwash measurements on a pitching canard-wing configuration
[AD-A239956] N92-10016

AIRFOILS
Dual strain gage balance system for measuring light loads
[NASA-CASE-LAR-14419-1] N92-10185

AIRFRAMES
Airframe noise N92-10605
Propulsive lift noise N92-10606

AIRLINE OPERATIONS
A comparison between the consequences of the liberal and non-liberal UK-Europe bilaterals
[TT-9101] N92-10018

ALBEDO
Variable features in the Valles Marineris region of Mars N92-10799
Mineralogy of the Martian surface from Mariner 6/7 infrared spectrometer data N92-10814
An infrared reflectance study of low albedo surface constituents N92-10830
Laboratory photometric measurement of particulate soils out to very large phase angles N92-10834
Disk resolved studies of the optical properties and physical nature of the surfaces of the outer planet satellites N92-10837
Planetary atlases N92-10925
Thermal and albedo mapping of the north and south polar regions of Mars N92-10943
Properties of dust and clouds in the Mars atmosphere: Analysis of Viking IRTM emission phase function sequences N92-10956

ALCOHOLS
The Alternative Fuels Data Center
[DE91-015003] N92-10111

ALGORITHMS
Recent advances on a finite element algorithm for computational aerodynamics: Transonics-hypersonics
[DE91-018176] N92-10010
A compensatory algorithm for the slow-down effect on constant-time-separation approaches
[NASA-TM-4265] N92-10024
The application of the ADSP-21020 40-bit floating point DSP microprocessor in a digital Doppler radar
[DE91-018005] N92-10135
A 3-D adaptive mesh refinement algorithm for multimaterial gas dynamics
[DE91-018040] N92-10169
A general-purpose finite-difference code for solving steady-state three-dimensional fluid-flow and heat transfer problems
[AD-A239857] N92-10175
A technique for estimating surface meteorological ranges over oceans from satellite measurements of aerosol optical depth
[AD-A239985] N92-10219
The SolarTrak solar array tracking controller
[DE91-017721] N92-10224
On the suitability of the connection machine for direct particle simulation
[NASA-CR-188863] N92-10293

Content addressable memory project
[NASA-CR-188981] N92-10299
Parallel machine architecture and compiler design facilities
[NASA-CR-188784] N92-10304
An implementation of the look-ahead Lanczos algorithm for non-Hermitian matrices, part 1
[NASA-CR-188909] N92-10311
An implementation of the look-ahead Lanczos algorithm for non-Hermitian matrices, part 2
[NASA-CR-188910] N92-10312
Performance of conjugate gradient-like algorithms in transient two-phase subchannel analysis
[DE91-013373] N92-10316
MERLIN 2: A computer program to transfer solution data betwwen finite element meshes
[DE91-018130] N92-10321
On adaptive multiband detection of targets in nonstationary nonhomogeneous interference
[AD-A239983] N92-10327
Totally parallel multilevel algorithms for sparse elliptic systems
[NASA-CR-188837] N92-10333
The improved robustness of multigrid elliptic solvers based on multiple semicoarsened grids
[NASA-CR-187633] N92-10348
Multi-dimensional ENO schemes for general geometries
[NASA-CR-187637] N92-10349
A polynomial-time algorithm for computing the yolk in fixed dimension
[AD-A240060] N92-10353
Using surrogate data to detect nonlinearity in time series
[DE91-018017] N92-10357
Running discrete cosine transform algorithm N92-10375
Waveguide Dammann gratings and kinoforms N92-10458
Tunneling in oscillating double barrier heterostructures N92-10496
Algorithm for detection of VFIB in real time from ECG N92-10542
Nonlinear RF processes in plasma
[DE91-017441] N92-10658
A reexamination of early numerical simulations of planetary accretion N92-10897

ALKALI HALIDES
An improved technique for electrolytic colouration of alkali halide crystals N92-10513

ALKALI METALS
Equivalence in the shell structure of the tight binding and free electron clusters N92-10441

ALKYL COMPOUNDS
Conducting polymers N92-10524

ALLOYS
BES Welding Science Contractors summary report, 1990--1991
[DE91-018510] N92-10198

ALLUVIUM
Characteristics of ejecta and alluvial deposits at Meteor Crater, Arizona and Odessa Craters, Texas: Results from ground penetrating radar N92-10872

ALPHA PARTICLES
Experimental investigations of electron capture from atomic hydrogen and deuterium by alpha particles
[DE91-018280] N92-10629

ALPHANUMERIC CHARACTERS
Display format, highlight validity, and highlight method: Their effects on search performance
[NASA-TM-104742] N92-10287

ALTIMETRY
Interpretation of the northern boundary of Ishtar Terra from Magellan images and altimetry N92-10745

ALUMINIDES
Oxide properties of a gamma titanium aluminide: A surface science study
[DE91-018024] N92-10095

ALUMINUM ALLOYS
In situ liquid-crystal-polymer fiber reinforced aluminum matrix composite
[AD-A239860] N92-10072
Microstructural stability and creep response of a new Al-Fe-W-Si alloy
[AD-A239861] N92-10087

ALUMINUM GALLIUM ARSENIDES
Tunneling calculations for GaAs-Al(x)Ga(1-x) as graded band-gap sawtooth superlattices
[NASA-TM-100726] N92-10680
Gallium arsenide pilot line for high performance components
[AD-A239955] N92-10704

ALUMINUM OXIDES
Surface characterization of coated powders with XPS: Al2O3-SiO2 coated TiO2 pigments N92-10520
Formation of small metallic precipitates of niobium in (alpha)-Al2O3 implanted with Nb ions
[DE91-015928] N92-10678

AMMONIUM COMPOUNDS
Transformation products of submicron-sized aluminum-substituted magnetite: Color and reductant solubility N92-10251

AMPLIFICATION
User antennas N92-10121

AMPOULES
Modelling crystal growth: Convection in an asymmetrically heated ampoule
[NASA-CR-184214] N92-10676

ANALOG DATA
Digital simulation of speech transmission channels
[IZF-1991-A-7] N92-10115

ANALOG TO DIGITAL CONVERTERS
The application of the ADSP-21020 40-bit floating point DSP microprocessor in a digital Doppler radar
[DE91-018005] N92-10135
Recovering signals from optical fiber interferometric sensors
[AD-A240062] N92-10644

ANGLE OF ATTACK
Transonic and supersonic Euler computations of vortex-dominated flow fields about a generic fighter
[NASA-TP-3156] N92-10011

ANGULAR CORRELATION
Influence of the angular correlation of fission neutrons on noise signatures
[DE91-014577] N92-10618

ANGULAR DISTRIBUTION
Limitations of the condensed history method for low energy electrons
[DE91-015764] N92-10619

ANGULAR MOMENTUM
Ring satellite interaction in planetary rings N92-10572
Understanding asteroid collisional history through experimental and numerical studies N92-10884
A geometrical model for shepherding N92-10901

ANHYDRIDES
A process for preparing 1,3-diamino-5-pentafluorosulfanylbenzene and polymers therefrom
[NASA-CASE-LAR-14773-1-CU] N92-10105

ANIMALS
Compilation of 1990 annual reports of the Navy ELF communications system ecological monitoring program. Volume 1: Tabs A, B
[AD-A239868] N92-10137

ANIONS
Quantum world in 2+1 dimensions N92-10365

ANISOTROPIC MEDIA
NMR-relaxation time measurements of noble gas isotope Xe-129 dissolved in isotropic and anisotropic liquids N92-10437

ANISOTROPY
The Kr-83 NMR in probing electric field gradients in thermotropic liquid crystals N92-10435
Vortex lattice: Vortex liquid states in anisotropic high-T(sub c) superconductors N92-10500
Anisotropic twin boundary pinning in YBa2Cu3O(x)
[DE91-018536] N92-10692

ANNEALING
Evaluation of advanced austenitic alloys relative to alloy design criteria for steam service
[DE91-017800] N92-10081
Gate matrix optimization using simulated annealing N92-10374

ANNUAL VARIATIONS
Ozone depletion rates in the late winter/early spring Arctic and Antarctic stratosphere according to recent ozone sounding observations N92-10547

ANODES
Alkali metal carbon dioxide electrochemical system for energy storage and/or conversion of carbon dioxide to oxygen
[NASA-CASE-LEW-14973-1] N92-10222
Numerical simulation of ion beam generated in the diode with anode plasma column
[IPPCZ-306] N92-10652

ANOMALIES
Anomalous scattering of light on Triton N92-10836

ANTARCTIC REGIONS
Ozone depletion rates in the late winter/early spring Arctic and Antarctic stratosphere according to recent ozone sounding observations N92-10547

ANTENNA COMPONENTS
PASS spacecraft antenna technology assessment N92-10123

ANTENNA DESIGN
User antennas N92-10121
Spacecraft antennas N92-10122
PASS spacecraft antenna technology assessment N92-10123
Laser interferometer (TENKO-10 and -100) for gravitational wave antenna development
[ISAS-640] N92-10189

ANTENNA FEEDS
Spacecraft antennas N92-10122

ANTENNA RADIATION PATTERNS
Antenna beam coverage concepts N92-10119

ANTENNAS
Radar applications of gigawatt sources at millimeter wave frequencies
[DE91-017541] N92-10133
Fast-wave ICRF minority-regime heating experiments on the Tore Supra tokamak
[DE91-018866] N92-10673

ANTIFERROMAGNETISM
Neutron diffraction experiments on nuclear magnetic order in copper N92-10507
Antiferromagnetic ordering in silver at picoKelvin temperatures N92-10509
Strong correlation theories of high temperature superconductors
[DE91-017479] N92-10688

ANTIICING ADDITIVES
Technical evaluation report, AGARD Fluid Dynamics Panel Symposium on Effects of Adverse Weather on Aerodynamics
[NASA-TM-105192] N92-10002

ANTIMISSILE DEFENSE
Massively parallel computing at Sandia and its application to national defense
[DE91-008178] N92-10334
Massively parallel computing and the mid-course tracking problem
[DE91-010864] N92-10335

ANTIMONY ALLOYS
OMVPE growth of InAsSbBi and related alloys using new organometallic group V sources
[AD-A239939] N92-10703

ANTIPROTONS
Measurements of the ratio R = sigma(sub W)Br(W to mu(nu))/sigma(sub Z)Br(Z to mu(mu)) and gamma(sup tot)(sub W) at the CERN proton-antiproton collider
[CERN-PPE/90-141] N92-10392

ANTIREFLECTION COATINGS
InP solar cells grown by gas-source molecular beam epitaxy N92-10531

ANXIETY
Test anxiety and post processing interference, 2
[AD-A239819] N92-10283

APPLICATION SPECIFIC INTEGRATED CIRCUITS
A digital ASIC implementation of a video filter for synthetic aperture radar
[DE91-018400] N92-10131

APPLICATIONS PROGRAMS (COMPUTERS)
The EH safety representative information system on the safety performance measurement system is where you will find... Word processing and helps with a V-PLUS
[DE91-018709] N92-10113
A method for determining spiral-bevel gear tooth geometry for finite element analysis
[NASA-TP-3096] N92-10195

APPROACH INDICATORS
A compensatory algorithm for the slow-down effect on constant-time-separation approaches
[NASA-TM-4285] N92-10024

APPROXIMATION
Overview of Krylov subspace methods with applications to control problems
[NASA-CR-188842] N92-10343
Double beta decay in the particle-number projected QRPA formalism N92-10408
Molecular dynamics using the tight-binding approximation: Application to liquid silicon N92-10465
Interatomic interactions in the local density approximation N92-10487

AQUEOUS SOLUTIONS
Definition and measurement at high temperatures of pH
[DE91-017945] N92-10077
Passivation of high temperature superconductors
[NASA-CASE-NPO-17949-1-CU] N92-10681

ARC JET ENGINES
MPD thruster research issues, activities, strategies N92-10051

ARC SPRAYING
Self-consistent modeling of plasma spraying processes
[DE91-018820] N92-10672

ARCHITECTURE (COMPUTERS)
BIRD: A general interface for sparse distributed memory simulators
[NASA-CR-188858] N92-10292
Measurement of memory access contentions in multiple vector processor systems
[DE91-013205] N92-10297

A performance comparison of three supercomputers: Fujitsu VP-2600, NEC SX-3, and CRAY Y-MP [DE91-016304] N92-10298
Content addressable memory project [NASA-CR-188981] N92-10299
Efficient multitasking of Choleski matrix factorization on CRAY supercomputers [NASA-TM-4259] N92-10302
Parallel machine architecture and compiler design facilities [NASA-CR-188784] N92-10304
Queueing in networks of computers [NASA-CR-188892] N92-10308
TAURUS: An interactive post-processor for the analysis codes NIKE3D, DYNA3D, and TOPAZ3D [DE91-019012] N92-10326
Fiber networking at Argonne: A distributed, multiapplication, multivendor computing environment [DE91-018560] N92-10338
A model for a data acquisition solution for a medium size accelerator laboratory N92-10376
Worldnet [NASA-CR-188845] N92-10711

ARCS
Studies in planetary rings N92-10949

ARCTIC REGIONS
Ozone depletion rates in the late winter/early spring Arctic and Antarctic stratosphere according to recent ozone sounding observations N92-10547

ARGON
Decay channels of resonantly excited 2p(-1)ns, md states of Ar and 3d(-1)np states of Kr N92-10426
Experimental study of interactions of highly charged ions with atoms at keV energies [DE91-016962] N92-10616

ARGON LASERS
Laser interferometer (TENKO-10 and -100) for gravitational wave antenna development [ISAS-640] N92-10189

ARGON PLASMA
Dependence of Au(-) production upon the target work function in a plasma-sputter-type negative ion source [NIFS-85] N92-10656

ARRAYS
Formation of self-aligned guard rings for monolithic Schottky-barrier diode arrays [NASA-CASE-NPO-17734-1-CU] N92-10146
Integrated array and 3-component processing using a seismic microarray [AD-A240139] N92-10265

ARSENIC ALLOYS
OMVPE growth of InAsSbBi and related alloys using new organometallic group V sources [AD-A239939] N92-10703

ARTIFICIAL INTELLIGENCE
Automated eddy current analysis of materials [NASA-CR-184216] N92-10200
Predicting cloud-to-ground lightning with neural networks [AD-A239989] N92-10270
IID: An intelligent information dictionary for managing semantic metadata [AD-A240022] N92-10715

ARTIFICIAL SATELLITES
Activities report of the Norwegian Space Center [ETN-91-90052] N92-10029

ASTEROID BELTS
An infrared reflectance study of low albedo surface constituents N92-10830
Asteroid families N92-10885

ASTEROIDS
Clay minerals in primitive meteorites and interplanetary dust 1 N92-10256
Theoretical studies of optical phenomena and related inverse problems of solar system bodies N92-10566
Infrared (2.08-14 micron) spectra of powered stony meteorites N92-10826
An infrared reflectance study of low albedo surface constituents N92-10830
Hydrocode predictions of collisional outcomes: Effects of target size N92-10861
Energy coupling in catastrophic collisions N92-10862
Continuum modeling of catastrophic collisions N92-10863
Asteroid flux and impact cratering rate on Venus N92-10880
Meteorite spectroscopy and characterization of asteroid surface materials N92-10881
Will Galileo resolve the S-asteroid controversy? N92-10882
Mapping the stability field of Jupiter Trojans N92-10883
Understanding asteroid collisional history through experimental and numerical studies N92-10884
Asteroid families N92-10885
Origin and evolution of the zodiacal dust cloud N92-10886
Asteroid surface processes: Experimental studies of the solar wind on reflectance and optical properties of asteroids N92-10941

ASTRONOMICAL CATALOGS
An atlas of optical counterparts of low mass x ray binaries. Part 1: The Northern Sample [MPE-PREPRINT-195-PT-1] N92-10723
A new catalog of planetary maps N92-10929
Image retrieval and processing system version 2.0 development work N92-10930

ASTRONOMICAL MAPS
An atlas of optical counterparts of low mass x ray binaries. Part 1: The Northern Sample [MPE-PREPRINT-195-PT-1] N92-10723

ASTRONOMICAL MODELS
Origin and evolution of the zodiacal dust cloud N92-10886
Water/rock interactions in experimentally simulated dirty snowball and dirty iceball cometary nuclei N92-10888
Formation of the protosolar nebula N92-10890
Fragmentation in stellar collapse N92-10891
Aerodynamic and gasdynamic effects in cosmogony N92-10892
Particle-gas dynamics in the protoplanetary nebula N92-10893
Accretion and evolution of solar system bodies N92-10895
Long-term evolution of a planetesimal swarm in the vicinity of a protoplanet N92-10896
A reexamination of early numerical simulations of planetary accretion N92-10897
Collision probabilities in the presence of nebular gas drag N92-10898
Growth of planets from planetesimals N92-10899
Planetary ring studies N92-10903
Models of planetary rings N92-10934
Optical properties of grains in molecular clouds and accretion disks N92-10948

ASTRONOMICAL PHOTOMETRY
Photometry of the comet 2060 Chiron N92-10887

ASTRONOMICAL SPECTROSCOPY
Remote sensing and geologic studies of the terrain northwest of Humorum basin N92-10810
Meteorite spectroscopy and characterization of asteroid surface materials N92-10881

ASTRONOMY
Finnish space projects: Planetary studies N92-10548

ASTROPHYSICS
Anomalous e(+)e(-) pairs in heavy ion collisions and solar neutrinos: Two puzzles with common solution? N92-10364
Origin and evolution of the zodiacal dust cloud N92-10886

ASYMMETRY
The effects of forebody strakes on asymmetric vortices on a vertically launched missile [AD-A239948] N92-10014
Modelling crystal growth: Convection in an asymmetrically heated ampoule [NASA-CR-184214] N92-10676

ASYMPTOTIC METHODS
Optical properties of grains in molecular clouds and accretion disks N92-10948

ASYMPTOTIC SERIES
A mathematical model for a paired comparison experiment on a continuum of response [AD-A239858] N92-10351

ATMOSPHERIC BOUNDARY LAYER
Free convection in the Martian atmosphere N92-10803
Characteristics of the Martian atmosphere surface layer N92-10804

ATMOSPHERIC CHEMISTRY
A novel technique for the measurement of photoenhanced electron attachment: Implications for an optically-controlled diffuse discharge opening switch [DE91-016226] N92-10621

ATMOSPHERIC CIRCULATION
Free convection in the Martian atmosphere N92-10803
Investigation of the small-scale structure and dynamics of Uranus' atmosphere [NASA-CR-188819] N92-10960

ATMOSPHERIC COMPOSITION
Greenhouse Warming: Abatement and Adaptation [ISBN-0-915707-50-0] N92-10228
The biological consequences of climate changes: An ecological and economic assessment N92-10235
Thoughts on abatement and adaptation N92-10239
Epilogue N92-10240
Processes for identifying regional influences of and responses to increasing atmospheric CO2 and climate change: The MINK project [DE91-018602] N92-10242
Processes for identifying regional influences of and responses to increasing atmospheric CO2 and climate change: The MINK project [DE91-018603] N92-10243
Processes for identifying regional influences of and responses to increasing atmospheric CO2 and climate change: The MINK project [DE91-018605] N92-10244
Abatement strategies based on critical loads N92-10533
Ozone depletion rates in the late winter/early spring Arctic and Antarctic stratosphere according to recent ozone sounding observations N92-10547
Mineralogy of the Martian surface from Mariner 6/7 infrared spectrometer data N92-10814
New spectral observations of Callisto and leading/trailing hemisphere distinctions N92-10839
Styles of ejecta emplacement under atmospheric conditions N92-10857

ATMOSPHERIC CORRECTION
Properties of dust and clouds in the Mars atmosphere: Analysis of Viking IRTM emission phase function sequences N92-10956

ATMOSPHERIC EFFECTS
Heat flow vs. atmospheric greenhouse on early Mars N92-10805
Venus impact craters: Implications for atmospheric and resurfacing processes from Magellan observations N92-10854
Breakup of meteoroids in the Venusian atmosphere and its effects on crater formation N92-10855
Atmospheric effects on oblique impacts N92-10856
Styles of ejecta emplacement under atmospheric conditions N92-10857
Impact cratering calculations N92-10933

ATMOSPHERIC HEATING
Greenhouse Warming: Abatement and Adaptation [ISBN-0-915707-50-0] N92-10228
Thoughts on abatement and adaptation N92-10239
The greenhouse effect N92-10587

ATMOSPHERIC IONIZATION
The structure and dynamics of the polar mesosphere investigated with the EISCAT radar systems N92-10368

ATMOSPHERIC MODELS
Processes for identifying regional influences of and responses to increasing atmospheric CO2 and climate change: The MINK project [DE91-018602] N92-10242
Free convection in the Martian atmosphere N92-10803

ATMOSPHERIC MOISTURE
Atmospheric measurements using a scanning, solar-blind Raman Lidar [DE91-016078] N92-10260
Meteo and irradiation data during BEST TWO, Mourmelon (Netherlands) [FEL-90-A368] N92-10966

ATMOSPHERIC PHYSICS
Investigation of the small-scale structure and dynamics of Uranus' atmosphere [NASA-CR-188819] N92-10960

ATMOSPHERIC RADIATION
Mission description and in-flight operations of ERBE instruments on ERBS and NOAA 9 spacecraft, November 1984 - January 1986 [NASA-RP-1256] N92-10208
Remote sensing of the Martian surface N92-10813

ATMOSPHERIC SCATTERING
Properties of dust and clouds in the Mars atmosphere: Analysis of Viking IRTM emission phase function sequences N92-10956

ATMOSPHERIC SOUNDING
Ozone depletion rates in the late winter/early spring Arctic and Antarctic stratosphere according to recent ozone sounding observations N92-10547

ATMOSPHERIC STRATIFICATION
Characteristics of the Martian atmosphere surface layer N92-10804

ATMOSPHERIC TEMPERATURE
Meteo and irradiation data during BEST TWO, Mourmelon (Netherlands) [FEL-90-A368] N92-10966

ATMOSPHERIC TIDES
Observations of semidiurnal atmospheric tides using the EISCAT incoherent scatter radar N92-10560

ATOMIC COLLISIONS
Differential collision cross-sections for atomic oxygen: Analysis of space flight instruments for solar terrestrial physics [NASA-CR-184235] N92-10613

ATOMIC ENERGY LEVELS
Ground state properties of a He-3 impurity in liquid He-4 monolayers [AD-A239993] N92-10078

ATOMIC EXCITATIONS
Super Coster Kronig and resonance super Coster Kronig spectra of solid Ge around 3p-ionization threshold N92-10517
Synchrotron radiation study of recombination processes in solid state Tb and Dy after 4d to 4f giant resonance excitation N92-10518
The N(4,5)N(6,7)N(6,7) and N(4,5)O(2,3)N(6,7) resonance Auger effects in the electron spectra of solid state Gd and Eu N92-10519
ATOMIC INTERACTIONS
Internal friction associated with interaction between carbon atoms and dislocations at low temperature N92-10471
Helium in silicon: A first principle molecular dynamics study N92-10473
Surface reconstruction and many-atom models N92-10483
Interatomic interactions in the local density approximation N92-10487
Polarizabilities of trans and cis polyacetylene and interactions among chains in crystalline polyacetylene [AD-A240025] N92-10705
ATOMIC PHYSICS
Proceedings of the 25th Annual Conference of the Finnish Physical Society [REPT-119(1991)] N92-10362
Atomic physics of strongly correlated systems [DE91-012259] N92-10617
Physics Division annual review, April 1, 1990 - March 31, 1991 [DE91-018704] N92-10707
ATOMIC STRUCTURE
Decay channels of resonantly excited 2p(-1)ns, md states of Ar and 3d(-1)np states of Kr N92-10426
Li 1s photoionization and photoexcitation with satellites N92-10427
Relaxation and final-state correlation effects in the 3p and 3s photoionization of Ar, K(+), and Ca(++) N92-10430
Isotope selective resonance ionization measurements of lithium N92-10442
Interatomic interactions in the local density approximation N92-10487
Scanning tunneling microscope measurements in air:Langmuir-Blodgett films on HOPG and growth of evaporated gold on HOPG N92-10497
Scanning tunneling microscopy of polysialic acid N92-10538
Strong correlation theories of high temperature superconductors [DE91-017479] N92-10688
Chemical thermodynamic equilibria and conductivity of nonstoichiometric YB2Cu3O7-(delta): A review [DE91-018638] N92-10701
ATOMIC THEORY
Vlasov-Maxwell system: 2-D equilibria, reversed field pinches [DE91-018421] N92-10595
ATOMS
Physics Division annual review, April 1, 1990 - March 31, 1991 [DE91-018704] N92-10707
AUDIO EQUIPMENT
Laser acoustic technology demonstration and equipment field trails [DE91-018759] N92-10193
Acoustic device and method for measuring gas densities [NASA-CASE-NPO-18155-1-CU] N92-10609
AUDIOMETRY
US TAG for ISO/TC43, acoustics, IEC/TC29 electroacoustics, ISO/TC108/SC4 human exposure to mechanical vibration and shock: Minutes of the Accredited Standards Committee on Bioacoustics, S3 [AD-A239918] N92-10610
AUDITORY DEFECTS
US TAG for ISO/TC43, acoustics, IEC/TC29 electroacoustics, ISO/TC108/SC4 human exposure to mechanical vibration and shock: Minutes of the Accredited Standards Committee on Bioacoustics, S3 [AD-A239918] N92-10610
The hazard of exposure to impulse noise as a function of frequency, volume 1 [AD-A239992] N92-10611
AUDITORY PERCEPTION
Auditory and visual evoked potentials as a function of sleep deprivation and irregular sleep [AD-A240097] N92-10281
US TAG for ISO/TC43, acoustics, IEC/TC29 electroacoustics, ISO/TC108/SC4 human exposure to mechanical vibration and shock: Minutes of the Accredited Standards Committee on Bioacoustics, S3 [AD-A239918] N92-10610
On categorizing sounds [AD-A240006] N92-10612
AUDITORY SIGNALS
On categorizing sounds [AD-A240006] N92-10612
AUDITORY STIMULI
On categorizing sounds [AD-A240006] N92-10612
AUGER EFFECT
The N(4,5)N(6,7)N(6,7) and N(4,5)O(2,3)N(6,7) resonance Auger effects in the electron spectra of solid state Gd and Eu N92-10519
Atomic physics of strongly correlated systems [DE91-012259] N92-10617
AUGER SPECTROSCOPY
Positron annihilation induced Auger-electron spectroscopy: A study of a Ge(100) surface N92-10515
AURORAL ZONES
Ionospheric and magnetospheric processes [AD-A239967] N92-10263
Examples of VLF emissions recorded in the auroral zone N92-10555
AURORAS
Examples of VLF emissions recorded in the auroral zone N92-10555
AUSTENITE
Evaluation of advanced austenitic alloys relative to alloy design criteria for steam service [DE91-017800] N92-10081
AUSTENITIC STAINLESS STEELS
Evaluation of advanced austenitic alloys relative to alloy design criteria for steam service [DE91-017800] N92-10081
AUSTRALIA
Gravity survey of the Mt. Toondina impact structure, South Australia N92-10879
AUTOMATIC CONTROL
A system performance throughput model applicable to advanced manned telescience systems [NASA-CR-188860] N92-10034
AUTOMATION
Computer assisted multiplex sequencing [DE91-017851] N92-10337
AVALANCHE DIODES
Sintered compacts for heat sinks and process for fabricating same [DE91-018438] N92-10153
In(0.5)3Ga(0.47)As/InP SAM avalanche photodiodes grown by gas source MBE N92-10530
AXISYMMETRIC BODIES
Geometrical effects of the magnetic field on the neoclassical flow, current, and rotation in general toroidal systems [NIFS-86] N92-10655
AXISYMMETRIC FLOW
Computer simulations on the orientation of molecular hydrogen in liquid crystals N92-10466

B

BACILLUS
Remote detection of atmospherically dispersed vegetative cells using fluorescence lidar [DE91-016077] N92-10218
BACKSCATTERING
Combined Backscatter Moessbauer Spectrometer and X Ray Fluorescence analyzer (BaMS/XRF) for planetary surface materials N92-10249
The structure and dynamics of the polar mesosphere investigated with the EISCAT radar systems N92-10368
Use of radar to assess aeolian processes N92-10802
The perplexing continuum slops of Mars: Effects of thin ferric coatings and viewing geometry N92-10816
The photometric roughness of Mimas N92-10835
Anomalous scattering of light on Triton N92-10836
Models of the diffuse radar backscatter from Mars N92-10846
Surface properties of Galilean satellites from bistatic radar experiments N92-10849
Radar backscattering by the icy Galilean satellites and the radar glory effect N92-10850
Regoliths of icy satellites: The coherent backscatter model N92-10851
BALLISTICS
Effects of wires on solid propellant ballistics N92-10109
BANACH SPACE
Some results on constrained controllability in discrete-time convex processes [MEMO-926] N92-10342
BAND STRUCTURE OF SOLIDS
Shape coexistence in transitional (132,133,134)Ba N92-10401
A band theoretical study on the electronic properties in the phase transition CuAu 1 to CuAu 2 N92-10488
BANDWIDTH
Development of a pressure transducer calibration system (dynamic pressure response caliber), phase 2 [AD-A239859] N92-10188
BARIUM
Electron correlation in the 4d hole state of Cs and Ba N92-10428
BARIUM ION CLOUDS
Plasma cloud behavior [AD-A240000] N92-10264
BARIUM ISOTOPES
Shape coexistence in transitional (132,133,134)Ba N92-10401
BARIUM OXIDES
Neutron irradiation effects on YBCO single crystals [DE91-018615] N92-10700
BARRIER LAYERS
Tunneling in oscillating double barrier heterostructures N92-10496
BASALT
Oxidation of basaltic tephras: Influence on reflectance in the 1 micron region N92-10817
Factors controlling the structures of magma chambers in basaltic volcanoes N92-10957
Workshop on Mare Volcanism and Basalt Petrogenesis: Astounding Fundamental Concepts (AFC) Developed Over the Last Fifteen Years --- Author [NASA-CR-188810] N92-10961
Formation of Apollo 14 aluminous mare basalts by replenishment fractional crystallization and assimilation of precursor crust N92-10963
Exploration of relationships between low-Ti and high-Ti pristine lunar glasses using an armalcolite assimilation model N92-10964
BAYES THEOREM
Detection of abrupt changes in statistical models [AD-A240116] N92-10360
BEAM CURRENTS
Synchrotron radiation research and Finnish beamline at MAX-lab N92-10377
BEAM INJECTION
Observation of plasma toroidal rotations driven by the electric field due to a loss of ions [NIFS-23] N92-10647
Density peaking in the JFT-2M tokamak plasma with counter neutral beam injection [NIFS-83] N92-10657
BEAM WAVEGUIDES
Study of different SX-700 designs for the undulator beamline (BL51) at MAX-LAB N92-10446
BEAMS (RADIATION)
Synchrotron radiation: New research opportunities for the next decade N92-10366
BEAT FREQUENCIES
Beat wave current drive experiment on DDT [DE91-017407] N92-10622
BERYLLIUM
Beryllium doping of InP grown by gas-source molecular beam epitaxy N92-10489
BESSEL FUNCTIONS
Abel inversion with the fast Fourier transform N92-10379
Exact strangeness conservation and particle production [BI-TP-90/35] N92-10385
BETA PARTICLES
Double beta decay in the particle-number projected QRPA formalism N92-10408
Neutrinoless beta decay in the framework of a relativistic quark model N92-10409
BIBLIOGRAPHIES
Aeronautical engineering: A continuing bibliography with indexes (supplement 267) [NASA-SP-7037(267)] N92-10001
Index to 1987 NASA Tech Briefs, volume 11, numbers 1-10 [NASA-TM-105024] N92-10717
Index to 1988 NASA Tech Briefs, volume 12, numbers 1-11 [NASA-TM-105077] N92-10718
Index to 1989 NASA Tech Briefs, volume 13, numbers 1-12 [NASA-TM-105109] N92-10719
Index to 1990 NASA Tech Briefs, volume 14, numbers 1-12 [NASA-TM-105110] N92-10720
Cumulative index to NASA Tech Briefs, 1976-1980, volumes 1-5 [NASA-TM-89327] N92-10721
Cumulative index to NASA Tech Briefs, 1981-1985, volumes 6-10 [NASA-TM-89326] N92-10722
BICRYSTALS
Electrical transport across grain boundaries in bicrystals of YBa2Cu3O7(delta) [DE91-018588] N92-10697

BIDIRECTIONAL REFLECTANCE
The bidirectional reflectance spectra of five gas-rich ordinary chondrites N92-10828
Surface scattering properties estimated from modeling airborne multiple emission angle reflectance data N92-10841
Application of Hapke photometric model to three geologic surfaces using PARABOLA bidirectional reflection data N92-10843
BINARY DATA
An alternative design for a sparse distributed memory [NASA-CR-188847] N92-10291
Sparse distributed memory: Principles and operation [NASA-CR-188901] N92-10294
A mathematical model for a paired comparison experiment on a continuum of response [AD-A239858] N92-10351
BINARY MIXTURES
Aerosol dynamics: Binary nucleation N92-10525
BINDING
Molecular dynamics using the tight-binding approximation: Application to liquid silicon N92-10465
BINOCULAR VISION
Three experiments with stereoscopic television: When it works and why [DE91-016277] N92-10129
BIOACOUSTICS
US TAG for ISO/TC43, acoustics, IEC/TC29 electroacoustics, ISO/TC108/SC4 human exposure to mechanical vibration and shock: Minutes of the Accredited Standards Committee on Bioacoustics, S3 [AD-A239918] N92-10610
BIOCHEMISTRY
Paucity of moderately repetitive sequences [DE91-017953] N92-10276
BIODYNAMICS
Holographic nondestructive testing in bone biomechanics N92-10451
BIOELECTRIC POTENTIAL
Auditory and visual evoked potentials as a function of sleep deprivation and irregular sleep [AD-A240097] N92-10281
BIOGEOCHEMISTRY
Regional scale dynamical modelling of biogeochemical processes [AD-A240115] N92-10246
BIOINSTRUMENTATION
Integration of magnetoencephalography and magnetic resonance imaging N92-10540
Proton NMR studies on human blood plasma: An application to cancer research N92-10545
BIOLOGICAL EFFECTS
Compilation of 1990 annual reports of the Navy ELF communications system ecological monitoring program. Volume 2: Tabs C thru F [AD-A239869] N92-10138
Processes for identifying regional influences of and responses to increasing atmospheric CO2 and climate change: The MINK project [DE91-018605] N92-10244
The hazard of exposure to impulse noise as a function of frequency, volume 1 [AD-A239992] N92-10611
BIOT NUMBER
Sea ice elastic moduli: Determination of Biot parameters using in-field velocity measurements [AD-A239803] N92-10275
BIRDS
Compilation of 1990 annual reports of the Navy ELF communications system ecological monitoring program. Volume 3: Tabs G thru I [AD-A239870] N92-10139
BISMUTH ALLOYS
OMVPE growth of InAsSbBi and related alloys using new organometallic group V sources [AD-A239939] N92-10703
BISTATIC REFLECTIVITY
Surface properties of Galilean satellites from bistatic radar experiments N92-10849
BLACKOUT (PHYSIOLOGY)
Physiologic Transection of the brain stem in healthy humans and the neurologic basis of unconsciousness [AD-A240122] N92-10023
BLAZARS
Explanation for optical frequency dependent polarization in blazars N92-10577
BLOOD PLASMA
Proton NMR studies on human blood plasma: An application to cancer research N92-10545
BODY TEMPERATURE
A computer simulation for predicting the time course of thermal and cardiovascular responses to various combinations of heat stress, clothing, and exercise [AD-A240023] N92-10288
BODY-WING CONFIGURATIONS
Transonic and supersonic Euler computations of vortex-dominated flow fields about a generic fighter [NASA-TP-3156] N92-10011
BOILING WATER REACTORS
Are limit cycle calculations a stochastic process? [DE91-017681] N92-10355
BOLIDES
Impact cratering calculations N92-10933
BONDING
Bond of reinforcement under controlled confinement [AD-A240142] N92-10207
BONES
Holographic nondestructive testing in bone biomechanics N92-10451
BORON
Diamond thin films grown by microwave plasma assisted chemical vapor deposition [DE91-018553] N92-10695
BORON COMPOUNDS
The shape effect of magnetic damages in irradiated Nd2Fe14B-permanent magnets N92-10468
BOSONS
Limits on t-quark decay into charged Higgs from a direct search at the CERN proton-antiproton collider [CERN-PPE/90-180] N92-10391
Measurements of the ratio R = sigma(sub W)Br(W to mu(nu))/sigma(sub Z)Br(Z to mu(mu)) and gamma(sup tot)(sub W) at the CERN proton-antiproton collider [CERN-PPE/90-141] N92-10392
Proton-neutron symmetry in boson models of nuclear structure N92-10406
Predictions of the electron-hole liquid model for high T(sub c) superconductors N92-10499
BOUNDARY LAYER FLOW
Hypersonic flows as related to the National Aerospace plane [NASA-CR-187985] N92-10004
The measurement of plate vibration and sound radiation from a turbulent boundary layer manipulator [AD-A240127] N92-10206
Airframe noise N92-10605
BOUNDARY LAYER SEPARATION
Hypersonic flows as related to the National Aerospace plane [NASA-CR-187985] N92-10004
Numerical investigation of the effect of leading edge geometry on dynamic stall of airfoils [AD-A239949] N92-10015
Management and control of unsteady and turbulent flows [AD-A240050] N92-10180
BOUNDARY LAYER STABILITY
Stability of the flow around a cylinder: The spin-up problem [NASA-CR-187636] N92-10171
BOUNDARY LAYERS
A grid-free method for high Reynolds number flow around an immersed elastic structure [AD-A239851] N92-10013
Regional scale dynamical modelling of biogeochemical processes [AD-A240115] N92-10246
BOUNDARY VALUE PROBLEMS
Steady flow of a fluid-solid mixture in a circular cylinder [DE91-018698] N92-10174
Totally parallel multilevel algorithms for sparse elliptic systems [NASA-CR-188837] N92-10333
Multi-dimensional ENO schemes for general geometries [NASA-CR-187637] N92-10349
BRAIN
Auditory and visual evoked potentials as a function of sleep deprivation and irregular sleep [AD-A240097] N92-10281
Fear-potentiated startle as a model system for analyzing learning and memory [AD-A239994] N92-10284
BRAIN STEM
Physiologic Transection of the brain stem in healthy humans and the neurologic basis of unconsciousness [AD-A240122] N92-10023
BRANCHING (MATHEMATICS)
Nonlinear interactions of tearing modes in the presence of shear flow [DE91-018420] N92-10173
The connectivity of the basis graph of a branching greedoid [MEMO-937] N92-10341
Applications of multiparameter bifurcations of period functions [AD-A240046] N92-10352
BRAZIL
UV, visible, and near-IR reflectivity data for magnetic soils/rocks from Brazil N92-10254
BRAZING
High temperature creep properties of eutectic and near eutectic silver-copper alloys: Application to metal/ceramic joining [DE91-017987] N92-10082
BRECCIA
Infrared reflectance spectra (4-12 micron) of lunar samples N92-10812
BREEDING (REPRODUCTION)
Compilation of 1990 annual reports of the Navy ELF communications system ecological monitoring program. Volume 3: Tabs G thru I [AD-A239870] N92-10139
BRIGHTNESS
Photometry of the comet 2060 Chiron N92-10887
BRINES
Physical properties of cryovolcanic brines: Applications to the evolution of Ganymede N92-10737
The magnesium sulfate-water system at pressures to 4 kilobars N92-10738
BRITTLE MATERIALS
The width of fault zones in a brittle-viscous lithosphere: Strike-slip faults N92-10944
BRITTLENESS
Probability of brittle failure [NASA-CR-187174] N92-10205
The strength of Miranda's lithosphere N92-10767
BROADBAND
An analysis of the frequency characteristics of corona discharge at low pressure [AD-A239940] N92-10674
BROADCASTING
Real-time data compression of broadcast video signals [NASA-CASE-LEW-14945-2] N92-10128
BROKEN SYMMETRY
Proton-neutron symmetry in boson models of nuclear structure N92-10406
Independent and cumulative yields of neutron-rich nuclei in symmetric fission induced by p and d on U-238 N92-10411
BROMINATION
Brominated graphitized carbon fibers [NASA-CASE-LEW-14698-2] N92-10090
BROMINE
Brominated graphitized carbon fibers [NASA-CASE-LEW-14698-2] N92-10090
BROWNIAN MOVEMENTS
Detection of abrupt changes in statistical models [AD-A240116] N92-10360
BUDGETING
Activities of the Board on Mathematical Sciences [DE91-017931] N92-10361
BULK MODULUS
Strong magnetic compression of spin-polarized hydrogen N92-10480
BUOYANCY
Process modelling for Space Station experiments [NASA-CR-184227] N92-10112
BURGER EQUATION
Optimal moving grids for time-dependent partial differential equations [NASA-CR-188850] N92-10344
BURNING RATE
Erosive burning of solid propellants N92-10108
Combustion and safety of solid propellant rocket motors N92-10110

C

CADMIUM ISOTOPES
High-spin states in Cd-109 N92-10403
Shapes of Cd-110 at high spins N92-10404
CALDERAS
Timing and formation of wrinkle ridges in the Tyrrhena Patera Region of Mars N92-10752
Physical properties of lava flows on the southwest flank of Tyrrhena Patera, Mars N92-10790
Factors controlling the structures of magma chambers in basaltic volcanoes N92-10957
CALIBRATING
The data book of ERS-1: The European Remote Sensing Satellite [ESA-BR-75] N92-10039
Development of a pressure transducer calibration system (dynamic pressure response caliber), phase 2 [AD-A239859] N92-10188
Calibration of scintillation cells for radon-222 measurements N92-10521
Crustal heterogeneity of the moon viewed from the Galileo SSI camera: Lunar sample calibrations and compositional implications N92-10808

Mineralogy of the Martian surface from Mariner 6/7 infrared spectrometer data N92-10814

CALLISTO
New spectral observations of Callisto and leading/trailing hemisphere distinctions N92-10839
Tidal evolution of planetary satellites N92-10953

CALORIMETERS
Thermal energy storage and heat transfer support program. Volume 1: Task-1 heat transport system study copper-water and steel-sodium DWAHP [AD-A239928] N92-10176

CAMERAS
Explosive Transient Camera (ETC) program [NASA-CR-188957] N92-10184
Geologic mapping of tunnels using photogrammetry: Camera and target positioning [DE91-018394] N92-10261

CANCER
Proton NMR studies on human blood plasma: An application to cancer research N92-10545

CANOPIES
An experimental evaluation of the impact resistance of recoated F-16A monolithic polycarbonate flat sheet [AD-A239984] N92-10101

CARBIDES
Evaluation of advanced austenitic alloys relative to alloy design criteria for steam service [DE91-017800] N92-10081

CARBOHYDRATES
Scanning tunneling microscopy of polysialic acid N92-10538

CARBON
Internal friction associated with interaction between carbon atoms and dislocations at low temperature N92-10471
High resolution spectroscopy of H(+) energy loss in thin carbon film [NIFS-88] N92-10654

CARBON COMPOUNDS
Torsional potential for the C(sp2)-C(sp2) bond N92-10443

CARBON CYCLE
Simulations of the carbon cycle in the oceans [DE91-018475] N92-10273

CARBON DIOXIDE
Alkali metal carbon dioxide electrochemical system for energy storage and/or conversion of carbon dioxide to oxygen [NASA-CASE-LEW-14973-1] N92-10222
Climate change: Problems of limits and policy responses N92-10232
Climate and forests N92-10234
Simulations of the carbon cycle in the oceans [DE91-018475] N92-10273
Fossil fuels and the environment N92-10586
Heat flow vs. atmospheric greenhouse on early Mars N92-10805
Degradation of Fe-Mg silicates in hot CO2 atmospheres: Applications to Venus N92-10806
Mineralogy of the Martian surface from Mariner 6/7 infrared spectrometer data N92-10814
Optical properties of CO2 ice and CO2 snow from ultraviolet to infrared: Application to frost deposits and clouds on Mars N92-10821

CARBON DIOXIDE CONCENTRATION
The greenhouse effect: Its causes, possible impacts, and associated uncertainties N92-10229
Human development and carbon dioxide emissions: The current picture and the long-term prospects N92-10230
Epilogue N92-10240
Processes for identifying regional influences of and responses to increasing atmospheric CO2 and climate change: The MINK project [DE91-018602] N92-10242
Processes for identifying regional influences of and responses to increasing atmospheric CO2 and climate change: The MINK project [DE91-018603] N92-10243
Processes for identifying regional influences of and responses to increasing atmospheric CO2 and climate change: The MINK project [DE91-018605] N92-10244
Heat flow vs. atmospheric greenhouse on early Mars N92-10805

CARBON FIBERS
Corrosion tests of meshes in carbon fiber laminates: Impact beam tests [INFORME-I-522/90] N92-10068
Quantitative nondestructive evaluation of materials and structures [NASA-CR-188975] N92-10071
Brominated graphitized carbon fibers [NASA-CASE-LEW-14698-2] N92-10090

CARBON MONOXIDE
Quantum state resolved desorption of CO from solid surface [DE91-017712] N92-10626

CARBONACEOUS CHONDRITES
Physical properties of cryovolcanic brines: Applications to the evolution of Ganymede N92-10737
The magnesium sulfate-water system at pressures to 4 kilobars N92-10738
Pre-terrestrial oxidation products in carbonaceous meteorites identified by Mossbauer spectroscopy N92-10824
Water/rock interactions in experimentally simulated dirty snowball and dirty iceball cometary nuclei N92-10888

CARBONACEOUS METEORITES
Pre-terrestrial oxidation products in carbonaceous meteorites identified by Mossbauer spectroscopy N92-10824

CARBONATES
Spectral evidence for carbonates on Mars: Hydrous carbonates N92-10820

CARBONYL COMPOUNDS
Diosmacycloalkanes as models for the formation of hydrocarbons from surface methylenes [DE91-017854] N92-10065

CARDIOVASCULAR SYSTEM
A computer simulation for predicting the time course of thermal and cardiovascular responses to various combinations of heat stress, clothing, and exercise [AD-A240023] N92-10288

CARGO SPACECRAFT
NEP mission sensitivities N92-10045

CARTESIAN COORDINATES
On the most general tensor B(sub ij) which is zero for i does not equal j, and the most general isotropic tensor I(sub ij) [NASA-TM-105236] N92-10289
Fragmentation in stellar collapse N92-10891

CASCADE FLOW
Multigrid calculation of three-dimensional viscous cascade flows [NASA-TM-105257] N92-10345

CASSINI MISSION
CAPS-plasma spectrometer for the Cassini spacecraft N92-10565

CASTING
Helmet of a laminate construction of polycarbonate and polysulfone polymeric material [NASA-CASE-MSC-21503-1] N92-10091

CATALYSIS
Chemisorption of CO on Mg-O/Co(0001) N92-10484

CATHODES
Experimental investigation of a 12 cm diameter Kaufman xenon ion thruster [NAL-TR-1099] N92-10056
Optical and electrical investigations into cathode ignition and diode closure [DE91-017823] N92-10191
Alkali metal carbon dioxide electrochemical system for energy storage and/or conversion of carbon dioxide to oxygen [NASA-CASE-LEW-14973-1] N92-10222
Numerical simulation of ion beam generated in the diode with anode plasma column [IPPCZ-306] N92-10652

CAUCHY PROBLEM
Mean estimation in highly skewed samples [DE91-018513] N92-10358

CAVITIES
Measurements of forces, moments, and pressures on a generic store separating from a box cavity at supersonic speeds [NASA-TP-3110] N92-10005
Automatic network analyzer procedures for 5045 klystron cavities [DE91-018015] N92-10149
Surface effect on optical bistability in coupled exciton-phonon systems inside a cavity [AD-A240026] N92-10643

CAVITY RESONATORS
High temperature ceramic superconductors [AD-A239813] N92-10154
Coupling between radiation and gas dynamics [AD-A240004] N92-10179

CENTRAL NERVOUS SYSTEM
Physiologic Transection of the brain stem in healthy humans and the neurologic basis of unconsciousness [AD-A240122] N92-10023

CENTRAL PROCESSING UNITS
The role of graphics super-workstations in a supercomputing environment [NASA-CR-188852] N92-10306
TAURUS: An interactive post-processor for the analysis codes NIKE3D, DYNA3D, and TOPAZ3D [DE91-019012] N92-10326

CERAMIC FIBERS
Relative sliding durability of two candidate high temperature oxide fiber seal materials [NASA-TM-105199] N92-10064

CERAMIC MATRIX COMPOSITES
Development of nondestructive characterization technologies for process control of ceramics [DE91-018540] N92-10097

CERAMICS
Development of nondestructive characterization technologies for process control of ceramics [DE91-018540] N92-10097
Update on the prospects for ceramic engine components [DE91-018574] N92-10098
High temperature ceramic superconductors [AD-A239813] N92-10154

CESIUM
Electron correlation in the 4d hole state of Cs and Ba N92-10428

CESIUM IONS
Instrumental design for measurement of surface charge on insulating materials [DE91-018695] N92-10099

CHANGE DETECTION
New methods of change detection using multispectral data [AD-A239370] N92-10217

CHANNEL FLOW
Superfluid vortex nucleation in He-3 flow N92-10479

CHANNELS (DATA TRANSMISSION)
Digital simulation of speech transmission channels [IZF-1991-A-7] N92-10115
Multi-gigabit fiber optic wide area network development [AD-A239850] N92-10642

CHAOS
Characterization of nonlinear input-output systems using time series analysis [DE91-018003] N92-10356
Using surrogate data to detect nonlinearity in time series [DE91-018017] N92-10357

CHARACTERIZATION
Glass sample characterization [NASA-CR-184230] N92-10088
Electromagnetic oil field mapping for improved process monitoring and reservoir characterization [DE91-017452] N92-10132

CHARGE TRANSFER
A band theoretical study on the electronic properties in the phase transition CuAu 1 to CuAu 2 N92-10488

CHARGED PARTICLES
Instrumental design for measurement of surface charge on insulating materials [DE91-018695] N92-10099
Ionospheric and magnetospheric processes [AD-A239967] N92-10263
Searches for heavy neutrinos from decays of the Z N92-10395
Single particle and fluid picture for the ponderomotive drift in nonuniform plasmas [NIFS-25] N92-10645
Composition and energetics of solar flare particle events measured by satellites, 1989 - 1991 [DE91-018028] N92-10969

CHASSIGNITES
Does Lafayette = Nakhla? Not necessarily so, based on 4.2K Mossbauer spectra of all of the SNC meteorites N92-10825

CHEMICAL ANALYSIS
Clay minerals in primitive meteorites and interplanetary dust 2. Smectites and micas N92-10252
Formation of Apollo 14 aluminous mare basalts by replenishment fractional crystallization and assimilation of precursor crust N92-10963

CHEMICAL BONDS
Torsional potential for the C(sp2)-C(sp2) bond N92-10443
Polarization dependent x ray spectroscopy of high T(sub c) superconductors [DE91-017475] N92-10683
Chemical thermodynamic equilibria and conductivity of nonstoichiometric YB2Cu3O7-(delta): A review [DE91-018638] N92-10701

CHEMICAL COMPOSITION
Brominated graphitized carbon fibers [NASA-CASE-LEW-14698-2] N92-10090
Mineralogy of Cretaceous/Tertiary boundary clays in the Chicxulub structure in northern Yucatan N92-10253
Clay minerals in primitive meteorites and interplanetary dust 1 N92-10256
The influence of growth conditions on the composition of GaInAsP grown by gas-source molecular beam epitaxy N92-10491

Structure and evolution of turbulent preplanetary disc N92-10571
Electronics of the cosmic ray air shower array at Turku (Finland) N92-10574
Test results of density detectors of the cosmic ray air shower array in Turku (Finland) N92-10575
The magnesium sulfate-water system at pressures to 4 kilobars N92-10738
Properties of planetary fluids at high pressures and temperatures N92-10739
Composition of Syrtis Major volcanic plateau N92-10815
Water detection at the moon, Mars and comets with a combined neutron gamma ray instrument N92-10819
Disk-resolved spectral reflectance properties of Phobos from 0.3-3.2 micron: Preliminary integrated results from Phobos 2 N92-10822
Compositional variability of the Martian surface N92-10931
Optical properties of grains in molecular clouds and accretion disks N92-10948

CHEMICAL ENGINEERING
Air pulsed plate liquid-liquid extractor simulation [DE91-018155] N92-10172

CHEMICAL EQUILIBRIUM
Chemical thermodynamic equilibria and conductivity of nonstoichiometric YB2Cu3O7-(delta): A review [DE91-018638] N92-10701

CHEMICAL EVOLUTION
Implications of convection in the moon and the terrestrial planets N92-10730

CHEMICAL FRACTIONATION
Chemical fractionation of siderophile elements in impactites from Australian meteorite craters N92-10875

CHEMICAL PROPERTIES
High temperature solar cell contacts [AD-A239932] N92-10227

CHEMICAL REACTIONS
Diosmacycloalkanes as models for the formation of hydrocarbons from surface methylenes [DE91-017854] N92-10065
Poly 1, 2, 4-triazoles via aromatic nucleophilic displacement [NASA-CASE-LAR-14440-1] N92-10066
Structure and optical polarizabilities of small silicon clusters N92-10425
Studies of volatiles and organic materials in early terrestrial and present-day outer solar system environments N92-10958

CHEMICAL WARFARE
Laser acoustic technology demonstration and equipment field trails [DE91-018759] N92-10193

CHEMISORPTION
Oxide properties of a gamma titanium aluminide: A surface science study [DE91-018024] N92-10095
Chemisorption of CO on Mg-O/Co(0001) N92-10484

CHIPS (ELECTRONICS)
Thermal management of high heat flux electronic components in space and aircraft systems, phase 1 [AD-A239982] N92-10157

CHIPS (MEMORY DEVICES)
Gallium arsenide pilot line for high performance components [AD-A239955] N92-10704

CHIRON
Photometry of the comet 2060 Chiron N92-10887

CHLORIDES
Poly 1, 2, 4-triazoles via aromatic nucleophilic displacement [NASA-CASE-LAR-14440-1] N92-10066

CHLORINE
Lifetime of the 1.959 MeV state in Cl-36 N92-10400

CHLORINE COMPOUNDS
Surface electrochemistry of Chloro(phthalocyaninato)rhodium(III) species, and oxygen reduction electrocatalysis, formation of a dimeric species [AD-A240148] N92-10104

CHLORINE FLUORIDES
Nonflammable hydraulic power system for tactical aircraft. Volume 2: Equipment and systems test and evaluation [AD-A239805] N92-10100

CHOLESKY FACTORIZATION
Efficient multitasking of Choleski matrix factorization on CRAY supercomputers [NASA-TM-4259] N92-10302

CHONDRITES
Clay minerals in primitive meteorites and interplanetary dust 1 N92-10256
Infrared (2.08-14 micron) spectra of powered stony meteorites N92-10826
Darkening in gas-rich ordinary chondrites: Spectral modelling and implications for the regoliths of ordinary chondrite parent bodies N92-10827
The bidirectional reflectance spectra of five gas-rich ordinary chondrites N92-10828
Reflectance spectra of some fractions of Migei and Murchison SM chondrites in the range of 0.3-2.6 microns N92-10829

CHONDRULE
Reflectance spectra of some fractions of Migei and Murchison SM chondrites in the range of 0.3-2.6 microns N92-10829

CHROMIUM ALLOYS
Evaluation of advanced austenitic alloys relative to alloy design criteria for steam service [DE91-017800] N92-10081
Transport properties and oxidation in chromium and Fe-Cr alloys exposed to oxygen at high temperatures [DE91-018571] N92-10086

CHRONOLOGY
Glacial and marine chronology of Mars N92-10772
Chronology of glaciation in the Hellas region of Mars N92-10773
Glacial geology of the Hellas region on Mars N92-10774

CIRCUITS
Diamond heat sinks for electronic circuits [AD-A239750] N92-10145

CIRCULAR CYLINDERS
A grid-free method for high Reynolds number flow around an immersed elastic structure [AD-A239851] N92-10013
Steady flow of a fluid-solid mixture in a circular cylinder [DE91-018698] N92-10174

CIRCULAR POLARIZATION
Spacecraft antennas N92-10122
Regoliths of icy satellites: The coherent backscatter model N92-10851

CITIES
Evaluation of high altitude photography for city regional areas [MGA-A-44] N92-10210
Possibilities of producing land use information for city regional area planning by high altitude photographs, taking south west Munich (Fed. Republic of Germany) regional area as an example N92-10212
Evaluation of high altitude photography for city cartography, with the example of Seattle, US N92-10214

CLASSIFICATIONS
Algorithm for detection of VFIB in real time from ECG N92-10542

CLASSIFIERS
New methods of change detection using multispectral data [AD-A239370] N92-10217

CLAYS
Program and Abstracts for Clay Minerals Society 28th Annual Meeting [NASA-TM-105098] N92-10248
Clays on Mars: Review of chemical and mineralogical evidence N92-10250
Clay minerals in primitive meteorites and interplanetary dust 2. Smectites and micas N92-10252
Mineralogy of Cretaceous/Tertiary boundary clays in the Chicxulub structure in northern Yucatan N92-10253
Clay minerals in primitive meteorites and interplanetary dust 1 N92-10256
Spectroscopic analyses of Fe and water in clays: A Martian surface weathering study N92-10818

CLIMATE
Processes for identifying regional influences of and responses to increasing atmospheric CO2 and climate change: The MINK project [DE91-018605] N92-10244
Paleolakes and lacustrine basins on Mars N92-10776
The gradational history of southern Ismenius Lacus N92-10785
Heat flow vs. atmospheric greenhouse on early Mars N92-10805

CLIMATE CHANGE
Greenhouse Warming: Abatement and Adaptation [ISBN-0-915707-50-0] N92-10228
The greenhouse effect: Its causes, possible impacts, and associated uncertainties N92-10229
Human development and carbon dioxide emissions: The current picture and the long-term prospects N92-10230
Sea-level rise: Regional consequences and responses N92-10231
Climate change: Problems of limits and policy responses N92-10232
Assessing and managing the risks of climate change N92-10233
Climate and forests N92-10234
The biological consequences of climate changes: An ecological and economic assessment N92-10235
Water resources and climate change N92-10236
Human dimensions of global change: Toward a research agenda N92-10238
Epilogue N92-10240
Processes for identifying regional influences of and responses to increasing atmospheric CO2 and climate change: The MINK project [DE91-018602] N92-10242
Processes for identifying regional influences of and responses to increasing atmospheric CO2 and climate change: The MINK project [DE91-018603] N92-10243
Solar energy in mitigating global environmental problems N92-10584
The greenhouse effect N92-10587

CLIMATOLOGY
The greenhouse effect: Its causes, possible impacts, and associated uncertainties N92-10229
Paleolakes and lacustrine basins on Mars N92-10776
Large impacts and climatic catastrophes on the early Earth N92-10865

CLINICAL MEDICINE
Program and abstracts of the 2nd Meeting of the Society for Research on Biological Rhythms [AD-A240007] N92-10280

CLOCKS
Method and apparatus for frequency spectrum analysis [NASA-CASE-NPO-17759-1-CU] N92-10125

CLOSURE LAW
Optical and electrical investigations into cathode ignition and diode closure [DE91-017823] N92-10191

CLOUD PHYSICS
Plasma cloud behavior [AD-A240000] N92-10264

CLOUDS
Variable features in the Valles Marineris region of Mars N92-10799
Origin and evolution of the zodiacal dust cloud N92-10886
Properties of dust and clouds in the Mars atmosphere: Analysis of Viking IRTM emission phase function sequences N92-10956

CLUMPS
Equivalence in the shell structure of the tight binding and free electron clusters N92-10441

CLUSTER ANALYSIS
Clustering: A powerful aid in classifying QRS waveforms N92-10541

CMOS
An assessment of the radiation tolerance of large satellite memories in low earth orbits [DE91-018353] N92-10040

COAGULATION
Aerodynamic and gasdynamic effects in cosmogony N92-10892
Dynamics of low velocity collisions of ice particle, coated with frost N92-10902

COAL
Electrostatic precipitator modelling N92-10532

COASTAL WATER
Sea-level rise: Regional consequences and responses N92-10231

COATING
Glass sample characterization [NASA-CR-184230] N92-10088
An experimental evaluation of the impact resistance of recoated F-16A monolithic polycarbonate flat sheet [AD-A239984] N92-10101
The perplexing continuum slope of Mars: Effects of thin ferric coatings and viewing geometry N92-10816

COATINGS
The perplexing continuum slope of Mars: Effects of thin ferric coatings and viewing geometry N92-10816
Oxidation of basaltic tephras: Influence on reflectance in the 1 micron region N92-10817

COBALT
Chemisorption of CO on Mg-O/Co(0001) N92-10484

CODE DIVISION MULTIPLE ACCESS
Multiple access trade study N92-10118

CODING
Real-time data compression of broadcast video signals [NASA-CASE-LEW-14945-2] N92-10128
A general-purpose finite-difference code for solving steady-state three-dimensional fluid-flow and heat transfer problems [AD-A239857] N92-10175

COEFFICIENTS
Calibration of scintillation cells for radon-222 measurements N92-10521

COGNITION
Auditory and visual evoked potentials as a function of sleep deprivation and irregular sleep [AD-A240097] N92-10281

COGNITIVE PSYCHOLOGY
Research into the development of a knowledge acquisition taxonomy
[NASA-CR-188948] N92-10712
COHERENT SCATTERING
Electronically resonant CARS spectroscopy of NO2 N92-10455
Regoliths of icy satellites: The coherent backscatter model N92-10851
COLD PLASMAS
Plasma Science Committee (PLSC)
[DE91-018011] N92-10594
COLD TOLERANCE
Physiological responses of the human extremities to cold water immersion
[IZF-1991-A-15] N92-10277
COLLIMATION
Spacecraft antennas N92-10122
Single-shot spectral measurements of multimode pulsed dye lasers N92-10452
COLLIMATORS
Study of different SX-700 designs for the undulator beamline (BL51) at MAX-LAB N92-10446
Optical signal multiplexer and demultiplexer
[DE91-017836] N92-10640
COLLISION PARAMETERS
Energy coupling in catastrophic collisions N92-10862
Growth of planets from planetesimals N92-10899
COLLISIONAL PLASMAS
Geometrical effects of the magnetic field on the neoclassical flow, current, and rotation in general toroidal systems
[NIFS-86] N92-10655
COLLISIONS
Dynamic screening and wake effects on electronic excitation in ion-solid and ion-surface collisions
[DE91-018224] N92-10687
Hydrocode predictions of collisional outcomes: Effects of target size N92-10861
Energy coupling in catastrophic collisions N92-10862
Continuum modeling of catastrophic collisions N92-10863
Long-term evolution of a planetesimal swarm in the vicinity of a protoplanet N92-10896
Collision probabilities in the presence of nebular gas drag N92-10898
Growth of planets from planetesimals N92-10899
COLLOCATION
Geoid undulations and gravity anomalies over the Aral Sea, the Black Sea and the Caspian Sea from a combined GEOS-3/SEASAT/GEOSAT altimeter data set
[NASA-TM-104543] N92-10257
COLOR
Transformation products of submicron-sized aluminum-substituted magnetite: Color and reductant solubility N92-10251
Recognizing of spectral mixtures, their components and spectral patterns N92-10447
An improved technique for electrolytic colouration of alkali halide crystals N92-10513
Spectral representation in vision N92-10539
Crustal heterogeneity of the moon viewed from the Galileo SSI camera: Lunar sample calibrations and compositional implications N92-10808
The bidirectional reflectance spectra of five gas-rich ordinary chondrites N92-10828
Digital cartography of Io N92-10927
COLOR CENTERS
An improved technique for electrolytic colouration of alkali halide crystals N92-10513
COLOR CODING
Color-coded global topographic map of Mars N92-10920
COLOR VISION
Spectral representation in vision N92-10539
COLUMBIA RIVER BASIN (ID-OR-WA)
Using LANDSAT to provide potato production estimates to Columbia Basin farmers and processors
[NASA-CR-188783] N92-10209
COLUMNS (PROCESS ENGINEERING)
Air pulsed plate liquid-liquid extractor simulation
[DE91-018155] N92-10172
COMBUSTION
Fire retardant performance of some interior shipboard paint schemes
[MRL-TR-91-31] N92-10089
Erosive burning of solid propellants N92-10108
COMBUSTION CHAMBERS
Gas turbine combuster exit temperature measurement
[AD-A239936] N92-10026
Combustion of Solid Propellants --- Author
[AGARD-LS-180] N92-10106
Fluidized bed combustion diagnostics by laser photocoustic spectroscopy N92-10380
Combustion and core noise N92-10607
COMBUSTION CHEMISTRY
Combustion of Solid Propellants --- Author
[AGARD-LS-180] N92-10106
COMBUSTION PHYSICS
Combustion of Solid Propellants --- Author
[AGARD-LS-180] N92-10106
Solid propellant steady combustion: Physical aspects N92-10107
Combustion and core noise N92-10607
COMBUSTION PRODUCTS
Electrostatic precipitator modelling N92-10532
COMBUSTION STABILITY
PC programs for the prediction of the linear stability behavior of liquid propellant propulsion systems and application to current MSFC rocket engine test programs, volume 1
[NASA-CR-184228] N92-10042
COMET NUCLEI
Photometry of the comet 2060 Chiron N92-10887
Water/rock interactions in experimentally simulated dirty snowball and dirty iceball cometary nuclei N92-10888
Thermal modeling of comet Kopff: Implications for the CRAF mission N92-10889
COMET RENDEZVOUS ASTEROID FLYBY MISSION
Thermal modeling of comet Kopff: Implications for the CRAF mission N92-10889
COMETARY ATMOSPHERES
New spectral observations of Callisto and leading/trailing hemisphere distinctions N92-10839
COMETS
Water detection at the moon, Mars and comets with a combined neutron gamma ray instrument N92-10819
Charged-particle induced alterations of surfaces in the outer solar system N92-10838
Photometry of the comet 2060 Chiron N92-10887
Water/rock interactions in experimentally simulated dirty snowball and dirty iceball cometary nuclei N92-10888
Thermal modeling of comet Kopff: Implications for the CRAF mission N92-10889
COMMAND AND CONTROL
C4I2 in space: Solving the SatCom shortfall
[AD-A239880] N92-10140
Software Technology for Adaptable, Reliable Systems (STARS): Domain specific environment repository composite paradigm report
[AD-A240107] N92-10328
Software Technology for Adaptable, Reliable Systems (STARS): UUS40 risk-reduction reasoning-based development paradigm tailored to Navy C2 systems
[AD-A240108] N92-10329
COMMERCE
Worldnet
[NASA-CR-188845] N92-10711
COMMERCIAL AIRCRAFT
A comparison between the consequences of the liberal and non-liberal UK-Europe bilaterals
[TT-9101] N92-10018
COMMUNICATION NETWORKS
Telescience testbed pilot program, volume 1: Executive summary
[NASA-CR-188833] N92-10031
Telescience testbed pilot program, volume 3: Experiment summaries
[NASA-CR-188834] N92-10032
Telescience testbed pilot program, volume 2: Program results
[NASA-CR-188835] N92-10033
C4I2 in space: Solving the SatCom shortfall
[AD-A239880] N92-10140
Human performance measurement: Validation procedures applicable to advanced manned telescience systems
[NASA-CR-185447] N92-10282
COMMUNICATION SATELLITES
Introduction to the Personal Access Satellite System study N92-10117
Spacecraft antennas N92-10122
C4I2 in space: Solving the SatCom shortfall
[AD-A239880] N92-10140
COMPACTING
Sintered compacts for heat sinks and process for fabricating same
[DE91-018438] N92-10153
COMPARISON
Retire FORTRAN? A debate rekindled
[DE91-016565] N92-10317
A mathematical model for a paired comparison experiment on a continuum of response
[AD-A239858] N92-10351
Earth, Uranus, and Neptune: A comparison of their magnetospheres N92-10567
COMPETITION
A comparison between the consequences of the liberal and non-liberal UK-Europe bilaterals
[TT-9101] N92-10018
COMPILERS
The paradigm compiler: Mapping a functional language for the connection machine
[NASA-CR-188839] N92-10290
Parallel machine architecture and compiler design facilities
[NASA-CR-188784] N92-10304
COMPLEX COMPOUNDS
Diosmacycloalkanes as models for the formation of hydrocarbons from surface methylenes
[DE91-017854] N92-10065
The crystal structure and moisture sensitivity of (+)-4-(1-(2,3 dimethylphenyl) ethyl) 1H-imidazole hydrochloride N92-10522
COMPLEX SYSTEMS
Glass sample characterization
[NASA-CR-184230] N92-10088
Software Technology for Adaptable, Reliable Systems (STARS): Domain specific environment repository composite paradigm report
[AD-A240107] N92-10328
COMPOSITE MATERIALS
Process for application of powder particles to filamentary materials
[NASA-CASE-LAR-14231-1] N92-10070
BES Welding Science Contractors summary report, 1990--1991
[DE91-018510] N92-10198
COMPOSITE PROPELLANTS
Erosive burning of solid propellants N92-10108
COMPOSITE STRUCTURES
Advanced thermoplastic resins, phase 1
[NASA-CR-178402] N92-10069
Software Technology for Adaptable, Reliable Systems (STARS): UUS40 risk-reduction reasoning-based development paradigm tailored to Navy C2 systems
[AD-A240108] N92-10329
COMPRESSION LOADS
Compressive strain in Lunae Planum-shortening across wrinkle ridges N92-10753
COMPRESSION TESTS
Properties of three graphite/toughened resin composites
[NASA-TP-3102] N92-10067
Quantitative nondestructive evaluation of materials and structures
[NASA-CR-188975] N92-10071
COMPTON EFFECT
Use of In-111 in quantitative SPECT N92-10544
COMPUTATION
A general-purpose finite-difference code for solving steady-state three-dimensional fluid-flow and heat transfer problems
[AD-A239857] N92-10175
Retire FORTRAN? A debate rekindled
[DE91-016565] N92-10317
Analytical and computational mathematical physics
[DE91-018965] N92-10596
COMPUTATIONAL FLUID DYNAMICS
Numerical simulation of hypersonic viscous flow for the design of H-2 orbiting plane (HOPE-2)
[NAL-TR-1093] N92-10009
Recent advances on a finite element algorithm for computational aerodynamics: Transonics-hypersonics
[DE91-018176] N92-10010
An additive turbulent decomposition of the Navier-Stokes equations implemented on highly parallel computer systems
[AD-A240131] N92-10181
COMPUTATIONAL GRIDS
A 3-D adaptive mesh refinement algorithm for multimaterial gas dynamics
[DE91-018040] N92-10169
Transformation of two and three-dimensional regions by elliptic systems
[NASA-CR-188982] N92-10170
Two-color holography concept (T-CHI)
[NASA-CR-184240] N92-10183
Performance of conjugate gradient-like algorithms in transient two-phase subchannel analysis
[DE91-013373] N92-10316
MERLIN 2: A computer program to transfer solution data betwwen finite element meshes
[DE91-018130] N92-10321
Optimal moving grids for time-dependent partial differential equations
[NASA-CR-188850] N92-10344
Multigrid calculation of three-dimensional viscous cascade flows
[NASA-TM-105257] N92-10345
The improved robustness of multigrid elliptic solvers based on multiple semicoarsened grids
[NASA-CR-187633] N92-10348
Analytical and computational mathematical physics
[DE91-018965] N92-10596

Electromagnetic plasma simulation in realistic geometries
[DE91-018651] N92-10670

COMPUTER AIDED DESIGN

Expert systems for superalloy studies
[NASA-CR-184236] N92-10080
Analysis of loss for inductive strips in finline
[AD-A239947] N92-10156
Air pulsed plate liquid-liquid extractor simulation
[DE91-018155] N92-10172
A method for determining spiral-bevel gear tooth geometry for finite element analysis
[NASA-TP-3096] N92-10195
PATRAN and P/THERMAL applications for thermal modeling
[DE91-017767] N92-10320

COMPUTER AIDED MAPPING

Triangulation using synthetic aperture radar images
N92-10914

COMPUTER AIDED TOMOGRAPHY

Use of In-111 in quantitative SPECT N92-10544

COMPUTER ASSISTED INSTRUCTION

Magneto-optical disk as a CD-ROM development tool
[DE91-009973] N92-10296

COMPUTER GRAPHICS

Composite video and graphics display for multiple camera viewing system in robotics and teleoperation
[NASA-CASE-NPO-17836-1-CU] N92-10126
The role of graphics super-workstations in a supercomputing environment
[NASA-CR-188852] N92-10306

COMPUTER NETWORKS

Queueing in networks of computers
[NASA-CR-188892] N92-10308
Fiber networking at Argonne: A distributed, multiapplication, multivendor computing environment
[DE91-018560] N92-10338
Parallel programming with PCN
[DE91-019005] N92-10339
Worldnet
[NASA-CR-188845] N92-10711

COMPUTER PROGRAMMING

The paradigm compiler: Mapping a functional language for the connection machine
[NASA-CR-188839] N92-10290
INTEGRA manual: Routines for electronic spreadsheet integration (under FRAMEWORK 3)
[DE91-017518] N92-10318
A portable run-time system for PCN
[DE91-017700] N92-10319
Software Technology for Adaptable, Reliable Systems (STARS): UUS40 risk-reduction reasoning-based development paradigm tailored to Navy C2 systems
[AD-A240108] N92-10329
Software Technology for Adaptable, Reliable Systems (STARS): US40-STARS reuse concept of operations. Volume 1: Version 0.5-draft
[AD-A240109] N92-10330

COMPUTER PROGRAMS

Numerical simulation of hypersonic viscous flow for the design of H-2 orbiting plane (HOPE-2)
[NAL-TR-1093] N92-10009
CH-53E/AV-8B aircraft sling load recovery system analysis
[AD-A239950] N92-10022
MPD thruster technology N92-10048
Thermal modeling of an epoxy encapsulation process
[DE91-017845] N92-10096
The SolarTrak solar array tracking controller
[DE91-017721] N92-10224
Solar Constant (SOLCON) Experiment: Ground Support Equipment (GSE) software development
[NASA-CR-187596] N92-10267
BIRD: A general interface for sparse distributed memory simulators
[NASA-CR-188858] N92-10292
A performance comparison of three supercomputers: Fujitsu VP-2600, NEC SX-3, and CRAY Y-MP
[DE91-016304] N92-10298
Methodology for automating software systems
[NASA-CR-184233] N92-10301
Efficient multitasking of Choleski matrix factorization on CRAY supercomputers
[NASA-TM-4259] N92-10302
Continuation of research into language concepts for the mission support environment: Source code
[NASA-CR-187816] N92-10303
Functional description for the Mapping And Graphic Information Capability (MAGIC)
[AD-A239436] N92-10305
Performance of conjugate gradient-like algorithms in transient two-phase subchannel analysis
[DE91-013373] N92-10316
INTEGRA manual: Routines for electronic spreadsheet integration (under FRAMEWORK 3)
[DE91-017518] N92-10318
PATRAN and P/THERMAL applications for thermal modeling
[DE91-017767] N92-10320
MERLIN 2: A computer program to transfer solution data betwwen finite element meshes
[DE91-018130] N92-10321
Solving problems under uncertainty
[DE91-017940] N92-10322
A brief introduction to CONDOR
[DE91-018652] N92-10325
Software Technology for Adaptable, Reliable Systems (STARS): Domain specific environment repository composite paradigm report
[AD-A240107] N92-10328
Software Technology for Adaptable, Reliable Systems (STARS): UUS40 risk-reduction reasoning-based development paradigm tailored to Navy C2 systems
[AD-A240108] N92-10329
Software Technology for Adaptable, Reliable Systems (STARS): US40-STARS reuse concept of operations. Volume 1: Version 0.5-draft
[AD-A240109] N92-10330
Massively parallel computing and the mid-course tracking problem
[DE91-010864] N92-10335
Computer assisted multiplex sequencing
[DE91-017851] N92-10337
Design controls for large order systems
[NASA-CR-184237] N92-10340
Magnetic field settings for the K130 cyclotron
N92-10421
Electromagnetic plasma simulation in realistic geometries
[DE91-018651] N92-10670
Worldnet
[NASA-CR-188845] N92-10711
Hydrocode predictions of collisional outcomes: Effects of target size N92-10861
Energy coupling in catastrophic collisions N92-10862
Continuum modeling of catastrophic collisions
N92-10863
Production of impact melt in craters on Venus, Earth, and the moon N92-10870
Understanding asteroid collisional history through experimental and numerical studies N92-10884
Aerodynamic and gasdynamic effects in cosmogony
N92-10892
Particle-gas dynamics in the protoplanetary nebula
N92-10893
Accretion and evolution of solar system bodies
N92-10895
Tidal disruption of inviscid protoplanets N92-10900
Image retrieval and processing system version 2.0 development work N92-10930

COMPUTER STORAGE DEVICES

An alternative design for a sparse distributed memory
[NASA-CR-188847] N92-10291

COMPUTER SYSTEMS DESIGN

Hardware description ADSP-21020 40-bit floating point DSP as designed in a remotely controlled digital CW Doppler radar
[DE91-018004] N92-10134
An alternative design for a sparse distributed memory
[NASA-CR-188847] N92-10291
Measurement of memory access contentions in multiple vector processor systems
[DE91-013205] N92-10297
Parallel machine architecture and compiler design facilities
[NASA-CR-188784] N92-10304
Design controls for large order systems
[NASA-CR-184237] N92-10340
A model for a data acquisition solution for a medium size accelerator laboratory N92-10376

COMPUTER SYSTEMS PERFORMANCE

The application of the ADSP-21020 40-bit floating point DSP microprocessor in a digital Doppler radar
[DE91-018005] N92-10135
Measurement of memory access contentions in multiple vector processor systems
[DE91-013205] N92-10297
A performance comparison of three supercomputers: Fujitsu VP-2600, NEC SX-3, and CRAY Y-MP
[DE91-016304] N92-10298
Methodology for automating software systems
[NASA-CR-184233] N92-10301
Modeling reality
[NASA-CR-188881] N92-10307
Integrity and security in an Ada runtime environment
[NASA-CR-188826] N92-10313
ART/Ada design project, phase 1. Task 3 report: Test plan
[NASA-CR-188945] N92-10314
Retire FORTRAN? A debate rekindled
[DE91-016565] N92-10317
Solving problems under uncertainty
[DE91-017940] N92-10322
Design controls for large order systems
[NASA-CR-184237] N92-10340

COMPUTER TECHNIQUES

Explosive Transient Camera (ETC) program
[NASA-CR-188957] N92-10184
Remote detection of atmospherically dispersed vegetative cells using fluorescence lidar
[DE91-016077] N92-10218
Parallel QR factorization on a hypercube using the torus wrap mapping
[DE91-011502] N92-10315
Retire FORTRAN? A debate rekindled
[DE91-016565] N92-10317
Computer assisted multiplex sequencing
[DE91-017851] N92-10337
Are limit cycle calculations a stochastic process?
[DE91-017681] N92-10355

COMPUTER VISION

Passive range estimation for rotorcraft low-altitude flight
[NASA-TM-103897] N92-10003

COMPUTERIZED SIMULATION

CH-53E/AV-8B aircraft sling load recovery system analysis
[AD-A239950] N92-10022
The determination of operational and support requirements and costs during the conceptual design of space systems
[NASA-CR-188817] N92-10037
MPD thruster research issues, activities, strategies
N92-10051
The generalized van der Waals theory of pure fluids and mixtures
[DE91-017549] N92-10093
Air pulsed plate liquid-liquid extractor simulation
[DE91-018155] N92-10172
Electron acceleration by laser fields in a gas
[DE91-018269] N92-10192
Using LANDSAT to provide potato production estimates to Columbia Basin farmers and processors
[NASA-CR-188783] N92-10209
Processes for identifying regional influences of and responses to increasing atmospheric CO2 and climate change: The MINK project
[DE91-018602] N92-10242
A computer simulation for predicting the time course of thermal and cardiovascular responses to various combinations of heat stress, clothing, and exercise
[AD-A240023] N92-10288
On the suitability of the connection machine for direct particle simulation
[NASA-CR-188863] N92-10293
Parallel machine architecture and compiler design facilities
[NASA-CR-188784] N92-10304
Modeling reality
[NASA-CR-188881] N92-10307
PATRAN and P/THERMAL applications for thermal modeling
[DE91-017767] N92-10320
A brief introduction to CONDOR
[DE91-018652] N92-10325
Cooperating systems: Layered MAS
[NASA-CR-184232] N92-10332
Massively parallel computing and the mid-course tracking problem
[DE91-010864] N92-10335
Gate matrix optimization using simulated annealing
N92-10374
Magnetic field settings for the K130 cyclotron
N92-10421
Optical correlators in texture analysis N92-10450
Molecular dynamics using the tight-binding approximation: Application to liquid silicon N92-10465
Computer simulations on the orientation of molecular hydrogen in liquid crystals N92-10466
Diffusion anomaly at a surface reconstruction
N92-10470
Superfluid vortex nucleation in He-3 flow N92-10479
Modeling the dynamics of molecular films by Monte Carlo simulation N92-10481
Numerical simulation studies of fluid spreading
N92-10482
Tunneling in oscillating double barrier heterostructures
N92-10496
Simulation study of scalings in scrape-off layer plasma by two-dimensional transport code
[NIFS-24] N92-10646
Electromagnetic plasma simulation in realistic geometries
[DE91-018651] N92-10670
Self-consistent modeling of plasma spraying processes
[DE91-018820] N92-10672

Langevin dynamics simulations of large frustrated Josephson junction arrays
[DE91-018046] N92-10686
Energy coupling in catastrophic collisions N92-10862
Understanding asteroid collisional history through experimental and numerical studies N92-10884
Aerodynamic and gasdynamic effects in cosmogony N92-10892
Accretion and evolution of solar system bodies N92-10895
A reexamination of early numerical simulations of planetary accretion N92-10897

COMPUTERS
The role of the computer in science fair projects: Current status and potential
[DE91-008606] N92-10295
Modeling reality
[NASA-CR-188881] N92-10307
Worldnet
[NASA-CR-188845] N92-10711

CONCENTRATION (COMPOSITION)
Definition and measurement at high temperatures of pH
[DE91-017945] N92-10077
Fourier component analysis of three Euler-Lagrangian methods applied to the one-dimensional advection-dispersion model
[DE91-017733] N92-10346

CONCENTRATORS
A generic guide for the preparation of a quality assurance/quality control manual for the design, production, and installation of photovoltaic concentrator systems
[DE91-017716] N92-10223
High efficiency GaAs/Ge monolithic tandem cells for space concentrator arrays, phase 1
[AD-A239931] N92-10226

CONCRETE STRUCTURES
Bond of reinforcement under controlled confinement
[AD-A240142] N92-10207

CONCURRENT PROCESSING
A portable run-time system for PCN
[DE91-017700] N92-10319

CONDENSATION
Aerosol dynamics: Binary nucleation N92-10525
Aerosol dynamics: Condensation and evaporation N92-10526

CONDENSED MATTER PHYSICS
Proceedings of the 25th Annual Conference of the Finnish Physical Society
[REPT-119(1991)] N92-10362
Superfluid interfaces in liquid He-3: Superconducting cosmic domain walls in the laboratory N92-10478

CONDUCTING POLYMERS
Highlights of material research for optoelectronics in the eighties, trends and challenges for the nineties N92-10486
Conducting polymers N92-10524

CONDUCTION ELECTRONS
Valence electron states of the Bi-Sr-Ca-Cu-O high-T(sub c) compound N92-10503

CONDUCTIVE HEAT TRANSFER
Optimal moving grids for time-dependent partial differential equations
[NASA-CR-188850] N92-10344

CONDUCTIVITY
Conducting polymers N92-10524

CONFERENCES
Magnetoplasmadynamic Thruster Workshop
[NASA-CP-10084] N92-10044
Proceedings of the Second Switch Tube Advanced Technology Meeting
[DE91-017718] N92-10148
The 14th International Conference on Combined Effect of Environmental Factors
[AD-A240045] N92-10245
Program and Abstracts for Clay Minerals Society 28th Annual Meeting
[NASA-TM-105098] N92-10248
Proceedings of the First Energy Research Power Supercomputer Users Symposium
[DE91-018877] N92-10300

CONGRESSIONAL REPORTS
NASA procurement: Management oversight of contract cost and time changes could be enhanced
[GAO/NSIAD-91-259] N92-10708

CONICS
Ionospheric and magnetospheric processes
[AD-A239967] N92-10263

CONIFERS
Spectral reflectance of pine and intensity of moose browsing N92-10514

CONJUGATE GRADIENT METHOD
Performance of conjugate gradient-like algorithms in transient two-phase subchannel analysis
[DE91-013373] N92-10316

CONNECTORS
Mechanized fluid connector and assembly tool system with ball detents
[NASA-CASE-MSC-21434-1] N92-10197

CONSERVATION LAWS
Multi-dimensional ENO schemes for general geometries
[NASA-CR-187637] N92-10349

CONTAMINANTS
A measuring robot for thermal environment, contaminant concentration and ventilation studies N92-10537
Contamination study
[NASA-CR-184225] N92-10639

CONTAMINATION
Contamination study
[NASA-CR-184225] N92-10639
Optical properties of CO2 ice and CO2 snow from ultraviolet to infrared: Application to frost deposits and clouds on Mars N92-10821

CONTINUOUS RADIATION
Preliminary comparison of 3.5-cm and 12.6-cm wavelength continuous wave observations of Mars N92-10848

CONTINUOUS WAVE RADAR
Hardware description ADSP-21020 40-bit floating point DSP as designed in a remotely controlled digital CW Doppler radar
[DE91-018004] N92-10134

CONTINUUM MECHANICS
Driven growth in the restricted solid on solid model N92-10373

CONTINUUM MODELING
Driven growth in the restricted solid on solid model N92-10373
Continuum modeling of catastrophic collisions N92-10863

CONTINUUMS
A mathematical model for a paired comparison experiment on a continuum of response
[AD-A239858] N92-10351
The probable continuum between emplacement of plutons and mare volcanism in lunar crustal evolution N92-10794
The perplexing continuum slope of Mars: Effects of thin ferric coatings and viewing geometry N92-10816
Oxidation of basaltic tephras: Influence on reflectance in the 1 micron region N92-10817

CONTRACT MANAGEMENT
NASA procurement: Management oversight of contract cost and time changes could be enhanced
[GAO/NSIAD-91-259] N92-10708

CONTROL SURFACES
Rotatable non-circular forebody flow controller
[NASA-CASE-LAR-14212-1-CU] N92-10021

CONTROL SYSTEMS DESIGN
On the formulation of a minimal uncertainty model for robust control with structured uncertainty
[NASA-TP-3094] N92-10027
Development of digital/optical rotary position transducer
[NAL-TR-1106] N92-10028
Instrumentation and control for space nuclear propulsion
[DE91-018351] N92-10061
Approximate evaluation of reliability and related quantities via perturbation techniques
[AD-A240049] N92-10201
Reconfigurable fuzzy cell
[NASA-CASE-MSC-21613-1] N92-10331
Design controls for large order systems
[NASA-CR-184237] N92-10340
Control system of the Jyvaskyla (Finland) K130 cyclotron N92-10419
Turbomachinery noise N92-10601

CONTROL THEORY
Overview of Krylov subspace methods with applications to control problems
[NASA-CR-188842] N92-10343
The control network of Mercury: April 1991 N92-10916
A unified lunar control network: April 1991 N92-10917
The control network of Mars: April 1991 N92-10918

CONTROLLABILITY
Some results on constrained controllability in discrete-time convex processes
[MEMO-926] N92-10342

CONTROLLED FUSION
Fast wave heating at intermediate ion cyclotron harmonics on the JIPP T-II U tokamak
[NIFS-21] N92-10649

CONTROLLERS
Rotatable non-circular forebody flow controller
[NASA-CASE-LAR-14212-1-CU] N92-10021
Control system for ruling blazed, aberration corrected diffraction gratings
[NASA-CASE-GSC-13240-1] N92-10186
The SolarTrak solar array tracking controller
[DE91-017721] N92-10224
Reconfigurable fuzzy cell
[NASA-CASE-MSC-21613-1] N92-10331

CONVECTION
Process modelling for Space Station experiments
[NASA-CR-184227] N92-10112
A general-purpose finite-difference code for solving steady-state three-dimensional fluid-flow and heat transfer problems
[AD-A239857] N92-10175
Modelling crystal growth: Convection in an asymmetrically heated ampoule
[NASA-CR-184214] N92-10676
Dynamic models for ridge belt formation on Venus N92-10731

CONVECTIVE HEAT TRANSFER
Implications of convection in the moon and the terrestrial planets N92-10730

CONVERGENCE
Transformation of two and three-dimensional regions by elliptic systems
[NASA-CR-188982] N92-10170
Globally convergent techniques in nonlinear Newton-Krylov
[NASA-CR-188894] N92-10309
The improved robustness of multigrid elliptic solvers based on multiple semicoarsened grids
[NASA-CR-187633] N92-10348
A new method to assess the statistical convergence of Monte Carlo solutions
[DE91-016013] N92-10354

CONVEXITY
Some results on constrained controllability in discrete-time convex processes
[MEMO-926] N92-10342

CONVULSIONS
Physiologic Transection of the brain stem in healthy humans and the neurologic basis of unconsciousness
[AD-A240122] N92-10023

COOLERS
Thermal management of high heat flux electronic components in space and aircraft systems, phase 1
[AD-A239982] N92-10157

COOLING
Electron temperatures in the E-region of the ionosphere
[ISAS-641] N92-10259

COOLING SYSTEMS
Thermal management of high heat flux electronic components in space and aircraft systems, phase 1
[AD-A239982] N92-10157

COORDINATES
The control network of Mercury: April 1991 N92-10916
The control network of Mars: April 1991 N92-10918

COPPER
Neutron diffraction experiments on nuclear magnetic order in copper N92-10507

COPPER ALLOYS
Corrosion tests of meshes in carbon fiber laminates: Impact beam tests
[INFORME-I-522/90] N92-10068
A band theoretical study on the electronic properties in the phase transition CuAu 1 to CuAu 2 N92-10488

COPPER COMPOUNDS
Photoemission in YbCu2Si2: Problems with the Kondo impurity model
[DE91-018018] N92-10684

COPPER OXIDES
Polarization dependent x ray spectroscopy of high T(sub c) superconductors
[DE91-017475] N92-10683
Initial magnetization and magnetic relaxation in a single crystal of Bi2Sr2CaCu2O(x)
[DE91-018537] N92-10693
Electrical transport across grain boundaries in bicrystals of YBa2Cu3O7(delta)
[DE91-018588] N92-10697
Reversible magnetization of Bi2Sr2CaCu2O8 single crystals
[DE91-018600] N92-10699
Neutron irradiation effects on YBCO single crystals
[DE91-018615] N92-10700

CORE SAMPLING
Mineralogy of Cretaceous/Tertiary boundary clays in the Chicxulub structure in northern Yucatan N92-10253

CORES
Processes of deep terrestrial mantles and cores N92-10729

CORONAS
The extension of solar magnetic fields into interplanetary space
[DE91-018052] N92-10970
CORRELATION
Erosive burning of solid propellants N92-10108
Normalization of correlations
[DE91-018398] N92-10324
CORRELATION DETECTION
The detection and location of near-regional seismic disturbances by the Eskdalemuir array: A study using noise and signal correlations
[AWE-RE-0-20/90] N92-10247
CORROSION PREVENTION
Evaluation of preservative engine oil containing vapor-phase corrosion inhibitor and a simplified engine preservation technique
[AD-A240100] N92-10103
CORROSION RESISTANCE
Corrosion tests of meshes in carbon fiber laminates: Impact beam tests
[INFORME-I-522/90] N92-10068
Evaluation of advanced austenitic alloys relative to alloy design criteria for steam service
[DE91-017800] N92-10081
COSINE SERIES
Running discrete cosine transform algorithm N92-10375
COSMIC DUST
Clay minerals in primitive meteorites and interplanetary dust 2. Smectites and micas N92-10252
Physical processes in planetary rings N92-10904
COSMIC RAY SHOWERS
Electronics of the cosmic ray air shower array at Turku (Finland) N92-10574
Test results of density detectors of the cosmic ray air shower array in Turku (Finland) N92-10575
COSMIC RAYS
Charged-particle induced alterations of surfaces in the outer solar system N92-10838
Long-term neutrino flux integrations
[DE91-013903] N92-10967
COSMOLOGY
Double radio sources as standard rods of testing cosmological models N92-10578
Quantum cosmology on the worldsheet
[DE91-018415] N92-10727
Aerodynamic and gasdynamic effects in cosmogony N92-10892
COST ANALYSIS
PASS spacecraft antenna technology assessment N92-10123
Climate change: Problems of limits and policy responses N92-10232
Climate and forests N92-10234
NASA maintenance: Stronger commitment needed to curb facility deterioration
[GAO/NSIAD-91-34] N92-10709
COST ESTIMATES
NASA procurement: Management oversight of contract cost and time changes could be enhanced
[GAO/NSIAD-91-259] N92-10708
COSTS
Nuclear energy: Its strengths, weaknesses and role in Finland N92-10585
COULOMB POTENTIAL
Magneto-optical transitions in a Coulomb coupled pair of quantum dots N92-10494
COUNTERS
Real-time data compression of broadcast video signals
[NASA-CASE-LEW-14945-2] N92-10128
COUPLED MODES
Coupled wave analysis in inverse grating diffraction problems N92-10456
COVARIANCE
Mean estimation in highly skewed samples
[DE91-018513] N92-10358
CRACK ARREST
Probability of brittle failure
[NASA-CR-187174] N92-10205
CRACK INITIATION
Prediction of matrix fatigue crack initiation in notched SCS-6/Ti-15-3 metal matrix composites
[NASA-TM-104141] N92-10203
Probability of brittle failure
[NASA-CR-187174] N92-10205
CRACK PROPAGATION
BES Welding Science Contractors summary report, 1990--1991
[DE91-018510] N92-10198
Probability of brittle failure
[NASA-CR-187174] N92-10205
CRACKS
Evaluation of advanced austenitic alloys relative to alloy design criteria for steam service
[DE91-017800] N92-10081
CRATERING
Gradational evolution of young, simple impact craters on the Earth N92-10783
Impact craters on Venus N92-10852
Breakup of meteoroids in the Venusian atmosphere and its effects on crater formation N92-10855
Atmospheric effects on oblique impacts N92-10856
Impact decapitation from laboratory to basin scales N92-10858
Laboratory simulation of cratering on small bodies N92-10859
Possible misinterpretation of lunar cratering record in Voyager team analyses of outer planet satellites N92-10860
Large impacts and climatic catastrophes on the early Earth N92-10865
Vapor plumes: A neglected aspect of impact cratering N92-10867
Production of impact melt in craters on Venus, Earth, and the moon N92-10870
Characteristics of ejecta and alluvial deposits at Meteor Crater, Arizona and Odessa Craters, Texas: Results from ground penetrating radar N92-10872
The scaling of secondary craters N92-10874
Asteroid flux and impact cratering rate on Venus N92-10880
Asteroid families N92-10885
Impact cratering calculations N92-10933
CRATERS
Structural geology and geological history of the Perrine and Nun Sulci Quadrangles (Jg-2 and Jg-5), Ganymede N92-10762
Mimas: Tectonic structure and geologic history N92-10764
Gradational evolution of young, simple impact craters on the Earth N92-10783
Large impacts and climatic catastrophes on the early Earth N92-10865
Characteristics of ejecta and alluvial deposits at Meteor Crater, Arizona and Odessa Craters, Texas: Results from ground penetrating radar N92-10872
Depth/diameter relationships of fresh craters within Hesperia Planum, Mars N92-10873
The spatial distribution and time evolution of impact-generated magnetic fields N92-10878
The violent side of mare volcanism N92-10962
CRAY COMPUTERS
Measurement of memory access contentions in multiple vector processor systems
[DE91-013205] N92-10297
Efficient multitasking of Choleski matrix factorization on CRAY supercomputers
[NASA-TM-4259] N92-10302
CREEP PROPERTIES
High temperature creep properties of eutectic and near eutectic silver-copper alloys: Application to metal/ceramic joining
[DE91-017987] N92-10082
Microstructural stability and creep response of a new Al-Fe-W-Si alloy
[AD-A239861] N92-10087
CREEP TESTS
High temperature creep properties of eutectic and near eutectic silver-copper alloys: Application to metal/ceramic joining
[DE91-017987] N92-10082
CRETACEOUS PERIOD
Gravity survey of the Mt. Toondina impact structure, South Australia N92-10879
CRETACEOUS-TERTIARY BOUNDARY
Mineralogy of Cretaceous/Tertiary boundary clays in the Chicxulub structure in northern Yucatan N92-10253
Melt droplet formation in energetic impacts N92-10869
CREW PROCEDURES (INFLIGHT)
Mission description and in-flight operations of ERBE instruments on ERBS and NOAA 9 spacecraft, November 1984 - January 1986
[NASA-RP-1256] N92-10208
CRITICAL TEMPERATURE
Work function changes of high-T(sub c) superconductors around the T(sub c) N92-10498
CROSS SECTIONS
Long-term evolution of a planetesimal swarm in the vicinity of a protoplanet N92-10896
CROSSED FIELDS
Magneto-optical transitions in a Coulomb coupled pair of quantum dots N92-10494
CRUSHING
Reflectance spectra of some fractions of Migei and Murchison SM chondrites in the range of 0.3-2.6 microns N92-10829
CRUSTS
Extension and strain in Northern Tharsis N92-10757
Crustal heterogeneity of the moon viewed from the Galileo SSI camera: Lunar sample calibrations and compositional implications N92-10808
CRYOGENIC FLUIDS
Novel type of cryogenic liquid level sensor with high sensitivity N92-10528
CRYOGENIC TEMPERATURE
Ultra-cold polarized hydrogen source N92-10423
CRYOSTATS
Experiments on the nuclear interactions of pions and electrons
[DE91-017929] N92-10623
CRYSTAL DEFECTS
Examination of mechanical behavior in nanocrystalline materials
[DE91-018552] N92-10085
High-temperature implantation of Au into Ni
[DE91-017304] N92-10682
CRYSTAL GROWTH
Characterization of electronic materials
[AD-A240063] N92-10159
Two-color holography concept (T-CHI)
[NASA-CR-184240] N92-10183
Driven growth in the restricted solid on solid model N92-10373
Chemisorption of CO on Mg-O/Co(0001) N92-10484
Modelling crystal growth: Convection in an asymmetrically heated ampoule
[NASA-CR-184214] N92-10676
CRYSTAL LATTICES
Computer simulations on the orientation of molecular hydrogen in liquid crystals N92-10466
Vortex lattice: Vortex liquid states in anisotropic high-T(sub c) superconductors N92-10500
CRYSTAL STRUCTURE
Computer simulations on the orientation of molecular hydrogen in liquid crystals N92-10466
Adsorbate induced surface reconstruction N92-10469
Surface reconstruction and many-atom models N92-10483
Vortex lattice: Vortex liquid states in anisotropic high-T(sub c) superconductors N92-10500
Valence electron states of the Bi-Sr-Ca-Cu-O high-T(sub c) compound N92-10503
Studies on superconducting Bi2Sr2Ca(n-1) Cu(n)O(4+2n) compounds with Fe-57 and Eu-151 Moessbauer spectroscopy N92-10504
Epitaxial high T(sub c) superconducting thin films and superlattices deposited by laser albation N92-10505
Antiferromagnetic ordering in silver at picoKelvin temperatures N92-10509
The crystal structure and moisture sensitivity of (+)-4-(1-(2,3 dimethylphenyl) ethyl) 1H-imidazole hydrochloride N92-10522
Diamond thin films grown by microwave plasma assisted chemical vapor deposition
[DE91-018553] N92-10695
CRYSTAL SURFACES
Determination of the (1x2) structure of a Pt film on Pd(110) N92-10463
Surface reconstruction and many-atom models N92-10483
CRYSTALLIZATION
Crystallization during emplacement of lava flows N92-10789
Exploration of relationships between low-Ti and high-Ti pristine lunar glasses using an armalcolite assimilation model N92-10964
CRYSTALLOGRAPHY
Synchrotron radiation: New research opportunities for the next decade N92-10366
The influence of growth conditions on the composition of GaInAsP grown by gas-source molecular beam epitaxy N92-10491
CRYSTALS
Helium in silicon: A first principle molecular dynamics study N92-10473
An improved technique for electrolytic colouration of alkali halide crystals N92-10513
Formation of small metallic precipitates of niobium in (alpha)-Al2O3 implanted with Nb ions
[DE91-015928] N92-10678
Neutron irradiation effects on YBCO single crystals
[DE91-018615] N92-10700
Crystallization during emplacement of lava flows N92-10789
CURIE TEMPERATURE
Ferromagnetism in small clusters N92-10508
CURING
Thermal modeling of an epoxy encapsulation process
[DE91-017845] N92-10096

CURRENT DENSITY
High temperature ceramic superconductors
[AD-A239813] N92-10154
CYANIDES
The nu(sub 4) and nu(sub 7) bands of CD3CN with coriolis coupling and other resonance perturbations N92-10432
The nu(sub 8) and 2nu(sub 8) bands of CD3CN N92-10433
CYCLONES
Annual tropical cyclone report, 1990
[AD-A239910] N92-10268
ONR tropical cyclone motion research initiative: Data users guide to observations
[AD-A240061] N92-10271
CYCLOTRON RADIATION
Status of the JYFL-ECR ion source N92-10422
CYCLOTRON RESONANCE DEVICES
Status of the JYFL-ECR ion source N92-10422
The 110 GHz ECH heating system for DIII-D
[DE91-018732] N92-10671
CYCLOTRONS
A model for a data acquisition solution for a medium size accelerator laboratory N92-10376
Control system of the Jyvaskyla (Finland) K130 cyclotron N92-10419
The Jyvaskyla (Finland) K130 cyclotron project N92-10420
Magnetic field settings for the K130 cyclotron N92-10421
Status of the JYFL-ECR ion source N92-10422
Inhomogeneity and nonlinearity effects on stop bands of Alfvenic ion cyclotron waves in multicomponent plasma N92-10557
CYLINDRICAL BODIES
Automated eddy current analysis of materials
[NASA-CR-184216] N92-10200
Vlasov-Maxwell system: 2-D equilibria, reversed field pinches
[DE91-018421] N92-10595
Modelling crystal growth: Convection in an asymmetrically heated ampoule
[NASA-CR-184214] N92-10676
CYLINDRICAL CHAMBERS
Laboratory simulation of cratering on small bodies N92-10859

D

D REGION
The structure and dynamics of the polar mesosphere investigated with the EISCAT radar systems N92-10368
EISCAT incoherent scatter radar observations and model studies on day to night variations in the ionospheric D-region during the PCA event of August 1989 N92-10559
Variation of D-region parameters during polar cap absorption events in the year 1989 N92-10561
DARK MATTER
IPC two-color analysis of x ray galaxy clusters
[NASA-CR-188980] N92-10724
Dark matter and the effective value of Newton's constant at large distances
[DE91-018152] N92-10726
DARKENING
Darkening in gas-rich ordinary chondrites: Spectral modelling and implications for the regoliths of ordinary chondrite parent bodies N92-10627
DATA ACQUISITION
The Alternative Fuels Data Center
[DE91-015003] N92-10111
Compilation of 1990 annual reports of the Navy ELF communications system ecological monitoring program. Volume 3: Tabs G thru I
[AD-A239870] N92-10139
Mean estimation in highly skewed samples
[DE91-018513] N92-10358
A model for a data acquisition solution for a medium size accelerator laboratory N92-10376
Research into the development of a knowledge acquisition taxonomy
[NASA-CR-188948] N92-10712
High resolution lunar radar studies: Preliminary results N92-10845
Gravity survey of the Mt. Toondina impact structure, South Australia N92-10879
DATA BASE MANAGEMENT SYSTEMS
The Alternative Fuels Data Center
[DE91-015003] N92-10111
ONR tropical cyclone motion research initiative: Data users guide to observations
[AD-A240061] N92-10271
INFOTECH '91: DOE Technical Infomation (TI) Meeting
[DE91-018074] N92-10713
MANPRINT reference retrieval system (user's guide)
[AD-A239915] N92-10714
Image retrieval and processing system version 2.0 development work N92-10930
DATA BASES
Recent changes of weather patterns in North America
[DE91-017706] N92-10266
Cooperating systems: Layered MAS
[NASA-CR-184232] N92-10332
MANPRINT reference retrieval system (user's guide)
[AD-A239915] N92-10714
IID: An intelligent information dictionary for managing semantic metadata
[AD-A240022] N92-10715
A new edition of the Mars 1:5,000,000 map series N92-10924
CD-ROM publication of the Mars digital cartographic data base N92-10926
A new catalog of planetary maps N92-10929
DATA COMPRESSION
Real-time data compression of broadcast video signals
[NASA-CASE-LEW-14945-2] N92-10128
DATA LINKS
Impact of non-geostationary orbits on PASS N92-10120
User antennas N92-10121
Technology assessment and experimentation plan N92-10124
DATA MANAGEMENT
Management of the Space Station Freedom onboard local area network
[NASA-TM-104741] N92-10036
Modeling of the Space Station Freedom data management system
[NASA-CR-188869] N92-10038
IID: An intelligent information dictionary for managing semantic metadata
[AD-A240022] N92-10715
DATA PROCESSING
Mission description and in-flight operations of ERBE instruments on ERBS and NOAA 9 spacecraft, November 1984 - January 1986
[NASA-RP-1256] N92-10208
Integrated array and 3-component processing using a seismic microarray
[AD-A240139] N92-10265
Recent changes of weather patterns in North America
[DE91-017706] N92-10266
The role of graphics super-workstations in a supercomputing environment
[NASA-CR-188852] N92-10306
Analysis of esophageal pH-recordings for reflux disease N92-10543
IID: An intelligent information dictionary for managing semantic metadata
[AD-A240022] N92-10715
High resolution lunar radar studies: Preliminary results N92-10845
DATA REDUCTION
The Alternative Fuels Data Center
[DE91-015003] N92-10111
Recent changes of weather patterns in North America
[DE91-017706] N92-10266
Retire FORTRAN? A debate rekindled
[DE91-016565] N92-10317
DATA RETRIEVAL
An alternative design for a sparse distributed memory
[NASA-CR-188847] N92-10291
Image retrieval and processing system version 2.0 development work N92-10930
DATA STRUCTURES
The paradigm compiler: Mapping a functional language for the connection machine
[NASA-CR-188839] N92-10290
DEATH VALLEY (CA)
Relationships between topographic roughness and aeolian processes N92-10801
Use of radar to assess aeolian processes N92-10802
DEBRIS
Models of the diffuse radar backscatter from Mars N92-10846
DECODERS
Solid-State Radar Beacon Decoder (SSRBD) Operational Test and Evaluation (OT/E) integration test plan
[DOT/FAA/CT-TN91/30] N92-10020
DECONTAMINATION
Solar detoxification technology: Using energy from the sun to destroy hazardous waste
[DE91-015007] N92-10241
DEFECTS
Automated eddy current analysis of materials
[NASA-CR-184216] N92-10200
DEFENSE PROGRAM
Massively parallel computing at Sandia and its application to national defense
[DE91-008178] N92-10334
DEFORMATION
An assessment of the crustal remelting hypothesis for volcanism in the Freyja Montes deformation zone N92-10732
Tectonic evolution of Lavinia Planitia, Venus N92-10741
Compressive strain in Lunae Planum-shortening across wrinkle ridges N92-10753
Tectonic deformation on icy satellites: A model of compensating horsts N92-10763
Wrinkle ridge-upland scarp transitions: Implications for the mechanical properties of the deformed materials N92-10954
DEGRADATION
An experimental evaluation of the impact resistance of recoated F-16A monolithic polycarbonate flat sheet
[AD-A239984] N92-10101
Degradation of Fe-Mg silicates in hot CO2 atmospheres: Applications to Venus N92-10806
DEICERS
Technical evaluation report, AGARD Fluid Dynamics Panel Symposium on Effects of Adverse Weather on Aerodynamics
[NASA-TM-105192] N92-10002
DEICING
Technical evaluation report, AGARD Fluid Dynamics Panel Symposium on Effects of Adverse Weather on Aerodynamics
[NASA-TM-105192] N92-10002
DEMAGNETIZATION
The short-circuited fluxgate sensitivity parameters
[ISSN-0109-6605] N92-10147
Antiferromagnetic ordering in silver at picoKelvin temperatures N92-10509
DEMODULATION
Recovering signals from optical fiber interferometric sensors
[AD-A240062] N92-10644
DENSITY (MASS/VOLUME)
Strong magnetic compression of spin-polarized hydrogen N92-10480
DENSITY DISTRIBUTION
Test results of density detectors of the cosmic ray air shower array in Turku (Finland) N92-10575
Properties of planetary fluids at high pressures and temperatures N92-10739
DENSITY MEASUREMENT
Interatomic interactions in the local density approximation N92-10487
Acoustic device and method for measuring gas densities
[NASA-CASE-NPO-18155-1-CU] N92-10609
DENSITY WAVE MODEL
Bending waves and orbital inclinations N92-10894
DEOXYRIBONUCLEIC ACID
Paucity of moderately repetitive sequences
[DE91-017953] N92-10276
DEPOSITION
High T(sub c) superconducting Li-doped Bi-Sr-Ca-Cu-O thin films deposited by laser ablation N92-10506
Preparation and characterization of high temperature superconductor film surfaces
[AD-A240118] N92-10706
Variable features in the Valles Marineris region of Mars N92-10799
DEPOSITS
Lunar western limb pyroclastic deposits N92-10795
Lunar and Hawaiian lava tubes: Analogs and uses based on terrestrial field data N92-10796
On using a pyroclastic deposit as a manned lunar base site N92-10797
Crustal heterogeneity of the moon viewed from the Galileo SSI camera: Lunar sample calibrations and compositional implications N92-10808
The violent side of mare volcanism N92-10962
DESERTS
Relationships between topographic roughness and aeolian processes N92-10801
Use of radar to assess aeolian processes N92-10802
Remote sensing observations of Kelso Dunes, California N92-10847
DESIGN ANALYSIS
The determination of operational and support requirements and costs during the conceptual design of space systems
[NASA-CR-188817] N92-10037

Evaluation of advanced austenitic alloys relative to alloy design criteria for steam service
[DE91-017800] N92-10081
The design of spaceborne synthetic aperture radar
[ETN-91-99986] N92-10114
Explosive Transient Camera (ETC) program
[NASA-CR-188957] N92-10184
Study of different SX-700 designs for the undulator beamline (BL51) at MAX-LAB N92-10446
Single-shot spectral measurements of multimode pulsed dye lasers N92-10452
Advanced photon source: Radiological design considerations
[DE91-018014] N92-10635

DESORPTION
Determining desorption pre-exponential factors from temperature-programmed desorption spectra when the surface is nonuniform
[DE91-009971] N92-10074
The search for low photodesorption coatings
[DE91-017473] N92-10092
Thermal helium desorption facility in Jyvaskyla (Finland) N92-10464
Quantum state resolved desorption of CO from solid surface
[DE91-017712] N92-10626

DESULFURIZING
Regenerative Cu/La zeolite supported desulfurizing sorbents
[NASA-CASE-NPO-17480-1-CU] N92-10073
Electrostatic precipitator modelling N92-10532

DETECTION
Algorithm for detection of VFIB in real time from ECG N92-10542
Water detection at the moon, Mars and comets with a combined neutron gamma ray instrument N92-10819

DEUTERIUM
Experimental investigations of electron capture from atomic hydrogen and deuterium by alpha particles
[DE91-018280] N92-10629

DEUTERIUM COMPOUNDS
The nu(sub 4) and nu(sub 7) bands of CD3CN with coriolis coupling and other resonance perturbations N92-10432
The nu(sub 8) and 2nu(sub 8) bands of CD3CN N92-10433

DEVELOPING NATIONS
Potential strategies for adapting to greenhouse warming: Perspectives from the developing world N92-10237

DEVICES
An overview of modern permanent magnet design
[AD-A240144] N92-10597

DIAMINES
A process for preparing 1,3-diamino-5-pentafluorosulfanylbenzene and polymers therefrom
[NASA-CASE-LAR-14773-1-CU] N92-10105

DIAMONDS
Diamond heat sinks for electronic circuits
[AD-A239750] N92-10145
Diamond thin films grown by microwave plasma assisted chemical vapor deposition
[DE91-018553] N92-10695

DICTIONARIES
IID: An intelligent information dictionary for managing semantic metadata
[AD-A240022] N92-10715

DIELECTRICS
Poly 1, 2, 4-triazoles via aromatic nucleophilic displacement
[NASA-CASE-LAR-14440-1] N92-10066
Constitutive parameter extraction for heated materials
[NASA-CR-186208] N92-10593
Character of the opposition effect and negative polarization N92-10833

DIESEL ENGINES
Update on the prospects for ceramic engine components
[DE91-018574] N92-10098

DIESEL FUELS
Regenerative Cu/La zeolite supported desulfurizing sorbents
[NASA-CASE-NPO-17480-1-CU] N92-10073

DIFFERENTIAL ANALYZERS
Recovering signals from optical fiber interferometric sensors
[AD-A240062] N92-10644

DIFFERENTIAL PULSE CODE MODULATION
Real-time data compression of broadcast video signals
[NASA-CASE-LEW-14945-2] N92-10128

DIFFRACTION RADIATION
The crystal structure and moisture sensitivity of (+)-4-(1-(2,3 dimethylphenyl) ethyl) 1H-imidazole hydrochloride N92-10522

DIFFUSION
Process modelling for Space Station experiments
[NASA-CR-184227] N92-10112
Fourier component analysis of three Euler-Lagrangian methods applied to the one-dimensional advection-dispersion model
[DE91-017733] N92-10346

DIFFUSIVITY
Characteristics of the Martian atmosphere surface layer N92-10804

DIGITAL DATA
Color-coded global topographic map of Mars N92-10920
Mars elevation distribution N92-10921
Mars high-resolution mapping N92-10923
A new edition of the Mars 1:5,000,000 map series N92-10924
CD-ROM publication of the Mars digital cartographic data base N92-10926
Digital solar system geology N92-10928

DIGITAL ELECTRONICS
Running discrete cosine transform algorithm N92-10375

DIGITAL RADAR SYSTEMS
Hardware description ADSP-21020 40-bit floating point DSP as designed in a remotely controlled digital CW Doppler radar
[DE91-018004] N92-10134
The application of the ADSP-21020 40-bit floating point DSP microprocessor in a digital Doppler radar
[DE91-018005] N92-10135

DIGITAL SIMULATION
Digital simulation of speech transmission channels
[IZF-1991-A-7] N92-10115
Numerical simulation of vortex breakdown
[ONERA-RSF-6/4368-AY-008A] N92-10162
Numerical simulation of vortex breakdown by solving the Euler equations for an incompressible fluid N92-10163
Numerical simulation of vortex breakdown via 3-D Euler equations N92-10164
Spectral representation in vision N92-10539
Energy-latitude dispersion of energetic ions in the dayside of the Earth's magnetosphere: A substorm-related phenomenon N92-10558
EISCAT incoherent scatter radar observations and model studies on day to night variations in the ionospheric D-region during the PCA event of August 1989 N92-10559
Numerical simulations of dense collisional systems N92-10573
N-body simulations of interacting galaxies N92-10579

DIGITAL SYSTEMS
Hardware description ADSP-21020 40-bit floating point DSP as designed in a remotely controlled digital CW Doppler radar
[DE91-018004] N92-10134
Reconfigurable fuzzy cell
[NASA-CASE-MSC-21613-1] N92-10331

DIGITAL TECHNIQUES
Digital cartography of Io N92-10927

DIGITAL TELEVISION
A digital ASIC implementation of a video filter for synthetic aperture radar
[DE91-018400] N92-10131

DIMENSIONAL ANALYSIS
RIPPLE: A new model for incompressible flows with free surfaces
[DE91-017830] N92-10168

DIMENSIONAL STABILITY
Microstructural stability and creep response of a new Al-Fe-W-Si alloy
[AD-A239861] N92-10087

DIODES
Optical and electrical investigations into cathode ignition and diode closure
[DE91-017823] N92-10191
Dual pin diode preamplifier for laser Doppler velocimetry N92-10382
Optical signal multiplexer and demultiplexer
[DE91-017836] N92-10640

DIRAC EQUATION
Nonperturbative electromagnetic muon-pair production with capture in peripheral relativistic heavy-ion collisions
[DE91-018247] N92-10624

DIRECTIONAL SOLIDIFICATION (CRYSTALS)
Process modelling for Space Station experiments
[NASA-CR-184227] N92-10112

DISCRIMINATION
Using surrogate data to detect nonlinearity in time series
[DE91-018017] N92-10357

DISEASES
Physiologic Transection of the brain stem in healthy humans and the neurologic basis of unconsciousness
[AD-A240122] N92-10023
Analysis of esophageal pH-recordings for reflux disease N92-10543

DISK GALAXIES
Self-regulation mechanisms in galactic discs N92-10576

DISKS (SHAPES)
Structure and evolution of turbulent preplanetary disc N92-10571

DISLOCATIONS (MATERIALS)
Internal friction associated with interaction between carbon atoms and dislocations at low temperature N92-10471

DISORIENTATION
Physiologic Transection of the brain stem in healthy humans and the neurologic basis of unconsciousness
[AD-A240122] N92-10023

DISPERSING
Fourier component analysis of three Euler-Lagrangian methods applied to the one-dimensional advection-dispersion model
[DE91-017733] N92-10346

DISPLACEMENT
Poly 1, 2, 4-triazoles via aromatic nucleophilic displacement
[NASA-CASE-LAR-14440-1] N92-10066
Martian seismicity through time from surface faulting N92-10759

DISPLAY DEVICES
Feasibility of using a knowledge-based system concept for in-flight primary flight display research
[NASA-TM-4279] N92-10017
Composite video and graphics display for multiple camera viewing system in robotics and teleoperation
[NASA-CASE-NPO-17836-1-CU] N92-10126
Three experiments with stereoscopic television: When it works and why
[DE91-016277] N92-10129
Display format, highlight validity, and highlight method: Their effects on search performance
[NASA-TM-104742] N92-10287
TAURUS: An interactive post-processor for the analysis codes NIKE3D, DYNA3D, and TOPAZ3D
[DE91-019012] N92-10326

DISSOLVED GASES
NMR determination of the Ne-21 quadrupole coupling for neon gas dissolved in liquid crystals N92-10436
NMR-relaxation time measurements of noble gas isotope Xe-129 dissolved in isotropic and anisotropic liquids N92-10437
Computer simulations on the orientation of molecular hydrogen in liquid crystals N92-10466

DISSOLVING
Transformation products of submicron-sized aluminum-substituted magnetite: Color and reductant solubility N92-10251

DISTORTION
Glass sample characterization
[NASA-CR-184230] N92-10088

DISTRIBUTED PROCESSING
An alternative design for a sparse distributed memory
[NASA-CR-188847] N92-10291
Cooperating systems: Layered MAS
[NASA-CR-184232] N92-10332
Fiber networking at Argonne: A distributed, multiapplication, multivendor computing environment
[DE91-018560] N92-10338

DISTRIBUTION FUNCTIONS
A new method to assess the statistical convergence of Monte Carlo solutions
[DE91-016013] N92-10354
Mean estimation in highly skewed samples
[DE91-018513] N92-10358

DIURNAL VARIATIONS
Remote sensing of the Martian surface N92-10813

DIVERTERS
Simulation study of scalings in scrape-off layer plasma by two-dimensional transport code
[NIFS-24] N92-10646
Overview of the 1990's D3-D research program
[DE91-018185] N92-10661

DOPED CRYSTALS
Beryllium doping of InP grown by gas-source molecular beam epitaxy N92-10489
Electrical characterization of Li and N doped ZnSe N92-10493
High T(sub c) superconducting Li-doped Bi-Sr-Ca-Cu-O thin films deposited by laser ablation N92-10506

DOPPLER EFFECT
Doppler shift velocimetry in disperse flows N92-10378

Preliminary comparison of 3.5-cm and 12.6-cm wavelength continuous wave observations of Mars N92-10848

DOPPLER RADAR
Hardware description ADSP-21020 40-bit floating point DSP as designed in a remotely controlled digital CW Doppler radar [DE91-018004] N92-10134
The application of the ADSP-21020 40-bit floating point DSP microprocessor in a digital Doppler radar [DE91-018005] N92-10135

DOUBLE BASE PROPELLANTS
Erosive burning of solid propellants N92-10108

DOWNLINKING
Personal Access Satellite System (PASS) study. Fiscal year 1989 results [NASA-CR-188808] N92-10116
Technology assessment and experimentation plan N92-10124

DOWNWASH
Downwash measurements on a pitching canard-wing configuration [AD-A239956] N92-10016

DRAINAGE
Evolution of the Martian hydrosphere N92-10768

DRIFT RATE
New observations of the low frequency interplanetary radio emissions [NASA-CR-188917] N92-10971

DROP TESTS
Quantitative nondestructive evaluation of materials and structures [NASA-CR-188975] N92-10071

DROPS (LIQUIDS)
Molecular dynamics studies of liquid-solid interfaces N92-10462
Melt droplet formation in energetic impacts N92-10869

DRUGS
Synaptic plasticity and memory formation [AD-A240121] N92-10285

DRYING APPARATUS
Absorption measurements with an integrating sphere and an FT-IR spectrometer N92-10445

DUNES
The potential scale of aeolian structures on Venus N92-10800
Remote sensing observations of Kelso Dunes, California N92-10847

DUNITE
Production of impact melt in craters on Venus, Earth, and the moon N92-10870

DUPLEXERS
Computer assisted multiplex sequencing [DE91-017851] N92-10337

DURABILITY
Relative sliding durability of two candidate high temperature oxide fiber seal materials [NASA-TM-105199] N92-10064

DUST
Variable features in the Valles Marineris region of Mars N92-10799
Optical properties of CO2 ice and CO2 snow from ultraviolet to infrared: Application to frost deposits and clouds on Mars N92-10821
Properties of dust and clouds in the Mars atmosphere: Analysis of Viking IRTM emission phase function sequences N92-10956

DYE LASERS
Single-shot spectral measurements of multimode pulsed dye lasers N92-10452

DYNAMIC CHARACTERISTICS
Mutual friction in superfluid He-3: Effects of bound states in the vortex core N92-10475
Modeling the dynamics of molecular films by Monte Carlo simulation N92-10481
The stability analysis of a double barrier resonant tunneling device N92-10485
Dynamics of vortices in high-temperature superconductors N92-10501
Aerosol dynamics: Binary nucleation N92-10525
Aerosol dynamics: Condensation and evaporation N92-10526
Physical processes in planetary rings N92-10904
Dynamics and structure of planetary rings N92-10935

DYNAMIC MODELS
Regional scale dynamical modelling of biogeochemical processes [AD-A240115] N92-10246
The stability analysis of a double barrier resonant tunneling device N92-10485
Dynamic models for ridge belt formation on Venus N92-10731

DYNAMIC PRESSURE
Development of a pressure transducer calibration system (dynamic pressure response caliber), phase 2 [AD-A239859] N92-10188

DYNAMIC RESPONSE
Development of a pressure transducer calibration system (dynamic pressure response caliber), phase 2 [AD-A239859] N92-10188

DYSPROSIUM
Synchrotron radiation study of recombination processes in solid state Tb and Dy after 4d to 4f giant resonance excitation N92-10518

E

E REGION
Electron temperatures in the E-region of the ionosphere [ISAS-641] N92-10259
Observations of semidiurnal atmospheric tides using the EISCAT incoherent scatter radar N92-10560

EAR
US TAG for ISO/TC43, acoustics, IEC/TC29 electroacoustics, ISO/TC108/SC4 human exposure to mechanical vibration and shock: Minutes of the Accredited Standards Committee on Bioacoustics, S3 [AD-A239918] N92-10610

EARTH (PLANET)
Earth, Uranus, and Neptune: A comparison of their magnetospheres N92-10567
Fluid dynamics of multiphase flow in volcanic environments on the Earth, Io, and other planets N92-10740
Gradational evolution of young, simple impact craters on the Earth N92-10783
Large impacts and climatic catastrophes on the early Earth N92-10865

EARTH ATMOSPHERE
Range reference atmosphere, Nellis Air Force Base, Nevada [AD-A239816] N92-10262
Impacts and atmospheric erosion on the early Earth N92-10871

EARTH IONOSPHERE
Theoretical estimation of the vibrational temperatures of N2 molecules in the ionosphere and in the laboratory simulated plasma [ISAS-642] N92-10258

EARTH MAGNETOSPHERE
Average properties of energetic ions in different parts of the cusp/cleft region N92-10556
Energy-latitude dispersion of energetic ions in the dayside of the Earth's magnetosphere: A substorm-related phenomenon N92-10558

EARTH OBSERVATIONS (FROM SPACE)
Activities report of the Norwegian Space Center [ETN-91-90052] N92-10029

EARTH ORBITAL ENVIRONMENTS
A neural network model of the relativistic electron flux at geosynchronous orbit [AD-A239827] N92-10030
An assessment of the radiation tolerance of large satellite memories in low earth orbits [DE91-018353] N92-10040

EARTH PLANETARY STRUCTURE
Lithosphere physics: Geoelectrics and seismics N92-10551

EARTH RADIATION BUDGET EXPERIMENT
Mission description and in-flight operations of ERBE instruments on ERBS and NOAA 9 spacecraft, November 1984 - January 1986 [NASA-RP-1256] N92-10208

EARTH SURFACE
A technique for estimating surface meteorological ranges over oceans from satellite measurements of aerosol optical depth [AD-A239985] N92-10219
Relationships between topographic roughness and aeolian processes N92-10801
Use of radar to assess aeolian processes N92-10802

EARTH TERMINALS
User antennas N92-10121

EARTH-MOON SYSTEM
Analyses of the lunar surface with advanced remote sensors: Expectations for the 1990's N92-10811

ECCENTRIC ORBITS
Studies in planetary rings N92-10949

ECCENTRICITY
Bending waves and orbital inclinations N92-10894

ECHOES
Gamma echo experiments N92-10512

ECONOMIC ANALYSIS
Climate and forests N92-10234

ECOSYSTEMS
The greenhouse effect: Its causes, possible impacts, and associated uncertainties N92-10229
The biological consequences of climate changes: An ecological and economic assessment N92-10235

EDDY CURRENTS
Automated eddy current analysis of materials [NASA-CR-184216] N92-10200

EDUCATION
Design restrictions and licensing for Petite Amateur Navy Satellite (PANSAT) [AD-A239951] N92-10041
The role of the computer in science fair projects: Current status and potential [DE91-008606] N92-10295

EIGENVALUES
A restricted signature normal form for Hermitian matrices, quasi-spectral decompositions, and applications [NASA-CR-188895] N92-10310
An implementation of the look-ahead Lanczos algorithm for non-Hermitian matrices, part 1 [NASA-CR-188909] N92-10311
An implementation of the look-ahead Lanczos algorithm for non-Hermitian matrices, part 2 [NASA-CR-188910] N92-10312
Overview of Krylov subspace methods with applications to control problems [NASA-CR-188842] N92-10343

EIGENVECTORS
Recognizing of spectral mixtures, their components and spectral patterns N92-10447

EISCAT RADAR SYSTEM (EUROPE)
The structure and dynamics of the polar mesosphere investigated with the EISCAT radar systems N92-10368
EISCAT research program N92-10553
EISCAT incoherent scatter radar observations and model studies on day to night variations in the ionospheric D-region during the PCA event of August 1989 N92-10559

EJECTA
Mineralogy of Cretaceous/Tertiary boundary clays in the Chicxulub structure in northern Yucatan N92-10253
Ancient fluvial processes in the equatorial highlands of Mars N92-10781
Venus impact craters: Implications for atmospheric and resurfacing processes from Magellan observations N92-10854
Styles of ejecta emplacement under atmospheric conditions N92-10857
Production of impact melt in craters on Venus, Earth, and the moon N92-10870
The scaling of secondary craters N92-10874

ELASTIC SCATTERING
Inclusive quasielastic and deep inelastic electron scattering at high energies [DE91-018755] N92-10633

ELASTOMERS
Evaluation of preservative engine oil containing vapor-phase corrosion inhibitor and a simplified engine preservation technique [AD-A240100] N92-10103

ELECTRIC CHARGE
Instrumental design for measurement of surface charge on insulating materials [DE91-018695] N92-10099

ELECTRIC COILS
Magnetic field settings for the K130 cyclotron N92-10421

ELECTRIC CONTACTS
Electrical characterization of Li and N doped ZnSe N92-10493

ELECTRIC CORONA
An analysis of the frequency characteristics of corona discharge at low pressure [AD-A239940] N92-10674

ELECTRIC CURRENT
Fear-potentiated startle as a model system for analyzing learning and memory [AD-A239994] N92-10284
Interface effects on electrical properties of high purity InP grown by gas-source molecular beam epitaxy N92-10490
Neutron irradiation effects on YBCO single crystals [DE91-018615] N92-10700

ELECTRIC DISCHARGES
A novel technique for the measurement of photoenhanced electron attachment: Implications for an optically-controlled diffuse discharge opening switch [DE91-016226] N92-10621

ELECTRIC ENERGY STORAGE
Alkali metal carbon dioxide electrochemical system for energy storage and/or conversion of carbon dioxide to oxygen [NASA-CASE-LEW-14973-1] N92-10222

ELECTRIC FIELDS
The Kr-83 NMR in probing electric field gradients in thermotropic liquid crystals N92-10435
The field drift of ions and its influence on the electrical properties of SnO2 N92-10492
Observation of plasma toroidal rotations driven by the electric field due to a loss of ions [NIFS-23] N92-10647
The meandering orbit effect on stabilization of the tilting instability in a field-reversed configuration [NIFS-22] N92-10648
Numerical simulation of ion beam generated in the diode with anode plasma column [IPPCZ-306] N92-10652
Dynamic screening and wake effects on electronic excitation in ion-solid and ion-surface collisions [DE91-018224] N92-10687

ELECTRIC MOTORS
Mechanized fluid connector and assembly tool system with ball detents [NASA-CASE-MSC-21434-1] N92-10197

ELECTRIC POTENTIAL
Experimental investigation of a 12 cm diameter Kaufman xenon ion thruster [NAL-TR-1099] N92-10056
Method and apparatus for frequency spectrum analysis [NASA-CASE-NPO-17759-1-CU] N92-10125

ELECTRIC POWER PLANTS
Evaluation of advanced austenitic alloys relative to alloy design criteria for steam service [DE91-017800] N92-10081
Electrostatic precipitator modelling N92-10532

ELECTRIC POWER SUPPLIES
Thermal management of high heat flux electronic components in space and aircraft systems, phase 1 [AD-A239982] N92-10157
Long pulse electron beams [DE91-018357] N92-10636

ELECTRIC PROPULSION
IRS organigram N92-10053

ELECTRIC ROCKET ENGINES
Magnetoplasmadynamic Thruster Workshop [NASA-CP-10084] N92-10044
The MPD thruster program at JPL N92-10046
LLNL contributions to MPD thrusters for SEI N92-10047
MPD thruster technology N92-10048
Los Alamos NEP research in advanced plasma thrusters N92-10049
Eppdyl: Research focus; past accomplishments; and current research N92-10052
IRS organigram N92-10053

ELECTRIC SWITCHES
Proceedings of the Second Switch Tube Advanced Technology Meeting [DE91-017718] N92-10148

ELECTRICAL IMPEDANCE
Development of a pressure transducer calibration system (dynamic pressure response caliber), phase 2 [AD-A239859] N92-10188

ELECTRICAL INSULATION
An analysis of the frequency characteristics of corona discharge at low pressure [AD-A239940] N92-10674

ELECTRICAL MEASUREMENT
Method and apparatus for frequency spectrum analysis [NASA-CASE-NPO-17759-1-CU] N92-10125
Constant frequency pulsed phase-locked loop measuring device [NASA-CASE-LAR-13823-1] N92-10182
Optical and electrical investigations into cathode ignition and diode closure [DE91-017823] N92-10191
Constitutive parameter extraction for heated materials [NASA-CR-186208] N92-10593

ELECTRICAL PROPERTIES
High temperature solar cell contacts [AD-A239932] N92-10227
A band theoretical study on the electronic properties in the phase transition CuAu 1 to CuAu 2 N92-10488
Beryllium doping of InP grown by gas-source molecular beam epitaxy N92-10489
Interface effects on electrical properties of high purity InP grown by gas-source molecular beam epitaxy N92-10490
The field drift of ions and its influence on the electrical properties of SnO2 N92-10492
Electrical characterization of Li and N doped ZnSe N92-10493
A novel technique for the measurement of photoenhanced electron attachment: Implications for an optically-controlled diffuse discharge opening switch [DE91-016226] N92-10621

ELECTRICAL RESISTIVITY
Brominated graphitized carbon fibers [NASA-CASE-LEW-14698-2] N92-10090
Electromagnetic oil field mapping for improved process monitoring and reservoir characterization [DE91-017452] N92-10132
Analysis of loss for inductive strips in finline [AD-A239947] N92-10156
Anisotropic twin boundary pinning in YBa2Cu3O(x) [DE91-018536] N92-10692
Chemical thermodynamic equilibria and conductivity of nonstoichiometric YB2Cu3O7-(delta): A review [DE91-018638] N92-10701

ELECTRO-OPTICS
Efficient, high-speed, monolithic optoelectronic circuits using quantum-confined structures [AD-A239841] N92-10155
Characterization of electronic materials [AD-A240063] N92-10159
Compound semiconductor technology: Materials and devices N92-10523

ELECTROACOUSTICS
US TAG for ISO/TC43, acoustics, IEC/TC29 electroacoustics, ISO/TC108/SC4 human exposure to mechanical vibration and shock: Minutes of the Accredited Standards Committee on Bioacoustics, S3 [AD-A239918] N92-10610

ELECTROCARDIOGRAPHY
Clustering: A powerful aid in classifying QRS waveforms N92-10541
Algorithm for detection of VFIB in real time from ECG N92-10542

ELECTROCHEMICAL CELLS
Alkali metal carbon dioxide electrochemical system for energy storage and/or conversion of carbon dioxide to oxygen [NASA-CASE-LEW-14973-1] N92-10222
Fuel cell systems program plan, fiscal year 1991 [DE91-017215] N92-10225

ELECTROCHEMICAL OXIDATION
Surface electrochemistry of Chloro(phthalocyaninato)rhodium(III) species, and oxygen reduction electrocatalysis, formation of a dimeric species [AD-A240148] N92-10104

ELECTROCHEMISTRY
Definition and measurement at high temperatures of pH [DE91-017945] N92-10077
Surface electrochemistry of Chloro(phthalocyaninato)rhodium(III) species, and oxygen reduction electrocatalysis, formation of a dimeric species [AD-A240148] N92-10104

ELECTROLYSIS
An improved technique for electrolytic colouration of alkali halide crystals N92-10513

ELECTROLYTES
Electromigration of carrier-free radionuclides [DE91-017840] N92-10076
Fuel cell systems program plan, fiscal year 1991 [DE91-017215] N92-10225

ELECTROLYTIC CELLS
Cold fusion verification [AD-A239957] N92-10675

ELECTROMAGNETIC COUPLING
Theory of Ion Bernstein wave coupling at low edge densities [DE91-018321] N92-10665

ELECTROMAGNETIC FIELDS
Electromagnetic oil field mapping for improved process monitoring and reservoir characterization [DE91-017452] N92-10132
Optimization methods in control of electromagnetic fields [AD-A240044] N92-10144
On acceleration of charged particles in intensity minima of laser fields [IPPCZ-307] N92-10653
Nonlinear RF processes in plasma [DE91-017441] N92-10658

ELECTROMAGNETIC INTERACTIONS
Fundamental studies in the molecular basis of laser induced retinal damage [AD-A239941] N92-10278
Investigations of the structure and electromagnetic interactions of few-body systems [DE91-017927] N92-10628

ELECTROMAGNETIC INTERFERENCE
On adaptive multiband detection of targets in nonstationary nonhomogeneous interference [AD-A239983] N92-10327

ELECTROMAGNETIC PROPERTIES
Optimization methods in control of electromagnetic fields [AD-A240044] N92-10144

ELECTROMAGNETIC RADIATION
Compilation of 1990 annual reports of the Navy ELF communications system ecological monitoring program. Volume 1: Tabs A, B [AD-A239868] N92-10137

ELECTROMAGNETIC SCATTERING
Optimization methods in control of electromagnetic fields [AD-A240044] N92-10144

ELECTROMAGNETIC SPECTRA
Interaction-induced light scattering as a source of information on properties and interactions of spherical top molecules N92-10439

ELECTROMETERS
Low pressure impactor with electrical concentration detection N92-10534

ELECTROMIGRATION
Electromigration of carrier-free radionuclides [DE91-017840] N92-10076

ELECTRON ACCELERATION
Electron acceleration by laser fields in a gas [DE91-018269] N92-10192

ELECTRON ATTACHMENT
A novel technique for the measurement of photoenhanced electron attachment: Implications for an optically-controlled diffuse discharge opening switch [DE91-016226] N92-10621

ELECTRON BEAMS
Optical and electrical investigations into cathode ignition and diode closure [DE91-017823] N92-10191
Electron acceleration by laser fields in a gas [DE91-018269] N92-10192
Ultra-cold polarized hydrogen source N92-10423
Long pulse electron beams [DE91-018357] N92-10636
Fiber-tile optical studies at Argonne [DE91-018591] N92-10641

ELECTRON CAPTURE
Experimental investigations of electron capture from atomic hydrogen and deuterium by alpha particles [DE91-018280] N92-10629
Dynamic screening and wake effects on electronic excitation in ion-solid and ion-surface collisions [DE91-018224] N92-10687

ELECTRON CYCLOTRON HEATING
The 110 GHz ECH heating system for DIII-D [DE91-018732] N92-10671

ELECTRON DENSITY (CONCENTRATION)
Variation of D-region parameters during polar cap absorption events in the year 1989 N92-10561

ELECTRON DIFFRACTION
Determination of the (1x2) structure of a Pt film on Pd(110) N92-10463

ELECTRON ENERGY
Electron temperatures in the E-region of the ionosphere [ISAS-641] N92-10259
Equivalence in the shell structure of the tight binding and free electron clusters N92-10441
Kinetic gas and electron temperatures in RF induction plasma N92-10460

ELECTRON GAS
Dynamic screening and wake effects on electronic excitation in ion-solid and ion-surface collisions [DE91-018224] N92-10687

ELECTRON MICROSCOPES
Control system for ruling blazed, aberration corrected diffraction gratings [NASA-CASE-GSC-13240-1] N92-10186

ELECTRON MICROSCOPY
Valence and phonon excitations in high-resolution electron microscopy [DE91-017684] N92-10625

ELECTRON OSCILLATIONS
On acceleration of charged particles in intensity minima of laser fields [IPPCZ-307] N92-10653

ELECTRON PARAMAGNETIC RESONANCE
NMR and ESR experiments on solid molecular hydrogen containing atomic hydrogen N92-10510

ELECTRON RECOMBINATION
Synchrotron radiation study of recombination processes in solid state Tb and Dy after 4d to 4f giant resonance excitation N92-10518
The N(4,5)N(6,7)N(6,7) and N(4,5)O(2,3)N(6,7) resonance Auger effects in the electron spectra of solid state Gd and Eu N92-10519

ELECTRON SCATTERING
Inclusive quasielastic and deep inelastic electron scattering at high energies [DE91-018755] N92-10633

ELECTRON SPECTROSCOPY
Positron annihilation induced Auger-electron spectroscopy: A study of a Ge(100) surface N92-10515

Super Coster Kronig and resonance super Coster Kronig spectra of solid Ge around 3p-ionization threshold N92-10517

Synchrotron radiation study of recombination processes in solid state Tb and Dy after 4d to 4f giant resonance excitation N92-10518

The N(4,5)N(6,7)N(6,7) and N(4,5)O(2,3)N(6,7) resonance Auger effects in the electron spectra of solid state Gd and Eu N92-10519

ELECTRON SPIN

Ultra-cold polarized hydrogen source N92-10423

NMR and ESR experiments on solid molecular hydrogen containing atomic hydrogen N92-10510

ELECTRON STATES

Decay channels of resonantly excited 2p(-1)ns, md states of Ar and 3d(-1)np states of Kr N92-10426

Li 1s photoionization and photoexcitation with satellites N92-10427

Electron correlation in the 4d hole state of Cs and Ba N92-10428

Krypton 4p,4s and 3d partial photoionization cross sections below 260 eV photon energy N92-10429

Relaxation and final-state correlation effects in the 3p and 3s photoionization of Ar, K(+), and Ca(++) N92-10430

Equivalence in the shell structure of the tight binding and free electron clusters N92-10441

Valence electron states of the Bi-Sr-Ca-Cu-O high-T(sub c) compound N92-10503

ELECTRON TRANSFER

Experimental study of interactions of highly charged ions with atoms at keV energies
[DE91-016962] N92-10616

Limitations of the condensed history method for low energy electrons
[DE91-015764] N92-10619

The response history Monte Carlo method for electron transport
[DE91-018295] N92-10631

ELECTRON TRANSITIONS

Electron correlation in the 4d hole state of Cs and Ba N92-10428

Synchrotron radiation study of recombination processes in solid state Tb and Dy after 4d to 4f giant resonance excitation N92-10518

The N(4,5)N(6,7)N(6,7) and N(4,5)O(2,3)N(6,7) resonance Auger effects in the electron spectra of solid state Gd and Eu N92-10519

ELECTRON TUNNELING

Control system for ruling blazed, aberration corrected diffraction gratings
[NASA-CASE-GSC-13240-1] N92-10186

ELECTRON-POSITRON PAIRS

Anomalous e(+)e(-) pairs in heavy ion collisions and solar neutrinos: Two puzzles with common solution? N92-10364

Recent physics results from DELPHI N92-10394

Heavy neutrinos in e(+)e(-) collisions N92-10398

ELECTRONIC COUNTERMEASURES

Integration of Electronic Support Measures (ESM) and alpha-beta radar tracker
[AD-A240031] N92-10143

ELECTRONIC EQUIPMENT

Thermal management of high heat flux electronic components in space and aircraft systems, phase 1
[AD-A239982] N92-10157

ELECTRONIC EQUIPMENT TESTS

Thermal energy storage and heat transfer support program. Volume 2: Task 4 Thermionic energy conversion studies
[AD-A239968] N92-10178

Gallium arsenide pilot line for high performance components
[AD-A239955] N92-10704

ELECTRONIC SPECTRA

Super Coster Kronig and resonance super Coster Kronig spectra of solid Ge around 3p-ionization threshold N92-10517

Experimental study of interactions of highly charged ions with atoms at keV energies
[DE91-016962] N92-10616

ELECTRONS

A neural network model of the relativistic electron flux at geosynchronous orbit
[AD-A239827] N92-10030

An improved technique for electrolytic colouration of alkali halide crystals N92-10513

Scale dependence of Lambda sub (MS bar) from deep inelastic scattering
[RAL-91-044] N92-10614

Experiments on the nuclear interactions of pions and electrons
[DE91-017929] N92-10623

The response history Monte Carlo method for electron transport
[DE91-018295] N92-10631

On acceleration of charged particles in intensity minima of laser fields
[IPPCZ-307] N92-10653

The influence of plasma motion on disruption generated runaway electrons
[DE91-018356] N92-10666

ELECTROSTATIC PRECIPITATORS

Electrostatic precipitator modelling N92-10532

ELECTROSTATIC WAVES

Beat wave current drive experiment on DDT
[DE91-017407] N92-10622

ELEMENTARY PARTICLE INTERACTIONS

Activities report of the Werner Heisenberg Institute for Physics, Munich (Federal Republic of Germany)
[ISSN-0173-6256] N92-10588

ELEMENTARY PARTICLES

The DELPHI microvertex detector, a silicon tracking chamber N92-10412

Activities report of the Werner Heisenberg Institute for Physics, Munich (Federal Republic of Germany)
[ISSN-0173-6256] N92-10588

ELEVATION

Mars elevation distribution N92-10921

ELLIPSES

Totally parallel multilevel algorithms for sparse elliptic systems
[NASA-CR-188837] N92-10333

ELLIPTIC DIFFERENTIAL EQUATIONS

Transformation of two and three-dimensional regions by elliptic systems
[NASA-CR-188982] N92-10170

EMISSION SPECTRA

Synthesis and properties of Ti-substituted goethites and hematites N92-10255

Infrared reflectance spectra (4-12 micron) of lunar samples N92-10812

Spectral evidence for carbonates on Mars: Hydrous carbonates N92-10820

Infrared (2.08-14 micron) spectra of powered stony meteorites N92-10826

Mapping compositional and particle size variations across Silver Lake Playa: Relevance to analyses of Mars TIR data N92-10842

ENCAPSULATING

Thermal modeling of an epoxy encapsulation process
[DE91-017845] N92-10096

ENERGETIC PARTICLES

Composition and energetics of solar flare particle events measured by satellites, 1989 - 1991
[DE91-018028] N92-10969

ENERGY BUDGETS

The role of nonuniform internal heating in Triton's energy budget N92-10736

ENERGY CONSUMPTION

Energy systems and their technical, economic and environmental boundary conditions N92-10581

The possibilities to control and to regulate the energy consumption N92-10582

ENERGY CONVERSION

Thermal energy storage and heat transfer support program. Volume 2: Task 4 Thermionic energy conversion studies
[AD-A239968] N92-10178

Energy systems and their technical, economic and environmental boundary conditions N92-10581

The possibilities to control and to regulate the energy consumption N92-10582

ENERGY CONVERSION EFFICIENCY

Energy systems and their technical, economic and environmental boundary conditions N92-10581

The possibilities to control and to regulate the energy consumption N92-10582

ENERGY DISSIPATION

Thermal management of high heat flux electronic components in space and aircraft systems, phase 1
[AD-A239982] N92-10157

Electron acceleration by laser fields in a gas
[DE91-018269] N92-10192

High resolution spectroscopy of H(+) energy loss in thin carbon film
[NIFS-88] N92-10654

ENERGY DISTRIBUTION

The stability analysis of a double barrier resonant tunneling device N92-10485

Average properties of energetic ions in different parts of the cusp/cleft region N92-10556

Nuclear physics at extreme energy density
[DE91-018012] N92-10637

ENERGY LEVELS

Li 1s photoionization and photoexcitation with satellites N92-10427

Analysis of the interacting levels V(sub 9) = 1 and V(sub 10) = 2 of propyne N92-10444

NMR pulse responses of pairs of triads of 1/2 spins in solids N92-10511

Super Coster Kronig and resonance super Coster Kronig spectra of solid Ge around 3p-ionization threshold N92-10517

Non-unicity of Gibbs states of Czech models in a half-space
[IPPCZ-311] N92-10679

Strong correlation theories of high temperature superconductors
[DE91-017479] N92-10688

ENERGY POLICY

The Alternative Fuels Data Center
[DE91-015003] N92-10111

Climate change: Problems of limits and policy responses N92-10232

ENERGY SPECTRA

Performance tests of ERNE HED sensor N92-10562

The hazard of exposure to impulse noise as a function of frequency, volume 1
[AD-A239992] N92-10611

An analysis of the frequency characteristics of corona discharge at low pressure
[AD-A239940] N92-10674

ENERGY TECHNOLOGY

Proceedings of the First Energy Research Power Supercomputer Users Symposium
[DE91-018877] N92-10300

Energy systems and their technical, economic and environmental boundary conditions N92-10581

ENERGY TRANSFER

Pulse thermal energy transport system
[NASA-CASE-LEW-15235-1] N92-10167

Electron temperatures in the E-region of the ionosphere
[ISAS-641] N92-10259

ENGINE AIRFRAME INTEGRATION

A computational and experimental investigation of a three-dimensional hypersonic scramjet inlet flow field N92-10007

ENGINE DESIGN

The space shuttle advanced solid rocket motor: Quality control and testing
[NASA-CR-188800] N92-10043

ENGINE NOISE

Combustion and core noise N92-10607

ENGINE PARTS

Update on the prospects for ceramic engine components
[DE91-018574] N92-10098

ENGINE TESTS

PC programs for the prediction of the linear stability behavior of liquid propellant propulsion systems and application to current MSFC rocket engine test programs, volume 1
[NASA-CR-184228] N92-10042

ENGINES

Evaluation of preservative engine oil containing vapor-phase corrosion inhibitor and a simplified engine preservation technique
[AD-A240100] N92-10103

ENTROPY

Information flow in quantum mechanics: The quantum Maxwell demon
[DE91-017659] N92-10725

ENVIRONMENT EFFECTS

The biological consequences of climate changes: An ecological and economic assessment N92-10235

Potential strategies for adapting to greenhouse warming: Perspectives from the developing world N92-10237

Epilogue N92-10240

Processes for identifying regional influences of and responses to increasing atmospheric CO2 and climate change: The MINK project
[DE91-018602] N92-10242

Processes for identifying regional influences of and responses to increasing atmospheric CO2 and climate change: The MINK project
[DE91-018605] N92-10244

The 14th International Conference on Combined Effect of Environmental Factors
[AD-A240045] N92-10245

Fossil fuels and the environment N92-10586

ENVIRONMENT MANAGEMENT

Assessing and managing the risks of climate change N92-10233

Human dimensions of global change: Toward a research agenda N92-10238

ENVIRONMENT PROTECTION

Climate change: Problems of limits and policy responses N92-10232

Solar energy in mitigating global environmental problems N92-10584

ENVIRONMENTAL ENGINEERING

MHD program plan, FY 1991
[DE91-017916] N92-10659

ENVIRONMENTAL MONITORING
Compilation of 1990 annual reports of the Navy ELF communications system ecological monitoring program. Volume 1: Tabs A, B
[AD-A239868] N92-10137
Compilation of 1990 annual reports of the Navy ELF communications system ecological monitoring program. Volume 2: Tabs C thru F
[AD-A239869] N92-10138
Compilation of 1990 annual reports of the Navy ELF communications system ecological monitoring program. Volume 3: Tabs G thru I
[AD-A239870] N92-10139
EPIDEMIOLOGY
The 14th International Conference on Combined Effect of Environmental Factors
[AD-A240045] N92-10245
EPITAXY
Epitaxial high T(sub c) superconducting thin films and superlattices deposited by laser albation N92-10505
Heteroepitaxial growth of TiO2, VO2, and TiO2/VO2 multilayers by MOCVD
[DE91-018543] N92-10694
Heteroepitaxy of MOCVD grown TiO2, VO2 films and TiO2/VO2 multilayers on sapphire (1120)
[DE91-018589] N92-10698
EPOXY COMPOUNDS
Thermal modeling of an epoxy encapsulation process
[DE91-017845] N92-10096
EPOXY RESINS
A process for preparing 1,3-diamino-5-pentafluorosulfanylbenzene and polymers therefrom
[NASA-CASE-LAR-14773-1-CU] N92-10105
Probability of brittle failure
[NASA-CR-187174] N92-10205
EQUATIONS OF MOTION
CH-53E/AV-8B aircraft sling load recovery system analysis
[AD-A239950] N92-10022
A 3-D adaptive mesh refinement algorithm for multimaterial gas dynamics
[DE91-018040] N92-10169
Stabilization of the m = 1 tearing mode by resonance detuning
[DE91-018423] N92-10668
EQUATIONS OF STATE
The generalized van der Waals theory of pure fluids and mixtures
[DE91-017549] N92-10093
Hadronic equation of state and the onset of kaon condensation N92-10386
Production of impact melt in craters on Venus, Earth, and the moon N92-10870
EROSION
Variable features in the Valles Marineris region of Mars N92-10799
Wrinkle ridges in the floor material of Kasei Valles, Mars: Nature and origin N92-10955
EROSIVE BURNING
Erosive burning of solid propellants N92-10108
ERROR ANALYSIS
Using surrogate data to detect nonlinearity in time series
[DE91-018017] N92-10357
ERS-1 (ESA SATELLITE)
The data book of ERS-1: The European Remote Sensing Satellite
[ESA-BR-75] N92-10039
ESCARPMENTS
Wrinkle ridge-upland scarp transitions: Implications for the mechanical properties of the deformed materials N92-10954
ESOPHAGUS
Analysis of esophageal pH-recordings for reflux disease N92-10543
ESSENTIALLY NON-OSCILLATORY SCHEMES
Multi-dimensional ENO schemes for general geometries
[NASA-CR-187637] N92-10349
ESTIMATING
Magma generation on Mars: Estimated volumes through time N92-10788
ETCHING
Glass sample characterization
[NASA-CR-184230] N92-10088
ETHYLENE
Nonflammable hydraulic power system for tactical aircraft. Volume 2: Equipment and systems test and evaluation
[AD-A239805] N92-10100
EULER EQUATIONS OF MOTION
Transonic and supersonic Euler computations of vortex-dominated flow fields about a generic fighter
[NASA-TP-3156] N92-10011
Numerical simulation of vortex breakdown by solving the Euler equations for an incompressible fluid N92-10163
Numerical simulation of vortex breakdown via 3-D Euler equations N92-10164
EULER-LAGRANGE EQUATION
Ground state properties of a He-3 impurity in liquid He-4 monolayers
[AD-A239993] N92-10078
EUROPA
Thermal models for icy satellites N92-10734
Tidal evolution of planetary satellites N92-10953
EUROPE
Abatement strategies based on critical loads N92-10533
EUROPIUM
The N(4,5)N(6,7)N(6,7) and N(4,5)O(2,3)N(6,7) resonance Auger effects in the electron spectra of solid state Gd and Eu N92-10519
EUTECTIC ALLOYS
High temperature creep properties of eutectic and near eutectic silver-copper alloys: Application to metal/ceramic joining
[DE91-017987] N92-10082
EUTROPHICATION
The remote sensing Loosdrecht Lakes (Netherlands) project
[BCRS-90-29] N92-10215
EVALUATION
Evaluation of high altitude photography for city cartography, with the example of Seattle, US N92-10214
EVAPORATION
Aerosol dynamics: Condensation and evaporation N92-10526
Evolution of the Martian hydrosphere N92-10768
EVAPORATORS
Pulse thermal energy transport system
[NASA-CASE-LEW-15235-1] N92-10167
EVEN-EVEN NUCLEI
Double beta decay in the particle-number projected QRPA formalism N92-10408
EVOKED RESPONSE (PSYCHOPHYSIOLOGY)
Auditory and visual evoked potentials as a function of sleep deprivation and irregular sleep
[AD-A240097] N92-10281
Fear-potentiated startle as a model system for analyzing learning and memory
[AD-A239994] N92-10284
EVOLUTION (DEVELOPMENT)
Gradational evolution of young, simple impact craters on the Earth N92-10783
New studies of Martian volcanoes N92-10793
EXCITATION
High-spin states in Cd-109 N92-10403
Shapes of Cd-110 at high spins N92-10404
Evidence for band termination in Xe-118 N92-10405
Atomic physics of strongly correlated systems
[DE91-012259] N92-10617
Valence and phonon excitations in high-resolution electron microscopy
[DE91-017684] N92-10625
Nuclear excitations and reaction mechanisms
[DE91-018968] N92-10634
Dynamic screening and wake effects on electronic excitation in ion-solid and ion-surface collisions
[DE91-018224] N92-10687
EXCITONS
Surface effect on optical bistability in coupled exciton-phonon systems inside a cavity
[AD-A240026] N92-10643
EXHAUST EMISSION
Human development and carbon dioxide emissions: The current picture and the long-term prospects N92-10230
EXHAUST GASES
Human development and carbon dioxide emissions: The current picture and the long-term prospects N92-10230
EXOSAT SATELLITE
An atlas of optical counterparts of low mass x ray binaries. Part 1: The Northern Sample
[MPE-PREPRINT-195-PT-1] N92-10723
EXPERIMENTATION
The B Experimental Division (of the Werner Heisenberg Institute of Physics) N92-10591
The Technical Division (of the Werner Heisenberg Institute of Physics) N92-10592
EXPERT SYSTEMS
Feasibility of using a knowledge-based system concept for in-flight primary flight display research
[NASA-TM-4279] N92-10017
Expert systems for superalloy studies
[NASA-CR-184236] N92-10080
Automated eddy current analysis of materials
[NASA-CR-184216] N92-10200
Research into the development of a knowledge acquisition taxonomy
[NASA-CR-188948] N92-10712
EXPLOSIONS
Thermal- and ignition-type steam explosions of single drops of molten aluminum
[DE91-014705] N92-10084
EXPLOSIVE DEVICES
Apparatus and method for explosive bonding to edge of flyer plate
[NASA-CASE-LAR-14096-1] N92-10196
EXPLOSIVE WELDING
Apparatus and method for explosive bonding to edge of flyer plate
[NASA-CASE-LAR-14096-1] N92-10196
EXPOSURE
Photoresist crossed gratings N92-10448
Charged-particle induced alterations of surfaces in the outer solar system N92-10838
EXTERNAL STORE SEPARATION
Measurements of forces, moments, and pressures on a generic store separating from a box cavity at supersonic speeds
[NASA-TP-3110] N92-10005
EXTRATERRESTRIAL RADIO WAVES
New observations of the low frequency interplanetary radio emissions
[NASA-CR-188917] N92-10971
EXTREMELY LOW FREQUENCIES
Compilation of 1990 annual reports of the Navy ELF communications system ecological monitoring program. Volume 1: Tabs A, B
[AD-A239868] N92-10137
Compilation of 1990 annual reports of the Navy ELF communications system ecological monitoring program. Volume 2: Tabs C thru F
[AD-A239869] N92-10138
EYE (ANATOMY)
Fundamental studies in the molecular basis of laser induced retinal damage
[AD-A239941] N92-10278
Two informative cases of Q-switched laser eye injury
[AD-A240001] N92-10279

F

FABRICATION
Gas turbine combuster exit temperature measurement
[AD-A239936] N92-10026
Formation of self-aligned guard rings for monolithic Schottky-barrier diode arrays
[NASA-CASE-NPO-17734-1-CU] N92-10146
Sintered compacts for heat sinks and process for fabricating same
[DE91-018438] N92-10153
Gallium arsenide pilot line for high performance components
[AD-A239955] N92-10704
FACE CENTERED CUBIC LATTICES
Surface reconstruction and many-atom models N92-10483
Ferromagnetism in small clusters N92-10508
FACTORIZATION
Parallel QR factorization on a hypercube using the torus wrap mapping
[DE91-011502] N92-10315
FAILURE
Probability of brittle failure
[NASA-CR-187174] N92-10205
FAILURE ANALYSIS
Thermal energy storage and heat transfer support program. Task-5 heat pipe life test study. Facilities upgrading and maintenance
[AD-A239929] N92-10177
Prediction of matrix fatigue crack initiation in notched SCS-6/Ti-15-3 metal matrix composites
[NASA-TM-104141] N92-10203
FAR ULTRAVIOLET RADIATION
Contamination study
[NASA-CR-184225] N92-10639
FARM CROPS
Using LANDSAT to provide potato production estimates to Columbia Basin farmers and processors
[NASA-CR-188783] N92-10209
FAST FOURIER TRANSFORMATIONS
Totally parallel multilevel algorithms for sparse elliptic systems
[NASA-CR-188837] N92-10333
Running discrete cosine transform algorithm N92-10375
Abel inversion with the fast Fourier transform N92-10379
Tunneling in oscillating double barrier heterostructures N92-10496

FATIGUE (MATERIALS)
Prediction of matrix fatigue crack initiation in notched SCS-6/Ti-15-3 metal matrix composites
[NASA-TM-104141] N92-10203
FAULT TOLERANCE
Approximate evaluation of reliability and related quantities via perturbation techniques
[AD-A240049] N92-10201
FEAR
Fear-potentiated startle as a model system for analyzing learning and memory
[AD-A239994] N92-10284
FEED SYSTEMS
PC programs for the prediction of the linear stability behavior of liquid propellant propulsion systems and application to current MSFC rocket engine test programs, volume 1
[NASA-CR-184228] N92-10042
FEEDBACK CONTROL
A compensatory algorithm for the slow-down effect on constant-time-separation approaches
[NASA-TM-4285] N92-10024
On the formulation of a minimal uncertainty model for robust control with structured uncertainty
[NASA-TP-3094] N92-10027
Approximate evaluation of reliability and related quantities via perturbation techniques
[AD-A240049] N92-10201
Recovering signals from optical fiber interferometric sensors
[AD-A240062] N92-10644
FERMI LIQUIDS
Predictions of the electron-hole liquid model for high T(sub c) superconductors N92-10499
FERMIONS
Photoemission in YbCu2Si2: Problems with the Kondo impurity model
[DE91-018018] N92-10684
FERROMAGNETISM
Ferromagnetism in small clusters N92-10508
Electronic and magnetic properties of strongly correlated systems
[DE91-018205] N92-10690
FERTILIZATION
Simulations of the carbon cycle in the oceans
[DE91-018475] N92-10273
FIBER COMPOSITES
Quantitative nondestructive evaluation of materials and structures
[NASA-CR-188975] N92-10071
In situ liquid-crystal-polymer fiber reinforced aluminum matrix composite
[AD-A239860] N92-10072
FIBER OPTICS
Fiber networking at Argonne: A distributed, multiapplication, multivendor computing environment
[DE91-018560] N92-10338
Multi-gigabit fiber optic wide area network development
[AD-A239850] N92-10642
FIBER STRENGTH
Relative sliding durability of two candidate high temperature oxide fiber seal materials
[NASA-TM-105199] N92-10064
FIBRILLATION
Algorithm for detection of VFIB in real time from ECG N92-10542
FIELD EFFECT TRANSISTORS
Fabrication of GaAs: MESFET's and test structures for electrical material characterization N92-10529
FIELD STRENGTH
Surface effect on optical bistability in coupled exciton-phonon systems inside a cavity
[AD-A240026] N92-10643
On acceleration of charged particles in intensity minima of laser fields
[IPPCZ-307] N92-10653
Anisotropic twin boundary pinning in YBa2Cu3O(x)
[DE91-018536] N92-10692
FIELD THEORY (PHYSICS)
Proceedings of the 25th Annual Conference of the Finnish Physical Society
[REPT-119(1991)] N92-10362
Activities report of the Werner Heisenberg Institute for Physics, Munich (Federal Republic of Germany)
[ISSN-0173-6256] N92-10588
Dark matter and the effective value of Newton's constant at large distances
[DE91-018152] N92-10726
Quantum cosmology on the worldsheet
[DE91-018415] N92-10727
FIGHTER AIRCRAFT
Transonic and supersonic Euler computations of vortex-dominated flow fields about a generic fighter
[NASA-TP-3156] N92-10011
FIGURE OF MERIT
User antennas N92-10121
FILAMENT WINDING
Automated eddy current analysis of materials
[NASA-CR-184216] N92-10200
FILAMENTS
Process for application of powder particles to filamentary materials
[NASA-CASE-LAR-14231-1] N92-10070
FINANCIAL MANAGEMENT
NASA procurement: Management oversight of contract cost and time changes could be enhanced
[GAO/NSIAD-91-259] N92-10708
Management issues at the National Aeronautics and Space Administration
[GAO/T-NSIAD-91-48] N92-10710
FINE STRUCTURE
Parsec-scale penetration of UV into molecular clouds: CII 158 micron mapping of W3, NGC 1977, and NGC 2023
[NASA-CR-188969] N92-10615
FINES
Clays on Mars: Review of chemical and mineralogical evidence N92-10250
FINITE DIFFERENCE THEORY
RIPPLE: A new model for incompressible flows with free surfaces
[DE91-017830] N92-10168
A 3-D adaptive mesh refinement algorithm for multimaterial gas dynamics
[DE91-018040] N92-10169
A general-purpose finite-difference code for solving steady-state three-dimensional fluid-flow and heat transfer problems
[AD-A239857] N92-10175
Fragmentation in stellar collapse N92-10891
FINITE ELEMENT METHOD
Recent advances on a finite element algorithm for computational aerodynamics: Transonics-hypersonics
[DE91-018176] N92-10010
A method for determining spiral-bevel gear tooth geometry for finite element analysis
[NASA-TP-3096] N92-10195
MERLIN 2: A computer program to transfer solution data betwwen finite element meshes
[DE91-018130] N92-10321
TAURUS: An interactive post-processor for the analysis codes NIKE3D, DYNA3D, and TOPAZ3D
[DE91-019012] N92-10326
Optimal moving grids for time-dependent partial differential equations
[NASA-CR-188850] N92-10344
FINITE VOLUME METHOD
Numerical analysis of fully developed laminar flow in curved rectangular channels
[NAL-TR-1111] N92-10166
FINLAND
The 1990 solar eclipse as seen by a torsion pendulum N92-10550
FINNISH SPACE PROGRAM
Finnish space projects: Planetary studies N92-10548
Finnish space projects: Space astronomy N92-10549
FISSION
Observations on very neutron-rich nuclei below Z = 50 N92-10402
Independent and cumulative yields of neutron-rich nuclei in symmetric fission induced by p and d on U-238 N92-10411
Influence of the angular correlation of fission neutrons on noise signatures
[DE91-014577] N92-10618
FLAME PROPAGATION
Fire retardant performance of some interior shipboard paint schemes
[MRL-TR-91-31] N92-10089
FLAME RETARDANTS
Fire retardant performance of some interior shipboard paint schemes
[MRL-TR-91-31] N92-10089
FLAME TEMPERATURE
Polarization spectroscopy in OH and flame temperature measurements N92-10454
FLAT PLATES
Measurements of forces, moments, and pressures on a generic store separating from a box cavity at supersonic speeds
[NASA-TP-3110] N92-10005
A grid-free method for high Reynolds number flow around an immersed elastic structure
[AD-A239851] N92-10013
FLIGHT CONTROL
Rotatable non-circular forebody flow controller
[NASA-CASE-LAR-14212-1-CU] N92-10021
FLIGHT CREWS
A system performance throughput model applicable to advanced manned telescience systems
[NASA-CR-188860] N92-10034
FLIGHT INSTRUMENTS
Differential collision cross-sections for atomic oxygen: Analysis of space flight instruments for solar terrestrial physics
[NASA-CR-184235] N92-10613
FLIGHT PATHS
A comparison between the consequences of the liberal and non-liberal UK-Europe bilaterals
[TT-9101] N92-10018
FLIGHT SAFETY
The space shuttle advanced solid rocket motor: Quality control and testing
[NASA-CR-188800] N92-10043
FLIGHT TESTS
Feasibility of using a knowledge-based system concept for in-flight primary flight display research
[NASA-TM-4279] N92-10017
FLOATING POINT ARITHMETIC
Hardware description ADSP-21020 40-bit floating point DSP as designed in a remotely controlled digital CW Doppler radar
[DE91-018004] N92-10134
The application of the ADSP-21020 40-bit floating point DSP microprocessor in a digital Doppler radar
[DE91-018005] N92-10135
FLOODS
Channeling episodes of Kasei Valles, Mars, and the nature of ridged plains material N92-10779
Flood routing of the Maja outflow across Xanthe Terra N92-10780
FLOORS
Igneous intrusion models for floor fracturing in lunar craters N92-10876
FLOW DISTRIBUTION
Hypersonic flows as related to the National Aerospace plane
[NASA-CR-187985] N92-10004
Measurements of forces, moments, and pressures on a generic store separating from a box cavity at supersonic speeds
[NASA-TP-3110] N92-10005
Mass flux similarity for slotted transonic-wind-tunnel walls
[NASA-TM-4281] N92-10006
A computational and experimental investigation of a three-dimensional hypersonic scramjet inlet flow field N92-10007
Transonic and supersonic Euler computations of vortex-dominated flow fields about a generic fighter
[NASA-TP-3156] N92-10011
Downwash measurements on a pitching canard-wing configuration
[AD-A239956] N92-10016
A non-isotropic multiple-scale turbulence model
[NASA-CR-184217] N92-10160
Numerical analysis and simulation of an assured crew return vehicle flow field
[NASA-TP-3101] N92-10161
Numerical simulation of vortex breakdown
[ONERA-RSF-6/4368-AY-008A] N92-10162
Numerical simulation of vortex breakdown by solving the Euler equations for an incompressible fluid N92-10163
Numerical simulation of vortex breakdown via 3-D Euler equations N92-10164
Nonequilibrium radiative heating prediction method for aeroassist flowfields with coupling to flowfield solvers N92-10165
Stability of the flow around a cylinder: The spin-up problem
[NASA-CR-187636] N92-10171
Management and control of unsteady and turbulent flows
[AD-A240050] N92-10180
Doppler shift velocimetry in disperse flows N92-10378
Turbomachinery noise N92-10601
Jet noise classical theory and experiments N92-10602
Jet noise generated by large-scale coherent motion N92-10604
FLOW EQUATIONS
Numerical simulation studies of fluid spreading N92-10482
FLOW GEOMETRY
Numerical analysis of fully developed laminar flow in curved rectangular channels
[NAL-TR-1111] N92-10166
FLOW MEASUREMENT
Reflection type skin friction meter
[NASA-CASE-LAR-14520-1-SB] N92-10008

Acoustic device and method for measuring gas densities
[NASA-CASE-NPO-18155-1-CU] N92-10609

FLOW REGULATORS
Rotatable non-circular forebody flow controller
[NASA-CASE-LAR-14212-1-CU] N92-10021

FLOW STABILITY
PC programs for the prediction of the linear stability behavior of liquid propellant propulsion systems and application to current MSFC rocket engine test programs, volume 1
[NASA-CR-184228] N92-10042
Stability of the flow around a cylinder: The spin-up problem
[NASA-CR-187636] N92-10171

FLOW VELOCITY
Velocimetry in gas flows using pulsed laser induced photothermal effects N92-10459
Propulsive lift noise N92-10606

FLUE GASES
Electrostatic precipitator modelling N92-10532

FLUID BOUNDARIES
A grid-free method for high Reynolds number flow around an immersed elastic structure
[AD-A239851] N92-10013

FLUID DYNAMICS
Technical evaluation report, AGARD Fluid Dynamics Panel Symposium on Effects of Adverse Weather on Aerodynamics
[NASA-TM-105192] N92-10002
Fluid dynamics of multiphase flow in volcanic environments on the Earth, Io, and other planets N92-10740

FLUID FILMS
Molecular dynamics studies of liquid-solid interfaces N92-10462

FLUID FILTERS
Evaluation of preservative engine oil containing vapor-phase corrosion inhibitor and a simplified engine preservation technique
[AD-A240100] N92-10103

FLUID FLOW
Reflection type skin friction meter
[NASA-CASE-LAR-14520-1-SB] N92-10008
Pulse thermal energy transport system
[NASA-CASE-LEW-15235-1] N92-10167
Steady flow of a fluid-solid mixture in a circular cylinder
[DE91-018698] N92-10174
A general-purpose finite-difference code for solving steady-state three-dimensional fluid-flow and heat transfer problems
[AD-A239857] N92-10175
Mechanized fluid connector and assembly tool system with ball detents
[NASA-CASE-MSC-21434-1] N92-10197
Numerical simulation studies of fluid spreading N92-10482
Magma generation on Mars: Estimated volumes through time N92-10788
Crystallization during emplacement of lava flows N92-10789
Physical properties of lava flows on the southwest flank of Tyrrhena Patera, Mars N92-10790
Rheological analyses of lava flows on Mars N92-10791
Factors controlling lava dome morphology N92-10792
Reflectance spectra of Fe(2+)-Mg(2+) disordered pyroxenes: Implications to remote-sensed spectra of planetary surfaces N92-10823
Mojave remote sensing field experiment N92-10840

FLUID MECHANICS
A grid-free method for high Reynolds number flow around an immersed elastic structure
[AD-A239851] N92-10013

FLUID POWER
Nonflammable hydraulic power system for tactical aircraft. Volume 2: Equipment and systems test and evaluation
[AD-A239805] N92-10100

FLUID-SOLID INTERACTIONS
Water/rock interactions in experimentally simulated dirty snowball and dirty iceball cometary nuclei N92-10888

FLUIDIZED BED PROCESSORS
Fluidized bed combustion diagnostics by laser photocoustic spectroscopy N92-10380
Simultaneous pyrometric measurement of temperature and size of fuel particles in fluidized bed combustions N92-10381

FLUORINE ORGANIC COMPOUNDS
Diosmacycloalkanes as models for the formation of hydrocarbons from surface methylenes
[DE91-017854] N92-10065

FLUX (RATE)
A neural network model of the relativistic electron flux at geosynchronous orbit
[AD-A239827] N92-10030

FLUX DENSITY
Nuclear physics at extreme energy density
[DE91-018012] N92-10637

FLUX PINNING
Electrical transport across grain boundaries in bicrystals of YBa2Cu3O7(delta)
[DE91-018588] N92-10697

FLUX QUANTIZATION
Properties of shocked relativistic jets N92-10564

FLY ASH
Electrostatic precipitator modelling N92-10532

FLYBY MISSIONS
Mineralogy of the Martian surface from Mariner 6/7 infrared spectrometer data N92-10814

FOILS
Antiferromagnetic ordering in silver at picoKelvin temperatures N92-10509

FOILS (MATERIALS)
Valence and phonon excitations in high-resolution electron microscopy
[DE91-017684] N92-10625

FOLDING STRUCTURES
Shuttle orbiter with telescoping main propulsion unit and payload
[NASA-CASE-LAR-13586-1] N92-10035

FOREBODIES
The effects of forebody strakes on asymmetric vortices on a vertically launched missile
[AD-A239948] N92-10014

FOREST MANAGEMENT
Climate and forests N92-10234

FORESTS
Climate and forests N92-10234
Processes for identifying regional influences of and responses to increasing atmospheric CO2 and climate change: The MINK project
[DE91-018605] N92-10244

FORM FACTORS
Electronic and magnetic properties of strongly correlated systems
[DE91-018205] N92-10690

FORMALISM
Exact strangeness conservation and particle production
[BI-TP-90/35] N92-10385

FORMAT
Display format, highlight validity, and highlight method: Their effects on search performance
[NASA-TM-104742] N92-10287

FORTRAN
Retire FORTRAN? A debate rekindled
[DE91-016565] N92-10317

FORWARD SCATTERING
Laboratory photometric measurement of particulate soils out to very large phase angles N92-10834
Anomalous scattering of light on Triton N92-10836

FOSSIL FUELS
Thoughts on abatement and adaptation N92-10239
Fossil fuels and the environment N92-10586

FOURIER ANALYSIS
Fourier component analysis of three Euler-Lagrangian methods applied to the one-dimensional advection-dispersion model
[DE91-017733] N92-10346

FOURIER SERIES
Coupled wave analysis in inverse grating diffraction problems N92-10456

FOURIER TRANSFORMATION
A new line-narrowing method LOMEP N92-10438

FRACTURE MECHANICS
Quantitative non-destructive evaluation of high-temperature superconducting materials
[DE91-018284] N92-10150

FRACTURE STRENGTH
Development of nondestructive characterization technologies for process control of ceramics
[DE91-018540] N92-10097

FRACTURES (MATERIALS)
Global relationships between volcanic vents and fractures radial to large impact basins on Mars N92-10750
Structural geology and geological history of the Perrine and Nun Sulci Quadrangles (Jg-2 and Jg-5), Ganymede N92-10762
Lunar western limb pyroclastic deposits N92-10795

FRACTURING
Microstructural stability and creep response of a new Al-Fe-W-Si alloy
[AD-A239861] N92-10087
Probability of brittle failure
[NASA-CR-187174] N92-10205
Flow and fracture of ice and ice mixtures N92-10735
The strength of Miranda's lithosphere N92-10767

FRAGMENTATION
Continuum modeling of catastrophic collisions N92-10863
Fragmentation in stellar collapse N92-10891

FRAGMENTS
Continuum modeling of catastrophic collisions N92-10863

FREE CONVECTION
Free convection in the Martian atmosphere N92-10803

FREE ELECTRON LASERS
Radar applications of gigawatt sources at millimeter wave frequencies
[DE91-017541] N92-10133

FREE ELECTRONS
Equivalence in the shell structure of the tight binding and free electron clusters N92-10441

FREE ENERGY
A statistical mechanics study of solid-solid interfaces
[DE91-017852] N92-10689

FREQUENCIES
Explanation for optical frequency dependent polarization in blazars N92-10577

FREQUENCY ANALYZERS
Parameter identification for nonlinear aerodynamic systems
[NASA-CR-188985] N92-10347

FREQUENCY CONTROL
Phase control in a two-element folded waveguide array
[DE91-018251] N92-10130

FREQUENCY DISTRIBUTION
Method and apparatus for frequency spectrum analysis
[NASA-CASE-NPO-17759-1-CU] N92-10125
A frequency domain method for the generation of partially coherent normal stationary time domain signals
[DE91-017058] N92-10204
An analysis of the frequency characteristics of corona discharge at low pressure
[AD-A239940] N92-10674

FREQUENCY DIVISION MULTIPLE ACCESS
Multiple access trade study N92-10118

FREQUENCY DIVISION MULTIPLEXING
Multi-gigabit fiber optic wide area network development
[AD-A239850] N92-10642

FREQUENCY MEASUREMENT
Constant frequency pulsed phase-locked loop measuring device
[NASA-CASE-LAR-13823-1] N92-10182

FREQUENCY RANGES
Method and apparatus for frequency spectrum analysis
[NASA-CASE-NPO-17759-1-CU] N92-10125

FREQUENCY STABILITY
A simple method to stabilize the frequency of semiconductor lasers N92-10453

FREQUENCY SYNTHESIZERS
Automatic network analyzer procedures for 5045 klystron cavities
[DE91-018015] N92-10149

FRICTION FACTOR
Numerical analysis of fully developed laminar flow in curved rectangular channels
[NAL-TR-1111] N92-10166

FRICTION MEASUREMENT
Reflection type skin friction meter
[NASA-CASE-LAR-14520-1-SB] N92-10008

FRONTS (METEOROLOGY)
The 1990 Airport Surveillance Radar Wind Shear Processor (ASR-WSP) operational test at Orlando International Airport
[AD-A239852] N92-10019

FROST
Optical properties of CO2 ice and CO2 snow from ultraviolet to infrared: Application to frost deposits and clouds on Mars N92-10821

FUEL CELL POWER PLANTS
Fuel cell systems program plan, fiscal year 1991
[DE91-017215] N92-10225

FUEL CELLS
Fuel cell systems program plan, fiscal year 1991
[DE91-017215] N92-10225

FUEL COMBUSTION
Electrostatic precipitator modelling N92-10532

FUEL CONSUMPTION
The Alternative Fuels Data Center
[DE91-015003] N92-10111

FUEL INJECTION
Extended temperature range rocket injector
[NASA-CASE-LEW-14846-1] N92-10054

FUEL SYSTEMS
Extended temperature range rocket injector
[NASA-CASE-LEW-14846-1] N92-10054

FUNCTION GENERATORS
A 500 MHz phase generator for synthetic aperture radar waveform synthesizers
[DE91-018399] N92-10136
FUNCTIONS (MATHEMATICS)
Applications of multiparameter bifurcations of period functions
[AD-A240046] N92-10352
FURNACES
Gas turbine combuster exit temperature measurement
[AD-A239936] N92-10026
FUSION REACTORS
Long pulse electron beams
[DE91-018357] N92-10636
FUZZY SYSTEMS
Reconfigurable fuzzy cell
[NASA-CASE-MSC-21613-1] N92-10331

G

GADOLINIUM
The N(4,5)N(6,7)N(6,7) and N(4,5)O(2,3)N(6,7) resonance Auger effects in the electron spectra of solid state Gd and Eu N92-10519
GALACTIC CLUSTERS
IPC two-color analysis of x ray galaxy clusters
[NASA-CR-188980] N92-10724
GALACTIC EVOLUTION
Long-term neutrino flux integrations
[DE91-013903] N92-10967
GALILEAN SATELLITES
Surface properties of Galilean satellites from bistatic radar experiments N92-10849
Radar backscattering by the icy Galilean satellites and the radar glory effect N92-10850
GALILEO SPACECRAFT
Surface properties of Galilean satellites from bistatic radar experiments N92-10849
Will Galileo resolve the S-asteroid controversy? N92-10882
GALLIUM ARSENIDES
A 500 MHz phase generator for synthetic aperture radar waveform synthesizers
[DE91-018399] N92-10136
Transport in heterostructures and devices in microwave and millimeter-wave regimes
[AD-A239943] N92-10142
High efficiency GaAs/Ge monolithic tandem cells for space concentrator arrays, phase 1
[AD-A239931] N92-10226
High temperature solar cell contacts
[AD-A239932] N92-10227
Observation of a monovacancy in the metastable state of the EL2 defect in GaAs by positron annihilation N92-10467
The influence of growth conditions on the composition of GaInAsP grown by gas-source molecular beam epitaxy N92-10491
Fabrication of GaAs: MESFET's and test structures for electrical material characterization N92-10529
Gallium arsenide pilot line for high performance components
[AD-A239955] N92-10704
GAME THEORY
A polynomial-time algorithm for computing the yolk in fixed dimension
[AD-A240060] N92-10353
GAMMA RAY ASTRONOMY
The measuring modes and observations with the x-ray spectrometer array SIXA onboard spectrum-x-gamma N92-10563
GAMMA RAY BURSTS
Explosive Transient Camera (ETC) program
[NASA-CR-188957] N92-10184
GAMMA RAY SPECTROMETERS
Water detection at the moon, Mars and comets with a combined neutron gamma ray instrument N92-10819
GAMMA RAYS
Thermal emission of gammas and lepton pairs from quark-gluon plasmas N92-10383
Lifetime of the 1.959 MeV state in Cl-36 N92-10400
Gamma-decay branching of 1(+)-states in Gd-156 and Dy-164 N92-10410
Radiation damage measurements on double-sided Si strip detectors N92-10415
Gamma echo experiments N92-10512
GANYMEDE
Structural geology and geological history of the Perrine and Nun Sulci Quadrangles (Jg-2 and Jg-5), Ganymede N92-10762
Stratigraphy of the Perrine and Nun Sulci quadrangles (Jg-2 and Jg-5), Ganymede N92-10911
Tidal evolution of planetary satellites N92-10953
GAS ANALYSIS
Fluidized bed combustion diagnostics by laser photocoustic spectroscopy N92-10380
Ion mobility spectrometer to trace gas analysis N92-10535
GAS DENSITY
Acoustic device and method for measuring gas densities
[NASA-CASE-NPO-18155-1-CU] N92-10609
GAS DYNAMICS
A 3-D adaptive mesh refinement algorithm for multimaterial gas dynamics
[DE91-018040] N92-10169
Coupling between radiation and gas dynamics
[AD-A240004] N92-10179
Analytical and computational mathematical physics
[DE91-018965] N92-10596
Particle-gas dynamics in the protoplanetary nebula N92-10893
GAS FLOW
Velocimetry in gas flows using pulsed laser induced photothermal effects N92-10459
GAS GIANT PLANETS
Flow and fracture of ice and ice mixtures N92-10735
Theoretical studies of volatile processes in the outer solar system N92-10807
Mapping the stability field of Jupiter Trojans N92-10883
Planetary origin, evolution, and structure N92-10952
Studies of volatiles and organic materials in early terrestrial and present-day outer solar system environments N92-10958
GAS MIXTURES
Theoretical estimation of the vibrational temperatures of N2 molecules in the ionosphere and in the laboratory simulated plasma
[ISAS-642] N92-10258
GAS TEMPERATURE
Gas turbine combuster exit temperature measurement
[AD-A239936] N92-10026
Theoretical estimation of the vibrational temperatures of N2 molecules in the ionosphere and in the laboratory simulated plasma
[ISAS-642] N92-10258
GAS TURBINE ENGINES
Combustion and core noise N92-10607
GAS TURBINES
Gas turbine combuster exit temperature measurement
[AD-A239936] N92-10026
Contractors Meeting in Propulsion
[AD-A240057] N92-10062
Combustion and core noise N92-10607
GAS-SOLID INTERACTIONS
The 14th International Conference on Combined Effect of Environmental Factors
[AD-A240045] N92-10245
GATES (CIRCUITS)
Gate matrix optimization using simulated annealing N92-10374
GAUGE THEORY
Quantum world in 2+1 dimensions N92-10365
GEAR TEETH
A method for determining spiral-bevel gear tooth geometry for finite element analysis
[NASA-TP-3096] N92-10195
GENES
Paucity of moderately repetitive sequences
[DE91-017953] N92-10276
GENETIC CODE
Paucity of moderately repetitive sequences
[DE91-017953] N92-10276
Computer assisted multiplex sequencing
[DE91-017851] N92-10337
GEOCHEMISTRY
Processes of deep terrestrial mantles and cores N92-10729
Water on Mars: Clue to accretional history N92-10798
Chemical fractionation of siderophile elements in impactites from Australian meteorite craters N92-10875
GEOCHRONOLOGY
Mineralogy of Cretaceous/Tertiary boundary clays in the Chicxulub structure in northern Yucatan N92-10253
Interactions of tectonic, igneous, and hydraulic processes in the North Tharsis Region of Mars N92-10755
Extension and strain in Northern Tharsis N92-10757
Valles Marineris, Mars: Are pit chains formed by erosion and troughs by tectonism? N92-10758
Iapetus: Tectonic structure and geologic history N92-10766
Large impacts and climatic catastrophes on the early Earth N92-10865
GEODESY
The control network of Mars: April 1991 N92-10918
GEODYNAMICS
SO2-rich equatorial basins and epeirogeny of Io N92-10761
GEOELECTRICITY
Lithosphere physics: Geoelectrics and seismics N92-10551
GEOGRAPHIC INFORMATION SYSTEMS
Remote sensing and watershed modeling: Towards a hydrological interface model
[BCRS-90-42] N92-10216
GEOGRAPHY
Functional description for the Mapping And Graphic Information Capability (MAGIC)
[AD-A239436] N92-10305
GEOIDS
Geoid undulations and gravity anomalies over the Aral Sea, the Black Sea and the Caspian Sea from a combined GEOS-3/SEASAT/GEOSAT altimeter data set
[NASA-TM-104543] N92-10257
GEOLOGICAL FAULTS
Interpretation of the northern boundary of Ishtar Terra from Magellan images and altimetry N92-10745
Modelled and measured strain in mascon basins on the moon N92-10747
Strain accommodation beneath structures on Mars N92-10748
Tectonic setting of Martian volcanoes and deep-seated intrusives N92-10751
Compressive strain in Lunae Planum-shortening across wrinkle ridges N92-10753
Interactions of tectonic, igneous, and hydraulic processes in the North Tharsis Region of Mars N92-10755
Extension and strain in Northern Tharsis N92-10757
Martian seismicity through time from surface faulting N92-10759
Structural geology and geological history of the Perrine and Nun Sulci Quadrangles (Jg-2 and Jg-5), Ganymede N92-10762
Tectonic deformation on icy satellites: A model of compensating horsts N92-10763
The width of fault zones in a brittle-viscous lithosphere: Strike-slip faults N92-10944
Wrinkle ridge-upland scarp transitions: Implications for the mechanical properties of the deformed materials N92-10954
Preliminary 1:500,000-scale geologic mapping of Claritas Fossae, Mars N92-10959
GEOLOGICAL SURVEYS
Geologic mapping of tunnels using photogrammetry: Camera and target positioning
[DE91-018394] N92-10261
Geologic history and channeling episodes of the Chryse Planitia region of Mars N92-10782
Surface scattering properties estimated from modeling airborne multiple emission angle reflectance data N92-10841
Application of Hapke photometric model to three geologic surfaces using PARABOLA bidirectional reflection data N92-10843
The Geologic Remote Sensing Field Experiment (GRSFE) N92-10844
Gravity survey of the Mt. Toondina impact structure, South Australia N92-10879
Preliminary geologic mapping of central Chryse Planitia, Mars N92-10906
Geologic mapping of northern Lunae Planun, Mars N92-10907
Mars geologic mapping: Dao, Harmakhis, and Reull Valles region N92-10908
Geologic mapping of MTM quads 40292 and 40297: In the Utopian lowlands north of the Nilosyrtis Mensae, Mars N92-10910
Mars geologic mapping program: Review and highlights N92-10912
Venus mapping N92-10913
Mars high-resolution mapping N92-10923
Planetary atlases N92-10925
Preliminary 1:500,000-scale geologic mapping of Claritas Fossae, Mars N92-10959
The violent side of mare volcanism N92-10962
GEOLOGY
Structural geology and geological history of the Perrine and Nun Sulci Quadrangles (Jg-2 and Jg-5), Ganymede N92-10762
GEOMAGNETIC LATITUDE
Variation of D-region parameters during polar cap absorption events in the year 1989 N92-10561
The effect of latitudinally varying solar wind flux on the Lyman alpha sky background N92-10570
GEOMAGNETIC MICROPULSATIONS
On the ionospheric influence upon the spectral structure on the Pc1 geomagnetic pulsations N92-10552
GEOMAGNETISM
On the ionospheric influence upon the spectral structure on the Pc1 geomagnetic pulsations N92-10552

GEOMETRICAL OPTICS
Numerical calculations of wave propagation in tokamak plasmas N92-10461
GEOMORPHOLOGY
The gradational history of southern Ismenius Lacus N92-10785
Jetting and the origin of tektites N92-10868
Melt droplet formation in energetic impacts N92-10869
Depth/diameter relationships of fresh craters within Hesperia Planum, Mars N92-10873
The scaling of secondary craters N92-10874
Planetary geomorphology research: FY 1990-1991 N92-10940
Are the Equatorial Highlands on Venus formed by mantle plume diapirs? N92-10942
Wrinkle ridge-upland scarp transitions: Implications for the mechanical properties of the deformed materials N92-10954
Wrinkle ridges in the floor material of Kasei Valles, Mars: Nature and origin N92-10955
Factors controlling the structures of magma chambers in basaltic volcanoes N92-10957
GEOPHYSICS
Lithosphere physics: Geoelectrics and seismics N92-10551
EISCAT research program N92-10553
Reports of Planetary Geology and Geophysics Program, 1990
[NASA-TM-4300] N92-10728
Horizontal stress in planetary lithospheres from vertical processes N92-10746
Heat flow vs. atmospheric greenhouse on early Mars N92-10805
GEOPOTENTIAL
Geoid undulations and gravity anomalies over the Aral Sea, the Black Sea and the Caspian Sea from a combined GEOS-3/SEASAT/GEOSAT altimeter data set
[NASA-TM-104543] N92-10257
GEOSYNCHRONOUS ORBITS
A neural network model of the relativistic electron flux at geosynchronous orbit
[AD-A239827] N92-10030
Impact of non-geostationary orbits on PASS N92-10120
GERMANIUM
High efficiency GaAs/Ge monolithic tandem cells for space concentrator arrays, phase 1
[AD-A239931] N92-10226
Positron annihilation induced Auger-electron spectroscopy: A study of a Ge(100) surface N92-10515
Super Coster Kronig and resonance super Coster Kronig spectra of solid Ge around 3p-ionization threshold N92-10517
GERMANY
Recording of urban land use by high altitude photography: The Munich (Fed. Republic of Germany) exampl N92-10211
Possibilities of producing land use information for city regional area planning by high altitude photographs, taking south west Munich (Fed. Republic of Germany) regional area as an example N92-10212
The A Experimental Division (of the Werner Heisenberg Institute for Physics) N92-10590
The B Experimental Division (of the Werner Heisenberg Institute of Physics) N92-10591
GIBBS FREE ENERGY
Non-unicity of Gibbs states of Czech models in a half-space
[IPPCZ-311] N92-10679
GLACIAL DRIFT
Terrestrial glacial eskers: Analogs for Martian sinuous ridges N92-10775
GLACIERS
Role of artesian groundwater in forming Martian permafrost features N92-10771
Glacial and marine chronology of Mars N92-10772
Chronology of glaciation in the Hellas region of Mars N92-10773
Glacial geology of the Hellas region on Mars N92-10774
Terrestrial glacial eskers: Analogs for Martian sinuous ridges N92-10775
Paleolakes and lacustrine basins on Mars N92-10776
GLASS
Glass sample characterization
[NASA-CR-184230] N92-10088
Characterization of electronic materials
[AD-A240063] N92-10159
Exploration of relationships between low-Ti and high-Ti pristine lunar glasses using an armalcolite assimilation model N92-10964
GLIDE PATHS
A compensatory algorithm for the slow-down effect on constant-time-separation approaches
[NASA-TM-4285] N92-10024
GLOBAL WARMING
Climate change: Problems of limits and policy responses N92-10232
Assessing and managing the risks of climate change N92-10233
Climate and forests N92-10234
Potential strategies for adapting to greenhouse warming: Perspectives from the developing world N92-10237
Human dimensions of global change: Toward a research agenda N92-10238
Epilogue N92-10240
Solar energy in mitigating global environmental problems N92-10584
The greenhouse effect N92-10587
GLOW DISCHARGES
An analysis of the frequency characteristics of corona discharge at low pressure
[AD-A239940] N92-10674
GLUONS
Gluon overlap factors extracted from Monte Carlo lattice calculations N92-10397
GOERTLER INSTABILITY
Stability of the flow around a cylinder: The spin-up problem
[NASA-CR-187636] N92-10171
GOLD
Dependence of Au(-) production upon the target work function in a plasma-sputter-type negative ion source
[NIFS-85] N92-10656
High-temperature implantation of Au into Ni
[DE91-017304] N92-10682
GOLD ALLOYS
A band theoretical study on the electronic properties in the phase transition CuAu 1 to CuAu 2 N92-10488
GOODNESS OF FIT
Identification of nonlinear times series from first order cumulative characteristics
[AD-A239822] N92-10350
GOVERNMENT PROCUREMENT
NASA procurement: Management oversight of contract cost and time changes could be enhanced
[GAO/NSIAD-91-259] N92-10708
GRAIN BOUNDARIES
Grain boundaries in nanophase materials
[DE91-018587] N92-10696
Electrical transport across grain boundaries in bicrystals of YBa2Cu3O7(delta)
[DE91-018588] N92-10697
Character of the opposition effect and negative polarization N92-10833
GRAIN SIZE
Examination of mechanical behavior in nanocrystalline materials
[DE91-018552] N92-10085
Effects of grain size and shape in modeling reflectance spectra of mineral mixtures N92-10831
GRAINS
Optical properties of grains in molecular clouds and accretion disks N92-10948
GRAPH THEORY
The connectivity of the basis graph of a branching greedoid
[MEMO-937] N92-10341
GRAPHITE
Automated eddy current analysis of materials
[NASA-CR-184216] N92-10200
GRAPHITE-EPOXY COMPOSITES
Properties of three graphite/toughened resin composites
[NASA-TP-3102] N92-10067
GRAPHITIZATION
Brominated graphitized carbon fibers
[NASA-CASE-LEW-14698-2] N92-10090
GRAPHS (CHARTS)
The connectivity of the basis graph of a branching greedoid
[MEMO-937] N92-10341
GRATINGS (SPECTRA)
Control system for ruling blazed, aberration corrected diffraction gratings
[NASA-CASE-GSC-13240-1] N92-10186
Photoresist crossed gratings N92-10448
Reconfigurable optical interconnections by acousto-optic holograms N92-10449
Coupled wave analysis in inverse grating diffraction problems N92-10456
Parametric optimization of synthetic gratings using vector diffraction theory N92-10457
The normal incidence grating inverse photoemission spectrometer in the energy range 8-28 eV N92-10516
Thermal infrared observations of Mars (7.5-12.8 microns) during the 1990 opposition N92-10951
GRAVITATION
Research program in particle physics
[DE91-018525] N92-10632
Quantum cosmology on the worldsheet
[DE91-018415] N92-10727
Mimas: Tectonic structure and geologic history N92-10764
Gravity survey of the Mt. Toondina impact structure, South Australia N92-10879
GRAVITATION THEORY
Studies in planetary rings N92-10949
GRAVITATIONAL COLLAPSE
Supernova neutrinos N92-10399
Formation of the protosolar nebula N92-10890
Fragmentation in stellar collapse N92-10891
GRAVITATIONAL EFFECTS
Gravitational spreading of Danu, Freyja and Maxwell Montes, Venus N92-10744
Energy coupling in catastrophic collisions N92-10862
Accretion rates of protoplanets N92-10936
The ring arcs of Neptune N92-10945
Studies in planetary rings N92-10949
GRAVITATIONAL FIELDS
Dynamic lattice computing in general relativity N92-10372
A 40th deg and order gravitational field model for Mars N92-10760
Gravity survey of the Mt. Toondina impact structure, South Australia N92-10879
GRAVITATIONAL WAVE ANTENNAS
Laser interferometer (TENKO-10 and -100) for gravitational wave antenna development
[ISAS-640] N92-10189
GRAVITY ANOMALIES
Geoid undulations and gravity anomalies over the Aral Sea, the Black Sea and the Caspian Sea from a combined GEOS-3/SEASAT/GEOSAT altimeter data set
[NASA-TM-104543] N92-10257
GRAZING INCIDENCE
The normal incidence grating inverse photoemission spectrometer in the energy range 8-28 eV N92-10516
GREEN'S FUNCTIONS
Mutual friction in superfluid He-3: Effects of bound states in the vortex core N92-10475
GREENHOUSE EFFECT
Greenhouse Warming: Abatement and Adaptation
[ISBN-0-915707-50-0] N92-10228
The greenhouse effect: Its causes, possible impacts, and associated uncertainties N92-10229
Human development and carbon dioxide emissions: The current picture and the long-term prospects N92-10230
Climate change: Problems of limits and policy responses N92-10232
The biological consequences of climate changes: An ecological and economic assessment N92-10235
Potential strategies for adapting to greenhouse warming: Perspectives from the developing world N92-10237
Human dimensions of global change: Toward a research agenda N92-10238
Thoughts on abatement and adaptation N92-10239
Epilogue N92-10240
Processes for identifying regional influences of and responses to increasing atmospheric CO2 and climate change: The MINK project
[DE91-018605] N92-10244
The greenhouse effect N92-10587
Thermal models for icy satellites N92-10734
Heat flow vs. atmospheric greenhouse on early Mars N92-10805
GRID GENERATION (MATHEMATICS)
Transformation of two and three-dimensional regions by elliptic systems
[NASA-CR-188982] N92-10170
Optimal moving grids for time-dependent partial differential equations
[NASA-CR-188850] N92-10344
GROOVES
Structural geology and geological history of the Perrine and Nun Sulci Quadrangles (Jg-2 and Jg-5), Ganymede N92-10762
GROUND BASED CONTROL
Remote sensing observations of Kelso Dunes, California N92-10847
GROUND STATE
Ground state properties of a He-3 impurity in liquid He-4 monolayers
[AD-A239993] N92-10078
Electronic and magnetic properties of strongly correlated systems
[DE91-018205] N92-10690
GROUND STATIONS
Personal Access Satellite System (PASS) study. Fiscal year 1989 results
[NASA-CR-186808] N92-10116

GROUND SUPPORT EQUIPMENT
Solar Constant (SOLCON) Experiment: Ground Support Equipment (GSE) software development
[NASA-CR-187596] N92-10267
GROUND WATER
A Martian global groundwater model N92-10769
Role of groundwater in formation of Martian channels N92-10770
Role of artesian groundwater in forming Martian permafrost features N92-10771
GUSTS
The 1990 Airport Surveillance Radar Wind Shear Processor (ASR-WSP) operational test at Orlando International Airport
[AD-A239852] N92-10019
GYRATION
The meandering orbit effect on stabilization of the tilting instability in a field-reversed configuration
[NIFS-22] N92-10648

H

HADRONS
The quark-hadron phase transition N92-10367
Thermal photon production from high-temperature nuclear matter N92-10384
Hadronic equation of state and the onset of kaon condensation N92-10386
Local charge compensation in Z(sup 0) hadronic decays N92-10393
Study of muon triggers and momentum reconstruction in a strong magnetic field for a muon detector at LHC N92-10413
Electronics of the cosmic ray air shower array at Turku (Finland) N92-10574
Test results of density detectors of the cosmic ray air shower array in Turku (Finland) N92-10575
Nuclear excitations and reaction mechanisms
[DE91-018968] N92-10634
HALF SPACES
Non-unicity of Gibbs states of Czech models in a half-space
[IPPCZ-311] N92-10679
HALL EFFECT
Interface effects on electrical properties of high purity InP grown by gas-source molecular beam epitaxy N92-10490
Recombination radiation in the fractional quantum Hall effect regime N92-10495
HAMILTONIAN FUNCTIONS
The Titan-Hyperion orbital resonance N92-10946
HARMONICS
Recovering signals from optical fiber interferometric sensors
[AD-A240062] N92-10644
Fast wave heating at intermediate ion cyclotron harmonics on the JIPP T-II U tokamak
[NIFS-21] N92-10649
HARRIER AIRCRAFT
CH-53E/AV-8B aircraft sling load recovery system analysis
[AD-A239950] N92-10022
HARTREE APPROXIMATION
Polarizabilities of trans and cis polyacetylene and interactions among chains in crystalline polyacetylene
[AD-A240025] N92-10705
HAWAII
Lunar and Hawaiian lava tubes: Analogs and uses based on terrestrial field data N92-10796
HAZARDS
Predicting cloud-to-ground lightning with neural networks
[AD-A239989] N92-10270
The hazard of exposure to impulse noise as a function of frequency, volume 1
[AD-A239992] N92-10611
HEALTH
The EH safety representative information system on the safety performance measurement system is where you will find... Word processing and helps with a V-PLUS
[DE91-018709] N92-10113
HEARING
US TAG for ISO/TC43, acoustics, IEC/TC29 electroacoustics, ISO/TC108/SC4 human exposure to mechanical vibration and shock: Minutes of the Accredited Standards Committee on Bioacoustics, S3
[AD-A239918] N92-10610
On categorizing sounds
[AD-A240006] N92-10612
HEART FUNCTION
A computer simulation for predicting the time course of thermal and cardiovascular responses to various combinations of heat stress, clothing, and exercise
[AD-A240023] N92-10288
HEART VALVES
A grid-free method for high Reynolds number flow around an immersed elastic structure
[AD-A239851] N92-10013
HEAT BUDGET
Crystallization during emplacement of lava flows N92-10789
HEAT FLUX
Thermal management of high heat flux electronic components in space and aircraft systems, phase 1
[AD-A239982] N92-10157
Thermal energy storage and heat transfer support program. Volume 1: Task-1 heat transport system study copper-water and steel-sodium DWAHP
[AD-A239928] N92-10176
Thermal models for icy satellites N92-10734
The role of nonuniform internal heating in Triton's energy budget N92-10736
HEAT PIPES
Thermal energy storage and heat transfer support program. Volume 1: Task-1 heat transport system study copper-water and steel-sodium DWAHP
[AD-A239928] N92-10176
Thermal energy storage and heat transfer support program. Task-5 heat pipe life test study. Facilities upgrading and maintenance
[AD-A239929] N92-10177
HEAT RESISTANT ALLOYS
Expert systems for superalloy studies
[NASA-CR-184236] N92-10080
HEAT SINKS
Diamond heat sinks for electronic circuits
[AD-A239750] N92-10145
Sintered compacts for heat sinks and process for fabricating same
[DE91-018438] N92-10153
HEAT STORAGE
Pulse thermal energy transport system
[NASA-CASE-LEW-15235-1] N92-10167
Thermal energy storage and heat transfer support program. Volume 1: Task-1 heat transport system study copper-water and steel-sodium DWAHP
[AD-A239928] N92-10176
Thermal energy storage and heat transfer support program. Task-5 heat pipe life test study. Facilities upgrading and maintenance
[AD-A239929] N92-10177
Thermal energy storage and heat transfer support program. Volume 2: Task 4 Thermionic energy conversion studies
[AD-A239968] N92-10178
HEAT TOLERANCE
A computer simulation for predicting the time course of thermal and cardiovascular responses to various combinations of heat stress, clothing, and exercise
[AD-A240023] N92-10288
HEAT TRANSFER
Hypersonic flows as related to the National Aerospace plane
[NASA-CR-187985] N92-10004
Pulse thermal energy transport system
[NASA-CASE-LEW-15235-1] N92-10167
A general-purpose finite-difference code for solving steady-state three-dimensional fluid-flow and heat transfer problems
[AD-A239657] N92-10175
Thermal energy storage and heat transfer support program. Volume 1: Task-1 heat transport system study copper-water and steel-sodium DWAHP
[AD-A239928] N92-10176
Thermal energy storage and heat transfer support program. Task-5 heat pipe life test study. Facilities upgrading and maintenance
[AD-A239929] N92-10177
Thermal energy storage and heat transfer support program. Volume 2: Task 4 Thermionic energy conversion studies
[AD-A239968] N92-10178
Performance of conjugate gradient-like algorithms in transient two-phase subchannel analysis
[DE91-013373] N92-10316
PATRAN and P/THERMAL applications for thermal modeling
[DE91-017767] N92-10320
Free convection in the Martian atmosphere N92-10803
Characteristics of the Martian atmosphere surface layer N92-10804
Planetary origin, evolution, and structure N92-10952
HEAT TRANSMISSION
Heat flow vs. atmospheric greenhouse on early Mars N92-10805
HEATERS
Thermal energy storage and heat transfer support program. Volume 1: Task-1 heat transport system study copper-water and steel-sodium DWAHP
[AD-A239928] N92-10176
HEATING
Electron temperatures in the E-region of the ionosphere
[ISAS-641] N92-10259
Self-regulation mechanisms in galactic discs N92-10576
Crystallization during emplacement of lava flows N92-10789
Impacts and atmospheric erosion on the early Earth N92-10871
HEATING EQUIPMENT
MHD program plan, FY 1991
[DE91-017916] N92-10659
HEAVY IONS
Status of the JYFL-ECR ion source N92-10422
Plan for the JYFL gas-filled recoil separator N92-10424
Nonperturbative electromagnetic muon-pair production with capture in peripheral relativistic heavy-ion collisions
[DE91-018247] N92-10624
HEAVY NUCLEI
Contribution of the delta resonance to the Gamow-Teller decay of heavy nuclei N92-10407
HELICOPTER PERFORMANCE
CH-53E/AV-8B aircraft sling load recovery system analysis
[AD-A239950] N92-10022
HELICOPTERS
CH-53E/AV-8B aircraft sling load recovery system analysis
[AD-A239950] N92-10022
HELIOSPHERE
New observations of the low frequency interplanetary radio emissions
[NASA-CR-188917] N92-10971
HELIOSTATS
The SolarTrak solar array tracking controller
[DE91-017721] N92-10224
HELIUM
Thermal helium desorption facility in Jyvaskyla (Finland) N92-10464
Helium in silicon: A first principle molecular dynamics study N92-10473
HELIUM IONS
Ion-Guide Quadrupole Mass Spectrometer (IGQMS) N92-10417
HELIUM ISOTOPES
Ground state properties of a He-3 impurity in liquid He-4 monolayers
[AD-A239993] N92-10078
Two-phonon absorption by the real squashing collective mode in superfluid He-3 N92-10474
Vortex nucleation in rotating superfluid He-3-B N92-10476
Superfluid interfaces in liquid He-3: Superconducting cosmic domain walls in the laboratory N92-10478
Superfluid vortex nucleation in He-3 flow N92-10479
Experiments on the nuclear interactions of pions and electrons
[DE91-017929] N92-10623
HELMETS
Helmet of a laminate construction of polycarbonate and polysulfone polymeric material
[NASA-CASE-MSC-21503-1] N92-10091
HEMATITE
Transformation products of submicron-sized aluminum-substituted magnetite: Color and reductant solubility N92-10251
Synthesis and properties of Ti-substituted goethites and hematites N92-10255
Degradation of Fe-Mg silicates in hot CO2 atmospheres: Applications to Venus N92-10806
HEMISPHERES
Core formation by giant impacts N92-10864
HERMITIAN POLYNOMIAL
A restricted signature normal form for Hermitian matrices, quasi-spectral decompositions, and applications
[NASA-CR-188895] N92-10310
HETEROJUNCTIONS
Transport in heterostructures and devices in microwave and millimeter-wave regimes
[AD-A239943] N92-10142
Tunneling in oscillating double barrier heterostructures N92-10496
HIGH ALTITUDE
Evaluation of high altitude photography for city regional areas
[MGA-A-44] N92-10210

Recording of urban land use by high altitude photography: The Munich (Fed. Republic of Germany) exampl N92-10211
Possibilities of producing land use information for city regional area planning by high altitude photographs, taking south west Munich (Fed. Republic of Germany) regional area as an example N92-10212
Image evaluation of high altitude photographs. Examples: Boston and Foster City (US) N92-10213
Evaluation of high altitude photography for city cartography, with the example of Seattle, US N92-10214

HIGH ENERGY INTERACTIONS
Intermittency studies in proton-antiproton collisions at square root of S = 630 GeV
[CERN-PPE/90-153] N92-10387
Research program in particle physics
[DE91-018525] N92-10632

HIGH LEVEL LANGUAGES
The paradigm compiler: Mapping a functional language for the connection machine
[NASA-CR-188839] N92-10290

HIGH PRESSURE
Properties of planetary fluids at high pressures and temperatures N92-10739
Jetting and the origin of tektites N92-10868

HIGH RESOLUTION
High resolution lunar radar studies: Preliminary results N92-10845

HIGH TEMPERATURE
High temperature creep properties of eutectic and near eutectic silver-copper alloys: Application to metal/ceramic joining
[DE91-017987] N92-10082
The field drift of ions and its influence on the electrical properties of SnO2 N92-10492
Properties of planetary fluids at high pressures and temperatures N92-10739
Degradation of Fe-Mg silicates in hot CO2 atmospheres: Applications to Venus N92-10806

HIGH TEMPERATURE ENVIRONMENTS
Gas turbine combuster exit temperature measurement
[AD-A239936] N92-10026
Definition and measurement at high temperatures of pH
[DE91-017945] N92-10077
High temperature solar cell contacts
[AD-A239932] N92-10227

HIGH TEMPERATURE RESEARCH
Transport properties and oxidation in chromium and Fe-Cr alloys exposed to oxygen at high temperatures
[DE91-018571] N92-10086

HIGH TEMPERATURE SUPERCONDUCTORS
Quantitative non-destructive evaluation of high-temperature superconducting materials
[DE91-018284] N92-10150
High temperature ceramic superconductors
[AD-A239813] N92-10154
Work function changes of high-T(sub c) superconductors around the T(sub c) N92-10498
Predictions of the electron-hole liquid model for high T(sub c) superconductors N92-10499
Vortex lattice: Vortex liquid states in anisotropic high-T(sub c) superconductors N92-10500
Dynamics of vortices in high-temperature superconductors N92-10501
Valence electron states of the Bi-Sr-Ca-Cu-O high-T(sub c) compound N92-10503
Studies on superconducting Bi2Sr2Ca(n-1) Cu(n)O(4+2n) compounds with Fe-57 and Eu-151 Moessbauer spectroscopy N92-10504
Epitaxial high T(sub c) superconducting thin films and superlattices deposited by laser albation N92-10505
High T(sub c) superconducting Li-doped Bi-Sr-Ca-Cu-O thin films deposited by laser ablation N92-10506
Novel type of cryogenic liquid level sensor with high sensitivity N92-10528
Passivation of high temperature superconductors
[NASA-CASE-NPO-17949-1-CU] N92-10681
Polarization dependent x ray spectroscopy of high T(sub c) superconductors
[DE91-017475] N92-10683
Mechanical after-effect studies of oxygen relaxation in YBa2Cu3O(7-delta)
[DE91-018043] N92-10685
Langevin dynamics simulations of large frustrated Josephson junction arrays
[DE91-018046] N92-10686
Strong correlation theories of high temperature superconductors
[DE91-017479] N92-10688
Initial magnetization and magnetic relaxation in a single crystal of Bi2Sr2CaCu2O(x)
[DE91-018537] N92-10693
Electrical transport across grain boundaries in bicrystals of YBa2Cu3O7(delta)
[DE91-018588] N92-10697
Preparation and characterization of high temperature superconductor film surfaces
[AD-A240118] N92-10706

HIGH TEMPERATURE TESTS
Constitutive parameter extraction for heated materials
[NASA-CR-186208] N92-10593

HIGH VOLTAGES
Compilation of 1990 annual reports of the Navy ELF communications system ecological monitoring program. Volume 2: Tabs C thru F
[AD-A239869] N92-10138
Proceedings of the Second Switch Tube Advanced Technology Meeting
[DE91-017718] N92-10148

HIGHLANDS
Are the Equatorial Highlands on Venus formed by mantle plume diapirs? N92-10942
The violent side of mare volcanism N92-10962

HISTORIES
The changing face of probability
[DE91-018857] N92-10359

HOLES (ELECTRON DEFICIENCIES)
Electron correlation in the 4d hole state of Cs and Ba N92-10428
Predictions of the electron-hole liquid model for high T(sub c) superconductors N92-10499

HOLLOW CATHODES
Experimental investigation of a 12 cm diameter Kaufman xenon ion thruster
[NAL-TR-1099] N92-10056

HOLOGRAPHIC INTERFEROMETRY
Two-color holography concept (T-CHI)
[NASA-CR-184240] N92-10183
Holographic nondestructive testing in bone biomechanics N92-10451

HOLOGRAPHY
Two-color holography concept (T-CHI)
[NASA-CR-184240] N92-10183
Control system for ruling blazed, aberration corrected diffraction gratings
[NASA-CASE-GSC-13240-1] N92-10186
Waveguide Dammann gratings and kinoforms N92-10458

HOMODYNE RECEPTION
Recovering signals from optical fiber interferometric sensors
[AD-A240062] N92-10644

HOMOGENEITY
On adaptive multiband detection of targets in nonstationary nonhomogeneous interference
[AD-A239983] N92-10327

HOMOJUNCTIONS
InP solar cells grown by gas-source molecular beam epitaxy N92-10531

HUMAN BEHAVIOR
New methods of change detection using multispectral data
[AD-A239370] N92-10217
Human dimensions of global change: Toward a research agenda N92-10238

HUMAN FACTORS ENGINEERING
Three experiments with stereoscopic television: When it works and why
[DE91-016277] N92-10129

HUMAN PERFORMANCE
A system performance throughput model applicable to advanced manned telescience systems
[NASA-CR-188860] N92-10034
Three experiments with stereoscopic television: When it works and why
[DE91-016277] N92-10129
Human performance measurement: Validation procedures applicable to advanced manned telescience systems
[NASA-CR-185447] N92-10282
Modeling reality
[NASA-CR-188881] N92-10307

HUMAN REACTIONS
Three experiments with stereoscopic television: When it works and why
[DE91-016277] N92-10129
Human dimensions of global change: Toward a research agenda N92-10238

HUMAN RESOURCES
Management issues at the National Aeronautics and Space Administration
[GAO/T-NSIAD-91-48] N92-10710

HYDRATES
Aerosol dynamics: Binary nucleation N92-10525

HYDRAULIC EQUIPMENT
Nonflammable hydraulic power system for tactical aircraft. Volume 2: Equipment and systems test and evaluation
[AD-A239805] N92-10100

HYDRAZINES
Poly 1, 2, 4-triazoles via aromatic nucleophilic displacement
[NASA-CASE-LAR-14440-1] N92-10066
A process for preparing 1,3-diamino-5-pentafluorosulfanylbenzene and polymers therefrom
[NASA-CASE-LAR-14773-1-CU] N92-10105

HYDROCARBON FUELS
Regenerative Cu/La zeolite supported desulfurizing sorbents
[NASA-CASE-NPO-17480-1-CU] N92-10073

HYDROCARBONS
Development and optimization of methodologies for analysis of complex hydrocarbon mixtures
[DE91-017954] N92-10075

HYDROCHLORIDES
The crystal structure and moisture sensitivity of (+)-4-(1-(2,3 dimethylphenyl) ethyl) 1H-imidazole hydrochloride N92-10522

HYDRODYNAMIC EQUATIONS
Fragmentation in stellar collapse N92-10891

HYDRODYNAMICS
RIPPLE: A new model for incompressible flows with free surfaces
[DE91-017830] N92-10168
Hydrocode predictions of collisional outcomes: Effects of target size N92-10861

HYDROGEN
Computer simulations on the orientation of molecular hydrogen in liquid crystals N92-10466
NMR and ESR experiments on solid molecular hydrogen containing atomic hydrogen N92-10510
Experimental investigations of electron capture from atomic hydrogen and deuterium by alpha particles
[DE91-018280] N92-10629

HYDROGEN ATOMS
Ultra-cold polarized hydrogen source N92-10423
Strong magnetic compression of spin-polarized hydrogen N92-10480
Energy partitioning in elementary gas phase reactions
[DE91-017783] N92-10627

HYDROGEN EMBRITTLEMENT
Test apparatus and tensile properties of LE-7 turbine blade materials in high pressure hydrogen conditions
[NAL-TR-1092] N92-10025
Expert systems for superalloy studies
[NASA-CR-184236] N92-10080

HYDROGEN IONS
High resolution spectroscopy of H(+) energy loss in thin carbon film
[NIFS-88] N92-10654

HYDROGEN OXYGEN ENGINES
Test apparatus and tensile properties of LE-7 turbine blade materials in high pressure hydrogen conditions
[NAL-TR-1092] N92-10025

HYDROGEN RECOMBINATIONS
Ultra-cold polarized hydrogen source N92-10423
NMR and ESR experiments on solid molecular hydrogen containing atomic hydrogen N92-10510

HYDROLOGICAL CYCLE
Evolution of the Martian hydrosphere N92-10768

HYDROLOGY
Remote sensing and watershed modelling: Towards a hydrological interface model
[BCRS-90-42] N92-10216
Processes for identifying regional influences of and responses to increasing atmospheric CO2 and climate change: The MINK project
[DE91-018605] N92-10244
Radiohydrophysical aerospace research of ocean
[SRI-PR-1749] N92-10272

HYDROLOGY MODELS
Remote sensing and watershed modelling: Towards a hydrological interface model
[BCRS-90-42] N92-10216
Water resources and climate change N92-10236
A Martian global groundwater model N92-10769
Role of groundwater in formation of Martian channels N92-10770
Glacial and marine chronology of Mars N92-10772
Terrestrial glacial eskers: Analogs for Martian sinuous ridges N92-10775

HYDROLYSIS
Electromigration of carrier-free radionuclides
[DE91-017840] N92-10076

HYDROSTATIC PRESSURE
Flow and fracture of ice and ice mixtures N92-10735

HYDROXYL RADICALS
Polarization spectroscopy in OH and flame temperature measurements N92-10454

HYPERCUBE MULTIPROCESSORS
Parallel QR factorization on a hypercube using the torus wrap mapping
[DE91-011502] N92-10315
Totally parallel multilevel algorithms for sparse elliptic systems
[NASA-CR-188837] N92-10333
HYPERION
The Titan-Hyperion orbital resonance N92-10946
HYPERSONIC FLOW
Hypersonic flows as related to the National Aerospace plane
[NASA-CR-187985] N92-10004
Numerical simulation of hypersonic viscous flow for the design of H-2 orbiting plane (HOPE-2)
[NAL-TR-1093] N92-10009
Recent advances on a finite element algorithm for computational aerodynamics: Transonics-hypersonics
[DE91-018176] N92-10010
Numerical analysis and simulation of an assured crew return vehicle flow field
[NASA-TP-3101] N92-10161
HYPERSONIC INLETS
A computational and experimental investigation of a three-dimensional hypersonic scramjet inlet flow field N92-10007
HYPERSONICS
Recent advances on a finite element algorithm for computational aerodynamics: Transonics-hypersonics
[DE91-018176] N92-10010
HYPERVELOCITY IMPACT
Impact decapitation from laboratory to basin scales N92-10858
Energy coupling in catastrophic collisions N92-10862
Continuum modeling of catastrophic collisions N92-10863
Core formation by giant impacts N92-10864
Impacts and the early environment and evolution of the terrestrial planets N92-10866
Vapor plumes: A neglected aspect of impact cratering N92-10867
Jetting and the origin of tektites N92-10868
Melt droplet formation in energetic impacts N92-10869
Production of impact melt in craters on Venus, Earth, and the moon N92-10870
Impacts and atmospheric erosion on the early Earth N92-10871
Depth/diameter relationships of fresh craters within Hesperia Planum, Mars N92-10873
Magnetic effects of large-scale impacts on airless planetary bodies N92-10877
Gravity survey of the Mt. Toondina impact structure, South Australia N92-10879
HYSTERESIS
Neutron irradiation effects on YBCO single crystals
[DE91-018615] N92-10700

I

IAPETUS
Iapetus: Tectonic structure and geologic history N92-10766
ICE
Flow and fracture of ice and ice mixtures N92-10735
Paleolakes and lacustrine basins on Mars N92-10776
Spectroscopic analyses of Fe and water in clays: A Martian surface weathering study N92-10818
Optical properties of CO2 ice and CO2 snow from ultraviolet to infrared: Application to frost deposits and clouds on Mars N92-10821
Water/rock interactions in experimentally simulated dirty snowball and dirty iceball cometary nuclei N92-10888
Planetary geomorphology research: FY 1990-1991 N92-10940
Properties of dust and clouds in the Mars atmosphere: Analysis of Viking IRTM emission phase function sequences N92-10956
ICE FORMATION
Technical evaluation report, AGARD Fluid Dynamics Panel Symposium on Effects of Adverse Weather on Aerodynamics
[NASA-TM-105192] N92-10002
ICE PREVENTION
Technical evaluation report, AGARD Fluid Dynamics Panel Symposium on Effects of Adverse Weather on Aerodynamics
[NASA-TM-105192] N92-10002
ICY SATELLITES
Thermal models for icy satellites N92-10734
The role of nonuniform internal heating in Triton's energy budget N92-10736
Physical properties of cryovolcanic brines: Applications to the evolution of Ganymede N92-10737
The magnesium sulfate-water system at pressures to 4 kilobars N92-10738
Tectonic deformation on icy satellites: A model of compensating horsts N92-10763
Mimas: Tectonic structure and geologic history N92-10764
Tethys geology and tectonics revisited N92-10765
The strength of Miranda's lithosphere N92-10767
Theoretical studies of volatile processes in the outer solar system N92-10807
Radar backscattering by the icy Galilean satellites and the radar glory effect N92-10850
Regoliths of icy satellites: The coherent backscatter model N92-10851
IDENTIFYING
Identification of nonlinear times series from first order cumulative characteristics
[AD-A239822] N92-10350
IGNEOUS ROCKS
The probable continuum between emplacement of plutons and mare volcanism in lunar crustal evolution N92-10794
Infrared reflectance spectra (4-12 micron) of lunar samples N92-10812
IGNITION
Combustion and safety of solid propellant rocket motors N92-10110
Optical and electrical investigations into cathode ignition and diode closure
[DE91-017823] N92-10191
ILMENITE
On using a pyroclastic deposit as a manned lunar base site N92-10797
IMAGE ANALYSIS
Passive range estimation for rotorcraft low-altitude flight
[NASA-TM-103897] N92-10003
Recording of urban land use by high altitude photography: The Munich (Fed. Republic of Germany) exampl N92-10211
Image evaluation of high altitude photographs. Examples: Boston and Foster City (US) N92-10213
Optical correlators in texture analysis N92-10450
IMAGE CORRELATORS
A miniature acousto-optic image correlator
[DE91-018002] N92-10151
IMAGE PROCESSING
Composite video and graphics display for multiple camera viewing system in robotics and teleoperation
[NASA-CASE-NPO-17836-1-CU] N92-10126
A digital ASIC implementation of a video filter for synthetic aperture radar
[DE91-018400] N92-10131
A 500 MHz phase generator for synthetic aperture radar waveform synthesizers
[DE91-018399] N92-10136
Continuation of research into language concepts for the mission support environment: Source code
[NASA-CR-187816] N92-10303
Normalization of correlations
[DE91-018398] N92-10324
Optical correlators in texture analysis N92-10450
Image retrieval and processing system version 2.0 development work N92-10930
Compositional variability of the Martian surface N92-10931
IMAGE RESOLUTION
A miniature acousto-optic image correlator
[DE91-018002] N92-10151
IMAGERY
A miniature acousto-optic image correlator
[DE91-018002] N92-10151
IMAGING SPECTROMETERS
Integration of magnetoencephalography and magnetic resonance imaging N92-10540
The perplexing continuum slope of Mars: Effects of thin ferric coatings and viewing geometry N92-10816
IMAGING TECHNIQUES
Use of In-111 in quantitative SPECT N92-10544
Remote sensing and geologic studies of the orientale basin region N92-10809
Surface scattering properties estimated from modeling airborne multiple emission angle reflectance data N92-10841
Digital cartography of Io N92-10927
IMPACT DAMAGE
Properties of three graphite/toughened resin composites
[NASA-TP-3102] N92-10067
Quantitative nondestructive evaluation of materials and structures
[NASA-CR-188975] N92-10071
The spatial distribution and time evolution of impact-generated magnetic fields N92-10878
IMPACT LOADS
Properties of three graphite/toughened resin composites
[NASA-TP-3102] N92-10067
Atmospheric effects on oblique impacts N92-10856
IMPACT MELTS
Melt droplet formation in energetic impacts N92-10869
Production of impact melt in craters on Venus, Earth, and the moon N92-10870
Chemical fractionation of siderophile elements in impactites from Australian meteorite craters N92-10875
IMPACT RESISTANCE
An experimental evaluation of the impact resistance of recoated F-16A monolithic polycarbonate flat sheet
[AD-A239984] N92-10101
IMPACT TESTS
Properties of three graphite/toughened resin composites
[NASA-TP-3102] N92-10067
Corrosion tests of meshes in carbon fiber laminates: Impact beam tests
[INFORME-I-522/90] N92-10068
Quantitative nondestructive evaluation of materials and structures
[NASA-CR-188975] N92-10071
Atmospheric effects on oblique impacts N92-10856
Impact and collisional processes in the solar system N92-10932
IMPACTORS
Low pressure impactor with electrical concentration detection N92-10534
Energy coupling in catastrophic collisions N92-10862
IMPLANTATION
Impact and collisional processes in the solar system N92-10932
IMPULSES
The hazard of exposure to impulse noise as a function of frequency, volume 1
[AD-A239992] N92-10611
IMPURITIES
Ground state properties of a He-3 impurity in liquid He-4 monolayers
[AD-A239993] N92-10078
Effective mass and excitation spectrum of He-3 impurities in superfluid He-4 N92-10477
Photoemission in YbCu2Si2: Problems with the Kondo impurity model
[DE91-018018] N92-10684
INCIDENT RADIATION
The normal incidence grating inverse photoemission spectrometer in the energy range 8-28 eV N92-10516
INCLINATION
Bending waves and orbital inclinations N92-10894
INCOHERENT SCATTER RADAR
Observations of semidiurnal atmospheric tides using the EISCAT incoherent scatter radar N92-10560
INCOHERENT SCATTERING
The structure and dynamics of the polar mesosphere investigated with the EISCAT radar systems N92-10368
INCOMPRESSIBLE FLOW
Numerical simulation of vortex breakdown
[ONERA-RSF-6/4368-AY-008A] N92-10162
Numerical analysis of fully developed laminar flow in curved rectangular channels
[NAL-TR-1111] N92-10166
RIPPLE: A new model for incompressible flows with free surfaces
[DE91-017830] N92-10168
INCOMPRESSIBLE FLUIDS
Numerical simulation of vortex breakdown by solving the Euler equations for an incompressible fluid N92-10163
INDEXES (DOCUMENTATION)
Index to 1987 NASA Tech Briefs, volume 11, numbers 1-10
[NASA-TM-105024] N92-10717
Index to 1988 NASA Tech Briefs, volume 12, numbers 1-11
[NASA-TM-105077] N92-10718
Index to 1989 NASA Tech Briefs, volume 13, numbers 1-12
[NASA-TM-105109] N92-10719
Index to 1990 NASA Tech Briefs, volume 14, numbers 1-12
[NASA-TM-105110] N92-10720
Cumulative index to NASA Tech Briefs, 1976-1980, volumes 1-5
[NASA-TM-89327] N92-10721
Cumulative index to NASA Tech Briefs, 1981-1985, volumes 6-10
[NASA-TM-89326] N92-10722
INDICATING INSTRUMENTS
Novel type of cryogenic liquid level sensor with high sensitivity N92-10528

INDICATORS
Novel type of cryogenic liquid level sensor with high sensitivity N92-10528
INDIUM ALLOYS
OMVPE growth of InAsSbBi and related alloys using new organometallic group V sources
[AD-A239939] N92-10703
INDIUM ARSENIDES
The influence of growth conditions on the composition of GaInAsP grown by gas-source molecular beam epitaxy N92-10491
INDIUM ISOTOPES
Use of in-111 in quantitative SPECT N92-10544
INDIUM PHOSPHIDES
Beryllium doping of InP grown by gas-source molecular beam epitaxy N92-10489
Interface effects on electrical properties of high purity InP grown by gas-source molecular beam epitaxy N92-10490
The influence of growth conditions on the composition of GaInAsP grown by gas-source molecular beam epitaxy N92-10491
InP solar cells grown by gas-source molecular beam epitaxy N92-10531
INDUCTANCE
Analysis of loss for inductive strips in finline
[AD-A239947] N92-10156
INDUCTION HEATING
Kinetic gas and electron temperatures in RF induction plasma N92-10460
INELASTIC SCATTERING
The A Experimental Division (of the Werner Heisenberg Institute for Physics) N92-10590
Scale dependence of Lambda sub (MS bar) from deep inelastic scattering
[RAL-91-044] N92-10614
Theoretical and experimental studies of elementary particles
[DE91-018285] N92-10630
Inclusive quasielastic and deep inelastic electron scattering at high energies
[DE91-018755] N92-10633
INERTIAL CONFINEMENT FUSION
The Magnetically Insulated Inertial Confinement Fusion: A novel approach
[DE91-018273] N92-10660
INFORMATION DISSEMINATION
INFOTECH '91: DOE Technical Infomation (TI) Meeting
[DE91-018074] N92-10713
INFORMATION FLOW
IID: An intelligent information dictionary for managing semantic metadata
[AD-A240022] N92-10715
Information flow in quantum mechanics: The quantum Maxwell demon
[DE91-017659] N92-10725
INFORMATION MANAGEMENT
Feasibility of using a knowledge-based system concept for in-flight primary flight display research
[NASA-TM-4279] N92-10017
Introduction to the Personal Access Satellite System study N92-10117
Management issues at the National Aeronautics and Space Administration
[GAO/T-NSIAD-91-48] N92-10710
INFOTECH '91: DOE Technical Infomation (TI) Meeting
[DE91-018074] N92-10713
INFORMATION PROCESSING (BIOLOGY)
Test anxiety and post processing interference, 2
[AD-A239819] N92-10283
INFORMATION RETRIEVAL
MANPRINT reference retrieval system (user's guide)
[AD-A239915] N92-10714
INFORMATION SYSTEMS
Aeronautical engineering: A continuing bibliography with indexes (supplement 267)
[NASA-SP-7037(267)] N92-10001
Telescience testbed pilot program, volume 1: Executive summary
[NASA-CR-188833] N92-10031
Telescience testbed pilot program, volume 3: Experiment summaries
[NASA-CR-188834] N92-10032
Telescience testbed pilot program, volume 2: Program results
[NASA-CR-188835] N92-10033
The EH safety representative information system on the safety performance measurement system is where you will find... Word processing and helps with a V-PLUS
[DE91-018709] N92-10113
Functional description for the Mapping And Graphic Information Capability (MAGIC)
[AD-A239436] N92-10305
INFOTECH '91: DOE Technical Infomation (TI) Meeting
[DE91-018074] N92-10713
INFORMATION THEORY
INFOTECH '91: DOE Technical Infomation (TI) Meeting
[DE91-018074] N92-10713
INFORMATION TRANSFER
Possibilities of producing land use information for city regional area planning by high altitude photographs, taking south west Munich (Fed. Republic of Germany) regional area as an example N92-10212
MERLIN 2: A computer program to transfer solution data betwwen finite element meshes
[DE91-018130] N92-10321
Multi-gigabit fiber optic wide area network development
[AD-A239850] N92-10642
INFRARED ASTRONOMY
Remote sensing and geologic studies of the terrain northwest of Humorum basin N92-10810
Thermal infrared observations of Mars (7.5-12.8 microns) during the 1990 opposition N92-10951
INFRARED ASTRONOMY SATELLITE
Origin and evolution of the zodiacal dust cloud N92-10886
INFRARED DETECTORS
Radiohydrophysical aerospace research of ocean
[SRI-PR-1749] N92-10272
INFRARED RADIATION
Optical properties of CO2 ice and CO2 snow from ultraviolet to infrared: Application to frost deposits and clouds on Mars N92-10821
Darkening in gas-rich ordinary chondrites: Spectral modelling and implications for the regoliths of ordinary chondrite parent bodies N92-10827
Mapping compositional and particle size variations across Silver Lake Playa: Relevance to analyses of Mars TIR data N92-10842
Meteo and irradiation data during BEST TWO, Mourmelon (Netherlands)
[FEL-90-A368] N92-10966
INFRARED SCANNERS
Mojave remote sensing field experiment N92-10840
INFRARED SPECTRA
The nu(sub 4) and nu(sub 7) bands of CD3CN with coriolis coupling and other resonance perturbations N92-10432
The nu(sub 8) and 2nu(sub 8) bands of CD3CN N92-10433
The infrared rotation-vibration spectrum of C2H2 in the nu(sub 2) + nu(sub 5) band region; l-resonances in the bands nu(sub 2) + nu(sub 5), nu(sub 2) + 2(nu(sub 5)) back arrow nu(sub 5) and nu(sub 1) back arrow nu(sub 5) N92-10434
Analysis of the interacting levels V(sub 9) = 1 and V(sub 10) = 2 of propyne N92-10444
Absorption measurements with an integrating sphere and an FT-IR spectrometer N92-10445
Parsec-scale penetration of UV into molecular clouds: CII 158 micron mapping of W3, NGC 1977, and NGC 2023
[NASA-CR-188969] N92-10615
Infrared reflectance spectra (4-12 micron) of lunar samples N92-10812
Mineralogy of the Martian surface from Mariner 6/7 infrared spectrometer data N92-10814
Infrared (2.08-14 micron) spectra of powered stony meteorites N92-10826
Mapping compositional and particle size variations across Silver Lake Playa: Relevance to analyses of Mars TIR data N92-10842
Derivation of mid-infrared (5-25 microns) optical constraints of some silicates and palagonite N92-10950
Thermal infrared observations of Mars (7.5-12.8 microns) during the 1990 opposition N92-10951
INFRARED SPECTROMETERS
Mineralogy of the Martian surface from Mariner 6/7 infrared spectrometer data N92-10814
Remote sensing observations of Kelso Dunes, California N92-10847
INFRARED TELESCOPES
New spectral observations of Callisto and leading/trailing hemisphere distinctions N92-10839
INFRARED WINDOWS
Chemical synthesis and microstructural toughening of infrared window materials
[AD-A239987] N92-10102
INJECTION
An improved technique for electrolytic colouration of alkali halide crystals N92-10513
INJECTORS
Extended temperature range rocket injector
[NASA-CASE-LEW-14846-1] N92-10054
INLET FLOW
A computational and experimental investigation of a three-dimensional hypersonic scramjet inlet flow field N92-10007
INPUT/OUTPUT ROUTINES
Hardware description ADSP-21020 40-bit floating point DSP as designed in a remotely controlled digital CW Doppler radar
[DE91-018004] N92-10134
INSPECTION
Laser acoustic technology demonstration and equipment field trails
[DE91-018759] N92-10193
Automated eddy current analysis of materials
[NASA-CR-184216] N92-10200
INSULATION
Instrumental design for measurement of surface charge on insulating materials
[DE91-018695] N92-10099
INTEGRAL EQUATIONS
Pion-nucleon sigma-term and the strange quark content of the proton N92-10396
INTEGRATED CIRCUITS
A 500 MHz phase generator for synthetic aperture radar waveform synthesizers
[DE91-018399] N92-10136
Efficient, high-speed, monolithic optoelectronic circuits using quantum-confined structures
[AD-A239841] N92-10155
Development of double-sided silicon strip detectors N92-10414
INTEGRATED OPTICS
Glass sample characterization
[NASA-CR-184230] N92-10088
Reconfigurable optical interconnections by acousto-optic holograms N92-10449
Waveguide Dammann gratings and kinoforms N92-10458
INTERACTING GALAXIES
N-body simulations of interacting galaxies N92-10579
INTERACTIONAL AERODYNAMICS
Airframe noise N92-10605
INTERATOMIC FORCES
Helium in silicon: A first principle molecular dynamics study N92-10473
Interatomic interactions in the local density approximation N92-10487
INTERFACES
Superfluid interfaces in liquid He-3: Superconducting cosmic domain walls in the laboratory N92-10478
INTERFACIAL TENSION
RIPPLE: A new model for incompressible flows with free surfaces
[DE91-017830] N92-10168
BES Welding Science Contractors summary report, 1990--1991
[DE91-018510] N92-10198
INTERFEROMETERS
Laser interferometer (TENKO-10 and -100) for gravitational wave antenna development
[ISAS-640] N92-10189
Recovering signals from optical fiber interferometric sensors
[AD-A240062] N92-10644
INTERFEROMETRY
Single-shot spectral measurements of multimode pulsed dye lasers N92-10452
INTERMITTENCY
Intermittency studies in proton-antiproton collisions at square root of S = 630 GeV
[CERN-PPE/90-153] N92-10387
INTERNAL ENERGY
The role of nonuniform internal heating in Triton's energy budget N92-10736
INTERNAL FRICTION
Internal friction associated with interaction between carbon atoms and dislocations at low temperature N92-10471
INTERNATIONAL COOPERATION
Worldnet
[NASA-CR-188845] N92-10711
INTERPLANETARY DUST
Clay minerals in primitive meteorites and interplanetary dust 2. Smectites and micas N92-10252
Clay minerals in primitive meteorites and interplanetary dust 1 N92-10256
INTERPLANETARY MAGNETIC FIELDS
The extension of solar magnetic fields into interplanetary space
[DE91-018052] N92-10970
INTERPLANETARY MEDIUM
The extension of solar magnetic fields into interplanetary space
[DE91-018052] N92-10970

INTERPLANETARY SPACE
The extension of solar magnetic fields into interplanetary space
[DE91-018052] N92-10970
INTERPROCESSOR COMMUNICATION
BIRD: A general interface for sparse distributed memory simulators
[NASA-CR-188858] N92-10292
INTERSTELLAR GAS
Collision probabilities in the presence of nebular gas drag N92-10898
INTERSTELLAR MATTER
Parsec-scale penetration of UV into molecular clouds: CII 158 micron mapping of W3, NGC 1977, and NGC 2023
[NASA-CR-188969] N92-10615
INTRUSION
Igneous intrusion models for floor fracturing in lunar craters N92-10876
INVARIANCE
Geometric phase, rotational transforms and adiabatic invariants in toroidal magnetic fields
[DE91-018419] N92-10667
INVERSIONS
Abel inversion with the fast Fourier transform N92-10379
INVISCID FLOW
Numerical analysis and simulation of an assured crew return vehicle flow field
[NASA-TP-3101] N92-10161
Stability of the flow around a cylinder: The spin-up problem
[NASA-CR-187636] N92-10171
IO
Fluid dynamics of multiphase flow in volcanic environments on the Earth, Io, and other planets N92-10740
SO2-rich equatorial basins and epeirogeny of Io N92-10761
Digital cartography of Io N92-10927
Tidal evolution of planetary satellites N92-10953
IODIDES
The rotational structure of the nu(sub 6) vibration band of CH3I N92-10431
IODINE
A simple method to stabilize the frequency of semiconductor lasers N92-10453
ION ACCELERATORS
Status of the JYFL-ECR ion source N92-10422
Numerical simulation of ion beam generated in the diode with anode plasma column
[IPPCZ-306] N92-10652
ION ATOM INTERACTIONS
Experimental study of interactions of highly charged ions with atoms at keV energies
[DE91-016962] N92-10616
Atomic physics of strongly correlated systems
[DE91-012259] N92-10617
ION BEAMS
Instrumental design for measurement of surface charge on insulating materials
[DE91-018695] N92-10099
Numerical simulation of ion beam generated in the diode with anode plasma column
[IPPCZ-306] N92-10652
ION CYCLOTRON RADIATION
Ionospheric and magnetospheric processes
[AD-A239967] N92-10263
Plan for the JYFL gas-filled recoil separator N92-10424
Observation of plasma toroidal rotations driven by the electric field due to a loss of ions
[NIFS-23] N92-10647
Fast wave heating at intermediate ion cyclotron harmonics on the JIPP T-II U tokamak
[NIFS-21] N92-10649
ION DISTRIBUTION
The field drift of ions and its influence on the electrical properties of SnO2 N92-10492
ION IMPLANTATION
Thermal helium desorption facility in Jyvaskyla (Finland) N92-10464
Formation of small metallic precipitates of niobium in (alpha)-Al2O3 implanted with Nb ions
[DE91-015928] N92-10678
High-temperature implantation of Au into Ni
[DE91-017304] N92-10682
ION MOTION
The field drift of ions and its influence on the electrical properties of SnO2 N92-10492
Ion mobility spectrometer to trace gas analysis N92-10535
ION PROPULSION
Experimental investigation of a 12 cm diameter Kaufman xenon ion thruster
[NAL-TR-1099] N92-10056
ION SOURCES
Status of the JYFL-ECR ion source N92-10422
Dependence of Au(-) production upon the target work function in a plasma-sputter-type negative ion source
[NIFS-85] N92-10656
ION STRIPPING
Ion-Guide Quadrupole Mass Spectrometer (IGQMS) N92-10417
IONIC COLLISIONS
Experimental study of interactions of highly charged ions with atoms at keV energies
[DE91-016962] N92-10616
Atomic physics of strongly correlated systems
[DE91-012259] N92-10617
IONIZATION
Definition and measurement at high temperatures of pH
[DE91-017945] N92-10077
Isotope selective resonance ionization measurements of lithium N92-10442
Thermal helium desorption facility in Jyvaskyla (Finland) N92-10464
Super Coster Kronig and resonance super Coster Kronig spectra of solid Ge around 3p-ionization threshold N92-10517
The effect of latitudinally varying solar wind flux on the Lyman alpha sky background N92-10570
The response history Monte Carlo method for electron transport
[DE91-018295] N92-10631
IONIZATION CROSS SECTIONS
Krypton 4p,4s and 3d partial photoionization cross sections below 260 eV photon energy N92-10429
Relaxation and final-state correlation effects in the 3p and 3s photoionization of Ar, K(+), and Ca(++) N92-10430
IONOSPHERES
Ionospheric and magnetospheric processes
[AD-A239967] N92-10263
IONOSPHERIC HEATING
Plasma Physics Research Institute, Lawrence Livermore National Laboratory, University of California, Davis annual report for fiscal year 1989
[DE91-018490] N92-10669
IONOSPHERIC PROPAGATION
On the ionospheric influence upon the spectral structure on the Pc1 geomagnetic pulsations N92-10552
IONOSPHERIC TEMPERATURE
Theoretical estimation of the vibrational temperatures of N2 molecules in the ionosphere and in the laboratory simulated plasma
[ISAS-642] N92-10258
IONS
Performance tests of ERNE HED sensor N92-10562
Atomic physics of strongly correlated systems
[DE91-012259] N92-10617
Dynamic screening and wake effects on electronic excitation in ion-solid and ion-surface collisions
[DE91-018224] N92-10687
Physics Division annual review, April 1, 1990 - March 31, 1991
[DE91-018704] N92-10707
Composition and energetics of solar flare particle events measured by satellites, 1989 - 1991
[DE91-018028] N92-10969
IRON
The perplexing continuum slope of Mars: Effects of thin ferric coatings and viewing geometry N92-10816
Oxidation of basaltic tephras: Influence on reflectance in the 1 micron region N92-10817
Pre-terrestrial oxidation products in carbonaceous meteorites identified by Mossbauer spectroscopy N92-10824
IRON ALLOYS
Evaluation of advanced austenitic alloys relative to alloy design criteria for steam service
[DE91-017800] N92-10081
Transport properties and oxidation in chromium and Fe-Cr alloys exposed to oxygen at high temperatures
[DE91-018571] N92-10086
Microstructural stability and creep response of a new Al-Fe-W-Si alloy
[AD-A239861] N92-10087
IRON COMPOUNDS
The shape effect of magnetic damages in irradiated Nd2Fe14B-permanent magnets N92-10468
IRON ISOTOPES
Gamma echo experiments N92-10512
IRON OXIDES
Clays on Mars: Review of chemical and mineralogical evidence N92-10250
Transformation products of submicron-sized aluminum-substituted magnetite: Color and reductant solubility N92-10251
IRRADIATION
On acceleration of charged particles in intensity minima of laser fields
[IPPCZ-307] N92-10653
Charged-particle induced alterations of surfaces in the outer solar system N92-10838
ISCHEMIA
Physiologic Transection of the brain stem in healthy humans and the neurologic basis of unconsciousness
[AD-A240122] N92-10023
ISING MODEL
Ferromagnetism in small clusters N92-10508
ISOMERS
Isotope selective resonance ionization measurements of lithium N92-10442
Torsional potential for the C(sp2)-C(sp2) bond N92-10443
ISOTOPE EFFECT
Isotope selective resonance ionization measurements of lithium N92-10442
ISOTOPES
Investigations of the effects of isotopic substitution and pressure on miscibility in polymer-polymer and polymer-solvent systems
[DE91-018010] N92-10094
ISOTOPIC LABELING
Studies on superconducting Bi2Sr2Ca(n-1) Cu(n)O(4+2n) compounds with Fe-57 and Eu-151 Moessbauer spectroscopy N92-10504
ISOTOPIC SPIN
High-spin states in Cd-109 N92-10403
Shapes of Cd-110 at high spins N92-10404
Evidence for band termination in Xe-118 N92-10405
ISOTROPIC MEDIA
NMR-relaxation time measurements of noble gas isotope Xe-129 dissolved in isotropic and anisotropic liquids N92-10437
ITERATION
Transformation of two and three-dimensional regions by elliptic systems
[NASA-CR-188982] N92-10170
ITERATIVE SOLUTION
Determining desorption pre-exponential factors from temperature-programmed desorption spectra when the surface is nonuniform
[DE91-009971] N92-10074
Optimization methods in control of electromagnetic fields
[AD-A240044] N92-10144
A general-purpose finite-difference code for solving steady-state three-dimensional fluid-flow and heat transfer problems
[AD-A239857] N92-10175
Globally convergent techniques in nonlinear Newton-Krylov
[NASA-CR-188894] N92-10309
Optimal diffusion synthetic acceleration of discrete ordinates transport calculations
[DE91-015924] N92-10620

J

JAHN-TELLER EFFECT
Structure and optical polarizabilities of small silicon clusters N92-10425
JET AIRCRAFT NOISE
Jet noise classical theory and experiments N92-10602
Noise from turbulent shear flows N92-10603
Jet noise generated by large-scale coherent motion N92-10604
JET ENGINES
Jet noise classical theory and experiments N92-10602
JETS
Jetting and the origin of tektites N92-10868
JFET
Studies on new low noise silicon radiation detector N92-10418
JOINTS (JUNCTIONS)
Bond of reinforcement under controlled confinement
[AD-A240142] N92-10207
JOSEPHSON JUNCTIONS
Langevin dynamics simulations of large frustrated Josephson junction arrays
[DE91-018046] N92-10686
Electrical transport across grain boundaries in bicrystals of YBa2Cu3O7(delta)
[DE91-018588] N92-10697
JUPITER (PLANET)
The stability of the planetary triangular Lagrange points N92-10568
Mapping the stability field of Jupiter Trojans N92-10883

JUPITER SATELLITES
Disk resolved studies of the optical properties and physical nature of the surfaces of the outer planet satellites N92-10837
Surface properties of Galilean satellites from bistatic radar experiments N92-10849

K

KALMAN FILTERS
Passive range estimation for rotorcraft low-altitude flight
[NASA-TM-103897] N92-10003
KAONS
Hadronic equation of state and the onset of kaon condensation N92-10386
KINOFORM
Waveguide Dammann gratings and kinoforms N92-10458
KLYSTRONS
Automatic network analyzer procedures for 5045 klystron cavities
[DE91-018015] N92-10149
KNOWLEDGE BASES (ARTIFICIAL INTELLIGENCE)
Expert systems for superalloy studies
[NASA-CR-184236] N92-10080
Cooperating systems: Layered MAS
[NASA-CR-184232] N92-10332
KNOWLEDGE REPRESENTATION
Expert systems for superalloy studies
[NASA-CR-184236] N92-10080
Methodology for automating software systems
[NASA-CR-184233] N92-10301
KNUDSEN FLOW
Superfluid vortex nucleation in He-3 flow N92-10479
KOLMOGOROFF THEORY
Aerodynamic and gasdynamic effects in cosmogony N92-10892
KONDO EFFECT
Photoemission in YbCu2Si2: Problems with the Kondo impurity model
[DE91-018018] N92-10684
KRYPTON
Decay channels of resonantly excited 2p(-1)ns, md states of Ar and 3d(-1)np states of Kr N92-10426
Krypton 4p,4s and 3d partial photoionization cross sections below 260 eV photon energy N92-10429
KRYPTON FLUORIDE LASERS
Optical and electrical investigations into cathode ignition and diode closure
[DE91-017823] N92-10191

L

LABORATORIES
LLNL contributions to MPD thrusters for SEI N92-10047
LAGRANGIAN EQUILIBRIUM POINTS
The stability of the planetary triangular Lagrange points N92-10568
LAKES
Paleolakes and lacustrine basins on Mars N92-10776
LAMINAR FLOW
Numerical analysis of fully developed laminar flow in curved rectangular channels
[NAL-TR-1111] N92-10166
LAMINATES
Properties of three graphite/toughened resin composites
[NASA-TP-3102] N92-10067
Corrosion tests of meshes in carbon fiber laminates: Impact beam tests
[INFORME-I-522/90] N92-10068
Quantitative nondestructive evaluation of materials and structures
[NASA-CR-188975] N92-10071
Helmet of a laminate construction of polycarbonate and polysulfone polymeric material
[NASA-CASE-MSC-21503-1] N92-10091
LAND ICE
Role of artesian groundwater in forming Martian permafrost features N92-10771
Glacial and marine chronology of Mars N92-10772
LAND USE
Evaluation of high altitude photography for city regional areas
[MGA-A-44] N92-10210
Recording of urban land use by high altitude photography: The Munich (Fed. Republic of Germany) exampl N92-10211
Possibilities of producing land use information for city regional area planning by high altitude photographs, taking south west Munich (Fed. Republic of Germany) regional area as an example N92-10212
LANDFORMS
Dynamic models for ridge belt formation on Venus N92-10731
Strain accommodation beneath structures on Mars N92-10748
Timing and formation of wrinkle ridges in the Tyrrhena Patera Region of Mars N92-10752
A 40th deg and order gravitational field model for Mars N92-10760
Mimas: Tectonic structure and geologic history N92-10764
Chronology of glaciation in the Hellas region of Mars N92-10773
Naming the newly found landforms on Venus N92-10915
The control network of Mercury: April 1991 N92-10916
LANDING SITES
Surface-material maps of Viking landing sites on Mars N92-10787
LANDSAT SATELLITES
Using LANDSAT to provide potato production estimates to Columbia Basin farmers and processors
[NASA-CR-188783] N92-10209
Mojave remote sensing field experiment N92-10840
Remote sensing observations of Kelso Dunes, California N92-10847
LANGEVIN FORMULA
Numerical simulation studies of fluid spreading N92-10482
Langevin dynamics simulations of large frustrated Josephson junction arrays
[DE91-018046] N92-10686
LARGE SPACE STRUCTURES
Development of a model of space station solar array
[NASA-CR-188911] N92-10220
LARMOR RADIUS
The meandering orbit effect on stabilization of the tilting instability in a field-reversed configuration
[NIFS-22] N92-10648
LASER APPLICATIONS
Laser acoustic technology demonstration and equipment field trails
[DE91-018759] N92-10193
A survey of laser lightning rod techniques
[AD-A239988] N92-10269
Epitaxial high T(sub c) superconducting thin films and superlattices deposited by laser albation N92-10505
High T(sub c) superconducting Li-doped Bi-Sr-Ca-Cu-O thin films deposited by laser ablation N92-10506
LASER BEAMS
Doppler shift velocimetry in disperse flows N92-10378
A novel technique for the measurement of photoenhanced electron attachment: Implications for an optically-controlled diffuse discharge opening switch
[DE91-016226] N92-10621
Surface effect on optical bistability in coupled exciton-phonon systems inside a cavity
[AD-A240026] N92-10643
Recovering signals from optical fiber interferometric sensors
[AD-A240062] N92-10644
LASER CAVITIES
Cavity issues for Ni-like Ta x ray lasers
[DE91-017668] N92-10190
LASER DAMAGE
Laser induced optical damage in solids
[AD-A240124] N92-10194
Fundamental studies in the molecular basis of laser induced retinal damage
[AD-A239941] N92-10278
Two informative cases of Q-switched laser eye injury
[AD-A240001] N92-10279
LASER DOPPLER VELOCIMETERS
Dual pin diode preamplifier for laser Doppler velocimetry N92-10382
LASER INDUCED FLUORESCENCE
Remote detection of atmospherically dispersed vegetative cells using fluorescence lidar
[DE91-016077] N92-10218
LASER INTERFEROMETRY
Laser interferometer (TENKO-10 and -100) for gravitational wave antenna development
[ISAS-640] N92-10189
Recovering signals from optical fiber interferometric sensors
[AD-A240062] N92-10644
LASER OUTPUTS
Electron acceleration by laser fields in a gas
[DE91-018269] N92-10192
A novel technique for the measurement of photoenhanced electron attachment: Implications for an optically-controlled diffuse discharge opening switch
[DE91-016226] N92-10621
On acceleration of charged particles in intensity minima of laser fields
[IPPCZ-307] N92-10653
LASER PLASMAS
The Magnetically Insulated Inertial Confinement Fusion: A novel approach
[DE91-018273] N92-10660
LASER PROPULSION
Contractors Meeting in Propulsion
[AD-A240057] N92-10062
LASER SPECTROSCOPY
Fluidized bed combustion diagnostics by laser photocoustic spectroscopy N92-10380
Polarization spectroscopy in OH and flame temperature measurements N92-10454
Electronically resonant CARS spectroscopy of NO2 N92-10455
LASER STABILITY
A simple method to stabilize the frequency of semiconductor lasers N92-10453
LASER TARGETS
Dependence of Au(-) production upon the target work function in a plasma-sputter-type negative ion source
[NIFS-85] N92-10656
LASER WELDING
Proceedings of the Second Switch Tube Advanced Technology Meeting
[DE91-017718] N92-10148
LASERS
Laser acoustic technology demonstration and equipment field trails
[DE91-018759] N92-10193
LATENT HEAT
Characteristics of the Martian atmosphere surface layer N92-10804
LATTICES (MATHEMATICS)
Dynamic lattice computing in general relativity N92-10372
Gluon overlap factors extracted from Monte Carlo lattice calculations N92-10397
Non-unicity of Gibbs states of Czech models in a half-space
[IPPCZ-311] N92-10679
LAUNCH VEHICLES
Test apparatus and tensile properties of LE-7 turbine blade materials in high pressure hydrogen conditions
[NAL-TR-1092] N92-10025
Small upper stage basic program
[AD-A240059] N92-10063
LAVA
Magma generation on Mars: Estimated volumes through time N92-10788
Crystallization during emplacement of lava flows N92-10789
Physical properties of lava flows on the southwest flank of Tyrrhena Patera, Mars N92-10790
Rheological analyses of lava flows on Mars N92-10791
Factors controlling lava dome morphology N92-10792
Lunar and Hawaiian lava tubes: Analogs and uses based on terrestrial field data N92-10796
Mojave remote sensing field experiment N92-10840
LAY-UP
Prediction of matrix fatigue crack initiation in notched SCS-6/Ti-15-3 metal matrix composites
[NASA-TM-104141] N92-10203
LEADING EDGES
Numerical investigation of the effect of leading edge geometry on dynamic stall of airfoils
[AD-A239949] N92-10015
LEARNING
Test anxiety and post processing interference, 2
[AD-A239819] N92-10283
Fear-potentiated startle as a model system for analyzing learning and memory
[AD-A239994] N92-10284
LEAST SQUARES METHOD
Optimal moving grids for time-dependent partial differential equations
[NASA-CR-188850] N92-10344
Early 19th-century least squares calculations in Finland repeated with modern techniques N92-10369
LEAVES
Spectral reflectance of pine and intensity of moose browsing N92-10514
LENSES
Optical signal multiplexer and demultiplexer
[DE91-017836] N92-10640
LEPTONS
Thermal emission of gammas and lepton pairs from quark-gluon plasmas N92-10383

LEVEL (QUANTITY)
Novel type of cryogenic liquid level sensor with high sensitivity N92-10528
LICENSING
Design restrictions and licensing for Petite Amateur Navy Satellite (PANSAT)
[AD-A239951] N92-10041
LIFT
Downwash measurements on a pitching canard-wing configuration
[AD-A239956] N92-10016
Propulsive lift noise N92-10606
LIFTING REENTRY VEHICLES
Numerical analysis and simulation of an assured crew return vehicle flow field
[NASA-TP-3101] N92-10161
LIGHT (VISIBLE RADIATION)
Spectral reflectance of pine and intensity of moose browsing N92-10514
LIGHT CURVE
Photometry of the comet 2060 Chiron N92-10887
LIGHT EMISSION
Examples of VLF emissions recorded in the auroral zone N92-10555
Optical signal multiplexer and demultiplexer
[DE91-017836] N92-10640
LIGHT SCATTERING
Investigations of the effects of isotopic substitution and pressure on miscibility in polymer-polymer and polymer-solvent systems
[DE91-018010] N92-10094
Dual pin diode preamplifier for laser Doppler velocimetry N92-10382
Interaction-induced light scattering as a source of information on properties and interactions of spherical top molecules N92-10439
Contamination study
[NASA-CR-184225] N92-10639
Light scattering by lunar-like particle size distributions N92-10832
LIGHT TRANSMISSION
Transport in heterostructures and devices in microwave and millimeter-wave regimes
[AD-A239943] N92-10142
LIGHTNING
A survey of laser lightning rod techniques
[AD-A239988] N92-10269
Predicting cloud-to-ground lightning with neural networks
[AD-A239989] N92-10270
LINE SHAPE
A new line-narrowing method LOMEP N92-10438
LINE SPECTRA
The remote sensing Loosdrecht Lakes (Netherlands) project
[BCRS-90-29] N92-10215
The rotational structure of the nu(sub 6) vibration band of CH3I N92-10431
Parsec-scale penetration of UV into molecular clouds: CII 158 micron mapping of W3, NGC 1977, and NGC 2023
[NASA-CR-188969] N92-10615
LINEAR ACCELERATORS
Theoretical and experimental studies of elementary particles
[DE91-018285] N92-10630
Advanced photon source: Radiological design considerations
[DE91-018014] N92-10635
LINEAR PREDICTION
A new line-narrowing method LOMEP N92-10438
LINEAR PROGRAMMING
Solving problems under uncertainty
[DE91-017940] N92-10322
LINEAR SYSTEMS
Transformation of two and three-dimensional regions by elliptic systems
[NASA-CR-188982] N92-10170
Globally convergent techniques in nonlinear Newton-Krylov
[NASA-CR-188894] N92-10309
An implementation of the look-ahead Lanczos algorithm for non-Hermitian matrices, part 1
[NASA-CR-188909] N92-10311
An implementation of the look-ahead Lanczos algorithm for non-Hermitian matrices, part 2
[NASA-CR-188910] N92-10312
Parameter identification for nonlinear aerodynamic systems
[NASA-CR-188985] N92-10347
LINEARITY
A new line-narrowing method LOMEP N92-10438
LIQUID CHROMATOGRAPHY
Development and optimization of methodologies for analysis of complex hydrocarbon mixtures
[DE91-017954] N92-10075
LIQUID CRYSTALS
In situ liquid-crystal-polymer fiber reinforced aluminum matrix composite
[AD-A239860] N92-10072
The Kr-83 NMR in probing electric field gradients in thermotropic liquid crystals N92-10435
NMR determination of the Ne-21 quadrupole coupling for neon gas dissolved in liquid crystals N92-10436
Computer simulations on the orientation of molecular hydrogen in liquid crystals N92-10466
Positron lifetime measurements in chiral nematic liquid crystals
[NASA-TP-3122] N92-10677
LIQUID HELIUM
Two-phonon absorption by the real squashing collective mode in superfluid He-3 N92-10474
Mutual friction in superfluid He-3: Effects of bound states in the vortex core N92-10475
Vortex nucleation in rotating superfluid He-3-B N92-10476
Effective mass and excitation spectrum of He-3 impurities in superfluid He-4 N92-10477
Superfluid interfaces in liquid He-3: Superconducting cosmic domain walls in the laboratory N92-10478
Superfluid vortex nucleation in He-3 flow N92-10479
Experiments on the nuclear interactions of pions and electrons
[DE91-017929] N92-10623
LIQUID LEVELS
Novel type of cryogenic liquid level sensor with high sensitivity N92-10528
LIQUID METAL FAST BREEDER REACTORS
Status of Rankine-cycle technology for space nuclear power applications
[DE91-017859] N92-10059
LIQUID METALS
Thermal- and ignition-type steam explosions of single drops of molten aluminum
[DE91-014705] N92-10084
LIQUID PHASES
Molecular dynamics using the tight-binding approximation: Application to liquid silicon N92-10465
Superfluid interfaces in liquid He-3: Superconducting cosmic domain walls in the laboratory N92-10478
LIQUID ROCKET PROPELLANTS
PC programs for the prediction of the linear stability behavior of liquid propellant propulsion systems and application to current MSFC rocket engine test programs, volume 1
[NASA-CR-184228] N92-10042
Extended temperature range rocket injector
[NASA-CASE-LEW-14846-1] N92-10054
LIQUID-LIQUID INTERFACES
Air pulsed plate liquid-liquid extractor simulation
[DE91-018155] N92-10172
LIQUID-SOLID INTERFACES
Molecular dynamics studies of liquid-solid interfaces N92-10462
LITHIUM
Alkali metal carbon dioxide electrochemical system for energy storage and/or conversion of carbon dioxide to oxygen
[NASA-CASE-LEW-14973-1] N92-10222
Li 1s photoionization and photoexcitation with satellites N92-10427
Electrical characterization of Li and N doped ZnSe N92-10493
High T(sub c) superconducting Li-doped Bi-Sr-Ca-Cu-O thin films deposited by laser ablation N92-10506
LITHIUM ISOTOPES
Isotope selective resonance ionization measurements of lithium N92-10442
LITHOSPHERE
Lithosphere physics: Geoelectrics and seismics N92-10551
Interpretation of the northern boundary of Ishtar Terra from Magellan images and altimetry N92-10745
Horizontal stress in planetary lithospheres from vertical processes N92-10746
Modelled and measured strain in mascon basins on the moon N92-10747
Martian seismicity through time from surface faulting N92-10759
The strength of Miranda's lithosphere N92-10767
The width of fault zones in a brittle-viscous lithosphere: Strike-slip faults N92-10944
LOADS (FORCES)
Dual strain gage balance system for measuring light loads
[NASA-CASE-LAR-14419-1] N92-10185
Horizontal stress in planetary lithospheres from vertical processes N92-10746
LOCAL AREA NETWORKS
Management of the Space Station Freedom onboard local area network
[NASA-TM-104741] N92-10036
A model for a data acquisition solution for a medium size accelerator laboratory N92-10376
LOGIC CIRCUITS
Reconfigurable fuzzy cell
[NASA-CASE-MSC-21613-1] N92-10331
Gate matrix optimization using simulated annealing N92-10374
LOGISTICS
A mathematical model for a paired comparison experiment on a continuum of response
[AD-A239858] N92-10351
LONG TERM EFFECTS
Sea-level rise: Regional consequences and responses N92-10231
LOW ALTITUDE
Passive range estimation for rotorcraft low-altitude flight
[NASA-TM-103897] N92-10003
LOW FREQUENCIES
New observations of the low frequency interplanetary radio emissions
[NASA-CR-188917] N92-10971
LOW PRESSURE
An analysis of the frequency characteristics of corona discharge at low pressure
[AD-A239940] N92-10674
LOW SPEED
Dynamics of low velocity collisions of ice particle, coated with frost N92-10902
LOW TEMPERATURE
Wettability of low temperature solder alloys for step-soldering
[DE91-018348] N92-10083
Internal friction associated with interaction between carbon atoms and dislocations at low temperature N92-10471
Redistribution of nitrogen atoms and magnetic ordering in Fe-N martensite at low temperatures N92-10472
LOW THRUST PROPULSION
Magnetoplasmadynamic Thruster Workshop
[NASA-CP-10084] N92-10044
LUMINOSITY
Double radio sources as standard rods of testing cosmological models N92-10578
LUNAR BASES
On using a pyroclastic deposit as a manned lunar base site N92-10797
LUNAR CRATERS
Remote sensing and geologic studies of the terrain northwest of Humorum basin N92-10810
Analyses of the lunar surface with advanced remote sensors: Expectations for the 1990's N92-10811
Igneous intrusion models for floor fracturing in lunar craters N92-10876
The history of lunar volcanism N92-10965
LUNAR CRUST
Crustal heterogeneity of the moon viewed from the Galileo SSI camera: Lunar sample calibrations and compositional implications N92-10808
Analyses of the lunar surface with advanced remote sensors: Expectations for the 1990's N92-10811
LUNAR EVOLUTION
The probable continuum between emplacement of plutons and mare volcanism in lunar crustal evolution N92-10794
Analyses of the lunar surface with advanced remote sensors: Expectations for the 1990's N92-10811
The history of lunar volcanism N92-10965
LUNAR EXPLORATION
NEP mission sensitivities N92-10045
LUNAR FAR SIDE
Crustal heterogeneity of the moon viewed from the Galileo SSI camera: Lunar sample calibrations and compositional implications N92-10808
LUNAR GEOLOGY
Lunar and Hawaiian lava tubes: Analogs and uses based on terrestrial field data N92-10796
On using a pyroclastic deposit as a manned lunar base site N92-10797
Crustal heterogeneity of the moon viewed from the Galileo SSI camera: Lunar sample calibrations and compositional implications N92-10808
Remote sensing and geologic studies of the orientale basin region N92-10809
Remote sensing and geologic studies of the terrain northwest of Humorum basin N92-10810
Analyses of the lunar surface with advanced remote sensors: Expectations for the 1990's N92-10811
Infrared reflectance spectra (4-12 micron) of lunar samples N92-10812
Magnetic effects of large-scale impacts on airless planetary bodies N92-10877
Workshop on Mare Volcanism and Basalt Petrogenesis: Astounding Fundamental Concepts (AFC) Developed Over the Last Fifteen Years --- Author
[NASA-CR-188810] N92-10961

LUNAR LIMB
Lunar western limb pyroclastic deposits N92-10795
LUNAR MANTLE
Exploration of relationships between low-Ti and high-Ti pristine lunar glasses using an armalcolite assimilation model N92-10964
The history of lunar volcanism N92-10965
LUNAR MARIA
Remote sensing and geologic studies of the orientale basin region N92-10809
Remote sensing and geologic studies of the terrain northwest of Humorum basin N92-10810
Igneous intrusion models for floor fracturing in lunar craters N92-10876
Workshop on Mare Volcanism and Basalt Petrogenesis: Astounding Fundamental Concepts (AFC) Developed Over the Last Fifteen Years --- Author [NASA-CR-188810] N92-10961
The violent side of mare volcanism N92-10962
The history of lunar volcanism N92-10965
LUNAR ROCKS
Crustal heterogeneity of the moon viewed from the Galileo SSI camera: Lunar sample calibrations and compositional implications N92-10808
Remote sensing and geologic studies of the orientale basin region N92-10809
Infrared reflectance spectra (4-12 micron) of lunar samples N92-10812
Exploration of relationships between low-Ti and high-Ti pristine lunar glasses using an armalcolite assimilation model N92-10964
The history of lunar volcanism N92-10965
LUNAR SOIL
Infrared reflectance spectra (4-12 micron) of lunar samples N92-10812
Light scattering by lunar-like particle size distributions N92-10832
LUNAR SURFACE
Modelled and measured strain in mascon basins on the moon N92-10747
Lunar and Hawaiian lava tubes: Analogs and uses based on terrestrial field data N92-10796
On using a pyroclastic deposit as a manned lunar base site N92-10797
Analyses of the lunar surface with advanced remote sensors: Expectations for the 1990's N92-10811
Infrared reflectance spectra (4-12 micron) of lunar samples N92-10812
Oxidation of basaltic tephras: Influence on reflectance in the 1 micron region N92-10817
High resolution lunar radar studies: Preliminary results N92-10845
Possible misinterpretation of lunar cratering record in Voyager team analyses of outer planet satellites N92-10860
Large impacts and climatic catastrophes on the early Earth N92-10865
Igneous intrusion models for floor fracturing in lunar craters N92-10876
A unified lunar control network: April 1991 N92-10917
Wrinkle ridge-upland scarp transitions: Implications for the mechanical properties of the deformed materials N92-10954
LUNAR TOPOGRAPHY
Lunar western limb pyroclastic deposits N92-10795
LYMAN ALPHA RADIATION
The effect of latitudinally varying solar wind flux on the Lyman alpha sky background N92-10570
LYMAN SPECTRA
Energy partitioning in elementary gas phase reactions [DE91-017783] N92-10627

M

MACH NUMBER
The measurement of plate vibration and sound radiation from a turbulent boundary layer manipulator [AD-A240127] N92-10206
MAGELLAN SPACECRAFT (NASA)
Venus behind the clouds N92-10569
Impact craters on Venus N92-10852
Venus impact craters: Implications for atmospheric and resurfacing processes from Magellan observations N92-10854
Breakup of meteoroids in the Venusian atmosphere and its effects on crater formation N92-10855
MAGMA
Magma generation on Mars: Estimated volumes through time N92-10788
Crystallization during emplacement of lava flows N92-10789
Physical properties of lava flows on the southwest flank of Tyrrhena Patera, Mars N92-10790
Factors controlling lava dome morphology N92-10792
Reflectance spectra of Fe(2+)-Mg(2+) disordered pyroxenes: Implications to remote-sensed spectra of planetary surfaces N92-10823
Factors controlling the structures of magma chambers in basaltic volcanoes N92-10957
Workshop on Mare Volcanism and Basalt Petrogenesis: Astounding Fundamental Concepts (AFC) Developed Over the Last Fifteen Years --- Author [NASA-CR-188810] N92-10961
Exploration of relationships between low-Ti and high-Ti pristine lunar glasses using an armalcolite assimilation model N92-10964
The history of lunar volcanism N92-10965
MAGNESIUM CELLS
Performance characterization of magnesium/manganese dioxide batteries [AD-A240037] N92-10158
MAGNESIUM OXIDES
Chemisorption of CO on Mg-O/Co(0001) N92-10484
MAGNESIUM SULFATES
Physical properties of cryovolcanic brines: Applications to the evolution of Ganymede N92-10737
The magnesium sulfate-water system at pressures to 4 kilobars N92-10738
MAGNET COILS
Status of the Repetitive High Energy Pulsed Power Project [DE91-018359] N92-10152
MAGNETIC COILS
Magnetic field settings for the K130 cyclotron N92-10421
MAGNETIC COMPRESSION
Status of the Repetitive High Energy Pulsed Power Project [DE91-018359] N92-10152
Strong magnetic compression of spin-polarized hydrogen N92-10480
MAGNETIC DISKS
Magneto-optical disk as a CD-ROM development tool [DE91-009973] N92-10296
MAGNETIC DISTURBANCES
Energy-latitude dispersion of energetic ions in the dayside of the Earth's magnetosphere: A substorm-related phenomenon N92-10558
MAGNETIC EFFECTS
Geometrical effects of the magnetic field on the neoclassical flow, current, and rotation in general toroidal systems [NIFS-86] N92-10655
Magnetic effects of large-scale impacts on airless planetary bodies N92-10877
The ring arcs of Neptune N92-10945
MAGNETIC FIELD CONFIGURATIONS
Vlasov-Maxwell system: 2-D equilibria, reversed field pinches [DE91-018421] N92-10595
Single particle and fluid picture for the ponderomotive drift in nonuniform plasmas [NIFS-25] N92-10645
The meandering orbit effect on stabilization of the tilting instability in a field-reversed configuration [NIFS-22] N92-10648
Geometrical effects of the magnetic field on the neoclassical flow, current, and rotation in general toroidal systems [NIFS-86] N92-10655
Geometric phase, rotational transforms and adiabatic invariants in toroidal magnetic fields [DE91-018419] N92-10667
MAGNETIC FIELDS
The short-circuited fluxgate sensitivity parameters [ISSN-0109-6605] N92-10147
Study of muon triggers and momentum reconstruction in a strong magnetic field for a muon detector at LHC N92-10413
Magnetic field settings for the K130 cyclotron N92-10421
Magneto-optical transitions in a Coulomb coupled pair of quantum dots N92-10494
Dynamics of vortices in high-temperature superconductors N92-10501
Beat wave current drive experiment on DDT [DE91-017407] N92-10622
On ponderomotive force effects on coupling of the LH and IBW grills for the FTU tokamak [IPPCZ-305] N92-10650
The Magnetically Insulated Inertial Confinement Fusion: A novel approach [DE91-018273] N92-10660
Geometric phase, rotational transforms and adiabatic invariants in toroidal magnetic fields [DE91-018419] N92-10667
Langevin dynamics simulations of large frustrated Josephson junction arrays [DE91-018046] N92-10686
Anomalous neutron scattering from the flux-line lattice in K(0.6)Ba(0.4)BiO3 [DE91-018233] N92-10691
Anisotropic twin boundary pinning in YBa2Cu3O(x) [DE91-018536] N92-10692
Reversible magnetization of Bi2Sr2CaCu2O8 single crystals [DE91-018600] N92-10699
Magnetic effects of large-scale impacts on airless planetary bodies N92-10877
The spatial distribution and time evolution of impact-generated magnetic fields N92-10878
Generation and behavior of solar system magnetic fields N92-10939
The ring arcs of Neptune N92-10945
MAGNETIC FLUX
The shape effect of magnetic damages in irradiated Nd2Fe14B-permanent magnets N92-10468
Dynamics of vortices in high-temperature superconductors N92-10501
An overview of modern permanent magnet design [AD-A240144] N92-10597
The extension of solar magnetic fields into interplanetary space [DE91-018052] N92-10970
MAGNETIC MATERIALS
UV, visible, and near-IR reflectivity data for magnetic soils/rocks from Brazil N92-10254
An overview of modern permanent magnet design [AD-A240144] N92-10597
MAGNETIC PROBES
Plasma cloud behavior [AD-A240000] N92-10264
MAGNETIC PROPERTIES
UV, visible, and near-IR reflectivity data for magnetic soils/rocks from Brazil N92-10254
Redistribution of nitrogen atoms and magnetic ordering in Fe-N martensite at low temperatures N92-10472
Photoinduced superconductivity in films of YBaCuO N92-10502
Neutron diffraction experiments on nuclear magnetic order in copper N92-10507
Ferromagnetism in small clusters N92-10508
Antiferromagnetic ordering in silver at picoKelvin temperatures N92-10509
Electronic and magnetic properties of strongly correlated systems [DE91-018205] N92-10690
MAGNETIC RELAXATION
Initial magnetization and magnetic relaxation in a single crystal of Bi2Sr2CaCu2O(x) [DE91-018537] N92-10693
MAGNETIC RESONANCE
Integration of magnetoencephalography and magnetic resonance imaging N92-10540
MAGNETITE
Transformation products of submicron-sized aluminum-substituted magnetite: Color and reductant solubility N92-10251
Degradation of Fe-Mg silicates in hot CO2 atmospheres: Applications to Venus N92-10806
MAGNETIZATION
Ferromagnetism in small clusters N92-10508
Initial magnetization and magnetic relaxation in a single crystal of Bi2Sr2CaCu2O(x) [DE91-018537] N92-10693
Reversible magnetization of Bi2Sr2CaCu2O8 single crystals [DE91-018600] N92-10699
Neutron irradiation effects on YBCO single crystals [DE91-018615] N92-10700
Magnetic effects of large-scale impacts on airless planetary bodies N92-10877
MAGNETO-OPTICS
Magneto-optical disk as a CD-ROM development tool [DE91-009973] N92-10296
Magneto-optical transitions in a Coulomb coupled pair of quantum dots N92-10494
Recombination radiation in the fractional quantum Hall effect regime N92-10495
MAGNETOHYDRODYNAMIC FLOW
MPD work at MIT N92-10050
Observations of semidiurnal atmospheric tides using the EISCAT incoherent scatter radar N92-10560
Single particle and fluid picture for the ponderomotive drift in nonuniform plasmas [NIFS-25] N92-10645
Geometrical effects of the magnetic field on the neoclassical flow, current, and rotation in general toroidal systems [NIFS-86] N92-10655

MAGNETOHYDRODYNAMIC GENERATORS
MHD program plan, FY 1991
[DE91-017916] N92-10659
MAGNETOHYDRODYNAMIC STABILITY
Nonlinear interactions of tearing modes in the presence of shear flow
[DE91-018420] N92-10173
The meandering orbit effect on stabilization of the tilting instability in a field-reversed configuration
[NIFS-22] N92-10648
Nonlinear RF processes in plasma
[DE91-017441] N92-10658
VH-mode: A new very high confinement regime in the boronized DIII-D tokamak
[DE91-018186] N92-10662
Ion temperature gradient driven transport in a density modification experiment on the TFTR tokamak
[DE91-018215] N92-10663
Stabilization of the m = 1 tearing mode by resonance detuning
[DE91-018423] N92-10668
Plasma Physics Research Institute, Lawrence Livermore National Laboratory, University of California, Davis annual report for fiscal year 1989
[DE91-018490] N92-10669
MAGNETOHYDRODYNAMIC WAVES
On the ionospheric influence upon the spectral structure on the Pc1 geomagnetic pulsations N92-10552
Inhomogeneity and nonlinearity effects on stop bands of Alfvenic ion cyclotron waves in multicomponent plasma N92-10557
MAGNETOHYDRODYNAMICS
Nonlinear interactions of tearing modes in the presence of shear flow
[DE91-018420] N92-10173
MHD program plan, FY 1991
[DE91-017916] N92-10659
Generation and behavior of solar system magnetic fields N92-10939
MAGNETOMETERS
The short-circuited fluxgate sensitivity parameters
[ISSN-0109-6605] N92-10147
MAGNETOPLASMADYNAMICS
Magnetoplasmadynamic Thruster Workshop
[NASA-CP-10084] N92-10044
The MPD thruster program at JPL N92-10046
LLNL contributions to MPD thrusters for SEI N92-10047
MPD thruster technology N92-10048
Los Alamos NEP research in advanced plasma thrusters N92-10049
MPD work at MIT N92-10050
MPD thruster research issues, activities, strategies N92-10051
Eppdyl: Research focus; past accomplishments; and current research N92-10052
IRS organigram N92-10053
MAGNETOSPHERES
Ionospheric and magnetospheric processes
[AD-A239967] N92-10263
MAGNETOSPHERIC ELECTRON DENSITY
The use of whistlers for magnetospheric diagnostics N92-10554
MAGNETOSPHERIC ION DENSITY
Inhomogeneity and nonlinearity effects on stop bands of Alfvenic ion cyclotron waves in multicomponent plasma N92-10557
Energy-latitude dispersion of energetic ions in the dayside of the Earth's magnetosphere: A substorm-related phenomenon N92-10558
MAGNETS
Neutron diffraction experiments on nuclear magnetic order in copper N92-10507
MAINTENANCE
NASA maintenance: Stronger commitment needed to curb facility deterioration
[GAO/NSIAD-91-34] N92-10709
MAN MACHINE SYSTEMS
A system performance throughput model applicable to advanced manned telescience systems
[NASA-CR-188860] N92-10034
Human performance measurement: Validation procedures applicable to advanced manned telescience systems
[NASA-CR-185447] N92-10282
Modeling reality
[NASA-CR-188881] N92-10307
Worldnet
[NASA-CR-188845] N92-10711
MAN-COMPUTER INTERFACE
Display format, highlight validity, and highlight method: Their effects on search performance
[NASA-TM-104742] N92-10287
TAURUS: An interactive post-processor for the analysis codes NIKE3D, DYNA3D, and TOPAZ3D
[DE91-019012] N92-10326
Control system of the Jyvaskyla (Finland) K130 cyclotron N92-10419
MANAGEMENT INFORMATION SYSTEMS
NASA procurement: Management oversight of contract cost and time changes could be enhanced
[GAO/NSIAD-91-259] N92-10708
MANAGEMENT PLANNING
Differential collision cross-sections for atomic oxygen: Analysis of space flight instruments for solar terrestrial physics
[NASA-CR-184235] N92-10613
Management issues at the National Aeronautics and Space Administration
[GAO/T-NSIAD-91-48] N92-10710
MANAGEMENT SYSTEMS
Management of the Space Station Freedom onboard local area network
[NASA-TM-104741] N92-10036
Modeling of the Space Station Freedom data management system
[NASA-CR-188809] N92-10038
MANGANESE OXIDES
Performance characterization of magnesium/manganese dioxide batteries
[AD-A240037] N92-10158
MANIFOLDS
Extended temperature range rocket injector
[NASA-CASE-LEW-14846-1] N92-10054
MANIFOLDS (MATHEMATICS)
Nonlinear interactions of tearing modes in the presence of shear flow
[DE91-018420] N92-10173
MANNED MARS MISSIONS
NEP mission sensitivities N92-10045
Multi-reactor power system configurations for multimegawatt nuclear electric propulsion
[NASA-TM-105212] N92-10057
Comparison of selected nuclear thermal propulsion concepts
[DE91-017982] N92-10060
MANNED ORBITAL LABORATORIES
Activities report of the Norwegian Space Center
[ETN-91-90052] N92-10029
MANUALS
A generic guide for the preparation of a quality assurance/quality control manual for the design, production, and installation of photovoltaic concentrator systems
[DE91-017716] N92-10223
MANY BODY PROBLEM
Investigations of the structure and electromagnetic interactions of few-body systems
[DE91-017927] N92-10628
MAPPING
Image evaluation of high altitude photographs. Examples: Boston and Foster City (US) N92-10213
Geologic mapping of tunnels using photogrammetry: Camera and target positioning
[DE91-018394] N92-10261
Functional description for the Mapping And Graphic Information Capability (MAGIC)
[AD-A239436] N92-10305
An atlas of optical counterparts of low mass x ray binaries. Part 1: The Northern Sample
[MPE-PREPRINT-195-PT-1] N92-10723
Channeling episodes of Kasei Valles, Mars, and the nature of ridged plains material N92-10779
Geologic history and channeling episodes of the Chryse Planitia region of Mars N92-10782
MAPS
Mars geologic mapping program: Review and highlights N92-10912
Naming the newly found landforms on Venus N92-10915
Planetary atlases N92-10925
Digital cartography of Io N92-10927
Digital solar system geology N92-10928
A new catalog of planetary maps N92-10929
Image retrieval and processing system version 2.0 development work N92-10930
Thermal and albedo mapping of the north and south polar regions of Mars N92-10943
MARIA
The probable continuum between emplacement of plutons and mare volcanism in lunar crustal evolution N92-10794
Lunar western limb pyroclastic deposits N92-10795
Formation of Apollo 14 aluminous mare basalts by replenishment fractional crystallization and assimilation of precursor crust N92-10963
MARINE BIOLOGY
Compilation of 1990 annual reports of the Navy ELF communications system ecological monitoring program. Volume 3: Tabs G thru I
[AD-A239870] N92-10139
MARINER SPACECRAFT
Mineralogy of the Martian surface from Mariner 6/7 infrared spectrometer data N92-10814
MARS (PLANET)
Clays on Mars: Review of chemical and mineralogical evidence N92-10250
Fluid dynamics of multiphase flow in volcanic environments on the Earth, Io, and other planets N92-10740
Martian seismicity through time from surface faulting N92-10759
Evolution of the Martian hydrosphere N92-10768
A Martian global groundwater model N92-10769
Surface-material maps of Viking landing sites on Mars N92-10787
Crystallization during emplacement of lava flows N92-10789
Physical properties of lava flows on the southwest flank of Tyrrhena Patera, Mars N92-10790
Rheological analyses of lava flows on Mars N92-10791
New studies of Martian volcanoes N92-10793
Water on Mars: Clue to accretional history N92-10798
Use of radar to assess aeolian processes N92-10802
Free convection in the Martian atmosphere N92-10803
Characteristics of the Martian atmosphere surface layer N92-10804
Heat flow vs. atmospheric greenhouse on early Mars N92-10805
Remote sensing of the Martian surface N92-10813
Mineralogy of the Martian surface from Mariner 6/7 infrared spectrometer data N92-10814
Composition of Syrtis Major volcanic plateau N92-10815
Spectroscopic analyses of Fe and water in clays: A Martian surface weathering study N92-10818
Water detection at the moon, Mars and comets with a combined neutron gamma ray instrument N92-10819
Spectral evidence for carbonates on Mars: Hydrous carbonates N92-10820
Mojave remote sensing field experiment N92-10840
Preliminary comparison of 3.5-cm and 12.6-cm wavelength continuous wave observations of Mars N92-10848
Preliminary geologic mapping of central Chryse Planitia, Mars N92-10906
Geologic mapping of northern Lunae Planun, Mars N92-10907
Evolution of the east rim of the Hellas basin, Mars N92-10909
Mars geologic mapping program: Review and highlights N92-10912
Planetary geomorphology research: FY 1990-1991 N92-10940
MARS ATMOSPHERE
Free convection in the Martian atmosphere N92-10803
Characteristics of the Martian atmosphere surface layer N92-10804
Heat flow vs. atmospheric greenhouse on early Mars N92-10805
Mineralogy of the Martian surface from Mariner 6/7 infrared spectrometer data N92-10814
Derivation of mid-infrared (5-25 microns) optical constraints of some silicates and palagonite N92-10950
Thermal infrared observations of Mars (7.5-12.8 microns) during the 1990 opposition N92-10951
Properties of dust and clouds in the Mars atmosphere: Analysis of Viking IRTM emission phase function sequences N92-10956
MARS CRATERS
The formation of antipodal-impact terrains on Mars N92-10749
Global relationships between volcanic vents and fractures radial to large impact basins on Mars N92-10750
Tectonic setting of Martian volcanoes and deep-seated intrusives N92-10751
Glacial and marine chronology of Mars N92-10772
Chronology of glaciation in the Hellas region of Mars N92-10773
Ancient fluvial processes in the equatorial highlands of Mars N92-10781
Styles of crater gradation in Southern Ismenius Lacus, Mars N92-10784
MARS ENVIRONMENT
Hydrologic activity during late Noachian and Early Hesperian downwarping of Borealis Basin, Mars N92-10778
MARS PHOTOGRAPHS
Surface-material maps of Viking landing sites on Mars N92-10787

Variable features in the Valles Marineris region of Mars N92-10799
The control network of Mars: April 1991 N92-10918
Mars high-resolution mapping N92-10923
Compositional variability of the Martian surface N92-10931

MARS PROBES
NEP mission sensitivities N92-10045

MARS SURFACE
Clays on Mars: Review of chemical and mineralogical evidence N92-10250
UV, visible, and near-IR reflectivity data for magnetic soils/rocks from Brazil N92-10254
Synthesis and properties of Ti-substituted goethites and hematites N92-10255
Martian seismicity N92-10733
Strain accommodation beneath structures on Mars N92-10748
The formation of antipodal-impact terrains on Mars N92-10749
Global relationships between volcanic vents and fractures radial to large impact basins on Mars N92-10750
Tectonic setting of Martian volcanoes and deep-seated intrusives N92-10751
Timing and formation of wrinkle ridges in the Tyrrhena Patera Region of Mars N92-10752
Compressive strain in Lunae Planum-shortening across wrinkle ridges N92-10753
Late Noachian development of the Coprates rise, Mars N92-10754
Interactions of tectonic, igneous, and hydraulic processes in the North Tharsis Region of Mars N92-10755
Valles Marineris tectonism: Questions and suggestions N92-10756
Extension and strain in Northern Tharsis N92-10757
Valles Marineris, Mars: Are pit chains formed by erosion and troughs by tectonism? N92-10758
Martian seismicity through time from surface faulting N92-10759
A 40th deg and order gravitational field model for Mars N92-10760
Evolution of the Martian hydrosphere N92-10768
A Martian global groundwater model N92-10769
Role of groundwater in formation of Martian channels N92-10770
Role of artesian groundwater in forming Martian permafrost features N92-10771
Glacial and marine chronology of Mars N92-10772
Chronology of glaciation in the Hellas region of Mars N92-10773
Glacial geology of the Hellas region on Mars N92-10774
Terrestrial glacial eskers: Analogs for Martian sinuous ridges N92-10775
Stratigraphy of the layered terrain in Valles Marineris, Mars N92-10777
Hydrologic activity during late Noachian and Early Hesperian downwarping of Borealis Basin, Mars N92-10778
Channeling episodes of Kasei Valles, Mars, and the nature of ridged plains material N92-10779
Flood routing of the Maja outflow across Xanthe Terra N92-10780
Ancient fluvial processes in the equatorial highlands of Mars N92-10781
Geologic history and channeling episodes of the Chryse Planitia region of Mars N92-10782
Styles of crater gradation in Southern Ismenius Lacus, Mars N92-10784
The gradational history of southern Ismenius Lacus N92-10785
Soil crusts on Mars N92-10786
Surface-material maps of Viking landing sites on Mars N92-10787
Magma generation on Mars: Estimated volumes through time N92-10788
Crystallization during emplacement of lava flows N92-10789
Physical properties of lava flows on the southwest flank of Tyrrhena Patera, Mars N92-10790
Rheological analyses of lava flows on Mars N92-10791
New studies of Martian volcanoes N92-10793
Water on Mars: Clue to accretional history N92-10798
Variable features in the Valles Marineris region of Mars N92-10799
Heat flow vs. atmospheric greenhouse on early Mars N92-10805
Remote sensing of the Martian surface N92-10813
Mineralogy of the Martian surface from Mariner 6/7 infrared spectrometer data N92-10814
Composition of Syrtis Major volcanic plateau N92-10815
The perplexing continuum slope of Mars: Effects of thin ferric coatings and viewing geometry N92-10816
Oxidation of basaltic tephras: Influence on reflectance in the 1 micron region N92-10817
Spectroscopic analyses of Fe and water in clays: A Martian surface weathering study N92-10818
Spectral evidence for carbonates on Mars: Hydrous carbonates N92-10820
Optical properties of CO2 ice and CO2 snow from ultraviolet to infrared: Application to frost deposits and clouds on Mars N92-10821
Models of the diffuse radar backscatter from Mars N92-10846
Depth/diameter relationships of fresh craters within Hesperia Planum, Mars N92-10873
Preliminary geologic mapping of Arsia Mons, Mars N92-10905
Preliminary geologic mapping of central Chryse Planitia, Mars N92-10906
Geologic mapping of northern Lunae Planun, Mars N92-10907
Mars geologic mapping: Dao, Harmakhis, and Reull Valles region N92-10908
Evolution of the east rim of the Hellas basin, Mars N92-10909
Geologic mapping of MTM quads 40292 and 40297: In the Utopian lowlands north of the Nilosyrtis Mensae, Mars N92-10910
Mars geologic mapping program: Review and highlights N92-10912
The control network of Mars: April 1991 N92-10918
Publication of topographic atlas and control network of Mars N92-10919
Color-coded global topographic map of Mars N92-10920
Mars elevation distribution N92-10921
Completion of compilation of the 1:2,000,000-scale topographic map series of Mars N92-10922
Mars high-resolution mapping N92-10923
A new edition of the Mars 1:5,000,000 map series N92-10924
CD-ROM publication of the Mars digital cartographic data base N92-10926
Compositional variability of the Martian surface N92-10931
Mud volcanoes on Mars? N92-10938
Thermal and albedo mapping of the north and south polar regions of Mars N92-10943
Derivation of mid-infrared (5-25 microns) optical constraints of some silicates and palagonite N92-10950
Thermal infrared observations of Mars (7.5-12.8 microns) during the 1990 opposition N92-10951
Wrinkle ridge-upland scarp transitions: Implications for the mechanical properties of the deformed materials N92-10954
Wrinkle ridges in the floor material of Kasei Valles, Mars: Nature and origin N92-10955
Preliminary 1:500,000-scale geologic mapping of Claritas Fossae, Mars N92-10959

MARS VOLCANOES
Martian seismicity N92-10733
The formation of antipodal-impact terrains on Mars N92-10749
Global relationships between volcanic vents and fractures radial to large impact basins on Mars N92-10750
Tectonic setting of Martian volcanoes and deep-seated intrusives N92-10751
Timing and formation of wrinkle ridges in the Tyrrhena Patera Region of Mars N92-10752
Interactions of tectonic, igneous, and hydraulic processes in the North Tharsis Region of Mars N92-10755
Extension and strain in Northern Tharsis N92-10757
Martian seismicity through time from surface faulting N92-10759
Stratigraphy of the layered terrain in Valles Marineris, Mars N92-10777
Hydrologic activity during late Noachian and Early Hesperian downwarping of Borealis Basin, Mars N92-10778
Ancient fluvial processes in the equatorial highlands of Mars N92-10781
The gradational history of southern Ismenius Lacus N92-10785
Magma generation on Mars: Estimated volumes through time N92-10788
Physical properties of lava flows on the southwest flank of Tyrrhena Patera, Mars N92-10790
Rheological analyses of lava flows on Mars N92-10791
New studies of Martian volcanoes N92-10793
Composition of Syrtis Major volcanic plateau N92-10815
The perplexing continuum slope of Mars: Effects of thin ferric coatings and viewing geometry N92-10816
Preliminary geologic mapping of Arsia Mons, Mars N92-10905
Mars geologic mapping: Dao, Harmakhis, and Reull Valles region N92-10908
Mud volcanoes on Mars? N92-10938

MARTENSITE
Redistribution of nitrogen atoms and magnetic ordering in Fe-N martensite at low temperatures N92-10472

MASCONS
Modelled and measured strain in mascon basins on the moon N92-10747

MASS DISTRIBUTION
IPC two-color analysis of x ray galaxy clusters [NASA-CR-188980] N92-10724

MASS SPECTROMETERS
Instrumental design for measurement of surface charge on insulating materials [DE91-018695] N92-10099
Ion-Guide Quadrupole Mass Spectrometer (IGQMS) N92-10417

MASS SPECTROSCOPY
Oxide properties of a gamma titanium aluminide: A surface science study [DE91-018024] N92-10095
Instrumental design for measurement of surface charge on insulating materials [DE91-018695] N92-10099

MASSIVELY PARALLEL PROCESSORS
The paradigm compiler: Mapping a functional language for the connection machine [NASA-CR-188839] N92-10290
BIRD: A general interface for sparse distributed memory simulators [NASA-CR-188858] N92-10292
On the suitability of the connection machine for direct particle simulation [NASA-CR-188863] N92-10293
Sparse distributed memory: Principles and operation [NASA-CR-188901] N92-10294
Totally parallel multilevel algorithms for sparse elliptic systems [NASA-CR-188837] N92-10333
Massively parallel computing at Sandia and its application to national defense [DE91-008178] N92-10334
Massively parallel computing and the mid-course tracking problem [DE91-010864] N92-10335

MATERIALS SCIENCE
Materials science and technology centra in Sweden and Denmark: A research policy for the future N92-10580

MATHEMATICAL LOGIC
Activities of the Board on Mathematical Sciences [DE91-017931] N92-10361

MATHEMATICAL MODELS
Gas turbine combuster exit temperature measurement [AD-A239936] N92-10026
A neural network model of the relativistic electron flux at geosynchronous orbit [AD-A239827] N92-10030
The determination of operational and support requirements and costs during the conceptual design of space systems [NASA-CR-188817] N92-10037
Modeling of the Space Station Freedom data management system [NASA-CR-188869] N92-10038
MPD work at MIT N92-10050
Thermal modeling of an epoxy encapsulation process [DE91-017845] N92-10096
Effects of wires on solid propellant ballistics N92-10109
Two-color holography concept (T-CHI) [NASA-CR-184240] N92-10183
Development of a pressure transducer calibration system (dynamic pressure response caliber), phase 2 [AD-A239859] N92-10188
A method for determining spiral-bevel gear tooth geometry for finite element analysis [NASA-TP-3096] N92-10195
Using LANDSAT to provide potato production estimates to Columbia Basin farmers and processors [NASA-CR-188783] N92-10209
Development of a model of space station solar array [NASA-CR-188911] N92-10220
Processes for identifying regional influences of and responses to increasing atmospheric CO2 and climate change: The MINK project [DE91-018603] N92-10243
Regional scale dynamical modelling of biogeochemical processes [AD-A240115] N92-10246

Range reference atmosphere, Nellis Air Force Base, Nevada
[AD-A239816] N92-10262
Fourier component analysis of three Euler-Lagrangian methods applied to the one-dimensional advection-dispersion model
[DE91-017733] N92-10346
Identification of nonlinear times series from first order cumulative characteristics
[AD-A239822] N92-10350
A mathematical model for a paired comparison experiment on a continuum of response
[AD-A239858] N92-10351
Mean estimation in highly skewed samples
[DE91-018513] N92-10358
Detection of abrupt changes in statistical models
[AD-A240116] N92-10360
Quantum world in 2+1 dimensions N92-10365
Early 19th-century least squares calculations in Finland repeated with modern techniques N92-10369
Dromions: The movie N92-10370
Structure and optical polarizabilities of small silicon clusters N92-10425
Coupled wave analysis in inverse grating diffraction problems N92-10456
Modeling the dynamics of molecular films by Monte Carlo simulation N92-10481
Predictions of the electron-hole liquid model for high T(sub c) superconductors N92-10499
Dynamics of vortices in high-temperature superconductors N92-10501
Aerosol dynamics: Binary nucleation N92-10525
Electrostatic precipitator modelling N92-10532
Abatement strategies based on critical loads N92-10533
Theoretical studies of optical phenomena and related inverse problems of solar system bodies N92-10566
Analytical and computational mathematical physics
[DE91-018965] N92-10596
Jet noise generated by large-scale coherent motion N92-10604
Airframe noise N92-10605
Sonic boom N92-10608
Plasma Physics Research Institute, Lawrence Livermore National Laboratory, University of California, Davis annual report for fiscal year 1989
[DE91-018490] N92-10669
Self-consistent modeling of plasma spraying processes
[DE91-018820] N92-10672
Modelling crystal growth: Convection in an asymmetrically heated ampoule
[NASA-CR-184214] N92-10676
Non-unicity of Gibbs states of Czech models in a half-space
[IPPCZ-311] N92-10679
A statistical mechanics study of solid-solid interfaces
[DE91-017852] N92-10689
Thermal models for icy satellites N92-10734
Models of the diffuse radar backscatter from Mars N92-10846
Atmospheric effects on oblique impacts N92-10856
Melt droplet formation in energetic impacts N92-10869
Production of impact melt in craters on Venus, Earth, and the moon N92-10870
Impacts and atmospheric erosion on the early Earth N92-10871
Igneous intrusion models for floor fracturing in lunar craters N92-10876
Thermal modeling of comet Kopff: Implications for the CRAF mission N92-10889
Tidal disruption of inviscid protoplanets N92-10900
A geometrical model for shepherding N92-10901
Planetary ring studies N92-10903
Color-coded global topographic map of Mars N92-10920
Mars elevation distribution N92-10921
Models of planetary rings N92-10934

MATRICES (MATHEMATICS)
On the formulation of a minimal uncertainty model for robust control with structured uncertainty
[NASA-TP-3094] N92-10027
A frequency domain method for the generation of partially coherent normal stationary time domain signals
[DE91-017058] N92-10204
A restricted signature normal form for Hermitian matrices, quasi-spectral decompositions, and applications
[NASA-CR-188895] N92-10310
An implementation of the look-ahead Lanczos algorithm for non-Hermitian matrices, part 1
[NASA-CR-188909] N92-10311
An implementation of the look-ahead Lanczos algorithm for non-Hermitian matrices, part 2
[NASA-CR-188910] N92-10312
Parallel QR factorization on a hypercube using the torus wrap mapping
[DE91-011502] N92-10315
Overview of Krylov subspace methods with applications to control problems
[NASA-CR-188842] N92-10343
Relaxation and final-state correlation effects in the 3p and 3s photoionization of Ar, K(+), and Ca(++) N92-10430
Polarization aberrations. 1: Rotationally symmetric optical systems
[NASA-CR-184218] N92-10638

MATRIX MATERIALS
Poly 1, 2, 4-triazoles via aromatic nucleophilic displacement
[NASA-CASE-LAR-14440-1] N92-10066
Advanced thermoplastic resins, phase 1
[NASA-CR-178402] N92-10069
Chemical synthesis and microstructural toughening of infrared window materials
[AD-A239987] N92-10102

MATRIX METHODS
Tunneling calculations for GaAs-Al(x)Ga(1-x) as graded band-gap sawtooth superlattices
[NASA-TM-100726] N92-10680

MAXIMUM ENTROPY METHOD
A new phase retrieval method for CARS spectrum analysis N92-10363
A new line-narrowing method LOMEP N92-10438

MAXIMUM LIKELIHOOD ESTIMATES
Detection of abrupt changes in statistical models
[AD-A240116] N92-10360

MAXWELL EQUATION
Optimization methods in control of electromagnetic fields
[AD-A240044] N92-10144
A brief introduction to CONDOR
[DE91-018652] N92-10325
Vlasov-Maxwell system: 2-D equilibria, reversed field pinches
[DE91-018421] N92-10595

MEAN SQUARE VALUES
A mathematical model for a paired comparison experiment on a continuum of response
[AD-A239858] N92-10351

MEASURING INSTRUMENTS
Reflection type skin friction meter
[NASA-CASE-LAR-14520-1-SB] N92-10008
Instrumentation and control for space nuclear propulsion
[DE91-018351] N92-10061
Constant frequency pulsed phase-locked loop measuring device
[NASA-CASE-LAR-13823-1] N92-10182
A measuring robot for thermal environment, contaminant concentration and ventilation studies N92-10537
Acoustic device and method for measuring gas densities
[NASA-CASE-NPO-18155-1-CU] N92-10609
Contamination study
[NASA-CR-184225] N92-10639

MECHANICAL DRIVES
Mechanized fluid connector and assembly tool system with ball detents
[NASA-CASE-MSC-21434-1] N92-10197

MECHANICAL PROPERTIES
Advanced thermoplastic resins, phase 1
[NASA-CR-178402] N92-10069
High temperature creep properties of eutectic and near eutectic silver-copper alloys: Application to metal/ceramic joining
[DE91-017987] N92-10082
Examination of mechanical behavior in nanocrystalline materials
[DE91-018552] N92-10085
Wrinkle ridge-upland scarp transitions: Implications for the mechanical properties of the deformed materials N92-10954

MELTING
An assessment of the crustal remelting hypothesis for volcanism in the Freyja Montes deformation zone N92-10732
Martian seismicity N92-10733
Melt droplet formation in energetic impacts N92-10869

MELTING POINTS
High temperature materials characterization
[NASA-CR-184231] N92-10079

MELTS (CRYSTAL GROWTH)
Process modelling for Space Station experiments
[NASA-CR-184227] N92-10112

MEMORY
Test anxiety and post processing interference, 2
[AD-A239819] N92-10283
Fear-potentiated startle as a model system for analyzing learning and memory
[AD-A239994] N92-10284
Synaptic plasticity and memory formation
[AD-A240121] N92-10285

MEMORY (COMPUTERS)
An assessment of the radiation tolerance of large satellite memories in low earth orbits
[DE91-018353] N92-10040
An alternative design for a sparse distributed memory
[NASA-CR-188847] N92-10291
BIRD: A general interface for sparse distributed memory simulators
[NASA-CR-188858] N92-10292
Sparse distributed memory: Principles and operation
[NASA-CR-188901] N92-10294
Measurement of memory access contentions in multiple vector processor systems
[DE91-013205] N92-10297
Content addressable memory project
[NASA-CR-188981] N92-10299

MERCATOR PROJECTION
Color-coded global topographic map of Mars N92-10920
Mars elevation distribution N92-10921
Mars high-resolution mapping N92-10923

MERCURY (PLANET)
The control network of Mercury: April 1991 N92-10916

MESH
Corrosion tests of meshes in carbon fiber laminates: Impact beam tests
[INFORME-I-522/90] N92-10068

MESONS
A search for rare B meson decays at the CERN proton-antiproton collider
[CERN-PPE/91] N92-10389

MESOSCALE PHENOMENA
VERMOD capabilities. VERMOD 1.0 and future
[AD-A239801] N92-10274

MESOSPHERE
The structure and dynamics of the polar mesosphere investigated with the EISCAT radar systems N92-10368

METAL BONDING
BES Welding Science Contractors summary report, 1990--1991
[DE91-018510] N92-10198

METAL COATINGS
The search for low photodesorption coatings
[DE91-017473] N92-10092

METAL CRYSTALS
Surface reconstruction and many-atom models N92-10483

METAL FILMS
Determination of the (1x2) structure of a Pt film on Pd(110) N92-10463

METAL IONS
Formation of small metallic precipitates of niobium in (alpha)-Al2O3 implanted with Nb ions
[DE91-015928] N92-10678

METAL MATRIX COMPOSITES
In situ liquid-crystal-polymer fiber reinforced aluminum matrix composite
[AD-A239860] N92-10072
Prediction of matrix fatigue crack initiation in notched SCS-6/Ti-15-3 metal matrix composites
[NASA-TM-104141] N92-10203

METAL PLATES
Corrosion tests of meshes in carbon fiber laminates: Impact beam tests
[INFORME-I-522/90] N92-10068
Apparatus and method for explosive bonding to edge of flyer plate
[NASA-CASE-LAR-14096-1] N92-10196

METAL SURFACES
In situ liquid-crystal-polymer fiber reinforced aluminum matrix composite
[AD-A239860] N92-10072
Determination of the (1x2) structure of a Pt film on Pd(110) N92-10463
Diffusion anomaly at a surface reconstruction N92-10470

METAL-METAL BONDING
Apparatus and method for explosive bonding to edge of flyer plate
[NASA-CASE-LAR-14096-1] N92-10196

METAL-WATER REACTIONS
Thermal- and ignition-type steam explosions of single drops of molten aluminum
[DE91-014705] N92-10084

METALLIZING
Diamond heat sinks for electronic circuits
[AD-A239750] N92-10145

METALORGANIC CHEMICAL VAPOR DEPOSITION
Heteroepitaxial growth of TiO2, VO2, and TiO2/VO2 multilayers by MOCVD
[DE91-018543] N92-10694
Heteroepitaxy of MOCVD grown TiO2, VO2 films and TiO2/VO2 multilayers on sapphire (1120)
[DE91-018589] N92-10698
METASTABLE STATE
Observation of a monovacancy in the metastable state of the EL2 defect in GaAs by positron annihilation N92-10467
METEORITE COLLISIONS
Mineralogy of Cretaceous/Tertiary boundary clays in the Chicxulub structure in northern Yucatan N92-10253
Martian seismicity through time from surface faulting N92-10759
Impacts and the early environment and evolution of the terrestrial planets N92-10866
Vapor plumes: A neglected aspect of impact cratering N92-10867
Depth/diameter relationships of fresh craters within Hesperia Planum, Mars N92-10873
Asteroid flux and impact cratering rate on Venus N92-10880
Understanding asteroid collisional history through experimental and numerical studies N92-10884
Impact and collisional processes in the solar system N92-10932
METEORITE CRATERS
Impact craters on Venus N92-10852
Venus impact craters: Implications for atmospheric and resurfacing processes from Magellan observations N92-10854
Breakup of meteoroids in the Venusian atmosphere and its effects on crater formation N92-10855
Atmospheric effects on oblique impacts N92-10856
Impact decapitation from laboratory to basin scales N92-10858
Laboratory simulation of cratering on small bodies N92-10859
Characteristics of ejecta and alluvial deposits at Meteor Crater, Arizona and Odessa Craters, Texas: Results from ground penetrating radar N92-10872
The scaling of secondary craters N92-10874
Chemical fractionation of siderophile elements in impactites from Australian meteorite craters N92-10875
Igneous intrusion models for floor fracturing in lunar craters N92-10876
Asteroid flux and impact cratering rate on Venus N92-10880
Impact cratering calculations N92-10933
METEORITES
Clays on Mars: Review of chemical and mineralogical evidence N92-10250
Clay minerals in primitive meteorites and interplanetary dust 1 N92-10256
Physical properties of cryovolcanic brines: Applications to the evolution of Ganymede N92-10737
An infrared reflectance study of low albedo surface constituents N92-10830
Chemical fractionation of siderophile elements in impactites from Australian meteorite craters N92-10875
Meteorite spectroscopy and characterization of asteroid surface materials N92-10881
Impact and collisional processes in the solar system N92-10932
METEORITIC COMPOSITION
Clays on Mars: Review of chemical and mineralogical evidence N92-10250
Does Lafayette = Nakhla? Not necessarily so, based on 4.2K Mossbauer spectra of all of the SNC meteorites N92-10825
Infrared (2.08-14 micron) spectra of powered stony meteorites N92-10826
The bidirectional reflectance spectra of five gas-rich ordinary chondrites N92-10828
Reflectance spectra of some fractions of Migei and Murchison SM chondrites in the range of 0.3-2.6 microns N92-10829
Meteorite spectroscopy and characterization of asteroid surface materials N92-10881
Will Galileo resolve the S-asteroid controversy? N92-10882
Water/rock interactions in experimentally simulated dirty snowball and dirty iceball cometary nuclei N92-10888
METEORITIC MICROSTRUCTURES
Reflectance spectra of some fractions of Migei and Murchison SM chondrites in the range of 0.3-2.6 microns N92-10829
METEOROIDS
Breakup of meteoroids in the Venusian atmosphere and its effects on crater formation N92-10855
METEOROLOGICAL RADAR
The 1990 Airport Surveillance Radar Wind Shear Processor (ASR-WSP) operational test at Orlando International Airport
[AD-A239852] N92-10019
Use of radar to assess aeolian processes N92-10802
METEOROLOGY
A technique for estimating surface meteorological ranges over oceans from satellite measurements of aerosol optical depth
[AD-A239985] N92-10219
Variable features in the Valles Marineris region of Mars N92-10799
METHANE
Interaction-induced light scattering as a source of information on properties and interactions of spherical top molecules N92-10439
Charged-particle induced alterations of surfaces in the outer solar system N92-10838
METHODOLOGY
The Technical Division (of the Werner Heisenberg Institute of Physics) N92-10592
METHYL ALCOHOL
The Alternative Fuels Data Center
[DE91-015003] N92-10111
METHYL COMPOUNDS
The rotational structure of the nu(sub 6) vibration band of CH3I N92-10431
The nu(sub 4) and nu(sub 7) bands of CD3CN with coriolis coupling and other resonance perturbations N92-10432
The nu(sub 8) and 2nu(sub 8) bands of CD3CN N92-10433
Analysis of the interacting levels V(sub 9) = 1 and V(sub 10) = 2 of propyne N92-10444
METHYLENE
Diosmacycloalkanes as models for the formation of hydrocarbons from surface methylenes
[DE91-017854] N92-10065
MICA
Clay minerals in primitive meteorites and interplanetary dust 2. Smectites and micas N92-10252
MICROELECTRONICS
A 500 MHz phase generator for synthetic aperture radar waveform synthesizers
[DE91-018399] N92-10136
MICROGRAVITY APPLICATIONS
Two-color holography concept (T-CHI)
[NASA-CR-184240] N92-10183
MICROPROCESSORS
The application of the ADSP-21020 40-bit floating point DSP microprocessor in a digital Doppler radar
[DE91-018005] N92-10135
MICROSTRIP DEVICES
Analysis of loss for inductive strips in finline
[AD-A239947] N92-10156
The DELPHI microvertex detector, a silicon tracking chamber N92-10412
Development of double-sided silicon strip detectors N92-10414
Radiation damage measurements on double-sided Si strip detectors N92-10415
Beam test results of ion-implanted silicon strip detectors on a 100 mm wafer N92-10416
MICROSTRUCTURE
High temperature creep properties of eutectic and near eutectic silver-copper alloys: Application to metal/ceramic joining
[DE91-017987] N92-10082
Microstructural stability and creep response of a new Al-Fe-W-Si alloy
[AD-A239861] N92-10087
BES Welding Science Contractors summary report, 1990--1991
[DE91-018510] N92-10198
Grain boundaries in nanophase materials
[DE91-018587] N92-10696
MICROWAVE AMPLIFIERS
The 110 GHz ECH heating system for DIII-D
[DE91-018732] N92-10671
Fast-wave ICRF minority-regime heating experiments on the Tore Supra tokamak
[DE91-018866] N92-10673
MICROWAVE COUPLING
Coupling between radiation and gas dynamics
[AD-A240004] N92-10179
MICROWAVE RADIOMETERS
Radiohydrophysical aerospace research of ocean
[SRI-PR-1749] N92-10272
MICROWAVE TRANSMISSION
Personal Access Satellite System (PASS) study. Fiscal year 1989 results
[NASA-CR-188808] N92-10116
Technology assessment and experimentation plan N92-10124
MICROWAVES
Transport in heterostructures and devices in microwave and millimeter-wave regimes
[AD-A239943] N92-10142
Diamond thin films grown by microwave plasma assisted chemical vapor deposition
[DE91-018553] N92-10695
Remote sensing observations of Kelso Dunes, California N92-10847
MIE SCATTERING
Light scattering by lunar-like particle size distributions N92-10832
MILITARY OPERATIONS
C4I2 in space: Solving the SatCom shortfall
[AD-A239880] N92-10140
MILLIMETER WAVES
Radar applications of gigawatt sources at millimeter wave frequencies
[DE91-017541] N92-10133
Transport in heterostructures and devices in microwave and millimeter-wave regimes
[AD-A239943] N92-10142
MIMAS
Mimas: Tectonic structure and geologic history N92-10764
The photometric roughness of Mimas N92-10835
MINERALOGY
Program and Abstracts for Clay Minerals Society 28th Annual Meeting
[NASA-TM-105098] N92-10248
Clays on Mars: Review of chemical and mineralogical evidence N92-10250
Mineralogy of Cretaceous/Tertiary boundary clays in the Chicxulub structure in northern Yucatan N92-10253
Synthesis and properties of Ti-substituted goethites and hematites N92-10255
Remote sensing and geologic studies of the orientale basin region N92-10809
Mineralogy of the Martian surface from Mariner 6/7 infrared spectrometer data N92-10814
Spectral evidence for carbonates on Mars: Hydrous carbonates N92-10820
Derivation of mid-infrared (5-25 microns) optical constraints of some silicates and palagonite N92-10950
MINERALS
Program and Abstracts for Clay Minerals Society 28th Annual Meeting
[NASA-TM-105098] N92-10248
Clay minerals in primitive meteorites and interplanetary dust 1 N92-10256
Effects of grain size and shape in modeling reflectance spectra of mineral mixtures N92-10831
Will Galileo resolve the S-asteroid controversy? N92-10882
Water/rock interactions in experimentally simulated dirty snowball and dirty iceball cometary nuclei N92-10888
Derivation of mid-infrared (5-25 microns) optical constraints of some silicates and palagonite N92-10950
MINIATURIZATION
A miniature acousto-optic image correlator
[DE91-018002] N92-10151
MINICOMPUTERS
ART/Ada design project, phase 1. Task 3 report: Test plan
[NASA-CR-188945] N92-10314
MIRRORS
Cavity issues for Ni-like Ta x ray lasers
[DE91-017668] N92-10190
Study of different SX-700 designs for the undulator beamline (BL51) at MAX-LAB N92-10446
MISSILE CONFIGURATIONS
The effects of forebody strakes on asymmetric vortices on a vertically launched missile
[AD-A239948] N92-10014
MISSILE CONTROL
Rotatable non-circular forebody flow controller
[NASA-CASE-LAR-14212-1-CU] N92-10021
MISSILES
The use and misuse of aircraft and missile RCS statistics
[AD-A239892] N92-10141
MISSION PLANNING
The data book of ERS-1: The European Remote Sensing Satellite
[ESA-BR-75] N92-10039
NEP mission sensitivities N92-10045
Thermal modeling of comet Kopff: Implications for the CRAF mission N92-10889
MIXING LAYERS (FLUIDS)
Jet noise generated by large-scale coherent motion N92-10604

MIXTURES
Investigations of the effects of isotopic substitution and pressure on miscibility in polymer-polymer and polymer-solvent systems
[DE91-018010] N92-10094
Recognizing of spectral mixtures, their components and spectral patterns N92-10447
Photoresist crossed gratings N92-10448
Effects of grain size and shape in modeling reflectance spectra of mineral mixtures N92-10831
MODELS
Dual strain gage balance system for measuring light loads
[NASA-CASE-LAR-14419-1] N92-10185
Fear-potentiated startle as a model system for analyzing learning and memory
[AD-A239994] N92-10284
Exploration of relationships between low-Ti and high-Ti pristine lunar glasses using an armalcolite assimilation model N92-10964
MODULARITY
Multi-reactor power system configurations for multimegawatt nuclear electric propulsion
[NASA-TM-105212] N92-10057
MODULUS OF ELASTICITY
High temperature materials characterization
[NASA-CR-184231] N92-10079
Sea ice elastic moduli: Determination of Biot parameters using in-field velocity measurements
[AD-A239803] N92-10275
MOISTURE
The crystal structure and moisture sensitivity of (+)-4-(1-(2,3 dimethylphenyl) ethyl) 1H-imidazole hydrochloride N92-10522
MOISTURE CONTENT
Atmospheric measurements using a scanning, solar-blind Raman Lidar
[DE91-016078] N92-10260
MOJAVE DESERT (CA)
Use of radar to assess aeolian processes N92-10802
Mojave remote sensing field experiment N92-10840
MOLECULAR BEAM EPITAXY
Efficient, high-speed, monolithic optoelectronic circuits using quantum-confined structures
[AD-A239841] N92-10155
Beryllium doping of InP grown by gas-source molecular beam epitaxy N92-10489
Interface effects on electrical properties of high purity InP grown by gas-source molecular beam epitaxy N92-10490
The influence of growth conditions on the composition of GaInAsP grown by gas-source molecular beam epitaxy N92-10491
Compound semiconductor technology: Materials and devices N92-10523
Fabrication of GaAs: MESFET's and test structures for electrical material characterization N92-10529
In(0.5)3Ga(0.47)As/InP SAM avalanche photodiodes grown by gas source MBE N92-10530
InP solar cells grown by gas-source molecular beam epitaxy N92-10531
MOLECULAR BEAMS
Supersonic molecular beam apparatus to study surface reactions N92-10440
MOLECULAR CHAINS
The generalized van der Waals theory of pure fluids and mixtures
[DE91-017549] N92-10093
Polarizabilities of trans and cis polyacetylene and interactions among chains in crystalline polyacetylene
[AD-A240025] N92-10705
MOLECULAR CLOUDS
Parsec-scale penetration of UV into molecular clouds: CII 158 micron mapping of W3, NGC 1977, and NGC 2023
[NASA-CR-188969] N92-10615
Formation of the protosolar nebula N92-10890
Fragmentation in stellar collapse N92-10891
Optical properties of grains in molecular clouds and accretion disks N92-10948
MOLECULAR COLLISIONS
Interaction-induced light scattering as a source of information on properties and interactions of spherical top molecules N92-10439
Supersonic molecular beam apparatus to study surface reactions N92-10440
Experimental study of interactions of highly charged ions with atoms at keV energies
[DE91-016962] N92-10616
MOLECULAR DIFFUSION
Diffusion anomaly at a surface reconstruction N92-10470
Internal friction associated with interaction between carbon atoms and dislocations at low temperature N92-10471
Helium in silicon: A first principle molecular dynamics study N92-10473
Modeling the dynamics of molecular films by Monte Carlo simulation N92-10481
Numerical simulation studies of fluid spreading N92-10482
MOLECULAR EXCITATION
Theoretical estimation of the vibrational temperatures of N2 molecules in the ionosphere and in the laboratory simulated plasma
[ISAS-642] N92-10258
Decay channels of resonantly excited 2p(-1)ns, nd states of Ar and 3d(-1)np states of Kr N92-10426
Krypton 4p,4s and 3d partial photoionization cross sections below 260 eV photon energy N92-10429
Effective mass and excitation spectrum of He-3 impurities in superfluid He-4 N92-10477
A novel technique for the measurement of photoenhanced electron attachment: Implications for an optically-controlled diffuse discharge opening switch
[DE91-016226] N92-10621
MOLECULAR GASES
Computer simulations on the orientation of molecular hydrogen in liquid crystals N92-10466
MOLECULAR INTERACTIONS
Interaction-induced light scattering as a source of information on properties and interactions of spherical top molecules N92-10439
Supersonic molecular beam apparatus to study surface reactions N92-10440
Molecular dynamics studies of liquid-solid interfaces N92-10462
MOLECULAR ORBITALS
Helium in silicon: A first principle molecular dynamics study N92-10473
MOLECULAR PHYSICS
Proceedings of the 25th Annual Conference of the Finnish Physical Society
[REPT-119(1991)] N92-10362
MOLECULAR RELAXATION
Relaxation and final-state correlation effects in the 3p and 3s photoionization of Ar, K(+), and Ca(++) N92-10430
Mechanical after-effect studies of oxygen relaxation in YBa2Cu3O(7-delta)
[DE91-018043] N92-10685
MOLECULAR ROTATION
The rotational structure of the nu(sub 6) vibration band of CH3I N92-10431
The nu(sub 4) and nu(sub 7) bands of CD3CN with coriolis coupling and other resonance perturbations N92-10432
Interaction-induced light scattering as a source of information on properties and interactions of spherical top molecules N92-10439
MOLECULAR SPECTRA
Analysis of the interacting levels V(sub 9) = 1 and V(sub 10) = 2 of propyne N92-10444
Effective mass and excitation spectrum of He-3 impurities in superfluid He-4 N92-10477
NMR pulse responses of pairs of triads of 1/2 spins in solids N92-10511
MOLECULAR SPECTROSCOPY
Polarization spectroscopy in OH and flame temperature measurements N92-10454
Electronically resonant CARS spectroscopy of NO2 N92-10455
MOLECULAR STRUCTURE
The rotational structure of the nu(sub 6) vibration band of CH3I N92-10431
NMR determination of the Ne-21 quadrupole coupling for neon gas dissolved in liquid crystals N92-10436
Interaction-induced light scattering as a source of information on properties and interactions of spherical top molecules N92-10439
Torsional potential for the C(sp2)-C(sp2) bond N92-10443
Molecular dynamics studies of liquid-solid interfaces N92-10462
Molecular dynamics using the tight-binding approximation: Application to liquid silicon N92-10465
Helium in silicon: A first principle molecular dynamics study N92-10473
Scanning tunneling microscope measurements in air:Langmuir-Blodgett films on HOPG and growth of evaporated gold on HOPG N92-10497
The crystal structure and moisture sensitivity of (+)-4-(1-(2,3 dimethylphenyl) ethyl) 1H-imidazole hydrochloride N92-10522
MOLECULES
Physics Division annual review, April 1, 1990 - March 31, 1991
[DE91-018704] N92-10707
MOMENTS
Measurements of forces, moments, and pressures on a generic store separating from a box cavity at supersonic speeds
[NASA-TP-3110] N92-10005
MONOMERS
Poly 1, 2, 4-triazoles via aromatic nucleophilic displacement
[NASA-CASE-LAR-14440-1] N92-10066
MONOMOLECULAR FILMS
Ground state properties of a He-3 impurity in liquid He-4 monolayers
[AD-A239993] N92-10078
MONTE CARLO METHOD
Recent changes of weather patterns in North America
[DE91-017706] N92-10266
A new method to assess the statistical convergence of Monte Carlo solutions
[DE91-016013] N92-10354
Gluon overlap factors extracted from Monte Carlo lattice calculations N92-10397
Computer simulations on the orientation of molecular hydrogen in liquid crystals N92-10466
Diffusion anomaly at a surface reconstruction N92-10470
Modeling the dynamics of molecular films by Monte Carlo simulation N92-10481
Ferromagnetism in small clusters N92-10508
The response history Monte Carlo method for electron transport
[DE91-018295] N92-10631
Electronic and magnetic properties of strongly correlated systems
[DE91-018205] N92-10690
MOON
Implications of convection in the moon and the terrestrial planets N92-10730
The probable continuum between emplacement of plutons and mare volcanism in lunar crustal evolution N92-10794
Lunar western limb pyroclastic deposits N92-10795
Lunar and Hawaiian lava tubes: Analogs and uses based on terrestrial field data N92-10796
On using a pyroclastic deposit as a manned lunar base site N92-10797
Crustal heterogeneity of the moon viewed from the Galileo SSI camera: Lunar sample calibrations and compositional implications N92-10808
Remote sensing and geologic studies of the orientale basin region N92-10809
Analyses of the lunar surface with advanced remote sensors: Expectations for the 1990's N92-10811
Infrared reflectance spectra (4-12 micron) of lunar samples N92-10812
Water detection at the moon, Mars and comets with a combined neutron gamma ray instrument N92-10819
A unified lunar control network: April 1991 N92-10917
The violent side of mare volcanism N92-10962
MORPHOLOGY
N-body simulations of interacting galaxies N92-10579
Tectonic evolution of Lavinia Planitia, Venus N92-10741
Morphology and evolution of coronae and ovoids on Venus N92-10742
Factors controlling lava dome morphology N92-10792
New studies of Martian volcanoes N92-10793
The potential scale of aeolian structures on Venus N92-10800
The violent side of mare volcanism N92-10962
MOSAICS
Venus mapping N92-10913
Mars high-resolution mapping N92-10923
A new edition of the Mars 1:5,000,000 map series N92-10924
Digital cartography of Io N92-10927
MOSSBAUER EFFECT
Combined Backscatter Moessbauer Spectrometer and X Ray Fluorescence analyzer (BaMS/XRF) for planetary surface materials N92-10249
Studies on superconducting Bi2Sr2Ca(n-1) Cu(n)O(4+2n) compounds with Fe-57 and Eu-151 Moessbauer spectroscopy N92-10504
Gamma echo experiments N92-10512
Does Lafayette = Nakhla? Not necessarily so, based on 4.2K Mossbauer spectra of all of the SNC meteorites N92-10825
MOTION PERCEPTION
Visual motion perception
[AD-A240133] N92-10286
MOUNTAINS
Gravity survey of the Mt. Toondina impact structure, South Australia N92-10879

MUD
Mud volcanoes on Mars? N92-10938
MULTIGRID METHODS
A non-isotropic multiple-scale turbulence model [NASA-CR-184217] N92-10160
Totally parallel multilevel algorithms for sparse elliptic systems [NASA-CR-188837] N92-10333
Multigrid calculation of three-dimensional viscous cascade flows [NASA-TM-105257] N92-10345
The improved robustness of multigrid elliptic solvers based on multiple semicoarsened grids [NASA-CR-187633] N92-10348
MULTIPHASE FLOW
Fluid dynamics of multiphase flow in volcanic environments on the Earth, Io, and other planets N92-10740
MULTIPHOTON ABSORPTION
Quantum state resolved desorption of CO from solid surface [DE91-017712] N92-10626
MULTIPLE ACCESS
Introduction to the Personal Access Satellite System study N92-10117
MULTIPLEXING
Computer assisted multiplex sequencing [DE91-017851] N92-10337
Optical signal multiplexer and demultiplexer [DE91-017836] N92-10640
MULTIPROCESSING (COMPUTERS)
Proceedings of the First Energy Research Power Supercomputer Users Symposium [DE91-018877] N92-10300
Massively parallel computing at Sandia and its application to national defense [DE91-008178] N92-10334
Massively parallel computing and the mid-course tracking problem [DE91-010864] N92-10335
Gang scheduling a parallel machine [DE91-011539] N92-10336
Parallel programming with PCN [DE91-019005] N92-10339
MULTISPECTRAL BAND SCANNERS
New methods of change detection using multispectral data [AD-A239370] N92-10217
Disk-resolved spectral reflectance properties of Phobos from 0.3-3.2 micron: Preliminary integrated results from Phobos 2 N92-10822
Mojave remote sensing field experiment N92-10840
Mapping compositional and particle size variations across Silver Lake Playa: Relevance to analyses of Mars TIR data N92-10842
MULTISPECTRAL PHOTOGRAPHY
Variable features in the Valles Marineris region of Mars N92-10799
Crustal heterogeneity of the moon viewed from the Galileo SSI camera: Lunar sample calibrations and compositional implications N92-10808
MULTISTATIC RADAR
Surface properties of Galilean satellites from bistatic radar experiments N92-10849
MUONS
Study of muon triggers and momentum reconstruction in a strong magnetic field for a muon detector at LHC N92-10413
Nonperturbative electromagnetic muon-pair production with capture in peripheral relativistic heavy-ion collisions [DE91-018247] N92-10624
Nuclear excitations and reaction mechanisms [DE91-018968] N92-10634

N

N-TYPE SEMICONDUCTORS
Formation of self-aligned guard rings for monolithic Schottky-barrier diode arrays [NASA-CASE-NPO-17734-1-CU] N92-10146
NAKHLITES
Does Lafayette = Nakhla? Not necessarily so, based on 4.2K Mossbauer spectra of all of the SNC meteorites N92-10825
NAMING
Naming the newly found landforms on Venus N92-10915
NAP-OF-THE-EARTH NAVIGATION
Passive range estimation for rotorcraft low-altitude flight [NASA-TM-103897] N92-10003
NARROWBAND
An analysis of the frequency characteristics of corona discharge at low pressure [AD-A239940] N92-10674
NASA PROGRAMS
The MPD thruster program at JPL N92-10046
NASA procurement: Management oversight of contract cost and time changes could be enhanced [GAO/NSIAD-91-259] N92-10708
NASA maintenance: Stronger commitment needed to curb facility deterioration [GAO/NSIAD-91-34] N92-10709
Management issues at the National Aeronautics and Space Administration [GAO/T-NSIAD-91-48] N92-10710
Index to 1987 NASA Tech Briefs, volume 11, numbers 1-10 [NASA-TM-105024] N92-10717
Index to 1988 NASA Tech Briefs, volume 12, numbers 1-11 [NASA-TM-105077] N92-10718
Index to 1989 NASA Tech Briefs, volume 13, numbers 1-12 [NASA-TM-105109] N92-10719
Index to 1990 NASA Tech Briefs, volume 14, numbers 1-12 [NASA-TM-105110] N92-10720
Cumulative index to NASA Tech Briefs, 1976-1980, volumes 1-5 [NASA-TM-89327] N92-10721
Cumulative index to NASA Tech Briefs, 1981-1985, volumes 6-10 [NASA-TM-89326] N92-10722
NATIONAL AEROSPACE PLANE PROGRAM
Hypersonic flows as related to the National Aerospace plane [NASA-CR-187985] N92-10004
NATURAL SATELLITES
Ring satellite interaction in planetary rings N92-10572
Possible misinterpretation of lunar cratering record in Voyager team analyses of outer planet satellites N92-10860
Planetary atlases N92-10925
Digital solar system geology N92-10928
Rotational properties of planetary satellites N92-10947
NAVIER-STOKES EQUATION
Numerical simulation of hypersonic viscous flow for the design of H-2 orbiting plane (HOPE-2) [NAL-TR-1093] N92-10009
Numerical investigation of the effect of leading edge geometry on dynamic stall of airfoils [AD-A239949] N92-10015
Numerical simulation of vortex breakdown [ONERA-RSF-6/4368-AY-008A] N92-10162
Numerical analysis of fully developed laminar flow in curved rectangular channels [NAL-TR-1111] N92-10166
An additive turbulent decomposition of the Navier-Stokes equations implemented on highly parallel computer systems [AD-A240131] N92-10181
NAVY
Compilation of 1990 annual reports of the Navy ELF communications system ecological monitoring program. Volume 1: Tabs A, B [AD-A239868] N92-10137
Compilation of 1990 annual reports of the Navy ELF communications system ecological monitoring program. Volume 2: Tabs C thru F [AD-A239869] N92-10138
NEAR INFRARED RADIATION
UV, visible, and near-IR reflectivity data for magnetic soils/rocks from Brazil N92-10254
Optical properties of CO2 ice and CO2 snow from ultraviolet to infrared: Application to frost deposits and clouds on Mars N92-10821
NEBULAE
Parsec-scale penetration of UV into molecular clouds: CII 158 micron mapping of W3, NGC 1977, and NGC 2023 [NASA-CR-188969] N92-10615
Formation of the protosolar nebula N92-10890
Aerodynamic and gasdynamic effects in cosmogony N92-10892
Particle-gas dynamics in the protoplanetary nebula N92-10893
NEGATIVE IONS
Dependence of Au(-) production upon the target work function in a plasma-sputter-type negative ion source [NIFS-85] N92-10656
NEODYMIUM COMPOUNDS
The shape effect of magnetic damages in irradiated Nd2Fe14B-permanent magnets N92-10468
NEPTUNE (PLANET)
Earth, Uranus, and Neptune: A comparison of their magnetospheres N92-10567
Thermal models for icy satellites N92-10734
Models of planetary rings N92-10934
The ring arcs of Neptune N92-10945
Studies in planetary rings N92-10949
NEPTUNE SATELLITES
The ring arcs of Neptune N92-10945
Studies in planetary rings N92-10949
NETWORK ANALYSIS
Automatic network analyzer procedures for 5045 klystron cavities [DE91-018015] N92-10149
NETWORKS
Spacecraft antennas N92-10122
The control network of Mercury: April 1991 N92-10916
A unified lunar control network: April 1991 N92-10917
The control network of Mars: April 1991 N92-10918
Publication of topographic atlas and control network of Mars N92-10919
NEURAL NETS
A neural network model of the relativistic electron flux at geosynchronous orbit [AD-A239827] N92-10030
Predicting cloud-to-ground lightning with neural networks [AD-A239989] N92-10270
Gate matrix optimization using simulated annealing N92-10374
Recognizing of spectral mixtures, their components and spectral patterns N92-10447
NEUTRAL BEAMS
Observation of plasma toroidal rotations driven by the electric field due to a loss of ions [NIFS-23] N92-10647
Density peaking in the JFT-2M tokamak plasma with counter neutral beam injection [NIFS-83] N92-10657
NEUTRINOS
Searches for heavy neutrinos from decays of the Z N92-10395
Heavy neutrinos in e(+)e(-) collisions N92-10398
Supernova neutrinos N92-10399
Double beta decay in the particle-number projected QRPA formalism N92-10408
Theoretical and experimental studies of elementary particles [DE91-018285] N92-10630
NEUTRON COUNTERS
Influence of the angular correlation of fission neutrons on noise signatures [DE91-014577] N92-10618
Water detection at the moon, Mars and comets with a combined neutron gamma ray instrument N92-10819
NEUTRON DIFFRACTION
Neutron diffraction experiments on nuclear magnetic order in copper N92-10507
Anomalous neutron scattering from the flux-line lattice in K(0.6)Ba(0.4)BiO3 [DE91-018233] N92-10691
NEUTRON FLUX DENSITY
Neutron irradiation effects on YBCO single crystals [DE91-018615] N92-10700
NEUTRON IRRADIATION
Neutron irradiation effects on YBCO single crystals [DE91-018615] N92-10700
NEUTRON SCATTERING
Anomalous neutron scattering from the flux-line lattice in K(0.6)Ba(0.4)BiO3 [DE91-018233] N92-10691
NEUTRONS
Observations on very neutron-rich nuclei below Z = 50 N92-10402
Proton-neutron symmetry in boson models of nuclear structure N92-10406
Influence of the angular correlation of fission neutrons on noise signatures [DE91-014577] N92-10618
Optimal diffusion synthetic acceleration of discrete ordinates transport calculations [DE91-015924] N92-10620
Cold fusion verification [AD-A239957] N92-10675
NEWTON METHODS
Globally convergent techniques in nonlinear Newton-Krylov [NASA-CR-188894] N92-10309
NICHROME (TRADEMARK)
Thermal energy storage and heat transfer support program. Volume 1: Task-1 heat transport system study copper-water and steel-sodium DWAHP [AD-A239928] N92-10176
NICKEL
High-temperature implantation of Au into Ni [DE91-017304] N92-10682

NICKEL ALLOYS
Evaluation of advanced austenitic alloys relative to alloy design criteria for steam service
[DE91-017800] N92-10081
NIOBIUM
Formation of small metallic precipitates of niobium in (alpha)-Al2O3 implanted with Nb ions
[DE91-015928] N92-10678
NITRIDES
Redistribution of nitrogen atoms and magnetic ordering in Fe-N martensite at low temperatures N92-10472
NITROGEN
Theoretical estimation of the vibrational temperatures of N2 molecules in the ionosphere and in the laboratory simulated plasma
[ISAS-642] N92-10258
Electrical characterization of Li and N doped ZnSe N92-10493
NITROGEN ATOMS
Redistribution of nitrogen atoms and magnetic ordering in Fe-N martensite at low temperatures N92-10472
NITROGEN DIOXIDE
Semiconducting organic thin films as monitoring devices for NO2 air pollution N92-10527
NITROGEN OXIDES
Electronically resonant CARS spectroscopy of NO2 N92-10455
NITROUS OXIDES
Simulations of the carbon cycle in the oceans
[DE91-018475] N92-10273
NOAA 9 SATELLITE
Mission description and in-flight operations of ERBE instruments on ERBS and NOAA 9 spacecraft, November 1984 - January 1986
[NASA-RP-1256] N92-10208
NOAA 10 SATELLITE
Mission description and in-flight operations of ERBE instruments on ERBS and NOAA 9 spacecraft, November 1984 - January 1986
[NASA-RP-1256] N92-10208
NOCTURNAL VARIATIONS
EISCAT incoherent scatter radar observations and model studies on day to night variations in the ionospheric D-region during the PCA event of August 1989 N92-10559
NOISE
Using surrogate data to detect nonlinearity in time series
[DE91-018017] N92-10357
NOISE (SOUND)
Turbomachinery noise N92-10601
The hazard of exposure to impulse noise as a function of frequency, volume 1
[AD-A239992] N92-10611
NOISE GENERATORS
Aeroacoustics of flight vehicles: Theory and practice. Volume 1: Noise sources
[NASA-RP-1258-VOL-1] N92-10598
Jet noise generated by large-scale coherent motion N92-10604
Combustion and core noise N92-10607
Sonic boom N92-10608
NOISE INJURIES
The hazard of exposure to impulse noise as a function of frequency, volume 1
[AD-A239992] N92-10611
NOISE MEASUREMENT
Influence of the angular correlation of fission neutrons on noise signatures
[DE91-014577] N92-10618
NOISE POLLUTION
Sonic boom N92-10608
NOISE PREDICTION
Propeller and propfan noise N92-10599
NOISE REDUCTION
Aeroacoustics of flight vehicles: Theory and practice. Volume 1: Noise sources
[NASA-RP-1258-VOL-1] N92-10598
Propeller and propfan noise N92-10599
Rotor noise N92-10600
Jet noise classical theory and experiments N92-10602
Airframe noise N92-10605
Sonic boom N92-10608
NOISE SPECTRA
Recognizing of spectral mixtures, their components and spectral patterns N92-10447
The hazard of exposure to impulse noise as a function of frequency, volume 1
[AD-A239992] N92-10611
NOISE TOLERANCE
The hazard of exposure to impulse noise as a function of frequency, volume 1
[AD-A239992] N92-10611
NOMENCLATURES
Naming the newly found landforms on Venus N92-10915
NONDESTRUCTIVE TESTS
Quantitative nondestructive evaluation of materials and structures
[NASA-CR-188975] N92-10071
Development of nondestructive characterization technologies for process control of ceramics
[DE91-018540] N92-10097
Quantitative non-destructive evaluation of high-temperature superconducting materials
[DE91-018284] N92-10150
Holographic nondestructive testing in bone biomechanics N92-10451
NONEQUILIBRIUM FLOW
Nonequilibrium radiative heating prediction method for aeroassist flowfields with coupling to flowfield solvers N92-10165
NONEQUILIBRIUM RADIATION
Nonequilibrium radiative heating prediction method for aeroassist flowfields with coupling to flowfield solvers N92-10165
NONLINEAR EQUATIONS
Dromions: The movie N92-10370
Dynamics of discrete quantum nonlinear Schroedinger equations N92-10371
Modelling crystal growth: Convection in an asymmetrically heated ampoule
[NASA-CR-184214] N92-10676
NONLINEAR SYSTEMS
Nonlinear interactions of tearing modes in the presence of shear flow
[DE91-018420] N92-10173
Globally convergent techniques in nonlinear Newton-Krylov
[NASA-CR-188894] N92-10309
Some results on constrained controllability in discrete-time convex processes
[MEMO-926] N92-10342
Parameter identification for nonlinear aerodynamic systems
[NASA-CR-188985] N92-10347
Identification of nonlinear times series from first order cumulative characteristics
[AD-A239822] N92-10350
Characterization of nonlinear input-output systems using time series analysis
[DE91-018003] N92-10356
Nonlinear RF processes in plasma
[DE91-017441] N92-10658
NONLINEARITY
Identification of nonlinear times series from first order cumulative characteristics
[AD-A239822] N92-10350
Using surrogate data to detect nonlinearity in time series
[DE91-018017] N92-10357
NONPARAMETRIC STATISTICS
Identification of nonlinear times series from first order cumulative characteristics
[AD-A239822] N92-10350
NONUNIFORM PLASMAS
Single particle and fluid picture for the ponderomotive drift in nonuniform plasmas
[NIFS-25] N92-10645
NORMAL DENSITY FUNCTIONS
Accretion rates of protoplanets 2: Gaussian distribution of planestesimal velocities N92-10937
NORWEGIAN SPACE PROGRAM
Activities report of the Norwegian Space Center
[ETN-91-90052] N92-10029
NOSES (FOREBODIES)
Rotatable non-circular forebody flow controller
[NASA-CASE-LAR-14212-1-CU] N92-10021
NOTCH TESTS
Prediction of matrix fatigue crack initiation in notched SCS-6/Ti-15-3 metal matrix composites
[NASA-TM-104141] N92-10203
NOZZLE FLOW
MPD thruster research issues, activities, strategies N92-10051
NUCLEAR CAPTURE
Atomic physics of strongly correlated systems
[DE91-012259] N92-10617
Nonperturbative electromagnetic muon-pair production with capture in peripheral relativistic heavy-ion collisions
[DE91-018247] N92-10624
NUCLEAR ELECTRIC POWER GENERATION
Multi-reactor power system configurations for multimegawatt nuclear electric propulsion
[NASA-TM-105212] N92-10057
NUCLEAR ELECTRIC PROPULSION
NEP mission sensitivities N92-10045
The MPD thruster program at JPL N92-10046
LLNL contributions to MPD thrusters for SEI N92-10047
Multi-reactor power system configurations for multimegawatt nuclear electric propulsion
[NASA-TM-105212] N92-10057
NUCLEAR ENERGY
Fusion energy: Status and prospects N92-10583
Nuclear energy: Its strengths, weaknesses and role in Finland N92-10585
NUCLEAR EXPLOSIONS
The detection and location of near-regional seismic disturbances by the Eskdalemuir array: A study using noise and signal correlations
[AWE-RE-0-20/90] N92-10247
NUCLEAR FUSION
Fusion energy: Status and prospects N92-10583
Plasma Science Committee (PLSC)
[DE91-018011] N92-10594
Overview of the 1990's D3-D research program
[DE91-018185] N92-10661
Cold fusion verification
[AD-A239957] N92-10675
Solar and supernova neutrino interactions
[DE91-013905] N92-10968
NUCLEAR INTERACTIONS
Experiments on the nuclear interactions of pions and electrons
[DE91-017929] N92-10623
NUCLEAR ISOBARS
Contribution of the delta resonance to the Gamow-Teller decay of heavy nuclei N92-10407
NUCLEAR MAGNETIC RESONANCE
The Kr-83 NMR in probing electric field gradients in thermotropic liquid crystals N92-10435
NMR determination of the Ne-21 quadrupole coupling for neon gas dissolved in liquid crystals N92-10436
NMR-relaxation time measurements of noble gas isotope Xe-129 dissolved in isotropic and anisotropic liquids N92-10437
Vortex nucleation in rotating superfluid He-3-B N92-10476
Antiferromagnetic ordering in silver at picoKelvin temperatures N92-10509
NMR and ESR experiments on solid molecular hydrogen containing atomic hydrogen N92-10510
NMR pulse responses of pairs of triads of 1/2 spins in solids N92-10511
Proton NMR studies on human blood plasma: An application to cancer research N92-10545
An overview of modern permanent magnet design
[AD-A240144] N92-10597
NUCLEAR MODELS
Neutron diffraction experiments on nuclear magnetic order in copper N92-10507
NMR pulse responses of pairs of triads of 1/2 spins in solids N92-10511
NUCLEAR PHYSICS
Proceedings of the 25th Annual Conference of the Finnish Physical Society
[REPT-119(1991)] N92-10362
Nuclear physics at extreme energy density
[DE91-018012] N92-10637
Physics Division annual review, April 1, 1990 - March 31, 1991
[DE91-018704] N92-10707
NUCLEAR POWER PLANTS
Nuclear energy: Its strengths, weaknesses and role in Finland N92-10585
NUCLEAR PROPULSION
Materials in space nuclear power systems
[DE91-017688] N92-10058
Comparison of selected nuclear thermal propulsion concepts
[DE91-017982] N92-10060
Instrumentation and control for space nuclear propulsion
[DE91-018351] N92-10061
Trade studies for nuclear space power systems
[NASA-TM-105231] N92-10221
NUCLEAR QUADRUPOLE RESONANCE
Ion-Guide Quadrupole Mass Spectrometer (IGQMS) N92-10417
NMR determination of the Ne-21 quadrupole coupling for neon gas dissolved in liquid crystals N92-10436
NUCLEAR REACTIONS
Nonperturbative electromagnetic muon-pair production with capture in peripheral relativistic heavy-ion collisions
[DE91-018247] N92-10624
Inclusive quasielastic and deep inelastic electron scattering at high energies
[DE91-018755] N92-10633
Nuclear excitations and reaction mechanisms
[DE91-018968] N92-10634

NUCLEAR REACTOR CONTROL
Instrumentation and control for space nuclear propulsion
[DE91-018351] N92-10061
NUCLEAR REACTORS
Thermal- and ignition-type steam explosions of single drops of molten aluminum
[DE91-014705] N92-10084
Nuclear energy: Its strengths, weaknesses and role in Finland N92-10585
NUCLEAR SPIN
Neutron diffraction experiments on nuclear magnetic order in copper N92-10507
NMR pulse responses of pairs of triads of 1/2 spins in solids N92-10511
NUCLEAR STRUCTURE
Proton-neutron symmetry in boson models of nuclear structure N92-10406
Neutrinoless beta decay in the framework of a relativistic quark model N92-10409
Independent and cumulative yields of neutron-rich nuclei in symmetric fission induced by p and d on U-238 N92-10411
Investigations of the structure and electromagnetic interactions of few-body systems
[DE91-017927] N92-10628
NUCLEATION
Vortex nucleation in rotating superfluid He-3-B N92-10476
Superfluid vortex nucleation in He-3 flow N92-10479
Aerosol dynamics: Binary nucleation N92-10525
NUCLEI (NUCLEAR PHYSICS)
Shape coexistence in transitional (132,133,134)Ba N92-10401
Observations on very neutron-rich nuclei below Z = 50 N92-10402
Contribution of the delta resonance to the Gamow-Teller decay of heavy nuclei N92-10407
Neutrinoless beta decay in the framework of a relativistic quark model N92-10409
Gamma-decay branching of 1(+)-states in Gd-156 and Dy-164 N92-10410
Independent and cumulative yields of neutron-rich nuclei in symmetric fission induced by p and d on U-238 N92-10411
NUCLEONS
Pion-nucleon sigma-term and the strange quark content of the proton N92-10396
NULL HYPOTHESIS
Using surrogate data to detect nonlinearity in time series
[DE91-018017] N92-10357
NUMERICAL ANALYSIS
Numerical investigation of the effect of leading edge geometry on dynamic stall of airfoils
[AD-A239949] N92-10015
Erosive burning of solid propellants N92-10108
Numerical analysis of fully developed laminar flow in curved rectangular channels
[NAL-TR-1111] N92-10166
Globally convergent techniques in nonlinear Newton-Krylov
[NASA-CR-188894] N92-10309
An implementation of the look-ahead Lanczos algorithm for non-Hermitian matrices, part 2
[NASA-CR-188910] N92-10312
Waveguide Dammann gratings and kinoforms N92-10458
Kinetic gas and electron temperatures in RF induction plasma N92-10460
Numerical calculations of wave propagation in tokamak plasmas N92-10461
Simulation study of scalings in scrape-off layer plasma by two-dimensional transport code
[NIFS-24] N92-10646
Formation of the protosolar nebula N92-10890
NUMERICAL CONTROL
Explosive Transient Camera (ETC) program
[NASA-CR-188957] N92-10184
The SolarTrak solar array tracking controller
[DE91-017721] N92-10224
NUMERICAL INTEGRATION
Long-term evolution of a planetesimal swarm in the vicinity of a protoplanet N92-10896
NUMERICAL STABILITY
Optimal diffusion synthetic acceleration of discrete ordinates transport calculations
[DE91-015924] N92-10620

O

OBJECT-ORIENTED PROGRAMMING
Object oriented programming
[DE91-018151] N92-10323
OBSERVATORIES
High resolution lunar radar studies: Preliminary results N92-10845
OBSTACLE AVOIDANCE
Passive range estimation for rotorcraft low-altitude flight
[NASA-TM-103897] N92-10003
OCCULTATION
Dynamics and structure of planetary rings N92-10935
OCEAN MODELS
Regional scale dynamical modelling of biogeochemical processes
[AD-A240115] N92-10246
Simulations of the carbon cycle in the oceans
[DE91-018475] N92-10273
VERMOD capabilities. VERMOD 1.0 and future
[AD-A239801] N92-10274
OCEANOGRAPHY
VERMOD capabilities. VERMOD 1.0 and future
[AD-A239801] N92-10274
OCEANS
A technique for estimating surface meteorological ranges over oceans from satellite measurements of aerosol optical depth
[AD-A239985] N92-10219
Radiohydrophysical aerospace research of ocean
[SRI-PR-1749] N92-10272
VERMOD capabilities. VERMOD 1.0 and future
[AD-A239801] N92-10274
OIL FIELDS
Electromagnetic oil field mapping for improved process monitoring and reservoir characterization
[DE91-017452] N92-10132
OILS
Reflection type skin friction meter
[NASA-CASE-LAR-14520-1-SB] N92-10008
Evaluation of preservative engine oil containing vapor-phase corrosion inhibitor and a simplified engine preservation technique
[AD-A240100] N92-10103
OLIVINE
Degradation of Fe-Mg silicates in hot CO2 atmospheres: Applications to Venus N92-10806
Reflectance spectra of some fractions of Migei and Murchison SM chondrites in the range of 0.3-2.6 microns N92-10829
ON-LINE SYSTEMS
Detection of abrupt changes in statistical models
[AD-A240116] N92-10360
OORT CLOUD
Charged-particle induced alterations of surfaces in the outer solar system N92-10838
OPERATING SYSTEMS (COMPUTERS)
Management of the Space Station Freedom onboard local area network
[NASA-TM-104741] N92-10036
ART/Ada design project, phase 1. Task 3 report: Test plan
[NASA-CR-188945] N92-10314
OPERATOR PERFORMANCE
A system performance throughput model applicable to advanced manned telescience systems
[NASA-CR-188860] N92-10034
Advances and experience with teleoperated systems incorporating remote presence
[AD-A239980] N92-10199
OPTICAL ACTIVITY
Positron lifetime measurements in chiral nematic liquid crystals
[NASA-TP-3122] N92-10677
OPTICAL BISTABILITY
Surface effect on optical bistability in coupled exciton-phonon systems inside a cavity
[AD-A240026] N92-10643
OPTICAL COMMUNICATION
Transport in heterostructures and devices in microwave and millimeter-wave regimes
[AD-A239943] N92-10142
Compound semiconductor technology: Materials and devices N92-10523
OPTICAL CORRELATORS
Optical correlators in texture analysis N92-10450
OPTICAL COUPLING
Surface effect on optical bistability in coupled exciton-phonon systems inside a cavity
[AD-A240026] N92-10643
OPTICAL DISKS
CD-ROM publication of the Mars digital cartographic data base N92-10926
OPTICAL EQUIPMENT
Contamination study
[NASA-CR-184225] N92-10639
Optical signal multiplexer and demultiplexer
[DE91-017836] N92-10640
OPTICAL FIBERS
Development of digital/optical rotary position transducer
[NAL-TR-1106] N92-10028
Two-color holography concept (T-CHI)
[NASA-CR-184240] N92-10183
OPTICAL FILTERS
Abel inversion with the fast Fourier transform N92-10379
Reconfigurable optical interconnections by acousto-optic holograms N92-10449
Optical correlators in texture analysis N92-10450
Waveguide Dammann gratings and kinoforms N92-10458
OPTICAL MEASUREMENT
Optical and electrical investigations into cathode ignition and diode closure
[DE91-017823] N92-10191
Absorption measurements with an integrating sphere and an FT-IR spectrometer N92-10445
Single-shot spectral measurements of multimode pulsed dye lasers N92-10452
Contamination study
[NASA-CR-184225] N92-10639
OPTICAL MEASURING INSTRUMENTS
Explosive Transient Camera (ETC) program
[NASA-CR-188957] N92-10184
Study of different SX-700 designs for the undulator beamline (BL51) at MAX-LAB N92-10446
OPTICAL MEMORY (DATA STORAGE)
Magneto-optical disk as a CD-ROM development tool
[DE91-009973] N92-10296
CD-ROM publication of the Mars digital cartographic data base N92-10926
OPTICAL POLARIZATION
Structure and optical polarizabilities of small silicon clusters N92-10425
OPTICAL PROPERTIES
Characterization of electronic materials
[AD-A240063] N92-10159
Laser induced optical damage in solids
[AD-A240124] N92-10194
Structure and optical polarizabilities of small silicon clusters N92-10425
Absorption measurements with an integrating sphere and an FT-IR spectrometer N92-10445
Theoretical studies of optical phenomena and related inverse problems of solar system bodies N92-10566
Explanation for optical frequency dependent polarization in blazars N92-10577
Optical properties of CO2 ice and CO2 snow from ultraviolet to infrared: Application to frost deposits and clouds on Mars N92-10821
Disk resolved studies of the optical properties and physical nature of the surfaces of the outer planet satellites N92-10837
Asteroid surface processes: Experimental studies of the solar wind on reflectance and optical properties of asteroids N92-10941
Optical properties of grains in molecular clouds and accretion disks N92-10948
Properties of dust and clouds in the Mars atmosphere: Analysis of Viking IRTM emission phase function sequences N92-10956
Studies of volatiles and organic materials in early terrestrial and present-day outer solar system environments N92-10958
OPTICAL RADAR
Remote detection of atmospherically dispersed vegetative cells using fluorescence lidar
[DE91-016077] N92-10218
Atmospheric measurements using a scanning, solar-blind Raman Lidar
[DE91-016078] N92-10260
OPTICAL REFLECTION
Reflection type skin friction meter
[NASA-CASE-LAR-14520-1-SB] N92-10008
Spectral reflectance of pine and intensity of moose browsing N92-10514
OPTICAL RESONANCE
Electronically resonant CARS spectroscopy of NO2 N92-10455
OPTICAL THICKNESS
A technique for estimating surface meteorological ranges over oceans from satellite measurements of aerosol optical depth
[AD-A239985] N92-10219
OPTICAL TRANSITION
Magneto-optical transitions in a Coulomb coupled pair of quantum dots N92-10494
Recombination radiation in the fractional quantum Hall effect regime N92-10495
Surface effect on optical bistability in coupled exciton-phonon systems inside a cavity
[AD-A240026] N92-10643

OPTIMIZATION
Development and optimization of methodologies for analysis of complex hydrocarbon mixtures [DE91-017954] N92-10075
Optimization methods in control of electromagnetic fields [AD-A240044] N92-10144
Computer assisted multiplex sequencing [DE91-017851] N92-10337
Gate matrix optimization using simulated annealing N92-10374
Parametric optimization of synthetic gratings using vector diffraction theory N92-10457
Abatement strategies based on critical loads N92-10533

OPTOELECTRONIC DEVICES
Highlights of material research for optoelectronics in the eighties, trends and challenges for the nineties N92-10486

ORBIT CALCULATION
Impact of non-geostationary orbits on PASS N92-10120
Asteroid flux and impact cratering rate on Venus N92-10880
Bending waves and orbital inclinations N92-10894
Collision probabilities in the presence of nebular gas drag N92-10898

ORBIT PERTURBATION
Bending waves and orbital inclinations N92-10894
Long-term evolution of a planetesimal swarm in the vicinity of a protoplanet N92-10896

ORBITAL ELEMENTS
Bending waves and orbital inclinations N92-10894

ORBITAL MANEUVERS
Small upper stage basic program [AD-A240059] N92-10063

ORBITAL MECHANICS
Asteroid flux and impact cratering rate on Venus N92-10880
The Titan-Hyperion orbital resonance N92-10946

ORBITAL RESONANCES (CELESTIAL MECHANICS)
The Titan-Hyperion orbital resonance N92-10946
Tidal evolution of planetary satellites N92-10953

ORDER-DISORDER TRANSFORMATIONS
Adsorbate induced surface reconstruction N92-10469

ORGANIC COMPOUNDS
Photoresist crossed gratings N92-10448

ORGANIC MATERIALS
Highlights of material research for optoelectronics in the eighties, trends and challenges for the nineties N92-10486
Studies of volatiles and organic materials in early terrestrial and present-day outer solar system environments N92-10958

ORGANIC SEMICONDUCTORS
Semiconducting organic thin films as monitoring devices for NO2 air pollution N92-10527

ORGANOMETALLIC COMPOUNDS
OMVPE growth of InAsSbBi and related alloys using new organometallic group V sources [AD-A239939] N92-10703

OSCILLATING FLOW
Downwash measurements on a pitching canard-wing configuration [AD-A239956] N92-10016

OSCILLATORS
Constant frequency pulsed phase-locked loop measuring device [NASA-CASE-LAR-13823-1] N92-10182
Characterization of nonlinear input-output systems using time series analysis [DE91-018003] N92-10356

OSEEN APPROXIMATION
The structure and development of streamwise vortex arrays embedded in a turbulent boundary layer [NASA-TM-105211] N92-10012

OVERPRESSURE
Sonic boom N92-10608

OXALATES
Transformation products of submicron-sized aluminum-substituted magnetite: Color and reductant solubility N92-10251

OXIDATION
Transport properties and oxidation in chromium and Fe-Cr alloys exposed to oxygen at high temperatures [DE91-018571] N92-10086
Oxide properties of a gamma titanium aluminide: A surface science study [DE91-018024] N92-10095
Transformation products of submicron-sized aluminum-substituted magnetite: Color and reductant solubility N92-10251
Chemisorption of CO on Mg-O/Co(0001) N92-10484
Degradation of Fe-Mg silicates in hot CO2 atmospheres: Applications to Venus N92-10806
Oxidation of basaltic tephras: Influence on reflectance in the 1 micron region N92-10817
Pre-terrestrial oxidation products in carbonaceous meteorites identified by Mossbauer spectroscopy N92-10824

OXIDE FILMS
Heteroepitaxial growth of TiO2, VO2, and TiO2/VO2 multilayers by MOCVD [DE91-018543] N92-10694
Heteroepitaxy of MOCVD grown TiO2, VO2 films and TiO2/VO2 multilayers on sapphire (1120) [DE91-018589] N92-10698

OXIDES
Activation energies in a Bi2Si2CaCu2O(x) single crystal [DE91-018640] N92-10702

OXYGEN
Transport properties and oxidation in chromium and Fe-Cr alloys exposed to oxygen at high temperatures [DE91-018571] N92-10086
Surface electrochemistry of Chloro(phthalocyaninato)rhodium(III) species, and oxygen reduction electrocatalysis, formation of a dimeric species [AD-A240148] N92-10104
On using a pyroclastic deposit as a manned lunar base site N92-10797

OXYGEN ATOMS
Differential collision cross-sections for atomic oxygen: Analysis of space flight instruments for solar terrestrial physics [NASA-CR-184235] N92-10613
Mechanical after-effect studies of oxygen relaxation in YBa2Cu3O(7-delta) [DE91-018043] N92-10685

OXYGEN PRODUCTION
Alkali metal carbon dioxide electrochemical system for energy storage and/or conversion of carbon dioxide to oxygen [NASA-CASE-LEW-14973-1] N92-10222
On using a pyroclastic deposit as a manned lunar base site N92-10797

OZONE DEPLETION
Ozone depletion rates in the late winter/early spring Arctic and Antarctic stratosphere according to recent ozone sounding observations N92-10547

OZONOSPHERE
Simulations of the carbon cycle in the oceans [DE91-018475] N92-10273

P

P-I-N JUNCTIONS
Dual pin diode preamplifier for laser Doppler velocimetry N92-10382

P-TYPE SEMICONDUCTORS
Formation of self-aligned guard rings for monolithic Schottky-barrier diode arrays [NASA-CASE-NPO-17734-1-CU] N92-10146

PACKET SWITCHING
Multi-gigabit fiber optic wide area network development [AD-A239850] N92-10642

PAINTS
Fire retardant performance of some interior shipboard paint schemes [MRL-TR-91-31] N92-10089

PAIR PRODUCTION
Anomalous e(+)e(-) pairs in heavy ion collisions and solar neutrinos: Two puzzles with common solution? N92-10364
Thermal emission of gammas and lepton pairs from quark-gluon plasmas N92-10383
Searches for heavy neutrinos from decays of the Z N92-10395
Heavy neutrinos in e(+)e(-) collisions N92-10398
Nonperturbative electromagnetic muon-pair production with capture in peripheral relativistic heavy-ion collisions [DE91-018247] N92-10624

PALEONTOLOGY
Mimas: Tectonic structure and geologic history N92-10764
Iapetus: Tectonic structure and geologic history N92-10766
Geologic history and channeling episodes of the Chryse Planitia region of Mars N92-10782

PALLADIUM
Determination of the (1x2) structure of a Pt film on Pd(110) N92-10463

PARABOLIC REFLECTORS
Solar detoxification technology: Using energy from the sun to destroy hazardous waste [DE91-015007] N92-10241

PARALLEL COMPUTERS
The paradigm compiler: Mapping a functional language for the connection machine [NASA-CR-188839] N92-10290

PARALLEL FLOW
Geometrical effects of the magnetic field on the neoclassical flow, current, and rotation in general toroidal systems [NIFS-86] N92-10655

PARALLEL PROCESSING (COMPUTERS)
An additive turbulent decomposition of the Navier-Stokes equations implemented on highly parallel computer systems [AD-A240131] N92-10181
On the suitability of the connection machine for direct particle simulation [NASA-CR-188863] N92-10293
Sparse distributed memory: Principles and operation [NASA-CR-188901] N92-10294
Content addressable memory project [NASA-CR-188981] N92-10299
Efficient multitasking of Choleski matrix factorization on CRAY supercomputers [NASA-TM-4259] N92-10302
Parallel machine architecture and compiler design facilities [NASA-CR-188784] N92-10304
Parallel QR factorization on a hypercube using the torus wrap mapping [DE91-011502] N92-10315
Retire FORTRAN? A debate rekindled [DE91-016565] N92-10317
Totally parallel multilevel algorithms for sparse elliptic systems [NASA-CR-188837] N92-10333
Massively parallel computing at Sandia and its application to national defense [DE91-008178] N92-10334
Massively parallel computing and the mid-course tracking problem [DE91-010864] N92-10335
Gang scheduling a parallel machine [DE91-011539] N92-10336
Parallel programming with PCN [DE91-019005] N92-10339
The improved robustness of multigrid elliptic solvers based on multiple semicoarsened grids [NASA-CR-187633] N92-10348

PARALLEL PROGRAMMING
Parallel programming with PCN [DE91-019005] N92-10339
Dynamic lattice computing in general relativity N92-10372

PARAMETER IDENTIFICATION
Optimization methods in control of electromagnetic fields [AD-A240044] N92-10144
Parameter identification for nonlinear aerodynamic systems [NASA-CR-188985] N92-10347

PARAMETERIZATION
Identification of nonlinear times series from first order cumulative characteristics [AD-A239822] N92-10350

PARTIAL DIFFERENTIAL EQUATIONS
Optimal moving grids for time-dependent partial differential equations [NASA-CR-188850] N92-10344
Modelling crystal growth: Convection in an asymmetrically heated ampoule [NASA-CR-184214] N92-10676

PARTICLE ACCELERATION
Ionospheric and magnetospheric processes [AD-A239967] N92-10263
Object oriented programming [DE91-018151] N92-10323
High-spin states in Cd-109 N92-10403
Shapes of Cd-110 at high spins N92-10404
Evidence for band termination in Xe-118 N92-10405

PARTICLE ACCELERATOR TARGETS
Evidence for band termination in Xe-118 N92-10405
Nonperturbative electromagnetic muon-pair production with capture in peripheral relativistic heavy-ion collisions [DE91-018247] N92-10624
Investigations of the structure and electromagnetic interactions of few-body systems [DE91-017927] N92-10628
Inclusive quasielastic and deep inelastic electron scattering at high energies [DE91-018755] N92-10633
Advanced photon source: Radiological design considerations [DE91-018014] N92-10635

PARTICLE ACCELERATORS
The DELPHI microvertex detector, a silicon tracking chamber N92-10412

PARTICLE BEAMS
Instrumental design for measurement of surface charge on insulating materials
[DE91-018695] N92-10099
PARTICLE COLLISIONS
Anomalous e(+)e(-) pairs in heavy ion collisions and solar neutrinos: Two puzzles with common solution? N92-10364
The quark-hadron phase transition N92-10367
Thermal emission of gammas and lepton pairs from quark-gluon plasmas N92-10383
Intermittency studies in proton-antiproton collisions at square root of S = 630 GeV
[CERN-PPE/90-153] N92-10387
Beauty production at the CERN proton-antiproton collider
[CERN-PPE/90-155] N92-10388
A search for rare B meson decays at the CERN proton-antiproton collider
[CERN-PPE/91] N92-10389
Recent physics results from DELPHI N92-10394
Heavy neutrinos in e(+)e(-) collisions N92-10398
Study of muon triggers and momentum reconstruction in a strong magnetic field for a muon detector at LHC N92-10413
Nuclear excitations and reaction mechanisms
[DE91-018968] N92-10634
Aerodynamic and gasdynamic effects in cosmogony N92-10892
Particle-gas dynamics in the protoplanetary nebula N92-10893
Dynamics of low velocity collisions of ice particle, coated with frost N92-10902
PARTICLE DENSITY (CONCENTRATION)
Low pressure impactor with electrical concentration detection N92-10534
PARTICLE DIFFUSION
Aerosol dynamics: Condensation and evaporation N92-10526
PARTICLE EMISSION
Abatement strategies based on critical loads N92-10533
PARTICLE INTERACTIONS
Relaxation and final-state correlation effects in the 3p and 3s photoionization of Ar, K(+), and Ca(++) N92-10430
The A Experimental Division (of the Werner Heisenberg Institute for Physics) N92-10590
Experiments on the nuclear interactions of pions and electrons
[DE91-017929] N92-10623
Physics Division annual review, April 1, 1990 - March 31, 1991
[DE91-018704] N92-10707
Solar and supernova neutrino interactions
[DE91-013905] N92-10968
PARTICLE MASS
Low pressure impactor with electrical concentration detection N92-10534
PARTICLE MOTION
The influence of plasma motion on disruption generated runaway electrons
[DE91-018356] N92-10666
Models of planetary rings N92-10934
The ring arcs of Neptune N92-10945
PARTICLE PRODUCTION
Thermal photon production from high-temperature nuclear matter N92-10384
Exact strangeness conservation and particle production
[BI-TP-90/35] N92-10385
Beauty production at the CERN proton-antiproton collider
[CERN-PPE/90-155] N92-10388
J/psi and psi' production at the CERN proton-antiproton collider
[CERN-PPE/90-154] N92-10390
Measurements of the ratio R = sigma(sub W)Br(W to mu(nu))/sigma(sub Z)Br(Z to mu(mu)) and gamma(sup tot)(sub W) at the CERN proton-antiproton collider
[CERN-PPE/90-141] N92-10392
Observations on very neutron-rich nuclei below Z = 50 N92-10402
Aerosol dynamics: Condensation and evaporation N92-10526
Cold fusion verification
[AD-A239957] N92-10675
PARTICLE SIZE DISTRIBUTION
Simultaneous pyrometric measurement of temperature and size of fuel particles in fluidized bed combustions N92-10381
Low pressure impactor with electrical concentration detection N92-10534
Light scattering by lunar-like particle size distributions N92-10832
Mapping compositional and particle size variations across Silver Lake Playa: Relevance to analyses of Mars TIR data N92-10842
PARTICLE SPIN
Quantum world in 2+1 dimensions N92-10365
Electronic and magnetic properties of strongly correlated systems
[DE91-018205] N92-10690
PARTICLE THEORY
A new method to assess the statistical convergence of Monte Carlo solutions
[DE91-016013] N92-10354
Activities report of the Werner Heisenberg Institute for Physics, Munich (Federal Republic of Germany)
[ISSN-0173-6256] N92-10588
The A Experimental Division (of the Werner Heisenberg Institute for Physics) N92-10590
The B Experimental Division (of the Werner Heisenberg Institute of Physics) N92-10591
Inclusive quasielastic and deep inelastic electron scattering at high energies
[DE91-018755] N92-10633
Quantum cosmology on the worldsheet
[DE91-018415] N92-10727
PARTICULATES
The 14th International Conference on Combined Effect of Environmental Factors
[AD-A240045] N92-10245
Laboratory photometric measurement of particulate soils out to very large phase angles N92-10834
PASSIVITY
Passivation of high temperature superconductors
[NASA-CASE-NPO-17949-1-CU] N92-10681
PATTERN RECOGNITION
Visual motion perception
[AD-A240133] N92-10286
Normalization of correlations
[DE91-018398] N92-10324
Recognizing of spectral mixtures, their components and spectral patterns N92-10447
Optical correlators in texture analysis N92-10450
Spectral representation in vision N92-10539
PAYLOADS
The data book of ERS-1: The European Remote Sensing Satellite
[ESA-BR-75] N92-10039
PENDULUMS
The 1990 solar eclipse as seen by a torsion pendulum N92-10550
Dynamics of low velocity collisions of ice particle, coated with frost N92-10902
PERFORMANCE PREDICTION
A system performance throughput model applicable to advanced manned telescience systems
[NASA-CR-188860] N92-10034
Glass sample characterization
[NASA-CR-184230] N92-10088
PERFORMANCE TESTS
Performance characterization of magnesium/manganese dioxide batteries
[AD-A240037] N92-10158
The Jyvaskyla (Finland) K130 cyclotron project N92-10420
Performance tests of ERNE HED sensor N92-10562
PERMAFROST
Role of artesian groundwater in forming Martian permafrost features N92-10771
PERMANENT MAGNETS
The shape effect of magnetic damages in irradiated Nd2Fe14B-permanent magnets N92-10468
An overview of modern permanent magnet design
[AD-A240144] N92-10597
PEROVSKITES
Processes of deep terrestrial mantles and cores N92-10729
PERTURBATION
Approximate evaluation of reliability and related quantities via perturbation techniques
[AD-A240049] N92-10201
Simulations of the carbon cycle in the oceans
[DE91-018475] N92-10273
Ring satellite interaction in planetary rings N92-10572
PERTURBATION THEORY
Thermal emission of gammas and lepton pairs from quark-gluon plasmas N92-10383
PETRI NETS
Methodology for automating software systems
[NASA-CR-184233] N92-10301
PETROLOGY
Clays on Mars: Review of chemical and mineralogical evidence N92-10250
Workshop on Mare Volcanism and Basalt Petrogenesis: Astounding Fundamental Concepts (AFC) Developed Over the Last Fifteen Years --- Author
[NASA-CR-188810] N92-10961
PH
Definition and measurement at high temperatures of pH
[DE91-017945] N92-10077
Analysis of esophageal pH-recordings for reflux disease N92-10543
PHARMACOLOGY
Synaptic plasticity and memory formation
[AD-A240121] N92-10285
PHASE CONTROL
Phase control in a two-element folded waveguide array
[DE91-018251] N92-10130
PHASE DIAGRAMS
Fluid dynamics of multiphase flow in volcanic environments on the Earth, Io, and other planets N92-10740
PHASE LOCKED SYSTEMS
Constant frequency pulsed phase-locked loop measuring device
[NASA-CASE-LAR-13823-1] N92-10182
PHASE MODULATION
Recovering signals from optical fiber interferometric sensors
[AD-A240062] N92-10644
PHASE SHIFT
Phase control in a two-element folded waveguide array
[DE91-018251] N92-10130
Constant frequency pulsed phase-locked loop measuring device
[NASA-CASE-LAR-13823-1] N92-10182
Character of the opposition effect and negative polarization N92-10833
Laboratory photometric measurement of particulate soils out to very large phase angles N92-10834
PHASE TRANSFORMATIONS
The quark-hadron phase transition N92-10367
A band theoretical study on the electronic properties in the phase transition CuAu 1 to CuAu 2 N92-10488
Strong correlation theories of high temperature superconductors
[DE91-017479] N92-10688
Flow and fracture of ice and ice mixtures N92-10735
Dynamics of low velocity collisions of ice particle, coated with frost N92-10902
PHASE VELOCITY
Constant frequency pulsed phase-locked loop measuring device
[NASA-CASE-LAR-13823-1] N92-10182
PHOBOS
Disk-resolved spectral reflectance properties of Phobos from 0.3-3.2 micron: Preliminary integrated results from Phobos 2 N92-10822
PHONONS
Two-phonon absorption by the real squashing collective mode in superfluid He-3 N92-10474
Tunneling in oscillating double barrier heterostructures N92-10496
Valence and phonon excitations in high-resolution electron microscopy
[DE91-017684] N92-10625
Surface effect on optical bistability in coupled exciton-phonon systems inside a cavity
[AD-A240026] N92-10643
PHOTOACOUSTIC SPECTROSCOPY
Fluidized bed combustion diagnostics by laser photocoustic spectroscopy N92-10380
PHOTOCATHODES
Subpicosecond x ray streak camera
[DE91-017664] N92-10187
PHOTOCHEMICAL REACTIONS
Photoinduced superconductivity in films of YBaCuO N92-10502
Energy partitioning in elementary gas phase reactions
[DE91-017783] N92-10627
PHOTOCONDUCTIVITY
Photoinduced superconductivity in films of YBaCuO N92-10502
PHOTOCONDUCTORS
Photoresist crossed gratings N92-10448
PHOTODIODES
In(0.5)3Ga(0.47)As/InP SAM avalanche photodiodes grown by gas source MBE N92-10530
PHOTODISSOCIATION
Energy partitioning in elementary gas phase reactions
[DE91-017783] N92-10627
PHOTOELECTRIC EMISSION
Synchrotron radiation research and Finnish beamline at MAX-lab N92-10377
The normal incidence grating inverse photoemission spectrometer in the energy range 8-28 eV N92-10516
Photoemission in YbCu2Si2: Problems with the Kondo impurity model
[DE91-018018] N92-10684

PHOTOELECTRON SPECTROSCOPY
Oxide properties of a gamma titanium aluminide: A surface science study
[DE91-018024] N92-10095
Surface characterization of coated powders with XPS: Al2O3-SiO2 coated TiO2 pigments N92-10520
PHOTOELECTRONS
Li 1s photoionization and photoexcitation with satellites N92-10427
Electron correlation in the 4d hole state of Cs and Ba N92-10428
PHOTOGEOLOGY
A 40th deg and order gravitational field model for Mars N92-10760
Tethys geology and tectonics revisited N92-10765
Magma generation on Mars: Estimated volumes through time N92-10788
PHOTOGRAMMETRY
Geologic mapping of tunnels using photogrammetry: Camera and target positioning
[DE91-018394] N92-10261
Late Noachian development of the Coprates rise, Mars N92-10754
Rheological analyses of lava flows on Mars N92-10791
The control network of Mercury: April 1991 N92-10916
The control network of Mars: April 1991 N92-10918
Completion of compilation of the 1:2,000,000-scale topographic map series of Mars N92-10922
PHOTOGRAPHS
Image evaluation of high altitude photographs. Examples: Boston and Foster City (US) N92-10213
PHOTOGRAPHY
Geologic mapping of tunnels using photogrammetry: Camera and target positioning
[DE91-018394] N92-10261
PHOTOINTERPRETATION
Spectral reflectance of pine and intensity of moose browsing N92-10514
PHOTOIONIZATION
Li 1s photoionization and photoexcitation with satellites N92-10427
Krypton 4p,4s and 3d partial photoionization cross sections below 260 eV photon energy N92-10429
Relaxation and final-state correlation effects in the 3p and 3s photoionization of Ar, K(+), and Ca(++) N92-10430
A novel technique for the measurement of photoenhanced electron attachment: Implications for an optically-controlled diffuse discharge opening switch
[DE91-016226] N92-10621
PHOTOLUMINESCENCE
Interface effects on electrical properties of high purity InP grown by gas-source molecular beam epitaxy N92-10490
PHOTOMAPPING
Magma generation on Mars: Estimated volumes through time N92-10788
Digital cartography of Io N92-10927
PHOTOMETRY
Character of the opposition effect and negative polarization N92-10833
Laboratory photometric measurement of particulate soils out to very large phase angles N92-10834
The photometric roughness of Mimas N92-10835
Anomalous scattering of light on Triton N92-10836
Application of Hapke photometric model to three geologic surfaces using PARABOLA bidirectional reflection data N92-10843
PHOTON BEAMS
The search for low photodesorption coatings
[DE91-017473] N92-10092
Use of In-111 in quantitative SPECT N92-10544
PHOTONS
Thermal photon production from high-temperature nuclear matter N92-10384
Advanced photon source: Radiological design considerations
[DE91-018014] N92-10635
High resolution spectroscopy of H(+) energy loss in thin carbon film
[NIFS-88] N92-10654
PHOTONUCLEAR REACTIONS
Investigations of the structure and electromagnetic interactions of few-body systems
[DE91-017927] N92-10628
PHOTOTHERMAL CONVERSION
Velocimetry in gas flows using pulsed laser induced photothermal effects N92-10459
PHOTOVOLTAIC CELLS
A generic guide for the preparation of a quality assurance/quality control manual for the design, production, and installation of photovoltaic concentrator systems
[DE91-017716] N92-10223
PHOTOVOLTAIC CONVERSION
A generic guide for the preparation of a quality assurance/quality control manual for the design, production, and installation of photovoltaic concentrator systems
[DE91-017716] N92-10223
PHYSICAL EXERCISE
A computer simulation for predicting the time course of thermal and cardiovascular responses to various combinations of heat stress, clothing, and exercise
[AD-A240023] N92-10288
PHYSICAL PROPERTIES
Solid propellant steady combustion: Physical aspects N92-10107
VERMOD capabilities. VERMOD 1.0 and future
[AD-A239801] N92-10274
PHYSICAL SCIENCES
The Technical Division (of the Werner Heisenberg Institute of Physics) N92-10592
PHYSIOLOGICAL EFFECTS
Fundamental studies in the molecular basis of laser induced retinal damage
[AD-A239941] N92-10278
PHYSIOLOGICAL FACTORS
Physiologic Transection of the brain stem in healthy humans and the neurologic basis of unconsciousness
[AD-A240122] N92-10023
On categorizing sounds
[AD-A240006] N92-10612
PHYSIOLOGICAL RESPONSES
Synaptic plasticity and memory formation
[AD-A240121] N92-10285
A computer simulation for predicting the time course of thermal and cardiovascular responses to various combinations of heat stress, clothing, and exercise
[AD-A240023] N92-10288
US TAG for ISO/TC43, acoustics, IEC/TC29 electroacoustics, ISO/TC108/SC4 human exposure to mechanical vibration and shock: Minutes of the Accredited Standards Committee on Bioacoustics, S3
[AD-A239918] N92-10610
PHYSIOLOGY
Physiologic Transection of the brain stem in healthy humans and the neurologic basis of unconsciousness
[AD-A240122] N92-10023
Physiological responses of the human extremities to cold water immersion
[IZF-1991-A-15] N92-10277
PIGMENTS
Surface characterization of coated powders with XPS: Al2O3-SiO2 coated TiO2 pigments N92-10520
PILOT PLANTS
Gallium arsenide pilot line for high performance components
[AD-A239955] N92-10704
PINNING
Dynamics of vortices in high-temperature superconductors N92-10501
Anisotropic twin boundary pinning in YBa2Cu3O(x)
[DE91-018536] N92-10692
PION BEAMS
Beam test results of ion-implanted silicon strip detectors on a 100 mm wafer N92-10416
PIONEER VENUS SPACECRAFT
Quantitative analysis of terrain units mapped in the northern quarter of Venus from Venera 15/16 data N92-10853
PIONS
Pion-nucleon sigma-term and the strange quark content of the proton N92-10396
Experiments on the nuclear interactions of pions and electrons
[DE91-017929] N92-10623
PIPE FLOW
Steady flow of a fluid-solid mixture in a circular cylinder
[DE91-018698] N92-10174
PIPELINES
Mechanized fluid connector and assembly tool system with ball detents
[NASA-CASE-MSC-21434-1] N92-10197
PIPELINING (COMPUTERS)
A model for a data acquisition solution for a medium size accelerator laboratory N92-10376
PISTON ENGINES
Combustion and core noise N92-10607
PLAINS
Channeling episodes of Kasei Valles, Mars, and the nature of ridged plains material N92-10779
Wrinkle ridges in the floor material of Kasei Valles, Mars: Nature and origin N92-10955
PLANETARY ATMOSPHERES
Planetary origin, evolution, and structure N92-10952
PLANETARY COMPOSITION
Synthesis and properties of Ti-substituted goethites and hematites N92-10255
Physical properties of cryovolcanic brines: Applications to the evolution of Ganymede N92-10737
The magnesium sulfate-water system at pressures to 4 kilobars N92-10738
Properties of planetary fluids at high pressures and temperatures N92-10739
Fluid dynamics of multiphase flow in volcanic environments on the Earth, Io, and other planets N92-10740
Role of groundwater in formation of Martian channels N92-10770
Soil crusts on Mars N92-10786
PLANETARY CORES
Processes of deep terrestrial mantles and cores N92-10729
The role of nonuniform internal heating in Triton's energy budget N92-10736
Properties of planetary fluids at high pressures and temperatures N92-10739
Tectonic evolution of Lavinia Planitia, Venus N92-10741
Growth of planets from planetesimals N92-10899
PLANETARY CRATERS
Iapetus: Tectonic structure and geologic history N92-10766
The strength of Miranda's lithosphere N92-10767
Role of artesian groundwater in forming Martian permafrost features N92-10771
Impact cratering calculations N92-10933
PLANETARY CRUSTS
An assessment of the crustal remelting hypothesis for volcanism in the Freyja Montes deformation zone N92-10732
The formation of antipodal-impact terrains on Mars N92-10749
The strength of Miranda's lithosphere N92-10767
Soil crusts on Mars N92-10786
Formation of Apollo 14 aluminous mare basalts by replenishment fractional crystallization and assimilation of precursor crust N92-10963
PLANETARY EVOLUTION
Structure and evolution of turbulent preplanetary disc N92-10571
Numerical simulations of dense collisional systems N92-10573
Reports of Planetary Geology and Geophysics Program, 1990
[NASA-TM-4300] N92-10728
Implications of convection in the moon and the terrestrial planets N92-10730
Martian seismicity N92-10733
Physical properties of cryovolcanic brines: Applications to the evolution of Ganymede N92-10737
Tectonic evolution of Lavinia Planitia, Venus N92-10741
Morphology and evolution of coronae and ovoids on Venus N92-10742
Hot-spot tectonics of Eistla Regio, Venus: Results from Magellan images and Pioneer Venus gravity N92-10743
Valles Marineris tectonism: Questions and suggestions N92-10756
Valles Marineris, Mars: Are pit chains formed by erosion and troughs by tectonism? N92-10758
Structural geology and geological history of the Perrine and Nun Sulci Quadrangles (Jg-2 and Jg-5), Ganymede N92-10762
Tectonic deformation on icy satellites: A model of compensating horsts N92-10763
Tethys geology and tectonics revisited N92-10765
Iapetus: Tectonic structure and geologic history N92-10766
The strength of Miranda's lithosphere N92-10767
Evolution of the Martian hydrosphere N92-10768
A Martian global groundwater model N92-10769
Role of groundwater in formation of Martian channels N92-10770
Glacial geology of the Hellas region on Mars N92-10774
Channeling episodes of Kasei Valles, Mars, and the nature of ridged plains material N92-10779
Flood routing of the Maja outflow across Xanthe Terra N92-10780
Ancient fluvial processes in the equatorial highlands of Mars N92-10781
Styles of crater gradation in Southern Ismenius Lacus, Mars N92-10784
Impact craters on Venus N92-10852
Venus impact craters: Implications for atmospheric and resurfacing processes from Magellan observations N92-10854
Core formation by giant impacts N92-10864
Large impacts and climatic catastrophes on the early Earth N92-10865
Impacts and the early environment and evolution of the terrestrial planets N92-10866

Vapor plumes: A neglected aspect of impact cratering N92-10867
Impacts and atmospheric erosion on the early Earth N92-10871
Formation of the protosolar nebula N92-10890
Accretion and evolution of solar system bodies N92-10895
Long-term evolution of a planetesimal swarm in the vicinity of a protoplanet N92-10896
A reexamination of early numerical simulations of planetary accretion N92-10897
Growth of planets from planetesimals N92-10899
Tidal disruption of inviscid protoplanets N92-10900
A geometrical model for shepherding N92-10901
Evolution of the east rim of the Hellas basin, Mars N92-10909
Impact and collisional processes in the solar system N92-10932
Accretion rates of protoplanets N92-10936
Accretion rates of protoplanets 2: Gaussian distribution of planestesimal velocities N92-10937
Are the Equatorial Highlands on Venus formed by mantle plume diapirs? N92-10942
Planetary origin, evolution, and structure N92-10952
Tidal evolution of planetary satellites N92-10953

PLANETARY GEOLOGY
Reports of Planetary Geology and Geophysics Program, 1990 [NASA-TM-4300] N92-10728
Morphology and evolution of coronae and ovoids on Venus N92-10742
Hot-spot tectonics of Eistla Regio, Venus: Results from Magellan images and Pioneer Venus gravity N92-10743
Strain accommodation beneath structures on Mars N92-10748
The formation of antipodal-impact terrains on Mars N92-10749
Interactions of tectonic, igneous, and hydraulic processes in the North Tharsis Region of Mars N92-10755
A 40th deg and order gravitational field model for Mars N92-10760
Chronology of glaciation in the Hellas region of Mars N92-10773
Terrestrial glacial eskers: Analogs for Martian sinuous ridges N92-10775
Stratigraphy of the layered terrain in Valles Marineris, Mars N92-10777
Hydrologic activity during late Noachian and Early Hesperian downwarping of Borealis Basin, Mars N92-10778
Flood routing of the Maja outflow across Xanthe Terra N92-10780
Styles of crater gradation in Southern Ismenius Lacus, Mars N92-10784
The gradational history of southern Ismenius Lacus N92-10785
Physical properties of lava flows on the southwest flank of Tyrrhena Patera, Mars N92-10790
Factors controlling lava dome morphology N92-10792
New studies of Martian volcanoes N92-10793
Water on Mars: Clue to accretional history N92-10798
Variable features in the Valles Marineris region of Mars N92-10799
The potential scale of aeolian structures on Venus N92-10800
Relationships between topographic roughness and aeolian processes N92-10801
Heat flow vs. atmospheric greenhouse on early Mars N92-10805
Remote sensing of the Martian surface N92-10813
Composition of Syrtis Major volcanic plateau N92-10815
The perplexing continuum slope of Mars: Effects of thin ferric coatings and viewing geometry N92-10816
Oxidation of basaltic tephras: Influence on reflectance in the 1 micron region N92-10817
Spectroscopic analyses of Fe and water in clays: A Martian surface weathering study N92-10818
Spectral evidence for carbonates on Mars: Hydrous carbonates N92-10820
Impact craters on Venus N92-10852
Quantitative analysis of terrain units mapped in the northern quarter of Venus from Venera 15/16 data N92-10853
Preliminary geologic mapping of Arsia Mons, Mars N92-10905
Preliminary geologic mapping of central Chryse Planitia, Mars N92-10906
Geologic mapping of northern Lunae Planun, Mars N92-10907
Mars geologic mapping: Dao, Harmakhis, and Reull Valles region N92-10908
Evolution of the east rim of the Hellas basin, Mars N92-10909
Geologic mapping of MTM quads 40292 and 40297: In the Utopian lowlands north of the Nilosyrtis Mensae, Mars N92-10910
Stratigraphy of the Perrine and Nun Sulci quadrangles (Jg-2 and Jg-5), Ganymede N92-10911
Mars geologic mapping program: Review and highlights N92-10912
Venus mapping N92-10913
Digital solar system geology N92-10928

PLANETARY GRAVITATION
Numerical simulations of dense collisional systems N92-10573
Hot-spot tectonics of Eistla Regio, Venus: Results from Magellan images and Pioneer Venus gravity N92-10743
Studies in planetary rings N92-10949

PLANETARY MAGNETIC FIELDS
Properties of planetary fluids at high pressures and temperatures N92-10739
Generation and behavior of solar system magnetic fields N92-10939

PLANETARY MAGNETOSPHERES
Earth, Uranus, and Neptune: A comparison of their magnetospheres N92-10567

PLANETARY MANTLES
Processes of deep terrestrial mantles and cores N92-10729
Are the Equatorial Highlands on Venus formed by mantle plume diapirs? N92-10942

PLANETARY MAPPING
Impact craters on Venus N92-10852
Quantitative analysis of terrain units mapped in the northern quarter of Venus from Venera 15/16 data N92-10853
Depth/diameter relationships of fresh craters within Hesperia Planum, Mars N92-10873
Preliminary geologic mapping of Arsia Mons, Mars N92-10905
Preliminary geologic mapping of central Chryse Planitia, Mars N92-10906
Geologic mapping of northern Lunae Planun, Mars N92-10907
Mars geologic mapping: Dao, Harmakhis, and Reull Valles region N92-10908
Geologic mapping of MTM quads 40292 and 40297: In the Utopian lowlands north of the Nilosyrtis Mensae, Mars N92-10910
Mars geologic mapping program: Review and highlights N92-10912
Venus mapping N92-10913
Triangulation using synthetic aperture radar images N92-10914
Naming the newly found landforms on Venus N92-10915
Completion of compilation of the 1:2,000,000-scale topographic map series of Mars N92-10922
Mars high-resolution mapping N92-10923
A new edition of the Mars 1:5,000,000 map series N92-10924
CD-ROM publication of the Mars digital cartographic data base N92-10926
Digital cartography of Io N92-10927
Thermal and albedo mapping of the north and south polar regions of Mars N92-10943
Preliminary 1:500,000-scale geologic mapping of Claritas Fossae, Mars N92-10959

PLANETARY NEBULAE
Collision probabilities in the presence of nebular gas drag N92-10898
Growth of planets from planetesimals N92-10899
A geometrical model for shepherding N92-10901
Generation and behavior of solar system magnetic fields N92-10939

PLANETARY ORBITS
The stability of the planetary triangular Lagrange points N92-10568
Long-term evolution of a planetesimal swarm in the vicinity of a protoplanet N92-10896
Collision probabilities in the presence of nebular gas drag N92-10898

PLANETARY RINGS
Bending waves and orbital inclinations N92-10894
A geometrical model for shepherding N92-10901
Planetary ring studies N92-10903
Models of planetary rings N92-10934
The ring arcs of Neptune N92-10945
Studies in planetary rings N92-10949

PLANETARY ROTATION
Planetary origin, evolution, and structure N92-10952

PLANETARY STRUCTURE
Dynamics and structure of planetary rings N92-10935
Planetary origin, evolution, and structure N92-10952

PLANETARY SURFACES
Combined Backscatter Moessbauer Spectrometer and X Ray Fluorescence analyzer (BaMS/XRF) for planetary surface materials N92-10249
Dynamic models for ridge belt formation on Venus N92-10731
Morphology and evolution of coronae and ovoids on Venus N92-10742
Timing and formation of wrinkle ridges in the Tyrrhena Patera Region of Mars N92-10752
Reflectance spectra of Fe(2+)-Mg(2+) disordered pyroxenes: Implications to remote-sensed spectra of planetary surfaces N92-10823
Charged-particle induced alterations of surfaces in the outer solar system N92-10838
The Geologic Remote Sensing Field Experiment (GRSFE) N92-10844
Impact decapitation from laboratory to basin scales N92-10858
Vapor plumes: A neglected aspect of impact cratering N92-10867
Characteristics of ejecta and alluvial deposits at Meteor Crater, Arizona and Odessa Craters, Texas: Results from ground penetrating radar N92-10872
The scaling of secondary craters N92-10874
Magnetic effects of large-scale impacts on airless planetary bodies N92-10877
The control network of Mercury: April 1991 N92-10916
Planetary atlases N92-10925
Digital solar system geology N92-10928
Planetary geomorphology research: FY 1990-1991 N92-10940

PLANETARY TEMPERATURE
Flow and fracture of ice and ice mixtures N92-10735
Remote sensing of the Martian surface N92-10813

PLANETARY WAVES
Investigation of the small-scale structure and dynamics of Uranus' atmosphere [NASA-CR-188819] N92-10960

PLANETS
Horizontal stress in planetary lithospheres from vertical processes N92-10746
Impacts and the early environment and evolution of the terrestrial planets N92-10866
Accretion and evolution of solar system bodies N92-10895
Planetary atlases N92-10925
A new catalog of planetary maps N92-10929
Image retrieval and processing system version 2.0 development work N92-10930

PLANTS (BOTANY)
Compilation of 1990 annual reports of the Navy ELF communications system ecological monitoring program. Volume 1: Tabs A, B [AD-A239868] N92-10137

PLASMA CLOUDS
Plasma cloud behavior [AD-A240000] N92-10264

PLASMA COMPOSITION
Ion temperature gradient driven transport in a density modification experiment on the TFTR tokamak [DE91-018215] N92-10663

PLASMA CONTROL
Approximate analytic theory of the multijunction grill [IPPCZ-309] N92-10127
Simulation study of scalings in scrape-off layer plasma by two-dimensional transport code [NIFS-24] N92-10646
The meandering orbit effect on stabilization of the tilting instability in a field-reversed configuration [NIFS-22] N92-10648
Density peaking in the JFT-2M tokamak plasma with counter neutral beam injection [NIFS-83] N92-10657
Overview of the 1990's D3-D research program [DE91-018185] N92-10661
VH-mode: A new very high confinement regime in the boronized DIII-D tokamak [DE91-018186] N92-10662
The DIII-D tokamak and energy confinement at low q [DE91-018317] N92-10664
Fast-wave ICRF minority-regime heating experiments on the Tore Supra tokamak [DE91-018866] N92-10673

PLASMA CURRENTS
Observation of plasma toroidal rotations driven by the electric field due to a loss of ions [NIFS-23] N92-10647
On ponderomotive force effects on coupling of the LH and IBW grills for the FTU tokamak [IPPCZ-305] N92-10650

PLASMA DENSITY
Beat wave current drive experiment on DDT [DE91-017407] N92-10622

Fast wave heating at intermediate ion cyclotron harmonics on the JIPP T-II U tokamak
[NIFS-21] N92-10649
Density peaking in the JFT-2M tokamak plasma with counter neutral beam injection
[NIFS-83] N92-10657

PLASMA DIAGNOSTICS
Beat wave current drive experiment on DDT
[DE91-017407] N92-10622
Experimental investigations of electron capture from atomic hydrogen and deuterium by alpha particles
[DE91-018280] N92-10629

PLASMA DIODES
Numerical simulation of ion beam generated in the diode with anode plasma column
[IPPCZ-306] N92-10652

PLASMA DRIFT
The use of whistlers for magnetospheric diagnostics . N92-10554
Single particle and fluid picture for the ponderomotive drift in nonuniform plasmas
[NIFS-25] N92-10645
Ion temperature gradient driven transport in a density modification experiment on the TFTR tokamak
[DE91-018215] N92-10663

PLASMA DYNAMICS
The influence of plasma motion on disruption generated runaway electrons
[DE91-018356] N92-10666

PLASMA ELECTRODES
Optical and electrical investigations into cathode ignition and diode closure
[DE91-017823] N92-10191

PLASMA ENGINES
Los Alamos NEP research in advanced plasma thrusters N92-10049

PLASMA EQUILIBRIUM
Nonlinear interactions of tearing modes in the presence of shear flow
[DE91-018420] N92-10173
VH-mode: A new very high confinement regime in the boronized DIII-D tokamak
[DE91-018186] N92-10662
Stabilization of the m = 1 tearing mode by resonance detuning
[DE91-018423] N92-10668

PLASMA HEATING
Ionospheric and magnetospheric processes
[AD-A239967] N92-10263
Fast wave heating at intermediate ion cyclotron harmonics on the JIPP T-II U tokamak
[NIFS-21] N92-10649
On ponderomotive force effects on coupling of the LH and IBW grills for the FTU tokamak
[IPPCZ-305] N92-10650
Experimental studies of tokamak plasma in IPP Prague
[IPPCZ-310] N92-10651
Overview of the 1990's D3-D research program
[DE91-018185] N92-10661
Theory of Ion Bernstein wave coupling at low edge densities
[DE91-018321] N92-10665
Plasma Physics Research Institute, Lawrence Livermore National Laboratory, University of California, Davis annual report for fiscal year 1989
[DE91-018490] N92-10669

PLASMA INTERACTIONS
Experimental studies of tokamak plasma in IPP Prague
[IPPCZ-310] N92-10651
Charged-particle induced alterations of surfaces in the outer solar system N92-10838
Magnetic effects of large-scale impacts on airless planetary bodies N92-10877

PLASMA JETS
Doppler shift velocimetry in disperse flows N92-10378
Explanation for optical frequency dependent polarization in blazars N92-10577
Self-consistent modeling of plasma spraying processes
[DE91-018820] N92-10672

PLASMA LAYERS
Simulation study of scalings in scrape-off layer plasma by two-dimensional transport code
[NIFS-24] N92-10646

PLASMA PHYSICS
Proceedings of the 25th Annual Conference of the Finnish Physical Society
[REPT-119(1991)] N92-10362
Kinetic gas and electron temperatures in RF induction plasma N92-10460
EISCAT research program N92-10553
Plasma Science Committee (PLSC)
[DE91-018011] N92-10594
Nuclear physics at extreme energy density
[DE91-018012] N92-10637
Overview of the 1990's D3-D research program
[DE91-018185] N92-10661
Plasma Physics Research Institute, Lawrence Livermore National Laboratory, University of California, Davis annual report for fiscal year 1989
[DE91-018490] N92-10669

PLASMA PINCH
Density peaking in the JFT-2M tokamak plasma with counter neutral beam injection
[NIFS-83] N92-10657

PLASMA POWER SOURCES
Coupling between radiation and gas dynamics
[AD-A240004] N92-10179

PLASMA PROPULSION
Magnetoplasmadynamic Thruster Workshop
[NASA-CP-10084] N92-10044
The MPD thruster program at JPL N92-10046
LLNL contributions to MPD thrusters for SEI N92-10047
MPD thruster technology N92-10048
Los Alamos NEP research in advanced plasma thrusters N92-10049
MPD work at MIT N92-10050
MPD thruster research issues, activities, strategies N92-10051
Eppdyl: Research focus; past accomplishments; and current research N92-10052
IRS organigram N92-10053
Coupling between radiation and gas dynamics
[AD-A240004] N92-10179

PLASMA RESONANCE
Stabilization of the m = 1 tearing mode by resonance detuning
[DE91-018423] N92-10668

PLASMA SLABS
Numerical simulation of ion beam generated in the diode with anode plasma column
[IPPCZ-306] N92-10652

PLASMA SPECTRA
High resolution spectroscopy of H(+) energy loss in thin carbon film
[NIFS-88] N92-10654

PLASMA SPRAYING
Doppler shift velocimetry in disperse flows N92-10378
Self-consistent modeling of plasma spraying processes
[DE91-018820] N92-10672

PLASMA TURBULENCE
Ionospheric and magnetospheric processes
[AD-A239967] N92-10263
Stabilization of the m = 1 tearing mode by resonance detuning
[DE91-018423] N92-10668

PLASMA WAVES
Beat wave current drive experiment on DDT
[DE91-017407] N92-10622
Fast wave heating at intermediate ion cyclotron harmonics on the JIPP T-II U tokamak
[NIFS-21] N92-10649

PLASMA-PARTICLE INTERACTIONS
Overview of the 1990's D3-D research program
[DE91-018185] N92-10661

PLASMAPAUSE
The use of whistlers for magnetospheric diagnostics N92-10554

PLASMAS (PHYSICS)
Proceedings of the Second Switch Tube Advanced Technology Meeting
[DE91-017718] N92-10148
A brief introduction to CONDOR
[DE91-018652] N92-10325
Thermal photon production from high-temperature nuclear matter N92-10384
Hadronic equation of state and the onset of kaon condensation N92-10386
Average properties of energetic ions in different parts of the cusp/cleft region N92-10556
Inhomogeneity and nonlinearity effects on stop bands of Alfvenic ion cyclotron waves in multicomponent plasma N92-10557
Energy-latitude dispersion of energetic ions in the dayside of the Earth's magnetosphere: A substorm-related phenomenon N92-10558
Observations of semidiurnal atmospheric tides using the EISCAT incoherent scatter radar N92-10560
Simulation study of scalings in scrape-off layer plasma by two-dimensional transport code
[NIFS-24] N92-10646
Electromagnetic plasma simulation in realistic geometries
[DE91-018651] N92-10670
Fast-wave ICRF minority-regime heating experiments on the Tore Supra tokamak
[DE91-018866] N92-10673
The spatial distribution and time evolution of impact-generated magnetic fields N92-10878

PLASTIC PROPERTIES
Synaptic plasticity and memory formation
[AD-A240121] N92-10285

PLATEAUS
Composition of Syrtis Major volcanic plateau N92-10815

PLATINUM
Determination of the (1x2) structure of a Pt film on Pd(110) N92-10463

PLUMES
Vapor plumes: A neglected aspect of impact cratering N92-10867

PLUTO (PLANET)
Charged-particle induced alterations of surfaces in the outer solar system N92-10838

PNEUMATIC EQUIPMENT
Air pulsed plate liquid-liquid extractor simulation
[DE91-018155] N92-10172

POLAR CAP ABSORPTION
EISCAT incoherent scatter radar observations and model studies on day to night variations in the ionospheric D-region during the PCA event of August 1989 N92-10559
Variation of D-region parameters during polar cap absorption events in the year 1989 N92-10561

POLAR CAPS
Thermal and albedo mapping of the north and south polar regions of Mars N92-10943

POLAR CUSPS
Average properties of energetic ions in different parts of the cusp/cleft region N92-10556

POLAR REGIONS
Thermal and albedo mapping of the north and south polar regions of Mars N92-10943

POLARIMETERS
Variable optical polarization in Her X-1 N92-10546

POLARIMETRY
Polarization spectroscopy in OH and flame temperature measurements N92-10454
Mojave remote sensing field experiment N92-10840

POLARIZATION (SPIN ALIGNMENT)
Ultra-cold polarized hydrogen source N92-10423
Strong magnetic compression of spin-polarized hydrogen N92-10480
Recombination radiation in the fractional quantum Hall effect regime N92-10495

POLARIZATION (WAVES)
Properties of shocked relativistic jets N92-10564
Polarization aberrations. 1: Rotationally symmetric optical systems
[NASA-CR-184218] N92-10638
Polarization dependent x ray spectroscopy of high T(sub c) superconductors
[DE91-017475] N92-10683

POLARIZATION CHARACTERISTICS
Structure and optical polarizabilities of small silicon clusters N92-10425
Variable optical polarization in Her X-1 N92-10546
Polarization aberrations. 1: Rotationally symmetric optical systems
[NASA-CR-184218] N92-10638
Polarizabilities of trans and cis polyacetylene and interactions among chains in crystalline polyacetylene
[AD-A240025] N92-10705
Character of the opposition effect and negative polarization N92-10833

POLARIZED LIGHT
Variable optical polarization in Her X-1 N92-10546

POLICIES
Assessing and managing the risks of climate change N92-10233

POLISHING
Glass sample characterization
[NASA-CR-184230] N92-10088
Characterization of electronic materials
[AD-A240063] N92-10159

POLLUTION CONTROL
Assessing and managing the risks of climate change N92-10233
Abatement strategies based on critical loads N92-10533
A simple radon well N92-10536
MHD program plan, FY 1991
[DE91-017916] N92-10659

POLLUTION MONITORING
Semiconducting organic thin films as monitoring devices for NO2 air pollution N92-10527
A simple radon well N92-10536

POLYACETYLENE
Polarizabilities of trans and cis polyacetylene and interactions among chains in crystalline polyacetylene
[AD-A240025] N92-10705
POLYAMIDE RESINS
A process for preparing 1,3-diamino-5-pentafluorosulfanylbenzene and polymers therefrom
[NASA-CASE-LAR-14773-1-CU] N92-10105
POLYATOMIC MOLECULES
Structure and optical polarizabilities of small silicon clusters N92-10425
POLYCARBONATES
Helmet of a laminate construction of polycarbonate and polysulfone polymeric material
[NASA-CASE-MSC-21503-1] N92-10091
An experimental evaluation of the impact resistance of recoated F-16A monolithic polycarbonate flat sheet
[AD-A239984] N92-10101
POLYCRYSTALS
Work function changes of high-T(sub c) superconductors around the T(sub c) N92-10498
Antiferromagnetic ordering in silver at picoKelvin temperatures N92-10509
Grain boundaries in nanophase materials
[DE91-018587] N92-10696
POLYIMIDE RESINS
Advanced thermoplastic resins, phase 1
[NASA-CR-178402] N92-10069
POLYMER CHEMISTRY
A process for preparing 1,3-diamino-5-pentafluorosulfanylbenzene and polymers therefrom
[NASA-CASE-LAR-14773-1-CU] N92-10105
POLYMER MATRIX COMPOSITES
Advanced thermoplastic resins, phase 1
[NASA-CR-178402] N92-10069
POLYMERS
Process for application of powder particles to filamentary materials
[NASA-CASE-LAR-14231-1] N92-10070
The generalized van der Waals theory of pure fluids and mixtures
[DE91-017549] N92-10093
Investigations of the effects of isotopic substitution and pressure on miscibility in polymer-polymer and polymer-solvent systems
[DE91-018010] N92-10094
POLYNOMIALS
A polynomial-time algorithm for computing the yolk in fixed dimension
[AD-A240060] N92-10353
PONDEROMOTIVE FORCES
Single particle and fluid picture for the ponderomotive drift in nonuniform plasmas
[NIFS-25] N92-10645
On ponderomotive force effects on coupling of the LH and IBW grills for the FTU tokamak
[IPPCZ-305] N92-10650
POROSITY
Regenerative Cu/La zeolite supported desulfurizing sorbents
[NASA-CASE-NPO-17480-1-CU] N92-10073
POROUS MATERIALS
Fourier component analysis of three Euler-Lagrangian methods applied to the one-dimensional advection-dispersion model
[DE91-017733] N92-10346
PORTABLE EQUIPMENT
The application of the ADSP-21020 40-bit floating point DSP microprocessor in a digital Doppler radar
[DE91-018005] N92-10135
POSITION (LOCATION)
Plasma cloud behavior
[AD-A240000] N92-10264
POSITION INDICATORS
Reflection type skin friction meter
[NASA-CASE-LAR-14520-1-SB] N92-10008
The detection and location of near-regional seismic disturbances by the Eskdalemuir array: A study using noise and signal correlations
[AWE-RE-0-20/90] N92-10247
POSITION SENSING
Development of digital/optical rotary position transducer
[NAL-TR-1106] N92-10028
POSITRON ANNIHILATION
Local charge compensation in Z(sup 0) hadronic decays N92-10393
Recent physics results from DELPHI N92-10394
Positron annihilation induced Auger-electron spectroscopy: A study of a Ge(100) surface N92-10515
Scale dependence of Lambda sub (MS bar) from deep inelastic scattering
[RAL-91-044] N92-10614
Positron lifetime measurements in chiral nematic liquid crystals
[NASA-TP-3122] N92-10677
POSITRONS
Observation of a monovacancy in the metastable state of the EL2 defect in GaAs by positron annihilation N92-10467
Scale dependence of Lambda sub (MS bar) from deep inelastic scattering
[RAL-91-044] N92-10614
Positron lifetime measurements in chiral nematic liquid crystals
[NASA-TP-3122] N92-10677
POTATOES
Using LANDSAT to provide potato production estimates to Columbia Basin farmers and processors
[NASA-CR-188783] N92-10209
POTENTIAL ENERGY
The stability analysis of a double barrier resonant tunneling device N92-10485
POWDER (PARTICLES)
Process for application of powder particles to filamentary materials
[NASA-CASE-LAR-14231-1] N92-10070
Surface characterization of coated powders with XPS: Al2O3-SiO2 coated TiO2 pigments N92-10520
Effects of grain size and shape in modeling reflectance spectra of mineral mixtures N92-10831
POWDERED ALUMINUM
In situ liquid-crystal-polymer fiber reinforced aluminum matrix composite
[AD-A239860] N92-10072
POWER CONDITIONING
Eppdyl: Research focus; past accomplishments; and current research N92-10052
Description of the PMAD DC test bed architecture and integration sequence
[NASA-TM-105284] N92-10055
POWER CONVERTERS
Description of the PMAD DC test bed architecture and integration sequence
[NASA-TM-105284] N92-10055
POWER PLANTS
MHD program plan, FY 1991
[DE91-017916] N92-10659
POWER SPECTRA
A frequency domain method for the generation of partially coherent normal stationary time domain signals
[DE91-017058] N92-10204
POWER TRANSMISSION
The 110 GHz ECH heating system for DIII-D
[DE91-018732] N92-10671
PREAMPLIFIERS
Dual pin diode preamplifier for laser Doppler velocimetry N92-10382
PRECIPITATES
Formation of small metallic precipitates of niobium in (alpha)-Al2O3 implanted with Nb ions
[DE91-015928] N92-10678
Charged-particle induced alterations of surfaces in the outer solar system N92-10838
PREDICTION ANALYSIS TECHNIQUES
Prediction of matrix fatigue crack initiation in notched SCS-6/Ti-15-3 metal matrix composites
[NASA-TM-104141] N92-10203
The biological consequences of climate changes: An ecological and economic assessment N92-10235
Water resources and climate change N92-10236
Characterization of nonlinear input-output systems using time series analysis
[DE91-018003] N92-10356
Predictions of the electron-hole liquid model for high T(sub c) superconductors N92-10499
PREDICTIONS
Predicting cloud-to-ground lightning with neural networks
[AD-A239989] N92-10270
A computer simulation for predicting the time course of thermal and cardiovascular responses to various combinations of heat stress, clothing, and exercise
[AD-A240023] N92-10288
Modeling reality
[NASA-CR-188881] N92-10307
PREPREGS
Process for application of powder particles to filamentary materials
[NASA-CASE-LAR-14231-1] N92-10070
PRESERVATIVES
Evaluation of preservative engine oil containing vapor-phase corrosion inhibitor and a simplified engine preservation technique
[AD-A240100] N92-10103
PRESSURE DEPENDENCE
On the most general tensor B(sub ij) which is zero for i does not equal j, and the most general isotropic tensor I(sub ij)
[NASA-TM-105236] N92-10289
PRESSURE DISTRIBUTION
Transonic and supersonic Euler computations of vortex-dominated flow fields about a generic fighter
[NASA-TP-3156] N92-10011
Performance of conjugate gradient-like algorithms in transient two-phase subchannel analysis
[DE91-013373] N92-10316
PRESSURE EFFECTS
Test apparatus and tensile properties of LE-7 turbine blade materials in high pressure hydrogen conditions
[NAL-TR-1092] N92-10025
Bond of reinforcement under controlled confinement
[AD-A240142] N92-10207
PRESSURE MEASUREMENT
Measurements of forces, moments, and pressures on a generic store separating from a box cavity at supersonic speeds
[NASA-TP-3110] N92-10005
Acoustic device and method for measuring gas densities
[NASA-CASE-NPO-18155-1-CU] N92-10609
PRESSURE SENSORS
Development of a pressure transducer calibration system (dynamic pressure response caliber), phase 2
[AD-A239859] N92-10188
PRINCIPAL COMPONENTS ANALYSIS
Spectral representation in vision N92-10539
PROBABILITY THEORY
Solving problems under uncertainty
[DE91-017940] N92-10322
Are limit cycle calculations a stochastic process?
[DE91-017681] N92-10355
The changing face of probability
[DE91-018857] N92-10359
Collision probabilities in the presence of nebular gas drag N92-10898
PROBLEM SOLVING
Dromions: The movie N92-10370
PROCESS CONTROL (INDUSTRY)
Development of nondestructive characterization technologies for process control of ceramics
[DE91-018540] N92-10097
A process for preparing 1,3-diamino-5-pentafluorosulfanylbenzene and polymers therefrom
[NASA-CASE-LAR-14773-1-CU] N92-10105
PROFILOMETERS
Models of the diffuse radar backscatter from Mars N92-10846
PROGRAM VERIFICATION (COMPUTERS)
Numerical simulation of hypersonic viscous flow for the design of H-2 orbiting plane (HOPE-2)
[NAL-TR-1093] N92-10009
PROGRAMMING LANGUAGES
Continuation of research into language concepts for the mission support environment: Source code
[NASA-CR-187816] N92-10303
A portable run-time system for PCN
[DE91-017700] N92-10319
Type abstraction rules for references: A comparison of four which have achieved notoriety
[AD-A240076] N92-10716
PROJECT MANAGEMENT
The determination of operational and support requirements and costs during the conceptual design of space systems
[NASA-CR-188817] N92-10037
The Theoretical Division (of the Werner Heisenberg Institute for Physics) N92-10589
The B Experimental Division (of the Werner Heisenberg Institute of Physics) N92-10591
The Technical Division (of the Werner Heisenberg Institute of Physics) N92-10592
Management issues at the National Aeronautics and Space Administration
[GAO/T-NSIAD-91-48] N92-10710
PROJECT PLANNING
Fuel cell systems program plan, fiscal year 1991
[DE91-017215] N92-10225
Software Technology for Adaptable, Reliable Systems (STARS): US40-STARS reuse concept of operations. Volume 1: Version 0.5-draft
[AD-A240109] N92-10330
Design controls for large order systems
[NASA-CR-184237] N92-10340
MHD program plan, FY 1991
[DE91-017916] N92-10659
PROJECTILES
Impact decapitation from laboratory to basin scales N92-10858

Production of impact melt in craters on Venus, Earth, and the moon N92-10870
Chemical fractionation of siderophile elements in impactites from Australian meteorite craters N92-10875
PROP-FAN TECHNOLOGY
Propeller and propfan noise N92-10599
PROPELLANT COMBUSTION
Combustion and safety of solid propellant rocket motors N92-10110
PROPELLANT GRAINS
Simultaneous pyrometric measurement of temperature and size of fuel particles in fluidized bed combustions N92-10381
PROPELLER FANS
Propeller and propfan noise N92-10599
PROPELLER NOISE
Propeller and propfan noise N92-10599
PROPELLERS
Propeller and propfan noise N92-10599
PROPORTIONAL COUNTERS
IPC two-color analysis of x ray galaxy clusters [NASA-CR-188980] N92-10724
PROPULSION SYSTEM CONFIGURATIONS
Shuttle orbiter with telescoping main propulsion unit and payload [NASA-CASE-LAR-13586-1] N92-10035
MPD work at MIT N92-10050
MPD thruster research issues, activities, strategies N92-10051
Multi-reactor power system configurations for multimegawatt nuclear electric propulsion [NASA-TM-105212] N92-10057
Comparison of selected nuclear thermal propulsion concepts [DE91-017982] N92-10060
Coupling between radiation and gas dynamics [AD-A240004] N92-10179
PROPULSION SYSTEM PERFORMANCE
The space shuttle advanced solid rocket motor: Quality control and testing [NASA-CR-188800] N92-10043
MPD work at MIT N92-10050
Comparison of selected nuclear thermal propulsion concepts [DE91-017982] N92-10060
PROTECTIVE CLOTHING
A computer simulation for predicting the time course of thermal and cardiovascular responses to various combinations of heat stress, clothing, and exercise [AD-A240023] N92-10288
PROTECTIVE COATINGS
Helmet of a laminate construction of polycarbonate and polysulfone polymeric material [NASA-CASE-MSC-21503-1] N92-10091
An experimental evaluation of the impact resistance of recoated F-16A monolithic polycarbonate flat sheet [AD-A239984] N92-10101
PROTON-PROTON REACTIONS
Intermittency studies in proton-antiproton collisions at square root of S = 630 GeV [CERN-PPE/90-153] N92-10387
Beauty production at the CERN proton-antiproton collider [CERN-PPE/90-155] N92-10388
A search for rare B meson decays at the CERN proton-antiproton collider [CERN-PPE/91] N92-10389
J/psi and psi' production at the CERN proton-antiproton collider [CERN-PPE/90-154] N92-10390
Limits on t-quark decay into charged Higgs from a direct search at the CERN proton-antiproton collider [CERN-PPE/90-180] N92-10391
Measurements of the ratio R = sigma(sub W)Br(W to mu(nu))/sigma(sub Z)Br(Z to mu(mu)) and gamma(sup tot)(sub W) at the CERN proton-antiproton collider [CERN-PPE/90-141] N92-10392
PROTONS
Pion-nucleon sigma-term and the strange quark content of the proton N92-10396
Proton-neutron symmetry in boson models of nuclear structure N92-10406
Proton NMR studies on human blood plasma: An application to cancer research N92-10545
PROTOPLANETS
Structure and evolution of turbulent preplanetary disc N92-10571
Mapping the stability field of Jupiter Trojans N92-10883
Particle-gas dynamics in the protoplanetary nebula N92-10893
Bending waves and orbital inclinations N92-10894
Accretion and evolution of solar system bodies N92-10895
Long-term evolution of a planetesimal swarm in the vicinity of a protoplanet N92-10896
A reexamination of early numerical simulations of planetary accretion N92-10897
Collision probabilities in the presence of nebular gas drag N92-10898
Growth of planets from planetesimals N92-10899
Tidal disruption of inviscid protoplanets N92-10900
A geometrical model for shepherding N92-10901
Impact and collisional processes in the solar system N92-10932
Accretion rates of protoplanets N92-10936
Accretion rates of protoplanets 2: Gaussian distribution of planestesimal velocities N92-10937
Generation and behavior of solar system magnetic fields N92-10939
Planetary origin, evolution, and structure N92-10952
PROTOSTARS
Formation of the protosolar nebula N92-10890
Fragmentation in stellar collapse N92-10891
PROTOTYPES
Explosive Transient Camera (ETC) program [NASA-CR-188957] N92-10184
PROVING
The data book of ERS-1: The European Remote Sensing Satellite [ESA-BR-75] N92-10039
PULSE DURATION
Cavity issues for Ni-like Ta x ray lasers [DE91-017668] N92-10190
PULSE GENERATORS
Status of the Repetitive High Energy Pulsed Power Project [DE91-018359] N92-10152
PULSED LASERS
Single-shot spectral measurements of multimode pulsed dye lasers N92-10452
Velocimetry in gas flows using pulsed laser induced photothermal effects N92-10459
PULSES
Status of the Repetitive High Energy Pulsed Power Project [DE91-018359] N92-10152
NMR pulse responses of pairs of triads of 1/2 spins in solids N92-10511
Long pulse electron beams [DE91-018357] N92-10636
PUMPS
Pulse thermal energy transport system [NASA-CASE-LEW-15235-1] N92-10167
PYROLYTIC GRAPHITE
Scanning tunneling microscope measurements in air:Langmuir-Blodgett films on HOPG and growth of evaporated gold on HOPG N92-10497
PYROMETERS
Simultaneous pyrometric measurement of temperature and size of fuel particles in fluidized bed combustions N92-10381
PYROXENES
Reflectance spectra of Fe(2+)-Mg(2+) disordered pyroxenes: Implications to remote-sensed spectra of planetary surfaces N92-10823

Q

Q FACTORS
Analysis of loss for inductive strips in finline [AD-A239947] N92-10156
Q SWITCHED LASERS
Two informative cases of Q-switched laser eye injury [AD-A240001] N92-10279
QUALITY CONTROL
The space shuttle advanced solid rocket motor: Quality control and testing [NASA-CR-188800] N92-10043
A generic guide for the preparation of a quality assurance/quality control manual for the design, production, and installation of photovoltaic concentrator systems [DE91-017716] N92-10223
QUANTUM CHROMODYNAMICS
The quark-hadron phase transition N92-10367
Beauty production at the CERN proton-antiproton collider [CERN-PPE/90-155] N92-10388
Scale dependence of Lambda sub (MS bar) from deep inelastic scattering [RAL-91-044] N92-10614
QUANTUM ELECTRONICS
Magneto-optical transitions in a Coulomb coupled pair of quantum dots N92-10494
QUANTUM MECHANICS
Quantum world in 2+1 dimensions N92-10365
Molecular dynamics using the tight-binding approximation: Application to liquid silicon N92-10465
Mutual friction in superfluid He-3: Effects of bound states in the vortex core N92-10475
Superfluid interfaces in liquid He-3: Superconducting cosmic domain walls in the laboratory N92-10478
Research program in particle physics [DE91-018525] N92-10632
Tunneling calculations for GaAs-Al(x)Ga(1-x) as graded band-gap sawtooth superlattices [NASA-TM-100726] N92-10680
Information flow in quantum mechanics: The quantum Maxwell demon [DE91-017659] N92-10725
QUANTUM STATISTICS
Exact strangeness conservation and particle production [BI-TP-90/35] N92-10385
Hadronic equation of state and the onset of kaon condensation N92-10386
Beauty production at the CERN proton-antiproton collider [CERN-PPE/90-155] N92-10388
A search for rare B meson decays at the CERN proton-antiproton collider [CERN-PPE/91] N92-10389
J/psi and psi' production at the CERN proton-antiproton collider [CERN-PPE/90-154] N92-10390
Limits on t-quark decay into charged Higgs from a direct search at the CERN proton-antiproton collider [CERN-PPE/90-180] N92-10391
Measurements of the ratio R = sigma(sub W)Br(W to mu(nu))/sigma(sub Z)Br(Z to mu(mu)) and gamma(sup tot)(sub W) at the CERN proton-antiproton collider [CERN-PPE/90-141] N92-10392
Local charge compensation in Z(sup 0) hadronic decays N92-10393
QUANTUM THEORY
Quantum world in 2+1 dimensions N92-10365
Dynamics of discrete quantum nonlinear Schroedinger equations N92-10371
Recombination radiation in the fractional quantum Hall effect regime N92-10495
Ion temperature gradient driven transport in a density modification experiment on the TFTR tokamak [DE91-018215] N92-10663
Stabilization of the m = 1 tearing mode by resonance detuning [DE91-018423] N92-10668
Dark matter and the effective value of Newton's constant at large distances [DE91-018152] N92-10726
Quantum cosmology on the worldsheet [DE91-018415] N92-10727
QUANTUM WELLS
The stability analysis of a double barrier resonant tunneling device N92-10485
QUARKS
The quark-hadron phase transition N92-10367
Limits on t-quark decay into charged Higgs from a direct search at the CERN proton-antiproton collider [CERN-PPE/90-180] N92-10391
Pion-nucleon sigma-term and the strange quark content of the proton N92-10396
Gluon overlap factors extracted from Monte Carlo lattice calculations N92-10397
Neutrinoless beta decay in the framework of a relativistic quark model N92-10409
Nonperturbative electromagnetic muon-pair production with capture in peripheral relativistic heavy-ion collisions [DE91-018247] N92-10624
QUARTZ CRYSTALS
Low pressure impactor with electrical concentration detection N92-10534
QUEUEING THEORY
Queueing in networks of computers [NASA-CR-188892] N92-10308

R

RADAR
EISCAT incoherent scatter radar observations and model studies on day to night variations in the ionospheric D-region during the PCA event of August 1989 N92-10559
RADAR BEACONS
Solid-State Radar Beacon Decoder (SSRBD) Operational Test and Evaluation (OT/E) integration test plan [DOT/FAA/CT-TN91/30] N92-10020
RADAR CROSS SECTIONS
The use and misuse of aircraft and missile RCS statistics [AD-A239892] N92-10141
Optimization methods in control of electromagnetic fields [AD-A240044] N92-10144

RADAR DATA
Late Noachian development of the Coprates rise, Mars N92-10754
Mojave remote sensing field experiment N92-10840
High resolution lunar radar studies: Preliminary results N92-10845
Regoliths of icy satellites: The coherent backscatter model N92-10851
RADAR DETECTION
The use and misuse of aircraft and missile RCS statistics [AD-A239892] N92-10141
RADAR ECHOES
Preliminary comparison of 3.5-cm and 12.6-cm wavelength continuous wave observations of Mars N92-10848
Radar backscattering by the icy Galilean satellites and the radar glory effect N92-10850
RADAR EQUIPMENT
The 1990 Airport Surveillance Radar Wind Shear Processor (ASR-WSP) operational test at Orlando International Airport [AD-A239852] N92-10019
The use and misuse of aircraft and missile RCS statistics [AD-A239892] N92-10141
RADAR IMAGERY
Gravitational spreading of Danu, Freyja and Maxwell Montes, Venus N92-10744
Venus mapping N92-10913
Triangulation using synthetic aperture radar images N92-10914
RADAR MAPS
Venus mapping N92-10913
Triangulation using synthetic aperture radar images N92-10914
RADAR MEASUREMENT
Studies of volatiles and organic materials in early terrestrial and present-day outer solar system environments N92-10958
RADAR SCATTERING
Use of radar to assess aeolian processes N92-10802
Models of the diffuse radar backscatter from Mars N92-10846
Radar backscattering by the icy Galilean satellites and the radar glory effect N92-10850
Regoliths of icy satellites: The coherent backscatter model N92-10851
RADAR TARGETS
Integration of Electronic Support Measures (ESM) and alpha-beta radar tracker [AD-A240031] N92-10143
RADAR TRACKING
Radar applications of gigawatt sources at millimeter wave frequencies [DE91-017541] N92-10133
Integration of Electronic Support Measures (ESM) and alpha-beta radar tracker [AD-A240031] N92-10143
RADIANT HEATING
Fire retardant performance of some interior shipboard paint schemes [MRL-TR-91-31] N92-10089
RADIATION ABSORPTION
The search for low photodesorption coatings [DE91-017473] N92-10092
Nonequilibrium radiative heating prediction method for aeroassist flowfields with coupling to flowfield solvers N92-10165
Two-phonon absorption by the real squashing collective mode in superfluid He-3 N92-10474
Polarization dependent x ray spectroscopy of high T(sub c) superconductors [DE91-017475] N92-10683
RADIATION DAMAGE
Radiation damage measurements on double-sided Si strip detectors N92-10415
The shape effect of magnetic damages in irradiated Nd2Fe14B-permanent magnets N92-10468
RADIATION DETECTORS
Searches for heavy neutrinos from decays of the Z N92-10395
Supernova neutrinos N92-10399
The DELPHI microvertex detector, a silicon tracking chamber N92-10412
Study of muon triggers and momentum reconstruction in a strong magnetic field for a muon detector at LHC N92-10413
Development of double-sided silicon strip detectors N92-10414
Beam test results of ion-implanted silicon strip detectors on a 100 mm wafer N92-10416
Cold fusion verification [AD-A239957] N92-10675
Long-term neutrino flux integrations [DE91-013903] N92-10967
RADIATION EFFECTS
An assessment of the radiation tolerance of large satellite memories in low earth orbits [DE91-018353] N92-10040
Compilation of 1990 annual reports of the Navy ELF communications system ecological monitoring program. Volume 1: Tabs A, B [AD-A239868] N92-10137
Compilation of 1990 annual reports of the Navy ELF communications system ecological monitoring program. Volume 2: Tabs C thru F [AD-A239869] N92-10138
Compilation of 1990 annual reports of the Navy ELF communications system ecological monitoring program. Volume 3: Tabs G thru I [AD-A239870] N92-10139
Fiber-tile optical studies at Argonne [DE91-018591] N92-10641
Formation of small metallic precipitates of niobium in (alpha)-Al2O3 implanted with Nb ions [DE91-015928] N92-10678
High-temperature implantation of Au into Ni [DE91-017304] N92-10682
Neutron irradiation effects on YBCO single crystals [DE91-018615] N92-10700
Remote sensing of the Martian surface N92-10813
RADIATION HARDENING
An assessment of the radiation tolerance of large satellite memories in low earth orbits [DE91-018353] N92-10040
RADIATION HAZARDS
Compilation of 1990 annual reports of the Navy ELF communications system ecological monitoring program. Volume 3: Tabs G thru I [AD-A239870] N92-10139
Advanced photon source: Radiological design considerations [DE91-018014] N92-10635
RADIATION INJURIES
Two informative cases of Q-switched laser eye injury [AD-A240001] N92-10279
RADIATION MEASUREMENT
Calibration of scintillation cells for radon-222 measurements N92-10521
RADIATION MEASURING INSTRUMENTS
Performance tests of ERNE HED sensor N92-10562
RADIATION PROTECTION
Advanced photon source: Radiological design considerations [DE91-018014] N92-10635
RADIATION SOURCES
Synchrotron radiation: New research opportunities for the next decade N92-10366
Advanced photon source: Radiological design considerations [DE91-018014] N92-10635
An atlas of optical counterparts of low mass x ray binaries. Part 1: The Northern Sample [MPE-PREPRINT-195-PT-1] N92-10723
RADIATIVE HEAT TRANSFER
Nonequilibrium radiative heating prediction method for aeroassist flowfields with coupling to flowfield solvers N92-10165
Implications of convection in the moon and the terrestrial planets N92-10730
RADIATIVE LIFETIME
Lifetime of the 1.959 MeV state in Cl-36 N92-10400
RADIATIVE RECOMBINATION
Recombination radiation in the fractional quantum Hall effect regime N92-10495
RADIATIVE TRANSFER
The Geologic Remote Sensing Field Experiment (GRSFE) N92-10844
RADICALS
Chemisorption of CO on Mg-O/Co(0001) N92-10484
RADIO BURSTS
Properties of shocked relativistic jets N92-10564
Explanation for optical frequency dependent polarization in blazars N92-10577
RADIO FREQUENCIES
Kinetic gas and electron temperatures in RF induction plasma N92-10460
Nonlinear RF processes in plasma [DE91-017441] N92-10658
RADIO FREQUENCY HEATING
Theory of Ion Bernstein wave coupling at low edge densities [DE91-018321] N92-10665
Plasma Physics Research Institute, Lawrence Livermore National Laboratory, University of California, Davis annual report for fiscal year 1989 [DE91-018490] N92-10669
RADIO JETS (ASTRONOMY)
Properties of shocked relativistic jets N92-10564
RADIO OCCULTATION
Investigation of the small-scale structure and dynamics of Uranus' atmosphere [NASA-CR-188819] N92-10960
RADIO RECEIVERS
Recovering signals from optical fiber interferometric sensors [AD-A240062] N92-10644
RADIO SOURCES (ASTRONOMY)
Double radio sources as standard rods of testing cosmological models N92-10578
RADIOACTIVE DECAY
A search for rare B meson decays at the CERN proton-antiproton collider [CERN-PPE/91] N92-10389
Limits on t-quark decay into charged Higgs from a direct search at the CERN proton-antiproton collider [CERN-PPE/90-180] N92-10391
Local charge compensation in Z(sup 0) hadronic decays N92-10393
Searches for heavy neutrinos from decays of the Z N92-10395
Heavy neutrinos in e(+)e(-) collisions N92-10398
Contribution of the delta resonance to the Gamow-Teller decay of heavy nuclei N92-10407
Double beta decay in the particle-number projected QRPA formalism N92-10408
Neutrinoless beta decay in the framework of a relativistic quark model N92-10409
Gamma-decay branching of 1(+)-states in Gd-156 and Dy-164 N92-10410
Decay channels of resonantly excited 2p(-1)ns, md states of Ar and 3d(-1)np states of Kr N92-10426
Gamma echo experiments N92-10512
Experiments on the nuclear interactions of pions and electrons [DE91-017929] N92-10623
Research program in particle physics [DE91-018525] N92-10632
RADIOACTIVE ISOTOPES
Electromigration of carrier-free radionuclides [DE91-017840] N92-10076
Lifetime of the 1.959 MeV state in Cl-36 N92-10400
RADIOISOTOPE BATTERIES
Materials in space nuclear power systems [DE91-017688] N92-10058
RADIOLOGY
Advanced photon source: Radiological design considerations [DE91-018014] N92-10635
RADIOMETERS
Application of Hapke photometric model to three geologic surfaces using PARABOLA bidirectional reflection data N92-10843
RADON
A simple radon well N92-10536
RADON ISOTOPES
Calibration of scintillation cells for radon-222 measurements N92-10521
RAMAN SPECTRA
Atmospheric measurements using a scanning, solar-blind Raman Lidar [DE91-016078] N92-10260
Electronically resonant CARS spectroscopy of NO2 N92-10455
Numerical calculations of wave propagation in tokamak plasmas N92-10461
RAMAN SPECTROSCOPY
A new phase retrieval method for CARS spectrum analysis N92-10363
RANDOM ACCESS
Multiple access trade study N92-10118
RANDOM ACCESS MEMORY
Sparse distributed memory: Principles and operation [NASA-CR-188901] N92-10294
RANDOM NOISE
The short-circuited fluxgate sensitivity parameters [ISSN-0109-6605] N92-10147
RANDOM PROCESSES
A frequency domain method for the generation of partially coherent normal stationary time domain signals [DE91-017058] N92-10204
Are limit cycle calculations a stochastic process? [DE91-017681] N92-10355
Detection of abrupt changes in statistical models [AD-A240116] N92-10360
RANDOM VARIABLES
A new method to assess the statistical convergence of Monte Carlo solutions [DE91-016013] N92-10354
RANGEFINDING
Passive range estimation for rotorcraft low-altitude flight [NASA-TM-103897] N92-10003

RANKINE CYCLE
Status of Rankine-cycle technology for space nuclear power applications
[DE91-017859] N92-10059
RARE GASES
Thermal helium desorption facility in Jyvaskyla (Finland) N92-10464
Impact and collisional processes in the solar system N92-10932
RATES (PER TIME)
Accretion rates of protoplanets N92-10936
RATS
Fear-potentiated startle as a model system for analyzing learning and memory
[AD-A239994] N92-10284
RAY TRACING
Study of different SX-700 designs for the undulator beamline (BL51) at MAX-LAB N92-10446
Numerical calculations of wave propagation in tokamak plasmas N92-10461
Polarization aberrations. 1: Rotationally symmetric optical systems
[NASA-CR-184218] N92-10638
REACTION KINETICS
Quantum state resolved desorption of CO from solid surface
[DE91-017712] N92-10626
Nuclear excitations and reaction mechanisms
[DE91-018968] N92-10634
REACTION PRODUCTS
Plan for the JYFL gas-filled recoil separator N92-10424
REACTOR DESIGN
Multi-reactor power system configurations for multimegawatt nuclear electric propulsion
[NASA-TM-105212] N92-10057
REACTORS
Aerosol dynamics: Condensation and evaporation N92-10526
READ-ONLY MEMORY DEVICES
Magneto-optical disk as a CD-ROM development tool
[DE91-009973] N92-10296
CD-ROM publication of the Mars digital cartographic data base N92-10926
REAL TIME OPERATION
Feasibility of using a knowledge-based system concept for in-flight primary flight display research
[NASA-TM-4279] N92-10017
Gas turbine combuster exit temperature measurement
[AD-A239936] N92-10026
Method and apparatus for frequency spectrum analysis
[NASA-CASE-NPO-17759-1-CU] N92-10125
Real-time data compression of broadcast video signals
[NASA-CASE-LEW-14945-2] N92-10128
The role of graphics super-workstations in a supercomputing environment
[NASA-CR-188852] N92-10306
RECOIL IONS
Plan for the JYFL gas-filled recoil separator N92-10424
RECOILINGS
Plan for the JYFL gas-filled recoil separator N92-10424
RECOMBINATION REACTIONS
Quantum state resolved desorption of CO from solid surface
[DE91-017712] N92-10626
RECONNAISSANCE
Annual tropical cyclone report, 1990
[AD-A239910] N92-10268
RECONSTRUCTION
Surface reconstruction and many-atom models N92-10483
RECTANGULAR WAVEGUIDES
Constitutive parameter extraction for heated materials
[NASA-CR-186208] N92-10593
RECYCLING
Heat flow vs. atmospheric greenhouse on early Mars N92-10805
RED SHIFT
Double radio sources as standard rods of testing cosmological models N92-10578
REDUCED GRAVITY
Process modelling for Space Station experiments
[NASA-CR-184227] N92-10112
REDUCTION
Surface electrochemistry of Chloro(phthalocyaninato)rhodium(III) species, and oxygen reduction electrocatalysis, formation of a dimeric species
[AD-A240148] N92-10104
REENTRY VEHICLES
Numerical simulation of hypersonic viscous flow for the design of H-2 orbiting plane (HOPE-2)
[NAL-TR-1093] N92-10009
REFERENCE ATMOSPHERES
Range reference atmosphere, Nellis Air Force Base, Nevada
[AD-A239816] N92-10262
REFLECTANCE
Approximate analytic theory of the multijunction grill
[IPPCZ-309] N92-10127
Transformation products of submicron-sized aluminum-substituted magnetite: Color and reductant solubility N92-10251
UV, visible, and near-IR reflectivity data for magnetic soils/rocks from Brazil N92-10254
Contamination study
[NASA-CR-184225] N92-10639
Infrared reflectance spectra (4-12 micron) of lunar samples N92-10812
The perplexing continuum slope of Mars: Effects of thin ferric coatings and viewing geometry N92-10816
Oxidation of basaltic tephras: Influence on reflectance in the 1 micron region N92-10817
Spectroscopic analyses of Fe and water in clays: A Martian surface weathering study N92-10818
Reflectance spectra of Fe(2+)-Mg(2+) disordered pyroxenes: Implications to remote-sensed spectra of planetary surfaces N92-10823
Darkening in gas-rich ordinary chondrites: Spectral modelling and implications for the regoliths of ordinary chondrite parent bodies N92-10827
Reflectance spectra of some fractions of Migei and Murchison SM chondrites in the range of 0.3-2.6 microns N92-10829
An infrared reflectance study of low albedo surface constituents N92-10830
Effects of grain size and shape in modeling reflectance spectra of mineral mixtures N92-10831
Charged-particle induced alterations of surfaces in the outer solar system N92-10838
Mapping compositional and particle size variations across Silver Lake Playa: Relevance to analyses of Mars TIR data N92-10842
Asteroid surface processes: Experimental studies of the solar wind on reflectance and optical properties of asteroids N92-10941
REFLECTED WAVES
Approximate analytic theory of the multijunction grill
[IPPCZ-309] N92-10127
REFLECTOR ANTENNAS
Antenna beam coverage concepts N92-10119
Spacecraft antennas N92-10122
REFLECTORS
PASS spacecraft antenna technology assessment N92-10123
REFRACTION
Derivation of mid-infrared (5-25 microns) optical constraints of some silicates and palagonite N92-10950
REFRACTIVITY
Coupled wave analysis in inverse grating diffraction problems N92-10456
Light scattering by lunar-like particle size distributions N92-10832
REFRACTORY MATERIALS
High temperature materials characterization
[NASA-CR-184231] N92-10079
REFRIGERATORS
Optical properties of CO2 ice and CO2 snow from ultraviolet to infrared: Application to frost deposits and clouds on Mars N92-10821
REGENERATION (ENGINEERING)
Regenerative Cu/La zeolite supported desulfurizing sorbents
[NASA-CASE-NPO-17480-1-CU] N92-10073
REGIONAL PLANNING
Evaluation of high altitude photography for city regional areas
[MGA-A-44] N92-10210
Possibilities of producing land use information for city regional area planning by high altitude photographs, taking south west Munich (Fed. Republic of Germany) regional area as an example N92-10212
REGIONS
Local charge compensation in Z(sup 0) hadronic decays N92-10393
REGOLITH
Darkening in gas-rich ordinary chondrites: Spectral modelling and implications for the regoliths of ordinary chondrite parent bodies N92-10827
Light scattering by lunar-like particle size distributions N92-10832
Anomalous scattering of light on Triton N92-10836
Charged-particle induced alterations of surfaces in the outer solar system N92-10838
Regoliths of icy satellites: The coherent backscatter model N92-10851
REINFORCEMENT (STRUCTURES)
Bond of reinforcement under controlled confinement
[AD-A240142] N92-10207
RELATIVISTIC PARTICLES
A neural network model of the relativistic electron flux at geosynchronous orbit
[AD-A239827] N92-10030
RELATIVITY
Dynamic lattice computing in general relativity N92-10372
RELAXATION (MECHANICS)
Mechanical after-effect studies of oxygen relaxation in YBa2Cu3O(7-delta)
[DE91-018043] N92-10685
Langevin dynamics simulations of large frustrated Josephson junction arrays
[DE91-018046] N92-10686
RELIABILITY
Approximate evaluation of reliability and related quantities via perturbation techniques
[AD-A240049] N92-10201
Modeling reality
[NASA-CR-188881] N92-10307
RELIABILITY ENGINEERING
Software Technology for Adaptable, Reliable Systems (STARS): US40-STARS reuse concept of operations. Volume 1: Version 0.5-draft
[AD-A240109] N92-10330
RELIEF MAPS
Geologic history and channeling episodes of the Chryse Planitia region of Mars N92-10782
Surface-material maps of Viking landing sites on Mars N92-10787
Publication of topographic atlas and control network of Mars N92-10919
Color-coded global topographic map of Mars N92-10920
Mars elevation distribution N92-10921
Completion of compilation of the 1:2,000,000-scale topographic map series of Mars N92-10922
A new edition of the Mars 1:5,000,000 map series N92-10924
Planetary atlases N92-10925
CD-ROM publication of the Mars digital cartographic data base N92-10926
REMOTE CONTROL
Hardware description ADSP-21020 40-bit floating point DSP as designed in a remotely controlled digital CW Doppler radar
[DE91-018004] N92-10134
Advances and experience with teleoperated systems incorporating remote presence
[AD-A239980] N92-10199
Human performance measurement: Validation procedures applicable to advanced manned telescience systems
[NASA-CR-185447] N92-10282
REMOTE SENSING
The data book of ERS-1: The European Remote Sensing Satellite
[ESA-BR-75] N92-10039
The remote sensing Loosdrecht Lakes (Netherlands) project
[BCRS-90-29] N92-10215
Remote sensing and watershed modelling: Towards a hydrological interface model
[BCRS-90-42] N92-10216
Remote detection of atmospherically dispersed vegetative cells using fluorescence lidar
[DE91-016077] N92-10218
Radiohydrophysical aerospace research of ocean
[SRI-PR-1749] N92-10272
Remote sensing and geologic studies of the orientale basin region N92-10809
Remote sensing and geologic studies of the terrain northwest of Humorum basin N92-10810
Remote sensing of the Martian surface N92-10813
Reflectance spectra of Fe(2+)-Mg(2+) disordered pyroxenes: Implications to remote-sensed spectra of planetary surfaces N92-10823
Mojave remote sensing field experiment N92-10840
Surface scattering properties estimated from modeling airborne multiple emission angle reflectance data N92-10841
Mapping compositional and particle size variations across Silver Lake Playa: Relevance to analyses of Mars TIR data N92-10842
Application of Hapke photometric model to three geologic surfaces using PARABOLA bidirectional reflection data N92-10843
The Geologic Remote Sensing Field Experiment (GRSFE) N92-10844
Remote sensing observations of Kelso Dunes, California N92-10847
The violent side of mare volcanism N92-10962

REMOTE SENSORS
Analyses of the lunar surface with advanced remote sensors: Expectations for the 1990's N92-10811
RESCUE OPERATIONS
Numerical analysis and simulation of an assured crew return vehicle flow field
[NASA-TP-3101] N92-10161
RESEARCH
EISCAT research program N92-10553
RESEARCH AND DEVELOPMENT
Explosive Transient Camera (ETC) program
[NASA-CR-188957] N92-10184
Compound semiconductor technology: Materials and devices N92-10523
Finnish space projects: Planetary studies N92-10548
The Theoretical Division (of the Werner Heisenberg Institute for Physics) N92-10589
MHD program plan, FY 1991
[DE91-017916] N92-10659
Index to 1987 NASA Tech Briefs, volume 11, numbers 1-10
[NASA-TM-105024] N92-10717
Index to 1988 NASA Tech Briefs, volume 12, numbers 1-11
[NASA-TM-105077] N92-10718
Index to 1989 NASA Tech Briefs, volume 13, numbers 1-12
[NASA-TM-105109] N92-10719
Index to 1990 NASA Tech Briefs, volume 14, numbers 1-12
[NASA-TM-105110] N92-10720
Cumulative index to NASA Tech Briefs, 1976-1980, volumes 1-5
[NASA-TM-89327] N92-10721
Cumulative index to NASA Tech Briefs, 1981-1985, volumes 6-10
[NASA-TM-89326] N92-10722
RESEARCH FACILITIES
Materials science and technology centra in Sweden and Denmark: A research policy for the future N92-10580
The Theoretical Division (of the Werner Heisenberg Institute for Physics) N92-10589
The A Experimental Division (of the Werner Heisenberg Institute for Physics) N92-10590
The B Experimental Division (of the Werner Heisenberg Institute of Physics) N92-10591
The Technical Division (of the Werner Heisenberg Institute of Physics) N92-10592
Differential collision cross-sections for atomic oxygen: Analysis of space flight instruments for solar terrestrial physics
[NASA-CR-184235] N92-10613
Physics Division annual review, April 1, 1990 - March 31, 1991
[DE91-018704] N92-10707
NASA maintenance: Stronger commitment needed to curb facility deterioration
[GAO/NSIAD-91-34] N92-10709
RESEARCH MANAGEMENT
MPD thruster research issues, activities, strategies N92-10051
Program and abstracts of the 2nd Meeting of the Society for Research on Biological Rhythms
[AD-A240007] N92-10280
Activities of the Board on Mathematical Sciences
[DE91-017931] N92-10361
Materials science and technology centra in Sweden and Denmark: A research policy for the future N92-10580
Activities report of the Werner Heisenberg Institute for Physics, Munich (Federal Republic of Germany)
[ISSN-0173-6256] N92-10588
The Theoretical Division (of the Werner Heisenberg Institute for Physics) N92-10589
The A Experimental Division (of the Werner Heisenberg Institute for Physics) N92-10590
The B Experimental Division (of the Werner Heisenberg Institute of Physics) N92-10591
The Technical Division (of the Werner Heisenberg Institute of Physics) N92-10592
Differential collision cross-sections for atomic oxygen: Analysis of space flight instruments for solar terrestrial physics
[NASA-CR-184235] N92-10613
Physics Division annual review, April 1, 1990 - March 31, 1991
[DE91-018704] N92-10707
RESEARCH PROJECTS
Investigations of the effects of isotopic substitution and pressure on miscibility in polymer-polymer and polymer-solvent systems
[DE91-018010] N92-10094
Explosive Transient Camera (ETC) program
[NASA-CR-188957] N92-10184
Program and abstracts of the 2nd Meeting of the Society for Research on Biological Rhythms
[AD-A240007] N92-10280
Content addressable memory project
[NASA-CR-188981] N92-10299
Activities report of the Werner Heisenberg Institute for Physics, Munich (Federal Republic of Germany)
[ISSN-0173-6256] N92-10588
The Theoretical Division (of the Werner Heisenberg Institute for Physics) N92-10589
The A Experimental Division (of the Werner Heisenberg Institute for Physics) N92-10590
The B Experimental Division (of the Werner Heisenberg Institute of Physics) N92-10591
The Technical Division (of the Werner Heisenberg Institute of Physics) N92-10592
Physics Division annual review, April 1, 1990 - March 31, 1991
[DE91-018704] N92-10707
RESERVOIRS
Electromagnetic oil field mapping for improved process monitoring and reservoir characterization
[DE91-017452] N92-10132
RESIDUAL STRESS
High temperature creep properties of eutectic and near eutectic silver-copper alloys: Application to metal/ceramic joining
[DE91-017987] N92-10082
RESIN MATRIX COMPOSITES
Poly 1, 2, 4-triazoles via aromatic nucleophilic displacement
[NASA-CASE-LAR-14440-1] N92-10066
RESONANCE
Contribution of the delta resonance to the Gamow-Teller decay of heavy nuclei N92-10407
Gamma-decay branching of 1(+)-states in Gd-156 and Dy-164 N92-10410
Decay channels of resonantly excited 2p(-1)ns, md states of Ar and 3d(-1)np states of Kr N92-10426
Isotope selective resonance ionization measurements of lithium N92-10442
Analysis of the interacting levels V(sub 9) = 1 and V(sub 10) = 2 of propyne N92-10444
Gamma echo experiments N92-10512
Super Coster Kronig and resonance super Coster Kronig spectra of solid Ge around 3p-ionization threshold N92-10517
RESONANT FREQUENCIES
Development of a model of space station solar array
[NASA-CR-188911] N92-10220
The nu(sub 4) and nu(sub 7) bands of CD3CN with coriolis coupling and other resonance perturbations N92-10432
The infrared rotation-vibration spectrum of C2H2 in the nu(sub 2) + nu(sub 5) band region; l-resonances in the bands nu(sub 2) + nu(sub 5), nu(sub 2) + 2(nu(sub 5)) back arrow nu(sub 5) and nu(sub 1) back arrow nu(sub 5) N92-10434
RESONANT TUNNELING
The stability analysis of a double barrier resonant tunneling device N92-10485
Tunneling in oscillating double barrier heterostructures N92-10496
Tunneling calculations for GaAs-Al(x)Ga(1-x) as graded band-gap sawtooth superlattices
[NASA-TM-100726] N92-10680
RESOURCES MANAGEMENT
Management issues at the National Aeronautics and Space Administration
[GAO/T-NSIAD-91-48] N92-10710
RESPONSE TIME (COMPUTERS)
Telescience testbed pilot program, volume 3: Experiment summaries
[NASA-CR-188834] N92-10032
Queueing in networks of computers
[NASA-CR-188892] N92-10308
RETINA
Fundamental studies in the molecular basis of laser induced retinal damage
[AD-A239941] N92-10278
Two informative cases of Q-switched laser eye injury
[AD-A240001] N92-10279
REVERSE FIELD PINCH
Vlasov-Maxwell system: 2-D equilibria, reversed field pinches
[DE91-018421] N92-10595
The meandering orbit effect on stabilization of the tilting instability in a field-reversed configuration
[NIFS-22] N92-10648
REYNOLDS NUMBER
A grid-free method for high Reynolds number flow around an immersed elastic structure
[AD-A239851] N92-10013
REYNOLDS STRESS
A non-isotropic multiple-scale turbulence model
[NASA-CR-184217] N92-10160
RHEOLOGY
Crystallization during emplacement of lava flows N92-10789
Rheological analyses of lava flows on Mars N92-10791
Factors controlling lava dome morphology N92-10792
Theoretical studies of volatile processes in the outer solar system N92-10807
RHODIUM
Surface electrochemistry of Chloro(phthalocyaninato)rhodium(III) species, and oxygen reduction electrocatalysis, formation of a dimeric species
[AD-A240148] N92-10104
RHYTHM (BIOLOGY)
Program and abstracts of the 2nd Meeting of the Society for Research on Biological Rhythms
[AD-A240007] N92-10280
RIDGES
Wrinkle ridge-upland scarp transitions: Implications for the mechanical properties of the deformed materials N92-10954
Wrinkle ridges in the floor material of Kasei Valles, Mars: Nature and origin N92-10955
RIGID STRUCTURES
PASS spacecraft antenna technology assessment N92-10123
RIPPLES
RIPPLE: A new model for incompressible flows with free surfaces
[DE91-017830] N92-10168
The potential scale of aeolian structures on Venus N92-10800
RISK
Assessing and managing the risks of climate change N92-10233
ROBOTS
A measuring robot for thermal environment, contaminant concentration and ventilation studies N92-10537
ROBUSTNESS (MATHEMATICS)
On the formulation of a minimal uncertainty model for robust control with structured uncertainty
[NASA-TP-3094] N92-10027
The improved robustness of multigrid elliptic solvers based on multiple semicoarsened grids
[NASA-CR-187633] N92-10348
Particle-gas dynamics in the protoplanetary nebula N92-10893
ROCHE LIMIT
Tidal disruption of inviscid protoplanets N92-10900
ROCKET ENGINE DESIGN
Combustion of Solid Propellants --- Author
[AGARD-LS-180] N92-10106
ROCKET ENGINES
Extended temperature range rocket injector
[NASA-CASE-LEW-14846-1] N92-10054
ROCKET LAUNCHING
Predicting cloud-to-ground lightning with neural networks
[AD-A239989] N92-10270
ROCKS
Clays on Mars: Review of chemical and mineralogical evidence N92-10250
UV, visible, and near-IR reflectivity data for magnetic soils/rocks from Brazil N92-10254
Surface-material maps of Viking landing sites on Mars N92-10787
RODS
A survey of laser lightning rod techniques
[AD-A239988] N92-10269
ROOM TEMPERATURE
High temperature materials characterization
[NASA-CR-184231] N92-10079
ROTARY WING AIRCRAFT
Passive range estimation for rotorcraft low-altitude flight
[NASA-TM-103897] N92-10003
Rotor noise N92-10600
ROTATING BODIES
Rotatable non-circular forebody flow controller
[NASA-CASE-LAR-14212-1-CU] N92-10021
ROTATING PLASMAS
Geometrical effects of the magnetic field on the neoclassical flow, current, and rotation in general toroidal systems
[NIFS-86] N92-10655
Density peaking in the JFT-2M tokamak plasma with counter neutral beam injection
[NIFS-83] N92-10657
ROTATION
Observation of plasma toroidal rotations driven by the electric field due to a loss of ions
[NIFS-23] N92-10647
ROTATIONAL SPECTRA
The rotational structure of the nu(sub 6) vibration band of CH3I N92-10431
ROTOR AERODYNAMICS
Rotor noise N92-10600

RULES
Type abstraction rules for references: A comparison of four which have achieved notoriety
[AD-A240076] N92-10716
RUN TIME (COMPUTERS)
Integrity and security in an Ada runtime environment
[NASA-CR-188826] N92-10313
A portable run-time system for PCN
[DE91-017700] N92-10319
RUNGE-KUTTA METHOD
Multigrid calculation of three-dimensional viscous cascade flows
[NASA-TM-105257] N92-10345

S

SACCADIC EYE MOVEMENTS
Visual motion perception
[AD-A240133] N92-10286
SAFETY FACTORS
Combustion and safety of solid propellant rocket motors N92-10110
The EH safety representative information system on the safety performance measurement system is where you will find... Word processing and helps with a V-PLUS
[DE91-018709] N92-10113
SALINITY
Sea ice elastic moduli: Determination of Biot parameters using in-field velocity measurements
[AD-A239803] N92-10275
SANDS
The potential scale of aeolian structures on Venus N92-10800
Relationships between topographic roughness and aeolian processes N92-10801
Remote sensing observations of Kelso Dunes, California N92-10847
SAPPHIRE
Heteroepitaxial growth of TiO2, VO2, and TiO2/VO2 multilayers by MOCVD
[DE91-018543] N92-10694
Heteroepitaxy of MOCVD grown TiO2, VO2 films and TiO2/VO2 multilayers on sapphire (1120)
[DE91-018589] N92-10698
SATELLITE ALTIMETRY
Geoid undulations and gravity anomalies over the Aral Sea, the Black Sea and the Caspian Sea from a combined GEOS-3/SEASAT/GEOSAT altimeter data set
[NASA-TM-104543] N92-10257
SATELLITE ATMOSPHERES
Theoretical studies of volatile processes in the outer solar system N92-10807
SATELLITE COMMUNICATION
Impact of non-geostationary orbits on PASS N92-10120
User antennas N92-10121
C4I2 in space: Solving the SatCom shortfall
[AD-A239880] N92-10140
SATELLITE CONTROL
C4I2 in space: Solving the SatCom shortfall
[AD-A239880] N92-10140
SATELLITE DESIGN
Design restrictions and licensing for Petite Amateur Navy Satellite (PANSAT)
[AD-A239951] N92-10041
Small upper stage basic program
[AD-A240059] N92-10063
Antenna beam coverage concepts N92-10119
SATELLITE NETWORKS
Introduction to the Personal Access Satellite System study N92-10117
SATELLITE OBSERVATION
Using LANDSAT to provide potato production estimates to Columbia Basin farmers and processors
[NASA-CR-188783] N92-10209
The remote sensing Loosdrecht Lakes (Netherlands) project
[BCRS-90-29] N92-10215
A technique for estimating surface meteorological ranges over oceans from satellite measurements of aerosol optical depth
[AD-A239985] N92-10219
Origin and evolution of the zodiacal dust cloud N92-10886
SATELLITE ORBITS
Impact of non-geostationary orbits on PASS N92-10120
The Titan-Hyperion orbital resonance N92-10946
Rotational properties of planetary satellites N92-10947
SATELLITE ROTATION
Rotational properties of planetary satellites N92-10947
SATELLITE TRANSMISSION
Technology assessment and experimentation plan N92-10124
SATURN (PLANET)
Charged-particle induced alterations of surfaces in the outer solar system N92-10838
SATURN RINGS
Ring satellite interaction in planetary rings N92-10572
Numerical simulations of dense collisional systems N92-10573
Planetary ring studies N92-10903
Physical processes in planetary rings N92-10904
Models of planetary rings N92-10934
SATURN SATELLITES
Disk resolved studies of the optical properties and physical nature of the surfaces of the outer planet satellites N92-10837
SAWTOOTH WAVEFORMS
The DIII-D tokamak and energy confinement at low q
[DE91-018317] N92-10664
SCANNERS
Automated eddy current analysis of materials
[NASA-CR-184216] N92-10200
Atmospheric measurements using a scanning, solar-blind Raman Lidar
[DE91-016078] N92-10260
SCANNING
Antenna beam coverage concepts N92-10119
SCANNING TUNNELING MICROSCOPY
Scanning tunneling microscope measurements in air:Langmuir-Blodgett films on HOPG and growth of evaporated gold on HOPG N92-10497
Scanning tunneling microscopy of polysialic acid N92-10538
SCATTERING
Limitations of the condensed history method for low energy electrons
[DE91-015764] N92-10619
Valence and phonon excitations in high-resolution electron microscopy
[DE91-017684] N92-10625
The response history Monte Carlo method for electron transport
[DE91-018295] N92-10631
Character of the opposition effect and negative polarization N92-10833
Surface scattering properties estimated from modeling airborne multiple emission angle reflectance data N92-10841
The Geologic Remote Sensing Field Experiment (GRSFE) N92-10844
SCATTERING COEFFICIENTS
Use of radar to assess aeolian processes N92-10802
SCATTERING CROSS SECTIONS
Differential collision cross-sections for atomic oxygen: Analysis of space flight instruments for solar terrestrial physics
[NASA-CR-184235] N92-10613
Experiments on the nuclear interactions of pions and electrons
[DE91-017929] N92-10623
SCATTERING FUNCTIONS
Inclusive quasielastic and deep inelastic electron scattering at high energies
[DE91-018755] N92-10633
SCHEDULING
Gang scheduling a parallel machine
[DE91-011539] N92-10336
SCHOOLS
The role of the computer in science fair projects: Current status and potential
[DE91-008606] N92-10295
SCHOTTKY DIODES
Formation of self-aligned guard rings for monolithic Schottky-barrier diode arrays
[NASA-CASE-NPO-17734-1-CU] N92-10146
Electrical characterization of Li and N doped ZnSe N92-10493
SCHROEDINGER EQUATION
Dynamics of discrete quantum nonlinear Schroedinger equations N92-10371
SCINTILLATION COUNTERS
Calibration of scintillation cells for radon-222 measurements N92-10521
Fiber-tile optical studies at Argonne
[DE91-018591] N92-10641
SEA ICE
Sea ice elastic moduli: Determination of Biot parameters using in-field velocity measurements
[AD-A239803] N92-10275
SEA LEVEL
Sea-level rise: Regional consequences and responses N92-10231
SEALING
Helmet of a laminate construction of polycarbonate and polysulfone polymeric material
[NASA-CASE-MSC-21503-1] N92-10091
SEALS (STOPPERS)
Relative sliding durability of two candidate high temperature oxide fiber seal materials
[NASA-TM-105199] N92-10064
SEARCHING
Display format, highlight validity, and highlight method: Their effects on search performance
[NASA-TM-104742] N92-10287
SEASAT SATELLITES
The design of spaceborne synthetic aperture radar
[ETN-91-99986] N92-10114
SECURITY
Integrity and security in an Ada runtime environment
[NASA-CR-188826] N92-10313
SEDIMENT TRANSPORT
Relationships between topographic roughness and aeolian processes N92-10801
Use of radar to assess aeolian processes N92-10802
SEDIMENTS
Mapping compositional and particle size variations across Silver Lake Playa: Relevance to analyses of Mars TIR data N92-10642
SEISMIC WAVES
The detection and location of near-regional seismic disturbances by the Eskdalemuir array: A study using noise and signal correlations
[AWE-RE-0-20/90] N92-10247
Lithosphere physics: Geoelectrics and seismics N92-10551
SEISMOGRAPHS
The detection and location of near-regional seismic disturbances by the Eskdalemuir array: A study using noise and signal correlations
[AWE-RE-0-20/90] N92-10247
Integrated array and 3-component processing using a seismic microarray
[AD-A240139] N92-10265
SEISMOLOGY
The detection and location of near-regional seismic disturbances by the Eskdalemuir array: A study using noise and signal correlations
[AWE-RE-0-20/90] N92-10247
Martian seismicity N92-10733
The formation of antipodal-impact terrains on Mars N92-10749
SELF ALIGNMENT
Formation of self-aligned guard rings for monolithic Schottky-barrier diode arrays
[NASA-CASE-NPO-17734-1-CU] N92-10146
SEMANTICS
IID: An intelligent information dictionary for managing semantic metadata
[AD-A240022] N92-10715
SEMICONDUCTING FILMS
Semiconducting organic thin films as monitoring devices for NO2 air pollution N92-10527
SEMICONDUCTOR DEVICES
Transport in heterostructures and devices in microwave and millimeter-wave regimes
[AD-A239943] N92-10142
Sintered compacts for heat sinks and process for fabricating same
[DE91-018438] N92-10153
Highlights of material research for optoelectronics in the eighties, trends and challenges for the nineties N92-10486
Compound semiconductor technology: Materials and devices N92-10523
Semiconducting organic thin films as monitoring devices for NO2 air pollution N92-10527
SEMICONDUCTOR DIODES
Efficient, high-speed, monolithic optoelectronic circuits using quantum-confined structures
[AD-A239841] N92-10155
SEMICONDUCTOR LASERS
A miniature acousto-optic image correlator
[DE91-018002] N92-10151
Sintered compacts for heat sinks and process for fabricating same
[DE91-018438] N92-10153
Two-color holography concept (T-CHI)
[NASA-CR-184240] N92-10183
A simple method to stabilize the frequency of semiconductor lasers N92-10453
SEMICONDUCTORS (MATERIALS)
High temperature solar cell contacts
[AD-A239932] N92-10227
Compound semiconductor technology: Materials and devices N92-10523

SENSITIVITY
Process modelling for Space Station experiments
[NASA-CR-184227] N92-10112
The crystal structure and moisture sensitivity of (+)-4-(1-(2,3 dimethylphenyl) ethyl) 1H-imidazole hydrochloride N92-10522
Novel type of cryogenic liquid level sensor with high sensitivity N92-10528

SENSORY PERCEPTION
Advances and experience with teleoperated systems incorporating remote presence
[AD-A239980] N92-10199

SEPARATED FLOW
Numerical investigation of the effect of leading edge geometry on dynamic stall of airfoils
[AD-A239949] N92-10015

SEPARATORS
Plan for the JYFL gas-filled recoil separator N92-10424

SEQUENCING
Paucity of moderately repetitive sequences
[DE91-017953] N92-10276
Computer assisted multiplex sequencing
[DE91-017851] N92-10337

SERVICE LIFE
Thermal energy storage and heat transfer support program. Task-5 heat pipe life test study. Facilities upgrading and maintenance
[AD-A239929] N92-10177

SHAPES
Effects of grain size and shape in modeling reflectance spectra of mineral mixtures N92-10831

SHEAR FLOW
A non-isotropic multiple-scale turbulence model
[NASA-CR-184217] N92-10160
Nonlinear interactions of tearing modes in the presence of shear flow
[DE91-018420] N92-10173
Noise from turbulent shear flows N92-10603

SHEAR LAYERS
Contractors Meeting in Propulsion
[AD-A240057] N92-10062

SHEAR STRESS
The strength of Miranda's lithosphere N92-10767

SHERGOTTITES
Does Lafayette = Nakhla? Not necessarily so, based on 4.2K Mossbauer spectra of all of the SNC meteorites N92-10825

SHOCK TESTS
Impact and collisional processes in the solar system N92-10932

SHOCK WAVE INTERACTION
Hypersonic flows as related to the National Aerospace plane
[NASA-CR-187985] N92-10004

SHOCK WAVES
Properties of shocked relativistic jets N92-10564
Explanation for optical frequency dependent polarization in blazars N92-10577
Sonic boom N92-10608

SHORT CIRCUITS
The short-circuited fluxgate sensitivity parameters
[ISSN-0109-6605] N92-10147

SHUTTLE DERIVED VEHICLES
Shuttle orbiter with telescoping main propulsion unit and payload
[NASA-CASE-LAR-13586-1] N92-10035

SIGNAL ANALYSIS
Automated eddy current analysis of materials
[NASA-CR-184216] N92-10200

SIGNAL DETECTION
Method and apparatus for frequency spectrum analysis
[NASA-CASE-NPO-17759-1-CU] N92-10125
On adaptive multiband detection of targets in nonstationary nonhomogeneous interference
[AD-A239983] N92-10327

SIGNAL PROCESSING
Real-time data compression of broadcast video signals
[NASA-CASE-LEW-14945-2] N92-10128
Hardware description ADSP-21020 40-bit floating point DSP as designed in a remotely controlled digital CW Doppler radar
[DE91-018004] N92-10134
The application of the ADSP-21020 40-bit floating point DSP microprocessor in a digital Doppler radar
[DE91-018005] N92-10135
A frequency domain method for the generation of partially coherent normal stationary time domain signals
[DE91-017058] N92-10204
The detection and location of near-regional seismic disturbances by the Eskdalemuir array: A study using noise and signal correlations
[AWE-RE-0-20/90] N92-10247
A new phase retrieval method for CARS spectrum analysis N92-10363
Running discrete cosine transform algorithm N92-10375
Studies on new low noise silicon radiation detector N92-10418
Algorithm for detection of VFIB in real time from ECG N92-10542

SIGNAL REFLECTION
Gamma echo experiments N92-10512

SIGNAL TO NOISE RATIOS
The short-circuited fluxgate sensitivity parameters
[ISSN-0109-6605] N92-10147
The detection and location of near-regional seismic disturbances by the Eskdalemuir array: A study using noise and signal correlations
[AWE-RE-0-20/90] N92-10247

SIGNATURES
A restricted signature normal form for Hermitian matrices, quasi-spectral decompositions, and applications
[NASA-CR-188895] N92-10310

SILICATES
Clays on Mars: Review of chemical and mineralogical evidence N92-10250
Clay minerals in primitive meteorites and interplanetary dust 1 N92-10256
Degradation of Fe-Mg silicates in hot CO2 atmospheres: Applications to Venus N92-10806
An infrared reflectance study of low albedo surface constituents N92-10830
Character of the opposition effect and negative polarization N92-10833
Jetting and the origin of tektites N92-10868
Chemical fractionation of siderophile elements in impactites from Australian meteorite craters N92-10875
Magnetic effects of large-scale impacts on airless planetary bodies N92-10877
Impact cratering calculations N92-10933
Derivation of mid-infrared (5-25 microns) optical constraints of some silicates and palagonite N92-10950

SILICON
The DELPHI microvertex detector, a silicon tracking chamber N92-10412
Development of double-sided silicon strip detectors N92-10414
Radiation damage measurements on double-sided Si strip detectors N92-10415
Beam test results of ion-implanted silicon strip detectors on a 100 mm wafer N92-10416
Structure and optical polarizabilities of small silicon clusters N92-10425
Molecular dynamics using the tight-binding approximation: Application to liquid silicon N92-10465
Helium in silicon: A first principle molecular dynamics study N92-10473
Fabrication of GaAs: MESFET's and test structures for electrical material characterization N92-10529

SILICON ALLOYS
Microstructural stability and creep response of a new Al-Fe-W-Si alloy
[AD-A239861] N92-10087

SILICON COMPOUNDS
Photoemission in YbCu2Si2: Problems with the Kondo impurity model
[DE91-018018] N92-10684

SILICON DIOXIDE
Development and optimization of methodologies for analysis of complex hydrocarbon mixtures
[DE91-017954] N92-10075

SILICON NITRIDES
Update on the prospects for ceramic engine components
[DE91-018574] N92-10098

SILICON OXIDES
Surface characterization of coated powders with XPS: Al2O3-SiO2 coated TiO2 pigments N92-10520

SILICON RADIATION DETECTORS
Studies on new low noise silicon radiation detector N92-10418

SILVER
Antiferromagnetic ordering in silver at picoKelvin temperatures N92-10509

SIMULATION
Plasma cloud behavior
[AD-A240000] N92-10264
Laboratory simulation of cratering on small bodies N92-10659

SIMULATORS
BIRD: A general interface for sparse distributed memory simulators
[NASA-CR-188858] N92-10292

SINE WAVES
Preliminary comparison of 3.5-cm and 12.6-cm wavelength continuous wave observations of Mars N92-10848
Color-coded global topographic map of Mars N92-10920
Mars elevation distribution N92-10921

SINGLE CRYSTALS
NMR pulse responses of pairs of triads of 1/2 spins in solids N92-10511
Anisotropic twin boundary pinning in YBa2Cu3O(x)
[DE91-018536] N92-10692
Initial magnetization and magnetic relaxation in a single crystal of Bi2Sr2CaCu2O(x)
[DE91-018537] N92-10693
Reversible magnetization of Bi2Sr2CaCu2O8 single crystals
[DE91-018600] N92-10699
Neutron irradiation effects on YBCO single crystals
[DE91-018615] N92-10700
Activation energies in a Bi2Si2CaCu2O(x) single crystal
[DE91-018640] N92-10702

SINGLE EVENT UPSETS
An assessment of the radiation tolerance of large satellite memories in low earth orbits
[DE91-018353] N92-10040

SINKS
Climate change: Problems of limits and policy responses N92-10232

SINTERING
Sintered compacts for heat sinks and process for fabricating same
[DE91-018438] N92-10153

SIZE DISTRIBUTION
Crystallization during emplacement of lava flows N92-10789
Light scattering by lunar-like particle size distributions N92-10832
Hydrocode predictions of collisional outcomes: Effects of target size N92-10861

SKEWNESS
Mean estimation in highly skewed samples
[DE91-018513] N92-10358

SKIN FRICTION
Reflection type skin friction meter
[NASA-CASE-LAR-14520-1-SB] N92-10008

SKIN TEMPERATURE (BIOLOGY)
Physiological responses of the human extremities to cold water immersion
[IZF-1991-A-15] N92-10277

SLEEP
Auditory and visual evoked potentials as a function of sleep deprivation and irregular sleep
[AD-A240097] N92-10281

SLEEP DEPRIVATION
Auditory and visual evoked potentials as a function of sleep deprivation and irregular sleep
[AD-A240097] N92-10281

SLIDING FRICTION
Relative sliding durability of two candidate high temperature oxide fiber seal materials
[NASA-TM-105199] N92-10064

SLOPES
The perplexing continuum slope of Mars: Effects of thin ferric coatings and viewing geometry N92-10816
Oxidation of basaltic tephras: Influence on reflectance in the 1 micron region N92-10817

SLOTTED WIND TUNNELS
Mass flux similarity for slotted transonic-wind-tunnel walls
[NASA-TM-4281] N92-10006

SLURRIES
Steady flow of a fluid-solid mixture in a circular cylinder
[DE91-018698] N92-10174

SMALL SCIENTIFIC SATELLITES
Design restrictions and licensing for Petite Amateur Navy Satellite (PANSAT)
[AD-A239951] N92-10041

SNOW
Optical properties of CO2 ice and CO2 snow from ultraviolet to infrared: Application to frost deposits and clouds on Mars N92-10821

SOFTWARE ENGINEERING
The EH safety representative information system on the safety performance measurement system is where you will find... Word processing and helps with a V-PLUS
[DE91-018709] N92-10113
Solar Constant (SOLCON) Experiment: Ground Support Equipment (GSE) software development
[NASA-CR-187596] N92-10267
Methodology for automating software systems
[NASA-CR-184233] N92-10301

Software Technology for Adaptable, Reliable Systems (STARS): Domain specific environment repository composite paradigm report
[AD-A240107] N92-10328
Clustering: A powerful aid in classifying QRS waveforms N92-10541

SOILS
Clays on Mars: Review of chemical and mineralogical evidence N92-10250
UV, visible, and near-IR reflectivity data for magnetic soils/rocks from Brazil N92-10254
Soil crusts on Mars N92-10786
Laboratory photometric measurement of particulate soils out to very large phase angles N92-10834

SOLAR ACTIVITY
New observations of the low frequency interplanetary radio emissions
[NASA-CR-188917] N92-10971

SOLAR ARRAYS
Development of a model of space station solar array
[NASA-CR-188911] N92-10220
The SolarTrak solar array tracking controller
[DE91-017721] N92-10224

SOLAR CELLS
A generic guide for the preparation of a quality assurance/quality control manual for the design, production, and installation of photovoltaic concentrator systems
[DE91-017716] N92-10223
The SolarTrak solar array tracking controller
[DE91-017721] N92-10224
High efficiency GaAs/Ge monolithic tandem cells for space concentrator arrays, phase 1
[AD-A239931] N92-10226
High temperature solar cell contacts
[AD-A239932] N92-10227
InP solar cells grown by gas-source molecular beam epitaxy N92-10531

SOLAR COLLECTORS
The SolarTrak solar array tracking controller
[DE91-017721] N92-10224
High efficiency GaAs/Ge monolithic tandem cells for space concentrator arrays, phase 1
[AD-A239931] N92-10226
Solar detoxification technology: Using energy from the sun to destroy hazardous waste
[DE91-015007] N92-10241

SOLAR CONSTANT
Solar Constant (SOLCON) Experiment: Ground Support Equipment (GSE) software development
[NASA-CR-187596] N92-10267

SOLAR CORONA
The extension of solar magnetic fields into interplanetary space
[DE91-018052] N92-10970

SOLAR CORPUSCULAR RADIATION
Composition and energetics of solar flare particle events measured by satellites, 1989 - 1991
[DE91-018028] N92-10969

SOLAR CYCLES
Composition and energetics of solar flare particle events measured by satellites, 1989 - 1991
[DE91-018028] N92-10969
New observations of the low frequency interplanetary radio emissions
[NASA-CR-188917] N92-10971

SOLAR ECLIPSES
The 1990 solar eclipse as seen by a torsion pendulum N92-10550

SOLAR ENERGY
The Alternative Fuels Data Center
[DE91-015003] N92-10111
Solar energy in mitigating global environmental problems N92-10584

SOLAR ENERGY CONVERSION
Trade studies for nuclear space power systems
[NASA-TM-105231] N92-10221
Solar detoxification technology: Using energy from the sun to destroy hazardous waste
[DE91-015007] N92-10241

SOLAR FLARES
Composition and energetics of solar flare particle events measured by satellites, 1989 - 1991
[DE91-018028] N92-10969

SOLAR FLUX
Long-term neutrino flux integrations
[DE91-013903] N92-10967

SOLAR FURNACES
Solar detoxification technology: Using energy from the sun to destroy hazardous waste
[DE91-015007] N92-10241

SOLAR INTERIOR
Long-term neutrino flux integrations
[DE91-013903] N92-10967

SOLAR MAGNETIC FIELD
The extension of solar magnetic fields into interplanetary space
[DE91-018052] N92-10970

SOLAR NEUTRINOS
Anomalous e(-+)e(-) pairs in heavy ion collisions and solar neutrinos: Two puzzles with common solution? N92-10364
Long-term neutrino flux integrations
[DE91-013903] N92-10967
Solar and supernova neutrino interactions
[DE91-013905] N92-10968

SOLAR OBSERVATORIES
Performance tests of ERNE HED sensor N92-10562

SOLAR OSCILLATIONS
Solar and supernova neutrino interactions
[DE91-013905] N92-10968

SOLAR POSITION
The role of nonuniform internal heating in Triton's energy budget N92-10736

SOLAR PROTONS
EISCAT incoherent scatter radar observations and model studies on day to night variations in the ionospheric D-region during the PCA event of August 1989 N92-10559

SOLAR RADIATION
Solar detoxification technology: Using energy from the sun to destroy hazardous waste
[DE91-015007] N92-10241
EISCAT incoherent scatter radar observations and model studies on day to night variations in the ionospheric D-region during the PCA event of August 1989 N92-10559
Meteo and irradiation data during BEST TWO, Mourmelon (Netherlands)
[FEL-90-A368] N92-10966

SOLAR SYSTEM
Theoretical studies of optical phenomena and related inverse problems of solar system bodies N92-10566
Energy coupling in catastrophic collisions N92-10862
Mapping the stability field of Jupiter Trojans N92-10883
Origin and evolution of the zodiacal dust cloud N92-10886
Formation of the protosolar nebula N92-10890
Accretion and evolution of solar system bodies N92-10895
Digital solar system geology N92-10928
Generation and behavior of solar system magnetic fields N92-10939

SOLAR WIND
The effect of latitudinally varying solar wind flux on the Lyman alpha sky background N92-10570
Asteroid surface processes: Experimental studies of the solar wind on reflectance and optical properties of asteroids N92-10941
The extension of solar magnetic fields into interplanetary space
[DE91-018052] N92-10970

SOLDERED JOINTS
High temperature creep properties of eutectic and near eutectic silver-copper alloys: Application to metal/ceramic joining
[DE91-017987] N92-10082
Wettability of low temperature solder alloys for step-soldering
[DE91-018348] N92-10083
Proceedings of the Second Switch Tube Advanced Technology Meeting
[DE91-017718] N92-10148

SOLDERING
Wettability of low temperature solder alloys for step-soldering
[DE91-018348] N92-10083
Proceedings of the Second Switch Tube Advanced Technology Meeting
[DE91-017718] N92-10148

SOLDERS
Wettability of low temperature solder alloys for step-soldering
[DE91-018348] N92-10083

SOLID ELECTROLYTES
Fuel cell systems program plan, fiscal year 1991
[DE91-017215] N92-10225

SOLID MECHANICS
Driven growth in the restricted solid on solid model N92-10373

SOLID PROPELLANT COMBUSTION
Combustion of Solid Propellants --- Author
[AGARD-LS-180] N92-10106
Solid propellant steady combustion: Physical aspects N92-10107
Effects of wires on solid propellant ballistics N92-10109
Simultaneous pyrometric measurement of temperature and size of fuel particles in fluidized bed combustions N92-10381

SOLID PROPELLANT ROCKET ENGINES
The space shuttle advanced solid rocket motor: Quality control and testing
[NASA-CR-188800] N92-10043
Combustion of Solid Propellants --- Author
[AGARD-LS-180] N92-10106
Effects of wires on solid propellant ballistics N92-10109
Combustion and safety of solid propellant rocket motors N92-10110

SOLID PROPELLANTS
Combustion of Solid Propellants --- Author
[AGARD-LS-180] N92-10106
Solid propellant steady combustion: Physical aspects N92-10107
Effects of wires on solid propellant ballistics N92-10109
Combustion and safety of solid propellant rocket motors N92-10110

SOLID STATE
Solid-State Radar Beacon Decoder (SSRBD) Operational Test and Evaluation (OT/E) integration test plan
[DOT/FAA/CT-TN91/30] N92-10020
Synchrotron radiation study of recombination processes in solid state Tb and Dy after 4d to 4f giant resonance excitation N92-10518
The N(4,5)N(6,7)N(6,7) and N(4,5)O(2,3)N(6,7) resonance Auger effects in the electron spectra of solid state Gd and Eu N92-10519

SOLID SURFACES
Quantum state resolved desorption of CO from solid surface
[DE91-017712] N92-10626

SOLID-SOLID INTERFACES
Driven growth in the restricted solid on solid model N92-10373
Interface effects on electrical properties of high purity InP grown by gas-source molecular beam epitaxy N92-10490
A statistical mechanics study of solid-solid interfaces
[DE91-017852] N92-10689

SOLIDIFICATION
Two-color holography concept (T-CHI)
[NASA-CR-184240] N92-10183

SOLIDIFIED GASES
NMR and ESR experiments on solid molecular hydrogen containing atomic hydrogen N92-10510

SOLIDS
Laser induced optical damage in solids
[AD-A240124] N92-10194

SOLIDS FLOW
Steady flow of a fluid-solid mixture in a circular cylinder
[DE91-018698] N92-10174

SOLITARY WAVES
Dromions: The movie N92-10370

SOLUBILITY
Investigations of the effects of isotopic substitution and pressure on miscibility in polymer-polymer and polymer-solvent systems
[DE91-018010] N92-10094
Transformation products of submicron-sized aluminum-substituted magnetite: Color and reductant solubility N92-10251
Photoresist crossed gratings N92-10448
Passivation of high temperature superconductors
[NASA-CASE-NPO-17949-1-CU] N92-10681

SOLVENT EXTRACTION
Air pulsed plate liquid-liquid extractor simulation
[DE91-018155] N92-10172

SONIC BOOMS
Sonic boom N92-10608

SORBATES
Adsorbate induced surface reconstruction N92-10469

SORBENTS
Regenerative Cu/La zeolite supported desulfurizing sorbents
[NASA-CASE-NPO-17480-1-CU] N92-10073

SOUND GENERATORS
Noise from turbulent shear flows N92-10603

SOUND INTENSITY
The measurement of plate vibration and sound radiation from a turbulent boundary layer manipulator
[AD-A240127] N92-10206

SOUND PRESSURE
Acoustic device and method for measuring gas densities
[NASA-CASE-NPO-18155-1-CU] N92-10609

SOUND WAVES
The measurement of plate vibration and sound radiation from a turbulent boundary layer manipulator [AD-A240127] N92-10206
Jet noise classical theory and experiments N92-10602
Propulsive lift noise N92-10606
SOURCE PROGRAMS
The paradigm compiler: Mapping a functional language for the connection machine [NASA-CR-188839] N92-10290
SPACE BASED RADAR
The design of spaceborne synthetic aperture radar [ETN-91-99986] N92-10114
SPACE EXPLORATION
The MPD thruster program at JPL N92-10046
LLNL contributions to MPD thrusters for SEI N92-10047
Trade studies for nuclear space power systems [NASA-TM-105231] N92-10221
SPACE PLASMAS
Plasma Science Committee (PLSC) [DE91-018011] N92-10594
Plasma Physics Research Institute, Lawrence Livermore National Laboratory, University of California, Davis annual report for fiscal year 1989 [DE91-018490] N92-10669
Magnetic effects of large-scale impacts on airless planetary bodies N92-10877
The extension of solar magnetic fields into interplanetary space [DE91-018052] N92-10970
SPACE PLATFORMS
Trade studies for nuclear space power systems [NASA-TM-105231] N92-10221
SPACE POWER REACTORS
Materials in space nuclear power systems [DE91-017688] N92-10058
Status of Rankine-cycle technology for space nuclear power applications [DE91-017859] N92-10059
Comparison of selected nuclear thermal propulsion concepts [DE91-017982] N92-10060
Instrumentation and control for space nuclear propulsion [DE91-018351] N92-10061
Trade studies for nuclear space power systems [NASA-TM-105231] N92-10221
High efficiency GaAs/Ge monolithic tandem cells for space concentrator arrays, phase 1 [AD-A239931] N92-10226
PATRAN and P/THERMAL applications for thermal modeling [DE91-017767] N92-10320
SPACE SHUTTLE MAIN ENGINE
Shuttle orbiter with telescoping main propulsion unit and payload [NASA-CASE-LAR-13586-1] N92-10035
SPACE SHUTTLE ORBITERS
Shuttle orbiter with telescoping main propulsion unit and payload [NASA-CASE-LAR-13586-1] N92-10035
SPACE SHUTTLE PAYLOADS
Telescience testbed pilot program, volume 3: Experiment summaries [NASA-CR-188834] N92-10032
Telescience testbed pilot program, volume 2: Program results [NASA-CR-188835] N92-10033
SPACE SHUTTLES
The space shuttle advanced solid rocket motor: Quality control and testing [NASA-CR-188800] N92-10043
SPACE STATION FREEDOM
Telescience testbed pilot program, volume 1: Executive summary [NASA-CR-188833] N92-10031
Telescience testbed pilot program, volume 3: Experiment summaries [NASA-CR-188834] N92-10032
Telescience testbed pilot program, volume 2: Program results [NASA-CR-188835] N92-10033
Management of the Space Station Freedom onboard local area network [NASA-TM-104741] N92-10036
Modeling of the Space Station Freedom data management system [NASA-CR-188869] N92-10038
Description of the PMAD DC test bed architecture and integration sequence [NASA-TM-105284] N92-10055
Numerical analysis and simulation of an assured crew return vehicle flow field [NASA-TP-3101] N92-10161
SPACE STATION PAYLOADS
Telescience testbed pilot program, volume 1: Executive summary [NASA-CR-188833] N92-10031
SPACE STATIONS
Process modelling for Space Station experiments [NASA-CR-184227] N92-10112
SPACE TRANSPORTATION
Activities report of the Norwegian Space Center [ETN-91-90052] N92-10029
IRS organigram N92-10053
SPACEBORNE ASTRONOMY
Finnish space projects: Space astronomy N92-10549
The measuring modes and observations with the x-ray spectrometer array SIXA onboard spectrum-x-gamma N92-10563
SPACEBORNE EXPERIMENTS
Process modelling for Space Station experiments [NASA-CR-184227] N92-10112
Solar Constant (SOLCON) Experiment: Ground Support Equipment (GSE) software development [NASA-CR-187596] N92-10267
SPACECRAFT ANTENNAS
Spacecraft antennas N92-10122
PASS spacecraft antenna technology assessment N92-10123
SPACECRAFT COMMUNICATION
Modeling of the Space Station Freedom data management system [NASA-CR-188869] N92-10038
Personal Access Satellite System (PASS) study. Fiscal year 1989 results [NASA-CR-188808] N92-10116
Technology assessment and experimentation plan N92-10124
SPACECRAFT CONFIGURATIONS
Numerical simulation of hypersonic viscous flow for the design of H-2 orbiting plane (HOPE-2) [NAL-TR-1093] N92-10009
Shuttle orbiter with telescoping main propulsion unit and payload [NASA-CASE-LAR-13586-1] N92-10035
Multi-reactor power system configurations for multimegawatt nuclear electric propulsion [NASA-TM-105212] N92-10057
SPACECRAFT INSTRUMENTS
The data book of ERS-1: The European Remote Sensing Satellite [ESA-BR-75] N92-10039
Performance tests of ERNE HED sensor N92-10562
CAPS-plasma spectrometer for the Cassini spacecraft N92-10565
SPACECRAFT POWER SUPPLIES
Description of the PMAD DC test bed architecture and integration sequence [NASA-TM-105284] N92-10055
Materials in space nuclear power systems [DE91-017688] N92-10058
Trade studies for nuclear space power systems [NASA-TM-105231] N92-10221
SPACECRAFT PROPULSION
Shuttle orbiter with telescoping main propulsion unit and payload [NASA-CASE-LAR-13586-1] N92-10035
NEP mission sensitivities N92-10045
The MPD thruster program at JPL N92-10046
SPACECRAFT STRUCTURES
Shuttle orbiter with telescoping main propulsion unit and payload [NASA-CASE-LAR-13586-1] N92-10035
SPATIAL DISTRIBUTION
The remote sensing Loosdrecht Lakes (Netherlands) project [BCRS-90-29] N92-10215
The spatial distribution and time evolution of impact-generated magnetic fields N92-10878
SPATIAL FILTERING
Abel inversion with the fast Fourier transform N92-10379
SPATIAL RESOLUTION
A 40th deg and order gravitational field model for Mars N92-10760
SPECIFIC HEAT
Characteristics of the Martian atmosphere surface layer N92-10804
SPECTRA
Determining desorption pre-exponential factors from temperature-programmed desorption spectra when the surface is nonuniform [DE91-009971] N92-10074
Transformation products of submicron-sized aluminum-substituted magnetite: Color and reductant solubility N92-10251
Variable features in the Valles Marineris region of Mars N92-10799
Remote sensing and geologic studies of the orientale basin region N92-10809
The perplexing continuum slope of Mars: Effects of thin ferric coatings and viewing geometry N92-10816
Oxidation of basaltic tephras: Influence on reflectance in the 1 micron region N92-10817
Spectral evidence for carbonates on Mars: Hydrous carbonates N92-10820
Optical properties of CO2 ice and CO2 snow from ultraviolet to infrared: Application to frost deposits and clouds on Mars N92-10821
Reflectance spectra of Fe(2+)-Mg(2+) disordered pyroxenes: Implications to remote-sensed spectra of planetary surfaces N92-10823
Pre-terrestrial oxidation products in carbonaceous meteorites identified by Mossbauer spectroscopy N92-10824
Does Lafayette = Nakhla? Not necessarily so, based on 4.2K Mossbauer spectra of all of the SNC meteorites N92-10825
Darkening in gas-rich ordinary chondrites: Spectral modelling and implications for the regoliths of ordinary chondrite parent bodies N92-10827
The bidirectional reflectance spectra of five gas-rich ordinary chondrites N92-10828
Reflectance spectra of some fractions of Migei and Murchison SM chondrites in the range of 0.3-2.6 microns N92-10829
Effects of grain size and shape in modeling reflectance spectra of mineral mixtures N92-10831
New spectral observations of Callisto and leading/trailing hemisphere distinctions N92-10839
Mojave remote sensing field experiment N92-10840
Application of Hapke photometric model to three geologic surfaces using PARABOLA bidirectional reflection data N92-10843
SPECTRAL BANDS
Shapes of Cd-110 at high spins N92-10404
Evidence for band termination in Xe-118 N92-10405
Proton-neutron symmetry in boson models of nuclear structure N92-10406
The rotational structure of the nu(sub 6) vibration band of CH3I N92-10431
The nu(sub 8) and 2nu(sub 8) bands of CD3CN N92-10433
The infrared rotation-vibration spectrum of C2H2 in the nu(sub 2) + nu(sub 5) band region; I-resonances in the bands nu(sub 2) + nu(sub 5), nu(sub 2) + 2(nu(sub 5)) back arrow nu(sub 5) and nu(sub 1) back arrow nu(sub 5) N92-10434
Analysis of the interacting levels V(sub 9) = 1 and V(sub 10) = 2 of propyne N92-10444
An infrared reflectance study of low albedo surface constituents N92-10830
SPECTRAL ENERGY DISTRIBUTION
A frequency domain method for the generation of partially coherent normal stationary time domain signals [DE91-017058] N92-10204
SPECTRAL METHODS
A frequency domain method for the generation of partially coherent normal stationary time domain signals [DE91-017058] N92-10204
SPECTRAL REFLECTANCE
Absorption measurements with an integrating sphere and an FT-IR spectrometer N92-10445
Spectral reflectance of pine and intensity of moose browsing N92-10514
Infrared reflectance spectra (4-12 micron) of lunar samples N92-10812
Disk-resolved spectral reflectance properties of Phobos from 0.3-3.2 micron: Preliminary integrated results from Phobos 2 N92-10822
Meteorite spectroscopy and characterization of asteroid surface materials N92-10881
Derivation of mid-infrared (5-25 microns) optical constraints of some silicates and palagonite N92-10950
SPECTROMETERS
Combined Backscatter Moessbauer Spectrometer and X Ray Fluorescence analyzer (BaMS/XRF) for planetary surface materials N92-10249
Ion mobility spectrometer to trace gas analysis N92-10535
The measuring modes and observations with the x-ray spectrometer array SIXA onboard spectrum-x-gamma N92-10563
CAPS-plasma spectrometer for the Cassini spacecraft N92-10565
Electronics of the cosmic ray air shower array at Turku (Finland) N92-10574
Experiments on the nuclear interactions of pions and electrons [DE91-017929] N92-10623
New spectral observations of Callisto and leading/trailing hemisphere distinctions N92-10839

SPECTRORADIOMETERS
Surface scattering properties estimated from modeling airborne multiple emission angle reflectance data N92-10841
SPECTROSCOPIC ANALYSIS
Observations on very neutron-rich nuclei below Z = 50 N92-10402
High-spin states in Cd-109 N92-10403
Shapes of Cd-110 at high spins N92-10404
Studies on superconducting Bi2Sr2Ca(n-1) Cu(n)O(4+2n) compounds with Fe-57 and Eu-151 Moessbauer spectroscopy N92-10504
Spectroscopic analyses of Fe and water in clays: A Martian surface weathering study N92-10818
SPECTROSCOPY
Proton NMR studies on human blood plasma: An application to cancer research N92-10545
High resolution spectroscopy of H(+) energy loss in thin carbon film
[NIFS-88] N92-10654
Remote sensing and geologic studies of the orientale basin region N92-10809
Spectroscopic analyses of Fe and water in clays: A Martian surface weathering study N92-10818
Water detection at the moon, Mars and comets with a combined neutron gamma ray instrument N92-10819
Pre-terrestrial oxidation products in carbonaceous meteorites identified by Mossbauer spectroscopy N92-10824
SPECTRUM ANALYSIS
Method and apparatus for frequency spectrum analysis
[NASA-CASE-NPO-17759-1-CU] N92-10125
New methods of change detection using multispectral data
[AD-A239370] N92-10217
UV, visible, and near-IR reflectivity data for magnetic soils/rocks from Brazil N92-10254
Synthesis and properties of Ti-substituted goethites and hematites N92-10255
A new phase retrieval method for CARS spectrum analysis N92-10363
Analysis of the interacting levels V(sub 9) = 1 and V(sub 10) = 2 of propyne N92-10444
Recognizing of spectral mixtures, their components and spectral patterns N92-10447
Single-shot spectral measurements of multimode pulsed dye lasers N92-10452
Electronically resonant CARS spectroscopy of NO2 N92-10455
NMR pulse responses of pairs of triads of 1/2 spins in solids N92-10511
Spectral reflectance of pine and intensity of moose browsing N92-10514
Spectral representation in vision N92-10539
On the ionospheric influence upon the spectral structure on the Pc1 geomagnetic pulsations N92-10552
Crustal heterogeneity of the moon viewed from the Galileo SSI camera: Lunar sample calibrations and compositional implications N92-10808
Does Lafayette = Nakhla? Not necessarily so, based on 4.2K Mossbauer spectra of all of the SNC meteorites N92-10825
Darkening in gas-rich ordinary chondrites: Spectral modelling and implications for the regoliths of ordinary chondrite parent bodies N92-10827
Effects of grain size and shape in modeling reflectance spectra of mineral mixtures N92-10831
New spectral observations of Callisto and leading/trailing hemisphere distinctions N92-10839
Compositional variability of the Martian surface N92-10931
Studies of volatiles and organic materials in early terrestrial and present-day outer solar system environments N92-10958
SPEECH RECOGNITION
Digital simulation of speech transmission channels
[IZF-1991-A-7] N92-10115
SPHERES
Jetting and the origin of tektites N92-10868
SPHERULES
Large impacts and climatic catastrophes on the early Earth N92-10865
SPIN-LATTICE RELAXATION
NMR-relaxation time measurements of noble gas isotope Xe-129 dissolved in isotropic and anisotropic liquids N92-10437
SPREAD SPECTRUM TRANSMISSION
Introduction to the Personal Access Satellite System study N92-10117
Multiple access trade study N92-10118
SPREADING
Numerical simulation studies of fluid spreading N92-10482
Gravitational spreading of Danu, Freyja and Maxwell Montes, Venus N92-10744
SPUTTERING
Dependence of Au(-) production upon the target work function in a plasma-sputter-type negative ion source
[NIFS-85] N92-10656
Preparation and characterization of high temperature superconductor film surfaces
[AD-A240118] N92-10706
STABILITY
The stability of the planetary triangular Lagrange points N92-10568
Mapping the stability field of Jupiter Trojans N92-10883
STANDARD DEVIATION
A new method to assess the statistical convergence of Monte Carlo solutions
[DE91-016013] N92-10354
STANDARDIZATION
Definition and measurement at high temperatures of pH
[DE91-017945] N92-10077
STATISTICAL ANALYSIS
Range reference atmosphere, Nellis Air Force Base, Nevada
[AD-A239816] N92-10262
Recent changes of weather patterns in North America
[DE91-017706] N92-10266
VERMOD capabilities. VERMOD 1.0 and future
[AD-A239801] N92-10274
On adaptive multiband detection of targets in nonstationary nonhomogeneous interference
[AD-A239983] N92-10327
A mathematical model for a paired comparison experiment on a continuum of response
[AD-A239858] N92-10351
A new method to assess the statistical convergence of Monte Carlo solutions
[DE91-016013] N92-10354
Using surrogate data to detect nonlinearity in time series
[DE91-018017] N92-10357
Mean estimation in highly skewed samples
[DE91-018513] N92-10358
The changing face of probability
[DE91-018857] N92-10359
Activities of the Board on Mathematical Sciences
[DE91-017931] N92-10361
Lifetime of the 1.959 MeV state in Cl-36 N92-10400
STATISTICAL DISTRIBUTIONS
Processes for identifying regional influences of and responses to increasing atmospheric CO2 and climate change: The MINK project
[DE91-018603] N92-10243
STATISTICAL MECHANICS
A statistical mechanics study of solid-solid interfaces
[DE91-017852] N92-10689
STEADY FLOW
Numerical analysis of fully developed laminar flow in curved rectangular channels
[NAL-TR-1111] N92-10166
Steady flow of a fluid-solid mixture in a circular cylinder
[DE91-018698] N92-10174
STEADY STATE
A general-purpose finite-difference code for solving steady-state three-dimensional fluid-flow and heat transfer problems
[AD-A239857] N92-10175
STEAM
Evaluation of advanced austenitic alloys relative to alloy design criteria for steam service
[DE91-017800] N92-10081
Thermal- and ignition-type steam explosions of single drops of molten aluminum
[DE91-014705] N92-10084
STELLAR EVOLUTION
Photometry of the comet 2060 Chiron N92-10887
Fragmentation in stellar collapse N92-10891
STELLAR MASS ACCRETION
Core formation by giant impacts N92-10864
STEREOSCOPIC VISION
Three experiments with stereoscopic television: When it works and why
[DE91-016277] N92-10129
STIFFNESS MATRIX
Development of a model of space station solar array
[NASA-CR-188911] N92-10220
STOCHASTIC PROCESSES
Approximate evaluation of reliability and related quantities via perturbation techniques
[AD-A240049] N92-10201
Solving problems under uncertainty
[DE91-017940] N92-10322
STOICHIOMETRY
Chemical thermodynamic equilibria and conductivity of nonstoichiometric YB2Cu3O7-(delta): A review
[DE91-018638] N92-10701
STONY METEORITES
Clay minerals in primitive meteorites and interplanetary dust 2. Smectites and micas N92-10252
STORAGE RINGS (PARTICLE ACCELERATORS)
The search for low photodesorption coatings
[DE91-017473] N92-10092
The A Experimental Division (of the Werner Heisenberg Institute for Physics) N92-10590
STORMS
The 1990 Airport Surveillance Radar Wind Shear Processor (ASR-WSP) operational test at Orlando International Airport
[AD-A239852] N92-10019
STRAIN GAGE BALANCES
Dual strain gage balance system for measuring light loads
[NASA-CASE-LAR-14419-1] N92-10185
STRAKES
The effects of forebody strakes on asymmetric vortices on a vertically launched missile
[AD-A239948] N92-10014
STRANGENESS
Exact strangeness conservation and particle production
[BI-TP-90/35] N92-10385
Hadronic equation of state and the onset of kaon condensation N92-10386
Pion-nucleon sigma-term and the strange quark content of the proton N92-10396
STRATIGRAPHY
Valles Marineris tectonism: Questions and suggestions N92-10756
Glacial and marine chronology of Mars N92-10772
Stratigraphy of the layered terrain in Valles Marineris, Mars N92-10777
Stratigraphy of the Perrine and Nun Sulci quadrangles (Jg-2 and Jg-5), Ganymede N92-10911
STRATOSPHERE
Ozone depletion rates in the late winter/early spring Arctic and Antarctic stratosphere according to recent ozone sounding observations N92-10547
Investigation of the small-scale structure and dynamics of Uranus' atmosphere
[NASA-CR-188819] N92-10960
STREAK CAMERAS
Subpicosecond x ray streak camera
[DE91-017664] N92-10187
STRESS ANALYSIS
Prediction of matrix fatigue crack initiation in notched SCS-6/Ti-15-3 metal matrix composites
[NASA-TM-104141] N92-10203
Bond of reinforcement under controlled confinement
[AD-A240142] N92-10207
Horizontal stress in planetary lithospheres from vertical processes N92-10746
STRESS TENSORS
On the most general tensor B(sub ij) which is zero for i does not equal j, and the most general isotropic tensor I(sub ij)
[NASA-TM-105236] N92-10289
STRESS-STRAIN RELATIONSHIPS
High temperature creep properties of eutectic and near eutectic silver-copper alloys: Application to metal/ceramic joining
[DE91-017987] N92-10082
STRESSES
Compressive strain in Lunae Planum-shortening across wrinkle ridges N92-10753
STRING THEORY
Quantum cosmology on the worldsheet
[DE91-018415] N92-10727
STRUCTURAL ANALYSIS
TAURUS: An interactive post-processor for the analysis codes NIKE3D, DYNA3D, and TOPAZ3D
[DE91-019012] N92-10326
STRUCTURAL BASINS
Global relationships between volcanic vents and fractures radial to large impact basins on Mars N92-10750
Tectonic setting of Martian volcanoes and deep-seated intrusives N92-10751
Chronology of glaciation in the Hellas region of Mars N92-10773
Remote sensing and geologic studies of the terrain northwest of Humorum basin N92-10810
Preliminary geologic mapping of central Chryse Planitia, Mars N92-10906
Mars geologic mapping: Dao, Harmakhis, and Reull Valles region N92-10908
Evolution of the east rim of the Hellas basin, Mars N92-10909
The history of lunar volcanism N92-10965
STRUCTURAL DESIGN
Mechanized fluid connector and assembly tool system with ball detents
[NASA-CASE-MSC-21434-1] N92-10197

Study of different SX-700 designs for the undulator beamline (BL51) at MAX-LAB N92-10446
STRUCTURAL PROPERTIES (GEOLOGY)
Reports of Planetary Geology and Geophysics Program, 1990
[NASA-TM-4300] N92-10728
Morphology and evolution of coronae and ovoids on Venus N92-10742
Valles Marineris tectonism: Questions and suggestions N92-10756
Valles Marineris, Mars: Are pit chains formed by erosion and troughs by tectonism? N92-10758
SO2-rich equatorial basins and epeirogeny of Io N92-10761
Structural geology and geological history of the Perrine and Nun Suici Quadrangles (Jg-2 and Jg-5), Ganymede N92-10762
Tectonic deformation on icy satellites: A model of compensating horsts N92-10763
Mimas: Tectonic structure and geologic history N92-10764
Iapetus: Tectonic structure and geologic history N92-10766
Hydrologic activity during late Noachian and Early Hesperian downwarping of Borealis Basin, Mars N92-10778
Flood routing of the Maja outflow across Xanthe Terra N92-10780
Ancient fluvial processes in the equatorial highlands of Mars N92-10781
Styles of crater gradation in Southern Ismenius Lacus, Mars N92-10784
The gradational history of southern Ismenius Lacus N92-10785
Are the Equatorial Highlands on Venus formed by mantle plume diapirs? N92-10942
Preliminary 1:500,000-scale geologic mapping of Claritas Fossae, Mars N92-10959
STRUCTURAL VIBRATION
Multi-degree of freedom, active vibration control method, and system
[NASA-CASE-LAR-14508-1-CU] N92-10202
STRUCTURAL WEIGHT
PASS spacecraft antenna technology assessment N92-10123
SUBDUCTION (GEOLOGY)
Interpretation of the northern boundary of Ishtar Terra from Magellan images and altimetry N92-10745
SUBLIMATION
Planetary geomorphology research: FY 1990-1991 N92-10940
SUBSIDENCE
Horizontal stress in planetary lithospheres from vertical processes N92-10746
Modelled and measured strain in mascon basins on the moon N92-10747
SUBSTITUTES
Investigations of the effects of isotopic substitution and pressure on miscibility in polymer-polymer and polymer-solvent systems
[DE91-018010] N92-10094
Synthesis and properties of Ti-substituted goethites and hematites N92-10255
SUBSTRATES
Scanning tunneling microscopy of polysialic acid N92-10538
SULFONES
Helmet of a laminate construction of polycarbonate and polysulfone polymeric material
[NASA-CASE-MSC-21503-1] N92-10091
SULFUR
Abatement strategies based on critical loads N92-10533
SULFUR COMPOUNDS
Conducting polymers N92-10524
SULFUR DIOXIDES
SO2-rich equatorial basins and epeirogeny of Io N92-10761
SULFUR FLUORIDES
Interaction-induced light scattering as a source of information on properties and interactions of spherical top molecules N92-10439
SULFUR OXIDES
Soil crusts on Mars N92-10786
SUNSPOT CYCLE
Variation of D-region parameters during polar cap absorption events in the year 1989 N92-10561
SUPERCOMPUTERS
The paradigm compiler: Mapping a functional language for the connection machine
[NASA-CR-188839] N92-10290
A performance comparison of three supercomputers: Fujitsu VP-2600, NEC SX-3, and CRAY Y-MP
[DE91-016304] N92-10298
Proceedings of the First Energy Research Power Supercomputer Users Symposium
[DE91-018877] N92-10300
The role of graphics super-workstations in a supercomputing environment
[NASA-CR-188852] N92-10306
SUPERCONDUCTING FILMS
Photoinduced superconductivity in films of YBaCuO N92-10502
Epitaxial high T(sub c) superconducting thin films and superlattices deposited by laser albation N92-10505
High T(sub c) superconducting Li-doped Bi-Sr-Ca-Cu-O thin films deposited by laser ablation N92-10506
Preparation and characterization of high temperature superconductor film surfaces
[AD-A240118] N92-10706
SUPERCONDUCTING SUPER COLLIDER
A search for rare B meson decays at the CERN proton-antiproton collider
[CERN-PPE/91] N92-10389
J/psi and psi' production at the CERN proton-antiproton collider
[CERN-PPE/90-154] N92-10390
Recent physics results from DELPHI N92-10394
Theoretical and experimental studies of elementary particles
[DE91-018285] N92-10630
Research program in particle physics
[DE91-018525] N92-10632
SUPERCONDUCTIVITY
Photoinduced superconductivity in films of YBaCuO N92-10502
Studies on superconducting Bi2Sr2Ca(n-1) Cu(n)O(4+2n) compounds with Fe-57 and Eu-151 Moessbauer spectroscopy N92-10504
Passivation of high temperature superconductors
[NASA-CASE-NPO-17949-1-CU] N92-10681
Strong correlation theories of high temperature superconductors
[DE91-017479] N92-10688
Electrical transport across grain boundaries in bicrystals of YBa2Cu3O7(delta)
[DE91-018588] N92-10697
Reversible magnetization of Bi2Sr2CaCu2O8 single crystals
[DE91-018600] N92-10699
SUPERCONDUCTORS
Transport in heterostructures and devices in microwave and millimeter-wave regimes
[AD-A239943] N92-10142
Highlights of material research for optoelectronics in the eighties, trends and challenges for the nineties N92-10486
Anisotropic twin boundary pinning in YBa2Cu3O(x)
[DE91-018536] N92-10692
SUPERFLUIDITY
Two-phonon absorption by the real squashing collective mode in superfluid He-3 N92-10474
Mutual friction in superfluid He-3: Effects of bound states in the vortex core N92-10475
Vortex nucleation in rotating superfluid He-3-B N92-10476
Effective mass and excitation spectrum of He-3 impurities in superfluid He-4 N92-10477
Superfluid interfaces in liquid He-3: Superconducting cosmic domain walls in the laboratory N92-10478
Superfluid vortex nucleation in He-3 flow N92-10479
SUPERLATTICES
Epitaxial high T(sub c) superconducting thin films and superlattices deposited by laser albation N92-10505
Tunneling calculations for GaAs-Al(x)Ga(1-x) as graded band-gap sawtooth superlattices
[NASA-TM-100726] N92-10680
SUPERNOVA 1987A
Supernova neutrinos N92-10399
SUPERNOVAE
Solar and supernova neutrino interactions
[DE91-013905] N92-10968
SUPERSONIC COMBUSTION RAMJET ENGINES
A computational and experimental investigation of a three-dimensional hypersonic scramjet inlet flow field N92-10007
Contractors Meeting in Propulsion
[AD-A240057] N92-10062
SUPERSONIC FLIGHT
Sonic boom N92-10608
SUPERSONIC FLOW
Recent advances on a finite element algorithm for computational aerodynamics: Transonics-hypersonics
[DE91-018176] N92-10010
Noise from turbulent shear flows N92-10603
SUPERSONIC JET FLOW
Jet noise generated by large-scale coherent motion N92-10604
SUPERSONIC SPEED
Measurements of forces, moments, and pressures on a generic store separating from a box cavity at supersonic speeds
[NASA-TP-3110] N92-10005
SUPERSONIC TEST APPARATUS
Supersonic molecular beam apparatus to study surface reactions N92-10440
SUPERSYMMETRY
Scale dependence of Lambda sub (MS bar) from deep inelastic scattering
[RAL-91-044] N92-10614
SUPPORT SYSTEMS
The determination of operational and support requirements and costs during the conceptual design of space systems
[NASA-CR-188817] N92-10037
SURFACE COOLING
Thermal management of high heat flux electronic components in space and aircraft systems, phase 1
[AD-A239982] N92-10157
SURFACE ENERGY
Surface reconstruction and many-atom models N92-10483
SURFACE GEOMETRY
A method for determining spiral-bevel gear tooth geometry for finite element analysis
[NASA-TP-3096] N92-10195
SURFACE LAYERS
Adsorbate induced surface reconstruction N92-10469
Diffusion anomaly at a surface reconstruction N92-10470
Free convection in the Martian atmosphere N92-10803
Characteristics of the Martian atmosphere surface layer N92-10804
SURFACE PROPERTIES
Oxide properties of a gamma titanium aluminide: A surface science study
[DE91-018024] N92-10095
Instrumental design for measurement of surface charge on insulating materials
[DE91-018695] N92-10099
Combined Backscatter Moessbauer Spectrometer and X Ray Fluorescence analyzer (BaMS/XRF) for planetary surface materials N92-10249
Thermal helium desorption facility in Jyvaskyla (Finland) N92-10464
Modeling the dynamics of molecular films by Monte Carlo simulation N92-10481
Scanning tunneling microscope measurements in air:Langmuir-Blodgett films on HOPG and growth of evaporated gold on HOPG N92-10497
Positron annihilation induced Auger-electron spectroscopy: A study of a Ge(100) surface N92-10515
Surface characterization of coated powders with XPS: Al2O3-SiO2 coated TiO2 pigments N92-10520
Quantum state resolved desorption of CO from solid surface
[DE91-017712] N92-10626
Surface-material maps of Viking landing sites on Mars N92-10787
Remote sensing and geologic studies of the orientale basin region N92-10809
Character of the opposition effect and negative polarization N92-10833
Surface scattering properties estimated from modeling airborne multiple emission angle reflectance data N92-10841
Mapping compositional and particle size variations across Silver Lake Playa: Relevance to analyses of Mars TIR data N92-10842
Application of Hapke photometric model to three geologic surfaces using PARABOLA bidirectional reflection data N92-10843
Surface properties of Galilean satellites from bistatic radar experiments N92-10849
Meteorite spectroscopy and characterization of asteroid surface materials N92-10881
Geologic mapping of northern Lunae Planun, Mars N92-10907
Evolution of the east rim of the Hellas basin, Mars N92-10909
Compositional variability of the Martian surface N92-10931
Asteroid surface processes: Experimental studies of the solar wind on reflectance and optical properties of asteroids N92-10941
SURFACE REACTIONS
Surface electrochemistry of Chloro(phthalocyaninato)rhodium(III) species, and oxygen reduction electrocatalysis, formation of a dimeric species
[AD-A240148] N92-10104
Supersonic molecular beam apparatus to study surface reactions N92-10440

SURFACE ROUGHNESS
Relationships between topographic roughness and aeolian processes N92-10801
Use of radar to assess aeolian processes N92-10802
The photometric roughness of Mimas N92-10835
Surface scattering properties estimated from modeling airborne multiple emission angle reflectance data N92-10841
High resolution lunar radar studies: Preliminary results N92-10845
Models of the diffuse radar backscatter from Mars N92-10846

SURFACE TEMPERATURE
Thermal models for icy satellites N92-10734
The role of nonuniform internal heating in Triton's energy budget N92-10736
Gravitational spreading of Danu, Freyja and Maxwell Montes, Venus N92-10744
Free convection in the Martian atmosphere N92-10803
Remote sensing of the Martian surface N92-10813
Thermal modeling of comet Kopff: Implications for the CRAF mission N92-10889

SURFACE TO AIR MISSILES
The effects of forebody strakes on asymmetric vortices on a vertically launched missile [AD-A239948] N92-10014

SURVEILLANCE RADAR
The 1990 Airport Surveillance Radar Wind Shear Processor (ASR-WSP) operational test at Orlando International Airport [AD-A239852] N92-10019

SURVEYS
Solid propellant steady combustion: Physical aspects N92-10107
Physics Division annual review, April 1, 1990 - March 31, 1991 [DE91-018704] N92-10707

SWITCHING
Antenna beam coverage concepts N92-10119

SWITCHING CIRCUITS
Technology assessment and experimentation plan N92-10124

SYNAPSES
Synaptic plasticity and memory formation [AD-A240121] N92-10285

SYNCHRONISM
Beat wave current drive experiment on DDT [DE91-017407] N92-10622
Multi-gigabit fiber optic wide area network development [AD-A239850] N92-10642

SYNCHROTRON RADIATION
Synchrotron radiation: New research opportunities for the next decade N92-10366
Synchrotron radiation research and Finnish beamline at MAX-lab N92-10377
Super Coster Kronig and resonance super Coster Kronig spectra of solid Ge around 3p-ionization threshold N92-10517
Synchrotron radiation study of recombination processes in solid state Tb and Dy after 4d to 4f giant resonance excitation N92-10518
Advanced photon source: Radiological design considerations [DE91-018014] N92-10635

SYNCHROTRONS
Theoretical and experimental studies of elementary particles [DE91-018285] N92-10630

SYNTAX
Type abstraction rules for references: A comparison of four which have achieved notoriety [AD-A240076] N92-10716

SYNTHESIS (CHEMISTRY)
Diosmacycloalkanes as models for the formation of hydrocarbons from surface methylenes [DE91-017854] N92-10065
Chemical synthesis and microstructural toughening of infrared window materials [AD-A239987] N92-10102

SYNTHETIC APERTURE RADAR
The design of spaceborne synthetic aperture radar [ETN-91-99986] N92-10114
A digital ASIC implementation of a video filter for synthetic aperture radar [DE91-018400] N92-10131
Triangulation using synthetic aperture radar images N92-10914

SYSTEM IDENTIFICATION
Parameter identification for nonlinear aerodynamic systems [NASA-CR-188985] N92-10347

SYSTEMS ANALYSIS
Design controls for large order systems [NASA-CR-184237] N92-10340

SYSTEMS ENGINEERING
Multi-reactor power system configurations for multimegawatt nuclear electric propulsion [NASA-TM-105212] N92-10057
The EH safety representative information system on the safety performance measurement system is where you will find... Word processing and helps with a V-PLUS [DE91-018709] N92-10113
The design of spaceborne synthetic aperture radar [ETN-91-99986] N92-10114
Software Technology for Adaptable, Reliable Systems (STARS): UUS40 risk-reduction reasoning-based development paradigm tailored to Navy C2 systems [AD-A240108] N92-10329
The measuring modes and observations with the x-ray spectrometer array SIXA onboard spectrum-x-gamma N92-10563

SYSTEMS INTEGRATION
Solid-State Radar Beacon Decoder (SSRBD) Operational Test and Evaluation (OT/E) integration test plan [DOT/FAA/CT-TN91/30] N92-10020
Functional description for the Mapping And Graphic Information Capability (MAGIC) [AD-A239436] N92-10305
Integration of magnetoencephalography and magnetic resonance imaging N92-10540

SYSTEMS STABILITY
The stability analysis of a double barrier resonant tunneling device N92-10485

T

TANTALUM
Cavity issues for Ni-like Ta x ray lasers [DE91-017668] N92-10190

TARGET ACQUISITION
On adaptive multiband detection of targets in nonstationary nonhomogeneous interference [AD-A239983] N92-10327

TARGETS
Styles of ejecta emplacement under atmospheric conditions N92-10857
Impact decapitation from laboratory to basin scales N92-10858
Hydrocode predictions of collisional outcomes: Effects of target size N92-10861

TAXONOMY
Research into the development of a knowledge acquisition taxonomy [NASA-CR-188948] N92-10712
Will Galileo resolve the S-asteroid controversy? N92-10882

TEARING
Nonlinear interactions of tearing modes in the presence of shear flow [DE91-018420] N92-10173

TECHNOLOGY ASSESSMENT
PASS spacecraft antenna technology assessment N92-10123
Technology assessment and experimentation plan N92-10124
A survey of laser lightning rod techniques [AD-A239988] N92-10269
Compound semiconductor technology: Materials and devices N92-10523
Materials science and technology centra in Sweden and Denmark: A research policy for the future N92-10580
Solar energy in mitigating global environmental problems N92-10584

TECHNOLOGY TRANSFER
INFOTECH '91: DOE Technical Infomation (TI) Meeting [DE91-018074] N92-10713
Index to 1987 NASA Tech Briefs, volume 11, numbers 1-10 [NASA-TM-105024] N92-10717
Index to 1988 NASA Tech Briefs, volume 12, numbers 1-11 [NASA-TM-105077] N92-10718
Index to 1989 NASA Tech Briefs, volume 13, numbers 1-12 [NASA-TM-105109] N92-10719
Index to 1990 NASA Tech Briefs, volume 14, numbers 1-12 [NASA-TM-105110] N92-10720
Cumulative index to NASA Tech Briefs, 1976-1980, volumes 1-5 [NASA-TM-89327] N92-10721
Cumulative index to NASA Tech Briefs, 1981-1985, volumes 6-10 [NASA-TM-89326] N92-10722

TECHNOLOGY UTILIZATION
MHD program plan, FY 1991 [DE91-017916] N92-10659
Index to 1987 NASA Tech Briefs, volume 11, numbers 1-10 [NASA-TM-105024] N92-10717
Index to 1988 NASA Tech Briefs, volume 12, numbers 1-11 [NASA-TM-105077] N92-10718
Index to 1989 NASA Tech Briefs, volume 13, numbers 1-12 [NASA-TM-105109] N92-10719
Index to 1990 NASA Tech Briefs, volume 14, numbers 1-12 [NASA-TM-105110] N92-10720
Cumulative index to NASA Tech Briefs, 1976-1980, volumes 1-5 [NASA-TM-89327] N92-10721
Cumulative index to NASA Tech Briefs, 1981-1985, volumes 6-10 [NASA-TM-89326] N92-10722

TECTONICS
Martian seismicity N92-10733
Flow and fracture of ice and ice mixtures N92-10735
Physical properties of cryovolcanic brines: Applications to the evolution of Ganymede N92-10737
Tectonic evolution of Lavinia Planitia, Venus N92-10741
Hot-spot tectonics of Eistla Regio, Venus: Results from Magellan images and Pioneer Venus gravity N92-10743
Horizontal stress in planetary lithospheres from vertical processes N92-10746
Modelled and measured strain in mascon basins on the moon N92-10747
Strain accommodation beneath structures on Mars N92-10748
Tectonic setting of Martian volcanoes and deep-seated intrusives N92-10751
Compressive strain in Lunae Planum-shortening across wrinkle ridges N92-10753
Late Noachian development of the Coprates rise, Mars N92-10754
Interactions of tectonic, igneous, and hydraulic processes in the North Tharsis Region of Mars N92-10755
Valles Marineris tectonism: Questions and suggestions N92-10756
Valles Marineris, Mars: Are pit chains formed by erosion and troughs by tectonism? N92-10758
Tectonic deformation on icy satellites: A model of compensating horsts N92-10763
Mimas: Tectonic structure and geologic history N92-10764
Tethys geology and tectonics revisited N92-10765
Iapetus: Tectonic structure and geologic history N92-10766
Stratigraphy of the layered terrain in Valles Marineris, Mars N92-10777
Hydrologic activity during late Noachian and Early Hesperian downwarping of Borealis Basin, Mars N92-10778
Geologic history and channeling episodes of the Chryse Planitia region of Mars N92-10782
Mars geologic mapping: Dao, Harmakhis, and Reull Valles region N92-10908
Planetary geomorphology research: FY 1990-1991 N92-10940
Are the Equatorial Highlands on Venus formed by mantle plume diapirs? N92-10942
Preliminary 1:500,000-scale geologic mapping of Claritas Fossae, Mars N92-10959

TEKTITES
Jetting and the origin of tektites N92-10868

TELECOMMUNICATION
Activities report of the Norwegian Space Center [ETN-91-90052] N92-10029
Compilation of 1990 annual reports of the Navy ELF communications system ecological monitoring program. Volume 1: Tabs A, B [AD-A239868] N92-10137
Compilation of 1990 annual reports of the Navy ELF communications system ecological monitoring program. Volume 2: Tabs C thru F [AD-A239869] N92-10138

TELEMETRY
Solar Constant (SOLCON) Experiment: Ground Support Equipment (GSE) software development [NASA-CR-187596] N92-10267

TELEOPERATORS
Composite video and graphics display for multiple camera viewing system in robotics and teleoperation [NASA-CASE-NPO-17836-1-CU] N92-10126
Three experiments with stereoscopic television: When it works and why [DE91-016277] N92-10129

Advances and experience with teleoperated systems incorporating remote presence
[AD-A239980] N92-10199

TELEROBOTICS

Composite video and graphics display for multiple camera viewing system in robotics and teleoperation
[NASA-CASE-NPO-17836-1-CU] N92-10126

TELEVISION CAMERAS

Composite video and graphics display for multiple camera viewing system in robotics and teleoperation
[NASA-CASE-NPO-17836-1-CU] N92-10126

TELEVISION SYSTEMS

Composite video and graphics display for multiple camera viewing system in robotics and teleoperation
[NASA-CASE-NPO-17836-1-CU] N92-10126

Three experiments with stereoscopic television: When it works and why
[DE91-016277] N92-10129

TEMPERATURE

Determining desorption pre-exponential factors from temperature-programmed desorption spectra when the surface is nonuniform
[DE91-009971] N92-10074

TEMPERATURE CONTROL

Thermal management of high heat flux electronic components in space and aircraft systems, phase 1
[AD-A239982] N92-10157

Mechanized fluid connector and assembly tool system with ball detents
[NASA-CASE-MSC-21434-1] N92-10197

A measuring robot for thermal environment, contaminant concentration and ventilation studies N92-10537

TEMPERATURE DEPENDENCE

Relative sliding durability of two candidate high temperature oxide fiber seal materials
[NASA-TM-105199] N92-10064

Thermal modeling of an epoxy encapsulation process
[DE91-017845] N92-10096

NMR-relaxation time measurements of noble gas isotope Xe-129 dissolved in isotropic and anisotropic liquids N92-10437

The shape effect of magnetic damages in irradiated Nd2Fe14B-permanent magnets N92-10468

Mechanical after-effect studies of oxygen relaxation in YBa2Cu3O(7-delta)
[DE91-018043] N92-10685

Langevin dynamics simulations of large frustrated Josephson junction arrays
[DE91-018046] N92-10686

A statistical mechanics study of solid-solid interfaces
[DE91-017852] N92-10689

Anisotropic twin boundary pinning in YBa2Cu3O(x)
[DE91-018536] N92-10692

Reversible magnetization of Bi2Sr2CaCu2O8 single crystals
[DE91-018600] N92-10699

TEMPERATURE DISTRIBUTION

Electron temperatures in the E-region of the ionosphere
[ISAS-641] N92-10259

Implications of convection in the moon and the terrestrial planets N92-10730

Thermal models for icy satellites N92-10734

Crystallization during emplacement of lava flows N92-10789

Thermal modeling of comet Kopff: Implications for the CRAF mission N92-10889

TEMPERATURE EFFECTS

High temperature materials characterization
[NASA-CR-184231] N92-10079

Fire retardant performance of some interior shipboard paint schemes
[MRL-TR-91-31] N92-10089

Physiological responses of the human extremities to cold water immersion
[IZF-1991-A-15] N92-10277

The Kr-83 NMR in probing electric field gradients in thermotropic liquid crystals N92-10435

The field drift of ions and its influence on the electrical properties of SnO2 N92-10492

Initial magnetization and magnetic relaxation in a single crystal of Bi2Sr2CaCu2O(x)
[DE91-018537] N92-10693

TEMPERATURE GRADIENTS

Heat flow vs. atmospheric greenhouse on early Mars N92-10805

TEMPERATURE MEASUREMENT

Gas turbine combuster exit temperature measurement
[AD-A239936] N92-10026

Early 19th-century least squares calculations in Finland repeated with modern techniques N92-10369

Polarization spectroscopy in OH and flame temperature measurements N92-10454

Kinetic gas and electron temperatures in RF induction plasma N92-10460

Work function changes of high-T(sub c) superconductors around the T(sub c) N92-10498

TEMPORAL DISTRIBUTION

The remote sensing Loosdrecht Lakes (Netherlands) project
[BCRS-90-29] N92-10215

TEMPORAL RESOLUTION

Subpicosecond x ray streak camera
[DE91-017664] N92-10187

TENSILE PROPERTIES

Test apparatus and tensile properties of LE-7 turbine blade materials in high pressure hydrogen conditions
[NAL-TR-1092] N92-10025

TERBIUM

Synchrotron radiation study of recombination processes in solid state Tb and Dy after 4d to 4f giant resonance excitation N92-10518

TERRAIN

Gravitational spreading of Danu, Freyja and Maxwell Montes, Venus N92-10744

Late Noachian development of the Coprates rise, Mars N92-10754

Role of groundwater in formation of Martian channels N92-10770

Role of artesian groundwater in forming Martian permafrost features N92-10771

Stratigraphy of the layered terrain in Valles Marineris, Mars N92-10777

Channeling episodes of Kasei Valles, Mars, and the nature of ridged plains material N92-10779

Ancient fluvial processes in the equatorial highlands of Mars N92-10781

Remote sensing and geologic studies of the terrain northwest of Humorum basin N92-10810

Anomalous scattering of light on Triton N92-10836

Quantitative analysis of terrain units mapped in the northern quarter of Venus from Venera 15/16 data N92-10853

TERRAIN ANALYSIS

Color-coded global topographic map of Mars N92-10920

Mars elevation distribution N92-10921

TERRESTRIAL PLANETS

Core formation by giant impacts N92-10864

Impacts and the early environment and evolution of the terrestrial planets N92-10866

Growth of planets from planetesimals N92-10899

Studies of volatiles and organic materials in early terrestrial and present-day outer solar system environments N92-10958

TEST CHAMBERS

Laboratory simulation of cratering on small bodies N92-10859

TEST FACILITIES

PC programs for the prediction of the linear stability behavior of liquid propellant propulsion systems and application to current MSFC rocket engine test programs, volume 1
[NASA-CR-184228] N92-10042

LLNL contributions to MPD thrusters for SEI N92-10047

Description of the PMAD DC test bed architecture and integration sequence
[NASA-TM-105284] N92-10055

NASA maintenance: Stronger commitment needed to curb facility deterioration
[GAO/NSIAD-91-34] N92-10709

TETHERING

Advances and experience with teleoperated systems incorporating remote presence
[AD-A239980] N92-10199

TETHYS

Tethys geology and tectonics revisited N92-10765

TETRAGONS

Redistribution of nitrogen atoms and magnetic ordering in Fe-N martensite at low temperatures N92-10472

TEXTURES

Optical correlators in texture analysis N92-10450

Mapping compositional and particle size variations across Silver Lake Playa: Relevance to analyses of Mars TIR data N92-10842

THEMATIC MAPPERS (LANDSAT)

Mojave remote sensing field experiment N92-10840

THEOREMS

Some results on constrained controllability in discrete-time convex processes
[MEMO-926] N92-10342

THEORETICAL PHYSICS

The Theoretical Division (of the Werner Heisenberg Institute for Physics) N92-10589

Analytical and computational mathematical physics
[DE91-018965] N92-10596

Research program in particle physics
[DE91-018525] N92-10632

Physics Division annual review, April 1, 1990 - March 31, 1991
[DE91-016704] N92-10707

THERMAL ANALYSIS

Thermal modeling of an epoxy encapsulation process
[DE91-017845] N92-10096

PATRAN and P/THERMAL applications for thermal modeling
[DE91-017767] N92-10320

Crystallization during emplacement of lava flows N92-10789

Thermal modeling of comet Kopff: Implications for the CRAF mission N92-10889

THERMAL CONDUCTIVITY

Sintered compacts for heat sinks and process for fabricating same
[DE91-018438] N92-10153

Thermal energy storage and heat transfer support program. Volume 1: Task-1 heat transport system study copper-water and steel-sodium DWAHP
[AD-A239928] N92-10176

Characteristics of the Martian atmosphere surface layer N92-10804

THERMAL DIFFUSION

Ion temperature gradient driven transport in a density modification experiment on the TFTR tokamak
[DE91-018215] N92-10663

THERMAL EMISSION

Thermal emission of gammas and lepton pairs from quark-gluon plasmas N92-10383

Thermal photon production from high-temperature nuclear matter N92-10384

Remote sensing of the Martian surface N92-10813

THERMAL ENERGY

Pulse thermal energy transport system
[NASA-CASE-LEW-15235-1] N92-10167

THERMAL INSULATION

Helmet of a laminate construction of polycarbonate and polysulfone polymeric material
[NASA-CASE-MSC-21503-1] N92-10091

THERMAL MAPPING

Thermal and albedo mapping of the north and south polar regions of Mars N92-10943

THERMAL RESISTANCE

Work function changes of high-T(sub c) superconductors around the T(sub c) N92-10498

THERMAL STABILITY

High temperature solar cell contacts
[AD-A239932] N92-10227

THERMAL STRESSES

Test apparatus and tensile properties of LE-7 turbine blade materials in high pressure hydrogen conditions
[NAL-TR-1092] N92-10025

A computer simulation for predicting the time course of thermal and cardiovascular responses to various combinations of heat stress, clothing, and exercise
[AD-A240023] N92-10288

THERMIONIC CONVERTERS

Thermal energy storage and heat transfer support program. Volume 2: Task 4 Thermionic energy conversion studies
[AD-A239968] N92-10178

THERMIONIC DIODES

Thermal energy storage and heat transfer support program. Volume 2: Task 4 Thermionic energy conversion studies
[AD-A239968] N92-10178

THERMIONIC POWER GENERATION

Thermal energy storage and heat transfer support program. Volume 2: Task 4 Thermionic energy conversion studies
[AD-A239968] N92-10178

THERMODYNAMIC EQUILIBRIUM

A statistical mechanics study of solid-solid interfaces
[DE91-017852] N92-10689

THERMODYNAMIC PROPERTIES

A statistical mechanics study of solid-solid interfaces
[DE91-017852] N92-10689

Chemical thermodynamic equilibria and conductivity of nonstoichiometric YB2Cu3O7-(delta): A review
[DE91-018638] N92-10701

THERMODYNAMICS

The generalized van der Waals theory of pure fluids and mixtures
[DE91-017549] N92-10093

Chemical thermodynamic equilibria and conductivity of nonstoichiometric YB2Cu3O7-(delta): A review
[DE91-018638] N92-10701

THERMOELECTRIC GENERATORS

Materials in space nuclear power systems
[DE91-017688] N92-10058

THERMOELECTRIC MATERIALS

Novel type of cryogenic liquid level sensor with high sensitivity N92-10528

THERMOPLASTIC RESINS
Advanced thermoplastic resins, phase 1 [NASA-CR-178402] N92-10069
THERMOREGULATION
A computer simulation for predicting the time course of thermal and cardiovascular responses to various combinations of heat stress, clothing, and exercise [AD-A240023] N92-10288
THICK FILMS
The field drift of ions and its influence on the electrical properties of SnO2 N92-10492
THIN FILMS
Reflection type skin friction meter [NASA-CASE-LAR-14520-1-SB] N92-10008
Modeling the dynamics of molecular films by Monte Carlo simulation N92-10481
Beryllium doping of InP grown by gas-source molecular beam epitaxy N92-10489
Scanning tunneling microscope measurements in air:Langmuir-Blodgett films on HOPG and growth of evaporated gold on HOPG N92-10497
Epitaxial high T(sub c) superconducting thin films and superlattices deposited by laser albation N92-10505
High T(sub c) superconducting Li-doped Bi-Sr-Ca-Cu-O thin films deposited by laser ablation N92-10506
Compound semiconductor technology: Materials and devices N92-10523
Semiconducting organic thin films as monitoring devices for NO2 air pollution N92-10527
High resolution spectroscopy of H(+) energy loss in thin carbon film [NIFS-88] N92-10654
Diamond thin films grown by microwave plasma assisted chemical vapor deposition [DE91-018553] N92-10695
THIN PLATES
Jetting and the origin of tektites N92-10868
THREE DIMENSIONAL FLOW
A computational and experimental investigation of a three-dimensional hypersonic scramjet inlet flow field N92-10007
Numerical simulation of vortex breakdown via 3-D Euler equations N92-10164
Performance of conjugate gradient-like algorithms in transient two-phase subchannel analysis [DE91-013373] N92-10316
Multigrid calculation of three-dimensional viscous cascade flows [NASA-TM-105257] N92-10345
THREE DIMENSIONAL MODELS
A 3-D adaptive mesh refinement algorithm for multimaterial gas dynamics [DE91-018040] N92-10169
A method for determining spiral-bevel gear tooth geometry for finite element analysis [NASA-TP-3096] N92-10195
N-body simulations of interacting galaxies N92-10579
Fragmentation in stellar collapse N92-10891
THRUST CHAMBERS
MPD thruster research issues, activities, strategies N92-10051
TIDES
Tidal disruption of inviscid protoplanets N92-10900
Tidal evolution of planetary satellites N92-10953
TILES
Fiber-tile optical studies at Argonne [DE91-018591] N92-10641
TIME
Dynamic lattice computing in general relativity N92-10372
TIME DEPENDENCE
Optimal moving grids for time-dependent partial differential equations [NASA-CR-188850] N92-10344
Contamination study [NASA-CR-184225] N92-10639
The spatial distribution and time evolution of impact-generated magnetic fields N92-10878
TIME DIVISION MULTIPLE ACCESS
Multiple access trade study N92-10118
Antenna beam coverage concepts N92-10119
TIME MEASUREMENT
Positron lifetime measurements in chiral nematic liquid crystals [NASA-TP-3122] N92-10677
TIME OF FLIGHT SPECTROMETERS
Quantum state resolved desorption of CO from solid surface [DE91-017712] N92-10626
TIME SERIES ANALYSIS
Recent changes of weather patterns in North America [DE91-017706] N92-10266
Identification of nonlinear times series from first order cumulative characteristics [AD-A239822] N92-10350
Characterization of nonlinear input-output systems using time series analysis [DE91-018003] N92-10356
Using surrogate data to detect nonlinearity in time series [DE91-018017] N92-10357
TIN OXIDES
The field drift of ions and its influence on the electrical properties of SnO2 N92-10492
TITAN
Theoretical studies of volatile processes in the outer solar system N92-10807
The Titan-Hyperion orbital resonance N92-10946
Planetary origin, evolution, and structure N92-10952
TITANIUM
Synthesis and properties of Ti-substituted goethites and hematites N92-10255
TITANIUM COMPOUNDS
Oxide properties of a gamma titanium aluminide: A surface science study [DE91-018024] N92-10095
TITANIUM OXIDES
Surface characterization of coated powders with XPS: Al2O3-SiO2 coated TiO2 pigments N92-10520
Heteroepitaxial growth of TiO2, VO2, and TiO2/VO2 multilayers by MOCVD [DE91-018543] N92-10694
Heteroepitaxy of MOCVD grown TiO2, VO2 films and TiO2/VO2 multilayers on sapphire (1120) [DE91-018589] N92-10698
Exploration of relationships between low-Ti and high-Ti pristine lunar glasses using an armalcolite assimilation model N92-10964
TOKAMAK DEVICES
Approximate analytic theory of the multijunction grill [IPPCZ-309] N92-10127
Fusion energy: Status and prospects N92-10583
Simulation study of scalings in scrape-off layer plasma by two-dimensional transport code [NIFS-24] N92-10646
Fast wave heating at intermediate ion cyclotron harmonics on the JIPP T-II U tokamak [NIFS-21] N92-10649
On ponderomotive force effects on coupling of the LH and IBW grills for the FTU tokamak [IPPCZ-305] N92-10650
Experimental studies of tokamak plasma in IPP Prague [IPPCZ-310] N92-10651
Density peaking in the JFT-2M tokamak plasma with counter neutral beam injection [NIFS-83] N92-10657
Overview of the 1990's D3-D research program [DE91-018185] N92-10661
VH-mode: A new very high confinement regime in the boronized DIII-D tokamak [DE91-018186] N92-10662
Ion temperature gradient driven transport in a density modification experiment on the TFTR tokamak [DE91-018215] N92-10663
The DIII-D tokamak and energy confinement at low q [DE91-018317] N92-10664
Theory of Ion Bernstein wave coupling at low edge densities [DE91-018321] N92-10665
The influence of plasma motion on disruption generated runaway electrons [DE91-018356] N92-10666
Stabilization of the m = 1 tearing mode by resonance detuning [DE91-018423] N92-10668
Plasma Physics Research Institute, Lawrence Livermore National Laboratory, University of California, Davis annual report for fiscal year 1989 [DE91-018490] N92-10669
The 110 GHz ECH heating system for DIII-D [DE91-018732] N92-10671
Fast-wave ICRF minority-regime heating experiments on the Tore Supra tokamak [DE91-018866] N92-10673
TOPOGRAPHY
Dynamic models for ridge belt formation on Venus N92-10731
An assessment of the crustal remelting hypothesis for volcanism in the Freyja Montes deformation zone N92-10732
Hot-spot tectonics of Eistla Regio, Venus: Results from Magellan images and Pioneer Venus gravity N92-10743
SO2-rich equatorial basins and epeirogeny of Io N92-10761
Flood routing of the Maja outflow across Xanthe Terra N92-10780
Ancient fluvial processes in the equatorial highlands of Mars N92-10781
New studies of Martian volcanoes N92-10793
Relationships between topographic roughness and aeolian processes N92-10801
Publication of topographic atlas and control network of Mars N92-10919
Color-coded global topographic map of Mars N92-10920
Mars elevation distribution N92-10921
Completion of compilation of the 1:2,000,000-scale topographic map series of Mars N92-10922
A new edition of the Mars 1:5,000,000 map series N92-10924
Planetary atlases N92-10925
Preliminary 1:500,000-scale geologic mapping of Claritas Fossae, Mars N92-10959
TOPOLOGY
Styles of crater gradation in Southern Ismenius Lacus, Mars N92-10784
TOROIDAL PLASMAS
Numerical calculations of wave propagation in tokamak plasmas N92-10461
Simulation study of scalings in scrape-off layer plasma by two-dimensional transport code [NIFS-24] N92-10646
Observation of plasma toroidal rotations driven by the electric field due to a loss of ions [NIFS-23] N92-10647
Geometrical effects of the magnetic field on the neoclassical flow, current, and rotation in general toroidal systems [NIFS-86] N92-10655
Nonlinear RF processes in plasma [DE91-017441] N92-10658
Geometric phase, rotational transforms and adiabatic invariants in toroidal magnetic fields [DE91-018419] N92-10667
TOROIDS
Geometric phase, rotational transforms and adiabatic invariants in toroidal magnetic fields [DE91-018419] N92-10667
TORQUE
A geometrical model for shepherding N92-10901
TORSION
Torsional potential for the C(sp2)-C(sp2) bond N92-10443
The 1990 solar eclipse as seen by a torsion pendulum N92-10550
TORUSES
Parallel QR factorization on a hypercube using the torus wrap mapping [DE91-011502] N92-10315
Experimental studies of tokamak plasma in IPP Prague [IPPCZ-310] N92-10651
TOUGHNESS
Chemical synthesis and microstructural toughening of infrared window materials [AD-A239987] N92-10102
TOXIC HAZARDS
Ion mobility spectrometer to trace gas analysis N92-10535
TOXICOLOGY
The 14th International Conference on Combined Effect of Environmental Factors [AD-A240045] N92-10245
TRACE ELEMENTS
Isotope selective resonance ionization measurements of lithium N92-10442
Formation of Apollo 14 aluminous mare basalts by replenishment fractional crystallization and assimilation of precursor crust N92-10963
TRACKING FILTERS
Integration of Electronic Support Measures (ESM) and alpha-beta radar tracker [AD-A240031] N92-10143
TRACKING PROBLEM
Massively parallel computing and the mid-course tracking problem [DE91-010864] N92-10335
TRANSDUCERS
Development of digital/optical rotary position transducer [NAL-TR-1106] N92-10026
Development of a pressure transducer calibration system (dynamic pressure response caliber), phase 2 [AD-A239859] N92-10188
TRANSFER FUNCTIONS
On the formulation of a minimal uncertainty model for robust control with structured uncertainty [NASA-TP-3094] N92-10027
Parameter identification for nonlinear aerodynamic systems [NASA-CR-188985] N92-10347
TRANSFER ORBITS
Small upper stage basic program [AD-A240059] N92-10063

TRANSFORMATIONS (MATHEMATICS)
Mass flux similarity for slotted transonic-wind-tunnel walls
[NASA-TM-4281] N92-10006
A restricted signature normal form for Hermitian matrices, quasi-spectral decompositions, and applications
[NASA-CR-188895] N92-10310
Geometric phase, rotational transforms and adiabatic invariants in toroidal magnetic fields
[DE91-018419] N92-10667
The Titan-Hyperion orbital resonance N92-10946
TRANSIENT HEATING
Generation and behavior of solar system magnetic fields N92-10939
TRANSITION POINTS
A band theoretical study on the electronic properties in the phase transition CuAu 1 to CuAu 2 N92-10488
TRANSITION TEMPERATURE
Diffusion anomaly at a surface reconstruction N92-10470
A band theoretical study on the electronic properties in the phase transition CuAu 1 to CuAu 2 N92-10488
Reversible magnetization of Bi2Sr2CaCu2O8 single crystals
[DE91-018600] N92-10699
TRANSONIC FLOW
Recent advances on a finite element algorithm for computational aerodynamics: Transonics-hypersonics
[DE91-018176] N92-10010
TRANSPORT PROPERTIES
Transport properties and oxidation in chromium and Fe-Cr alloys exposed to oxygen at high temperatures
[DE91-018571] N92-10086
Transport in heterostructures and devices in microwave and millimeter-wave regimes
[AD-A239943] N92-10142
Planetary ring studies N92-10903
Models of planetary rings N92-10934
TRANSPORT THEORY
Limitations of the condensed history method for low energy electrons
[DE91-015764] N92-10619
Optimal diffusion synthetic acceleration of discrete ordinates transport calculations
[DE91-015924] N92-10620
Ion temperature gradient driven transport in a density modification experiment on the TFTR tokamak
[DE91-018215] N92-10663
TRAPPED PARTICLES
Ion temperature gradient driven transport in a density modification experiment on the TFTR tokamak
[DE91-018215] N92-10663
TRIANGULATION
Triangulation using synthetic aperture radar images N92-10914
The control network of Mercury: April 1991 N92-10916
TRITIUM
The Magnetically Insulated Inertial Confinement Fusion: A novel approach
[DE91-018273] N92-10660
TROJAN ORBITS
The stability of the planetary triangular Lagrange points N92-10568
Mapping the stability field of Jupiter Trojans N92-10883
TROPICAL STORMS
Annual tropical cyclone report, 1990
[AD-A239910] N92-10268
TROUGHS
Late Noachian development of the Coprates rise, Mars N92-10754
Interactions of tectonic, igneous, and hydraulic processes in the North Tharsis Region of Mars N92-10755
Valles Marineris tectonism: Questions and suggestions N92-10756
Tectonic deformation on icy satellites: A model of compensating horsts N92-10763
TUNABLE LASERS
A simple method to stabilize the frequency of semiconductor lasers N92-10453
TUNGSTEN
Adsorbate induced surface reconstruction N92-10469
Diffusion anomaly at a surface reconstruction N92-10470
TUNGSTEN ALLOYS
Microstructural stability and creep response of a new Al-Fe-W-Si alloy
[AD-A239861] N92-10087
TUNING
Stabilization of the m = 1 tearing mode by resonance detuning
[DE91-018423] N92-10668
TUNNEL DIODES
The stability analysis of a double barrier resonant tunneling device N92-10485
TURBIDITY
Styles of ejecta emplacement under atmospheric conditions N92-10857
TURBINE BLADES
Test apparatus and tensile properties of LE-7 turbine blade materials in high pressure hydrogen conditions
[NAL-TR-1092] N92-10025
TURBINE PUMPS
Test apparatus and tensile properties of LE-7 turbine blade materials in high pressure hydrogen conditions
[NAL-TR-1092] N92-10025
Thermal helium desorption facility in Jyvaskyla (Finland) N92-10464
TURBOFAN ENGINES
Turbomachinery noise N92-10601
TURBOMACHINE BLADES
Turbomachinery noise N92-10601
TURBOMACHINERY
Turbomachinery noise N92-10601
TURBULENCE
Numerical investigation of the effect of leading edge geometry on dynamic stall of airfoils
[AD-A239949] N92-10015
TURBULENCE EFFECTS
A non-isotropic multiple-scale turbulence model
[NASA-CR-184217] N92-10160
Noise from turbulent shear flows N92-10603
Jet noise generated by large-scale coherent motion N92-10604
Propulsive lift noise N92-10606
Aerodynamic and gasdynamic effects in cosmogony N92-10892
TURBULENCE MODELS
A non-isotropic multiple-scale turbulence model
[NASA-CR-184217] N92-10160
An additive turbulent decomposition of the Navier-Stokes equations implemented on highly parallel computer systems
[AD-A240131] N92-10181
TURBULENT BOUNDARY LAYER
The structure and development of streamwise vortex arrays embedded in a turbulent boundary layer
[NASA-TM-105211] N92-10012
Management and control of unsteady and turbulent flows
[AD-A240050] N92-10180
The measurement of plate vibration and sound radiation from a turbulent boundary layer manipulator
[AD-A240127] N92-10206
TURBULENT DIFFUSION
Structure and evolution of turbulent preplanetary disc N92-10571
TURBULENT FLOW
Numerical simulation of vortex breakdown
[ONERA-RSF-6/4368-AY-008A] N92-10162
Management and control of unsteady and turbulent flows
[AD-A240050] N92-10180
On the most general tensor B(sub ij) which is zero for i does not equal j, and the most general isotropic tensor I(sub ij)
[NASA-TM-105236] N92-10289
Noise from turbulent shear flows N92-10603
Propulsive lift noise N92-10606
TWO DIMENSIONAL MODELS
Vlasov-Maxwell system: 2-D equilibria, reversed field pinches
[DE91-018421] N92-10595
Continuum modeling of catastrophic collisions N92-10863
TWO PHASE FLOW
Steady flow of a fluid-solid mixture in a circular cylinder
[DE91-018698] N92-10174
Performance of conjugate gradient-like algorithms in transient two-phase subchannel analysis
[DE91-013373] N92-10316

U

ULTRASONIC RADIATION
High temperature materials characterization
[NASA-CR-184231] N92-10079
Constant frequency pulsed phase-locked loop measuring device
[NASA-CASE-LAR-13823-1] N92-10182
ULTRASONIC TESTS
Quantitative non-destructive evaluation of high-temperature superconducting materials
[DE91-018284] N92-10150
ULTRASONICS
Two-phonon absorption by the real squashing collective mode in superfluid He-3 N92-10474
ULTRAVIOLET ABSORPTION
Oxidation of basaltic tephras: Influence on reflectance in the 1 micron region N92-10817
ULTRAVIOLET RADIATION
Remote detection of atmospherically dispersed vegetative cells using fluorescence lidar
[DE91-016077] N92-10218
Parsec-scale penetration of UV into molecular clouds: CII 158 micron mapping of W3, NGC 1977, and NGC 2023
[NASA-CR-188969] N92-10615
ULTRAVIOLET SPECTROMETERS
The normal incidence grating inverse photoemission spectrometer in the energy range 8-28 eV N92-10516
ULTRAVIOLET SPECTROSCOPY
The normal incidence grating inverse photoemission spectrometer in the energy range 8-28 eV N92-10516
UNITED STATES
Image evaluation of high altitude photographs. Examples: Boston and Foster City (US) N92-10213
Evaluation of high altitude photography for city cartography, with the example of Seattle, US N92-10214
The Geologic Remote Sensing Field Experiment (GRSFE) N92-10844
UNIVERSE
IPC two-color analysis of x ray galaxy clusters
[NASA-CR-188980] N92-10724
UNSTEADY FLOW
Numerical investigation of the effect of leading edge geometry on dynamic stall of airfoils
[AD-A239949] N92-10015
Management and control of unsteady and turbulent flows
[AD-A240050] N92-10180
Jet noise classical theory and experiments N92-10602
A Martian global groundwater model N92-10769
UPLINKING
Personal Access Satellite System (PASS) study. Fiscal year 1989 results
[NASA-CR-188808] N92-10116
Technology assessment and experimentation plan N92-10124
UPPER STAGE ROCKET ENGINES
Small upper stage basic program
[AD-A240059] N92-10063
URANIUM 238
Independent and cumulative yields of neutron-rich nuclei in symmetric fission induced by p and d on U-238 N92-10411
URANUS (PLANET)
Earth, Uranus, and Neptune: A comparison of their magnetospheres N92-10567
Investigation of the small-scale structure and dynamics of Uranus' atmosphere
[NASA-CR-188819] N92-10960
URANUS ATMOSPHERE
Dynamics and structure of planetary rings N92-10935
Investigation of the small-scale structure and dynamics of Uranus' atmosphere
[NASA-CR-188819] N92-10960
URANUS RINGS
Models of planetary rings N92-10934
Dynamics and structure of planetary rings N92-10935
URANUS SATELLITES
Disk resolved studies of the optical properties and physical nature of the surfaces of the outer planet satellites N92-10837
URBAN PLANNING
Recording of urban land use by high altitude photography: The Munich (Fed. Republic of Germany) exampl N92-10211
USER MANUALS (COMPUTER PROGRAMS)
INTEGRA manual: Routines for electronic spreadsheet integration (under FRAMEWORK 3)
[DE91-017518] N92-10318
TAURUS: An interactive post-processor for the analysis codes NIKE3D, DYNA3D, and TOPAZ3D
[DE91-019012] N92-10326
MANPRINT reference retrieval system (user's guide)
[AD-A239915] N92-10714

V

VACANCIES (CRYSTAL DEFECTS)
Observation of a monovacancy in the metastable state of the EL2 defect in GaAs by positron annihilation N92-10467

VACUUM
Information flow in quantum mechanics: The quantum Maxwell demon
[DE91-017659] N92-10725
VACUUM CHAMBERS
The Jyvaskyla (Finland) K130 cyclotron project N92-10420
Thermal helium desorption facility in Jyvaskyla (Finland) N92-10484
VACUUM SYSTEMS
PATRAN and P/THERMAL applications for thermal modeling
[DE91-017767] N92-10320
VALENCE
Valence electron states of the Bi-Sr-Ca-Cu-O high-T(sub c) compound N92-10503
Valence and phonon excitations in high-resolution electron microscopy
[DE91-017684] N92-10625
VAN DER WAALS FORCES
The generalized van der Waals theory of pure fluids and mixtures
[DE91-017549] N92-10093
VANADIUM OXIDES
Heteroepitaxial growth of TiO2, VO2, and TiO2/VO2 multilayers by MOCVD
[DE91-018543] N92-10694
Heteroepitaxy of MOCVD grown TiO2, VO2 films and TiO2/VO2 multilayers on sapphire (1120)
[DE91-018589] N92-10698
VAPOR DEPOSITION
Process modelling for Space Station experiments
[NASA-CR-184227] N92-10112
Diamond thin films grown by microwave plasma assisted chemical vapor deposition
[DE91-018553] N92-10695
VAPOR PHASE EPITAXY
OMVPE growth of InAsSbBi and related alloys using new organometallic group V sources
[AD-A239939] N92-10703
VAPOR PHASES
Evaluation of preservative engine oil containing vapor-phase corrosion inhibitor and a simplified engine preservation technique
[AD-A240100] N92-10103
Energy partitioning in elementary gas phase reactions
[DE91-017783] N92-10627
VAPORIZING
Vapor plumes: A neglected aspect of impact cratering N92-10867
Melt droplet formation in energetic impacts N92-10869
Impacts and atmospheric erosion on the early Earth N92-10871
VAPORS
The role of nonuniform internal heating in Triton's energy budget N92-10736
The spatial distribution and time evolution of impact-generated magnetic fields N92-10878
VARIABILITY
Compositional variability of the Martian surface N92-10931
VARIATIONS
Variation of D-region parameters during polar cap absorption events in the year 1989 N92-10561
Variable features in the Valles Marineris region of Mars N92-10799
VECTOR ANALYSIS
Parametric optimization of synthetic gratings using vector diffraction theory N92-10457
VECTOR PROCESSING (COMPUTERS)
Measurement of memory access contentions in multiple vector processor systems
[DE91-013205] N92-10297
A performance comparison of three supercomputers: Fujitsu VP-2600, NEC SX-3, and CRAY Y-MP
[DE91-016304] N92-10298
Efficient multitasking of Choleski matrix factorization on CRAY supercomputers
[NASA-TM-4259] N92-10302
VECTOR SPACES
Overview of Krylov subspace methods with applications to control problems
[NASA-CR-188842] N92-10343
VECTORS (MATHEMATICS)
Particle-gas dynamics in the protoplanetary nebula N92-10893
VEGETATION
Atmospheric measurements using a scanning, solar-blind Raman Lidar
[DE91-016078] N92-10260
VEGETATION GROWTH
Compilation of 1990 annual reports of the Navy ELF communications system ecological monitoring program. Volume 1: Tabs A, B
[AD-A239868] N92-10137
VEGETATIVE INDEX
Using LANDSAT to provide potato production estimates to Columbia Basin farmers and processors
[NASA-CR-188783] N92-10209
VELOCITY DISTRIBUTION
The structure and development of streamwise vortex arrays embedded in a turbulent boundary layer
[NASA-TM-105211] N92-10012
Dual pin diode preamplifier for laser Doppler velocimetry N92-10382
Velocimetry in gas flows using pulsed laser induced photothermal effects N92-10459
The effect of latitudinally varying solar wind flux on the Lyman alpha sky background N92-10570
N-body simulations of interacting galaxies N92-10579
Accretion rates of protoplanets 2: Gaussian distribution of planestesimal velocities N92-10937
VELOCITY MEASUREMENT
Sea ice elastic moduli: Determination of Biot parameters using in-field velocity measurements
[AD-A239803] N92-10275
Velocimetry in gas flows using pulsed laser induced photothermal effects N92-10459
Observations of semidiurnal atmospheric tides using the EISCAT incoherent scatter radar N92-10560
VENERA SATELLITES
Quantitative analysis of terrain units mapped in the northern quarter of Venus from Venera 15/16 data N92-10853
VENTILATION
A measuring robot for thermal environment, contaminant concentration and ventilation studies N92-10537
VENTS
Global relationships between volcanic vents and fractures radial to large impact basins on Mars N92-10750
VENUS (PLANET)
Venus behind the clouds N92-10569
Processes of deep terrestrial mantles and cores N92-10729
Implications of convection in the moon and the terrestrial planets N92-10730
Dynamic models for ridge belt formation on Venus N92-10731
Morphology and evolution of coronae and ovoids on Venus N92-10742
Factors controlling lava dome morphology N92-10792
The potential scale of aeolian structures on Venus N92-10800
Use of radar to assess aeolian processes N92-10802
Degradation of Fe-Mg silicates in hot CO2 atmospheres: Applications to Venus N92-10806
Reflectance spectra of Fe(2+)-Mg(2+) disordered pyroxenes: Implications to remote-sensed spectra of planetary surfaces N92-10823
Mojave remote sensing field experiment N92-10840
Impact craters on Venus N92-10852
Quantitative analysis of terrain units mapped in the northern quarter of Venus from Venera 15/16 data N92-10853
Asteroid flux and impact cratering rate on Venus N92-10880
Venus mapping N92-10913
Triangulation using synthetic aperture radar images N92-10914
Naming the newly found landforms on Venus N92-10915
Planetary geomorphology research: FY 1990-1991 N92-10940
Are the Equatorial Highlands on Venus formed by mantle plume diapirs? N92-10942
VENUS ATMOSPHERE
The potential scale of aeolian structures on Venus N92-10800
Degradation of Fe-Mg silicates in hot CO2 atmospheres: Applications to Venus N92-10806
Breakup of meteoroids in the Venusian atmosphere and its effects on crater formation N92-10855
Impact cratering calculations N92-10933
VENUS SURFACE
Venus behind the clouds N92-10569
An assessment of the crustal remelting hypothesis for volcanism in the Freyja Montes deformation zone N92-10732
Tectonic evolution of Lavinia Planitia, Venus N92-10741
Hot-spot tectonics of Eistla Regio, Venus: Results from Magellan images and Pioneer Venus gravity N92-10743
Gravitational spreading of Danu, Freyja and Maxwell Montes, Venus N92-10744
Interpretation of the northern boundary of Ishtar Terra from Magellan images and altimetry N92-10745
Factors controlling lava dome morphology N92-10792
The potential scale of aeolian structures on Venus N92-10800
Degradation of Fe-Mg silicates in hot CO2 atmospheres: Applications to Venus N92-10806
Reflectance spectra of Fe(2+)-Mg(2+) disordered pyroxenes: Implications to remote-sensed spectra of planetary surfaces N92-10823
Impact craters on Venus N92-10852
Quantitative analysis of terrain units mapped in the northern quarter of Venus from Venera 15/16 data N92-10853
Venus impact craters: Implications for atmospheric and resurfacing processes from Magellan observations N92-10854
Breakup of meteoroids in the Venusian atmosphere and its effects on crater formation N92-10855
Asteroid flux and impact cratering rate on Venus N92-10880
Venus mapping N92-10913
Triangulation using synthetic aperture radar images N92-10914
Naming the newly found landforms on Venus N92-10915
Impact cratering calculations N92-10933
Are the Equatorial Highlands on Venus formed by mantle plume diapirs? N92-10942
VERY LOW FREQUENCIES
Examples of VLF emissions recorded in the auroral zone N92-10555
VESTIBULES
The 14th International Conference on Combined Effect of Environmental Factors
[AD-A240045] N92-10245
VIBRATION
Theoretical estimation of the vibrational temperatures of N2 molecules in the ionosphere and in the laboratory simulated plasma
[ISAS-642] N92-10258
VIBRATION DAMPING
Multi-degree of freedom, active vibration control method, and system
[NASA-CASE-LAR-14508-1-CU] N92-10202
VIBRATION MEASUREMENT
The measurement of plate vibration and sound radiation from a turbulent boundary layer manipulator
[AD-A240127] N92-10206
VIBRATION MODE
Development of a model of space station solar array
[NASA-CR-188911] N92-10220
VIBRATIONAL SPECTRA
The rotational structure of the nu(sub 6) vibration band of CH3I N92-10431
The nu(sub 4) and nu(sub 7) bands of CD3CN with coriolis coupling and other resonance perturbations N92-10432
The nu(sub 8) and 2nu(sub 8) bands of CD3CN N92-10433
The infrared rotation-vibration spectrum of C2H2 in the nu(sub 2) + nu(sub 5) band region; l-resonances in the bands nu(sub 2) + nu(sub 5), nu(sub 2) + 2(nu(sub 5)) back arrow nu(sub 5) and nu(sub 1) back arrow nu(sub 5) N92-10434
Analysis of the interacting levels V(sub 9) = 1 and V(sub 10) = 2 of propyne N92-10444
VIDEO SIGNALS
Real-time data compression of broadcast video signals
[NASA-CASE-LEW-14945-2] N92-10128
VIKING LANDER SPACECRAFT
Clays on Mars: Review of chemical and mineralogical evidence N92-10250
Surface-material maps of Viking landing sites on Mars N92-10787
VIKING MARS PROGRAM
Surface-material maps of Viking landing sites on Mars N92-10787
Magma generation on Mars: Estimated volumes through time N92-10788
VISCOSITY
Tidal disruption of inviscid protoplanets N92-10900
VISCOUS FLOW
Numerical simulation of hypersonic viscous flow for the design of H-2 orbiting plane (HOPE-2)
[NAL-TR-1093] N92-10009
Multigrid calculation of three-dimensional viscous cascade flows
[NASA-TM-105257] N92-10345
VISIBLE SPECTRUM
UV, visible, and near-IR reflectivity data for magnetic soils/rocks from Brazil N92-10254
Spectral reflectance of pine and intensity of moose browsing N92-10514

VISUAL ACUITY
Two informative cases of Q-switched laser eye injury [AD-A240001] N92-10279
VISUAL PERCEPTION
Auditory and visual evoked potentials as a function of sleep deprivation and irregular sleep [AD-A240097] N92-10281
Visual motion perception [AD-A240133] N92-10286
VISUAL PIGMENTS
Fundamental studies in the molecular basis of laser induced retinal damage [AD-A239941] N92-10278
VISUAL STIMULI
Display format, highlight validity, and highlight method: Their effects on search performance [NASA-TM-104742] N92-10287
VLASOV EQUATIONS
Vlasov-Maxwell system: 2-D equilibria, reversed field pinches [DE91-018421] N92-10595
VOICE COMMUNICATION
Digital simulation of speech transmission channels [IZF-1991-A-7] N92-10115
VOLATILITY
Impact and collisional processes in the solar system N92-10932
Studies of volatiles and organic materials in early terrestrial and present-day outer solar system environments N92-10958
VOLCANOES
Venus behind the clouds N92-10569
Fluid dynamics of multiphase flow in volcanic environments on the Earth, Io, and other planets N92-10740
Chronology of glaciation in the Hellas region of Mars N92-10773
Physical properties of lava flows on the southwest flank of Tyrrhena Patera, Mars N92-10790
Factors controlling lava dome morphology N92-10792
Lunar and Hawaiian lava tubes: Analogs and uses based on terrestrial field data N92-10796
On using a pyroclastic deposit as a manned lunar base site N92-10797
Oxidation of basaltic tephras: Influence on reflectance in the 1 micron region N92-10817
Mojave remote sensing field experiment N92-10840
Planetary geomorphology research: FY 1990-1991 N92-10940
Factors controlling the structures of magma chambers in basaltic volcanoes N92-10957
VOLCANOLOGY
An assessment of the crustal remelting hypothesis for volcanism in the Freyja Montes deformation zone N92-10732
Magma generation on Mars: Estimated volumes through time N92-10788
The probable continuum between emplacement of plutons and mare volcanism in lunar crustal evolution N92-10794
Lunar western limb pyroclastic deposits N92-10795
Remote sensing and geologic studies of the orientale basin region N92-10809
Composition of Syrtis Major volcanic plateau N92-10815
Oxidation of basaltic tephras: Influence on reflectance in the 1 micron region N92-10817
Mud volcanoes on Mars? N92-10938
Factors controlling the structures of magma chambers in basaltic volcanoes N92-10957
Workshop on Mare Volcanism and Basalt Petrogenesis: Astounding Fundamental Concepts (AFC) Developed Over the Last Fifteen Years --- Author [NASA-CR-188810] N92-10961
The violent side of mare volcanism N92-10962
The history of lunar volcanism N92-10965
VOLT-AMPERE CHARACTERISTICS
Thermal energy storage and heat transfer support program. Volume 2: Task 4 Thermionic energy conversion studies [AD-A239968] N92-10178
VORTEX BREAKDOWN
Numerical simulation of vortex breakdown [ONERA-RSF-6/4368-AY-008A] N92-10162
Numerical simulation of vortex breakdown by solving the Euler equations for an incompressible fluid N92-10163
Numerical simulation of vortex breakdown via 3-D Euler equations N92-10164
VORTEX GENERATORS
The structure and development of streamwise vortex arrays embedded in a turbulent boundary layer [NASA-TM-105211] N92-10012
VORTICES
The structure and development of streamwise vortex arrays embedded in a turbulent boundary layer [NASA-TM-105211] N92-10012
The effects of forebody strakes on asymmetric vortices on a vertically launched missile [AD-A239948] N92-10014
Stability of the flow around a cylinder: The spin-up problem [NASA-CR-187636] N92-10171
Mutual friction in superfluid He-3: Effects of bound states in the vortex core N92-10475
Vortex nucleation in rotating superfluid He-3-B N92-10476
Superfluid vortex nucleation in He-3 flow N92-10479
Vortex lattice: Vortex liquid states in anisotropic high-T(sub c) superconductors N92-10500
Dynamics of vortices in high-temperature superconductors N92-10501
VOYAGER PROJECT
Possible misinterpretation of lunar cratering record in Voyager team analyses of outer planet satellites N92-10860

W

WAFERS
Diamond heat sinks for electronic circuits [AD-A239750] N92-10145
Beam test results of ion-implanted silicon strip detectors on a 100 mm wafer N92-10416
Studies on new low noise silicon radiation detector N92-10418
WAKES
Dynamic screening and wake effects on electronic excitation in ion-solid and ion-surface collisions [DE91-018224] N92-10687
WASTE DISPOSAL
Solar detoxification technology: Using energy from the sun to destroy hazardous waste [DE91-015007] N92-10241
WATER
Solar detoxification technology: Using energy from the sun to destroy hazardous waste [DE91-015007] N92-10241
The magnesium sulfate-water system at pressures to 4 kilobars N92-10738
Evolution of the Martian hydrosphere N92-10768
Paleolakes and lacustrine basins on Mars N92-10776
Water on Mars: Clue to accretional history N92-10798
Spectroscopic analyses of Fe and water in clays: A Martian surface weathering study N92-10818
Water detection at the moon, Mars and comets with a combined neutron gamma ray instrument N92-10819
Water/rock interactions in experimentally simulated dirty snowball and dirty iceball cometary nuclei N92-10888
WATER MANAGEMENT
Water resources and climate change N92-10236
Processes for identifying regional influences of and responses to increasing atmospheric CO2 and climate change: The MINK project [DE91-018603] N92-10243
Atmospheric measurements using a scanning, solar-blind Raman Lidar [DE91-016078] N92-10260
WATER QUALITY
The remote sensing Loosdrecht Lakes (Netherlands) project [BCRS-90-29] N92-10215
Sea-level rise: Regional consequences and responses N92-10231
Processes for identifying regional influences of and responses to increasing atmospheric CO2 and climate change: The MINK project [DE91-018605] N92-10244
WATER RESOURCES
Water resources and climate change N92-10236
Processes for identifying regional influences of and responses to increasing atmospheric CO2 and climate change: The MINK project [DE91-018605] N92-10244
WATER VAPOR
Atmospheric measurements using a scanning, solar-blind Raman Lidar [DE91-016078] N92-10260
Free convection in the Martian atmosphere N92-10803
WATERSHEDS
Remote sensing and watershed modelling: Towards a hydrological interface model [BCRS-90-42] N92-10216
WAVE DIFFRACTION
Coupled wave analysis in inverse grating diffraction problems N92-10456
Parametric optimization of synthetic gratings using vector diffraction theory N92-10457
Waveguide Dammann gratings and kinoforms N92-10458
WAVE FRONTS
Waveguide Dammann gratings and kinoforms N92-10458
WAVE FUNCTIONS
Ground state properties of a He-3 impurity in liquid He-4 monolayers [AD-A239993] N92-10078
Mutual friction in superfluid He-3: Effects of bound states in the vortex core N92-10475
Effective mass and excitation spectrum of He-3 impurities in superfluid He-4 N92-10477
WAVE INTERACTION
Self-regulation mechanisms in galactic discs N92-10576
WAVE PROPAGATION
Reconfigurable optical interconnections by acousto-optic holograms N92-10449
Waveguide Dammann gratings and kinoforms N92-10458
Numerical calculations of wave propagation in tokamak plasmas N92-10461
Inhomogeneity and nonlinearity effects on stop bands of Alfvenic ion cyclotron waves in multicomponent plasma N92-10557
Nonlinear RF processes in plasma [DE91-017441] N92-10658
WAVE REFLECTION
Approximate analytic theory of the multijunction grill [IPPCZ-309] N92-10127
On ponderomotive force effects on coupling of the LH and IBW grills for the FTU tokamak [IPPCZ-305] N92-10650
WAVEFORMS
Characterization of nonlinear input-output systems using time series analysis [DE91-018003] N92-10356
Clustering: A powerful aid in classifying QRS waveforms N92-10541
WAVEGUIDES
Approximate analytic theory of the multijunction grill [IPPCZ-309] N92-10127
Phase control in a two-element folded waveguide array [DE91-018251] N92-10130
Coupling between radiation and gas dynamics [AD-A240004] N92-10179
Waveguide Dammann gratings and kinoforms N92-10458
WEAK ENERGY INTERACTIONS
Recent physics results from DELPHI N92-10394
WEAPONS
Laser acoustic technology demonstration and equipment field trails [DE91-018759] N92-10193
WEAR
Relative sliding durability of two candidate high temperature oxide fiber seal materials [NASA-TM-105199] N92-10064
WEATHER
Recent changes of weather patterns in North America [DE91-017706] N92-10266
WEATHER FORECASTING
Annual tropical cyclone report, 1990 [AD-A239910] N92-10268
VERMOD capabilities. VERMOD 1.0 and future [AD-A239801] N92-10274
WEATHERING
Clays on Mars: Review of chemical and mineralogical evidence N92-10250
Spectroscopic analyses of Fe and water in clays: A Martian surface weathering study N92-10818
WELDABILITY
Proceedings of the Second Switch Tube Advanced Technology Meeting [DE91-017718] N92-10148
WELDED JOINTS
Proceedings of the Second Switch Tube Advanced Technology Meeting [DE91-017718] N92-10148
WELDING
BES Welding Science Contractors summary report, 1990--1991 [DE91-018510] N92-10198
WELLS
A simple radon well N92-10536
WETTABILITY
Wettability of low temperature solder alloys for step-soldering [DE91-018348] N92-10083

WETTING
Molecular dynamics studies of liquid-solid interfaces N92-10462
Numerical simulation studies of fluid spreading N92-10482
WHISKERS (CRYSTALS)
Chemical synthesis and microstructural toughening of infrared window materials
[AD-A239987] N92-10102
WHISTLERS
The use of whistlers for magnetospheric diagnostics N92-10554
WHITE NOISE
Influence of the angular correlation of fission neutrons on noise signatures
[DE91-014577] N92-10618
WIND (METEOROLOGY)
The potential scale of aeolian structures on Venus N92-10800
WIND EFFECTS
Relationships between topographic roughness and aeolian processes N92-10801
Use of radar to assess aeolian processes N92-10802
WIND MEASUREMENT
Use of radar to assess aeolian processes N92-10802
WIND PROFILES
Relationships between topographic roughness and aeolian processes N92-10801
Use of radar to assess aeolian processes N92-10802
WIND SHEAR
The 1990 Airport Surveillance Radar Wind Shear Processor (ASR-WSP) operational test at Orlando International Airport
[AD-A239852] N92-10019
WIND TUNNEL MODELS
Downwash measurements on a pitching canard-wing configuration
[AD-A239956] N92-10016
WIND TUNNEL TESTS
Mass flux similarity for slotted transonic-wind-tunnel walls
[NASA-TM-4281] N92-10006
The effects of forebody strakes on asymmetric vortices on a vertically launched missile
[AD-A239948] N92-10014
Dual strain gage balance system for measuring light loads
[NASA-CASE-LAR-14419-1] N92-10185
WIND TUNNEL WALLS
Mass flux similarity for slotted transonic-wind-tunnel walls
[NASA-TM-4281] N92-10006
WIND TUNNELS
Numerical simulation of hypersonic viscous flow for the design of H-2 orbiting plane (HOPE-2)
[NAL-TR-1093] N92-10009
WIND VELOCITY
Free convection in the Martian atmosphere N92-10803
Meteo and irradiation data during BEST TWO, Mourmelon (Netherlands)
[FEL-90-A368] N92-10966
WIRE
Effects of wires on solid propellant ballistics N92-10109
WORD PROCESSING
The EH safety representative information system on the safety performance measurement system is where you will find... Word processing and helps with a V-PLUS
[DE91-018709] N92-10113
WORK FUNCTIONS
Work function changes of high-T(sub c) superconductors around the T(sub c) N92-10498
Dependence of Au(-) production upon the target work function in a plasma-sputter-type negative ion source
[NIFS-85] N92-10656
WORKSTATIONS
The role of graphics super-workstations in a supercomputing environment
[NASA-CR-188852] N92-10306
Worldnet
[NASA-CR-188845] N92-10711

X

X RAY ANALYSIS
IPC two-color analysis of x ray galaxy clusters
[NASA-CR-188980] N92-10724
X RAY BINARIES
Variable optical polarization in Her X-1 N92-10546
An atlas of optical counterparts of low mass x ray binaries. Part 1: The Northern Sample
[MPE-PREPRINT-195-PT-1] N92-10723
X RAY DIFFRACTION
Studies on superconducting Bi2Sr2Ca(n-1) Cu(n)O(4+2n) compounds with Fe-57 and Eu-151 Moessbauer spectroscopy N92-10504
X RAY FLUORESCENCE
Combined Backscatter Moessbauer Spectrometer and X Ray Fluorescence analyzer (BaMS/XRF) for planetary surface materials N92-10249
X RAY LASERS
Cavity issues for Ni-like Ta x ray lasers
[DE91-017668] N92-10190
X RAY SPECTROSCOPY
Oxide properties of a gamma titanium aluminide: A surface science study
[DE91-018024] N92-10095
Combined Backscatter Moessbauer Spectrometer and X Ray Fluorescence analyzer (BaMS/XRF) for planetary surface materials N92-10249
Studies on new low noise silicon radiation detector N92-10418
Surface characterization of coated powders with XPS: Al2O3-SiO2 coated TiO2 pigments N92-10520
The measuring modes and observations with the x-ray spectrometer array SIXA onboard spectrum-x-gamma N92-10563
Polarization dependent x ray spectroscopy of high T(sub c) superconductors
[DE91-017475] N92-10683
X RAYS
Characterization of electronic materials
[AD-A240063] N92-10159
Subpicosecond x ray streak camera
[DE91-017664] N92-10187
XENON
Experimental investigation of a 12 cm diameter Kaufman xenon ion thruster
[NAL-TR-1099] N92-10056
XENON ISOTOPES
Evidence for band termination in Xe-118 N92-10405
NMR-relaxation time measurements of noble gas isotope Xe-129 dissolved in isotropic and anisotropic liquids N92-10437

Y

YIELD STRENGTH
Physical properties of lava flows on the southwest flank of Tyrrhena Patera, Mars N92-10790
Factors controlling lava dome morphology N92-10792
YTTERBIUM COMPOUNDS
Photoemission in YbCu2Si2: Problems with the Kondo impurity model
[DE91-018018] N92-10684
YTTRIUM OXIDES
Neutron irradiation effects on YBCO single crystals
[DE91-018615] N92-10700

Z

ZEOLITES
Regenerative Cu/La zeolite supported desulfurizing sorbents
[NASA-CASE-NPO-17480-1-CU] N92-10073
ZINC SELENIDES
Electrical characterization of Li and N doped ZnSe N92-10493
ZINC SULFIDES
Chemical synthesis and microstructural toughening of infrared window materials
[AD-A239987] N92-10102
ZODIACAL DUST
Origin and evolution of the zodiacal dust cloud N92-10886

Typical Personal Author Index Listing

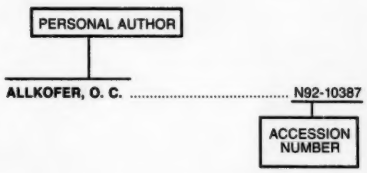

Listings in this index are arranged alphabetically by personal author. The accession number denotes the number by which the citation is identified.

A

AABERG, T. N92-10428
AAKKO, KYLLIKKI N92-10521
AALTO, J. P. S. N92-10538
ABBOTT, TERENCE S. N92-10024
ABLIN, KARYN K. N92-10920
N92-10921
N92-10922
ABRAHAM, D. B. N92-10481
ACHARYA, MUKUND N92-10180
ACHENBACH, J. D. N92-10150
ADAMS, JOHN B. N92-10931
ADATI, K. N92-10647
N92-10649
ADCOCK, J. N92-10152
AGARICI, G. N92-10673
AGRESTI, D. G. N92-10249
AHMAD, ANEES N92-10088
AHONEN, P. N92-10401
N92-10403
N92-10404
N92-10405
AHRENS, THOMAS J. N92-10932
N92-10933
AKIMOTO, TOSHIO N92-10009
AKIYAMA, R. N92-10647
AKSELA, H. N92-10426
N92-10427
N92-10428
N92-10429
N92-10517
AKSELA, SEPPO N92-10377
N92-10426
N92-10427
N92-10428
N92-10429
N92-10446
N92-10517
N92-10518
N92-10519
ALA-KORPELA, M. N92-10545
ALA-NISSILA, TAPIO N92-10373
N92-10469
N92-10470
ALANKO, S. N92-10431
N92-10434
ALATALO, M. N92-10473
ALBAJAR, C. N92-10387
N92-10388
N92-10389
N92-10390
N92-10391
N92-10392
ALBROW, M. G. N92-10387
ALEXANDER, J. IWAN D. N92-10112
N92-10676
ALEXANDER, M. JOAN N92-10813
ALLEN, BRADLEY P. N92-10314
ALLES, H. N92-10474
ALLKOFER, O. C. N92-10387
ALLTON, JUDITH H. N92-10888
AMBROSIANO, J. J. N92-10325
N92-10670
AMIET, R. K. N92-10599
AMINOFF, C. G. N92-10454
N92-10455
AMIROUDINE, SAKIR N92-10112
ANAND, HARSH N92-10274
ANDERSON, J. V. N92-10241
ANDERSSON, MIKAEL N92-10416
ANDO, A. N92-10647
ANDO, R. N92-10649
ANDRIEU, B. N92-10387
ANGELL, THOMAS S. N92-10144
ANKOVIAK, K. N92-10387
ANNILA, A. J. N92-10507
ANTAYA, T. A. N92-10422
ANTTILA, R. N92-10432
N92-10433
AOKI, T. N92-10649
APAJA, V. N92-10499
APSIMON, R. N92-10387
ARJE, J. N92-10422
ARKO, A. J. N92-10684
ARMSTRONG, W. C. N92-10042
ARNONE, A. N92-10345
ARVELA, H. N92-10574
N92-10575
ARVELA, P. N92-10480
ARVIDSON, RAYMOND E. N92-10840
N92-10841
N92-10842
N92-10843
N92-10844
ASONEN, H. N92-10489
N92-10490
N92-10491
N92-10523
N92-10530
N92-10531
ASPAUG, ERIK N92-10863
ASPHAUG, ERIK N92-10861
ATTREP, A., JR. N92-10875
AU, ANDREW Y. N92-10257
AUBELE, JAYNE C. N92-10906
AUBERT, B. N92-10387
AUSTIN, R. T. N92-10846
AVIV, DAVID N92-10360
AYDEMIR, A. Y. N92-10668
AYSTO, J. N92-10402
N92-10411
N92-10424
AZMY, Y. Y. N92-10620

B

BABCOCK, S. E. N92-10697
BACA, R. G. N92-10096
BACCI, C. N92-10387
N92-10413
BACK, LLOYD N92-10609
BADALEC, J. N92-10651
BAITY, F. W. N92-10673
BAKER, A. J. N92-10010
BAKER, V. N92-10768
BALDO, P. M. N92-10682
BALLINGER, C. T. N92-10619
N92-10631
BALSER, R. A. N92-10758
BANDYOPADHYAY, PROMODE R. N92-10008
BANERDT, W. B. N92-10746
N92-10748
N92-10759
BANIN, AMOS N92-10250
BARNES, ARNOLD A., JR. N92-10269
N92-10270
BARNES, SCOTT P. N92-10128
BARNETT, JOHN N92-10046
BARRINGTON, C. A. N92-10172
BARTHA, S. N92-10387
BARTON, TIMOTHY J. N92-10303
BATIE, SANDRA S. N92-10235
BATSON, R. M. N92-10913
N92-10915
N92-10923
N92-10924
N92-10925
N92-10926
N92-10928
N92-10929
BATTERMAN, BORIS W. N92-10366
BAUCOM, ROBERT M. N92-10070
BAUER, G. N92-10387
BEACH, R. F. N92-10055
BEAUMONT, B. N92-10673
BEAVIS, L. C. N92-10148
BECK, S. T. N92-10099
BECKER, R. N92-10932
BECKER, T. N92-10808
BECKWITH, S. N92-10948
BECOULET, A. N92-10673
BELCASTRO, CHRISTINE M. N92-10027
BELCHER, M. L. N92-10133
BELIAN, R. D. N92-10969
BELL, JEFFREY F. N92-10809
N92-10810
N92-10882
BELTON, M. N92-10808
BEMENT, LAURENCE J. N92-10196
BENCI, JOHN N92-10087
BENTLEY, J. N92-10625
BENTS, DAVID J. N92-10221
BENZ, W. N92-10900
BERSOHN, R. N92-10627
BERTAUX, J.-L. N92-10570
BERTHEL, ROBERT O. N92-10269
BERTOLINI, L. M. N92-10758
BESANCON, JAMES R. N92-10823
BETTINI, S. N92-10413
BHADKAMKAR, N. N92-10294
BHATTACHARJEE, A. N92-10667
BHATTACHARYYA, B. N92-10645
BIBRING, JEAN-PIERRE N92-10815
N92-10822
BILLIDEAU, JENNIFER S. N92-10919
BINDSCHADLER, DUANE L. N92-10742
BIRKAN, M. A. N92-10082
BISHOP, A. R. N92-10686
BISHOP, J. L. N92-10818
BISHOP, LEE R. N92-10141
BJORKSTEN, M. F. N92-10496
BLEWETT, D. N92-10809
N92-10810
N92-10851
BLOOMFIELD, HARVEY S. N92-10221
BLUMBERG, D. N92-10802
BODEK, A. N92-10630
BOGGS, T. L. N92-10110
BOLERJACK, B. N92-10055
BONNE, ULRICH A. N92-10834
BOONE, L. N92-10902
BORDWELL, KEVIN N92-10611
BOSELA, PAUL A. N92-10220
BOSNYAK, C. P. N92-10205
BOSS, ALAN P. N92-10890
N92-10900
BOUCHARD, MICHAEL P. N92-10101
BOWERS, M. W. N92-10187
BOWN, RODNEY L. N92-10313
BRANDON, S. N92-10325
N92-10670
BRATTON, THOMAS D. N92-10020
BRENNER, R. N92-10412
N92-10416
BRENNER, RICHARD N92-10414
BRIDGES, F. N92-10902
BRIDGES, NATHAN N92-10792
BRITT, DANIEL T. N92-10822
N92-10827
N92-10828
BROERSMA, H. J. N92-10341
BROOKS, E. D., III N92-10336
BROPHY, T. G. N92-10934
BROWN, L. F. N92-10074
BROWN, PETER N. N92-10309
BROWN, R. H. N92-10736

BROWN, RICHARD D. N92-10257
BROWN, ROBERT H. N92-10734
BROWNING, J. S. N92-10040
BRUDER, J. A. N92-10133
BRUNEL, M. N92-10678
BUCHER, I. Y. N92-10297
BUGLANOV, G. V. N92-10076
BULATOV, M. G. N92-10272
BULLOCK, HAROLD E. N92-10140
BUNKOV, Y. M. N92-10476
BURATTI, BONNIE J. N92-10837
N92-10887
BURCHETT, S. N. N92-10082
BURGDOERFER, J. N92-10687
BURKHALTER, JOHN E. N92-10016
BURLAK, A. V. N92-10492
BURNS, JOSEPH A. N92-10904
BURNS, ROGER G. N92-10806
N92-10823
N92-10824
N92-10825
BURTON, IAN N92-10238
BUSCHHORN, G. N92-10590
BUSH, KATHRYN A. N92-10208
BUTLER, M. N92-10152

C

CAI, L. N92-10327
CAI, X. Y. N92-10697
CALLIS, R. N92-10671
CALVIN, W. M. N92-10820
N92-10839
CAMERON, A. G. W. N92-10900
CAMERON, CHARLES B. N92-10644
CAMMARATA, STEPHANIE N92-10715
CAMPBELL, B. N92-10810
CAMPBELL, DONALD B. N92-10845
CANFIELD, P. C. N92-10684
CANN, D. N92-10317
CANTRELL, JOHN H. N92-10182
CANUT, B. N92-10678
CARDARELLI, R. N92-10413
CARPENTER, M. N92-10401
CARR, M. H. N92-10798
N92-10808
CARRIER, MELVIN, JR. N92-10611
CARY, W. N92-10671
CAULFIELD, H. J. N92-10183
CAVES, ROBERT N92-10018
CAYTON, T. E. N92-10969
CEDERWALL, B N92-10405
CENTRO, S. N92-10413
CERADINI, F. N92-10413
CHAKRABORTY, TAPASH N92-10494
N92-10495
CHAKRAVARTHY, SUKUMAR R. N92-10349
CHAMPNEY, JOELLE M. N92-10893
CHAN, MATTHEW T. N92-10181
CHAN, TONY F. N92-10181
CHANG, B.-C. N92-10027
CHANG, C. H. N92-10672
CHANG, H. L. M. N92-10694
N92-10698
CHANG, S. N92-10818
CHANG, TOM N92-10263
CHANG, Y. C. N92-10699
CHAPLINE, G. F. N92-10725
CHAPMAN, MARY G. N92-10756
N92-10779
CHAPMANN, C. N92-10808
CHEMBURKAR, R. M. N92-10074
CHEN, C. P. N92-10160
CHEN, K. C. N92-10154
CHEN, X. L. N92-10173
CHICONE, CARMEN N92-10352
CHIPMAN, RUSSELL A. N92-10638
CHIU, S. C. N92-10665
CHOE, K. Y. N92-10862
CHOINSKI, J. N92-10422
CHOW, J. N92-10131
CHRISTOPHOROU, L. G. N92-10621
CHUDNOVSKY, A. N92-10205
CHURCH, G. M. N92-10337
CHYBA, CHRISTOPHER F. N92-10958
CIAPETTI, G. N92-10413
CLANCY, R. T. N92-10956
CLARK, R. L. N92-10183
CLARK, R. N. N92-10839
CLAUSE, CELIA N92-10889
CLAUSEN, K. N. N92-10507
CLEYMANS, J. N92-10385
N92-10386
CLINE, D. N92-10413
CLOW, G. D. N92-10803
N92-10804
CLYNE, R. J. N92-10241
COE, J. A. N92-10261
COEY, J. M. D. N92-10254
COLDREN, LARRY A. N92-10155
COLE, STEVEN W. N92-10125
CONAHAN, FRANK C. N92-10710
CONNELL, JOHN W. N92-10066
COOGAN, J. J. N92-10191
COOMBS, CASSANDRA R. N92-10795
N92-10796
N92-10797
N92-10810
N92-10962
COOPER, A. R. N92-10727
COOPER, CHESTER L. N92-10240
COOPER, D. I. N92-10260
COOPER, F. N92-10726
COOPER, R. H. N92-10058
CORBEL, C. N92-10467
CORKE, THOMAS C. N92-10180
COST, J. R. N92-10685
COYNE, L. M. N92-10818
CRABTREE, G. W. N92-10692
N92-10693
N92-10699
N92-10700
N92-10702
CRADDOCK, ROBERT A. N92-10781
N92-10906
N92-10907
N92-10955
CRAMER, PAUL N92-10121
N92-10122
CRAWFORD, D. A. N92-10878
CREA, B. A. N92-10320
CRIGHTON, DAVID G. N92-10605
CRISP, J. N92-10789
CROFT, STEVEN K. N92-10764
N92-10765
N92-10766
N92-10874
CRONIN, R. N92-10932
CROSSON, PIERRE R. N92-10228
N92-10232
N92-10242
CROWN, DAVID A. N92-10752
N92-10790
N92-10909
CRUMPLER, L. S. N92-10906
CUBITT, R. N92-10691
CULLEN, J. A. N92-10019
CUZZI, JEFFREY N. N92-10893
N92-10903

D

DAANEN, H. A. M. N92-10277
DAGUM, LEONARD N92-10293
DALE-BANNISTER, MARY A. N92-10844
DARIA, D. M. N92-10826
DARKNELL, D. N92-10902
DARMSTADTER, JOEL N92-10228
N92-10230
DAS, A. N92-10630
DASILVA, L. B. N92-10190
DAU, D. N92-10413
DAVID, S. A. N92-10198
DAVIES, MERTON E. N92-10916
N92-10917
N92-10918
DAVIS, DONALD R. N92-10884
N92-10895
DAVIS, MICHAEL N92-10284
DAVIS, P. A. N92-10755
N92-10791
DAWN, FREDERIC S. N92-10091
DAY, D. B. N92-10633
DEBROVOLSKIS, A. N92-10802
DECROCK, P. N92-10411
DEERING, DONALD W. N92-10843
DEHART, J. N92-10255
DEHON, R. A. N92-10780
DEISSLER, ROBERT G. N92-10289
DEKKER, A. G. N92-10215
DELANO, JOHN W. N92-10964
DELLACORTE, CHRISTOPHER N92-10064
DELLANEGRA, M. N92-10413
DEMAISON, J. N92-10444
DENDOOVEN, P. N92-10411
DENNING, PETER J. N92-10307
N92-10308
N92-10711
DENNIS, JACK B. N92-10290
DERMOTT, S. F. N92-10886
DERUIZ, KAYE A. N92-10351
DICKEY, F. M. N92-10324
DICKINSON, TAMMY L. N92-10963
DICUS, D. A. N92-10632
DIECKMAN, S. L. N92-10097
DIEHL, P. N92-10436
DIEU, TRINH CONG N92-10342
DIFILIPPO, F. C. N92-10618
DINER, DANIEL B. N92-10126
DOANE, GEORGE B., III N92-10042
N92-10340
DOBROVOLSKIS, ANTHONY R. N92-10801
N92-10893
N92-10903
DOHM, JAMES M. N92-10751
N92-10776
DOMINEK, A. N92-10593
DONES, LUKE N92-10903
DONG, J. Q. N92-10663
DONNER, KIMBERLY A. N92-10287
DOSANJH, S. S. N92-10334
DOSTER, M. J. N92-10316
DOW, MARVIN B. N92-10067
DOWNEY, J. N92-10692
DRAGER, G. N92-10503
DRAKE, R. P. N92-10669
DRAPER, J. V. N92-10129
DRAPER, JAMES S. N92-10270
DREYER, R. N92-10076
DUCHARME, M. B. N92-10277
DUCK, B. N92-10927
DUDA, P. M. N92-10084
DUEHOLM, K. S. N92-10261
DUERR, H.-P. N92-10589
DUEX, P. N92-10442
DUFFY, T. N92-10932
DUNBAR, R. SCOTT N92-10887
DURDA, D. N92-10886
DURHAM, W. B. N92-10735
DURISEN, RICHARD H. N92-10903
DUTERQUE, JEAN-ROBERT N92-10107

E

EASTERLING, WILLIAM E., III N92-10228
N92-10243
EBELING, CHARLES N92-10037
EDER, D. C. N92-10190
EDMONDS, JAE N92-10230
EDWARDS, J. O. N92-10818
EDWARDS, KATHLEEN N92-10926
N92-10927
EEROLA, P. N92-10393
EFTEKHARI, ABE N92-10677
EGGERT, K. N92-10413
EGONSSON, J. N92-10546
EICHINGER, W. E. N92-10218
N92-10260
EL-SHEIKH, S. M. N92-10439
ELIASON, E. M. N92-10926
ELLINGSON, W. A. N92-10097
ELO, A.-M. N92-10574
N92-10575
ELSBERRY, RUSSELL L. N92-10271
EMERY, V. J. N92-10688
ENGLAND, A. W. N92-10846
ENQVIST, T. N92-10424
EOYANG, C. N92-10298
ERARD, S. N92-10815
ERARD, STEPHANE N92-10822
ERONEN, T. N92-10562
ESHLEMAN, VON R. N92-10850
N92-10960
ESKELINEN, S. N92-10545
ESKOLA, K. N92-10402
N92-10411
N92-10424
ESPOSITO, L. W. N92-10934
ESTABROOK, POLLY N92-10119
N92-10120
N92-10124
ETKIN, V. S. N92-10272
EUBANK, S. N92-10357
EVANS, D. N92-10840
EVERHART, JOEL L. N92-10006

F

FAESSLER, A. N92-10410
FAHLANDER, C. N92-10401
N92-10404
FALCONE, A. N92-10069
FALLSTROEM, K. N92-10497
FANALE, F. P. N92-10805
N92-10808

FANT, B. N92-10405
FARMER, J. D. N92-10357
FARR, T. N92-10840
FARRAND, WILLIAM H. N92-10817
FAUCI, LISA J. N92-10013
FECHTER, LAWRENCE D. N92-10245
FELLIEROS, S. N92-10634
FERBEL, T. N92-10630
FEYGIN, F. Z. N92-10552
FIELD, M. B. N92-10697
FINK, JONATHAN N92-10792
FINK, MARTIN R. N92-10606
FINK, PAMELA K. N92-10712
FINNE, J. N92-10538
FISCHER, ERICH M. N92-10808
N92-10816
FISCHL, ROBERT N92-10027
FISHER, DUNCAN S. N92-10824
FISK, Z. N92-10684
FLESHLER, S. N92-10692
FLODSTROEM, A. N92-10580
FLYNN, M. J. N92-10294
FOERSTER, C. L. N92-10092
FONG, D. N92-10055
FONG, W. N92-10948
FONSECA, M. G. N92-10318
FONTANA, J. R. N92-10192
FORGAN, E. M. N92-10691
FORREST, DANA K. N92-10005
FORREST, KATHRINE A. N92-10680
FORSTER, R. A. N92-10354
FOSTER, C. M. N92-10694
FOSTER, I. N92-10319
N92-10339
FOSTER, MICHAEL S. N92-10274
FRAME, EDWIN A. N92-10103
FRANCOIS, R. E. N92-10275
FRANK, SHARON L. N92-10741
FRANKEL, DONALD N92-10270
FRANKLIN, B. J. N92-10747
FRAZIER, WILLIAM E. N92-10072
N92-10087
FREAR, D. R. N92-10083
FREDERICK, KENNETH D. N92-10236
N92-10244
FREDERICKSON, PAUL O. N92-10333
FREELAND, R. E. N92-10123
FREELS, J. D. N92-10010
FREEMAN, R. N92-10671
FREI, T. E. N92-10063
FRENCH, R. G. N92-10935
FREUND, ROLAND W. N92-10310
N92-10311
N92-10312
FRIBERG, ARI T. N92-10449
FRICKE, S. K. N92-10760
FROLOV, A. N92-10510
FUJITA, JUNJI N92-10656
FULLER, CHRIS R. N92-10202
FUNK, L. N92-10682
FURUSAWA, Y. N92-10426
N92-10427
N92-10429

G

GADDIS, L. N92-10801
N92-10802
N92-10808
N92-10840
N92-10847
GAFFEY, MICHAEL J. N92-10881
GAGLIANO, D. N92-10279
GALDRIKIAN, B. N92-10357
GANASAN, J. P. N92-10738
GAO, Y. N92-10694
N92-10697
N92-10698
GAPONENKO, N. I. N92-10652
GARCIA, PATRICIA A. N92-10922
GARTLING, D. K. N92-10321
GASCON, J. N92-10401
GASSER, J. N92-10396
GAULT, D. E. N92-10858
GAUTIER, ILIA M. N92-10611
GAVRILJUK, V. G. N92-10472
GAZIS, C. N92-10932
GEA, L. N92-10678
GEISSLER, PAUL E. N92-10799
GENZEL, R. N92-10615
GEOFFROY, GREGORY N92-10102
GEORGE, JEFFREY A. N92-10057
GEORGE, THOMAS F. N92-10078
N92-10425
N92-10643
GERKEN, N. T. N92-10069
GERWIN, RICHARD N92-10049
GIBBS, GARY P. N92-10202
GIBSON, M. ALAN N92-10267
GIERLOFF-EMDEN, H.-G. N92-10210
N92-10213
GILLAND, JAMES H. N92-10045
GISLER, G. R. N92-10969
GLEICK, PETER H. N92-10236
GLIEBE, PHILLIP R. N92-10601
GODON, JEAN-CLAUDE N92-10107
GOGUEN, JAY D. N92-10832
GOLDEN, D. C. N92-10251
GOLDMAN, T. N92-10726
GOLDSTEIN, M. E. N92-10603
GOLOMBEK, M. P. N92-10747
N92-10748
N92-10755
N92-10759
GOMES, R. S. N92-10886
GOODFELLOW, KEITH N92-10046
GOODING, JAMES L. N92-10250
N92-10888
GOODSELL, AGA M. N92-10011
GOPALSAMI, N. N92-10097
GORADIA, SURESH H. N92-10006
GORDA, B. C. N92-10336
GORNEY, DAVID J. N92-10030
GOTTWALD, M. N92-10723
GOW, P. J. N92-10114
GRAEFFE, GUNNAR N92-10536
GRAHN, K. N92-10418
GRANER, G. N92-10444
GRANT, J. A. N92-10783
N92-10784
N92-10785
N92-10872
GRAPS, A. N92-10951
GRASER, U. N92-10723
GREBER, ISAAC N92-10012
GREELEY, RONALD N92-10749
N92-10750
N92-10752
N92-10763
N92-10767
N92-10788
N92-10790
N92-10800
N92-10801
N92-10802
N92-10808
N92-10840
N92-10847
N92-10909
GREEN, A. M. N92-10397
GREENBERG, R. N92-10808
N92-10897
GREENE, FRANCIS A. N92-10161
GREENE, J. B. N92-10100
GREENZWEIG, YUVAL N92-10936
N92-10937
GRIFFEE, J. W. N92-10040
GRIFFITHS, ROSS N92-10792
GRIMM, ROBERT E. N92-10733
N92-10743
N92-10745
GROENEWEG, JOHN F. N92-10601
GROHSMEYER, STEVEN P. N92-10015
GRONBECH-JENSEN, N. N92-10686
GUARD, CHARLES P. N92-10268
GUINNESS, EDWARD A. N92-10841
N92-10930
GUINNESS, EDWARD E. N92-10844
GUO, J. N92-10694
GURNETT, D. A. N92-10971
GURROLA, ERIC M. N92-10850
GUSTAFSON, B. N92-10886
GUTKNECHT, MARTIN H. N92-10311

H

HABERLE, R. M. N92-10803
N92-10804
HAGBERG, J. N92-10528
HAGEDORN, NORMAN H. N92-10222
HAGEN, C. R. N92-10630
HAGER, BRADFORD H. N92-10731
HAIKKILA, L. N92-10538
HAINES, ELDON L. N92-10819
HAINES, RICHARD F. N92-10034
N92-10282
HAKALA, P. J. N92-10546
HAKKARAINEN, T. N92-10489
N92-10490
N92-10491
N92-10523
N92-10530
HAKKINEN, H. N92-10483
HAKONEN, P. J. N92-10509
HALL, DAVID W. N92-10305
HALL, JOSH N92-10299
HALLIKAINEN, J. N92-10539
HALONEN, V. N92-10494
HAMADA, Y. N92-10649
HAMAGUCHI, S. N92-10663
HAMALAINEN, M. S. N92-10540
HAMALAINEN, RAUNO N92-10514
HAMEEN-ANTTILA, K. A. N92-10571
HAMERI, KAARLE N92-10525
N92-10526
HAMERNIK, ROGER P. N92-10611
HAMMAREN, E. N92-10410
N92-10441
HAMMETT, G. W. N92-10663
HAN, W. K. N92-10470
HANDEL, S. N92-10129
HANDSCHUH, ROBERT F. N92-10195
HANNINEN, J. N92-10572
HANNINEN, V. N92-10419
HANSEN, GARY B. N92-10821
HANSON, D. B. N92-10599
HANSSON, H. N92-10365
HAPKE, B. N92-10851
HARA, AKIO N92-10153
HARADA, HIROO N92-10298
HARDING, D. J. N92-10841
HARJES, H. C. N92-10152
HARMON, A. O. N92-10100
HARR, PATRICK A. N92-10271
HARRIS, CHRIS J. N92-10208
HARSH, JOHN R. N92-10281
HARTEN, AMI N92-10349
HARTMANN, WILLIAM K. N92-10860
HARTUNG, LIN CLARA N92-10165
HASTE, G. R. N92-10130
N92-10673
HATTULA, J. N92-10403
N92-10404
HAUKENES, LARRY O. N92-10175
HAUTANEN, JUKKA N92-10532
HAUTOJARVI, P. N92-10467
N92-10484
HAWKE, B. RAY N92-10795
N92-10796
N92-10797
N92-10809
N92-10810
N92-10962
HAXTON, W. C. N92-10967
N92-10968
HAYAKAWA, YUKIO N92-10056
HAYASHI, J. N. N92-10873
HAYRINEN, V. N92-10378
HAZELTINE, R. D. N92-10668
HEAD, JAMES W. N92-10815
N92-10822
N92-10957
HEALD, S. M. N92-10683
HEIKEN, GRANT N92-10797
HEIKKINEN, P. N92-10410
N92-10424
HEILMANN, A. N92-10527
HEINIG, N. F. N92-10697
HEINIO, J. N92-10481
N92-10482
HEKSTRA, GJERRIT P. N92-10231
HELFENSTEIN, PAUL N92-10834
N92-10836
HELISTO, P. N92-10512
HENDERSON, BRADLEY G. N92-10813
HENDRICKS, C. L. N92-10069
HENDRICKSON, B. N92-10315
HERBERT, K. N92-10206
HERGENROTHER, PAUL M. N92-10066
HERNBERG, ROLF G. N92-10378
N92-10379
N92-10380
N92-10381
N92-10459
N92-10460
HERREN, KENNETH A. N92-10639
HERREN, L. TANDY N92-10712
HERRICK, R. R. N92-10855
HEYMANN, G. N92-10529
HIDEKUMA, S. N92-10657
HIETANEN, IIRO N92-10412
N92-10414
N92-10415
N92-10416
HIETANIEMI, J. N92-10504
HIETARINTA, JARMO N92-10370
HIGGINS, CHRISTOPHER N92-10018

HILL, S. G. N92-10069
HILLBERRY, B. M. N92-10203
HILTUNEN, Y. N92-10545
HINGST, WARREN R. N92-10012
HINSON, DAVID P. N92-10960
HIROI, T. N92-10831
HIROKURA, S. N92-10649
HOF, D. E. N92-10218
HOGENBOOM, D. L. N92-10738
HOLCOMB, R. S. N92-10059
HOLLAND, SCOTT DOUGLAS N92-10007
HOLLBERG, MATTI R. N92-10438
HOLLENBACH, D. N92-10948
HOLMES, H. F. N92-10077
HOLMES, N. C. N92-10739
HOLMLUND, CHRISTER N92-10453
HOLOPAINEN, E. N92-10587
HOLSAPPLE, K. A. N92-10862
HOLTKAMP, D. B. N92-10040
N92-10218
N92-10260
HONKONEN, V. N92-10450
HOOD, C. C. N92-10129
HOOD, L. L. N92-10877
HOOPER, EDWIN BICKFORD N92-10047
HORIUCHI, RITOKU N92-10648
HORN, LINDA N92-10903
HORNEMAN, V.-M. N92-10433
HORTON, K. N92-10809
HORTON, W. N92-10663
HOSKING, F. M. N92-10082
N92-10083
HOUGHTON, F. K. N92-10296
HOVINEN, M. N92-10489
N92-10491
N92-10523
HOWARD, ALAN D. N92-10769
N92-10770
N92-10771
HOWE, J. E. N92-10615
HOWERTON, CLAYTON E. N92-10208
HOWINGTON-KRAUS, ANNIE E. N92-10914
N92-10920
N92-10921
HUANG, Z. N92-10705
N92-10877
HUBBARD, HARVEY H. N92-10598
HUBBELING, L. N92-10416
HUCKLE, THOMAS N92-10310
HUMMEL, JOHN R. N92-10219
HUNG, CHING-CHEH N92-10090
HUNTER, DAVID R. N92-10714
HUNTER, N. F. N92-10356
HUOMO, H. N92-10565
HUOVELIN, J. N92-10563
HURTAK, O. N92-10127
HUSSIEN, B. N92-10003
HUTTUNEN, JUHANI N92-10458
HUUSKONEN, A. N92-10560
HUYSE, M. N92-10411
HWANG, D. Q. N92-10622
HYLIN, E. C. N92-10181
HYNDMAN, D. A. N92-10084

I

IANELLI, G. S. N92-10010
IDA, K. N92-10647
N92-10649
N92-10657
IGNATOV, A. V. N92-10492
IIVONEN, A. N92-10417
IKONEN, ERKKI N92-10453
IMAI, K. N92-10493
IMMONEN, E. N92-10528
INGE, J. L. N92-10925
N92-10929
INGMAN, L. P. N92-10435
INNANEN, K. A. N92-10568
IRISOV, V. G. N92-10272
IRONS, J. R. N92-10841
ISBELL, NANCY K. N92-10756
N92-10928
ISHIGAKI, HIROSHI N92-10166
ISHIGURO, MISAKO N92-10298
ITOH, KIMITAKA N92-10646
N92-10657
ITOH, SANAE-I. N92-10646
N92-10657
IVERSEN, ARTHUR H. N92-10157
IVERSEN, J. D. N92-10801
N92-10802
IVLEV, B. I. N92-10500

J

JAAKKOLA, S. N92-10480
JAAKKOLA, T. N92-10578
JAASKELAINEN, T. N92-10447
N92-10450
N92-10456
N92-10539
JAECKEL, LOUIS A. N92-10291
JAFFE, D. T. N92-10615
JAFFE, S. M. N92-10379
N92-10460
JAKOSKY, BRUCE M. N92-10813
JAKUBKA, K. N92-10651
JALAS, P. N92-10418
JAMES, M. R. N92-10682
JAMNEJAD, VAHRAZ N92-10121
N92-10122
JAMSA, SAULI N92-10566
JANES, DANIEL M. N92-10742
JANSSEN, Y. H. L. N92-10966
JAROSEWICH, E. N92-10826
JARVILUOTO, M. N92-10541
JARVINEN, K. N92-10543
JARVIS, LOUIS N92-10158
JAUHO, P. P. N92-10402
N92-10411
JAYARAMAN, S. N92-10886
JEANLOZ, RAYMOND N92-10729
JELSKI, D. A. N92-10705
JELSKI, DANIEL A. N92-10425
JENA, P. N92-10508
JIANG, P. Z. N92-10699
JODHA, N. S. N92-10237
JOHANSSON, LEENA-SISKO N92-10520
JOHANSSON, M. N92-10533
JOHNSON, A. N92-10405
JOHNSON, G. N92-10174
JOHNSON, MARJORY J. N92-10038
JOHNSON, N. N92-10773
JOHNSON, NATASHA N92-10772
N92-10774
JOHNSON, R. BARRY N92-10639
JOHNSON, R. E. N92-10838
JOHNSON, T. V. N92-10837
JOHNSON, W. S. N92-10203
JOKINEN, A. N92-10402
N92-10411
JOKISAARI, JUKKA N92-10362
N92-10435
N92-10436
N92-10437
N92-10545
JONES, JOHN H. N92-10964
JOOSTEN, H. P. N92-10485
JORDAN, RAYMOND N92-10922
JOSEPH, R. J. N92-10218
JOSHI, YOGENDRA N92-10175
JOYCE, J. J. N92-10684
JUDKINS, J. G. N92-10149
JULIN, R. N92-10401
N92-10403
N92-10404
N92-10405
N92-10424
JUNTUNEN, M. N92-10418
JURGENS, R. F. N92-10848
JUUTINEN, S. N92-10401
N92-10403
N92-10404
N92-10405

K

KAASALAINEN, MIKKO K. J. N92-10566
KAEHKOENEN, O.-P. N92-10464
N92-10468
KAELLMAN, K.-M. N92-10401
KAEMAERAEINEN, V. N92-10563
KAERNAE, MARKKU N92-10451
KAHLE, A. B. N92-10842
KAIVOLA, M. N92-10454
N92-10455
KAJAVA, T. N92-10442
N92-10452
KALKKINNE, JUSSI N92-10526
KALLIO, A. N92-10499
KALPURI, K. S. N92-10258
KAMIJO, KENJIRO N92-10025
KAMMASH, T. N92-10660
KANEKO, O. N92-10647
KANERVA, P. N92-10294
KANG, H. C. N92-10463
KANGAS, JORMA N92-10552
N92-10553
N92-10557
KANGASMAKI, A. N92-10400
KANKAALA, K. N92-10469
KANKARE, J. N92-10544
KAPUSTA, J. N92-10384
KARADY, GEORGE G. N92-10674
KARCHMER, ALLEN N92-10607
KARGEL, JEFFREY S. N92-10737
N92-10738
N92-10772
N92-10773
N92-10774
N92-10775
KARHUNEN, M. N92-10480
KARIMAKI, V. N92-10388
N92-10389
N92-10390
N92-10391
N92-10392
KARL, R. R., JR. N92-10218
N92-10260
KARLEMO, T. N92-10504
KARPPINEN, M. N92-10504
KARTTUNEN, M. N92-10462
KARTTUNEN, S. N92-10461
KARY, DAVID M. N92-10896
N92-10898
KASKI, KIMMO N92-10374
N92-10462
N92-10481
N92-10482
N92-10485
KAST, B. A. N92-10324
KATHMAN, A. D. N92-10183
KATILA, T. N92-10504
N92-10512
KATTO, TERO N92-10535
KATUNIN, A. N92-10480
KATZ, L. A. N92-10242
KAUHANEN, K. N92-10569
KAUKASOINA, P. N92-10463
KAUKLER, WILLIAM F. N92-10080
KAULA, W. M. N92-10891
KAUPPINEN, JYRKI K. N92-10438
KAUTTO, E. N92-10464
KAWAHATA, K. N92-10647
KAWASHIMA, H. N92-10657
KAWASHIMA, NOBUKI N92-10189
KEEGAN, K. D. N92-10943
KEINONEN, J. N92-10400
KEINONEN, TUULA N92-10448
KELHA, V. N92-10565
KELLEHER, MATTHEW D. N92-10175
KELLER, J. M. N92-10787
KELLER, L. P. N92-10252
N92-10256
KENDALL, JOHN E. N92-10026
KERANEN, REINO N92-10394
KESKINEN, J. N92-10523
N92-10534
KETOLAINEN, P. N92-10513
KHALKIN, V. A. N92-10076
KHARE, B. N. N92-10958
KIEFFER, SUSAN WERNER N92-10740
KIENHOLZ, DAVID A. N92-10188
KILLEEN, J. N92-10669
KILPELAINEN, MARKKU N92-10532
KIM, A. N92-10205
KIM, J. M. N92-10373
KIM, J. Y. N92-10663
KIM, KWANG H. N92-10143
KING, D. B. N92-10061
KING, MERRILL K. N92-10108
N92-10109
KING, T. V. V. N92-10820
N92-10839
KINNUNEN, R. N92-10388
N92-10389
N92-10390
N92-10391
N92-10392
KIRBY, S. H. N92-10735
KIRILYUK, A. I. N92-10502
KIRK, R. L. N92-10736
KITAMURA, SHOJI N92-10056
KITOH, KENSHIN N92-10654
KIURU, A. N92-10544
KIVIMAKI, A. N92-10446
N92-10517
KIVINIITTY, K. N92-10545
KLEINMAN, RALPH E. N92-10144
KNIGHT, CHRISTINE N92-10772
N92-10773
KOBAYASHI, N. N92-10104
KOIVISTOINEN, I. N92-10410
KOIVUSAARI, M. N92-10432
N92-10433

KOKKO, K. N92-10488
KOLVOORD, R. A. N92-10897
KOMAR, PAUL D. N92-10938
KOMATSU, G. N92-10777
KONDO, Y. N92-10476
KOONS, HARRY C. N92-10030
KOPNIN, N. B. N92-10475
N92-10476
N92-10479
N92-10500
N92-10501
KORHONEN, J. S. N92-10476
KORJA, T. N92-10551
KORN, G. N92-10092
KORTEOJA, M. N92-10523
KOSKELA, H. N92-10537
KOSMO, JOSEPH J. N92-10091
KOSTERLITZ, J. M. N92-10373
KOSTROUN, V. O. N92-10616
KOTALIK, PAVEL N92-10679
KOTHE, D. B. N92-10168
KOTILAINEN, J. N92-10578
KOZAK, R. C. N92-10928
KRANING, KENNETH K., II N92-10288
KRAUSE, R. N92-10467
KREINES, N. M. N92-10502
KREMSER, G. N92-10556
N92-10558
N92-10567
KRING, C. T. N92-10129
KRISHNAMAGARU, RAMESH N92-10274
KRITSCHA, W. N92-10699
N92-10702
KRUEGER, UTE N92-10210
N92-10214
KRUKOWSKI, S. N92-10676
KRUSIUS, M. N92-10476
KRYSKA, L. N92-10651
KUCK, DAVID J. N92-10304
KUDINOV, V. I. N92-10502
KUHFUSS, T. C. N92-10338
KUITTINEN, M. N92-10456
KULMALA, MARKKU N92-10525
N92-10526
KUMAZAWA, R. N92-10649
KUMPULAINEN, J. N92-10403
N92-10404
N92-10424
KUNZ, P. F. N92-10323
KURONEN, A. N92-10400
KURTH, W. S. N92-10971
KURTOGLU, LEVENT N92-10156
KUSHNICK, ANNE C. N92-10196
KUSHNICK, PETER W. N92-10182
KUSSOY, MARVIN N92-10004
KUUS, H. N92-10673
KUUSISTO, E. N92-10493
KUZMIN, A. V. N92-10272
KVAERNA, T. N92-10265
KWACK, EUG Y. N92-10609
KWOK, W. K. N92-10692
KYRO, ESKO N92-10547
KYROLA, E. N92-10570
KYYNARAINEN, J. M. N92-10474

L

LAAKSO, MIKKO N92-10415
N92-10418
LAAKSONEN, ARI N92-10525
N92-10526
LAASONEN, K. N92-10465
N92-10473
N92-10496
LADERACH, G. E. N92-10152
LAHDERANTA, E. N92-10502
LAHTI, KATARIINA N92-10536
LAHTINEN, J. N92-10484
LAHTINEN, M. N92-10376
LAIHO, R. N92-10490
N92-10502
N92-10538
LAINE, E. N92-10522
LAINELA, MARKKU N92-10564
LALLEMENT, R. N92-10570
LAM, D. J. N92-10694
N92-10698
LAM, H. N92-10104
LAM, N. Q. N92-10682
LAMMASNIEMI, J. N92-10523
N92-10531
LAMPINEN, A. N92-10376
N92-10401
N92-10403
N92-10404
LAMPINEN, J. N92-10419
LAMPINEN, M. J. N92-10445
LANCASTER, N. N92-10801
N92-10802
N92-10840
N92-10847
LANGEVIN, YVES N92-10815
N92-10822
LANSIMIES, E. N92-10543
LANTTO, V. N92-10492
N92-10498
N92-10527
LAPHAM, E. F. N92-10704
LARBALESTIER, D. C. N92-10697
LARJO, J. N92-10379
N92-10460
LARSEN, R. P. N92-10098
LAUB, R. J. N92-10075
LAUER, H. V., JR. N92-10251
N92-10254
N92-10255
LAURANTO, H. N92-10442
N92-10452
LAWRENCE, J. M. N92-10684
LAZARIDIS, MIHALIS N92-10525
LE, T. H. N92-10162
N92-10163
N92-10164
LEBOFSKY, LARRY A. N92-10830
LEE, PASCAL N92-10836
LEE, S. L. N92-10691
LEE, S. W. N92-10956
LEEHEY, P. N92-10206
LEEPER, ARTHUR J. N92-10140
LEHMAN, D. R. N92-10628
LEINER, BARRY M. N92-10031
N92-10032
N92-10033
LEINO, M. N92-10402
N92-10411
N92-10424
LEINONEN, KARI N92-10414
N92-10416
N92-10418
LEIRO, J. A. N92-10503
LEKSONO, M. N92-10695
LEMON, K. M. N92-10243
LENGELLE, GUY N92-10107
LENSTRA, D. N92-10485
LEOVY, CONWAY B. N92-10821
LEPISTO, A. N92-10582
LEPPAVUORI, S. N92-10492
N92-10505
N92-10506
N92-10528
LERCH, F. J. N92-10760
LEUNG, TSAN-CHUEN N92-10690
LEUPOLD, HERBERT A. N92-10597
LEUTTGEN, A. L. N92-10296
LEUTWYLER, H. N92-10396
LEVASALMI, MAARIT N92-10362
N92-10427
LEVIN, E. N92-10306
LEVIN, F. S. N92-10634
LEVISON, H. F. N92-10883
LEVITON, DOUGLAS B. N92-10186
LEVOSKA, J. N92-10505
N92-10506
LEVY, EUGENE H. N92-10939
LEVY, LIONEL N92-10004
LEVY, SAUL N92-10299
LEWIS, AARON N92-10278
LEWIS, J. S. N92-10738
LEWIS, T. G. N92-10674
LEZNOFF, C. C. N92-10104
LI, CHOU H. N92-10145
LI, W. Q. N92-10595
LI, X. N92-10643
LI, XUELIANG N92-10341
LICHARD, P. N92-10384
LILJA, J. N92-10493
LILLEY, G. M. N92-10602
LILWALL, R. C. N92-10247
LIN, C. D. N92-10617
LIN, D. N92-10902
LIN, D. L. N92-10643
LIN, TRUE-LON N92-10146
LINDBERG, D. N92-10663
LINDEN, J. N92-10504
LINDGREN, JUKKA N92-10412
N92-10414
N92-10416
LINDROOS, M. N92-10463
LINDSTROM, F. T. N92-10346
LINSON, LEWIS M. N92-10264
LIOU, M.-S. N92-10345
LIPAS, P. O. N92-10406
LIPPMAA, M. N92-10504
N92-10512
LISSAUER, JACK J. N92-10896
N92-10898
N92-10899
N92-10901
N92-10936
N92-10937
LITOVCHENKO, K. TS. N92-10272
LITVIN, FAYDOR L. N92-10195
LIU, J. Z. N92-10692
LIU, Y. N92-10471
LIU, YONG N92-10550
LIU, Z. D. N92-10643
LIUKKONEN, ESKO N92-10420
LOBERG, K. N92-10376
LOCKHEAD, GREGORY R. N92-10612
LOENNROTH, T. N92-10401
N92-10404
LOHIKOSKI, R. N92-10371
LOMDAHL, P. S. N92-10686
LONDON, GILBERT J. N92-10072
LONDON, R. A. N92-10190
LONGDON, NORMAN N92-10039
LONGI, JOHN N92-10961
LONGTIN, A. N92-10357
LONGTIN, DAVID R. N92-10219
LOO, P. I. N92-10113
LOSOI, TUOMO N92-10520
LOUNILA, JUHANI N92-10466
LUBECK, O. M. N92-10298
LUCCHITTA, BAERBEL K. N92-10756
N92-10758
LUCEY, P. G. N92-10809
N92-10810
LUCY, P. G. N92-10951
LUDVIGSEN, HANNE N92-10453
LUETHI, T. N92-10097
LUKASHEVICH, I. I. N92-10480
N92-10510
LUKKARI, J. N92-10572
LUKKARINEN, A. N92-10482
LUMME, KARI N92-10548
N92-10566
LUMME, M. N92-10562
LUND, J. N92-10279
LUND, P. D. N92-10584
LUNINE, JONATHAN I. N92-10807
LUPPOV, V. G. N92-10423
LYNCH, GARY N92-10285
LYNN, K. G. N92-10515

M

MAALAMPI, J. N92-10398
MACCONOCHIE, IAN O. N92-10035
MACGOWAN, B. J. N92-10190
MAEKELA, JYRKI N92-10526
MAEKINEN, S. N92-10464
N92-10468
MAGLIERI, DOMENIC J. N92-10608
MAGLIOZZI, B. N92-10599
MAHAJAN, S. M. N92-10595
MAHAN, J. ROBERT N92-10607
MAHONEN, M. N92-10562
MAHONEN, P. N92-10364
N92-10372
MAISH, A. B. N92-10224
MAKELA, JYRKI N92-10525
MALIN, M. C. N92-10940
MALM, S. N92-10402
MALTHUS, T. J. N92-10215
MALTSEVA, N. F. N92-10557
MALVAR, L. J. N92-10207
MALY, JOSEPH R. N92-10188
MANN, G. A. N92-10152
MANNFORS, B. N92-10443
MANNGAARD, P. N92-10401
MANNINEN, A. J. N92-10474
MANNINEN, JYRKI N92-10554
N92-10555
MANNINEN, M. N92-10441
N92-10464
N92-10468
N92-10483
N92-10508
MANSHADI, FARZIN N92-10122
MANSIKKA-AHO, J. N92-10441
MANSURE, A. J. N92-10132
MANTERE, K. N92-10447
MANTYKENTTA, A. N92-10428
MARCH-LEUBA, J. N92-10355
MARCHELLO, JOSEPH M. N92-10070
MARCIALIS, ROBERT L. N92-10887

MARSHALL, J. R. N92-10800
MARTIN, A. D. N92-10614
MARTIN, G. N92-10673
MARTIN, T. Z. N92-10814
MARTIN, W. R. N92-10619
MARTINEZ-SANCHEZ, MANUEL N92-10050
MARTINEZ, L. N92-10152
MARTINEZ, R. J. N92-10218
MASSOUDI, M. N92-10174
MASTIN, C. WAYNE N92-10170
MASTNY, G. F. N92-10675
MATHUR, M. P. N92-10174
MATSUDA, T. N92-10657
MATSUNAMI, NORIAKI N92-10654
MAXON, S. N92-10190
MAXWELL, TED A. N92-10781
N92-10907
MAYANAGI, MITSUYOSHI N92-10028
MAYBERRY, M. J. N92-10665
MAZDIYASNI, K. S. N92-10154
MAZIASZ, P. J. N92-10081
MCCARTHY, DEREK N92-10836
MCCLENAHAN, C. R. N92-10152
MCCOLLOM, THOMAS M. N92-10813
MCCOMAS, D. J. N92-10970
MCDONOUGH, J. M. N92-10181
MCEWEN, ALFRED S. N92-10761
N92-10924
N92-10927
MCFADDEN, LUCY-ANN N92-10941
MCGILL, GEORGE E. N92-10741
N92-10762
N92-10911
MCGUIRE, JAMES P., JR. N92-10638
MCGUIRE, MICHAEL S. N92-10140
MCKAY, DAVID S. N92-10797
N92-10962
MCKAY, GORDON N92-10246
MCKAY, TIM D. N92-10287
MCKEAGUE, IAN W. N92-10350
MCKENNEY, M. S. N92-10243
MEGE, P. N92-10162
N92-10163
N92-10164
MEIER, R. N92-10454
MEIJER, PAUL H. E. N92-10680
MEINANDER, N. N92-10439
MELISSINOS, A. C. N92-10630
MELOSH, H. J. N92-10861
N92-10863
N92-10864
N92-10865
N92-10866
N92-10867
N92-10869
N92-10870
MELTON, JOHN E. N92-10011
MENDEZ, R. N92-10298
MENTER, F. N92-10004
MERIKOSKI, J. N92-10483
N92-10508
MERKLE, CHARLES L. N92-10179
MERKLE, K. L. N92-10697
MERTIG, M. N92-10423
MESMER, R. E. N92-10077
MESSERSCHMID, ERNST N92-10053
MESSING, GARY L. N92-10102
METZGER, ALBERT E. N92-10819
MICCI, MICHAEL M. N92-10179
MIKKOLA, SEPPO N92-10568
MILANOV, M. N92-10076
MILITSKY, YU. A. N92-10272
MILLER, FRANK W. N92-10036
MINEHART, R. C. N92-10623
MING, D. W. N92-10251
N92-10253
MINNI, E. N92-10537
MITARAI, S. N92-10405
MITCHELL, A. C. N92-10739
MITCHELL, RANDY C. N92-10036
MIURA, Y. N92-10657
MIYAKE, K. N92-10299
MIYAZAKI, KATSUHIRO N92-10056
MIZSEI, J. N92-10498
MJOLSNESS, R. C. N92-10168
MOCHIZUKI, MUNEKAZU N92-10166
MOE, H. J. N92-10635
MOELLER, C. N92-10671
MOFFATT, DOUGLAS J. N92-10438
MOLLEY, P. A. N92-10151
MOOK, H. A. N92-10691
MOORE, D. S. N92-10218
MOORE, H. J. N92-10786
N92-10787
N92-10791
N92-10848
MOORE, J. P. N92-10058
MORCHOISNE, Y. N92-10163
N92-10164
MORGAN, D. J. N92-10641
MORGAN, H. F. N92-10913
N92-10925
MORGAN, W. W. N92-10338
MORI, M. N92-10657
MORIMATSU, O. N92-10397
MORITA, K. N92-10417
MOROZ, L. V. N92-10829
MORRIS, R. V. N92-10249
N92-10254
N92-10255
MORRISON, P. J. N92-10173
MORRISON, R. E. N92-10134
N92-10135
MORSE, E. N92-10658
MOSELEY, WARREN N92-10301
MOSHER, J. A. N92-10837
MOSKOVITZ, CARY N92-10021
MOTAMEDI, MASOUD N92-10118
N92-10119
N92-10120
MOUGINIS-MARK, P. J. N92-10793
N92-10873
MOUROU, GERARD A. N92-10142
MUELLER, B. N92-10837
MUELLER, D. N92-10403
N92-10404
MUELLER, S. N92-10745
MUENSTER, O. N92-10436
MUINONEN, KARRI O. N92-10566
MUKAI, J. N92-10405
MUNK, J. N92-10593
MURCHIE, SCOTT L. N92-10822
MURDOCCA, M. N92-10299
MURPHY, D. W. N92-10199
MURSULA, K. N92-10398
N92-10552
N92-10556
N92-10557
N92-10565
MURTONIEMI, T. N92-10505
N92-10506
MURTY, V. S. N92-10223
MUSTARD, JOHN F. N92-10815
N92-10822
MYERS, ROGER M. N92-10048
MYHILL, E. M. N92-10891

N

NACHTIGAL, NOEL M. N92-10311
N92-10312
NADARAJAH, ARUNAN N92-10112
NADUTOV, V. M. N92-10472
NAGIB, HASSAN M. N92-10180
NAIK, NAOMI H. N92-10348
NAKAJIMA, N. N92-10655
NAMIKI, NORIYUKI N92-10732
NAPPI, J. N92-10523
NASH, DOUGLAS B. N92-10812
NATESAN, K. N92-10086
NEKRASOV, A. K. N92-10552
N92-10557
NELLIS, W. J. N92-10739
NELSON, DENNIS O. N92-10963
NELSON, L. S. N92-10084
NEREM, R. S. N92-10760
NETA, TAMAR N92-10271
NEWELL, O. J. N92-10019
NICHOLSON, P. D. N92-10886
NIELSEN, D. N92-10670
NIELSEN, D. E., JR. N92-10325
NIELSEN, O. V. N92-10147
NIEMAN, G. W. N92-10085
NIEMELA, R. N92-10537
NIEMI, H. N92-10497
NIEMINEN, A. N92-10542
N92-10562
NIEMINEN, J. A. N92-10462
NIEMINEN, R. M. N92-10465
N92-10473
N92-10487
N92-10496
NIEMINEN, V. N92-10422
NIETO, M. M. N92-10726
NIININEN, H. N92-10586
NIINISTO, L. N92-10504
NIITTYLAHTI, JARKKO N92-10374
NILSSON, K. N92-10578
NISHIKAWA, KYOJI N92-10645
NOPONEN, EERO N92-10457
NORRIS, THEODORE B. N92-10142
NORTH, M. H. N92-10675
NORTON, J. R. N92-10065
NOTEBORN, H. J. M. F. N92-10485
NOYES, T. A. N92-10019
NUMMILA, K. K. N92-10509
NYBERG, J. N92-10404
NYGREN, KAARLO N92-10451
N92-10514
NYGREN, T. N92-10560
NYHOLM, K. N92-10454
N92-10455
NYHOLM, R. N92-10446
NYQUIST, LAURENCE E. N92-10965

O

OBERACKER, V. E. N92-10624
OBRIEN, KEVIN M. N92-10287
OBRIEN, T. C. N92-10848
OGAWA, Y. N92-10647
OHARU, NOBUAKI N92-10640
OIKARINEN, KARI N92-10437
OIKARINEN, L. N92-10455
OJA, A. S. N92-10507
OJALA, K. T. N92-10445
OKABE, YUSHIROU N92-10656
OKAMOTO, M. N92-10655
OKEEFE, J. D. N92-10933
OKSANEN, EERO N92-10521
OKUBO, S. N92-10630
OLKKONEN, H. N92-10375
N92-10382
OLLONQVIST, T. N92-10516
OLSEN, S. L. N92-10630
OLSON, PETER N92-10942
ONEAL, J. B., JR. N92-10642
ORAVA, R. N92-10393
N92-10412
N92-10416
ORENBERG, J. B. N92-10950
ORF, M. A. N92-10100
ORTH, C. J. N92-10875
OSTERBERG, KENNETH N92-10395
OTOOLE, JAMES W., JR. N92-10716
OTTO, S. R. N92-10171
OUAZZANI, JALIL N92-10112
N92-10676
OVERMAN, ANDREA L. N92-10302
OYAMA, K.-I. N92-10258
N92-10259

P

PAATSAMA, JUHA N92-10451
PADUA, DAVID N92-10304
PAEIVIKE, H. N92-10563
PAEZ, T. L. N92-10204
PAFFETT, M. T. N92-10095
PAGUIO, S. N92-10154
PAIGE, D. A. N92-10943
PAISLEY, E. C. I. N92-10847
PAKKANEN, A. N92-10403
PALMO, K. N92-10443
PANTANO, CARLO G. N92-10102
PAPPALARDO, ROBERT N92-10763
N92-10767
PARK, J. H. N92-10086
PARKKINEN, J. N92-10447
N92-10450
N92-10539
PARMAR, DEVENDRA S. N92-10677
PARMENTIER, E. M. N92-10944
PARMLEY, V. C. N92-10279
PARMONEN, J. N92-10402
PARMONEN, J. M. N92-10411
PARTS, U. N92-10476
PASO, R. N92-10431
PASSI, RANJIT M. N92-10274
PATEL, G. B. N92-10760
PATOMAKI, L. N92-10541
N92-10542
N92-10543
PATON, J. N92-10397
PATTERSON, JAMES H., JR. N92-10611
PATTIKANGAS, T. N92-10461
PAUL, D. M. N92-10691
PEALE, S. J. N92-10945
N92-10946
N92-10947
PEARSON, ALLAN E. N92-10347
PEDERSON, S. P. N92-10358
PEIPONEN, K.-E. N92-10363
PEKKALA, K. N92-10444
PEKKARINEN, J. N92-10537

PEKOLA, J. P. N92-10474
PELLINIEMI, L. J. N92-10538
PELTONEN, J. N92-10562
N92-10575
PELTONIEMI, JOUNI I. N92-10566
PELTONIEMI, JUHA T. N92-10399
PENN, K. J. N92-10152
PENNANEN, J. N92-10393
PENTTILA, H. N92-10402
N92-10411
PEPIN, R. N92-10932
PEREZ-MERCADER, J. N92-10726
PESSA, M. N92-10489
N92-10490
N92-10493
N92-10523
N92-10529
N92-10530
PETERS, S. W. M. N92-10215
PETERSEN, J. R. N92-10147
PETERSON, C. A. N92-10809
N92-10810
PETROY, S. B. N92-10840
N92-10842
PETRZILKA, V. N92-10650
N92-10653
PETTY, C. C. N92-10665
PHAT, VU NGOC N92-10342
PHILLIPS, J. L. N92-10970
PHILLIPS, M. N92-10206
PHILLIPS, P. T. N92-10338
PHILLIPS, ROGER J. N92-10733
N92-10743
N92-10745
N92-10854
N92-10855
PIETARINEN, E. N92-10388
N92-10389
N92-10390
N92-10391
N92-10392
PIETARINEN, KIMMO N92-10534
N92-10535
PIETERS, CARLE M. N92-10794
N92-10808
N92-10811
N92-10815
N92-10816
N92-10818
N92-10822
N92-10827
N92-10828
N92-10829
N92-10831
N92-10833
PIETIKAINEN, J. N92-10471
PIETILA, L.-O. N92-10443
PIETILAINEN, P. N92-10494
N92-10495
PIETSCH, W. N92-10723
PIIPARINEN, M. N92-10403
PIKKARAINEN, T. N92-10552
N92-10557
PILIPENKO, Y. K. N92-10423
PIMIA, M. N92-10388
N92-10389
N92-10390
N92-10391
N92-10392
PIMPERL, M. M. N92-10249
PINNADUWAGE, L. A. N92-10621
PINSKER, R. I. N92-10665
PIRTTIMAKI, J. N92-10522
PITKANEN, M. N92-10364
PIVIROTTO, THOMAS N92-10046
PLAUT, J. J. N92-10840
PLESCIA, J. B. N92-10753
N92-10755
N92-10757
N92-10879
PLOTKIN, KENNETH J. N92-10608
POLANSKY, G. F. N92-10060
POLK, JAMES N92-10046
POLLACK, J. B. N92-10948
N92-10950
N92-10951
PONNAPPAN, R. N92-10176
N92-10177
POOLE, EUGENE L. N92-10302
PORCO, CAROLYN C. N92-10949
PORJESZ, T. N92-10528
PORKOLAB, M. N92-10665
PORTER, TRACY K. N92-10752
N92-10790
PORTNEY, PAUL R. N92-10233
POSTAWKO, S. E. N92-10805
POTENZIANI, ERNEST, II N92-10597
POVINELLI, L. A. N92-10345
PRATER, R. N92-10671
PRATT, STEPHEN F. N92-10816
N92-10823
PRECHTEL, NICOLAS N92-10210
PRECHTEL, NIKOLAS N92-10211
N92-10212
PREINHAELTER, J. N92-10127
PRICE, KATHERINE H. N92-10908
N92-10909
PRIEDHORSKY, W. C. N92-10040
PRIMDAHL, F. N92-10147
PROBER, DANIEL E. N92-10706
PROUDFOOT, J. N92-10641
PUCKETT, E. G. N92-10169
PULICANI, J. P. N92-10676
PULKKINEN, O. N92-10426
PUNKKA, V. N92-10372
PUNKKINEN, MATTI N92-10510
N92-10511
PUSKA, M. J. N92-10487

Q

QUICK, C. R. N92-10218
N92-10260
QUINTANA, L. R. N92-10875

R

RAERINNE, P. N92-10513
RAEV, M. D. N92-10272
RAGNARSSON, I. N92-10405
RAHMAT-SAMII, YAHYA N92-10122
RAITALA, J. N92-10569
RAITTINEN, HARRI N92-10374
RAIZER, V. YU. N92-10272
RAJAGOPAL, K. R. N92-10174
RAJALA, R. N92-10522
RAJEEV, S. G. N92-10630
RAKENNUS, K. N92-10489
N92-10490
N92-10491
N92-10523
N92-10530
N92-10531
RAM, PRASAD N92-10715
RAMALINGAM, MYSORE L. N92-10178
RAMOS, S. N92-10678
RAMSHAW, J. D. N92-10672
RANDALL, CORA E. N92-10813
RANTA, H. N92-10561
RANTALA, TAPIO T. N92-10425
N92-10466
RASINKANGAS, R. N92-10558
RASMUSSEN, K. R. N92-10801
N92-10802
RATHKOPF, J. A. N92-10619
RATNER, JEREMIAH M. N92-10303
RAUMA, J. N92-10376
RAY, S. N92-10325
RAZEGHI, M. N92-10486
REDLICH, K. N92-10385
REED, K. W. N92-10152
REEVES, G. D. N92-10969
REHN, L. E. N92-10682
REIMANN, T. N92-10076
REINMANN, J. J. N92-10002
REISENTHEL, PATRICK H. N92-10180
REISSNER, M. N92-10702
REMSEN, D. N92-10671
REMUND, B. L. N92-10131
N92-10136
REVELLE, ROGER R. N92-10239
RICE, EDWARD J. N92-10601
RICE, JAMES W., JR. N92-10776
RICHARDSON, GIL N92-10217
RICKER, GEORGE N92-10184
RICKS, WENDELL R. N92-10017
RINGDAL, F. N92-10265
RINTA-NIKKOLA, M. N92-10421
RIPKA, P. N92-10147
RITCHIE, J. L. N92-10632
ROBERTS, PAUL W. N92-10185
ROBERTS, R. G. N92-10614
ROBINSON, ALLAN R. N92-10246
ROBINSON, M. S. N92-10793
ROBINSON, S. H. N92-10134
N92-10135
ROCHOWIAK, DANIEL N92-10332
RODRIGUEZ, J. G. N92-10193
ROESCH, F. N92-10076
ROETTGER, J. N92-10368
ROGERS, DAVID N92-10292
ROGERS, PATRICIA G. N92-10916
N92-10918
ROMANA, L. N92-10678
ROMEO, ALESSANDRO B. N92-10576
RONKAINEN, HANNU N92-10414
N92-10416
RONNQVIST, C. N92-10412
ROSE, E. A. N92-10191
ROSENBERG, NORMAN J. N92-10228
N92-10229
N92-10243
ROSENBERGER, FRANZ N92-10112
N92-10676
ROTTO, SUSAN L. N92-10782
ROUSH, T. L. N92-10948
N92-10950
N92-10951
ROUTTI, JORMA N92-10581
ROWAN, L. N92-10932
ROWSEY, ROBERT R. N92-10041
RUDISILL, MARIANNE N92-10287
RUDOLPH, DIETER K. N92-10268
RUGGIERO, R. M. N92-10183
RUOKOLAINEN, J. N92-10370
RUSSELL, J. F. N92-10915
RUSSO, A. J. N92-10666
RUUSKANEN, A. N92-10585
RUUSKANEN, P. V. N92-10383
RYAN, EILEEN V. N92-10861
N92-10863
N92-10884

S

SAAD, YOUCEF N92-10309
N92-10343
SAARELA, M. N92-10477
SAARINEN, JYRKI N92-10458
SAARINEN, K. N92-10467
SACKS, JOANNE N92-10283
SAFONOV, A. N92-10480
SAGAN, CARL N92-10958
SAINIO, M. E. N92-10396
SAINTOLA, R. N92-10417
SAIRANEN, O.-P. N92-10517
N92-10518
N92-10519
SAISA, L. N92-10516
SALAZAR, GEORGE A. N92-10331
SALIN, ARTO N92-10458
SALINAS, J. N92-10131
SALISBURY, J. W. N92-10826
SALMINEN, H. N92-10402
SALMINEN, OLLI N92-10448
SALO, H. N92-10572
N92-10573
N92-10579
SALOKATVE, A. N92-10523
SALOMAA, M. M. N92-10475
N92-10478
N92-10479
N92-10500
SALOMAA, RAINER N92-10442
N92-10452
N92-10461
N92-10583
SALTZMAN, J. S. N92-10169
SAMEH, AHMED N92-10304
SANDLER, S. I. N92-10093
SANUKI, H. N92-10647
SAOUTIC, B. N92-10673
SARMIENTO, J. L. N92-10273
SASAO, MAMIKO N92-10656
SASHIDA, KIYOSHI N92-10640
SATHE, SANJEEV B. N92-10175
SATO, HIDEO N92-10140
SATO, TETSUYA N92-10648
SATZ, HELMUT N92-10367
SAUERZOPF, F. M. N92-10699
N92-10700
N92-10702
SAUNDERS, R. S. N92-10801
N92-10802
SAVANDER, PEKKA N92-10448
SAVOLAINEN, I. N92-10533
SAVOLAINEN, S. N92-10544
SCHABER, G. G. N92-10852
N92-10853
SCHMID, C. W. N92-10276
SCHMID, K. W. N92-10410
SCHMIDT, ROBERT M. N92-10859
SCHMITZ, F. H. N92-10600
SCHMITZ, N. N92-10590
SCHMITZ, P. J. N92-10463

SCHMUECKER, H. N92-10592
SCHNEID, B. N92-10788
SCHNEID, BYRON D. N92-10750
SCHNEIDER, STEPHEN H. N92-10229
SCHNEIDER, STEVEN J. N92-10054
SCHOENBERG, KURT N92-10049
SCHREIBER, G. M. N92-10667
SCHUBERT, GERALD N92-10742
SCHULMAN, TOM N92-10415
SCHULTZ, P. H. N92-10783
N92-10784
N92-10785
N92-10856
N92-10857
N92-10858
N92-10872
N92-10876
N92-10878
SCHULTZ, RICHARD A. N92-10754
SCHURAYTZ, B. C. N92-10253
SCHUTT, J. A. N92-10096
SCHWAB, A. N92-10515
SCOTT, DAVID H. N92-10751
N92-10776
N92-10912
SCOTT, S. D. N92-10663
SEDJO, ROGER A. N92-10234
SEIBERT, D. N92-10384
SEITSONEN, A. P. N92-10487
SEKI, T. N92-10649
SEN, A. N92-10595
SERDYUK, V. V. N92-10492
SERGATSKOV, D. A. N92-10476
SEVIER, L. N92-10671
SEYHAN, E. N92-10215
SEYMOUR, P. N92-10104
SHAKKOTTAI, PARTHASARATHY N92-10609
SHALKAUSER, MARY JO W. N92-10128
SHANE, DARRELL N92-10715
SHARMA, PRAMOD K. N92-10073
SHARP, EDWARD J. N92-10194
SHARPTON, VIRGIL L. N92-10253
N92-10742
SHEAHAN, J. J. N92-10100
SHEFFIELD, CHARLES N92-10217
SHELFER, T. D. N92-10249
SHEPARD, MICHAEL K. N92-10840
N92-10843
SHEPARD, T. D. N92-10673
SHEPHERD, R. L. N92-10187
SHETTLE, ERIC P. N92-10219
SHEVTSOV, V. A. N92-10510
SHIGEMASA, E. N92-10429
SHIH, C.-Y. N92-10965
SHKURATOV, YU. G. N92-10833
SHLYAPNIKOV, G. N92-10480
SHOEMAKER, C. S. N92-10875
N92-10879
N92-10880
SHOEMAKER, E. M. N92-10875
N92-10879
N92-10880
N92-10883
SHOKAIR, I. R. N92-10636
SHOWALTER, MARK R. N92-10903
SHUGART, HERMAN H. N92-10235
SHURTER, R. P. N92-10191
SIEGEL, R. W. N92-10085
N92-10696
SILCOX, RICHARD J. N92-10202
SILLANPAA, R. N92-10522
SILVENNOINEN, RAIMO N92-10451
N92-10514
SIMMONS, M. L. N92-10297
N92-10298
SIMONELLI, D. N92-10948
SIMONEN, T. C. N92-10661
N92-10662
SIMONS, MARK N92-10731
SIMPSON, DEBRA N92-10954
SIMPSON, R. A. N92-10849
SINGER, DONALD J. N92-10140
SINGER, ROBERT B. N92-10799
N92-10817
SINGH, JAG J. N92-10677
SIPILA, S. N92-10461
SIRKIS, MURRAY D. N92-10674
SLADE, M. A. N92-10848
SLATTERY, P. N92-10630
SLAVNEY, SUSAN H. N92-10844
N92-10930
SLAWSON, MICHAEL R. N92-10642
SMALLWOOD, D. O. N92-10204
SMIRNOV, A. V. N92-10272
SMITH, BARRY T. N92-10071
SMITH, D. N92-10299
SMITH, D. E. N92-10760
SMITH, DONALD L. N92-10067
SMITH, J. R. N92-10636
SMITH, JOHN M. N92-10221
SMITH, MILTON O. N92-10931
SMITH, ROBERT E., JR. N92-10161
SMITH, STEVEN N92-10227
SMITH, STEVEN A. N92-10197
SMITHER, C. N92-10933
SMREKAR, SUZANNE E. N92-10744
SNIDER, R. N92-10664
SNOHA, JOHN J. N92-10070
SODERBLOM, L. A. N92-10926
SOFRIN, THOMAS G. N92-10601
SOININEN, E. N92-10515
SOININEN, P. I. N92-10479
SOLOMON, ALLEN M. N92-10234
SOLOMON, SEAN C. N92-10731
N92-10732
N92-10741
N92-10744
SORAAS, F. N92-10558
SPARE, BETH A. N92-10919
SPELCE, T. N92-10326
SPERLING, GEORGE N92-10286
SPUDIS, P. D. N92-10809
N92-10810
SQUYRES, STEVEN W. N92-10741
N92-10742
N92-10762
N92-10911
SRICHANDER, RAMASWAMY N92-10201
SRIDHAR, B. N92-10003
SRIVATSA, C. R. N92-10136
ST.CLAIR, ANNE K. N92-10105
ST.CLAIR, TERRY L. N92-10105
STAALNACKE, J. N92-10386
STACEY, G. J. N92-10615
STACY, NICHOLAS J. S. N92-10845
STALLINGS, ROBERT L., JR. N92-10005
STANKEVICH, D. G. N92-10833
STANLEY, J. T. N92-10685
STEENEKEN, H. J. M. N92-10115
STEIN, THOMAS C. N92-10844
STEINER, W. N92-10702
STEINETZ, BRUCE M. N92-10064
STEINLE, H. N92-10723
STENBERG, JARI N92-10380
N92-10381
STEPHENS, J. J. N92-10082
STEVENSON, DAVID J. N92-10952
STEWART, GLEN R. N92-10899
N92-10934
STEWART, R. E. N92-10187
STIERLIN, U. N92-10591
STIRLING, W. J. N92-10614
STOCKMAN, MARK I. N92-10425
STODOLSKY, L. N92-10589
STOECKEL, J. N92-10651
STOFAN, ELLEN R. N92-10742
STOLOVY, SUSAN N92-10834
STRATHMANN, FRANK W. N92-10210
N92-10211
STRAUB, DARCY W. N92-10806
STRINGFELLOW, G. B. N92-10703
STROM, ROBERT G. N92-10772
N92-10774
STROM, ROGER G. N92-10773
N92-10775
N92-10777
STRONG, D. S. N92-10151
STRUVE, K. W. N92-10636
STUBBINS, J. F. N92-10682
STUCK, B. E. N92-10279
SUCHARSKI, ROBERT N92-10913
SUDARSHAN, E. C. G. N92-10632
SUE, MILES K. N92-10116
N92-10117
SUHONEN, E. N92-10385
N92-10386
SUHONEN, J. N92-10407
N92-10408
N92-10409
SULLIVAN, JOHN D. N92-10026
SUMMANEN, T. N92-10570
SUNDIUS, T. N92-10369
SUNKA, P. N92-10652
SUORSA, R. N92-10003
SUSSKIND, L. N92-10727
SUZUKI, N. N92-10657
SVENSSON, S. N92-10446
SWEATT, W. C. N92-10151
SWINDEMAN, R. W. N92-10081

T

TAALAS, P. N92-10547
TABISZ, G. C. N92-10439
TAHTINEN, M. N92-10533
TAJIMA, YOSHIMASA N92-10025
TAKA, TAPANI N92-10524
TAKASE, Y. N92-10649
TAKATA, T. N92-10933
TAKIZAWA, MINORU N92-10028
TALO, A. N92-10484
TALVITIE, M. N92-10468
TAM, CHRISTOPHER K. W. N92-10604
TAMAI, H. N92-10657
TANAKA, KENNETH L. N92-10748
N92-10754
N92-10755
N92-10759
N92-10778
N92-10779
N92-10782
TANSKANEN, P. N92-10565
TAPPURA, K. N92-10489
N92-10490
N92-10491
N92-10530
N92-10531
TAYLOR, G. J. N92-10809
N92-10810
TAYLOR, J. B. N92-10667
TAYLOR, LAWRENCE A. N92-10961
TAYLOR, S. N92-10319
TAYLOR, S. R. N92-10875
TAYLOR, T. N. N92-10095
TERVONEN, EERO N92-10449
THEILER, J. N92-10356
N92-10357
THEVENARD, P. N92-10678
THIEL, P. A. N92-10463
THOMAS, G. J. N92-10696
THOMAS, P. K. N92-10923
THOMAS, SUSAN N92-10267
THOME, F. V. N92-10061
THOMPSON, J. D. N92-10684
THOMPSON, T. W. N92-10848
THOMPSON, W. REID N92-10958
THORLACIUS, L. N92-10727
THORN, R. J. N92-10701
THRASHER, JOSEPH S. N92-10105
THYAGARAJA, A. N92-10668
TIEE, J. J. N92-10218
N92-10260
TIKKANEN, P. N92-10400
TIKKANEN, T. N92-10418
TIMONEN, J. N92-10371
N92-10508
TINGLE, T. N92-10932
TIPTON, P. N92-10630
TISHKOFF, J. M. N92-10062
TISSARI, S. O. N92-10540
TITTEMORE, WILLIAM C. N92-10953
TITTONEN, I. N92-10504
N92-10512
TJUKANOV, E. N92-10480
TOBIAS, SIGMUND N92-10283
TOERMAENEN, S. N92-10403
TOI, K. N92-10647
TOLONEN, A.-M. N92-10434
TOLSON, CAROL J. N92-10208
TOMKINS, J. L. N92-10335
TONKS, W. B. N92-10864
TONN, BRUCE E. N92-10359
TORIZUKA, K. N92-10474
TORMANEN, S. N92-10405
TORMANEN, T. N92-10569
TORR, DOUGLAS G. N92-10613
TORSTI, J. J. N92-10562
N92-10574
N92-10575
TOVEY, CRAIG A. N92-10353
TOW, D. M. N92-10193
TOWNSEND, J. K. N92-10642
TRAINOR, M. S. N92-10295
TRALLI, D. N92-10759
TRANQUADA, J. M. N92-10683
TRASH, L. N92-10055
TROKHIMOVSKY, YU. A. N92-10272
TROLINGER, J. D. N92-10183
TROXEL, S. W. N92-10019
TRUBERT, JEAN-FRANCOIS N92-10107
TSCHARNUTER, WERNER M. N92-10890
TSE, Y.-H. N92-10104
TSUBATA, HIDEO N92-10640
TUECKE, S. N92-10319
N92-10339

TULKKI, J. N92-10428
N92-10429
N92-10430
TUOMINEN, E. N92-10418
TUOMINIEMI, J. N92-10388
N92-10389
N92-10390
N92-10391
N92-10392
TUORINIEMI, J. T. N92-10507
TURALA, M. N92-10416
TURCOTTE, DONALD L. N92-10730
TUREK, FRED W. N92-10280
TURNER, J. A. N92-10316
TURUNEN, E. N92-10559
TURUNEN, JARI N92-10449
N92-10457
N92-10458
TURUNEN, TAUNO N92-10555
TURUNEN, TIMO N92-10555
TUTTLE, MICHAEL J. N92-10954
TUUVA, T. N92-10412
TUUVA, TUURE N92-10414
N92-10415
N92-10416
TYBURCZY, J. N92-10932
TYLER, G. L. N92-10849
TYRVAINEN, HARRI N92-10535

U

UCHIDA, TADAO N92-10028
UEDA, NORIAKI N92-10646
ULLAKKO, K. N92-10471
N92-10472
N92-10504
N92-10550
UM, C. I. N92-10078
UMAR, A. S. N92-10624
UMEZAWA, A. N92-10693
UNDERWOOD, D. G. N92-10641
UNDERWOOD, JAMES R., JR. N92-10959
URPONEN, M. N92-10381
UUSIMAKI, A. N92-10498
N92-10528

V

VAARI, J. N92-10484
VAINIO, P. N92-10543
VALDEN, M. N92-10440
VALDIVIEZ, R. N92-10320
VALLI, K. N92-10417
VALOVIC, M. N92-10651
VALTAOJA, ESKO N92-10564
VALTAOJA, L. N92-10577
VALTONEN, E. N92-10562
N92-10574
N92-10575
VALTONEN, M. N92-10578
VALVERDEA, L. JAMES., JR. N92-10359
VANDEVOORT, K. G. N92-10692
VANDYKE, J. P. N92-10335
VANHALA, H. N92-10571
VANHOOK, A. N92-10094
VANRAAIJ, J. L. N92-10115
VANROSENDALE, JOHN N92-10348
VARRIO, J. N92-10529
VARTIAINEN, E. M. N92-10363
VASARA, ANTTI N92-10457
N92-10458
VASILYEV, S. N92-10480
VASQUEZ, RICHARD P. N92-10681
VATTULAINEN, I. N92-10440
VATTULAINEN, J. P. N92-10459
N92-10460
VAYRYNEN, J. N92-10516
VEHSE, ROBERT C. N92-10704
VEIDENBAUM, ALEX N92-10304
VEMPATI, R. K. N92-10254
N92-10255
VENEMA, STEVEN C. N92-10126
VERBISCER, A. N92-10835
VERRONEN, M. N92-10571
VESALA, TIMO N92-10525
N92-10526
VEVERKA, JOSEPH N92-10834
N92-10835
N92-10836
VIANCO, P. T. N92-10083
VIANO, J. B. N92-10562
VICKERY, A. M. N92-10866
N92-10868
N92-10869
N92-10870
N92-10871
VIITALA, E. N92-10371
VIKRAM, C. S. N92-10183
VILHU, O. N92-10549
N92-10563
VIRKKUNEN, R. N92-10465
VOECKS, GERALD E. N92-10073
VONWEISSENBERG, KIM N92-10514
VRBA, P. N92-10652
VUOPIONPERA, R. N92-10398
VUORIMAKI, ANTTI N92-10511
VUORINEN, R. N92-10509
VYAS, A. D. N92-10098

W

WADA, MOTOI N92-10656
WAGGONER, J. R. N92-10132
WAKE, L. V. N92-10089
WALKER, BRUCE K. N92-10201
WALL, S. N92-10801
N92-10802
WANG, H. N92-10327
WANG, Q. N92-10440
WANG, R. N92-10705
WANG, Z. L. N92-10625
WARD, WILLIAM R. N92-10894
WAREKOIS, EDWARD P. N92-10159
WARK, CANDACE C. N92-10180
WARREN, O. L. N92-10463
WARREN, STEPHEN G. N92-10821
WASSERMAN, H. J. N92-10298
WATANABE, T. N92-10645
WATANABE, YOSHIAKI N92-10025
WATARI, T. N92-10647
N92-10649
WATHEN, A. J. N92-10344
WATTERS, THOMAS R. N92-10954
N92-10955
WAVRIK, R. W. N92-10152
WEAVER, WILLIAM L. N92-10208
WEBER, H. W. N92-10699
N92-10700
N92-10702
WEBER, M. E. N92-10019
WEERTMAN, J. R. N92-10085
WEI, S. N92-10299
WEIDENSCHILLING, S. J. N92-10884
N92-10892
N92-10895
WEILMUENSTER, K. JAMES N92-10161
WEINFURTER, H. N92-10507
WEINSTEIN, LEONARD M. N92-10008
WEISLOGEL, MARK W. N92-10167
WEISSMAN, PAUL N92-10889
WELKER, JEAN E. N92-10257
WELLS, J. C. N92-10624
WELP, U. N92-10692
WENDT, BRUCE J. N92-10012
WERFEL, F. N92-10503
WESLEY, E. J. N92-10675
WESS, J. N92-10589
WHINNERY, JAMES E. N92-10023
WHITAKER, JOHN F. N92-10142
WHITE, B. N92-10802
WHITE, B. R. N92-10801
WHITE, RAYMOND E., III N92-10724
WHYTE, WAYNE A., JR. N92-10128
WICHMAN, R. W. N92-10876
WIELDT, J. A. N92-10100
WIESINGER, H. P. N92-10700
WILCOX, FLOYD J., JR. N92-10005
WILHELM, F. N92-10210
WILKE, K. N92-10529
WILKEN, B. N92-10556
N92-10558
WILLIAMS, D. A. N92-10749
WILLIAMS, JAMES G. N92-10885
WILLIAMS, K. L. N92-10275
WILLIAMS, L. K. N92-10697
WILLIAMS, STEVEN H. N92-10910
WILLS, E. L. N92-10249
WILSON, L. N92-10957
WILSON, ROBERT N92-10267
WINGARD, J. N92-10242
WITTEBORN, F. N92-10951
WLODARCZAK, G. N92-10444
WOJTCZUK, STEVEN J. N92-10226
WOLF, PETER N92-10066
WOLFE, R. F. N92-10880
N92-10883
WOOD, C. P. N92-10183
WOOD, GARY L. N92-10194
WORKMAN, G. L. N92-10183
WORKMAN, GARY L. N92-10079
N92-10080
N92-10200
WU, SHERMAN S. C. N92-10914
N92-10919
N92-10920
N92-10921
N92-10922
N92-10924
N92-10926

X

XIE, D. N92-10705
XIE, ZELIANG N92-10550
XIONG, X. N92-10499
XU, MING N92-10693
XU, Y.-L. N92-10686

Y

YAGISHITA, A. N92-10426
N92-10427
N92-10429
YAMADA, HITOSHI N92-10166
YAMAMOTO, YUKIMITSU N92-10009
YAMAOKA, HITOSHI N92-10656
YANAMANDRA-FISHER, P. A. N92-10934
YANG, Y. N92-10181
YATSU, SHUJI N92-10153
YEW, PEN-CHUNG N92-10304
YIN, S. N92-10509
YING, S.-C. N92-10469
N92-10470
YLINEN, E. E. N92-10510
YOO, S. K. N92-10078
YOSHIDA, A. N92-10417
YOSHIDA, MAKOTO N92-10025
YOST, WILLIAM T. N92-10182
YOU, H. N92-10694
YUAN, CHIH-CHUNG N92-10014

Z

ZACEK, F. N92-10651
ZAHO, C. N92-10705
ZALPURI, K. S N92-10259
ZAMMIT, ROSE M. N92-10022
ZAPOTOSKY, J. E. N92-10137
N92-10138
N92-10139
ZARNSTORFF, M. C. N92-10663
ZENTNER, RONALD C. N92-10197
ZHANG, G. N92-10530
N92-10531
ZHANG, MEI-JIE N92-10350
ZHANG, N. N92-10697
ZHANG, T. J. N92-10694
N92-10698
ZIBIN, J. P. N92-10531
ZIMBELMAN, JAMES R. N92-10905
N92-10910
ZIMMERMANN, W. N92-10589
ZIOCK, K. O. H. N92-10623
ZISK, S. H. N92-10793
ZOLENSKY, M. E. N92-10252
N92-10256
ZUBER, M. T. N92-10760
ZWICK, H. N92-10279

Typical Corporate Source Index Listing

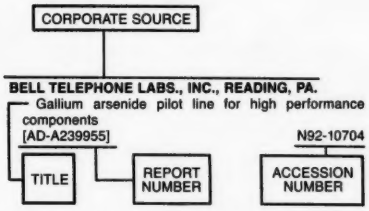

Listings in this index are arranged alphabetically by corporate source. The title of the document provides the user with a brief description of the subject matter. The report number helps to indicate the type of document cited (e.g., NASA report, translation, NASA contractor report). The accession number denotes the number by which the citation is identified. The titles are arranged under each corporate source in ascending accession number order.

A

ACADEMY OF SCIENCES (USSR), MOSCOW.
Radiohydrophysical aerospace research of ocean
[SRI-PR-1749] N92-10272
On the ionospheric influence upon the spectral structure on the Pc1 geomagnetic pulsations N92-10552
Inhomogeneity and nonlinearity effects on stop bands of Alfvenic ion cyclotron waves in multicomponent plasma N92-10557
Reflectance spectra of some fractions of Migei and Murchison SM chondrites in the range of 0.3-2.6 microns N92-10829

ACOUSTICAL SOCIETY OF AMERICA, NEW YORK, NY.
US TAG for ISO/TC43, acoustics, IEC/TC29 electroacoustics, ISO/TC108/SC4 human exposure to mechanical vibration and shock: Minutes of the Accredited Standards Committee on Bioacoustics, S3
[AD-A239918] N92-10610

ADVISORY GROUP FOR AEROSPACE RESEARCH AND DEVELOPMENT, NEUILLY-SUR-SEINE (FRANCE).
Combustion of Solid Propellants
[AGARD-LS-180] N92-10106

AEROSPACE CORP., EL SEGUNDO, CA.
A neural network model of the relativistic electron flux at geosynchronous orbit
[AD-A239827] N92-10030

AIR FORCE ACADEMY, CO.
Downwash measurements on a pitching canard-wing configuration
[AD-A239956] N92-10016

AIR FORCE INST. OF TECH., WRIGHT-PATTERSON AFB, OH.
A mathematical model for a paired comparison experiment on a continuum of response
[AD-A239858] N92-10351

ALABAMA UNIV., HUNTSVILLE.
PC programs for the prediction of the linear stability behavior of liquid propellant propulsion systems and application to current MSFC rocket engine test programs, volume 1
[NASA-CR-184228] N92-10042
High temperature materials characterization
[NASA-CR-184231] N92-10079
Expert systems for superalloy studies
[NASA-CR-184236] N92-10080
Glass sample characterization
[NASA-CR-184230] N92-10088
Process modelling for Space Station experiments
[NASA-CR-184227] N92-10112
A non-isotropic multiple-scale turbulence model
[NASA-CR-184217] N92-10160
Automated eddy current analysis of materials
[NASA-CR-184216] N92-10200
Methodology for automating software systems
[NASA-CR-184233] N92-10301
Cooperating systems: Layered MAS
[NASA-CR-184232] N92-10332
Design controls for large order systems
[NASA-CR-184237] N92-10340
Differential collision cross-sections for atomic oxygen: Analysis of space flight instruments for solar terrestrial physics
[NASA-CR-184235] N92-10613
Polarization aberrations. 1: Rotationally symmetric optical systems
[NASA-CR-184218] N92-10638
Contamination study
[NASA-CR-184225] N92-10639
Modelling crystal growth: Convection in an asymmetrically heated ampoule
[NASA-CR-184214] N92-10676
IPC two-color analysis of x ray galaxy clusters
[NASA-CR-188980] N92-10724

AMES LAB., IA.
Electronic and magnetic properties of strongly correlated systems
[DE91-018205] N92-10690
Diamond thin films grown by microwave plasma assisted chemical vapor deposition
[DE91-018553] N92-10695

ARGONNE NATIONAL LAB., IL.
Examination of mechanical behavior in nanocrystalline materials
[DE91-018552] N92-10085
Transport properties and oxidation in chromium and Fe-Cr alloys exposed to oxygen at high temperatures
[DE91-018571] N92-10086
Development of nondestructive characterization technologies for process control of ceramics
[DE91-018540] N92-10097
Update on the prospects for ceramic engine components
[DE91-018574] N92-10098
A portable run-time system for PCN
[DE91-017700] N92-10319
Fiber networking at Argonne: A distributed, multiapplication, multivendor computing environment
[DE91-018560] N92-10338
Parallel programming with PCN
[DE91-019005] N92-10339
Advanced photon source: Radiological design considerations
[DE91-018014] N92-10635
Optical signal multiplexer and demultiplexer
[DE91-017836] N92-10640
Fiber-tile optical studies at Argonne
[DE91-018591] N92-10641
High-temperature implantation of Au into Ni
[DE91-017304] N92-10682
Anisotropic twin boundary pinning in YBa2Cu3O(x)
[DE91-018536] N92-10692
Initial magnetization and magnetic relaxation in a single crystal of Bi2Sr2CaCu2O(x)
[DE91-018537] N92-10693
Heteroepitaxial growth of TiO2, VO2, and TiO2/VO2 multilayers by MOCVD
[DE91-018543] N92-10694
Grain boundaries in nanophase materials
[DE91-018587] N92-10696
Electrical transport across grain boundaries in bicrystals of YBa2Cu3O7(delta)
[DE91-018588] N92-10697
Heteroepitaxy of MOCVD grown TiO2, VO2 films and TiO2/VO2 multilayers on sapphire (1120)
[DE91-018589] N92-10698
Reversible magnetization of Bi2Sr2CaCu2O8 single crystals
[DE91-018600] N92-10699
Neutron irradiation effects on YBCO single crystals
[DE91-018615] N92-10700
Chemical thermodynamic equilibria and conductivity of nonstoichiometric YB2Cu3O7-(delta): A review
[DE91-018638] N92-10701
Activation energies in a Bi2Si2CaCu2O(x) single crystal
[DE91-018640] N92-10702
Physics Division annual review, April 1, 1990 - March 31, 1991
[DE91-018704] N92-10707

ARIZONA STATE UNIV., TEMPE.
Fluid dynamics of multiphase flow in volcanic environments on the Earth, Io, and other planets N92-10740
The formation of antipodal-impact terrains on Mars N92-10749
Global relationships between volcanic vents and fractures radial to large impact basins on Mars N92-10750
Timing and formation of wrinkle ridges in the Tyrrhena Patera Region of Mars N92-10752
Tectonic deformation on icy satellites: A model of compensating horsts N92-10763
The strength of Miranda's lithosphere N92-10767
Magma generation on Mars: Estimated volumes through time N92-10788
Physical properties of lava flows on the southwest flank of Tyrrhena Patera, Mars N92-10790
Factors controlling lava dome morphology N92-10792
The potential scale of aeolian structures on Venus N92-10800
Remote sensing observations of Kelso Dunes, California N92-10847
Evolution of the east rim of the Hellas basin, Mars N92-10909
Planetary geomorphology research: FY 1990-1991 N92-10940

ARIZONA UNIV., TUCSON.
Physical properties of cryovolcanic brines: Applications to the evolution of Ganymede N92-10737
Mimas: Tectonic structure and geologic history N92-10764
Tethys geology and tectonics revisited N92-10765
Iapetus: Tectonic structure and geologic history N92-10766
Evolution of the Martian hydrosphere N92-10768
Glacial and marine chronology of Mars N92-10772
Chronology of glaciation in the Hellas region of Mars N92-10773
Glacial geology of the Hellas region on Mars N92-10774
Terrestrial glacial eskers: Analogs for Martian sinuous ridges N92-10775
Stratigraphy of the layered terrain in Valles Marineris, Mars N92-10777
Variable features in the Valles Marineris region of Mars N92-10799
Theoretical studies of volatile processes in the outer solar system N92-10807
Oxidation of basaltic tephras: Influence on reflectance in the 1 micron region N92-10817
An infrared reflectance study of low albedo surface constituents N92-10830
Core formation by giant impacts N92-10864
Large impacts and climatic catastrophes on the early Earth N92-10865
Impacts and the early environment and evolution of the terrestrial planets N92-10866
Vapor plumes: A neglected aspect of impact cratering N92-10867
Jetting and the origin of tektites N92-10868
Melt droplet formation in energetic impacts N92-10869
Production of impact melt in craters on Venus, Earth, and the moon N92-10870
Impacts and atmospheric erosion on the early Earth N92-10871
The scaling of secondary craters N92-10874
Magnetic effects of large-scale impacts on airless planetary bodies N92-10877
A reexamination of early numerical simulations of planetary accretion N92-10897
Generation and behavior of solar system magnetic fields N92-10939
Studies in planetary rings N92-10949

Tidal evolution of planetary satellites N92-10953

ARMY AEROMEDICAL RESEARCH LAB., FORT RUCKER, AL.

The hazard of exposure to impulse noise as a function of frequency, volume 1
[AD-A239992] N92-10611

ARMY LAB. COMMAND, FORT MONMOUTH, NJ.

Performance characterization of magnesium/manganese dioxide batteries
[AD-A240037] N92-10158

An overview of modern permanent magnet design
[AD-A240144] N92-10597

ARMY RESEARCH INST. FOR THE BEHAVIORAL AND SOCIAL SCIENCES, ALEXANDRIA, VA.

MANPRINT reference retrieval system (user's guide)
[AD-A239915] N92-10714

ARMY RESEARCH INST. OF ENVIRONMENTAL MEDICINE, NATICK, MA.

A computer simulation for predicting the time course of thermal and cardiovascular responses to various combinations of heat stress, clothing, and exercise
[AD-A240023] N92-10288

ASTRON RESEARCH AND ENGINEERING, SUNNYVALE, CA.

Gas turbine combuster exit temperature measurement
[AD-A239936] N92-10026

ATOMIC WEAPONS RESEARCH ESTABLISHMENT, ALDERMASTON (ENGLAND).

The detection and location of near-regional seismic disturbances by the Eskdalemuir array: A study using noise and signal correlations
[AWE-RE-0-20/90] N92-10247

B

BELEIDSCOMMISSIE REMOTE SENSING, DELFT (NETHERLANDS).

The remote sensing Loosdrecht Lakes (Netherlands) project
[BCRS-90-29] N92-10215

Remote sensing and watershed modelling: Towards a hydrological interface model
[BCRS-90-42] N92-10216

BELL TELEPHONE LABS., INC., READING, PA.

Gallium arsenide pilot line for high performance components
[AD-A239955] N92-10704

BERN UNIV. (SWITZERLAND).

Pion-nucleon sigma-term and the strange quark content of the proton N92-10396

BOEING CO., SEATTLE, WA.

Advanced thermoplastic resins, phase 1
[NASA-CR-178402] N92-10069

Software Technology for Adaptable, Reliable Systems (STARS): US40-STARS reuse concept of operations. Volume 1: Version 0.5-draft
[AD-A240109] N92-10330

Laboratory simulation of cratering on small bodies N92-10859

BROOKHAVEN NATIONAL LAB., UPTON, NY.

The search for low photodesorption coatings
[DE91-017473] N92-10092

Positron annihilation induced Auger-electron spectroscopy: A study of a Ge(100) surface N92-10515

Polarization dependent x ray spectroscopy of high T(sub c) superconductors
[DE91-017475] N92-10683

Strong correlation theories of high temperature superconductors
[DE91-017479] N92-10688

BROWN UNIV., PROVIDENCE, RI.

Parameter identification for nonlinear aerodynamic systems
[NASA-CR-188985] N92-10347

Nuclear excitations and reaction mechanisms
[DE91-018968] N92-10634

Gradational evolution of young, simple impact craters on the Earth N92-10783

Styles of crater gradation in Southern Ismenius Lacus, Mars N92-10784

The gradational history of southern Ismenius Lacus N92-10785

The probable continuum between emplacement of plutons and mare volcanism in lunar crustal evolution N92-10794

Analyses of the lunar surface with advanced remote sensors: Expectations for the 1990's N92-10811

Composition of Syrtis Major volcanic plateau N92-10815

The perplexing continuum slope of Mars: Effects of thin ferric coatings and viewing geometry N92-10816

Disk-resolved spectral reflectance properties of Phobos from 0.3-3.2 micron: Preliminary integrated results from Phobos 2 N92-10822

Darkening in gas-rich ordinary chondrites: Spectral modelling and implications for the regoliths of ordinary chondrite parent bodies N92-10827

The bidirectional reflectance spectra of five gas-rich ordinary chondrites N92-10828

Effects of grain size and shape in modeling reflectance spectra of mineral mixtures N92-10831

Character of the opposition effect and negative polarization N92-10833

Atmospheric effects on oblique impacts N92-10856

Styles of ejecta emplacement under atmospheric conditions N92-10857

Impact decapitation from laboratory to basin scales N92-10858

Characteristics of ejecta and alluvial deposits at Meteor Crater, Arizona and Odessa Craters, Texas: Results from ground penetrating radar N92-10872

Igneous intrusion models for floor fracturing in lunar craters N92-10876

The spatial distribution and time evolution of impact-generated magnetic fields N92-10878

The width of fault zones in a brittle-viscous lithosphere: Strike-slip faults N92-10944

C

CALIFORNIA INST. OF TECH., PASADENA.

Impact and collisional processes in the solar system N92-10932

Impact cratering calculations N92-10933

Planetary origin, evolution, and structure N92-10952

CALIFORNIA UNIV., BERKELEY.

Nonlinear RF processes in plasma
[DE91-017441] N92-10658

Processes of deep terrestrial mantles and cores N92-10729

CALIFORNIA UNIV., DAVIS.

Paucity of moderately repetitive sequences
[DE91-017953] N92-10276

Beat wave current drive experiment on DDT
[DE91-017407] N92-10622

CALIFORNIA UNIV., IRVINE.

Synaptic plasticity and memory formation
[AD-A240121] N92-10285

CALIFORNIA UNIV., LOS ANGELES.

An additive turbulent decomposition of the Navier-Stokes equations implemented on highly parallel computer systems
[AD-A240131] N92-10181

Fragmentation in stellar collapse N92-10891

Thermal and albedo mapping of the north and south polar regions of Mars N92-10943

CALIFORNIA UNIV., SAN DIEGO, LA JOLLA.

Thoughts on abatement and adaptation N92-10239

Asteroid surface processes: Experimental studies of the solar wind on reflectance and optical properties of asteroids N92-10941

CALIFORNIA UNIV., SANTA BARBARA.

Efficient, high-speed, monolithic optoelectronic circuits using quantum-confined structures
[AD-A239841] N92-10155

Electron acceleration by laser fields in a gas
[DE91-018269] N92-10192

Accretion rates of protoplanets N92-10936

Accretion rates of protoplanets 2: Gaussian distribution of planetesimal velocities N92-10937

The ring arcs of Neptune N92-10945

The Titan-Hyperion orbital resonance N92-10946

Rotational properties of planetary satellites N92-10947

CALIFORNIA UNIV., SANTA CRUZ.

Dynamics of low velocity collisions of ice particle, coated with frost N92-10902

CAMBRIDGE UNIV. (ENGLAND).

Airframe noise N92-10605

CAPE TOWN UNIV., RONDEBOSCH (SOUTH AFRICA).

Exact strangeness conservation and particle production
[BI-TP-90/35] N92-10385

Hadronic equation of state and the onset of kaon condensation N92-10386

CARNEGIE INSTITUTION OF WASHINGTON, DC.

Tidal disruption of inviscid protoplanets N92-10900

CENTER FOR NIGHT VISION AND ELECTRO-OPTICS, FORT BELVOIR, VA.

Laser induced optical damage in solids
[AD-A240124] N92-10194

CENTRE FOR SCIENTIFIC COMPUTING, ESPOO (FINLAND).

Adsorbate induced surface reconstruction N92-10469

CESKOSLOVENSKA AKADEMIE VED, PRAGUE.

Approximate analytic theory of the multijunction grill
[IPPCZ-309] N92-10127

On ponderomotive force effects on coupling of the LH and IBW grills for the FTU tokamak
[IPPCZ-305] N92-10650

Experimental studies of tokamak plasma in IPP Prague
[IPPCZ-310] N92-10651

Numerical simulation of ion beam generated in the diode with anode plasma column
[IPPCZ-306] N92-10652

On acceleration of charged particles in intensity minima of laser fields
[IPPCZ-307] N92-10653

Non-unicity of Gibbs states of Czech models in a half-space
[IPPCZ-311] N92-10679

CINCINNATI UNIV., OH.

Approximate evaluation of reliability and related quantities via perturbation techniques
[AD-A240049] N92-10201

CITY UNIV. OF NEW YORK, NY.

Test anxiety and post processing interference, 2
[AD-A239819] N92-10283

CLEVELAND STATE UNIV., OH.

Development of a model of space station solar array
[NASA-CR-188911] N92-10220

COLLEGE OF WILLIAM AND MARY, WILLIAMSBURG, VA.

Quantitative nondestructive evaluation of materials and structures
[NASA-CR-188975] N92-10071

COLORADO STATE UNIV., FORT COLLINS.

Diosmacycloalkanes as models for the formation of hydrocarbons from surface methylenes
[DE91-017854] N92-10065

COLORADO UNIV., BOULDER.

Contractors Meeting in Propulsion
[AD-A240057] N92-10062

Remote sensing of the Martian surface N92-10813

Models of planetary rings N92-10934

Properties of dust and clouds in the Mars atmosphere: Analysis of Viking IRTM emission phase function sequences N92-10956

COLUMBIA UNIV., NEW YORK, NY.

Energy partitioning in elementary gas phase reactions
[DE91-017783] N92-10627

CONSTRUCCIONES AERONAUTICAS S.A., MADRID (SPAIN).

Corrosion tests of meshes in carbon fiber laminates: Impact beam tests
[INFORME-I-522/90] N92-10068

CORIOLIS CORP., SARATOGA, CA.

Thermal management of high heat flux electronic components in space and aircraft systems, phase 1
[AD-A239982] N92-10157

CORNELL UNIV., ITHACA, NY.

Synchrotron radiation: New research opportunities for the next decade N92-10366

Experimental study of interactions of highly charged ions with atoms at keV energies
[DE91-016962] N92-10616

Implications of convection in the moon and the terrestrial planets N92-10730

Tectonic evolution of Lavinia Planitia, Venus N92-10741

Morphology and evolution of coronae and ovoids on Venus N92-10742

Laboratory photometric measurement of particulate soils out to very large phase angles N92-10834

The photometric roughness of Mimas N92-10835

Anomalous scattering of light on Triton N92-10836

High resolution lunar radar studies: Preliminary results N92-10845

Physical processes in planetary rings N92-10904

Studies of volatiles and organic materials in early terrestrial and present-day outer solar system environments N92-10958

CSA ENGINEERING, INC., PALO ALTO, CA.

Development of a pressure transducer calibration system (dynamic pressure response caliber), phase 2
[AD-A239659] N92-10188

D

DANISH SPACE RESEARCH INST., LYNGBY.

The short-circuited fluxgate sensitivity parameters
[ISSN-0109-6605] N92-10147

DAYTON UNIV., OH.

The determination of operational and support requirements and costs during the conceptual design of space systems
[NASA-CR-188817] N92-10037

An experimental evaluation of the impact resistance of recoated F-16A monolithic polycarbonate flat sheet
[AD-A239984] N92-10101

High temperature solar cell contacts
[AD-A239932] N92-10227

DEFENSE SYSTEMS SUPPORT ORGANIZATION, ARLINGTON, VA.
Functional description for the Mapping And Graphic Information Capability (MAGIC)
[AD-A239436] N92-10305

DELAWARE UNIV., NEWARK.
The generalized van der Waals theory of pure fluids and mixtures
[DE91-017549] N92-10093
Optimization methods in control of electromagnetic fields
[AD-A240044] N92-10144

DEPARTMENT OF ENERGY, OAK RIDGE, TN.
INFOTECH '91: DOE Technical Infomation (TI) Meeting
[DE91-018074] N92-10713

DEPARTMENT OF ENERGY, WASHINGTON, DC.
Fuel cell systems program plan, fiscal year 1991
[DE91-017215] N92-10225
Proceedings of the First Energy Research Power Supercomputer Users Symposium
[DE91-018877] N92-10300
MHD program plan, FY 1991
[DE91-017916] N92-10659

DEPAUW UNIV., GREENCASTLE, IN.
Mars geologic mapping: Dao, Harmakhis, and Reull Vailes region N92-10908

DUKE UNIV., DURHAM, NC.
On categorizing sounds
[AD-A240006] N92-10612
Nuclear physics at extreme energy density
[DE91-018012] N92-10637

E

EAGLE ENGINEERING, INC., HAMPTON, VA.
Sonic boom N92-10608

EARTH SATELLITE CORP., ROCKVILLE, MD.
New methods of change detection using multispectral data
[AD-A239370] N92-10217

EDGERTON, GERMESHAUSEN AND GRIER, INC., IDAHO FALLS, ID.
Instrumental design for measurement of surface charge on insulating materials
[DE91-018695] N92-10099
The EH safety representative information system on the safety performance measurement system is where you will find... Word processing and helps with a V-PLUS
[DE91-018709] N92-10113
Laser acoustic technology demonstration and equipment field trails
[DE91-018759] N92-10193
Self-consistent modeling of plasma spraying processes
[DE91-018820] N92-10672

EISCAT SCIENTIFIC ASSOCIATION, KIRUNA (SWEDEN).
The structure and dynamics of the polar mesosphere investigated with the EISCAT radar systems N92-10368

ELORET CORP., SUNNYVALE, CA.
Hypersonic flows as related to the National Aerospace plane
[NASA-CR-187985] N92-10004

ENVIRONICS OY, MIKKELI (FINLAND).
Ion mobility spectrometer to trace gas analysis N92-10535

EUROPEAN ORGANIZATION FOR NUCLEAR RESEARCH, GENEVA (SWITZERLAND).
The quark-hadron phase transition N92-10367
Intermittency studies in proton-antiproton collisions at square root of S = 630 GeV
[CERN-PPE/90-153] N92-10387
Beauty production at the CERN proton-antiproton collider
[CERN-PPE/90-155] N92-10388
A search for rare B meson decays at the CERN proton-antiproton collider
[CERN-PPE/91] N92-10389
J/psi and psi' production at the CERN proton-antiproton collider
[CERN-PPE/90-154] N92-10390
Limits on t-quark decay into charged Higgs from a direct search at the CERN proton-antiproton collider
[CERN-PPE/90-180] N92-10391
Measurements of the ratio R = sigma(sub W)Br(W to mu(nu))/sigma(sub Z)Br(Z to mu(mu)) and gamma(sup tot)(sub W) at the CERN proton-antiproton collider
[CERN-PPE/90-141] N92-10392
Study of muon triggers and momentum reconstruction in a strong magnetic field for a muon detector at LHC N92-10413

EUROPEAN SPACE AGENCY, PARIS (FRANCE).
The data book of ERS-1: The European Remote Sensing Satellite
[ESA-BR-75] N92-10039

F

FEDERAL AVIATION ADMINISTRATION, ATLANTIC CITY, NJ.
Solid-State Radar Beacon Decoder (SSRBD) Operational Test and Evaluation (OT/E) integration test plan
[DOT/FAA/CT-TN91/30] N92-10020

FINNISH CENTRE FOR RADIATION AND NUCLEAR SAFETY, HELSINKI.
Calibration of scintillation cells for radon-222 measurements N92-10521

FINNISH METEOROLOGICAL INST., HELSINKI.
The effect of latitudinally varying solar wind flux on the Lyman alpha sky background N92-10570

FINNISH NATIONAL FUND FOR RESEARCH AND DEVELOPMENT, HELSINKI.
Energy systems and their technical, economic and environmental boundary conditions N92-10581

FLORIDA STATE UNIV., TALLAHASSEE.
Identification of nonlinear times series from first order cumulative characteristics
[AD-A239822] N92-10350
Jet noise generated by large-scale coherent motion N92-10604

FLORIDA UNIV., GAINESVILLE.
Origin and evolution of the zodiacal dust cloud N92-10886

G

GENERAL ACCOUNTING OFFICE, WASHINGTON, DC.
NASA procurement: Management oversight of contract cost and time changes could be enhanced
[GAO/NSIAD-91-259] N92-10708
NASA maintenance: Stronger commitment needed to curb facility deterioration
[GAO/NSIAD-91-34] N92-10709
Management issues at the National Aeronautics and Space Administration
[GAO/T-NSIAD-91-48] N92-10710

GENERAL ATOMIC CO., SAN DIEGO, CA.
High temperature ceramic superconductors
[AD-A239813] N92-10154
Overview of the 1990's D3-D research program
[DE91-018185] N92-10661
VH-mode: A new very high confinement regime in the boronized DIII-D tokamak
[DE91-018186] N92-10662
The DIII-D tokamak and energy confinement at low q
[DE91-018317] N92-10664
Theory of Ion Bernstein wave coupling at low edge densities
[DE91-018321] N92-10665
The 110 GHz ECH heating system for DIII-D
[DE91-018732] N92-10671

GEOLOGICAL SURVEY, DENVER, CO.
Geologic mapping of tunnels using photogrammetry: Camera and target positioning
[DE91-018394] N92-10261
Spectral evidence for carbonates on Mars: Hydrous carbonates N92-10820
New spectral observations of Callisto and leading/trailing hemisphere distinctions N92-10839

GEOLOGICAL SURVEY, FLAGSTAFF, AZ.
Tectonic setting of Martian volcanoes and deep-seated intrusives N92-10751
Late Noachian development of the Coprates rise, Mars N92-10754
Valles Marineris tectonism: Questions and suggestions N92-10756
Valles Marineris, Mars: Are pit chains formed by erosion and troughs by tectonism? N92-10758
SO2-rich equatorial basins and epeirogeny of Io N92-10761
Paleolakes and lacustrine basins on Mars N92-10776
Hydrologic activity during late Noachian and Early Hesperian downwarping of Borealis Basin, Mars N92-10778
Channeling episodes of Kasei Valles, Mars, and the nature of ridged plains material N92-10779
Geologic history and channeling episodes of the Chryse Planitia region of Mars N92-10782
Impact craters on Venus N92-10852
Quantitative analysis of terrain units mapped in the northern quarter of Venus from Venera 15/16 data N92-10853
Asteroid flux and impact cratering rate on Venus N92-10880
Mars geologic mapping program: Review and highlights N92-10912
Venus mapping N92-10913
Triangulation using synthetic aperture radar images N92-10914
Naming the newly found landforms on Venus N92-10915
Publication of topographic atlas and control network of Mars N92-10919
Color-coded global topographic map of Mars N92-10920
Mars elevation distribution N92-10921
Completion of compilation of the 1:2,000,000-scale topographic map series of Mars N92-10922
Mars high-resolution mapping N92-10923
A new edition of the Mars 1:5,000,000 map series N92-10924
Planetary atlases N92-10925
CD-ROM publication of the Mars digital cartographic data base N92-10926
Digital cartography of Io N92-10927
Digital solar system geology N92-10928
A new catalog of planetary maps N92-10929

GEOLOGICAL SURVEY, MENLO PARK, CA.
Soil crusts on Mars N92-10786
Surface-material maps of Viking landing sites on Mars N92-10787
Rheological analyses of lava flows on Mars N92-10791
Water on Mars: Clue to accretional history N92-10798
Preliminary comparison of 3.5-cm and 12.6-cm wavelength continuous wave observations of Mars N92-10848

GEOPHYSICAL OBSERVATORY, SODANKYLA (FINLAND).
Ozone depletion rates in the late winter/early spring Arctic and Antarctic stratosphere according to recent ozone sounding observations N92-10547
EISCAT incoherent scatter radar observations and model studies on day to night variations in the ionospheric D-region during the PCA event of August 1989 N92-10559
Variation of D-region parameters during polar cap absorption events in the year 1989 N92-10561

GEORGE WASHINGTON UNIV., WASHINGTON, DC.
Investigations of the structure and electromagnetic interactions of few-body systems
[DE91-017927] N92-10628

H

HAMILTON STANDARD, WINDSOR LOCKS, CT.
Propeller and propfan noise N92-10599

HARVARD UNIV., BOSTON, MA.
Computer assisted multiplex sequencing
[DE91-017851] N92-10337

HARVARD UNIV., CAMBRIDGE, MA.
Regional scale dynamical modelling of biogeochemical processes
[AD-A240115] N92-10246

HAWAII UNIV., HONOLULU.
New studies of Martian volcanoes N92-10793
Heat flow vs. atmospheric greenhouse on early Mars N92-10805
Remote sensing and geologic studies of the orientale basin region N92-10809
Depth/diameter relationships of fresh craters within Hesperia Planum, Mars N92-10873
Will Galileo resolve the S-asteroid controversy? N92-10882

HEBREW UNIV., JERUSALEM (ISRAEL).
Fundamental studies in the molecular basis of laser induced retinal damage
[AD-A239941] N92-10278

HEIDELBERG UNIV. (GERMANY, F.R.).
Formation of the protosolar nebula N92-10890

HELSINKI UNIV. OF TECHNOLOGY, ESPOO (FINLAND).
Early 19th-century least squares calculations in Finland repeated with modern techniques N92-10369
Local charge compensation in Z(sup 0) hadronic decays N92-10393
Recent physics results from DELPHI N92-10394
Gluon overlap factors extracted from Monte Carlo lattice calculations N92-10397
Heavy neutrinos in e(+)e(-) collisions N92-10398
Supernova neutrinos N92-10399
Lifetime of the 1.959 MeV state in Cl-36 N92-10400
Independent and cumulative yields of neutron-rich nuclei in symmetric fission induced by p and d on U-238 N92-10411
The DELPHI microvertex detector, a silicon tracking chamber N92-10412

Development of double-sided silicon strip detectors N92-10414
Radiation damage measurements on double-sided Si strip detectors N92-10415
Beam test results of ion-implanted silicon strip detectors on a 100 mm wafer N92-10416
Studies on new low noise silicon radiation detector N92-10418
Krypton 4p,4s and 3d partial photoionization cross sections below 260 eV photon energy N92-10429
Relaxation and final-state correlation effects in the 3p and 3s photoionization of Ar, K(+), and Ca(++) N92-10430
Interaction-induced light scattering as a source of information on properties and interactions of spherical top molecules N92-10439
Isotope selective resonance ionization measurements of lithium N92-10442
Torsional potential for the C(sp2)-C(sp2) bond N92-10443
Absorption measurements with an integrating sphere and an FT-IR spectrometer N92-10445
Reconfigurable optical interconnections by acousto-optic holograms N92-10449
Single-shot spectral measurements of multimode pulsed dye lasers N92-10452
A simple method to stabilize the frequency of semiconductor lasers N92-10453
Polarization spectroscopy in OH and flame temperature measurements N92-10454
Electronically resonant CARS spectroscopy of NO2 N92-10455
Parametric optimization of synthetic gratings using vector diffraction theory N92-10457
Waveguide Dammann gratings and kinoforms N92-10458
Numerical calculations of wave propagation in tokamak plasmas N92-10461
Molecular dynamics using the tight-binding approximation: Application to liquid silicon N92-10465
Observation of a monovacancy in the metastable state of the EL2 defect in GaAs by positron annihilation N92-10467
Internal friction associated with interaction between carbon atoms and dislocations at low temperature N92-10471
Redistribution of nitrogen atoms and magnetic ordering in Fe-N martensite at low temperatures N92-10472
Helium in silicon: A first principle molecular dynamics study N92-10473
Two-phonon absorption by the real squashing collective mode in superfluid He-3 N92-10474
Vortex nucleation in rotating superfluid He-3-B N92-10476
Superfluid interfaces in liquid He-3: Superconducting cosmic domain walls in the laboratory N92-10478
Superfluid vortex nucleation in He-3 flow N92-10479
Chemisorption of CO on Mg-O/Co(0001) N92-10484
Interatomic interactions in the local density approximation N92-10487
Tunneling in oscillating double barrier heterostructures N92-10496
Scanning tunneling microscope measurements in air:Langmuir-Blodgett films on HOPG and growth of evaporated gold on HOPG N92-10497
Dynamics of vortices in high-temperature superconductors N92-10501
Studies on superconducting Bi2Sr2Ca(n-1) Cu(n)O(4+2n) compounds with Fe-57 and Eu-151 Moessbauer spectroscopy N92-10504
Neutron diffraction experiments on nuclear magnetic order in copper N92-10507
Antiferromagnetic ordering in silver at picoKelvin temperatures N92-10509
Gamma echo experiments N92-10512
Aerosol dynamics: Binary nucleation N92-10525
Aerosol dynamics: Condensation and evaporation N92-10526
Integration of magnetoencephalography and magnetic resonance imaging N92-10540
Use of In-111 in quantitative SPECT N92-10544
Variable optical polarization in Her X-1 N92-10546
Finnish space projects: Planetary studies N92-10548
Finnish space projects: Space astronomy N92-10549
The 1990 solar eclipse as seen by a torsion pendulum N92-10550
The measuring modes and observations with the x-ray spectrometer array SIXA onboard spectrum-x-gamma N92-10563
Theoretical studies of optical phenomena and related inverse problems of solar system bodies N92-10566
Fusion energy: Status and prospects N92-10583
Solar energy in mitigating global environmental problems N92-10584
The greenhouse effect N92-10587

HUMBOLDT UNIV., BERLIN (GERMAN D.R.).
Fabrication of GaAs: MESFET's and test structures for electrical material characterization N92-10529

I

IBM FEDERAL SYSTEMS CENTER, GAITHERSBURG, MD.
Software Technology for Adaptable, Reliable Systems (STARS): US40-STARS reuse concept of operations. Volume 1: Version 0.5-draft [AD-A240109] N92-10330

IIT RESEARCH INST., CHICAGO, IL.
Compilation of 1990 annual reports of the Navy ELF communications system ecological monitoring program. Volume 1: Tabs A, B [AD-A239868] N92-10137
Compilation of 1990 annual reports of the Navy ELF communications system ecological monitoring program. Volume 2: Tabs C thru F [AD-A239869] N92-10138
Compilation of 1990 annual reports of the Navy ELF communications system ecological monitoring program. Volume 3: Tabs G thru I [AD-A239870] N92-10139

ILLINOIS INST. OF TECH., CHICAGO.
Management and control of unsteady and turbulent flows [AD-A240050] N92-10180

ILLINOIS UNIV., CHICAGO.
Probability of brittle failure [NASA-CR-187174] N92-10205

ILLINOIS UNIV., URBANA.
Parallel machine architecture and compiler design facilities [NASA-CR-188784] N92-10304

IMATRAN VOIMA OY, HELSINKI (FINLAND).
Nuclear energy: Its strengths, weaknesses and role in Finland N92-10585

IMATRAN VOIMA OY, VANTAA (FINLAND).
Fossil fuels and the environment N92-10586

INSTITUTE FOR COMPUTER APPLICATIONS IN SCIENCE AND ENGINEERING, HAMPTON, VA.
Stability of the flow around a cylinder: The spin-up problem [NASA-CR-187636] N92-10171
The improved robustness of multigrid elliptic solvers based on multiple semicoarsened grids [NASA-CR-187633] N92-10348
Multi-dimensional ENO schemes for general geometries [NASA-CR-187637] N92-10349

INSTITUTE FOR NAVAL OCEANOGRAPHY, BAY SAINT LOUIS, MS.
VERMOD capabilities. VERMOD 1.0 and future [AD-A239801] N92-10274

INSTITUTE FOR PERCEPTION RVO-TNO, SOESTERBERG (NETHERLANDS).
Digital simulation of speech transmission channels [IZF-1991-A-7] N92-10115
Physiological responses of the human extremities to cold water immersion [IZF-1991-A-15] N92-10277

INSTITUTE OF OCCUPATIONAL HEALTH, TURKU (FINLAND).
A measuring robot for thermal environment, contaminant concentration and ventilation studies N92-10537

INTERNATIONAL CENTRE FOR INTEGRATED MOUNTAIN DEVELOPMENT, KATHMANDU (NEPAL).
Potential strategies for adapting to greenhouse warming: Perspectives from the developing world N92-10237

INTERNATIONAL FEDERATION OF INST. FOR ADVANCED STUDY, TORONTO (ONTARIO).
Human dimensions of global change: Toward a research agenda N92-10238

INTERNATIONAL INST. FOR AEROSPACE SURVEY AND EARTH SCIENCES, ENSCHEDE (NETHERLANDS).
Remote sensing and watershed modelling: Towards a hydrological interface model [BCRS-90-42] N92-10216

IOWA UNIV., IOWA CITY.
New observations of the low frequency interplanetary radio emissions [NASA-CR-188917] N92-10971

IWACO B.V., ROTTERDAM (NETHERLANDS).
Remote sensing and watershed modelling: Towards a hydrological interface model [BCRS-90-42] N92-10216

J

JET PROPULSION LAB., CALIFORNIA INST. OF TECH., PASADENA.
The MPD thruster program at JPL N92-10046
Regenerative Cu/La zeolite supported desulfurizing sorbents [NASA-CASE-NPO-17480-1-CU] N92-10073
Personal Access Satellite System (PASS) study. Fiscal year 1989 results [NASA-CR-188808] N92-10116
Introduction to the Personal Access Satellite System study N92-10117
Multiple access trade study N92-10118
Antenna beam coverage concepts N92-10119
Impact of non-geostationary orbits on PASS N92-10120
User antennas N92-10121
Spacecraft antennas N92-10122
PASS spacecraft antenna technology assessment N92-10123
Technology assessment and experimentation plan N92-10124
Method and apparatus for frequency spectrum analysis [NASA-CASE-NPO-17759-1-CU] N92-10125
Composite video and graphics display for multiple camera viewing system in robotics and teleoperation [NASA-CASE-NPO-17836-1-CU] N92-10126
Formation of self-aligned guard rings for monolithic Schottky-barrier diode arrays [NASA-CASE-NPO-17734-1-CU] N92-10146
Acoustic device and method for measuring gas densities [NASA-CASE-NPO-18155-1-CU] N92-10609
Passivation of high temperature superconductors [NASA-CASE-NPO-17949-1-CU] N92-10681
Thermal models for icy satellites N92-10734
The role of nonuniform internal heating in Triton's energy budget N92-10736
Horizontal stress in planetary lithospheres from vertical processes N92-10746
Modelled and measured strain in mascon basins on the moon N92-10747
Strain accommodation beneath structures on Mars N92-10748
Compressive strain in Lunae Planum-shortening across wrinkle ridges N92-10753
Interactions of tectonic, igneous, and hydraulic processes in the North Tharsis Region of Mars N92-10755
Extension and strain in Northern Tharsis N92-10757
Martian seismicity through time from surface faulting N92-10759
Crystallization during emplacement of lava flows N92-10789
Use of radar to assess aeolian processes N92-10802
Crustal heterogeneity of the moon viewed from the Galileo SSI camera: Lunar sample calibrations and compositional implications N92-10808
Mineralogy of the Martian surface from Mariner 6/7 infrared spectrometer data N92-10814
Water detection at the moon, Mars and comets with a combined neutron gamma ray instrument N92-10819
Light scattering by lunar-like particle size distributions N92-10832
Disk resolved studies of the optical properties and physical nature of the surfaces of the outer planet satellites N92-10837
Mojave remote sensing field experiment N92-10840
Mapping compositional and particle size variations across Silver Lake Playa: Relevance to analyses of Mars TIR data N92-10842
Gravity survey of the Mt. Toondina impact structure, South Australia N92-10879
Asteroid families N92-10885
Photometry of the comet 2060 Chiron N92-10887
Thermal modeling of comet Kopff: Implications for the CRAF mission N92-10889
Bending waves and orbital inclinations N92-10894

JOENSUU UNIV. (FINLAND).
A new phase retrieval method for CARS spectrum analysis N92-10363
Photoresist crossed gratings N92-10448
Holographic nondestructive testing in bone biomechanics N92-10451
An improved technique for electrolytic colouration of alkali halide crystals N92-10513
Spectral reflectance of pine and intensity of moose browsing N92-10514

JOHNS HOPKINS UNIV., BALTIMORE, MD.
The 14th International Conference on Combined Effect of Environmental Factors [AD-A240045] N92-10245

Infrared (2.08-14 micron) spectra of powered stony meteorites N92-10826
Are the Equatorial Highlands on Venus formed by mantle plume diapirs? N92-10942

JYVASKYLA UNIV. (FINLAND).
Dynamics of discrete quantum nonlinear Schroedinger equations N92-10371
A model for a data acquisition solution for a medium size accelerator laboratory N92-10376
Thermal emission of gammas and lepton pairs from quark-gluon plasmas N92-10383
Thermal photon production from high-temperature nuclear matter N92-10384
Observations on very neutron-rich nuclei below Z = 50 N92-10402
High-spin states in Cd-109 N92-10403
Shapes of Cd-110 at high spins N92-10404
Evidence for band termination in Xe-118 N92-10405
Proton-neutron symmetry in boson models of nuclear structure N92-10406
Double beta decay in the particle-number projected QRPA formalism N92-10408
Neutrinoless beta decay in the framework of a relativistic quark model N92-10409
Gamma-decay branching of 1(+)-states in Gd-156 and Dy-164 N92-10410
Ion-Guide Quadrupole Mass Spectrometer (IGQMS) N92-10417
Control system of the Jyvaskyla (Finland) K130 cyclotron N92-10419
The Jyvaskyla (Finland) K130 cyclotron project N92-10420
Magnetic field settings for the K130 cyclotron N92-10421
Status of the JYFL-ECR ion source N92-10422
Plan for the JYFL gas-filled recoil separator N92-10424
Equivalence in the shell structure of the tight binding and free electron clusters N92-10441
Thermal helium desorption facility in Jyvaskyla (Finland) N92-10464
The shape effect of magnetic damages in irradiated Nd2Fe14B-permanent magnets N92-10468
Surface reconstruction and many-atom models N92-10483
Ferromagnetism in small clusters N92-10508

K

KANSAS STATE UNIV., MANHATTAN.
Atomic physics of strongly correlated systems [DE91-012259] N92-10617
Preliminary 1:500,000-scale geologic mapping of Claritas Fossae, Mars N92-10959

KATHOLIEKE UNIV. TE LEUVEN (BELGIUM).
Observations on very neutron-rich nuclei below Z = 50 N92-10402

KENTUCKY UNIV., LEXINGTON.
An additive turbulent decomposition of the Navier-Stokes equations implemented on highly parallel computer systems [AD-A240131] N92-10181

KUOPIO UNIV. (FINLAND).
Running discrete cosine transform algorithm N92-10375
Dual pin diode preamplifier for laser Doppler velocimetry N92-10382
Recognizing of spectral mixtures, their components and spectral patterns N92-10447
Optical correlators in texture analysis N92-10450
Coupled wave analysis in inverse grating diffraction problems N92-10456
Spectral representation in vision N92-10539
Clustering: A powerful aid in classifying QRS waveforms N92-10541
Algorithm for detection of VFIB in real time from ECG N92-10542
Analysis of esophageal pH-recordings for reflux disease N92-10543

KURCHATOV (I. V.) INST. OF ATOMIC ENERGY, MOSCOW (USSR).
NMR and ESR experiments on solid molecular hydrogen containing atomic hydrogen N92-10510

L

LAFAYETTE COLL., EASTON, PA.
The magnesium sulfate-water system at pressures to 4 kilobars N92-10738

LAMONT-DOHERTY GEOLOGICAL OBSERVATORY, PALISADES, NY.
Recent changes of weather patterns in North America [DE91-017706] N92-10266

LANCASTER UNIV. (ENGLAND).
Factors controlling the structures of magma chambers in basaltic volcanoes N92-10957

LANDAU INST. FOR THEORETICAL PHYSICS, MOSCOW (USSR).
Mutual friction in superfluid He-3: Effects of bound states in the vortex core N92-10475
Vortex lattice: Vortex liquid states in anisotropic high-T(sub c) superconductors N92-10500

LAWRENCE LIVERMORE NATIONAL LAB., CA.
LLNL contributions to MPD thrusters for SEI N92-10047
Radar applications of gigawatt sources at millimeter wave frequencies [DE91-017541] N92-10133
Subpicosecond x ray streak camera [DE91-017664] N92-10187
Cavity issues for Ni-like Ta x ray lasers [DE91-017668] N92-10190
Retire FORTRAN? A debate rekindled [DE91-016565] N92-10317
A brief introduction to CONDOR [DE91-018652] N92-10325
TAURUS: An interactive post-processor for the analysis codes NIKE3D, DYNA3D, and TOPAZ3D [DE91-019012] N92-10326
Gang scheduling a parallel machine [DE91-011539] N92-10336
Limitations of the condensed history method for low energy electrons [DE91-015764] N92-10619
The response history Monte Carlo method for electron transport [DE91-018295] N92-10631
Nonlinear RF processes in plasma [DE91-017441] N92-10658
Plasma Physics Research Institute, Lawrence Livermore National Laboratory, University of California, Davis annual report for fiscal year 1989 [DE91-018490] N92-10669
Electromagnetic plasma simulation in realistic geometries [DE91-018651] N92-10670
Information flow in quantum mechanics: The quantum Maxwell demon [DE91-017659] N92-10725
Flow and fracture of ice and ice mixtures N92-10735
Properties of planetary fluids at high pressures and temperatures N92-10739

LETTERMAN ARMY INST. OF RESEARCH, SAN FRANCISCO, CA.
Two informative cases of Q-switched laser eye injury [AD-A240001] N92-10279

LINTEL TECHNOLOGY, INC., ROSLYN, NY.
Diamond heat sinks for electronic circuits [AD-A239750] N92-10145

LOS ALAMOS NATIONAL LAB., NM.
Los Alamos NEP research in advanced plasma thrusters N92-10049
Determining desorption pre-exponential factors from temperature-programmed desorption spectra when the surface is nonuniform [DE91-009971] N92-10074
Oxide properties of a gamma titanium aluminide: A surface science study [DE91-018024] N92-10095
Hardware description ADSP-21020 40-bit floating point DSP as designed in a remotely controlled digital CW Doppler radar [DE91-018004] N92-10134
The application of the ADSP-21020 40-bit floating point DSP microprocessor in a digital Doppler radar [DE91-018005] N92-10135
RIPPLE: A new model for incompressible flows with free surfaces [DE91-017830] N92-10168
A 3-D adaptive mesh refinement algorithm for multimaterial gas dynamics [DE91-018040] N92-10169
Optical and electrical investigations into cathode ignition and diode closure [DE91-017823] N92-10191
Remote detection of atmospherically dispersed vegetative cells using fluorescence lidar [DE91-016077] N92-10218
Atmospheric measurements using a scanning, solar-blind Raman Lidar [DE91-016078] N92-10260
The role of the computer in science fair projects: Current status and potential [DE91-008606] N92-10295
Magneto-optical disk as a CD-ROM development tool [DE91-009973] N92-10296
Measurement of memory access contentions in multiple vector processor systems [DE91-013205] N92-10297
A performance comparison of three supercomputers: Fujitsu VP-2600, NEC SX-3, and CRAY Y-MP [DE91-016304] N92-10298
Performance of conjugate gradient-like algorithms in transient two-phase subchannel analysis [DE91-013373] N92-10316
INTEGRA manual: Routines for electronic spreadsheet integration (under FRAMEWORK 3) [DE91-017518] N92-10318
A new method to assess the statistical convergence of Monte Carlo solutions [DE91-016013] N92-10354
Using surrogate data to detect nonlinearity in time series [DE91-018017] N92-10357
Mean estimation in highly skewed samples [DE91-018513] N92-10358
Photoemission in YbCu2Si2: Problems with the Kondo impurity model [DE91-018018] N92-10684
Mechanical after-effect studies of oxygen relaxation in YBa2Cu3O(7-delta) [DE91-018043] N92-10685
Langevin dynamics simulations of large frustrated Josephson junction arrays [DE91-018046] N92-10686
Dark matter and the effective value of Newton's constant at large distances [DE91-018152] N92-10726
Chemical fractionation of siderophile elements in impactites from Australian meteorite craters N92-10875
Composition and energetics of solar flare particle events measured by satellites, 1989 - 1991 [DE91-018028] N92-10969
The extension of solar magnetic fields into interplanetary space [DE91-018052] N92-10970

LOS ALAMOS NUCLEAR CORP., NM.
Characterization of nonlinear input-output systems using time series analysis [DE91-018003] N92-10356

LOUGHBOROUGH UNIV. OF TECHNOLOGY (ENGLAND).
A comparison between the consequences of the liberal and non-liberal UK-Europe bilaterals [TT-9101] N92-10018
The design of spaceborne synthetic aperture radar [ETN-91-99986] N92-10114

LUNAR AND PLANETARY INST., HOUSTON, TX.
Program and Abstracts for Clay Minerals Society 28th Annual Meeting [NASA-TM-105098] N92-10248
Geologic mapping of MTM quads 40292 and 40297: In the Utopian lowlands north of the Nilosyrtis Mensae, Mars N92-10910
Workshop on Mare Volcanism and Basalt Petrogenesis: Astounding Fundamental Concepts (AFC) Developed Over the Last Fifteen Years [NASA-CR-188810] N92-10961

LUND OBSERVATORY (SWEDEN).
Variable optical polarization in Her X-1 N92-10546

LYON-1 UNIV. (FRANCE).
Observations on very neutron-rich nuclei below Z = 50 N92-10402

M

MANLABS, INC., CAMBRIDGE, MA.
Characterization of electronic materials [AD-A240063] N92-10159

MARINE CORPS, WASHINGTON, DC.
C4I2 in space: Solving the SatCom shortfall [AD-A239880] N92-10140

MASSACHUSETTS INST. OF TECH., CAMBRIDGE.
MPD work at MIT N92-10050
Explosive Transient Camera (ETC) program [NASA-CR-188957] N92-10184
The measurement of plate vibration and sound radiation from a turbulent boundary layer manipulator [AD-A240127] N92-10206
Ionospheric and magnetospheric processes [AD-A239967] N92-10263
Type abstraction rules for references: A comparison of four which have achieved notoriety [AD-A240076] N92-10716
Dynamic models for ridge belt formation on Venus N92-10731
An assessment of the crustal remelting hypothesis for volcanism in the Freyja Montes deformation zone N92-10732
Gravitational spreading of Danu, Freyja and Maxwell Montes, Venus N92-10744
Degradation of Fe-Mg silicates in hot CO2 atmospheres: Applications to Venus N92-10806

Reflectance spectra of Fe(2+)-Mg(2+) disordered pyroxenes: Implications to remote-sensed spectra of planetary surfaces N92-10823

Pre-terrestrial oxidation products in carbonaceous meteorites identified by Mossbauer spectroscopy N92-10824

Does Lafayette = Nakhla? Not necessarily so, based on 4.2K Mossbauer spectra of all of the SNC meteorites N92-10825

MASSACHUSETTS INST. OF TECH., LEXINGTON.

The 1990 Airport Surveillance Radar Wind Shear Processor (ASR-WSP) operational test at Orlando International Airport
[AD-A239852] N92-10019

MASSACHUSETTS UNIV., AMHERST.

Structural geology and geological history of the Perrine and Nun Sulci Quadrangles (Jg-2 and Jg-5), Ganymede N92-10762

Stratigraphy of the Perrine and Nun Sulci quadrangles (Jg-2 and Jg-5), Ganymede N92-10911

MATERIALS RESEARCH LABS., MELBOURNE (AUSTRALIA).

Fire retardant performance of some interior shipboard paint schemes
[MRL-TR-91-31] N92-10089

MAX-PLANCK-INST. FUER PHYSIK UND ASTROPHYSIK, GARCHING (GERMANY, F.R.).

Activities report of the Werner Heisenberg Institute for Physics, Munich (Federal Republic of Germany)
[ISSN-0173-6256] N92-10588

The Theoretical Division (of the Werner Heisenberg Institute for Physics) N92-10589

The A Experimental Division (of the Werner Heisenberg Institute for Physics) N92-10590

The B Experimental Division (of the Werner Heisenberg Institute of Physics) N92-10591

The Technical Division (of the Werner Heisenberg Institute of Physics) N92-10592

Parsec-scale penetration of UV into molecular clouds: CII 158 micron mapping of W3, NGC 1977, and NGC 2023
[NASA-CR-188969] N92-10615

An atlas of optical counterparts of low mass x ray binaries. Part 1: The Northern Sample
[MPE-PREPRINT-195-PT-1] N92-10723

MCDONNELL AIRCRAFT CO., SAINT LOUIS, MO.

Nonflammable hydraulic power system for tactical aircraft. Volume 2: Equipment and systems test and evaluation
[AD-A239805] N92-10100

MICHIGAN UNIV., ANN ARBOR.

Transport in heterostructures and devices in microwave and millimeter-wave regimes
[AD-A239943] N92-10142

The Magnetically Insulated Inertial Confinement Fusion: A novel approach
[DE91-018273] N92-10660

A statistical mechanics study of solid-solid interfaces
[DE91-017852] N92-10689

Models of the diffuse radar backscatter from Mars N92-10846

MIDWEST RESEARCH INST., GOLDEN, CO.

The Alternative Fuels Data Center
[DE91-015003] N92-10111

Solar detoxification technology: Using energy from the sun to destroy hazardous waste
[DE91-015007] N92-10241

MINISTRY OF HOUSING, PHYSICAL PLANNING, AND ENVIRONMENT, LEIDSCHENDAM (NETHERLANDS).

Sea-level rise: Regional consequences and responses N92-10231

MISSISSIPPI STATE UNIV., MISSISSIPPI STATE.

Transformation of two and three-dimensional regions by elliptic systems
[NASA-CR-188982] N92-10170

MISSOURI UNIV., COLUMBIA.

Applications of multiparameter bifurcations of period functions
[AD-A240046] N92-10352

MISSOURI UNIV., ROLLA.

Experimental investigations of electron capture from atomic hydrogen and deuterium by alpha particles
[DE91-018280] N92-10629

MITRE CORP., BEDFORD, MA.

Integration of Electronic Support Measures (ESM) and alpha-beta radar tracker
[AD-A240031] N92-10143

N

NATIONAL ACADEMY OF SCIENCES - NATIONAL RESEARCH COUNCIL, WASHINGTON, DC.

The space shuttle advanced solid rocket motor: Quality control and testing
[NASA-CR-188800] N92-10043

Activities of the Board on Mathematical Sciences
[DE91-017931] N92-10361

Plasma Science Committee (PLSC)
[DE91-018011] N92-10594

NATIONAL AERONAUTICS AND SPACE ADMINISTRATION, WASHINGTON, DC.

Aeronautical engineering: A continuing bibliography with indexes (supplement 267)
[NASA-SP-7037(267)] N92-10001

Index to 1987 NASA Tech Briefs, volume 11, numbers 1-10
[NASA-TM-105024] N92-10717

Index to 1988 NASA Tech Briefs, volume 12, numbers 1-11
[NASA-TM-105077] N92-10718

Index to 1989 NASA Tech Briefs, volume 13, numbers 1-12
[NASA-TM-105109] N92-10719

Index to 1990 NASA Tech Briefs, volume 14, numbers 1-12
[NASA-TM-105110] N92-10720

Cumulative index to NASA Tech Briefs, 1976-1980, volumes 1-5
[NASA-TM-89327] N92-10721

Cumulative index to NASA Tech Briefs, 1981-1985, volumes 6-10
[NASA-TM-89326] N92-10722

Reports of Planetary Geology and Geophysics Program, 1990
[NASA-TM-4300] N92-10728

NATIONAL AERONAUTICS AND SPACE ADMINISTRATION. AMES RESEARCH CENTER, MOFFETT FIELD, CA.

Passive range estimation for rotorcraft low-altitude flight
[NASA-TM-103897] N92-10003

Transonic and supersonic Euler computations of vortex-dominated flow fields about a generic fighter
[NASA-TP-3156] N92-10011

Clays on Mars: Review of chemical and mineralogical evidence N92-10250

Rotor noise N92-10600

Relationships between topographic roughness and aeolian processes N92-10801

Free convection in the Martian atmosphere N92-10803

Characteristics of the Martian atmosphere surface layer N92-10804

Spectroscopic analyses of Fe and water in clays: A Martian surface weathering study N92-10818

Particle-gas dynamics in the protoplanetary nebula N92-10893

Planetary ring studies N92-10903

Optical properties of grains in molecular clouds and accretion disks N92-10948

Derivation of mid-infrared (5-25 microns) optical constraints of some silicates and palagonite N92-10950

Thermal infrared observations of Mars (7.5-12.8 microns) during the 1990 opposition N92-10951

NATIONAL AERONAUTICS AND SPACE ADMINISTRATION. GODDARD SPACE FLIGHT CENTER, GREENBELT, MD.

Control system for ruling blazed, aberration corrected diffraction gratings
[NASA-CASE-GSC-13240-1] N92-10186

Geoid undulations and gravity anomalies over the Aral Sea, the Black Sea and the Caspian Sea from a combined GEOS-3/SEASAT/GEOSAT altimeter data set
[NASA-TM-104543] N92-10257

Tunneling calculations for GaAs-Al(x)Ga(1-x) as graded band-gap sawtooth superlattices
[NASA-TM-100726] N92-10680

A 40th deg and order gravitational field model for Mars N92-10760

Surface scattering properties estimated from modeling airborne multiple emission angle reflectance data N92-10841

Application of Hapke photometric model to three geologic surfaces using PARABOLA bidirectional reflection data N92-10843

NATIONAL AERONAUTICS AND SPACE ADMINISTRATION. LYNDON B. JOHNSON SPACE CENTER, HOUSTON, TX.

Management of the Space Station Freedom onboard local area network
[NASA-TM-104741] N92-10036

Helmet of a laminate construction of polycarbonate and polysulfone polymeric material
[NASA-CASE-MSC-21503-1] N92-10091

Two-color holography concept (T-CHI)
[NASA-CR-184240] N92-10183

Mechanized fluid connector and assembly tool system with ball detents
[NASA-CASE-MSC-21434-1] N92-10197

Program and Abstracts for Clay Minerals Society 28th Annual Meeting
[NASA-TM-105098] N92-10248

Combined Backscatter Moessbauer Spectrometer and X Ray Fluorescence analyzer (BaMS/XRF) for planetary surface materials N92-10249

Transformation products of submicron-sized aluminum-substituted magnetite: Color and reductant solubility N92-10251

Clay minerals in primitive meteorites and interplanetary dust 2. Smectites and micas N92-10252

Mineralogy of Cretaceous/Tertiary boundary clays in the Chicxulub structure in northern Yucatan N92-10253

UV, visible, and near-IR reflectivity data for magnetic soils/rocks from Brazil N92-10254

Synthesis and properties of Ti-substituted goethites and hematites N92-10255

Clay minerals in primitive meteorites and interplanetary dust 1 N92-10256

Display format, highlight validity, and highlight method: Their effects on search performance
[NASA-TM-104742] N92-10287

Reconfigurable fuzzy cell
[NASA-CASE-MSC-21613-1] N92-10331

Lunar western limb pyroclastic deposits N92-10795

Lunar and Hawaiian lava tubes: Analogs and uses based on terrestrial field data N92-10796

On using a pyroclastic deposit as a manned lunar base site N92-10797

Remote sensing and geologic studies of the terrain northwest of Humorum basin N92-10810

Water/rock interactions in experimentally simulated dirty snowball and dirty iceball cometary nuclei N92-10888

The violent side of mare volcanism N92-10962

Formation of Apollo 14 aluminous mare basalts by replenishment fractional crystallization and assimilation of precursor crust N92-10963

Exploration of relationships between low-Ti and high-Ti pristine lunar glasses using an armalcolite assimilation model N92-10964

The history of lunar volcanism N92-10965

NATIONAL AERONAUTICS AND SPACE ADMINISTRATION. LANGLEY RESEARCH CENTER, HAMPTON, VA.

Measurements of forces, moments, and pressures on a generic store separating from a box cavity at supersonic speeds
[NASA-TP-3110] N92-10005

Mass flux similarity for slotted transonic-wind-tunnel walls
[NASA-TM-4281] N92-10006

Reflection type skin friction meter
[NASA-CASE-LAR-14520-1-SB] N92-10008

Feasibility of using a knowledge-based system concept for in-flight primary flight display research
[NASA-TM-4279] N92-10017

Rotatable non-circular forebody flow controller
[NASA-CASE-LAR-14212-1-CU] N92-10021

A compensatory algorithm for the slow-down effect on constant-time-separation approaches
[NASA-TM-4285] N92-10024

On the formulation of a minimal uncertainty model for robust control with structured uncertainty
[NASA-TP-3094] N92-10027

Shuttle orbiter with telescoping main propulsion unit and payload
[NASA-CASE-LAR-13586-1] N92-10035

Poly 1, 2, 4-triazoles via aromatic nucleophilic displacement
[NASA-CASE-LAR-14440-1] N92-10066

Properties of three graphite/toughened resin composites
[NASA-TP-3102] N92-10067

Process for application of powder particles to filamentary materials
[NASA-CASE-LAR-14231-1] N92-10070

A process for preparing 1,3-diamino-5-pentafluorosulfanylbenzene and polymers therefrom
[NASA-CASE-LAR-14773-1-CU] N92-10105

Numerical analysis and simulation of an assured crew return vehicle flow field
[NASA-TP-3101] N92-10161

Constant frequency pulsed phase-locked loop measuring device
[NASA-CASE-LAR-13823-1] N92-10182

Dual strain gage balance system for measuring light loads
[NASA-CASE-LAR-14419-1] N92-10185

Apparatus and method for explosive bonding to edge of flyer plate
[NASA-CASE-LAR-14096-1] N92-10196

Multi-degree of freedom, active vibration control method, and system
[NASA-CASE-LAR-14508-1-CU] N92-10202

Prediction of matrix fatigue crack initiation in notched SCS-6/Ti-15-3 metal matrix composites
[NASA-TM-104141] N92-10203

Mission description and in-flight operations of ERBE instruments on ERBS and NOAA 9 spacecraft, November 1984 - January 1986
[NASA-RP-1256] N92-10208

Efficient multitasking of Choleski matrix factorization on CRAY supercomputers
[NASA-TM-4259] N92-10302

Aeroacoustics of flight vehicles: Theory and practice. Volume 1: Noise sources
[NASA-RP-1258-VOL-1] N92-10598

Positron lifetime measurements in chiral nematic liquid crystals
[NASA-TP-3122] N92-10677

NATIONAL AERONAUTICS AND SPACE ADMINISTRATION. LEWIS RESEARCH CENTER, CLEVELAND, OH.

Technical evaluation report, AGARD Fluid Dynamics Panel Symposium on Effects of Adverse Weather on Aerodynamics
[NASA-TM-105192] N92-10002

The structure and development of streamwise vortex arrays embedded in a turbulent boundary layer
[NASA-TM-105211] N92-10012

Magnetoplasmadynamic Thruster Workshop
[NASA-CP-10084] N92-10044

Extended temperature range rocket injector
[NASA-CASE-LEW-14846-1] N92-10054

Description of the PMAD DC test bed architecture and integration sequence
[NASA-TM-105284] N92-10055

Multi-reactor power system configurations for multimegawatt nuclear electric propulsion
[NASA-TM-105212] N92-10057

Relative sliding durability of two candidate high temperature oxide fiber seal materials
[NASA-TM-105199] N92-10064

Brominated graphitized carbon fibers
[NASA-CASE-LEW-14698-2] N92-10090

Real-time data compression of broadcast video signals
[NASA-CASE-LEW-14945-2] N92-10128

Pulse thermal energy transport system
[NASA-CASE-LEW-15235-1] N92-10167

A method for determining spiral-bevel gear tooth geometry for finite element analysis
[NASA-TP-3096] N92-10195

Trade studies for nuclear space power systems
[NASA-TM-105231] N92-10221

Alkali metal carbon dioxide electrochemical system for energy storage and/or conversion of carbon dioxide to oxygen
[NASA-CASE-LEW-14973-1] N92-10222

On the most general tensor B(sub ij) which is zero for i does not equal j, and the most general isotropic tensor I(sub ij)
[NASA-TM-105236] N92-10289

Multigrid calculation of three-dimensional viscous cascade flows
[NASA-TM-105257] N92-10345

Turbomachinery noise N92-10601

Noise from turbulent shear flows N92-10603

Combustion and core noise N92-10607

NATIONAL AERONAUTICS AND SPACE ADMINISTRATION. PASADENA OFFICE, CA.

Regenerative Cu/La zeolite supported desulfurizing sorbents
[NASA-CASE-NPO-17480-1-CU] N92-10073

Method and apparatus for frequency spectrum analysis
[NASA-CASE-NPO-17759-1-CU] N92-10125

Composite video and graphics display for multiple camera viewing system in robotics and teleoperation
[NASA-CASE-NPO-17836-1-CU] N92-10126

Formation of self-aligned guard rings for monolithic Schottky-barrier diode arrays
[NASA-CASE-NPO-17734-1-CU] N92-10146

Acoustic device and method for measuring gas densities
[NASA-CASE-NPO-18155-1-CU] N92-10609

Passivation of high temperature superconductors
[NASA-CASE-NPO-17949-1-CU] N92-10681

NATIONAL AEROSPACE LAB., TOKYO (JAPAN).

Numerical simulation of hypersonic viscous flow for the design of H-2 orbiting plane (HOPE-2)
[NAL-TR-1093] N92-10009

Test apparatus and tensile properties of LE-7 turbine blade materials in high pressure hydrogen conditions
[NAL-TR-1092] N92-10025

Development of digital/optical rotary position transducer
[NAL-TR-1106] N92-10028

Experimental investigation of a 12 cm diameter Kaufman xenon ion thruster
[NAL-TR-1099] N92-10056

Numerical analysis of fully developed laminar flow in curved rectangular channels
[NAL-TR-1111] N92-10166

NATIONAL AIR AND SPACE MUSEUM, WASHINGTON, DC.

Ancient fluvial processes in the equatorial highlands of Mars N92-10781

Preliminary geologic mapping of Arsia Mons, Mars N92-10905

Preliminary geologic mapping of central Chryse Planitia, Mars N92-10906

Geologic mapping of northern Lunae Planun, Mars N92-10907

Wrinkle ridge-upland scarp transitions: Implications for the mechanical properties of the deformed materials N92-10954

Wrinkle ridges in the floor material of Kasei Valles, Mars: Nature and origin N92-10955

NATIONAL CENTER FOR ATMOSPHERIC RESEARCH, BOULDER, CO.

The greenhouse effect: Its causes, possible impacts, and associated uncertainties N92-10229

NATIONAL INST. FOR FUSION SCIENCE, NAGOYA (JAPAN).

Single particle and fluid picture for the ponderomotive drift in nonuniform plasmas
[NIFS-25] N92-10645

Simulation study of scalings in scrape-off layer plasma by two-dimensional transport code
[NIFS-24] N92-10646

Observation of plasma toroidal rotations driven by the electric field due to a loss of ions
[NIFS-23] N92-10647

The meandering orbit effect on stabilization of the tilting instability in a field-reversed configuration
[NIFS-22] N92-10648

Fast wave heating at intermediate ion cyclotron harmonics on the JIPP T-II U tokamak
[NIFS-21] N92-10649

High resolution spectroscopy of H(+) energy loss in thin carbon film
[NIFS-88] N92-10654

Geometrical effects of the magnetic field on the neoclassical flow, current, and rotation in general toroidal systems
[NIFS-86] N92-10655

Dependence of Au(-) production upon the target work function in a plasma-sputter-type negative ion source
[NIFS-85] N92-10656

Density peaking in the JFT-2M tokamak plasma with counter neutral beam injection
[NIFS-83] N92-10657

NATIONAL RESEARCH COUNCIL OF CANADA, OTTAWA (ONTARIO).

Magneto-optical transitions in a Coulomb coupled pair of quantum dots N92-10494

Recombination radiation in the fractional quantum Hall effect regime N92-10495

NATIONAL SCIENCE FOUNDATION, WASHINGTON, DC.

Erosive burning of solid propellants N92-10108

Effects of wires on solid propellant ballistics N92-10109

NAVAL AIR DEVELOPMENT CENTER, WARMINSTER, PA.

Physiologic Transection of the brain stem in healthy humans and the neurologic basis of unconsciousness
[AD-A240122] N92-10023

In situ liquid-crystal-polymer fiber reinforced aluminum matrix composite
[AD-A239860] N92-10072

Microstructural stability and creep response of a new Al-Fe-W-Si alloy
[AD-A239861] N92-10087

NAVAL CIVIL ENGINEERING LAB., PORT HUENEME, CA.

Bond of reinforcement under controlled confinement
[AD-A240142] N92-10207

NAVAL OBSERVATORY, FLAGGSTAFF, AZ.

Mapping the stability field of Jupiter Trojans N92-10883

NAVAL OCEAN SYSTEMS CENTER, SAN DIEGO, CA.

Advances and experience with teleoperated systems incorporating remote presence
[AD-A239980] N92-10199

Cold fusion verification
[AD-A239957] N92-10675

NAVAL OCEANOGRAPHY COMMAND CENTER/JOINT TYPHOON WARNING CENTER, FPO SAN FRANCISCO, CA.

Annual tropical cyclone report, 1990
[AD-A239910] N92-10268

NAVAL POSTGRADUATE SCHOOL, MONTEREY, CA.

The effects of forebody strakes on asymmetric vortices on a vertically launched missile
[AD-A239948] N92-10014

Numerical investigation of the effect of leading edge geometry on dynamic stall of airfoils
[AD-A239949] N92-10015

CH-53E/AV-8B aircraft sling load recovery system analysis
[AD-A239950] N92-10022

Design restrictions and licensing for Petite Amateur Navy Satellite (PANSAT)
[AD-A239951] N92-10041

Analysis of loss for inductive strips in finline
[AD-A239947] N92-10156

A general-purpose finite-difference code for solving steady-state three-dimensional fluid-flow and heat transfer problems
[AD-A239857] N92-10175

ONR tropical cyclone motion research initiative: Data users guide to observations
[AD-A240061] N92-10271

A polynomial-time algorithm for computing the yolk in fixed dimension
[AD-A240060] N92-10353

Detection of abrupt changes in statistical models
[AD-A240116] N92-10360

Recovering signals from optical fiber interferometric sensors
[AD-A240062] N92-10644

NAVAL WEAPONS CENTER, CHINA LAKE, CA.

Combustion and safety of solid propellant rocket motors N92-10110

NESTE OY, PORVOO (FINLAND).

Conducting polymers N92-10524

NEW YORK UNIV., NEW YORK.

Visual motion perception
[AD-A240133] N92-10286

Analytical and computational mathematical physics
[DE91-018965] N92-10596

NORDEN, NORWALK, CT.

Propulsive lift noise N92-10606

NORTH CAROLINA STATE UNIV., RALEIGH.

A computational and experimental investigation of a three-dimensional hypersonic scramjet inlet flow field N92-10007

Nonequilibrium radiative heating prediction method for aeroassist flowfields with coupling to flowfield solvers N92-10165

Multi-gigabit fiber optic wide area network development
[AD-A239850] N92-10642

NORTHWESTERN UNIV., EVANSTON, IL.

Quantitative non-destructive evaluation of high-temperature superconducting materials
[DE91-018284] N92-10150

Program and abstracts of the 2nd Meeting of the Society for Research on Biological Rhythms
[AD-A240007] N92-10280

NORWEGIAN SPACE CENTER, OSLO.

Activities report of the Norwegian Space Center
[ETN-91-90052] N92-10029

O

OAK RIDGE ASSOCIATED UNIVERSITIES, INC., TN.

Steady flow of a fluid-solid mixture in a circular cylinder
[DE91-018698] N92-10174

OAK RIDGE NATIONAL LAB., TN.

Recent advances on a finite element algorithm for computational aerodynamics: Transonics-hypersonics
[DE91-018176] N92-10010

Materials in space nuclear power systems
[DE91-017688] N92-10058

Status of Rankine-cycle technology for space nuclear power applications
[DE91-017859] N92-10059

Definition and measurement at high temperatures of pH
[DE91-017945] N92-10077

Evaluation of advanced austenitic alloys relative to alloy design criteria for steam service
[DE91-017800] N92-10081

Three experiments with stereoscopic television: When it works and why
[DE91-016277] N92-10129

Phase control in a two-element folded waveguide array
[DE91-018251] N92-10130

BES Welding Science Contractors summary report, 1990--1991
[DE91-018510] N92-10198

Are limit cycle calculations a stochastic process?
[DE91-017681] N92-10355

The changing face of probability
[DE91-018857] N92-10359
Influence of the angular correlation of fission neutrons on noise signatures
[DE91-014577] N92-10618
Optimal diffusion synthetic acceleration of discrete ordinates transport calculations
[DE91-015924] N92-10620
A novel technique for the measurement of photoenhanced electron attachment: Implications for an optically-controlled diffuse discharge opening switch
[DE91-016226] N92-10621
Nonperturbative electromagnetic muon-pair production with capture in peripheral relativistic heavy-ion collisions
[DE91-018247] N92-10624
Valence and phonon excitations in high-resolution electron microscopy
[DE91-017684] N92-10625
Fast-wave ICRF minority-regime heating experiments on the Tore Supra tokamak
[DE91-018866] N92-10673
Formation of small metallic precipitates of niobium in (alpha)-Al2O3 implanted with Nb ions
[DE91-015928] N92-10678
Dynamic screening and wake effects on electronic excitation in ion-solid and ion-surface collisions
[DE91-018224] N92-10687
Anomalous neutron scattering from the flux-line lattice in K(0.6)Ba(0.4)BiO3
[DE91-018233] N92-10691

ODESSA STATE UNIV. (USSR).
The field drift of ions and its influence on the electrical properties of SnO2 N92-10492

OFFICE NATIONAL D'ETUDES ET DE RECHERCHES AEROSPATIALES, PARIS (FRANCE).
Solid propellant steady combustion: Physical aspects N92-10107
Numerical simulation of vortex breakdown
[ONERA-RSF-6/4368-AY-008A] N92-10162
Numerical simulation of vortex breakdown by solving the Euler equations for an incompressible fluid N92-10163
Numerical simulation of vortex breakdown via 3-D Euler equations N92-10164

OHIO STATE UNIV., COLUMBUS.
MPD thruster research issues, activities, strategies N92-10051
Constitutive parameter extraction for heated materials
[NASA-CR-186208] N92-10593

OREGON STATE UNIV., CORVALLIS.
Using LANDSAT to provide potato production estimates to Columbia Basin farmers and processors
[NASA-CR-188783] N92-10209
Mud volcanoes on Mars? N92-10938

OULU UNIV. (FINLAND).
Proceedings of the 25th Annual Conference of the Finnish Physical Society
[REPT-119(1991)] N92-10362
Anomalous e(+)e(-) pairs in heavy ion collisions and solar neutrinos: Two puzzles with common solution? N92-10364
Dynamic lattice computing in general relativity N92-10372
Synchrotron radiation research and Finnish beamline at MAX-lab N92-10377
Contribution of the delta resonance to the Gamow-Teller decay of heavy nuclei N92-10407
Structure and optical polarizabilities of small silicon clusters N92-10425
Decay channels of resonantly excited 2p(-1)ns, md states of Ar and 3d(-1)np states of Kr N92-10426
Li 1s photoionization and photoexcitation with satellites N92-10427
Electron correlation in the 4d hole state of Cs and Ba N92-10428
The rotational structure of the nu(sub 6) vibration band of CH3I N92-10431
The nu(sub 4) and nu(sub 7) bands of CD3CN with coriolis coupling and other resonance perturbations N92-10432
The nu(sub 8) and 2nu(sub 8) bands of CD3CN N92-10433
The infrared rotation-vibration spectrum of C2H2 in the nu(sub 2) + nu(sub 5) band region; l-resonances in the bands nu(sub 2) + nu(sub 5), nu(sub 2) + 2(nu(sub 5)) back arrow nu(sub 5) and nu(sub 1) back arrow nu(sub 5) N92-10434
The Kr-83 NMR in probing electric field gradients in thermotropic liquid crystals N92-10435
NMR determination of the Ne-21 quadrupole coupling for neon gas dissolved in liquid crystals N92-10436
NMR-relaxation time measurements of noble gas isotope Xe-129 dissolved in isotropic and anisotropic liquids N92-10437
Analysis of the interacting levels V(sub 9) = 1 and V(sub 10) = 2 of propyne N92-10444
Study of different SX-700 designs for the undulator beamline (BL51) at MAX-LAB N92-10446
Computer simulations on the orientation of molecular hydrogen in liquid crystals N92-10466
Effective mass and excitation spectrum of He-3 impurities in superfluid He-4 N92-10477
Predictions of the electron-hole liquid model for high T(sub c) superconductors N92-10499
Epitaxial high T(sub c) superconducting thin films and superlattices deposited by laser albation N92-10505
High T(sub c) superconducting Li-doped Bi-Sr-Ca-Cu-O thin films deposited by laser ablation N92-10506
Super Coster Kronig and resonance super Coster Kronig spectra of solid Ge around 3p-ionization threshold N92-10517
Synchrotron radiation study of recombination processes in solid state Tb and Dy after 4d to 4f giant resonance excitation N92-10518
The N(4,5)N(6,7)N(6,7) and N(4,5)O(2,3)N(6,7) resonance Auger effects in the electron spectra of solid state Gd and Eu N92-10519
Novel type of cryogenic liquid level sensor with high sensitivity N92-10528
Proton NMR studies on human blood plasma: An application to cancer research N92-10545
Lithosphere physics: Geoelectrics and seismics N92-10551
EISCAT research program N92-10553
The use of whistlers for magnetospheric diagnostics N92-10554
Examples of VLF emissions recorded in the auroral zone N92-10555
Average properties of energetic ions in different parts of the cusp/cleft region N92-10556
Energy-latitude dispersion of energetic ions in the dayside of the Earth's magnetosphere: A substorm-related phenomenon N92-10558
Observations of semidiurnal atmospheric tides using the EISCAT incoherent scatter radar N92-10560
CAPS-plasma spectrometer for the Cassini spacecraft N92-10565
Earth, Uranus, and Neptune: A comparison of their magnetospheres N92-10567
Venus behind the clouds N92-10569
Structure and evolution of turbulent preplanetary disc N92-10571
Ring satellite interaction in planetary rings N92-10572
Numerical simulations of dense collisional systems N92-10573
Test results of density detectors of the cosmic ray air shower array in Turku (Finland) N92-10575
N-body simulations of interacting galaxies N92-10579

P

PACIFIC NORTHWEST LAB., RICHLAND, WA.
Electromigration of carrier-free radionuclides
[DE91-017840] N92-10076

PENNSYLVANIA STATE UNIV., UNIVERSITY PARK.
Chemical synthesis and microstructural toughening of infrared window materials
[AD-A239987] N92-10102
Coupling between radiation and gas dynamics
[AD-A240004] N92-10179

PHILLIPS LAB., HANSCOM AFB, MA.
A survey of laser lightning rod techniques
[AD-A239988] N92-10269
Predicting cloud-to-ground lightning with neural networks
[AD-A239989] N92-10270

PHILLIPS LAB., KIRKLAND AFB, NM.
An analysis of the frequency characteristics of corona discharge at low pressure
[AD-A239940] N92-10674

PHYSICS AND ELECTRONICS LAB. TNO, THE HAGUE (NETHERLANDS).
Meteo and irradiation data during BEST TWO, Mourmelon (Netherlands)
[FEL-90-A368] N92-10966

PITTSBURGH ENERGY TECHNOLOGY CENTER, PA.
Steady flow of a fluid-solid mixture in a circular cylinder
[DE91-018698] N92-10174

PITTSBURGH UNIV., PA.
Quantum state resolved desorption of CO from solid surface
[DE91-017712] N92-10626
Regoliths of icy satellites: The coherent backscatter model N92-10851

PLANETARY SCIENCE INST., TUCSON, AZ.
Possible misinterpretation of lunar cratering record in Voyager team analyses of outer planet satellites N92-10860
Hydrocode predictions of collisional outcomes: Effects of target size N92-10861
Continuum modeling of catastrophic collisions N92-10863
Understanding asteroid collisional history through experimental and numerical studies N92-10884
Aerodynamic and gasdynamic effects in cosmogony N92-10892
Accretion and evolution of solar system bodies N92-10895

PRINCETON UNIV., NJ.
Eppdyl: Research focus; past accomplishments; and current research N92-10052
Simulations of the carbon cycle in the oceans
[DE91-018475] N92-10273

R

RAND CORP., SANTA MONICA, CA.
IID: An intelligent information dictionary for managing semantic metadata
[AD-A240022] N92-10715
The control network of Mercury: April 1991 N92-10916
A unified lunar control network: April 1991 N92-10917
The control network of Mars: April 1991 N92-10918

RANGE COMMANDERS COUNCIL, WHITE SANDS MISSILE RANGE, NM.
Range reference atmosphere, Nellis Air Force Base, Nevada
[AD-A239816] N92-10262

RENSSELAER POLYTECHNIC INST., TROY, NY.
Meteorite spectroscopy and characterization of asteroid surface materials N92-10881

RESEARCH INST. FOR ADVANCED COMPUTER SCIENCE, MOFFETT FIELD, CA.
Telescience testbed pilot program, volume 1: Executive summary
[NASA-CR-188833] N92-10031
Telescience testbed pilot program, volume 3: Experiment summaries
[NASA-CR-188834] N92-10032
Telescience testbed pilot program, volume 2: Program results
[NASA-CR-188835] N92-10033
A system performance throughput model applicable to advanced manned telescience systems
[NASA-CR-188860] N92-10034
Modeling of the Space Station Freedom data management system
[NASA-CR-188869] N92-10038
Human performance measurement: Validation procedures applicable to advanced manned telescience systems
[NASA-CR-185447] N92-10282
The paradigm compiler: Mapping a functional language for the connection machine
[NASA-CR-188839] N92-10290
An alternative design for a sparse distributed memory
[NASA-CR-188847] N92-10291
BIRD: A general interface for sparse distributed memory simulators
[NASA-CR-188858] N92-10292
On the suitability of the connection machine for direct particle simulation
[NASA-CR-188863] N92-10293
Sparse distributed memory: Principles and operation
[NASA-CR-188901] N92-10294
The role of graphics super-workstations in a supercomputing environment
[NASA-CR-188852] N92-10306
Modeling reality
[NASA-CR-188881] N92-10307
Queueing in networks of computers
[NASA-CR-188892] N92-10308
Globally convergent techniques in nonlinear Newton-Krylov
[NASA-CR-188894] N92-10309
A restricted signature normal form for Hermitian matrices, quasi-spectral decompositions, and applications
[NASA-CR-188895] N92-10310
An implementation of the look-ahead Lanczos algorithm for non-Hermitian matrices, part 1
[NASA-CR-188909] N92-10311
An implementation of the look-ahead Lanczos algorithm for non-Hermitian matrices, part 2
[NASA-CR-188910] N92-10312
Integrity and security in an Ada runtime environment
[NASA-CR-188826] N92-10313
ART/Ada design project, phase 1. Task 3 report: Test plan
[NASA-CR-188945] N92-10314

Totally parallel multilevel algorithms for sparse elliptic systems
[NASA-CR-188837] N92-10333
Overview of Krylov subspace methods with applications to control problems
[NASA-CR-188842] N92-10343
Optimal moving grids for time-dependent partial differential equations
[NASA-CR-188850] N92-10344
Worldnet
[NASA-CR-188845] N92-10711
Research into the development of a knowledge acquisition taxonomy
[NASA-CR-188948] N92-10712

RESOURCES FOR THE FUTURE, INC., WASHINGTON, DC.
Greenhouse Warming: Abatement and Adaptation
[ISBN-0-915707-50-0] N92-10228
Human development and carbon dioxide emissions: The current picture and the long-term prospects N92-10230
Climate change: Problems of limits and policy responses N92-10232
Assessing and managing the risks of climate change N92-10233
Climate and forests N92-10234
Water resources and climate change N92-10236
Epilogue N92-10240
Processes for identifying regional influences of and responses to increasing atmospheric CO2 and climate change: The MINK project
[DE91-018602] N92-10242
Processes for identifying regional influences of and responses to increasing atmospheric CO2 and climate change: The MINK project
[DE91-018603] N92-10243
Processes for identifying regional influences of and responses to increasing atmospheric CO2 and climate change: The MINK project
[DE91-018605] N92-10244

REYNOLDS ELECTRICAL AND ENGINEERING CO., INC., LAS VEGAS, NV.
Fourier component analysis of three Euler-Lagrangian methods applied to the one-dimensional advection-dispersion model
[DE91-017733] N92-10346

ROCHESTER UNIV., NY.
Theoretical and experimental studies of elementary particles
[DE91-018285] N92-10630

ROCKET RESEARCH CORP., REDMOND, WA.
Small upper stage basic program
[AD-A240059] N92-10063

ROYAL INST. OF TECH., STOCKHOLM (SWEDEN).
Materials science and technology centra in Sweden and Denmark: A research policy for the future N92-10580

ROYAL NORWEGIAN COUNCIL FOR SCIENTIFIC AND INDUSTRIAL RESEARCH, KJELLER.
Integrated array and 3-component processing using a seismic microarray
[AD-A240139] N92-10265

RUTGERS - THE STATE UNIV., NEW BRUNSWICK, NJ.
Content addressable memory project
[NASA-CR-188981] N92-10299

RUTHERFORD APPLETON LAB., CHILTON (ENGLAND).
Scale dependence of Lambda sub (MS bar) from deep inelastic scattering
[RAL-91-044] N92-10614

S

SAN DIEGO STATE UNIV., CA.
Development and optimization of methodologies for analysis of complex hydrocarbon mixtures
[DE91-017954] N92-10075

SAN JUAN CAPISTRANO RESEARCH INST., CA.
Infrared reflectance spectra (4-12 micron) of lunar samples N92-10812

SANDIA NATIONAL LABS., ALBUQUERQUE, NM.
An assessment of the radiation tolerance of large satellite memories in low earth orbits
[DE91-018353] N92-10040
Comparison of selected nuclear thermal propulsion concepts
[DE91-017982] N92-10060
Instrumentation and control for space nuclear propulsion
[DE91-018351] N92-10061
High temperature creep properties of eutectic and near eutectic silver-copper alloys: Application to metal/ceramic joining
[DE91-017987] N92-10082
Wettability of low temperature solder alloys for step-soldering
[DE91-018348] N92-10083
Thermal- and ignition-type steam explosions of single drops of molten aluminum
[DE91-014705] N92-10084
Thermal modeling of an epoxy encapsulation process
[DE91-017845] N92-10096
A digital ASIC implementation of a video filter for synthetic aperture radar
[DE91-018400] N92-10131
Electromagnetic oil field mapping for improved process monitoring and reservoir characterization
[DE91-017452] N92-10132
A 500 MHz phase generator for synthetic aperture radar waveform synthesizers
[DE91-018399] N92-10136
Proceedings of the Second Switch Tube Advanced Technology Meeting
[DE91-017718] N92-10148
A miniature acousto-optic image correlator
[DE91-018002] N92-10151
Status of the Repetitive High Energy Pulsed Power Project
[DE91-018359] N92-10152
Sintered compacts for heat sinks and process for fabricating same
[DE91-018438] N92-10153
A frequency domain method for the generation of partially coherent normal stationary time domain signals
[DE91-017058] N92-10204
A generic guide for the preparation of a quality assurance/quality control manual for the design, production, and installation of photovoltaic concentrator systems
[DE91-017716] N92-10223
The SolarTrak solar array tracking controller
[DE91-017721] N92-10224
Parallel QR factorization on a hypercube using the torus wrap mapping
[DE91-011502] N92-10315
MERLIN 2: A computer program to transfer solution data betwwen finite element meshes
[DE91-018130] N92-10321
Normalization of correlations
[DE91-018398] N92-10324
Massively parallel computing at Sandia and its application to national defense
[DE91-008178] N92-10334
Massively parallel computing and the mid-course tracking problem
[DE91-010864] N92-10335
Long pulse electron beams
[DE91-018357] N92-10636
The influence of plasma motion on disruption generated runaway electrons
[DE91-018356] N92-10666

SCIENCE APPLICATIONS INTERNATIONAL CORP., SAN DIEGO, CA.
Plasma cloud behavior
[AD-A240000] N92-10264

SOUTHAMPTON UNIV. (ENGLAND).
Jet noise classical theory and experiments N92-10602

SOUTHERN METHODIST UNIV., DALLAS, TX.
Martian seismicity N92-10733
Hot-spot tectonics of Eistla Regio, Venus: Results from Magellan images and Pioneer Venus gravity N92-10743
Interpretation of the northern boundary of Ishtar Terra from Magellan images and altimetry N92-10745
Venus impact craters: Implications for atmospheric and resurfacing processes from Magellan observations N92-10854
Breakup of meteoroids in the Venusian atmosphere and its effects on crater formation N92-10855

SOUTHWEST RESEARCH INST., SAN ANTONIO, TX.
Evaluation of preservative engine oil containing vapor-phase corrosion inhibitor and a simplified engine preservation technique
[AD-A240100] N92-10103
Continuation of research into language concepts for the mission support environment: Source code
[NASA-CR-187816] N92-10303

SPARTA, INC., LEXINGTON, MA.
A technique for estimating surface meteorological ranges over oceans from satellite measurements of aerosol optical depth
[AD-A239985] N92-10219

SPIRE CORP., BEDFORD, MA.
High efficiency GaAs/Ge monolithic tandem cells for space concentrator arrays, phase 1
[AD-A239931] N92-10226

ST SYSTEMS CORP., HAMPTON, VA.
Solar Constant (SOLCON) Experiment: Ground Support Equipment (GSE) software development
[NASA-CR-187596] N92-10267

STANFORD LINEAR ACCELERATOR CENTER, CA.
Automatic network analyzer procedures for 5045 klystron cavities
[DE91-018015] N92-10149
Object oriented programming
[DE91-018151] N92-10323
Quantum cosmology on the worldsheet
[DE91-018415] N92-10727

STANFORD UNIV., CA.
Solving problems under uncertainty
[DE91-017940] N92-10322
Surface properties of Galilean satellites from bistatic radar experiments N92-10849
Radar backscattering by the icy Galilean satellites and the radar glory effect N92-10850
Investigation of the small-scale structure and dynamics of Uranus' atmosphere
[NASA-CR-188819] N92-10960

STATE UNIV. OF NEW YORK, STONY BROOK.
Long-term evolution of a planetesimal swarm in the vicinity of a protoplanet N92-10896
Collision probabilities in the presence of nebular gas drag N92-10898
Growth of planets from planetesimals N92-10899
A geometrical model for shepherding N92-10901
Accretion rates of protoplanets N92-10936
Accretion rates of protoplanets 2: Gaussian distribution of planestesimal velocities N92-10937

STOCKHOLM UNIV. (SWEDEN).
Quantum world in 2+1 dimensions N92-10365

STUTTGART UNIV. (GERMANY, F.R.).
IRS organigram N92-10053

SVERDRUP TECHNOLOGY, INC., CLEVELAND, OH.
NEP mission sensitivities N92-10045
MPD thruster technology N92-10048

SYRACUSE UNIV., NY.
On adaptive multiband detection of targets in nonstationary nonhomogeneous interference
[AD-A239983] N92-10327

T

TAMPERE UNIV. OF TECHNOLOGY (FINLAND).
Driven growth in the restricted solid on solid model N92-10373
Gate matrix optimization using simulated annealing N92-10374
Doppler shift velocimetry in disperse flows N92-10378
Abel inversion with the fast Fourier transform N92-10379
Fluidized bed combustion diagnostics by laser photocoustic spectroscopy N92-10380
Simultaneous pyrometric measurement of temperature and size of fuel particles in fluidized bed combustions N92-10381
Supersonic molecular beam apparatus to study surface reactions N92-10440
Velocimetry in gas flows using pulsed laser induced photothermal effects N92-10459
Kinetic gas and electron temperatures in RF induction plasma N92-10460
Molecular dynamics studies of liquid-solid interfaces N92-10462
Determination of the (1x2) structure of a Pt film on Pd(110) N92-10463
Diffusion anomaly at a surface reconstruction N92-10470
Modeling the dynamics of molecular films by Monte Carlo simulation N92-10481
Numerical simulation studies of fluid spreading N92-10482
The stability analysis of a double barrier resonant tunneling device N92-10485
Beryllium doping of InP grown by gas-source molecular beam epitaxy N92-10489
Interface effects on electrical properties of high purity InP grown by gas-source molecular beam epitaxy N92-10490
The influence of growth conditions on the composition of GaInAsP grown by gas-source molecular beam epitaxy N92-10491
Electrical characterization of Li and N doped ZnSe N92-10493
Compound semiconductor technology: Materials and devices N92-10523
In(0.5)3Ga(0.47)As/InP SAM avalanche photodiodes grown by gas source MBE N92-10530
InP solar cells grown by gas-source molecular beam epitaxy N92-10531
Electrostatic precipitator modelling N92-10532
Low pressure impactor with electrical concentration detection N92-10534
A simple radon well N92-10536

TECHNICAL RESEARCH CENTRE OF FINLAND, ESPOO.
Abatement strategies based on critical loads N92-10533
The possibilities to control and to regulate the energy consumption N92-10582
TECHNICAL UNIV. OF BUDAPEST (HUNGARY).
Work function changes of high-T(sub c) superconductors around the T(sub c) N92-10498
TECHNISCHE UNIV., CHEMNITZ (GERMANY, F.R.).
Semiconducting organic thin films as monitoring devices for NO2 air pollution N92-10527
TECHNISCHE UNIV., DRESDEN (GERMAN D.R.).
Ultra-cold polarized hydrogen source N92-10423
TECHNISCHE UNIV., MUNICH (GERMANY, F.R.).
Evaluation of high altitude photography for city regional areas
[MGA-A-44] N92-10210
Recording of urban land use by high altitude photography: The Munich (Fed. Republic of Germany) exampl N92-10211
Possibilities of producing land use information for city regional area planning by high altitude photographs, taking south west Munich (Fed. Republic of Germany) regional area as an example N92-10212
Image evaluation of high altitude photographs. Examples: Boston and Foster City (US) N92-10213
Evaluation of high altitude photography for city cartography, with the example of Seattle, US N92-10214
TENNESSEE UNIV., KNOXVILLE.
Investigations of the effects of isotopic substitution and pressure on miscibility in polymer-polymer and polymer-solvent systems
[DE91-018010] N92-10094
TEST GROUP (6585TH), HOLLOMAN AFB, NM.
The use and misuse of aircraft and missile RCS statistics
[AD-A239892] N92-10141
TEXAS SOUTHERN UNIV., HOUSTON.
A generic guide for the preparation of a quality assurance/quality control manual for the design, production, and installation of photovoltaic concentrator systems
[DE91-017716] N92-10223
TEXAS UNIV., AUSTIN.
Nonlinear interactions of tearing modes in the presence of shear flow
[DE91-018420] N92-10173
Vlasov-Maxwell system: 2-D equilibria, reversed field pinches
[DE91-018421] N92-10595
Research program in particle physics
[DE91-018525] N92-10632
Ion temperature gradient driven transport in a density modification experiment on the TFTR tokamak
[DE91-018215] N92-10663
Geometric phase, rotational transforms and adiabatic invariants in toroidal magnetic fields
[DE91-018419] N92-10667
Stabilization of the m = 1 tearing mode by resonance detuning
[DE91-018423] N92-10668
THOMSON-CSF, ORSAY (FRANCE).
Highlights of material research for optoelectronics in the eighties, trends and challenges for the nineties N92-10486
TOKYO UNIV. (JAPAN).
Laser interferometer (TENKO-10 and -100) for gravitational wave antenna development
[ISAS-640] N92-10189
Theoretical estimation of the vibrational temperatures of N2 molecules in the ionosphere and in the laboratory simulated plasma
[ISAS-642] N92-10258
Electron temperatures in the E-region of the ionosphere
[ISAS-641] N92-10259
TULANE UNIV., NEW ORLEANS, LA.
A grid-free method for high Reynolds number flow around an immersed elastic structure
[AD-A239851] N92-10013
TURKU UNIV. (FINLAND).
Dromions: The movie N92-10370
Searches for heavy neutrinos from decays of the Z N92-10395
Shape coexistence in transitional (132,133,134)Ba N92-10401
A new line-narrowing method LOMEP N92-10438
Strong magnetic compression of spin-polarized hydrogen N92-10480
A band theoretical study on the electronic properties in the phase transition CuAu 1 to CuAu 2 N92-10488
Photoinduced superconductivity in films of YBaCuO N92-10502
Valence electron states of the Bi-Sr-Ca-Cu-O high-T(sub c) compound N92-10503
NMR and ESR experiments on solid molecular hydrogen containing atomic hydrogen N92-10510
NMR pulse responses of pairs of triads of 1/2 spins in solids N92-10511
The normal incidence grating inverse photoemission spectrometer in the energy range 8-28 eV N92-10516
Surface characterization of coated powders with XPS: Al2O3-SiO2 coated TiO2 pigments N92-10520
The crystal structure and moisture sensitivity of (+)-4-(1-(2,3 dimethylphenyl) ethyl) 1H-imidazole hydrochloride N92-10522
Scanning tunneling microscopy of polysialic acid N92-10538
Performance tests of ERNE HED sensor N92-10562
Properties of shocked relativistic jets N92-10564
The stability of the planetary triangular Lagrange points N92-10568
Electronics of the cosmic ray air shower array at Turku (Finland) N92-10574
Self-regulation mechanisms in galactic discs N92-10576
Explanation for optical frequency dependent polarization in blazars N92-10577
Double radio sources as standard rods of testing cosmological models N92-10578

U

UNISYS CORP., RESTON, VA.
Software Technology for Adaptable, Reliable Systems (STARS): Domain specific environment repository composite paradigm report
[AD-A240107] N92-10328
Software Technology for Adaptable, Reliable Systems (STARS): UUS40 risk-reduction reasoning-based development paradigm tailored to Navy C2 systems
[AD-A240108] N92-10329
Software Technology for Adaptable, Reliable Systems (STARS): US40-STARS reuse concept of operations. Volume 1: Version 0.5-draft
[AD-A240109] N92-10330
UNIVERSAL ENERGY SYSTEMS, INC., DAYTON, OH.
Thermal energy storage and heat transfer support program. Volume 1: Task-1 heat transport system study copper-water and steel-sodium DWAHP
[AD-A239928] N92-10176
Thermal energy storage and heat transfer support program. Task-5 heat pipe life test study. Facilities upgrading and maintenance
[AD-A239929] N92-10177
Thermal energy storage and heat transfer support program. Volume 2: Task 4 Thermionic energy conversion studies
[AD-A239968] N92-10178
UNIVERSITEIT TWENTE, ENSCHEDE (NETHERLANDS).
The connectivity of the basis graph of a branching greedoid
[MEMO-937] N92-10341
Some results on constrained controllability in discrete-time convex processes
[MEMO-926] N92-10342
UNIVERSITY OF NORTHEAST LOUISIANA, MONROE.
Flood routing of the Maja outflow across Xanthe Terra N92-10780
UNIVERSITY OF SOUTHERN MISSISSIPPI, HATTIESBURG.
Auditory and visual evoked potentials as a function of sleep deprivation and irregular sleep
[AD-A240097] N92-10281
UTAH UNIV., SALT LAKE CITY.
OMVPE growth of InAsSbBi and related alloys using new organometallic group V sources
[AD-A239939] N92-10703

V

VIRGINIA POLYTECHNIC INST. AND STATE UNIV., BLACKSBURG.
The biological consequences of climate changes: An ecological and economic assessment N92-10235
VIRGINIA UNIV., CHARLOTTESVILLE.
Experiments on the nuclear interactions of pions and electrons
[DE91-017929] N92-10623
Inclusive quasielastic and deep inelastic electron scattering at high energies
[DE91-018755] N92-10633
A Martian global groundwater model N92-10769
Role of groundwater in formation of Martian channels N92-10770
Role of artesian groundwater in forming Martian permafrost features N92-10771
Charged-particle induced alterations of surfaces in the outer solar system N92-10838

W

WARSAW UNIV. (POLAND).
Observations on very neutron-rich nuclei below Z = 50 N92-10402
WASHINGTON STATE UNIV., PULLMAN.
Ground state properties of a He-3 impurity in liquid He-4 monolayers
[AD-A239993] N92-10078
Surface effect on optical bistability in coupled exciton-phonon systems inside a cavity
[AD-A240026] N92-10643
Polarizabilities of trans and cis polyacetylene and interactions among chains in crystalline polyacetylene
[AD-A240025] N92-10705
WASHINGTON UNIV., SAINT LOUIS, MO.
The Geologic Remote Sensing Field Experiment (GRSFE) N92-10844
Image retrieval and processing system version 2.0 development work N92-10930
WASHINGTON UNIV., SEATTLE.
Sea ice elastic moduli: Determination of Biot parameters using in-field velocity measurements
[AD-A239803] N92-10275
Optical properties of CO2 ice and CO2 snow from ultraviolet to infrared: Application to frost deposits and clouds on Mars N92-10821
Energy coupling in catastrophic collisions N92-10862
Compositional variability of the Martian surface N92-10931
Long-term neutrino flux integrations
[DE91-013903] N92-10967
Solar and supernova neutrino interactions
[DE91-013905] N92-10968
WELLESLEY COLL., MA.
Dynamics and structure of planetary rings N92-10935
WESTINGHOUSE HANFORD CO., RICHLAND, WA.
Air pulsed plate liquid-liquid extractor simulation
[DE91-018155] N92-10172
PATRAN and P/THERMAL applications for thermal modeling
[DE91-017767] N92-10320
WINAND STARING CENTRE, WAGENINGEN (NETHERLANDS).
Remote sensing and watershed modelling: Towards a hydrological interface model
[BCRS-90-42] N92-10216

Y

YALE UNIV., NEW HAVEN, CT.
Fear-potentiated startle as a model system for analyzing learning and memory
[AD-A239994] N92-10284
Preparation and characterization of high temperature superconductor film surfaces
[AD-A240118] N92-10706
YORK UNIV. (ONTARIO).
Surface electrochemistry of Chloro(phthalocyaninato)rhodium(III) species, and oxygen reduction electrocatalysis, formation of a dimeric species
[AD-A240148] N92-10104

Typical Contract Number Index Listing

Listings in this index are arranged alphanumerically by contract number. Under each contract number the accession numbers denoting documents that have been produced as a result of research done under that contract are arranged in ascending order. The accession number denotes the number by which the citation is identified.

AF PROJ. ILIR N92-10269
AF PROJ. 2304 ..... N92-10144
N92-10201
N92-10352
AF PROJ. 2305 ..... N92-10706
AF PROJ. 2307 ..... N92-10016
AF PROJ. 2308 ..... N92-10062
N92-10179
AF PROJ. 2312 ..... N92-10245
N92-10280
N92-10284
N92-10285
AF PROJ. 2313 ..... N92-10286
N92-10612
AF PROJ. 2707 ..... N92-10181
AF PROJ. 3484 ..... N92-10142
AF PROJ. 6670 ..... N92-10270
AF PROJ. 7755 ..... N92-10013
AF PROJ. 9993 ..... N92-10674
AF-AFOSR-0078-89 ..... N92-10352
AF-AFOSR-0140-88 ..... N92-10286
AF-AFOSR-0214-90 ..... N92-10142
AF-AFOSR-0269-86 ..... N92-10144
AF-AFOSR-0270-90 ..... N92-10280
AF-AFOSR-0271-90 ..... N92-10181
AF-AFOSR-0295-89 ..... N92-10013
AF-AFOSR-0306-90 ..... N92-10706
AF-AFOSR-0312-89 ..... N92-10179
AF-AFOSR-0336-87 ..... N92-10284
AF-AFOSR-0344-90 ..... N92-10245
AF-AFOSR-0353-87 ..... N92-10612
AF-AFOSR-0383-89 ..... N92-10285
AF-AFOSR-0486-89 ..... N92-10201
AF-AFOSR-0541-89 ..... N92-10062
A87/M/124 ..... N92-10277
A89/KLU/321 ..... N92-10115
A90/KL/621 ..... N92-10966
DA PROJ. 1L1-61102-AH-47 ..... N92-10597
DA PROJ. 1L1-62211-A-47A N92-10195
DA PROJ. 1L7-62786-AH-20 ..... N92-10103
DA PROJ. 3E1-62777-A-878 ..... N92-10611
DA PROJ. 3E1-62777-A-879 ..... N92-10281
DA PROJ. 3M1-62787-A-878 ..... N92-10278
DAAK70-85-C-0007 ..... N92-10103
DAAK70-87-C-0043 ..... N92-10103
DAAL03-86-G-0204 ..... N92-10350
DAAL03-89-K-0078 ..... N92-10155
DAAL03-90-G-0103 ..... N92-10350
DACA76-86-C-0018 ..... N92-10217
DAMD17-88-C-8016 ..... N92-10281
DAMD17-88-Z-8008 ..... N92-10278
DE-AC02-76CH-00016 ..... N92-10092
N92-10683
N92-10688
DE-AC02-76CH-03073 ..... N92-10663
DE-AC02-76ER-13065 ..... N92-10630
DE-AC02-78ET-51013 ..... N92-10649
DE-AC02-83CH-10093 ..... N92-10111
N92-10241
DE-AC03-76SF-00515 ..... N92-10149
N92-10323
N92-10727
DE-AC03-82ER-13000 ..... N92-10683
DE-AC03-89ER-51114 ..... N92-10661
N92-10662
N92-10664
N92-10665
N92-10671
DE-AC04-76DP-00789 ..... N92-10040
N92-10060
N92-10061
N92-10082
N92-10083
N92-10084
N92-10096
N92-10131
N92-10132
N92-10136
N92-10148
N92-10151
N92-10152
N92-10153
N92-10204
N92-10223
N92-10224
N92-10315
N92-10321
N92-10324
N92-10334
N92-10335
N92-10636
N92-10666
N92-10696
DE-AC05-76OR-00033 ..... N92-10174
DE-AC05-84OR-21400 ..... N92-10010
N92-10058
N92-10059
N92-10077
N92-10081
N92-10129
N92-10130
N92-10198
N92-10355
N92-10359
N92-10618
N92-10620
N92-10621
N92-10624
N92-10625
N92-10673
N92-10678
N92-10687
N92-10691
DE-AC06-76RL-01830 ..... N92-10076
N92-10242
N92-10243
N92-10244
DE-AC06-87RL-10930 ..... N92-10172
N92-10320
DE-AC07-76ID-01570 ..... N92-10099
N92-10113
N92-10193
N92-10672
DE-AC08-89NV-10630 ..... N92-10346
DE-AI08-78ET-44802 ..... N92-10261
DE-AS03-84ER-40136 ..... N92-10192
DE-AS05-80ER-10742 ..... N92-10683
DE-FG02-84ER-13299 ..... N92-10065
DE-FG02-84ER-53188 ..... N92-10629
DE-FG02-85ER-13436 ..... N92-10093
DE-FG02-85ER-60372 ..... N92-10266
DE-FG02-86ER-13484 ..... N92-10150
DE-FG02-86ER-13492 ..... N92-10627
DE-FG02-86ER-13519 ..... N92-10616
DE-FG02-86ER-13596 ..... N92-10617
DE-FG02-86ER-45229 ..... N92-10085
DE-FG02-87ER-13723 ..... N92-10660
DE-FG02-87ER-40334 ..... N92-10634
DE-FG02-87ER-60565 ..... N92-10337
DE-FG02-88ER-13933 ..... N92-10626
DE-FG02-88ER-25053 ..... N92-10596
DE-FG02-88ER-45367 ..... N92-10689
DE-FG02-90ER-61052 ..... N92-10273
DE-FG03-87ER-13658 ..... N92-10075
DE-FG03-87ER-25028 ..... N92-10322
DE-FG03-88ER-60693 ..... N92-10276
DE-FG03-89ER-53289 ..... N92-10622
DE-FG05-80ET-53088 ..... N92-10173
N92-10595
N92-10663
N92-10667
N92-10668
DE-FG05-85ER-40200 ..... N92-10632
DE-FG05-86ER-40261 ..... N92-10633
DE-FG05-86ER-40270 ..... N92-10628
DE-FG05-88ER-40390 ..... N92-10623
DE-FG05-88ER-45374 ..... N92-10094
DE-FG05-88ER-53279 ..... N92-10594
DE-FG05-89ER-25080 ..... N92-10361
DE-FG05-90ER-40592 ..... N92-10637
DE-FG06-88ER-40427 ..... N92-10967
N92-10968
DNA PROJ. 125-AAXH N92-10264
DNA001-80-C-0246H N92-10264
DRET-89-34-001 ..... N92-10162
DTFA-01-L-83-4-10579 ..... N92-10019
F19628-86-K-0005 ..... N92-10263
F19628-87-C-0125 ..... N92-10159
F19628-88-C-0038 ..... N92-10219
F19628-88-D-0031 ..... N92-10328
N92-10329
N92-10330
F19628-89-C-0001 ..... N92-10143
F19628-90-C-0002 ..... N92-10019
F29601-87-C-0202 ..... N92-10704
F30602-88-D-0025 ..... N92-10642
F30602-88-D-0027 ..... N92-10327
F33615-84-C-3202 ..... N92-10598
F33615-84-C-3404 ..... N92-10101
F33615-86-C-2600 ..... N92-10100
F33615-86-C-2722 ..... N92-10227
F33615-87-C-2738 ..... N92-10176
N92-10177
N92-10178
F33615-88-C-2844 ..... N92-10226
F33615-89-C-2970 ..... N92-10157
F40600-87-C-0002 ..... N92-10026
F40600-89-C-0004 ..... N92-10188
F40701-88-C-0089 ..... N92-10030
F49620-86-C-0133 ..... N92-10180
F49620-89-C-0038 ..... N92-10265
JPL-957723 ..... N92-10971
MDA903-82-0353 ..... N92-10283
MDA903-90-C-0004 ..... N92-10715
NAGW-1 ..... N92-10940
NAGW-28 ..... N92-10828
NAGW-129 ..... N92-10781
NAGW-185 ..... N92-10952
NAGW-285 ..... N92-10768
NAGW-310 ..... N92-10904
NAGW-419 ..... N92-10294
NAGW-437 ..... N92-10793
N92-10873
NAGW-590 ..... N92-10902
NAGW-642 ..... N92-10881
NAGW-748 ..... N92-10816
N92-10818
N92-10823
N92-10828
N92-10831
NAGW-769 ..... N92-10899
NAGW-940 ..... N92-10954
N92-10955
NAGW-960 ..... N92-10949
NAGW-965 ..... N92-10293
NAGW-1107 ..... N92-10896
N92-10898
N92-10899
N92-10901
N92-10937
NAGW-1172 ..... N92-10954
N92-10955
NAGW-1180 ..... N92-10960
NAGW-1378 ..... N92-10956
NAGW-1390 ..... N92-10905
NAGW-1720 ..... N92-10953
NAGW-1734 ..... N92-10821

NAGW-1780 ..... N92-10907
N92-10955
NAGW-1881 ..... N92-10877
NAGW-1941 ..... N92-10932
NAGW-1953 ..... N92-10933
NAGW-2037 ..... N92-10806
N92-10823
N92-10824
N92-10825
NAGW-2061 ..... N92-10936
N92-10937
N92-10945
N92-10946
N92-10947
NAGW-2084 ..... N92-10836
NAGW-2085 ..... N92-10891
NAGW-2171 ..... N92-10906
NAGW-2176 ..... N92-10939
NAGW-2187 ..... N92-10906
NAGW-2199 ..... N92-10846
NAGW-2215 ..... N92-10941
NAGW-2336 ..... N92-10908
NAG1-1063 ..... N92-10071
NAG1-1065 ..... N92-10347
NAG1-1327 ..... N92-10037
NAG2-419 ..... N92-10615
NAG2-668 ..... N92-10299
NAG3-520 ..... N92-10012
NAG3-1008 ..... N92-10220
NAG3-1034 ..... N92-10205
NAG3-1108 ..... N92-10593
NAG5-1188 ..... N92-10724
NAG8-790 ..... N92-10676
NAG9-435 ..... N92-10303
NASA ORDER C-99066-G N92-10345
NASA ORDER W-16180 ..... N92-10739
NASA-PGP-151-01-70-56-00 ..... N92-10832
NASW-4003 ..... N92-10043
NASW-4234 ..... N92-10031
N92-10032
N92-10033
NASW-4495 ..... N92-10895
NASW-4574 ..... N92-10248
N92-10961
NASW-4618 ..... N92-10892
NAS1-17432 ..... N92-10069
NAS1-18460 ..... N92-10267
NAS1-18605 ..... N92-10171
N92-10348
N92-10349
NAS7-918 ..... N92-10125
N92-10126
N92-10146
N92-10609
NAS8-36955 ..... N92-10042
N92-10079
N92-10080
N92-10088
N92-10112
N92-10160
N92-10200
N92-10301
N92-10332
N92-10340
N92-10613
N92-10638
N92-10639
N92-10676
NAS8-38078 ..... N92-10183
NCA2-313 ..... N92-10293
NCC2-387 ..... N92-10034
N92-10036
N92-10282
N92-10290
N92-10291
N92-10292
N92-10293
N92-10294
N92-10306
N92-10307
N92-10308
N92-10309
N92-10310
N92-10311
N92-10312
N92-10333
N92-10343
N92-10344
N92-10711
NCC2-408 ..... N92-10291
NCC2-452 ..... N92-10004
NCC2-559 ..... N92-10304
NCC2-569 ..... N92-10209
NCC9-16 ..... N92-10313
N92-10314
N92-10712
NCC9-19 ..... N92-10846
NGL-05-020-014 ..... N92-10850
NGT-50482 ..... N92-10835
NGT-70056 ..... N92-10850
NR PROJ. RM3-5-G-97 ..... N92-10274
NR PROJ. RR0-00-N-0 ..... N92-10675
NR PROJ. RS3-4-A-50 ..... N92-10072
NSF AST-87-21880 ..... N92-10850
NSF DMS-88-11863 ..... N92-10349
NSG-1577 ..... N92-10170
NSG-7156 ..... N92-10835
N92-10836
NSG-7339 ..... N92-10184
N00014-83-K-0125 ..... N92-10716
N00014-84-G-0201 ..... N92-10104
N00014-86-K-0191 ..... N92-10102
N00014-86-K-0691 ..... N92-10349
N00014-88-C-0714 ..... N92-10154
N00014-88-K-0617 ..... N92-10246
N00014-89-J-1176 ..... N92-10206
N00014-90-C-0143 ..... N92-10145
N00014-90-C-2309 ..... N92-10063
N00014-90-J-1193 ..... N92-10078
N92-10643
N92-10705
N00014-91-J-1447 ..... N92-10703
N00039-88-C-0065 ..... N92-10137
N92-10138
N92-10139
N00039-91-C-0072 ..... N92-10275
RICIS PROJ. ET-26 ..... N92-10712
RICIS PROJ. SE-19 ..... N92-10314
RICIS PROJ. SE-26 ..... N92-10313
SWRI PROJ. 05-3531 ..... N92-10303
SWRI PROJ. 05-3744 ..... N92-10712
W-31-109-ENG-38 ..... N92-10085
N92-10086
N92-10097
N92-10098
N92-10319
N92-10338
N92-10339
N92-10635
N92-10640
N92-10641
N92-10682
N92-10692
N92-10693
N92-10694
N92-10696
N92-10697
N92-10698
N92-10699
N92-10700
N92-10701
N92-10702
N92-10707
W-7405-ENG-36 ..... N92-10074
N92-10095
N92-10134
N92-10135
N92-10168
N92-10169
N92-10191
N92-10218
N92-10260
N92-10295
N92-10296
N92-10297
N92-10298
N92-10316
N92-10318
N92-10354
N92-10356
N92-10357
N92-10358
N92-10684
N92-10685
N92-10686
N92-10726
N92-10969
N92-10970
W-7405-ENG-48 ..... N92-10133
N92-10187
N92-10190
N92-10309
N92-10317
N92-10325
N92-10326
N92-10336
N92-10619
N92-10631
N92-10658
N92-10669
N92-10670
N92-10725
N92-10739
W-7405-ENG-82 ..... N92-10690
N92-10693
N92-10695
474-42-10 ..... N92-10055
505-60-11 ..... N92-10011
505-62-21 ..... N92-10345
505-62-52 ..... N92-10012
505-63-1A N92-10064
505-63-40 ..... N92-10205
505-63-50-05 ..... N92-10067
505-63-51 ..... N92-10195
505-64-13 ..... N92-10024
505-64-13-22 ..... N92-10017
505-66-01-02 ..... N92-10027
505-68-11 ..... N92-10003
505-68-10 ..... N92-10002
505-68-91-12 ..... N92-10005
505-90-52 ..... N92-10289
505-90-52-01 ..... N92-10171
N92-10348
N92-10349
505-90-52-02 ..... N92-10302
506-40-41-02 ..... N92-10006
506-40-91-01 ..... N92-10161
506-42-31 ..... N92-10044
506-43-11-01 ..... N92-10069
506-44-21 ..... N92-10680
535-03-11-03 ..... N92-10598
590-13-00 ..... N92-10221
650-60-15 ..... N92-10116
665-45-20 ..... N92-10208
665-45-30-01 ..... N92-10267
763-23-41-85 ..... N92-10203
920-00-00 ..... N92-10057

Typical Report Number Index Listing

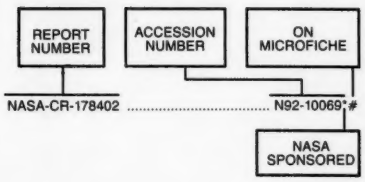

Listings in this index are arranged alphanumerically by report number. The accession number denotes the number by which the citation is identified. An asterisk (*) indicates that the item is a NASA report. A pound sign (#) indicates that the item is available on microfiche.

A-90161 ..... N92-10011* #
A-91242 ..... N92-10003* #

AD-A239370 ..... N92-10217 #
AD-A239436 ..... N92-10305 #
AD-A239750 ..... N92-10145 #
AD-A239801 ..... N92-10274 #
AD-A239803 ..... N92-10275 #
AD-A239805 ..... N92-10100 #
AD-A239813 ..... N92-10154 #
AD-A239816 ..... N92-10262 #
AD-A239819 ..... N92-10283 #
AD-A239822 ..... N92-10350 #
AD-A239827 ..... N92-10030 #
AD-A239841 ..... N92-10155 #
AD-A239850 ..... N92-10642 #
AD-A239851 ..... N92-10013 #
AD-A239852 ..... N92-10019 #
AD-A239857 ..... N92-10175 #
AD-A239858 ..... N92-10351 #
AD-A239859 ..... N92-10188 #
AD-A239860 ..... N92-10072 #
AD-A239861 ..... N92-10087 #
AD-A239868 ..... N92-10137 #
AD-A239869 ..... N92-10138 #
AD-A239870 ..... N92-10139 #
AD-A239880 ..... N92-10140 #
AD-A239892 ..... N92-10141 #
AD-A239910 ..... N92-10268 #
AD-A239915 ..... N92-10714 #
AD-A239918 ..... N92-10610 #
AD-A239928 ..... N92-10176 #
AD-A239929 ..... N92-10177 #
AD-A239931 ..... N92-10226 #
AD-A239932 ..... N92-10227 #
AD-A239936 ..... N92-10026 #
AD-A239939 ..... N92-10703 #
AD-A239940 ..... N92-10674 #
AD-A239941 ..... N92-10278 #
AD-A239943 ..... N92-10142 #
AD-A239947 ..... N92-10156 #
AD-A239948 ..... N92-10014 #
AD-A239949 ..... N92-10015 #
AD-A239950 ..... N92-10022 #
AD-A239951 ..... N92-10041 #
AD-A239955 ..... N92-10704 #
AD-A239956 ..... N92-10016 #
AD-A239957 ..... N92-10675 #
AD-A239967 ..... N92-10263 #
AD-A239968 ..... N92-10178 #
AD-A239980 ..... N92-10199 #
AD-A239982 ..... N92-10157 #
AD-A239983 ..... N92-10327 #
AD-A239984 ..... N92-10101 #
AD-A239985 ..... N92-10219 #
AD-A239987 ..... N92-10102 #
AD-A239988 ..... N92-10269 #
AD-A239989 ..... N92-10270 #
AD-A239992 ..... N92-10611 #
AD-A239993 ..... N92-10078 #
AD-A239994 ..... N92-10284 #

AD-A240000 ..... N92-10264 #
AD-A240001 ..... N92-10279 #
AD-A240004 ..... N92-10179 #
AD-A240006 ..... N92-10612 #
AD-A240007 ..... N92-10280 #
AD-A240022 ..... N92-10715 #
AD-A240023 ..... N92-10288 #
AD-A240025 ..... N92-10705 #
AD-A240026 ..... N92-10643 #
AD-A240031 ..... N92-10143 #
AD-A240037 ..... N92-10158 #
AD-A240044 ..... N92-10144 #
AD-A240045 ..... N92-10245 #
AD-A240046 ..... N92-10352 #
AD-A240049 ..... N92-10201 #
AD-A240050 ..... N92-10180 #
AD-A240057 ..... N92-10062 #
AD-A240059 ..... N92-10063 #
AD-A240060 ..... N92-10353 #
AD-A240061 ..... N92-10271 #
AD-A240062 ..... N92-10644 #
AD-A240063 ..... N92-10159 #
AD-A240076 ..... N92-10716 #
AD-A240097 ..... N92-10281 #
AD-A240100 ..... N92-10103 #
AD-A240107 ..... N92-10328 #
AD-A240108 ..... N92-10329 #
AD-A240109 ..... N92-10330 #
AD-A240115 ..... N92-10246 #
AD-A240116 ..... N92-10360 #
AD-A240118 ..... N92-10706 #
AD-A240121 ..... N92-10285 #
AD-A240122 ..... N92-10023 #
AD-A240124 ..... N92-10194 #
AD-A240127 ..... N92-10206 #
AD-A240131 ..... N92-10181 #
AD-A240133 ..... N92-10286 #
AD-A240139 ..... N92-10265 #
AD-A240142 ..... N92-10207 #
AD-A240144 ..... N92-10597 #
AD-A240148 ..... N92-10104 #

AD-E040098 ..... N92-10274 #
AD-E040115 ..... N92-10275 #

AEDC-TR-91-11 ..... N92-10026 #
AEDC-TR-91-13-PHASE-2 ..... N92-10188 #

AFIT/CI/CIA-90-041D ..... N92-10351 #

AFOSR-91-0708TR ..... N92-10285 #
AFOSR-91-0713TR ..... N92-10062 #
AFOSR-91-0715TR ..... N92-10179 #
AFOSR-91-0716TR ..... N92-10201 #
AFOSR-91-0719TR ..... N92-10144 #
AFOSR-91-0722TR ..... N92-10352 #
AFOSR-91-0725TR ..... N92-10280 #
AFOSR-91-0726TR ..... N92-10180 #
AFOSR-91-0731TR ..... N92-10612 #
AFOSR-91-0732TR ..... N92-10245 #
AFOSR-91-0733TR ..... N92-10181 #
AFOSR-91-0744TR ..... N92-10706 #
AFOSR-91-0749TR ..... N92-10284 #
AFOSR-91-0757TR ..... N92-10286 #

AGARD-LS-180 ..... N92-10106 #

AIAA-91-3518 ..... N92-10221* #

AL-TR-1991-0045 ..... N92-10013 #

ALS/TR-90-021 ..... N92-10153 #

AMSEL-NV-TR-0097 ..... N92-10194 #

ANL-HEP-TR-91-69 ..... N92-10641 #

ANL-TRANS-90-19 ..... N92-10640 #

ANL-91/12 ..... N92-10707 #
ANL-91/32 ..... N92-10339 #

ANL/CP-71551 ..... N92-10086 #

ANL/CP-72131 ..... N92-10694 #
ANL/CP-72749 ..... N92-10097 #
ANL/CP-73356 ..... N92-10698 #
ANL/CP-73571 ..... N92-10098 #
ANL/CP-73745 ..... N92-10682 #
ANL/CP-73930 ..... N92-10702 #
ANL/CP-73957 ..... N92-10701 #
ANL/CP-74007 ..... N92-10338 #
ANL/CP-74017 ..... N92-10697 #
ANL/CP-74018 ..... N92-10696 #
ANL/CP-74019 ..... N92-10085 #
ANL/CP-74039 ..... N92-10693 #
ANL/CP-74040 ..... N92-10692 #
ANL/CP-74043 ..... N92-10700 #
ANL/CP-74044 ..... N92-10699 #

ANL/MCS-TM-137 ..... N92-10319 #

APS-LS-141-REV ..... N92-10635 #

AR-006-821 ..... N92-10089 #

ARI-RN-91-88 ..... N92-10283 #

ARI-RP-91-10 ..... N92-10714 #

ARO-26922.13-EL ..... N92-10155 #
ARO-27868.10-MA ..... N92-10350 #

ATC-178 ..... N92-10019 #

AVSCOM-TR-91-C-020 ..... N92-10195* #

AWE-RE-0-20/90 ..... N92-10247 #

B-240547 ..... N92-10709 #
B-245559 ..... N92-10708 #

BCRS-90-29 ..... N92-10215 #
BCRS-90-42 ..... N92-10216 #

BFLRF-269 ..... N92-10103 #

BI-TP-90/35 ..... N92-10385 #

BNL-45591 ..... N92-10683 #
BNL-46454 ..... N92-10688 #
BNL-46492 ..... N92-10092 #

BR116726 ..... N92-10247 #

CERN-PPE/90-141 ..... N92-10392 #
CERN-PPE/90-153 ..... N92-10387 #
CERN-PPE/90-154 ..... N92-10390 #
CERN-PPE/90-155 ..... N92-10388 #
CERN-PPE/90-180 ..... N92-10391 #
CERN-PPE/91 ..... N92-10389 #

CONF-900986-1 ..... N92-10357 #
CONF-910197-2 ..... N92-10696 #
CONF-910505-405 ..... N92-10636 #
CONF-910572-2 ..... N92-10097 #
CONF-910609-21 ..... N92-10662 #
CONF-910635-13 ..... N92-10699 #
CONF-910635-14 ..... N92-10700 #
CONF-910640-5 ..... N92-10621 #
CONF-910640-43 ..... N92-10191 #
CONF-910640-44 ..... N92-10152 #
CONF-910707-1 ..... N92-10678 #
CONF-910707-5 ..... N92-10682 #
CONF-910736-18 ..... N92-10691 #
CONF-910736-19 ..... N92-10692 #
CONF-910736-20 ..... N92-10693 #
CONF-910736-22 ..... N92-10697 #
CONF-910736-23 ..... N92-10702 #
CONF-910855-1 ..... N92-10701 #
CONF-910867-1 ..... N92-10672 #
CONF-910869-3 ..... N92-10130 #
CONF-910869-4 ..... N92-10665 #
CONF-910869-6 ..... N92-10671 #
CONF-910869-8 ..... N92-10673 #
CONF-910881-2 ..... N92-10726 #
CONF-910903-11 ..... N92-10684 #

CONF-910909-9 ..... N92-10098 #
CONF-910909-12 ..... N92-10086 #
CONF-910938-1 ..... N92-10095 #
CONF-910972-1 ..... N92-10625 #
CONF-911003-10 ..... N92-10082 #
CONF-911003-14 ..... N92-10085 #
CONF-911103-1 ..... N92-10335 #
CONF-911103-3-REV-1 ..... N92-10317 #
CONF-911103-4 ..... N92-10336 #
CONF-911103-5 ..... N92-10315 #
CONF-911103-6 ..... N92-10297 #
CONF-911107-3 ..... N92-10316 #
CONF-911107-6 ..... N92-10618 #
CONF-911107-8 ..... N92-10084 #
CONF-911107-15 ..... N92-10619 #
CONF-911107-16 ..... N92-10620 #
CONF-911107-19 ..... N92-10354 #
CONF-911107-27-EXTD-ABST ..... N92-10355 #
CONF-911107-28-EXTD-ABST ..... N92-10058 #
CONF-911125-1 ..... N92-10132 #
CONF-911129-1 ..... N92-10334 #
CONF-911130-1 ..... N92-10295 #
CONF-911130-2 ..... N92-10296 #
CONF-911133-1 ..... N92-10074 #
CONF-911147-1-EXTD-ABST ..... N92-10617 #
CONF-911152-1 ..... N92-10968 #
CONF-911153-1 ..... N92-10967 #
CONF-911162-1 ..... N92-10129 #
CONF-911164-1 ..... N92-10298 #
CONF-911165-1 ..... N92-10218 #
CONF-911165-2 ..... N92-10260 #
CONF-911178-1 ..... N92-10092 #
CONF-9010183-5 ..... N92-10633 #
CONF-9102131 ..... N92-10148 #
CONF-9105113-2 ..... N92-10727 #
CONF-9105153 ..... N92-10713 #
CONF-9105202 ..... N92-10300 #
CONF-9105238-5 ..... N92-10624 #
CONF-9105251-1 ..... N92-10725 #
CONF-9105252-1 ..... N92-10169 #
CONF-9106182-2 ..... N92-10661 #
CONF-9106265-1 ..... N92-10688 #
CONF-9107115-35 ..... N92-10683 #
CONF-9107115-37 ..... N92-10190 #
CONF-9107115-38 ..... N92-10187 #
CONF-9107115-44 ..... N92-10151 #
CONF-9107115-45 ..... N92-10324 #
CONF-9107155-3 ..... N92-10687 #
CONF-9107171-1 ..... N92-10698 #
CONF-9108114-3 ..... N92-10077 #
CONF-9108133-2 ..... N92-10113 #
CONF-9108140-1 ..... N92-10686 #
CONF-9108141-1 ..... N92-10969 #
CONF-9108146-1 ..... N92-10133 #
CONF-9108155-1 ..... N92-10323 #
CONF-9109121-4 ..... N92-10359 #
CONF-9109156-2 ..... N92-10694 #
CONF-9109213-1 ..... N92-10685 #
CONF-9109226-10 ..... N92-10168 #
CONF-9109226-11 ..... N92-10059 #
CONF-9109226-13 ..... N92-10060 #
CONF-9109226-14 ..... N92-10061 #
CONF-9109230-5 ..... N92-10338 #
CONF-9109232-2 ..... N92-10040 #
CONF-9109252-1 ..... N92-10666 #
CONF-9109254-1 ..... N92-10970 #
CONF-9109255-1 ..... N92-10241 #
CONF-9109257-1 ..... N92-10010 #
CONF-9110189-1 ..... N92-10204 #
CONF-9110196-1 ..... N92-10320 #
CONF-9110196-2 ..... N92-10096 #
CONF-9110199-1 ..... N92-10134 #
CONF-9110199-2 ..... N92-10135 #
CONF-9110200-1 ..... N92-10356 #
CONF-9110202-1 ..... N92-10131 #
CONF-9110202-2 ..... N92-10136 #

CSL-TR-89-400 ..... N92-10294* #

DE91-008178 ..... N92-10334 #
DE91-008606 ..... N92-10295 #
DE91-009971 ..... N92-10074 #
DE91-009973 ..... N92-10296 #
DE91-010864 ..... N92-10335 #
DE91-011502 ..... N92-10315 #
DE91-011539 ..... N92-10336 #
DE91-012259 ..... N92-10617 #
DE91-013205 ..... N92-10297 #
DE91-013373 ..... N92-10316 #
DE91-013903 ..... N92-10967 #
DE91-013905 ..... N92-10968 #
DE91-014577 ..... N92-10618 #
DE91-014705 ..... N92-10084 #
DE91-015003 ..... N92-10111 #
DE91-015007 ..... N92-10241 #
DE91-015764 ..... N92-10619 #
DE91-015924 ..... N92-10620 #
DE91-015928 ..... N92-10678 #
DE91-016013 ..... N92-10354 #
DE91-016077 ..... N92-10218 #
DE91-016078 ..... N92-10260 #
DE91-016226 ..... N92-10621 #
DE91-016277 ..... N92-10129 #
DE91-016304 ..... N92-10298 #
DE91-016565 ..... N92-10317 #
DE91-016962 ..... N92-10616 #
DE91-017058 ..... N92-10204 #
DE91-017215 ..... N92-10225 #
DE91-017304 ..... N92-10682 #
DE91-017407 ..... N92-10622 #
DE91-017441 ..... N92-10658 #
DE91-017452 ..... N92-10132 #
DE91-017473 ..... N92-10092 #
DE91-017475 ..... N92-10683 #
DE91-017479 ..... N92-10688 #
DE91-017518 ..... N92-10318 #
DE91-017541 ..... N92-10133 #
DE91-017549 ..... N92-10093 #
DE91-017659 ..... N92-10725 #
DE91-017664 ..... N92-10187 #
DE91-017668 ..... N92-10190 #
DE91-017681 ..... N92-10355 #
DE91-017684 ..... N92-10625 #
DE91-017688 ..... N92-10058 #
DE91-017700 ..... N92-10319 #
DE91-017706 ..... N92-10266 #
DE91-017712 ..... N92-10626 #
DE91-017716 ..... N92-10223 #
DE91-017718 ..... N92-10148 #
DE91-017721 ..... N92-10224 #
DE91-017733 ..... N92-10346 #
DE91-017767 ..... N92-10320 #
DE91-017783 ..... N92-10627 #
DE91-017800 ..... N92-10081 #
DE91-017823 ..... N92-10191 #
DE91-017830 ..... N92-10168 #
DE91-017836 ..... N92-10640 #
DE91-017840 ..... N92-10076 #
DE91-017845 ..... N92-10096 #
DE91-017851 ..... N92-10337 #
DE91-017852 ..... N92-10689 #
DE91-017854 ..... N92-10065 #
DE91-017859 ..... N92-10059 #
DE91-017916 ..... N92-10659 #
DE91-017927 ..... N92-10628 #
DE91-017929 ..... N92-10623 #
DE91-017931 ..... N92-10361 #
DE91-017940 ..... N92-10322 #
DE91-017945 ..... N92-10077 #
DE91-017953 ..... N92-10276 #
DE91-017954 ..... N92-10075 #
DE91-017982 ..... N92-10060 #
DE91-017987 ..... N92-10082 #
DE91-018002 ..... N92-10151 #
DE91-018003 ..... N92-10356 #
DE91-018004 ..... N92-10134 #
DE91-018005 ..... N92-10135 #
DE91-018010 ..... N92-10094 #
DE91-018011 ..... N92-10594 #
DE91-018012 ..... N92-10637 #
DE91-018014 ..... N92-10635 #
DE91-018015 ..... N92-10149 #
DE91-018017 ..... N92-10357 #
DE91-018018 ..... N92-10684 #
DE91-018024 ..... N92-10095 #
DE91-018028 ..... N92-10969 #
DE91-018040 ..... N92-10169 #
DE91-018043 ..... N92-10685 #
DE91-018046 ..... N92-10686 #
DE91-018052 ..... N92-10970 #
DE91-018074 ..... N92-10713 #
DE91-018130 ..... N92-10321 #
DE91-018151 ..... N92-10323 #
DE91-018152 ..... N92-10726 #
DE91-018155 ..... N92-10172 #
DE91-018176 ..... N92-10010 #
DE91-018185 ..... N92-10661 #
DE91-018186 ..... N92-10662 #
DE91-018205 ..... N92-10690 #
DE91-018215 ..... N92-10663 #
DE91-018224 ..... N92-10687 #
DE91-018233 ..... N92-10691 #
DE91-018247 ..... N92-10624 #
DE91-018251 ..... N92-10130 #
DE91-018269 ..... N92-10192 #
DE91-018273 ..... N92-10660 #
DE91-018280 ..... N92-10629 #
DE91-018284 ..... N92-10150 #
DE91-018285 ..... N92-10630 #
DE91-018295 ..... N92-10631 #
DE91-018317 ..... N92-10664 #
DE91-018321 ..... N92-10665 #
DE91-018348 ..... N92-10083 #
DE91-018351 ..... N92-10061 #
DE91-018353 ..... N92-10040 #
DE91-018356 ..... N92-10666 #
DE91-018357 ..... N92-10636 #
DE91-018359 ..... N92-10152 #
DE91-018394 ..... N92-10261 #
DE91-018398 ..... N92-10324 #
DE91-018399 ..... N92-10136 #
DE91-018400 ..... N92-10131 #
DE91-018415 ..... N92-10727 #
DE91-018419 ..... N92-10667 #
DE91-018420 ..... N92-10173 #
DE91-018421 ..... N92-10595 #
DE91-018423 ..... N92-10668 #
DE91-018438 ..... N92-10153 #
DE91-018475 ..... N92-10273 #
DE91-018490 ..... N92-10669 #
DE91-018510 ..... N92-10198 #
DE91-018513 ..... N92-10358 #
DE91-018525 ..... N92-10632 #
DE91-018536 ..... N92-10692 #
DE91-018537 ..... N92-10693 #
DE91-018540 ..... N92-10097 #
DE91-018543 ..... N92-10694 #
DE91-018552 ..... N92-10085 #
DE91-018553 ..... N92-10695 #
DE91-018560 ..... N92-10338 #
DE91-018571 ..... N92-10086 #
DE91-018574 ..... N92-10098 #
DE91-018587 ..... N92-10696 #
DE91-018588 ..... N92-10697 #
DE91-018589 ..... N92-10698 #
DE91-018591 ..... N92-10641 #
DE91-018600 ..... N92-10699 #
DE91-018602 ..... N92-10242 #
DE91-018603 ..... N92-10243 #
DE91-018605 ..... N92-10244 #
DE91-018615 ..... N92-10700 #
DE91-018638 ..... N92-10701 #
DE91-018640 ..... N92-10702 #
DE91-018651 ..... N92-10670 #
DE91-018652 ..... N92-10325 #
DE91-018695 ..... N92-10099 #
DE91-018698 ..... N92-10174 #
DE91-018704 ..... N92-10707 #
DE91-018709 ..... N92-10113 #
DE91-018732 ..... N92-10671 #
DE91-018755 ..... N92-10633 #
DE91-018759 ..... N92-10193 #
DE91-018820 ..... N92-10672 #
DE91-018857 ..... N92-10359 #
DE91-018866 ..... N92-10673 #
DE91-018877 ..... N92-10300 #
DE91-018965 ..... N92-10596 #
DE91-018968 ..... N92-10634 #
DE91-019005 ..... N92-10339 #
DE91-019012 ..... N92-10326 #

DISA/DSSO-FD-4-91 ..... N92-10305 #

DNA-TR-89-55 ..... N92-10264 #

DOE/ER-13065/672 ..... N92-10630 #
DOE/ER-13299/7 ..... N92-10065 #
DOE/ER-13436/6 ..... N92-10093 #
DOE/ER-13484/5 ..... N92-10150 #
DOE/ER-13492/13 ..... N92-10627 #
DOE/ER-13519/5 ..... N92-10616 #
DOE/ER-13596/18 ..... N92-10617 #
DOE/ER-13658/T1 ..... N92-10075 #
DOE/ER-13723/3 ..... N92-10660 #
DOE/ER-13933/2 ..... N92-10626 #
DOE/ER-25028/T2 ..... N92-10322 #
DOE/ER-25053/6 ..... N92-10596 #
DOE/ER-25080/2 ..... N92-10361 #
DOE/ER-40136/T10 ..... N92-10192 #
DOE/ER-40200/261 ..... N92-10632 #
DOE/ER-40270/28 ..... N92-10628 #
DOE/ER-40334/7 ..... N92-10634 #
DOE/ER-40390/4 ..... N92-10623 #
DOE/ER-40427/09-N91 ..... N92-10968 #
DOE/ER-40427/10-N91 ..... N92-10967 #
DOE/ER-40592/1 ..... N92-10637 #
DOE/ER-45367/3 ..... N92-10689 #
DOE/ER-45374/3 ..... N92-10094 #
DOE/ER-53188/8 ..... N92-10629 #
DOE/ER-53279/1 ..... N92-10594 #
DOE/ER-53289/T1 ..... N92-10622 #
DOE/ER-60372/6 ..... N92-10266 #
DOE/ER-60565/5 ..... N92-10337 #
DOE/ER-60693/T1 ..... N92-10276 #
DOE/ER-61052/1 ..... N92-10273 #

DOE/ET-53088/501 ..... N92-10663 #
DOE/ET-53088/509 ..... N92-10667 #

DOE/ET-53088/511 ..... N92-10173 #
DOE/ET-53088/512 ..... N92-10595 #
DOE/ET-53088/516 ..... N92-10668 #

DOE/FE-0238P ..... N92-10225 #
DOE/FE-0239P ..... N92-10659 #

DOE/NV-10630/21 ..... N92-10346 #

DOE/PETC-TR/91/10 ..... N92-10174 #

DOE/RL-01830T-H7 ..... N92-10242 #
DOE/RL-01830T-H8 ..... N92-10243 #
DOE/RL-01830T-H10 ..... N92-10244 #

DOT/FAA/CT-TN91/30 ..... N92-10020 #

DOT/FAA/NR-91/1 ..... N92-10019 #

DTP/91/24 ..... N92-10614 #

D180-32725-1 ..... N92-10069* #

E-5837 ..... N92-10195* #
E-6460 ..... N92-10002* #
E-6502 ..... N92-10064* #
E-6518 ..... N92-10044* #
E-6523 ..... N92-10012* #
E-6554 ..... N92-10221* #
E-6561 ..... N92-10289* #
E-6587 ..... N92-10345* #
E-6607 ..... N92-10057* #
E-6614 ..... N92-10055* #

EGG-CS-9762 ..... N92-10099 #

EGG-M-91232 ..... N92-10113 #
EGG-M-91257 ..... N92-10672 #

EGG-MS-9726 ..... N92-10193 #

ESA-BR-75 ..... N92-10039 #

ESD-TR-91-208 ..... N92-10143 #

ETL-0586 ..... N92-10217 #

ETN-91-90016 ..... N92-10723
ETN-91-90020 ..... N92-10615*
ETN-91-90027 ..... N92-10162 #
ETN-91-90049 ..... N92-10215 #
ETN-91-90051 ..... N92-10216 #
ETN-91-90052 ..... N92-10029 #
ETN-91-90059 ..... N92-10068 #
ETN-91-90073 ..... N92-10039 #
ETN-91-99727 ..... N92-10342 #
ETN-91-99735 ..... N92-10341 #
ETN-91-99832 ..... N92-10210
ETN-91-99833 ..... N92-10588 #
ETN-91-99838 ..... N92-10362 #
ETN-91-99862 ..... N92-10247 #
ETN-91-99885 ..... N92-10614 #
ETN-91-99891 ..... N92-10018 #
ETN-91-99986 ..... N92-10114 #
ETN-91-99989 ..... N92-10115
ETN-91-99992 ..... N92-10277
ETN-91-99998 ..... N92-10966

FEL-90-A368 ..... N92-10966

FJSRL-TR-91-0001 ..... N92-10016 #

FSU-STATISTICS-TR-M-853 ..... N92-10350 #

GA-A-20552 ..... N92-10662 #
GA-A-20556 ..... N92-10664 #
GA-A-20569 ..... N92-10661 #
GA-A-20608 ..... N92-10665 #
GA-A-20627 ..... N92-10671 #

GA-C19465 ..... N92-10154 #

GAO/NSIAD-91-34 ..... N92-10709 #
GAO/NSIAD-91-259 ..... N92-10708 #

GAO/T-NSIAD-91-48 ..... N92-10710 #

GL-TR-90-0284 ..... N92-10219 #

GR-7670-1195(NP) ..... N92-10328 #
GR-7670-1219(NP) ..... N92-10329 #
GR-7670-1259(NP) ..... N92-10330 #

ICASE-91-70 ..... N92-10348* #
ICASE-91-74 ..... N92-10171* #
ICASE-91-76 ..... N92-10349* #

ICOMP-91-18 ..... N92-10345* #

IFSR-501 ..... N92-10663 #
IFSR-509 ..... N92-10667 #
IFSR-511 ..... N92-10173 #
IFSR-512 ..... N92-10595 #
IFSR-516 ..... N92-10668 #

IITRI-E06628-4-VOL-1 ..... N92-10137 #
IITRI-E06628-4-VOL-2 ..... N92-10138 #
IITRI-E06628-4-VOL-3 ..... N92-10139 #

INFORME-I-522/90 ..... N92-10068 #

INO-TM-4 ..... N92-10274 #

INT-PATENT-CLASS-B01J-29/10 ..... N92-10073*
INT-PATENT-CLASS-B05D-1/24 ..... N92-10070*
INT-PATENT-CLASS-B05D-5/12 ..... N92-10681*
INT-PATENT-CLASS-B43L-13/24 ..... N92-10186*

INT-PATENT-CLASS-C01B-31/04 ..... N92-10090*
INT-PATENT-CLASS-C23F-1/00 ..... N92-10681*

INT-PATENT-CLASS-F02R-9/52 ..... N92-10054*
INT-PATENT-CLASS-F16L-15/00 ..... N92-10197*

INT-PATENT-CLASS-G01L-5/16 ..... N92-10185*
INT-PATENT-CLASS-G01M-9/00 ..... N92-10185*

INT-PATENT-CLASS-H04N-7/13 ..... N92-10128*

IPPCZ-305 ..... N92-10650 #
IPPCZ-306 ..... N92-10652 #
IPPCZ-307 ..... N92-10653 #
IPPCZ-309 ..... N92-10127 #
IPPCZ-310 ..... N92-10651 #
IPPCZ-311 ..... N92-10679 #

IS-T-1545 ..... N92-10690 #
IS-T-1558 ..... N92-10695 #

ISAS-640 ..... N92-10189 #
ISAS-641 ..... N92-10259 #
ISAS-642 ..... N92-10258 #

ISBN-0-904947-30-0 ..... N92-10018 #
ISBN-0-915707-50-0 ..... N92-10228 #
ISBN-3-925-308-66-0 ..... N92-10210
ISBN-92-835-0630-8 ..... N92-10106 #
ISBN-92-9092-079-3 ..... N92-10039 #
ISBN-951-42-3087-6 ..... N92-10362 #

ISSN-0109-6605 ..... N92-10147 #
ISSN-0169-2690 ..... N92-10341 #
ISSN-0169-2690 ..... N92-10342 #
ISSN-0173-6256 ..... N92-10588 #
ISSN-0178-0719 ..... N92-10723
ISSN-0250-1589 ..... N92-10039 #
ISSN-0285-6808 ..... N92-10189 #
ISSN-0285-6808 ..... N92-10258 #
ISSN-0285-6808 ..... N92-10259 #
ISSN-0356-1852 ..... N92-10362 #
ISSN-0389-4010 ..... N92-10009 #
ISSN-0389-4010 ..... N92-10025 #
ISSN-0389-4010 ..... N92-10028 #
ISSN-0389-4010 ..... N92-10056 #
ISSN-0389-4010 ..... N92-10166 #
ISSN-0915-633X ..... N92-10645 #
ISSN-0915-633X ..... N92-10646 #
ISSN-0915-633X ..... N92-10647 #
ISSN-0915-633X ..... N92-10648 #
ISSN-0915-633X ..... N92-10649 #
ISSN-0915-633X ..... N92-10654 #
ISSN-0915-633X ..... N92-10655 #
ISSN-0915-633X ..... N92-10656 #
ISSN-0915-633X ..... N92-10657 #
ISSN-0932-3147 ..... N92-10210

IZF-1991-A-7 ..... N92-10115
IZF-1991-A-15 ..... N92-10277

JPL-D-7382 ..... N92-10116* #

JRC-RR-90-21 ..... N92-10332* #

L-16836 ..... N92-10161* #
L-16864 ..... N92-10006* #
L-16866 ..... N92-10005* #
L-16893 ..... N92-10027* #
L-16895 ..... N92-10208* #
L-16901 ..... N92-10302* #
L-16910 ..... N92-10067* #
L-16917 ..... N92-10017* #
L-16922 ..... N92-10024* #
L-16926-VOL-1 ..... N92-10598* #
L-16948 ..... N92-10677* #

LA-UR-91-702 ..... N92-10295 #
LA-UR-91-1031 ..... N92-10074 #
LA-UR-91-1100 ..... N92-10296 #
LA-UR-91-1665 ..... N92-10297 #
LA-UR-91-1802 ..... N92-10316 #
LA-UR-91-1955 ..... N92-10191 #
LA-UR-91-2184 ..... N92-10260 #
LA-UR-91-2185 ..... N92-10218 #
LA-UR-91-2391 ..... N92-10354 #
LA-UR-91-2554 ..... N92-10298 #
LA-UR-91-2613 ..... N92-10684 #
LA-UR-91-2615 ..... N92-10357 #
LA-UR-91-2637 ..... N92-10969 #
LA-UR-91-2679 ..... N92-10095 #
LA-UR-91-2736 ..... N92-10685 #
LA-UR-91-2745 ..... N92-10169 #
LA-UR-91-2756 ..... N92-10686 #
LA-UR-91-2781 ..... N92-10970 #
LA-UR-91-2792 ..... N92-10726 #
LA-UR-91-2803 ..... N92-10135 #
LA-UR-91-2804 ..... N92-10134 #
LA-UR-91-2816 ..... N92-10356 #
LA-UR-91-2818 ..... N92-10168 #

LA-12114-MS ..... N92-10358 #
LA-12182-M ..... N92-10318 #

LAIR-IR-463 ..... N92-10279 #

LC-89-8483 ..... N92-10228 #

LPI-CONTRIB-773 ..... N92-10248* #

LPI-TR-91-03 ..... N92-10961* #

LTR90-010 ..... N92-10219 #

MEMO-926 ..... N92-10342 #
MEMO-937 ..... N92-10341 #

MGA-A-44 ..... N92-10210

MIT-85469 ..... N92-10184* #

MIT/LCS/TM-390 ..... N92-10716 #

MPE-PREPRINT-195-PT-1 ..... N92-10723
MPE-PREPRINT-199 ..... N92-10615*

MRL-TR-91-31 ..... N92-10089 #

MTR-11093 ..... N92-10143 #

NADC-91030-60 ..... N92-10087 #
NADC-91041-60 ..... N92-10072 #
NADC-91053-60 ..... N92-10023 #

NAL-TR-1092 ..... N92-10025 #
NAL-TR-1093 ..... N92-10009 #
NAL-TR-1099 ..... N92-10056 #
NAL-TR-1106 ..... N92-10028 #
NAL-TR-1111 ..... N92-10166 #

NAS 1.15:4259 ..... N92-10302* #
NAS 1.15:4279 ..... N92-10017* #
NAS 1.15:4281 ..... N92-10006* #
NAS 1.15:4285 ..... N92-10024* #
NAS 1.15:4300 ..... N92-10728* #
NAS 1.15:89326 ..... N92-10722*
NAS 1.15:89327 ..... N92-10721*
NAS 1.15:100726 ..... N92-10680* #
NAS 1.15:103897 ..... N92-10003* #
NAS 1.15:104141 ..... N92-10203* #
NAS 1.15:104543 ..... N92-10257* #
NAS 1.15:104741 ..... N92-10036* #
NAS 1.15:104742 ..... N92-10287* #
NAS 1.15:105024 ..... N92-10717*
NAS 1.15:105077 ..... N92-10718*
NAS 1.15:105098 ..... N92-10248* #
NAS 1.15:105109 ..... N92-10719*
NAS 1.15:105110 ..... N92-10720*
NAS 1.15:105192 ..... N92-10002* #
NAS 1.15:105199 ..... N92-10064* #
NAS 1.15:105211 ..... N92-10012* #
NAS 1.15:105212 ..... N92-10057* #
NAS 1.15:105231 ..... N92-10221* #
NAS 1.15:105236 ..... N92-10289* #
NAS 1.15:105257 ..... N92-10345* #
NAS 1.15:105284 ..... N92-10055* #
NAS 1.21:7037(267) N92-10001*
NAS 1.26:178402 ..... N92-10069* #
NAS 1.26:184214 ..... N92-10676* #
NAS 1.26:184216 ..... N92-10200* #
NAS 1.26:184217 ..... N92-10160* #

NAS 1.26:184218 ..... N92-10638* #
NAS 1.26:184225 ..... N92-10639* #
NAS 1.26:184227 ..... N92-10112* #
NAS 1.26:184228 ..... N92-10042* #
NAS 1.26:184230 ..... N92-10088* #
NAS 1.26:184231 ..... N92-10079* #
NAS 1.26:184232 ..... N92-10332* #
NAS 1.26:184233 ..... N92-10301* #
NAS 1.26:184235 ..... N92-10613* #
NAS 1.26:184236 ..... N92-10080* #
NAS 1.26:184237 ..... N92-10340* #
NAS 1.26:184240 ..... N92-10183* #
NAS 1.26:185447 ..... N92-10282* #
NAS 1.26:186208 ..... N92-10593* #
NAS 1.26:187174 ..... N92-10205* #
NAS 1.26:187596 ..... N92-10267* #
NAS 1.26:187633 ..... N92-10348* #
NAS 1.26:187636 ..... N92-10171* #
NAS 1.26:187637 ..... N92-10349* #
NAS 1.26:187816 ..... N92-10303* #
NAS 1.26:187985 ..... N92-10004* #
NAS 1.26:188783 ..... N92-10209* #
NAS 1.26:188784 ..... N92-10304* #
NAS 1.26:188800 ..... N92-10043* #
NAS 1.26:188808 ..... N92-10116* #
NAS 1.26:188810 ..... N92-10961* #
NAS 1.26:188817 ..... N92-10037* #
NAS 1.26:188819 ..... N92-10960* #
NAS 1.26:188826 ..... N92-10313* #
NAS 1.26:188833 ..... N92-10031* #
NAS 1.26:188834 ..... N92-10032* #
NAS 1.26:188835 ..... N92-10033* #
NAS 1.26:188837 ..... N92-10333* #
NAS 1.26:188839 ..... N92-10290* #
NAS 1.26:188842 ..... N92-10343* #
NAS 1.26:188845 ..... N92-10711* #
NAS 1.26:188847 ..... N92-10291* #
NAS 1.26:188850 ..... N92-10344* #
NAS 1.26:188852 ..... N92-10306* #
NAS 1.26:188858 ..... N92-10292* #
NAS 1.26:188860 ..... N92-10034* #
NAS 1.26:188863 ..... N92-10293* #
NAS 1.26:188869 ..... N92-10038* #
NAS 1.26:188881 ..... N92-10307* #
NAS 1.26:188892 ..... N92-10308* #
NAS 1.26:188894 ..... N92-10309* #
NAS 1.26:188895 ..... N92-10310* #
NAS 1.26:188901 ..... N92-10294* #
NAS 1.26:188909 ..... N92-10311* #
NAS 1.26:188910 ..... N92-10312* #
NAS 1.26:188911 ..... N92-10220* #
NAS 1.26:188917 ..... N92-10971* #
NAS 1.26:188945 ..... N92-10314* #
NAS 1.26:188948 ..... N92-10712* #
NAS 1.26:188957 ..... N92-10184* #
NAS 1.26:188969 ..... N92-10615*
NAS 1.26:188975 ..... N92-10071* #
NAS 1.26:188980 ..... N92-10724* #
NAS 1.26:188981 ..... N92-10299* #
NAS 1.26:188982 ..... N92-10170* #
NAS 1.26:188985 ..... N92-10347* #
NAS 1.55:10084 ..... N92-10044* #
NAS 1.60:3094 ..... N92-10027* #
NAS 1.60:3096 ..... N92-10195* #
NAS 1.60:3101 ..... N92-10161* #
NAS 1.60:3102 ..... N92-10067* #
NAS 1.60:3110 ..... N92-10005* #
NAS 1.60:3122 ..... N92-10677* #
NAS 1.60:3156 ..... N92-10011* #
NAS 1.61:1256 ..... N92-10208* #
NAS 1.61:1258-VOL-1 ..... N92-10598* #
NAS 1.71:LAR-13586-1 ..... N92-10035* #
NAS 1.71:LAR-13823-1 ..... N92-10182* #
NAS 1.71:LAR-14096-1 ..... N92-10196* #
NAS 1.71:LAR-14212-1-CU ..... N92-10021* #
NAS 1.71:LAR-14440-1 ..... N92-10066* #
NAS 1.71:LAR-14508-1-CU ..... N92-10202* #
NAS 1.71:LAR-14520-1-SB ..... N92-10008* #
NAS 1.71:LAR-14773-1 ..... N92-10105* #
NAS 1.71:LEW-14973-1 ..... N92-10222* #
NAS 1.71:LEW-15235-1 ..... N92-10167* #
NAS 1.71:MSC-21613-1 ..... N92-10331* #
NAS 1.71:NPO-17734-1-CU ..... N92-10146* #
NAS 1.71:NPO-17759-1-CU ..... N92-10125* #
NAS 1.71:NPO-17836-1-CU ..... N92-10126* #
NAS 1.71:NPO-18155-1-CU ..... N92-10609* #

NASA-CASE-GSC-13240-1 ..... N92-10186*

NASA-CASE-LAR-13586-1 ..... N92-10035* #
NASA-CASE-LAR-13823-1 ..... N92-10182* #
NASA-CASE-LAR-14096-1 ..... N92-10196* #
NASA-CASE-LAR-14212-1-CU ..... N92-10021* #
NASA-CASE-LAR-14231-1 ..... N92-10070*
NASA-CASE-LAR-14419-1 ..... N92-10185*
NASA-CASE-LAR-14440-1 ..... N92-10066* #
NASA-CASE-LAR-14508-1-CU ..... N92-10202* #
NASA-CASE-LAR-14520-1-SB ..... N92-10008* #
NASA-CASE-LAR-14773-1-CU ..... N92-10105* #

NASA-CASE-LEW-14698-2 ..... N92-10090*
NASA-CASE-LEW-14846-1 ..... N92-10054*
NASA-CASE-LEW-14945-2 ..... N92-10128*
NASA-CASE-LEW-14973-1 ..... N92-10222* #
NASA-CASE-LEW-15235-1 ..... N92-10167* #

NASA-CASE-MSC-21434-1 ..... N92-10197*
NASA-CASE-MSC-21503-1 ..... N92-10091*
NASA-CASE-MSC-21613-1 ..... N92-10331* #

NASA-CASE-NPO-17480-1-CU N92-10073*
NASA-CASE-NPO-17734-1-CU ..... N92-10146* #
NASA-CASE-NPO-17759-1-CU ..... N92-10125* #
NASA-CASE-NPO-17836-1-CU ..... N92-10126* #
NASA-CASE-NPO-17949-1-CU N92-10681*
NASA-CASE-NPO-18155-1-CU ..... N92-10609* #

NASA-CP-10084 ..... N92-10044* #

NASA-CR-178402 ..... N92-10069* #
NASA-CR-184214 ..... N92-10676* #
NASA-CR-184216 ..... N92-10200* #
NASA-CR-184217 ..... N92-10160* #
NASA-CR-184218 ..... N92-10638* #
NASA-CR-184225 ..... N92-10639* #
NASA-CR-184227 ..... N92-10112* #
NASA-CR-184228 ..... N92-10042* #
NASA-CR-184230 ..... N92-10088* #
NASA-CR-184231 ..... N92-10079* #
NASA-CR-184232 ..... N92-10332* #
NASA-CR-184233 ..... N92-10301* #
NASA-CR-184235 ..... N92-10613* #
NASA-CR-184236 ..... N92-10080* #
NASA-CR-184237 ..... N92-10340* #
NASA-CR-184240 ..... N92-10183* #
NASA-CR-185447 ..... N92-10282* #
NASA-CR-186208 ..... N92-10593* #
NASA-CR-187174 ..... N92-10205* #
NASA-CR-187596 ..... N92-10267* #
NASA-CR-187633 ..... N92-10348* #
NASA-CR-187636 ..... N92-10171* #
NASA-CR-187637 ..... N92-10349* #
NASA-CR-187816 ..... N92-10303* #
NASA-CR-187985 ..... N92-10004* #
NASA-CR-188783 ..... N92-10209* #
NASA-CR-188784 ..... N92-10304* #
NASA-CR-188800 ..... N92-10043* #
NASA-CR-188808 ..... N92-10116* #
NASA-CR-188810 ..... N92-10961* #
NASA-CR-188817 ..... N92-10037* #
NASA-CR-188819 ..... N92-10960* #
NASA-CR-188826 ..... N92-10313* #
NASA-CR-188833 ..... N92-10031* #
NASA-CR-188834 ..... N92-10032* #
NASA-CR-188835 ..... N92-10033* #
NASA-CR-188837 ..... N92-10333* #
NASA-CR-188839 ..... N92-10290* #
NASA-CR-188842 ..... N92-10343* #
NASA-CR-188845 ..... N92-10711* #
NASA-CR-188847 ..... N92-10291* #
NASA-CR-188850 ..... N92-10344* #
NASA-CR-188852 ..... N92-10306* #
NASA-CR-188858 ..... N92-10292* #
NASA-CR-188860 ..... N92-10034* #
NASA-CR-188863 ..... N92-10293* #
NASA-CR-188869 ..... N92-10038* #
NASA-CR-188881 ..... N92-10307* #
NASA-CR-188892 ..... N92-10308* #
NASA-CR-188894 ..... N92-10309* #
NASA-CR-188895 ..... N92-10310* #
NASA-CR-188901 ..... N92-10294* #
NASA-CR-188909 ..... N92-10311* #
NASA-CR-188910 ..... N92-10312* #
NASA-CR-188911 ..... N92-10220* #
NASA-CR-188917 ..... N92-10971* #
NASA-CR-188945 ..... N92-10314* #
NASA-CR-188948 ..... N92-10712* #
NASA-CR-188957 ..... N92-10184* #
NASA-CR-188969 ..... N92-10615*
NASA-CR-188975 ..... N92-10071* #
NASA-CR-188980 ..... N92-10724* #
NASA-CR-188981 ..... N92-10299* #
NASA-CR-188982 ..... N92-10170* #
NASA-CR-188985 ..... N92-10347* #

NASA-RP-1256 ..... N92-10208* #
NASA-RP-1258-VOL-1 ..... N92-10598* #

NASA-SP-7037(267) N92-10001*

NASA-TM-4259 ..... N92-10302* #
NASA-TM-4279 ..... N92-10017* #
NASA-TM-4281 ..... N92-10006* #
NASA-TM-4285 ..... N92-10024* #
NASA-TM-4300 ..... N92-10728* #
NASA-TM-89326 ..... N92-10722*
NASA-TM-89327 ..... N92-10721*
NASA-TM-100726 ..... N92-10680* #
NASA-TM-103897 ..... N92-10003* #
NASA-TM-104141 ..... N92-10203* #
NASA-TM-104543 ..... N92-10257* #
NASA-TM-104741 ..... N92-10036* #
NASA-TM-104742 ..... N92-10287* #
NASA-TM-105024 ..... N92-10717*
NASA-TM-105077 ..... N92-10718*
NASA-TM-105098 ..... N92-10248* #
NASA-TM-105109 ..... N92-10719*
NASA-TM-105110 ..... N92-10720*
NASA-TM-105192 ..... N92-10002* #
NASA-TM-105199 ..... N92-10064* #
NASA-TM-105211 ..... N92-10012* #
NASA-TM-105212 ..... N92-10057* #
NASA-TM-105231 ..... N92-10221* #
NASA-TM-105236 ..... N92-10289* #
NASA-TM-105257 ..... N92-10345* #
NASA-TM-105284 ..... N92-10055* #

NASA-TP-3094 ..... N92-10027* #
NASA-TP-3096 ..... N92-10195* #
NASA-TP-3101 ..... N92-10161* #
NASA-TP-3102 ..... N92-10067* #
NASA-TP-3110 ..... N92-10005* #
NASA-TP-3122 ..... N92-10677* #
NASA-TP-3156 ..... N92-10011* #

NCEL-TN-1833 ..... N92-10207 #

NIFS-21 ..... N92-10649 #
NIFS-22 ..... N92-10648 #
NIFS-23 ..... N92-10647 #
NIFS-24 ..... N92-10646 #
NIFS-25 ..... N92-10645 #
NIFS-83 ..... N92-10657 #
NIFS-85 ..... N92-10656 #
NIFS-86 ..... N92-10655 #
NIFS-88 ..... N92-10654 #

NOARL-CR-036-91 ..... N92-10275 #

NOSC/TR-1412 ..... N92-10675 #

NPS-EC-91-005 ..... N92-10644 #

NPS-ME-91-001 ..... N92-10175 #

NPS-MR-91-002 ..... N92-10271 #

NPSOR-91-024 ..... N92-10353 #

OAL91-2 ..... N92-10613* #

OCNR-10P ..... N92-10675 #

ONERA-RSF-6/4368-AY-008A ..... N92-10162 #

ORNL-6629/P2 ..... N92-10081 #

ORNL/M-1677 ..... N92-10198 #

PL-TR-91-1043 ..... N92-10674 #
PL-TR-91-2117 ..... N92-10263 #
PL-TR-91-2142 ..... N92-10265 #
PL-TR-91-2199 ..... N92-10270 #
PL-TR-91-2201 ..... N92-10269 #

PNL-TR-484 ..... N92-10076 #

RAL-91-044 ..... N92-10614 #

RAND/R-3856-DARPA ..... N92-10715 #

RATSCAT-TM-91-001 ..... N92-10141 #

RCC-377-91 ..... N92-10262 #

REPT-5-32176-VOL-1 ..... N92-10042* #
REPT-89B00121 ..... N92-10680* #
REPT-91E02481 ..... N92-10257* #
REPT-119(1991) ..... N92-10362 #
REPT-71435-2 ..... N92-10206 #
REPT-026845-910719 ..... N92-10142 #
REPT-723224-2 ..... N92-10593* #

RIACS-TR-89-7 ..... N92-10031* #
RIACS-TR-89-8 ..... N92-10033* #
RIACS-TR-89-9 ..... N92-10032* #
RIACS-TR-89-10 ..... N92-10333* #
RIACS-TR-89-15 ..... N92-10290* #

RIACS-TR-89-23 ..... N92-10343* #
RIACS-TR-89-26 ..... N92-10711* #
RIACS-TR-89-28 ..... N92-10291* #
RIACS-TR-89-37 ..... N92-10306* #
RIACS-TR-89-42 ..... N92-10344* #
RIACS-TR-89-53 ..... N92-10294* #
RIACS-TR-89-55 ..... N92-10310* #
RIACS-TR-89-57 ..... N92-10309* #
RIACS-TR-90-1 ..... N92-10034* #
RIACS-TR-90-3 ..... N92-10292* #
RIACS-TR-90-10 ..... N92-10282* #
RIACS-TR-90-26 ..... N92-10293* #
RIACS-TR-90-32 ..... N92-10038* #
RIACS-TR-90-45 ..... N92-10311* #
RIACS-TR-90-46 ..... N92-10312* #
RIACS-TR-90-49 ..... N92-10307* #
RIACS-TR-91-14 ..... N92-10308* #

RL-TR-91-118 ..... N92-10159 #
RL-TR-91-119 ..... N92-10327 #
RL-TR-91-132 ..... N92-10642 #

RRC-91-R-1511 ..... N92-10063 #

S-649 ..... N92-10036* #
S-654 ..... N92-10287* #

SAIC-89/1097 ..... N92-10264 #

SAND-89-0167C ..... N92-10040 #
SAND-89-2989 ..... N92-10321 #
SAND-90-1471 ..... N92-10224 #
SAND-90-3048C ..... N92-10096 #
SAND-90-3139C ..... N92-10636 #
SAND-90-3161C ..... N92-10151 #
SAND-90-3204C ..... N92-10324 #
SAND-90-3248C ..... N92-10083 #
SAND-91-8-0874C ..... N92-10315 #
SAND-91-0006C ..... N92-10082 #
SAND-91-0178C ..... N92-10152 #
SAND-91-0278C ..... N92-10334 #
SAND-91-0765C ..... N92-10335 #
SAND-91-0966C ..... N92-10136 #
SAND-91-0967C ..... N92-10131 #
SAND-91-0980C ..... N92-10132 #
SAND-91-0983C ..... N92-10204 #
SAND-91-1045 ..... N92-10148 #
SAND-91-1354C ..... N92-10084 #
SAND-91-1905C ..... N92-10060 #
SAND-91-1937C ..... N92-10666 #
SAND-91-1987C ..... N92-10061 #
SAND-91-7010 ..... N92-10223 #

SDC-91-00052 ..... N92-10641 #

SERI/SP-220-4403 ..... N92-10111 #

SERI/TP-250-4474 ..... N92-10241 #

SLCET-TR-90-6 ..... N92-10597 #
SLCET-TR-91-22 ..... N92-10158 #

SR-5 ..... N92-10219 #
SR-9 ..... N92-10265 #

SRI-PR-1749 ..... N92-10272 #

SSD-TR-91-14 ..... N92-10030 #

STARS-SC-03068/001/00 ..... N92-10328 #
STARS-SC-03070/001/00 ..... N92-10329 #
STARS-SC-03725/001/00 ..... N92-10330 #

SU-SLAC-PUB-5629 ..... N92-10323 #
SU-SLAC-PUB-5639 ..... N92-10727 #

SU-SLAC-TN-91-10 ..... N92-10149 #

TD-91-0035 ..... N92-10115
TD-91-0044 ..... N92-10277
TD-91-2194 ..... N92-10215 #
TD-91-2195 ..... N92-10216 #
TD-99-0403 ..... N92-10966

TR-42 ..... N92-10104 #
TR-0090(5940-06)-5 ..... N92-10030 #

TT-9101 ..... N92-10018 #

U-OF-IOWA-91-19 ..... N92-10971* #

UAH-5-32180 ..... N92-10639* #
UAH-5-32323 ..... N92-10340* #

UCRL-CR-107206 ..... N92-10133 #
UCRL-CR-107855 ..... N92-10658 #

UCRL-ID-108037 ..... N92-10325 #
UCRL-ID-108040 ..... N92-10631 #
UCRL-ID-108042 ..... N92-10670 #
UCRL-ID-108096 ..... N92-10669 #

UCRL-JC-105900 ..... N92-10190 #
UCRL-JC-107018-REV-1 ..... N92-10317 #
UCRL-JC-107020 ..... N92-10336 #
UCRL-JC-107753 ..... N92-10619 #
UCRL-JC-107942 ..... N92-10725 #
UCRL-JC-107984 ..... N92-10187 #

UCRL-MA-105401 ..... N92-10326 #

UDR-TR-89-41 ..... N92-10101 #

UDRI-FR-60136 ..... N92-10227 #

UES-799-TR-90-001-VOL-1 ..... N92-10176 #
UES-799-TR-90-004-VOL-2 ..... N92-10178 #
UES-799-TR-90-005-VOL-3 ..... N92-10177 #

US-PATENT-APPL-SN-219016 ..... N92-10090*
US-PATENT-APPL-SN-433881 ..... N92-10197*
US-PATENT-APPL-SN-443289 ..... N92-10090*
US-PATENT-APPL-SN-443414 ..... N92-10091*
US-PATENT-APPL-SN-443523 ..... N92-10054*
US-PATENT-APPL-SN-508386 ..... N92-10073*
US-PATENT-APPL-SN-524109 ..... N92-10070*
US-PATENT-APPL-SN-540976 ..... N92-10128*
US-PATENT-APPL-SN-545016 ..... N92-10681*
US-PATENT-APPL-SN-565090 ..... N92-10021* #
US-PATENT-APPL-SN-571344 ..... N92-10186*
US-PATENT-APPL-SN-584018 ..... N92-10185*
US-PATENT-APPL-SN-591644 ..... N92-10196* #
US-PATENT-APPL-SN-611214 ..... N92-10128*
US-PATENT-APPL-SN-650336 ..... N92-10066* #
US-PATENT-APPL-SN-658477 ..... N92-10609* #
US-PATENT-APPL-SN-660371 ..... N92-10125* #
US-PATENT-APPL-SN-664194 ..... N92-10202* #
US-PATENT-APPL-SN-700830 ..... N92-10146* #
US-PATENT-APPL-SN-716150 ..... N92-10126* #
US-PATENT-APPL-SN-736145 ..... N92-10167* #
US-PATENT-APPL-SN-743238 ..... N92-10008* #
US-PATENT-APPL-SN-743469 ..... N92-10035* #
US-PATENT-APPL-SN-749737 ..... N92-10182* #
US-PATENT-APPL-SN-755207 ..... N92-10105* #
US-PATENT-APPL-SN-761566 ..... N92-10331* #
US-PATENT-APPL-SN-766593 ..... N92-10222* #

US-PATENT-CLASS-2-2.1A N92-10091*
US-PATENT-CLASS-2-411 ..... N92-10091*
US-PATENT-CLASS-2-424 ..... N92-10091*
US-PATENT-CLASS-33-19.2 ..... N92-10186*
US-PATENT-CLASS-33-23.02 ..... N92-10186*
US-PATENT-CLASS-60-39.281 ..... N92-10054*
US-PATENT-CLASS-60-240 ..... N92-10054*
US-PATENT-CLASS-60-258 ..... N92-10054*
US-PATENT-CLASS-73-147 ..... N92-10185*
US-PATENT-CLASS-73-862.04 ..... N92-10185*
US-PATENT-CLASS-73-862.65 ..... N92-10185*
US-PATENT-CLASS-118-DIG.5 ..... N92-10070*
US-PATENT-CLASS-156-166 ..... N92-10070*
US-PATENT-CLASS-156-283 ..... N92-10070*
US-PATENT-CLASS-156-637 ..... N92-10681*
US-PATENT-CLASS-252-502 ..... N92-10090*
US-PATENT-CLASS-285-23 ..... N92-10197*
US-PATENT-CLASS-285-39 ..... N92-10197*
US-PATENT-CLASS-285-353 ..... N92-10197*
US-PATENT-CLASS-285-912 ..... N92-10197*
US-PATENT-CLASS-358-133 ..... N92-10128*
US-PATENT-CLASS-358-135 ..... N92-10128*
US-PATENT-CLASS-423-439 ..... N92-10090*
US-PATENT-CLASS-423-448 ..... N92-10090*
US-PATENT-CLASS-423-460 ..... N92-10090*
US-PATENT-CLASS-427-62 ..... N92-10681*
US-PATENT-CLASS-427-185 ..... N92-10070*
US-PATENT-CLASS-427-195 ..... N92-10070*
US-PATENT-CLASS-427-343 ..... N92-10681*
US-PATENT-CLASS-427-375 ..... N92-10070*
US-PATENT-CLASS-428-215 ..... N92-10091*
US-PATENT-CLASS-428-412 ..... N92-10091*
US-PATENT-CLASS-428-419 ..... N92-10091*
US-PATENT-CLASS-428-458 ..... N92-10091*
US-PATENT-CLASS-502-73 ..... N92-10073*
US-PATENT-CLASS-505-1 ..... N92-10681*
US-PATENT-CLASS-505-728 ..... N92-10681*

US-PATENT-5,054,287 ..... N92-10054*
US-PATENT-5,056,156 ..... N92-10091*
US-PATENT-5,056,361 ..... N92-10185*
US-PATENT-5,057,338 ..... N92-10070*
US-PATENT-5,057,473 ..... N92-10073*
US-PATENT-5,057,917 ..... N92-10128*
US-PATENT-5,058,281 ..... N92-10186*
US-PATENT-5,058,929 ..... N92-10197*

US-PATENT-5,059,409 ..... N92-10090*
US-PATENT-5,059,581 ..... N92-10681*

USAARL-91-18-VOL-1 ..... N92-10611 #

USARIEM-T13-91 ..... N92-10268 #

USGS-OFR-90-49 ..... N92-10261 #

WHC-MR-0187 ..... N92-10172 #

WHC-SA-1076 ..... N92-10320 #

WL-TR-91-2044 ..... N92-10227 #
WL-TR-91-2047-PHASE-1 ..... N92-10226 #

WRDC-TR-89-2026-VOL-2 ..... N92-10100 #
WRDC-TR-90-2121-VOL-1 ..... N92-10176 #
WRDC-TR-90-2121-VOL-2 ..... N92-10178 #
WRDC-TR-90-2121-VOL-3 ..... N92-10177 #
WRDC-TR-90-2122-PHASE-1 ..... N92-10157 #
WRDC-TR-90-3052-VOL-1 ..... N92-10598* #
WRDC-TR-90-3078 ..... N92-10101 #

WSU/DC/91/TR-58 ..... N92-10643 #
WSU/DC/91/TR-59 ..... N92-10705 #
WSU/DC/91/TR-60 ..... N92-10078 #

ZFK-634 ..... N92-10076 #

Appendix

NASA SCIENTIFIC AND TECHNICAL INFORMATION PROGRAM PRODUCTS AND SERVICES

The NASA Scientific and Technical Information (STI) Program provides for the collection and announcement of aerospace-related reports and literature obtained worldwide through agreements and exchanges. The result of the collection is the comprehensive NASA STI Database that covers aeronautics, space, and supporting disciplines.

The STI Database, documents generated or obtained by NASA, and products and services derived from or supporting the database are made available to the NASA research community and to the public. Descriptions and sources of these items are presented in the following pages.

Scientific and Technical Aerospace Reports (*STAR*) is an abstract journal, listing citations with abstracts for aerospace-related reports obtained from worldwide sources. *STAR* is issued on the 8th and 23rd of each month and announces current documents that have been entered into the NASA STI Database during the previous two weeks. The reports are of the following types:

- NASA, NASA contractor, and NASA grantee reports;
- Reports issued by other U.S. Government agencies, domestic and foreign institutions, universities, and private firms;
- Translations in report form;
- NASA-owned patents and patent applications;
- Other U.S. Government agency and foreign patents and patent applications;
- Domestic and foreign dissertations and theses.

Journal, book, and conference literature, journal translations, and certain foreign dissertations having the same subject scope as *STAR* are announced in a companion journal, *International Aerospace Abstracts* (*IAA*). *IAA* is issued on the 1st and 15th of each month and is available from the American Institute of Aeronautics and Astronautics, Technical Information Service, 555 West 57th Street, 12th Floor, New York, NY 10019.

ELIGIBILITY AND REGISTRATION FOR NASA STI PRODUCTS AND SERVICES

Organizations of the type listed below that have registered with NASA can receive products and services.

- NASA offices and installations, contractors, subcontractors, grantees, and consultants;
- Other U.S. Government agencies and their contractors;
- Libraries in the United States that have arrangements with NASA to maintain collections of NASA documents for public reference;
- Other organizations in the United States having a need for NASA documents in work related to aeronautics and space research;
- Organizations abroad that have established reciprocal documents exchange arrangements with NASA.

Only the central service points or central points of document acquisition and control within qualified organizations are eligible to register for NASA STI products and services. Domestic organizations that may be eligible to receive various classes of NASA publications and services should address their requests for registration or further information to:

NASA Center for AeroSpace Information
ATTN: Registration Services
P.O. Box 8757
Baltimore, MD 21240-0757
301-621-0153

Organizations abroad should direct requests to:

National Aeronautics and Space Administration
Director, Scientific and Technical Information Program
Code JTT
Washington, DC 20546
USA
703-271-5640

SUBJECT SCOPE

The subject scope of *STAR* and *IAA* includes all aspects of aeronautics and space research and development, supporting basic and applied research, and applications. Aerospace aspects of Earth resources, energy development, conservation, oceanography, environmental protection, urban transportation, and other topics of high national priority are also covered.

HOW TO USE *STAR* SUBJECT CATEGORIES

Abstracts in *STAR* are categorized by 10 major subject divisions that are divided further into 76 specific subject categories. The subject divisions and categories are listed in the Table of Contents together with a note for each that defines its scope and provides any cross-references. For example:

16 SPACE TRANSPORTATION
Includes passenger and cargo space transportation, e.g., shuttle operations; and space rescue techniques. For related information see also *03 Air Transportation and Safety* and *18 Spacecraft Design, Testing and Performance.* For space suits see *54 Man/System Technology and Life Support.*

CROSS-REFERENCES

Individual *STAR* abstracts are not ordinarily cross-referenced, except for certain conference reports or book translations that have had separate abstracts written for their component papers or chapters. Citations and abstracts of the components follow immediately after those of the parent document. When the subject content of a component differs sufficiently from the general content of the parent, a cross-reference citation also is printed at the end of the category to which it normally would have been assigned if it were independent.

DOCUMENTS ON MICROFICHE

Documents available on microfiche are designated by a pound sign (#) following the accession number.

LIMITED REPRODUCIBILITY

A note of limited reproducibility appears in the citation, if there are factors affecting the reproducibility of more than 20% of the document. These factors include faint or broken type, color photographs, black and white photographs, foldouts, dot matrix print, or some other factor that limits the reproducibility of the document. This notation also appears on the microfiche header with the specific factor checked off on a list visible in the second frame.

COLOR COPIES

An increasing number of NASA scientific and technical reports are being produced with color graphs, charts, illustrations, and photographs. An indication that a document has color pages follows the source and pricing (SAP) information in the *STAR* citation.

Registered users of the NASA Scientific and Technical Information Program will receive ordered documents with color at no additional cost, as long as stock copies of the document are available. Otherwise, an additional fee of $2.00 per color page will be charged. The NASA Center for AeroSpace Information staff will contact registered users to determine individual user's needs.

NASA PATENTS AND PATENT APPLICATIONS

Patents and patent applications owned by NASA are announced in *STAR* under appropriate subject categories and are referenced in the *STAR* indexes. In the Report/Accession Number Index, patents are indexed by the NASA Case Number, and the U.S. Patent Class. Patent applications are indexed by the NASA Case Number and the U.S. Patent Application Serial Number.

Printed copies of patents (which are not microfiched) are available for purchase from the U.S. Patent and Trademark Office.

NASA patent application specifications are sold in both paper copy and microfiche by the National Technical Information Service (NTIS). The US-Patent-Appl-SN-number should be used in ordering either paper copy or microfiche from NTIS.

When ordering patents, the U.S. Patent Number should be used, and payment must be remitted in advance, by money order or check payable to the Commissioner of Patents and Trademarks. Prepaid purchase coupons for ordering are also available from the U.S. Patent and Trademark Office.

The patents and patent applications announced in *STAR* are owned by NASA and are available for royalty-free licensing. Requests for licensing terms and further information should be addressed to:

National Aeronautics and Space Administration
Associate General Counsel for Intellectual Property
Code GP
Washington, DC 20546

SOURCES FOR DOCUMENTS

One or more sources from which a document announced in *STAR* is available to the public is given in each citation. The most commonly indicated sources and their acronyms or abbreviations are listed on page A-6. If the publication is available from a source other than those listed, the publisher and address will be displayed on the availability line or in combination with the corporate source line.

Avail: NTIS. Sold by the National Technical Information Service. Prices for hard copy (HC) and microfiche (MF) are indicated by a price code following the letters HC or MF in the *STAR* citation. Current values for the price codes are given in the tables on page A-7.

Initially distributed microfiche under the NTIS SRIM (Selected Research in Microfiche) is available at greatly reduced unit prices. For this service and for information concerning subscription to NASA printed reports, consult the NTIS Subscription Section, Springfield, VA 22161.

NOTE ON ORDERING DOCUMENTS: When ordering NASA publications (those followed by the * symbol), use the N accession number. NASA patent applications (only the specifications are offered) should be ordered by the US-Patent-Appl-SN number. Non-NASA publications (no asterisk) should be ordered by the AD, PB, or other *report number* shown on the last line of the citation, not by the N accession number. It is also advisable to cite the title and other bibliographic identification.

Avail: SOD (or GPO). Sold by the Superintendent of Documents, U.S. Government Printing Office, in hard copy. The current price and order number are given following the availability line. (NTIS will fill microfiche requests, as indicated above, for those documents identified by a # symbol.)

Avail: BLL (formerly NLL): British Library Lending Division, Boston Spa, Wetherby, Yorkshire, England. Photocopies available from this organization at the price shown. (If none is given, address inquiry to the BLL.)

Avail: DOE Depository Libraries. Organizations in U.S. cities and abroad that maintain collections of Department of Energy reports, usually in microfiche form, are listed in *Energy Research Abstracts.* Services available from the DOE and its depositories are described in a booklet, *DOE Technical Information Center - Its Functions and Services* (TID-4660), which may be obtained without charge from the DOE Technical Information Center.

Avail: ESDU. Pricing information on specific data, computer programs, and details on Engineering Sciences Data Unit (ESDU) topic categories can be obtained from ESDU International Ltd. Requesters in North America should use the Virginia address while all other requesters should use the London address, both of which are on page A-6.

Avail: Fachinformationszentrum, Karlsruhe. Sold by the Fachinformationszentrum Energie, Physik, Mathematik GMBH, Eggenstein Leopoldshafen, Federal Republic of Germany, at the price shown in deutschmarks (DM).

Avail: HMSO. Publications of Her Majesty's Stationery Office are sold in the U.S. by Pendragon House, Inc. (PHI), Redwood City, CA. The U.S. price (including a service and mailing charge) is given, or a conversion table may be obtained from PHI.

Avail: NASA Public Document Rooms. Documents so indicated may be examined at or purchased from the National Aeronautics and Space Administration, Public Documents Room (Room 126), 600 Independence Ave., S.W., Washington, DC 20546, or public document rooms located at NASA installations, and the NASA Pasadena Office at the Jet Propulsion Laboratory.

Avail: Univ. Microfilms. Documents so indicated are dissertations selected from *Dissertation Abstracts* and are sold by University Microfilms as xerographic copy (HC) and microfilm. All requests should cite the author and the Order Number as they appear in the citation.

Avail: US Patent and Trademark Office. Sold by Commissioner of Patents and Trademarks, U.S. Patent and Trademark Office, at the standard price of $1.50 each, postage free. (See discussion of NASA patents and patent applications below.)

Avail: (US Sales Only). These foreign documents are available to users within the United States from the National Technical Information Service (NTIS). They are available to users outside the United States through the International Nuclear Information Service (INIS) representative in their country, or by applying directly to the issuing organization.

Avail: USGS. Originals of many reports from the U.S. Geological Survey, which may contain color illustrations, or otherwise may not have the quality of illustrations preserved in the microfiche or facsimile reproduction, may be examined by the public at the libraries of the USGS field offices whose addresses are listed on page A-6. The libraries may be queried concerning the availability of specific documents and the possible utilization of local copying services, such as color reproduction.

Avail: Issuing Activity, or Corporate Author, or no indication of availability. Inquiries as to the availability of these documents should be addressed to the organization shown in the citation as the corporate author of the document.

FEDERAL DEPOSITORY LIBRARIES: To provide the general public with greater access to U.S. Government publications, Congress established the Federal Depository Library Program under the Government Printing Office (GPO), with 52 regional depositories responsible for permanent retention of material, inter-library loan, and reference services. (These libraries are not sales outlets.) At least one copy of nearly every NASA and NASA-sponsored publication, either in printed or microfiche format, is received and retained by the 52 regional depositories. A list of the regional GPO libraries, appears on page A-8. A local library can contact a regional depository library to help locate specific reports, or direct contact may be made by an individual.

PUBLIC COLLECTION OF NASA DOCUMENTS

An extensive collection of NASA and NASA-sponsored publications is maintianed by the British Library Lending Divison, Boston Spa, Wetherby, Yorkshire, England, for public access. The British Library Lending Division also has available many of the non-NASA publications cited in *STAR*.

European requesters may purchase facsimile copy or microfiche of NASA and NASA-sponsored documents, those identified by both the symbols # and * from ESA—Information Retrieval Service, European Space Agency, 8-10 rue Mario-Nikis, 75738 Paris CEDEX 15, France.

SUBMITTING DOCUMENTS

All users of this abstract service are urged to forward reports to be considered for announcement in *STAR*. This will aid NASA in its efforts to provide the fullest possible coverage of all scientific and technical publications that might support aeronautics and space research and development. If you have prepared relevant reports (other than those you will transmit to NASA, DOD, or DOE through the usual contract- or grant-reporting channels), please send them for consideration to the NASA Center for AeroSpace Information, P.O. Box 8757, Baltimore, MD 21240-0757.

Reprints of journal articles, book chapters, and conference papers are also welcome. These will be considered for announcement in *STAR*'s companion journal, *IAA*.

You may specify a particular source to be included in a report announcement if you wish; otherwise the report will be placed on a public sale at the National Technical Information Service. Copyrighted publications will be announced but not distributed or sold.

PURCHASE OF *STAR*

STAR is publicly available on annual subscription from the Superintendent of Documents, U.S. Government Printing Office, Washington, DC 20402.

STAR is available to registered users on annual subscription from the NASA Center for AeroSpace Information, ATTN: Registration Services, P.O. Box 8757, Baltimore, MD 21240-0757.

Microfiche of the abstract sections of *STAR* are available, on annual subscription only, from NTIS as PB92-911300, Attn: Subscriptions, 5285 Port Royal Road, Springfield, VA 22161. Annual subscription rates are $100.00 North America; $200.00 foreign. Abstract sections for previous years retroactive to 1964 are available at the current rates.

ADDRESSES OF ORGANIZATIONS

American Institute of Aeronautics and Astronautics
Technical Information Service
555 West 57th Street, 12th Floor
New York, New York 10019

British Library Lending Division,
Boston Spa, Wetherby, Yorkshire,
England

Commissioner of Patents and Trademarks
U.S. Patent and Trademark Office
Washington, DC 20231

Department of Energy
Technical Information Center
P.O. Box 62
Oak Ridge, Tennessee 37830

European Space Agency-Information Retrieval Service
ESRIN
Via Galileo Galilei
00044 Frascati (Rome) Italy

Engineering Sciences Data Unit International
P.O. Box 1633
Manassas, Virginia 22110

Engineering Sciences Data Unit International, Ltd.
251-259 Regent Street
London, W1R 7AD, England

Fachinformationszentrum Energie, Physik, Mathematik
GMBH
7514 Eggenstein Leopoldshafen
Federal Republic of Germany

Her Majesty's Stationery Office
P.O. Box 569, S.E. 1
London, England

NASA Center for AeroSpace Information
P.O. Box 8757
Baltimore, Maryland 21240-0757

National Aeronautics and Space Administration
Scientific and Technical Information Program (JTT)
Washington, DC 20546

National Technical Information Service
5285 Port Royal Road
Springfield, Virginia 22161

Pendragon House, Inc.
899 Broadway Avenue
Redwood City, California 94063

Superintendent of Documents
U.S. Government Printing Office
Washington, DC 20402

University Microfilms
A Xerox Company
300 North Zeeb Road
Ann Arbor, Michigan 48106

University Microfilms, Ltd.
Tylers Green
London, England

U.S. Geological Survey Library National Center
MS 950
12201 Sunrise Valley Drive
Reston, Virginia 22092

U.S. Geological Survey Library
2255 North Gemini Drive
Flagstaff, Arizona 86001

U.S. Geological Survey
345 Middlefield Road
Menlo Park, California 94025

U.S. Geological Survey Library
Box 25046
Denver Federal Center, MS914
Denver, Colorado 80225

NTIS PRICE SCHEDULES

(Effective October 1, 1991)

Schedule A
STANDARD PRICE DOCUMENTS AND MICROFICHE**

PRICE CODE	NORTH AMERICAN PRICE	FOREIGN PRICE
A01	$ 9.00	$ 18.00
A02	12.50	25.00
A03	17.00	34.00
A04-A05	19.00	38.00
A06-A09	26.00	52.00
A10-A13	35.00	70.00
A14-A17	43.00	86.00
A18-A21	50.00	100.00
A22-A25	59.00	118.00
A99	*	*
N01	60.00	120.00
N02	59.00	118.00
N03	20.00	40.00

Schedule E
EXCEPTION PRICE DOCUMENTS AND MICROFICHE**

PRICE CODE	NORTH AMERICAN PRICE	FOREIGN PRICE
E01	$11.00	$ 22.00
E02	14.00	28.00
E03	16.00	32.00
E04	19.00	38.00
E05	21.00	42.00
E06	24.00	48.00
E07	27.00	54.00
E08	30.00	60.00
E09	33.00	66.00
E10	36.00	72.00
E11	39.00	78.00
E12	43.00	86.00
E13	46.00	92.00
E14	50.00	100.00
E15	54.00	108.00
E16	59.00	118.00
E17	64.00	128.00
E18	69.00	138.00
E19	76.00	152.00
E20	88.00	176.00
E99	*	*

* Contact NTIS for price quote.

** Effective January 1, 1991, the microfiche copy of any new document entering the NTIS collection will be priced the same as the paper copy of the document.

IMPORTANT NOTICE

NTIS Shipping and Handling Charges

U.S., Canada, Mexico — ADD $3.00 per TOTAL ORDER

All Other Countries — ADD $4.00 per TOTAL ORDER

Exceptions — Does NOT apply to:

ORDERS REQUESTING NTIS RUSH HANDLING

ORDERS FOR SUBSCRIPTION OR STANDING ORDER PRODUCTS *ONLY*

NOTE: Each additional delivery address on an order requires a separate shipping and handling charge.

FEDERAL REGIONAL DEPOSITORY LIBRARIES

ALABAMA

AUBURN UNIV. AT MONTGOMERY LIBRARY
Documents Dept.
7300 University Drive
Montgomery, AL 36117-3596
(205) 244-3650 FAX: (205) 244-0678

UNIV. OF ALABAMA
Amelia Gayle Gorgas Library
Govt. Documents
Box 870266
Tuscaloosa, AL 35487-0266
(205) 348-6046 FAX: (205) 348-8833

ARIZONA

DEPT. OF LIBRARY, ARCHIVES, AND PUBLIC RECORDS
Federal Documents
Third Floor State Capitol
1700 West Washington
Phoenix, AZ 85007
(602) 542-4121 FAX: (602) 542-4400; 542-4500

ARKANSAS

ARKANSAS STATE LIBRARY
State Library Services
One Capitol Mall
Little Rock, AR 72201
(501) 682-2869

CALIFORNIA

CALIFORNIA STATE LIBRARY
Govt. Publications Section
914 Capitol Mall - P.O. Box 942837
Sacramento, CA 94237-0001
(916) 322-4572 FAX: (916) 324-8120

COLORADO

UNIV. OF COLORADO - BOULDER
Norlin Library
Govt. Publications
Campus Box 184
Boulder, CO 80309-0184
(303) 492-8834 FAX: (303) 492-2185

DENVER PUBLIC LIBRARY
Govt. Publications Dept. BS/GPD
1357 Broadway
Denver, CO 80203
(303) 571-2135

CONNECTICUT

CONNECTICUT STATE LIBRARY
231 Capitol Avenue
Hartford, CT 06106
(203) 566-4971 FAX: (203) 566-3322

FLORIDA

UNIV. OF FLORIDA LIBRARIES
Documents Dept.
Library West
Gainesville, FL 32611-2048
(904) 392-0366 FAX: (904) 392-7251

GEORGIA

UNIV. OF GEORGIA LIBRARIES
Govt. Documents Dept.
Jackson Street
Athens, GA 30602
(404) 542-8949 FAX: (404) 542-6522

HAWAII

UNIV. OF HAWAII
Hamilton Library
Govt. Documents Collection
2550 The Mall
Honolulu, HI 96822
(808) 948-8230 FAX: (808) 956-5968

IDAHO

UNIV. OF IDAHO LIBRARY
Documents Section
Moscow, ID 83843
(208) 885-6344 FAX: (208) 885-6817

ILLINOIS

ILLINOIS STATE LIBRARY
Reference Dept.
300 South Second
Springfield, IL 62701-1796
(217) 782-7596 FAX: (217) 524-0041

INDIANA

INDIANA STATE LIBRARY
Serials/Documents Section
140 North Senate Avenue
Indianapolis, IN 46204
(317) 232-3678 FAX: (317) 232-3728

IOWA

UNIV. OF IOWA LIBRARIES
Govt. Publications Dept.
Washington & Madison Streets
Iowa City, IA 52242
(319) 335-5926 FAX: (319) 335-5830

KANSAS

UNIV. OF KANSAS
Govt. Documents & Map Library
6001 Malatt Hall
Lawrence, KS 66045-2800
(913) 864-4660 FAX: (913) 864-5380

KENTUCKY

UNIV. OF KENTUCKY LIBRARIES
Govt. Publications/Maps Dept.
Lexington, KY 40506-0039
(606) 257-3139 FAX: (606) 257-1563; 257-8379

LOUISIANA

LOUISIANA STATE UNIV.
Middleton Library
Govt. Documents Dept.
Baton Rouge, LA 70803
(504) 388-2570 FAX: (504) 388-6992

LOUISIANA TECHNICAL UNIV.
Prescott Memorial Library
Govt. Documents Dept.
305 Wisteria Street
Ruston, LA 71270-9985
(318) 257-4962 FAX: (318) 257-2447

MAINE

TRI-STATE DOCUMENTS DEPOSITORY
Raymond H. Fogler Library
Govt. Documents & Microforms Dept.
Univ. of Maine
Orono, ME 04469
(207) 581-1680

MARYLAND

UNIV. OF MARYLAND
Hornbake Library
Govt. Documents/Maps Unit
College Park, MD 20742
(301) 454-3034 FAX: (301) 454-4985

MASSACHUSETTS

BOSTON PUBLIC LIBRARY
Govt. Documents Dept.
666 Boylston Street
Boston, MA 02117
(617) 536-5400 ext. 226
FAX: (617) 267-8273; 267-8248

MICHIGAN

DETROIT PUBLIC LIBRARY
5201 Woodward Avenue
Detroit, MI 48202-4093
(313) 833-1440; 833-1409
FAX: (313) 833-5039

LIBRARY OF MICHIGAN
Govt. Documents Unit
P.O. Box 30007
Lansing, MI 48909
(517) 373-0640 FAX: (517) 373-3381

MINNESOTA

UNIV. OF MINNESOTA
Wilson Library
Govt. Publications Library
309 19th Avenue South
Minneapolis, MN 55455
(612) 624-5073 FAX: (612) 626-9353

MISSISSIPPI

UNIV. OF MISSISSIPPI
J.D. Williams Library
Federal Documents Dept.
106 Old Gym Bldg.
University, MS 38677
(601) 232-5857 FAX: (601) 232-5453

MISSOURI

UNIV. OF MISSOURI - COLUMBIA
Ellis Library
Govt. Documents
Columbia, MO 65201
(314) 882-6733 FAX: (314) 882-8044

MONTANA

UNIV. OF MONTANA
Maureen & Mike Mansfield Library
Documents Div.
Missoula, MT 59812-1195
(406) 243-6700 FAX: (406) 243-2060

NEBRASKA

UNIV. OF NEBRASKA - LINCOLN
D.L. Love Memorial Library
Documents Dept.
Lincoln, NE 68588
(402) 472-2562

NEVADA

UNIV. OF NEVADA
Reno Library
Govt. Publications Dept.
Reno, NV 89557
(702) 784-6579 FAX: (702) 784-1751

NEW JERSEY

NEWARK PUBLIC LIBRARY
U.S. Documents Div.
5 Washington Street - P.O. Box 630
Newark, NJ 07101-0630
(201) 733-7812 FAX: (201) 733-5648

NEW MEXICO

UNIV. OF NEW MEXICO
General Library
Govt. Publications Dept.
Albuquerque, NM 87131-1466
(505) 277-5441 FAX: (505) 277-6019

NEW MEXICO STATE LIBRARY
325 Don Gaspar Avenue
Santa Fe, NM 87503
(505) 827-3826 FAX: (505) 827-3820

NEW YORK

NEW YORK STATE LIBRARY
Documents/Gift & Exchange Section
Federal Depository Program
Cultural Education Center
Albany, NY 12230
(518) 474-5563 FAX: (518) 474-5786

NORTH CAROLINA

UNIV. OF NORTH CAROLINA - CHAPEL HILL
CB#3912, Davis Library
BA/SS Dept.—Documents
Chapel Hill, NC 27599
(919) 962-1151 FAX: (919) 962-0484

NORTH DAKOTA

NORTH DAKOTA STATE UNIV. LIBRARY
Documents Office
Fargo, ND 58105
(701) 237-8886 FAX: (701) 237-7138
In cooperation with Univ. of North Dakota, Chester Fritz Library Grand Forks

OHIO

STATE LIBRARY OF OHIO
Documents Dept.
65 South Front Street
Columbus, OH 43266
(614) 644-7051 FAX: (614) 752-9178

OKLAHOMA

OKLAHOMA DEPT. OF LIBRARIES
U.S. Govt. Information Div.
200 NE 18th Street
Oklahoma City, OK 73105-3298
(405) 521-2502, ext. 252, 253
FAX: (405) 525-7804

OKLAHOMA STATE UNIV.
Edmon Low Library
Documents Dept.
Stillwater, OK 74078
(405) 744-6546 FAX: (405) 744-5183

OREGON

PORTLAND STATE UNIV.
Millar Library
934 SW Harrison - P.O. Box 1151
Portland, OR 97207
(503) 725-3673 FAX: (503) 725-4527

PENNSYLVANIA

STATE LIBRARY OF PENN.
Govt. Publications Section
Walnut St. & Commonwealth Ave. - P.O. Box 1601
Harrisburg, PA 17105
(717) 787-3752

SOUTH CAROLINA

CLEMSON UNIV.
Cooper Library
Public Documents Unit
Clemson, SC 29634-3001
(803) 656-5174 FAX: (803) 656-3025
In cooperation with Univ. of South Carolina, Thomas Cooper Library, Columbia

TENNESSEE

MEMPHIS STATE UNIV. LIBRARIES
Govt. Documents
Memphis, TN 38152
(901) 678-2586 FAX: (901) 678-2511

TEXAS

TEXAS STATE LIBRARY
United States Documents
P.O. Box 12927 - 1201 Brazos
Austin, TX 78711
(512) 463-5455 FAX: (512) 463-5436

TEXAS TECH. UNIV. LIBRARY
Documents Dept.
Lubbock, TX 79409
(806) 742-2268 FAX: (806) 742-1920

UTAH

UTAH STATE UNIV.
Merrill Library & Learning Resources Center, UMC-3000
Documents Dept.
Logan, UT 84322-3000
(801) 750-2684 FAX: (801) 750-2677

VIRGINIA

UNIV. OF VIRGINIA
Alderman Library
Govt. Documents
Charlottesville, VA 22903-2498
(804) 924-3133 FAX: (804) 924-4337

WASHINGTON

WASHINGTON STATE LIBRARY
Document Section
MS AJ-11
Olympia, WA 98504-0111
(206) 753-4027 FAX: (206) 753-3546

WEST VIRGINIA

WEST VIRGINIA UNIV. LIBRARY
Govt. Documents Section
P.O. Box 6069
Morgantown, WV 26506
(304) 293-3640

WISCONSIN

ST. HIST. SOC. OF WISCONSIN LIBRARY
Govt. Publications Section
816 State Street
Madison, WI 53706
(608) 262-2781 FAX: (608) 262-4711
In cooperation with Univ. of Wisconsin-Madison, Memorial Library

MILWAUKEE PUBLIC LIBRARY
Documents Div.
814 West Wisconsin Avenue
Milwaukee, WI 53233
(414) 278-2167 FAX: (414) 278-2137

WYOMING

WYOMING STATE LIBRARY
Supreme Court & Library Bldg.
Govt. Publications
Cheyenne, WY 82002
(307) 777-5920 FAX: (307) 777-6289

* U.S. G.P.O.:1992-313-125:60001

National Aeronautics and
Space Administration
Code JTT
Washington, D.C.
20546-0001

Official Business
Penalty for Private Use, $300

SPECIAL FOURTH-CLASS RATE
POSTAGE & FEES PAID
NASA
PERMIT No. G27

POSTMASTER: If Undeliverable (Section 158
Postal Manual) Do Not Return